HUMAN MICROBIOME: SYMBIOSIS TO PATHOGENESIS

EDITED BY: Learn-Han Lee, Nurul-Syakima Ab Mutalib, Sunny Hei Wong, Siok-Fong Chin and Vishal Singh

PUBLISHED IN: Frontiers in Microbiology

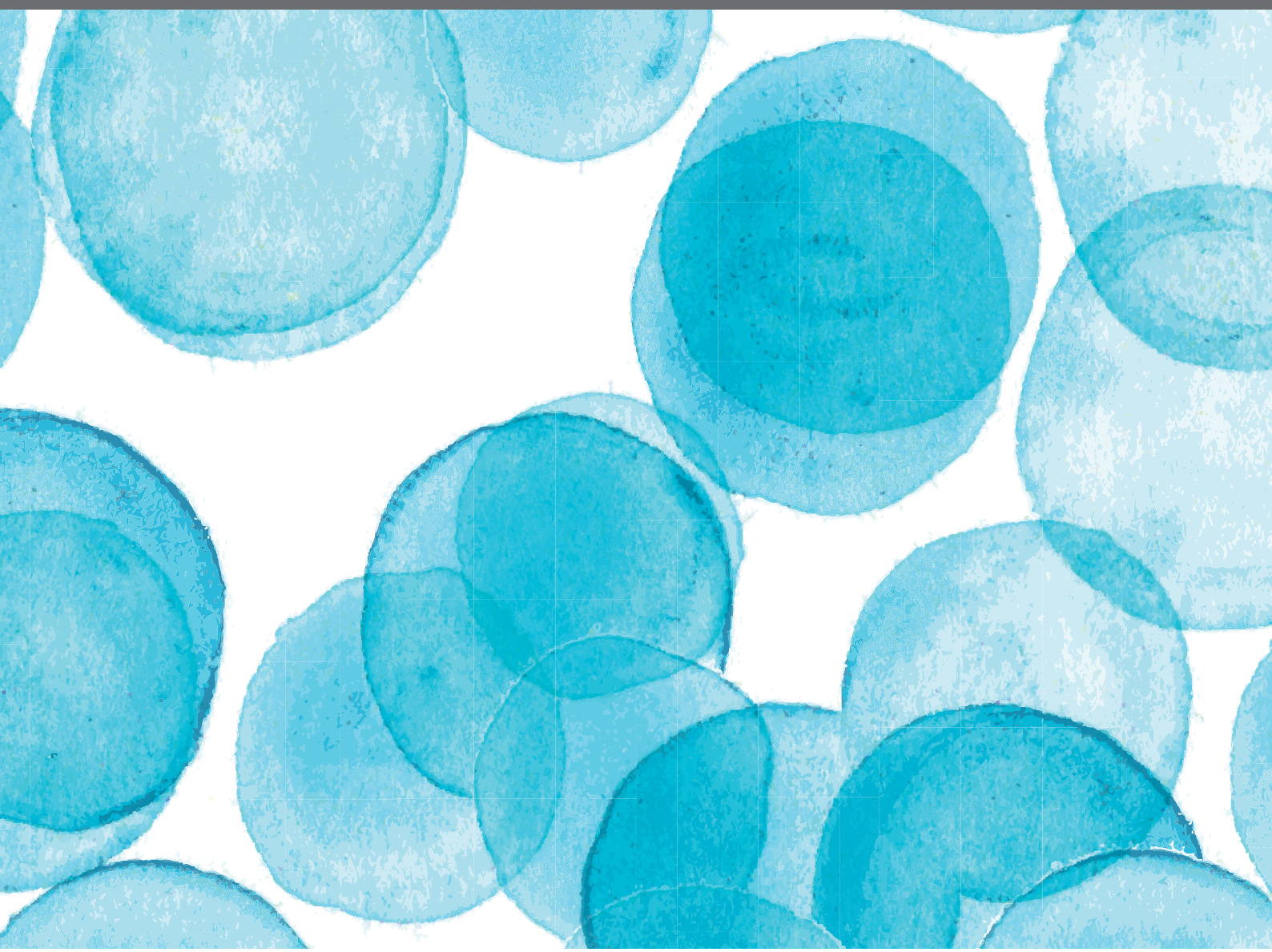

frontiers Research Topics

frontiers

Frontiers eBook Copyright Statement

The copyright in the text of individual articles in this eBook is the property of their respective authors or their respective institutions or funders. The copyright in graphics and images within each article may be subject to copyright of other parties. In both cases this is subject to a license granted to Frontiers.

The compilation of articles constituting this eBook is the property of Frontiers.

Each article within this eBook, and the eBook itself, are published under the most recent version of the Creative Commons CC-BY licence. The version current at the date of publication of this eBook is CC-BY 4.0. If the CC-BY licence is updated, the licence granted by Frontiers is automatically updated to the new version.

When exercising any right under the CC-BY licence, Frontiers must be attributed as the original publisher of the article or eBook, as applicable.

Authors have the responsibility of ensuring that any graphics or other materials which are the property of others may be included in the CC-BY licence, but this should be checked before relying on the CC-BY licence to reproduce those materials. Any copyright notices relating to those materials must be complied with.

Copyright and source acknowledgement notices may not be removed and must be displayed in any copy, derivative work or partial copy which includes the elements in question.

All copyright, and all rights therein, are protected by national and international copyright laws. The above represents a summary only. For further information please read Frontiers' Conditions for Website Use and Copyright Statement, and the applicable CC-BY licence.

ISSN 1664-8714
ISBN 978-2-88966-623-2
DOI 10.3389/978-2-88966-623-2

About Frontiers

Frontiers is more than just an open-access publisher of scholarly articles: it is a pioneering approach to the world of academia, radically improving the way scholarly research is managed. The grand vision of Frontiers is a world where all people have an equal opportunity to seek, share and generate knowledge. Frontiers provides immediate and permanent online open access to all its publications, but this alone is not enough to realize our grand goals.

Frontiers Journal Series

The Frontiers Journal Series is a multi-tier and interdisciplinary set of open-access, online journals, promising a paradigm shift from the current review, selection and dissemination processes in academic publishing. All Frontiers journals are driven by researchers for researchers; therefore, they constitute a service to the scholarly community. At the same time, the Frontiers Journal Series operates on a revolutionary invention, the tiered publishing system, initially addressing specific communities of scholars, and gradually climbing up to broader public understanding, thus serving the interests of the lay society, too.

Dedication to Quality

Each Frontiers article is a landmark of the highest quality, thanks to genuinely collaborative interactions between authors and review editors, who include some of the world's best academicians. Research must be certified by peers before entering a stream of knowledge that may eventually reach the public - and shape society; therefore, Frontiers only applies the most rigorous and unbiased reviews.
Frontiers revolutionizes research publishing by freely delivering the most outstanding research, evaluated with no bias from both the academic and social point of view. By applying the most advanced information technologies, Frontiers is catapulting scholarly publishing into a new generation.

What are Frontiers Research Topics?

Frontiers Research Topics are very popular trademarks of the Frontiers Journals Series: they are collections of at least ten articles, all centered on a particular subject. With their unique mix of varied contributions from Original Research to Review Articles, Frontiers Research Topics unify the most influential researchers, the latest key findings and historical advances in a hot research area! Find out more on how to host your own Frontiers Research Topic or contribute to one as an author by contacting the Frontiers Editorial Office: frontiersin.org/about/contact

HUMAN MICROBIOME: SYMBIOSIS TO PATHOGENESIS

Topic Editors:
Learn-Han Lee, Monash University Malaysia, Malaysia
Nurul-Syakima Ab Mutalib, National University of Malaysia, Malaysia
Sunny Hei Wong, The Chinese University of Hong Kong, China
Siok-Fong Chin, National University of Malaysia, Malaysia
Vishal Singh, Pennsylvania State University (PSU), United States

Citation: Lee, L.-H., Ab Mutalib, N.-S., Wong, S. H., Chin, S.-F., Singh, V., eds. (2021). Human Microbiome: Symbiosis to Pathogenesis. Lausanne: Frontiers Media SA. doi: 10.3389/978-2-88966-623-2

Table of Contents

06 ***Editorial: Human Microbiome: Symbiosis to Pathogenesis***
Learn-Han Lee, Sunny Hei Wong, Siok-Fong Chin, Vishal Singh and Nurul-Syakima Ab Mutalib

12 ***16S rRNA Gene Sequencing for Deciphering the Colorectal Cancer Gut Microbiome: Current Protocols and Workflows***
Muhammad-Afiq Osman, Hui-min Neoh, Nurul-Syakima Ab Mutalib, Siok-Fong Chin and Rahman Jamal

22 ***Microbial Similarity and Preference for Specific Sites in Healthy Oral Cavity and Esophagus***
Li Dong, Jian Yin, Jing Zhao, Shan-rui Ma, Hai-rui Wang, Meng Wang, Wen Chen and Wen-qiang Wei

32 ***Genetically Obese Human Gut Microbiota Induces Liver Steatosis in Germ-Free Mice Fed on Normal Diet***
Ruirui Wang, Hui Li, Xin Yang, Xinhe Xue, Liman Deng, Jian Shen, Menghui Zhang, Liping Zhao and Chenhong Zhang

44 ***Bacterial Communities in the Womb During Healthy Pregnancy***
Lihong Zhu, Fei Luo, Wenjing Hu, Yang Han, Yuezhu Wang, Huajun Zheng, Xiaokui Guo and Jinhong Qin

50 ***Alterations in the Urinary Microbiota are Associated With Cesarean Delivery***
Fengping Liu, Longxian Lv, Huiyong Jiang, Ren Yan, Shurong Dong, Liping Chen, Wei Wang and Yong Q. Chen

62 ***The Gut Microbiota in the Pathogenesis and Therapeutics of Inflammatory Bowel Disease***
Tao Zuo and Siew C. Ng

75 ***Keystone Species in Pregnancy Gingivitis: A Snapshot of Oral Microbiome During Pregnancy and Postpartum Period***
Preethi Balan, Yap Seng Chong, Shivshankar Umashankar, Sanjay Swarup, Wong Mun Loke, Violeta Lopez, Hong Gu He and Chaminda Jayampath Seneviratne

86 ***Clinical Efficacy and Microbiome Changes Following Fecal Microbiota Transplantation in Children With Recurrent Clostridium Difficile Infection***
Xiaolu Li, Xuefeng Gao, Hui Hu, Yongmei Xiao, Dan Li, Guangjun Yu, Dongbao Yu, Ting Zhang and Yizhong Wang

94 ***Alterations of Gut Microbiota in Cholestatic Infants and Their Correlation With Hepatic Function***
Cheng Guo, Yinhu Li, Peipei Wang, Yingchao Li, Chuangzhao Qiu, Muxia Li, Daxi Wang, Ruiqin Zhao, Dongfang Li, Ye Wang, Shuaicheng Li, Wenkui Dai and Lin Zhang

105 ***Corrigendum: Alterations of Gut Microbiota in Cholestatic Infants and Their Correlation With Hepatic Function***
Cheng Guo, Yinhu Li, Peipei Wang, Yingchao Li, Chuangzhao Qiu, Muxia Li, Daxi Wang, Ruiqin Zhao, Dongfang Li, Ye Wang, Shuaicheng Li, Wenkui Dai and Lin Zhang

106 ***Gut Microbiota Features in Young Children With Autism Spectrum Disorders***
Lorena Coretti, Lorella Paparo, Maria Pia Riccio, Felice Amato, Mariella Cuomo, Alessandro Natale, Luca Borrelli, Giusi Corrado, Carmen De Caro, Marika Comegna, Elisabetta Buommino, Giuseppe Castaldo, Carmela Bravaccio, Lorenzo Chiariotti, Roberto Berni Canani and Francesca Lembo

118 ***Corrigendum: Gut Microbiota Features in Young Children With Autism Spectrum Disorders***
Lorena Coretti, Lorella Paparo, Maria Pia Riccio, Felice Amato, Mariella Cuomo, Alessandro Natale, Luca Borrelli, Giuseppina Corrado, Carmen De Caro, Marika Comegna, Elisabetta Buommino, Giuseppe Castaldo, Carmela Bravaccio, Lorenzo Chiariotti, Roberto Berni Canani and Francesca Lembo

119 ***Identification of Specific Oral and Gut Pathogens in Full Thickness Colon of Colitis Patients: Implications for Colon Motility***
Vasudevan Dinakaran, Sammed N. Mandape, Kristina Shuba, Siddharth Pratap, Shruti S. Sakhare, Mohammad Ali Tabatabai, Duane T. Smoot, Cherae M. Farmer-Dixon, Lakshmyya N. Kesavalu, Samuel Evans Adunyah, Janet Hayes Southerland and Pandu R. Gangula

142 ***Elucidating the Immune-Related Mechanisms by Which Probiotic Strain* Lactobacillus casei *BL23 Displays Anti-tumoral Properties***
Elsa Jacouton, Marie-Laure Michel, Edgar Torres-Maravilla, Florian Chain, Philippe Langella and Luis G. Bermúdez-Humarán

152 ***Intestinal Microbiota as a Host Defense Mechanism to Infectious Threats***
Simona Iacob, Diana Gabriela Iacob and Luminita Monica Luminos

161 ***Nasopharyngeal Microbiota in Children With Invasive Pneumococcal Disease: Identification of Bacteria With Potential Disease-Promoting and Protective Effects***
Anny Camelo-Castillo, Desirée Henares, Pedro Brotons, Antonio Galiana, Juan Carlos Rodríguez, Alex Mira and Carmen Muñoz-Almagro on behalf of the Catalan Study Group of Host- Pathogen Interaction in Patients With IPD

175 ***Comparison of Small Gut and Whole Gut Microbiota of First-Degree Relatives With Adult Celiac Disease Patients and Controls***
Rahul Bodkhe, Sudarshan A. Shetty, Dhiraj P. Dhotre, Anil K. Verma, Khushbo Bhatia, Asha Mishra, Gurvinder Kaur, Pranav Pande, Dhinoth K. Bangarusamy, Beena P. Santosh, Rajadurai C. Perumal, Vineet Ahuja, Yogesh S. Shouche and Govind K. Makharia

187 ***Comparison of the Vaginal Microbiomes of Premenopausal and Postmenopausal Women***
Karol Gliniewicz, G. Maria Schneider, Benjamin J. Ridenhour, Christopher J. Williams, Yuli Song, Miranda A. Farage, Kenneth Miller and Larry J. Forney

196 ***Elucidation of* Akkermansia muciniphila *Probiotic Traits Driven by Mucin Depletion***
Jongoh Shin, Jung-Ran Noh, Dong-Ho Chang, Yong-Hoon Kim, Myung Hee Kim, Eaum Seok Lee, Suhyung Cho, Bon Jeong Ku, Moon-Soo Rhee, Byoung-Chan Kim, Chul-Ho Lee and Byung-Kwan Cho

208 ***Investigating Host Microbiota Relationships Through Functional Metagenomics***
Elisabeth Laville, Josette Perrier, Nada Bejar, Marc Maresca, Jeremy Esque, Alexandra S. Tauzin, Emna Bouhajja, Marion Leclerc, Elodie Drula, Bernard Henrissat, Stephane Berdah, Eric Di Pasquale, Patrick Robe and Gabrielle Potocki-Veronese

220 ***The Microbiome and Irritable Bowel Syndrome – A Review on the Pathophysiology, Current Research and Future Therapy***
Pei Pei Chong, Voon Kin Chin, Chung Yeng Looi, Won Fen Wong, Priya Madhavan and Voon Chen Yong

243 ***Corrigendum: The Microbiome and Irritable Bowel Syndrome – A Review on the Pathophysiology, Current Research and Future Therapy***
Pei Pei Chong, Voon Kin Chin, Chung Yeng Looi, Won Fen Wong, Priya Madhavan and Voon Chen Yong

244 ***Micronutrient Requirements and Sharing Capabilities of the Human Gut Microbiome***
Dmitry A. Rodionov, Aleksandr A. Arzamasov, Matvei S. Khoroshkin, Stanislav N. Iablokov, Semen A. Leyn, Scott N. Peterson, Pavel S. Novichkov and Andrei L. Osterman

266 ***B-Vitamin Sharing Promotes Stability of Gut Microbial Communities***
Vandana Sharma, Dmitry A. Rodionov, Semen A. Leyn, David Tran, Stanislav N. Iablokov, Hua Ding, Daniel A. Peterson, Andrei L. Osterman and Scott N. Peterson

281 ***Fecal Microbiome Data Distinguish Liver Recipients With Normal and Abnormal Liver Function From Healthy Controls***
Hai-Feng Lu, Zhi-Gang Ren, Ang Li, Hua Zhang, Shao-Yan Xu, Jian-Wen Jiang, Lin Zhou, Qi Ling, Bao-Hong Wang, Guang-Ying Cui, Xin-Hua Chen, Shu-Sen Zheng and Lan-Juan Li

294 ***miRNA-Gene Regulatory Network in Gnotobiotic Mice Stimulated by Dysbiotic Gut Microbiota Transplanted From a Genetically Obese Child***
Liman Deng, Ruirui Wang, Hui Li, Chenhong Zhang, Liping Zhao and Menghui Zhang

314 ***The Microbiome of Prostate Fluid is Associated With Prostate Cancer***
Xiaowei Ma, Chenfei Chi, Liancheng Fan, Baijun Dong, Xiaoguang Shao, Shaowei Xie, Min Li and Wei Xue

frontiers in Microbiology

EDITORIAL
published: 17 February 2021
doi: 10.3389/fmicb.2021.605783

Editorial: Human Microbiome: Symbiosis to Pathogenesis

Learn-Han Lee[1]*, *Sunny Hei Wong*[2]*, *Siok-Fong Chin*[3], *Vishal Singh*[4] and *Nurul-Syakima Ab Mutalib*[3]*

[1] Novel Bacteria and Drug Discovery (NBDD) Research Group, Microbiome and Bioresource Research Strength (MBRS), Jeffrey Cheah School of Medicine and Health Sciences, Monash University Malaysia, Subang Jaya, Malaysia, [2] Li Ka Shing Institute of Health Sciences, Department of Medicine and Therapeutics, The Chinese University of Hong Kong, Shatin, Hong Kong, [3] UKM Medical Molecular Biology Institute (UMBI), Universiti Kebangsaan Malaysia, Kuala Lumpur, Malaysia, [4] Department of Nutritional Sciences, The Pennsylvania State University, State College, PA, United States

Keywords: human microbiome, symbiosis, pathogenesis, fecal microbiome transplant, gut microbiome

Editorial on the Research Topic

Human Microbiome: Symbiosis to Pathogenesis

OPEN ACCESS

Edited by:
Marius Vital,
Hannover Medical School, Germany

Reviewed by:
M. Pilar Francino,
Fundación para el Fomento de la Investigación Sanitaria y Biomédica de la Comunitat Valenciana (FISABIO), Spain

***Correspondence:**
Learn-Han Lee
lee.learn.han@monash.edu
Sunny Hei Wong
wonghei@cuhk.edu.hk
Nurul-Syakima Ab Mutalib
syakima@ppukm.ukm.edu.my

Specialty section:
This article was submitted to Microbial Symbioses, a section of the journal Frontiers in Microbiology

Received: *13 September 2020*
Accepted: *26 January 2021*
Published: *17 February 2021*

Citation:
Lee L-H, Wong SH, Chin S-F, Singh V and Ab Mutalib N-S (2021) Editorial: Human Microbiome: Symbiosis to Pathogenesis. Front. Microbiol. 12:605783. doi: 10.3389/fmicb.2021.605783

INTRODUCTION

Researchers have come a long way in microorganism research since the first discovery of microbes as seen through an ingenious hand-held microscope over 300 years ago. In late 1600, the father of microbiology, Antonie van Leeuwenhoek, came up with his microscope design and observed tiny moving objects. He named the tiny objects animalcules (Leeuwenhoek, 1963; Smit and Heniger, 1975; Gest, 2004). Since then, the number of studies on microbes began to increase, opening up for a new horizon for research—the roles of microbes living not just in the environment but also throughout the human body.

The human microbiome consists of microbial communities, such as bacteria, virus, and fungi, which resides in and on our bodies. As the gut microbiome shifts toward a mature state after 2 years of human growth, numerous factors, such as drug use (e.g., antibiotics), dietary intake, and nutritional supplements, can lead to bacterial composition differences (Cho and Blaser, 2012; Voreades et al., 2014).

In this Research Topic, the Human Microbiome: Symbiosis to Pathogenesis, a total of 27 articles have been published, covering several exciting aspects that highlight the role of microbiota in humans, how microbes interact with the host, and how they subsequently contribute to the pathogenesis of chronic inflammatory diseases as well as metabolic disorders. Based on the gathered information, some research groups have also presented the potential of exploiting these data to design effective preventive and therapeutic options targeting specific bacterial communities.

REVOLUTIONARY TOOLS OF SCIENTIFIC RESEARCH: MORE SENSITIVE, ADVANCED, AND ACCURATE METHODS FOR MICROBIOME RESEARCH

On top of its current affordable pricing, next-generation sequencing speeds up the bacterial identification processes (by bypassing the need for culturing process) while providing enormous valuable information when combined with big data from other analytical techniques such as flow cytometry and gas or liquid chromatographic methods (Lagier et al., 2012; Escobar-Zepeda et al., 2015; Fouhy et al., 2015; Wang et al., 2015; Jovel et al., 2016; Lin et al., 2019; Osman et al.). A recent

study has proposed a new, revised estimated ratio of 1:1 bacterial to human cells after studying the human microbiome thoroughly a few years ago (Sender et al., 2016). Specifically, the colon contains ∼10 trillion cells, or 33% of the total bacterial cells in the human body, making it a site with the most microbes compared to other gastrointestinal system sites. Interestingly, Dong et al. shared their findings in this Research Topic, where they observed specific site-preferable bacterial signatures in the oral cavity and other parts of the gastrointestinal tract. These findings are significant in serving as a form of "baseline" to improving the understanding of the microbiome in human health.

HOW DOES THE MICROBIOME REFLECT ONE'S STATE OF HEALTH?

Till now, the relationship between humans and microbes appears to be rather complicated; one may even refer to it as a dramatic love-hate relationship as some can cause deadly infections while a portion of them improves the health of the host (Rosenstiel, 2013; Tomkovich and Jobin, 2016; Postler and Ghosh, 2017). As hosts, humans provide a habitat for microbes. In exchange, most microbes return the "favor" in a different form(s), including providing nutrients for the host by breaking down specific substrates (i.e., supporting the host's metabolism) and defending the host against harmful, opportunistic pathogens via habitat colonization and immunomodulatory responses (Iacob et al., Laville et al., Rodionov et al., Sharma et al., Shin et al.). Iacob et al. discussed the importance of the intestinal microbiome in maintaining barrier integrity while promoting and preserving immune homeostasis during intestinal infections. Whether or not the infant's gut is sterile or without microorganisms at birth remains a hot debate among the scientific community. The infant's gut microbiota begins to flourish within hours after birth and starts to stabilize upon reaching 2 years of age (Backhed et al., 2015; Bokulich et al., 2016; Yang et al., 2016; Chong et al., 2018; Mohammadkhah et al., 2018). Several factors lead to the microbiome's differences, including delivery mode, breastfeeding history, and drug use (e.g., direct antibiotic use, or mother antenatally). For example, infants delivered via cesarean delivery who lack exposure to the vaginal microbiome have a higher risk of developing asthma, autoimmune diseases, and metabolic diseases. Thus, it is now widely recognized that exposure to the vaginal microbiome of the mother or "vaginal seeding" assist in the formation of a healthy gut microbiome and "priming" the immune system of the infant (Dominguez-Bello et al., 2010; Ferretti et al., 2018; Stinson et al., 2018; Zhu et al.). Zhu et al. challenged the idea of a "sterile" healthy uterine cavity for pregnancy and discussed that bacterial colonization does occur during pregnancy. Even though a metagenomic study based on the 16S rRNA gene revealed certain bacterial groups, these microbes were either non-viable or rarely culturable. On the contrary, the team managed to recover, culture, and identify bacteria from the placenta, which led to the speculation that the bacteria recovered from amniotic fluid might spread through other locations (e.g., blood or placenta). Be that as it may, findings from Liu et al. further supported the notion that the delivery mode affects more than just the infant's microbiome. The team observed a rather peculiar change in the maternal urinary microbiome after cesarean delivery: many beneficial bacteria (including those affiliated with the phylum *Firmicutes*) dramatically reduced with an increment of potentially pathogenic bacterial populations such as *Pseudomonas* spp. (under the phylum *Proteobacteria* and family *Pseudomonadaceae*). These results suggest these microbial populations' potential, which may serve as risk markers for clinicians to consider protecting these mothers from infectious diseases.

Gut dysbiosis can directly affect gastrointestinal health (Zuo and Ng, Wang et al., Li et al., Guo et al., Bodkhe et al., Lu et al., Dinakaran et al., Chong et al., Jacouton et al., Deng et al.). The dysbiosis can occur due to overgrowth or invasion of pathogens in the gut, compromising the gut epithelial barrier integrity and exacerbating inflammation (Natividad and Verdu, 2013; Zhang et al., 2015; Wong et al., 2017). As chronic inflammation in the colon can lead to colon cancer development, Osman et al. reviewed the methods and databases available to help determine dysbiosis and summarized a list of bacteria associated with colorectal cancer based on previous literature. On the other hand, Wang et al. presented a piece of evidence suggesting the gut microbiome's causative role in non-alcoholic fatty liver disease. Gnotobiotic mice that received gut microbiota from genetically obese human donors developed liver macrovesicular steatosis with a higher concentration of hepatic triglyceride and cholesterol. These symptoms were not observed in those receiving gut microbiota from a genetically obese human donor after a dietary weight loss program. Similarly, Deng et al. also used gnotobiotic mice in their study, which showed that two groups of mice receiving gut microbiota from a child before and after dietary intervention (i.e., the WTP diet, composed of whole grains, traditional Chinese medicine food, and prebiotics) resulted in very different physiological phenotypes, each of which was similar to the donor's phenotype. The group analyzed differentially expressed (DE) miRNAs and genes in the colon and liver, which subsequently suggested the causative role of gut dysbiosis in obesity. Dinakaran et al. studied an array of full-thickness colon specimens of inflammatory bowel disease (IBD) patients. They found a significant difference in dysbiosis between African Americans compared to Caucasian patients along with a higher abundance of pathogenic bacteria at the diseased site than adjacent healthy colon specimens.

Apart from colon cancer and liver diseases, Chong et al. performed a thorough literature search and gathered necessary information highlighting the association between gut dysbiosis and irritable bowel syndrome (IBS). As a multifactorial disease, IBS is a chronic, functional bowel disorder that requires long-term management, including dietary and lifestyle changes (Selvaraj et al., 2020). The most striking part was the presence of co-morbid disorders among these patients, particularly anxiety and depression. There is still an apparent lack of explanations as to how microbes in the gut communicate with neurons in the brain that drives behavioral or emotional changes, but more clues are emphasizing the importance of the gut–brain axis (Foster and Neufeld, 2013; Kennedy et al., 2014; Lee et al., 2018, 2019; Quigley, 2018; Johnson et al., 2020). Coretti et al. observed a

substantial increase of *Bacteroidetes* and *Proteobacteria*, with a decrease of *Actinobacteria* in young children (aged 2–4 years of age) with autism spectrum disorder (ASD). The same team examined fecal short-chain fatty acid (SCFA) levels and discovered a significant increase of butyrate in ASD patients compared to healthy controls. Even though their levels were still within the normal range, the study pointed out that the over-representation of butyrate-producing bacteria can potentially result in neurologic and neuropsychiatric disorders.

Besides supporting the host's metabolism, microbes produce a wide array of beneficial compounds, including antibiotics and certain SCFAs that can function as "signaling molecules" and modulate the host's immune response (Ganapathy et al., 2013). Zuo and Ng published a review under this Research Topic, emphasizing the role of the gut microbiome in IBD. They indicated that a low intake of dietary fiber and low levels of SCFAs were associated with the development of IBD. Aside from that, the gut microbiome's stability and composition can be influenced by the host's dietary intake and dietary supplements like probiotics and prebiotics, emphasizing the importance of changing the host's eating behavior to restore health by boosting the balance in microbial composition.

MICROBIOME CHANGES AS BIOMARKERS AND POTENTIAL TREATMENT TARGET

Microbes within us could be the answer to identifying and resolving a plethora of health conditions. Instead of using invasive methods such as blood drawing or endoscopy examination, some teams have advocated the idea of screening fecal microbiome to identify specific bacterial signatures that may be used as a biomarker or even prognostic marker. Lu et al. discussed the unique gut microbial characteristics of liver recipients with abnormal and normal liver functions. The study described the fecal microbiome index measuring specific alterations of *Staphylococcus* and *Prevotella* spp. that could be used to distinguish liver recipients with abnormal and normal liver function. These findings could then help clinicians make subsequent decisions to ensure the swift recovery of liver function and restore the intestinal microbiota in patients after transplantation.

One of the easiest ways to manipulate the gut microbiome is via alterations in dietary intake. The concept of pre-and probiotics has always been under the limelight in the food industry. Probiotics are microbes that promote health effects in the host (when administered in adequate amounts), while prebiotics consists of non-digestible food or compounds that can be metabolized by microbes and grant beneficial physiological effects to the host via modulation of microbial composition or activity (Ziemer and Gibson, 1998; Martín and Langella, 2019). For instance, *Lactococcus* spp. is a frequently used probiotic in dairy products, and they can regulate the immune response via direct production of cytokines or induction of cytokines in immune cells (Del Carmen et al., 2011; Xu and Kong, 2013; Yin et al., 2014). Jacouton et al. presented that *Lactobacillus casei* BL23 confers antitumor activity against colorectal cancer via the regulation of natural killer cell activity and stimulation of IL-2 production. Undeniably, further in-depth investigations into the stability and persistence of beneficial microbes via supplementation and prebiotics can improve host-microbe relationships. Researchers can apply this knowledge to therapeutic and preventive measures strategy against diseases by reversing dysbiosis in the microbiome and improving humans' overall health (Ma et al., 2020; Yue et al., 2020). Rodionov et al. and Sharma et al. emphasized the idea of the dietary response of gut microbial communities when it came to designing treatment for dysbiosis-related syndromes and diseases via rational nutritional supplementation. Rodionov et al. utilized genomics and a predictive modeling approach to study eight B vitamins, queuosine utilization, and sharing capabilities in the gut microbiome. Likewise, experimental studies by Sharma et al. supported the hypothesis of B vitamin sharing among gut microbes as the relative abundance of auxotrophic species remained unchanged in the absence of B-vitamins or significant excess. In summary, understanding the interactions between microbe–microbe interactions is just as vital as host–microbe interactions when it comes to formulating preventive and therapeutic strategies targeting microbiome restoration.

Besides that, FMT is a procedure that delivers specially packed stool material from healthy donors to the recipient to improve health conditions by restoring the balance in the gut microbial community (Aroniadis and Brandt, 2013). FMT utilization began during the Chinese civilization: a traditional Chinese medicine doctor cured patients who had food poisoning and severe diarrhea by consuming "yellow soup" containing human fecal suspension (Zhang et al., 2012; Shi and Yang, 2018). In modern days, FMT is used to treat patients with multiple recurrent *Clostridium difficile* infections and who failed to respond to conventional antibiotics treatment (Liubakka and Vaughn, 2016; Nagy, 2018; Nicholson et al., 2020; Perler et al., 2020; Li et al.). Li et al. examined fecal samples from children with recurrent *C. difficile* infection (RCDI) after undergoing FMT. They noticed a shift in microbiome composition with similarity leaning toward the donor and healthy control group, possibly with a better gut health state. Even though four of them received more than a single FMT session as they did not exhibit clinical improvement after the first FMT, they still achieved remission after multiple FMT.

Other than the gut microbiomes, there is potentially increasing attention placed on studying the microbiomes of organs other than the gastrointestinal system for humanity's benefits, especially for the development of biomarkers. Under this Research Topic, there are a total of six articles exploring the microbiome of other organs such as the nasal, vaginal, urinary, and prostate microbiomes (Balan et al., Zhu et al., Liu et al., Gliniewicz et al., Ma et al., Camelo-Castillo et al.). Ma et al. compared the microbiome profiles of prostatic fluid samples from prostate cancer patients with healthy controls. Typically, detection of prostate cancer is performed using invasive procedures like biopsies and the measurement of prostate-specific antigen, which frequently leads to misdiagnosis due to its high sensitivity and low

specificity (Etzioni et al., 2002; Welch and Albertsen, 2009; Kasivisvanathan et al., 2018). This pilot study presented by Ma et al. demonstrated a lower microbial diversity in the prostate fluid of prostate cancer patients compared to healthy controls. Camelo-Castillo et al. compared the nasopharyngeal microbiota of children with invasive pneumococcal disease (IPD) to matched controls by performing a principal coordinate analysis. While pointing out that specific microbiota profiles should be studied thoroughly as potential biomarkers for IPD or asymptomatic colonization, the study emphasized that identifying beneficial bacteria through this type of study could help fight against pneumococcal infections, possibly by integrating these microorganisms in a probiotic formula. Having that said, these studies serve as an essential steppingstone in identifying specific bacterial species as novel diagnostic biomarkers. They offer an exciting perspective to consider capitalizing on their roles in different diseases to formulate better therapeutic and prevention strategies in the nearest future.

CONCLUSION

With the increasing ability to understand microbial metabolic and functional capabilities, the microbiome's contribution to human health and various diseases is becoming more evident. Researchers are attempting to untangle the complicated relationships between microbes and humans as the host. More work is needed to move toward personalized medicine by restoring balance in the gut microbiome, regardless of population replacement via FMT or introduction of prebiotics or probiotics. Just as insinuated by Bodkhe et al., it might be worthwhile to investigate the microbiome of close relatives of patients suffering heritable diseases such as celiac disease. The investigation may give a better overview of alterations in the microbiome during disease progression or transition. Given the complexity of interactions between host-microbe and microbe-microbe, defining the "baseline" for a healthy gut microbiome seems like the next hurdle for everyone in microbiome research. Nonetheless, the Research Topic's findings strengthen the current opinion on dysbiosis and human health and suggest the importance of seeking an association between different microbiomes in the human body. Understanding the symbiotic relationships between the human host and microbiome will guarantee success in the restoration of the microbiome for disease prevention, management, and treatment.

AUTHOR CONTRIBUTIONS

L-HL, SHW, and N-SAM wrote the editorial. L-HL, SHW, S-FC, VS, and N-SAM participated in reviewing, editing, and proofreading of the editorial. L-HL, SHW, and N-SAM conceptualized the project. All authors read and approved the final editorial.

FUNDING

Seed Funding supported this project from Microbiome and Bioresource Research Strength (MBRS), Jeffrey Cheah School of Medicine and Health Sciences (JCSMHS) (Vote Number: MBRS/JCSMHS/01/2020).

ACKNOWLEDGMENTS

This work was inspired by Microbiome and Bioresource Research Strength (MBRS) in Jeffrey Cheah School of Medicine and Health Sciences, Monash University Malaysia. Also, the authors thank Dr. Hooi-Leng Ser for the kind contribution in making the project a success.

REFERENCES

Aroniadis, O. C., and Brandt, L. J. (2013). Fecal microbiota transplantation: past, present and future. *Curr. Opin. Gastroenterol.* 29, 79–84. doi: 10.1097/MOG.0b013e32835a4b3e

Backhed, F., Roswall, J., Peng, Y., Feng, Q., Jia, H., Kovatcheva-Datchary, P., et al. (2015). Dynamics and stabilization of the human gut microbiome during the first year of life. *Cell Host Microbe* 17, 690–703. doi: 10.1016/j.chom.2015.04.004

Bokulich, N. A., Chung, J., Battaglia, T., Henderson, N., Jay, M., Li, H., et al. (2016). Antibiotics, birth mode, and diet shape microbiome maturation during early life. *Sci. Trans. Med.* 8:343ra82. doi: 10.1126/scitranslmed.aad7121

Cho, I., and Blaser, M. J. (2012). The human microbiome: at the interface of health and disease. *Nat. Rev. Gen.* 13, 260–270. doi: 10.1038/nrg3182

Chong, C. Y. L., Bloomfield, F. H., and O'Sullivan, J. M. (2018). Factors affecting gastrointestinal microbiome development in neonates. *Nutrients* 10:274. doi: 10.3390/nu10030274

Del Carmen, S., De Leblanc, A. D. M., Perdigon, G., Pereira, V. B., Miyoshi, A., Azevedo, V., et al. (2011). Evaluation of the anti-inflammatory effect of milk fermented by a strain of IL-10-producing *Lactococcus lactis* using a murine model of Crohn's disease. *J. Mol. Microbiol. Biotech.* 21, 138–146. doi: 10.1159/000333830

Dominguez-Bello, M. G., Costello, E. K., Contreras, M., Magris, M., Hidalgo, G., Fierer, N., et al. (2010). Delivery mode shapes the acquisition and structure of the initial microbiota across multiple body habitats in newborns. *Proc. Nat. Acad. Sci. U.S.A.* 107, 11971–11975. doi: 10.1073/pnas.1002601107

Escobar-Zepeda, A., Vera-Ponce de Leon, A., and Sanchez-Flores, A. (2015). The road to metagenomics: from microbiology to DNA sequencing technologies and bioinformatics. *Front. Genet.* 6:348. doi: 10.3389/fgene.2015.00348

Etzioni, R., Penson, D. F., Legler, J. M., Di Tommaso, D., Boer, R., Gann, P. H., et al. (2002). Overdiagnosis due to prostate-specific antigen screening: lessons from US prostate cancer incidence trends. *J. Nat. Cancer Inst.* 94, 981–990. doi: 10.1093/jnci/94.13.981

Ferretti, P., Pasolli, E., Tett, A., Asnicar, F., Gorfer, V., Fedi, S., et al. (2018). Mother-to-infant microbial transmission from different body sites shapes the developing infant gut microbiome. *Cell Host Microbe* 24, 133–145. doi: 10.1016/j.chom.2018.06.005

Foster, J. A., and Neufeld, K. A. M. (2013). Gut-brain axis: how the microbiome influences anxiety and depression. *Trends Neurosci.* 36, 305–312. doi: 10.1016/j.tins.2013.01.005

Fouhy, F., Stanton, C., Cotter, P. D., Hill, C., and Walsh, F. (2015). Proteomics as the final step in the functional metagenomics study of antimicrobial resistance. *Front. Microbiol.* 6:172. doi: 10.3389/fmicb.2015.00172

Ganapathy, V., Thangaraju, M., Prasad, P. D., Martin, P. M., and Singh, N. (2013). Transporters and receptors for short-chain fatty acids as the molecular link between colonic bacteria and the host. *Curr. Opin. Pharmacol.* 13, 869–874. doi: 10.1016/j.coph.2013.08.006

Gest, H. (2004). The discovery of microorganisms by Robert Hooke and Antoni Van Leeuwenhoek, fellows of the Royal Society. *Notes Rec. Royal Soc. Lond.* 58, 187–201. doi: 10.1098/rsnr.2004.0055

Johnson, D., Letchumanan, V., Thurairajasingam, S., and Lee, L. H. (2020). A revolutionizing approach to autism spectrum disorder using the microbiome. *Nutrients* 12:1983. doi: 10.3390/nu12071983

Jovel, J., Patterson, J., Wang, W., Hotte, N., O'Keefe, S., Mitchel, T., et al. (2016). Characterization of the gut microbiome using 16S or shotgun metagenomics. *Front. Microbiol.* 7:459. doi: 10.3389/fmicb.2016.00459

Kasivisvanathan, V., Rannikko, A. S., Borghi, M., Panebianco, V., Mynderse, L. A., Vaarala, M. H., et al. (2018). MRI-targeted or standard biopsy for prostate-cancer diagnosis. *New Eng. J. Med.* 378, 1767–1777. doi: 10.1056/NEJMoa1801993

Kennedy, P. J., Cryan, J. F., Dinan, T. G., and Clarke, G. (2014). Irritable bowel syndrome: a microbiome-gut-brain axis disorder?. *World J. Gastroenterol.* 20:14105. doi: 10.3748/wjg.v20.i39.14105

Lagier, J. C., Armougom, F., Million, M., Hugon, P., Pagnier, I., Robert, C., et al. (2012). Microbial culturomics: paradigm shift in the human gut microbiome study. *Clin. Microbiol. Infect.* 18, 1185–1193. doi: 10.1111/1469-0691.12023

Lee, L. H., Ser, H. L., Khan, T. M., Gan, K. G., Goh, B. H., and Ab Mutalib, N. S. (2019). IDDF2019-ABS-0321 Relationship between autism and gut microbiome: current status and update. *Gut* 68 (Suppl. 1), A40–A41. doi: 10.1136/gutjnl-2019-IDDFAbstracts.76

Lee, L. H., Ser, H. L., Khan, T. M., Long, M., Chan, K. G., Goh, B. H., et al. (2018). IDDF2018-ABS-0239 dissecting the gut and brain: potential links between gut microbiota in development of Alzheimer's disease?. *Gut* 67(Suppl. 2):A18. doi: 10.1136/gutjnl-2018-IDDFabstracts.37

Leeuwenhoek, A. V. (1963). IV. An extract of a letter from Mr. Anth. Van Leuwenhoek, concerning animalcules found on the teeth; of the scaleyness of the skin, andc. *Philos. Trans. R. Soc. Lond.* 17, 646–649. doi: 10.1098/rstl.1693.0012

Lin, H., He, Q. Y., Shi, L., Sleeman, M., Baker, M. S., and Nice, E. C. (2019). Proteomics and the microbiome: pitfalls and potential. *Exp. Rev. Proteomics* 16, 501–511. doi: 10.1080/14789450.2018.1523724

Liubakka, A., and Vaughn, B. P. (2016). *Clostridium difficile* infection and fecal microbiota transplant. *AACN Adv. Crit. Care* 27, 324–337. doi: 10.4037/aacnacc2016703

Ma, C., Wasti, S., Huang, S., Zhang, Z., Mishra, R., Jiang, S., et al. (2020). The gut microbiome stability is altered by probiotic ingestion and improved by the continuous supplementation of galactooligosaccharide. *Gut Microbes* 12:1785252. doi: 10.1080/19490976.2020.1785252

Martín, R., and Langella, P. (2019). Emerging health concepts in the probiotics field: streamlining the definitions. *Front. Microbiol.* 10:1047. doi: 10.3389/fmicb.2019.01047

Mohammadkhah, A. I., Simpson, E. B., Patterson, S. G., and Ferguson, J. F. (2018). Development of the gut microbiome in children, and lifetime implications for obesity and cardiometabolic disease. *Children* 5:160. doi: 10.3390/children5120160

Nagy, E. (2018). What do we know about the diagnostics, treatment and epidemiology of *Clostridioides* (*Clostridium*) *difficile* infection in Europe?. *J. Infect. Chemother.* 24, 164–170. doi: 10.1016/j.jiac.2017.12.003

Natividad, J. M., and Verdu, E. F. (2013). Modulation of intestinal barrier by intestinal microbiota: pathological and therapeutic implications. *Pharm. Res.* 69, 42–51. doi: 10.1016/j.phrs.2012.10.007

Nicholson, M. R., Mitchell, P. D., Alexander, E., Ballal, S., Bartlett, M., Becker, P., et al. (2020). Efficacy of fecal microbiota transplantation for *Clostridium difficile* infection in children. *Clin. Gastroenterol. Hepatol.* 18, 612–619. doi: 10.1016/j.cgh.2019.04.037

Perler, B. K., Chen, B., Phelps, E., Allegretti, J. R., Fischer, M., Ganapini, V., et al. (2020). Long-Term efficacy and safety of fecal microbiota transplantation for treatment of recurrent clostridioides difficile infection. *J. Clin. Gastroenterol.* 54, 701–706. doi: 10.1097/MCG.0000000000001281

Postler, T. S., and Ghosh, S. (2017). Understanding the holobiont: how microbial metabolites affect human health and shape the immune system. *Cell Metabol.* 26, 110–130. doi: 10.1016/j.cmet.2017.05.008

Quigley, E. M. (2018). The gut-brain axis and the microbiome: clues to pathophysiology and opportunities for novel management strategies in irritable bowel syndrome (IBS). *J. Clin. Med.* 7:6. doi: 10.3390/jcm7010006

Rosenstiel, P. (2013). Stories of love and hate: innate immunity and host-microbe crosstalk in the intestine. *Curr. Op. Gastroenterol.* 29, 125–132. doi: 10.1097/MOG.0b013e32835da2c7

Selvaraj, S. M., Wong, S. H., Ser, H. L., and Lee, L. H. (2020). Role of low FODMAP diet and probiotics on gut microbiome in irritable bowel syndrome (IBS). *Prog. Microbes Mol. Biol.* 3:a0000069. doi: 10.36877/pmmb.a0000069

Sender, R., Fuchs, S., and Milo, R. (2016). Revised estimates for the number of human and bacteria cells in the body. *PLoS Biol.* 14:e1002533. doi: 10.1371/journal.pbio.1002533

Shi, Y. C., and Yang, Y. S. (2018). Fecal microbiota transplantation: current status and challenges in China. *JGH Open* 2, 114–116. doi: 10.1002/jgh3.12071

Smit, P., and Heniger, J. (1975). Antoni van Leeuwenhoek (1632–1723) and the discovery of bacteria. *Antonie van Leeuwenhoek* 41, 217–228. doi: 10.1007/BF02565057

Stinson, L. F., Payne, M. S., and Keelan, J. A. (2018). A critical review of the bacterial baptism hypothesis and the impact of cesarean delivery on the infant microbiome. *Front. Med.* 5:135. doi: 10.3389/fmed.2018.00135

Tomkovich, S., and Jobin, C. (2016). Microbiota and host immune responses: a love–hate relationship. *Immunology* 147, 1–10. doi: 10.1111/imm.12538

Voreades, N., Kozil, A., and Weir, T. L. (2014). Diet and the development of the human intestinal microbiome. *Front. Microbiol.* 5:494. doi: 10.3389/fmicb.2014.00494

Wang, W. L., Xu, S. Y., Ren, Z. G., Tao, L., Jiang, J. W., and Zheng, S. S. (2015). Application of metagenomics in the human gut microbiome. *World J. Gastroenterol.* 21, 803–814. doi: 10.3748/wjg.v21.i3.803

Welch, H. G., and Albertsen, P. C. (2009). Prostate cancer diagnosis and treatment after the introduction of prostate-specific antigen screening: 1986–2005. *J. Nat. Cancer Inst.* 101, 1325–1329. doi: 10.1093/jnci/djp278

Wong, S. H., Zhao, L., Zhang, X., Nakatsu, G., Han, J., Xu, W., et al. (2017). Gavage of fecal samples from patients with colorectal cancer promotes intestinal carcinogenesis in germ-free and conventional mice. *Gastroenterology* 153, 1621–1633. doi: 10.1053/j.gastro.2017.08.022

Xu, Y., and Kong, J. (2013). Construction and potential application of controlled autolytic systems for *Lactobacillus casei* in cheese manufacture. *J. Food Protect.* 76, 1187–1193. doi: 10.4315/0362-028X.JFP-12-307

Yang, I., Corwin, E. J., Brennan, P. A., Jordan, S., Murphy, J. R., and Dunlop, A. (2016). The infant microbiome: implications for infant health and neurocognitive development. *Nurs. Res.* 65, 76–88. doi: 10.1097/NNR.0000000000000133

Yin, X., Yan, Y., Kim, E. B., Lee, B., and Marco, M. L. (2014). Effect of milk and milk containing *Lactobacillus casei* on the intestinal microbiota of mice. *J. Dairy Sci.* 97, 2049–2055. doi: 10.3168/jds.2013-7477

Yue, Y., Xu, X., Yang, B., Lu, J., Zhang, S., Liu, L., et al. (2020). Stable colonization of orally administered *Lactobacillus casei* SY13 alters the gut microbiota. *BioMed Res. Int.* 2020:5281639. doi: 10.1155/2020/5281639

Zhang, F., Luo, W., Shi, Y., Fan, Z., and Ji, G. (2012). Should we standardize the 1,700-year-old fecal microbiota transplantation? *Am. J. Gastroenterol.* 107:1755. doi: 10.1038/ajg.2012.251

Zhang, K., Hornef, M. W., and Dupont, A. (2015). The intestinal epithelium as guardian of gut barrier integrity. *Cell. Microbiol.* 17, 1561–1569. doi: 10.1111/cmi.12501

Ziemer, C. J., and Gibson, G. R. (1998). An overview of probiotics, prebiotics and synbiotics in the functional food concept: perspectives and future strategies. *Int. Dairy J.* 8, 473–479. doi: 10.1016/S0958-6946(98)00071-5

Conflict of Interest: The authors declare that the research was conducted in the absence of any commercial or financial relationships that could be construed as a potential conflict of interest.

Copyright © 2021 Lee, Wong, Chin, Singh and Ab Mutalib. This is an open-access article distributed under the terms of the Creative Commons Attribution License (CC BY). The use, distribution or reproduction in other forums is permitted, provided the original author(s) and the copyright owner(s) are credited and that the original publication in this journal is cited, in accordance with accepted academic practice. No use, distribution or reproduction is permitted which does not comply with these terms.

frontiers in Microbiology

MINI REVIEW
published: 27 April 2018
doi: 10.3389/fmicb.2018.00767

16S rRNA Gene Sequencing for Deciphering the Colorectal Cancer Gut Microbiome: Current Protocols and Workflows

Muhammad-Afiq Osman, Hui-min Neoh, Nurul-Syakima Ab Mutalib, Siok-Fong Chin and Rahman Jamal*

UKM Medical Molecular Biology Institute, Universiti Kebangsaan Malaysia, Kuala Lumpur, Malaysia

The human gut holds the densest microbiome ecosystem essential in maintaining a healthy host physiology, whereby disruption of this ecosystem has been linked to the development of colorectal cancer (CRC). The advent of next-generation sequencing technologies such as the 16S rRNA gene sequencing has enabled characterization of the CRC gut microbiome architecture in an affordable and culture-free approach. Nevertheless, the lack of standardization in handling and storage of biospecimens, nucleic acid extraction, 16S rRNA gene primer selection, length, and depth of sequencing and bioinformatics analyses have contributed to discrepancies found in various published studies of this field. Accurate characterization of the CRC microbiome found in different stages of CRC has the potential to be developed into a screening tool in the clinical setting. This mini review aims to concisely compile all available CRC microbiome studies performed till end of 2016 and to suggest standardized protocols that are crucial in developing a gut microbiome screening panel for CRC.

Keywords: gut microbiome, metagenomics, next-generation sequencing, 16S rRNA gene, 16S rRNA gene sequencing, colorectal cancer, colorectal cancer screening

OPEN ACCESS

Edited by:
Marius Vital,
Helmholtz-Zentrum für Infektionsforschung (HZI), Germany

Reviewed by:
Richard Allen White III,
RAW Molecular Systems (RMS) LLC, United States
Yuji Naito,
Kyoto Prefectural University of Medicine, Japan

****Correspondence:***
Hui-min Neoh
hui-min@ppukm.ukm.edu.my

Specialty section:
This article was submitted to Microbial Symbioses, a section of the journal Frontiers in Microbiology

Received: *30 December 2017*
Accepted: *04 April 2018*
Published: *27 April 2018*

Citation:
Osman M-A, Neoh H, Ab Mutalib N-S, Chin S-F and Jamal R (2018) 16S rRNA Gene Sequencing for Deciphering the Colorectal Cancer Gut Microbiome: Current Protocols and Workflows. Front. Microbiol. 9:767. doi: 10.3389/fmicb.2018.00767

INTRODUCTION

The human gut harbors an enormous, diverse, and dynamic microbiome, consisting primarily of bacteria and archaea, as well as fungi, protozoa and viruses. There are at least 100 trillion (10^{14}) microbial cells in the human gut, almost outnumbering the eukaryotic cells that reside together (Whitman et al., 1998; Costello et al., 2012; Sender et al., 2016). The gut microbiome is known to play a vital role in health, contributing toward the host's energy harvest and storage via various metabolic functions (Gill et al., 2006). In good health, our gut microbiota is mainly subdivided into two categories; commensal symbionts and commensal pathobionts. Commensal bacteria has been acknowledged to be important for host physiology through provision of essential nutrients and providing protection against colonization by opportunistic pathogens (Hooper and Gordon, 2001).

The gut microbiota has been typically controlled by environmental factors such as adoption of westernized diet and lifestyle (David et al., 2014). Incidentally, there is growing evidence to suggest that environmental factors such as obesity and diet are associated with the pathogenesis of colorectal cancer (CRC). As the mechanism of sporadic CRC is still poorly understood, an individual's gut microbiome landscape may reflect his or her dietary patterns which can either promote or protect against CRC (Bultman, 2017).

Bacterial composition in the gut helps to maintain its host's mucosal and systemic immunity homeostasis, avoiding any immunity trigger that might lead to physiological impairment. A shift of gut commensal microbiota toward opportunistic pathogens is a condition designated as dysbiosis (Barman et al., 2008). A few studies suggested dysbiosis as the scenario that will impact numerous physiological functions and that this will serve as a primary driver for inflammation in the colon leading to increased risk for CRC (Nistal et al., 2015). Many recent studies have started to disclose that the gut microbiome plays a role in oncogenesis, where their interaction with the immune system might either maintain a healthy host or drive tumor progression (Gagliani et al., 2014).

Unlike gastric cancer which is solely associated with *Helicobacter pylori* infection, metagenomics studies showed that fecal and mucosal samples of CRC patients and non-CRC individuals are enriched in different microbiome composition (Uemura et al., 2001; Thomas et al., 2016; Flemer et al., 2017). Most studies reported *Bacteroides, Fusobacterium,* and *Peptostreptococcus* as the more prominent genera in CRC samples compared to controls (**Table 1**). CRC patients also showed an increase in the abundance of *Gemella, Parvimonas,* and *Porphorymonas* (Chen et al., 2012; Allali et al., 2015; Sinha et al., 2016).

In conjunction with the acknowledgement of gut microbiome contribution toward health and disease, developments in next-generation sequencing provided many breakthroughs for taxonomic, phylogenetic or functional profiling of the gut microbiome. A metagenomics approach toward gut microbiome profiling will confer the added advantage of not only metagenome community characterization, but also provides answers on its physiological impact to the human host. Furthermore, via metagenomics sequencing, measurements of bacterial taxa abundance within a sample as well as identification of dysbiosis events within its tumor microenvironment could be carried out. Indeed, the Metagenomics of Human Intestinal Tract (MetaHIT) project was initiated to study associations between genes of the gut microbiome with health and disease (Qin et al., 2010).

Nevertheless, despite similar approaches being used in several gut microbiome studies on CRC patients, dissimilarities in results were still apparent (**Table 1**). These dissimilarities may either be caused by differences in the patients' dietary customs specific to a certain geographical location (**Figure 1**) or caused by the technical aspects of next-generation sequencing experiments due to variations in sample handling and processing, and bioinformatics analysis pipelines. Lack of standardization in human microbiome studies may cause repetitive discrepancies if no baseline protocol is available. To this end, recently, The Microbiome Quality Control (MBQC) project (http://www.mbqc.org/)has been initiated to expand and encourage open sharing of standard operating procedures and best practices in the metagenomics field (Sinha et al., 2015).

To elucidate the gut microbiome landscape in tumor microenvironments, specific study design and experiment protocols are required for metagenomics sequencing and analyses. In this review, we discuss the culture-independent application of 16S rRNA gene sequencing in cataloguing the CRC gut microbiome. This review will also cover the assessment of 16S rRNA gene sequencing of the CRC gut microbiome, covering steps from nucleic acid extraction, sample preparation, selection of hypervariable regions, sequencing platforms, and the determination of algorithms for bioinformatics analyses, which we believe will provide an insight into CRC gut microbiome characterization via the next-generation sequencing approach.

HIGH-THROUGHPUT MICROBIOME SEQUENCING

Advances in high-throughput sequencing technologies have enabled researchers to explore microbiome complexity associated with the human body and diseases. In the past decade, application of high-throughput DNA sequencing to profile the genomic composition of a microbial community in a culture-independent manner has expanded immensely. This high resolution molecular sequencing technique, designated as metagenomics, can be further sub-divided into two different approaches, namely 16S rRNA gene and shotgun metagenomics sequencing. The 16S rRNA gene sequencing approach relies on sequencing of the 16S ribosomal RNA (rRNA) gene as the genetic marker to study bacterial phylogeny and taxonomy. This genetic marker contains conserved hypervariable regions which can be used for bacteria identification. Selection of hypervariable regions for sequencing as well as amplicon primer design are important for 16S rRNA gene sequencing as these factors might contribute to differences in the results.

On the other hand, whole genome or shotgun metagenomics sequencing, an alternative to 16S rRNA gene sequencing, refers to massive parallel sequencing of DNA samples. This technique also identifies gene functions of the sequenced microbiome. Shotgun metagenomics sequencing involves random fragmentation of DNA, sequencing of these fragments, followed by reconstruction and assembly of overlapping sequences into a continuous sequence (Fraher et al., 2012). Researchers have used shotgun metagenomics sequencing to discover interactions between microbiota and its host. The disadvantages of this technique are that it is costly and it produces a huge amount of data that requires advanced bioinformatics analyses.

16S rRNA GENE SEQUENCING AND ITS IMPACT ON HUMAN GUT MICROBIOME

Many studies have employed 16S rRNA gene sequencing to profile the gut microbiota composition (Gill et al., 2006; Huse et al., 2012; Yatsunenko et al., 2012). The 16S small subunit ribosomal gene is an exclusive housekeeping gene in prokaryotes which can be used to determine microbial communities within samples; it is highly-conserved and contains hypervariable regions ranging from region V1 to V9. Sequencing of the 16S rRNA gene requires amplification of a selected variable region via PCR using a variety of "universal" primers followed by sequencing. The V4 region of 16S rRNA gene has been highly recommended as the gold standard for profiling of

TABLE 1 | CRC-associated bacteria of different geographical locations.

Publication	Location	CRC-associated Bacteria
Baxter et al., 2016	Canada & USA	*F. nucleatum, P. assaccharolytica, P. stomatis, Gemella sp., Prevotella sp. P. micra*
Flemer et al., 2017	Cork, Ireland	*Bacteroides, Roseburia, Ruminococcus, Oscillibacter, Porphyromonas, Peptostreptococcus, Parvimonas, Fusobacterium*
Sinha et al., 2016/ Ahn et al., 2013	Maryland/New York, USA	*Fusobacterium, Porphyromonas, Atobium*
Allali et al., 2015	US & Spain	*US: Eikenella Spain: Fusobacterium, Bulleida, Gemella, Parvimonas, Campylobacter, and Streptococcus*
Burns et al., 2015	Minneapolis, USA	*Fusobacterium, Providencia*
Gao et al., 2015	Shanghai, China	*Bacteroides, Prevotella, Streptococcus, Lactococcus, Fusobacterium*
Nakatsu et al., 2015	Guanzhou & Hong Kong, China	*B. fragilis, Gemella, Parvimonas, Peptostreptococcus, Granulicatella*
Zeller et al., 2014	Heidelberg, Germany & Créteil, France	*F. nucleatum, P. asaccharolytica, B. fragilis, E. ventriosum, E. eligens C. symbiosum, S. salivarus*
Dejea et al., 2014	Marryland, USA	*Lactococcus, Leuconostoc, Comamonas*
Mira-Pascual et al., 2015	Spain	*Fusobacterium, Bacteroides, and Methanobacteriales*
Zackular et al., 2014	UK	*Fusobacterium, Porphyromonas, Lachnospiraceae, and Enterobacteriaceae*
Geng et al., 2013	China	*Roseburia*
Weir et al., 2013	Colorado, USA	*Acidaminobacter unclassified, Phascolarctobacterium unclassified, Citrobacter farmeri and Akkermansia muciniphila*
Wu et al., 2013	Beijing, China	*Bacteroides, Campylobacter and Fusobacterium*
Chen et al., 2012	China	*Peptostreptococcus, Parvimonas, Fusobacterium, Mogibacterium, Porphyromonas*
Kostic et al., 2012	Spain	*Fusobacterium*
Wang et al., 2012	Shanghai, China	*Enterococcus, Escherichia/Shigella, Klebsiella, Streptococcus* and *Peptostreptococcus*
Marchesi et al., 2011	Netherland	*Slackia, Collinsella*
Sobhani et al., 2011	Paris, France	*Bacteroides/Prevotella*

human gut microbiome by the MetaHIT consortium (Qin et al., 2010; Lozupone et al., 2013). Besides selection of a suitable hypervariable region, compatibility of amplification fragment lengths with the read length capacity of the intended sequencing platform has to be confirmed.

The number of microbiome studies has increased enormously in concert with technological developments of DNA sequencing that facilitate culture- and cloning-free analyses. When it was first released in 2005, the first next-generation sequencer (Roche 454 pyrosequencer), can only sequence ∼120 bases of bacterial genome in a single run (Margulies et al., 2005). In recent years, this technology has enabled the coverage of up to 1000 bp and can span multiple hypervariable regions of the 16S rRNA gene. Due to its high resolution and cost-effective approach, 16S rRNA gene sequencing has become the commonest approach for microbial community profiling of the human gut.

16S rRNA GENE SEQUENCING AS A MOLECULAR SCREENING TOOL FOR CRC

Guaiac fecal occult blood test (gFOBT) and the immunochemical-based fecal occult blood test (iFOBT/FIT) are current screening tools for CRC via detection of gastrointestinal bleeding. Nevertheless, these tests are not specific for CRC as pathologies such as ulcerative colitis and polyps could also cause bleeding in the gut. Gut microbiome profiling studies based on 16S rRNA gene sequencing has identified bacterial genus frequently associated with CRC, including *Fusobacterium, Bacteroides,* and *Peptostreptococcus* (Nakatsu et al., 2015; Baxter et al., 2016; Flemer et al., 2017; **Table 1**). In particular, the role of *F. nucleatum* in CRC tumorigenesis and metastasis has been consistently reported in animal models and cell culture experiments (Kostic et al., 2013; Rubinstein et al., 2013). Recent, additional studies confirmed the importance of *F. nucleatum* in CRC, where the bacteria was shown to modulate tumorigenesis in the colon via miRNA-21 expression, which subsequently suppresses the immune response and activate oncogenic pathways (Nosho et al., 2016; Yang et al., 2017). Zackular et al's study demonstrated the feasibility of using microbial biomarkers such as *F. nucleatum* for CRC screening (Zackular et al., 2014). In addition, Liang et al established a species-level microbiome panel that could distinguish between CRC patients and healthy individuals of the Hong Kong population with greater accuracy and sensitivity than the current screening kit (Liang et al., 2017). Recently, it has been suggested that FOBT coupled with 16S rRNA gene sequencing will serve as a better screening approach for CRC, where stool-containing buffer samples from the FOBT kits could be used for sequencing (Liang et al., 2017; Taylor et al., 2017). To this end, standardized workflows for 16S rRNA gene sequencing will be crucial to produce results which are accurate and reproducible.

FIGURE 1 | CRC-associated bacteria from different geographical locations of the world. [1](Baxter et al., 2016) [2](Ahn et al., 2013; Sinha et al., 2016) [3] (Weir et al., 2013) [4](Burns et al., 2015) [5](Allali et al., 2015) [6](Thomas et al., 2016) [7](Marchesi et al., 2011) [8](Flemer et al., 2017) [9](Mira-Pascual et al., 2015) [10](Zackular et al., 2014) [11](Kostic et al., 2012) [12](Sobhani et al., 2011) [13](Gao et al., 2015) [14](Geng et al., 2013) [15](Wu et al., 2013) [16](Wang et al., 2012) [17] (Nakatsu et al., 2015) [18](Zeller et al., 2014).

SAMPLE COLLECTION AND STORAGE

An important but seldom emphasized aspect of 16S rRNA gene sequencing studies is sample integrity. For gut microbiome profiling studies, biopsy, surgical tissues and stool samples are the common biospecimens collected for characterization. Among these, stool samples were the first to be used for 16S rRNA gene sequencing to study the CRC microbiome. Subsequent studies used swabs, surgical or biopsy tissues as the starting material with different sample handling procedures. Minimization of sample contamination ensures that each biospecimen retains as much as possible of its original microbiome and contributes toward accurate results in gut microbiome profiling. Nevertheless, studies comparing methods of biospecimen handling remain few. Many published studies did not comprehensively disclose methods used for sample handling. Sobhani et al published the first 16S rRNA gene sequencing study on CRC microbiome in 2011. Their protocol used stool samples; samples were placed in a sterile carrier box, transported to the laboratory within 4 h and later stored at −20°C prior to DNA extraction. Subsequent studies published improvements in handling the biosamples and transportation protocols, including steps such as transportation of samples on ice (Wu et al., 2010) and storage at −80°C to preserve sample integrity (Consortium, 2012).

Stool samples require non-invasive techniques for collection and they are sufficient for researchers to obtain an overview of the gut microbiome spectrum in our colon. These samples could be studied using leftover stool-containing buffer from used FOBT and FIT cartridges (Baxter et al., 2016; Taylor et al., 2017). However, stool samples might not be able to provide a clear picture for studies exploring site-specific microbiome which would require a tissue biopsy. On the other hand, despite the invasiveness of tissue biopsy, these samples would enable in-depth studies into tumor-specific microbiota in comparison to stool sampling.

Short and long-term storage conditions post-transportation of samples is important to minimize differences in the microbiome spectrum caused by storage conditions. Sample transportation and storage conditions for fecal samples used in CRC gut microbiome characterization have been studied. Low temperature transportation, such as on ice or dry ice, ethanol-stored and long-term storage in −80°C are strongly recommended to maximize microbiome recovery within the sample prior nucleic acid extraction (Choo et al., 2015; Fouhy et al., 2015; Gorzelak et al., 2015; Blekhman et al., 2016). This also applies to biopsy and surgical tissue samples. Tissue handling protocols such snap-freezing cryovials in liquid nitrogen or usage of RNAlater medium will ensure optimum conditions for sample storage prior to nucleic acid extraction, leading to better microbiome recovery.

From the available literature, seven studies on CRC profiled the fecal microbiome, while others used colon tissue samples for their analyses (**Table 1**). Some studies investigated both fecal and tissue samples from the same individual to differentiate the microbiome compositions (**Table 1**). The authors from these studies applied various approaches for sample handling and

storage of the biospecimens. For studies using fecal samples, samples were all transported fresh and on ice to the research laboratory in <24 h; all samples except the ones used in a particular study were stored in −80°C. For the exception, DNA was directly extracted from samples and stored at −20°C until library preparation (Weir et al., 2013). On the other hand, for studies using tissue samples as the starting material, samples were usually snap-frozen in liquid nitrogen. Flemer et al. and Dejea et al. chose to use RNAlater as a preservative medium to ensure maximum recovery of nucleic acids; while the studies by Burns et al. and Gao et al. performed nucleic acid extraction right after sample collection (**Table 2**). Overall, perhaps due to the fact that 16S rRNA gene sequencing studies are still new, long-term effects of sampling and storage conditions for gut microbiome specimens have not been described.

METHODS IN NUCLEIC ACID EXTRACTION FOR PERCEIVING THE GUT MICROBIOME COMPOSITION

Nucleic acid extraction of samples is a simple but critical step in microbiome studies. In recent years, a few debates have risen about the best isolation protocol which will give the most accurate representation of the microbial spectrum. Most isolation protocols comprise of three basic steps that include cellular lysis, non-DNA macromolecule elimination together with DNA detachment and collection. In general, cell lysis protocols have received the most scrutiny, as complete cell disruption achieved from either enzymatic and/or mechanical processes will enable subsequent comprehensive DNA isolation, and vice versa. Gram positive organisms require stronger lysis conditions due to their thicker cell walls, unlike gram negative organisms which require only gentle lysis (Brown et al., 2015). Several studies have been carried out with modifications of the nucleic acid extraction protocols compared with earlier published studies. These modifications include incorporation of additional procedures such as mechanical homogenization of cells with glass or silica beads, enzymatic lysis reaction with lysozyme, or a combination of both mechanical and enzymatic reactions (**Table 2**). Once cellular lysis has been accomplished, DNA clean-up, concentration, and elution were routinely carried out.

On the other hand, there were studies that achieved success in microbiome profiling without modifications toward standard lysis protocols (**Table 2**). Nevertheless, it should be noted that no isolation protocol works equally well on different sample types or produces completely unbiased results. The prevention of sample contamination during nucleic acid extraction is also vital to eliminate DNA from non-indigenous microbes. Proper sample handling such as working in clean laboratory environments and using commercially available DNA/RNA-free nucleic acid extraction reagents will decrease the risk of contamination. The operator should also don proper attire, gloves and face mask to protect samples from contamination with their own microbiota.

SELECTION OF UNIVERSAL 16S rRNA GENE PRIMERS, SEQUENCING TECHNOLOGIES AND DATABASES

As described in an earlier section of this manuscript, the 16S rRNA gene consists of nine hypervariable conserved regions (V1 to V9) separated by ten highly conserved regions (Cox et al., 2013). The first 16S rRNA gene sequencing of CRC gut microbiome was completed 6 years ago using stool samples from 6 CRC patients (Sobhani et al., 2011). The study targeted the 16S rRNA V3/V4 regions, while its sequencing analyses relied on the database from the Ribosomal Database Project (RDP) using the RDP classifier (Cole et al., 2005). Similar studies targeting the same hypervariable regions were carried out a few years later using larger sample sizes and different biospecimens such as endoscopic biopsies and surgical tissues (Ahn et al., 2013; Flemer et al., 2017). Only very few studies were carried out to compare sequencing results obtained using primers targeting different hypervariable regions; most studies were done via sequencing of either one of the V3 or V4 regions, otherwise, a combination of two or more 16S rRNA gene hypervariable regions, whereby the most commonly used were the V3/V4 regions. Nevertheless, one study showed that while choice of primers had considerable effect, usage of matched primers on different sequencing platforms yielded little difference in results. (Tremblay et al., 2015). Differences obtained from the results of the various studies are conceivably due to factors such as selection of 16S rRNA gene primers and number of sequencing reads produced, as well as differences in classification techniques and bioinformatics analysis parameters. There is currently still no consensus on the best approach (Caporaso et al., 2011; Mizrahi-Man et al., 2013; Zheng et al., 2015).

Earlier gut microbiome studies in CRC were performed using the Roche 454 pyrosequencing technology (**Table 2**). Recently, the use of the Illumina MiSeq sequencer with paired-end reads and enhanced sequencing chemistry for microbiome studies has also increased (Caporaso et al., 2012). A study has been carried out to compare sequencing results produced between benchtop sequencers commonly used for 16S rRNA gene sequencing studies, including the Illumina MiSeq, Ion torrent Personal Genome Machine (PGM) and 454 GS Junior. Illumina MiSeq was found to generate data of the highest quality with almost no indel error compared to the other platforms (Loman et al., 2012).

Another important parameter in microbiome research is bioinformatics analysis. Most CRC microbiome studies rely on either the Greengenes or RDP database (**Table 1;** DeSantis et al., 2006; Cole et al., 2009). To the best of our knowledge, only RDP and SILVA are frequently updated; the Greengenes database has not been updated since 2013. On the other hand, the RefSeq Targeted Loci has been proposed to be the "gold standard" by the National Centre for Biotechnology Information (NCBI) for 16S rRNA gene sequencing data analysis (Tatusova et al., 2015). The NCBI database is also recommended for both 16S rRNA gene and shotgun metagenomics sequencing studies (Balvočiute and Huson, 2017). In addition, the SILVA database which covers phylogenies for small subunit rRNAs (16S for prokaryotes and 18S for eukaryotes) is also a resource for—aligning and/or

TABLE 2 | Published CRC 16S rRNA sequencing for gut microbiome studies, 2011–2016.

Publication	Sample Type	No. of CRC patients	Tissue samples	Sample handling	Sample storage	DNA Extraction kit	Hypervariable region	Sequencing Platform	OTU Classification Database	No. of Reads for Downstream/Total Reads	Bioinformatics Pipeline
Thomas et al., 2016	Biopsy Tissue	18	Non-cancer (18)	N/A	N/A	Phenol-Chloroform & Ethanol Precipitation	V4/V5	Ion Torrent PGM	RDP	17, 414 reads/sample	QIIME
Baxter et al., 2016	Stool	120	Adenoma (198) Normal (172)	Prior bowel prep, ship on ice next day	−80°C	MoBio Kit, 50 mg	V4	Illumina MiSeq	RDP	10, 000 reads/sample	MOTHUR
Flemer et al., 2017	Stool, Surgical Tissue, Biopsy Tissue	59	Adenoma (21), Control (56)	RNAlater (4°C, 12H)—Tissue, Ice box—Fecal (prior bowel prep)	−20°C (Tissue), −80°C (Fecal)	QIAGEN AllPrep DNA/RNA kit plus with glass bead homogenization)	V3/V4	Illumina MiSeq	RDP	5, 000 reads/sample	QIIME
Sinha et al., 2016/ Ahn et al., 2013	Stool	42	Normal (89)	Dry ice	−40°C	MoBio PowerSoil DNA Isolation kit	V3/V4	454 Pyro sequencing	Greengenes	5, 000 reads/sample	QIIME
Allali et al., 2015	Surgical Tissue	90	Adjacent-Normal	Snap-frozen in Isopentane	−80°C	QIAGEN Dneasy Blood and Tissue with Lysozyme in ATL buffer	V1/V2	454 Pyro sequencing	Greengenes	719 reads/sample	QIIME
Burns et al., 2015	Surgical Tissue	44	Adjacent-Normal	Flash-frozen Liquid Nitrogen	Not stored	QIAzol, Sonicate Water bath @65°C	V5/V6	Illumina MiSeq	Greengenes	5, 000 reads/sample	QIIME
Gao et al. 2015	Surgical Tissue	30	Adjacent-Normal, Normal (31)	N/A	Not stored	MoBio PowerSoil DNA Isolation kit	V3	454 Pyro sequencing	RDP, Greengenes, ITS Fungus, FGR	17, 018 reads/sample	QIIME
Nakatsu et al., 2015	Biopsy Tissue	52	Adenoma (47), Normal (61)	Flash-frozen Liquid Nitrogen	−80°C	QIAGEN QIAamp Mini kit with beads beating & lysozyme	V1-V4	454 Pyro sequencing	Greengenes	1, 000 reads/sample	MOTHUR
Zeller et al., 2014	Stool & Surgical tissue	89	Adjacent-normal (48), Normal (75)	Flash-frozen liquid nitrogen	−80°C	GNOME® DNA Isolation Kit	V4	Illumina MiSeq	SILVA	10, 000 reads/sample	MOTHUR
Dejea et al., 2014	Surgical & Biopsy tissue	23	Adenoma (2), Normal (22)	RNAlater	−80°C	QIAGEN QIAamp Stool DNA kit	V3-V5	454 Pyro sequencing	RDP	N/A	QIIME

(Continued)

TABLE 2 | Continued

Publication	Sample Type	No. of CRC patients	Tissue samples	Sample handling	Sample storage	DNA Extraction kit	Hypervariable region	Sequencing Platform	OTU Classification Database	No. of Reads for Downstream/Total Reads	Bioinformatics Pipeline
Mira-Pascual et al., 2015	Stool & Biopsy tissue	7	Adenoma (11), Normal (10)	N/A	−80°C	Machery-Nagel DNA kit with glass beads	V1/V2	454 Pyro sequencing	RDP	Biopsy/stool−6, 000 reads/sample, Biopsy-3groups−18, 000 reads/sample	MOTHUR
Zackular et al., 2014	Stool	30	Adenoma (30), Normal (30)	On ice (next day)	−80°C	MoBio PowerSoil DNA Isolation kit	V4	Illumina MiSeq	RDP	25, 993 reads/sample	MOTHUR
Geng et al., 2013	Biopsy Tissue	8	Adjacent-normal	Flash-frozen Liquid Nitrogen	−80°C	QIAGEN QIAamp DNA Mini kit with Silica beads	V1/V2	454 Pyro sequencing	BLAST	1, 400 reads/sample	QIIME
Weir et al., 2013	Stool	10	Normal (11)	Transport < 24 h	N/A	MoBio PowerSoil DNA Isolation kit	V4	454 Pyro sequencing	Greengenes	125 sequence/sample	MOTHUR
Wu et al., 2013	Stool	20	Normal (20)	Frozen	−80°C	QIAGEN QIAamp Stool DNA kit	V3	454 Pyro sequencing	RDP	N/A	MOTHUR
Chen et al., 2012	Surgical Tissue, Stool & Swab	47	Normal (9)	N/A	−80°C	QIAamp DNA Mini/Stool kit with lysozyme	V1-V3	454 Pyro sequencing	N/A	N/A	MOTHUR
Kostic et al., 2012	Surgical tissue	95	Adjacent-Normal	Flash-frozen Liquid Nitrogen	−80°C	N/A	V3-V5	454 Pyro sequencing	RDP	N/A	MOTHUR
Wang et al., 2012	Stool	46	Normal (56)	Frozen	−80°C	Bead-beating + Phenol-Chloroform Purification	V3	454 Pyro sequencing	RDP	N/A	DOTUR
Marchesi et al., 2011	Surgical tissue	6	Adjacent-Normal	N/A	−80°C	QIAGEN AllPrep DNA/RNA kit	V1-V3	454 Pyro sequencing	RDP	N/A	MOTHUR
Sobhani et al., 2011	Stool	6	Normal (6)	N/A	N/A	GNOME® DNA Isolation kit with Silica beads	V3/V4	454 Pyro sequencing	BLAST	N/A	R Package: VEGAN

N/A, Data/method was not described/stated.

quality-checking of rRNA sequence data (Pruesse et al., 2007; Quast et al., 2013). Recently, the EzBioCloud Genome database (previously known as EzTaxon) has been officially released. This database is well-curated; however, as it was recently launched, the database has yet been adapted in any 16S rRNA gene sequencing studies (Yoon et al., 2017). Despite the availability of numerous databases for 16S rRNA gene sequencing data analysis, a single, standardized database for this purpose is still unavailable.

The selection of appropriate computational tools for 16S rRNA gene sequencing dataset analysis is also crucial. Three commonly used bioinformatics pipelines were evaluated to determine the most precise tool available for unraveling the microbiome landscape via 16S rRNA gene sequencing (Plummer et al., 2015). Nevertheless, the comparison of findings from currently available studies showed that different results were obtained when analyses were run using different software or different databases. For all CRC gut microbiome studies carried out so far, most datasets were analyzed using Quantitative Insight into Microbial Ecology (QIIME) and MOTHUR (Schloss et al., 2009; Caporaso et al., 2010). Both tools were found to be precise for 16S rRNA gene sequencing dataset analysis.

CONCLUDING REMARKS AND FUTURE PERSPECTIVES

Initiatives on method standardization to study the human microbiome has been proposed by many research organizations such as the International Human Microbiome Standard (IHMS), MBQC and the well-known HMP project which acts as a baseline reference. In this mini review, we compiled and concisely compared all CRC 16S rRNA gene sequencing studies that have been carried out until 2016. As far as we know, no study is completely similar to another in terms of sample type and laboratory transfer, sequencing platform and primers, and bioinformatics database and analysis; therefore, the reproducibility of results obtained from a specific workflow could not be determined. Nevertheless, from our compilation, we found that most studies used the following workflow for CRC 16S rRNA gene sequencing: DNA extraction with mechanical homogenization, sequencing of the 16S rRNA V3/V4 regions, OTU picking using either the QIIME or MOTHUR software, and microbial classification against the Greengenes or RDP database. This commonly-used workflow was found to provide good quality sequencing reads and a comprehensive profile of CRC-associated gut microbiome. The reproducibility of 16S rRNA gene sequencing results from a specific workflow could only be tested via replicate experiments using identical workflow on the same DNA sample; this research approach could be further explored in future studies to build a sensitive, specific and non-invasive CRC molecular screening tool based on 16S rRNA gene sequencing.

AUTHOR CONTRIBUTIONS

M-AO and HN drafted and wrote this manuscript. HN, N-SA, S-FC, and RJ were responsible for idea conception, critical evaluation, and manuscript review.

ACKNOWLEDGMENTS

This mini review is part of a study funded by the Transdisciplinary Research Grant Scheme (TRGS/2/2014/UKM/02/3/1) awarded by the Ministry of Higher Education, Malaysia.

REFERENCES

Ahn, J., Sinha, R., Pei, Z., Dominianni, C., Wu, J., Shi, J., et al. (2013). Human gut microbiome and risk for colorectal cancer. *J. Natl. Cancer Inst.* 105, 1907–1911. doi: 10.1093/jnci/djt300

Allali, I., Delgado, S., Marron, P. I., Astudillo, A., Yeh, J. J., Ghazal, H., et al. (2015). Gut microbiome compositional and functional differences between tumor and non-tumor adjacent tissues from cohorts from the US and Spain. *Gut Microbes* 6, 161–172. doi: 10.1080/19490976.2015.1039223

Balvočiute, M., and Huson, D. H. (2017). SILVA, RDP, Greengenes, NCBI and OTT—how do these taxonomies compare? *BMC Genomics* 18(Suppl. 2):114. doi: 10.1186/s12864-017-3501-4

Barman, M., Unold, D., Shifley, K., Amir, E., Hung, K., Bos, N., et al. (2008). Enteric salmonellosis disrupts the microbial ecology of the murine gastrointestinal tract. *Infect. Immun.* 76, 907–915. doi: 10.1128/IAI.01432-07

Baxter, N. T., Ruffin, M. T., Rogers, M. A., and Schloss, P. D. (2016). Microbiota-based model improves the sensitivity of fecal immunochemical test for detecting colonic lesions. *Genome Med.* 8:37. doi: 10.1186/s13073-016-0290-3

Blekhman, R., Tang, K., Archie, E. A., Barreiro, L. B., Johnson, Z. P., Wilson, M. E., et al. (2016). Common methods for fecal sample storage in field studies yield consistent signatures of individual identity in microbiome sequencing data. *Sci. Rep.* 6:31519. doi: 10.1038/srep31519

Brown, L., Wolf, J. M., Prados-Rosales, R., and Casadevall, A. (2015). Through the wall: extracellular vesicles in Gram-positive bacteria, mycobacteria and fungi. *Nat. Rev. Microbiol.* 13, 620–630. doi: 10.1038/nrmicro3480

Bultman, S. J. (2017). Interplay between diet, gut microbiota, epigenetic events, and colorectal cancer. *Mol. Nutr. Food Res.* 61:1500902. doi: 10.1002/mnfr.201500902

Burns, M. B., Lynch, J., Starr, T. K., Knights, D., and Blekhman, R. (2015). Virulence genes are a signature of the microbiome in the colorectal tumor microenvironment. *Genome Med.* 7:55. doi: 10.1186/s13073-015-0177-8

Caporaso, J. G., Kuczynski, J., Stombaugh, J., Bittinger, K., Bushman, F. D., Costello, E. K., et al. (2010). QIIME allows analysis of high-throughput community sequencing data. *Nat. Methods* 7, 335–336. doi: 10.1038/nmeth.f.303

Caporaso, J. G., Lauber, C. L., Walters, W. A., Berg-Lyons, D., Huntley, J., Fierer, N., et al. (2012). Ultra-high-throughput microbial community analysis on the Illumina HiSeq and MiSeq platforms. *ISME J.* 6, 1621–1624. doi: 10.1038/ismej.2012.8

Caporaso, J. G., Lauber, C. L., Walters, W. A., Berg-Lyons, D., Lozupone, C. A., Turnbaugh, P. J., et al. (2011). Global patterns of 16S rRNA diversity at a depth of millions of sequences per sample. *Proc. Natl Acad. Sci. U.S.A.* 108(Suppl. 1), 4516–4522. doi: 10.1073/pnas.1000080107

Chen, W., Liu, F., Ling, Z., Tong, X., and Xiang, C. (2012). Human intestinal lumen and mucosa-associated microbiota in patients with colorectal cancer. *PLoS ONE* 7:e39743. doi: 10.1371/journal.pone.0039743

Choo, J. M., Leong, L. E. X., and Rogers, G. B. (2015). Sample storage conditions significantly influence faecal microbiome profiles. *Sci. Rep.* 5:16350. doi: 10.1038/srep16350

Cole, J. R., Chai, B., Farris, R. J., Wang, Q., Kulam, S., McGarrell, D. M., et al. (2005). The Ribosomal Database Project (RDP-II): sequences and tools for

high-throughput rRNA analysis. *Nucleic Acids Res.* 33(Suppl. 1), D294–D296. doi: 10.1093/nar/gki038

Cole, J. R., Wang, Q., Cardenas, E., Fish, J., Chai, B., Farris, R. J., et al. (2009). The Ribosomal Database Project: improved alignments and new tools for rRNA analysis. *Nucleic Acids Res.* 37(Suppl. 1), D141–D145. doi: 10.1093/nar/gkn879

Consortium, H. M. P. (2012). A framework for human microbiome research. *Nature* 486, 215–221. doi: 10.1038/nature11209

Costello, E. K., Stagaman, K., Dethlefsen, L., Bohannan, B. J., and Relman, D. A. (2012). The application of ecological theory toward an understanding of the human microbiome. *Science* 336, 1255–1262. doi: 10.1126/science.1224203

Cox, M. J., Cookson, W. O., and Moffatt, M. F. (2013). Sequencing the human microbiome in health and disease. *Hum. Mol. Genet.* 22, R88–R94. doi: 10.1093/hmg/ddt398

David, L. A., Maurice, C. F., Carmody, R. N., Gootenberg, D. B., Button, J. E., Wolfe, B. E., et al. (2014). Diet rapidly and reproducibly alters the human gut microbiome. *Nature* 505, 559–563. doi: 10.1038/nature12820

Dejea, C. M., Wick, E. C., Hechenbleikner, E. M., White, J. R., Mark Welch, J. L., Rossetti, B. J., et al. (2014). Microbiota organization is a distinct feature of proximal colorectal cancers. *Proc. Natl. Acad. Sci. U.S.A.* 111, 18321–18326. doi: 10.1073/pnas.1406199111

DeSantis, T. Z., Hugenholtz, P., Larsen, N., Rojas, M., Brodie, E. L., Keller, K., et al. (2006). Greengenes, a chimera-checked 16S rRNA gene database and workbench compatible with ARB. *Appl. Environ. Microbiol.* 72, 5069–5072. doi: 10.1128/AEM.03006-05

Flemer, B., Lynch, D. B., Brown, J. M., Jeffery, I. B., Ryan, F. J., Claesson, M. J., et al. (2017). Tumour-associated and non-tumour-associated microbiota in colorectal cancer. *Gut* 66, 633–643. doi: 10.1136/gutjnl-2015-309595

Fouhy, F., Deane, J., Rea, M. C., O'Sullivan, Ó., Ross, R. P., O'Callaghan, G., et al. (2015). The effects of freezing on faecal microbiota as determined using miseq sequencing and culture-based investigations. *PLoS ONE* 10:e0119355. doi: 10.1371/journal.pone.0119355

Fraher, M. H., O'Toole, P. W., and Quigley, E. M. (2012). Techniques used to characterize the gut microbiota: a guide for the clinician. *Nat. Rev. Gastroenterol. Hepatol.* 9, 312–322. doi: 10.1038/nrgastro.2012.44

Gagliani, N., Hu, B., Huber, S., Elinav, E., and Flavell, R. A. (2014). The fire within: microbes inflame tumors. *Cell* 157, 776–783. doi: 10.1016/j.cell.2014.03.006

Gao, Z., Guo, B., Gao, R., Zhu, Q., and Qin, H. (2015). Microbiota disbiosis is associated with colorectal cancer. *Front. Microbiol.* 6:20. doi: 10.3389/fmicb.2015.00020

Geng, J., Fan, H., Tang, X., Zhai, H., and Zhang, Z. (2013). Diversified pattern of the human colorectal cancer microbiome. *Gut Pathog.* 5, 1. doi: 10.1186/1757-4749-5-2

Gill, S. R., Pop, M., DeBoy, R. T., Eckburg, P. B., Turnbaugh, P. J., Samuel, B. S., et al. (2006). Metagenomic analysis of the human distal gut microbiome. *Science* 312, 1355–1359.

Gorzelak, M. A., Gill, S. K., Tasnim, N., Ahmadi-Vand, Z., Jay, M., and Gibson, D. L. (2015). Methods for improving human gut microbiome data by reducing variability through sample processing and storage of stool. *PLoS ONE* 10:e0134802. doi: 10.1371/journal.pone.0134802

Hooper, L. V., and Gordon, J. I. (2001). Commensal host-bacterial relationships in the gut. *Science* 292, 1115–1118. doi: 10.1126/science.1058709

Huse, S. M., Ye, Y., Zhou, Y., and Fodor, A. A. (2012). A core human microbiome as viewed through 16S rRNA sequence clusters. *PLoS ONE* 7:e34242. doi: 10.1371/journal.pone.0034242

Kostic, A. D., Chun, E., Robertson, L., Glickman, J. N., Gallini, C. A., Michaud, M., et al. (2013). Fusobacterium nucleatum potentiates intestinal tumorigenesis and modulates the tumor-immune microenvironment. *Cell Host Microbe* 14, 207–215. doi: 10.1016/j.chom.2013.07.007

Kostic, A. D., Gevers, D., Pedamallu, C. S., Michaud, M., Duke, F., Earl, A. M., et al. (2012). Genomic analysis identifies association of Fusobacterium with colorectal carcinoma. *Genome Res.* 22, 292–298. doi: 10.1101/gr.126573.111

Liang, Q., Chiu, J., Chen, Y., Huang, Y., Higashimori, A., Fang, J., et al. (2017). Fecal bacteria act as novel biomarkers for noninvasive diagnosis of colorectal cancer. *Clin. Cancer Res.* 23, 2061–2070. doi: 10.1158/1078-0432.CCR-16-1599

Loman, N. J., Misra, R. V., Dallman, T. J., Constantinidou, C., Gharbia, S. E., Wain, J., et al. (2012). Performance comparison of benchtop high-throughput sequencing platforms. *Nat. Biotechnol.* 30, 434–439. doi: 10.1038/nbt.2198

Lozupone, C. A., Stombaugh, J., Gonzalez, A., Ackermann, G., Wendel, D., Vázquez-Baeza, Y., et al. (2013). Meta-analyses of studies of the human microbiota. *Genome Res.* 23, 1704–1714. doi: 10.1101/gr.151803.112

Marchesi, J. R., Dutilh, B. E., Hall, N., Peters, W. H., Roelofs, R., Boleij, A., et al. (2011). Towards the human colorectal cancer microbiome. *PLoS ONE* 6:e20447. doi: 10.1371/journal.pone.0020447

Margulies, M., Egholm, M., Altman, W. E., Attiya, S., Bader, J. S., Bemben, L. A., et al. (2005). Genome sequencing in microfabricated high-density picolitre reactors. *Nature* 437, 376–380. doi: 10.1038/nature03959

Mira-Pascual, L., Cabrera-Rubio, R., Ocon, S., Costales, P., Parra, A., Suarez, A., et al. (2015). Microbial mucosal colonic shifts associated with the development of colorectal cancer reveal the presence of different bacterial and archaeal biomarkers. *J. Gastroenterol.* 50, 167–179. doi: 10.1007/s00535-014-0963-x

Mizrahi-Man, O., Davenport, E. R., and Gilad, Y. (2013). Taxonomic classification of bacterial 16S rRNA genes using short sequencing reads: evaluation of effective study designs. *PLoS ONE* 8:e53608. doi: 10.1371/journal.pone.0053608

Nakatsu, G., Li, X., Zhou, H., Sheng, J., Wong, S. H., Wu, W. K., et al. (2015). Gut mucosal microbiome across stages of colorectal carcinogenesis. *Nat. Commun.* 6:8727. doi: 10.1038/ncomms9727

Nistal, E., Fernández-Fernández, N., Vivas, S., and Olcoz, J. L. (2015). Factors determining colorectal cancer: the role of the intestinal microbiota. *Front.Oncol.* 5:220. doi: 10.3389/fonc.2015.00220

Nosho, K., Sukawa, Y., Adachi, Y., Ito, M., Mitsuhashi, K., Kurihara, H., et al. (2016). Association of Fusobacterium nucleatum with immunity and molecular alterations in colorectal cancer. *World J. Gastroenterol.* 22:557. doi: 10.3748/wjg.v22.i2.557

Plummer, E., Twin, J., Bulach, D. M., Garland, S. M., and Tabrizi, S. N. (2015). A comparison of three bioinformatics pipelines for the analysis of preterm gut microbiota using 16S rRNA gene sequencing data. *J. Proteomics Bioinform.* 8, 283–291. doi: 10.4172/jpb.1000381

Pruesse, E., Quast, C., Knittel, K., Fuchs, B. M., Ludwig, W., Peplies, J., et al. (2007). SILVA: a comprehensive online resource for quality checked and aligned ribosomal RNA sequence data compatible with ARB. *Nucleic Acids Res.* 35, 7188–7196. doi: 10.1093/nar/gkm864

Qin, J., Li, R., Raes, J., Arumugam, M., Burgdorf, K. S., Manichanh, C., et al. (2010). A human gut microbial gene catalogue established by metagenomic sequencing. *Nature* 464, 59–65. doi: 10.1038/nature08821

Quast, C., Pruesse, E., Yilmaz, P., Gerken, J., Schweer, T., Yarza, P., et al. (2013). The SILVA ribosomal RNA gene database project: improved data processing and web-based tools. *Nucleic Acids Res.* 41, D590–D596. doi: 10.1093/nar/gks1219

Rubinstein, M. R., Wang, X., Liu, W., Hao, Y., Cai, G., and Han, Y. W. (2013). Fusobacterium nucleatum promotes colorectal carcinogenesis by modulating E-cadherin/β-catenin signaling via its FadA adhesin. *Cell Host Microbe* 14, 195–206. doi: 10.1016/j.chom.2013.07.012

Schloss, P. D., Westcott, S. L., Ryabin, T., Hall, J. R., Hartmann, M., Hollister, E. B., et al. (2009). Introducing mothur: open-source, platform-independent, community-supported software for describing and comparing microbial communities. *Appl. Environ. Microbiol.* 75, 7537–7541. doi: 10.1128/AEM.01541-09

Sender, R., Fuchs, S., and Milo, R. (2016). Revised estimates for the number of human and bacteria cells in the body. *PLoS Biol.* 14:e1002533. doi: 10.1371/journal.pbio.1002533

Sinha, R., Abnet, C. C., White, O., Knight, R., and Huttenhower, C. (2015). The microbiome quality control project: baseline study design and future directions. *Genome Biol.* 16, 1. doi: 10.1186/s13059-015-0841-8

Sinha, R., Ahn, J., Sampson, J. N., Shi, J., Yu, G., Xiong, X., et al. (2016). Fecal microbiota, fecal metabolome, and colorectal cancer interrelations. *PLoS ONE* 11:e0152126. doi: 10.1371/journal.pone.0152126

Sobhani, I., Tap, J., Roudot-Thoraval, F., Roperch, J. P., Letulle, S., Langella, P., et al. (2011). Microbial dysbiosis in colorectal cancer (CRC) patients. *PLoS ONE* 6:e16393. doi: 10.1371/journal.pone.0016393

Tatusova, T., Ciufo, S., Federhen, S., Fedorov, B., McVeigh, R., O'Neill, K., et al. (2015). Update on RefSeq microbial genomes resources. *Nucleic Acids Res.* 43, D599–D605. doi: 10.1093/nar/gku1062

Taylor, M., Wood, H. M., Halloran, S. P., and Quirke, P. (2017). Examining the potential use and long-term stability of guaiac faecal occult blood test cards for microbial DNA 16S rRNA sequencing. *J. Clin. Pathol.* 70, 600–606. doi: 10.1136/jclinpath-2016-204165

Thomas, A. M., Jesus, E. C., Lopes, A., Aguiar, S. Jr., Begnami, M. D., Rocha, R. M., et al. (2016). Tissue-Associated bacterial alterations in rectal carcinoma patients revealed by 16S rRNA community profiling. *Front. Cell. Infect. Microbiol.* 6:179. doi: 10.3389/fcimb.2016.00179

Tremblay, J., Singh, K., Fern, A., Kirton, E. S., He, S., Woyke, T., et al. (2015). Primer and platform effects on 16S rRNA tag sequencing. *Front. Microbiol.* 6:771. doi: 10.3389/fmicb.2015.00771

Uemura, N., Okamoto, S., Yamamoto, S., Matsumura, N., Yamaguchi, S., Yamakido, M., et al. (2001). *Helicobacter pylori* infection and the development of gastric cancer. *New Engl. J. Med.* 345, 784–789. doi: 10.1056/NEJMoa001999

Wang, T., Cai, G., Qiu, Y., Fei, N., Zhang, M., Pang, X., et al. (2012). Structural segregation of gut microbiota between colorectal cancer patients and healthy volunteers. *ISME J.* 6, 320–329. doi: 10.1038/ismej.2011.109

Weir, T. L., Manter, D. K., Sheflin, A. M., Barnett, B. A., Heuberger, A. L., and Ryan, E. P. (2013). Stool microbiome and metabolome differences between colorectal cancer patients and healthy adults. *PLoS ONE* 8:e70803. doi: 10.1371/journal.pone.0070803

Whitman, W. B., Coleman, D. C., and Wiebe, W. J. (1998). Prokaryotes: the unseen majority. *Proc. Natl. Acad. Sci. U.S.A.* 95, 6578–6583. doi: 10.1073/pnas.95.12.6578

Wu, G. D., Lewis, J. D., Hoffmann, C., Chen, Y.-Y., Knight, R., Bittinger, K., et al. (2010). Sampling and pyrosequencing methods for characterizing bacterial communities in the human gut using 16S sequence tags. *BMC Microbiol.* 10:206. doi: 10.1186/1471-2180-10-206

Wu, N., Yang, X., Zhang, R., Li, J., Xiao, X., Hu, Y., et al. (2013). Dysbiosis signature of fecal microbiota in colorectal cancer patients. *Microb. Ecol.* 66, 462–470. doi: 10.1007/s00248-013-0245-9

Yang, Y., Weng, W., Peng, J., Hong, L., Yang, L., Toiyama, Y., et al. (2017). *Fusobacterium nucleatum* increases proliferation of colorectal cancer cells and tumor development in mice by activating toll-like receptor 4 signaling to nuclear factor– κB, and Up-regulating expression of MicroRNA-21. *Gastroenterology* 152, 851.e24–866.e24. doi: 10.1053/j.gastro.2016.11.018

Yatsunenko, T., Rey, F. E., Manary, M. J., Trehan, I., Dominguez-Bello, M. G., Contreras, M., et al. (2012). Human gut microbiome viewed across age and geography. *Nature* 486, 222–227. doi: 10.1038/nature11053

Yoon, S.-H., Ha, S.-M., Kwon, S., Lim, J., Kim, Y., Seo, H., et al. (2017). Introducing EzBioCloud: a taxonomically united database of 16S rRNA gene sequences and whole-genome assemblies. *Int. J. Syst. Evol. Microbiol.* 67, 1613–1617. doi: 10.1099/ijsem.0.001755

Zackular, J. P., Rogers, M. A., Ruffin, M. T.,t., and Schloss, P. D. (2014). The human gut microbiome as a screening tool for colorectal cancer. *Cancer Prev. Res.* 7, 1112–1121. doi: 10.1158/1940-6207.CAPR-14-0129

Zeller, G., Tap, J., Voigt, A. Y., Sunagawa, S., Kultima, J. R., Costea, P. I., et al. (2014). Potential of fecal microbiota for early-stage detection of colorectal cancer. *Mol. Syst. Biol.* 10:766. doi: 10.15252/msb.20145645

Zheng, W., Tsompana, M., Ruscitto, A., Sharma, A., Genco, R., Sun, Y., et al. (2015). An accurate and efficient experimental approach for characterization of the complex oral microbiota. *Microbiome* 3:48. doi: 10.1186/s40168-015-0110-9

Conflict of Interest Statement: The authors declare that the research was conducted in the absence of any commercial or financial relationships that could be construed as a potential conflict of interest.

Copyright © 2018 Osman, Neoh, Ab Mutalib, Chin and Jamal. This is an open-access article distributed under the terms of the Creative Commons Attribution License (CC BY). The use, distribution or reproduction in other forums is permitted, provided the original author(s) and the copyright owner are credited and that the original publication in this journal is cited, in accordance with accepted academic practice. No use, distribution or reproduction is permitted which does not comply with these terms.

frontiers in Microbiology

ORIGINAL RESEARCH
published: 17 July 2018
doi: 10.3389/fmicb.2018.01603

Microbial Similarity and Preference for Specific Sites in Healthy Oral Cavity and Esophagus

Li Dong[1,2†], Jian Yin[1†], Jing Zhao[1], Shan-rui Ma[1], Hai-rui Wang[1], Meng Wang[1], Wen Chen[1] and Wen-qiang Wei[1]**

[1] *Department of Epidemiology, National Cancer Center/National Clinical Research Center for Cancer/Cancer Hospital, Chinese Academy of Medical Sciences and Peking Union Medical College, Beijing, China,* [2] *Institutes of Biomedical Sciences, Shanxi University, Taiyuan, China*

Human microbial communities are highly complex ecosystems, but it remains unclear if microbial compositions have any similarity in distinct sites of the oral cavity and esophagus in particular. Clinical samples were collected from three niches (saliva, tongue dorsum and supragingival plaque) of the oral cavity and three segments (upper, middle, and lower) of the esophagus in 27 healthy individuals. Bacterial V3-V4 region of 16S rRNA gene in these samples was amplified and sequenced on Illumina sequencing platform, followed by data analysis using QIIME and LEfSe softwares. Highly diverse bacterial flora with 365 genera belonging to 29 phyla resided in the oral cavity and 594 genera belonging to 29 phyla in the esophagus. The phyla Proteobacteria, Firmicutes, Bacteroidetes, Actinobacteria, Fusobacteria, and TM7 were most abundant in both the oral cavity and the esophagus, but the phyla Actinobacteria and Bacteroidetes were preferable in the oral cavity and Firmicutes in the esophagus. The genera *Streptococcus, Neisseria, Prevotella, Actinobacillus,* and *Veillonella* were most abundant in both oral cavity and esophagus, but *Neisseri*a was preferable in the oral cavity and *Streptococcus* in the esophagus. Different niche-specific bacterial signatures were found in the oral cavity, e.g., the class Flavobacteria in the supragingival plaque, class Bacteroides in the saliva and the class Clostridia in the tongue dorsum. By contrast, no site specific bacteria for three different segments of esophagus were found. However, high variability of microbial compositions between individuals was observed. In conclusion, this study confirmed microbial diversity at different taxonomic levels in healthy oral cavity and esophagus, and identified the site-preferable bacterial signatures in six niches of the upper digestive tract. These findings provide a critical baseline for future studies interpreting microbiome-related diseases.

Keywords: microbial similarity, microbial preference, oral cavity, esophagus, 16S rRNA gene sequencing

OPEN ACCESS

Edited by:
Sunny Hei Wong,
The Chinese University of Hong Kong, Hong Kong

Reviewed by:
Yuji Naito,
Kyoto Prefectural University of Medicine, Japan
Alex Mira,
Center for Public Health Research (CSISP), Spain

****Correspondence:***
Wen Chen
Chenwen@cicams.ac.cn
Wen-qiang Wei
Weiwq@cicams.ac.cn

† These authors have contributed equally to this work.

Specialty section:
This article was submitted to Microbial Symbioses, a section of the journal Frontiers in Microbiology

Received: *29 March 2018*
Accepted: *27 June 2018*
Published: *17 July 2018*

Citation:
Dong L, Yin J, Zhao J, Ma S-r, Wang H-r, Wang M, Chen W and Wei W-q (2018) Microbial Similarity and Preference for Specific Sites in Healthy Oral Cavity and Esophagus. Front. Microbiol. 9:1603. doi: 10.3389/fmicb.2018.01603

INTRODUCTION

Human microbiome in the upper digestive tract is a very complex and highly diverse ecosystem (Bashan et al., 2016). Homeostasis of microbial diversity is vital for the development of mucosal barrier functions and immune responses to the invasion of pathogens leading to the diseases (Frank et al., 2011; Tlaskalova-Hogenova et al., 2011; Segata et al., 2012). Oral cavity, as the initial gateway of the integral digestive tract, is constantly exposed to both the inhaled and ingested microbes with more than 700 bacterial species or phylotypes (Aas et al., 2005; Nasidze et al., 2009), part

of which have been reported to be associated with the cancer and other systemic diseases (Abusleme et al., 2013; Kerr, 2015; Fan et al., 2016). It has been estimated that about 10^{11} bacterial cells flow from the mouth to the stomach per day (Socransky and Haffajee, 2002; Segata et al., 2012), and microbial compositions are overlapped along the oral, pharyngeal, esophageal and intestinal locations (Segata et al., 2012; Norder Grusell et al., 2013; Gall et al., 2015). However, it remains unclear to date if microbial compositions have any similarity in distinct sites of the upper digestive tract, oral cavity and esophagus in particular.

Esophagus plays a critical anatomic role in transferring the alimentary bolus from the mouth to the stomach and also in receiving the reflux from the stomach. Therefore, these varied microenvironments in the esophagus, e.g., the exposure to oral-like environment in the proximal esophagus and a sudden lowering of pH values in the distal esophagus might lead to microbial diversity in different segments (Di Pilato et al., 2016). Meanwhile, the esophagus is characterized with three physiological stenosis where residual food and microbes are more prone to retain and the risk of invasive cancer or esophageal lesions might be increased (Rice et al., 2009). Microbial diversity in the distal esophagus in patients with esophagitis has been reported (Pei et al., 2005). However, few studies analyze microbial compositions that resided in different esophageal segments, particularly in healthy individuals. This is in part due to the difficulty in procuring the esophageal samples that always requires an invasive method or limited capability of traditionally culture-based methods to identify the unknown, uncultivable and unclassified species (Pozhitkov et al., 2011). Not until recently, Pei et al. (2004) firstly found the most six prevalent phyla in four healthy individuals using 16S rDNA sequencing and widened our knowledge about microbial spectrum in distal esophagus. Similar investigations have been performed in different countries (Yu et al., 2014; Gall et al., 2015; Feng et al., 2017). Nevertheless, some limitations such as only distal or proximal esophagus sampled, biopsy-based rather than mucosal brushes sampling, culture-based method rather than sequencing in these studies precluded us from revealing a detailed spectrum of microbiome along healthy esophageal tract (Gall et al., 2015). In addition, fewer studies reported the similarity and specificity of microbial communities that reside in the oral cavity and the esophagus.

Understanding microbial spectrum in healthy population is of great value to demonstrate the bacteria-associated diseases affecting human health. The focus of this present study is to measure and compare the composition and relative abundance of the bacterial population inhabiting: (1) the oral cavity and esophagus; (2) three distinct oral niches including the saliva, tongue dorsum and supragingival plaque; (3) three distinct esophagus segments including upper, middle and lower esophagus, in a population with high-risk of esophagus cancer.

MATERIALS AND METHODS

Study Population

Participants were recruited for the upper digestive tract cancer screening in June 2015 in Linzhou county, China, a region with high incidence of esophageal cancer. The inclusion criteria were as follows: aged from 40 to 69 years old, local residents living in Linzhou county for at least 5 years, no contraindications for endoscopic examinations (e.g., history of allergy to iodine or lidocaine), mentally and physically competent to provide written informed consent, and no consumption of any food or beverage at least 6 hours prior to sample collection. For explorative reasons, a total of 27 dental and esophageal disease-free individuals (4 men and 23 women) were included in final analysis (Supplementary Table S1). Those dental disease-free individuals were those dentist-confirmed free of periodontal diseases and no incident caries at the time of sampling. Among some people who had a past history of caries, only those people whose caries had been filled at the time of sampling were eligible for this study. Those esophageal disease-free individuals were confirmed by endoscopic examination and then biopsy-based pathological diagnosis if necessary. This study was performed in accordance with the recommendations of the Declaration of Helsinki, Institutional Review Board approval of Cancer Hospital, Chinese Academy of Medical Sciences.

Clinical Procedures and Sample Collection

With the signed consent from each participant, we collected the information related with socio-demographics, lifestyle, eating habits and history of antibiotics use. Subsequently, visual inspection for oral health was conducted by the dentists and then the samples were collected from the oral cavity in the order of the tongue dorsum using sterile swab, the supragingival plaque using sterile forceps and the saliva by drooling. Thereafter, each participant underwent general anesthesia prior to the endoscopic examination of esophagus. The samples were collected from the upper third, middle third and lower third along esophageal tract surface in order with new sterile head-covered brushes, respectively. Biopsy would be taken at the suspicious locations and then pathological diagnosis was made. All samples were preserved in PreservCyt solution (Hologic, Bedford, MA, United States), transported with dry ice and stored in −70°C for use.

Quality Control

Minimization of the contamination from handling environment and adjacent tract sites was essential to accurately determine site-specific microbial compositions. Three important measures were deployed besides meticulous items such as disposable sampling devices and sterile equipment: Firstly, a covered esophageal sampling brush by a protective sheath was used so that it was threaded through the endoscope channel, deployed at the site of sampling and then re-sheathed before being retracted through the endoscope. Secondly, sample collection began with the upper third of the esophagus, followed with middle third using a new brush and ended at lower third with a new brush to avoid cross contamination along the surface of endoscope channel. Once being retracted the head

of the brush enriched with bacterial cells was re-sheathed, cut by a sterile scissor, immersed into the preservation solution and sealed immediately. Finally, three brushes without samples as the negative control were exposed at the same sampling room and concurrently processed with the samples in the same batch. The amount of DNA extracted from the negative control was beyond the detection limitation of Qubit ($<<$0.01 ng/μL).

DNA Extraction and 16S rRNA Gene Sequencing

Genomic DNA was extracted from each sample using a series of phenol and chloroform method. Each sample was subjected to a bead beating prior to DNA extraction using Lysing Matrix-B (MP Bio) to maximize the release of the microbial genomic DNA. The V3-V4 hypervariable region of 16S rRNA gene was amplified using the forward primer (5′-GTACTCCTACGGGAGGCAGCA-3′) and reverse primer (5′-GTGGACTACHVGGGTWTCTAAT-3′) with eight base pair barcodes (Caporaso et al., 2011a,b; Fierer et al., 2012). PCR reactions were performed using TransStart Fast PfuDNA Polymerase (TransStart®, TransGenBiotech, Beijing, China) with the following cycling parameters: 94°C for 3 min, followed by 23 cycles of 94°C for 30 s, 60°C for 40 s, 72°C for 60 s, and a final elongation at 72°C for 10 min. Three 16S gene amplicons for each sample were pooled and their resulting bands with a correct size on a 1% agarose gel were excised. Amplicons were further purified using Gel Extraction Kit (Omega Biotek, United States) and quantified with Qubit. All samples were pooled together with equal molar amount from each sample. The sequencing library was constructed using TruSeq DNA kit according to the manufacturer's instruction (Illumina, San Diego, CA, United States). The purified library was diluted, denatured, re-diluted, mixed with PhiX (equal to 30% of final DNA amount) as described in the Illumina library preparation protocols, and then applied to an Illumina Miseq system for sequencing with the Reagent Kit v3 600 cycles (Illumina, San Diego, CA, United States) as described in the manufacturer's manual.

OTU Picking

Raw sequencing data were demultiplexed, quality filtered, denoised, and then clear overlap paired end reads were joined together using fastq-join program. The 16S rRNA operational taxonomic units (OTUs) were clustered using "open-reference OTU" of QIIME (Caporaso et al., 2010). In this open-reference OTU picking process, reads were firstly clustered with reference to the Greengenes database (Release 13.8) using closed-reference OTUs picking. Subsequently, 0.1% of the reads which failed to hit the reference sequence collection were randomly subsampled and clustered de novo using UCLUST (v1.2.22q), with an OTU cluster defined by a sequence similarity of 97%. Chimeric sequences were removed using PYNAST (v1.2.2). OTUs were rarefied at a depth of 5,598 sequences. The operational taxonomic units (OTUs) were assigned to taxa (domain, kingdom, phylum, class, order, family, genus and species) by matching to the Greengenes database.

Phylogenetic Diversity Analysis and Statistical Analysis

Bacterial compositions and relative abundances at each taxonomic level in each specimen, were measured. Alpha diversity was estimated for each sample using the Chao1 richness (representing the community richness), Shannon's Diversity and Simpson Index (representing the community diversity) and then plotted using Origin 7.5. Statistical difference of the alpha diversity between two groups was determined by Student's *t*-tests and that among three or more groups by one-way ANOVA tests followed by Dunnet's test for multiple comparisons. Beta diversity was estimated by the Bray-Curtis distance and visualized by box plot. The difference of microbial spectrum between the oral cavity and the esophagus was revealed by the principal coordinate analysis (PCoA). PCoA was generated with QIIME platform based on the Bray-Curtis distance of OTU profile to ordinate dissimilarity matrices, in which complex dimensionality of the database indicating the beta diversity was reduced to its compositions of greatest variation. All statistical tests were performed using SPSS 18.0 with two-sided 0.05 as the significance level.

Linear discriminant effect size analysis (LEfSe) (Segata et al., 2011) based on the non-parametric factorial Kruskal–Wallis test was performed using the default parameters at any taxonomic level to find microbial biomarkers for the oral cavity and the esophagus. The threshold on the linear discriminant analysis (LDA) score for discriminative biomarkers was 2.0. All statistical analyses were conducted using R 3.1.1.

RESULTS

Composition of Microbial Community in the Oral Cavity and the Esophagus

A great diversity of microbial community was observed in the oral cavity and the esophagus (**Figure 1** and Supplementary Table S2). A total of 365 genera belonging to 29 phyla of bacteria in the oral cavity and 594 genera belonging to 29 phyla of bacteria in the esophagus were found. The most abundant microbiome at the phylum level predominant in both the oral cavity and esophagus were: Proteobacteria, Firmicutes, Bacteroidetes, Actinobacteria, Fusobacteria and TM7. Compared with the oral cavity, the esophagus had an increased relative abundance of Proteobacteria (43.6 ± 22.7% vs. 35.3 ± 15.4%, $p < 0.001$) and Firmicutes (37.4 ± 20.8% vs. 14.5 ± 10.3%, $p < 0.001$), and decreased abundance of Bacteroidetes (13.2 ± 8.6% vs. 32.2 ± 11.3%, $p < 0.01$), Actinobacteria (2.5 ± 2.0% vs. 9.3 ± 9.3%, $p < 0.01$), Fusobacteria (1.2 ± 0.9% vs. 3.8 ± 3.3%, $p < 0.05$) and TM7 (1.1 ± 1.4% vs. 3.3 ± 3.4%, $p < 0.01$).

At the genus level, the bacteria in both the oral cavity and the esopagus were characterized by high relative abundances of *Streptococcus*, *Neisseria*, *Prevotella*, *Actinobacillus*, and *Veillonella* (**Figure 1B** and Supplementary Table S2). *Neisseria* was predominant in the oral cavity, while *Streptococcus* in the esophagus. In addition, the bacteria with each relative abundance of over 1% were *Prevotella*, *Porphyromonas*, *Capnocytophaga*,

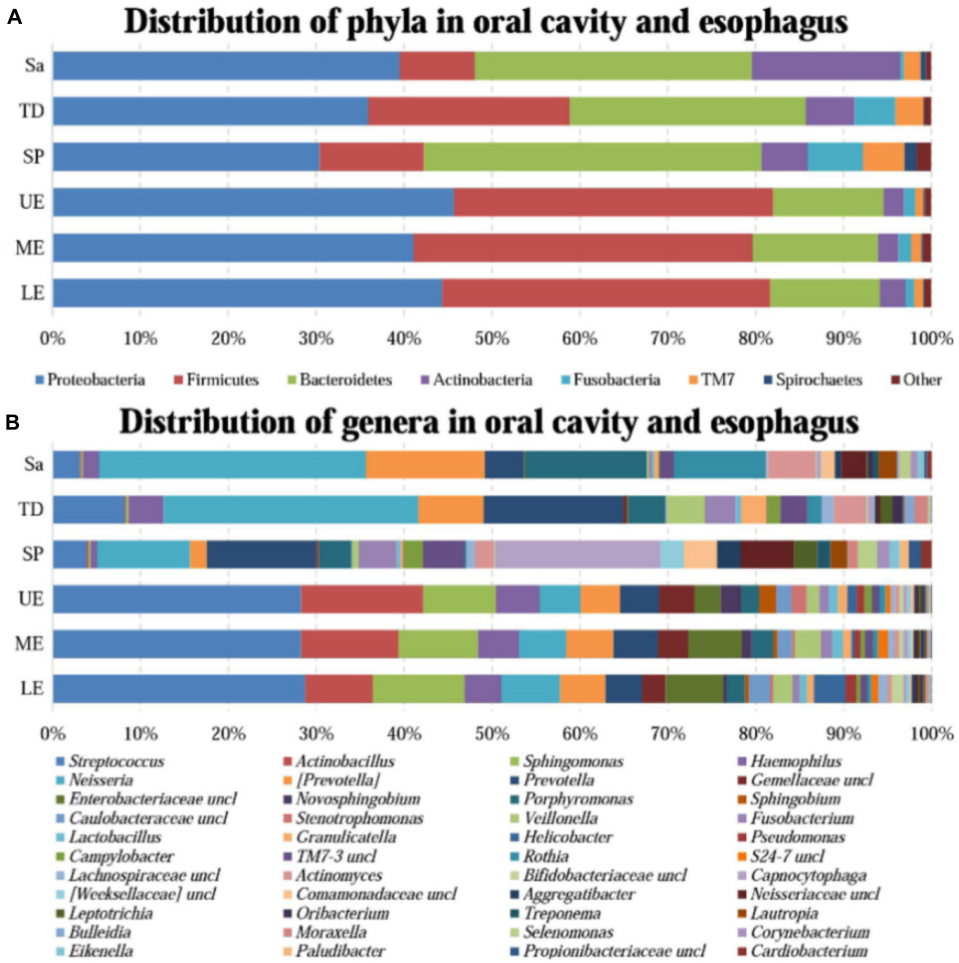

FIGURE 1 | The relative abundance of human microbiome in the oral cavity and esophagus. **(A)** At the phylum level. **(B)** At the genus level. Sa, saliva; TD, tongue dorsum; SP, supragingival plaque; UE, upper esophagus; ME, middle esophagus; LE, lower esophagus.

Streptococcus, and *Rothia* in the oral cavity, and *Actinobacillus*, *Sphingomonas*, *Neisseria*, *Haemophilus*, and *Prevotella* in the esophagus.

An interesting finding was that the phyla TM7 and Spirochaetes had low relative abundance but high prevalence in both the oral cavity and the esophagus. TM7 was detected in at least one of three sampling sites of the oral cavity of all subjects and in the esophagus of 96.7% subjects. Spirochaetes were detected in at least one of three sampling sites in the oral cavity of 95.0% subjects and in the esophagus of 85.0% subjects (Supplementary Table S3).

Distinct Microbial Preference in the Oral Cavity and the Esophagus

All samples from the oral cavity were significantly clustered together in PCoA plots based on the Bray-Curtis distance of microbial composition, but not the case for those from the esophagus, indicating lower variability of microbial composition in the oral cavity than that in the esophagus (**Figure 2A,B**, $p < 0.001$). Many microbial taxa significantly differed between the oral cavity and esophagus with LDA score >2 using LEfse analysis (**Figure 3** and Supplementary Figure S1). Both the phyla Actinobacteria and Bacteroidetes were more abundant in the oral cavity than those in the esophagus. By contrast, most taxa within the phylum Firmicutes such as the class of Bacilli and Alpha proteobacteria and most taxa within the phylum Proteobacteria such as the class Gamma proteobacteria were consistently more abundant in the esophagus than that in the oral cavity (**Figure 1**, all $p < 0.05$). Notably, the phylum TM7, originally thought to be exclusively environmental was present in any site of the oral cavity at greatly higher relative abundance than that in the esophagus ($3.3 \pm 3.6\%$ vs. $1.1 \pm 1.4\%$, $p < 0.05$) (**Figures 1**, **3** and Supplementary Table S2).

LEfSe analysis identified 37 genus-level signatures whose relative abundance significantly differed between the samples from the oral cavity and esophagus (**Figures 1**, **4**). Genus *Neisseria* of the phylum Proteobacteria was apparently more abundant in the oral cavity than that in the esophagus ($21.9 \pm 15.0\%$ vs. $4.8 \pm 4.1\%$, $p < 0.001$), so did *Actinomyces* of

the phylum Actinobacteria (3.5 ± 3.4% vs. 0.5 ± 0.5%, $p < 0.001$). The genus *Streptococcus* of the phylum Firmicutes and the genera *Actinobacillus* and *Sphingomonas* belonging to the phylum Proteobacteria could be considered as the genus-level biomarkers with significantly higher abundance in the esophagus than that in the oral cavity ($p < 0.001$). Another genus-level biomarker for the esophagus detected at >1% on the relative abundance was *Novosphingobium,* but its relative abundance much less in the oral cavity (**Figures 3**, **4** and Supplementary Table S2).

Microbial Ecological Diversity in the Oral Cavity and the Esophagus

Phylogenetic difference of microbiome between the oral cavity and esophagus extended to several ecological statistics including alpha diversity estimated by Chao1 richness, Shannon's Diversity and Simpson Index (**Table 1**) and beta diversity estimated by the Bray-Curtis distances (**Figure 2A**). Microbial profiles from esophageal specimens were statistically less diverse than those from oral specimens estimated by Shannon Diversity and Simpson Index ($p < 0.001$). However, no similar trends were found when the Chao1 richness was used (**Table 1**). These distinctions of alpha diversity in the level of OTU between the oral cavity and the esophagus reflected their physiological anatomic characteristics. Notably, after adjusting the beta diversity for each pair of samples using Bray-Curtis distances, within-group distance in each site was significantly lower than between-group distance between the oral cavity and the esophagus (**Figure 2B**, both $p < 0.05$).

Notable Preference of Microbial Communities for Three Sites of the Oral Cavity

Bacterial communities differed by the sites of the oral cavity (**Figure 5** and Supplementary Table S2). The class Bacteroides of the phylum Bacteroidetes appeared to be more abundant in the saliva. The class Clostridia from the phylum Firmicutes was preferable in the tongue dorsum. All taxa of the phylum TM7 and the class Flavobacteria of the phylum Bacteroidetes were prone to reside in the supragingival plaque.

At the genus level, *Neisseria* was more represented in the saliva and the tongue dorsum (28.4 ± 11.6% and 27.3 ± 16.5% respectively) than the supragingival plaque (9.7 ± 7.7%). *Porphyromonas*, *Rothia,* and *Actinomyces* were considerably abundant in the saliva. *Streptococcus*, *Veillonella*, *Haemophilus*, *Granulicatella*, *Oribacterium*, and *Bulleidia* dominated the tongue dorsum. The genus *Capnocytophaga* was well represented in the supragingival plaque but undetectable in the saliva and tongue dorsum. In contrast, the genus *Fusobacterium* accounted for higher relative abundance in the tongue dorsum and supragingival plaque than that in the saliva.

Regarding alpha diversity, Shannon Diversity and Simpson Index revealed that microbial profiles in the specimens from both the saliva and the tongue dorsum were statistically less diverse compared to those from the supragingival plaque, but no apparent differences among three sites measured by the Chao1 richness ($p < 0.001$, **Table 1**).

No Distinct Microbial Preference for Three Segments of the Esophagus

Microbial compositions from three anatomically separated segments along the esophageal tract were examined to identify segment-specific bacteria. LEfSe analysis did not discern any microbial difference among the upper third, middle third and lower third of esophagus at any clade level (Supplementary Tables S2, S4). Ecological summary statistics of both alpha diversity and beta diversity were employed to further analyze the difference of microbial abundance (**Figure 2B** and **Table 1**). No apparent clustering pattern was observed for the samples

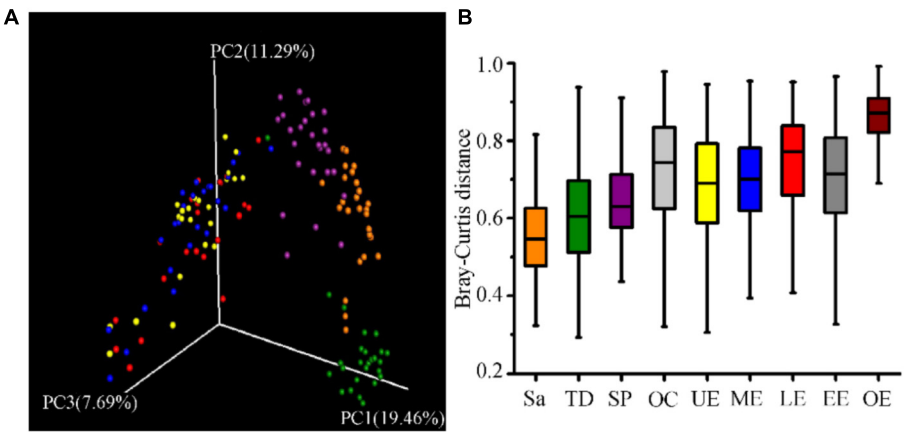

FIGURE 2 | The similarity of community structure within and between the oral cavity and esophagus. **(A)** Three-dimensional ordination of human microbial profiles by principal coordinate analysis (PCoA) of average Bray-Curtis index in different body sites. Red indicating LE, Blue indicating ME, Brown indicating Sa, Green indicating SP, Purple indicating TD, and Yellow indicating UE. **(B)** The similarity of microbial diversity in three sites of the esophagus estimated by Bray-Curtis index. Values expressed as the median and quartile of Bray-Curtis index. Sa, saliva; TD, tongue dorsum; SP, supragingival plaque; OC, oral cavity; UE, upper esophagus; ME, middle esophagus; LE, lower esophagus; EE, entire esophagus; OE, oral cavity and esophagus.

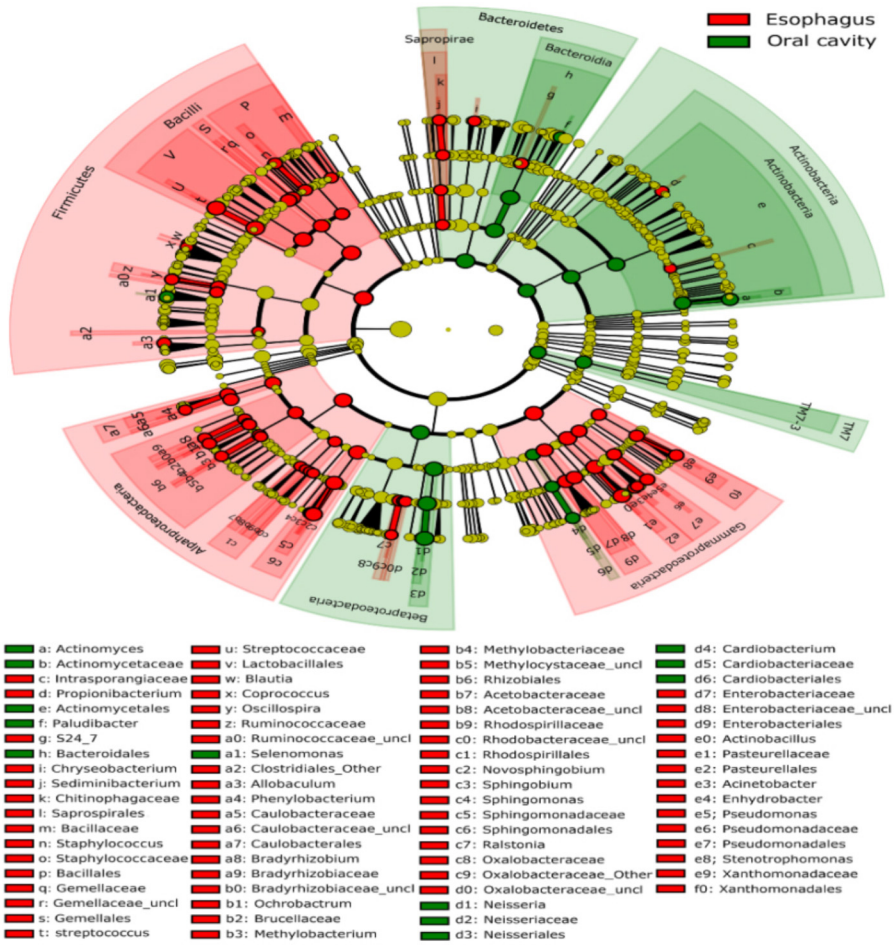

FIGURE 3 | Circular cladogram for niche specialization of microbial compositions in the oral cavity and esophagus using the linear discriminant analysis effect size (LEfSe) analysis of the abundance patterns of bacterial taxa. The circles used in this diagram represent the taxonomic categories of organisms from the phylum level as the outermost circle to genus (or species) level as the innermost cycle. Within each given taxon, each small cycle represents its lower taxon. The yellow nodes indicate no statistically significant differences of specific taxa between the samples from the oral cavity and the esophagus, the red nodes indicate significantly higher relative abundance in the esophagus than in the oral cavity, and the green nodes indicate significantly higher relative abundance in the oral cavity than the esophagus. The size of the node is in proportion to the linear discriminant analysis (LDA) score (detailed in Supplementary Figure S1). The links (lines) between the nodes mean hypothetically phylogenetic relationships among organisms, which can be traced back to where the lines branch off (hypothetical ancestor).

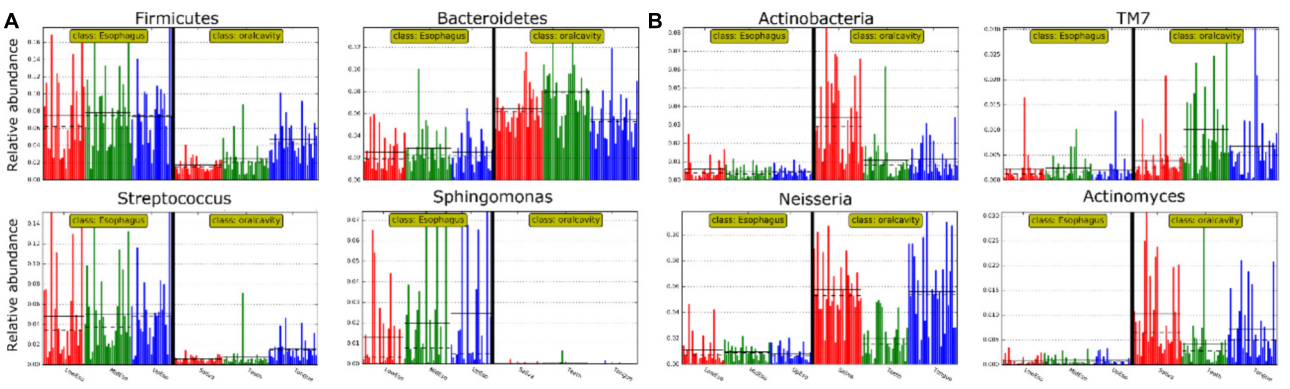

FIGURE 4 | Relative abundance of most predominant discriminative microbiota between the oral cavity and the esophagus in terms of the phylum level **(A)** and the genus level **(B)**.

TABLE 1 | Within-community alpha diversity of microbiome in the oral cavity and the esophagus.

Body habitats	Chao1 richness				Shannon Diversity				Simpson Index			
	Min	Max	Mean	*SD*	Min	Max	Mean	*SD*	Min	Max	Mean	*SD*
Oral cavity	291.18	1404.04	593.90	261.99	4.16	7.50	5.89	0.74	0.87	0.99	0.95	0.03
Sa	320.87	1355.30	645.79	289.93	4.16	6.92	5.69	0.63	0.87	0.98	0.94	0.03
TD	291.18	1085.69	535.37	264.48	4.44	6.19	5.49	0.53	0.87	0.97	0.94	0.03
SP	335.58	1404.04	600.79	223.76	4.98	7.50	6.53	0.59	0.88	0.99	0.97	0.02
Esophagus	237.50	1830.54	636.79	400.65	2.70	7.42	5.30	1.12	0.53	0.99	0.88	0.10
UE	247.24	1409.90	643.83	341.39	2.74	6.67	5.24	1.05	0.56	0.97	0.88	0.10
ME	237.50	1830.54	622.39	409.65	3.55	7.33	5.33	1.01	0.61	0.98	0.89	0.09
LE	238.91	1638.12	646.03	458.71	2.70	7.42	5.33	1.30	0.53	0.99	0.88	0.12

Min, minimal; Max, maximal; SD, standard deviation; Sa, saliva; TD, tongue dorsum; SP, supragingival plaque; UE, upper esophagus; ME, middle esophagus; LE, lower esophagus.

from three esophagus segments weighted by the Bray-Curtis distance of beta diversity (**Figure 2A**), and also no statistical differences of alpha diversity estimated by Shannon Diversity and Simpson Index (**Table 1**). Furthermore, within-group distance was comparable to between-group distance for all three habitats, indicating that the inter-individual variability of microbial diversity in the esophagus was so wide that the between-group diversity of microbes was covered.

DISCUSSION

We conducted a baseline study in a healthy population from a high-incidence region of esophageal cancer in China to demonstrate the contiguity and preference of microbiota in three niches of the oral cavity and three segments of the esophagus by 16S rRNA gene sequencing. Highly diverse bacterial flora with hundreds of genera belonging to 29 phyla resided in the oral cavity and the esophagus. Six most abundant phyla in both upper digestive tracts were Proteobacteria, Firmicutes, Bacteroidetes, Actinobacteria, Fusobacteria, and TM7. Meanwhile, several site-specific bacterial biomarkers both at the phylum and genus levels for the oral cavity and the esophagus were identified.

This investigation corroborated the diversity and complexity of bacterial profiles in the oral cavity reported by previous findings (Aas et al., 2005; Keijser et al., 2008; Bik et al., 2010; Segata et al., 2012; Norder Grusell et al., 2013), in which the phyla Proteobacteria, Firmicutes, Bacteroidetes, Actinobacteria, Fusobacteria, and TM7 were frequently detected and the genera *Neisseria, Prevotella*, *Porphyromonas*, *Capnocytophaga, Streptococcus*, *Rothia*, and *Actinomyces* were most predominant. The similarity of microbial compositions among three niches in the oral cavity coincided with their spatial continuity. The saliva is directly exposed to the ingested and inhaled substances, the tongue dorsum provides soft tissues medium for the dynamic bacterial flora and the supragingival plaque bathed in the saliva offers a hard tissue medium for the transitory reservoir of bacterial flora. These specific microenvironments in three oral niches might lead to microbial preference for the colonizing medium (Nasidze et al., 2009; Segata et al., 2012). Our results showed that the phylum Bacteroidetes apparently preferred to colonizing on the tooth surfaces than colonizing in the saliva or the supragingival plague, consistent with Segas's findings (Segata et al., 2012). The phylum TM7, originally thought to be exclusively environmental, was detected in healthy oral cavity (Kelsen et al., 2015; Ren et al., 2016; Xiao et al., 2016). In our study, TM7 apparently has a predilection for the supragingival plaque, indicating that 'environmental' phyla once resided in the oral cavity would select suitable anatomic niches and create microbial environment to conversely influence the ecology of these habitats (Aas et al., 2005). Microbial differences from three oral habitats in healthy individuals at the genus level were further analyzed in our study. The genus *Neisseria* appeared to be transient because it was more abundant in the tongue dorsum and the saliva than that in the supragingival plaque. The genus *Capnocytophaga* was a predominant composition of biofilm in the supragingival plaque, but undetectable in the saliva and the tongue dorsum, indicating the possibility of its involvement in the periodontal and systematic diseases in the immunocompromised and immunocompetent hosts (Bonatti et al., 2003; Piau et al., 2013). The findings of site-specific bacteria in the oral cavity have been reported by Aas et al. (2005) who utilized 16S PCR cloning molecular technique to analyze microbial compositions in nine sites of oral cavity from five clinically healthy subjects. Meanwhile, the US HMP study has re-categorized nine distinct mouth surfaces into three distinct community groups based on phylogenetic relationships of bacterial communities using 16S rRNA gene sequencing (Segata et al., 2012). Microbial preference to the oral niches might be a result of specific adhesions of bacterial surface binding to complementary specific receptors on a given oral surface (Gibbons et al., 1976; Gibbons, 1989).

Healthy esophagus was colonized by its own residential bacteria (Pei et al., 2004; Norder Grusell et al., 2013). Six predominant phylum-level bacteria in the esophagus identified by our study are generally in consistent with the findings in the distal esophagus using the same 16S rRNA gene sequencing technique (Pei et al., 2004), more diverse than those found in the studies using culture-based technique (Norder Grusell et al., 2013). However, our findings in esophageal microbiota at the genus level diverge from previous studies. Apart from the predominance of *Streptococcus*, other twelve members of genera found by Pei et al. (2004) were of different abundances. For

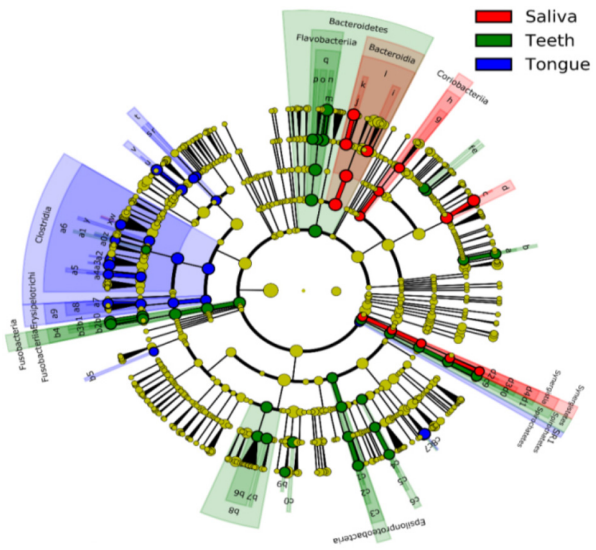

FIGURE 5 | Circular cladogram for niche specialization of microbial compositions in three sites in the oral cavity using the linear discriminant analysis effect size (LEfSe) analysis of the abundance patterns of bacterial taxa. The circles used in this diagram represent the taxonomic categories of organisms from the phylum level as the outermost circle to genus (or species) level as the innermost cycle. Within each given taxon, each small cycle represents its lower clade. The yellow nodes indicate no statistically significant differences of a given taxon between the samples of three sites, the red nodes indicate significantly higher relative abundance in saliva than other two sites, the green nodes indicate significantly higher relative abundance in the supragingival plagues than other two sites, and the blue nodes indicate significantly higher relative abundance in tongue dorsum than other two sites in oral cavity. The size of the node is in proportion to the LDA score. The links (lines) between the nodes mean hypothetically phylogenetic relationships among organisms, which can be traced back to where the lines branch off (hypothetical ancestor). Sa, saliva; TD, tongue dorsum; SP, supragingival plaque.

instances, the top two common bacteria in the esophagus were *Prevotella* and *Veillonella*, in combination, accounting for 30% of the bacterial taxa in their studies compared with approximately 5% in our study. *Gemella* and *Clostridium* presented in all subjects in their studies while in 30% of subjects in our study. *Actinobacillus* was not the predominant bacteria in their study but the second most common in our study. It might be explained by the populations residing in different geographical regions, having different life styles and different sampling methods. Besides, sex proportions could be also an impact factor. Four subjects including three males and one females, were recruited by Pei et al. (2005). while 27 subjects including four males and 23 females in our study. The divergence in gut microbiota in relation to age, gender, and geographic regions has been evaluated (Mueller et al., 2006; Haro et al., 2016). The last, more microbial diversity identified in brushes samples than the biopsies could also explain the difference between our study and Pei Z's study. Whatever, it is still uncertain which method or technique is suitable for specimen collection of the upper digestive tract.

Another intriguing finding is that *Sphingomonas* was present at least one site of the oral cavity and esophageal segments. The presence of this bacterium in human samples is normally related to contamination during the handling or DNA extraction process in samples with low bacterial load, where the contribution of water-associated or environmental bacteria is potentially higher. Although we did not sequence the negative controls, the small DNA amounts in these controls (<0.01 ng/μL) in relation to the DNA amounts in our samples (2–30 ng/μL) makes us think that the relative contribution of contaminants is low. In addition, recent studies also reported that it is an opportunistic pathogen of concern in drinking water and might cause the Bacteremia in patient with sickle cell disease and in a patient with cancer (Angelakis et al., 2009; Garcia-Lozano et al., 2015; Gulati et al., 2016). Therefore, its role in healthy upper digestive tract remains to be determined in future studies.

As reported by global esophageal cancer collaboration groups, the occurrence rates of esophageal cancer varied by specific esophageal segments (Rice et al., 2009). Considering the exposure of the reflux acid contents from the stomach in distal esophagus, we tried to investigate the differences among indigenous biota from three distinct esophageal segments. However, this study did not identify any segment-specific microbiota of healthy esophagus, which suggests that the samples from any one of esophagus segments are representative for investigating the microbiome. This finding might simplify the procedure of sampling esophagus and the resulting reduction of costs, especially for esophageal cancer screening. Nevertheless, given the bacterial compositions in abnormal esophagus different from those in healthy esophagus (Pei et al., 2005; Yang et al., 2009; Liu et al., 2013), the conclusion of random sampling at any segment should be generalized to the population with high-risk of esophagus cancer or other patients cautiously.

The esophagus may not only be colonized by the bacteria from the oral cavity but also its own specific residential bacteria. Our study confirmed the overall similarity of microbial biota at each clade level between the oral cavity and the esophagus, indicating that the oral microbiota might significantly contribute to the microbiota of down-stream digestive tract including intestine (Dal Bello and Hertel, 2006; Maukonen et al., 2008; Segata et al., 2012). However, certain bacteria, such as the genera *Neisseria*, *Prevotella*, *Capnocytophaga,* and *Porphyromonas,* were detected highly abundant in the oral cavity but moderately abundant in the esophagus where genus *Streptococcus* had pronounced predominance. These divergences could be explained by either selective passage of bacteria from the oropharynx or the selective retention of particular oral bacteria by the esophagus (Segata et al., 2012). Furthermore, similar bacteria from the samples between the esophagus and the stomach were also found if microbial compositions in the esophagus in our study were linked with those in the stomach reported by other studies (Hsieh et al., 2018), despite no direct comparison of the microbial communities between the samples of esophagus and stomach at the same individual to date.

The present study has several strengths in stringent inclusion criteria of the participants confirmed by the dentists and physicians aided with esophageal endoscopy to avoid the bias of

disease misclassification, and a series of quality control methods for the minimization of the contamination of microbiota from handling environment and adjacent tracts. However, a few of drawbacks still need to be addressed. Firstly, small sample size of healthy individuals limited the evaluation of the effects of social-demographic characteristics on microbial diversity. Secondly, microbiome diversity at the specie-level in high phylogenetic resolution couldn't be reached by 16S rRNA gene sequencing (Sundquist et al., 2007), compared to whole genome shotgun sequencing. Thirdly, most participants enrolled in our study were women, which might lead to microbial bias in term of sex-relevance. Finally, since this study just focused on healthy subjects, not on both patients of esophageal cancer and healthy subjects correspondingly, the association between microbial microbiome and esophageal cancer needs to be investigated in future studies.

CONCLUSION

Our study demonstrated microbial diversity at different taxonomic level in healthy oral cavity and esophagus, and identified site-preferable bacterial signatures in six niches of the upper digestive tract. We also found microbial differences between individuals caused by different genetic background and lifestyles. Further investigations with consideration of demographics variation including gender, age, health condition and life-styles are likely to comprehensively deepen our understanding of microbial characteristics in healthy population and to elucidate the disease-associated microbiota in local and systemic diseases affecting human health.

AUTHOR CONTRIBUTIONS

W-QW, WC, and LD designed this study. LD and JY wrote the manuscript. JY, WC, LD, and JZ cleaned, analyzed, and interpreted the data. W-QW, LD, S-RM, H-RW, and MW collected and detected clinical samples. All authors revised the manuscript and approved the final manuscript.

FUNDING

This work was supported by the CAMS Innovation Fund for Medical Sciences (CIFMS) (2016-I2M-3-001), Natural Science Fund from the National Natural Science Foundation of China (81573224), and Fundamental Research Funds for the Central Universities (2016ZX310178).

ACKNOWLEDGMENTS

We wish to thank Dr. Changxin Wu for his careful editing of the language, Mingyue Jiang for her designing questionnaire, Junjie Qin and Dongqian Shen for their technic supports. We also thank the local doctors and people who participated in our study from Linzhou cancer hospital.

SUPPLEMENTARY MATERIAL

The Supplementary Material for this article can be found online at: https://www.frontiersin.org/articles/10.3389/fmicb.2018.01603/full#supplementary-material

REFERENCES

Aas, J. A., Paster, B. J., Stokes, L. N., Olsen, I., and Dewhirst, F. E. (2005). Defining the normal bacterial flora of the oral cavity. *J. Clin. Microbiol.* 43, 5721–5732. doi: 10.1128/JCM.43.11.5721-5732.2005

Abusleme, L., Dupuy, A. K., Dutzan, N., Silva, N., Burleson, J. A., Strausbaugh, L. D., et al. (2013). The subgingival microbiome in health and periodontitis and its relationship with community biomass and inflammation. *ISME J.* 7, 1016–1025. doi: 10.1038/ismej.2012.174ismej2012174

Angelakis, E., Roux, V., and Raoult, D. (2009). Sphingomonas mucosissima Bacteremia in patient with sickle cell disease. *Emerg. Infect. Dis.* 15, 133–134. doi: 10.3201/eid1501.080465

Bashan, A., Gibson, T. E., Friedman, J., Carey, V. J., Weiss, S. T., Hohmann, E. L., et al. (2016). Universality of human microbial dynamics. *Nature* 534, 259–262. doi: 10.1038/nature18301nature18301

Bik, E. M., Long, C. D., Armitage, G. C., Loomer, P., Emerson, J., Mongodin, E. F., et al. (2010). Bacterial diversity in the oral cavity of 10 healthy individuals. *ISME J.* 4, 962–974. doi: 10.1038/ismej.2010.30ismej201030

Bonatti, H., Rossboth, D. W., Nachbaur, D., Fille, M., Aspock, C., Hend, I., et al. (2003). A series of infections due to *Capnocytophaga* spp in immunosuppressed and immunocompetent patients. *Clin. Microbiol. Infect.* 9, 380–387. doi: 10.1046/j.1469-0691.2003.00538.x

Caporaso, J. G., Kuczynski, J., Stombaugh, J., Bittinger, K., Bushman, F. D., Costello, E. K., et al. (2010). QIIME allows analysis of high-throughput community sequencing data. *Nat. Methods* 7, 335–336. doi: 10.1038/nmeth.f.303nmeth.f.303

Caporaso, J. G., Lauber, C. L., Costello, E. K., Berg-Lyons, D., Gonzalez, A., Stombaugh, J., et al. (2011a). Moving pictures of the human microbiome. *Genome Biol.* 12:R50. doi: 10.1186/gb-2011-12-5-r50gb-2011-12-5-r50

Caporaso, J. G., Lauber, C. L., Walters, W. A., Berg-Lyons, D., Lozupone, C. A., Turnbaugh, P. J., et al. (2011b). Global patterns of 16S rRNA diversity at a depth of millions of sequences per sample. *Proc. Natl. Acad. Sci. U.S.A.* 108(Suppl. 1), 4516–4522. doi: 10.1073/pnas.1000080107 1000080107

Dal Bello, F., and Hertel, C. (2006). Oral cavity as natural reservoir for intestinal lactobacilli. *Syst. Appl. Microbiol.* 29, 69–76. doi: 10.1016/j.syapm.2005.07.002

Di Pilato, V., Freschi, G., Ringressi, M. N., Pallecchi, L., Rossolini, G. M., and Bechi, P. (2016). The esophageal microbiota in health and disease. *Ann. N. Y. Acad. Sci.* 1381, 21–33. doi: 10.1111/nyas.13127

Fan, X., Alekseyenko, A. V., Wu, J., Peters, B. A., Jacobs, E. J., Gapstur, S. M., et al. (2016). Human oral microbiome and prospective risk for pancreatic cancer: a population-based nested case-control study. *Gut* 67, 120–127. doi: 10.1136/gutjnl-2016-312580

Feng, Z. H., Li, Q., Liu, S. R., Du, X. N., Wang, C., Nie, X. H., et al. (2017). Comparison of composition and diversity of bacterial microbiome in human upper and lower respiratory tract. *Chin. Med. J.* 130, 1122–1124. doi: 10.4103/0366-6999.204934

Fierer, N., Leff, J. W., Adams, B. J., Nielsen, U. N., Bates, S. T., Lauber, C. L., et al. (2012). Cross-biome metagenomic analyses of soil microbial communities and their functional attributes. *Proc. Natl. Acad. Sci. U.S.A.* 109, 21390–21395. doi: 10.1073/pnas.1215210110 1215210110

Frank, D. N., Zhu, W., Sartor, R. B., and Li, E. (2011). Investigating the biological and clinical significance of human dysbioses. *Trends Microbiol.* 19, 427–434. doi: 10.1016/j.tim.2011.06.005

Gall, A., Fero, J., McCoy, C., Claywell, B. C., Sanchez, C. A., Blount, P. L., et al. (2015). Bacterial composition of the human upper gastrointestinal tract microbiome is dynamic and associated with genomic instability in a Barrett's esophagus cohort. *PLoS One* 10:e0129055. doi: 10.1371/journal.pone.0129055

Garcia-Lozano, T., Garcia-Garcia, A. M., Iranzo-Tatay, A., and Aznar-Oroval, E. (2015). [First case of bacteremia by *Sphingomonas anadarae* in an patient with cancer]. *Med. Clin.* 145, 459–460. doi: 10.1016/j.medcle.2016.03.019

Gibbons, R. J. (1989). Bacterial adhesion to oral tissues: a model for infectious diseases. *J. Dent. Res.* 68, 750–760. doi: 10.1177/00220345890680050101

Gibbons, R. J., Spinell, D. M., and Skobe, Z. (1976). Selective adherence as a determinant of the host tropisms of certain indigenous and pathogenic bacteria. *Infect. Immun.* 13, 238–246.

Gulati, P., Singh, P., Chatterjee, A. K., and Ghosh, M. (2016). Monitoring of biofilm ageing in a *Sphingomonas* sp. strain from public drinking water sites through changes in capacitance. *Environ. Technol.* 38, 2344–2351. doi: 10.1080/09593330.2016.1260164

Haro, C., Rangel-Zuniga, O. A., Alcala-Diaz, J. F., Gomez-Delgado, F., Perez-Martinez, P., Delgado-Lista, J., et al. (2016). Intestinal microbiota is influenced by gender and body mass index. *PLoS One* 11:e0154090. doi: 10.1371/journal.pone.0154090

Hsieh, Y. Y., Tung, S. Y., and Pan, H. Y. (2018). Increased abundance of *Clostridium* and *Fusobacterium* in gastric microbiota of patients with gastric cancer in Taiwan. *Sci. Rep.* 8, 158–168. doi: 10.1038/s41598-017-18596-0

Keijser, B. J., Zaura, E., Huse, S. M., van der Vossen, J. M., Schuren, F. H., Montijn, R. C., et al. (2008). Pyrosequencing analysis of the oral microflora of healthy adults. *J. Dent. Res.* 87, 1016–1020. doi: 10.1177/154405910808701104

Kelsen, J., Bittinger, K., Pauly-Hubbard, H., Posivak, L., Grunberg, S., Baldassano, R., et al. (2015). Alterations of the subgingival microbiota in pediatric Crohn's disease studied longitudinally in discovery and validation cohorts. *Inflamm. Bowel Dis.* 21, 2797–2805. doi: 10.1097/MIB.0000000000000557

Kerr, A. R. (2015). The oral microbiome and cancer. *J. Dent. Hyg.* 89(Suppl. 1), 20–23.

Liu, N., Ando, T., Ishiguro, K., Maeda, O., Watanabe, O., Funasaka, K., et al. (2013). Characterization of bacterial biota in the distal esophagus of Japanese patients with reflux esophagitis and Barrett's esophagus. *BMC Infect. Dis.* 13:130. doi: 10.1186/1471-2334-13-130

Maukonen, J., Matto, J., Suihko, M. L., and Saarela, M. (2008). Intra-individual diversity and similarity of salivary and faecal microbiota. *J. Med. Microbiol.* 57(Pt 12), 1560–1568. doi: 10.1099/jmm.0.47352-0

Mueller, S., Saunier, K., Hanisch, C., Norin, E., Alm, L., Midtvedt, T., et al. (2006). Differences in fecal microbiota in different European study populations in relation to age, gender, and country: a cross-sectional study. *Appl. Environ. Microbiol.* 72, 1027–1033. doi: 10.1128/AEM.72.2.1027-1033.2006

Nasidze, I., Li, J., Quinque, D., Tang, K., and Stoneking, M. (2009). Global diversity in the human salivary microbiome. *Genome Res.* 19, 636–643. doi: 10.1101/gr.084616.108

Norder Grusell, E., Dahlen, G., Ruth, M., Ny, L., Quiding-Jarbrink, M., Bergquist, H., et al. (2013). Bacterial flora of the human oral cavity, and the upper and lower esophagus. *Dis. Esophagus* 26, 84–90. doi: 10.1111/j.1442-2050.2012.01328.x

Pei, Z., Bini, E. J., Yang, L., Zhou, M., Francois, F., and Blaser, M. J. (2004). Bacterial biota in the human distal esophagus. *Proc. Natl. Acad. Sci. U.S.A.* 101, 4250–4255. doi: 10.1073/pnas.0306398101

Pei, Z., Yang, L., Peek, R. M. Jr., Levine, S. M., Pride, D. T., and Blaser, M. J. (2005). Bacterial biota in reflux esophagitis and Barrett's esophagus. *World J. Gastroenterol.* 11, 7277–7283. doi: 10.3748/wjg.v11.i46.7277

Piau, C., Arvieux, C., Bonnaure-Mallet, M., and Jolivet-Gougeon, A. (2013). *Capnocytophaga* spp. involvement in bone infections: a review. *Int. J. Antimicrob. Agents* 41, 509–515. doi: 10.1016/j.ijantimicag.2013.03.001

Pozhitkov, A. E., Beikler, T., Flemmig, T., and Noble, P. A. (2011). High-throughput methods for analysis of the human oral microbiome. *Periodontol. 2000* 55, 70–86. doi: 10.1111/j.1600-0757.2010.00380.x

Ren, W., Zhang, Q., Liu, X., Zheng, S., Ma, L., Chen, F., et al. (2016). Supragingival plaque microbial community analysis of children with halitosis. *J. Microbiol. Biotechnol.* 26, 2141–2147. doi: 10.4014/jmb.1605.05012

Rice, T. W., Rusch, V. W., Apperson-Hansen, C., Allen, M. S., Chen, L. Q., Hunter, J. G., et al. (2009). Worldwide esophageal cancer collaboration. *Dis. Esophagus* 22, 1–8. doi: 10.1111/j.1442-2050.2008.00901.x

Segata, N., Haake, S. K., Mannon, P., Lemon, K. P., Waldron, L., Gevers, D., et al. (2012). Composition of the adult digestive tract bacterial microbiome based on seven mouth surfaces, tonsils, throat and stool samples. *Genome Biol.* 13:R42. doi: 10.1186/gb-2012-13-6-r42

Segata, N., Izard, J., Waldron, L., Gevers, D., Miropolsky, L., Garrett, W. S., et al. (2011). Metagenomic biomarker discovery and explanation. *Genome Biol.* 12:R60. doi: 10.1186/gb-2011-12-6-r60

Socransky, S. S., and Haffajee, A. D. (2002). Dental biofilms: difficult therapeutic targets. *Periodontol. 2000*, 28, 12–55. doi: 10.1034/j.1600-0757.2002.280102.x

Sundquist, A., Bigdeli, S., Jalili, R., Druzin, M. L., Waller, S., Pullen, K. M., et al. (2007). Bacterial flora-typing with targeted, chip-based Pyrosequencing. *BMC Microbiol.* 7:108. doi: 10.1186/1471-2180-7-108

Tlaskalova-Hogenova, H., Stepankova, R., Kozakova, H., Hudcovic, T., Vannucci, L., Tuckova, L., et al. (2011). The role of gut microbiota (commensal bacteria) and the mucosal barrier in the pathogenesis of inflammatory and autoimmune diseases and cancer: contribution of germ-free and gnotobiotic animal models of human diseases. *Cell. Mol. Immunol.* 8, 110–120. doi: 10.1038/cmi.2010.67

Xiao, C., Ran, S., Huang, Z., and Liang, J. (2016). Bacterial diversity and community structure of supragingival plaques in adults with dental health or caries revealed by 16S pyrosequencing. *Front. Microbiol.* 7:1145. doi: 10.3389/fmicb.2016.01145

Yang, L., Lu, X., Nossa, C. W., Francois, F., Peek, R. M., and Pei, Z. (2009). Inflammation and intestinal metaplasia of the distal esophagus are associated with alterations in the microbiome. *Gastroenterology* 137, 588–597. doi: 10.1053/j.gastro.2009.04.046

Yu, G., Gail, M. H., Shi, J., Klepac-Ceraj, V., Paster, B. J., Dye, B. A., et al. (2014). Association between upper digestive tract microbiota and cancer-predisposing states in the esophagus and stomach. *Cancer Epidemiol. Biomarkers Prev.* 23, 735–741. doi: 10.1158/1055-9965.EPI-13-0855

Conflict of Interest Statement: The authors declare that the research was conducted in the absence of any commercial or financial relationships that could be construed as a potential conflict of interest.

Copyright © 2018 Dong, Yin, Zhao, Ma, Wang, Wang, Chen and Wei. This is an open-access article distributed under the terms of the Creative Commons Attribution License (CC BY). The use, distribution or reproduction in other forums is permitted, provided the original author(s) and the copyright owner(s) are credited and that the original publication in this journal is cited, in accordance with accepted academic practice. No use, distribution or reproduction is permitted which does not comply with these terms.

frontiers in Microbiology

ORIGINAL RESEARCH
published: 20 July 2018
doi: 10.3389/fmicb.2018.01602

Genetically Obese Human Gut Microbiota Induces Liver Steatosis in Germ-Free Mice Fed on Normal Diet

*Ruirui Wang[1], Hui Li[1], Xin Yang[1], Xinhe Xue[1], Liman Deng[1], Jian Shen[2], Menghui Zhang[1], Liping Zhao[1,2,3] and Chenhong Zhang[1]**

[1] State Key Laboratory of Microbial Metabolism, School of Life Sciences and Biotechnology, Shanghai Jiao Tong University, Shanghai, China, [2] Ministry of Education Key Laboratory of Systems Biomedicine, Shanghai Center for Systems Biomedicine, Shanghai Jiao Tong University, Shanghai, China, [3] Department of Biochemistry and Microbiology, School of Environmental and Biological Sciences, Rutgers New Jersey Institute for Food, Nutrition, and Health, Rutgers University–New Brunswick, New Brunswick, NJ, United States

Dysbiotic gut microbiota contributes to genetically obese phenotype in human. However, the effect of genetic obesity-associated gut microbiota on host hepatic metabolic deteriorations remains largely unknown. Gut microbiota from a genetically obese human donor before and after a dietary weight loss program was transplanted into germ-free C57BL/6J male mice, grouped as PreM and PostM groups, respectively. The gut microbiome, liver pathology and transcriptome response in the gnotobiotic mice were evaluated. After being fed on normal chow diet for 4 weeks, PreM group developed liver macrovesicular steatosis accompanied with higher concentrations of hepatic triglyceride and cholesterol, while PostM group exhibited normal hepatic physiology. The gut microbiota in PreM and PostM groups was significantly different from each other and was more resembling with their respective donor. RNA-sequencing revealed that, in comparison with PostM group, PreM group showed a foregoing pro-steatotic transcriptional response in liver featuring by the repression of lipid beta-oxidation and the activation of lipid absorption and cholesterol uptake before the pathology of liver steatosis. Moreover, peroxisome proliferator-activated receptor alpha (PPARα), which was repressed in PreM group, may act as crucial regulator of the hepatic transcriptional profile of lipid metabolism between two groups. Our results show that gut microbiota from a genetically obese human promotes the onset of liver steatosis by impacting hepatic transcriptional profile of lipid metabolism in mice. This adds new evidence that gut microbiota may play a causative role in the development of non-alcoholic fatty liver disease.

Keywords: gut microbiota, genetic obesity, germ-free mice, liver steatosis, hepatic lipid metabolism

OPEN ACCESS

Edited by:
Sunny Hei Wong, The Chinese University of Hong Kong, Hong Kong

Reviewed by:
Phillipp Hartmann, University of California, San Diego, United States
Vishal Singh, University of Toledo, United States

****Correspondence:***
Chenhong Zhang
zhangchenhong@sjtu.edu.cn

Specialty section:
This article was submitted to Microbial Symbioses, a section of the journal Frontiers in Microbiology

Received: *08 April 2018*
Accepted: *27 June 2018*
Published: *20 July 2018*

Citation:
Wang R, Li H, Yang X, Xue X, Deng L, Shen J, Zhang M, Zhao L and Zhang C (2018) Genetically Obese Human Gut Microbiota Induces Liver Steatosis in Germ-Free Mice Fed on Normal Diet. Front. Microbiol. 9:1602. doi: 10.3389/fmicb.2018.01602

INTRODUCTION

Recently, non-alcoholic fatty liver disease (NAFLD) has become one of the most prevalent chronic liver diseases along with the worldwide epidemic of obesity (Bedogni et al., 2005; Younossi et al., 2016). The onset of NAFLD is featured by an excessive accumulation of triglyceride in the cytoplasm of hepatocytes, which brings potentially serious sequelae, such as non-alcoholic steatohepatitis, cirrhosis, and even hepatocellular carcinoma (Petta et al., 2016).

Notably, recent studies have highlighted the pivotal role of gut microbiota in the onset of NAFLD (Bashiardes et al., 2016; Boursier et al., 2016). Fat accumulation in liver induced by diet could be transferred to germ-free (GF) animal through gut microbiota transplantation (Le Roy et al., 2012; Duca et al., 2014). Backhed et al. (2004) has reported that the conventionalization of GF mice could promote the hepatic expression of genes involved in lipid uptake and de novo lipogenesis. Moreover, the persistent activation of genes involved in fatty acid oxidation in liver and skeletal muscle was speculated to be one of the crucial reasons for the resistance to diet-induced obesity in GF mice (Backhed et al., 2007). More recently, Murakami et al. (2016) found that in response to a high-fat diet, gut microbiota could drive the peroxisome proliferator-activated receptor gamma (PPARγ)-mediated activation of hepatic transcriptional circadian oscillation. Therefore, gut microbiota may contribute to the onset of diet-induced obesity and NAFLD through distal regulation of the host hepatic transcriptional response related with lipid metabolism.

In our previous cohort study of children with Prader−Willi syndrome (PWS), one of the most common human genetic diseases leading to obesity (Butler, 2011), we showed that a diet rich in non-digestible carbohydrates could modulate the structure and function of gut microbiota in PWS children and consequently improve their obesity-related phenotypes (Zhang et al., 2015). A human genetic obesity microbiota-associated mouse model was established through conventionalization of GF mice with the gut microbiota from one PWS child before and after diet intervention. We found that the pre-intervention gut microbiota induced a higher level of body fat accumulation and inflammation in the gnotobiotic mice. These results suggest that the dysbiotic, pre-intervention gut microbiota indeed has a greater capacity to induce metabolic deterioration in mice than the post-intervention gut microbiota, implicating a similar role in its PWS hosts (Zhang et al., 2015). However, the effects of gut microbiota associated with genetically predisposed obesity on host hepatic lipid metabolism are still unclear.

In the current study, we conducted an in-depth analysis of hepatic physiology, gut microbiome, and hepatic transcriptome in the human genetic obesity microbiota-associated mouse model. We found that the gut microbiota from a genetically obese child induced liver steatosis in GF mice fed on normal chow diet and revealed the underlying transcriptional process mediated by gut microbiota.

MATERIALS AND METHODS

The Conventionalization of GF Mice

The clinical trial of the PWS cohort (GD58 included) was approved by the Ethics Committee of the School of Life Sciences and Biotechnology, Shanghai Jiao Tong University (No. 2012-016) and registered at Chinese Clinical Trial Registry (No. ChiCTR-ONC-12002646) as described before (Zhang et al., 2015). Written informed consent was obtained from the guardian of the PWS donor (GD58, 8 years old). The procedures and protocols for the animal experiments were approved by Institutional Animal Care and Use Committee of SLAC Inc. Details of the fecal suspension preparation and gut microbiota transplantation of GF male C57BL/6J mice were described previously (Zhang et al., 2015). Mice that received gut microbiota from the PWS human donor pre-intervention (PreH) constituted the PreM group, and mice that received gut microbiota from the PWS human donor post-intervention (PostH) constituted the PostM group. Both PreM (n = 10) and PostM (n = 9) groups were fed a sterile normal chow diet (D12450B, Research Diets, Inc., United States) in separate plastic isolators for 4 weeks. Feces were collected from each mouse every week. Half of the mice in each group were sacrificed after being colonized for 2 or 4 weeks. Blood, liver, and colon tissues were harvested following refined protocols.

Liver Histology and Hepatic Lipid Level Assessment

Specific parts of fresh liver from each mouse were fixed in paraformaldehyde for 48 h at room temperature and embedded in paraffin. Five-micrometer-thick sections were stained with hematoxylin and eosin. Images of each liver section were obtained tripartitely by experienced staff who was blinded to the experiment. The liver steatosis score was assessed using Image-Pro Plus, version 7.01 for Windows (Media Cybernetics, Silver Springs, MD, United States) as described previously (Catta-Preta et al., 2011).

A frozen pellet of liver sample was homogenized in a corresponding volume (W/V:1/9) of homogenizing buffer (pH 7.4, 0.01 mol/L Tris-HCl, 1 mmol/L EDTA, 0.8% NaCl). The supernatant was collected after being centrifuged at 2000 g for 25 min at 4°C. Assay kits (NanJing Jiancheng Bioengineering Institute, China) were used to measure the hepatic and serum triglyceride and cholesterol concentrations. The results of hepatic lipids were corrected for total protein concentration (Yeasen Biotechnology Co., Ltd., China).

Enzyme-Linked Immunosorbent Assay

Enzyme-linked immunosorbent assay kits were used to determine the serum concentration of leptin (R&D Systems, United States), lipopolysaccharide (LPS)-binding protein (LBP) (Cell Sciences, United States), and serum amyloid A protein (SAA, Tridelta, Ireland) according to the manufacturer's instructions.

Gut Microbiota Profiling

The bacterial DNA from feces of the human donor and mouse recipients after transplantation for 1, 2, 3, and 4 weeks was extracted as previously described (Godon et al., 1997) and checked for concentration and purity (Qubit2.0, Thermo Fisher). The variable region 3 (V3) of bacterial 16S rRNA gene in all samples from the donor and recipients were sequenced in the same run by Ion Torrent^{TM} Next-Generation Sequencing (Thermo Fisher). The barcode library was prepared following the Ion Torrent PGM protocol for short amplicons (<350 bp). The primers were composed of a universal primer (341F: 5′ CCTACGGGAGGCAGCAG 3′, 518R: 5′

ATTACCGCGGCTGCTGG 3′) for the bacterial 16s rRNA gene V3 region, a sample-specific barcode, and a PGM sequencing adaptor. PCR was conducted using amplification conditions as described previously (Milani et al., 2013). After checking for size and concentration, the purified PCR product of each sample was mixed equally. The mixture was then pretreated on Ion OneTouch^{TM} using Ion PGM Template OT2 200 Kit and sequenced on PGM system using Ion 314 Chip Kit v2.

The raw reads were pretreated as described previously (Milani et al., 2013). High-quality reads were then assigned to closed reference operational taxonomic units (OTUs) at 97% similarity levels following the procedure in QIIME platform (version 1.8) (Caporaso et al., 2010). Using the rarefaction OTU table, we performed principal coordinate analysis (PCoA) based on weighted UniFrac distances. Multivariate analysis of variance using PCoA accounting for 80% of total variations was conducted in R version 3.4.0[1]. The alpha diversity of each sample was calculated based on the number of observed OTUs and the Shannon index.

Considering the stability of the gut microbiota in each group of recipient mice over time, all time points in different groups were merged to identify discriminating OTUs between two groups by a random forest model through leave-one-out cross-validation (Breiman, 2001). A visually selected cut-off value for discriminating OTUs was chosen according to the descending accuracy of discrimination of all the OTUs. The abundance variations in OTUs between different groups in donor (PostH divided by PreH) and recipients (PostM divided by PreM) were assessed. A heat map of the key OTUs was generated in R version 3.4.0 (see footnote 1), with the abundance of the OTUs which was log2-transformed.

Hepatic Transcriptome Profiling

Total RNA in mice livers was extracted using the RNeasy mini kit (Qiagen, Germany). After purification using the RNase-Free DNase Set (Qiagen), the concentration and quality of the purified RNA were determined using the NanoDrop ND-1000 (Thermo Scientific, United States) and Agilent Bioanalyzer 2100 systems (Agilent Technologies, United States). Libraries for sequencing were generated according to the Ilumina TrueSeq protocol. Paired-end RNA sequencing was performed on an Illummina HiSeq 2500 according to the manufacturer's instructions with a quality control standard (each sample sequencing depth higher than 7 GB, read length higher than 90 nt, and Q30 > 85%).

The raw RNA-seq reads in FASTQ format were processed to trim the adaptor using Flexbar (Dodt et al., 2012), and the reads containing ploy-N and the low-quality reads were removed using Prinseq (Schmieder and Edwards, 2011). The high-quality reads from each sample were aligned to the Mus musculus reference genome, GRCm38 (Genome Reference Consortium mouse build 38[2]), using HISAT (Hierarchical Indexing for Spliced Alignment of Transcripts, version 0.1.7-beta) with default parameters (Kim et al., 2015). The unambiguous alignments of each sample were quantified by HTSeq-count (version 0.6.1p1) (Anders et al., 2015) with the mouse genome annotation GTF file[3], and the gene expression profile in terms of the read counts was acquired. After obtaining the gene counts of each sample, differential expression analysis was performed using DESeq2 (version 1.9.23) (Love et al., 2014). Differentially expressed genes (DEGs) between PreM and PostM groups were determined by Deseq2 with the standard of $|\log2\text{FoldChange}| \geq 1$ on each time point. The normalized gene count matrix constructed by DESeq2 was extracted for further statistical analysis. Hierarchical clustering (spearman correlation) and expression visualization of all the DEGs were performed in R version 3.4.0, with the abundance of the DEGs transformed by *z*-score (standard score).The DEGs were analyzed using Ingenuity Pathway Analysis (IPA, QIAGEN[4]) for further functional analysis. Fisher's exact right-tailed test identified statistically significantly different [$-\log(P\text{-value}) \geq 1.3$] pathways or biological functions. Taken the change fold and direction of DEGs into account, an IPA *z*-score was computed to determine whether the pathway or biological functions were significantly activated or inhibited ($|z\text{-score}| \geq 2$). Network analysis was performed with selected biological functions and related genes to identify the crucial regulators.

Quantitative Real-Time PCR

Total RNA isolated from the liver and colon was reverse-transcribed to cDNA using a SuperScriptTM first-strand synthesis system for RT-PCR (Invitrogen, United States). Quantitative real-time PCR (qRT-PCR) was performed on a LightCycler96 (Roche, Switzerland) using iQ SYBR Green Supermix (BIO-RAD, United States). The relative expression of *Pparα*, *Pparγ*, *Alt* (gene encode alanine aminotransferase), and *Ast* (gene encode aspartate aminotransferase) were adjusted with Glyceraldehyde-3-phosphate dehydrogenase (*Gapdh*) as the housekeeping gene and then normalized to that in PreM group on the 2nd week. The primer sequences for qRT-PCR were as follows:

Pparα (F: 5′ AACATCGAGTGTCGAATATGTGG 3′, R: 5′ AGCCGAATAGTTCGCCGAAAG 3′);
Pparγ (F: 5′ TCGCTGATGCACTGCCTATG 3′, R: 5′ GA GAGGTCCACAGAGCTGATT 3′);
Alt (F: 5′ CTGCAGACCCGAACAACATA 3′, R: 5′ CAG CTCAGCGATGTCAAGAG 3′);
Ast (F: 5′ GCTGACTTCTTAGGGCGATG 3′, R: 5′ TCA TTCAGGAAACCCTGGAG 3′);
Gapdh (F: 5′ GTGTTCCTACCCCCAATGTGT 3′, R: 5′ AT TGTCATACCAGGAAATGAGCTT 3′).

Western Blot Analysis

Frozen pellets of liver and colon sample were homogenized in modified RIPA buffer (50 mmol/L Tris Base, 1% TritonX-100, 0.5% sodium deoxycholate, 0.1% sodium dodecyl sulfate (SDS), phosphatase inhibitor cocktail (Biotool, Houston, TX, United States), and protease inhibitor cocktail (Biotool,

[1]https://www.r-project.org/
[2]ftp://ftp.ensembl.org/pub/release-80/fasta/mus_musculus/dna/
[3]ftp://ftp.ensembl.org/pub/release-80/gtf/mus_musculus
[4]http://www.ingenuity.com

Houston, TX, United States). After centrifugation at 2000 × *g* for 25 min at 4°C, the resulting supernatant was collected. Aliquots (50,000 ng of protein) of the protein were separated through SDS-polyacrylamide gel electrophoresis and transferred to nitrocellulose filter membranes (ExCell Bio, Shanghai, China). Membranes were blocked with 5% (w/v) bull serum albumin (BSA; MP Biomedicals New Zealand Limited, New Zealand) in Tris-buffered saline containing 0.1% Tween 20 (TBS-T) and incubated with antibody in TBS-T containing 5% BSA and anti-rabbit PPARα or β-ACTIN antibody (1:1000; Abcam, Cambridge, United Kingdom). After incubation overnight, the membranes were washed with TBS-T and then incubated with anti-rabbit IgG secondary antibody (Gibco BRL, Gaithersburg, MD, United States) in 5% BSA in TBS-T. After the membranes were washed, the immune complexes were detected using a chemiluminescence system (LI-COR, Lincoln, NE, United States). Then PPARα immunoblots were quantified by densitometry analysis using ImageJ software against β-ACTIN as internal controls.

Immunohistochemistry

After deparaffinized and processed for antigen retrieval, the blank liver sections were incubated with anti-rabbit PPARα antibody (1:1000; Abcam, United States) for 37°C for 2 h. Then incubated with anti-rabbit IgG secondary antibody (KPL, Massachusetts, United States) for 30 min at room temperature. After washed by PBS, DAB Substrate kit (Solarbio, Beijing, China) was used to develop color. Images of each liver section were obtained tripartitely by experienced staff who was blinded to the experiment under 100 times magnification using Leica DMRBE microscope.

Statistical Analysis

Differences in the biochemical index and the distance of the gut microbiota between groups were assessed by the Mann-Whitney *U* test using GraphPad Prism 7 software. $P < 0.05$ was used to indicate significant differences. Other statistical analyses are described in the corresponding results section.

Sequence Data Accession Numbers

The 16S rRNA gene sequencing and hepatic transcriptome data have been submitted to the GenBank Sequence Read Archive database, with accession numbers of SRP132268 and SRP132325, respectively.

RESULTS

During our previous dietary intervention program of genetically obese children with PWS, we selected an eight-year-old boy (GD58) as the representative of the cohort for the subsequent gut microbiota transplantation experiment (Zhang et al., 2015). During the dietary intervention, this child showed substantial improvement of NAFLD and liver function, along with systemic alleviation of other obesity-related phenotypes (Supplementary Table S1). Meanwhile, the shift of the gut microbiota in this PWS child was concordant with that in the PWS cohort during the dietary intervention (Supplementary Figure S1). The fecal samples from this PWS donor were collected before (PreH) and after (PostH) dietary intervention and transplanted into GF mice which were named PreM and PostM groups, respectively.

Pre-intervention Gut Microbiota Induces Hepatic Steatosis in Recipient Mice Fed on Normal Chow Diet

To evaluate the effect of human genetic obesity-associated gut microbiota on host hepatic lipid metabolism, we assessed the lipid concentration and fat accumulation in the liver of the gnotobiotic mice. Hematoxylin and eosin staining of mouse liver sections showed that both groups exhibited normal liver histology 2 weeks after transplantation (**Figures 1A,B**). However, PreM group showed a higher level of serum LBP on the 2nd week (**Figure 1F**), reflecting a higher level of endotoxemia. The increased SAA on the 2nd week (**Figure 1G**) also suggested a higher level of systemic inflammation in PreM group compared with PostM group. During the following 2 weeks, PreM group developed liver macrovesicular steatosis, while PostM group remained normal morphology (**Figure 1A**). The steatosis score was significantly higher in PreM group than that in PostM group on the 4th week (**Figure 1B**). Accordingly, the concentrations of hepatic triglyceride and total cholesterol of PreM group were significantly higher than PostM group on the 4th week (**Figures 1C,D**), so is the serum triglyceride (Supplementary Figure S2). The expression of *Ast*, which encode aspartate aminotransferase, was significantly higher in PreM group compared to PostM group on the 4th week, while the expression of *Alt*, which encode alanine aminotransferase, showed no difference between groups (Supplementary Figure S3), indicating the heavier liver function in PreM group. Meanwhile, the concentration of leptin, which is an adipocytokine, was also significantly higher in PreM group on the 4th week (**Figure 1E**). These results suggested that the pre-intervention gut microbiota induced a higher level of bacterial stimuli and subsequently increased hepatic lipid concentration and accumulation in gnotobiotic mice.

The Gut Microbiota of Recipient Mice Was More Similar to Their Respective Donor

The gut microbiota of the human donor (PreH and PostH) and mice recipients (PreM and PostM) were profiled by sequencing of the bacterial 16S rRNA gene V3 region on Ion Torrent PGM System. On average, each sample obtained 20,727 ± 5173 high-quality reads. The high-quality reads were then delineated into 1123 OTUs at the similarity cutoff of 97% (Supplementary Table S2). PCoA analysis of weighted UniFrac distances based on OTUs revealed a clear separation of gut microbiota between PreM and PostM groups as well as the PreH and PostH groups on the first principal coordinate (PC1, accounting for 73.4% of the total variance) (**Figure 2A**). Multivariate analysis of variance analysis derived from PCoA scores confirmed a statistically significant (p-value < 0.001) separation of PreM and PostM group. Gut microbiota in each group showed little changes over time,

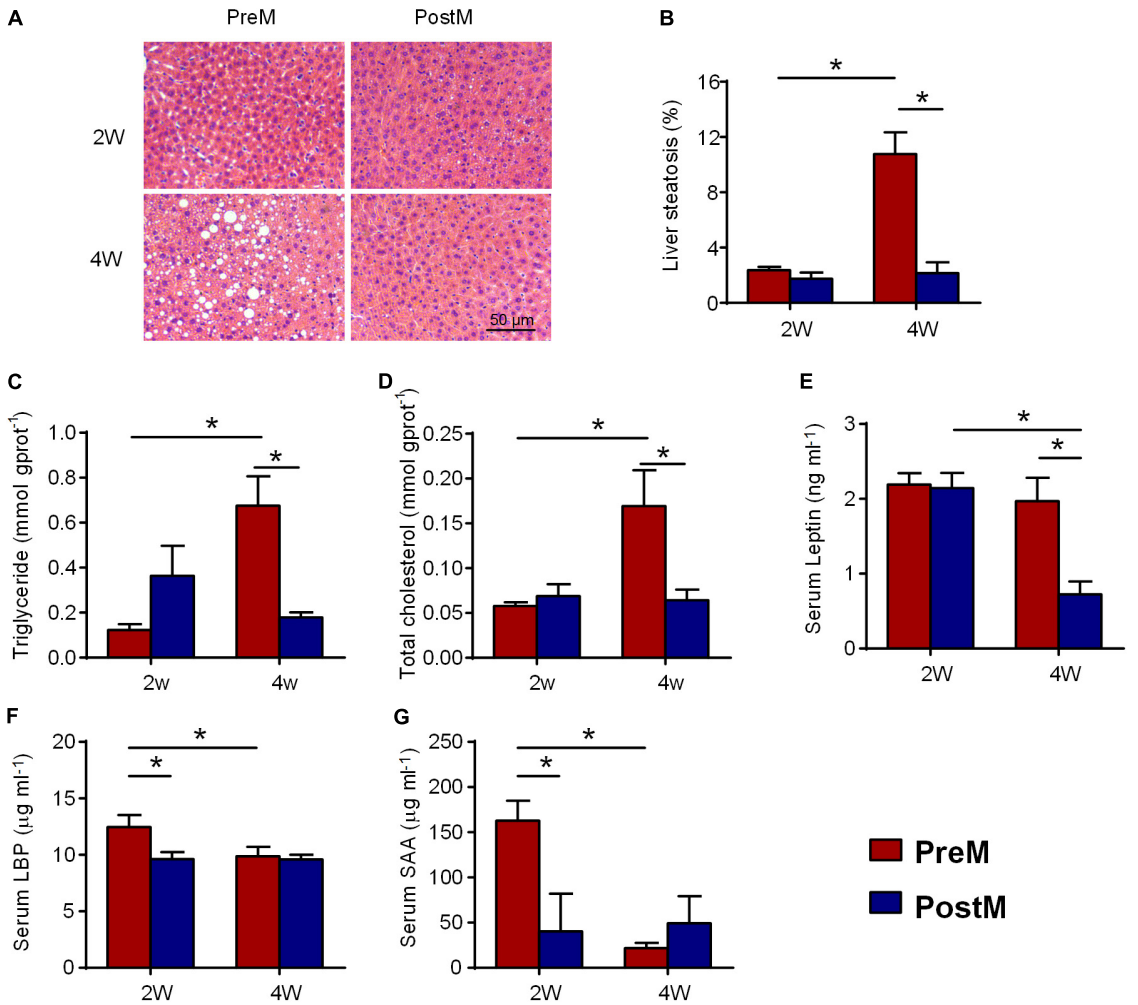

FIGURE 1 | PreM group showed increased lipid concentration and fat accumulation in liver after transplantation for 4 weeks; **(A)** Representative photomicrographs of hematoxylin- and eosin-stained sections of the liver (100× magnification); **(B)** bar graph of the volume density of liver steatosis; **(C)** hepatic triglyceride; **(D)** hepatic total cholesterol; **(E)** serum leptin; **(F)** serum LBP; and **(G)** serum SAA levels. Data are shown as the mean ± SEM and were compared between groups and time points using the Mann–Whitney *U* test; $^*P < 0.05$. $n = 4$ or 5 for each group. LBP, lipopolysaccharide binding protein; SAA, serum amyloid A protein.

indicating the gut microbiota kept stable after transplantation (**Figure 2B**). The gut microbiota of the donor and recipients were mainly distributed on PC2 (accounting for 8.7% of the total variance), reflecting the selectivity of the microbiota during the transplantation from the human to the mice (**Figure 2A**). The weighted UniFrac distance between the gut microbiota of the donor and recipients further revealed that each recipient group was more similar to their own donor (**Figure 2C** and Supplementary Figure S4). Nevertheless, decreased diversity and richness of gut microbiota in the PostH group were also recurred in PostM group, as measured by the Shannon index and the number of OTUs (**Figures 2D,E**).

Using a random forest model, 45 OTUs were picked out as discriminating features between PreM and PostM groups (Supplementary Figure S5 and Supplementary Table S2). These key OTUs accounts for 52.8% of the abundance of all the OTUs. Through the abundance pairwise comparisons of these OTUs between the donor (axis *X*) and recipients (axis *Y*) (**Figure 2F**), 38 OTUs showed consistent abundance variation between different groups in the donor and recipients. Six OTUs in the first quartile, including OTUs from *Bifidobacterium* and *Lactobacillus*, were less abundant in PreM group as in PreH. 32 OTUs in the third quartile were more abundant in PreM group as in PreH, while almost diminished in PostM group as in PostH, which are primarily belonged to Bacteroidetes (e.g., *Bacteroides* and *Parabacteroides*) and Firmicutes (e.g., *Ruminococcus*), as well as one belonged to Proteobacteria (*Bilophila*) (**Figures 2F,G**).

Meanwhile, the microbial fermentation products, short-chain fatty acids (SCFAs), showed a lower ratio of acetate and a higher ratio of propionate in PreM group as in PreH donor, compared with PostM group and PostH donor (**Figures 2H–J**). So, on the whole structure, bacteria species and bacterial product level of the gut microbiota, our results showed that the major features of

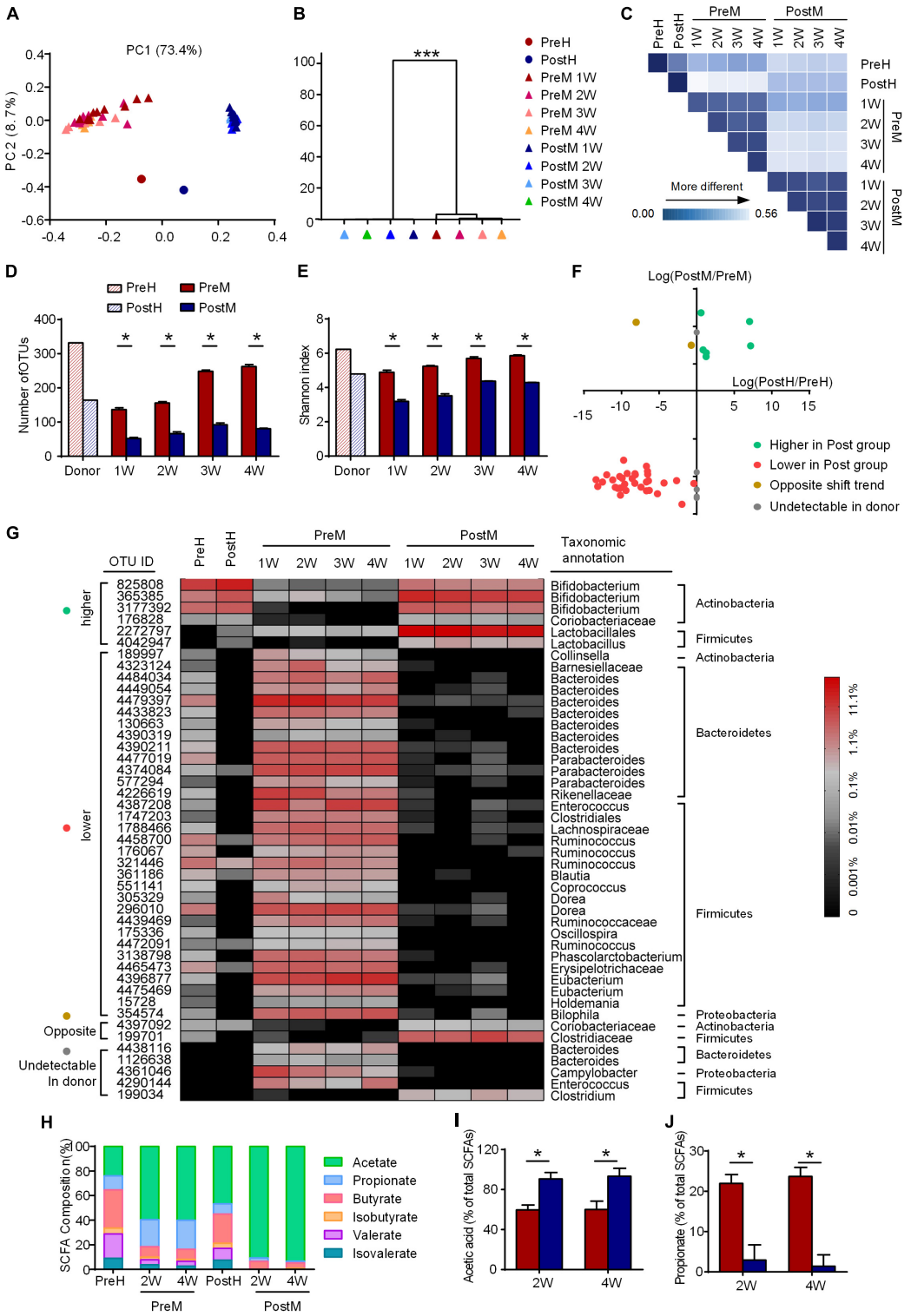

FIGURE 2 | The features of gut microbiota are transferrable from the human donor to the GF mice. **(A)** Weighted UniFrac PCoA plot and **(B)** multivariate analysis of variance analysis of gut microbiota based on OTUs, ***$P < 0.001$; **(C)** weighted UniFrac distances of gut microbiota between the donor and recipients; **(D)** OTU richness; **(E)** Shannon index; **(F)** abundance variation of 45 discriminatory OTUs in the donor and recipients; **(G)** heat map of 45 discriminatory OTUs, with the color of the spot corresponding to the normalized and log-transformed relative abundance; **(H)** the composition of SCFA in feces of donor and the cecum of the recipients; **(I)** relative concentrations of acetate; and **(J)** relative concentrations of propionate. For the recipient groups, $n = 9$ on the 1st and 2nd week; $n = 4$ or 5 on the 3rd and 4th week. In **D,E,I**, and **J**, data are shown as the mean ± SEM and were compared between groups using the Mann–Whitney U test. *$P < 0.05$. PC, principal coordinate; OTU, operational taxonomic unit; SCFA, short chain fatty acid.

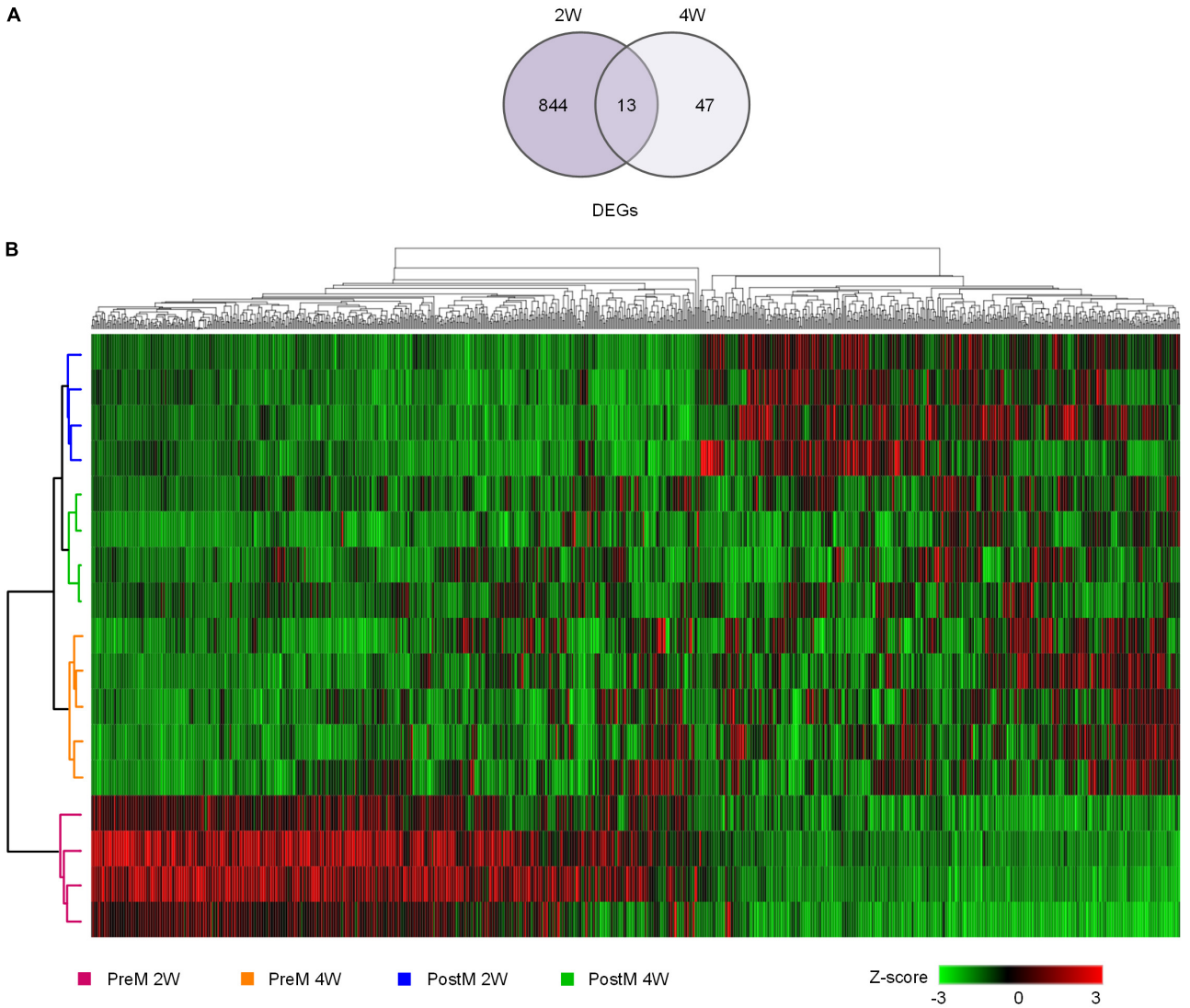

FIGURE 3 | The expression pattern of DEGs in the liver of gnotobiotic mice over time. **(A)** Venn diagrams of the DEGs between the two groups on week two and week four determined by Deseq2 with the standard of |log2FoldChange| ≥ 1; **(B)** hierarchical clustering of all the DEGs, with the color of the spot corresponding to the normalized and *z*-score transformed relative abundance. *n* = 4 or 5 for each group. DEGs, differentially expressed genes.

the gut microbiota were transferrable from the PWS donor to the recipient mice.

Pre-intervention Gut Microbiota Induces a Steatosis-Prone Transcriptional Program

To explore the biological process and mechanism underlying the development of liver steatosis mediated by gut microbiota, the hepatic transcriptional response in the recipient mice was monitored by mRNA sequencing on the 2nd and 4th week after transplantation. Deseq2 was used to identify DEGs between the two groups (|Log2(foldchange)| > 1). In total, 857 DEGs were identified on the 2nd week, while only 60 DEGs were identified on the 4th week (**Figure 3A**). All the DEGs (904 genes in total) were hierarchically clustered and revealed that hepatic gene expression patterns in PreM group on the 2nd week were distinct from those of other groups (**Figure 3B**), indicating that pre-intervention gut microbiota induced a specific disturbance on the transcriptional level in the liver of gnotobiotic mice after colonization for 2 weeks.

We then interpreted the data using IPA (QIAGEN see footnote 4) based on the comprehensive, manually curated content of the Ingenuity Knowledge Base. All the DEGs were input into the IPA software to identify statistically significantly different (calculated by Fisher's exact test, right-tailed, *P*-value < 0.05) and biologically significantly modulated (using an algorithm to predict the direction of change, *z*-score ≥ 2 for suppression and *z*-score ≤ −2 for activation in PreM compared to PostM group) biological functions and pathways between the two groups.

On the 2nd week, over 500 biological functions mainly related with small molecule biochemistry, lipid metabolism and molecular transport were significantly enriched (Supplementary Table S3), therein, 24 of which showed a significantly activated or suppressed state between PreM and PostM groups (**Figure 4**). Most notably, in PreM group, functions related to lipid catabolism including oxidation of fatty acid, oxidation of lipid and fatty acid metabolism were significantly repressed. While functions related to lipid anabolism, including absorption of lipid, uptake of cholesterol and synthesis of steroid were significantly activated. Two functions related to lipid transport, i.e., quantity of HDL cholesterol and protein lipid complex in blood, were also significantly repressed by the pre-intervention gut microbiota. The functions of alpha-amino acid and L-amino acid synthesis were significantly repressed in PreM group reflecting a decreased level of amino acid anabolism. Meanwhile, functions related to oxidative stress and apoptosis were significantly activated in PreM group. Additionally, the functions related to adaptive immune responses (i.e., biological function "quantity of T lymphocytes and regulatory T lymphocytes") were also significantly activated in PreM group.

We further identified 71 pathways that were significantly enriched between PreM and PostM group on the second week using IPA (Supplementary Table S4). These pathways were involved in various biological processes, including metabolism, signal transduction, and immune response. Of these 71 pathways, four were significantly activated or repressed between the two groups (**Table 1**). The PPARα/RXRα activation pathway was significantly suppressed in PreM group. Meanwhile, the PI3K/AKT signaling pathway and two pathways related to coagulation (extrinsic prothrombin activation and coagulation system pathway) were significantly activated in PreM group.

No function or pathway was significantly repressed or activated between the two groups 4 weeks after transplantation, indicating that the difference on the transcriptional level between PreM and PostM groups got diminished along with time. Taken together, the results indicate that before the pathology of steatosis was diagnosed, the pre-intervention gut microbiota induced a foregoing pro-steatotic transcriptional pattern in the liver of gnotobiotic mice.

TABLE 1 | Significantly repressed or activated pathways in liver between the two groups on the second week.

No.	Ingenuity Canonical Pathways	*z*-score*	−log (*P*-value)	Molecules
1	PPARα/RXRα activation	2	1.73	10
2	Extrinsic prothrombin activation	−2	3.20	4
3	Coagulation system	−2.24	2.71	5
4	PI3K/AKT signaling	−2.45	1.38	7

**z-scores ≥ 2 represent significantly repressed functions, while z-scores ≤ −2 represent significantly activated functions in PreM group compared to PostM group.*

PPARα May Play a Crucial Role in Regulating Hepatic Transcriptional Profile of Lipid Metabolism in Gnotobiotic Mice

The six significantly modulated lipid metabolism functions associated with 53 DEGs, which all differed on the 2nd week, and only one (fatty acid binding protein 1, FABP1) remained different until the 4th week (Supplementary Table S5). We then profiled the lipid metabolism network of the functions and DEGs using IPA (**Figure 5A**). Genes encoding crucial enzymes in lipid catabolism, especially lipid beta-oxidation, were down-regulated in PreM group, such as patatin-like phospholipase domain containing 2 (*Pnpla2*), acyl-CoA synthetase long-chain family member 1 (*Acsl1*) and enoyl CoA hydratase, short chain, 1 (*Echs1*). Meanwhile, the expression of genes involved in lipid binding and transport, such as fatty acid binding protein 1 (*Fabp1*), apolipoprotein A1 (*Apoa1*), apolipoprotein A4 (*Apoa4*), and apolipoprotein E (*Apoe*), was also decreased in PreM group.

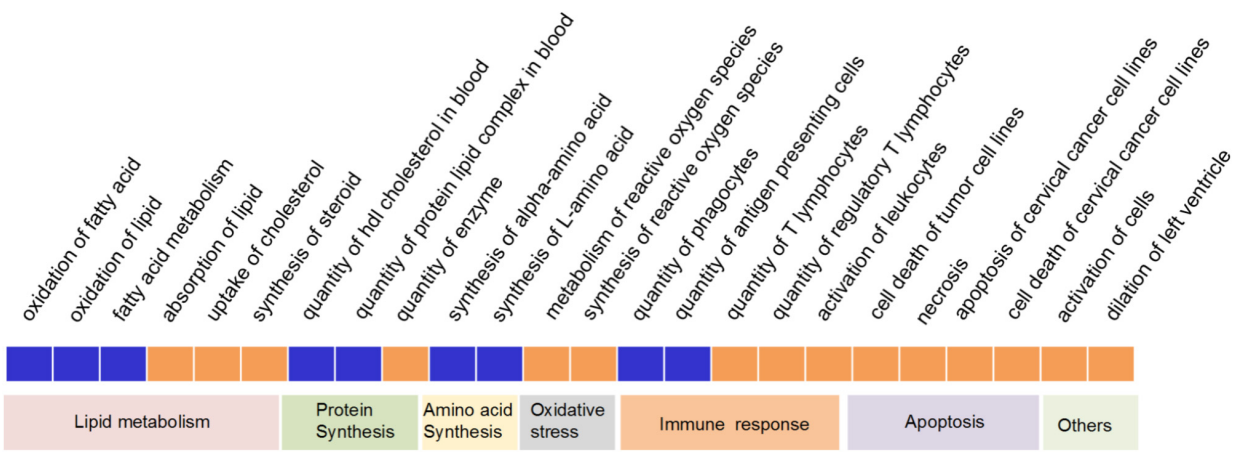

FIGURE 4 | Significantly repressed or activated functions in the liver of gnotobiotic mice on the 2nd week based on IPA. Blue represent significantly repressed functions (*z*-score ≥ 2), while red represent significantly activated (*z*-score ≤ −2) functions in PreM group compared to PostM group.

In contrast, genes involved in lipid absorption, steroids, and cholesterol metabolism, such as cytochrome P450 family 7 subfamily A member 1 (*Cyp7a1*), cytochrome P450 family 8 subfamily B member 1 (*Cyp8b1*), scavenger receptor class B member 1 (*Scarb1*), and adenylate cyclase type 10 (*Adcy10*), were up-regulated in PreM group (**Figure 5A**).

Notably, PPARα contributed to all the significantly modulated functions in the network (**Figure 5A**). PPARα is a transcriptional factor that plays a crucial role in lipid metabolism by directly inducing the expression of downstream genes (Pawlak et al., 2015). Seventeen of the 53 DEGs in the lipid metabolism network could be targeted by PPARα (Supplementary Figure S6). The suppression of *Pparα* contributed to the suppression of genes related to lipid catabolism, such as *Acsl1*, *Apoa1*, *Apoa4*, *Apoae*, and *Fabp1*, and the activation of *Cyp7a1* as predicted in the network. As verified by quantitative real-time PCR, the expression of *Pparα* was significantly suppressed not only in the liver but also in the colon of PreM group on the 2nd week compared to PostM group (**Figures 5B,C**). Western blot and immunohistochemical analysis also indicated a suppression of PPARα on protein level in PreM group compared to PostM group (**Figure 5D** and Supplementary Figures S7 and S8). Whereas, the expression of another key modulator of lipid metabolism in PPARs family – *Pparγ* showed no difference between two group on both 2nd and 4th week (Supplementary Figure S9). Our results indicates that the suppression of PPARα may play a regulating role contributing to the pro-steatotic transcriptional profile in PreM group.

DISCUSSION

In previous study, we showed that genetically obese children with PWS showed significantly improved liver functions after they have lost substantial amount of body weight on a dietary program targeting the gut microbiota [11]. In the current study, we showed that the baseline (pre-intervention) gut microbiota from one genetically obese child with PWS induced liver steatosis in GF mice fed on normal chow diet, while the gut microbiota from the same donor after the dietary intervention did not induce this early form of NAFLD.

Germ-free mice is considered as a powerful animal model to demonstrate the causal role of gut microbiota in the development of many metabolic diseases (Turnbaugh et al., 2009; Faith et al., 2014). Previous studies usually studied the contribution of gut microbiota to human disease using gnotobiotic animal model established through the conventionalization of GF animal by gut microbiota from disease or healthy control individuals (Ridaura et al., 2013; Llopis et al., 2016; Nagao-Kitamoto et al., 2016). However, the configurations of gut microbiota which could be affected by genetic and environmental variables vary substantially among individuals (Human Microbiome Project Consortium, 2012), which may confound the phenotype-associated microbial features. In our study, GF mice were conventionalized by gut microbiota from one PWS child before and after a dietary intervention, which significantly alleviated his obesity-related phenotypes. The comparison of gnotobiotic mice associated with gut microbiota from the same individual but having a distinct metabolic phenotype could minimize the individual-related variations, therefore, providing an opportunity to reveal the interaction between the host and gut microbiota which is more relevant with the metabolic phenotypes. More importantly, the liver steatosis observed in the GF mice receiving baseline gut microbiota from the PWS child was independent of diet, the major environmental factor to induce NAFLD. In this case, the baseline pre-intervention gut microbiota from the PWS donor is the only driver of liver steatosis in the gnotobiotic mice.

Microbiome-wide association studies make it possible to discover the disease-modulating microbes (Qin et al., 2010). Recently, Surana and Kasper (2017) proposed a microbe-phenotype triangulation to narrow the scope of the causal microbes, which is persistently correlated with defined phenotypes under different conditions. Given the reproducibility of the obesity-related phenotype in GF mice from the human PWS donor, the transferrable configurations of gut microbiota have a high probability acting as contributors causally associated with the metabolic phenotype in mice, which could also be implicated in the PWS donor. Through the metagenomics analysis in our previous cohort study, we found that co-abundance gene groups identified as *Bacteroides*, *Parabacteroides*, and *Ruminococcus* were abundant in the PWS cohort before diet intervention and regarded as potential pathogens on account of their genetic potential to produce toxic co-metabolites such as trimethylamine N-oxide and indoxyl sulfate (Zhang et al., 2015). The higher abundance of these OTUs may have exerted the same deteriorating effect in PreM group. Another abundant OTU in PreM group belongs to *Bilophila*, an opportunistic pathogen that has been correlated with many human inflammatory diseases (Baron et al., 1989; Feng et al., 2017). Bacteria from *Bifidobacterium* and *Lactobacillus* are generally regarded as beneficial, which have been reported having the capacity to attenuate weight gain and hepatic steatosis (Reichold et al., 2014; Wang et al., 2015). Furthermore, *Bifidobacterium* and its fermented product acetate have been reported having an inhibitory effect on many species of detrimental bacteria (Lievin et al., 2000; Fooks and Gibson, 2002). The higher level of the relative concentration of acetate among SCFAs and *Bifidobacterium* may have contributed to the decrease of the potential pathogenic bacteria in PostM group. These bacteria are highly indicated as functional bacteria relevant with host metabolic phenotypes. Functional validation and the underlying mechanism of these phenotype-associated bacteria should be further investigated.

The conventionalization of GF mice has been reported to induce metabolic reorientation and immune responses by process in both liver and intestine (Claus et al., 2011; El Aidy et al., 2012, 2013). PPARα serves as a crucial regulator of lipid metabolism in liver, while its deficiency can induce liver steatosis (Akiyama et al., 2001; Kersten and Stienstra, 2017). GF mice showed significantly higher expression of PPARα in the liver and intestine compared to conventionalized mice, indicating the expression of PPARα in peripheral tissues could be affected by the commensal bacteria in gut (El Aidy et al., 2013; Selwyn et al., 2015). Notably, LPS, a constituent of the outer membrane of gram-negative bacteria,

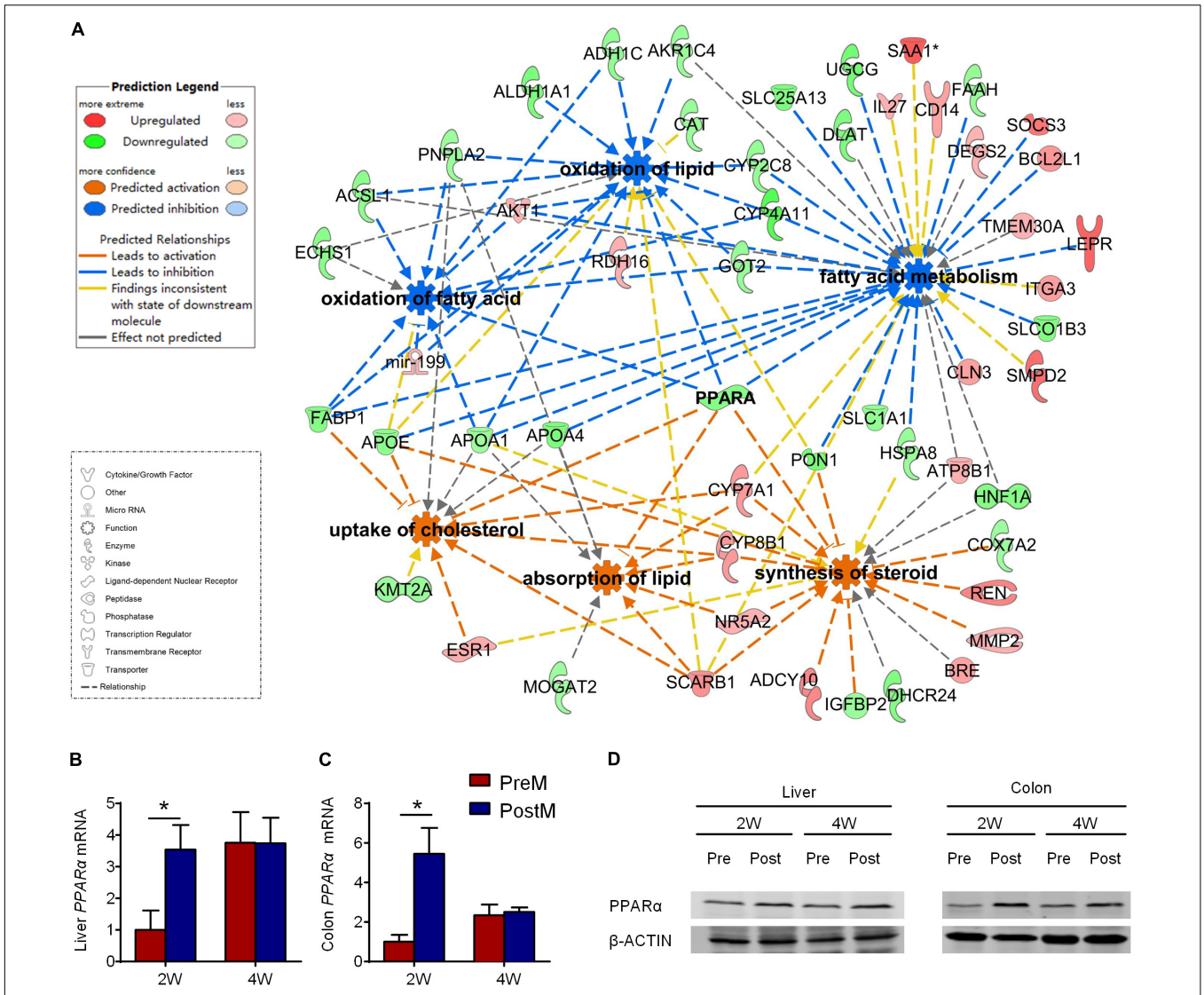

FIGURE 5 | The hepatic transcriptional profile of lipid metabolism in gnotobiotic mice. **(A)** IPA ingenuity interaction network of six significantly modulated biological functions (circle with eight arises) and 53 DEGs (configuration corresponding to the type of gene product as showed in the lower figure legend) related to lipid metabolism in liver on the 2nd week. As showed in the upper legend, DEGs with red color represent for upregulated while green color represent for downregulated in PreM group compared to PostM group, biological functions with blue color are predicted to be significantly repressed, while orange color are predicted to be significantly activated in PreM group compared to PostM group. Lines represent the relationship between the biological functions and DEGs. **(B)** RT-PCR of *pparα* expression in liver. **(C)** RT-PCR of *pparα* expression in colon. The relative expression of *Pparα* was adjusted with *Gapdh* as the housekeeping gene. **(D)** Western blot of PPARα and β-ACTIN in liver and colon. Data are shown as the mean ± SEM and were analyzed by the Mann–Whitney *U* test between groups; $^*P < 0.05$. $n = 4$ or 5 for each group. The details of the DEGs refer to Supplementary Table S5.

exhibits the capability to repress the hepatic expression of PPARα (Beigneux et al., 2000). In our study, the increased level of serum LBP and the higher hepatic expression of the membrane receptors of LPS, *Cd14* and *Tlr4* (Zhang et al., 2015), reflected a higher level of serum LPS in PreM group, which may have contributed to the suppression of PPARα in liver. On the contrary, prebiotic or probiotic treatment could increase the PPARα expression in liver (Pachikian et al., 2013; Mei et al., 2015). Meanwhile, acetate, the product of many probiotics, may significantly increase the hepatic expression of PPARα and its downstream genes related to fatty acid oxidation (Kondo et al., 2009). In the current study, the acetate concentration and the abundance of its producer were both significantly higher in PostM group. These results indicate that the suppression of hepatic expression of PPARα by pre-intervention gut microbiota may be due to the increased production of LPS and the decreased production of acetate. Our results also indicated a time-resolved hepatic transcriptional response mediated by gut microbiota and a delayed development "catching up" of liver steatosis. This temporal order of events from microbiota-induced gene expression changes in liver lipid metabolism to the actual manifestation of liver steatosis strongly implicates a causative role of gut microbiota in NAFLD.

SUMMARY

The effect of gut microbiota in the development of obesity and NAFLD has been widely realized. The current study show that the gut microbiota from a genetically obese human could promote the onset of liver steatosis in mice independent from diet and genetic factors. Our result also give a comprehensive profile of hepatic lipid metabolism and suggested that PPARα may be the key regulator in the gut microbiota induced hepatic steatosis. The plasticity of gut microbiota makes it a potentially preventive and therapeutic target of NAFLD and other metabolic diseases.

AUTHOR CONTRIBUTIONS

RW, CZ, and LZ conceived the project, designed the experiments, and wrote the manuscript. RW, XY, and XX performed and analyzed the animal experiments. RW carried out the gut microbiome analysis. HL, RW, LD, and MZ established the RNA sequencing analysis pipeline and carried out the analysis. RW and JS prepared the fecal suspension for the transplantation experiment. All authors commented on and approved the manuscript.

FUNDING

This work was supported by grants from the National Natural Science Foundation of China (Grant Nos. 31330005 and 81401141) and the Science and Technology Commission of Shanghai Municipality (Grant No. 14YF1402200). A computing facility award on the PI cluster at Shanghai Jiao Tong University is acknowledged.

SUPPLEMENTARY MATERIAL

The Supplementary Material for this article can be found online at: https://www.frontiersin.org/articles/10.3389/fmicb.2018.01602/full#supplementary-material

REFERENCES

Akiyama, T. E., Nicol, C. J., Fievet, C., Staels, B., Ward, J. M., Auwerx, J., et al. (2001). Peroxisome proliferator-activated receptor-alpha regulates lipid homeostasis, but is not associated with obesity: studies with congenic mouse lines. *J. Biol. Chem.* 276, 39088–39093. doi: 10.1074/jbc.M107073200

Anders, S., Pyl, P. T., and Huber, W. (2015). HTSeq–a Python framework to work with high-throughput sequencing data. *Bioinformatics* 31, 166–169. doi: 10.1093/bioinformatics/btu638

Backhed, F., Ding, H., Wang, T., Hooper, L. V., Koh, G. Y., Nagy, A., et al. (2004). The gut microbiota as an environmental factor that regulates fat storage. *Proc. Natl. Acad. Sci. U.S.A.* 101, 15718–15723. doi: 10.1073/pnas.0407076101

Backhed, F., Manchester, J. K., Semenkovich, C. F., and Gordon, J. I. (2007). Mechanisms underlying the resistance to diet-induced obesity in germ-free mice. *Proc. Natl. Acad. Sci. U.S.A.* 104, 979–984. doi: 10.1073/pnas.0605374104

Baron, E. J., Summanen, P., Downes, J., Roberts, M. C., Wexler, H., and Finegold, S. M. (1989). *Bilophila wadsworthia*, gen. nov. and sp. nov., a unique gram-negative anaerobic rod recovered from appendicitis specimens and human faeces. *J. Gen. Microbiol.* 135, 3405–3411. doi: 10.1099/00221287-135-12-3405

Bashiardes, S., Shapiro, H., Rozin, S., Shibolet, O., and Elinav, E. (2016). Non-alcoholic fatty liver and the gut microbiota. *Mol. Metab.* 5, 782–794. doi: 10.1016/j.molmet.2016.06.003

Bedogni, G., Miglioli, L., Masutti, F., Tiribelli, C., Marchesini, G., and Bellentani, S. (2005). Prevalence of and risk factors for nonalcoholic fatty liver disease: the dionysos nutrition and liver study. *Hepatology* 42, 44–52. doi: 10.1002/hep.20734

Beigneux, A. P., Moser, A. H., Shigenaga, J. K., Grunfeld, C., and Feingold, K. R. (2000). The acute phase response is associated with retinoid X receptor repression in rodent liver. *J. Biol. Chem.* 275, 16390–16399. doi: 10.1074/jbc.M000953200

Boursier, J., Mueller, O., Barret, M., Machado, M., Fizanne, L., Araujo-Perez, F., et al. (2016). The severity of nonalcoholic fatty liver disease is associated with gut dysbiosis and shift in the metabolic function of the gut microbiota. *Hepatology* 63, 764–775. doi: 10.1002/hep.28356

Breiman, L. (2001). Random forests. *Mach. Learn.* 45, 5–32. doi: 10.1023/a:1010933404324

Butler, M. G. (2011). Prader-Willi syndrome: obesity due to genomic imprinting. *Curr. Genomics* 12, 204–215. doi: 10.2174/138920211795677877

Caporaso, J. G., Kuczynski, J., Stombaugh, J., Bittinger, K., Bushman, F. D., Costello, E. K., et al. (2010). QIIME allows analysis of high-throughput community sequencing data. *Nat. Methods* 7, 335–336. doi: 10.1038/nmeth.f.303

Catta-Preta, M., Mendonca, L. S., Fraulob-Aquino, J., Aguila, M. B., and Mandarim-de-Lacerda, C. A. (2011). A critical analysis of three quantitative methods of assessment of hepatic steatosis in liver biopsies. *Virchows Arch.* 459, 477–485. doi: 10.1007/s00428-011-1147-1

Claus, S. P., Ellero, S. L., Berger, B., Krause, L., Bruttin, A., Molina, J., et al. (2011). Colonization-induced host-gut microbial metabolic interaction. *mBio* 2:e00271-10. doi: 10.1128/mBio.00271-10

Dodt, M., Roehr, J. T., Ahmed, R., and Dieterich, C. (2012). FLEXBAR-Flexible Barcode and adapter processing for next-generation sequencing platforms. *Biology* 1, 895–905. doi: 10.3390/biology1030895

Duca, F. A., Sakar, Y., Lepage, P., Devime, F., Langelier, B., Dore, J., et al. (2014). Replication of obesity and associated signaling pathways through transfer of microbiota from obese-prone rats. *Diabetes Metab. Res. Rev.* 63, 1624–1636. doi: 10.2337/db13-1526

El Aidy, S., Merrifield, C. A., Derrien, M., van Baarlen, P., Hooiveld, G., Levenez, F., et al. (2013). The gut microbiota elicits a profound metabolic reorientation in the mouse jejunal mucosa during conventionalisation. *Gut* 62, 1306–1314. doi: 10.1136/gutjnl-2011-301955

El Aidy, S., van Baarlen, P., Derrien, M., Lindenbergh-Kortleve, D. J., Hooiveld, G., Levenez, F., et al. (2012). Temporal and spatial interplay of microbiota and intestinal mucosa drive establishment of immune homeostasis in conventionalized mice. *Mucosal Immunol.* 5, 567–579. doi: 10.1038/mi.2012.32

Faith, J. J., Ahern, P. P., Ridaura, V. K., Cheng, J., and Gordon, J. I. (2014). Identifying gut microbe-host phenotype relationships using combinatorial communities in gnotobiotic mice. *Sci. Transl. Med.* 6:220ra11. doi: 10.1126/scitranslmed.3008051

Feng, Z., Long, W., Hao, B., Ding, D., Ma, X., Zhao, L., et al. (2017). A human stool-derived *Bilophila wadsworthia* strain caused systemic inflammation in specific-pathogen-free mice. *Gut Pathog.* 9, 59–68. doi: 10.1186/s13099-017-0208-7

Fooks, L. J., and Gibson, G. R. (2002). Probiotics as modulators of the gut flora. *Br. J. Nutr.* 88(Suppl. 1), S39–S49. doi: 10.1079/bjn2002628

Godon, J. J., Zumstein, E., Dabert, P., Habouzit, F., and Moletta, R. (1997). Molecular microbial diversity of an anaerobic digestor as determined by small-subunit rDNA sequence analysis. *Appl. Environ. Microbiol.* 63, 2802–2813.

Human Microbiome Project Consortium (2012). Structure, function and diversity of the healthy human microbiome. *Nature* 486, 207–214. doi: 10.1038/nature11234

Kersten, S., and Stienstra, R. (2017). The role and regulation of the peroxisome proliferator activated receptor alpha in human liver. *Biochimie* 136, 75–84. doi: 10.1016/j.biochi.2016.12.019

Kim, D., Langmead, B., and Salzberg, S. L. (2015). HISAT: a fast spliced aligner with low memory requirements. *Nat. Methods* 12, 357–360. doi: 10.1038/nmeth.3317

Kondo, T., Kishi, M., Fushimi, T., and Kaga, T. (2009). Acetic acid upregulates the expression of genes for fatty acid oxidation enzymes in liver to suppress body fat accumulation. *J. Agric. Food Chem.* 57, 5982–5986. doi: 10.1021/jf900470c

Le Roy, T., Llopis, M., Lepage, P., Bruneau, A., Rabot, S., Bevilacqua, C., et al. (2012). Intestinal microbiota determines development of non-alcoholic fatty liver disease in mice. *Gut* 62, 1787–1794. doi: 10.1136/gutjnl-2012-303816

Lievin, V., Peiffer, I., Hudault, S., Rochat, F., Brassart, D., Neeser, J. R., et al. (2000). Bifidobacterium strains from resident infant human gastrointestinal microflora exert antimicrobial activity. *Gut* 47, 646–652. doi: 10.1136/gut.47.5.646

Llopis, M., Cassard, A. M., Wrzosek, L., Boschat, L., Bruneau, A., Ferrere, G., et al. (2016). Intestinal microbiota contributes to individual susceptibility to alcoholic liver disease. *Gut* 65, 830–839. doi: 10.1136/gutjnl-2015-310585

Love, M. I., Huber, W., and Anders, S. (2014). Moderated estimation of fold change and dispersion for RNA-seq data with DESeq2. *Genome Biol.* 15:550. doi: 10.1186/s13059-014-0550-8

Mei, L., Tang, Y., Li, M., Yang, P., Liu, Z., Yuan, J., et al. (2015). Co-Administration of cholesterol-lowering probiotics and anthraquinone from *Cassia obtusifolia* L. *PLoS One* 10:e0138078. doi: 10.1371/journal.pone.0138078

Milani, C., Hevia, A., Foroni, E., Duranti, S., Turroni, F., Lugli, G. A., et al. (2013). Assessing the fecal microbiota: an optimized ion torrent 16S rRNA gene-based analysis protocol. *PLoS One* 8:e68739. doi: 10.1371/journal.pone.0068739

Murakami, M., Tognini, P., Liu, Y., Eckel-Mahan, K. L., Baldi, P., and Sassone-Corsi, P. (2016). Gut microbiota directs PPARgamma-driven reprogramming of the liver circadian clock by nutritional challenge. *EMBO Rep.* 17, 1292–1303. doi: 10.15252/embr.201642463

Nagao-Kitamoto, H., Shreiner, A. B., Gillilland, M. G., Kitamoto, S., Ishii, C., Hirayama, A., et al. (2016). Functional characterization of inflammatory bowel disease-associated gut dysbiosis in gnotobiotic mice. *Cell. Mol. Gastroenterol. Hepatol.* 2, 468–481. doi: 10.1016/j.jcmgh.2016.02.003

Pachikian, B. D., Essaghir, A., Demoulin, J. B., Catry, E., Neyrinck, A. M., Dewulf, E. M., et al. (2013). Prebiotic approach alleviates hepatic steatosis: implication of fatty acid oxidative and cholesterol synthesis pathways. *Mol. Nutr. Food Res.* 57, 347–359. doi: 10.1002/mnfr.201200364

Pawlak, M., Lefebvre, P., and Staels, B. (2015). Molecular mechanism of PPARalpha action and its impact on lipid metabolism, inflammation and fibrosis in non-alcoholic fatty liver disease. *J. Hepatol.* 62, 720–733. doi: 10.1016/j.jhep.2014.10.039

Petta, S., Gastaldelli, A., Rebelos, E., Bugianesi, E., Messa, P., Miele, L., et al. (2016). Pathophysiology of non alcoholic fatty liver disease. *Int. J. Mol. Sci.* 17, 2082–2107. doi: 10.3390/ijms17122082

Qin, J., Li, R., Raes, J., Arumugam, M., Burgdorf, K. S., Manichanh, C., et al. (2010). A human gut microbial gene catalogue established by metagenomic sequencing. *Nature* 464, 59–65. doi: 10.1038/nature08821

Reichold, A., Brenner, S. A., Spruss, A., Forster-Fromme, K., Bergheim, I., and Bischoff, S. C. (2014). *Bifidobacterium adolescentis* protects from the development of nonalcoholic steatohepatitis in a mouse model. *J. Nutr. Biochem.* 25, 118–125. doi: 10.1016/j.jnutbio.2013.09.011

Ridaura, V. K., Faith, J. J., Rey, F. E., Cheng, J., Duncan, A. E., Kau, A. L., et al. (2013). Gut microbiota from twins discordant for obesity modulate metabolism in mice. *Science* 341:1241214. doi: 10.1126/science.1241214

Schmieder, R., and Edwards, R. (2011). Quality control and preprocessing of metagenomic datasets. *Bioinformatics* 27, 863–864. doi: 10.1093/bioinformatics/btr026

Selwyn, F. P., Cheng, S. L., Bammler, T. K., Prasad, B., Vrana, M., Klaassen, C., et al. (2015). Developmental regulation of drug-processing genes in livers of germ-free mice. *Toxicol. Sci.* 147, 84–103. doi: 10.1093/toxsci/kfv110

Surana, N. K., and Kasper, D. L. (2017). Moving beyond microbiome-wide associations to causal microbe identification. *Nature* 552, 244–247. doi: 10.1038/nature25019

Turnbaugh, P. J., Ridaura, V. K., Faith, J. J., Rey, F. E., Knight, R., and Gordon, J. I. (2009). The effect of diet on the human gut microbiome: a metagenomic analysis in humanized gnotobiotic mice. *Sci. Transl. Med.* 1:6ra14. doi: 10.1126/scitranslmed.3000322

Wang, J., Tang, H., Zhang, C., Zhao, Y., Derrien, M., Rocher, E., et al. (2015). Modulation of gut microbiota during probiotic-mediated attenuation of metabolic syndrome in high fat diet-fed mice. *ISME J.* 9, 1–15. doi: 10.1038/ismej.2014.99

Younossi, Z. M., Koenig, A. B., Abdelatif, D., Fazel, Y., Henry, L., and Wymer, M. (2016). Global epidemiology of nonalcoholic fatty liver disease-Meta-analytic assessment of prevalence, incidence, and outcomes. *Hepatology* 64, 73–84. doi: 10.1002/hep.28431

Zhang, C., Yin, A., Li, H., Wang, R., Wu, G., Shen, J., et al. (2015). Dietary modulation of gut microbiota contributes to alleviation of both genetic and simple obesity in children. *EBioMedicine* 2, 968–984. doi: 10.1016/j.ebiom.2015.07.007

Conflict of Interest Statement: The authors declare that the research was conducted in the absence of any commercial or financial relationships that could be construed as a potential conflict of interest.

Copyright © 2018 Wang, Li, Yang, Xue, Deng, Shen, Zhang, Zhao and Zhang. This is an open-access article distributed under the terms of the Creative Commons Attribution License (CC BY). The use, distribution or reproduction in other forums is permitted, provided the original author(s) and the copyright owner(s) are credited and that the original publication in this journal is cited, in accordance with accepted academic practice. No use, distribution or reproduction is permitted which does not comply with these terms.

frontiers in Microbiology

ORIGINAL RESEARCH
published: 06 September 2018
doi: 10.3389/fmicb.2018.02163

Bacterial Communities in the Womb During Healthy Pregnancy

Lihong Zhu[1], Fei Luo[2], Wenjing Hu[2], Yang Han[3], Yuezhu Wang[4], Huajun Zheng[4], Xiaokui Guo[2] and Jinhong Qin[2]**

[1] Department of Gynecology, Huadong Hospital, Fudan University, Shanghai, China, [2] Department of Microbiology and Immunology, Institutes of Medical Sciences, Shanghai Jiao Tong University School of Medicine, Shanghai, China, [3] Department of Microbiology, Guizhou Medical University, Guiyang, China, [4] Shanghai-MOST Key Laboratory of Health and Disease Genomics, Chinese National Human Genome Center at Shanghai, Shanghai, China

The idea that healthy uterine cavity is sterile is challenged nowadays. It is still debatable whether the bacteria present in the uterine cavity during pregnancy are residents or invaders. To reveal microbiome composition and its characteristics in the womb of pregnant women, 41 decidual tissue samples and 64 amniotic fluid samples were taken from pregnant Chinese women. DNA extraction was followed by pyrosequencing of the hypervariable V4 region of the 16S rDNA gene to characterize womb microbiome. Both types of samples had low diversity microbiome with Enterobacteriaceae being the dominant phylotypes at family level. To characterize the nature of colonization during pregnancy, the presence of endogenous biomass was confirmed by cultivation. Surprisingly, all of the 50 amniotic fluid samples studied were culture-negative, whereas 379 out of 1,832 placenta samples were culture-positive. Our results suggested that womb contained microbiome with low diversity. Culture-based investigation of amniotic fluid and placenta samples confirmed the presence of cultivable microorganisms in the placenta but not in amniotic fluid. Thus it suggests that bacterial colonization does occur during healthy pregnancy.

Keywords: decidual tissue, amniotic fluid, V4 region of 16S rDNA, microbiome, proteobacteria, firmicutes

OPEN ACCESS

Edited by:
Learn-Han Lee, Monash University Malaysia, Malaysia

Reviewed by:
Clarissa Schwab, ETH Zürich, Switzerland
Siti Aishah Sulaiman, UKM Medical Molecular Biology Institute (UMBI), Malaysia

****Correspondence:***
Xiaokui Guo
xkguo@shsmu.edu.cn
Jinhong Qin
jinhongqin@sjtu.edu.cn

Specialty section:
This article was submitted to Microbial Symbioses, a section of the journal Frontiers in Microbiology

Received: *21 April 2018*
Accepted: *23 August 2018*
Published: *06 September 2018*

Citation:
Zhu L, Luo F, Hu W, Han Y, Wang Y, Zheng H, Guo X and Qin J (2018) Bacterial Communities in the Womb During Healthy Pregnancy. Front. Microbiol. 9:2163. doi: 10.3389/fmicb.2018.02163

INTRODUCTION

It was widely thought that the womb is a sterile environment during healthy pregnancy (Funkhouser and Bordenstein, 2013). The presence of bacteria in uterine cavity was considered as a risk factor because they could potentially affect the fetus and cause systemic inflammation and multiple organ damage (Martius and Eschenbach, 1990). The bacteria invading uterine cavity have been postulated to emerge mainly from the lower urogenital tract, ascending upward through the cervix to the uterus and then breaching the placental barrier to amniotic fluid and placenta (Goldenberg et al., 2000; Keelan and Payne, 2015). The presence of microorganisms such as *Ureaplasma* sp. and *Fusobacterium* sp. in uterine cavity confirmed by culture-dependent or culture-independent methods has been frequently associated with negative pregnancy outcomes (Han et al., 2004, 2009, 2010). However, despite the undoubtedly strong associations, these species have not been conclusively shown to be pathological agents. This circumstance indicates that available findings may have complex interpretation.

Recent advances in human microbiome investigations revealed an important role of microbes for human health (Human Microbiome Project Consortium, 2012). By using current sequencing technologies, multiple recent studies have challenged the traditional view of the womb as a sterile compartment. Amniotic fluid, the uterus, and the placenta, conventionally thought to be sterile, have recently been demonstrated to harbor unique microbiomes (Aagaard et al., 2014; Collado et al., 2016; Franasiak and Scott, 2017). We report here microbiomes of decidual tissue and amniotic fluid from healthy pregnancies elucidated by high-throughput sequencing technology and cultivable biomass of amniotic fluid and placenta by culture-based method.

MATERIALS AND METHODS

Patient Recruitment and Ethical Considerations

Decidual tissue samples were obtained by curettage with vacuum aspiration from 41 pregnant women aged from 18 to 41 years with gestational age between 30 and 60 days. All cases were confirmed as normal intrauterine pregnancies by ultrasonography at the outpatient clinic of the Obstetrics and Gynecology Hospital before eligible artificial abortion. Women were excluded if: (1) they had been diagnosed with lower genital tract infections or other gynecological diseases; (2) had used any antimicrobials in the past 7 days; and (3) had used any vaginal devices or vaginally applied products in the past 30 days. The vulva, vagina, and cervix of the uterus were adequately sterilized before the operation. Specimens of decidual tissue were obtained from the participants after curettage with vacuum aspiration, and blood clots were removed. The samples were stored at −80°C for microbiome analysis.

Samples of amniotic fluid were collected from 64 Chinese women aged from 22 to 44 years with gestational age between 17 and 20 weeks in which the result of screening for Down's syndrome in the fetus indicated high risk. Thus, amniocentesis for fetal karyotyping was recommended to these women at the Obstetrics and Gynecology Hospital. Women were excluded if: (1) they had been diagnosed with Down's syndrome, lower genital tract infections, or other gynecological diseases; (2) had used any antimicrobials in the past 7 days; and (3) had used any vaginal devices or vaginally applied products in the past 17–20 weeks. After amniocentesis, amniotic fluid was centrifuged at 1,000 × *g* to obtain cells for fetal karyotyping, and the remaining supernatant was further centrifuged at 10,000 × *g* for microbiome analysis.

The clinical trial was registered with clinical trials (2017K055). All experiments were performed in accordance with guidelines and regulations of clinical trials (2017K055) approved by the Medical Ethics Committee of Huadong Hospital affiliated to Fudan University. All study participants gave their written informed consent for sample collection and subsequent microbiological analysis.

Culturing Microbes From the Placenta and Amniotic Fluid

Amniotic fluid samples were collected from 50 pregnant women for medical diagnostics of aneuploidy as above. After centrifugation at 10,000 × *g*, cells were plated onto brain heart infusion (Oxoid, Cambridge, United Kingdom) and Columbia blood agar plates (Oxoid, Cambridge, United Kingdom), which were aerobically incubated at 37°C for 48 h. A total of 1,832 placenta samples were collected by sterile swabs by using obstetrical standard operating procedures. Women aged 23–42 years were included if: (1) singleton gestation; (2) delivered at term ($38^{0/7}$ to $41^{6/7}$ weeks gestational age); and (3) without clinical chorioamnionitis and other anomaly. Following standard obstetrical practices, after cesarean delivery of the infant and before the delivery of the placenta, swabs for microbial collection were swirled to fetal side to collect samples while taking care to avoid contamination from the maternal side. All the swabs were streak plated onto brain heart infusion (Oxoid, Cambridge, United Kingdom) and Columbia blood agar plates (Oxoid, Cambridge, United Kingdom), and cultivated aerobically at 37°C for 48 h. Conventional microbiological methods including analysis of colony and cellular morphology were used to preliminarily identify the isolates. Three clones each colony type was random selected to do Gram staining and observed. After preliminary identification, the same type clone was re-streaked to prepare a pure culture. Identification of viable organisms was carried out using VITEK 2 compact system (BioMerieux Inc., Marcy l'Etoil, France). GP, GN, NH, YST, and ANC cards were used.

DNA Isolation and 16S rDNA Sequencing

Total genomic DNA of decidual tissue and amniotic fluid samples was extracted with a Power Soil DNA isolation Kit (cat. no. G-3246-50; Mo Bio Laboratories Inc., Carlsbad, CA, United States) according to manufacturer's instructions. The quantity and quality of extracted DNA of each isolate was measured by PCR amplified with V3V5 primer (357F: 5′-CCTACGGGAGGCAGCAG-3′, 926R: 5′-CCGTCAATTCMTTTRAGT-3′). The amplification products were measured using a NanoDrop ND-1000 spectrophotometer (Thermo Fisher Scientific, Waltham, MA, United States) and agarose gel electrophoresis. When the amplicons were <500 ng, the extraction were not used as appropriate for sequencing. For sequencing, PCR amplification of hypervariable V4 regions of bacterial 16S rDNA genes was performed using forward primer 520F (5′-AYTGGGYDTAAAGNG-3′) and reverse primer 802R (5′-TACNVGGGTATCTAATCC-3′). Sample-specific 7-bp barcodes were incorporated into the primers for multiplex sequencing. After purification, PCR amplicons were pooled in equal amounts and pair-end 2 bp × 300 bp sequencing was performed using the Illlumina MiSeq platform with a MiSeq Reagent Kit v3 at Shanghai Personal Biotechnology Co., Ltd. (Shanghai, China).

The Quantitative Insights Into Microbial Ecology (QIIME, v. 1.8.0) pipeline was employed to process sequencing data as previously described (Caporaso et al., 2010). Briefly, raw

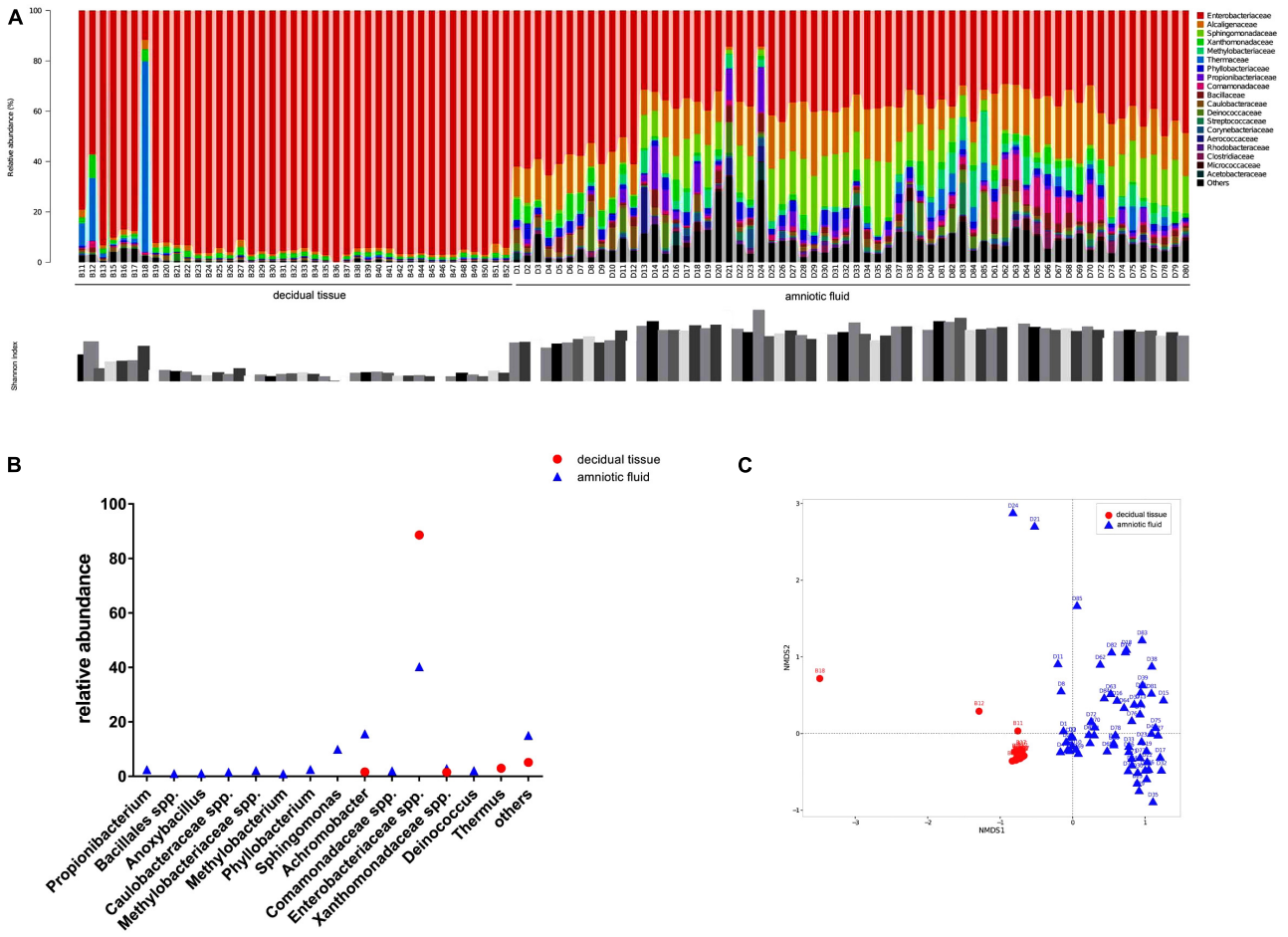

FIGURE 1 | Bacterial profiling and diversity in each sample analyzed by 16S rDNA gene pyrosequencing. **(A)** Bacterial profiling plot of relative abundances of operational taxonomic units (OTUs) at the family level. Points plot of Estimators of the Shannon index are shown below. **(B)** Difference of bacterial taxa at the genus level between decidual tissue and amniotic fluid samples. **(C)** Non-metric multidimensional scaling of microbiome structure based on weighted UniFrac distance. Relative abundances of OTUs accounting for >0.1% of the total bacterial community are shown.

sequencing reads with exact matches to the barcodes were assigned to respective samples and identified as valid sequences. The low-quality sequences, namely sequences that had a length of <150 bp, sequences that had average Phred scores of <20, sequences that contained ambiguous bases, and sequences that contained mononucleotide repeats of >8 bp were filtered out. Paired-end reads were assembled using FLASH (Magoc and Salzberg, 2011). After chimera detection, bacterial operation taxonomic units (OTUs) were clustered by UCLUST (QIIME[1]) based on 97% nucleotide similarity. A representative sequence selected from each OTU using default parameters. OTU taxonomic classification was conducted by using BLAST comparisons of the representative sequences set against the Greengenes Database using best hits. An OTU table was further generated to record the abundance of each OTU in each sample and taxonomy of these OTUs. OTUs containing <0.001% of total sequences across all samples were discarded. To minimize the difference of sequencing depth across the samples, an averaged, rounded, and rarefied OTU table was generated by averaging 100 evenly resampled OTU subsets under 90% of the minimal sequencing depth for further analysis.

Bioinformatics and Statistical Analysis

Bioinformatics and statistical analyses of sequencing data were mainly performed using QIIME and R packages (v. 3.2.0). Relative abundance profiles at taxa levels (phylum, class, order, family, and genus) were generated based on OTU annotation. OTU-level alpha diversity indices such as Shannon diversity index were calculated using the OTU table in QIIME and plotted by GraphPad Prism 5 (GraphPad Software, Inc., San Diego, CA, United States). Beta diversity analysis was performed to investigate the structural variation of microbial communities across the samples using UniFrac distance metrics and visualized via non-metric multidimensional scaling (NMDS). Taxon abundances at the family and genus levels were statistically compared among the samples and plotted by GraphPad Prism 5.

[1]http://qiime.org/scripts/pick_otus.html

RESULTS

Diversity and Composition of Bacterial Communities in Decidual Tissues and Amniotic Fluids

Total DNA was isolated from collected samples, and the V4 region of the 16S rDNA gene was amplified and sequenced. A total of 2,401,802 filtered, high-quality sequences were produced in this study, with an average of 22,658 reads per sample. The validation sequences were clustered into 740 OTUs. All decidual tissue sample OTUs (100% of phylotypes) could be annotated at the phylogenetic level, as well as on family (99.9% of phylotypes) and genus levels (92.082% of phylotypes). Nearly all OTUs in amniotic fluid samples (99.976% of phylotypes) were also annotated at the phylogenetic level, including 97.823% of phylotypes at the family level and 54.091% of phylotypes at the genus level.

The diversity of microbes within a habitat was defined as the number and abundance distribution of distinct types of organisms. **Figure 1A** presents the relative abundances of OTUs at the family level in each sample along with the Shannon index. Microorganisms with relative abundance of >0.1% at the family level in two types of samples showed that Enterobacteriaceae accounted for 88.6% of the relative abundance in decidual tissue and for 40.3% in amniotic fluid. Detailed comparisons at the genus level across the two types of samples showed that Firmicutes were more abundant in decidual tissue than in amniotic fluid (**Figure 1B**) and 10 taxa, e.g., *Propionibacterium*, *Bacillales* spp., *Anoxybacillus*, *Caulobacteraceae* spp., *Methylobacteriaceae* spp., *Methylobacterium*, *Phyllobacterium*, *Sphingomonas*, *Comamonadaceae* spp., and *Deinococcus* were unique in amniotic fluid. Although Enterobacteriaceae were most abundant in most samples, differences in the compositions of bacterial communities were observed between decidual tissue and amniotic fluid. The Shannon indices indicated low diversity in both decidual tissue and amniotic fluid, although amniotic fluid diversity tended to be higher. When the community structures of decidual tissue and amniotic fluid were assessed by NMDS analysis of relative genus abundances, significantly separated clusters representing the two types of samples was demonstrated (**Figure 1C**).

Recovery of Cultivable Biomass From Placental Samples but Not From Amniotic Fluid

In our studies, we further cultured 50 amniotic fluid samples and 1,832 placental samples. Out of 1,832 placental samples, 379 were culture-positive, whereas all 50 amniotic fluid samples were culture-negative in this study. In total, 447 strains of microorganisms were recovered from 1,832 placental samples (**Supplementary Table S1**). Of those, 428 were bacteria and 19 were fungi. All 19 fungi taxa were identified as belonging to the three species of the genus *Candida*: *Candida albicans*, *Candida tropicalis*, and *Candida glabrata*. Of the 428 recovered bacteria, 30 species were identified (**Table 1**). *Escherichia coli*, belonging to the family Enterobacteriaceae, accounted for 57.71% of the isolated strains, whereas *Enterococcus faecalis*, belonging to the family Enterococcaceae, accounted for 21.03% of the isolated strains.

DISCUSSION

The uterine cavity of healthy pregnant women has long been considered sterile, and it is traditionally believed that bacterial colonization of the womb is associated with adverse reproductive health outcomes, including miscarriage, chorioamnionitis, and preterm delivery. In recent years, although reports have shown that the womb is not a sterile environment, it is still debated if the microbiome detected in uterine cavity samples during healthy pregnancy represents real endogenous womb microflora or is a result of contamination

TABLE 1 | Bacteria recovered from the placenta under aerobic condition.

Strain	No.	Percentage
Firmicutes		
Staphylococcus aureus	8	1.87%
Staphylococcus sp.	8	1.87%
Enterococcus faecium	9	2.10%
Enterococcus faecalis	90	21.03%
Enterococcus durans	2	0.47%
Enterococcus hirae	1	0.23%
Streptococcus salivarius	1	0.23%
Streptococcus pyogenes	1	0.23%
Streptococcus agalactiae	22	5.14%
Streptococcus bovis	2	0.47%
Streptococcus sp.	2	0.47%
Streptococcus pasteurianus	1	0.23%
Streptococcus mitis	3	0.23%
Listeria monocytogenes	1	1.87%
Proteobacteria		
Escherichia coli	247	57.71%
Klebsiella pneumoniae	10	2.34%
Klebsiella oxytoca	1	0.23%
Enterobacter aerogenes	2	0.47%
Proteus mirabilis	1	0.23%
Proteus vulgaris	1	0.23%
Proteus penneri	1	0.23%
Morganella morganii	1	0.23%
Citrobacter koseri	3	0.70%
Citrobacter braakii	1	0.23%
Citrobacter freundii	3	0.70%
Ewingella americana	1	0.23%
Raoultella planticola	1	0.23%
Aeromonas sp.	1	0.23%
Acinetobacter baumannii	1	0.23%
Sphingomonas sp.	1	0.23%
Actinobacteria		
Micrococcus sp.	1	0.23%

(Jimenez et al., 2005, 2008; Stout et al., 2013; Aagaard et al., 2014; Wassenaar and Panigrahi, 2014; Lauder et al., 2016; Arora et al., 2017; Hornef and Penders, 2017). In our study, in order to avoid contamination, we obtained decidual tissue samples after curettage with vacuum aspiration. Our results showed that decidual tissue microbiome was low diversity and composed predominant phyla such as Proteobacteria, Thermus, and Firmicutes. *Enterobacteriaceae* sp. and *Thermus* were the dominant organisms at the genus level. Consistent with previous limited data on uterine microbiome composition from both culture-dependent and culture-independent assays, our experiments confirmed that uterine cavity harbored a limited number of particular phylotypes with low abundance and low diversity (Verstraelen et al., 2016; Walther-Antonio et al., 2016). However, our results showed that Proteobacteria taxa, such as Enterobacteriaceae, were the dominant organisms in the uterus of pregnant women, whereas previous reports indicated that Bacteroidetes were dominant organisms in the uterus of non-pregnant women (Verstraelen et al., 2016; Walther-Antonio et al., 2016).

Amniotic fluid samples in our study were collected in the middle trimester stage at the gestation age of 17 to 20 weeks by amniocentesis rather than at delivery in order to avoid contamination. We could recover microorganisms from the placenta by culture, but not from amniotic fluid. Thus, our results suggested that commensal and cultivable microbiota colonized the placenta. By using histological tissue staining, it has been previously demonstrated that the maternal basal plate of the placenta harbored microbes (Jimenez et al., 2005). Those data supported the idea that the placenta was not sterile. However, amniotic fluid samples in our study were culture-negative under both aerobic and anaerobic conditions. Recently, culture-based studies confirmed that amniotic fluid samples often (in >90% of cases) did not contain viable bacteria and only rarely were culture-positive (DiGiulio et al., 2010; Wassenaar and Panigrahi, 2014). In our study, although 16S rDNA sequencing detected microbiome in amniotic fluid, the samples were all culture-negative. It is possible that commensal microbiota in amniotic fluid has low abundance and thus, can only occasionally be isolated by culture, as noted by others. Another explanation is that commensal microbiota in amniotic fluid is adapted to specific environmental conditions and resists cultivation (a phenomenon called "the great plate count anomaly") as suggested previously (Staley and Konopka, 1985; Romero et al., 2008). Finally, it is possible that healthy amniotic fluid indeed did not contain viable bacteria, and the detected microbiome actually is DNA release of microorganisms originating from other sites, such as from blood or placenta.

In summary, we present here a high-throughput assessment of womb microbiome. Microbiome structure of amniotic fluid was more diverse than that of decidual tissue, which supported the previous reports that bacteria could be hematogenously spread from blood to amniotic cavity (Aagaard et al., 2014). Thus, possibly, during healthy pregnancy, bacterial colonization occurs, however, chronological and mechanistic aspects of this phenomenon remain to be elucidated.

AUTHOR CONTRIBUTIONS

JQ and XG conceived the study. LZ, FL, WH, and YH performed the experiments. YW and HZ analyzed sequencing data. All authors contributed to the writing of the manuscript.

FUNDING

This work was supported by the Shanghai 3-Year Plan of the Key Subjects Construction in Public Health-Infectious Diseases and Pathogenic Microorganisms (15GWZK0102) and Natural Science Foundation of Shanghai (17ZR1415900 and 16ZR1420800).

SUPPLEMENTARY MATERIAL

The Supplementary Material for this article can be found online at: https://www.frontiersin.org/articles/10.3389/fmicb.2018.02163/full#supplementary-material

TABLE S1 | Detailed information of cultured organism from placenta.

REFERENCES

Aagaard, K., Ma, J., Antony, K. M., Ganu, R., Petrosino, J., and Versalovic, J. (2014). The placenta harbors a unique microbiome. *Sci. Transl. Med.* 6:237ra265. doi: 10.1126/scitranslmed.3008599

Arora, N., Sadovsky, Y., Dermody, T. S., and Coyne, C. B. (2017). Microbial vertical transmission during human pregnancy. *Cell Host Microbe* 21, 561–567. doi: 10.1016/j.chom.2017.04.007

Caporaso, J. G., Kuczynski, J., Stombaugh, J., Bittinger, K., Bushman, F. D., Costello, E. K., et al. (2010). QIIME allows analysis of high-throughput community sequencing data. *Nat. Methods* 7, 335–336. doi: 10.1038/nmeth.f.303

Collado, M. C., Rautava, S., Aakko, J., Isolauri, E., and Salminen, S. (2016). Human gut colonisation may be initiated in utero by distinct microbial communities in the placenta and amniotic fluid. *Sci. Rep.* 6:23129. doi: 10.1038/srep23129

DiGiulio, D. B., Romero, R., Kusanovic, J. P., Gomez, R., Kim, C. J., Seok, K. S., et al. (2010). Prevalence and diversity of microbes in the amniotic fluid, the fetal inflammatory response, and pregnancy outcome in women with preterm pre-labor rupture of membranes. *Am. J. Reprod. Immunol.* 64, 38–57. doi: 10.1111/j.1600-0897.2010.00830.x

Franasiak, J. M., and Scott, R. T. (2017). Endometrial microbiome. *Curr. Opin. Obstet. Gynecol.* 29, 146–152. doi: 10.1097/GCO.0000000000000357

Funkhouser, L. J., and Bordenstein, S. R. (2013). Mom knows best: the universality of maternal microbial transmission. *PLoS Biol.* 11:e1001631. doi: 10.1371/journal.pbio.1001631

Goldenberg, R. L., Hauth, J. C., and Andrews, W. W. (2000). Intrauterine infection and preterm delivery. *N. Engl. J. Med.* 342, 1500–1507. doi: 10.1056/NEJM200005183422007

Han, Y. W., Fardini, Y., Chen, C., Iacampo, K. G., Peraino, V. A., Shamonki, J. M., et al. (2010). Term stillbirth caused by oral *Fusobacterium nucleatum*. *Obstet. Gynecol.* 115(2 Pt 2), 442–445. doi: 10.1097/AOG.0b013e3181cb9955

Han, Y. W., Redline, R. W., Li, M., Yin, L., Hill, G. B., and McCormick, T. S. (2004). *Fusobacterium nucleatum* induces premature and term stillbirths in pregnant mice: implication of oral bacteria in preterm birth. *Infect. Immun.* 72, 2272–2279. doi: 10.1128/IAI.72.4.2272-2279.2004

Han, Y. W., Shen, T., Chung, P., Buhimschi, I. A., and Buhimschi, C. S. (2009). Uncultivated bacteria as etiologic agents of intra-amniotic inflammation leading to preterm birth. *J. Clin. Microbiol.* 47, 38–47. doi: 10.1128/JCM.01206-08

Hornef, M., and Penders, J. (2017). Does a prenatal bacterial microbiota exist? *Mucosal Immunol.* 10, 598–601. doi: 10.1038/mi.2016.141

Human Microbiome Project Consortium (2012). Structure, function and diversity of the healthy human microbiome. *Nature* 486, 207–214. doi: 10.1038/nature11234

Jimenez, E., Fernandez, L., Marin, M. L., Martin, R., Odriozola, J. M., Nueno-Palop, C., et al. (2005). Isolation of commensal bacteria from umbilical cord blood of healthy neonates born by cesarean section. *Curr. Microbiol.* 51, 270–274. doi: 10.1007/s00284-005-0020-3

Jimenez, E., Marin, M. L., Martin, R., Odriozola, J. M., Olivares, M., Xaus, J., et al. (2008). Is meconium from healthy newborns actually sterile? *Res. Microbiol.* 159, 187–193. doi: 10.1016/j.resmic.2007.12.007

Keelan, J. A., and Payne, M. S. (2015). Vaginal microbiota during pregnancy: pathways of risk of preterm delivery in the absence of intrauterine infection? *Proc. Natl. Acad. Sci. U.S.A.* 112, E6414. doi: 10.1073/pnas.1517346112

Lauder, A. P., Roche, A. M., Sherrill-Mix, S., Bailey, A., Laughlin, A. L., Bittinger, K., et al. (2016). Comparison of placenta samples with contamination controls does not provide evidence for a distinct placenta microbiota. *Microbiome* 4:29. doi: 10.1186/s40168-016-0172-3

Magoc, T., and Salzberg, S. L. (2011). FLASH: fast length adjustment of short reads to improve genome assemblies. *Bioinformatics* 27, 2957–2963. doi: 10.1093/bioinformatics/btr507

Martius, J., and Eschenbach, D. A. (1990). The role of bacterial vaginosis as a cause of amniotic fluid infection, chorioamnionitis and prematurity–a review. *Arch. Gynecol. Obstet.* 247, 1–13. doi: 10.1007/BF02390649

Romero, R., Schaudinn, C., Kusanovic, J. P., Gorur, A., Gotsch, F., Webster, P., et al. (2008). Detection of a microbial biofilm in intraamniotic infection. *J. Obstet. Gynecol.* 198, 135.e1–135.e5. doi: 10.1016/j.ajog.2007.11.026

Staley, J. T., and Konopka, A. (1985). Measurement of in situ activities of nonphotosynthetic microorganisms in aquatic and terrestrial habitats. *Annu. Rev. Microbiol.* 39, 321–346. doi: 10.1146/annurev.mi.39.100185.001541

Stout, M. J., Conlon, B., Landeau, M., Lee, I., Bower, C., Zhao, Q., et al. (2013). Identification of intracellular bacteria in the basal plate of the human placenta in term and preterm gestations. *Am. J. Obstet. Gynecol.* 208, 226.e1–226.e7. doi: 10.1016/j.ajog.2013.01.018

Verstraelen, H., Vilchez-Vargas, R., Desimpel, F., Jauregui, R., Vankeirsbilck, N., Weyers, S., et al. (2016). Characterisation of the human uterine microbiome in non-pregnant women through deep sequencing of the V1-2 region of the 16S rRNA gene. *PeerJ* 4:e1602. doi: 10.7717/peerj.1602

Walther-Antonio, M. R., Chen, J., Multinu, F., Hokenstad, A., Distad, T. J., Cheek, E. H., et al. (2016). Potential contribution of the uterine microbiome in the development of endometrial cancer. *Genome Med.* 8:122. doi: 10.1186/s13073-016-0368-y

Wassenaar, T. M., and Panigrahi, P. (2014). Is a foetus developing in a sterile environment? *Lett. Appl. Microbiol.* 59, 572–579. doi: 10.1111/lam.12334

Conflict of Interest Statement: The authors declare that the research was conducted in the absence of any commercial or financial relationships that could be construed as a potential conflict of interest.

Copyright © 2018 Zhu, Luo, Hu, Han, Wang, Zheng, Guo and Qin. This is an open-access article distributed under the terms of the Creative Commons Attribution License (CC BY). The use, distribution or reproduction in other forums is permitted, provided the original author(s) and the copyright owner(s) are credited and that the original publication in this journal is cited, in accordance with accepted academic practice. No use, distribution or reproduction is permitted which does not comply with these terms.

frontiers in Microbiology

ORIGINAL RESEARCH
published: 12 September 2018
doi: 10.3389/fmicb.2018.02193

Alterations in the Urinary Microbiota Are Associated With Cesarean Delivery

Fengping Liu[1†], Longxian Lv[2†], Huiyong Jiang[2†], Ren Yan[2], Shurong Dong[3], Liping Chen[4], Wei Wang[5*] and Yong Q. Chen[1*]*

[1] Wuxi School of Medicine, Jiangnan University, Wuxi, China, [2] Collaborative Innovation Center for Diagnosis and Treatment of Infectious Diseases, State Key Laboratory for Diagnosis and Treatment of Infectious Diseases, The First Affiliated Hospital, School of Medicine, Zhejiang University, Hangzhou, China, [3] Key Laboratory of Advanced Micro/Nano Electronic Devices and Smart Systems of Zhejiang, College of Information Science and Electronic Engineering, Zhejiang University, Hangzhou, China, [4] Intensive Unit, Affiliated Yancheng Hospital, School of Medicine, Southeast University, Nanjing, China, [5] Department of Urology, The First Affiliated Hospital, College of Medicine, Zhejiang University, Hangzhou, China

Similar to the gut, the bladder contains urinary microbiota, and its bacterial composition and structure are determined by the individual's health status. Cesarean section is a traumatic event for women and it is correlated with postpartum complications. To better understand the urinary microbiota alterations caused by cesarean section, 16S rDNA sequencing was used to assess urine specimens collected by transurethral catheterization from 30 healthy women undergoing cesarean section pre-delivery (PreD) and post-delivery (PostD). A significant increase in bacterial diversity and more detectable bacteria at the phylum, family, and genus levels was observed in the PostD group compared to the PreD group, indicating that cesarean delivery (a process that includes surgery and delivery) altered the bacterial community. Specifically, the phylum Firmicutes and its affiliated family Lactobacillaceae and genus *Lactobacillus* dramatically decreased in the PostD group, suggesting that beneficial bacteria decreased after cesarean section, and clinicians should be aware that this might increase the risk of complications. Concurrently, the phylum Proteobacteria and its affiliated bacteria Pseudomonadaceae and *Pseudomonas* increased in the PostD group compared to the PreD group. This indicates that pathogen growth increases after cesarean section, making it important for clinicians to combat these changes to protect women from infectious diseases. Interestingly, several metabolic pathways, such as metabolism of energy, cofactors and vitamins were strengthened in the PostD group, whereas membrane transport was lessened in this group. This suggests that women's metabolic disorders might be cured by balancing urinary microbiota. In conclusion, the altered urinary microbiota between the PreD and PostD periods appears to provide insight into how to prevent postpartum metabolic disorders.

Keywords: cesarean section, delivery, *Lactobacillus*, Proteobacteria, urinary microbiota

OPEN ACCESS

Edited by:
Learn-Han Lee,
Monash University Malaysia, Malaysia

Reviewed by:
Anastasia N. Vlasova,
The Ohio State University, United States
Bernard La Scola,
Aix-Marseille Université, France

Correspondence:
Fengping Liu
liulaoshiyc@163.com
Wei Wang
wangw2005@zju.edu.cn
Yong Q. Chen
yqchen@jiangnan.edu.cn

† These authors have contributed equally to this work

Specialty section:
This article was submitted to Microbial Symbioses, a section of the journal Frontiers in Microbiology

Received: *05 May 2018*
Accepted: *27 August 2018*
Published: *12 September 2018*

Citation:
Liu F, Lv L, Jiang H, Yan R, Dong S, Chen L, Wang W and Chen YQ (2018) Alterations in the Urinary Microbiota Are Associated With Cesarean Delivery. Front. Microbiol. 9:2193. doi: 10.3389/fmicb.2018.02193

INTRODUCTION

Cesarean sections have risen in frequency in many countries around the world. Globally, the cesarean rate was 12.0% in 2000 and 15.5% in 2012 (Ye et al., 2016), while in developing countries, including China, it was 13.1% in 2000 and 16.9% in 2012 (Ye et al., 2016). Cesarean section is associated with future complications (Zakerihamidi et al., 2015), including hemorrhage, surgical

site infections, chest infections, and urinary tract infection (UTI), etc. (Yang and Sun, 2017). UTI and surgical site infections are the two infections that most commonly occur after cesarean delivery (Vincent et al., 2008). The prevalence of postpartum UTI in women who underwent cesarean section was 2.8%, and it was 1.50% in women who underwent vaginal delivery (Leth et al., 2009).

Traditionally, clinicians have always associated microorganisms in an individual's bladder with UTI. An individual is diagnosed with a UTI or asymptomatic bacteriuria if urine culture shows that an individual bacterial count is $>10^5$ CFU/mL (Vasudevan, 2014). However, metagenomic analyses have demonstrated that the female bladder harbors an indigenous microbiota (Thomas-White et al., 2018). Therefore, the presence of bacteria in the bladder does not necessarily indicate UTI. Moreover, the composition of the urinary microbiota is affected by the individual's health status. For example, Pearce et al. (2014) reported that patients with urgent urinary incontinence had higher abundance of *Gardnerella* and lower abundance of *Lactobacillus*. Thomas-White et al. (2018) found that urgent urinary incontinence patients had increased bacterial diversity compared to healthy controls. Furthermore, bacterial diversity affects patients' treatment response (Karstens et al., 2016). Siddiqui et al. (2012) noted that patients with interstitial cystitis had lower bacterial diversity, with increased *Lactobacillus*. In a study by Abernethy et al. (2017) interstitial cystitis patients had fewer *Lactobacillus* than healthy females. In addition, they found that the urinary microbiota was affected by the patients' characteristics. For instance, patients with *Lactobacillus* species had lower Female Genitourinary Pain Index, Interstitial Cystitis Symptom Index, and Interstitial Cystitis Problem Index scores than patients without isolated *Lactobacillus* species (Abernethy et al., 2017).

Recently, researchers have begun to explore the correlations between the urinary microbiota and pregnancy and preterm delivery. Yoo et al. (2016) found that bacteria-derived extracellular vesicles (EVs) excreted via the urinary tract were significantly different between pregnant and non-pregnant women. For example, *Bacillus* spp. EVs predominated in the urine of pregnant women, while *Pseudomonas* spp. EVs predominated in the urine of non-pregnant women (Yoo et al., 2016). Furthermore, pregnant women who underwent normal delivery had different EVs profiles from preterm delivery women, such as *Ureaplasma* spp. and Veillonellaceae EVs being more frequently detected in the urine of preterm delivery women (Yoo et al., 2016). However, in another study conducted by Ollberding et al. (2016) no differences in taxa richness, evenness, and bacterial communities were found in the urine from women with preterm or normal deliveries.

Although alteration in the urinary microbiota is associated with pregnancy and preterm delivery, no study has explored whether cesarean section can lead to dysbiosis of the urinary microbiota or whether the composition of the urinary microbiota affects puerperium complications. Our primary aim was to investigate differences in the urinary microbiota between the pre-delivery (PreD) and post-delivery (PostD) periods.

MATERIALS AND METHODS

Recruitment of Subjects

A self-controlled case series approach was used in the design of the present study. The participants were pregnant women who were going to undergo cesarean section. The present study is the first self-controlled case series on the urinary bacterial community in women undergoing cesarean section. It was impossible to obtain the values for the mean and standard deviation from previous studies, so the appropriate sample size was determined according to a recommendation from Benner, who suggested that the sample size should be $>$ 25 cases (Benner, 1999). At least 28 participants were needed in the present study as approximately 10% of patients have negative sequencing results in urinary microbiota studies (Karstens et al., 2016).

Thirty participants were recruited from the Obstetrics Department of the Sixth People's Hospital of Hangzhou from April to June 2017. The inclusion criteria were as follows: willingness to participate the study; aged $\geq$ 18 years; pregnant women who were going to undergo an elective cesarean section; consciousness; no history of iodine allergy; and no fever. The exclusion criteria were as follows: UTI in the past month; use of antibiotics, probiotics, or synbiotics in the past month; current abnormal vaginal discharge or itching; or intestinal cystitis, urinary incontinence, urinary tract deformity, bladder protrusion, hydronephrosis, renal atrophy, neurogenic cystitis, or kidney transplantation.

Before collecting the first urine specimen, data on each participant's characteristics, such as age, parity, gravidity, vital signs, and medication history, were collected. The Ethics Committee of the First Affiliated Hospital of the School of Medicine at Zhejiang University approved the study (reference number: 413). Written informed consent was obtained from each patient before enrollment.

Urine Specimen Collection

On the day of the cesarean section, a 50 mL urine specimen was collected in two sterile centrifuge tubes using a 50 mL sterile syringe via an indwelling urinary transurethral catheter while conducting transurethral catheterization before surgery. 40 mL urine was collected in a tube for urinary microbiota sequencing and the remaining urine was collected in another tube for standard urine culture. After 24 h, another 50 mL urine specimen was collected while withdrawing the catheter. Prior to collecting the urine using a sterile syringe, the junction between the catheter and the urine collection bag was disinfected with a poly (vinylpyrrolidone) –iodine antiseptic solution (Dian'erkang, Shanghai, China) twice.

Urine Specimen Processing

The procedure for urine specimen processing was described in our previous study (Ling et al., 2017). Briefly, the urine specimen was discarded if it was confirmed to be contaminated (based on standard urine culture). Non-contaminated specimens were given an anonymous identification code, and they were then immediately transferred to the laboratory and stored

at −80°C until DNA extraction. 40 mL urine was used for the urinary microbiota analysis. Magnetic bead-based isolation of bacterial genomic DNA was carried out according to the manufacturer's protocol with minor modifications (Beckman Coulter, United States) (Ling et al., 2017). The processes of DNA extraction and PCR set up were performed in a laminar air flow bench, illuminated with a UV lamp prior to use, in order to avoid possible contamination. Negative DNA extraction controls (containing lysis buffer and kit reagents only) were amplified and sequenced as the contamination controls. The amplicons were normalized, pooled, and sequenced on an Illumina MiSeq platform using a V3 reagent kit with 2 × 300 cycles. The 16S rRNA gene V3–V4 regions were amplified from the microbial genomic DNA (forward primer, 5′-ACTCCTACGGGAGGCAGCAG-3′; reverse primer, 5′-GGACTACHVGGGTWTCTAAT-3′). The 16S metagenomic sequencing data of the PreD group have also been used in a study (which is currently under review for publication) that compared the effect on urine microbiota of a transurethral catheterization sampling method to the effect of a new specially designed midstream urine collection technique.

Bioinformatic and Statistical Analyses

The Quantitative Insights Into Microbial Ecology (QIIME, v1.9.0) pipeline was employed to process the sequencing data, as previously described (Caporaso et al., 2010). Raw sequencing reads with exact matches to the barcodes were assigned to respective samples and identified as valid sequences. The low-quality sequences were filtered out using the following criteria (Gill et al., 2006; Chen and Jiang, 2014): length < 150 bp, average Phred score < 20, contained ambiguous bases, and contained mononucleotide repeats > 8 bp. Paired-end reads were assembled using FLASH (Magoc and Salzberg, 2011). Operational taxonomic unit (OTU) picking using Vsearch v1.11.1, included dereplication(–derep_fulllength), cluster(–cluster_fast,–id 0.97), detectection of chimeras(–uchime_ref) (Rognes et al., 2016). The index of alpha diversity was calculated with QIIME based on a sequence similarity of 97%. Beta diversity was measured by unweighted UniFrac distance, which was also calculated by QIIME. The diversity and richness of the bacteria in the urine specimens were calculated using several estimates, such as OTUs, Chao1, and the Shannon and Simpson indices (which are measures of bacterial diversity). Principal coordinates analysis (PCoA) of weighted UniFrac distance was used to demonstrate the beta diversity. The taxonomic tree was visualized using GraPhlAn. Kruskal–Wallis rank sum tests and pairwise Wilcoxon tests were used to identify the different markers, and linear discriminant analysis (LDA) was used to score each feature in the LDA effect size (LEfSe) analysis. The output file was further analyzed using the Statistical Analysis of Metagenomic Profiles software package (version 2.1.3). To obtain insight into the possible functional pathways that differ between the PreD and PostD groups, PicRUst was used to calculate the contributions of various OTUs to known biological pathways using Kyoto Encyclopedia of Genes and Genomes (KEGG) databases (Langille et al., 2013; Vernocchi et al., 2017). KEGG pathways that were non-prokaryotic, had <2 sequences in each group, or had a difference in mean proportions < 0.1% were excluded from the analysis (Shoskes et al., 2016). White's non-parametric *t*-test, using an alpha value of 0.05 with the Story false discovery rate (FDR)-controlling procedure, was used to control the FDR linked to multiple testing (Shoskes et al., 2016). Also, bacterial taxa with < 2 sequences in either group because they were suspected to contain contaminants, a relative abundance < 0.01% in either group, or a difference in mean proportions < 0.10% were removed from the analysis of the between-group differences in the relative abundance of bacterial taxa (Logares et al., 2014; Shoskes et al., 2016; Legione et al., 2018). All tests of significance were two-sided, and p/q < 0.05 was considered statistically significant.

The sequence data from this study were deposited in the GenBank Sequence Read Archive under accession number SRP 126710.

RESULTS

Participant Characteristics

Thirty women undergoing cesarean section participated in the present study. Their characteristics are shown in **Table 1**. Their temperatures on the day PostD were slightly higher than PreD.

Sequencing Results

The mean bacterial DNA concentration was 25.54 ng/μL for the 60 samples (the individual concentrations are shown in **Supplementary Table S1**). There were no bands on the gel after PCR amplification. When the negative control was sequenced, it yielded < 100 reads, and the sequences could not be assembled.

From the 60 samples, 2,367,239 raw sequences were produced, and 2,352,732 high-quality sequences remained after filtering out low-quality and short-length sequences, with a median read length of 420 bp (range, 391–528 bp). After filtering out the chimera, the mean number of sequences per barcoded sample used for downstream analysis was 32,972 reads. The total number of unique sequences from the PreD and PostD groups was

TABLE 1 | Characteristics of participants (*n* = 30).

Parameter	Range and/or number of patients	Mean ± SD
Age (years)	19–43	31.43 ± 4.37
Gravidity (times)	1–5	2.57 ± 1.04
Parity (times)	1–2	1.80 ± 0.41
Temperature (°C) on the day of the first urine sample collection	36.30–37.30	36.80 ± 0.26
Temperature (°C) on the day after cesarean section	36.40–37.50	36.90 ± 0.31
Pulse (times/min)	72–100	85.00 ± 6.78
Respiration (times/min)	18–20	18.47 ± 0.57
Body mass index (kg/m^2)	34.84–56.97	43.68 ± 4.72
Systolic blood pressure (mmHg)	93–138	114.80 ± 13.22
Diastolic blood pressure (mmHg)	50–88	71.00 ± 10.04
Fluid transfused (mL)	2200–4420	3635.87 ± 449.79

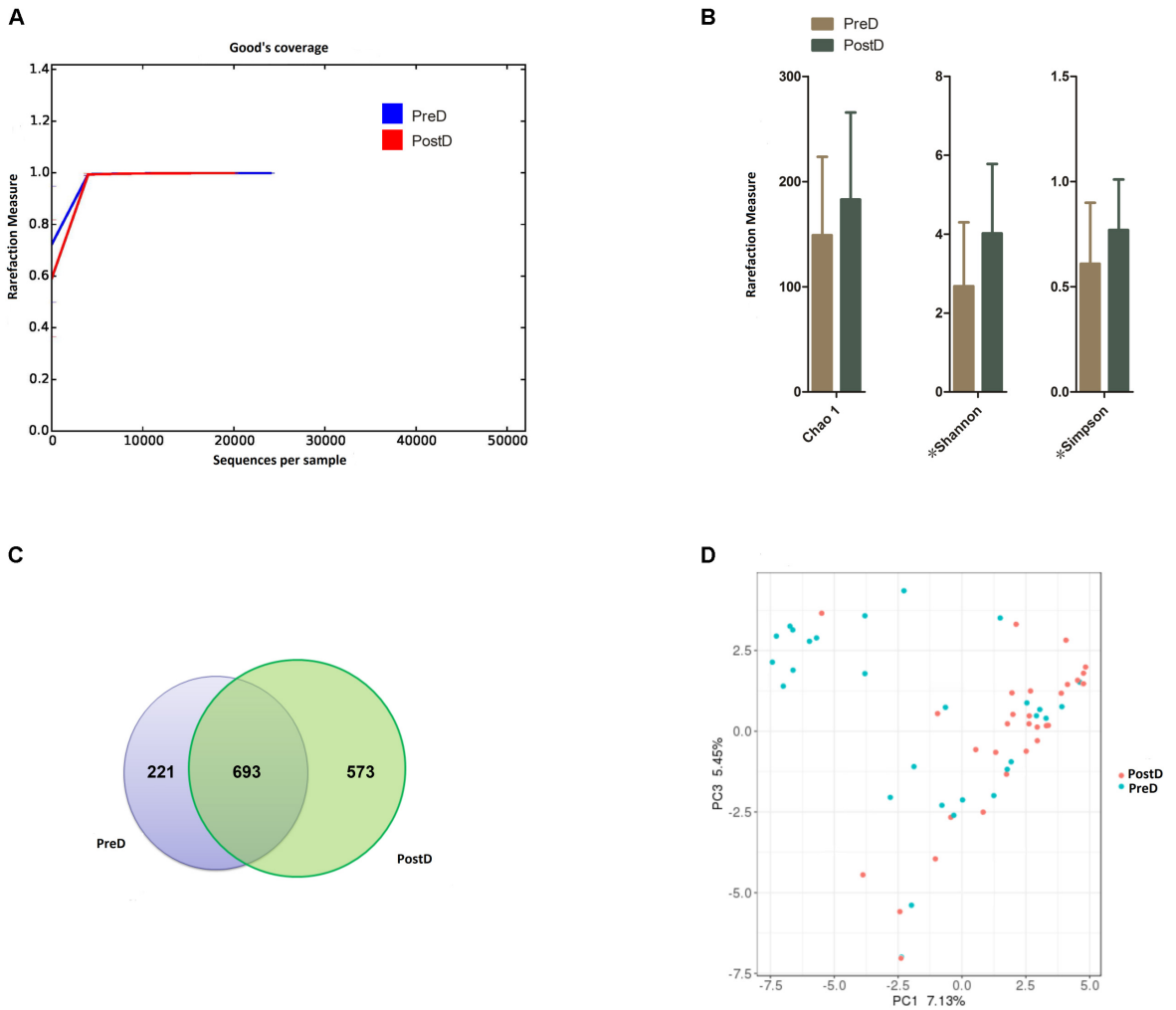

FIGURE 1 | Bacterial diversity. **(A)** Good's coverage was used to assess sequencing depth. **(B)** The Chao 1 index was used to measure richness, and the Shannon and Simpson rarefaction indices were applied to estimate diversity. *Indicates that a significant difference was found between groups ($p < 0.05$). **(C)** Venn diagram showing the number of OTUs shared between the PreD and PostD groups. **(D)** Principal coordinates analysis plot of the urinary microbiota based on the unweighted UniFrac metric. Blue and red dots represent the PostD and PreD groups, respectively. PreD means pre-delivery and PostD means post-delivery.

1,134,258, and they represented all phylotypes. Good's coverage values in both the PreD and PostD groups were nearly 100% and the curves again level off, showing that the sequencing effort was sufficient to detect most of the OTUs (**Figure 1A**).

The PostD Group Had Higher Bacterial Richness and Diversity Compared to the PreD Group

Chao 1, a bacterial richness index, was increased in the PostD group compared to the PreD group, but not significantly (**Figure 1B**) ($p = 0.101$). The Shannon and Simpson indices, measures of bacterial diversity, were significantly higher in the PostD group than the PreD group ($p = 0.003$; $p = 0.020$) (**Figure 1B**). The Venn diagram illustrated that 693 bacterial OTUs (accounting for 46.60%) were shared by the PreD and PostD groups (**Figure 1C**). The PCoA illustrated that the OTUs in the PreD and PostD groups could not completely separated (**Figure 1D**).

The PostD Group Had More Detectable Bacteria at All Taxon Levels, With Some Bacteria Showing Differences Between Groups

When the bacterial phyla were analyzed, 21 bacterial phyla were detected and all of them were detectable in the PostD group, while 6 were non-detectable in the PreD group, including Gemmatimonadetes and Planctomycetes. Although Firmicutes, Actinobacteria, Proteobacteria, Bacteroidetes, and Thermi were the most abundant bacteria in both the PreD and PostD groups, Firmicutes was significantly enriched in the PreD group compared to the PostD group ($q = 0.000$). In addition, the relative abundance of Proteobacteria was significantly decreased

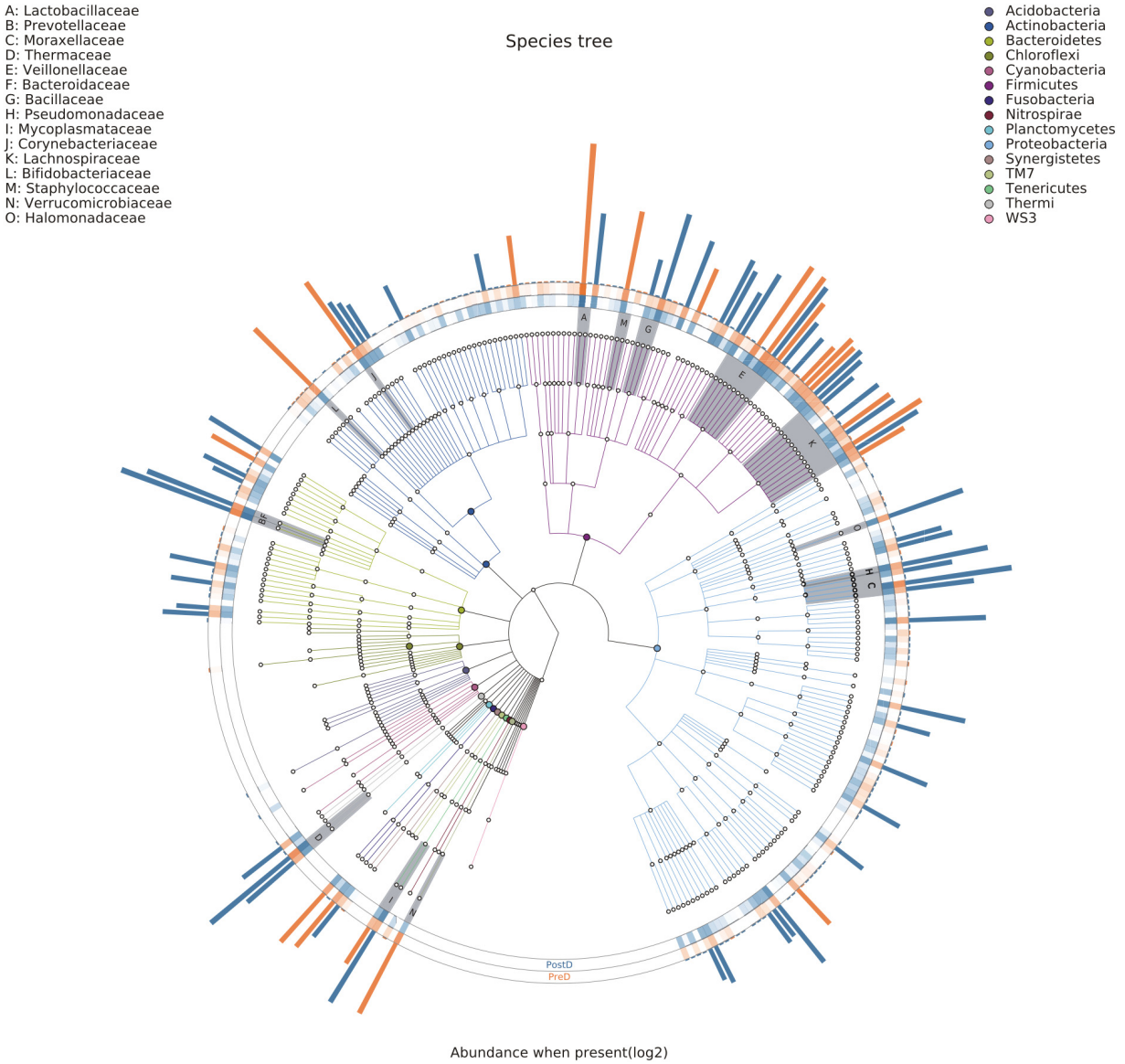

FIGURE 2 | Taxonomic visualization. Taxonomic tree visualized using GraPhlAn. The color of each node is consistent with the color of the corresponding bacterial phylum node located in the upper left corner of the graph. Each letter in the inner circle is consistent with the letter located in the upper right corner of the graph. The orange and blue columns around the circle represent the relative abundances of bacterial families in the PreD and PostD groups, respectively. PreD means pre-delivery and PostD means post-delivery.

in the PreD group compared to the PostD group (q = 0.000) (**Supplementary Table S2**).

At the family level, 135 and 116 bacteria families were present in the PostD and PreD groups, respectively. The bacterial families present in the PreD and PostD groups are shown in **Supplementary Table S3**. Bifidobacteriaceae, Lactobacillaceae, Lachnospiraceae, Thermaceae, and Prevotellaceae were the most abundant bacterial families in the present study (**Supplementary Figure S1**). The PreD group had higher levels of Lactobacillaceae and Coriobacteriaceae than the PostD group (q = 0.003; q = 0.044), while the PostD group had more abundant Bacteroidaceae, Comamonadaceae, Halomonadaceae, Methylobacteriaceae, and Micrococcaceae than the PreD group (q = 0.020; q = 0.016; q = 0.031; p = 0.007; p = 0.023) (**Supplementary Figure S2**). Bacterial families belonging to the phylum Proteobacteria were mainly found in the PostD group, such as Pseudomonadaceae, Halomonadaceae, and Moraxellaceae. Similarly, bacterial families belonging to the phylum Bacteroidetes were also mainly found in the PostD group. Bacterial families in the phylum Firmicutes were frequently detected; half of them were found in the PreD group, including Lactobacillaceae, Staphylococcaceae, and Veillonellaceae (**Figure 2**).

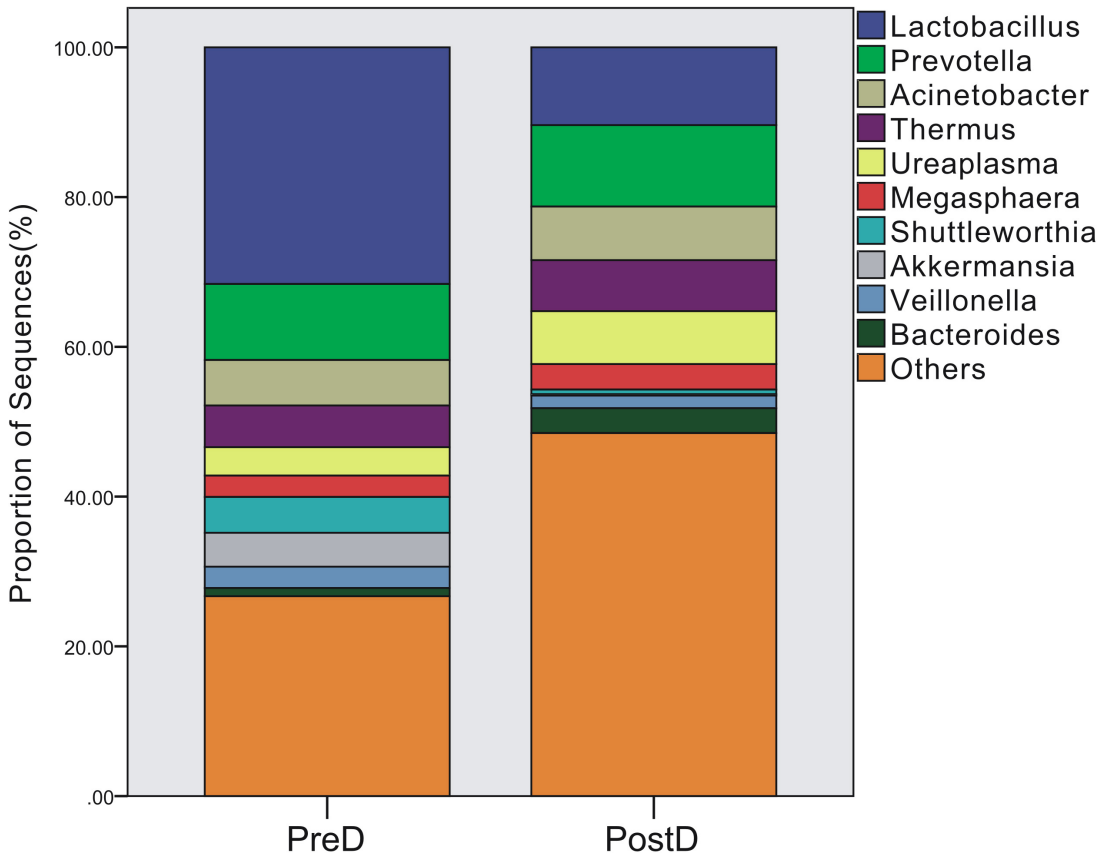

FIGURE 3 | Bacterial genera profile. Top 10 most abundant bacterial genera in the PreD and PostD groups. PreD means pre-delivery and PostD means post-delivery.

A total of 219 bacterial genera were found in the present study, and 181 genera were detected in the PreD group, while 209 genera were noted in the PostD group. The most abundant bacterial genus in the PreD group was *Lactobacillus* (accounting for 31.61%), while *Prevotella* was ranked as the most abundant bacteria in the PostD group (accounting for 10.88%). The top 10 most abundant bacteria in the PreD and PostD groups are shown in **Figure 3**. *Lactobacillus* was significantly lower in the PostD group compared to the PreD group, whereas *Ruminococcus* and *Bacteroides* were significantly increased in the PostD group compared to the PreD group (**Figure 4**).

Biomarkers Associated With Cesarean Section

The LEfSe analysis demonstrated that Bacilli, Lactobacillaceae, *Lactobacillus*, Lactobacillales, Firmicutes, Mobiluncus, and Actinomycetaceae could differentiate PreD specimens from the PostD specimens (**Supplementary Figure S3**).

Metabolic Pathways Were Correlated With Cesarean Delivery

Twenty metabolic pathways were associated with the PreD and PostD groups. Energy metabolism, metabolism of cofactors and vitamins, and amino acid metabolism were strengthened in the PostD group compared to the PreD group. However, membrane transport, nucleotide metabolism, and replication and repair lessened in the PostD group (**Figure 5**).

DISCUSSION

The associations between the human microbiota and health status have been of great concern to researchers and clinicians in recent decades. Although some studies have demonstrated that delivery mode impacted on the human microbiota, the focus of these studies was on the infant gut microbiota (Dominguez-Bello et al., 2010; Jakobsson et al., 2014; Liu et al., 2015; Chu et al., 2017), and few focused on the effects of delivery mode on the maternal microbiota. The bladder, previously considered sterile, has been demonstrated to have a unique bacterial community and the urinary microbiota has been found to be associated with diseases including urologic disorders, cancer, burn injuries, sexually transmitted infection, metabolic disease, bacterial vaginosis, etc. (Nelson et al., 2010; Aragon et al., 2016; Gottschick et al., 2017; Ling et al., 2017; Plichta et al., 2017; Shrestha et al., 2018). As previous studies reported that postpartum complications such as UTI are associated with the mode of delivery (Leth et al., 2009; Hung et al., 2016), the present study explored whether the characteristics of the urinary

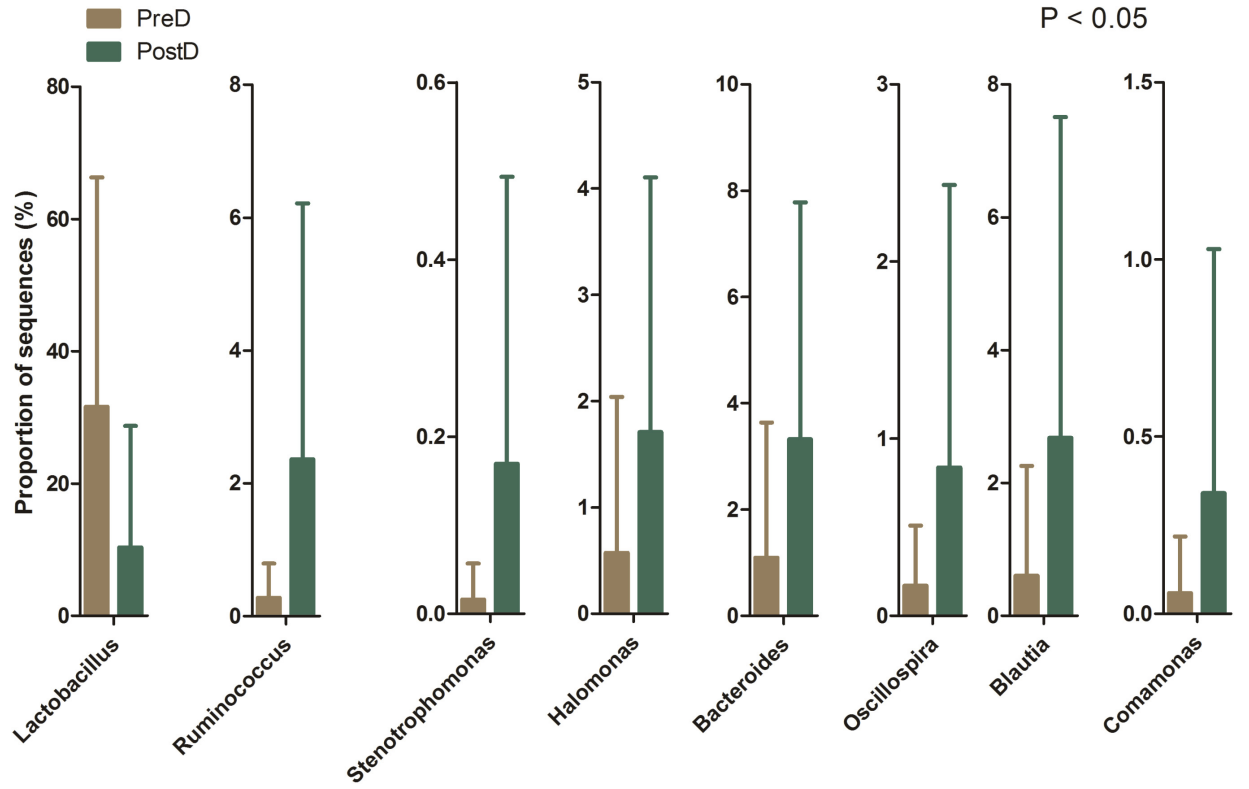

FIGURE 4 | Bacterial genera differences. Bacterial genera showing significant differences in relative abundance between the PreD and PostD groups. PreD means pre-delivery and PostD means post-delivery.

microbiota are associated with cesarean section and postpartum health status.

The present study indicates that there is a greater microbial diversity and a greater bacterial relative abundance at all taxonomic levels (including phylum, family, and genus) in the PostD group compared to the PreD group. This shows that cesarean section, which consists of surgery and delivery, has a profound influence on women's urinary microbial composition. Interestingly, urinary microbial diversity has also been found to be significantly increased in burn patients compared to controls (Plichta et al., 2017). This phenomenon is also similar to that identified in a study by Howard et al. (2017) which found that significant changes in gut microbial diversity occurred early after severe injury. Cesarean section is a traumatic experience for women (Ryding et al., 1997), and the above phenomena suggest that microbial diversity increases after trauma such as cesarean section. The PCoA indicated that cesarean section was not the only influencing factor responsible for the urinary microbiota changes in women undergoing cesarean section. As demonstrated by studies of the human gut and vaginal microbiota, the sharp decline in estrogen and progesterone levels after delivery may also affect the urinary microbiota (Koren et al., 2012; MacIntyre et al., 2015; Neuman et al., 2015). Therefore, the alteration of urinary microbiota caused by delivery via cesarean section may not only be associated with the cesarean section, but also with changes in hormone levels resulting from delivery (which can also occur after vaginal delivery). The number of OTUs shared between the PreD and PostD groups was lower than the number of OTUs detected overall, illustrating that cesarean section delivery played an important role in the dysbiosis of the urinary microbiota in women. Clinicians may need to be aware of possible cesarean section delivery-related complications associated with the imbalance of urinary microbiota.

Gemmatimonadetes and Planctomycetes were not found in the PreD group, while they were found in the PostD group. In addition, Cyanobacteria, Chloroflexi, and Acidobacteria showed a great shift after delivery. Little is known about these bacteria and further research should be carried out to assess their roles in the urinary microbiota and the possible connection to delivery modes.

Some genera belonging to the phylum Firmicutes such as *Lactobacillus* sharply decreased in the PostD group, which is similar to the change in *Lactobacillus* shown in a previous study by Plichta et al. (2017) on the urinary microbiota in burn patients. In their study, the relative abundance of *Lactobacillus* continuously decreased after burn injury. Both cesarean section and burn injuries can lead to post-traumatic stress disorder (Lopez et al., 2017; Plichta et al., 2017). Post-traumatic stress disorder occurs more frequently in women following cesarean section than in women with normal delivery (Lopez et al., 2017). The elevated stress disorder can predict reduced estrogen level in women (Roney and Simmons, 2015). The postpartum period is

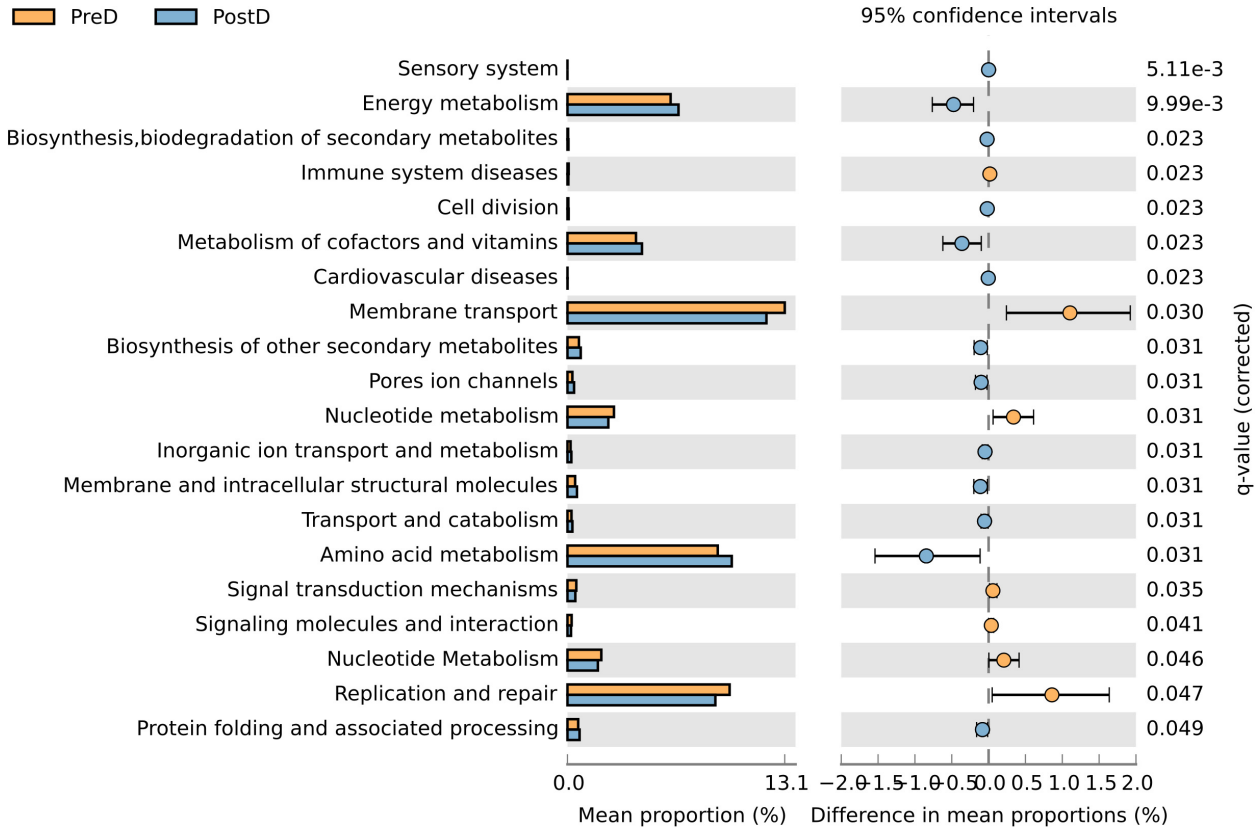

FIGURE 5 | Contributions of OTUs to known biological metabolic pathways. Functional analysis of urinary microbiota from the PreD and PostD groups. Microbial pathways predicted to be differentially regulated based on microbiome differences between the PreD (orange) and PostD (blue) groups. Upregulated pathways are represented by a higher mean proportion of expression. *q*-values are based on White's nonparametric *t*-test and corrected using the Story false discovery rate-controlling procedure.

associated with a significant decrease in estrogen (Nuriel-Ohayon et al., 2016), and the level of estrogen has been demonstrated to be responsible for the proportion of *Lactobacillus* in the bladder (Karstens et al., 2016). Post-delivery disturbances in the vaginal bacterial community, in terms of a decreased proportion of *Lactobacillus*, have also been demonstrated to occur. A study by Digiulio et al. found that *Lactobacillus* significantly decreased and was replaced by *Peptoniphilus*, *Prevotella*, and *Anaerococcus* after delivery (DiGiulio et al., 2015). These findings suggest that hormone alterations caused by delivery play an important role in regulating the microbiota, including the urinary microbiota and vaginal microbiota, after delivery (DiGiulio et al., 2015; Nuriel-Ohayon et al., 2016). Therefore, the alteration of urinary microbiota is not only attributed to cesarean section, but also to the hormonal changes associated with the cesarean section delivery mode. Proteobacteria increased in the PostD group compared to the PreD group and detectable bacterial families in the phylum Proteobacteria were mainly found in the PostD group, suggesting that it may play a role in postpartum diseases including infections. Emerging evidence has demonstrated that increases in the expression of genes associated with inflammatory disease coincide with expansion of Proteobacteria blooms (Miyasaka et al., 2013; Mizuta et al., 2016; Nagao-Kitamoto et al., 2016). For example, the genus *Pseudomonas* (which belongs to the phylum Proteobacteria) has been frequently found to be correlated with infections (Micek et al., 2005; Pobiega et al., 2016; Boutin et al., 2017). In our study, the bacterial order Pseudomonadales and genus *Pseudomonas* (which both belong to the phylum Proteobacteria) were distinguishing markers for PostD specimens. Several recent studies reported that Proteobacteria was frequently detected in subjects with asymptomatic sexually transmitted infection (Nelson et al., 2010), urgency urinary incontinence patients (Karstens et al., 2016), and UTI patients (Willner et al., 2014; Santiago-Rodriguez et al., 2015), indicating that Proteobacteria might play a role in complications in postpartum women. Yoo et al. (2016) reported that women who had undergone delivery had a lower abundance of *Pseudomonas* than non-pregnant women. We found that *Pseudomonas* was enriched in the PostD specimens; similar results were reported in a study by Toscano et al., 2017 who compared the vaginal microbiota between women with cesarean section and those who underwent vaginal delivery: women who underwent cesarean section had a higher abundance of *Pseudomonas* than women who delivered vaginally. The present results as well as those of Toscano et al. (2017) suggest that low levels of *Pseudomonas* may play a role

in maintaining the vaginal health and normal urinary functions of pregnant women, and that cesarean section might disrupt this balance.

Although 22 bacterial families were not found in the PreD group, they were detectable in the PostD group. Their function in the human urinary microbiota is unclear, as almost all of them have not previously been reported. Interestingly, Bacteroidaceae increased after cesarean section, which was similar to another urinary microbiota study on chronic prostatitis/chronic pelvic pain syndrome patients (Shoskes et al., 2016). In their study, Shoskes et al. (2016) reported that the urinary microbiota of patients with gastrointestinal symptoms was dominated by Bacteroidaceae (Shoskes et al., 2016). This suggests that Bacteroidaceae in the urinary microbiota is not indicative of health.

Ollberding et al. (2016) reported that the relative abundance of *Ruminococcus* was higher in women who underwent preterm delivery than normal delivery controls. In addition, Ling et al. (2017) noted that *Ruminococcus* could explain the presence of interleukin-8 in urine. Hence, the increased level of *Ruminococcus* spp. in our present study may be correlated with complications after cesarean section.

After delivery, the woman subjects initiated lactation. During the lactation stage, basal metabolic rates and mobilization of fat stores increase (Gunderson, 2014), which might be responsible for the strengthened energy metabolism in the PostD group. Interestingly, although women who underwent cesarean section would theoretically have had many complications, none the subjects in our present study had postpartum complications (except for back pain). This might be due to the higher proportion of pathways related to the metabolism of cofactors and vitamins resulting from the urinary microbiota alterations in the PostD group, as some vitamins (such as vitamins A, B, and C) play roles in boosting the immune system (Arigony et al., 2013). Notably, the pathway related to membrane transport proteins was reduced in the present study. This suggests that clinicians should consider taking measures to restore the membrane transport proteins, as they play important roles in cellular functions (Mishra et al., 2014), which are correlated with women's recovery after delivery (Groer et al., 2015). In addition, the pathway related to replication and repair was impaired after delivery, which suggests that tissue injury caused by cesarean section is correlated with urinary microbiota alteration, indicating that measures for balancing urinary microbiota dysbiosis may play a role in the recovery of postpartum women.

Limitations

The main limitation in our present study is the lack of control group. Therefore, it is hard to rule out the influences on urinary microbiota caused by hormonal changes correlated with delivery. We could not perform a case control study as it was impossible to collect urine specimens from pregnant women who did not need a cesarean section, because transurethral catheterization is an invasive procedure and it is unnecessary for women undergoing normal delivery. Importantly, performing transurethral catheterization in this population does not meet our ethical standards. Although midstream urine specimens are thought to be representative of the microbiota in the bladder, they are likely to contain traces of contaminating bacteria from the genital tract (Ainsworth, 2017), so we could not use midstream urine specimens. Thus, we could not use a case control study approach in the present study. There is an urgent need to design a non-invasive urine specimen collection technique in the future, which would be useful for comparing urinary microbiota alterations caused by various surgeries such as cesarean section, as the alterations might provide hints for preventing complications after surgery.

Another limitation is that the present study could not rule out the potential effects of anesthesia, which has been demonstrated to increase the abundance of *Ruminococcus* in horse fecal microbiota, 48 h after anesthesia (Schoster et al., 2016). Firstly, this limitation arose due to the inability to recruit women who had elected to receive epidural analgesia during labor, owing to widespread belief (among both pregnant women and health care providers in China) that epidural analgesia is harmful to the mother and baby (Hu et al., 2016). Secondly, catheterization was refused, even among women who elected to receive epidural analgesia. Thirdly, women exhibit high levels of lochia (vaginal discharge following delivery). It is difficult to obtain urine samples in which lochia is absent, as participants refused to undergo sample collection procedures owing to the discomfort involved. Finally, it is difficult to disinfect the perineum area because the flow of lochia; as a result, the collection of uncontaminated urine samples was difficult to achieve.

In addition, our present study only explored the urinary microbiota changes caused by cesarean section. Future work needs to be focused on animal models to explain why cesarean section leads to the alterations, which might be helpful to guide clinicians to take more specific measures to prevent urinary microbiota-related disease.

CONCLUSION

To our knowledge, this is the first study investigating the alterations in bladder microbiota caused by cesarean section. Firstly, women's urinary microbiota is significantly altered before and after delivery. It is valuable to note that pathogenic bacteria dramatically increased in the PostD group compared to the PreD group; therefore, clinicians should consider therapy for women who have given birth to depress the growth of bladder pathogens, which might be helpful to prevent postpartum complications such as infections. Secondly, the changes in the metabolic pathways reflected the composition of the urinary microbiota, which might be useful information for clinicians investigating the etiological factors of metabolic disease in postpartum women. Future work using a larger sample size is needed to confirm this result and future work is needed to explore how the alteration of urinary microbiota leads to changes in metabolic pathways in postpartum women. Finally, alterations in the PostD group may be responsible for postpartum symptoms including back pain. Thus, regulation of the urinary microbiota is a potential new therapy to control back pain in postpartum women.

AUTHOR CONTRIBUTIONS

YC and WW conceived and designed the study. FL generated the sequencing data. FL and LL collected the samples. HJ and RY conducted the urine culturing. SD and FL extracted the bacterial DNA. LL, LC, and FL analyzed the data. FL carried out the computational analysis. YC interpreted the data. FL and YC drafted the manuscript.

FUNDING

This study was supported by the Health and Family Planning Commission of Zhejiang Province (grant no: 2018ZD006).

ACKNOWLEDGMENTS

We gratefully acknowledge the volunteers who participated in our study. We also thank the Charlesworth Group for language editing the manuscript.

SUPPLEMENTARY MATERIAL

The Supplementary Material for this article can be found online at: https://www.frontiersin.org/articles/10.3389/fmicb.2018.02193/full#supplementary-material

FIGURE S1 | Bacterial family profile. Top 10 most abundant bacterial families in the PreD and PostD groups. PreD means pre-delivery and PostD means post-delivery.

FIGURE S2 | Bacterial family differences. Bacterial genera showing significant differences in relative abundance between the PreD and PostD groups. PreD means pre-delivery and PostD means post-delivery.

FIGURE S3 | Cladogram of differentially abundant microbiota taxa. **(A)** LEfSe cladogram showing the most differentially abundant taxa between the PreD and PostD groups. Taxonomic cladogram obtained from LEfSe analysis of 16S rRNA sequences. Blue and red represents taxa enriched in the PreD and PostD groups, respectively. The brightness of each dot is proportional to its effect size. **(B)** Only taxa meeting an LDA threshold > 2.0 are shown. PreD means pre-delivery and PostD means post-delivery.

TABLE S1 | Relative abundance of bacterial phyla in the PreD and PostD groups.

TABLE S2 | Presence of bacterial families.

REFERENCES

Abernethy, M. G., Rosenfeld, A., White, J. R., Mueller, M. G., Lewicky-Gaupp, C., and Kenton, K. (2017). Urinary microbiome and cytokine levels in women with interstitial cystitis. *Obstet. Gynecol.* 129, 500–506. doi: 10.1097/AOG.0000000000001892

Ainsworth, C. (2017). Microbiome: a bag of surprises. *Nature* 551, S40–S41. doi: 10.1038/551S40a

Aragon, I. M., Herrera-Imbroda, B., Queipo-Ortuno, M. I., Castillo, E., Del, M. J., Gomez-Millan, J., et al. (2016). The urinary tract microbiome in health and disease. *Eur. Urol. Focus* 4, 128–138. doi: 10.1016/j.euf.2016.11.001

Arigony, A. L. V., de Oliveira, I. M., Machado, M., Bordin, D. L., Bergter, L., Prá, D., et al. (2013). The influence of micronutrients in cell culture: a reflection on viability and genomic stability. *Biomed Res. Int.* 2013: 597282. doi: 10.1155/2013/597282

Benner, A. (1999). Sample size tables for clinical studies. *Stat. Med.* 18, 494–495. doi: 10.1002/(SICI)1097-0258(19990228)18:4<494::AID-SIM56>3.0.CO;2-T

Boutin, S., Graeber, S. Y., Stahl, M., Dittrich, A. S., Mall, M. A., and Dalpke, A. H. (2017). Chronic but not intermittent infection with *Pseudomonas aeruginosa* is associated with global changes of the lung microbiome in cystic fibrosis. *Eur. Respir. J.* 50:1701086. doi: 10.1183/13993003.01086-2017

Caporaso, J. G., Kuczynski, J., Stombaugh, J., Bittinger, K., Bushman, F. D., Costello, E. K., et al. (2010). QIIME allows analysis of high-throughput community sequencing data. *Nat. Methods* 7, 335–336. doi: 10.1038/nmeth.f.303

Chen, H., and Jiang, W. (2014). Application of high-throughput sequencing in understanding human oral microbiome related with health and disease. *Front. Microbiol.* 5:508. doi: 10.3389/fmicb.2014.00508

Chu, D. M., Ma, J., Prince, A. L., Antony, K. M., Seferovic, M. D., and Aagaard, K. M. (2017). Maturation of the infant microbiome community structure and function across multiple body sites and in relation to mode of delivery. *Nat. Med.* 23, 314–326. doi: 10.1038/nm.4272

DiGiulio, D. B., Callahan, B. J., McMurdie, P. J., Costello, E. K., Lyell, D. J., Robaczewska, A., et al. (2015). Temporal and spatial variation of the human microbiota during pregnancy. *Proc. Natl. Acad. Sci. U.S.A.* 112, 11060–11065. doi: 10.1073/pnas.1502875112

Dominguez-Bello, M. G., Costello, E. K., Contreras, M., Magris, M., Hidalgo, G., Fierer, N., et al. (2010). Delivery mode shapes the acquisition and structure of the initial microbiota across multiple body habitats in newborns. *Proc. Natl. Acad. Sci. U.S.A.* 107, 11971–11975. doi: 10.1073/pnas.1002601107

Gill, S. R., Pop, M., Deboy, R. T., Eckburg, P. B., Turnbaugh, P. J., Samuel, B. S., et al. (2006). Metagenomic analysis of the human distal gut microbiome. *Science* 312, 1355–1359. doi: 10.1126/science.1124234

Gottschick, C., Deng, Z. L., Vital, M., Masur, C., Abels, C., Pieper, D. H., et al. (2017). The urinary microbiota of men and women and its changes in women during bacterial vaginosis and antibiotic treatment. *Microbiome* 5:99. doi: 10.1186/s40168-017-0305-3

Groer, M. E., Jevitt, C., and Ji, M. (2015). Immune changes and dysphoric moods across the postpartum. *Am. J. Reprod. Immunol.* 73, 193–198. doi: 10.1111/aji.12322

Gunderson, E. P. (2014). Impact of breastfeeding on maternal metabolism: implications for women with gestational diabetes. *Curr. Diabetes Rep.* 14:460. doi: 10.1007/s11892-013-0460-2

Howard, B. M., Kornblith, L. Z., Christie, S. A., Conroy, A. S., Nelson, M. F., Campion, E. M., et al. (2017). Characterizing the gut microbiome in trauma: significant changes in microbial diversity occur early after severe injury. *Trauma Surg. Acute Care Open* 2:e108. doi: 10.1136/tsaco-2017-000108

Hu, L., Flood, P., Li, Y., Tao, W., Zhao, P., Xia, Y., et al. (2016). No pain labor & delivery. *Anesth. Analg.* 122, 1931–1938. doi: 10.1213/ANE.0000000000001328

Hung, H. W., Yang, P. Y., Yan, Y. H., Jou, H. J., Lu, M. C., and Wu, S. C. (2016). Increased postpartum maternal complications after cesarean section compared with vaginal delivery in 225 304 Taiwanese women. *J. Matern. Fetal Neonatal Med.* 29, 1665–1672. doi: 10.3109/14767058.2015.1059806

Jakobsson, H. E., Abrahamsson, T. R., Jenmalm, M. C., Harris, K., Quince, C., Jernberg, C., et al. (2014). Decreased gut microbiota diversity, delayed Bacteroidetes colonisation and reduced Th1 responses in infants delivered by Caesarean section. *Gut* 63, 559–566. doi: 10.1136/gutjnl-2012-303249

Karstens, L., Asquith, M., Davin, S., Stauffer, P., Fair, D., Gregory, W. T., et al. (2016). Does the urinary microbiome play a role in urgency urinary incontinence and its severity? *Front. Cell. Infect. Microbiol.* 6:78. doi: 10.3389/fcimb.2016.00078

Koren, O., Goodrich, J. K., Cullender, T. C., Spor, A., Laitinen, K., Kling Bäckhed, H., et al. (2012). Host remodeling of the gut microbiome and metabolic changes during pregnancy. *Cell* 150, 470–480. doi: 10.1016/j.cell.2012.07.008

Langille, M. G., Zaneveld, J., Caporaso, J. G., McDonald, D., Knights, D., Reyes, J. A., et al. (2013). Predictive functional profiling of microbial communities using 16S rRNA marker gene sequences. *Nat. Biotechnol.* 31, 814–821. doi: 10.1038/nbt.2676

Legione, A. R., Amery-Gale, J., Lynch, M., Haynes, L., Gilkerson, J. R., Sansom, F. M., et al. (2018). Variation in the microbiome of the urogenital tract of

Chlamydia-free female koalas (*Phascolarctos cinereus*) with and without 'wet bottom'. *PLoS One* 13:e194881. doi: 10.1371/journal.pone.0194881

Leth, R. A., Moller, J. K., Thomsen, R. W., Uldbjerg, N., and Norgaard, M. (2009). Risk of selected postpartum infections after cesarean section compared with vaginal birth: a five-year cohort study of 32,468 women. *Acta Obstet. Gynecol. Scand.* 88, 976–983. doi: 10.1080/00016340903147405

Ling, Z., Liu, F., Shao, L., Cheng, Y., and Li, L. (2017). Dysbiosis of the urinary microbiota associated with urine levels of proinflammatory chemokine interleukin-8 in female type 2 diabetic patients. *Front. Immunol.* 8:1032. doi: 10.3389/fimmu.2017.01032

Liu, D., Yu, J., Li, L., Ai, Q., Feng, J., Song, C., et al. (2015). Bacterial community structure associated with elective cesarean section versus vaginal delivery in Chinese newborns. *J. Pediatr. Gastroenterol. Nutr.* 60, 240–246. doi: 10.1097/MPG.0000000000000606

Logares, R., Audic, S., Bass, D., Bittner, L., Boutte, C., Christen, R., et al. (2014). Patterns of rare and abundant marine microbial eukaryotes. *Curr. Biol.* 24, 813–821. doi: 10.1016/j.cub.2014.02.050

Lopez, U., Meyer, M., Loures, V., Iselin-Chaves, I., Epiney, M., Kern, C., et al. (2017). Post-traumatic stress disorder in parturients delivering by caesarean section and the implication of anaesthesia: a prospective cohort study. *Health Qual. Life Outcomes* 15:118. doi: 10.1186/s12955-017-0692-y

MacIntyre, D. A., Chandiramani, M., Lee, Y. S., Kindinger, L., Smith, A., Angelopoulos, N., et al. (2015). The vaginal microbiome during pregnancy and the postpartum period in a European population. *Sci. Rep.* 5:8988. doi: 10.1038/srep08988

Magoc, T., and Salzberg, S. L. (2011). FLASH: fast length adjustment of short reads to improve genome assemblies. *Bioinformatics* 27, 2957–2963. doi: 10.1093/bioinformatics/btr507

Micek, S. T., Lloyd, A. E., Ritchie, D. J., Reichley, R. M., Fraser, V. J., and Kollef, M. H. (2005). *Pseudomonas aeruginosa* bloodstream infection: importance of appropriate initial antimicrobial treatment. *Antimicrob. Agents Chemother.* 49, 1306–1311. doi: 10.1128/AAC.49.4.1306-1311.2005

Mishra, N. K., Chang, J., and Zhao, P. X. (2014). Prediction of membrane transport proteins and their substrate specificities using primary sequence information. *PLoS One* 9:e100278. doi: 10.1371/journal.pone.0100278

Miyasaka, E. A., Feng, Y., Poroyko, V., Falkowski, N. R., Erb-Downward, J., Gillilland, M. R., et al. (2013). Total parenteral nutrition-associated lamina propria inflammation in mice is mediated by a MyD88-dependent mechanism. *J. Immunol.* 190, 6607–6615. doi: 10.4049/jimmunol.1201746

Mizuta, M., Endo, I., Yamamoto, S., Inokawa, H., Kubo, M., Udaka, T., et al. (2016). Perioperative supplementation with bifidobacteria improves postoperative nutritional recovery, inflammatory response, and fecal microbiota in patients undergoing colorectal surgery: a prospective, randomized clinical trial. *Biosci. Microbiota Food Health* 35, 77–87. doi: 10.12938/bmfh.2015-017

Nagao-Kitamoto, H., Shreiner, A. B., Gillilland, M. G., Kitamoto, S., Ishii, C., Hirayama, A., et al. (2016). Functional characterization of inflammatory bowel disease-associated gut dysbiosis in gnotobiotic mice. *Cell. Mol. Gastroenterol. Hepatol.* 2, 468–481. doi: 10.1016/j.jcmgh.2016.02.003

Nelson, D. E., Van Der Pol, B., Dong, Q., Revanna, K. V., Fan, B., Easwaran, S., et al. (2010). Characteristic male urine microbiomes associate with asymptomatic sexually transmitted infection. *PLoS One* 5:e14116. doi: 10.1371/journal.pone.0014116

Neuman, H., Debelius, J. W., Knight, R., and Koren, O. (2015). Microbial endocrinology: the interplay between the microbiota and the endocrine system. *FEMS Microbiol. Rev.* 39, 509–521. doi: 10.1093/femsre/fuu010

Nuriel-Ohayon, M., Neuman, H., and Koren, O. (2016). Microbial changes during pregnancy, birth, and infancy. *Front. Microbiol.* 7:1031. doi: 10.3389/fmicb.2016.01031

Ollberding, N. J., Volgyi, E., Macaluso, M., Kumar, R., Morrow, C., Tylavsky, F. A., et al. (2016). Urinary microbiota associated with preterm birth: results from the conditions affecting neurocognitive development and learning in early childhood (CANDLE) study. *PLoS One* 11:e162302. doi: 10.1371/journal.pone.0162302

Pearce, M. M., Hilt, E. E., Rosenfeld, A. B., Zilliox, M. J., Thomas-White, K., Fok, C., et al. (2014). The female urinary microbiome: a comparison of women with and without urgency urinary incontinence. *mBio* 5:e01283-14. doi: 10.1128/mBio.01283-14

Plichta, J. K., Holmes, C. J., Nienhouse, V., Puszynski, M., Gao, X., Dong, Q., et al. (2017). Cutaneous burn injury modulates urinary antimicrobial peptide responses and the urinary microbiome. *Crit. Care Med.* 45, e543–e551. doi: 10.1097/CCM.0000000000002304

Pobiega, M., Maciag, J., Pomorska-Wesolowska, M., Chmielarczyk, A., Romaniszyn, D., Ziolkowski, G., et al. (2016). Urinary tract infections caused by *Pseudomonas aeruginosa* among children in Southern Poland: virulence factors and antibiotic resistance. *J. Pediatr. Urol.* 12, 31–36. doi: 10.1016/j.jpurol.2015.05.034

Rognes, T., Flouri, T., Nichols, B., Quince, C., and Mahe, F. (2016). VSEARCH: a versatile open source tool for metagenomics. *PeerJ* 4:e2584. doi: 10.7717/peerj.2584

Roney, J. R., and Simmons, Z. L. (2015). Elevated psychological stress predicts reduced estradiol concentrations in young women. *Adapt. Hum. Behav. Physiol.* 1, 30–40. doi: 10.1007/s40750-014-0004-2

Ryding, E. L., Wijma, B., and Wijma, K. (1997). Posttraumatic stress reactions after emergency cesarean section. *Acta Obstet. Gynecol. Scand.* 76, 856–861. doi: 10.3109/00016349709024365

Santiago-Rodriguez, T. M., Ly, M., Bonilla, N., and Pride, D. T. (2015). The human urine virome in association with urinary tract infections. *Front. Microbiol.* 6:14. doi: 10.3389/fmicb.2015.00014

Schoster, A., Mosing, M., Jalali, M., Staempfli, H. R., and Weese, J. S. (2016). Effects of transport, fasting and anaesthesia on the faecal microbiota of healthy adult horses. *Equine Vet. J.* 48, 595–602. doi: 10.1111/evj.12479

Shoskes, D. A., Altemus, J., Polackwich, A. S., Tucky, B., Wang, H., and Eng, C. (2016). The urinary microbiome differs significantly between patients with chronic prostatitis/chronic pelvic pain syndrome and controls as well as between patients with different clinical phenotypes. *Urology* 92, 26–32. doi: 10.1016/j.urology.2016.02.043

Shrestha, E., White, J. R., Yu, S. H., Kulac, I., Ertunc, O., De Marzo, A. M., et al. (2018). Profiling the urinary microbiome in men with positive versus negative biopsies for prostate cancer. *J. Urol.* 199, 161–171. doi: 10.1016/j.juro.2017.08.001

Siddiqui, H., Lagesen, K., Nederbragt, A. J., Jeansson, S. L., and Jakobsen, K. S. (2012). Alterations of microbiota in urine from women with interstitial cystitis. *BMC Microbiol.* 12:205. doi: 10.1186/1471-2180-12-205

Thomas-White, K., Forster, S. C., Kumar, N., Van Kuiken, M., Putonti, C., Stares, M. D., et al. (2018). Culturing of female bladder bacteria reveals an interconnected urogenital microbiota. *Nat. Commun.* 9:1557. doi: 10.1038/s41467-018-03968-5

Toscano, M., De Grandi, R., Peroni, D. G., Grossi, E., Facchin, V., Comberiati, P., et al. (2017). Impact of delivery mode on the colostrum microbiota composition. *BMC Microbiol.* 17:205. doi: 10.1186/s12866-017-1109-0

Vasudevan, R. (2014). Urinary tract infection: an overview of the infection and the associated risk factors. *J. Microbiol. Exp.* 1:8. doi: 10.15406/jmen.2014.01.00008

Vernocchi, P., Del Chierico, F., Quagliariello, A., Ercolini, D., Lucidi, V., and Putignani, L. A. (2017). Metagenomic and in silico functional prediction of gut microbiota profiles may concur in discovering new cystic fibrosis patient-targeted probiotics. *Nutrients* 9:1342. doi: 10.3390/nu9121342

Vincent, A., Ayzac, L., Girard, R., Caillat-Vallet, E., Chapuis, C., Depaix, F., et al. (2008). Downward trends in surgical site and urinary tract infections after cesarean delivery in a French surveillance network, 1997-2003. *Infect. Control Hosp. Epidemiol.* 29, 227–233. doi: 10.1086/527512

Willner, D., Low, S., Steen, J. A., George, N., Nimmo, G. R., Schembri, M. A., et al. (2014). Single clinical isolates from acute uncomplicated urinary tract infections are representative of dominant in situ populations. *mBio* 5:e01064-13. doi: 10.1128/mBio.01064-13

Yang, X., and Sun, S. (2017). Comparison of maternal and fetal complications in elective and emergency cesarean section: a systematic review and meta-analysis. *Arch. Gynecol. Obstet.* 296, 503–512. doi: 10.1007/s00404-017-4445-2

Ye, J., Zhang, J., Mikolajczyk, R., Torloni, M. R., Gülmezoglu, A. M., and Betran, A. P. (2016). Association between rates of caesarean section and maternal and neonatal mortality in the 21st century: a worldwide population-based ecological

study with longitudinal data. *Arch. Gynecol. Obstet.* 123, 745–753. doi: 10.1111/1471-0528.13592

Yoo, J. Y., Rho, M., You, Y. A., Kwon, E. J., Kim, M. H., Kym, S., et al. (2016). 16S rRNA gene-based metagenomic analysis reveals differences in bacteria-derived extracellular vesicles in the urine of pregnant and non-pregnant women. *Exp. Mol. Med.* 48:e208. doi: 10.1038/emm.2015.110

Zakerihamidi, M., Latifnejad, R. R., and Merghati, K. E. (2015). Vaginal delivery vs. cesarean section: a focused ethnographic study of women's perceptions in the north of Iran. *Int. J. Community Based Nurs. Midwifery* 3, 39–50.

Conflict of Interest Statement: The authors declare that the research was conducted in the absence of any commercial or financial relationships that could be construed as a potential conflict of interest.

Copyright © 2018 Liu, Lv, Jiang, Yan, Dong, Chen, Wang and Chen. This is an open-access article distributed under the terms of the Creative Commons Attribution License (CC BY). The use, distribution or reproduction in other forums is permitted, provided the original author(s) and the copyright owner(s) are credited and that the original publication in this journal is cited, in accordance with accepted academic practice. No use, distribution or reproduction is permitted which does not comply with these terms.

frontiers in Microbiology

REVIEW
published: 25 September 2018
doi: 10.3389/fmicb.2018.02247

The Gut Microbiota in the Pathogenesis and Therapeutics of Inflammatory Bowel Disease

Tao Zuo [1,2] *and Siew C. Ng* [1,2]*

[1] *Department of Medicine and Therapeutics, Institute of Digestive Disease, LKS Institute of Health Science, The Chinese University of Hong Kong, Hong Kong, China,* [2] *Faculty of Medicine, Center for Gut Microbiota Research, The Chinese University of Hong Kong, Hong Kong, China*

In the twenty first century, the changing epidemiology of inflammatory bowel disease (IBD) globally with increasing disease incidence across many countries relates to the altered gut microbiota, due to a combinatorial effect of environmental factors, human immune responses and genetics. IBD is a gastrointestinal disease associated with a gut microbial dysbiosis, including an expansion of facultative anaerobic bacteria of the family Enterobacteriaceae. Advances in high-throughput sequencing enable us to entangle the gut microbiota in human health and IBD beyond the gut bacterial microbiota, expanding insights into the mycobiota, virobiota and helminthes. *Caudovirales* (viruses) and *Basidiomycota*, *Ascomycota*, and *Candida albicans* (fungi) are revealed to be increased in IBD. The deconvolution of the gut microbiota in IBD lays the basis for unveiling the roles of these various gut microbiota components in IBD pathogenesis and being conductive to instructing on future IBD diagnosis and therapeutics. Here we comprehensively elucidate the alterations in the gut microbiota in IBD, discuss the effect of diets in the gut microbiota in relation to IBD, and illustrate the potential of manipulation of gut microbiota for IBD therapeutics. The therapeutic strategy of antibiotics, prebiotics, probiotics and fecal microbiota transplantation will benefit the effective application of precision microbiome manipulation in IBD.

Keywords: gut microbiota, bacteria, virobiota, mycobiota, helminths, diet, inflammatory bowel disease, fecal microbiota transplantation

OPEN ACCESS

Edited by:
Learn-Han Lee,
Monash University Malaysia, Malaysia

Reviewed by:
Maryam Dadar,
Razi Vaccine and Serum Research Institute, Iran
Hui-min Neoh,
UKM Medical Molecular Biology Institute (UMBI), Malaysia
Wei Li Thong,
University of Manchester, United Kingdom

***Correspondence:**
Siew C. Ng
siewchienng@cuhk.edu.hk

Specialty section:
This article was submitted to Microbial Symbioses, a section of the journal Frontiers in Microbiology

Received: *20 February 2018*
Accepted: *03 September 2018*
Published: *25 September 2018*

Citation:
Zuo T and Ng SC (2018) The Gut Microbiota in the Pathogenesis and Therapeutics of Inflammatory Bowel Disease. Front. Microbiol. 9:2247. doi: 10.3389/fmicb.2018.02247

INTRODUCTION

Inflammatory bowel diseases (IBD), including Crohn's disease (CD) and ulcerative disease (UC), are proposed to result from an inappropriate immune response to the gut microbes in a genetically susceptible host. It is a chronic inflammatory disorder of the intestinal tract of an unknown cause. The incidence of IBD has increased in the western world since the midst of the twentieth century (Molodecky et al., 2012; Rocchi et al., 2012; Hammer et al., 2016). At the turn of the twenty-first century, it plateaued in some developed nations with a prevalence of up to 0.5% of the general population, while it is continuing to rise in developing nations (Benchimol et al., 2009, 2014; Kaplan, 2015). Etiological studies on IBD have centered on several factors, including host genetics and immune responses, the gut microbiota, and the importance of environmental stimuli in disease

pathogenesis (**Figure 1**). Gut dysbiosis has been consistently shown to be associated with IBD. Due to the expansion in application of high-throughput deep sequencing technology in the past decade, we are able to gradually unveiling the role of the microbiome in development of IBD. These findings have improved our knowledge on the functional mechanisms of the microbiome in the pathogenesis of IBD.

The gut microbiota, comprising bacteria, fungi, viruses, and other microorganisms, operate as a secondary organ system with critical functions to the host. IBD is amongst the most extensively studied of all inflammatory diseases that are closely associated with the gut microbiome. In this review, we discuss the role of the gut microbiota, including the bacterial microbiota, mycobiota and virobiota in the development of IBD as well as microbiota-based therapeutic approaches in the treatment of IBD.

GUT MICROBIOME AND INFLAMMATORY BOWEL DISEASE (IBD)

Bacterial Microbiota

Bacterial microbiota is the most well-studied component of the gut microbiota, which inhabit its host in variable concentrations. In the gastrointestinal (GI) tract, it reaches an upper level in the colon of 10^{11} or 10^{12} cells/g of luminal contents (Dave et al., 2012). It was estimated that our gut contains ∼1,000 bacterial species and 100-fold more genes than that found in the human genome (Ley et al., 2006; Qin et al., 2010). This bacterial community performs a diversity of important functions in the host, including educating the immune system (Round and Mazmanian, 2009), secreting enzymes for digesting substrates inaccessible to the host (El Kaoutari et al., 2013), and repressing detrimental microorganisms (O'Hara and Shanahan, 2006). Overall, the phyla *Firmicutes*, *Bacteroidetes*, *Actinobacteria* and *Verrucomicrobia* are the predominant constituents in the healthy gut microbiota (Jandhyala et al., 2015). The gut bacterial microbiome exhibit differences with regard to both the mucosal-to-luminal and proximal-to-distal gradients, displaying substantial variations between individuals (Turnbaugh et al., 2009; Qin et al., 2010; Bäckhed et al., 2012). The gut bacterial microbiota develops from a low diverse community at birth into a highly complex community with the introduction of diets by 9–12 months of age (Koenig et al., 2011; Backhed et al., 2015). The microbiota becomes stable and resilient to environmental perturbations, such as dietary changes or short-term antibiotic exposure (Dethlefsen and Relman, 2011; Wu et al., 2011). A multitude of factors have been shown to intervene with the gut microbiome, including age, genetics, diet and drugs (Yatsunenko et al., 2012; Maier et al., 2018; Zuo et al., 2018).

Gut microbes were demonstrated to be an essential factor in intestinal inflammation in IBD (Tamboli et al., 2004; Sartor, 2008). Some studies suggest that dysbiosis occur in IBD (Frank et al., 2007; Casen et al., 2015; Putignani et al., 2016; Halfvarson et al., 2017), and a broad microbial alteration pattern was revealed including reduction in diversity, decreased abundances of bacterial taxa within the Phyla *Firmicutes* and *Bacteroides*, and increases in the *Gammaproteobacteria* (**Table 1**; Frank et al., 2011; Morgan et al., 2012). In IBD, it has been consistently shown that there is a decrease in biodiversity, knowingly α diversity, and in species richness, a measure of the total number of species in a community. Patients with CD exhibited a reduced α diversity in the fecal microbiome, compared with healthy controls (Manichanh et al., 2006), and similar findings were found in monozygotic twins discordant for CD (Dicksved et al., 2008). This decreased diversity was partly linked to the temporal instability of the dominant taxa in IBD (Martinez et al., 2008). There is also reduced diversity in inflamed vs. non-inflamed tissues even within the same patient, and a lower bacterial load was observed at the inflamed regions in CD patients (Sepehri et al., 2007). A multicenter study that they investigated >1,000 treatment-naïve pediatric CD samples collected from multiple concurrent gastrointestinal locations (Gevers et al., 2014). They found that changes in bacteria, including increased *Veillonellaceae*, *Pasteurellacaea*, *Enterobacteriaceae*, and *Fusobacteriaceae*, and decreased *Bacteroidales*, *Erysipelotrichales*, and *Clostridiale*s, strongly correlated with disease status. This study also showed that rectal mucosa-associated microbiome profiling offered a feasible biomarker for the diagnosis of CD at the early stage of disease.

Human studies have shown that abundance of specific bacteria taxa were altered in IBD (**Table 1**). *Enterobacteriacae* bacteria are augmented both in patients with IBD and in mice (Lupp et al., 2007). *Escherichia coli*, particularly adherent-invasive *E. coli* (AIEC) strains, were isolated from ileal CD biopsies (Darfeuille-Michaud et al., 2004) and were also found in UC patients (Sokol et al., 2006). Meanwhile, mucosal samples showed more pronounced enrichment than fecal samples (Chassaing and Darfeuille-Michaud, 2011). It indicates that the inflammatory environment in IBD may favor the growth of this bacterial clade, *Enterobacteriaceae*. Anti-inflammatory drug, mesalamine, could attenuate intestinal inflammation and decrease the abundance of *Escherichia*/*Shigella* in IBD (Benjamin et al., 2012; Morgan et al., 2012).

Fusobacteria is another clade of adherent and invasive bacteria. Bacteria of the genus *Fusobacterium* principally colonize both the oral cavity and the gut. *Fusobacterium* species were present at a higher abundance in the colonic mucosa of patients with UC compared to healthy controls (Ohkusa et al., 2002, 2009). When administered by rectal enema in mice, *Fusobacterium varium* was able to cause colonic mucosal inflammation (Ohkusa et al., 2003). The invasive ability of human *Fusobacterium* bacteria correlate positively with host IBD severity (Strauss et al., 2011), indicating that invasive *Fusobacterium* species may impact IBD pathology. Beyond that, *Fusobacterium* species were documented to be abundantly present in tumor than in adjacent normal tissue in colorectal cancer (Castellarin et al., 2012; Kostic et al., 2012; Yu et al., 2017). Besides, human *Fusobacterium* isolates were reported to have a tumorigenesis role in mice (Kostic et al., 2013).

There are also specific groups of gut bacteria that may play a protective role against IBD. A range of bacterial species, most notably the genera *Lactobacillus*, *Bifidobacterium*, and

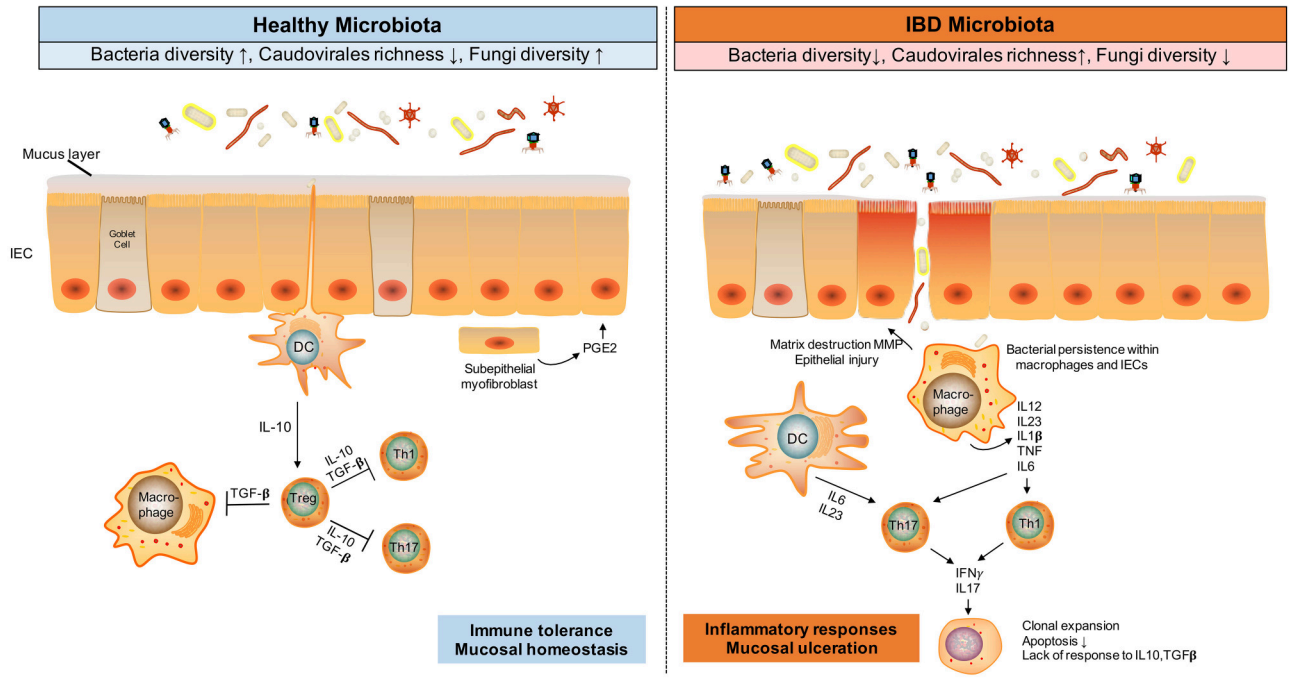

FIGURE 1 | Gut microbiota alteration and immune responses in IBD. The gut microbes, including bacteria, viruses and fungi, and dysfunctional immune responses, engaging Tregs, T-helper 1 (Th1), and Th17, are implicated in IBD pathogenesis. During homestasis, gut microbes induce an immune tolerance phenotype in the host, whilst in inflammatory conditions like IBD, antigens from dysbiotic microbes activate Th1 and Th17 cells, resulting in tissue injury, decreased mucus layer, and microbial penetration and persistence in the intestinal tissues. This mucosal injury results in further uptake of microbial antigens, TLR ligands, and viable organisms that perpetuate the immune responses. TGF, transforming growth factor; TGF, transforming growth factor; MMP, matrix metalloproteinase; DC, dendritic cell.

Faecalibacterium, have been shown to be protective of the host from mucosal inflammation via several mechanisms, including the stimulation of the anti-inflammatory cytokine (Sokol et al., 2008), including IL-10 and down-regulation of inflammatory cytokines (Llopis et al., 2009). *Faecalibacterium prausnitzii*, has been shown to have anti-inflammatory properties and was undererrepresented in IBD (Sokol et al., 2009). The abundance of *F. prausnitzii* is significantly decreased while the abundance of *E. coli* is increased in ileal biopsies of CD specimens (Willing et al., 2009). CD patients with low abundances of *F. prausnitzii* in the mucosa are more likely have relapse after surgery (Sokol et al., 2008). In contrast, restoration of *F. prausnitzii* after recurrence is associated with maintenance of clinical remission of UC (Varela et al., 2013). Epidemiological data in humans suggested a protective effect of *Helicobacter pylori* (*H. pylori*) infection against the development of autoimmune diseases, including IBD (Papamichael et al., 2014; Rokkas et al., 2015). Laboratory data demonstrated that *H. pylori* could induce immune tolerance and limit inflammatory responses (Arnold et al., 2011; Oertli and Müller, 2012; Oertli et al., 2012).

In chemically-induced mice with colitis, the colitis phenotype is more severe in germ-free mice than in conventionally reared mice (Kitajima et al., 2001). The commensal microbes protect the host via colonization resistance, where commensals occupy niches within the host and prevent invasion by pathogens (Callaway et al., 2008), outcompete pathogenic bacteria (Kamada et al., 2012). Commensals have also showed functional effects on pathogens, such as dampening virulence-related gene expression (Medellin-Pena et al., 2007). In addition, the gut microbiota can modulate the host mucosal immune response. *Clostridium* and *Bacteroides* species could induce the expansion of regulatory T cells (Treg) and to mitigate intestinal inflammation (Atarashi et al., 2013). Other gut bacterial members can alleviate mucosal inflammation by regulating NF-κB activation (Kelly et al., 2004).

Some members of the gut microbiota have the ability to ferment dietary fiber resulting in the production of short-chain fatty acids (SCFAs), including acetate, propionate, and butyrate. SCFAs have been shown to exert multiple beneficial effects on mammalian energy metabolism. They are the primary energy source for colonic epithelial cells (Ahmad et al., 2000) and can induce the expansion of colonic Treg cells (Atarashi et al., 2013; Smith et al., 2013). The butyrate-producing genus *Faecalibacterium*, which belonged to *Ruminococcaceae*, is decreased in IBD, especially in ileal CD (Sokol et al., 2008, 2009; Xenoulis et al., 2008; Kang et al., 2010; Morgan et al., 2012). Other SCFA-producing bacteria, *Phascolarctobacterium* and *Roseburia* are also reduced in CD, whilst *Leuconostocaceae* is depleted in UC (Morgan et al., 2012). The gut microbiota co-evolves with the polysaccharide-rich diet, to synergistically enable the host efficiently extract energy from dietary fiber and protect them from inflammation (Willing et al., 2009). Lack of dietary fiber intake has been associated with the development of IBD (Galvez

TABLE 1 | Altered gut microbiota in IBD compared to healthy individuals in humans.

	Decreased in IBD	Increased in IBD
Microbial composition	*Bifidobacterium* sp.	*Proteobacteria*
	Groups IV and XIVA Clostridium	*Escherichia coli*, adherent/invasivea
	Faecalibacterium prausnitzii	*Fusobacterium* species
	Roseburia species	*Ruminococcus gnavusa*
	Suterella species	*Pasteurellaceae*
	Bacteroides	*Veillonellaceae*
	Saccharomyces cerevisiae	*Caudovirales*
		Clavispora lusitaniae
		Kluyveromyces marxianus
		Candida albicans
		Candida tropicalis
		Cyberlindnera jadinii
Microbial function	SCFAs, butyrate	Auxotrophy
	Butanoate and propanoate metabolism	Amino acid transport
		Sulfate transport
	Amino acid biosynthesis	Oxidative stress
		Type II secretion system
		Secretion of toxins

et al., 2005; Chiba et al., 2015; Pituch-Zdanowska et al., 2015). In addition, low fiber diet is associated with a low concentration of SCFAs (Galvez et al., 2005; Maslowski and Mackay, 2011).

Fungal Microbiota (Mycobiota)

Fungi represent only a minor constituent of the gut microbiota and account for <0.1% of the total microbes (Qin et al., 2010). This may be an underestimation due to our current challenge to annotate fungi as a result of an incomplete fungal genomic database (Underhill and Iliev, 2014). Nevertheless, target region sequencing of marker genes, such as internal transcribed spacer (ITS) and 18S rRNA, mapping to annotated databases has contributed to an improved understanding of the mycobiota in the gut (Qin et al., 2010).

Fungi vary in composition at different body sites in humans (Underhill and Iliev, 2014). The GI tract, urogenital tract and oral cavity have the largest proportion of the taxa of the *Candida* genus which comprises up to 160 species (Soll et al., 1991; Huffnagle and Noverr, 2013). Species-specific colonization patterns of *Candida* are observed in mammals. *Candida albicans*, *C. parapsilosis* and *C. blabrata* are common in humans whereas *C. tropicalis* predominates in mice (Underhill and Iliev, 2014). In contrary to the relative stability of the bacterial microbiota over time, the mouse gut mycobiota have been observed to vary over time among mouse reared in cages suggesting an environmental influence on the gut fungi (Dollive et al., 2013). Competition between gut bacteria and fungi was observed. In humans and mice, a relatively long-term use of antibiotics can promote fungal overgrowth and infection (Noverr et al., 2004; Dollive et al., 2013). In line with these findings, antibiotic-induced fungal overgrowth in the gut predispose the host to the development of allergic airway in response to mold spore exposures (Noverr et al., 2004). These observations support a role for the gut mycobiota in the development of immune-mediated diseases.

In healthy individuals, *Saccharomyces*, *Candida*, and *Cladosporium* were the most predominate genera (Hoffmann et al., 2013). *Basidiomycota*, *Ascomycota*, and *C. albicans* have been shown to be significantly elevated in IBD patients (Ott et al., 2008; Hoffmann et al., 2013; Sokol et al., 2017). However, until recently the fungi composition in the mucosa is beginning to be elucidated. Liguori et al. evaluated the gut fungal composition in patients with CD and healthy individuals (Liguori et al., 2016). *Saccharomycetes* and *Tremellomycetes* classes, which belong to the phyla *Ascomycota* and *Basidiomycota*, respectively, are the most abundant taxa in the mucosal samples from healthy individuals. At a lower taxonomic level, these two classes can be divided into the genera *Candida, Debaryomyces, Saccharomyces, Malassezia, Sporobolomyces, Trichosporon, Wallemia*, together with a smaller proportion of unidentified *Filobasidiaceae* and *Xylariales*, In samples from CD subjects, the genus *Dioszegia* and species *Candida glabrata* predominate especially during a disease flare whereas *Trichosporon* and *Leptosphaeria* genera are decreased (Mckenzie et al., 1990; Standaert-Vitse et al., 2009; Schwiertz et al., 2010; Hansen et al., 2013; Mukhopadhya et al., 2015; Liguori et al., 2016). In addition, *Filobasidium uniguttulatum* and *Saccharomyces cerevisiae* were significantly elevated in non-inflamed mucosa, whereas *Xylariales* were increased in inflamed mucosa of CD (Liguori et al., 2016). In contrast with CD patients, UC patients showed a relatively decreased diversity of fungi. This might be due to an impairment of the inhibition of antimicrobial peptides against bacteria in the small bowel and altered bile acid reabsorption which can benefit the growth of fungi in patients with CD and not in UC. Overall these preliminary data suggest that an increased fungal load of *Candida* species and altered bacteria diversity may be associated with the pathogenic feature of CD.

There is also emerging evidence favoring a role for the gut mycobiota in IBD pathogenesis. A number of studies have investigated host immune responses against fungal cell wall derived molecules (Levitz, 2010). The glycoprotein cell wall components of the fungi, chitin, β-glucans and mannans can trigger the innate immune response, through receptors, such as dectin-1 (a C-type lectin receptor), Toll-like receptors (TLR2 and TLR4), components of the complement system, and members of the scavenger receptor family (CD5, SCARF1, and CD36). Activation of these molecules leads to downstream immune cascades engaging molecules, such as CARD9, IL-17, IL-22, ITAM, NFAT, and NF-κB (Sartor and Wu, 2017). Colitis in mouse can be exacerbated due to infiltration of fungi through disrupted mucosal barrier. Brun et al. and Iliev et al. suggested that fungi can invade the host by breaking down the mucosal barrier (Brun et al., 2007; Underhill and Iliev, 2014). Intestinal epithelial cells (IECs) act as a physical barrier to prevent foreign pathogens from invading the host. However, in IBD in humans and mice, prolonged inflammation along with the disruption of tight junction (TJ) Occludin and ZO-1, leads to loss of integrity of IECs. Pathogens like fungi and bacteria can therefore penetrate the mucosal barrier and activate TLRs, Dectin-1 and CARD9 in the lamina propria resulting into a more severe inflammatory phenotype (Brun et al., 2007; Iliev et al., 2012).

Viral Microbiota (Virobiota)

With the thriving of high-throughput sequencing technologies (Virgin, 2014), the importance of the gut virobiota is being better appreciated. The virobiota (which is referred to as the viral component of the microbiota) comprises both eukaryotic viruses and prokaryotic bacteriophages. They contain more diverse biological entities than the gut bacterial microbiota (Lecuit and Eloit, 2013; Ogilvie and Jones, 2015). The gut virome in healthy humans is characterized predominantly by the bacteriophages temperate dsDNA *Caudovirales* and ssDNA *Microviridae* that latently infect their bacterial hosts but can generate progenies that may infect and kill other bacteria when under stress (Reyes et al., 2010; Minot et al., 2012, 2013; Waller et al., 2014). In health, gut bacteriophages show intensive variation between subjects while temporally are stable in each individual (Reyes et al., 2010; Minot et al., 2013).

Bacteriophages are posited to play a role in IBD, though their function in disease pathogenesis remains unequivocal (Perez-Brocal et al., 2013; Norman et al., 2015). Patients with CD exhibited a lower diversity but higher variability of the gut virome relative to controls (Perez-Brocal et al., 2013). The virome richness was increased in CD and UC patients from the United Kingdom, Chicago and Boston (Norman et al., 2015). Children with CD have more bacteriophages from the order *Caudovirales* in their tissues and intestinal washings compared to non-inflammatory controls (Wagner et al., 2013). Furthermore, *Caudovirales* virions have been obtained from washings of CD biopsies observed under electron microscopy (Lepage et al., 2008).

The expansion in bacteriophages in IBD could arise from commensal microbes entering lytic cycles or from new viruses introduction from the surrounding environment. Meanwhile, alteration in bacteriophage composition might have further impact on the bacterial microbiota ecology. Bacteriophages are shown to be primary drivers of bacterial fitness and diversity (Brüssow et al., 2004). Moreover, the gut microbiome is prone to be affected by bacteriophage invasion, resulting in changes in the bacterial abundance of specific species (Reyes et al., 2013). In the GI tract, bacteriophages engage in the horizontal transfer of genetic elements between bacterial populations, including those for antibiotic resistance and disease pathogenesis (Maiques et al., 2006; Zhang and LeJeune, 2008; Reyes et al., 2013). Hence, increased virome richness with widespread bacteriophage acquisition in IBD, potentially from external sources, could effectively change bacterial fitness. In mice, western diet could induce an expansion of *Caudovirales* (Kim and Bae, 2016), implicating a role for diet in altering the gut virome.

One potential role of enteric bacteriophages in IBD might be their direct interaction with the mammalian host. Bacteriophages can translocate from the GI lumen to systemic sites in murines (Górski et al., 2006), patients with CD and healthy controls (Parent and Wilson, 1971). They can also induce humoral immune responses (Uhr et al., 1962). Altogether, bacteriophages may act as immune ligands or antigens that boost host immunity and inflammation. On the other hand, some viruses, such as norovirus, can functionally replace the beneficial effect of commensal bacteria, ameliorating intestinal abnormalities in germ-free mice and diminishing susceptibility to intestinal damage caused by chemical injury and bacterial infection (Kernbauer et al., 2014). Beyond that, viruses attached to the mucosa could protect the epithelium against bacteria invasion, through binding interactions between Ig-like proteins exposed on the phage capsid and mucin glycoproteins on the mucosal surface (Barr J. et al., 2013; Barr J. J. et al., 2013).

There is also compelling evidence from mice showing that gut viruses play a causal role in chronic GI inflammation (Cadwell et al., 2010). Mice with a mutation in the gene ATG16L1 (an autophagy gene), which in humans predisposes to CD, are developed without symptom. However, gut norovirus infection led to the manifestation of the disease, although solely harboring the susceptible allele or having the virus alone did not produce the disease, suggesting the combinatorial effect of susceptibility gene and virus in disease pathogenesis and/or progression. In a chemically induced colitis mouse model, the beneficial effect of the gut virome on the gut mucosal immune homeostasis was demonstrated (Yang et al., 2016). Mice, administered a cocktail of anti-viral drugs followed by dextran sulfate sodium (DSS), had more severe colitis than animals treated with DSS alone, along with greater reduction in colon length and weight loss. The observed protective effects of the gut viruses were mediated synergistically by TLR3 and TLR7, but not individually. In favor of this, patients carrying mutations in both TLR3 and TLR7 have been shown to have higher rates of hospitalization when compared with IBD patients without mutations (Yang et al., 2016).

Helminths

Gut helminthes are also considered to be one important gut microbial component coexisting in the gut with gut bacteria, fungi and viruses. The hygiene hypothesis suggests that a lack of early childhood exposure to symbiotic microorganisms and helminthic parasites increases susceptibility to immune mediated diseases in later life. Autoimmune and other immunologic diseases, such as IBD are highly prevalent in developed countries. However, with urbanization and environmental changes toward a more hygienic status, the uprising incidence of IBD appears to conincide with a diminished prevalence of helminth colonization in the host (Weinstock and Elliott, 2009).

Helminths are worm-like parasites, some of which have the potential to inhabit the GI tract and other regions of the body. Improvement in living standards in industrialized countries brings about environmental changes, which disrupt helminthic life cycles and lead to de-worming in humans. Before the twentieth century, every individual was likely to have at least one helminthic infection, mostly during early childhood, but this universal exposure has become rare in the twenty-first century (Elliott and Weinstock, 2012).

Helminths play an important immunoregulatory role in the host, and a lack of their presence has been associated with IBD development (Weinstock et al., 2002; Weinstock and Elliott, 2009; Ramanan et al., 2016). It was demonstrated by Ramanan et al. that helminths *Trichuris muris* and *Heligmosoides polygyrus* protected NOD2-deficient mice against intestinal inflammation, through inhibiting inflammatory *Bacteroides*

species. This protective effect could be attributed to the functional influence of certain helminths on host physiology, exemplified by *Trichinella spiralis* (Motomura et al., 2009; Yang et al., 2014) and *Schistosoma mansoni* (Ruyssers et al., 2009) modulating Treg expansion, *Trichuris trichiura* (Broadhurst et al., 2010) upregulating Th22 response, and *Heligmosomoides polygyrus* (Elliott et al., 2008; Hang et al., 2013) down-regulating Th17 responses while expanding Treg population.

Compared with helminth-negative individuals, helminth-colonized subjects displayed higher gut bacterial diversity, in an indigenous Malaysian cohort (Lee et al., 2014). Orang Asli of the Temuan subtribe are helminthes-positive and they predominantly formed a cluster driven by the gut bacteria *Faecalibacterium* and *Prevotella,* compared with subjects in Kuala Lumpur (Ramanan et al., 2016). Those residing in the city in Kuala Lumpur clustered into another group characterized by *Bacteroides* (Ramanan et al., 2016). The concurrent disparity in helminth prevalence and microbiome configuration between rural and urban dwellers favors a linkage between helminth presence and bacterial microbiome structure, implicating a potential protective role for helminths in rural dwellers against IBD microbiota.

Helminth infections could cause increases in mucus and water secretion into the gut lumen, as measures for anti-inflammatory responses in the host (Stepek et al., 2002; Harnett and Harnett, 2006). In clinical trials of IBD, *Trichiuris suis* or pig whip worm were shown to be efficacious in patients with CD and UC (Summers et al., 2005a,b; Velthuis et al., 2010; Helmby, 2015).

DIET AND THE GUT MICROBIOME

Diet is among the most important factors influencing the gut microbiota (Albenberg and Wu, 2014). Western diet is shown to predispose individuals to diseases including IBD, diabetes, obesity, hypercholesterolemia, and cardiovascular disease (Ley et al., 2008; Turnbaugh et al., 2008; Conlon and Bird, 2015; Agus et al., 2016; Carrillo-Larco et al., 2016). However, what or how certain diets protect against IBD is unclear, considering that urbanization is a significant risk factor for IBD (Soon et al., 2012). Study has shown that long-term diet can influence the composition and function of the gut microbiota (Muegge et al., 2011; Wu et al., 2011). Similarly, short-term diet can rapidly and reproducibly alter the gut microbiota (David et al., 2014). Compared to westerners on a western diet, inhabitants consuming a rural agrarian diet in rural areas and hunter–gatherers times showed a substantial higher diversity of the gut microbiota (De Filippo et al., 2010; Yatsunenko et al., 2012; Schnorr et al., 2014; Martínez et al., 2015; Obregon-Tito et al., 2015).

A western diet is associated with a decreased ratio of *Bacteroides* to *Firmicutes* and enhanced susceptibility to an increased presence of Adherent-Invasive *E. coli* (AIEC) infection (Agus et al., 2016). A recent review assessing the relationship between global IBD incidence and regional diets showed significant correlations between increased incidence of CD and increased consumptions of animal products, beer, honey, animal fats, and ghee, typical constituents of western diets. In contrast, an increased incidence of UC correlated with an increased consumption of pineapples and coffee products (Shivashankar et al., 2017). How these dietary products influence the gut microbiota and predispose individuals to IBD remains to be determined. Diet low in fiber was shown to be associated with a depletion of the microbial ecosystem in mice; this microbial extinction became irreversible and aggressive in the offspring over generations (Agus et al., 2016). The taxa driven to low abundances due to low-level intake of dietary microbiota-accessible carbohydrates were inefficiently transferred to the progeny (El Kaoutari et al., 2013). Mice transplanted with microbiota from humans on a typical unrestricted American diet (AMER) responded incompletely to plant-rich, calorie-restricted diet with optimized nutrient intake (CRON), while those transplanted with microbiota from CRON-consuming individuals responded strongly to both CRON and AMER diets (Griffin et al., 2017). These data imply that western diet may foster an irreversible microbial dysbiosis. In addition, a low-fiber diet was shown to exacerbate colitis and the expansion and activity of colonic mucus-degrading bacteria (Desai et al., 2016). Neither purified prebiotic fibers nor time-to-time diet oscillations between fiber-rich and fiber-deprived diet alleviate mucus layer degradation (Desai et al., 2016).

Specific types of diet are associated with alteration in the *Prevotella* to *Bacteroides* ratio. For instance, high consumption of amino acids, cholesterol, lipids and dairy products were shown to increase *Bacteroides* (Wu et al., 2011), while increase in *Prevotella* is boosted by consumption of sugar and other complex carbohydrates (De Filippo et al., 2010; Wu et al., 2011; Schnorr et al., 2014). The increased *Alistipes* and *Bilophila* were also linked to an animal-based diet (Wu et al., 2011; David et al., 2014). Vegans from non-westernized societies displayed an under-representation of *Bifidobacterium* (Wu et al., 2011), which might be ascribed to the absence of dairy products on their diet (Schnorr et al., 2014).

Diet has also been shown to impact on the gut mycobiota. In humans, increased *Candida* abundance is associated with diet high in carbohydrates, but not with diets high in protein, fatty acids and amino acids (Hoffmann et al., 2013). Consistently, in controlled feeding human study, *Candida* species in fecal samples were reduced in subjects consuming an animal-based diet and increased in subjects on a plant-based diet (David et al., 2014). The effects of diet on gut virobiota were also shown in humans and mice. In humans, dietary intervention was associated with a change in the virome to a new profile, in which individuals on the same diet converged (Minot et al., 2011). In mice, "western diet" could significantly enrich temperate bacteriophage *Caudovriales* both in the mucosa and luminal content (Kim and Bae, 2016). Interestingly, the community alteration of the virobiota occurred to a greater extent in the mucosa than in the lumen. Overall, diet has an impact on the gut mycobiota and virobiota. However, data and mechanistic study are still lacking, especially the associations among diet, mycobiota, virobiota and IBD.

Collectively, emerging animal and epidemiological studies have highlighted the necessity of preserving a diversified microbiome via diet.

MANIPULATION OF THE MICROBIOTA IN IBD THERAPEUTICS

Antibiotics, Probiotics and Prebiotics

Antibiotics, probiotics and prebiotics have been utilized to treat IBD with varying results. Antibiotics have a modest effect in CD but data for probiotics and prebiotics are generally disappointing (Sartor and Wu, 2017). Single antibiotics could ameliorate Crohn's colitis and septic complications, and prevent post-resection recurrence, but has not been shown to be effective in patients with UC. Combinations of antibiotics might improve outcomes (Ohkusa et al., 2010; Turner et al., 2014) but the long-term use of antibiotics may induce development of antibiotic resistance in gut microbes.

Traditional probiotics have demonstrated limited effect in treating UC, the probiotic combination VSL#3 however (a probiotic preparation of eight live freeze-dried bacterial species, including *Lactobacillus casei*, *L. delbrueckii subsp. Bulgaricus*, *L. acidophilus*, *L. plantarum*, *Bifidobacterium longum*, *B. infantis*, *B. breve*, and *Streptococcus salivarius subsp. Thermophiles*; Bibiloni et al., 2005) and *E. coli* Nissle were shown to reduce active inflammation and sustain remission (Wehkamp et al., 2004; Schultz, 2008). Contrarily, they do not benefit patients with CD. *F. prausnitzii* may have a protective effect on the intestine by producing barrier-enhancing and immunosuppressive SCFAs, stimulating Tregs to produce IL-10 thereby inhibiting exaggerated immune responses in IBD. In multiple mouse models, *F. prausnitzii, Clostridia* strains, and *B. fragilis* could reduce the severity of colitis (Sokol et al., 2008; Round et al., 2011; Atarashi et al., 2013). These beneficial microbes and their metabolites should be explored as therapeutic agents in treatment of IBD. Although the idea of providing dietary substrates, such as oligosaccharides and fiber, as a prebiotic means to selectively increase the abundance of SCFA-producing commensals is tantalizing, results to date have been not satisfactory (Sartor and Wu, 2017). Alternatively, it is feasible to block AIEC epithelial adherence, invasion and translocation via use of antibodies to flagellin and of antagonists to glycopolymers or FimH (Yan et al., 2015; Chassaing et al., 2016). Blocking the protease activity of *E. faecalis* or protease receptor binding has been shown to inhibit mucosal permeability (Steck et al., 2011; Maharshak et al., 2015). Thus, selectively blocking the virulence products of pathogenic microbes or their activity may diminish the dysbiotic bacteria in the gut in IBD. Recently, it is shown that precision editing of the gut microbiota by tungstate ameliorates colitis in mice (Zhu et al., 2018). Tungstate treatment could prevent gut inflammation as well as the dysbiotic expansion of Enterobacteriaceae by selectively inhibitting molybdenum-cofactor-dependent microbial respiratory pathways, while causing minimal changes in the microbiota composition under homeostatic conditions (Zhu et al., 2018).

Microbial markers have been shown to help in predicting which subset of patients are likely to have a positive response to treatment or who may undergo an aggressive disease course. Studies have shown that prognostic biomarkers from microbial profiling are instrumental to personalized therapy. For instance, microbial structure data, combined with level of apolipoprotein A1, can predict steroid-free remission in children newly diagnosed with CD (Haberman et al., 2014). Risk for post-operative recurrence of CD is linked to preoperative ileal concentrations of *F. prausnitzii* (Sokol et al., 2008). Risks for pouchitis post-colectomy in patients with UC can be predicted by the bacterial configuration (Machiels et al., 2017). In addition, microbial signatures correlate with response to therapy (Shaw et al., 2016) and dysbiosis is associated with relapse in patients after cessation of infliximab (Rajca et al., 2014).

There are a multitude of modern lifestyle associated factors that potentially associate with alterations of the gut microbiota (**Table 2**, any of these exposures may occur early in life). Studies from the West have shown that exposure of infants to antibiotics increases their risk for developing IBD (Patwa et al., 2011; Brito and Alm, 2016). More compelling evidence has been derived from human migration studies where migrants showed increased risks for IBD after migrating from developing to developed countries adopting an urbanized lifestyle (Probert et al., 1992; Barreiro-de Acosta et al., 2011). In a Canadian population-based inception and birth cohort study, rural residence in the first 1–5 years of life was associated with a lower risk of IBD (Benchimol et al., 2017). Early life colonization of microbes plays an essential role in the host immune system development (Gensollen et al., 2016). Further comprehensive appreciation of the underlying mechanisms would provide insights into the role of gut microbes in childhood in IBD pathogenesis.

Fecal Microbiota Transplantation

Fecal microbiota transplantation (FMT), a highly effective therapy for recurrent *Clostridium difficile* infection (CDI) (Kassam et al., 2013), has gained substantial interest as a novel treatment for inflammatory bowel disease (IBD). The success of FMT in treating CDI is ascribed to restoration of the gut microbial homeostasis in patients with dysbiosis (Khoruts and Sadowsky, 2016). This approach was later extended to studies of other diseases, such as IBD (Borody et al., 2003) and metabolic syndrome (Vrieze et al., 2013). The evidence for the efficacy of FMT in treating IBD is equivocal. A systematic analysis of 18 studies that included 122 patients with IBD found that around 36–45% of patients achieved clinical remission during follow-up (Colman and Rubin, 2014). Subgroup analyses demonstrated a pooled estimate of clinical remission rate of 22% for UC and 61% for CD (Colman and Rubin, 2014).

Two placebo-controlled trials of FMT on patients with UC have shown conflicting results with one study demonstrating the importance of the donor effect. It was documented that some patients with UC experienced fevers and increased levels of C-reactive protein post-FMT (Angelberger et al., 2013). Disease flares in patients with UC or CD after FMT were also observed in the treatment of CDI (De Leon et al., 2013; Kelly et al., 2014a,b).

A recent multicenter, double-blind, randomized, placebo-controlled trial showed that intensive-dosing, with multidonor FMT induces clinical remission and endoscopic improvement in active ulcerative colitis and is associated with distinct microbial changes related to the outcome (Paramsothy et al., 2017). The primary outcome was achieved in 11 (27%) of 41 patients

TABLE 2 | Factors associated with modern lifestyle that is potentially associated with alterations of the gut microbiota.

Modern lifestyle	Often live in an urban setting, surrounded by concrete
	Increased urbanization and migration to urban areas
	Birth in a hospital; increasing rate of cesarean delivery
	Small family size
	Sanitation of living spaces: environment colonized by resistant microorganisms (including resistant bacteria, fungi, and acari)
	Antibiotic usage early in life
	Frequent body wash with hot water and soap
	Low rate of *Helicobacter pylori* colonization
	Decline in endemic parasitism
	Food conserved by refrigeration
	Consumption of processed foods and food additives
	Increased pollution in developing nations
Traditional lifestyle	Vaginal delivery at home
	Large family size, crowding
	Livingin a rural setting in contact with soil microorganisms
	Ancestral colonization of the living environment
	No antibiotics in infant life
	Limited access to hot water and soap
	High rate of *Helicobacter pylori* colonization
	Parasitic worms common
	Food conserved by microbial fermentation
	Consumption of natural foods

allocated to FMT compared with 3 (8%) of 40 subjects who were assigned to placebo (risk ratio 3.6, $p = 0.021$). Importantly, the microbial diversity increased and persisted after FMT (Paramsothy et al., 2017). These data are consistent with a more recent study showing the low intensity pooled donor FMT is also effective in active UC (Costello et al., 2017).

It has been reported that 30–50% of the donor's bacterial microbiota persist in the recipient after FMT (Li et al., 2016). Two studies have shown bacteriophage transfer from donor to recipient (Chehoud et al., 2016; Zuo et al., 2017) and in a pilot study donor virome richness is associated with the efficacy of FMT (Zuo et al., 2017). When donor Caudovirales virome richness was higher than that of the recipient, the recipient was more likely to be cured after FMT treatment (Zuo et al., 2017). Patients with IBD have been shown to harbor significantly higher virome richness than healthy household controls (Norman et al., 2015), which may account for the higher failure rate of FMT in treating IBD than in treating CDI (De Leon et al., 2013; Colman and Rubin, 2014; Kelly et al., 2015). These data highlights the importance of donor selection, where inclusion of a donor with high virome richness or pooled multiple donors is preferred.

The long-term consequence of FMT in treating diseases remains unclear. In the future, FMT will be likely substituted by the use of defined microbial consortia. It was proven in animals that such an approach was feasible and effective for the treatment of IBD (Atarashi et al., 2013).

PERSPECTIVES

Efforts to date have effectively characterized the diverse constituents of the human gut microbiota in health and IBD. Bacterial microbiota is the most studied gut microbiota component though the function and strain-level resolution studies are still lacking. Beyond that, the under-studied gut microbiota components, viruses and fungi, and their inter-kingdom interactions with gut bacteria may have high impact in human health and IBD. These studies are still in its infancy. In summary, understanding the complexity of this gut ecosystem will require thorough mechanistic studies involving sophisticated molecular microbiologic techniques and animal studies to better define the role of different gut microbes in IBD pathogenesis and disease evolution. Precise interpretation of the cause and consequence of these microbial alterations will also require integration with host genetic polymorphisms and gene expression to allow proper comprehension of microbial-host interaction. Although microbe-based therapeutics is appealing, effective application of probiotics, prebiotics, antibiotics and FMT will require a personalized approach to identify defined subsets of patients that will benefit most from such a strategy.

AUTHOR CONTRIBUTIONS

TZ and SN devised the concept, acquired data, and wrote the manuscript.

ACKNOWLEDGMENTS

SN is supported by The Helmsley Charitable Trust through the ENIGMA study. SN and TZ are supported by a seed fund for Gut Microbiome Research provided by the Faculty of Medicine, The Chinese University of Hong Kong.

REFERENCES

Agus, A., Denizot, J., Thevenot, J., Martinez-Medina, M., Massier, S., Sauvanet, P., et al. (2016). Western diet induces a shift in microbiota composition enhancing susceptibility to Adherent-Invasive, *E. coli* infection and intestinal inflammation. *Sci. Rep.* 6:19032. doi: 10.1038/srep19032

Ahmad, M. S., Krishnan, S., Ramakrishna, B. S., Mathan, M., Pulimood, A. B., and Murthy, S. N. (2000). Butyrate and glucose metabolism by colonocytes in experimental colitis in mice. *Gut* 46, 493–499. doi: 10.1136/gut.46.4.493

Albenberg, L. G., and Wu, G. D. (2014). Diet and the intestinal microbiome: associations, functions, and implications for health and disease. *Gastroenterology* 146, 1564–1572. doi: 10.1053/j.gastro.2014.01.058

Angelberger, S., Reinisch, W., Makristathis, A., Lichtenberger, C., Dejaco, C., Papay, P., et al. (2013). Temporal bacterial community dynamics vary among ulcerative colitis patients after fecal microbiota transplantation. *Am. J. Gastroenterol.* 108, 1620–1630. doi: 10.1038/ajg.2013.257

Arnold, I. C., Lee, J. Y., Amieva, M. R., Roers, A., Flavell, R. A., Sparwasser, T., et al. (2011). Tolerance rather than immunity protects from *Helicobacter*

pylori–induced gastric preneoplasia. *Gastroenterology* 140, 199–209. doi: 10.1053/j.gastro.2010.06.047

Atarashi, K., Tanoue, T., Oshima, K., Suda, W., Nagano, Y., Nishikawa, H., et al. (2013). T-reg induction by a rationally selected mixture of Clostridia strains from the human microbiota. *Nature* 500, 232–236. doi: 10.1038/nature12331

Bäckhed, F., Fraser, C. M., Ringel, Y., Sanders, M. E., Sartor, R. B., Sherman, P. M., et al. (2012). Defining a healthy human gut microbiome: current concepts, future directions, and clinical applications. *Cell Host Microbe* 12, 611–622. doi: 10.1016/j.chom.2012.10.012

Backhed, F., Roswall, J., Peng, Y., Feng, Q., Jia, H., Kovatcheva-Datchary, P., et al. (2015). Dynamics and stabilization of the human gut microbiome during the first year of life. *Cell Host Microbe* 17:852. doi: 10.1016/j.chom.2015.05.012

Barr, J., Auro, R., Furlan, M., Whiteson, K., Talago, N., Paul, L., et al. (2013). Bacteriophage adhered to mucus provide a novel mucosal immune system. *J. Immunol.* 190:61.8.

Barr, J. J., Auro, R., Furlan, M., Whiteson, K. L., Erb, M. L., Pogliano, J., et al. (2013). Bacteriophage adhering to mucus provide a non-host-derived immunity. *Proc. Natl. Acad. Sci. U.S.A.* 110, 10771–10776. doi: 10.1073/pnas.1305923110

Barreiro-de Acosta, M., Alvarez Castro, A., Souto, R., Iglesias, M., Lorenzo, A., and Dominguez-Munoz, J. E. (2011). Emigration to western industrialized countries: a risk factor for developing inflammatory bowel disease. *J. Crohns Colitis* 5, 566–569. doi: 10.1016/j.crohns,.2011.05.009

Benchimol, E. I., Guttmann, A., Griffiths, A. M., Rabeneck, L., Mack, D. R., Brill, H., et al. (2009). Increasing incidence of paediatric inflammatory bowel disease in Ontario, Canada: evidence from health administrative data. *Gut* 58, 1490–1497. doi: 10.1136/gut.2009.188383

Benchimol, E. I., Kaplan, G. G., Otley, A. R., Nguyen, G. C., Underwood, F. E., Guttmann, A., et al. (2017). Rural and urban residence during early life is associated with a lower risk of inflammatory bowel disease: a population-based inception and birth cohort study. *Am. J. Gastroenterol.* 112, 1412–1422. doi: 10.1038/ajg.2017.208

Benchimol, E. I., Manuel, D. G., Guttmann, A., Nguyen, G. C., Mojaverian, N., Quach, P., et al. (2014). Changing age demographics of inflammatory bowel disease in ontario, canada: a population-based cohort study of epidemiology trends. *Inflamm. Bowel Dis.* 20, 1761–1769. doi: 10.1097/MIB.0000000000000103

Benjamin, J. L., Hedin, C. R., Koutsoumpas, A., Ng, S. C., McCarthy, N. E., Prescott, N. J., et al. (2012). Smokers with active Crohn's disease have a clinically relevant dysbiosis of the gastrointestinal microbiota. *Inflamm. Bowel Dis.* 18, 1092–1100. doi: 10.1002/ibd.21864

Bibiloni, R., Fedorak, R. N., Tannock, G. W., Madsen, K. L., Gionchetti, P., Campieri, M., et al. (2005). VSL# 3 probiotic-mixture induces remission in patients with active ulcerative colitis. *Am. J. Gastroenterol.* 100, 1539–1546. doi: 10.1111/j.1572-0241.2005.41794.x

Borody, T. J., Warren, E. F., Leis, S., Surace, R., and Ashman, O. (2003). Treatment of ulcerative colitis using fecal bacteriotherapy. *J. Clin. Gastroenterol.* 37, 42–47. doi: 10.1097/00004836-200307000-00012

Brito, I. L., and Alm, E. J. (2016). Tracking strains in the microbiome: insights from metagenomics and models. *Front. Microbiol.* 7:712. doi: 10.3389/fmicb.2016.00712

Broadhurst, M. J., Leung, J. M., Kashyap, V., McCune, J. M., Mahadevan, U., McKerrow, J. H., et al. (2010). IL-22(+) CD4(+) T Cells are associated with therapeutic trichuris trichiura infection in an ulcerative colitis patient. *Sci. Transl. Med.* 2:60ra88. doi: 10.1126/scitranslmed.3001500

Brun, P., Castagliuolo, I., Di Leo, V., Buda, A., Pinzani, M., Palù, G., et al. (2007). Increased intestinal permeability in obese mice: new evidence in the pathogenesis of nonalcoholic steatohepatitis. *Am. J. Physiol. Gastr. L* 292, G518–G525. doi: 10.1152/ajpgi.00024.2006

Brüssow, H., Canchaya, C., and Hardt, W. D. (2004). Phages and the evolution of bacterial pathogens: From genomic rearrangements to lysogenic conversion. *Microbiol. Mol. Biol. R* 68, 560-602. doi: 10.1128/MMBR.68.3.560-602.2004

Cadwell, K., Patel, K. K., Maloney, N. S., Liu, T. C., Ng, A. C., Storer, C. E., et al. (2010). Virus-plus-susceptibility gene interaction determines Crohn's disease gene Atg16L1 phenotypes in intestine. *Cell* 141, 1135–1145. doi: 10.1016/j.cell.2010.05.009

Callaway, T. R., Edrington, T. S., Anderson, R. C., Harvey, R. B., Genovese, K. J., Kennedy, C. N., et al. (2008). Probiotics, prebiotics and competitive exclusion for prophylaxis against bacterial disease. *Anim. Health Res. Rev.* 9, 217–225. doi: 10.1017/S1466252308001540

Carrillo-Larco, R. M., Bernabé-Ortiz, A., Pillay, T. D., Gilman, R. H., Sanchez, J. F., Poterico, J. A., et al. (2016). Obesity risk in rural, urban and rural-to-urban migrants: prospective results of the PERU MIGRANT study. *Int. J. Obes.* 40, 181–185. doi: 10.1038/ijo.2015.140

Casen, C., Vebo, H. C., Sekelja, M., Hegge, F. T., Karlsson, M. K., Ciemniejewska, E., et al. (2015). Deviations in human gut microbiota: a novel diagnostic test for determining dysbiosis in patients with IBS or IBD. *Aliment. Pharmacol. Ther.* 42, 71–83. doi: 10.1111/apt.13236

Castellarin, M., Warren, R. L., Freeman, J. D., Dreolini, L., Krzywinski, M., Strauss, J., et al. (2012). *Fusobacterium* nucleatum infection is prevalent in human colorectal carcinoma. *Genome Res.* 22, 299–306. doi: 10.1101/gr.126516.111

Chassaing, B., and Darfeuille-Michaud, A. (2011). The commensal microbiota and enteropathogens in the pathogenesis of inflammatory bowel diseases. *Gastroenterology* 140, 1720–1728. doi: 10.1053/j.gastro.2011.01.054

Chassaing, B., Tran, H., and Gewirtz, A. (2016). O-007 Colitis vaccine: flagellin-elicited immunity keeps motile bacteria in check and protects against intestinal inflammation. *Inflamm. Bowel Dis.* 22:S3. doi: 10.1097/01.MIB.0000480045.11503.c5

Chehoud, C., Dryga, A., Hwang, Y., Nagy-Szakal, D., Hollister, E. B., Luna, R. A., et al. (2016). Transfer of viral communities between human individuals during fecal microbiota transplantation. *mBio* 7:e00322. doi: 10.1128/mBio.00322-16

Chiba, M., Tsuji, T., Nakane, K., and Komatsu, M. (2015). High amount of dietary fiber not harmful but favorable for Crohn disease. *Perm. J.* 19, 58–91. doi: 10.7812/TPP/14-124

Colman, R. J., and Rubin, D. T. (2014). Fecal microbiota transplantation as therapy for inflammatory bowel disease: a systematic review and meta-analysis. *J. Crohns Colitis* 8, 1569–1581. doi: 10.1016/j.crohns.2014.08.006

Conlon, M. A., and Bird, A. R. (2015). The impact of diet and lifestyle on gut microbiota and human health. *Nutrients* 7, 17–44. doi: 10.3390/nu7010017

Costello, S., Waters, O., Bryant, R., Katsikeros, R., Makanyanga, J., Schoeman, M., et al. (2017). Short duration, low intensity pooled faecal microbiota transplantation induces remission in patients with mild-moderately active ulcerative colitis: a randomised controlled trial. *J. Crohns Colitis* 11, S23. doi: 10.1093/ecco-jcc/jjx002.035

Darfeuille-Michaud, A., Boudeau, J., Bulois, P., Neut, C., Glasser, A. L., Barnich, N., et al. (2004). High prevalence of adherent-invasive *Escherichia coli* associated with ileal mucosa in Crohn's disease. *Gastroenterology* 127, 412–421. doi: 10.1053/j.gastro.2004.04.061

Dave, M., Higgins, P. D., Middha, S., and Rioux, K. P. (2012). The human gut microbiome: current knowledge, challenges, and future directions. *Transl. Res.* 160, 246–257. doi: 10.1016/j.trsl.2012.05.003

David, L. A., Maurice, C. F., Carmody, R. N., Gootenberg, D. B., Button, J. E., Wolfe, B. E., et al. (2014). Diet rapidly and reproducibly alters the human gut microbiome. *Nature* 505, 559-563. doi: 10.1038/nature12820

De Filippo, C., Cavalieri, D., Di Paola, M., Ramazzotti, M., Poullet, J. B., Massart, S., et al. (2010). Impact of diet in shaping gut microbiota revealed by a comparative study in children from Europe and rural Africa. *Proc. Natl. Acad. Sci. U.S.A.* 107, 14691–14696. doi: 10.1073/pnas.1005963107

De Leon, L. M., Watson, J. B., and Kelly, C. R. (2013). Transient flare of ulcerative colitis after fecal microbiota transplantation for recurrent clostridium difficile infection. *Clin. Gastroenterol. Hepatol.* 11, 1036–1038. doi: 10.1016/j.cgh.2013.04.045

Desai, M. S., Seekatz, A. M., Koropatkin, N. M., Kamada, N., Hickey, C. A., Wolter, M., et al. (2016). A dietary fiber-deprived gut microbiota degrades the colonic mucus barrier and enhances pathogen susceptibility. *Cell* 167, 1339–1353.e21. doi: 10.1016/j.cell.2016.10.043

Dethlefsen, L., and Relman, D. A. (2011). Incomplete recovery and individualized responses of the human distal gut microbiota to repeated antibiotic perturbation. *Proc. Natl. Acad. Sci. U.S.A.* 108, 4554–4561. doi: 10.1073/pnas.1000087107

Dicksved, J., Halfvarson, J., Rosenquist, M., Järnerot, G., Tysk, C., Apajalahti, J., et al. (2008). Molecular analysis of the gut microbiota of identical twins with Crohn's disease. *Isme J.* 2, 716–727. doi: 10.1038/ismej.2008.37

Dollive, S., Chen, Y. Y., Grunberg, S., Bittinger, K., Hoffmann, C., Vandivier, L., et al. (2013). Fungi of the murine gut: episodic variation

and proliferation during antibiotic treatment. *PLoS ONE* 8: 71806. doi: 10.1371/journal.pone.0071806

El Kaoutari, A., Armougom, F., Gordon, J. I., Raoult, D., and Henrissat, B. (2013). The abundance and variety of carbohydrate-active enzymes in the human gut microbiota. *Nat. Rev. Microbiol.* 11, 497–504. doi: 10.1038/nrmicro3050

Elliott, D. E., Metwali, A., Leung, J., Setiawan, T., Blum, A. M., Ince, M. N., et al. (2008). Colonization with *Heligmosomoides polygyrus* suppresses mucosal IL-17 production. *J. Immunol.* 181, 2414–2419. doi: 10.4049/jimmunol.181.4.2414

Elliott, D. E., and Weinstock, J. V. (2012). Helminth-host immunological interactions: prevention and control of immune-mediated diseases. *Ann. N. Y. Acad. Sci.* 1247, 83–96. doi: 10.1111/j.1749-6632.2011.06292.x

Frank, D. N., Robertson, C. E., Hamm, C. M., Kpadeh, Z., Zhang, T., Chen, H., et al. (2011). Disease phenotype and genotype are associated with shifts in intestinal-associated microbiota in inflammatory bowel diseases. *Inflamm. Bowel Dis.* 17, 179–184. doi: 10.1002/ibd.21339

Frank, D. N., St Amand, A. L., Feldman, R. A., Boedeker, E. C., Harpaz, N., and Pace, N. R. (2007). Molecular-phylogenetic characterization of microbial community imbalances in human inflammatory bowel diseases. *Proc. Natl. Acad. Sci. U.S.A.* 104, 13780–13785. doi: 10.1073/pnas.0706625104

Galvez, J., Rodríguez-Cabezas, M. E., and Zarzuelo, A. (2005). Effects of dietary fiber on inflammatory bowel disease. *Mol. Nutr. Food Res.* 49, 601–608. doi: 10.1002/mnfr.200500013

Gensollen, T., Iyer, S. S., Kasper, D. L., and Blumberg, R. S. (2016). How colonization by microbiota in early life shapes the immune system. *Science* 352, 539–544. doi: 10.1126/science.aad9378

Gevers, D., Kugathasan, S., Denson, L. A., Vázquez-Baeza, Y., Van Treuren, W., Ren, B., et al. (2014). The treatment-naive microbiome in new-onset Crohn's disease. *Cell Host Microbe* 15, 382–392. doi: 10.1016/j.chom.2014.02.005

Górski, A., Wazna, E., Dabrowska, B. W., Dabrowska, K., Switala-Jelen, K., and Miedzybrodzki, R. (2006). Bacteriophage translocation. *FEMS Immunol. Med. Mic.* 46, 313–319. doi: 10.1111/j.1574-695X.2006.00044.x

Griffin, N. W., Ahern, P. P., Cheng, J., Heath, A. C., Ilkayeva, O., Newgard, C. B., et al. (2017). Prior dietary practices and connections to a human gut microbial metacommunity alter responses to diet interventions. *Cell Host Microbe* 21, 84–96. doi: 10.1016/j.chom.2016.12.006

Haberman, Y., Tickle, T. L., Dexheimer, P. J., Kim, M. O., Tang, D., Karns, R., et al. (2014). Pediatric Crohn disease patients exhibit specific ileal transcriptome and microbiome signature. *J. Clin. Invest.* 124, 3617–3633. doi: 10.1172/JCI75436

Halfvarson, J., Brislawn, C. J., Lamendella, R., Vázquez-Baeza, Y., Walters, W. A., Bramer, L. M., et al. (2017). Dynamics of the human gut microbiome in inflammatory bowel disease. *Nat. Microbiol.* 2:17004 doi: 10.1038/nmicrobiol.2017.4

Hammer, T., Nielsen, K. R., Munkholm, P., Burisch, J., and Lynge, E. (2016). The faroese IBD study: incidence of inflammatory bowel diseases across 54 years of population-based data. *J. Crohns Colitis* 10, 934–942. doi: 10.1093/ecco-jcc/jjw050

Hang, L., Blum, A. M., Setiawan, T., Urban, J. P., Stoyanoff, K. M., and Weinstock, J. V. (2013). Heligmosomoides polygyrus bakeri infection activates colonic Foxp3(+) T cells enhancing their capacity to prevent colitis. *J. Immunol.* 191, 1927–1934. doi: 10.4049/jimmunol.1201457

Hansen, R., Mukhopadhya, I., Meharg, C., Russell, R., Berry, S., El-Omar, E., et al. (2013). The role of the fungal microbiota in the pathogenesis of de-novo paediatric inflammatory bowel disease using next generation sequencing. *Gut* 62, A32. doi: 10.1136/gutjnl-2013-304907.073

Harnett, W., and Harnett, M. M. (2006). Filarial nematode secreted product ES-62 is an anti-inflammatory agent: therapeutic potential of small molecule derivatives and ES-62 peptide mimetics. *Clin. Exp. Pharmacol. Physiol.* 33, 511–518. doi: 10.1111/j.1440-1681.2006.04400.x

Helmby, H. (2015). Human helminth therapy to treat inflammatory disorders-where do we stand? *BMC Immunol.* 16:12. doi: 10.1186/s12865-015-0074-3

Hoffmann, C., Dollive, S., Grunberg, S., Chen, J., Li, H. Z., Wu, G. D., et al. (2013). Archaea and fungi of the human gut microbiome: correlations with diet and bacterial residents. *PLoS ONE* 8:e66019. doi: 10.1371/journal.pone.0066019

Huffnagle, G. B., and Noverr, M. C. (2013). The emerging world of the fungal microbiome. *Trends Microbiol.* 21, 334–341. doi: 10.1016/j.tim.2013.04.002

Iliev, I. D., Funari, V. A., Taylor, K. D., Nguyen, Q., Reyes, C. N., Strom, S. P., et al. (2012). Interactions between commensal fungi and the C-type lectin receptor dectin-1 influence colitis. *Science* 336, 1314–1317. doi: 10.1126/science.1221789

Jandhyala, S. M., Talukdar, R., Subramanyam, C., Vuyyuru, H., Sasikala, M., and Nageshwar Reddy, D. (2015). Role of the normal gut microbiota. *World J. Gastroenterol.* 21, 8787–8803. doi: 10.3748/wjg.v21.i29.8787

Kamada, N., Chen, G., and Núñez, G. (2012). A complex microworld in the gut: harnessing pathogen-commensal relations. *Nat. Med.* 18, 1190–1191. doi: 10.1038/nm.2900

Kang, S., Denman, S. E., Morrison, M., Yu, Z., Dore, J., Leclerc, M., et al. (2010). Dysbiosis of fecal microbiota in Crohn's disease patients as revealed by a custom phylogenetic microarray. *Inflamm. Bowel Dis.* 16, 2034–2042. doi: 10.1002/ibd.21319

Kaplan, G. G. (2015). The global burden of IBD: from 2015 to 2025. *Nat. Rev. Gastro. Hepat.* 12, 720–727. doi: 10.1038/nrgastro.2015.150

Kassam, Z., Lee, C. H., Yuan, Y., and Hunt, R. H. (2013). Fecal microbiota transplantation for Clostridium difficile infection: systematic review and meta-analysis. *Am. J. Gastroenterol.* 108, 500–508. doi: 10.1038/ajg.2013.59

Kelly, C. R., Ihunnah, C., Fischer, M., Khoruts, A., Surawicz, C., Afzali, A., et al. (2014b). Fecal microbiota transplant for treatment of clostridium difficile infection in immunocompromised patients. *Am. J. Gastroenterol.* 109, 1065–1071. doi: 10.1038/ajg.2014.133

Kelly, C. R., Kahn, S. A., and Kashyap, P. (2015). Update on fecal microbiota transplantation 2015: indications, methodologies, mechanisms, and outlook (vol 149, pg 223, 2015). *Gastroenterology* 149, 1644–1644. doi: 10.1053/j.gastro.2015.05.008

Kelly, C. R., Ziud, H., and Kahn, S. (2014a). New diagnosis of Crohn's colits 6 weeks after fecal microbiota transplantation. *Inflamm. Bowel Dis.* 20:S21. doi: 10.1097/01.MIB.0000456762.32133.2e

Kelly, D., Campbell, J. I., King, T. P., Grant, G., Jansson, E. A., Coutts, A. G., et al. (2004). Commensal anaerobic gut bacteria attenuate inflammation by regulating nuclear-cytoplasmic shuttling of PPAR-[gamma] and RelA. *Nat. Immunol.* 5, 104–112. doi: 10.1038/ni1018

Kernbauer, E., Ding, Y., and Cadwell, K. (2014). An enteric virus can replace the beneficial function of commensal bacteria. *Nature* 516, 94–98. doi: 10.1038/nature13960

Khoruts, A., and Sadowsky, M. J. (2016). Understanding the mechanisms of faecal microbiota transplantation. *Nat. Rev. Gastro. Hepat.* 13, 508–516. doi: 10.1038/nrgastro.2016.98

Kim, M. S., and Bae, J. W. (2016). Spatial disturbances in altered mucosal and luminal gut viromes of diet-induced obese mice. *Environ. Microbiol.* 18, 1498–1510. doi: 10.1111/1462-2920.13182

Kitajima, S., Morimoto, M., Sagara, E., Shimizu, C., and Ikeda, Y. (2001). Dextran sodium sulfate-induced colitis in germ-free IQI/Jic mice. *Exp. Anim. Tokyo* 50, 387–395. doi: 10.1538/expanim.50.387

Koenig, J. E., Spor, A., Scalfone, N., Fricker, A. D., Stombaugh, J., Knight, R., et al. (2011). Succession of microbial consortia in the developing infant gut microbiome. *Proc. Natl. Acad. Sci. U.S.A.* 108, 4578–4585. doi: 10.1073/pnas.1000081107

Kostic, A. D., Chun, E., Robertson, L., Glickman, J. N., Gallini, C. A., Michaud, M., et al. (2013). *Fusobacterium* nucleatum potentiates intestinal tumorigenesis and modulates the tumor-immune microenvironment. *Cell Host Microbe* 14, 207–215. doi: 10.1016/j.chom.2013.07.007

Kostic, A. D., Gevers, D., Pedamallu, C. S., Michaud, M., Duke, F., Earl, A. M., et al. (2012). Genomic analysis identifies association of *Fusobacterium* with colorectal carcinoma. *Genome Res.* 22, 292–298. doi: 10.1101/gr.126573.111

Lecuit, M., and Eloit, M. (2013). The human virome: new tools and concepts. *Trends Microbiol.* 21, 510–515. doi: 10.1016/j.tim.2013.07.001

Lee, S. C., Tang, M. S., Lim, Y. A., Choy, S. H., Kurtz, Z. D., Cox, L. M., et al. (2014). Helminth colonization is associated with increased diversity of the gut microbiota. *PLoS Negl. Trop. Dis.* 8:e2880. doi: 10.1371/journal.pntd.0002880

Lepage, P., Colombet, J., Marteau, P., Sime-Ngando, T., Doré, J., and Leclerc, M., (2008). Dysbiosis in inflammatory bowel disease: a role for bacteriophages? *Gut* 57, 424–425. doi: 10.1136/gut.2007.134668

Levitz, S. M. (2010). Innate recognition of fungal cell walls. *PLoS Pathog.* 6:1000758. doi: 10.1371/journal.ppat.1000758

Ley, R. E., Hamady, M., Lozupone, C., Turnbaugh, P. J., Ramey, R. R., Bircher, J. S., et al. (2008). Evolution of mammals and their gut microbes. *Science* 320, 1647–1651. doi: 10.1126/science.1155725

Ley, R. E., Peterson, D. A., and Gordon, J. I. (2006). Ecological and evolutionary forces shaping microbial diversity in the human intestine. *Cell* 124, 837–848. doi: 10.1016/j.cell.2006.02.017

Li, S. S., Zhu, A., Benes, V., Costea, P. I., Hercog, R., Hildebrand, F., et al. (2016). Durable coexistence of donor and recipient strains after fecal microbiota transplantation. *Science* 352, 586–589. doi: 10.1126/science.aad8852

Liguori, G., Lamas, B., Richard, M. L., Brandi, G., da Costa, G., Hoffmann, T. W., et al. (2016). Fungal dysbiosis in mucosa-associated microbiota of Crohn's disease patients. *J. Crohns Colitis* 10, 296–305. doi: 10.1093/ecco-jcc/jjv209

Llopis, M., Antolin, M., Carol, M., Borruel, N., Casellas, F., Martinez, C., et al. (2009). *Lactobacillus* casei downregulates commensals' inflammatory signals in Crohn's disease mucosa. *Inflamm. Bowel Dis.* 15, 275–283. doi: 10.1002/ibd.20736

Lupp, C., Robertson, M. L., Wickham, M. E., Sekirov, I., Champion, O. L., Gaynor, E. C., et al. (2007). Host-mediated inflammation disrupts the intestinal microbiota and promotes the overgrowth of Enterobacteriaceae. *Cell Host Microbe* 2, 119–129. doi: 10.1016/j.chom.2007.06.010

Machiels, K., Sabino, J., Vandermosten, L., Joossens, M., Arijs, I., de Bruyn, M., et al. (2017). Specific members of the predominant gut microbiota predict pouchitis following colectomy and IPAA in UC. *Gut* 66, 79–88. doi: 10.1136/gutjnl-2015-309398

Maharshak, N., Huh, E. Y., Paiboonrungruang, C., Shanahan, M., Thurlow, L., Herzog, J., et al. (2015). Enterococcus faecalis gelatinase mediates intestinal permeability via protease-activated receptor 2. *Infect. Immun.* 83, 2762–2770. doi: 10.1128/IAI.00425-15

Maier, L., Pruteanu, M., Kuhn, M., Zeller, G., Telzerow, A., Anderson, E. E., et al. (2018). Extensive impact of non-antibiotic drugs on human gut bacteria. *Nature* 555, 623–628. doi: 10.1038/nature25979

Maiques, E., Ubeda, C., Campoy, S., Salvador, N., Lasa, I., Novick, R. P., et al. (2006). Beta-lactam antibiotics induce the SOS response and horizontal transfer of virulence factors in Staphylococcus aureus. *J. Bacteriol.* 188, 2726–2729. doi: 10.1128/JB.188.7.2726-2729.2006

Manichanh, C., Rigottier-Gois, L., Bonnaud, E., Gloux, K., Pelletier, E., Frangeul, L., et al. (2006). Reduced diversity of faecal microbiota in Crohn's disease revealed by a metagenomic approach. *Gut* 55, 205–211. doi: 10.1136/gut.2005.073817

Martinez, C., Antolin, M., Santos, J., Torrejon, A., Casellas, F., Borruel, N., et al. (2008). Unstable composition of the fecal microbiota in ulcerative colitis during clinical remission. *Am. J. Gastroenterol.* 103, 643–648. doi: 10.1111/j.1572-0241.2007.01592.x

Martínez, I., Stegen, J. C., Maldonado-Gomez, M. X., Eren, A. M., Siba, P. M., Greenhill, A. R., et al. (2015). The gut microbiota of rural papua new guineans: composition, diversity patterns, and ecological processes. *Cell Rep.* 11, 527–538. doi: 10.1016/j.celrep.2015.03.049

Maslowski, K. M., and Mackay, C. R. (2011). Diet, gut microbiota and immune responses. *Nat. Immunol.* 12, 5–9. doi: 10.1038/ni0111-5

Mckenzie, H., Main, J., Pennington, C. R., and Parratt, D. (1990). Antibody to selected strains of saccharomyces-cerevisiae (Bakers and Brewers-Yeast) and Candida-Albicans in Crohns-disease. *Gut* 31, 536–538. doi: 10.1136/gut.31.5.536

Medellin-Pena, M. J., Wang, H. F., Johnson, R., Anand, S., and Griffiths, M. W. (2007). Probiotics affect virulence-related gene expression in *Escherichia coli* O157: H7. *Appl. Environ. Microb.* 73, 4259–4267. doi: 10.1128/AEM.00159-07

Minot, S., Bryson, A., Chehoud, C., Wu, G. D., Lewis, J. D., and Bushman, F. D. (2013). Rapid evolution of the human gut virome. *Proc. Natl. Acad. Sci. U.S.A.* 110, 12450–12455. doi: 10.1073/pnas.1300833110

Minot, S., Grunberg, S., Wu, G. D., Lewis, J. D., and Bushman, F. D. (2012). Hypervariable loci in the human gut virome. *Proc. Natl. Acad. Sci. U.S.A.* 109, 3962–3966. doi: 10.1073/pnas.1119061109

Minot, S., Sinha, R., Chen, J., Li, H. Z., Keilbaugh, S. A., Wu, G. D., et al. (2011). The human gut virome: inter-individual variation and dynamic response to diet. *Genome Res.* 21, 1616–1625. doi: 10.1101/gr.122705.111

Molodecky, N. A., Soon, I. S., Rabi, D. M., Ghali, W. A., Ferris, M., Chernoff, G., et al. (2012). Increasing incidence and prevalence of the inflammatory bowel diseases with time, based on systematic review. *Gastroenterology* 142, 46–54. doi: 10.1053/j.gastro.2011.10.001

Morgan, X. C., Tickle, T. L., Sokol, H., Gevers, D., Devaney, K. L., Ward, D. V., et al. (2012). Dysfunction of the intestinal microbiome in inflammatory bowel disease and treatment. *Genome Biol.* 13:R79. doi: 10.1186/gb-2012-13-9-r79

Motomura, Y., Wang, H., Deng, Y., El-Sharkawy, R. T., Verdu, E. F., and Khan, W. I. (2009). Helminth antigen-based strategy to ameliorate inflammation in an experimental model of colitis. *Clin. Exp. Immunol.* 155, 88–95. doi: 10.1111/j.1365-2249.2008.03805.x

Muegge, B. D., Kuczynski, J., Knights, D., Clemente, J. C., González, A., Fontana, L., et al. (2011). Diet drives convergence in gut microbiome functions across mammalian phylogeny and within humans. *Science* 332, 970–974. doi: 10.1126/science.1198719

Mukhopadhya, I., Hansen, R., Meharg, C., Thomson, J. M., Russell, R. K., Berry, S. H., et al. (2015). The fungal microbiota of de-novo paediatric inflammatory bowel disease. *Microbes Infect.* 17, 304–310. doi: 10.1016/j.micinf.2014.12.001

Norman, J. M., Handley, S. A., Baldridge, M. T., Droit, L., Liu, C. Y., Keller, B. C., et al. (2015). Disease-specific alterations in the enteric virome in inflammatory bowel disease. *Cell* 160, 447–460. doi: 10.1016/j.cell.2015.01.002

Noverr, M. C., Noggle, R. M., Toews, G. B., and Huffnagle, G. B. (2004). Role of antibiotics and fungal microbiota in driving pulmonary allergic responses. *Infect. Immun.* 72, 4996–5003. doi: 10.1128/IAI.72.9.4996-5003.2004

Obregon-Tito, A. J., Tito, R. Y., Metcalf, J., Sankaranarayanan, K., Clemente, J. C., Ursell, L. K., et al. (2015). Subsistence strategies in traditional societies distinguish gut microbiomes. *Nat. Commun.* 6:6505. doi: 10.1038/ncomms7505

Oertli, M., and Müller, A. (2012). *Helicobacter pylori* targets dendritic cells to induce immune tolerance, promote persistence and confer protection against allergic asthma. *Gut Microbes* 3, 566–571. doi: 10.4161/gmic.21750

Oertli, M., Sundquist, M., Hitzler, I., Engler, D. B., Arnold, I. C., Reuter, S., et al. (2012). DC-derived IL-18 drives Treg differentiation, murine *Helicobacter* pylori–specific immune tolerance, and asthma protection. *J. Clin. Invest.* 122, 1082–1096. doi: 10.1172/JCI61029

Ogilvie, L. A., and Jones, B. V. (2015). The human gut virome: a multifaceted majority. *Front. Microbiol.* 6:918. doi: 10.3389/fmicb.2015.00918

O'Hara, A. M., and Shanahan, F. (2006). The gut flora as a forgotten organ. *EMBO Rep.* 7, 688–693. doi: 10.1038/sj.embor.7400731

Ohkusa, T., Kato, K., Terao, S., Chiba, T., Mabe, K., Murakami, K., et al. (2010). Newly developed antibiotic combination therapy for ulcerative colitis: a double-blind placebo-controlled multicenter trial. *Am. J. Gastroenterol.* 105, 1820–1829. doi: 10.1038/ajg.2010.84

Ohkusa, T., Okayasu, I., Ogihara, T., Morita, K., Ogawa, M., and Sato, N. (2003). Induction of experimental ulcerative colitis by *Fusobacterium varium* isolated from colonic mucosa of patients with ulcerative colitis. *Gut* 52, 79–83. doi: 10.1136/gut.52.1.79

Ohkusa, T., Sato, N., Ogihara, T., Morita, K., Ogawa, M., and Okayasu, I. (2002). Fusobacterium varium localized in the colonic mucosa of patients with ulcerative colitis stimulates species-specific antibody. *J. Gastroenterol. Hepatol.* 17, 849–853. doi: 10.1046/j.1440-1746.2002.02834.x

Ohkusa, T., Yoshida, T., Sato, N., Watanabe, S., Tajiri, H., and Okayasu, I. (2009). Commensal bacteria can enter colonic epithelial cells and induce proinflammatory cytokine secretion: a possible pathogenic mechanism of ulcerative colitis. *J. Med. Microbiol.* 58, 535–545. doi: 10.1099/jmm.0.005801-0

Ott, S. J., Kuhbacher, T., Musfeldt, M., Rosenstiel, P., Hellmig, S., Rehman, A., et al. (2008). Fungi and inflammatory bowel diseases: alterations of composition and diversity. *Scand. J. Gastroentero.* 43, 831–841. doi: 10.1080/00365520801935434

Papamichael, K., Konstantopoulos, P., and Mantzaris, G. J. (2014). *Helicobacter* pylori infection and inflammatory bowel disease: is there a link? *World J. Gastroenterol.* 20:6374. doi: 10.3748/wjg.v20.i21.6374

Paramsothy, S., Kamm, M. A., Kaakoush, N. O., Walsh, A. J., van den Bogaerde, J., Samuel, D., et al. (2017). Multidonor intensive faecal microbiota transplantation for active ulcerative colitis: a randomised placebo-controlled trial. *Lancet* 389, 1218–1228. doi: 10.1016/S0140-6736(17)30182-4

Parent, K., and Wilson, I. D. (1971). Mycobacteriophage in Crohn's disease. *Gut* 12, 1019–1020. doi: 10.1136/gut.12.12.1019

Patwa, L. G., Fan, T. J., Tchaptchet, S., Liu, Y., Lussier, Y. A., Sartor, R. B., et al. (2011). Chronic intestinal inflammation induces stress-response genes in commensal *Escherichia coli*. *Gastroenterology* 141, 1842–1851.e1-10. doi: 10.1053/j.gastro,.2011.06.064

Perez-Brocal, V., Garcia-Lopez, R., Vazquez-Castellanos, J. F., Nos, P., Beltran, B., Latorre, A., et al. (2013). Study of the viral and microbial communities associated with Crohn's disease: a metagenomic approach. *Clin. Transl. Gastroen.* 4:e36. doi: 10.1038/ctg.2013.9

Pituch-Zdanowska, A., Banaszkiewicz, A., and Albrecht, P. (2015). The role of dietary fibre in inflammatory bowel disease. *Prz. Gastroenterol.* 10, 135–141. doi: 10.5114/pg.2015.52753

Probert, C. S., Jayanthi, V., Pinder, D., Wicks, A. C., and Mayberry, J. F. (1992). Epidemiologic-study of ulcerative proctocolitis in indian migrants and the indigenous population of leicestershire. *Gut* 33, 687–693. doi: 10.1136/gut.33.5.687

Putignani, L., Del Chierico, F., Vernocchi, P., Cicala, M., Cucchiara, S., Dallapiccola, B., et al. (2016). Gut microbiota dysbiosis as risk and premorbid factors of IBD and IBS along the childhood-adulthood transition. *Inflamm. Bowel Dis.* 22, 487–504. doi: 10.1097/MIB.0000000000000602

Qin, J., Li, R., Raes, J., Arumugam, M., Burgdorf, K. S., Manichanh, C., et al. (2010). A human gut microbial gene catalog established by metagenomic sequencing. *Nature* 464, 59–65. doi: 10.1038/nature08821

Rajca, S., Grondin, V., Louis, E., Vernier-Massouille, G., Grimaud, J. C., Bouhnik, Y., et al. (2014). Alterations in the intestinal microbiome (Dysbiosis) as a predictor of relapse after infliximab withdrawal in Crohn's disease. *Inflamm. Bowel Dis.* 20, 978–986. doi: 10.1097/MIB.0000000000000036

Ramanan, D., Bowcutt, R., Lee, S. C., Tang, M. S., Kurtz, Z. D., Ding, Y., et al. (2016). Helminth infection promotes colonization resistance via type 2 immunity. *Science* 352, 608–612. doi: 10.1126/science.aaf3229

Reyes, A., Haynes, M., Hanson, N., Angly, F. E., Heath, A. C., Rohwer, F., et al. (2010). Viruses in the faecal microbiota of monozygotic twins and their mothers. *Nature* 466, 334–338. doi: 10.1038/nature09199

Reyes, A., Wu, M., McNulty, N. P., Rohwer, F. L., and Gordon, J. I. (2013). Gnotobiotic mouse model of phage-bacterial host dynamics in the human gut. *Proc. Natl. Acad. Sci. U.S.A.* 110, 20236–20241. doi: 10.1073/pnas.1319470110

Rocchi, A., Benchimol, E. I., Bernstein, C. N., Bitton, A., Feagan, B., Panaccione, R., et al. (2012). Inflammatory bowel disease: a Canadian burden of illness review. *Can J. Gastroenterol.* 26, 811–817. doi: 10.1155/2012/984575

Rokkas, T., Gisbert, J. P., Niv, Y., and O'morain, C. (2015). The association between *Helicobacter pylori* infection and inflammatory bowel disease based on meta-analysis. *United Eur Gastroenterol. J.* 3, 539–550. doi: 10.1177/2050640615580889

Round, J. L., Lee, S. M., Li, J., Tran, G., Jabri, B., Chatila, T. A., et al. (2011). The toll-like receptor 2 pathway establishes colonization by a commensal of the human microbiota. *Science* 332, 974–977. doi: 10.1126/science.1206095

Round, J. L., and Mazmanian, S. K. (2009). The gut microbiota shapes intestinal immune responses during health and disease. *Nat. Rev. Immunol.* 9, 313–323. doi: 10.1038/nri2515

Ruyssers, N. E., De Winter, B. Y., De Man, J. G., Loukas, A., Pearson, M. S., Weinstock, J. V., et al. (2009). Therapeutic potential of helminth soluble proteins in TNBS-induced colitis in mice. *Inflamm. Bowel Dis.* 15, 491–500. doi: 10.1002/ibd.20787

Sartor, R. B. (2008). Microbial influences in inflammatory bowel diseases. *Gastroenterology* 134, 577–594. doi: 10.1053/j.gastro.2007.11.059

Sartor, R. B., and Wu, G. D. (2017). Roles for intestinal bacteria, viruses, and fungi in pathogenesis of inflammatory bowel diseases and therapeutic approaches. *Gastroenterology* 152, 327–339. doi: 10.1053/j.gastro.2016.10.012

Schnorr, S. L., Candela, M., Rampelli, S., Centanni, M., Consolandi, C., Basaglia, G., et al. (2014). Gut microbiome of the Hadza hunter-gatherers. *Nat. Commun.* 5:3654 doi: 10.1038/ncomms4654

Schultz, M. (2008). Clinical use of *E. coli* Nissle 1917 in inflammatory bowel disease. *Inflamm. Bowel Dis.* 14, 1012–1018. doi: 10.1002/ibd.20377

Schwiertz, A., Jacobi, M., Frick, J., Markus, R., Rusch, K., and Kohler, H. (2010). Microbiota in pediatric inflammatory bowel disease. *J. Pediatr. Gastroenterol. Nutri.* 50, E105–E105. doi: 10.1016/j.jpeds.2010.02.046

Sepehri, S., Kotlowski, R., Bernstein, C. N., and Krause, D. O. (2007). Microbial diversity of inflamed and noninflamed gut biopsy tissues in inflammatory bowel disease. *Inflamm. Bowel Dis.* 13, 675–683. doi: 10.1002/ibd.20101

Shaw, K. A., Bertha, M., Hofmekler, T., Chopra, P., Vatanen, T., Srivatsa, A., et al. (2016). Dysbiosis, inflammation, and response to treatment: a longitudinal study of pediatric subjects with newly diagnosed inflammatory bowel disease. *Genome Med.* 8:75. doi: 10.1186/s13073-016-0331-y

Shivashankar, R., Beauvais, J. C., and Lewis, J. D. (2017). The relationship of regional diets with global incidence rates of inflammatory bowel disease. *Gastroenterology* 152, S975–S976. doi: 10.1016/S0016-5085(17)33306-1

Smith, P. M., Howitt, M. R., Panikov, N., Michaud, M., Gallini, C., Bohlooly-y, M., et al. (2013). The microbial metabolites, short-chain fatty acids, regulate colonic Treg cell homeostasis. *Science* 341, 569–573. doi: 10.1126/science.1241165

Sokol, H., Leducq, V., Aschard, H., Pham, H. P., Jegou, S., Landman, C., et al. (2017). Fungal microbiota dysbiosis in IBD. *Gut* 66, 1039–1048. doi: 10.1136/gutjnl-2015-310746

Sokol, H., Lepage, P., Seksik, P., Dore, J., and Marteau, P. (2006). Temperature gradient gel electrophoresis of fecal 16S rRNA reveals active *Escherichia coli* in the microbiota of patients with ulcerative colitis. *J. Clin. Microbiol.* 44, 3172–3177. doi: 10.1128/JCM.02600-05

Sokol, H., Pigneur, B., Watterlot, L., Lakhdari, O., Bermudez-Humaran, L. G., Gratadoux, J. J., et al. (2008). *Faecalibacterium* prausnitzii is an anti-inflammatory commensal bacterium identified by gut microbiota analysis of Crohn disease patients. *Proc. Natl. Acad. Sci. U.S.A.* 105, 16731–16736. doi: 10.1073/pnas.0804812105

Sokol, H., Seksik, P., Furet, J. P., Firmesse, O., Nion-Larmurier, I., Beaugerie, L., et al. (2009). Low counts of *Faecalibacterium* prausnitzii in colitis microbiota. *Inflamm. Bowel Dis.* 15, 1183–1189. doi: 10.1002/ibd.20903

Soll, D. R., Galask, R., Schmid, J., Hanna, C., Mac, K., and Morrow, B. (1991). Genetic dissimilarity of commensal strains of candida spp carried in different anatomical locations of the same healthy women. *J. Clin. Microbiol.* 29, 1702–1710.

Soon, S., Molodecky, N. A., Rabi, D. M., Ghali, W. A., Barkema, H. W., and Kaplan, G. G. (2012). The relationship between urban environment and the inflammatory bowel diseases: a systematic review and meta-analysis. *BMC Gastroenterol.* 12:51. doi: 10.1186/1471-230X-12-51

Standaert-Vitse, A., Sendid, B., Joossens, M., Francois, N., Vandewalle-El Khoury, P., Branche, J., et al. (2009). Candida albicans Colonization and ASCA in familial Crohn's Disease. *Am. J. Gastroenterol.* 104, 1745–1753. doi: 10.1038/ajg.2009.225

Steck, N., Hoffmann, M., Sava, I., Kim, S., Hahne, H., Schemann, M., et al. (2011). *Enterococcus faecalis* metalloprotease compromises epithelial barrier and contributes to intestinal inflammation. *Int. J. Med. Microbiol.* 301, 106–106. doi: 10.1053/j.gastro.2011.05.035

Stepek, G., Auchie, M., Tate, R., Watson, K., Russell, D. G., Devaney, E., et al. (2002). Expression of the filarial nematode phosphorylcholine-containing glycoprotein, ES62, is stage specific. *Parasitology* 125, 155–164. doi: 10.1017/S0031182002001920

Strauss, J., Kaplan, G. G., Beck, P. L., Rioux, K., Panaccione, R., Devinney, R., et al. (2011). Invasive potential of gut mucosa-derived *Fusobacterium* nucleatum positively correlates with IBD status of the host. *Inflamm. Bowel Dis.* 17, 1971–1978. doi: 10.1002/ibd.21606

Summers, R. W., Elliott, D. E., Urban, J. F., Thompson, R., and Weinstock, J. V. (2005a). Trichuris suis therapy in Crohn's disease. *Gut* 54, 87–90. doi: 10.1136/gut.2004.041749

Summers, R. W., Elliott, D. E., Urban, J. F., Thompson, R. A., and Weinstock, J. V. (2005b). Trichuris suis therapy for active ulcerative colitis: a randomized controlled trial. *Gastroenterology* 128, 825–832. doi: 10.1053/j.gastro.2005.01.005

Tamboli, C. P., Neut, C., Desreumaux, P., and Colombel, J. F. (2004). Dysbiosis as a prerequisite for IBD. *Gut* 53, 1057. doi: 10.1136/gut.53.1.1

Turnbaugh, P. J., Baeckhed, F., Fulton, L., and Gordon, J. I. (2008). Diet-induced obesity is linked to marked but reversible alterations in the mouse distal gut microbiome. *Cell Host Microbe* 3, 213–223. doi: 10.1016/j.chom.2008.02.015

Turnbaugh, P. J., Hamady, M., Yatsunenko, T., Cantarel, B. L., Duncan, A., Ley, R. E., et al. (2009). A core gut microbiome in obese and lean twins. *Nature* 457, 480–484. doi: 10.1038/nature07540

Turner, D., Levine, A., Kolho, K. L., Shaoul, R., and Ledder, O. (2014). Combination of oral antibiotics may be effective in severe pediatric ulcerative colitis: a preliminary report. *J. Crohns Colitis* 8, 1464–1470. doi: 10.1016/j.crohns.2014.05.010

Uhr, J. W., Dancis, J., Franklin, E. C., Finkelstein, M. S., and Lewis, E. W. (1962). The antibody response to bacteriophage phi-X 174 in newborn premature infants. *J. Clin. Invest.* 41, 1509–1513. doi: 10.1172/JCI104606

Underhill, D. M., and Iliev, I. D. (2014). The mycobiota: interactions between commensal fungi and the host immune system. *Nat. Rev. Immunol.* 14, 405–416. doi: 10.1038/nri3684

Varela, E., Manichanh, C., Gallart, M., Torrejón, A., Borruel, N., Casellas, F., et al. (2013). Colonisation by *Faecalibacterium prausnitzii* and maintenance of clinical remission in patients with ulcerative colitis. *Aliment. Pharmacol. Ther.* 38, 151–161. doi: 10.1111/apt.12365

Velthuis, J. H., Unger, W. W., Abreu, J. R., Duinkerken, G., Franken, K., Peakman, M, et al. (2010). Simultaneous detection of circulating autoreactive CD8(+) T-cells specific for different islet cell-associated epitopes using combinatorial MHC multimers. *Diabetes* 59, 1721–1730. doi: 10.2337/db09-1486

Virgin, H. W. (2014). The virome in mammalian physiology and disease. *Cell* 157, 142–150. doi: 10.1016/j.cell.2014.02.032

Vrieze, A., Van Nood, E., and Holleman, F. (2013). Transfer of intestinal microbiota from lean donors increases insulin sensitivity in individuals with metabolic syndrome (vol 143, pg 913, 2012). *Gastroenterology* 144, 250–250. doi: 10.1053/j.gastro.2012.11.032

Wagner, J., Maksimovic, J., Farries, G., Sim, W. H., Bishop, R. F., Cameron, D. J., et al. (2013). Bacteriophages in gut samples from pediatric Crohn's disease patients: metagenomic analysis using 454 pyrosequencing. *Inflamm. Bowel Dis.* 19, 1598–1608. doi: 10.1097/MIB.0b013e318292477c

Waller, A. S., Yamada, T., Kristensen, D. M., Kultima, J. R., Sunagawa, S., Koonin, E. V., et al. (2014). Classification and quantification of bacteriophage taxa in human gut metagenomes. *ISME J.* 8, 1391–1402. doi: 10.1038/ismej.2014.30

Wehkamp, J., Harder, J., Wehkamp, K. B., Wehkamp-von Meissner, B., Schlee, M., Enders, C., et al. (2004). NF-κB-and AP-1-mediated induction of human beta defensin-2 in intestinal epithelial cells by *Escherichia coli* Nissle 1917: a novel effect of a probiotic bacterium. *Infect. Immun.* 72, 5750–5758. doi: 10.1128/IAI.72.10.5750-5758.2004

Weinstock, J. V., and Elliott, D. E. (2009). Helminths and the IBD hygiene hypothesis. *Inflamm. Bowel Dis.* 15, 128–133. doi: 10.1002/ibd.20633

Weinstock, J. V., Summers, R. W., Elliott, D. E., Qadir, K., Urban, J. F., and Thompson, R. (2002). The possible link between de-worming and the emergence of immunological disease. *J. Lab. Clin. Med.* 139, 334–338. doi: 10.1067/mlc.2002.124343

Willing, B., Halfvarson, J., Dicksved, J., Rosenquist, M., Järnerot, G., Engstrand, L., et al. (2009). Twin studies reveal specific imbalances in the mucosa-associated microbiota of patients with ileal Crohn's disease. *Inflamm. Bowel Dis.* 15, 653–660. doi: 10.1002/ibd.20783

Wu, G. D., Chen, J., Hoffmann, C., Bittinger, K., Chen, Y. Y., Keilbaugh, S. A., et al. (2011). Linking long-term dietary patterns with gut microbial enterotypes. *Science* 334, 105–108. doi: 10.1126/science.1208344

Xenoulis, P. G., Palculict, B., Allenspach, K., Steiner, J. M., Van House, A. M., and Suchodolski, J. S. (2008). Molecular-phylogenetic characterization of microbial communities imbalances in the small intestine of dogs with inflammatory bowel disease. *FEMS Microbiol. Ecol.* 66, 579–589. doi: 10.1111/j.1574-6941.2008.00556.x

Yan, X., Sivignon, A., Yamakawa, N., Crepet, A., Travelet, C., Borsali, R., et al. (2015). Glycopolymers as antiadhesives of *E. coli* strains inducing inflammatory bowel diseases. *Biomacromolecules* 16, 1827–1836. doi: 10.1021/acs.biomac.5b00413

Yang, X. D., Yang, Y. P., Wang, Y. Y., Zhan, B., Gu, Y., Cheng, Y. L., et al. (2014)Excretory/secretory products from trichinella spiralis adult worms ameliorate DSS-induced colitis in mice. *PLoS ONE* 9:96454. doi: 10.1371/journal.pone.0096454

Yang, YJ., Kim, M.-S., Kim, E., Cheon, J. H., Lee, Y.-S., Choi, S. S., et al. (2016). Enteric viruses ameliorate gut inflammation via toll-like receptor 3 and toll-like receptor 7-mediated interferon-β production. *Immunity* 44, 889–900. doi: 10.1016/j.immuni.2016.03.009

Yatsunenko, T., Rey, F. E., Manary, M. J., Trehan, I., Dominguez-Bello, M. G., Contreras, M., et al. (2012). Human gut microbiome viewed across age and geography. *Nature* 486, 222–227. doi: 10.1038/nature11053

Yu, T., Guo, F., Yu, Y., Sun, T., Ma, D., Han, J., et al. (2017). *Fusobacterium* nucleatum promotes chemoresistance to colorectal cancer by modulating autophagy. *Cell* 170, 548–563.e16. doi: 10.1016/j.cell.2017.07.008

Zhang, Y. F., and LeJeune, J. T. (2008). Transduction of bla(CMY-2), tet(A), and tet(B) from Salmonella enterica subspecies enterica serovar Heidelberg to S-Typhimurium. *Vet. Microbiol.* 129, 418–425. doi: 10.1016/j.vetmic.2007.11.032

Zhu, W. H., Winter, M. G., Byndloss, M. X., Spiga, L., Duerkop, B. A., Hughes, E. R., et al. (2018). Precision editing of the gut microbiota ameliorates colitis. *Nature* 553, 208–211. doi: 10.1038/nature25172

Zuo, T., Kamm, M. A., Colombel, J.-F., and Ng, S. C. (2018). Urbanization and the gut microbiota in health and inflammatory bowel disease. *Nat. Rev. Gastro. Hepat*. 15:440–452. doi: 10.1038/s41575-018-0003-z.

Zuo, T., Wong, S. H., Lam, L. Y. K., Lui, R., Cheung, K., Tang, W., et al. (2017). Bacteriophage transfer during fecal microbiota transplantation is associated with treatment response in clostridium difficile infection. *Gastroenterology* 152, S140–S141. doi: 10.1016/S0016-5085(17)30798-9

Conflict of Interest Statement: The authors declare that the research was conducted in the absence of any commercial or financial relationships that could be construed as a potential conflict of interest.

Copyright © 2018 Zuo and Ng. This is an open-access article distributed under the terms of the Creative Commons Attribution License (CC BY). The use, distribution or reproduction in other forums is permitted, provided the original author(s) and the copyright owner(s) are credited and that the original publication in this journal is cited, in accordance with accepted academic practice. No use, distribution or reproduction is permitted which does not comply with these terms.

frontiers in Microbiology

ORIGINAL RESEARCH
published: 09 October 2018
doi: 10.3389/fmicb.2018.02360

Keystone Species in Pregnancy Gingivitis: A Snapshot of Oral Microbiome During Pregnancy and Postpartum Period

*Preethi Balan[1], Yap Seng Chong[2], Shivshankar Umashankar[3,4], Sanjay Swarup[3,4,5], Wong Mun Loke[1], Violeta Lopez[6], Hong Gu He[6] and Chaminda Jayampath Seneviratne[1]**

[1] Discipline of Oral Sciences, Faculty of Dentistry, National University of Singapore, Singapore, Singapore, [2] Department of Obstetrics and Gynaecology, Yong Loo Lin School of Medicine, National University Hospital, Singapore, Singapore, [3] Department of Biological Sciences, Faculty of Science, National University of Singapore, Singapore, Singapore, [4] Singapore Centre for Environmental Life Sciences Engineering, National University of Singapore, Singapore, Singapore, [5] Synthetic Biology for Clinical and Technological Innovation, Centre for Life Sciences, National University of Singapore, Singapore, Singapore, [6] Alice Lee Centre for Nursing Studies, Yong Loo Lin School of Medicine, National University of Singapore, Singapore, Singapore

OPEN ACCESS

Edited by:
Nurul-Syakima Ab Mutalib, UKM Medical Molecular Biology Institute (UMBI), Malaysia

Reviewed by:
Christian T. K.-H. Stadtlander, Independent Researcher, St. Paul, MN, United States
Digvijay Verma, Babasaheb Bhimrao Ambedkar University, India

***Correspondence:**
Chaminda Jayampath Seneviratne
jaya@nus.edu.sg

Specialty section:
This article was submitted to Microbial Symbioses, a section of the journal Frontiers in Microbiology

Received: *15 July 2018*
Accepted: *14 September 2018*
Published: *09 October 2018*

Citation:
Balan P, Chong YS, Umashankar S, Swarup S, Loke WM, Lopez V, He HG and Seneviratne CJ (2018) Keystone Species in Pregnancy Gingivitis: A Snapshot of Oral Microbiome During Pregnancy and Postpartum Period. Front. Microbiol. 9:2360. doi: 10.3389/fmicb.2018.02360

It is well known that pregnancy is under the constant influence of hormonal, metabolic and immunological factors and this may impact the oral microbiota toward pregnancy gingivitis. However, it is still not clear how the oral microbial dysbiosis can modulate oral diseases as oral microbiome during pregnancy is very poorly characterized. In addition, the recent revelation that placental microbiome is akin to oral microbiome further potentiates the importance of oral dysbiosis in adverse pregnancy outcomes. Hence, leveraging on the 16S rRNA gene sequencing technology, we present a snapshot of the variations in the oral microbial composition with the progression of pregnancy and in the postpartum period and its association with pregnancy gingivitis. Despite the stability of oral microbial diversity during pregnancy and postpartum period, we observed that the microbiome makes a pathogenic shift during pregnancy and reverts back to a healthy microbiome during the postpartum period. Co-occurrence network analysis provided a mechanistic explanation of the pathogenicity of the microbiome during pregnancy and predicted taxa at hubs of interaction. Targeting the taxa which form the ecological guilds in the underlying microbiome would help to modulate the microbial pathogenicity during pregnancy, thereby alleviating risk for oral diseases and adverse pregnancy outcomes. Our study has also uncovered the possibility of novel species in subgingival plaque and saliva as the key players in the causation of pregnancy gingivitis. The keystone species hold the potential to open up avenues for designing microbiome modulation strategies to improve host health during pregnancy.

Keywords: pregnancy, microbiome, gingivitis, oral health, adverse pregnancy (birth) outcomes

Abbreviations: ANOVA, analysis of variance; BGI, Beijing Genome Institute; FDR, False Discovery Rate; GBI, gingival bleeding index; HMP, human microbiome project; NHG DSRB, National Health Group Domain Specific Review Boards; OTU, operational taxonomic units; PCoA, principal coordinates analysis; PERMANOVA, Permutational Multivariate Analysis of Variance Using Distance Matrices; RDP, Ribosomal Database Project; SGP, subgingival plaque.

INTRODUCTION

The oral cavity is one of the most clinically relevant habitats in humans. The diverse microorganisms of the oral cavity have been associated with numerous oral and systemic diseases (He et al., 2015; Simpson and Thomas, 2016). Currently, the expanded Human Oral Microbiome Database (eHOMD) contains a total of 770 microbial species, which includes 687 species from version 14.51 of HOMD and 83 species have been added based on publicly available data on the microbiota of the aerodigestive tract outside of the mouth (Chen et al., 2010; Dewhirst et al., 2010; Verma et al., 2018) The diversity and richness of the oral microbial community can be modified by fluctuations in the oral environment that may occur as a consequence of the systemic changes in the human body (Avila et al., 2009). Pregnancy represents one such altered environment where the body undergoes hormonal, metabolic, and immunological changes (Kumar and Magon, 2012). A dramatic rise in the level of sex hormones like progesterone and estrogens and altered immune responses during pregnancy can cause a significant impact on the human oral microbiome (Kumar and Magon, 2012; Nuriel-Ohayon et al., 2016).

Changes in the oral microbiota and the oral ecosystem may predispose the pregnant women to a higher risk of developing "gingival diseases" or exacerbated gingival inflammation. As a result, pregnancy gingivitis has been reported to be the most common oral manifestation during pregnancy with a prevalence of 35–100%, depending on the study cohort (Onigbinde et al., 2014). Moreover, gingival inflammation is also considered to be a potential risk factor for developing adverse pregnancy outcomes (Han, 2011). Interestingly, a recent sequencing-based study has shown that the microbial taxa detected in the placenta are akin to the commensal species in the oral microbiome rather than microbes derived from the urogenital tract (Aagaard et al., 2014). Hence, it is likely that the oral microbiome plays an important role in the health and disease status of the pregnant mother as well as the developing fetus.

Previous studies using culture-based and PCR-based methods have identified the association of anaerobic species such as *Porphyromonas gingivalis, Prevotella intermedia, Treponema denticola, Tannerella forsythia, Campylobacter rectus, Prevotella nigrescens,* and *Treponema denticola* with gingival bleeding during pregnancy (Kornman and Loesche, 1980; Jensen et al., 1981; Gursoy et al., 2009; Carrillo-de-Albornoz et al., 2010). However, this knowledge has been challenged by current studies based on DNA-sequencing platforms. Apparently, only one prospective study on the oral microbiome of pregnant women has been reported in the literature and none in the Chinese population (DiGiulio et al., 2015). Therefore, taking this research gap into consideration, the present study examined the changes in the oral microbiome that occur during pregnancy and the postpartum period of the Chinese population in Singapore. Both saliva and subgingival samples were collected from 24 patients across the three trimesters of pregnancy and during the postpartum period. Herein, we present a snapshot of the variations in the oral microbial composition and diversity with the progression of pregnancy and in the postpartum period, leveraging on the 16S rRNA gene sequencing technology.

MATERIALS AND METHODS

Cohort Design

Twenty-four participants were enrolled in this study through the prenatal clinic of a tertiary public hospital in Singapore. The study was approved by the National Health Group Domain Specific Review Boards (NHG DSRB Ref: 2014/00979). The inclusion criteria for the study were Singaporean Chinese pregnant women aged 21 years or older, with a gestational age of $\leq$12 weeks for the first trimester; 21–24 weeks for the second trimester; and 32–36 weeks for the third trimester; and 6 weeks for the postpartum analysis. The exclusion criteria were non-Chinese pregnant women and Chinese pregnant women with known systemic diseases and smoking habit; participants who have visited the dental clinic in the past 6 months for any gingival complaints; and prior gingival bleeding before the start of pregnancy. The study comprised 10 participants each across the three trimesters of pregnancy and 10 participants in the postpartum period, from whom a total of 40 saliva samples and 40 SGP samples were collected. Of these 40 participants, none in the first trimester attended any further follow-up sampling; six women in the second trimester attended sampling until the postpartum period; nine women in the second trimester attended sampling till the third trimester and seven women in the third trimester attended sampling till the postpartum period. The recruitment algorithm is represented in **Supplementary Figure S1**. A self-reported questionnaire was employed to obtain participants' demographic data and assess their oral health characteristics.

Clinical Assessment and Sample Collection

The clinical assessment of gingival bleeding was performed using the GBI of Ainamo and Bay (1975). A blunt periodontal probe was passed along the gingival crevice at the labial and lingual surfaces of the teeth. If bleeding occurred within 10–15 s, a positive score of "1" was given while a negative score of "0" was given for surfaces with no bleeding. The number of elicited bleeding points was totaled and divided by the number of gingival margins examined. The plaque index was graded on a scale of 1–3, where a score of 1 was considered "good" when dental plaque covered less than one third of all teeth present, score of 2 was considered "average" when dental plaque covered more than one third of the teeth but less than half of all teeth present, and a score of 3 was considered "poor" when half or more than half of all teeth present had dental plaque/calculus.

Unstimulated saliva was collected in a sterile, disposable 15 ml tube after thorough rinsing of the mouth. Samples of SGP were collected from all teeth between the incisors and the first molars in each of the four quadrants by inserting sterile paper points for 15 s. The plaque samples collected on the paper points were then suspended in a 2 ml tube containing 200 μL of TE buffer solution (pH 8.0). The saliva and SGP samples were frozen instantaneously on ice, transported, and stored at $-80°$C until

further analysis. All samples used in this study were collected by the same clinician and the same protocol was used to limit sampling variability.

DNA Extraction, Amplicon Synthesis, and Sequencing

Saliva and SGP samples were centrifuged at 8000 rpm for 10 min at 4°C to collect the cell pellet containing total DNA. Supernatant was separated from the cell pellet and DNA was extracted from the pellet using QiAamp UCP Pathogen Mini-kit (Qiagen Inc., Valencia, CA, United States) according to the manufacturer's instructions. A quantitative 16S rRNA PCR was performed to determine the amount of bacterial template DNA in the samples and a bacterial 16S rRNA amplicon library spanning the variable region V4 was generated. The DNA sequences of the amplicon library were determined using Illumina MiSeq technology at the Beijing Genome Institute [(BGI Tech Solutions (Hongkong) Co., Ltd., Hongkong].

Sequence Analysis

Paired-end reads were generated using the Illumina MiSeq platform. The tags were clustered into OTUs with a 97% threshold using UPARSE, and chimeras were filtered out by using UCHIME (v4.2.40) to form OTU representative sequences, with singleton OTUs excluded. Sequences representative of OTUs were taxonomically classified using the RDP Classifier v.2.2 against the Greengenes database, using 0.8 confidence value as cut-off. The representative sequences were aligned against the Silva core set (Silva_108_core_aligned_seqs) using PyNAST by 'align_seqs.py'. Alpha-diversity indices were estimated based on Observed species, Chao1, Shannon, and Simpson values (Shannon, 1948; Chao, 1984), which reflect the species diversity of the community, and are affected by both species richness and species evenness. These indices were calculated using Mothur (v1.31.2) and the corresponding rarefaction curves were drawn by R (v3.0.3). Fishers alpha diversity was calculated using fisher.alpha function of 'vegan' package (Oksanen et al., 2013), while the good coverage was calculated using the goods function of 'QsrUtils' package, and the boxplot was plotted using the 'ggplot2' package in R (Wickham, 2018). UniFrac-based PCoA was performed using QIIME. Metastats and R (v3.0.3) were used to determine differentially abundant taxonomic groups.

Statistical Analysis

Paired *t*-tests were performed to compare the alpha diversity among the trimester groups and with the postpartum group. PERMANOVA with 999 permutations was performed on the unweighted UniFrac distances using the *adonis* function in 'vegan' package in R (Oksanen et al., 2013). The distance-based tests of homogeneity of multivariate dispersions, to evaluate differences in structure centroid and dispersion (beta diversity), were performed using both the ANOVA and permutation test for homogeneity. Wilcoxon rank sum test was used to compare taxonomic abundance in the cross-sectional analysis. Spearman correlation was used to obtain pairwise score and to construct microbial interaction network models for pregnant and postpartum subjects. Pairwise network comparisons were carried out at global and module levels. Cytoscape 'Network Analyzer' plugin (Shannon et al., 2003) was used to characterize the global topological properties of networks during the three trimesters of pregnancy and the postpartum period. For module level comparisons, Molecular Complex Detection (MCODE) (Bader and Hogue, 2003) was used to extract the top highly connected modules in both pregnant and the postpartum groups. Spearman correlation coefficients were used to assess the bacterial association with GBI. Identification of keystone species was done using the CytoHubba plugin (Chin et al., 2014), which provided topological analysis by Degree, Edge Percolated Component, Maximum Neighborhood Component, Density of Maximum Neighborhood Component, and Maximal Clique Centrality (MCC) and six centralities (Bottleneck, EcCentricity, Closeness, Radiality, Betweenness, and Stress) based on the shortest paths. To assess the predictive power of the keystone species in identifying pregnancy gingivitis, a receiver operating characteristic (ROC) curve was constructed with true positive rate (Sensitivity) as a function of the false positive rate (1-Specificity) using XLSTAT add-on.

RESULTS

Participant Characteristics

The mean age of the participants in the study was 31.9 (SD ± 5.4) years and the mean gestational age was 8.9 weeks (SD ± 3.3), 21.7 weeks (SD ± 1.4), and 31.6 weeks (SD ± 1.5) in the first, second, and third trimesters respectively. All participants were reported to be non-smokers. Majority of the participants (83.3%) brushed their teeth twice a day. A good Plaque Index score was obtained for 66.7% of participants, while the remaining 33.3% obtained an average plaque score. Demographic and baseline clinical characteristics of the study population have been detailed in **Supplementary Table S1**. A total number of 3,052,703 reads were obtained from the 80 saliva and SGP samples with an average of 38,158 reads per sample and an average length of 252 bp. Of these, 2,787,452 sequences were filtered from the dataset, aligned with the Greengenes database, and clustered to 736 OTUs, which were non-singletons at 97% sequence similarity. OTUs were classified into a total of 12 phyla, 65 genera, and 131 species.

Oral Microbiome Remains Stable During the Course of Pregnancy

Good's coverage is an estimator of the proportion of non-singleton OTUs in the dataset as a measure of overall OTU sampling completion and was used to assess the adequacy of sampling. The Good's coverage of bacteria reached 99.8% in our dataset with majority of microbial diversity being captured. Alpha diversity analysis of the forty samples of SGP showed that three of the alpha diversity measures (Observed species, Chao 1, and Simpson index) were significantly different for only SGP samples between the second and third trimesters (**Figure 1**). Fisher's alpha diversity, which is an indicator for logarithmic changes in relative abundances corroborated these findings and

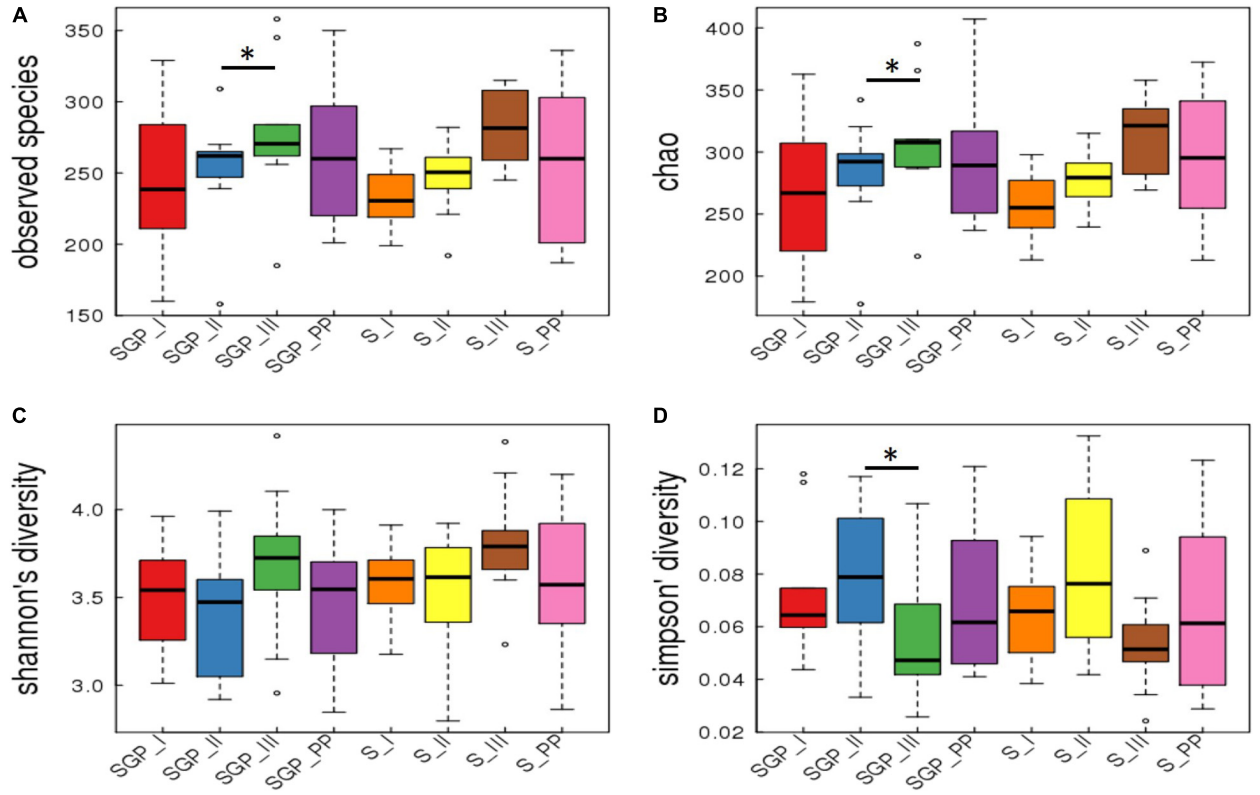

FIGURE 1 | Alpha diversity indices in subgingival plaque and saliva samples. Cross sectional analysis of alpha diversity measures in SGP and saliva samples across pregnancy and postpartum period. The indices are plotted with four alpha diversity indicators; **(A)** Observed species; **(B)** Chao1; **(C)** Shannon diversity; **(D)** Simpson's diversity. SGP, Subgingival plaque; S, Saliva; I, II, III indicate 3 trimesters of pregnancy; PP, Postpartum (*$p < 0.05$).

has been represented in **Supplementary Figure S2** On further analysis, it was observed that the significant differences in taxa arose due to inter-patient differences, which accounted for nearly 76% of the total microbial variation (**Supplementary Table S2**). Hence, analysis was performed among the longitudinal samples of six participants, who completed the sampling from the second trimester until the postpartum period. The longitudinal comparison showed that, in SGP samples, the observed number of species and Chao_1 index was significantly higher in the third trimester compared to the second trimester (**Supplementary Figure S3**). However, the Shannon and Simpson diversity index, which is a mathematical measure of diversity in a community, did not show any significant difference across the pregnancy trimesters and postpartum period. The saliva samples did not show any significant trend in any of the alpha diversity indices in both cross sectional and longitudinal analysis. These results indicate that the alpha diversity, in both inter-individual and intra-individual samples, remains stable across the pregnancy trimesters and postpartum period.

Beta diversity analysis demonstrated a distinct separation between saliva and SGP samples. However, the PCoA ordination did not reveal any distinct grouping of the bacterial communities across any of the trimesters of pregnancy or the postpartum period from both the niches ($p = 0.209$) (**Figure 2A**). In addition, distance-based tests of homogeneity of multivariate dispersions, also did not show any significant difference between trimesters (**Figure 2B**). Taken together, these results suggest that the oral microbial community structure is closely related and does not dramatically remodel in its diversity with the progression of pregnancy.

Oral Microbiome Is Pathogenic During Pregnancy and Reverts to Healthy During Postpartum Period

The bacterial community of SGP and saliva was examined at different taxonomic levels. At the phylum level, the microbial composition during pregnancy was dominated by members of Firmicutes (>30%), Bacteroidetes (>20%), and Actinobacteria (>5%) in both saliva and SGP samples (**Supplementary Figure S5A**). At the genus level, the genera Prevotella (15.65%), Fusobacterium (15.63%), Streptococcus (13.30%), Veillonella (6.80%) and Terrahaemophilus (5.01%) were most abundant in SGP and collectively represented more than 50% of sequences identified in SGP (**Supplementary Figures S4, S5B**). In saliva, the genera Prevotella (21.8%), Streptococcus (17.74%), Veillonella (10.17%), Neisseria (9.50%), and Terrahaemophilus (7.60%), along with some unclassified genera (6.92%) were detected at more than 5% abundance and comprised over 70% of all detected sequences in saliva.

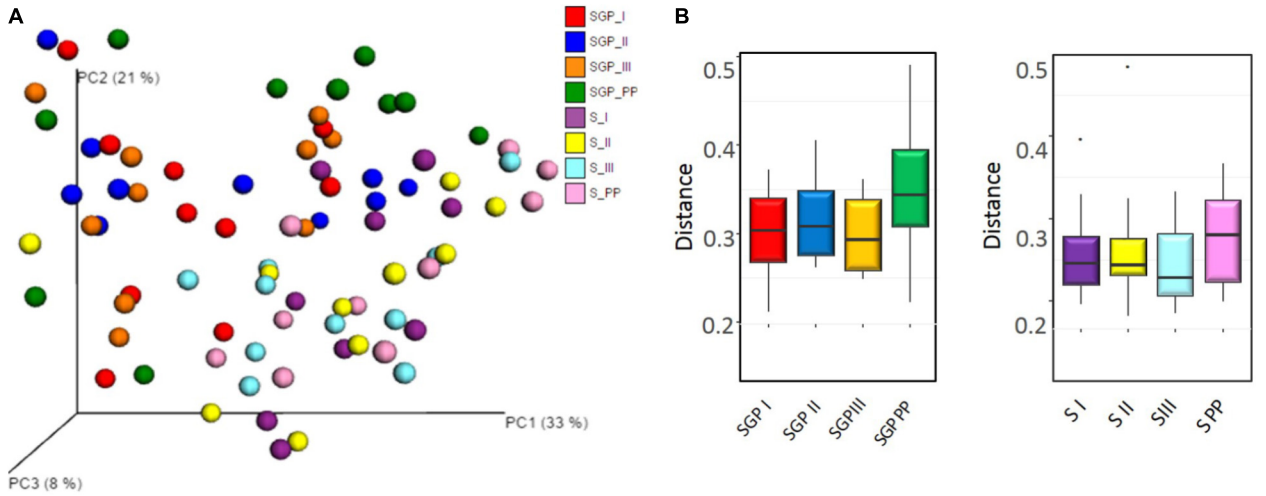

FIGURE 2 | Community structure analysis of sub gingival plaque and saliva samples **(A)** Principal Coordinate analysis (PCoA) based on weighted UniFrac distance. No distinct grouping of the bacterial communities across any trimesters of pregnancy and the postpartum period in saliva and SGP samples. **(B)** Boxplot showing the distance-based tests of homogeneity of multivariate dispersions. No significant differences in the distances of group members to the group centroid was observed. SGP, Subgingival plaque; S, Saliva; I, II, III indicate 3 trimesters of pregnancy; PP, Postpartum.

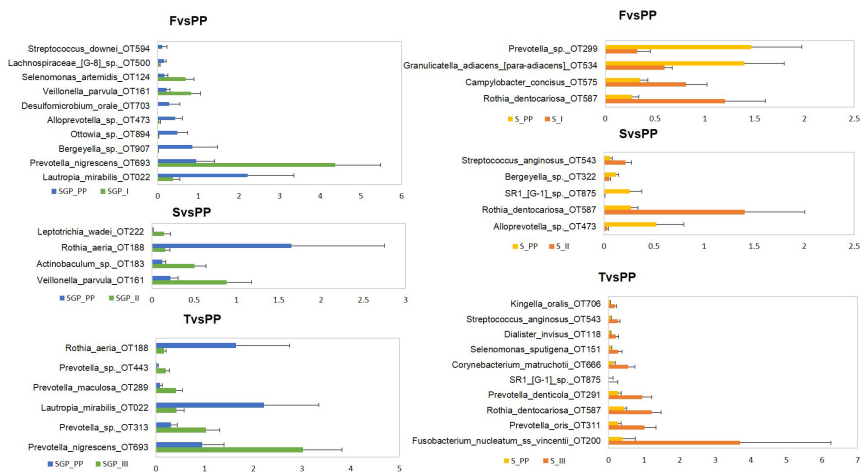

FIGURE 3 | Differential abundance of subgingival and saliva samples at species level. F, First trimester; S, Second trimester; T, Third trimester; PP, Postpartum ($p < 0.05$).

At species level, *unclassified species, Streptococcus sp. OT 058* and *Terrahaemophilus aromaticivorans* formed the highest abundance in both saliva and SGP samples during pregnancy (**Supplementary Figure S5C**). The pathogenic species *Prevotella nigrescens, Prevotella oris* and *Porphyromonas gingivalis* were most abundant in SGP, while *Prevotella_sp._oral_taxon_313* and *Prevotella melaninogenica* were most abundant in saliva. *Fusobacterium_nucleatum ss vincentii* showed higher abundance in SGP (13–15%) as compared to saliva (<4%) samples. Comparison of species with relative abundance that surpassed the 0.1% threshold in SGP showed that there was a significant drop in the abundance levels of pathogenic species—*Veillonella parvula*, *Prevotella species* and *Actinobaculum species* ($p < 0.05$) in the postpartum period compared with the three trimesters of pregnancy (**Figure 3**). Similarly, in the saliva samples, the pathogenic species *Fusobacteium nucleatum vincentii, Dialister invisus, Prevotella oris, Prevotella denticola, Cornybacterium matruchotii, Rothia dentocariosa, Streptococcus anginosus, Selenomonas sputigena,* and *Kingella oralis* were decreased significantly ($p < 0.05$) in the postpartum period than the pregnant condition. Conversely, bacterial species associated with health such as *Lautropia mirabilis*, *Rothia aeria, Granulicatella adiacens* and *SR1 species* repopulated in the oral microbiome during the postpartum period. It is likely that the pathogenic bacterial species in the oral microbiota thrive during the course of pregnancy, but their abundance declines during the postpartum period with the re-establishment of healthy oral microbiota.

Network Analysis

To compare the ecological relationships across the bacterial communities, correlation based networks were generated for the pregnancy group (by merging all three trimesters) and for the postpartum group. The networks were then analyzed at the global and module levels. The topological properties at the global level of the two networks are shown in **Table 1**. The topological properties showed that the network heterogeneity was more during pregnancy than postpartum period (1.26 vs. 0.59), while the network density was low during pregnancy (0.029) as compared to the postpartum period (0.128) (**Table 1**). There were 53 connected components in the pregnant group, while only 5 components were detected in the postpartum group. The average number of neighbors were observed to be higher in postpartum period (33.66) than pregnancy (7.66). These topological network properties of the pregnant and postpartum group suggest that the microbial community during pregnancy tend to have natural divisions within them which were not well connected. In contrast, the microbial community during the postpartum period was more coherent with strong inter-dependency within the members of the group. Thus it can be deduced that the microbial communities in the pregnant and postpartum conditions have different co-occurrences and mutual exclusion relationships.

To gain deeper insights into these differences, microbial communities were analyzed at the module level. As a result, we uncovered 8 modules (cluster) in the pregnancy group (**Supplementary Figure S6**) and 11 modules in the postpartum group (**Supplementary Figure S7**). **Supplementary Tables S3, S4** lists the results of MCODE cluster-detection in the two bacterial interaction networks. Interestingly, in the pregnant group, there was only a single strong cluster (score 20.51) with 36 nodes and 359 edges, while the other clusters were small with 3–7 nodes and 3–16 edges. The postpartum network also showed a strong cluster (score 40.83) with 44 nodes and 878 edges. However, unlike the pregnant group network, the postpartum network demonstrated additional 5 large but moderately strong clusters with 21–36 nodes and 47–180 edges. This indicates that oral microbiome during pregnancy is dominated by a single cluster of taxa, while the postpartum period promotes development of other clusters of taxa with strong interdependencies. Due to space constraints, we limited our analysis to the top module in each of pregnant and postpartum network. The top modules in both pregnant (**Figure 4A**) and postpartum group (**Figure 4B**) were dominated by pathogenic species which have been implicated in gingival or periodontal diseases. When the networks were connected by their first neighbors (direct correlations), we observed that *Filifactor alocis* formed the hub OTU around which maximum associations were centered in both the pregnant and postpartum networks. Interestingly, in the top module of pregnant group, the nodes were linked with only positive edges, suggestive of a synergistic relationship between the pathogenic species. In contrast, the positive interactions in the postpartum microbial network was also accompanied by negative interactions by health associated species such as *Bergeyella sp OT 322, Capnocytophaga leadbetteri OT 329, Eikenella corrodens OT 577,* and *Granulicatella_adiacens para-adiacens OT 534*. This invasion of negative interactions by health-associated taxa into the cluster of pathogenic species during the postpartum period explains partly how the microbiome restores to health after pregnancy.

TABLE 1 | Topological properties of interaction networks.

Network property	Pregnant group	Postpartum group
Nodes	264	264
Edges	1012	4444
Edge to node ratio	3.8:1	16.8:1
Clustering coefficient	0.300	0.464
Connected components	53	5
Network diameter	11	5
Network centralization	0.124	0.181
Shortest path	40240 (57%)	67340 (96%)
Characteristic path length	4.045	2.212
Average number of neighbors	7.667	33.667
Network density	0.029	0.128
Network heterogeneity	1.264	0.593
Isolated nodes	46	4

Oral Microbial Keystone Species Associated With Pregnancy Gingivitis

Deciphering microbial interactions and detecting the keystone species associated with disease are of great value for understanding the diseases pathologies. Hence, to identify the keystone species associated with pregnancy gingivitis, firstly, the level of pregnancy gingivitis was analyzed during each trimester of pregnancy and in the postpartum period using Ainamo GBI. The gingival bleeding was observed to increase from the first to the second trimester and decreased thereafter toward the postpartum period (**Supplementary Table S1**). Pairwise Spearman correlation analysis was then performed to assess whether the GBI correlated with specific bacterial groups in saliva and SGP. The Spearman correlation results showed that 31 species from SGP and 27 species from saliva significantly correlated with the GBI (defined as FDR < 0.200) (**Supplementary Figure S8**). Notably, the identified species that were present in more than 0.5% abundance included the periopathogens such as *Porphyromonas gingivalis* (2.22%), *Treponema denticola* (1.10%) and *Fretibacterium* sp. *OT 361* (0.67%) in SGP samples and *Prevotella_intermedia* (0.56%) in the saliva samples. In addition, *Porphyromonas endodontalis* was also observed in both SGP (0.89%) and saliva (0.91%) in high abundance. Intriguingly, the majority of the species associated with gingival bleeding were present in low abundance indicating the possibility of novel phylotypes being associated with pregnancy gingivitis, an observation that has not been reported before.

Subsequently, an interaction network of the species associated with gingival bleeding during pregnancy was constructed based on Spearman's correlation of the 31 species from SGP and 27 species from saliva. To identify the hubs or keystone species in the network, the nodes (species) were ranked by MCC algorithm (Chin et al., 2014) into top 20 species (**Figure 5A**). The species ranking were further substantiated by other algorithms

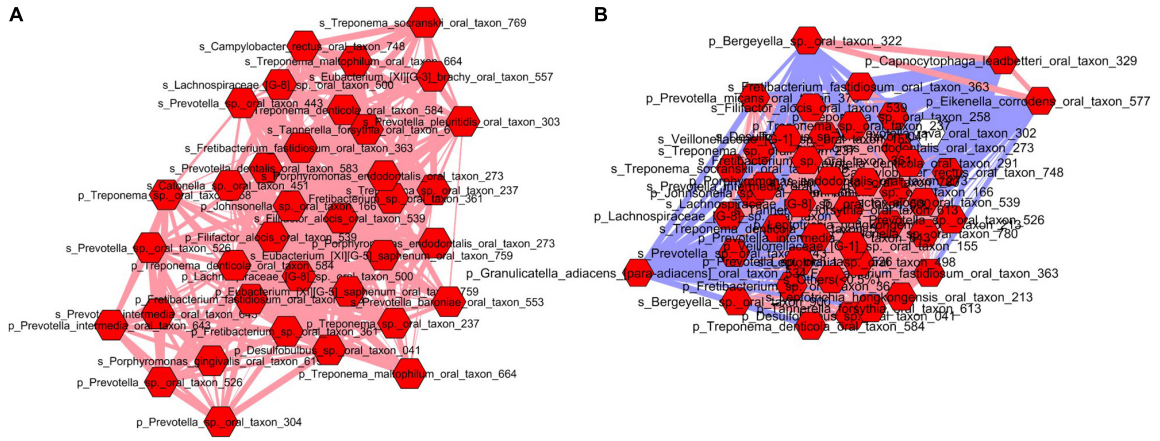

FIGURE 4 | Top module in pregnant **(A)** and postpartum **(B)** subgingival and salivary microbiome. Each node represents a bacterial species and each edge represents a co-occurrence/co-exclusion relationship. Nodes are colored based on first neighbors of *Filifactor alocis* sp. in both saliva and subgingival plaque. Edge width is proportional to the correlation coefficient and color indicates the sign of the association (blue: negative, pink: positive). Prefix 'p' and 's' denote species from subgingival plaque and saliva respectively.

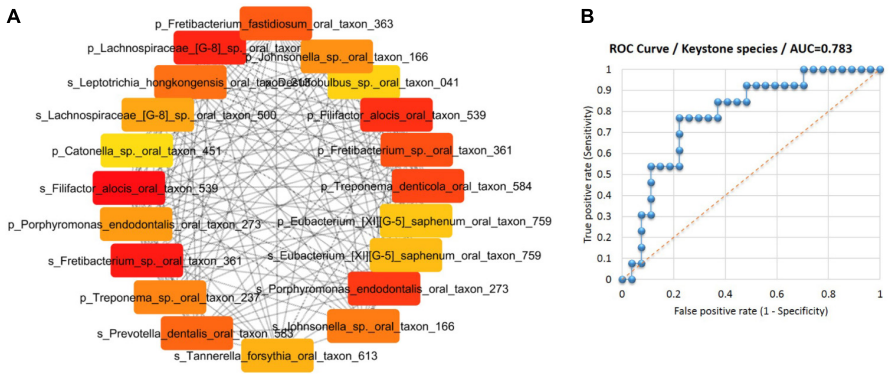

FIGURE 5 | Identification of keystone species for pregnancy gingivitis. **(A)** Top 20 nodes (species) ranked by Maximal Clique Centrality and displayed in circular layout. Nodes colored based on rank; dark color denotes high ranks **(B)** ROC curves of the keystone species in the identification of pregnancy gingivitis based on its relative abundance in saliva or subgingival plaque. (AUC denotes areas under the ROC curve).

of CytoHubba plugin (**Supplementary Data Sheet S3**). Thus, 11 SGP species and 9 saliva species were identified as the keystone players in the pathogenesis of pregnancy gingivitis.

To determine the diagnostic values of keystone species in pregnancy gingivitis, ROC curve was constructed. The area under the ROC curve (AUC) of the key species group was 0.783, indicating a good diagnostic performance (**Figure 5B**). The cut-off points of the key species group were determined at 5.28% (p = 0.001, sensitivity 0.76, specificity 0.77). These results indicate that women who have an abundance threshold of keystone species over 5.28% in SGP and saliva pose a high risk of developing gingivitis during pregnancy.

DISCUSSION

The high prevalence of gingival bleeding among women during pregnancy, could be due to the microbial perturbations influenced by immune modulations and hormonal changes (Mealey and Rose, 2008; Wu et al., 2015). Despite having a significant clinical relevance, high-resolution data on the oral microbiome during pregnancy and postpartum period are scarcely available. Therefore, using 80 samples of SGP and saliva, we analyzed the structure and composition of microbial community during pregnancy and identified the bacterial associations within the community that predispose women to pregnancy gingivitis.

Firstly, we observed that the inter-patient differences accounted for nearly 76% of the total microbial variation and was the predominant source of variation in the dataset. After offsetting the inter-patient variability, it was observed that species richness and diversity of the SGP and saliva samples were relatively stable during the course of pregnancy. Beta diversity analysis also showed that the differences in microbiome of patients is independent of the trimester and is more of an innate property of the patients themselves. These findings were

similar to that of a previous study, which demonstrated that the temporal and spatial variations in the oral microbiota tends to remain stable over gestational time (DiGiulio et al., 2015).

Despite the stability of the oral microbiome during pregnancy, it was intriguing to observe the dominance of pathogenic bacterial community during pregnancy, which attempts to re-establish into a healthy community during the postpartum period. We observed that the abundance of pathogenic taxa from genera *Prevotella, Streptococcus* and *Veillonella* in both SGP and saliva samples were more during pregnancy. This finding was in accordance with the recent study on oral microbiome in a similar population of pregnant Chinese women (Lin et al., 2018). However, the abundance of taxa observed in our study was higher than this study due to the discrepancies in sampling habitats. In contrast to the pregnant state, the genera most abundant in healthy non-pregnant subjects have been reported to be *Haemophilus*, *Neisseria*, *Streptocoocus* and *Rothia*, while the genera *Fusobacteria* and *Spirochaetes* were reported be in less abundance (Aas et al., 2005; Bik et al., 2010). In our cohort, the genera *Fusobacteria* was more prevalent with SGP (15.63%) showing more abundance than saliva (3.82%). The increased relative abundance of pathogenic taxa was observed at the species level as well with *Prevotella species, Porphyromonas gingivalis,* and *Fusobacterium nucleatum* showing higher abundance during pregnancy. The species *Prevotella intermedia, Prevotella melaninogenica,* and *Porphyromonas gingivalis*, have been reported to be abundant in previous culture based studies on pregnant women and have shown association with pregnancy gingivitis (Adriaens et al., 2009; Gursoy et al., 2009; Fujiwara et al., 2017). Interestingly, we observed that there was a significant decline in the abundance of pathogenic species from pregnancy to postpartum period. The species which showed significant drop in abundance in our cohort have not been identified previously and were largely in accordance with the comprehensive description of the microbiota in gingivitis of non-pregnant subjects (Kistler et al., 2013; Huang et al., 2014). This observation furthermore supports the pathogenicity of taxa during pregnancy. The decrease in the abundance levels of pathogenic species in the postpartum period was accompanied by simultaneous repopulation of healthy microbiome such as *Lautropis mirabilis* sp., *Rothia aeria, Granulicatella adiacens and SR1 sp* (Bik et al., 2010; Segata et al., 2012; Tsuzukibashi et al., 2017). These species have been reported to be dominating in the health-associated microbial communities in healthy subjects in previous studies (Abusleme et al., 2013; Hong et al., 2015). Pregnancy-related transition to pathogenic microbiome and its restoration to health during the postpartum period could be a result of complex host–microbial interactions that may be taking place under the influence of hormonal and immunological factors (Wu et al., 2015). In addition, pregnancy-induced perturbations in the oral cavity may disrupt the ecological balance maintained by interspecies interactions (Avila et al., 2009). These may trigger the overgrowth of species with pathogenic potential and suppress the healthy microbiome (Jenkinson and Lamont, 2005).

Further, our network analysis revealed that bacterial communities have different co-occurrence and co-exclusion relationships during pregnancy and postpartum period. The microbial network during pregnancy was observed to be inhomogeneous and sparse due to the development of natural divisions in the network. Analysis at the module level identified 8 clusters in the pregnancy network, of which only one was observed to have exceptional strength, and this module included positively associated pathogenic species centered on *Filifactor alocis species*. This was similar to the synergistic ecological pattern involving *Filifactor alocis* observed in a study of Chinese population with periodontitis (Chen et al., 2015). The clustering of potentially pathogenic groups into distinct hubs suggests how these pathogens mutually cooperate to create an imbalance in the microbial community. This in turn may lead to the creation of a milieu that is progressively pathogenic and detrimental to health. Contrary to this, the postpartum microbial network was more cohesive and included variable modules of optimum strength reflecting strong inter-dependencies. These relationships may be crucial for maintaining good health, and disruption of these interactions may lead to instability in the ecosystem or disease. However, the strongest cluster in the postpartum period microbial network was also centered on *Filifactor alocis* similar to the pregnancy microbial network. Previous studies have reported that in healthy non-pregnant population, the largest microbial representation is by *Actinomyces* spp., *Bergeyella* sp., *Kingella oralis, Lautropia mirabilis, Rothia aeria,* and *Streptococcus* spp. *Granulicatella_adiacens, Eikenella corrodens,* and *Capnocytophaga leadbetteri* (Abusleme et al., 2013; Diaz et al., 2016). The key finding in our study was the identification of negative interactions of majority of these health-associated species with the likely pathogens, indicating the restoration of the microbiome to health during the postpartum period. Given that all the negative interactions were associated with the pathogenic taxa in the post-partum period, the absence of these negative links in the pregnancy microbial network could be a possible cause for the decline of inhibitive effects on the pathogenic taxa in the microbiome. This also explains partly the pathogenic predisposition of the oral microbiome during pregnancy.

The dominance of pathogenic taxa could be the cause for pregnancy gingivitis, which is a most common manifestation of during this period (Silk et al., 2008). Pregnancy gingivitis shows a gradual increase during the progression of pregnancy, with an apparent resolution following parturition (Loe and Silness, 1963; Gursoy et al., 2008). The trend seen in our study cohort was concurrent with this observation. We identified 31 species from SGP and 27 species from saliva that were significantly associated with pregnancy gingivitis. These findings were concurrent with the majority of the previously well-studied anaerobes which showed high abundance in the setting of pregnancy gingivitis such as *Prevotella intermedia, Porphyromonas gingivalis, Treponema forsythia, Campylobacter rectus, Fusobacterium nucleatum,* and *Actinobacillus actinomycetemcomitans* (Kornman and Loesche, 1982; Yokoyama et al., 2008; Adriaens et al., 2009; Gursoy et al., 2009; Carrillo-de-Albornoz et al., 2010). Of these, *Prevotella intermedia species* is speculated as the most abundant species in pregnancy gingivitis and its growth was found to be stimulated by direct interaction of female sex hormones on the fumarate reductase system (Kornman and

Loesche, 1982; Wu et al., 2015). Contradictory to this general understanding of pathogens being abundant in disease, our microbiome data revealed that the majority of species associated with gingival bleeding were present in low abundance. Thus, high throughput sequencing platform used in our study has uncovered the possibility of novel low abundant species being key players in pregnancy gingivitis. However, their role in infections remains elusive, as they have not been cultivated yet.

As gingival diseases are polymicrobial diseases that require synergistic contribution of pathogens for disease progression (Short et al., 2014), it is comprehensible that it is not the mere presence of the pathogenic species, but rather the interactions between specific microbes that determines the course of disease. In this context, measuring the nodes of the interaction network by their network features would help to infer their biological importance in the functioning of the ecosystem. The ranking of species associated with pregnancy gingivitis using topological algorithms helped in the identification of keystone species. Interestingly, of the 20 keystone species identified, only *Porphyromonas endodontalis* and *Fretibacterium sp. OT 361* were present in more than 0.5% abundance. This finding is in line with the "keystone bacterial hypothesis" that suggests the role of low-abundance bacterial species in modulating the oral microbiome and orchestrating the disease process (Hajishengallis et al., 2012). Moreover, the low abundance species ranked more than the previously known players of pregnancy gingivitis such as *Prevotella intermedia* and *Porphyromonas gingivalis*, indicative of their presence having more biological importance in pregnancy gingivitis.

The synergistic interactions between cultivable oral pathogens have been studied previously. An *in vitro* study has shown that steroid dependent metabolism of *Prevotella intermedia* produces large amounts of fumarate, which in turn is taken up by *Campylobacter rectus* for its growth (Grenier and Mayrand, 1986). Similarly, *Porphyromonas gingivalis* can produce isobutyric acid to enhance the growth of *Treponema denticola* and utilize the succinate produced by *Treponema denticola* for its own growth (Grenier, 1992). Saito et al. (2008) have demonstrated the invasive abilities of *Porphyromonas gingivalis* strains in the presence of *Fusobacterium nucleatum*. However, these studies have studied the mutual symbiotic enhancement of microbial growth focussing two arbitrarily selected potential pathogen. Our study has identified the novel coordinated co-occurrence of 20 species present in low abundance along with the established oral pathogens. Furthermore we have evaluated the diagnostic value of this cluster using ROC curves and demonstrated that it has the potential to identify women at high-risk to develop pregnancy gingivitis.

CONCLUSION

In summary, the present study provides invaluable new insights on the modulation in the oral microbiome during pregnancy and the postpartum period. Contrary to the traditional understanding, our study has identified a potential synergistic network involving the low abundant "keystone" SGP and salivary species during pregnancy gingivitis. The keystone species hold potential to open up avenues for designing microbiome modulation strategies to improve host health during pregnancy. Considering the pilot nature of the study with limited sample size, our conclusions may be an over-simplification of the disease process. In order to obtain a definitive picture of the underlying changes associated with pregnancy gingivitis, a longitudinal study is obligatory. Nevertheless, our study lends a robust foundation for future research to develop management strategies which would help to obtain a microbial community structure favoring health during pregnancy.

AVAILABILITY OF DATA AND MATERIAL

The datasets used and/or analyzed during the current study are available from the corresponding author on reasonable request.

ETHICS STATEMENT

The study was approved by the Institutional Review Board of the study hospital (NHG DSRB Ref: 2014/00979). Signed informed consent was obtained from all participants upon recruitment.

AUTHOR CONTRIBUTIONS

CS, PB, YC, WL, HH, and VL conceived and designed the study. PB helped in data acquisition. PB, SS, and SU analyzed and interpreted the data. CS, PB, WL, HH, VL, YC, SS, and SU contributed to the writing of the manuscript. All the authors read and approved the final manuscript.

FUNDING

This study was supported by the Oral Health Seed Grant (R-221-000-076-733), Faculty of Dentistry, and Sunstar Donation Grant (R-221-000-111-720) to CS.

ACKNOWLEDGMENTS

We thank the study participants, study coordinators and the nursing staff in the Obstetrical and Gynaecology clinics of National University Health System, Singapore (NUHS).

SUPPLEMENTARY MATERIAL

The Supplementary Material for this article can be found online at: https://www.frontiersin.org/articles/10.3389/fmicb.2018.02360/full#supplementary-material

REFERENCES

Aagaard, K., Ma, J., Antony, K. M., Ganu, R., Petrosino, J., and Versalovic, J. (2014). The placenta harbors a unique microbiome. *Sci. Transl. Med.* 6:237ra65. doi: 10.1126/scitranslmed.3008599

Aas, J. A., Paster, B. J., Stokes, L. N., Olsen, I., and Dewhirst, F. E. (2005). Defining the normal bacterial flora of the oral cavity. *J. Clin. Microbiol.* 43, 5721–5732. doi: 10.1128/JCM.43.11.5721-5732.2005

Abusleme, L., Dupuy, A. K., Dutzan, N., Silva, N., Burleson, J. A., Strausbaugh, L. D., et al. (2013). The subgingival microbiome in health and periodontitis and its relationship with community biomass and inflammation. *ISME J.* 7, 1016–1025. doi: 10.1038/ismej.2012.174

Adriaens, L. M., Alessandri, R., Spörri, S., Lang, N. P., and Persson, G. R. (2009). Does pregnancy have an impact on the subgingival microbiota? *J. Periodontol.* 80, 72–81. doi: 10.1902/jop.2009.080012

Ainamo, J., and Bay, I. (1975). Problems and proposals for recording gingivitis and plaque. *Int. Dent. J.* 25, 229–235.

Avila, M., Ojcius, D. M., and Yilmaz, Ö. (2009). The oral microbiota: living with a permanent guest. *DNA Cell Biol.* 28, 405–411. doi: 10.1089/dna.2009.0874

Bader, G. D., and Hogue, C. W. (2003). An automated method for finding molecular complexes in large protein interaction networks. *BMC Bioinformatics* 4:2. doi: 10.1186/1471-2105-4-2

Bik, E. M., Long, C. D., Armitage, G. C., Loomer, P., Emerson, J., and Mongodin, E. F. et al. (2010). Bacterial diversity in the oral cavity of ten healthy individuals. *ISME J.* 4, 962–974. doi: 10.1038/ismej.2010.30

Carrillo-de-Albornoz, A., Figuero, E., Herrera, D., and Bascones-Martínez, A. (2010). Gingival changes during pregnancy: II. Influence of hormonal variations on the subgingival biofilm. *J. Clin. Periodontol.* 37, 230–240. doi: 10.1111/j.1600-051X.2009.01514.x

Chao, A. (1984). Nonparametric estimation of the number of classes in a population. *Scand. J. Stat.* 11, 265–270.

Chen, H., Liu, Y., Zhang, M., Wang, G., and Qi, Z. (2015). A filifactor alocis-centered co-occurrence group associates with periodontitis across different oral habitats. *Sci. Rep.* 5:9053. doi: 10.1038/srep09053

Chen, T., Yu, W. H., Izard, J., Baranova, O. V., Lakshmanan, A., and Dewhirst, F. E. (2010). The human oral microbiome database: a web accessible resource for investigating oral microbe taxonomic and genomic information. *Database* 2010:baq013. doi: 10.1093/database/baq013

Chin, C.-H., Chen, S. H., Wu, H. H., Ho, C. W., Ko, M. T., and Lin, C. Y. (2014). Cytohubba: identifying hub objects and sub-networks from complex interactome. *BMC Syst. Biol.* 8, S11–S11. doi: 10.1186/1752-0509-8-S4-S11

Dewhirst, F. E., Chen, T., Izard, J., Paster, B. J., Tanner, A. C. R., Yu, W. H., et al. (2010). The human oral microbiome. *J. Bacteriol.* 192, 5002–5017. doi: 10.1128/JB.00542-10

Diaz, P. I., Hoare, A., and Hong, B. Y. (2016). Subgingival microbiome shifts and community dynamics in periodontal diseases. *J. Calif. Dent. Assoc.* 44, 421–435.

DiGiulio, D. B., Callahan, B. J., McMurdie, P. J., Costello, E. K., Lyell, D. J., and Robaczewska, A. et al. (2015). Temporal and spatial variation of the human microbiota during pregnancy. *Proc. Natl. Acad. Sci. U.S.A.* 112, 11060–11065. doi: 10.1073/pnas.1502875112

Fujiwara, N., Tsuruda, K., Iwamoto, Y., Kato, F., Odaki, T., Yamane, N. et al. (2017). Significant increase of oral bacteria in the early pregnancy period in Japanese women. *J. Investig. Clin. Dent.* 8:1. doi: 10.1111/jicd.12189

Grenier, D. (1992). Nutritional interactions between two suspected periodontopathogens, *Treponema denticola* and *Porphyromonas gingivalis*. *Infect. Immun.* 60, 5298–5301.

Grenier, D., and Mayrand, D. (1986). Nutritional relationships between oral bacteria. *Infect. Immun.* 53, 616–620.

Gursoy, M., Haraldsson, G., Hyvönen, M., Sorsa, T., Pajukanta, R., and Könönen, E. (2009). Does the frequency of prevotella intermedia increase during pregnancy? *Oral Microbial. Immunol.* 24, 299–303. doi: 10.1111/j.1399-302X.2009.00509.x

Gursoy, M., Pajukanta, R., Sorsa, T., and Könönen, E. (2008). Clinical changes in periodontium during pregnancy and post-partum. *J. Clin. Periodontol.* 35, 576–583. doi: 10.1111/j.1600-051X.2008.01236.x

Hajishengallis, G., Darveau, R. P., and Curtis, M. A. (2012). The keystone pathogen hypothesis. *Nat. Rev. Microbiol.* 10, 717–725. doi: 10.1038/nrmicro2873

Han, Y. W. (2011). Oral health and adverse pregnancy outcomes - what's next? *J. Dent. Res.* 90, 289–293. doi: 10.1177/0022034510381905

He, J., Li, Y., Cao, Y., Xue, J., and Zhou, X. (2015). The oral microbiome diversity and its relation to human diseases. *Folia Microbiol.* 60, 69–80. doi: 10.1007/s12223-014-0342-2

Hong, B.-Y., Furtado Araujo, M. V., Strausbaugh, L. D., Terzi, E., Ioannidou, E., and Diaz, P. I. (2015). Microbiome profiles in periodontitis in relation to host and disease characteristics. *PLoS One* 10:e0127077. doi: 10.1371/journal.pone.0127077

Huang, S., Li, R., Zeng, X., He, T., Zhao, H., Chang, A., et al. (2014). Predictive modeling of gingivitis severity and susceptibility via oral microbiota. *ISME J.* 8, 1768–1780. doi: 10.1038/ismej.2014.32

Jenkinson, H. F., and Lamont, R. J. (2005). Oral microbial communities in sickness and in health. *Trends Microbiol.* 13, 589–595. doi: 10.1016/j.tim.2005.09.006

Jensen, J., Liljemark, W., and Bloomquist, W. (1981). The effect of female sex hormones on subgingival plaque. *J. Periodontol.* 52, 599–602. doi: 10.1902/jop.1981.52.10.599

Kistler, J. O., Booth, V., Bradshaw, D. J., and Wade, W. G. (2013). Bacterial community development in experimental gingivitis. *PLoS One* 8:e71227. doi: 10.1371/journal.pone.0071227

Kornman, K. S., and Loesche, W. J. (1980). The subgingival microbial flora during pregnancy. *J. Periodontal. Res.* 15, 111–122. doi: 10.1111/j.1600-0765.1980.tb00265.x

Kornman, K. S., and Loesche, W. J. (1982). Effects of estradiol and progesterone on bacteroides melaninogenicus and bacteroides gingivalis. *Infect. Immun.* 35, 256–263.

Kumar, P., and Magon, N. (2012). Hormones in pregnancy. *Niger Med. J.* 53, 179–183. doi: 10.4103/0300-1652.107549

Lin, W., Jiang, W., Hu, X., Gao, L., Ai, D., Pan, H., et al. (2018). Ecological shifts of supragingival microbiota in association with pregnancy. *Front. Cell. Infect. Microbiol.* 8:24. doi: 10.3389/fcimb.2018.00024

Loe, H., and Silness, J. (1963).Periodontal disease in pregnancy. I. prevalence and severity. *Acta Odontol. Scand.* 21, 533–551. doi: 10.3109/00016356309011240

Mealey, B. L., and Rose, L. F. (2008). Diabetes mellitus and inflammatory periodontal diseases. *Curr. Opin. Endocrinol. Diabetes Obes.* 15, 135–141. doi: 10.1097/MED.0b013e3282f824b7

Nuriel-Ohayon, M., Neuman, H., and Koren, O. (2016). Microbial changes during pregnancy, birth, and infancy. *Front. Microbiol.* 7:1031, doi: 10.3389/fmicb.2016.01031

Oksanen, J., Kindt, R., Blachet, F. G., and Wagner, H. H. (2013). *Package Vegan: Community Ecology package, version 2.0 10*. Available at: https://cran.r-project.org

Onigbinde, O. O., Sorunke, M. E., Braimoh, M. O., and Adeniyi, A. O. (2014). Periodontal status and some variables among pregnant women in a nigeria tertiary institution. *Ann. Med. Health Sci. Res.* 4, 852–857. doi: 10.4103/2141-9248.144876

Saito, A., Inagaki, S., Kimizuka, R., Okuda, K., Hosaka, Y., Nakagawa, T., et al. (2008). *Fusobacterium nucleatum* enhances invasion of human gingival epithelial and aortic endothelial cells by *Porphyromonas gingivalis*. *FEMS Immun. Med. Microbiol.* 54, 349–355. doi: 10.1111/j.1574-695X.2008.00481.x

Segata, N., Haake, S. K., Mannon, P., Lemon, K. P., Waldron, L., Gevers, D., et al. (2012). Composition of the adult digestive tract bacterial microbiome based on seven mouth surfaces, tonsils, throat and stool samples. *Genome Biol.* 13:R42. doi: 10.1186/gb-2012-13-6-r42

Shannon, C. E. (1948). A mathematical theory of communication. *Bell Syst. Techn. J.* 27, 379–423. doi: 10.1002/j.1538-7305.1948.tb01338.x

Shannon, P., Markiel, A., Ozier, O., Baliga, N. S., Wang, J. T., Ramage, D., et al. (2003). Cytoscape: a software environment for integrated models of biomolecular interaction networks. *Genome Res.* 13, 2498–2504. doi: 10.1101/gr.1239303

Short, F. L., Murdoch, S. L., and Ryan, R. P. (2014). Polybacterial human disease: the ills of social networking. *Trends Microbiol.* 22, 508–516. doi: 10.1016/j.tim.2014.05.007

Silk, H., Douglass, A. B., Douglass, J. M., and Silk, L. (2008). Oral health during pregnancy. *Am. Fam. Phys.* 77, 1139–1144.

Simpson, K. T., and Thomas, J. G. (2016). Oral microbiome: contributions to local and systemic infections. *Curr. Oral Health Rep.* 3, 45–55. doi: 10.1007/s40496-016-0079-x

Tsuzukibashi, O., Uchibori, S., Kobayashi, T., Umezawa, K., Mashimo, C., Nambu, T., et al. (2017). Isolation and identification methods of Rothia species in oral cavities. *J. Microbiol. Methods* 134, 21–26. doi: 10.1016/j.mimet.2017.01.005

Verma, D., Garg, P. K., and Dubey, A. K. (2018). Insights into the human oral microbiome. *Arch. Microbiol.* 200, 525–540. doi: 10.1007/s00203-018-1505-3

Wickham, H. (2018). *ggplot2: Elegant Graphics for Data Analysis*. New York, NY: Springer-Verlag.

Wu, M., Chen, S. W., and Jiang, S. Y. (2015). Relationship between gingival inflammation and pregnancy. *Med. Inflamm.* 2015:623427. doi: 10.1155/2015/623427

Yokoyama, M., Hinode, D., Yoshioka, M., Fukui, M., Tanabe, S., Grenier, D., et al. (2008). Relationship between *Campylobacter rectus* and periodontal status during pregnancy. *Oral Microbiol. Immunol.* 23, 55–59. doi: 10.1111/j.1399-302X.2007.00391.x

Conflict of Interest Statement: The authors declare that the research was conducted in the absence of any commercial or financial relationships that could be construed as a potential conflict of interest.

Copyright © 2018 Balan, Chong, Umashankar, Swarup, Loke, Lopez, He and Seneviratne. This is an open-access article distributed under the terms of the Creative Commons Attribution License (CC BY). The use, distribution or reproduction in other forums is permitted, provided the original author(s) and the copyright owner(s) are credited and that the original publication in this journal is cited, in accordance with accepted academic practice. No use, distribution or reproduction is permitted which does not comply with these terms.

frontiers in Microbiology

ORIGINAL RESEARCH
published: 02 November 2018
doi: 10.3389/fmicb.2018.02622

Clinical Efficacy and Microbiome Changes Following Fecal Microbiota Transplantation in Children With Recurrent Clostridium Difficile Infection

Xiaolu Li[1†], Xuefeng Gao[2,3†], Hui Hu[1], Yongmei Xiao[1], Dan Li[1], Guangjun Yu[1], Dongbao Yu[4], Ting Zhang[1] and Yizhong Wang[1*]*

[1] Department of Gastroenterology, Hepatology and Nutrition, Shanghai Children's Hospital, Shanghai Jiao Tong University, Shanghai, China, [2] Shenzhen University General Hospital, Shenzhen, China, [3] Shenzhen University Clinical Medical Academy, Shenzhen, China, [4] Shenzhen Hoiracle Bio-Tech Co., Ltd., Shenzhen, China

Fecal microbiota transplantation (FMT) has been shown as an effective treatment for recurrent clostridium difficile infection (RCDI) in adults. In this study, we aim to evaluate the clinical efficacy of FMT in treating children with RCDI, and explore fecal microbiota changes during FMT treatment. A total of 11 RCDI subjects with a median age of 3.5 years were enrolled in this single-center prospective pilot study. All patients were cured (11/11, 100%) by FMT either through upper gastrointestinal tract route with a nasointestinal tube (13/16, 81.2%) or lower gastrointestinal tract route with a rectal tube (3/16, 18.8%). The cure rate of single FMT was 63.6% (7/11), and 4 (4/11, 36.4%) cases were performed with 2 or 3 times of FMT. Mild adverse events were reported in 4 children (4/11, 36.4%), including transient diarrhea, mild abdominal pain, transient fever and vomit. Gut microbiota composition analysis of 59 fecal samples collected from 34 participants (9 RCDI children, 9 donors and 16 health controls) showed that the *alpha* diversity was lower in pediatric RCDI patients before FMT than the healthy controls and donors, and fecal microbial community of pre-FMT samples (*beta* diversity) was apart from that of healthy controls and donors. No significant differences in *alpha* diversity, *beta* diversity or phylogenetic distance were detected between donors and healthy controls. Both the richness and diversity of gut microbiota were improved in the pediatric RCDI patients after FMT, and the bacteria community was shifted closer to the donor and healthy control group. Furthermore, FMT re-directed gut microbiome functions of pediatric RCDI toward a health state. Our results indicate that it is safe and tolerant to use FMT in treating pediatric RCDI. FMT shifted the gut microbiome composition and function in children with RCDI toward a healthy state.

Keywords: fecal microbiota transplantation, recurrent clostridium difficile infection, gut microbiota, 16S rRNA gene sequencing, children

OPEN ACCESS

Edited by:
Nurul-Syakima Ab Mutalib, UKM Medical Molecular Biology Institute (UMBI), Malaysia

Reviewed by:
Yuji Naito, Kyoto Prefectural University of Medicine, Japan
Alejandro Arias-Vasquez, Radboud University Nijmegen Medical Centre, Netherlands

****Correspondence:***
Ting Zhang
zhangt@shchildren.com.cn
Yizhong Wang
wangyz@shchildren.com.cn

† These authors have contributed equally to this work

Specialty section:
This article was submitted to Microbial Symbioses, a section of the journal Frontiers in Microbiology

Received: *12 June 2018*
Accepted: *12 October 2018*
Published: *02 November 2018*

Citation:
Li X, Gao X, Hu H, Xiao Y, Li D, Yu G, Yu D, Zhang T and Wang Y (2018) Clinical Efficacy and Microbiome Changes Following Fecal Microbiota Transplantation in Children With Recurrent Clostridium Difficile Infection. Front. Microbiol. 9:2622. doi: 10.3389/fmicb.2018.02622

INTRODUCTION

Clostridium difficile (CD) is a leading causative pathogen of antibiotic-associated and healthcare-associated infective diarrhea. CD infection (CDI) is determined by the presence of symptoms (diarrhea) and either a detection of toxin producing *C. difficile* in stool, or findings of pseudomembranous colitis by colonoscopy or histopathology (McDonald et al., 2018). Due to the emergence of more virulent CD strains, the prevalence and severity of CDI in children increased in past decades (Khanna et al., 2013; Sammons and Toltzis, 2013; Wendt et al., 2014; Gupta et al., 2016; Spigaglia et al., 2017). Clinical treatment with metronidazole, vancomycin or fidaxomicin is successful in most of CDI subjects, however, recurrence after completion of a first treatment course ranges from 15 to 20%, and increases up to 45–60% after the first recurrence (McFarland et al., 2002; Kelly and LaMont, 2008; Brandt, 2013). Studies revealed that the recurrence rate of pediatric RCDI after first-line treatment varied from 2.6 to 30% in different examined population, with the frequency of recurrence rising further after subsequent infections (Barbut et al., 2000; McFarland et al., 2002; Pai et al., 2012; Khanna et al., 2013; Nicholson et al., 2015). Conventional antibiotic treatment is less ineffective for refractory, recurrent and complicated CDI, and new therapeutic approaches are needed for managing RCDI.

The normal intestinal microbiome plays an important physiological role in the prevention of infection, maintenance barriers, immunity, metabolism, and nutrition of the host (Lloyd-Price et al., 2016). It has been shown that either colonization or infection with CD is associated with reduced microbiota diversity in human gut (Samarkos et al., 2018). Fecal microbiota transplantation (FMT), first described in 1958 (Eiseman et al., 1958), is known as the administration of a solution of fecal matter from a donor into the intestinal tract of a recipient in order to cure a specific pathology (Aroniadis and Brandt, 2013; Mattner et al., 2016), which has been received increasing attention as an effective treatment for RCDI with cure rates of 90–100% in adults (Drekonja et al., 2015). However, the data of FMT for pediatric RCDI are rare. This study aimed to evaluate the clinical efficacy and safety of FMT and examine the influence of FMT on the diversity, structure, and function of gut microbiome in pediatric RCDI patients.

MATERIALS AND METHODS

Study Cohort

Eleven children with RCDI underwent FMT from Shanghai Children's Hospital, China, between September 2014 and December 2017, were enrolled to the study cohort. This study was approved by the Regional Ethical Review Board in Shanghai Children's Hospital. Data including demographics, clinical history, CDI treatment history, and clinical response to FMT were collected and analyzed. Clinical cure was defined as the resolution of diarrhea attributable to CDI, and without recurrence of CDI in 3 months after FMT. Nine stool donors and 16 health individuals were included in the study for gut microbiome analysis. Written informed consent was obtained from parents of all pediatric subjects, donors, and health controls.

FMT Procedure

Stool donors including healthy family members and unrelated volunteers were screened based on medical history and laboratory testing. Donor being on prescription drugs, antibiotic exposure in recent 3 months, body mass index >30 were excluded. Donors have history of malignancy, chemotherapy, chronic systemic or gastrointestinal disease, or functional disorders were also excluded. Informed consents were obtained before screening procedures. Laboratory testing including blood tests of syphilis, HIV, hepatitis A, B, and C, and stool tests including CD toxin, bacterial culture for enteric pathogens, ova and parasites, Giardia antigen and cryptosporidium antigen were performed. Fresh stool from donor was collected and blended using 200–250 mL sterilized saline per 150 g stool at high speed for 2–3 min. Stool suspension was filtered by 2 layers of medical gauze to remove large particles. Stool filtrate was drawn into 50 mL syringes for immediate FMT, or collected in 50 mL tubes frozen in -80°C for further FMT. Recipients were stopped antibiotic prescription for CDI 48 h prior to the FMT procedure. FMT was initially performed using an upper route to the distal duodenum with a nasal jejunal tube, and 50–100 mL of a processed donor stool suspension was instilled during the procedure. In the case of a failure of the upper route for FMT, a second FMT was performed via a lower route by retention enema with 100–200 mL donor stool suspension. If clinical symptoms were not improved after 2 days of FMT, the second FMT was administrated. Clinical efficacy and adverse events were assessed at 1, 2 weeks, and 3 months after FMT.

Fecal Microbiome Analysis

Stool samples of patients were collected 1 day before FMT, and on days 1, 3, 7, 30+ after FMT. All samples were stored at −80°C until shipping to the HRK-biotech lab for DNA extraction and sequencing. The isolation methods are described as previously (Wang et al., 2018). Isolated genomic DNA was amplified for the V3–V4 hypervariable regions of the 16S rRNA gene and sequenced using an Illumina Miseq platform. USEARCH (Edgar, 2010) *cluster_otus* command was employed to filter chimeric sequences and generate cluster operational taxonomic units (OTUs) based on 97% nucleotide similarity. Taxonomic assignment was performed by using the Ribosomal Database Project (RDP) classifier. The statistical analysis was performed with SHAMAN (shaman.c3bi.pasteur.fr). OTU counts were normalized by taking into account the confounding effect of sex and age. Overall differences in microbiome structure were evaluated through Principal Coordinate Analysis (PCoA) to Bray-Curtis distance. A generalized linear model (GLM) with contrast vectors was defined to evaluate the significant differences in the gut microbiome compositions among the sample groups. The resulting *p*-values were adjusted for multiple testing according to the Benjamini-Hochberg procedure. PICRUSt (Phylogenetic Investigation of Communities by Reconstruction of Unobserved States) was applied to predict the metagenomes from 16S rRNA data (Langille et al., 2013). The organism-level

microbiome phenotypes were predicted by using BugBase (Ward et al., 2017).

RESULTS

Characteristics of Pediatric RCDI

The characteristics of the 11 patients were summarized in **Table 1**. Of all these patients (5 boys and 6 girls), the median age at the time of FMT was 3.5 years (range, 0.5–12 years). All subjects were treated with 1–2 episodes of oral antibiotics before FMT, 7 patients (7/11, 63.6%) were given oral vancomycin, and all 11 (11/11, 100%) subjects received metronidazole treatment. Seven children (7/11, 63.6%) were diagnosed as pseudomembranous colitis based on the results of endoscopy. The main manifestations of abdominal CT scan were effusion and pneumatosis in 10 (10/11, 90.9%) patients.

Clinical Responses to FMT

Total 16 FMT were performed, 81.2% (13/16) using an upper route with a nasointestinal tube and 18.8% (3/16) through lower route by retention enema. Six donors (6/11, 54.5%) are parents of children and 5 (5/11, 45.5%) are unrelated donors. Seven (7/11, 63.6%) children were cured by single FMT, and 4 (4/11, 36.4%) children were cured with 2–3 times of FMT (**Table 2**). There was no recurrence of diarrhea during 3 months after FMT, and CD toxin tests were negative. There is no difference in clinical response to FMT related to the sources and ages of donors.

There were no serious adverse events reported after 3 months of FMT. Four children (4/11, 36.4%) were reported with mild and self-limited adverse events. Transient diarrhea was reported in 1 patient on the day of FMT, and disappeared after 2 days. Transient mild abdominal pain was reported in 1 child immediately after the procedure. One patient had transient fever and returned to normal on the time of second FMT. In addition, 1 child had vomit during FMT procedure. All subjects were followed up in every 3 months after FMT by phone call. The average follow-up time was 18 (range: 9–36) months (**Table 2**). No recurrence of CDI and FMT-related adverse events were reported by the parents of subjects.

TABLE 1 | Characteristics of RCDI children treated with FMT.

	n (%)
Gender (Female)	6 (54.5)
Median age at FMT (years, range)	3.5 (0.5–12)
Clinical symptoms	
Diarrhea	7 (63.6)
Bloating	1 (9.1)
Abdominal pain	1 (9.1)
Blood stool	2 (18.2)
Median duration of symptoms in months (range)	4 (1–12)
Endoscopy	
Pseudomembranous colitis	7 (63.6)
Inflammation	4 (36.4)
Abdominal CT scan	
Effusion	10 (90.9)
Pneumatosis	10 (90.9)
Antibiotics received for CDI beforeFMT	
Metronidazole	11 (100)
Vancomycin	7 (63.6)

RCDI, recurrent clostridium difficile infection; FMT, fecal microbiota transplantation.

TABLE 2 | Characteristic and clinical response of FMT for RCDI children.

	n (%)
Donors' relationship to patient	
Parent	6 (54.5)
Unrelated volunteer	5 (45.5)
Donors' gender (Female)	4 (36.4)
Median age of donors (years, range)	31 (27–49)
Number of previous CDI episodes	1.5 (1–2)
Route of FMT, n (%)	
Nasal jejunal tube	13 (81.2)
Retention enema	3 (18.8)
Cure of CDI, n (%)	11 (100)
Single	7 (63.6)
Multiple (2–3 times)	4 (36.4)
Time from FMT to resolution of diarrhea (days)	1 (1–2)
Adverse events, n (%)	4 (36.4)
Transient diarrhea	1 (9.1)
Fever	1 (9.1)
Transient mild abdominal	1 (9.1)
Vomit	1 (9.1)
Median follow-up time, in months (range)	18 (9–36)

RCDI, recurrent clostridium difficile infection; FMT, fecal microbiota transplantation.

FMT Corrected Dysbiosis and Re-established Intestinal Homeostasis in Pediatric RCDI

For characterizing gut microbiota associated with pediatric RCDI, a total of 59 fecal samples were collected from 34 participants including 9 RCDI children, 9 donors and 16 health individuals. Thirty-eight fecal samples from RCDI children were included: 9 at baseline (prior to FMT, FMT0) and 29 at various days (1, 3, 7, and 30+ days) after FMT. For children treated with multiple FMT, pre-FMT fecal samples were collected before the first time of FMT, and post-FMT samples were collected from post days of last FMT procedure. Each donor (n = 9, between the ages of 27 and 49 years with a mean of 31 years) and health subjects (n = 16, between the ages of 4 and 17 years with a mean of 12 years) provided a single stool sample. The *alpha* diversity was found lower in pediatric RCDI patients before FMT treatment (herein after termed FMT0) than the healthy controls and donors (**Figure 1A**). Analysis of the *beta* diversity calculated on the Bray-Curtis dissimilarity, unweighted and weighted UniFrac distances (**Figure 1B**) revealed that fecal microbial community of pre-FMT samples apart from that of healthy controls and donors. No significant differences in *alpha* diversity, *beta* diversity or phylogenetic distance were detected between donors and healthy controls.

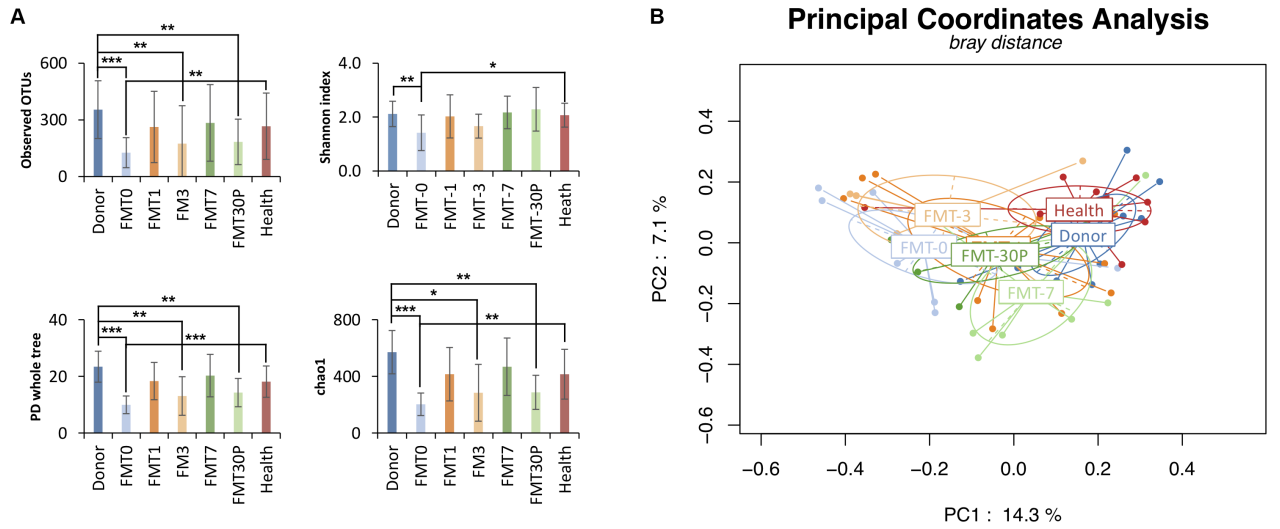

FIGURE 1 | FMT increases bacterial diversity of pediatric RCDI, and re-directs the gut microbiome toward a health state. **(A)** *Alpha* diversity was calculated using the number of overserved OTUs, Shannon index, PD whole tree, and chao1, with $*p < 0.05$, $**p < 0.01$, and $***p < 0.001$ (Student *T*-test). **(B)** Principal coordinate analysis (PCoA) profile of microbial diversity across all samples using Bray-Curtis distance. Each dot stands for one sample, and the ellipses stand for sample groups. The clustering based on microbial distribution is significant (analysis of variance using PERMANOVA test, *p*-value = 0.001).

Inter-group comparisons of taxonomic profiles revealed that gut microbiome from patients prior to FMT therapy exhibited alterations in the abundance of several taxa. At the phylum level, Proteobacteria was enriched in the children with RCDI (**Figure 2**). At the genus level, relative abundances of *Escherichia/Shigella*, *Lactobacillus*, *Streptococcus*, *Enterococcus*, *Akkermansia*, *Clostridium_sensu_stricto*, and *Flavonifractor* were significantly higher in the pre-FMT samples, while *Phascolarctobacterium*, *Fusicatenibacter*, *Ruminococcus*, *Coprococcus*, *Dorea*, *Gemmiger*, *Collinsella*, *Megamonas*, *Roseburia*, *Megasphaera*, *Bacteroides*, and *Oscillibacter* were significantly reduced compared to the controls and/or donors.

Following FMT treatment (herein after termed FMT-x, which indicated the samples were collected at x days after FMT, FMT-30P group includes samples collected at 30 and plus days after FMT), the bacterial diversity of intestinal microbiota was increased in the pediatric RCDI patients, and was maintained through the study (**Figure 1A**). PCoA showed that the bacterial communities of the FMT-1, -7, and -30P samples were shifted toward the healthy control and donor groups (**Figure 1B**). Statistical analysis of bacterial taxa revealed that the fecal microbiota of the pediatric RCDI patients was shifted toward a healthy composition by adopting a donor-like configuration after FMT (**Figure 2**). In specific, the relative abundances of Proteobacteria phylum declined significantly 7 days after FMT (**Figure 2**). At the genus level, some bacteria (indicated by solid outline in **Figure 2**) that depleted in the RCDI patients were uplifted after FMT. Some genera (indicated by dashed outline in **Figure 2**) that enriched in the pediatric RCDI patients were reduced following FMT and maintained during the study period. The microbiome composition changed rapidly after FMT, however, some bacteria drifted toward the baseline after 30 days post-FMT, such as *Escherichia/Shigella*, *Flavonifractor*, *Fusicatenibacter*, *Dorea*, *Gemmiger*, and *Collinsella*.

In our study, all 11 children with RCDI were cured, albeit a proportion (7/11) achieved remission after single FMT while remission occurred after multiple FMT for the others (4/11) (**Table 2**). We thus the patients into single-FMT and multiple-FMT and compared their gut bacterial composition. The *alpha* diversity was significantly lower in the pediatric patients achieved cure after multiple FMT compared to the donors and healthy controls (**Supplementary Figure S1**). Taxonomically, the Actinobacteria phylum and *Lachnospiracea incertae sedis* genus were significantly more abundant in the patients that achieved cure with multiple FMT while the genera *Bifidobacterium*, *Enterococcus*, *Alistipes*, *Dialister*, *Streptococcus*, *Oscillibacter*, and *Flavonifractor* were enriched in patients with symptom improvement sooner after a single FMT (**Figure 2**).

FMT Re-directed Gut Microbiome Functions of Pediatric RCDI Toward a Health State

We used BugBase to analyze community-wide phenotypes of the stool microbiome. We observed that the microbiome phenotypes were similar between the donors and health controls, indicating a common healthy state was shared by these individuals (**Figure 3**). The gram-positive species and gene functions associated with anaerobiosis were the lowest in the pre-FMT samples, and mainly due to some reduced taxa that belong to Firmicutes. The gram-negative taxa and gene functions associated with facultative anaerobiosis, biofilms forming, mobile element content, pathogenesis, and oxidative stress tolerance were enriched in the pediatric RCDI subjects prior to FMT, and the major contributors came from Proteobacteria. After FMT,

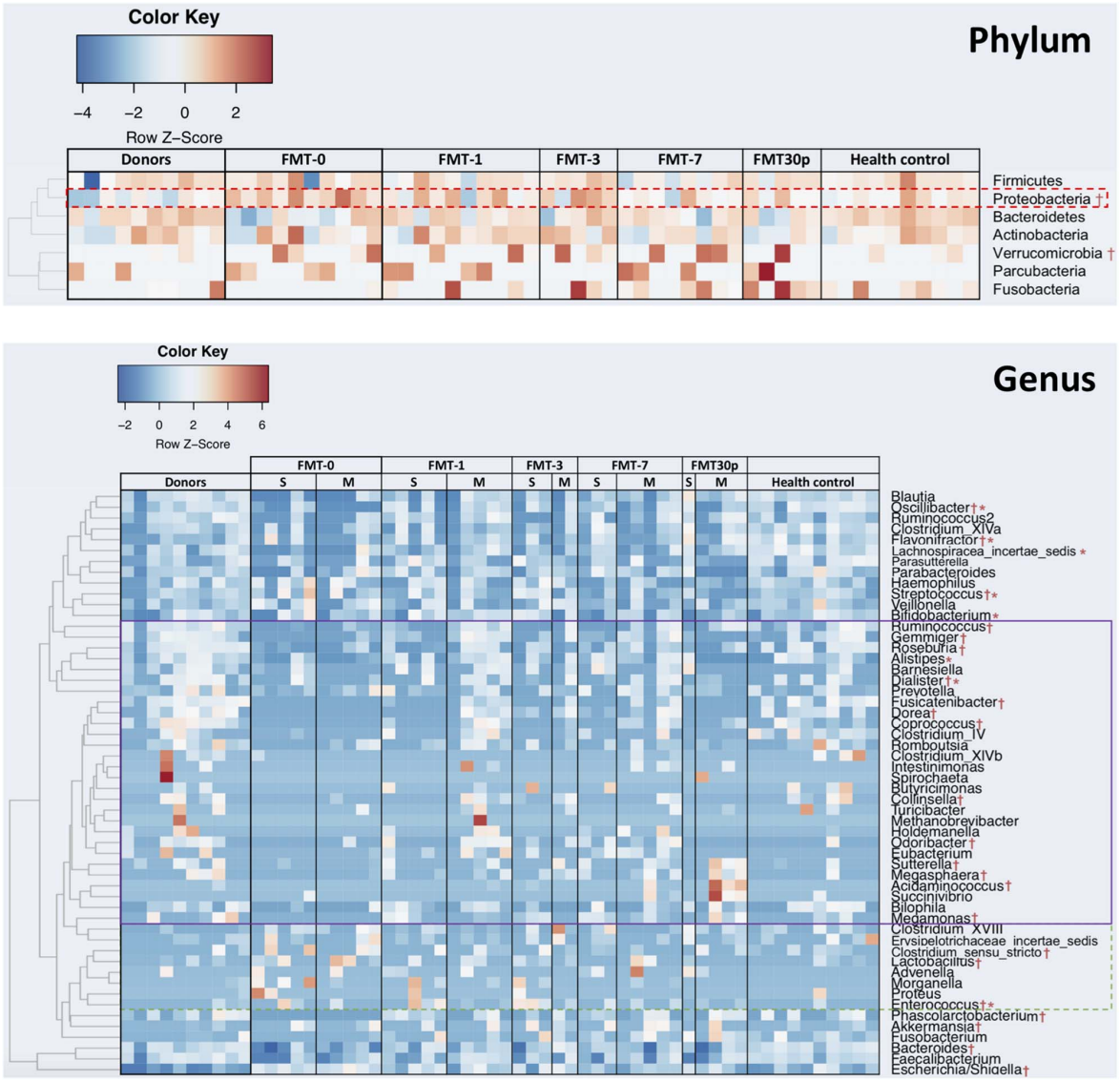

FIGURE 2 | FMT shifts the gut bacterial composition in children with RCDI toward a healthy state. Phyla and genera that were statistically different in abundance between the FMT-0 and donor/health control groups are identified by † ($p < 0.05$), and between the single-FMT-0 and multiple-FMT-0 are identified by * ($p < 0.05$). Heatmap is color-coded based on row z-scores. Genera having increased and decreased relative abundances after FMT are highlighted by a solid and dashed outlines, respectively. S, Single-FMT; M, Multiple-FMT.

most of the functional capacities were re-directed rapidly to a healthy level and maintained through the study. However, the proportions of anaerobic bacteria and that associated with biofilm forming changed slowly after FMT, and approached a healthy level 30 days (or longer) after treatment.

DISCUSSION

As an emerging and promising treatment in RCDI, FMT was proved to be more effective than conventional antibiotics treatment (van Nood et al., 2013; Drekonja et al., 2015). FMT has been strong recommended for adult patients with multiple recurrences of CDI who have failed appropriate antibiotic treatments for its high success rate (McDonald et al., 2018). However, study focused on FMT for pediatric RCDI was still limited. A recent review summarized the published data in FMT for pediatric RCDI showed that 89% (40/45) of patients had symptom improvement (Chen et al., 2017). An emerging study showed that 15 children with RCDI were cured by FMT, including five children with underlying IBD (Fareed et al., 2018). In the present study, a total of 11 RCDI subjects with a median age of 3.5 years were cured by FMT. The cure rate of single FMT was 63.6% (7/11), and 36.4% (4/11) cases performed with 2 or 3 times of FMT. The lower cure rate of single FMT may due to the low

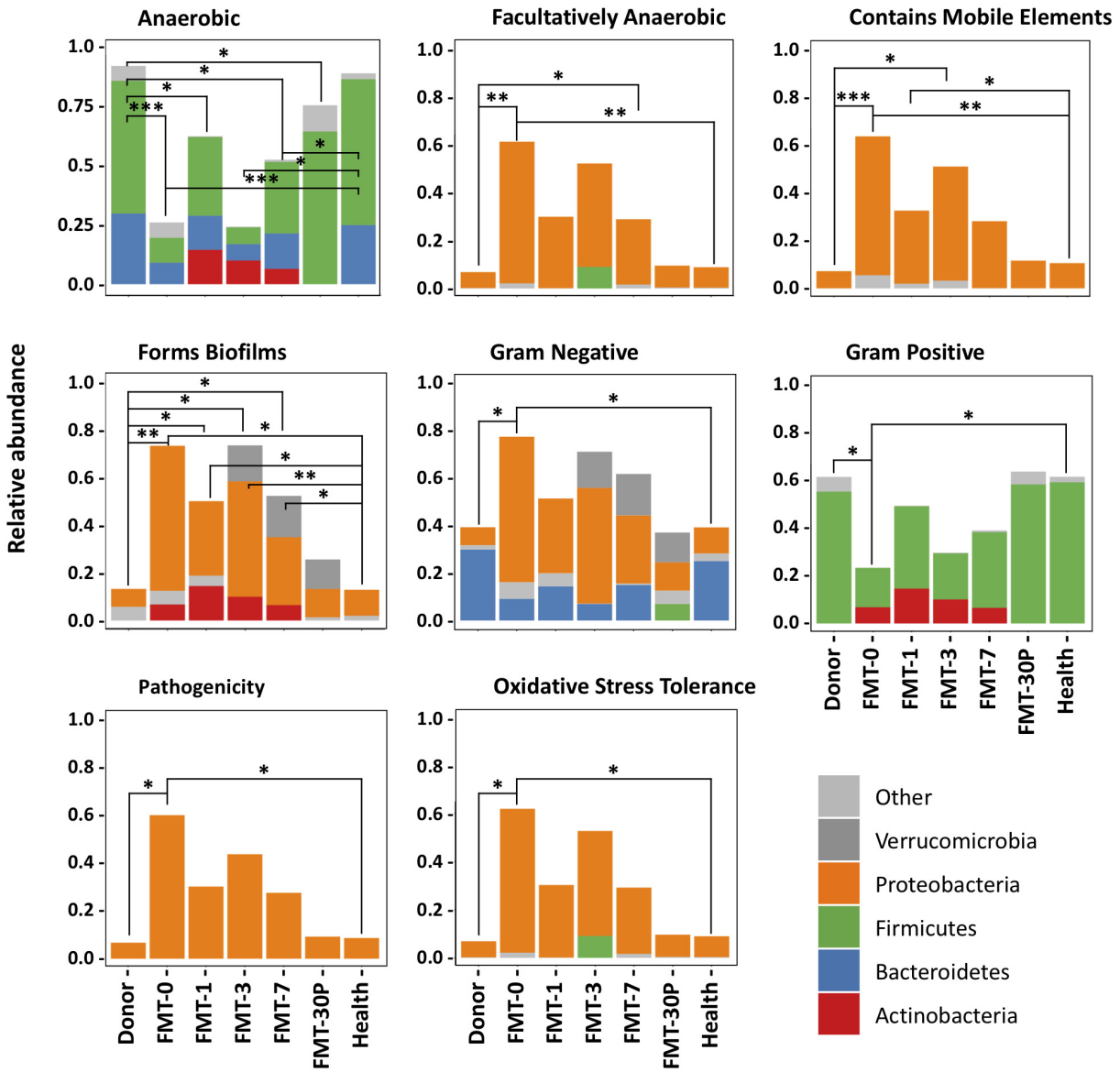

FIGURE 3 | BugBase predicts microbial community phenotypes and the corresponding contributions from different phyla. Statistical significance was determined by Pairwise Mann-Whitney-Wilcoxon tests. FDR-corrected pairwise *p*-value ranges are: $*p < 0.05$, $**p < 0.01$, and $***p < 0.001$.

feces dose infused to the gut or short retention time. There was no recurrence of diarrhea during the 6–36 months of follow up after FMT. No serious adverse event was observed after 3 months of FMT. Four children (36.4%) were reported with mild and self-limited adverse events, including transient diarrhea, transient mild abdominal pain, transient fever and vomit during FMT procedure. Our data showed that the cure rate of pediatric RCDI by FMT was comparable to adults (Drekonja et al., 2015), however, due to the limited number of pediatric RCDI treated with FMT, it is important to study the effect of FMT on pediatric RCDI in large cohort and well designed randomized controlled trial in the future.

Fecal microbiome profiles of pediatric RCDI patients were analyzed and compared with the donors and a control group of healthy children. Our data showed that the fecal microbial community of pre-FMT samples apart from that of healthy controls and donors. *Alpha* diversity in pediatric RCDI patients prior to FMT, especially those who occurred remission after multiple FMT, was much lower compared with both the healthy controls and the donors. Inter-group comparisons of taxonomic profiles revealed that samples from patients prior to FMT exhibited alterations in the gut microbiome composition. Interestingly, we also observed that seven genera were enriched in the patients that were cured by a single FMT while the *Lachnospiracea incertae sedis* genus was more abundant in those

achieved cure after multiple FMT. Previous study has shown that the genus *Lachnospiracea incertae sedis* is significantly enriched in CD-associated disease and irritable bowel syndrome (IBS) patients (Frank et al., 2007). In fact, members of the family Lachnospiraceae are able to induce an elevated immune reactivity in Crohn's disease patients and a subset of IBS patients through expressing highly antigenic flagellins (Duck et al., 2007; Schoepfer et al., 2008). Nevertheless, data characterizing gut microbiota changes after FMT in children are limited. In our study, the microbiota diversity increased in fecal samples of RCDI children after FMT, which agrees with previous findings (Walia et al., 2014; Hourigan et al., 2015). Further analysis of bacterial taxa revealed that the fecal microbiota of the pediatric RCDI patients after FMT was shifted toward a healthy composition by adopting a donor/health-control-like structure. In addition, the gut microbiome functions were re-directed by FMT to a healthy state. Although the abundances of some taxa moved toward baseline at 30 and more days post-FMT, the gut microbiome functions maintained as a similar status as the donors and healthy controls.

CONCLUSION

In this study, all 11 pediatric RCDI subjects were cured by FMT. FMT increased the diversity of the gut microbiota in children with RCDI, and shifted their microbiota composition and functions toward that of the donors and health controls. FMT is likely safe and tolerant in treating children with RCDI.

ETHICS STATEMENT

This study was carried out in accordance with the recommendations of the Declaration of Helsinki, World Medical Association. The study protocol was approved by the Regional Ethical Review Board of Shanghai Children's Hospital. Written informed consent was obtained from parents or legal guardians of all children eligible for study enrollment.

AUTHOR CONTRIBUTIONS

YW and TZ designed the study. XL, XG, and DY interpreted the data, created figures, and wrote the manuscript. HH, XL, YX, DL, and GY analyzed and interpreted the patient data regarding the RCDI. All authors read and approved the final manuscript.

FUNDING

This work was supported by grants from the National Natural Science Foundation of China (Grant No. 81500449 to YW), the Scientific Research Foundation for the Returned Overseas Chinese Scholars, and State Education Ministry of China (Grant No. 20150909-6 to YW), the Natural Science Foundation of Shanghai (Grant No. 16ZR1428700 to TZ), and Shanghai Hospital Development Center New Frontier Technology Joint Research Project (Grant No. SHDC12017115 to TZ).

SUPPLEMENTARY MATERIAL

The Supplementary Material for this article can be found online at: https://www.frontiersin.org/articles/10.3389/fmicb.2018.02622/full#supplementary-material

FIGURE S1 | Biodiversity of gut bacterial community is lower in pediatric RCDI patients that achieved cure after multiple FMT. *Alpha* diversity was calculated using the number of overserved OTUs, Shannon index, PD whole tree, and chao1. *P*-value ranges are: $*p < 0.05$, $**p < 0.01$, $***p < 0.001$ (Student *T*-test).

REFERENCES

Aroniadis, O. C., and Brandt, L. J. (2013). Fecal microbiota transplantation: past, present and future. *Curr. Opin. Gastroenterol.* 29, 79–84. doi: 10.1097/MOG.0b013e32835a4b3e

Barbut, F., Richard, A., Hamadi, K., Chomette, V., Burghoffer, B., and Petit, J. C. (2000). Epidemiology of recurrences or reinfections of *Clostridium difficile*-associated diarrhea. *J. Clin. Microbiol.* 38, 2386–2388.

Brandt, L. J. (2013). American journal of gastroenterology lecture: intestinal microbiota and the role of fecal microbiota transplant (FMT) in treatment of C. difficile infection. *Am. J. Gastroenterol.* 108, 177–185. doi: 10.1038/ajg.2012.450

Chen, B., Avinashi, V., and Dobson, S. (2017). Fecal microbiota transplantation for recurrent *Clostridium difficile* infection in children. *J. Infect.* 74(Suppl. 1), S120–S127. doi: 10.1016/S0163-4453(17)30202-5

Drekonja, D., Reich, J., Gezahegn, S., Greer, N., Shaukat, A., MacDonald, R., et al. (2015). Fecal microbiota transplantation for *Clostridium difficile* infection: a systematic review. *Ann. Intern. Med.* 162, 630–638. doi: 10.7326/M14-2693

Duck, L. W., Walter, M. R., Novak, J., Kelly, D., Tomasi, M., Cong, Y., et al. (2007). Isolation of flagellated bacteria implicated in Crohn's disease. *Inflamm. Bowel Dis.* 13, 1191–1201. doi: 10.1002/ibd.20237

Edgar, R. C. (2010). Search and clustering orders of magnitude faster than BLAST. *Bioinformatics* 26, 2460–2461. doi: 10.1093/bioinformatics/btq461

Eiseman, B., Silen, W., Bascom, G. S., and Kauvar, A. J. (1958). Fecal enema as an adjunct in the treatment of pseudomembranous enterocolitis. *Surgery* 44, 854–859.

Fareed, S., Sarode, N., Stewart, F. J., Malik, A., Laghaie, E., Khizer, S., et al. (2018). Applying fecal microbiota transplantation (FMT) to treat recurrent *Clostridium difficile* infections (rCDI) in children. *PeerJ* 6:e4663. doi: 10.7717/peerj.4663

Frank, D. N., St Amand, A. L., Feldman, R. A., Boedeker, E. C., Harpaz, N., and Pace, N. R. (2007). Molecular-phylogenetic characterization of microbial community imbalances in human inflammatory bowel diseases. *Proc. Natl. Acad. Sci. U.S.A.* 104, 13780–13785. doi: 10.1073/pnas.0706625104

Gupta, A., Pardi, D. S., Baddour, L. M., and Khanna, S. (2016). Outcomes in children with *Clostridium difficile* infection: results from a nationwide survey. *Gastroenterol. Rep.* 4, 293–298. doi: 10.1093/gastro/gow007

Hourigan, S. K., Chen, L. A., Grigoryan, Z., Laroche, G., Weidner, M., Sears, C. L., et al. (2015). Microbiome changes associated with sustained eradication of *Clostridium difficile* after single faecal microbiota transplantation in children with and without inflammatory bowel disease. *Aliment. Pharmacol. Ther.* 42, 741–752. doi: 10.1111/apt.13326

Kelly, C. P., and LaMont, J. T. (2008). *Clostridium difficile*–more difficult than ever. *N. Engl. J. Med.* 359, 1932–1940. doi: 10.1056/NEJMra0707500

Khanna, S., Baddour, L. M., Huskins, W. C., Kammer, P. P., Faubion, W. A., Zinsmeister, A. R., et al. (2013). The epidemiology of *Clostridium difficile* infection in children: a population-based study. *Clin. Infect. Dis.* 56, 1401–1406. doi: 10.1093/cid/cit075

Langille, M. G., Zaneveld, J., Caporaso, J. G., McDonald, D., Knights, D., Reyes, J. A., et al. (2013). Predictive functional profiling of microbial communities using 16S rRNA marker gene sequences. *Nat. Biotechnol.* 31, 814–821. doi: 10.1038/nbt.2676

Lloyd-Price, J., Abu-Ali, G., and Huttenhower, C. (2016). The healthy human microbiome. *Genome Med.* 8:51. doi: 10.1186/s13073-016-0307

Mattner, J., Schmidt, F., and Siegmund, B. (2016). Faecal microbiota transplantation-A clinical view. *Int. J. Med. Microbiol.* 306, 310–315. doi: 10.1016/j.ijmm.2016.02.003

McDonald, L. C., Gerding, D. N., Johnson, S., Bakken, J. S., Carroll, K. C., Coffin, S. E., et al. (2018). Clinical practice guidelines for *Clostridium difficile* infection in adults and children: 2017 update by the infectious diseases society of america (IDSA) and society for healthcare epidemiology of america (SHEA). *Clin. Infect. Dis.* 66, 987–994. doi: 10.1093/cid/ciy149

McFarland, L. V., Elmer, G. W., and Surawicz, C. M. (2002). Breaking the cycle: treatment strategies for 163 cases of recurrent *Clostridium difficile* disease. *Am. J. Gastroenterol.* 97, 1769–1775. doi: 10.1111/j.1572-0241.2002.05839.x

Nicholson, M. R., Thomsen, I. P., Slaughter, J. C., Creech, C. B., and Edwards, K. M. (2015). Novel risk factors for recurrent *Clostridium difficile* infection in children. *J. Pediatr. Gastroenterol. Nutr.* 60, 18–22. doi: 10.1097/MPG.0000000000000553

Pai, S., Aliyu, S. H., Enoch, D. A., and Karas, J. A. (2012). Five years experience of *Clostridium difficile* infection in children at a UK tertiary hospital: proposed criteria for diagnosis and management. *PLoS One* 7:e51728. doi: 10.1371/journal.pone.0051728

Samarkos, M., Mastrogianni, E., and Kampouropoulou, O. (2018). The role of gut microbiota in *Clostridium difficile* infection. *Eur. J. Intern. Med.* 50, 28–32. doi: 10.1016/j.ejim.2018.02.006

Sammons, J. S., and Toltzis, P. (2013). Recent trends in the epidemiology and treatment of C. difficile infection in children. *Curr. Opin. Pediatr.* 25, 116–121. doi: 10.1097/MOP.0b013e32835bf6c0

Schoepfer, A. M., Schaffer, T., Seibold-Schmid, B., Muller, S., and Seibold, F. (2008). Antibodies to flagellin indicate reactivity to bacterial antigens in IBS patients. *Neurogastroenterol. Motil.* 20, 1110–1118. doi: 10.1111/j.1365-2982.2008.01166.x

Spigaglia, P., Barbanti, F., Castagnola, E., Diana, M. C., Pescetto, L., and Bandettini, R. (2017). *Clostridium difficile* causing pediatric infections: new findings from a hospital-based study in Italy. *Anaerobe* 48, 262–268. doi: 10.1016/j.anaerobe.2017.10.008

van Nood, E., Vrieze, A., Nieuwdorp, M., Fuentes, S., Zoetendal, E. G., de Vos, W. M., et al. (2013). Duodenal infusion of donor feces for recurrent *Clostridium difficile*. *N. Engl. J. Med.* 368, 407–415. doi: 10.1056/NEJMoa1205037

Walia, R., Garg, S., Song, Y., Girotra, M., Cuffari, C., Fricke, W. F., et al. (2014). Efficacy of fecal microbiota transplantation in 2 children with recurrent *Clostridium difficile* infection and its impact on their growth and gut microbiome. *J. Pediatr. Gastroenterol. Nutr.* 59, 565–570. doi: 10.1097/MPG.0000000000000495

Wang, Y., Gao, X., Ghozlane, A., Hu, H., Li, X., Xiao, Y., et al. (2018). Characteristics of faecal microbiota in paediatric Crohn's disease and their dynamic changes during infliximab therapy. *J. Crohns Colitis* 12, 337–346. doi: 10.1093/ecco-jcc/jjx153

Ward, T., Larson, J., Meulemans, J., Hillmann, B., Lynch, J., Sidiropoulos, D., et al. (2017). BugBase predicts organism level microbiome phenotypes. *bioRxiv* [Preprint]. doi: 10.1101/133462

Wendt, J. M., Cohen, J. A., Mu, Y., Dumyati, G. K., Dunn, J. R., Holzbauer, S. M., et al. (2014). *Clostridium difficile* infection among children across diverse US geographic locations. *Pediatrics* 133, 651–658. doi: 10.1542/peds.2013-3049

Conflict of Interest Statement: The authors declare that the research was conducted in the absence of any commercial or financial relationships that could be construed as a potential conflict of interest.

Copyright © 2018 Li, Gao, Hu, Xiao, Li, Yu, Yu, Zhang and Wang. This is an open-access article distributed under the terms of the Creative Commons Attribution License (CC BY). The use, distribution or reproduction in other forums is permitted, provided the original author(s) and the copyright owner(s) are credited and that the original publication in this journal is cited, in accordance with accepted academic practice. No use, distribution or reproduction is permitted which does not comply with these terms.

frontiers in Microbiology

ORIGINAL RESEARCH
published: 13 November 2018
doi: 10.3389/fmicb.2018.02682

Alterations of Gut Microbiota in Cholestatic Infants and Their Correlation With Hepatic Function

Cheng Guo[1†], Yinhu Li[2†], Peipei Wang[1], Yingchao Li[3], Chuangzhao Qiu[4], Muxia Li[1], Daxi Wang[4], Ruiqin Zhao[5], Dongfang Li[4], Ye Wang[1], Shuaicheng Li[2], Wenkui Dai[4] and Lin Zhang[1]**

[1] Department of Pediatrics, The Third Hospital of Hebei Medical University, Shijiazhuang, China, [2] Department of Computer Science, City University of Hong Kong, Kowloon Tong, Hong Kong, [3] Department of Pediatrics, The Second Hospital of Hebei Medical University, Shijiazhuang, China, [4] Department of Microbial Research, WeHealthGene Institute, Shenzhen, China, [5] Department of Pediatrics, Children's Hospital of Hebei Province, Shijiazhuang, China

OPEN ACCESS

Edited by:
Learn-Han Lee,
Monash University Malaysia, Malaysia

Reviewed by:
Alinne Castro,
Universidade Católica Dom Bosco (UCDB), Brazil
Adil Mardinoglu,
Chalmers University of Technology, Sweden
Adam C. N. Wong,
University of Florida, United States
Daniele Zama,
Policlinico S.Orsola-Malpighi, Italy

***Correspondence:**
Wenkui Dai
daiwk@wehealthgene.com
Lin Zhang
lzhang_79@163.com

[†] These authors have contributed equally to this work

Specialty section:
This article was submitted to Microbial Symbioses, a section of the journal Frontiers in Microbiology

Received: 10 July 2018
Accepted: 19 October 2018
Published: 13 November 2018

Citation:
Guo C, Li Y, Wang P, Li Y, Qiu C, Li M, Wang D, Zhao R, Li D, Wang Y, Li S, Dai W and Zhang L (2018) Alterations of Gut Microbiota in Cholestatic Infants and Their Correlation With Hepatic Function. Front. Microbiol. 9:2682. doi: 10.3389/fmicb.2018.02682

Cholestasis is a major hepatic disease in infants, with increasing morbidity in recent years. Accumulating evidence has revealed that the gut microbiota (GM) is associated with liver diseases, such as non-alcoholic steatohepatitis, cirrhosis, and hepatocellular carcinoma. However, GM alterations in cholestatic infants and the correlation between the GM and hepatic functions remain uninvestigated. In this study, 43 cholestatic infants (IC group) and 37 healthy infants (H group) were enrolled to detect GM discrepancies using 16S rDNA analysis. The diversity in the bacterial community was significantly lower in the IC group than that in the H group (P = 0.013). After determining the top 10 abundant genera of microbes in the IC and H groups, we found that 13 of them were differentially enriched, including *Bifidobacterium*, *Bacteroides*, *Streptococcus*, *Enterococcus*, and *Staphylococcus*. As compared with the H group, the IC group had a more complex GM co-occurrence network featured by three core nodes: *Phyllobacterium*, *Ruminococcus*, and *Anaerostipes*. In addition, the positive correlation between *Faecalibacterium* and *Erysipelatoclostridium* (r = 0.689, P = 0.000, FDR = 0.009) was not observed in the IC patients. Using the GM composition, the cholestatic patients can be distinguished from healthy infants with high accuracy [areas under receiver operating curve (AUC) $>$ 0.97], wherein *Rothia*, *Eggerthella*, *Phyllobacterium*, and *Blautia* are identified as valuable biomarkers. Using KEGG annotation, we identified 32 functional categories with significant difference in enrichment of the GM of IC patients, including IC-enriched functional categories that were related to lipid metabolism, biodegradation and metabolism of xenobiotics, and various diseases. In contrast, the number of functions associated with amino acid metabolism, nucleotide metabolism, and vitamins metabolism was reduced in the IC patients. We also identified significant correlation between GM composition and indicators of hepatic function. *Megasphaera* positively correlated with total bilirubin (r = 0.455, P = 0.002) and direct bilirubin (r = 0.441, P = 0.003), whereas γ-glutamyl transpeptidase was positively associated with *Parasutterella* (r = 0.466, P = 0.002) and

negatively related to *Streptococcus* ($r = -0.450$, $P = 0.003$). This study describes the GM characteristics in the cholestatic infants, illustrates the association between the GM components and the hepatic function, and provides a solid theoretical basis for GM intervention for the treatment of infantile cholestasis.

Keywords: infantile cholestasis, 16S rRNA, hepatic function, bacterial biomarkers, co-abundance network

INTRODUCTION

Cholestasis is a major hepatic disease in infants, with increasing incidence, with nearly one in every 2,500 individuals being affected (Fischler and Lamireau, 2014). Numerous studies have reported that infantile cholestasis (IC) can be caused by infection of the liver (e.g., hepatitis A, B, and C viral infection, Epstein-Barr virus infection, and cytomegalovirus infection) (Delemos and Friedman, 2013; Fawaz et al., 2017), abnormal structure of the biliary tract (e.g., biliary atresia and choledochal cyst) (Hoerning et al., 2014; Fawaz et al., 2017), hereditary diseases (e.g., Alagille syndrome, progressive familial intrahepatic cholestasis, and Aagenaes syndrome) (Hartley et al., 2013; Fawaz et al., 2017), and metabolic disorders [e.g., abnormal amino acid metabolism (Reichardt and Woo, 1991), abnormal carbohydrate metabolism (Phaneuf et al., 1991), and abnormal lipid metabolism (Vance, 2006)]. This disease can further injure hepatocytes, leading to hyperbilirubinemia (Brumbaugh and Mack, 2012), cirrhosis (Li et al., 2017) and may be fatal. As a key feature of IC, bile acids (BAs) closely interact with gut microbiota (GM) through the gut-liver axis (Li et al., 2017; Tripathi et al., 2018).

Previous research indicates that the GM participates in BA enterohepatic circulation and affects the secretion of BAs (Long et al., 2017; Tripathi et al., 2018). Bile salt hydrolases (BSH) are enzymes derived from the GM, which metabolize primary BAs into secondary BAs that, in turn, activate the synthesis of primary BAs through farnesoid X-activated receptor (FXR) and G protein-coupled BA receptor 1 (TGR5) in enterocytes (Long et al., 2017; Schneider et al., 2018). BAs also affect GM composition by controlling the PH of the gut environment, repressing the growth of pathogens and maintaining the balance of the GM (Islam et al., 2011).

To date, the association between GM alteration and hepatic diseases, including alcoholic fatty liver disease (ALD) (Cassard and Ciocan, 2017), non-alcoholic fatty liver disease (NAFLD) (Li et al., 2018), cirrhosis (Chen et al., 2011), and hepatocellular carcinoma (HCC) (Garrett, 2015), has been mainly studied in adults, whereas reports of studies in infants with immature GM are rare (de Muinck and Trosvik, 2018). Currently, the characteristics of GM in infants with IC and their association with hepatic function remain uninvestigated.

In this study, we enrolled a total of 43 IC patients and 37 healthy infants to investigate the roles of GM in the IC patients. In addition, to characterize the GM of the patients, we aimed to: (I) evaluate bacterial correlation and their contribution to hepatic function; (II) identify GM biomarkers for non-invasive diagnosis of IC; (III) elucidate GM discrepancy among patients with IC owing to different causes. These findings enhance our understanding of the pathogenic mechanism of dysbiotic GM, and provide a solid theoretical basis for GM intervention for the treatment of IC.

MATERIALS AND METHODS

Ethics Statement

This study was approved by the Ethics Committee of The Third Hospital of Hebei Medical University under the registration number 2017-009-1. All the infants' parents provided written informed consent, and volunteered to allow their children to participate in the investigation for scientific research.

Participant Enrollment

The IC infants in this study were enrolled from the Third Hospital of Hebei Medical University, Children's Hospital of Hebei Province, and Second Hospital of Hebei Medical University if they satisfied the following criteria: (I) age below 3 years; (II) levels of γ-glutamyl transpeptidase (GGT) were higher than 40 U/L, or the levels of total bilirubin (TBIL) were higher than 20 μmol/L (Cholestasis, 2015). In addition, the patients who met the following criteria were excluded from the study: (I) If their mother suffered from diabetes, high blood pressure, or chronic liver disease during the pregnancy; (II) If their mother had been continually exposed to drugs or probiotics during pregnancy or lactation; (III) If the patients suffered from allergic diseases (e.g., food allergy, eczema, and allergic gastroenteritis); (IV) If the patients had been exposed to antibiotic, probiotic, or proton pump inhibitors 4 weeks before fecal sample collection.

Healthy infants were selected from among the subjects if they passed infantile physical examinations of Third Hospital of Hebei Medical University and met the following standards: (I) The candidate should be younger than 3 years old; (II) The candidate should not have a history of allergic diseases (e.g., food allergy, eczema, and allergic gastroenteritis); (III) The candidate should not have had diarrhea 2 weeks prior to the study; (IV) The candidate should not have been administered any antibiotic, probiotic, or proton pump inhibitors 4 weeks prior to the study. Finally, 37 healthy infants (H group) and 43 cholestatic infants (IC group) were enrolled for the study between December 2016 and January 2018 (**Table 1**).

Sample Collection

Fresh stools from the IC patients were collected in the morning after their admission to the hospital, and fresh stools from the healthy subjects were collected during their physical examination. The blood samples were collected from the participants, and

TABLE 1 | Background information of participants.

	Healthy (*n* = 37)	Infantile cholestasis (*n* = 43)	*P*-value
Gender			0.967
Male	23	28	
Female	14	15	
Age (mo)	12.03 ± 8.75	2.25 ± 1.79	0.000
Feeding pattern			0.041
Breastfeeding	25	31	
Formula feeding	2	8	
Mixed	10	4	
Delivery pattern			0.011
Natural delivery	31	29	
Cesarean section	6	23	
Indicators of hepatic function			
TBA (1–10 μmol/L)*	5.76 ± 2.43	146.71 ± 217.20	0.000
TBIL (3–20 μmol/L)*	8.39 ± 4.38	133.60 ± 86.05	0.000
DBIL (2–6 μmol/L)*	3.08 ± 1.16	90.46 ± 56.12	0.000
TP (60–80 g/L)*	65.70 ± 4.78	56.01 ± 8.33	0.000
CHOL (0–5.2 mmol/L)*	4.31 ± 0.46	3.43 ± 0.96	0.000
ALT (5–40 U/L)*	14.30 ± 3.81	284.22 ± 354.20	0.000
AST (5–35 U/L)*	24.27 ± 4.13	357.73 ± 467.64	0.000
GGT (7–40 U/L)*	16.89 ± 4.43	212.39 ± 180.72	0.000

**TBA, total bile acids; TBIL, total bilirubin; DBIL, direct bilirubin; TP, total protein; CHOL, total cholesterol; ALT, serum alanine aminotransferase; AST, aspartate aminotransferase; GGT, γ-glutamyl transpeptidase.*

hepatic function was examined using the blood autoanalyzer (Beckman Coulter AU5800, Brea, CA, United States). The clinical indices for the assessment of hepatic function consist of total bile acids (TBA), total bilirubin (TBIL), direct bilirubin (DBIL), total protein (TP), total cholesterol (CHOL), serum alanine aminotransferase (ALT), aspartate aminotransferase (AST), and γ-glutamyl transpeptidase (GGT) (**Supplementary Table S1**).

DNA Extraction, Library Construction, and Sequencing

Bacterial DNA was extracted from stools using the E.Z.N.A.® Soil DNA Kit (Omega BioTek, Norcross, GA, United States) according to the manufacturer's protocols. The V3–V4 region of the 16S rRNA gene was amplified by primers 338F and 806R, using the PCR kit (TransGenAP221-02, Peking). The quality of the PCR product was determined (Qubit, Thermo Fisher Scientific, Singapore), and it was then prepared for library construction (TruSeq DNA PCR-Free kit, Illumina, San Diego, CA, United States). Then the eligible libraries were paired-end sequenced as 300 (nt) reads using the MiSeq platform (Illumina, San Diego, CA, United States). The raw reads were uploaded to the NCBI Sequence Read Archive (SRA) Database (Accession Number: SRP151718).

Taxonomical Annotation

Raw reads were filtered if they contained more than 10 low-quality (<Q20) bases, or a 15-base adapter contamination owing to a self-edited program. The paired reads were connected into tags on the basis of an overlap of at least 50 bases. Then, the tags were clustered into Operational Taxonomic Units (OTUs) with 97% similarity using the USEARCH (v7.0.1090) program. After the elimination of the chimeras, the OTUs were aligned to the RDP 16S rRNA databases (trainset 16/release 11.5) (Cole et al., 2014) and their corresponding taxonomic positions were defined. The Shannon index was calculated using the "vegan" package in R (version 3.4.1).

PERMANOVA Analysis

The impact of physical indices (e.g., gender, age, delivery pattern, and feeding pattern) on GM distributions was assessed using Permutational Multivariate Analysis of Variance (PERMANOVA) (Tang et al., 2016) with 9,999 permutations and Euclidean distances (package "vegan" in R).

Selection of Biomarkers and Validation Test

For biomarker identification, a two-step schema was adopted. First, a random forest model (Liaw and Wiener, 2002) was constructed for the discrimination between the H and IC groups, and candidate biomarkers were selected on the basis of the Gini values and optimal variation numbers (using the R package "random-Forest"). Second, the GM between the two groups was compared using the Wilcoxon rank-sum test (using "wilcox.test" in R). Candidate biomarkers with a significant adjusted difference ($P < 0.05$, FDR < 0.05) were selected as final biomarkers for cholestatic patients.

All the samples were randomized into two sets (one training set and one testing set). The training set was used to construct a random forest model and the test set was used to validate final biomarkers. The accuracy of biomarkers for screening of

cholestatic infants was estimated using area under the curve (AUC) values with five repeats (using the R package "pROC").

Functional Prediction and Enrichment

Gut microbiota functions were predicted on the basis of 16S rRNA OTUs profiling using PICRUST with default setting (Langille et al., 2013). KEGG Orthology (KO) abundances were calculated for each sample, and the abundances of functional categories on level III of the KEGG database were detected. The differentially enriched categories between the H group and the IC group were identified using the Wilcoxon rank-sum test ($P < 0.05$). The associations between the KEGG pathways and the clinical indices were estimated with Spearman coefficient using "cor" in R.

Statistical Analysis

The Wilcoxon rank-sum test (using "wilcox.test" in R) was used to detect differentially enriched genera between the H and IC groups ($P < 0.05$). The Spearman correlation analysis was executed on the genus level, and the relationships whose *r*-values were higher than 0.6 or lower than −0.6 were retained. The co-occurrence networks were visualized using the Cytoscape software (v2.2.0) (Shannon et al., 2003). For the 43 IC patients and the 37 healthy infants, the relationships between the GM and eight clinical indices were evaluated using the Spearman coefficient. The statistical results from the Wilcoxon rank-sum test and Spearman correlation analysis were adjusted with the Benjamini and Hochberg method (FDR < 0.05) using "p.adjust" in R.

RESULTS

Sample Characteristics and Data Output

A total of 37 healthy infants (H group) and 43 cholestatic infants (IC group) were enrolled for stool sample collection (**Table 1**). Among the IC patients, 5 had cholestasis due to cytomegalovirus hepatitis, 9 had cholestasis due to biliary atresia, and the rest of the patients were diagnosed without any discernible cause (**Supplementary Table S1**). 16S rRNA sequencing of the samples and the connection of high-quality pair-end reads finally yielded 17,889 ± 5,012 (mean ± SD) tags, which ranged from 4,863 to 25,213. The number of OTUs ranged from 112 to 244 for the H group and from 54 to 245 for the IC group. After RDP database alignment, 93 genera of 7 phyla were identified from the samples, and the feeding pattern of the infants had an impact on the difference in GM between the H and IC groups ($P = 0.009$, PERMANOVA analysis, **Supplementary Table S2**). All the samples predominantly showed the following genera: *Bifidobacterium*, *Bacteroides*, *Enterococcus*, *Blautia*, *Roseburia*, and *Faecalibacterium* (**Figure 1A**). Principal component analysis (PCA) showed that the samples from the IC group clustered together and were separated from the H group (**Figure 1A**). Moreover, the IC patients exhibited a significantly lower diversity in the bacterial community: the average value of the Shannon index was 2.222 ± 0.790 for the IC group and 2.669 ± 0.753 for the H group ($P = 0.013$, **Figure 1B**).

IC and H Groups Showed Discrepancy in GM Structure, and GM Biomarkers Were Identified for Screening of IC Infants

Among the top 10 abundant genera found in the IC and H groups, 13 were differentially enriched (**Figure 2A**). *Streptococcus* (10.449 ± 13.479%, $P = 0.002$, FDR = 0.002), *Enterococcus* (8.301 ± 20.546%, $P = 0.003$, FDR = 0.003), *Staphylococcus* (3.520 ± 11.728%, $P = 0.000$, FDR = 0.000), *Megasphaera* (0.443 ± 0.755%, $P = 0.018$, FDR = 0.018), *Phyllobacterium* (1.401 ± 4.770%, $P = 0.000$, FDR = 0.000), and *Megamonas* (0.841 ± 3.248%, $P = 0.0124$, FDR = 0.013) were found to be enriched in the IC infants. Conversely, the relative abundance of *Bifidobacterium* (14.006 ± 21.753%, $P = 0.000$, FDR = 0.000), *Bacteroides* (5.699 ± 9.514%, $P = 0.026$, FDR = 0.026), *Blautia* (0.788 ± 1.313%, $P = 0.000$, FDR = 0.000), *Faecalibacterium* (2.482 ± 8.204%, $P = 0.041$, FDR = 0.041), *Roseburia* (1.215 ± 2.270%, $P = 0.017$, FDR = 0.018), *Anaerostipes* (0.143 ± 0.296%, $P = 0.000$, FDR = 0.000), and *Collinsella* (0.351 ± 1.412%, $P = 0.000$, FDR = 0.000) was reduced in the IC group (**Figure 2A**).

The GM co-occurrence networks were constructed for the H and IC groups, respectively, and the cholestatic infants showed a greater complexity in networks (**Figure 2B**). For healthy infants, *Ruminococcus* was the core node of the network, and enrichment of *Faecalibacterium* was positively associated with *Erysipelatoclostridium* ($r = 0.689$, $P = 0.000$, FDR = 0.009). Such a correlation was not observed in the IC group. Instead, the IC group contained three novel positive correlations between *Bacteroides* and *Ruminococcus* ($r = 0.611$, $P = 0.000$, FDR = 0.048), *Staphylococcus* and *Phyllobacterium* ($r = 0.672$, $P = 0.000$, FDR = 0.048), *Megamonas*, and *Prevotella* ($r = 0.638$, $P = 0.000$, FDR = 0.015) (**Figure 2B**). *Phyllobacterium*, *Ruminococcus*, and *Anaerostipes* were the core nodes of co-occurrence in the network for the IC group.

Using the Random forest classifier, 28 biomarkers were identified to differentiate IC infants from healthy infants (**Figure 3A**) with high accuracy (AUC > 0.97, **Figure 3B**). Among them, *Rothia* (Gini = 4.480), *Eggerthella* (Gini = 4.399), *Phyllobacterium* (Gini = 2.637), and *Blautia* (Gini = 2.172) were found to be the four genera with the highest Gini values, and helped in distinguishing between the two groups.

GM Functional Categories Were Differentially Enriched Between the H and IC Groups

Using KO distributions of GM in all the infants, 32 differentially enriched KEGG functional modules between the IC and H groups were identified (**Figure 4**). The enriched functional categories in the IC patients included "Lipid metabolism" ($P = 0.000$, FDR = 0.000), "Glycan biosynthesis and metabolism"($P = 0.000$, FDR = 0.000), and "Xenobiotics biodegradation and metabolism" ($P = 0.000$, FDR = 0.000) (**Figure 4**). Contrastingly, the abundance of "Amino acid metabolism" ($P = 0.000$, FDR = 0.000), "Nucleotide metabolism" ($P = 0.000$, FDR = 0.000), and "Metabolism of cofactors and

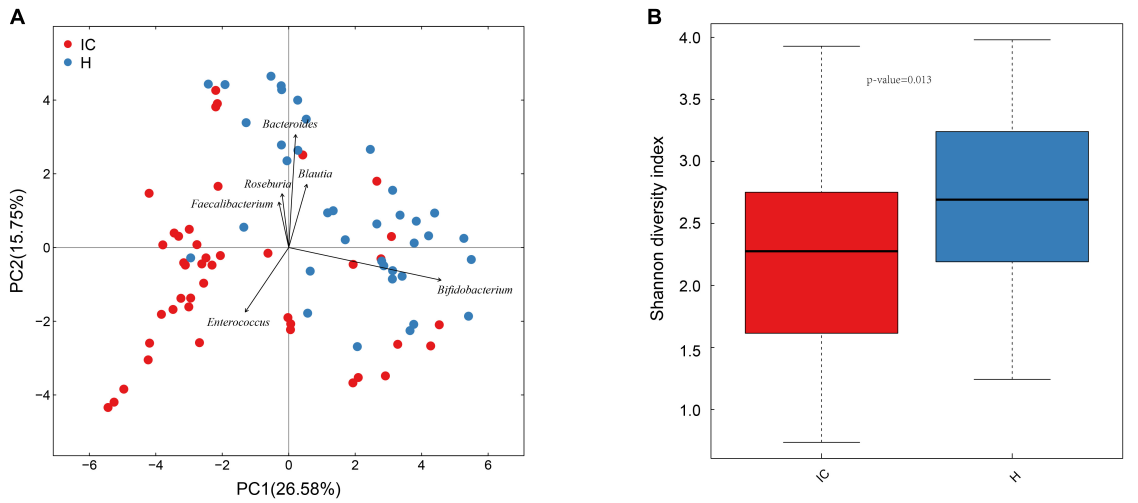

FIGURE 1 | Principal component analysis (PCA) distribution and bacterial diversity in IC and healthy infants. **(A)** Using PCA analysis, the samples from the IC group were clustered together, and they were separated from those of the H group. The GM of the participants predominantly included *Bacteroides*, *Bifidobacterium*, and *Enterococcus*. **(B)** The diversity in the bacterial community was significantly lower in the IC infants (2.222 ± 0.790) than that in the H group (2.669 ± 0.753) (P = 0.013).

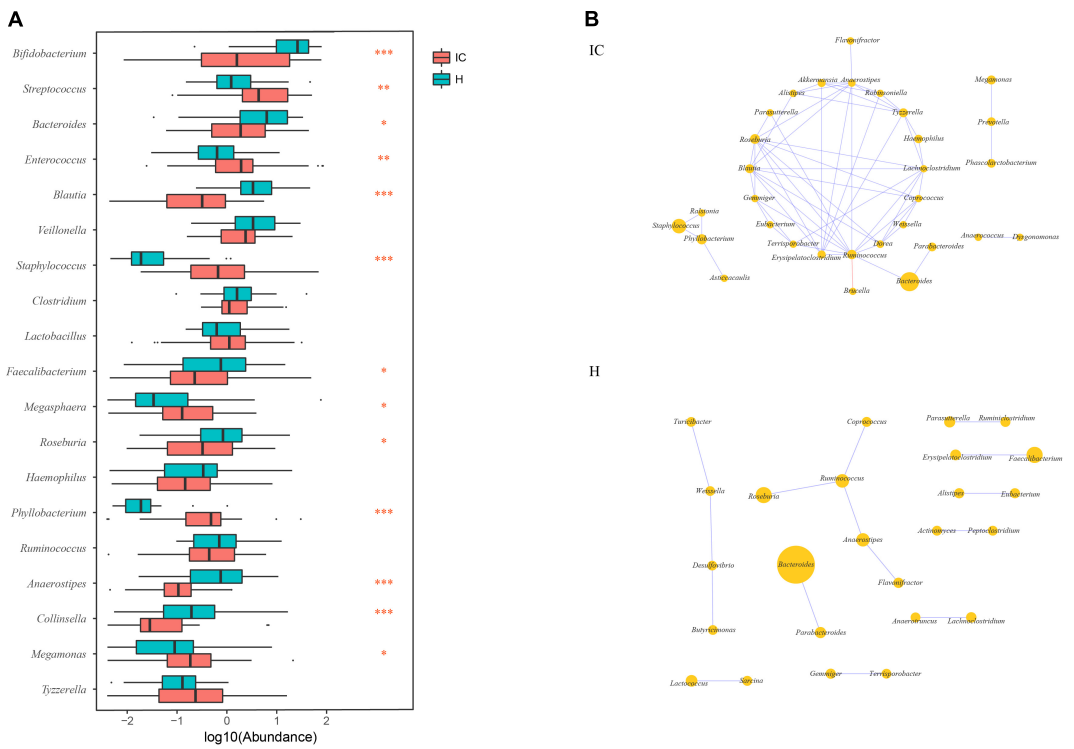

FIGURE 2 | Discrepancy in GM components and networks between the IC and H groups. **(A)** A total of 13 taxa are differentially enriched between the IC and H groups. *Streptococcus*, *Enterococcus*, *Staphylococcus*, *Megasphaera*, *Phyllobacterium*, and *Megamonas* are enriched in the IC infants, whereas the numbers of *Bifidobacterium*, *Bacteroides*, *Blautia*, *Faecalibacterium*, *Roseburia*, *Anaerostipes*, and *Collinsella* are lower than those in the H group. One, two, and three asterisks stand for the *P*-value lesser than 0.05, 0.01, and 0.001, respectively. **(B)** The GM co-occurrence network was constructed for the IC and H groups, respectively. The purple and red edges stand for the positive and negative correlations, respectively. The diameter of the circle is proportional to the relative abundance. The bacterial network in the IC group is more complicated than that in the H group, and some correlations in the H group are disrupted.

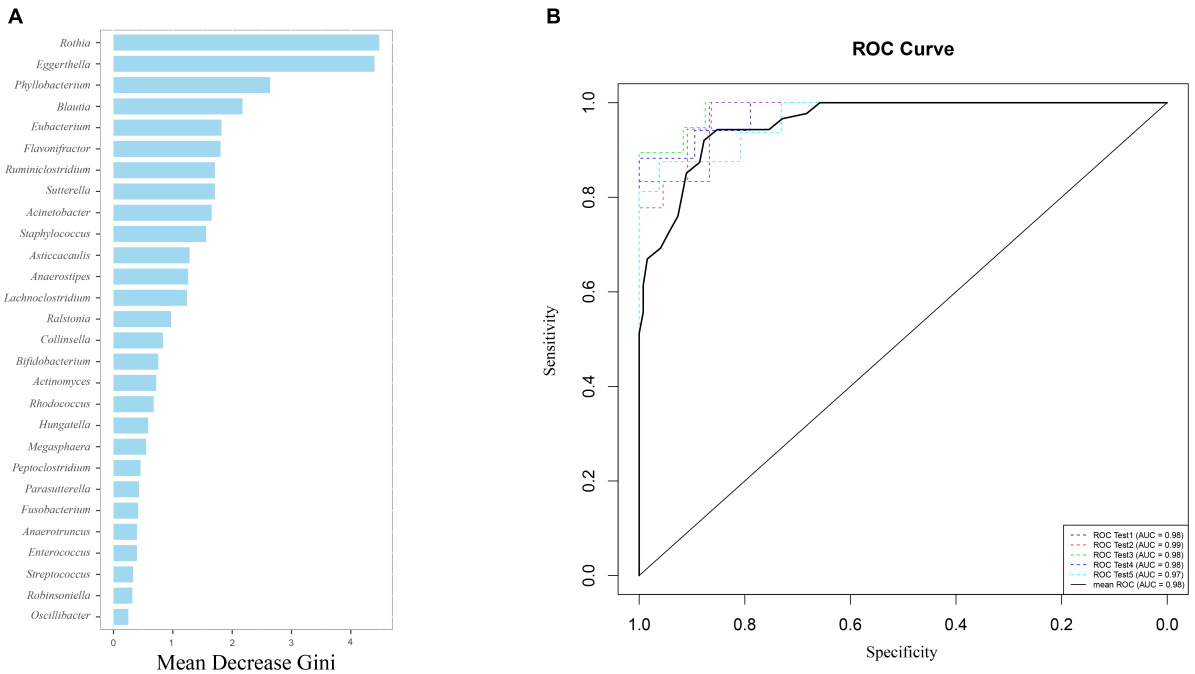

FIGURE 3 | Gut microbiota (GM) biomarkers help to differentiate between the IC and H groups. **(A)** Following optimal variation numbers were indicated by random forest classifiers, 28 GM biomarkers were examined for the IC group as compared with those for the H group. Their Gini values are shown in the picture. **(B)** The accuracy of biomarkers was verified using cross-validation, and their AUC values were calculated. The ROC curves were drawn with five repeats by different colors.

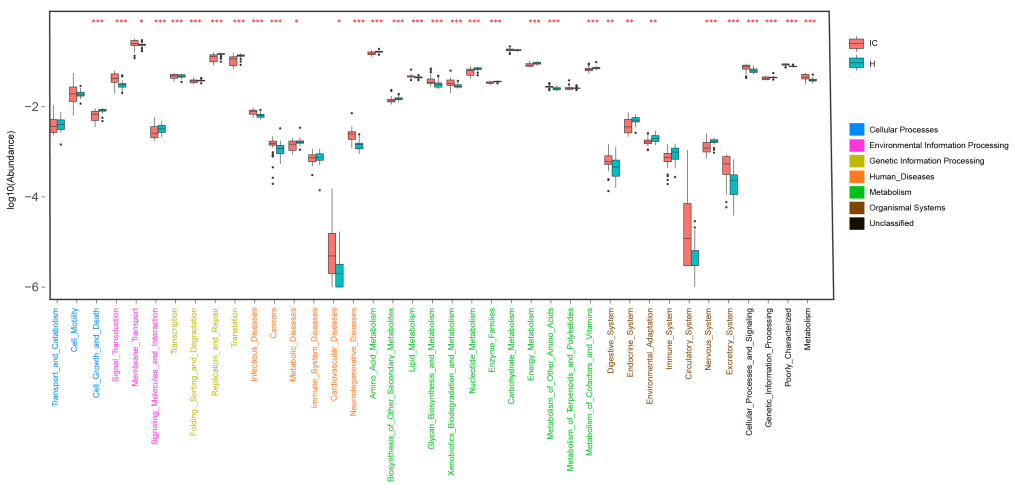

FIGURE 4 | Distribution of KEGG level II pathways in the IC and H groups. Relying on the functional classifications of the KEGG database, the enriched pathways were determined for the IC and H groups, and the functional categories between these two groups were compared. *P*-values are indicated by asterisks on the top (one, two, and three asterisks stand for a *P*-value smaller than 0.05, 0.01, and 0.001, respectively). In addition, level I classification of these KEGG functional categories is suggested by different colors on the right.

vitamins" (P = 0.000, FDR = 0.000) was reduced, and more bacterial genes participated in the hosts "Digestive system" (P = 0.000, FDR = 0.000) and "Excretory system" (P = 0.000, FDR = 0.000) in the IC group (**Figure 4**). We also found that the IC-enriched functional modules were associated with the occurrence of diseases, including infectious diseases (P = 0.000, FDR = 0.000), metabolic diseases (P = 0.000, FDR = 0.000), cardiovascular diseases (P = 0.000, FDR = 0.000), neurodegenerative diseases (P = 0.000, FDR = 0.000), and even cancer (P = 0.000, FDR = 0.000). Additionally, the GM of the IC group showed enrichment in "Signal transduction" (P = 0.000, FDR = 0.000), "membrane transport" (P = 0.000, FDR = 0.000), and "Cellular processing and signaling" (P = 0.000, FDR = 0.000) (**Figure 4**).

Taxonomic and Functional Composition of the GM Were Correlated With Hepatic Function

Pairwise correlations between GM genera and eight clinical indicators of hepatic function were estimated in healthy infants (**Figure 5A**). AST negatively and positively correlated with *Enterococcus* ($r = -0.356$, $P = 0.031$) and *Parasutterella* ($r = -0.330$, $P = 0.046$). Negative associations between GGT and *Acinetobacter* ($r = -0.458$, $P = 0.004$), AST and *Rothia* ($r = -0.332$, $P = 0.045$) were also found. In contrast, the relationships between the GM components and the hepatic functional indices were also constructed for the 43 cholestatic infants, and altered associations were observed (**Figure 5D**). For instance, *Oscillibacter* negatively correlated with AST ($r = -0.322$, $P = 0.0350$), whereas it was positively associated with TP ($r = 0.352$, $P = 0.021$). *Streptococcus* was also negatively associated with ALT ($r = -0.342$, $P = 0.025$) and GGT ($r = -0.450$, $P = 0.0026$). Positive correlations were found between *Megasphaera* and indicators of hepatic synthesis [TBIL ($r = 0.455$, $P = 0.002$), and DBIL ($r = 0.441$, $P = 0.003$)]. In addition, *Parasutterella* positively correlated with GGT ($r = 0.466$, $P = 0.002$).

The associations between the GM functional categories and the hepatic function were also investigated (**Figures 5B,E**). For healthy infants, TBIL positively correlated with "Metabolism of other amino acids" ($r = 0.373$, $P = 0.023$) and "Glycan biosynthesis and metabolism" ($r = 0.413$, $P = 0.011$) (**Figure 5B**). TP was negatively associated with the bacterial function "Replication and repair" ($r = -0.351$, $P = 0.034$), and "Signaling molecules and interaction" ($r = -0.349$, $P = 0.035$). In the IC group, the functional items "Metabolism of terpenoids and polyketides" and "Energy metabolism" negatively correlated with TBIL ($r = -0.489$ and $r = -0.515$, respectively) and DBIL ($r = -0.486$ and $r = -0.458$, respectively), and both of them positively correlated with TP ($r = 0.350$ and $r = 0.370$, respectively) (**Figure 5E**). Positive associations were identified between "Membrane transport" and indicators of hepatic

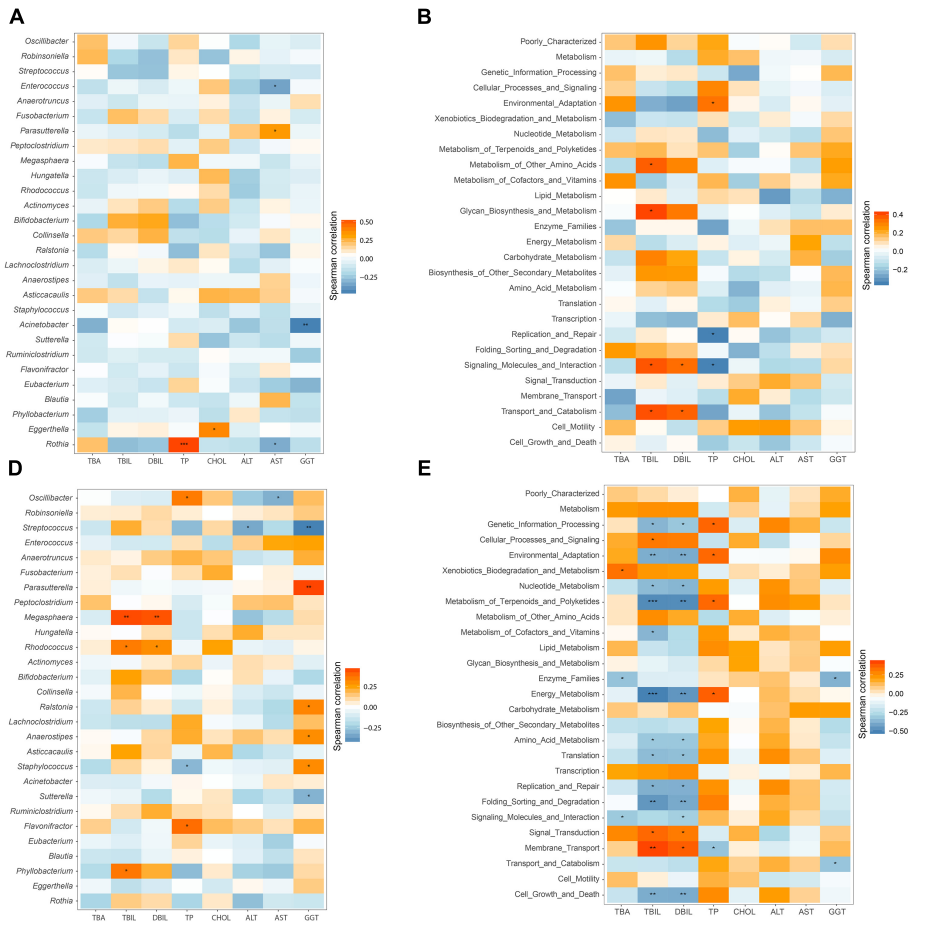

FIGURE 5 | Relationships between GM and hepatic function, and associations among indicators of hepatic function. Spearman correlation analysis was performed between GM components and eight indicators of hepatic function, and the results for the H and IC groups are shown in panels **(A,D)**, respectively. The relationships between the GM functional categories and the hepatic function are shown for healthy infants **(B)** and IC patients **(E)**. In these pictures, orange and blue colors stand for the positive and negative relationships, respectively. One, two, and three asterisks stand for a *P*-value smaller than 0.05, 0.01, and 0.001, respectively. In panels **(C,F)**, the significant relationships ($r > 0.5$ or $r < -0.6$, $P < 0.05$) among different indicators of hepatic function are shown for the H and IC groups.

synthesis [TBIL (r = 0.372, P = 0.005) and DBIL (r = 0.372, P = 0.014)]. In addition, AST positively correlated with ALT (r = 0.590, P = 0.000), and TBIL was positively associated with DBIL (r = 0.672, P = 0.000) (**Figures 5C,F**).

No Apparent GM Difference Was Detected Between IC Cohorts With Different Causes

The IC patients were sorted on the basis of clinical causes for their condition: biliary atresia (BA-IC cohort) or cytomegalovirus hepatitis (CMV-IC cohort). These two cohorts exhibited no significant difference in bacterial diversity (2.259 ± 0.912 and 1.956 ± 0.962 for the BA-IC and CMV-IC cohorts, respectively, **Supplementary Figure S1A**). We did not detect any significant differences in GM composition (**Supplementary Figure S2B**).

With decreasing GGT levels, the distribution of the diversity in the bacterial community, top 5 genera, and hepatic functional indicators were determined for the 43 IC patients (**Figure 6**). Special incidence was found although the GM-liver associations were illustrated. With low abundance of *Bifidobacterium* (0.391%) and *Bacteroides* (0.181%), the levels of GGT (324U/L) were found to be high in IC5; however, the concentrations of TBA (3.2 μmol/L) remained normal (**Figure 6**).

DISCUSSION

In this study, we mainly elucidated the discrepancy in GM between the IC patients and the healthy infants. Between the two groups, we observed lower diversity in the bacterial community in the IC patients, which is probably associated with the reduced inflow of BAs (Fischler and Lamireau, 2014) and GM dysbiosis (Islam et al., 2011). Although significant differences in age, delivery pattern, and feeding pattern were detected between the IC and H groups (P < 0.05), inter-group GM discrepancy was mainly attributed to the feeding pattern after PERMANOVA analysis (**Supplementary Table S2**), and the results also emphasized the impact of diet on GM components (Sonnenburg et al., 2016).

Analysis of GM composition showed low proportions of *Bifidobacterium*, *Bacteroides*, and *Faecalibacterium* in IC patients. Long et al. (2017) study reported that *Bifidobacterium* and *Bacteroides* could secrete BSH enzymes, which liberate conjugated bile acids and facilitate BA enterohepatic circulation. Furthermore, *Bifidobacterium* (Odenwald and Turner, 2017) and *Faecalibacterium* (Miquel et al., 2013) could reinforce the barrier integrity of epidermal cells (Odenwald and Turner, 2017), and repress systemic inflammation reactions through the production of SCFAs (Li et al., 2017). The low abundance of *Bifidobacterium* and *Bacteroides* partly explained the high GGT levels and severe liver injury in IC5. In addition, increased *Streptococcus* numbers in IC patients might raise the levels of TNF-α, IL-6, and IFN-γ, and hence, contribute to systematic inflammations (Jiang et al., 2015). Similarly, in adult patients with cholestatic liver disease, the IC patients showed an increased number of *Enterococcus*; however, overrepresented *Lactobacillus* and *Fusobacterium* were not found in the infantile patients (Sabino et al., 2016), which also suggested a different dysbiotic pattern in infants and adults with related diseases.

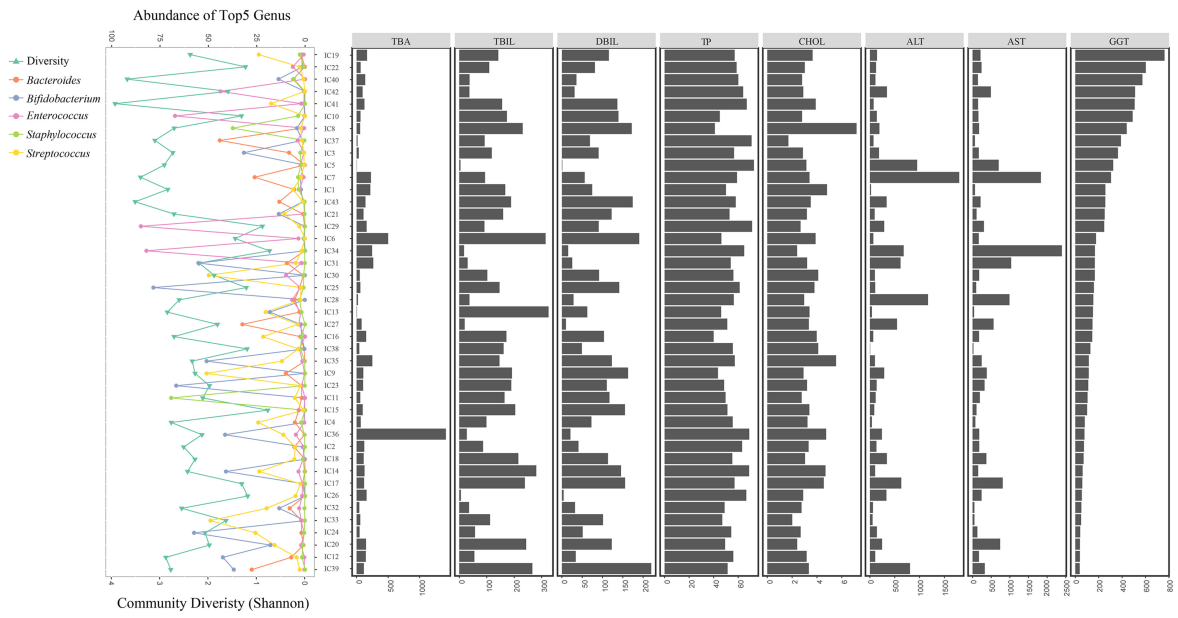

FIGURE 6 | Distribution of GM components and hepatic function in all IC patients. All IC patients were sorted into groups based on decreasing GGT concentrations. The distribution of bacterial diversity and top 5 genera in each sample is shown on the left. Levels of eight hepatic indicators are indicated by the histograms on the right.

Differentiated GM composition in IC patients also contributes to its unique co-occurrence network. For instance, a novel positive association between *Ruminococcus* and *Bacteroides* was discovered in the IC patients. As *Ruminococcus* can generate ursodeoxycholic acid (UDCA) to remiss cholestasis (Lee et al., 2013), decreased *Bacteroides* in IC patients suggest a reduction in *Ruminococcus* numbers, which might further aggravate cholestasis. Another core node for IC patients, *Anaerostipes* was found to contribute to host health improvement by producing SCFAs (Strati et al., 2016), which warranted further investigation in its potential associations with IC. These results suggest that the dynamic changes in GM co-occurrence networks in IC infants correspond to their health status.

Based on GM discrepancy, 28 GM biomarkers were identified for the diagnosis of IC with high precision. As the major biomarkers, *Eggerthella* can produce ω muricholic acid (ωMCA), which can be processed for deoxycholic acid (DCA) synthesis (Long et al., 2017), and participates in inflammation and insulin signaling (Wahlstrom et al., 2016). Therefore, GM biomarkers provided a promising approach for non-invasive diagnosis of IC.

A functional comparison between the H and IC groups revealed differential nutrient metabolism in the GM of IC patients. In the IC patients, more undigested lipids accumulate in the large intestine upon reduction in levels of BAs (Fischler and Lamireau, 2014), and become an important energy source for GM. This hypothesis explained the increase in relative abundance of lipid metabolic modules in IC patients. In addition, elevated levels of functional categories in biodegradation of xenobiotics might be related to the overgrowth of pathogens (Islam et al., 2011) due to the decrease in influx of BAs (Fischler and Lamireau, 2014). Previous research suggests that gut pathogens can be inhibited by BAs through spore germination (Sorg and Sonenshein, 2010) and by regulating vegetative cells (Buffie et al., 2015). With a reduction in the influx of BAs, the increase in number of pathogens might promote toxin secretion, aggravate GM dysbiosis, and injure the immune system (Abt et al., 2016), which also explained the increasing risks of infectious diseases, metabolic diseases, cardiovascular diseases, and neurodegenerative diseases in IC patients.

Discrepancies in relationships between GM and indicators of hepatic functions were further seen in IC infants. *Megasphaera* disrupts metabolic functions of the liver (suggested by TBIL and DBIL), via an unknown mechanism (Lv et al., 2016), which supports their positive correlation in IC patients. Correlating positively with inflammatory cells, *Parasutterella* triggers inflammatory responses (Chen et al., 2018), and positively correlates with indicators of hepatic injury (suggested by GGT). In healthy infants, such relationships were not found as the GM component was shaped by other factors than BAs, such as diet (Sonnenburg et al., 2016), delivery pattern (Rutayisire et al., 2016), and ethnicity (Gupta et al., 2017). Without apparent GM differences among IC patients with different causes for their condition, we suspect that similar GM alterations are driven by the reduced influx of BAs (Fischler and Lamireau, 2014). GM intervention can be adopted to ameliorate hepatic burdens and IC symptoms through the liver-BAs-microbiota associations.

This study presents data for GM alterations in IC patients, provides GM biomarkers for IC diagnosis, and describes the associations between bacterial commensals and hepatic function. However, there are some limitations to the research: (I) A greater number of IC patients with different causes for their condition should be enrolled; (II) GM biomarkers should be validated in populations of different ethnicities. In further studies, additional work is required, such as: (I) A large-cohort study needs to be performed to test the identified biomarkers; (II) Alterations in the microbiome and metabolite alterations in the GM of IC patients need to be investigated; (III) Changes in the immune system and its correlation with GM need be determined. In summary, this research provides a better understanding of the pathogenesis of IC, and emphasizes the therapeutic potential of GM in IC intervention.

AUTHOR CONTRIBUTIONS

LZ and WD managed the project. CG, PW, YCL, and RZ performed the sampling and information collection. ML and YW prepared the DNA. YHL, CQ, and DL performed the bioinformatics analysis in this work. CG and YHL interpreted the analysis results and wrote the paper. SL, DW, and WD optimized the graphs. SL, WD, DL, and LZ guided the statistic analysis and polished the article. All authors reviewed the manuscript.

FUNDING

This work was supported by the Natural Science Foundation of Hebei Province (No. H2018206310) and Shenzhen Science and Technology Project (No. JCYJ20170816170527583).

ACKNOWLEDGMENTS

We thank the nurses who helped with clinical examination and fecal collection at The Third Hospital of Hebei Medical University, and the technicians who give suggestions on data analyzing at WeHealthGene Institute. We also thank Mr. Xiaofeng (Lawrence) Lin from EasyPub for polishing the manuscript.

SUPPLEMENTARY MATERIAL

The Supplementary Material for this article can be found online at: https://www.frontiersin.org/articles/10.3389/fmicb.2018.02682/full#supplementary-material

FIGURE S1 | Comparison on bacterial diversity and GM components between IC cohorts with different causes. **(A)** No significant difference in bacterial diversity was detected between BA-IC cohort and CMV-IC cohort. **(B)** No taxa was differentially enriched between BA-IC and CMV-IC cohorts.

TABLE S1 | Detailed background information of the participants.

TABLE S2 | PERMANOVA ranking associations between GM and indicators of hepatic function.

REFERENCES

Abt, M. C., McKenney, P. T., and Pamer, E. G. (2016). *Clostridium difficile* colitis: pathogenesis and host defence. *Nat. Rev. Microbiol.* 14, 609–620. doi: 10.1038/nrmicro.2016.108

Brumbaugh, D., and Mack, C. (2012). Conjugated hyperbilirubinemia in children. *Pediatr. Rev.* 33, 291–302. doi: 10.1542/pir.33-7-291

Buffie, C. G., Bucci, V., Stein, R. R., McKenney, P. T., Ling, L., Gobourne, A., et al. (2015). Precision microbiome reconstitution restores bile acid mediated resistance to *Clostridium difficile*. *Nature* 517, 205–208. doi: 10.1038/nature13828

Cassard, A. M., and Ciocan, D. (2017). Microbiota, a key player in alcoholic liver disease. *Clin. Mol. Hepatol.* 24, 100–107. doi: 10.3350/cmh.2017.0067

Chen, Y., Yang, F., Lu, H., Wang, B., Chen, Y., Lei, D., et al. (2011). Characterization of fecal microbial communities in patients with liver cirrhosis. *Hepatology* 54, 562–572. doi: 10.1002/hep.24423

Chen, Y. J., Wu, H., Wu, S. D., Lu, N., Wang, Y. T., Liu, H. N., et al. (2018). Parasutterella, in association with irritable bowel syndrome and intestinal chronic inflammation. *J. Gastroenterol. Hepatol.* 33, 1844–1852. doi: 10.1111/jgh.14281

Cholestasis, C. (2015). Expert consensus for diagnosis and treatment of intrahepatic cholestasis. *Chin. J. Clin. Infect. Dis.* 8, 402–406.

Cole, J. R., Wang, Q., Fish, J. A., Chai, B., McGarrell, D. M., Sun, Y., et al. (2014). Ribosomal database project: data and tools for high throughput rRNA analysis. *Nucleic Acids Res.* 42, D633–D642. doi: 10.1093/nar/gkt1244

de Muinck, E. J., and Trosvik, P. (2018). Individuality and convergence of the infant gut microbiota during the first year of life. *Nat. Commun.* 9:2233. doi: 10.1038/s41467-018-04641-7

Delemos, A. S., and Friedman, L. S. (2013). Systemic causes of cholestasis. *Clin. Liver Dis.* 17, 301–317. doi: 10.1016/j.cld.2012.11.001

Fawaz, R., Baumann, U., Ekong, U., Fischler, B., Hadzic, N., Mack, C. L., et al. (2017). Guideline for the evaluation of cholestatic jaundice in infants: joint recommendations of the North American society for pediatric gastroenterology, hepatology, and nutrition and the European society for pediatric gastroenterology, hepatology, and nutrition. *J. Pediatr. Gastroenterol. Nutr.* 64, 154–168. doi: 10.1097/MPG.0000000000001334

Fischler, B., and Lamireau, T. (2014). Cholestasis in the newborn and infant. *Clin. Res. Hepatol. Gastroenterol.* 38, 263–267. doi: 10.1016/j.clinre.2014.03.010

Garrett, W. S. (2015). Cancer and the microbiota. *Science* 348, 80–86. doi: 10.1126/science.aaa4972

Gupta, V. K., Paul, S., and Dutta, C. (2017). Geography, ethnicity or subsistence-specific variations in human microbiome composition and diversity. *Front. Microbiol.* 8:1162. doi: 10.3389/fmicb.2017.01162

Hartley, J. L., Gissen, P., and Kelly, D. A. (2013). Alagille syndrome and other hereditary causes of cholestasis. *Clin. Liver Dis.* 17, 279–300. doi: 10.1016/j.cld.2012.12.004

Hoerning, A., Raub, S., Dechene, A., Brosch, M. N., Kathemann, S., Hoyer, P. F., et al. (2014). Diversity of disorders causing neonatal cholestasis - the experience of a tertiary pediatric center in Germany. *Front. Pediatr.* 2:65. doi: 10.3389/fped.2014.00065

Islam, K. B., Fukiya, S., Hagio, M., Fujii, N., Ishizuka, S., Ooka, T., et al. (2011). Bile acid is a host factor that regulates the composition of the cecal microbiota in rats. *Gastroenterology* 141, 1773–1781. doi: 10.1053/j.gastro.2011.07.046

Jiang, W., Wu, N., Wang, X., Chi, Y., Zhang, Y., Qiu, X., et al. (2015). Dysbiosis gut microbiota associated with inflammation and impaired mucosal immune function in intestine of humans with non-alcoholic fatty liver disease. *Sci. Rep.* 5:8096. doi: 10.1038/srep08096

Langille, M. G., Zaneveld, J., Caporaso, J. G., Huttenhower, C. (2013). Predictive functional profiling of microbial communities using 16S rRNA marker gene sequences. *Nat. Biotechnol.* 31, 814–821. doi: 10.1038/nbt.2676

Lee, J. Y., Arai, H., Nakamura, Y., Fukiya, S., Wada, M., and Yokota, A. (2013). Contribution of the 7beta-hydroxysteroid dehydrogenase from Ruminococcus gnavus N53 to ursodeoxycholic acid formation in the human colon. *J. Lipid Res.* 54, 3062–3069. doi: 10.1194/jlr.M039834

Li, F., Sun, G., Wang, Z.,Wu, W., Guo, H., Peng, L., et al. (2018). Characteristics of fecal microbiota in non-alcoholic fatty liver disease patients. *Sci. Chin. Life Sci.* 61, 770–778. doi: 10.1007/s11427-017-9303-9

Li, Y., Tang, R., Leung, P. S. C., Gershwin, M. E., and Ma, X. (2017). Bile acids and intestinal microbiota in autoimmune cholestatic liver diseases. *Autoimmun. Rev.* 16, 885–896. doi: 10.1016/j.autrev.2017.07.002

Liaw, A., and Wiener, W. (2002). Classification and regression by random forest. *R News.* 2, 18–22.

Long, S. L., Gahan, C. G. M., and Joyce, S. A. (2017). Interactions between gut bacteria and bile in health and disease. *Mol. Aspects Med.* 56, 54–65. doi: 10.1016/j.mam.2017.06.002

Lv, L. X., Fang, D. Q., Shi, D., Chen, D. Y., Yan, R., Zhu, Y. X., et al. (2016). Alterations and correlations of the gut microbiome, metabolism and immunity in patients with primary biliary cirrhosis. *Environ. Microbiol.* 18, 2272–2286. doi: 10.1111/1462-2920.13401

Miquel, S., Martin, R., Rossi, O., Bermúdez-Humarán, L. G., Chatel, J. M., Sokol, H., et al. (2013). Faecalibacterium Prausnitzii and human intestinal health. *Curr. Opin. Microbiol.* 16, 255–261. doi: 10.1016/j.mib.2013.06.003

Odenwald, M. A., and Turner, J. R. (2017). The intestinal epithelial barrier: a therapeutic target? *Nat. Rev. Gastroenterol. Hepatol.* 14, 9–21. doi: 10.1038/nrgastro.2016.169

Phaneuf, D., Labelle, Y., Berube, D., Arden, K., Cavenee, W., Gagné, R., et al. (1991). Cloning and expression of the cDNA encoding human fumarylacetoacetate hydrolase, the enzyme deficient in hereditary tyrosinemia: assignment of the gene to chromosome 15. *Am. J. Hum. Genet.* 48, 525–535.

Reichardt, J. K., and Woo, S. L. (1991). Molecular basis of galactosemia: mutations and polymorphisms in the gene encoding human galactose-1-phosphate uridylyltransferase. *Proc. Natl. Acad. Sci. U.S.A.* 88, 2633–2637. doi: 10.1073/pnas.88.7.2633

Rutayisire, E., Huang, K., Liu, Y., and Tao, F. (2016). The mode of delivery affects the diversity and colonization pattern of the gut microbiota during the first year of infants' life: a systematic review. *BMC Gastroenterol.* 16:86. doi: 10.1186/s12876-016-0498-0

Sabino, J., Vieira-Silva, S., Machiels, K., Joossens, M., Falony, G., Ballet, V., et al. (2016). Primary sclerosing cholangitis is characterised by intestinal dysbiosis independent from IBD. *Gut* 65, 1681–1689. doi: 10.1136/gutjnl-2015-311004

Schneider, K. M., Albers, S., and Trautwein, C. (2018). Role of bile acids in the gut-liver axis. *J. Hepatol.* 68, 1083–1085. doi: 10.1016/j.jhep.2017.11.025

Shannon, P., Markiel, A., Ozier, O., Baliga, N. S., Wang, J. T., Ramage, D., et al. (2003). Cytoscape: a software environment for integrated models of biomolecular interaction networks. *Genome Res.* 13, 2498–2504. doi: 10.1101/gr.1239303

Sonnenburg, E. D., Smits, S. A., Tikhonov, M., Higginbottom, S. K., Wingreen, N. S., and Sonnenburg, J. L. (2016). Diet-induced extinctions in the gut microbiota compound over generations. *Nature* 529, 212–215. doi: 10.1038/nature16504

Sorg, J. A., and Sonenshein, A. L. (2010). Inhibiting the initiation of *Clostridium difficile* spore germination using analogs of chenodeoxycholic acid, a bile acid. *J. Bacteriol.* 192, 4983–4990. doi: 10.1128/JB.00610-10

Strati, F., Cavalieri, D., Albanese, D., De Felice, C., Donati, C., Hayek, J., et al. (2016). Altered gut microbiota in rett syndrome. *Microbiome* 4:41. doi: 10.1186/s40168-016-0185-y

Tang, Z. Z., Chen, G., and Alekseyenko, A. V. (2016). Permanova-s: association test for microbial community composition that accommodates confounders and multiple distances. *Bioinformatics* 32, 2618–2625. doi: 10.1093/bioinformatics/btw311

Tripathi, A., Debelius, J., Brenner, D. A., Karin, M., Loomba, R., Schnabl, B., et al. (2018). The gut-liver axis and the intersection with the microbiome. *Nat. Rev. Gastroenterol. Hepatol.* 15, 397–411. doi: 10.1038/s41575-018-0011-z

Vance, J. E. (2006). Lipid imbalance in the neurological disorder, Niemann-Pick C disease. *FEBS Lett.* 580, 5518–5524. doi: 10.1016/j.febslet.2006.06.008

Wahlstrom, A., Sayin, S. I., Marschall, H. U., and Bäckhed, F. (2016). Intestinal crosstalk between bile acids and microbiota and its impact on host metabolism. *Cell Metab.* 24, 41–50. doi: 10.1016/j.cmet.2016.05.005

Conflict of Interest Statement: The authors declare that the research was conducted in the absence of any commercial or financial relationships that could be construed as a potential conflict of interest.

Copyright © 2018 Guo, Li, Wang, Li, Qiu, Li, Wang, Zhao, Li, Wang, Li, Dai and Zhang. This is an open-access article distributed under the terms of the Creative Commons Attribution License (CC BY). The use, distribution or reproduction in other forums is permitted, provided the original author(s) and the copyright owner(s) are credited and that the original publication in this journal is cited, in accordance with accepted academic practice. No use, distribution or reproduction is permitted which does not comply with these terms.

frontiers in Microbiology

CORRECTION
published: 24 July 2020
doi: 10.3389/fmicb.2020.01599

Corrigendum: Alterations of Gut Microbiota in Cholestatic Infants and Their Correlation With Hepatic Function

Cheng Guo[1†], Yinhu Li[2†], Peipei Wang[1], Yingchao Li[3], Chuangzhao Qiu[4], Muxia Li[1], Daxi Wang[4], Ruiqin Zhao[5], Dongfang Li[4], Ye Wang[1], Shuaicheng Li[2], Wenkui Dai[4] and Lin Zhang[1*]*

[1] Department of Pediatrics, The Third Hospital of Hebei Medical University, Shijiazhuang, China, [2] Department of Computer Science, City University of Hong Kong, Kowloon Tong, Hong Kong, [3] Department of Pediatrics, The Second Hospital of Hebei Medical University, Shijiazhuang, China, [4] Department of Microbial Research, WeHealthGene Institute, Shenzhen, China, [5] Department of Pediatrics, Children's Hospital of Hebei Province, Shijiazhuang, China

Keywords: infantile cholestasis, 16S rRNA, hepatic function, bacterial biomarkers, co-abundance network

OPEN ACCESS

Approved by:
Frontiers Editorial Office, Frontiers Media SA, Switzerland

***Correspondence:**
Wenkui Dai
daiwk@wehealthgene.com
Lin Zhang
lzhang_79@163.com

[†] These authors have contributed equally to this work

Specialty section:
This article was submitted to Microbial Symbioses, a section of the journal Frontiers in Microbiology

Received: *11 June 2020*
Accepted: *18 June 2020*
Published: *24 July 2020*

Citation:
Guo C, Li Y, Wang P, Li Y, Qiu C, Li M, Wang D, Zhao R, Li D, Wang Y, Li S, Dai W and Zhang L (2020) Corrigendum: Alterations of Gut Microbiota in Cholestatic Infants and Their Correlation With Hepatic Function. Front. Microbiol. 11:1599. doi: 10.3389/fmicb.2020.01599

A Corrigendum on

Alterations of Gut Microbiota in Cholestatic Infants and Their Correlation With Hepatic Function

by Guo, C., Li, Y., Wang, P., Li, Y., Qiu, C., Li, M., et al. (2018). Front. Microbiol. 9:2682. doi: 10.3389/fmicb.2018.02682

In the original article, there was an error in the Funding statement. The correct name for the funder is **Natural Science Foundation of Hebei Province** (No. H2018206310).

The authors apologize for this error and state that this does not change the scientific conclusions of the article in any way. The original article has been updated.

Copyright © 2020 Guo, Li, Wang, Li, Qiu, Li, Wang, Zhao, Li, Wang, Li, Dai and Zhang. This is an open-access article distributed under the terms of the Creative Commons Attribution License (CC BY). The use, distribution or reproduction in other forums is permitted, provided the original author(s) and the copyright owner(s) are credited and that the original publication in this journal is cited, in accordance with accepted academic practice. No use, distribution or reproduction is permitted which does not comply with these terms.

frontiers in Microbiology

ORIGINAL RESEARCH
published: 19 December 2018
doi: 10.3389/fmicb.2018.03146

Gut Microbiota Features in Young Children With Autism Spectrum Disorders

Lorena Coretti[1,2,3], Lorella Paparo[4], Maria Pia Riccio[4], Felice Amato[1,5], Mariella Cuomo[1], Alessandro Natale[1], Luca Borrelli[3,6], Giusi Corrado[4], Carmen De Caro[7], Marika Comegna[1,5], Elisabetta Buommino[3,7], Giuseppe Castaldo[1,5], Carmela Bravaccio[4], Lorenzo Chiariotti[1,3,8], Roberto Berni Canani[3,4,5,9]* and Francesca Lembo[3,7]**

[1] Department of Molecular Medicine and Medical Biotechnology, University of Naples Federico II, Naples, Italy, [2] Department of Physiology and Biochemistry, Faculty of Medicine and Surgery, University of Malta, Msida, Malta, [3] Task Force on Microbiome Studies, University of Naples Federico II, Naples, Italy, [4] Department of Translational Medical Science – Pediatric Section, University of Naples Federico II, Naples, Italy, [5] CEINGE Advanced Biotechnologies, University of Naples Federico II, Naples, Italy, [6] Department of Veterinary Medicine and Animal Productions, University of Naples Federico II, Naples, Italy, [7] Department of Pharmacy, University of Naples Federico II, Naples, Italy, [8] Istituto di Endocrinologia ed Oncologia Sperimantale, Naples, Italy, [9] European Laboratory for the Investigation of Food-Induced Diseases, University of Naples Federico II, Naples, Italy

OPEN ACCESS

Edited by:
Sunny Hei Wong,
The Chinese University of Hong Kong, China

Reviewed by:
Maria Jose Gosalbes,
Centro de Investigación Biomédica en Red (CIBER), Spain
Aymé Spor,
INRA UMR1347 Agroécologie, France

***Correspondence:**
Lorena Coretti
lorena.coretti@tiscali.it
Roberto Berni Canani
berni@unina.it
Francesca Lembo
frlembo@unina.it

Specialty section:
This article was submitted to Microbial Symbioses, a section of the journal Frontiers in Microbiology

Received: 02 August 2018
Accepted: 04 December 2018
Published: 19 December 2018

Citation:
Coretti L, Paparo L, Riccio MP, Amato F, Cuomo M, Natale A, Borrelli L, Corrado G, De Caro C, Comegna M, Buommino E, Castaldo G, Bravaccio C, Chiariotti L, Berni Canani R and Lembo F (2018) Gut Microbiota Features in Young Children With Autism Spectrum Disorders. Front. Microbiol. 9:3146. doi: 10.3389/fmicb.2018.03146

Proliferation and/or depletion of clusters of specific bacteria regulate intestinal functions and may interfere with neuro-immune communication and behavior in patients with autism spectrum disorder (ASD). Consistently, qualitative and quantitative alteration of bacterial metabolites may functionally affect ASD pathophysiology. Up to date, age-restricted cohort studies, that may potentially help to identify specific microbial signatures in ASD, are lacking. We investigated the gut microbiota (GM) structure and fecal short chain fatty acids (SCFAs) levels in a cohort of young children (2–4 years of age) with ASD, with respect to age-matched neurotypical healthy controls. Strong increase of Bacteroidetes and Proteobacteria and decrease of Actinobacteria was observed in these patients. Among the 91 OTUs whose relative abundance was altered in ASD patients, we observed a striking depletion of *Bifidobacterium longum*, one of the dominant bacteria in infant GM and, conversely, an increase of *Faecalibacterium prausnitzii*, a late colonizer of healthy human gut and a major butyrate producer. High levels of *F. prausnitzii* were associated to increase of fecal butyrate levels within normal range, and over representation of KEGG functions related to butyrate production in ASD patients. Here we report unbalance of GM structure with a shift in colonization by gut beneficial bacterial species in ASD patients as off early childhood.

Keywords: gut microbiome, ASD, short chain fatty acids, *Faecalibacterium prausnitzii*, *Bifidobacterium longum*, butyrate, propionate

INTRODUCTION

Autism spectrum disorders (ASD) are a group of severe neurodevelopmental conditions characterized by stereotypic behavior with defective communication and social interaction deriving from a combination of genetic and environmental factors (Hallmayer et al., 2011). The influence of early life alteration in GM and its metabolites on the development of ASD symptoms is emerging.

In animal models with ASD behavioral traits, GM dysbiosis was correlated to behavioral alterations, gastrointestinal tract abnormalities and immunologic alterations (Hsiao et al., 2013; Coretti et al., 2017), mimicking clinical features reported in ASD patients (de Magistris et al., 2010; Estes and McAllister, 2015). Several human pre-clinical studies have described abnormal gut bacteria in children with ASD. An unbalance in Bacteroidetes and Firmicutes phyla have been described with a decrease of Bacteriodetes/Firmicutes ratio in fecal samples of autistic children (Tomova et al., 2015). Higher abundance of *Clostridiun*, *Sutterella, Lactobacillus, Desulfovibrio* genera, and *Bacteroides vulgatus* was found in ASD patients with respect to neurotypical subjects (Song et al., 2004; Parracho et al., 2005; Finegold et al., 2010; Williams et al., 2011; De Angelis et al., 2013). Conversely, in some studies, *Bifidobacterium*, *Prevotella,* and *Akkermansia muciniphila* were found reduced in GM of ASD children (Finegold et al., 2010; Wang et al., 2011; Kang et al., 2013). More recently, reduction of Bacteroidetes in ASD young subjects and, at genus level, increase of *Collinsella*, *Corynebacterium*, *Dorea*, and *Lactobacillus* together with significant reduction of *Alistipes*, *Bilophila*, *Dialister*, *Parabacteroides, and Veillonella* have been reported (Strati et al., 2017). Inconsistently with previous studies, the ratio of Bacteroidetes/Firmicutes was significantly higher in Chinese children with ASD probably due to different living environment and eating habits (Zhang et al., 2018). Along with GM composition, also SCFAs levels, which are modulated by functional gut microbes, showed changes both in human patients and mouse models of ASD, possibly contributing to ASD symptoms. Butyric, propionic, acetic, valeric acids were found increased in ASD patients compared to controls and decreased in association with probiotic use (Wang et al., 2012). Abnormal levels of SCFAs in the systemic circulation may cause metabolic and neurological effects relevant to ASD (Thomas et al., 2012; Frye et al., 2016). Findings in animal models also supported this hypothesis (MacFabe et al., 2007; de Theije et al., 2014).

Several attempts have been made in elucidating GM features and to predict GM related activities in ASD, unfortunately heterogeneity in age, enrollment criteria, and methods used for GM analysis limit our knowledge in this area. In this study, we comparatively evaluated the GM composition and fecal levels of short chain fatty acids (SCFAs) in young ASD children, with a very restricted range of age, next ending from 2 to 4 years, and in age matched healthy controls.

MATERIALS AND METHODS

Study Subjects

ASD patients (both sexes, age 2–4 years), consecutively observed at a tertiary Center for Pediatric Neuropsychiatry, were evaluated for the study.

Exclusion criteria were: ASD secondary to genetic syndromes; concomitant other neurological diseases: obesity; genetic and metabolic syndromes; immunodeficiencies; chronic diseases of the GI or respiratory tract; congenital cardiac defects; hepatic diseases; allergic diseases; food intolerances; use of antibiotics, pre-/pro- or synbiotics in the previous 4 weeks.

Patients recruitment occurred in 8 months. Twenty-five children, with suspected diagnosis of ASD, were evaluated. All children therefore carried out a full anamnestic and clinical evaluation including genetic and metabolic evaluation, eye counseling, Auditory Brainstem Response (ABR), Magnetic Resonance Imaging (MRI), electroencephalography (EEG). Children were evaluated by the pediatric neuropsychiatrist and underwent to the clinical protocol for evaluation of ASD; 20 out of 25 received a final diagnosis of ASD (first diagnosis) whereas five children did not have diagnostic confirmation or had other concurrent medical conditions (brain abnormalities, epilepsy, other genetic or metabolic diseases) and were excluded from the study. Nine out of 20 children were excluded from the study because of a recent antibiotic treatment or because of food selectivity, with dietary habits significantly different from that of the healthy controls. A total of 11 ASD patients (ASD) were recruited in this study. During the same study period 14 age matched healthy controls (HCs) visiting our Center because minor surgical procedures were enrolled (**Table 1**).

In all patients the diagnosis of ASD was made according to the Diagnostic and Statistical Manual of Mental Disorders, Fifth edition (DSM-5; American Psychiatric Association, 2013). In order to validate the ASD diagnosis according to Italian Guideline, all patients underwent to the Autism Diagnostic Observation Schedule – 2 (ADOS 2; Lord et al., 2012) and Autism Diagnostic Interview, Revised Version (ADI-R; Rutter et al., 2005) was administered to parents; moreover, the Griffiths Mental Development Scales (Gagliano et al., 2014), Vineland Adaptive Behavior Scales (VABS; Sparrow et al., 2003) and Childhood Autism Rating Scale (CARS; Schopler et al., 1988) were administered to better characterize the patients.

According to DSM-5 ASD criteria includes three levels of severity: Level 1 ("Requiring support"), Level 2 ("Requiring substantial support"), and Level 3 ("Requiring very substantial support"). The classification is split across two areas, Social Communication (SC) and Restricted and Repetitive Behaviors (RRB), mirroring core ASD symptoms. The notion of "level

TABLE 1 | Descriptive data of study participants.

	ASD	HCs
Subjects (*n*)	11	14
Age (months)	35 ± 5.7	35 ± 8.4
Gender (*n*)		
Male	81.8% (9)	57.1% (8)
Female	18.2% (2)	42.9% (6)
GI disorders (*n*)	2	0
DSM-5 (*n*)		
Level-1	1	–
Level-2	5	–
Level-3	5	–
ADOS (Total score)	16 ± 5.7	–

ASD, autistic patients; HCs, neurotypical healthy controls; DSM-5 levels, Level 1 ("Requiring support"), Level 2 ("Requiring substantial support"), and Level 3 ("Requiring very substantial support"); ADOS, Autism Diagnostic Observation Schedules – total score. Age and ADOS scores are reported as mean ± SD.

of support" is considered as severity of impairment, the environmental modifications required for managing day-to-day life (Kats et al., 2013). ADOS total-scores overcame the cut-off for the presence of Autism in all the evaluated subjects. Based on neuropsychiatric assessment, according to DSM-5 severity-levels, 5 patients obtained scores indicating a requiring very substantial support, 5 had a requiring substantial support, and 1 showed requiring support (**Table 1**).

In all study subjects we evaluated dietary habits, with the use of a 3 days diary and results evaluated with a specific software (WinFood, Medimatica Srl Colonnella (TE), Italy), and the possible presence of functional gastrointestinal disorders using a validated questionnaire (Rome III Criteria questionnaire, Italian Version) (Walker et al., 2006). All the enrolled children were from an urban area and presented similar dietary habits.

For all study subjects a stool samples (3 g) was collected in sterile vials and immediately frozen at −80°C.

The study was approved by the Ethics Committee of the University of Naples "Federico II" and all enrolled tutors give written informed consent in accordance with the sampling protocol approved by the local ethical committee (No. 312/17). Written informed consent was obtained from the parents of the participants in this study.

V3–V4 16S rRNA Gene Sequencing and Data Analysis

Bacterial genomic DNA was extracted from frozen fecal samples using the QIAamp DNA Stool Mini Kit (Qiagen) according to manufacturer's instructions. Extracted DNAs were checked for quality and quantity by spectrophotometric measurements with NanoDrop (ThermoFisher Scientific Inc) and stored at -20°C until processed for amplification. Sequencing samples were prepared according to the protocol 16S Metagenomic Sequencing Library Preparation for Illumina Miseq System with some modifications as previously described (Coretti et al., 2017). The V3–V4 regions of the 16S rDNA gene were firstly amplified starting from 200 ng genomic DNA with Fast Start High Fidelity PCR System (Roche Applied Science) and subsequently indexed with Nextera XT Index Kit (Illumina) in 10 cycles of PCR using KAPA HiFi HotStart System according to Illumina guidelines. After each PCR step, amplicons were purified with Agencourt AMPure XP beads (Beckman Coulter Inc.). Then, library sizes and concentrations of barcoded amplicons were assessed using Bioanalyzer DNA 1000 chip (Agilent technologies) and Qubit dsDNA BR assay kit (Invitrogen), respectively. Normalized libraries were pooled, denatured with NaOH, diluted to 10pM and combined with 25% (v/v) denatured 10pM PhiX, according to Illumina guidelines. Sequencing run was performed on an Illumina Miseq system using v3 reagents for 2 × 281 cycles.

V3-V4 16S rDNA FASTQ paired-end reads were quality filtered and assembled using PEAR (Zhang et al., 2014), retaining only those sequences showing average PHRED score≥30, read length between 400 and 500 bp and overlapping regions between mate-pair end of at least 40 nucleotides. Passing filter sequences were processed with PRINSEQ in order to obtain FASTA and quality files for further analyses (Schmieder and Edwards, 2011). Metagenomic analyses on the resulting data were conducted using Quantitative Insights Into Microbial Ecology (QIIME, version 1.9.1) (Caporaso et al., 2010). 16S rRNA gene sequencing reads were collapsed to operational taxonomic units (OTUs) using closed reference-based OTU picking method against Greengenes 16S gene database (GG, may 2013 version) (DeSantis et al., 2006) at 97% of sequences similarity; picked OTUs were classified at different taxonomic levels with the GG database. Species and Clostridium cluster classification was performed using SPINGO version 1.3 with default parameters on a representative sequence of each OTU (Allard et al., 2015). To avoid sample size biases in subsequent analyses, a sequence rarefaction procedure was applied using a maximum depth of 45,038 sequences/sample.

To assess sampling depth coverage and species heterogeneity in each sample, alpha diversity metrics were employed on rarefied OTU table using Good's coverage, Observed species and Shannon's diversity index. A two-sample permutation *t*-test, using 999 Monte Carlo permutations to compute *p*-value, was performed to compare the alpha diversities between sample groups. Diversity among sample communities (beta diversity) was assessed by calculating weighted and unweighted Unifrac distance matrices and then represented by two dimensional principal coordinates analysis (PCoA) plot. Statistical significance of beta diversities was assessed on weighted and unweighted UniFrac distances matrixes using ANOSIM and ADONIS methods with 999 permutations and a two-sided Student's two-sample *t*-test. The Microbiome Regression-based Kernel Association Test (MiRKAT) (Zhao et al., 2015), a kernel-based regression method, was used to evaluate the effect of confounders by using a kernel metric constructed from weighted and unweighted UniFrac distances and adjusting for the small-sample size of the covariates. The significant associations were assessed using 9,999 permutations to verify the asymptotic *p*-value approximations.

Statistical differences in OTUs frequencies between sample groups at different taxonomic levels were assessed using nonparametric Kruskal–Wallis test taking into account False Discovery Rate (FDR) corrected *p*-values. Next, two analyses were applied on OTU tables generated by QIIME to identify key OTUs that discriminate ASD and HCs groups: Metastats comparison using the online interfaces (White et al., 2009) and LDA Effect Size analysis (LEfSe) (Segata et al., 2011). Only those OTUs reported by both methods to be significantly different between the two groups ($p < 0.05$ for Metastats, LDA > 2 and $p < 0.05$ for LEfSe) have been considered as key discriminatory OTUs.

The Phylogenetic Investigation of Communities by Reconstruction of Unobserved States (PICRUSt) was employed to predict the functional profile of the microbial communities in ASD and HC samples (Langille et al., 2013). In particular, the rarefied OTU table produced within QIIME was first corrected for multiple 16S rRNA gene copy number by using the normalize_by_copy_number.py script, then the obtained normalized OTU table was used as input in the predict_metagenomes.py script obtaining the Kyoto encyclopedia of genes and genomes (KEGG) ortholog (KOs)

predictions for each sample (Kanehisa et al., 2016). KOs abundances of selected functions were compared between groups by using nonparametric Kruskal–Wallis test taking into account FDR corrected *p*-values.

Microbial interactions were investigated by generating the Spearman co-occurrence network on the basis of the relative abundances of key OTUs. The network was generated using the CoNet plugin (Faust and Raes, 2016) for Cytoscape (3.7.0, Shannon et al., 2003) by applying the following parameters: nonparametric Spearman correlation coefficients with a minimal cut-off threshold of 0.5 ($P < 0.05$, FDR corrected), null distribution generated by 1000 permutations with renormalization, and 1000 iterations for bootstraps. Network was built taking in consideration the ADOS scores, and the fecal butyrate concentrations. Autism and butyrate's adjacent edges and connected nodes are reported as sub-networks.

Droplet Digital PCR (ddPCR)

Absolute quantification of bacteria was examined by ddPCR using a DNA binding dye (EvaGreen) according to the manufacturer's instructions. Species-specific primers for *F. prausnitzii* (Pfra-f: GATGGCCTCGCGTCCGATTAG and Pfra-r: CCGAAGACCTTCTTCCTCC) were designed by Chen et al. (2011). Total bacteria load in each sample was assessed using universal primers targeting the V7 region of the 16S rRNA gene (1048f: GTGSTGCAYGGYYGTCGTCA, 1194r: ACGTCRTCCMCNCCTTCCTC) (Raveh-Sadka et al., 2015). The ddPCR reaction mixture consisting of 10 μl QX200 EvaGreen ddPCR Supermix, 100 nM primers, and 0.5 ng of DNA extracted from fecal samples was mixed with 70 μl of droplet generator oil to create droplets following the manufacture's instructions. The following thermocycling parameters were used to PCR amplify the droplets generated from each sample: one denaturation cycle at 95°C for 10 min, 40 cycles composed of 95°C for 30 s, 61°C for 30 s, and 72°C for 30 s, followed by a stabilization cycle at 98°C for 10 min. All ramp rates were at 2.5°C/s. The copies/μl output from QuantaSoft software was used to calculate the number of bacterial cells, assuming four copies for bacteria (Hospodsky et al., 2012), normalized by grams of fecal mass used for each gDNA extraction reaction (Raveh-Sadka et al., 2015).

Determination of Fecal Butyrate and Propionate Concentration

Frozen feces weighing 1 g were diluted with saline, vortexed and centrifuged at 13,000 r.p.m. for 10 min in 2 ml tubes. The supernatants were filtered (0.45 μm) and used as the fecal extracts, which were stored at -20°C until analysis. To determine fecal butyrate and propionate concentration, frozen fecal extracts were acidified with 20 μl 85% phosphoric acid and 0.5 ml ethyl acetate, mixed, centrifuged at 14,000 r.p.m. for 1 h and extracted in duplicate. A quantity of the pooled extract containing the acidified butyrate was transferred into a 2 ml glass vial and loaded onto an Agilent Technologies (Santa Clara, CA, United States) 7890 gas chromatograph (GC) system with automatic loader/injector. The GC column was an Agilent J&W DB-FFAP (Agilent Technologies) with the length 30 m, internal diameter 0.25 mm and film thickness 0.25 μm. The GC was programmed to achieve the following run parameters: initial temperature 90°C, hold 0.5 min, ramp 20°C min^{-1}, final temperature 190°C, total run time 8.0 min, gas flow 7.7 ml min^{-1} split less to maintain 3.26 p.s.i. column head pressure, septum purge 2.0 ml min^{-1}. Detection was achieved using a flame ionization detector. Peaks were identified using a mixed external standard and quantified by peak height/internal standard ratio.

Statistical Analysis

ddPCR assay and fecal butyrate and propionate measurement results in ASD and HCs samples were compared using two tailed Student's *t*-test assuming equal variance. In this study results were considered statistically significant at *p*-value < 0.05. Significant differences were indicated in figures by $^{*}p < 0.05$, $^{**}p < 0.01$, $^{***}p < 0.001$. ANOSIM, ADONIS and permutation *t*-test were performed using QIIME scripts, all other analyses were performed using R 3.2.0 (R Core Team, 2015). Bar plots were created by using GraphPad Prism 6.0.

Data Deposition

The sequences reported in this study are deposited on the 'European Nucleotide Archive' under the accession number PRJEB29421[1].

RESULTS AND DISCUSSION

16S Sequencing for GM Structure Evaluation of ASD Young Children

We attempted to identify the key features of GM in very young children (2–4 years of age) at first diagnosis of ASD. High-throughput sequencing analysis of bacterial 16S rRNA V3–V4 regions was conducted on fecal samples of ASD and HCs. In total, over 3.078 million of high-quality sequences (123,138.64 ± 47,651.53 reads/sample) were obtained from all 25 fecal samples, representing 4,870 operational taxonomic units (OTUs). We used a depth of 45,038 sequences/sample clustered in 4,129 OTUs. Good's coverage > of 99% for all sequences in the two groups suggested that the majority of the phylotypes present in the samples had been identified, indicating good sequencing depth for investigation of ASD associated fecal microbiota (**Table 2**). Bacterial diversity within communities was significantly higher in the ASD group than in the controls, as indicated by the Shannon index, while no significant differences in number of observed species were detected between the two groups (**Table 2**). To date, conflicting data are available on the microbial richness of GM in patients with ASD, probably for the diverse enrollment criteria adopted worldwide and age dissimilarity of the studies participants. Therefore, the different bacterial diversity here observed in the

[1]https://www.ebi.ac.uk/ena/data/view/PRJEB29421

TABLE 2 | Observed diversity and estimated phylotype coverage for 16S rRNA gene sequences at 97% similarity from NGS analysis.

	Alpha diversity				Beta diversity			
Group	**No. of reads**	**Observed species**	**Shannon**	**Good's coverage**		**Student's *t*-test**	**ANOSIM**	**ADONIS**
ASD patients	495,418	920.5 ± 120.0	5.79 ± 0.53*	0.993 ± 0.001	Unweighted UniFrac distances	t = -3.001 (p = 0.003)	R = 0.199 (p = 0.006)	R^2 = 0.074 (p < 0.001)
HCs	630,532	789.2 ± 255.5	4.73 ± 1.07	0.994 ± 0.002	Weighted UniFrac distances	t = -6.076 (p = 3.76E-09)	R = 0.368 (p = 0.001)	R^2 = 0.246 (p < 0.001)

*Alpha diversity indexes are reported as mean ± SD; *values are significantly different at $p < 0.05$.*

two groups might be a distinctive factor in studies involving toddlers/preschoolers.

To evaluate differences in phylogenetic diversity among samples and between groups, beta diversity analysis was conducted by means of unweighted and weighted UniFrac distance metrics. Both measures, represented in two-dimentional principal coordinate analysis (PCoA) plots, showed a clustering of ASD away from the control samples (**Figures 1A,B**). In particular, the three different statistical methods used to compare beta diversity results showed that a more marked difference was estimated by considering weighted analysis of UniFrac distances. Results indicated that the differences in ASD and HCs microbial communities were prevalently due to changes in OTUs relative abundances (**Table 2** and **Figures 1A,B**). Since two out of 11 patients were female and 2 patients (one male and one female) had symptoms of constipation, we evaluated the impact of these potential confounders on the differences in GM composition between the two groups. Applying MiRKAT to the weighted and unweighted UniFrac distances and adjusting for the small-sample size of the covariates, the described differences in GM composition between ASD and HCs were further confirmed ($p < 0.01$ for both weighted and unweighted UniFrac distances after gender and constipation covariate adjustments; **Supplementary Figure S1**).

Phylogenetic Shift in GM of ASD Patients

At phylum level, ASD group was characterized by a marked reduction of Actinobacteria (12.18% vs. 47.30% in ASD and HCs, respectively; p = 0.004), and a significant increase in Bacteroidetes (19.34% vs. 1.53% in ASD and HCs, respectively; p = 0.04) and Proteobacteria (9.27% vs. 0.55% in ASD and HCs, respectively; p = 0.004; **Figure 2A**). Firmicutes represented the most abundant phylum both in HCs and ASD patients, without showing significant differences between the two groups. Bacteroidetes/Firmicutes ratio was significantly higher in ASD patients due to an increase in Bacteroidetes. At family level Actinomycetaceae, Coriobacteriaceae, Bifidobacteriaceae, Gemellaceae and Streptococcaceae were significantly reduced in ASD group (**Figure 2B**).

Then we identified specific phylotypes marking the differences in GM composition between the ASD and HCs groups. For 16S rRNA gene analyses a very conservative approach was applied

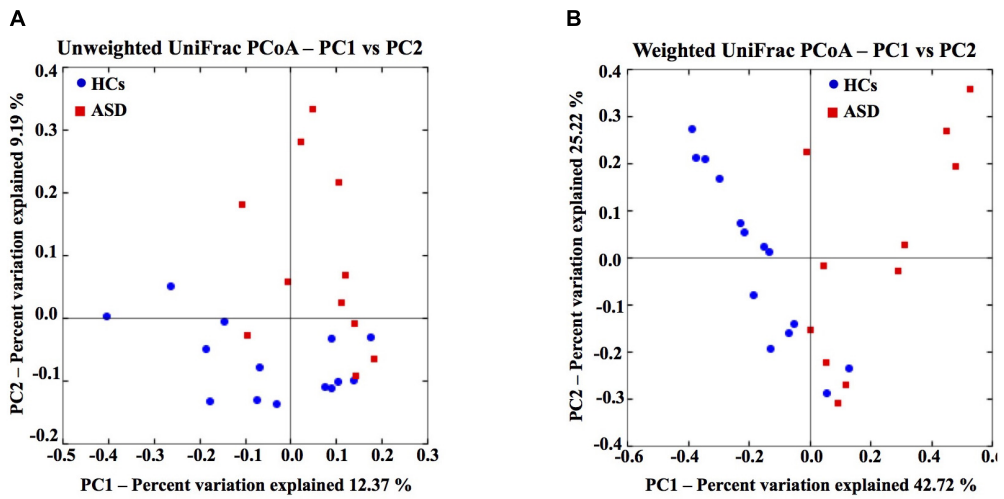

FIGURE 1 | Gut microbiota structure of HCs and ASD patients. Unweighted **(A)** and weighted **(B)** UniFrac-based PCoA plot based on all OTUs of gut microbial communities (45,038 sequences/sample).

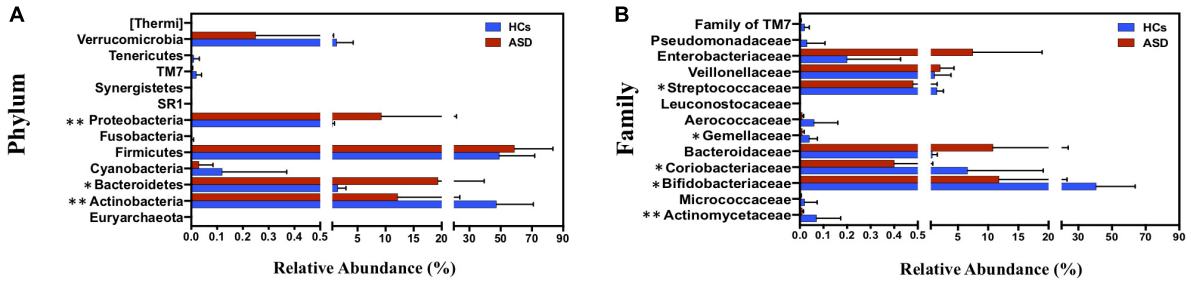

FIGURE 2 | Taxonomic differences of gut microbiota between HCs and ASD groups. **(A)** Percentage distribution of all bacterial phyla identified and **(B)** percentage distribution of significant bacterial families ($p < 0.05$) between HCs and ASD. *$p < 0.05$, **$p < 0.01$ after FDR correction. Mean values ± SD are plotted.

using LefSe algorithm and Metastats comparison to detect key OTUs responsible for the differences between ASD and HCs groups (White et al., 2009; Segata et al., 2011). Among total 4,129 OTUs, we found 91 key OTUs (relative abundance >0.01%) defining the GM of ASD patients; specifically, 65/91 OTUs were found more abundant and 26/91 OTUs less abundant in ASD patients with respect to controls (**Table 3**). To obtain bacterial species assignment of key OTUs, sequencing data were reprocessed using SPINGO high-resolution approach (Allard et al., 2015). This analysis resolved at species level the taxonomic classification of the 91 key OTUs identifying 40 distinct bacterial species (**Figure 3**).

Low Abundance of Specific Actinobacteria Phylum Components

Among Actinobacteria, ASD patients showed a significant decrease of OTUs assigned to unclassified genus of Coriobacteriaceae, *Actinomyces, Corynebacterium* and of OTUs corresponding to *Bifidobacterium longum* and *Eggerthella lenta* (**Table 3** and **Figure 3**). Notably, members of Actinobacteria, in particular *Bifidobacterium* spp., form a dominant fraction of the human GM, particularly in infants (Rajilić-Stojanović and de Vos, 2014). In accordance with our results, several studies reported decrease of Bifidobacteria in ASD patients (Adams et al., 2011; Wang et al., 2011; De Angelis et al., 2013;

TABLE 3 | Greengenes taxonomic classification and relative abundance of key OTUs defining the GM differences between ASD and HCs.

Phylum	Family	Genus	Number of OTUs	ASD	HCs
Actinobacteria	Actinomycetaceae	*Actinomyces*	1	0.002 ± 0.001	0.039 ± 0.02
	Corynebacteriaceae	*Corynebacterium*	1	0.001 ± 0.001	0.021 ± 0.007
	Bifidobacteriaceae	*Bifidobacterium (longum)*	1	6.904 ± 2.021	15.302 ± 2.943
	Coriobacteriaceae	–	1	0	0.026 ± 0.016
	Coriobacteriaceae	*Eggerthella (lenta)*	1	0.081 ± 0.031	0.408 ± 0.113
Bacteroidetes	Porphyromonadaceae	*Parabacteroides (distasonis)*	1	0.043 ± 0.028	0
	Bacteroidaceae	*Bacteroides*	22	1.606 ± 1.121	0.003 ± 0.002
Firmicutes	Aerococcaceae	–	1	0.006 ± 0.002	0.059 ± 0.027
	Streptococcaceae	*Streptococcus*	5	0.065 ± 0.03	0.704 ± 0.176
	U. Clostridiales	–	3	0.09 ± 0.05	0.1 ± 0.07
		–	2	0.16 ± 0.15	0
		Ruminococcus	3	0.42 ± 0.19	0.04 ± 0.02
	Lachnospiraceae	*Blautia*	10	1.06 ± 0.38	2.99 ± 0.55
		Coprococcus	4	0.06 ± 0.02	0.3 ± 0.08
		Lachnospira	1	0.04 ± 0.03	0
		Roseburia	1	0.06 ± 0.05	0
	Peptostreptococcaceae	–	1	0.02 ± 0.02	0
		–	18	0.97 ± 0.36	0.1 ± 0.02
	Ruminococcaceae	*Faecalibacterium (prausnitzii)*	6	0.51 ± 0.31	0.04 ± 0.01
		Oscillospira	3	1.21 ± 0.5	0.15 ± 0.05
Proteobacteria	Enterobacteriaceae	–	4	0.407 ± 0.368	0.002 ± 0.002
	Pasteurellaceae	–	1	0.057 ± 0.049	0

Discriminant OTUs were identified using LEfSe algorithm and Metastats comparison ($p < 0.05$ for Metastats comparison and LDA > 2 with alpha < 0.05 for LEfSe). Mean ± SEM of key OTUs with relative abundance > 0.01% is reported. A more detailed table with average and SEM for each discriminatory OTU is provided as ***Supplementary Table S1****.*

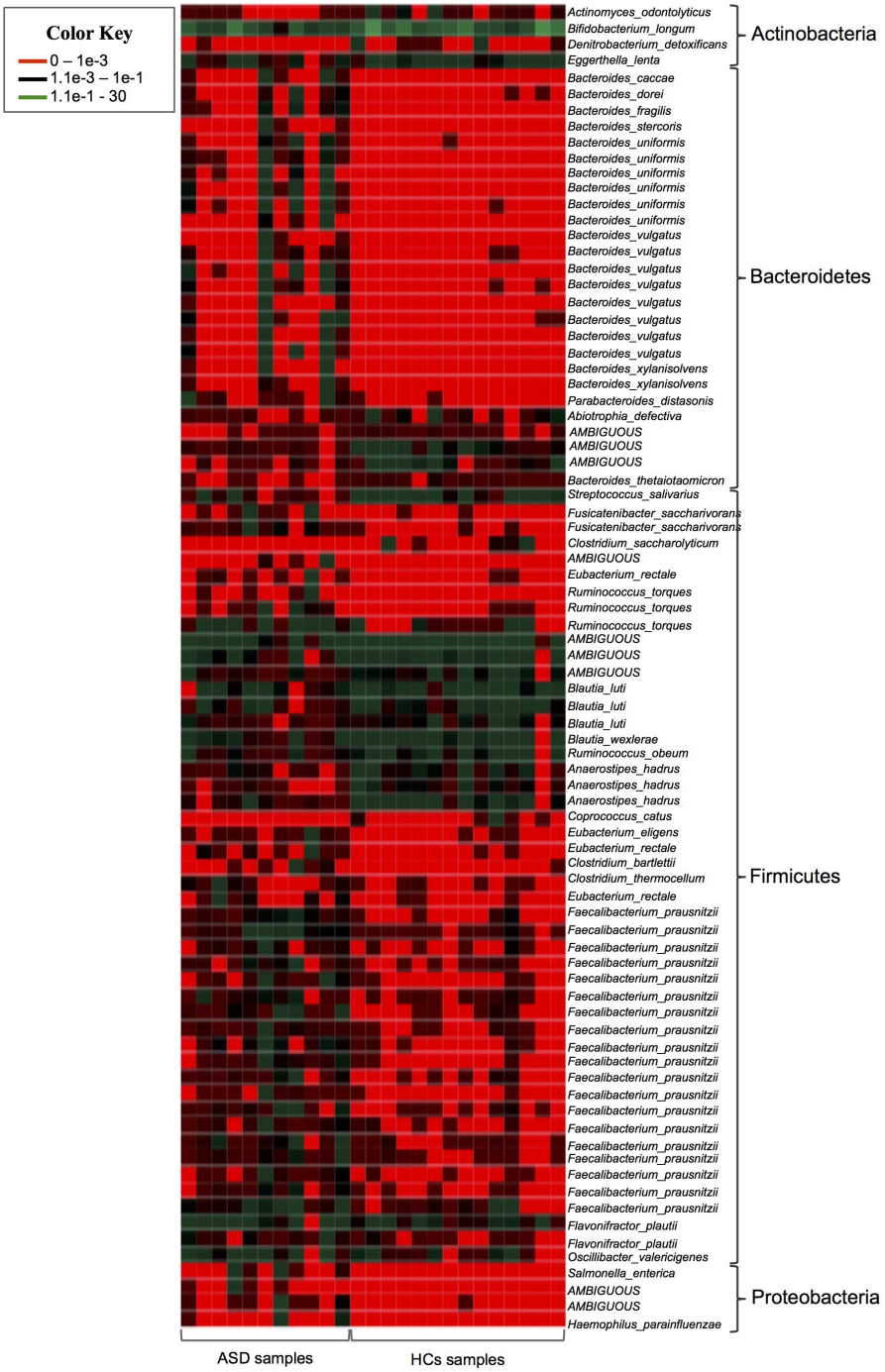

FIGURE 3 | Heatmap showing the SPINGO species classification of the key OTUs with a relative abundance >0.01% (y-axis) for individual fecal samples (x-axis).

Kang et al., 2013, 2017). *Bifidobacterium* is known as a promoter of healthy status and, recently, it has been proposed as a "psycobiotic" for its ability to produce neuromodulators and influence gut–brain relationship through interaction with other commensal bacteria (Sarkar et al., 2016). The administration of *B. longum* in animal models improves anxiety, depression, and memory related behaviors (Bercik et al., 2011). In a clinical study a mixture of probiotics including *B. longum* alleviated psychological distress and urinary cortisol levels (Messaoudi et al., 2011). The severe reduction of *B. longum* in ASD young children here reported, indicates a re-assortment of key microbes of infants GM in these patients, possibly contributing to some ASD symptoms by affecting gut ecosystem and functionality.

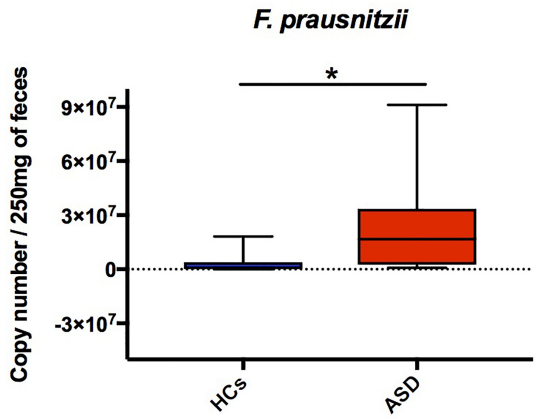

FIGURE 4 | DdPCR assay showing differences of *F. prausnitzii* copy number in ASD and HCs groups. The central line within each box represents the median of the data (*$p < 0.05$, Student's *t*-test).

Increase in Members of Gram-Negative Bacterial Phyla

Our data also showed an increase of several gram-negative bacteria with potential pathogenic features in GM of young children with ASD. Lipopolysaccharide (LPS), the major component of gram-negative cell wall, has been found increased in the serum of ASD patients and was associated with impaired social behavioral scores (Emanuele et al., 2010). LPS stimulates the secretion of proinflammatory cytokines from peripheral blood mononuclear cells and lymphoblasts of ASD children (Jyonouchi et al., 2001), probably contributing to both peripheral and brain inflammation associated with the disease (Patterson, 2011; Depino, 2013; Onore et al., 2013). In our study, among gram-negative bacteria, 22 Bacteroidetes OTUs owing to genus *Bacteroides*, mainly assigned to *B. uniformis* and *B. vulgatus* and *P. distasonis* species, were more abundant in ASD patients as well as Enterobacteriaceae and Pasteurellaceae OTUs belonging to Proteobacteria phylum (**Table 3** and **Figure 3**).

Reassortment of Firmicutes Phylum Components

The majority of key phylotypes were taxonomically classified in Firmicutes phylum (58/91 OTUs; **Table 3** and **Supplementary Table S1** and **Figure 3**), depicting that, changes within Firmicutes taxa typically characterized the GM of ASD patients. *Streptococcus* OTUs were markedly reduced in ASD patients and *Clostridium* clusters were differently represented in ASD and control groups (**Table 3**). Notably, *Clostridium* cluster IV discriminatory OTUs assigned to unclassified genus of Ruminococcaceae, *Faecalibacterium prausnitzii* and *Oscillospira* were all significantly increased in ASD patients. SPINGO analysis showed that 13/18 OTUs of unclassified genus of Ruminococcaceae were taxonomically classified as *F. prausnitzii,* revealing that increase in relative abundance of *F. prausnitzii* marked the GM of ASD children (**Figure 3**). GM studies involving ASD patients have shown inconsistent results regarding the abundance of *F. prausnitzii* (Wang et al., 2011; De Angelis et al., 2013; Kang et al., 2013, 2017). These conflicting data might depend on several factors ranging from the sampling cohort to the techniques and software used to identify the GM composition. To complement and support our findings, the copy number of *F. prausnitzii* was accurately quantified using Droplet digital PCR (ddPCR) as adjunctive approach to microbiota sequencing. The analysis revealed that *F. prausnitzii* was numerically more abundant in ASD patients compared to HCs (**Figure 4**). The ddPCR assay also showed no significant differences in number of total bacteria in fecal samples between ASD patients and controls (data not shown). Differently from Bifidobacteria, *F. prausnitzii* is a late GM colonizer in healthy subjects and it is present at very low levels until childhood (Miquel et al., 2014). The high levels of *F. prausnitzii* in ASD patients indicate its gut premature colonization possibly at the expense of other beneficial bacteria such as *B. longum*.

Evaluation of Fecal SCFAs Levels and Analysis of KEGG Functions Related to Butyrate Production and Mucin Degradation in ASD Patients

The higher amount of Bacteroidetes together with the altered assortment in Firmicutes taxa in ASD patients can impact on fecal SCFAs levels. SCFAs are the main end-products of bacterial fermentation in the gut and are among the most important components of microbe-host signaling, able to modulate gene

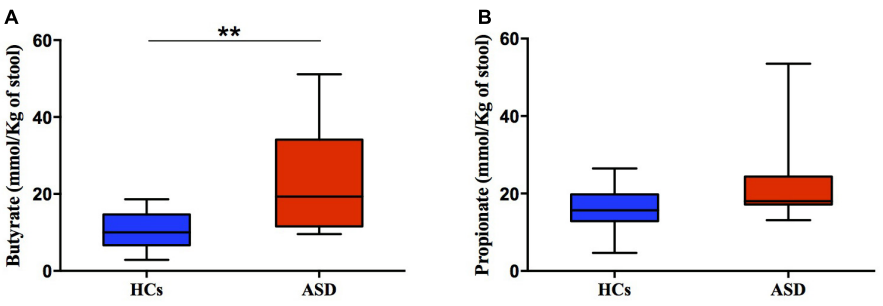

FIGURE 5 | Fecal concentration (mmol/Kg) of butyric **(A)** and propionic acid **(B)** in ASD and HCs samples. **$p < 0.01$ for comparisons of ASD vs. HCs using Mann-Whitney test.

TABLE 4 | PICRUSt KEGG Ortholog count prediction of genes codifying for key enzymes involved in butyrate production in ASD and HCs samples.

KEGG ortholog: description	ASD	HCs
K00626: acetyl-CoA C-acetyltransferase	11104 ± 1470.89	7656.86 ± 1303.27
K00074: 3-hydroxybutyryl-CoA dehydrogenase]	11688.64 ± 1977.89	12879.64 ± 1142.51
K01692: enoyl-CoA hydratase	2083.91 ± 486.13	1547.21 ± 232.23
K01715: 3-hydroxybutyryl-CoA dehydratase	7977.64 ± 2070.13	6119.93 ± 1372
K00248: butyryl-CoA dehydrogenase	11984.45 ± 2138.89	8469.43 ± 1746.3
K00634: phosphate butyryltransferase	2770.27 ± 621.97*	505.71 ± 99.14
K00929: butyrate kinase	6114.18 ± 867.86	3918.14 ± 883.67
K01034: acetate CoA-transferase alpha subunit	649.36 ± 167.35*	148.07 ± 44.15
K00016: L-lactate dehydrogenase	17782.91 ± 3128.77	24697.43 ± 2038.36

Data are mean ± SEM. Significant differences ($p < 0.05$) were assessed using nonparametric Kruskal–Wallis test taking into account False Discovery Rate (FDR) corrected p-values.*

expression in host cells, brain function and behavior, host energy metabolism and immune functions (Kim et al., 2016; Russo et al., 2016).

Here, analysis of fecal SCFAs levels, namely butyrate and propionate, revealed a trend toward an increase in ASD patients (**Figures 5A,B**). Butyrate and propionate fecal levels resulted within the normal range in all study subjects. But butyrate levels, even though remaining in normal limits, were significantly higher in ASD (median = 19.30 mmol/kg) compared to HCs group (median = 10.00 mmol/kg, $p = 0.005$; **Figure 5A**). Results suggest differences in the colonic fermentation in the two groups. In particular, data show that marked increase of *F. prausnitzii*, one of the most human butyrogenic bacteria, could account for augment of fiber fermentation capability and higher butyrate levels from gut microbes in ASD children.

PICRUSt analysis was used to predict and analyze the KEGG functions involved in butyrate production (**Table 4**; Langille et al., 2013; Borrelli et al., 2017). Notably, the majority of the analyzed functions were enriched in ASD patients compared to controls. In particular, phosphate butyryltransferase (K00634) and acetate CoA-transferase alpha subunit (K01034), enzymatic functions involved in the final conversion of butyryl-CoA in butyrate, were both significantly higher in ASD microbial communities (**Table 4**). Butyrate can also be produced from mucin degradation, thus we searched for the counts of beta-hexosaminidases, a mucin-degrading enzyme. We found beta-hexosaminidase (K12373) significantly more abundant in ASD group (13,815.45 ± 3,547.44 and 3,582.57 ± 564.94 in ASD and HCs, respectively, $p < 0.05$ after FDR correction); we also observed that high abundance of the mucin-degrading enzyme in ASD patients was concurrent with the increased level of *Ruminococcus torques* which is known to be a mucin-degrading bacterium (**Figure 3**). Cross-feeding mechanisms in gut ecosystem have been defined to connect metabolic activity of lactic acid-producing and mucin degrading bacteria (e.g., *Bifidobacterium* and *Ruminococcus*, respectively) with butyrate producing pathways (Duncan et al., 2004; Schwab et al., 2014). Our data pinpoint the possibility that the reduction of Bifidobacteria could be counterweighed by increase of mucin degrading bacteria to sustain augment of butyrogenic *F. prausnitzii* in ASD young children. Our observations were also sustained by results obtained from co-occurrence and exclusion network analysis based on Spearman's correlation coefficients, among microbial community structure of ASD patients and HCs, autism indices (ADOS score) and fecal butyrate levels (**Figure 6**). Co-occurrence network analysis revealed three ASD-enriched OTUs belonging to *F. prausnitzii, B. uniformis,* and *B. vulgatus*

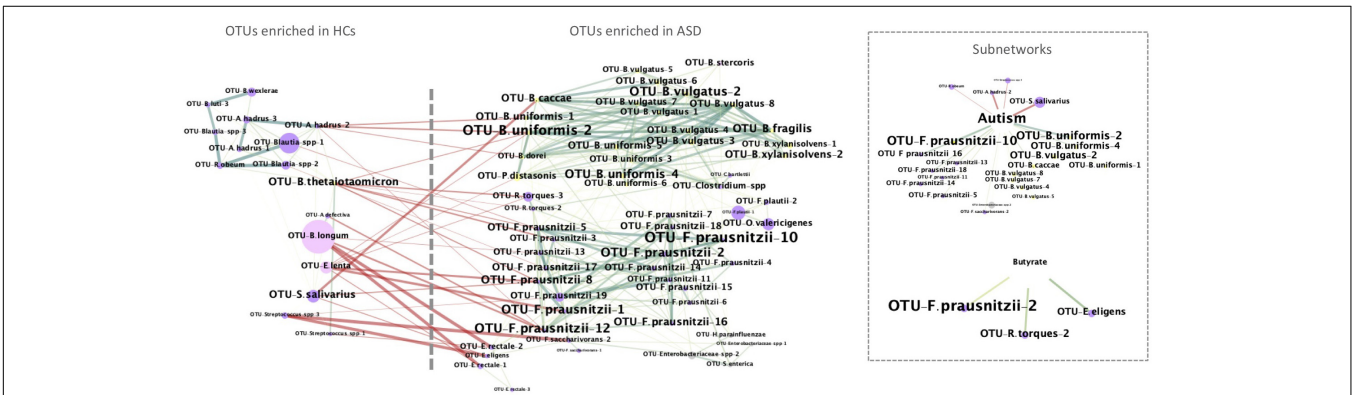

FIGURE 6 | Co-occurrence network analysis of identified key OTUs and their correlation with level of ASD and butyrate. In the networks: OTUs and samples' properties (ADOS score and fecal butyrate concentration) are depicted as nodes; an edge represents a spearman correlation with a correlation coefficient > 0.5 (green) or < -0.5 (red) that is statistically significant (FDR < 0.05); the size of each node represents the relative abundance, while the size of each label node is proportional to its degree (the number of edges and nodes connected to each node); the colors of nodes represent their classification at phylum level (pink, Actinobacteria; yellow, Bacteroidetes; violet, Firmicutes; gray, Proteobacteria). In the **Supplementary Tables S2**, **S3** are reported the significant nodes and edges, respectively.

species as highly interconnected and potentially able to drive, in the gut of ASD patients, the presence of other 35 OTUs and generate high bacterial co-occurrence network complexity. The three mentioned ASD-enriched OTUs were also the phylotypes most negatively correlated with HCs-enriched OTUs annotated to *B. longum*, *E. lenta,* and *Streptococcus* OTUs, suggesting their antagonistic or mutual exclusion relationship (**Figure 6**). The analysis also showed few OTUs directly associated with the level of ASD and concentrations of fecal butyrate. Notably, most ASD-enriched phylotypes, such as *F. prausnitzii* and *B. uniformis*, were positively correlated to the ADOS score ($R = 0.767$ and $R = 0.84$ with $p < 0.001$ for correlation with *F. prausnitzii* and *B. uniformis*, respectively), to which HCs-enriched phylotypes were negatively correlated (**Figure 6**, sub-networks). Finally, 3 OTUs taxonomically classified as *F. prausnitzii*, *R. torques,* and *E. eligens,* were found positively associated to butyrate levels (**Figure 6**, sub-networks).

Overall we observed a reassortment of gut ecosystem in young ASD patients as off early childhood characterized by shift in colonization of gut beneficial bacterial species. The majority of patients enrolled did not suffer from GI symptoms or comorbidities, thus the observed changes in microbial colonization depended primarily on autistic disorder itself. We reported a strong depletion of *B. longum,* with *Bifidobacterium* species defined as psicobiotics (Sarkar et al., 2016), preservers of gut barrier function and immune homeostasis (Sarkar et al., 2016). Concurrently, in accordance with a previous study (Wang et al., 2013), we also detected increased levels of the mucin-degrading *R. torques* in feces of ASD children. Mucus degradation might affect intestinal epithelium permeability contributing to the development of leaky gut phenotype also described for ASD children (Li et al., 2017). Moreover, we detected significant higher levels of butyrogenic *F. prausnitzii* and butyrate in feces of ASD patients with respect to controls. Other authors also reported overrepresentation of butyrate producing bacteria in patients with major depressive disorders (Zheng et al., 2016). Butyrate has beneficial effects on human gut homeostasis (Berni Canani et al., 2011; Macia et al., 2015), host immune functions (Kim et al., 2016) and is considered a resourceful compound with promising effects in several neurologic and neuropsichiatric disorders (Bourassa et al., 2016; Stilling et al., 2016; Dinan and Cryan, 2017). Preliminary data from animal models suggested a dose-dependency of butyrate effects on the brain development and function. With positive effects on brain functions and behavior of low doses of butyrate (<500 mg/kg) and stress-like response elicited by high doses of butyrate (>1,000 mg/kg) (Gagliano et al., 2014; Takuma et al., 2014; Kratsman et al., 2016). The butyrate fecal concentration observed in ASD children in our study was within the normal range and significantly lower compared with the butyrate concentration potentially responsible for brain stress. This data strongly limits the hypothesis of a pathogenetic action elicited by butyrate in ASD. We are conscious that variations of fecal SCFAs levels in feces could depend on either poor absorption due to increased gut permeability or excessive colonic fermentation, or different exposure to environmental factors. Our data suggest that both, microbial composition (namely increase of *R. torques* and *F. prausnitzii)* and microbial predicted metabolic activity (namely increase in mucin degradation and butyrate formation enzymes) may be accountable for the observed higher level of butyrate in fecal content of ASD patients.

This study, despite limitations relative to the small number of children evaluated, encourage to further investigate the role of GM-brain axis in the critical neurodevelopmental window of early life.

CONCLUSION

Our findings sustain the global alteration of GM equilibrium in ASD young children, including abnormalities in temporal colonization by *B. longum* and F. *prausnitzii*. The parallel development between GM and brain circuits, especially those required for social and emotional cognition, strongly suggest a role for GM and their metabolites in ASD symptoms and progress. In this view, it is very important to identify age-related bacterial signatures in ASD in order to develop GM-based therapies.

AUTHOR CONTRIBUTIONS

LCo performed microbiota analysis, statistically analyzed all data and wrote the manuscript. LP produced and analyzed butyrate and propionate data and contributed to manuscript writing. MR and GCo organized the clinical work and performed the subject's enrolment. FA, MCo, and GCa performed ddPCR and revised the manuscript. CD produced butyrate and propionate data. MCu, AN, LB, and EB contributed to the metagenomic analysis and to the interpretation of the data. LCh conceived the investigation and contributed to the interpretation of the data. CB designed the epidemiological study, organized the clinical work, and performed the subject's enrolment. RB conceived the investigation, designed the epidemiological study, supervised the general aspects of the work and contributed to manuscript writing. FL conceived the investigation, interpreted the data, wrote the manuscript, and critically supervised the work. All authors reviewed the manuscript.

ACKNOWLEDGMENTS

We would like to thank Domenico Palumbo and Ornella Affinito for help in statistical analysis.

SUPPLEMENTARY MATERIAL

The Supplementary Material for this article can be found online at: https://www.frontiersin.org/articles/10.3389/fmicb.2018.03146/full#supplementary-material

REFERENCES

Adams, J. B., Johansen, L. J., Powell, L. D., Quig, D., and Rubin, R. A. (2011). Gastrointestinal flora and gastrointestinal status in children with autism–comparisons to typical children and correlation with autism severity. *BMC Gastroenterol.* 11:22. doi: 10.1186/1471-230X-11-22

Allard, G., Ryan, F. J., Jeffery, I. B., and Claesson, M. J. (2015). SPINGO: a rapid species-classifier for microbial amplicon sequences. *BMC Bioinformatics* 16:324. doi: 10.1186/s12859-015-0747-1

American Psychiatric Association. (2013). *Cautionary Statement for Forensic Use of DSM-5. In Diagnostic and Statistical Manual of Mental Disorders*, 5th Edn. Washington, DC: American Psychiatric Association Publishing, 280. doi: 10.1176/appi.books.9780890425596.744053

Bercik, P., Park, A. J., Sinclair, D., Khoshdel, A., Lu, J., Huang, X., et al. (2011). The anxiolytic effect of *Bifidobacterium longum* NCC3001 involves vagal pathways for gut-brain communication. *Neurogastroenterol. Motil.* 23, 1132–1139. doi: 10.1111/j.1365-2982.2011.01796.x

Berni Canani, R., Costanzo, M. D., Leone, L., Pedata, M., Meli, R., and Calignano, A. (2011). Potential beneficial effects of butyrate in intestinal and extraintestinal diseases. *World J. Gastroenterol.* 17, 1519–1528. doi: 10.3748/wjg.v17.i12

Borrelli, L., Coretti, L., Dipineto, L., Bovera, F., Menna, F., Chiariotti, L., et al. (2017). Insect-based diet, a promising nutritional source, modulates gut microbiota composition and SCFAs production in laying hens. *Sci. Rep.* 7:16269. doi: 10.1038/s41598-017-16560-6

Bourassa, M. W., Alim, I., Bultman, S. J., and Ratan, R. R. (2016). Butyrate, neuroepigenetics and the gut microbiome: can a high fiber diet improve brain health? *Neurosci. Lett.* 625, 56–63. doi: 10.1016/j.neulet.2016.02.009

Caporaso, J. G., Kuczynski, J., Stombaugh, J., Bittinger, K., Bushman, F. D., Costello, E. K., et al. (2010). QIIME allows analysis of high-throughput community sequencing data. *Nat. Methods* 7, 335–336. doi: 10.1038/nmeth.f.303

Chen, Y., Yang, F., Lu, H., Wang, B., Chen, Y., Lei, D., et al. (2011). Characterization of fecal microbial communities in patients with liver cirrhosis. *Hepatology* 54, 562–572. doi: 10.1002/hep.24423

Core Team, R. (2015). *R: A Language and Environment for Statistical Computing*. Vienna: R Found. Stat. Comput.

Coretti, L., Cristiano, C., Florio, E., Scala, G., Lama, A., Keller, S., et al. (2017). Sex-related alterations of gut microbiota composition in the BTBR mouse model of autism spectrum disorder. *Sci. Rep.* 7:45356. doi: 10.1038/srep45356

De Angelis, M., Piccolo, M., Vannini, L., Siragusa, S., De Giacomo, A., Serrazzanetti, D. I., et al. (2013). Fecal microbiota and metabolome of children with autism and pervasive developmental disorder not otherwise specified. *PLoS One* 8:e76993. doi: 10.1371/journal.pone.0076993

de Magistris, L., Familiari, V., Pascotto, A., Sapone, A., Frolli, A., Iardino, P., et al. (2010). Alterations of the intestinal barrier in patients with autism spectrum disorders and in their first-degree relatives. *J. Pediatr. Gastroenterol. Nutr.* 51, 418–424. doi: 10.1097/MPG.0b013e3181dcc4a5

de Theije, C. G. M., Wopereis, H., Ramadan, M., van Eijndthoven, T., Lambert, J., Knol, J., et al. (2014). Altered gut microbiota and activity in a murine model of autism spectrum disorders. *Brain Behav. Immun.* 37, 197–206. doi: 10.1016/j.bbi.2013.12.005

Depino, A. M. (2013). Peripheral and central inflammation in autism spectrum disorders. *Mol. Cell. Neurosci.* 53, 69–76. doi: 10.1016/j.mcn.2012.10.003

DeSantis, T. Z., Hugenholtz, P., Larsen, N., Rojas, M., Brodie, E. L., Keller, K., et al. (2006). Greengenes, a chimera-checked 16S rRNA gene database and workbench compatible with ARB. *Appl. Environ. Microbiol.* 72, 5069–5072. doi: 10.1128/AEM.03006-05

Dinan, T. G., and Cryan, J. F. (2017). The microbiome-gut-brain axis in health and disease. *Gastroenterol. Clin. North Am.* 46, 77–89. doi: 10.1016/j.gtc.2016.09.007

Duncan, S. H., Louis, P., and Flint, H. J. (2004). Lactate-utilizing bacteria, isolated from human feces, that produce butyrate as a major fermentation product. *Appl. Environ. Microbiol.* 70, 5810–5817.

Emanuele, E., Orsi, P., Boso, M., Broglia, D., Brondino, N., Barale, F., et al. (2010). Low-grade endotoxemia in patients with severe autism. *Neurosci. Lett.* 471, 162–165. doi: 10.1016/j.neulet.2010.01.033

Estes, M. L., and McAllister, A. K. (2015). Immune mediators in the brain and peripheral tissues in autism spectrum disorder. *Nat. Rev. Neurosci.* 16, 469–486. doi: 10.1038/nrn3978

Faust, K., and Raes, J. (2016). CoNet app: inference of biological association networks using cytoscape. *F1000Res.* 5:1519.

Finegold, S. M., Dowd, S. E., Gontcharova, V., Liu, C., Henley, K. E., Wolcott, R. D., et al. (2010). Pyrosequencing study of fecal microflora of autistic and control children. *Anaerobe* 16, 444–453. doi: 10.1016/j.anaerobe.2010.06.008

Frye, R. E., Rose, S., Chacko, J., Wynne, R., Bennuri, S. C., Slattery, J. C., et al. (2016). Modulation of mitochondrial function by the microbiome metabolite propionic acid in autism and control cell lines. *Transl. Psychiatry* 6:e927. doi: 10.1038/tp.2016.189

Gagliano, H., Delgado-Morales, R., Sanz-Garcia, A., and Armario, A. (2014). High doses of the histone deacetylase inhibitor sodium butyrate trigger a stress-like response. *Neuropharmacology* 79, 75–82. doi: 10.1016/j.neuropharm.2013.10.031

Griffiths, R. (2006). *Griffiths Mental Developmental Scales Extended Revised Manual*. Firenze: Giunti Organizzazioni Speciali.

Hallmayer, J., Cleveland, S., Torres, A., Phillips, J., Cohen, B., Torigoe, T., et al. (2011). Genetic heritability and shared environmental factors among twin pairs with autism. *Arch. Gen. Psychiatry* 68, 1095–1102. doi: 10.1001/archgenpsychiatry.2011.76

Hospodsky, D., Qian, J., Nazaroff, W. W., Yamamoto, N., Bibby, K., Rismani-Yazdi, H., et al. (2012). Human occupancy as a source of indoor airborne bacteria. *PLoS One* 7:e34867. doi: 10.1371/journal.pone.0034867

Hsiao, E. Y., McBride, S. W., Hsien, S., Sharon, G., Hyde, E. R., McCue, T., et al. (2013). Microbiota modulate behavioral and physiological abnormalities associated with neurodevelopmental disorders. *Cell* 155, 1451–1463. doi: 10.1016/j.cell.2013.11.024

Jyonouchi, H., Sun, S., and Le, H. (2001). Proinflammatory and regulatory cytokine production associated with innate and adaptive immune responses in children with autism spectrum disorders and developmental regression. *J. Neuroimmunol.* 120, 170–179. doi: 10.1016/S0165-5728(01)00421-0

Kanehisa, M., Sato, Y., Kawashima, M., Furumichi, M., and Tanabe, M. (2016). KEGG as a reference resource for gene and protein annotation. *Nucleic Acids Res.* 44, D457–D462. doi: 10.1093/nar/gkv1070

Kang, D. W., Adams, J. B., Gregory, A. C., Borody, T., Chittick, L., Fasano, A., et al. (2017). Microbiota transfer therapy alters gut ecosystem and improves gastrointestinal and autism symptoms: an open-label study. *Microbiome* 5:10. doi: 10.1186/s40168-016-0225-7

Kang, D. W., Park, J. G., Ilhan, Z. E., Wallstrom, G., LaBaer, J., Adams, J. B., et al. (2013). Reduced incidence of prevotella and other fermenters in intestinal microflora of autistic children. *PLoS One* 8:e68322. doi: 10.1371/journal.pone.0068322

Kats, D., Payne, L., Parlier, M., and Piven, J. (2013). Prevalence of selected clinical problems in older adults with autism and intellectual disability. *J. Neurodev. Disord.* 5, 1–27. doi: 10.1186/1866-1955-5-27

Kim, M., Qie, Y., Park, J., and Kim, C. H. (2016). Gut microbial metabolites fuel host antibody responses. *Cell Host Microbe* 20, 202–214. doi: 10.1016/j.chom.2016.07.001

Kratsman, N., Getselter, D., and Elliott, E. (2016). Sodium butyrate attenuates social behavior deficits and modifies the transcription of inhibitory/excitatory genes in the frontal cortex of an autism model. *Neuropharmacology* 102, 136–145. doi: 10.1016/j.neuropharm.2015.11.003

Langille, M., Zaneveld, J., Caporaso, J. G., McDonald, D., Knights, D., Reyes, J., et al. (2013). Predictive functional profiling of microbial communities using 16S rRNA marker gene sequences. *Nat. Biotechnol.* 31, 814–821. doi: 10.1038/nbt.2676

Li, Q., Han, Y., Dy, A. B. C., and Hagerman, R. J. (2017). The gut microbiota and autism spectrum disorders. *Front. Cell. Neurosci.* 11:120. doi: 10.3389/fncel.2017.00120

Lord, C., Rutter, M., DiLavore, P., Risi, S., and Gotham, K. (2012). *Autism Diagnostic Observation Schedule, (ADOS-2)*. Los Angeles, CA: Western Psychological Services.

MacFabe, D. F., Cain, D. P., Rodriguez-Capote, K., Franklin, A. E., Hoffman, J. E., Boon, F., et al. (2007). Neurobiological effects of intraventricular propionic acid in rats: possible role of short chain fatty acids on the pathogenesis and

characteristics of autism spectrum disorders. *Behav. Brain Res.* 176, 149–169. doi: 10.1016/j.bbr.2006.07.025

Macia, L., Tan, J., Vieira, A. T., Leach, K., Stanley, D., Luong, S., et al. (2015). Metabolite-sensing receptors GPR43 and GPR109A facilitate dietary fibre-induced guthomeostasis through regulation of the inflammasome. *Nat. Commun.* 6:6734. doi: 10.1038/ncomms7734

Messaoudi, M., Violle, N., Bisson, J. F., Desor, D., Javelot, H., and Rougeot, C. (2011). Beneficial psychological effects of a probiotic formulation (*Lactobacillus helveticus* R0052 and *Bifidobacterium longum* R0175) in healthy human volunteers. *Gut Microbes* 2, 256–261. doi: 10.4161/gmic.2.4.16108

Miquel, S., Martin, R., Bridonneau, C., Robert, V., Sokol, H., Bermúdez-Humarán, L. G., et al. (2014). Ecology and metabolism of the beneficial intestinal commensal bacterium *Faecalibacterium prausnitzii*. *Gut Microbes* 5, 146–151. doi: 10.4161/gmic.27651

Onore, C. E., Careaga, M., Babineau, B. A., Schwartzer, J. J., Berman, R. F., and Ashwood, P. (2013). Inflammatory macrophage phenotype in BTBR T+tf/J mice. *Front. Neurosci.* 7:158. doi: 10.3389/fnins.2013.00158

Parracho, H. M., Bingham, M. O., Gibson, G. R., and McCartney, A. L. (2005). Differences between the gut microflora of children with autistic spectrum disorders and that of healthy children. *J. Med. Microbiol.* 54, 987–991. doi: 10.1099/jmm.0.46101-0

Patterson, P. H. (2011). Maternal infection and immune involvement in autism. *Trends Mol. Med.* 17, 389–394. doi: 10.1016/j.molmed.2011.03.001

Rajilić-Stojanović, M., and de Vos, W. M. (2014). The first 1000 cultured species of the human gastrointestinal microbiota. *FEMS Microbiol. Rev.* 38, 996–1047. doi: 10.1111/1574-6976.12075

Raveh-Sadka, T., Thomas, B. C., Singh, A., Firek, B., Brooks, B., Castelle, C. J., et al. (2015). Gut bacteria are rarely shared by co-hospitalized premature infants, regardless of necrotizing enterocolitis development. *Elife* 4:e05477. doi: 10.7554/eLife.05477

Russo, R., De Caro, C., Avagliano, C., Cristiano, C., La Rana, G., Mattace Raso, G., et al. (2016). Sodium butyrate and its synthetic amide derivative modulate nociceptive behaviors in mice. *Pharmacol. Res.* 103, 279–291. doi: 10.1016/j.phrs.2015.11.026

Rutter, M., Le Couteur, A., and Lord, C. (2005). *Autism Diagnostic Interview – Revised*. Firenze: Giunti Organizzazioni Speciali.

Sarkar, A., Lehto, S. M., Harty, S., Dinan, T. G., Cryan, J. F., and Burnet, P. W. J. (2016). Psychobiotics and the manipulation of bacteria–gut–brain signals. *Trends Neurosci.* 39, 763–781. doi: 10.1016/j.tins.2016.09.002

Schmieder, R., and Edwards, R. (2011). Quality control and preprocessing of metagenomic datasets. *Bioinformatics* 27, 863–864. doi: 10.1093/bioinformatics/btr026

Schopler, E., Reichler, R. J., and Renner, B. R. (1988). *Childhood Autism Rating Scale (CARS)*. Los Angeles, CA: West. Psychol. Serv, 59804.

Schwab, C., Berry, D., Rauch, I., Rennisch, I., Ramesmayer, J., Hainzl, E., et al. (2014). Longitudinal study of murine microbiota activity and interactions with the host during acute inflammation and recovery. *ISME J.* 8, 1101–1114. doi: 10.1038/ismej.2013.223

Segata, N., Izard, J., Waldron, L., Gevers, D., Miropolsky, L., Garrett, W. S., et al. (2011). Metagenomic biomarker discovery and explanation. *Genome Biol.* 12:R60. doi: 10.1186/gb-2011-12-6-r60

Shannon, P., Markiel, A., Ozier, O., Baliga, N. S., Wang, J. T., Ramage, D., et al. (2003). Cytoscape: a software environment for integrated models of biomolecular interaction networks. *Genome Res.* 13, 2498–2504.

Song, Y., Liu, C., and Finegold, S. M. (2004). Real-time PCR quantitation of clostridia in feces of autistic children. *Appl. Environ. Microbiol.* 70, 6459–6465. doi: 10.1128/AEM.70.11.6459-6465.2004

Sparrow, S. E., Balla, D. A., and Cicchetti, D. V. (2003). *Vineland Adaptive Behavior Scales. Intervista – Forma Completa*. Firenze: Giunti Organizzazioni Speciali.

Stilling, R. M., van de Wouw, M., Clarke, G., Stanton, C., Dinan, T. G., and Cryan, J. F. (2016). The neuropharmacology of butyrate: the bread and butter of the microbiota-gut-brain axis? *Neurochem. Int.* 99, 110–132. doi: 10.1016/j.neuint.2016.06.011

Strati, F., Cavalieri, D., Albanese, D., De Felice, C., Donati, C., Hayek, J., et al. (2017). New evidences on the altered gut microbiota in autism spectrum disorders. *Microbiome* 5:24. doi: 10.1186/s40168-017-0242-1

Takuma, K., Hara, Y., Kataoka, S., Kawanai, T., Maeda, Y., Watanabe, R., et al. (2014). Chronic treatment with valproic acid or sodium butyrate attenuates novel object recognition deficits and hippocampal dendritic spine loss in a mouse model of autism. *Pharmacol. Biochem. Behav.* 126, 43–49. doi: 10.1016/j.pbb.2014.08.013

Thomas, R. H., Meeking, M. M., Mepham, J. R., Tichenoff, L., Possmayer, F., Liu, S., et al. (2012). The enteric bacterial metabolite propionic acid alters brain and plasma phospholipid molecular species: further development of a rodent model of autism spectrum disorders. *J. Neuroinflammation* 9:153. doi: 10.1186/1742-2094-9-153

Tomova, A., Husarova, V., Lakatosova, S., Bakos, J., Vlkova, B., Babinska, K., et al. (2015). Gastrointestinal microbiota in children with autism in Slovakia. *Physiol. Behav.* 138, 179–187. doi: 10.1016/j.physbeh.2014.10.033

Walker, L., SCaplan, A., and Rasquin, A. (2006). *Rome III Diagnostic Questionnaire for the Pediatric Functional GI Disorders*. Rome: The Functional Gastrointestinal Disorders, 961–990.

Wang, L., Christophersen, C. T., Sorich, M. J., Gerber, J. P., Angley, M. T., and Conlon, M. A. (2011). Low relative abundances of the mucolytic bacterium *Akkermansia muciniphila* and *Bifidobacterium* spp. in feces of children with autism. *Appl. Environ. Microbiol.* 77, 6718–6721. doi: 10.1128/AEM.05212-11

Wang, L., Christophersen, C. T., Sorich, M. J., Gerber, J. P., Angley, M. T., and Conlon, M. A. (2012). Elevated fecal short chain fatty acid and ammonia concentrations in children with autism spectrum disorder. *Dig. Dis. Sci.* 57, 2096–2102. doi: 10.1007/s10620-012-2167-7

Wang, L., Christophersen, C. T., Sorich, M. J., Gerber, J. P., Angley, M. T., and Conlon, M. A. (2013). Increased abundance of *Sutterella* spp. and *Ruminococcus* torques in feces of children with autism spectrum disorder. *Mol. Autism* 4:42. doi: 10.1186/2040-2392-4-42

White, J. R., Nagarajan, N., and Pop, M. (2009). Statistical methods for detecting differentially abundant features in clinical metagenomic samples. *PLoS Comput. Biol.* 5:e1000352. doi: 10.1371/journal.pcbi.1000352

Williams, B. L., Hornig, M., Buie, T., Bauman, M. L., Cho Paik, M., Wick, I., et al. (2011). Impaired carbohydrate digestion and transport and mucosal dysbiosis in the intestines of children with autism and gastrointestinal disturbances. *PLoS One* 6:e24585. doi: 10.1371/journal.pone.0024585

Zhang, J., Kobert, K., Flouri, T., and Stamatakis, A. (2014). PEAR: a fast and accurate illumina paired-end reAd mergeR. *Bioinformatics* 30, 614–620. doi: 10.1093/bioinformatics/btt593

Zhang, M., Ma, W., Zhang, J., He, Y., and Wang, J. (2018). Analysis of gut microbiota profiles and microbe-disease associations in children with autism spectrum disorders in China. *Sci. Rep.* 18:13981. doi: 10.1038/s41598-018-32219-2

Zhao, N., Chen, J., Carroll, I. M., Ringel-Kulka, T., Epstein, M. P., Zhou, H., et al. (2015). Testing in microbiome-profiling studies with MiRKAT, the microbiome regression-based kernel association test. *Am. J. Hum. Genet.* 96, 797–807.

Zheng, P., Zeng, B., Zhou, C., Liu, M., Fang, Z., Xu, X., et al. (2016). Gut microbiome remodeling induces depressive-like behaviors through a pathway mediated by the host's metabolism. *Mol. Psychiatry* 21, 786–796. doi: 10.1038/mp.2016.44

Conflict of Interest Statement: The authors declare that the research was conducted in the absence of any commercial or financial relationships that could be construed as a potential conflict of interest.

Copyright © 2018 Coretti, Paparo, Riccio, Amato, Cuomo, Natale, Borrelli, Corrado, De Caro, Comegna, Buommino, Castaldo, Bravaccio, Chiariotti, Berni Canani and Lembo. This is an open-access article distributed under the terms of the Creative Commons Attribution License (CC BY). The use, distribution or reproduction in other forums is permitted, provided the original author(s) and the copyright owner(s) are credited and that the original publication in this journal is cited, in accordance with accepted academic practice. No use, distribution or reproduction is permitted which does not comply with these terms.

frontiers in Microbiology

CORRECTION
published: 03 May 2019
doi: 10.3389/fmicb.2019.00920

Corrigendum: Gut Microbiota Features in Young Children With Autism Spectrum Disorders

Lorena Coretti[1,2,3], Lorella Paparo[4], Maria Pia Riccio[4], Felice Amato[1,5], Mariella Cuomo[1], Alessandro Natale[1], Luca Borrelli[3,6], Giuseppina Corrado[4], Carmen De Caro[7], Marika Comegna[1,5], Elisabetta Buommino[3,7], Giuseppe Castaldo[1,5], Carmela Bravaccio[4], Lorenzo Chiariotti[1,3,8], Roberto Berni Canani[3,4,5,9]* and Francesca Lembo[3,7]**

[1] Department of Molecular Medicine and Medical Biotechnology, University of Naples Federico II, Naples, Italy, [2] Department of Physiology and Biochemistry, Faculty of Medicine and Surgery, University of Malta, Msida, Malta, [3] Task Force on Microbiome Studies, University of Naples Federico II, Naples, Italy, [4] Department of Translational Medical Science - Pediatric Section, University of Naples Federico II, Naples, Italy, [5] CEINGE Advanced Biotechnologies, University of Naples Federico II, Naples, Italy, [6] Department of Veterinary Medicine and Animal Productions, University of Naples Federico II, Naples, Italy, [7] Department of Pharmacy, University of Naples Federico II, Naples, Italy, [8] Istituto di Endocrinologia ed Oncologia Sperimantale, Naples, Italy, [9] European Laboratory for the Investigation of Food-Induced Diseases, University of Naples Federico II, Naples, Italy

Keywords: gut microbiome, ASD, short chain fatty acids, *Faecalibacterium prausnitzii*, *Bifidobacterium longum*, butyrate, propionate

OPEN ACCESS

Approved by:
Frontiers Editorial Office, Frontiers Media SA, Switzerland

***Correspondence:**
Lorena Coretti
lorena.coretti@tiscali.it
Roberto Berni Canani
berni@unina.it
Francesca Lembo
frlembo@unina.it

Specialty section:
This article was submitted to Microbial Symbioses, a section of the journal Frontiers in Microbiology

Received: *20 March 2019*
Accepted: *11 April 2019*
Published: *03 May 2019*

Citation:
Coretti L, Paparo L, Riccio MP, Amato F, Cuomo M, Natale A, Borrelli L, Corrado G, De Caro C, Comegna M, Buommino E, Castaldo G, Bravaccio C, Chiariotti L, Berni Canani R and Lembo F (2019) Corrigendum: Gut Microbiota Features in Young Children With Autism Spectrum Disorders. Front. Microbiol. 10:920. doi: 10.3389/fmicb.2019.00920

A Corrigendum on

Gut Microbiota Features in Young Children With Autism Spectrum Disorders
by Coretti, L., Paparo, L., Riccio, M. P., Amato, F., Cuomo, M., Natale, A., et al. (2018). Front. Microbiol. 9:3146. doi: 10.3389/fmicb.2018.03146

"Carmen De Caro" was not included as an author in the published article. The corrected Author Contributions Statement appears below.

The authors apologize for this error and state that this does not change the scientific conclusions of the article in any way. The original article has been updated.

AUTHOR CONTRIBUTIONS

LCo performed microbiota analysis, statistically analyzed all data and wrote the manuscript. LP produced and analyzed butyrate and propionate data and contributed to manuscript writing. MR and GCo organized the clinical work and performed the subject's enrolment. FA, MCo, and GCa performed ddPCR and revised the manuscript. CD produced butyrate and propionate data. MCu, AN, LB, and EB contributed to the metagenomic analysis and to the interpretation of the data. LCh conceived the investigation and contributed to the interpretation of the data. CB designed the epidemiological study, organized the clinical work, and performed the subject's enrolment. RB conceived the investigation, designed the epidemiological study, supervised the general aspects of the work and contributed to manuscript writing. FL conceived the investigation, interpreted the data, wrote the manuscript, and critically supervised the work. All authors reviewed the manuscript.

Copyright © 2019 Coretti, Paparo, Riccio, Amato, Cuomo, Natale, Borrelli, Corrado, De Caro, Comegna, Buommino, Castaldo, Bravaccio, Chiariotti, Berni Canani and Lembo. This is an open-access article distributed under the terms of the Creative Commons Attribution License (CC BY). The use, distribution or reproduction in other forums is permitted, provided the original author(s) and the copyright owner(s) are credited and that the original publication in this journal is cited, in accordance with accepted academic practice. No use, distribution or reproduction is permitted which does not comply with these terms.

frontiers in Microbiology

ORIGINAL RESEARCH
published: 04 January 2019
doi: 10.3389/fmicb.2018.03220

Identification of Specific Oral and Gut Pathogens in Full Thickness Colon of Colitis Patients: Implications for Colon Motility

Vasudevan Dinakaran[1†], Sammed N. Mandape[2†], Kristina Shuba[1], Siddharth Pratap[2], Shruti S. Sakhare[2], Mohammad Ali Tabatabai[3], Duane T. Smoot[4], Cherae M. Farmer-Dixon[1], Lakshmyya N. Kesavalu[5], Samuel Evans Adunyah[6], Janet Hayes Southerland[7] and Pandu R. Gangula[1]*

[1] Department of ODS & Research, School of Dentistry, Meharry Medical College, Nashville, TN, United States, [2] Bioinformatics Core, School of Graduate Studies/Research & School of Medicine, Meharry Medical College, Nashville, TN, United States, [3] Department of Public Health, School of Graduate Studies & Research, Meharry Medical College, Nashville, TN, United States, [4] Department of Internal Medicine, Division of Gastroenterology & Hepatology, Meharry Medical College, Nashville, TN, United States, [5] Department of Periodontology, College of Dentistry, University of Florida, Gainesville, FL, United States, [6] Department of Biochemistry, Cancer Biology, Neuroscience & Pharmacology, Meharry Medical College, Nashville, TN, United States, [7] Department of Nutrition Metabolism & Oral Surgery, University of Texas Medical Branch at Galveston, Galveston, TX, United States

OPEN ACCESS

Edited by:
Nurul-Syakima Ab Mutalib, UKM Medical Molecular Biology Institute (UMBI), Malaysia

Reviewed by:
Christopher L. Hemme, University of Rhode Island, United States
Chenyang Wang, Nanjing University Medical School, China

***Correspondence:**
Pandu R. Gangula
pgangula@mmc.edu

[†] These authors have contributed equally to this work

Specialty section:
This article was submitted to Microbial Symbioses, a section of the journal Frontiers in Microbiology

Received: 11 September 2018
Accepted: 11 December 2018
Published: 04 January 2019

Citation:
Dinakaran V, Mandape SN, Shuba K, Pratap S, Sakhare SS, Tabatabai MA, Smoot DT, Farmer-Dixon CM, Kesavalu LN, Adunyah SE, Southerland JH and Gangula PR (2019) Identification of Specific Oral and Gut Pathogens in Full Thickness Colon of Colitis Patients: Implications for Colon Motility. Front. Microbiol. 9:3220. doi: 10.3389/fmicb.2018.03220

Impaired colon motility is one of the leading problems associated with inflammatory bowel disease (IBD). An expanding body of evidence supports the role of microbiome in normal gut function and in progression of IBD. The objective of this work is to determine whether diseased full thickness colon specimens, including the neuromuscular region (critical for colon motility function), contain specific oral and gut pathogens. In addition, we compared the differences in colon microbiome between Caucasians (CA) and African Americans (AA). Thirty-nine human full thickness colon (diseased colon and adjacent healthy colon) specimens were collected from Crohn's Colitis (CC) or Ulcerative Colitis (UC) patients while they underwent elective colon surgeries. We isolated and analyzed bacterial ribosomal RNA (rRNA) from colon specimens by amplicon sequencing of the 16S rRNA gene region. The microbiome proportions were quantified into Operational Taxonomic Units (OTUs) by analysis with Quantitative Insights Into Microbial ecology (QIIME) platform. Two hundred twenty-eight different bacterial species were identified by QIIME analysis. However, we could only decipher the species name of fifty-three bacteria. Our results show that proportion of non-detrimental bacteria in CC or UC colon samples were altered compared to adjacent healthy colon specimens. We further show, for the first time in full thickness colon specimens, that microbiome of CC and UC diseased specimens is dominated by putative oral pathogens belonging to the Phyla Firmicutes (*Streptococcus*, *Staphylococcus*, *Peptostreptococcus*), and Fusobacteria (*Fusobacterium*). In addition, we have identified patterns of differences in microbiome levels between CA and AA specimens with potential implications for health disparities research. Overall, our results suggest a significant association between oral and gut microbes in the modulation of colon motility in colitis patients.

Keywords: colitis, colon motility, nitric oxide (NO), antioxidants, oral microbiome, operational taxonomic units (OTUs), gut microbiome

INTRODUCTION

Inflammatory bowel disease (IBD) is comprised of Crohn's disease / Crohn's colitis (CC) and Ulcerative colitis (UC). The term Colitis, refers to general inflammation of the inner lining of the colon arising from numerous underlying causes including idiopathic infection, IBD (either CC or UC), ischemic colitis, allergic reactions, and/or microscopic colitis. Distally, gingivitis, and periodontal disease are chronic inflammatory gum diseases associated with orange, red, yellow, purple, and green complex bacterial infections in sub-gingival areas of oral cavity (Popova et al., 2013).

Previous studies have shown that periodontal disease (PD) is a significant risk factor and contributor to many systemic diseases, including IBD (Vavricka et al., 2013). Several factors including genetic, dietary, and environmental factors could influence the pathogenesis of microbiome (oral and gut) which in turn may increase the incidence of periodontitis and IBD (Lira-Junior and Figueredo, 2016; Agossa et al., 2017). In addition, *Porphyromonas gingivalis* known to cause PD altered the gut microbiota leading to increased gut epithelial permeability and endotoxemia, which causes systemic inflammation (Hajishengallis, 2015). In addition, many earlier studies have shown intestinal colonization of oral bacteria in the pathogenesis of IBD (Strauss et al., 2011; Atarashi et al., 2017).

Innumerable number of studies have shown that the gut microbiome including Phyla Proteobacteria, Firmicutes, and Bacteroidetes contribute to normal gut function (Mariat et al., 2009; Koliada et al., 2017; Walker et al., 2018; Zhao et al., 2018). Colon motility is mainly regulated by neuromuscular portion of the colon and this was shown to be impaired in colitis patients; putatively due to a reduction in neuronal nitric oxide (NO) synthase (nNOS) protein expression and/or neuronal degeneration (Bassotti et al., 2014; Gangula et al., 2017). Previous studies have analyzed the microbiome in feces and/or colon mucosal biopsy specimens of colitis patients (Gibson et al., 1991; Bibiloni et al., 2006). However, the relationship/interaction between oral and gut bacteria in the development and/or exacerbation of inflammatory disease in the colon (containing neuromuscular tissue) was under studied. In addition, data is limited on how oral bacteria interact with and influence the large intestinal flora, thereby contributing to colitis. Since motility of the colon is impaired in colitis patients and neuromuscular tissue play a role in the motility function (Geboes and Collins, 1998; Poli et al., 2001), we hypothesize that the interaction between oral and gut microbiome may play a significant role in the inflammatory processes associated with the development and progression of colitis seen in certain patient populations. Furthermore, we hypothesize that difference in microbiome may exist between CA and AA colitis patients, potentially contributing to health disparities in IBD.

METHODS

Ethics Statement

The participants provided both written and verbal informed consent to Collaborative Human Tissue Networking (CHTN) Consortium to collect specimens while they underwent elective colon surgeries.

Collection of Specimens

Frozen full thickness colon specimens were obtained from Cooperative Human Tissue Networking (CHTN). Thirty-nine human full thickness colon (moderate to severe diseased colon and adjacent healthy colon) specimens were collected from CC and UC male and female patients (ages between 18 and 75 years old) while they underwent elective colon surgeries. The specimens include Ulcerative ($n = 13$), Crohn's ($n = 13$) and adjacent healthy ($n = 13$) specimens. Characteristics of participants included Caucasians (CA) ($n = 30$) and African Americans (AA) ($n = 9$). CC male and female patients presented with symptoms like fever, fatigue, diarrhea, blood in stool, mouth sores, abdominal cramping, and pain around the anus, reduced appetite, and weight loss. While UC male and female patients presented with additional signs like rectal pain, rectal bleeding, and inability to defecate despite urgency.

Extraction of DNA, Amplification of 16S rRNA Gene and Amplicon Sequencing

DNA extraction and microbial analysis were performed in the University of North Carolina at Chapel Hill School of Medicine Microbiome Core Facility (UNC: MC). We identified a conserved region of the 16S rRNA gene of 550 bp to amplify. This encompassed variable regions V3–V4 from the colon genomic DNA using primers 16S rRNA-F 5′-AGAGTTTGATCCTGGCTCAG-3′and 16S rRNA-R 5′-GCTGCCTCCCGTAGGAGT-3′ and overhang adapter sequences appended to the primer pair for compatibility with Illumina index and sequencing adapters. Briefly, each 16SrRNA amplicon was purified using AMPure XP reagent (Beckman Coulter, Indianapolis, IN, USA). Specifically, each sample was amplified using a limited cycle PCR program, adding Illumina sequencing adapters and optional dual-index barcodes [index 1(i7) and index 2(i5)] (Illumina, San Diego, CA, USA) to the amplicon target. The final libraries were purified using AMPure XP reagent, quantified and normalized prior to pooling. The DNA library pool was denatured with NaOH, diluted with hybridization buffer and heat denatured before loading on to the MiSeq reagent cartridge and to the MiSeq instrument (Illumina). The standard Illumina paired-end 250 base pair (PE250) protocol was used for sequencing the16S rRNA amplicons (Illumina, CA, USA).

Processing of Sequence Reads

Data was analyzed and microbial proportions using Operational Taxonomic Units (OTUs) were determined using Quantitative Insights Into Microbial ecology (QIIME) pipeline (Caporaso et al., 2010a) in the Meharry Medical College Bioinformatics Core. Briefly, generated raw reads were preprocessed for adapter removal. Processed sequence reads were obtained as fastq files and were converted into fasta, quality and flow files using Mothur package (Schloss et al., 2009). The initial number of fasta sequences obtained were 31,09,793. First, the fasta files were cleaned of host reads by mapping on to 9 mm mouse

genome. Then, the primer sequences and barcode sequences were removed, demultiplexed and quality filtered. The number of high quality sequences remaining after quality filtering was 16,64,769. The OTUs were picked by *de novo* strategy. The high quality sequences were clustered at 97% identity using UCLUST inbuilt in QIIME pipeline to generate 3994 OTUs and taxonomy was assigned to OTU representative sequences using UCLUST (Edgar, 2010). The picked sequences were aligned using PyNAST aligner (Caporaso et al., 2010b). The chimeric sequences and singleton OTUs were removed using ChimeraSlayer (Haas et al., 2011). We constructed a phylogenetic tree for the sequences using FastTree version 2.1.3 (data not shown) (Price et al., 2010). Next, an OTU table was constructed and taxa were summarized using the 894 OTUs obtained from QIIME pipeline. α-diversity metrics was computed using Chao1 (abundance-based richness estimator) and Shannon analysis (diversity index) and Rarefaction plots were constructed (data not shown). β-diversity metrics was computed using weighted and unweighted Principal Coordinates Analysis (PCoA) (data not shown) (Gower, 2005). A Taxonomic Summary Bar plot showing OTUs assigned to Phyla-level taxonomy per sample was subsequently constructed (**Figure 1**). Bar Plots showing the relative abundance of bacteria at the Phyla-level between races, diseased tissue and healthy tissue groups is shown in **Figure 3**. Sample-specific sequences were deposited in the MGRAST database (accession number: b3b851ba2c6d676d343739393937332e33) and was assigned an MG-RAST project ID (mgs675214) (Keegan et al., 2016). In addition, sample-specific sequences were deposited in the NCBI (BioProject: PRJNA496071).

The pathogenic and beneficial oral and gut bacteria were identified using the NCBI Genome database (https://www.ncbi.nlm.nih.gov/genome/). This analysis was performed to assess the pathogenic and healthy bacterial proportions in human full thickness colon specimens (**Tables 1–3**).

Statistical Analysis and Evaluation

Statistical analysis was performed between the healthy and diseased groups and based on race classification ($n = 13$ CC, $n = 13$ UC, $n = 13$ non-disease healthy patients, $n = 30$ CA and $n = 9$ AA). A non-parametric Mann-Whitney *U* Test *p*-value < 0.05 of bacterial 16S rRNA OTUs between the groups was considered statistically significant. IBM SPSS software package version 23 (IBM Analytics, USA) was used to conduct statistical analysis.

RESULTS

Relative Abundance Analysis

QIIME analysis showed about two hundred twenty-eight bacterial species in entire 39 specimens (**Tables 1–5**). However, non-ambiguous annotation at the species name resulted in fifty-three bacterial identifications. The dominant phyla across all samples (both diseased and healthy specimens) were Bacteroidetes (46.92%), followed by Firmicutes

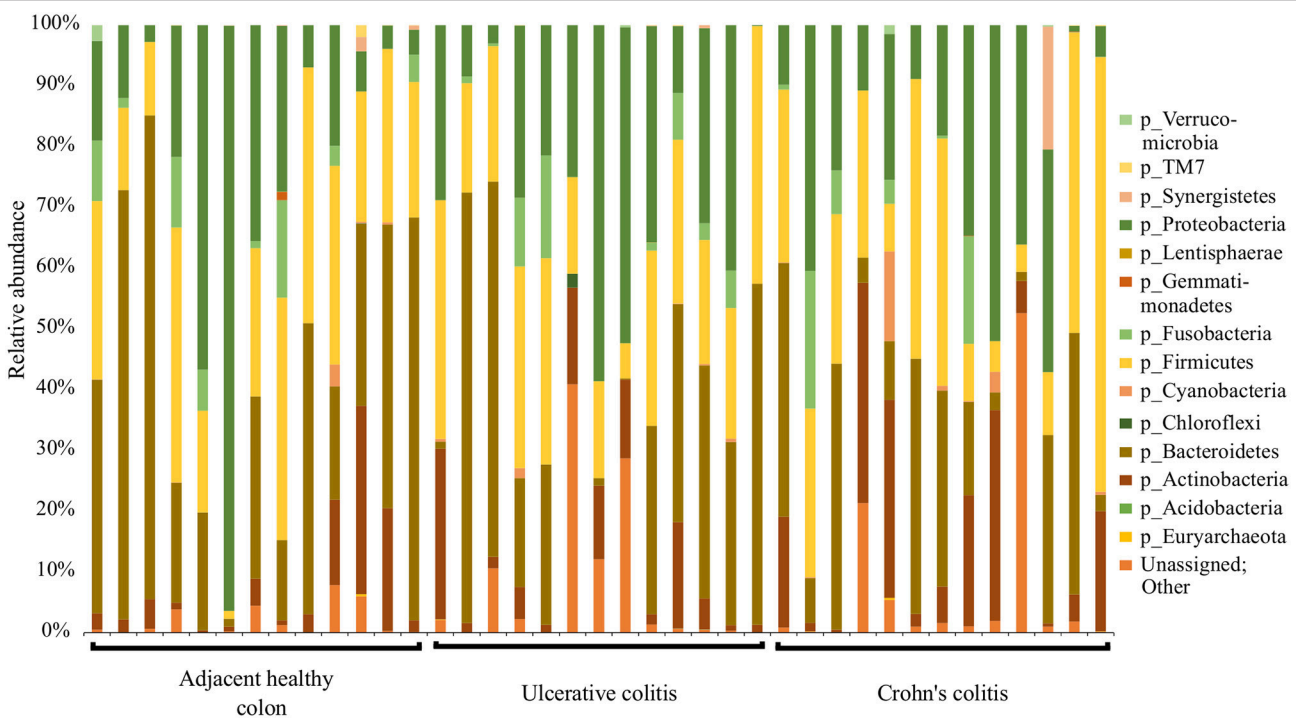

FIGURE 1 | Summary of major bacterial taxa contributing to the communities detected in the 39 specimens at the Phylum level in the colitis and adjacent healthy specimen groups. Specimens are categorized into adjacent healthy colon ($n = 13$), Ulcerative colitis (UC, $n = 13$), and Crohn's colitis (CC, $n = 13$). Data represented are the relative abundances (%) of each phylum identified in each specimen.

TABLE 1 | Functions and proportions of specific pathogenic Oral bacteria colonized in full thickness colon specimens.

Sl. No.	Bacteria genus	Bacteria species	Proportion (%)	Bacteria phylum	Function in IBD	NCBI genome database link
ADJACENT HEALTHY COLON						
1	Prevotella	stercorea	2.3	Bacteroidetes	Alters mucosal microbiota in the colon of patients with IBD	H
2	Prevotella	Other	0.3	Bacteroidetes	A microbial signature of Crohn's disease	GS
3	Gemella	s__	0.1	Firmicutes	Microbiome in New-Onset Crohn's Disease	CP
4	Staphylococcus	sciuri	0.1	Firmicutes	Develops intestinal inflammation in acute and chronic colitis	I
5	Staphylococcus	aureus	0.6	Firmicutes	Causes Crohn's disease	AU
6	Abiotrophia	s__	0.1	Firmicutes	Causes fecal microbial dysbiosis in IBD	CS
7	Lactobacillus	zeae	1.9	Firmicutes	Maintains remission of ulcerative colitis	A
8	Lactobacillus	s__	0.4	Firmicutes	Maintains remission of ulcerative colitis	CW
9	Lactococcus	s__	0.7	Firmicutes	Used in the treatment of Crohn's disease	CX
10	Peptostreptococcus	anaerobius	11.6	Firmicutes	Causes dysbiosis in IBD	AW
11	Peptostreptococcus	s__	0.5	Firmicutes	Causes gut microbiota dysbiosis in IBD	DR
12	Selenomonas	s__	0.2	Firmicutes	Causes dysbiosis in colorectal cancer	EB
13	Eubacterium	dolichum	1.0	Firmicutes	Causes dysbiosis of the intestinal microbiota	AL
14	Fusobacterium	s__	2.2	Fusobacteria	Identified from colonic biopsies of IBD patients	EN
15	Pseudomonas	alcaligenes	1.8	Proteobacteria	Identified in the gut microbiota of IBD	AX
16	Pseudomonas	s__	0.1	Proteobacteria	Causes infection in Children with Early-onset Crohn's Disease	GG
17	Pseudomonas	Other	0.2	Proteobacteria	Gut microbe in children with early onset Crohn's disease	HR
18	Corynebacterium	durum	0.1	Actinobacteria	Gut microbe in IBD patients	AK
19	Corynebacterium	s__	0.8	Actinobacteria	Causes experimental colitis	BI
20	Pseudoramibacter_Eubacterium	s__	1.6	Firmicutes	Metabolizes Linoleic acid in the Gut	DF
DISEASED COLON (ULCERATIVE COLITIS)						
1	Prevotella	stercorea	1.0	Bacteroidetes	Alters mucosal microbiota in the colon of patients with IBD	H
2	Prevotella	s__	0.3	Bacteroidetes	A microbial signature of Crohn's disease	BZ
3	Prevotella	Other	0.3	Bacteroidetes	A microbial signature of Crohn's disease	GS
4	Staphylococcus	aureus	0.3	Firmicutes	Causes Crohn's disease	AU
5	Lactobacillus	zeae	7.6	Firmicutes	Maintains remission of ulcerative colitis	A
6	Lactobacillus	s__	0.3	Firmicutes	Maintains remission of ulcerative colitis	CW
7	Lactococcus	s__	0.6	Firmicutes	Used in the treatment of Crohn's disease	CX
8	Peptostreptococcus	anaerobius	12.7	Firmicutes	Causes dysbiosis in IBD	AW
9	Peptostreptococcus	s__	0.3	Firmicutes	Causes gut microbiota dysbiosis in IBD	DR
10	Selenomonas	s__	0.1	Firmicutes	Causes dysbiosis in colorectal cancer	EB
11	Eubacterium	dolichum	0.5	Firmicutes	Causes dysbiosis of the intestinal microbiota	AL

(Continued)

TABLE 1 | Continued

Sl. No.	Bacteria genus	Bacteria species	Proportion (%)	Bacteria phylum	Function in IBD	NCBI genome database link
12	Pseudoramibacter_ Eubacterium	s__	1.9	Firmicutes	Metabolizes Linoleic acid in the Gut	DF
13	Fusobacterium	s__	3.0	Fusobacteria	Identified from colonic biopsies of IBD patients	EN
14	Pseudomonas	alcaligenes	0.4	Proteobacteria	Identified in the gut microbiota of IBD	AX
15	Pseudomonas	s__	0.8	Proteobacteria	Infection in Children with Early-onset Crohn's Disease	GG
16	Aggregatibacter	s__	1.4	Proteobacteria	Causes fungal microbiota dysbiosis in IBD	
17	Corynebacterium	s__	1.0	Actinobacteria	Causes experimental colitis	BI
DISEASED COLON (CROHN'S COLITIS)						
1	Prevotella	tannerae	0.2	Bacteroidetes	Prevalent in colitis	F
2	Prevotella	stercorea	3.3	Bacteroidetes	Alters mucosal microbiota in the colon of patients with IBD	H
3	Prevotella	melaninogenica	0.4	Bacteroidetes	Gut microbiome biomarker in ankylosing spondylitis	U
4	Prevotella	Other	3.3	Bacteroidetes	A microbial signature of Crohn's disease	GS
5	Gemella	s__	0.1	Firmicutes	Microbiome in New-Onset Crohn's Disease	CP
6	Staphylococcus	sciuri	0.1	Firmicutes	Develops intestinal inflammation in acute and chronic colitis	I
7	Staphylococcus	aureus	0.5	Firmicutes	Causes Crohn's disease	AU
8	Abiotrophia	s__	0.2	Firmicutes	Causes fecal microbial dysbiosis in IBD	CS
9	Lactobacillus	zeae	6.8	Firmicutes	Maintains remission of ulcerative colitis	A
10	Lactobacillus	reuteri	0.1	Firmicutes	Prevents colitis as a probiotic	M
11	Lactobacillus	s__	0.6	Firmicutes	Maintains remission of ulcerative colitis	CW
12	Lactococcus	s__	0.7	Firmicutes	Used in the treatment of Crohn's disease	CX
13	Peptostreptococcus	anaerobius	4.0	Firmicutes	Causes dysbiosis in IBD	AW
14	Peptostreptococcus	s__	0.1	Firmicutes	causes gut microbiota dysbiosis in IBD	DR
15	Selenomonas	s__	0.4	Firmicutes	Causes dysbiosis in colorectal cancer	EB
16	Eubacterium	dolichum	0.8	Firmicutes	Causes dysbiosis of the intestinal microbiota	AL
17	Pseudoramibacter_ Eubacterium	s__	1.3	Firmicutes	Metabolizes Linoleic acid in the Gut	DF
18	Fusobacterium	s__	2.4	Fusobacteria	Identified from colonic biopsies of IBD patients	EN
19	Pseudomonas	alcaligenes	0.8	Proteobacteria	Identified in the gut microbiota of IBD	AX
20	Pseudomonas	s__	1.0	Proteobacteria	Infection in Children with Early-onset Crohn's Disease	GG
21	Corynebacterium	durum	0.2	Actinobacteria	Gut microbe in IBD patients	AK
22	Corynebacterium	s__	0.1	Actinobacteria	Causes experimental colitis	BI
23	Pyramidobacter	piscolens	0.1	Synergistetes	Oral bacteria in IBD	P

Specific Information of functions was adapted from NCBI Genome Database (https://www.ncbi.nlm.nih.gov/genome/).
The bacterial species that could not be identified at the genus level are mentioned as g___ and the bacterial species that could not be identified at the species level are mentioned as s___.

(27.8%), and Proteobacteria (24.5%). Most importantly, our results indicate that putative oral pathogens (belonging to mostly Phylum Firmicutes) dominated the microbiome of diseased specimens (**Figure 1**). Adjacent healthy specimens show an increased abundance of Phylum Bacteroidetes (∼ 57%, containing mostly symbiotic and/or beneficial bacteria) population, which is altered in disease categories (**Figure 2**).

TABLE 2 | Functions and proportions of specific beneficial Gut bacteria colonized in full thickness colon specimens.

Sl. No.	Bacteria genus	Bacteria species	Proportion (%)	Bacteria phylum	Function in IBD	NCBI genome database link
ADJACENT HEALTHY COLON						
1	Shuttleworthia	satelles	0.2	Firmicutes	Identified in the human ileum	J
2	Bifidobacterium	longum	0.1	Actinobacteria	Attenuates acute murine experimental model of IBD	Y
3	Rhizobium	leguminosarum	0.1	Proteobacteria	Identified commensal gut microbe	AB
4	Lysinibacillus	boronitolerans	12.1	Firmicutes	Identified commensal gut microbe	AT
5	Alloiococcus	s__	1.7	Firmicutes	Identified commensal gut microbe	CT
6	Christensenella	s__	2.2	Firmicutes	Identified gut microbe	DC
7	Blautia	s__	0.3	Firmicutes	Butyrate-producing bacterial species in Gut	DH
8	Coprococcus	s__	0.1	Firmicutes	Butyrate-producing bacterial species in Gut	DI
9	g__	s__	0.7	Gemmatimonadetes	Identified commensal gut microbe	EP
10	g__	s__	0.7	Lentisphaerae	Normal gut microbe	EQ
11	g__	s__	0.4	Proteobacteria	Identified commensal gut microbe	FC
12	Comamonas	s__	1.0	Proteobacteria	Identified commensal gut microbe	FL
13	Desulfovibrio	s__	0.3	Proteobacteria	Sulfate reducing bacteria in IBD	FV
14	Paracoccus	Other	0.1	Proteobacteria	Identified commensal gut microbe	HH
15	Other	Other	0.2	Proteobacteria	Mucosal and fecal microbe	HP
DISEASED COLON (ULCERATIVE COLITIS)						
1	Lysinibacillus	boronitolerans	8.2	Firmicutes	Identified commensal gut microbe	AT
2	Varibaculum	s__	0.2	Actinobacteria	Identified in the gut of a premature infant	BH
3	Alloiococcus	s__	3.1	Firmicutes	Identified commensal gut microbe	CT
4	Christensenella	s__	0.6	Firmicutes	Identified gut microbe	DC
5	Blautia	s__	0.3	Firmicutes	Butyrate-producing bacterial species in Gut	DH
6	Coprococcus	s__	0.2	Firmicutes	Butyrate-producing bacterial species in Gut	DI
7	g__	s__	0.3	Gemmatimonadetes	Identified commensal gut microbe	EP
8	g__	s__	0.3	Proteobacteria	Identified commensal gut microbe	FC
9	Comamonas	s__	2.7	Proteobacteria	Identified commensal gut microbe	FL
10	Desulfovibrio	s__	0.1	Proteobacteria	Sulfate reducing bacteria in IBD	FV
11	Morganella	s__	0.1	Proteobacteria	Sulfate reducing bacteria in IBD	FZ
12	g__	s__	0.6	TM7	Identified commensal gut microbe	
13	Other	Other	0.1	Actinobacteria	Commensal gut bacteria in IBD	GN
14	Other	Other	0.5	Proteobacteria	Adult fecal microbe	HO
DISEASED COLON (CROHN'S COLITIS)						
1	Akkermansia	muciniphila	0.1	Verrucomicrobia	Adheres to enterocytes and strengthens the integrity of the epithelial cell layer	S
2	Bifidobacterium	longum	0.4	Actinobacteria	Attenuates acute murine experimental model of IBD	Y

(Continued)

TABLE 2 | Continued

Sl. No.	Bacteria genus	Bacteria species	Proportion (%)	Bacteria phylum	Function in IBD	NCBI genome database link
3	Rhizobium	leguminosarum	0.2	Proteobacteria	Identified commensal gut microbe	AB
4	Anoxybacillus	kestanbolensis	0.3	Firmicutes	Identified commensal gut microbe	AD
5	Lysinibacillus	boronitolerans	11.5	Firmicutes	Identified commensal gut microbe	AT
6	g__	s__	0.1	Acidobacteria	Identified in human gut microbiota	BC
7	Varibaculum	s__	0.1	Actinobacteria	Identified in the gut of a premature infant	BH
8	SHD-231	s__	0.1	Chloroflexi	Identified in the fecal microbiome of Gout patients	CH
9	g__	s__	0.1	Cyanobacteria	Identified in human gut microbiota	CJ
10	Alloiococcus	s__	7.1	Firmicutes	Identified commensal gut microbe	CT
11	Christensenella	s__	0.1	Firmicutes	Identified gut microbe	DC
12	g__	s__	0.1	Firmicutes	Commensal gut bacteria in IBD	DG
13	Blautia	s__	0.1	Firmicutes	Butyrate-producing bacterial species in Gut	DH
14	Coprococcus	s__	0.1	Firmicutes	Butyrate-producing bacterial species in Gut	DI
15	g__	s__	0.3	Gemmatimonadetes	Identified commensal gut microbe	EP
16	g__	s__	0.3	Lentisphaerae	Normal gut microbe	EQ
17	Comamonas	s__	2.4	Proteobacteria	Identified commensal gut microbe	FL
18	g__	s__	0.1	Proteobacteria	Identified commensal gut microbe	FT
19	Desulfovibrio	s__	0.2	Proteobacteria	Sulfate reducing bacteria in IBD	FV
20	g__	s__	0.3	TM7	Identified commensal gut microbe	
21	Other	Other	0.2	Firmicutes	Commensal gut bacteria in IBD	HA
22	Paracoccus	Other	0.7	Proteobacteria	Identified commensal gut microbe	HH
23	Other	Other	0.1	Proteobacteria	Identified commensal gut microbe	HN
24	Other	Other	0.7	Proteobacteria	Adult fecal microbe	HO

Specific Information of functions was adapted from NCBI Genome Database (https://www.ncbi.nlm.nih.gov/genome/).
The bacterial species that could not be identified at the genus level are mentioned as g___ and the bacterial species that could not be identified at the species level are mentioned as s___.

Differential Expression of Microbiomes in the Colon of CA and AA Patients

Figure 3 show racial differences of various bacterial phyla in adjacent healthy, UC and CC full thickness colon specimens. The tissue specimens from Caucasians represented a significantly higher proportion ($p < 0.05$) of the oral pathogen, *Fusobacterium*, and gut bacteria, *Parabacteroides* (Bacteroidetes). CA specimens also showed significantly higher levels ($p < 0.05$) of Phyla Proteobacteria including *Citrobacter*, *Hemophilus*, *Acinetobacter*, *Pseudomonas,* and *Stenotrophomonas* as compared to AA. Whereas, the AA specimens were observed to have a significantly higher proportion ($p < 0.05$) of *Prevotella* (Bacteroidetes) and *Clostridia* (Firmicutes) (**Figure 3**; **Table 4**).

As depicted in **Figure 3**, the adjacent healthy colon specimens, UC and CC contained ∼ 1%, ∼ 7% and ∼ 7% of sequence reads, respectively that were un-assignable to any taxon with a larger proportion of them identified in AA Colitis patients. Other major phyla observed among these specimens also include Proteobacteria (Adjacent healthy: 23.8%; UC: 26.5% and CC: 23.1%), Actinobacteria (Adjacent healthy: 6.7%; UC: 8.1% and CC: 14.1%), Fusobacteria (Adjacent healthy: 4.2%; UC: 3.6% and CC: 4.0%), and Synergistetes (Adjacent healthy: 0.2%; UC: 0.04% and CC: 1.5%). The Phylum Proteobacteria did not show

TABLE 3 | Functions and proportions of specific pathogenic Gut bacteria colonized in full thickness colon specimens.

Sl. No.	Bacteria genus	Bacteria species	Proportion (%)	Bacteria phylum	Function in IBD	NCBI Genome database link
ADJACENT HEALTHY COLON						
1	Ochrobactrum	s__	0.1	Proteobacteria	Causes early bacterial dependent induction of inducible nitric oxide synthase (iNOS) in epithelial cells in experimental colitis	EU
2	Sphingomonas	s__	0.2	Proteobacteria	Tissue associated intestinal microflora	FF
3	Burkholderia	s__	1.2	Proteobacteria	causes dysfunction of GALT and gut flora in IBD	FI
4	Acinetobacter	rhizosphaerae	0.3	Proteobacteria	Identified gut bacteria in IBD	K
5	Acinetobacter	lwoffii	0.3	Proteobacteria	gut bacteria in multiple sclerosis patients	W
6	Stenotrophomonas	geniculata	1.2	Proteobacteria	Identified gut bacteria in IBD	AG
7	Staphylococcus	sciuri	0.1	Firmicutes	Develops intestinal inflammation in acute and chronic colitis	I
8	Staphylococcus	aureus	0.6	Firmicutes	Causes Crohn's disease	AU
9	Lactobacillus	zeae	1.9	Firmicutes	Maintains remission of ulcerative colitis	A
10	Lactobacillus	s__	0.4	Firmicutes	Maintains remission of ulcerative colitis	CW
11	Lactococcus	s__	0.7	Firmicutes	Used in the treatment of Crohn's disease	CX
12	Pseudomonas	alcaligenes	1.8	Proteobacteria	Identified in the gut microbiota of IBD	AX
13	Pseudomonas	s__	0.1	Proteobacteria	Infection in Children with Early-onset Crohn's Disease	GG
14	Pseudomonas	Other	0.2	Proteobacteria	Gut microbe in children with early onset Crohn's disease	HR
15	Bacillus	s__	0.2	Firmicutes	Increases cytokine levels in IBD	CL
16	Bacteroides	Other	0.1	Bacteroidetes	Commensal bacteria that induces colitis	GR
17	Microbacterium	maritypicum	0.1	Actinobacteria	Fecal microbiome in Obesity	V
18	Eggerthella	lenta	0.8	Actinobacteria	Causes bacteremia in Crohn's disease patient	AA
19	Brevundimonas	diminuta	0.1	Proteobacteria	Identified in the adult fecal microbiota of allergy patients	AO
20	Propionibacterium	acnes	5.3	Actinobacteria	Intestinal microbe in Liver disease	BA
21	Methanobrevibacter	s__	0.7	Euryarchaeota	Identified in the gut of IBD	BB
22	g__	s__	2.4	Acidobacteria	Identified in the gut microbiome of Type 2 Diabetes patients	BD
23	g__	s__	1.1	Actinobacteria	Identified in gut microbiota in IBD	BF
24	Actinomyces	s__	0.1	Actinobacteria	Identified in Abdominopelvic actinomycosis involving the GIT	BG
25	Varibaculum	s__	0.2	Actinobacteria	Identified in the gut of a premature infant	BH
26	Microbacterium	s__	0.1	Actinobacteria	Identified in the duodenum of children with ulcerative colitis	BK
27	g__	s__	0.2	Actinobacteria	Identified in fecal microbiota of pediatric IBD patients	BP
28	Atopobium	s__	0.1	Actinobacteria	Altered intestinal microbiota in Crohn's disease	BR
29	Slackia	s__	0.2	Actinobacteria	Human gut bacteria in Multiple Sclerosis	BS
30	g__	s__	0.1	Bacteroidetes	Characterized in intestinal biopsies in IBD patients	CB
31	g__	s__	0.1	Bacteroidetes	Human gut microbe in Obesity and IBD	CC
32	Cloacibacterium	s__	1.1	Bacteroidetes	Identified in the rectum of human colorectal adenoma patients	CG
33	g__	s__	0.2	Cyanobacteria	Identified in the gut microbiome of IBD patients	CI
34	g__	s__	0.6	Firmicutes	Causes microbiota dysbiosis in IBD	CO
35	g__	s__	0.7	Firmicutes	A microbial signature of Crohn's disease	DB
36	Clostridium	s__	0.9	Firmicutes	Causes infection of the gut in IBD	DE
37	Dorea	s__	0.1	Firmicutes	Causes dysfunction of the intestinal microbiome in IBD	DJ
38	Lachnospira	s__	0.1	Firmicutes	Gut bacteria in Crohn's disease patients	DK
39	Ruminococcus	s__	0.1	Firmicutes	Dominant in gut microbiome of IBD patients	DO
40	g__	s__	0.2	Firmicutes	Gut microbe in IBD	DP

(Continued)

TABLE 3 | Continued

Sl. No.	Bacteria genus	Bacteria species	Proportion (%)	Bacteria phylum	Function in IBD	NCBI genome database link
41	g__	s__	0.6	Firmicutes	A microbial signature of Crohn's disease	DQ
42	Anaerotruncus	s__	0.2	Firmicutes	Tissue associated intestinal microflora	DT
43	Oscillospira	s__	0.4	Firmicutes	Gut microbe in IBD patients	DU
44	Ruminococcus	s__	0.7	Firmicutes	Dominant in gut microbiome of IBD patients	DV
45	g__	s__	0.4	Firmicutes	Gut microbe underlying the onset of IBD	DW
46	Acidaminococcus	s__	1.3	Firmicutes	Gut microbe in IBD	DX
47	Phascolarctobacterium	s__	1.9	Firmicutes	Causes dysfunction of the intestinal microbiome in IBD	DZ
48	Schwartzia	s__	0.5	Firmicutes	causes fecal microbial dysbiosis in IBD	EA
49	g__	s__	0.2	Firmicutes	A microbial signature of Crohn's disease	EC
50	Anaerococcus	s__	1.3	Firmicutes	Microbe in Inflammatory Pouch Complications	EE
51	Finegoldia	s__	0.3	Firmicutes	Intestinal microbe in colorectal cancer	EF
52	g__	s__	0.3	Firmicutes	Gut microbe in GI diseases	EI
53	Bulleidia	s__	0.1	Firmicutes	Fecal-associated and mucosalassociated microbiota in irritable bowel syndrome patients	EJ
54	Coprobacillus	s__	0.3	Firmicutes	Alters Gut Microbiota in Psoriatic Arthritis	EL
55	Leptotrichia	s__	0.7	Fusobacteria	Causes gut mucosal inflammation in Rheumatoid arthritis patients	EO
56	g__	s__	4.2	Proteobacteria	Intestinal microbe in children with severe and complicated acute viral gastroenteritis	EV
57	Methylobacterium	s__	0.1	Proteobacteria	Causes microbial dysbiosis in pediatric Crohn's disease	EW
58	g__	s__	0.1	Proteobacteria	Intestinal microbe in children with severe and complicated acute viral gastroenteritis	EX
59	g__	s__	1.2	Proteobacteria	Involved in host-microbial cross talk in IBD	FG
60	Lautropia	s__	0.3	Proteobacteria	causes fecal microbial dysbiosis in IBD	FJ
61	g__	s__	0.1	Proteobacteria	Fecal and mucosa associated microbe in IBD	FK
62	Citrobacter	s__	0.1	Proteobacteria	Gut microbe in newly diagnosed with treatment-naïve Crohn's disease patients	FY
63	Halomonas	s__	1.4	Proteobacteria	Intestinal microflora in chronic kidney disease	GB
64	g__	s__	0.1	Proteobacteria	Microbe in colon tissue from IBD subjects	GE
65	g__	s__	0.1	Proteobacteria	bacteria in human Ulcerative Colitis patients	GH
66	Other	Other	0.1	Actinobacteria	Alters fecal microbiota in pediatric IBD patients	GO
67	Other	Other	3.6	Firmicutes	gut microbe in experimental colitis	GT
68	Other	Other	12.5	Firmicutes	Fecal and mucosa associated microbe in IBD	GW
69	Weissella	Other	0.2	Firmicutes	Gut microbe in IBD patients	GX
70	Other	Other	0.1	Proteobacteria	Fecal and mucosa associated microbe in IBD	HL
71	Other	Other	0.1	Proteobacteria	Involved in host-microbial cross talk in IBD	HM
DISEASED COLON (ULCERATIVE COLITIS)						
1	Ochrobactrum	s__	0.1	Proteobacteria	Causes early bacterial dependent induction of inducible nitric oxide synthase (iNOS) in epithelial cells in experimental colitis	EU
2	Delftia	s__	0.1	Proteobacteria	Fecal and mucosa associated microbe in IBD	FM
3	Sphingomonas	s__	0.5	Proteobacteria	Tissue associated intestinal microflora	FF
4	Burkholderia	s__	0.2	Proteobacteria	Causes dysfunction of GALT and gut flora in IBD	FI
5	Acinetobacter	rhizosphaerae	0.7	Proteobacteria	Identified gut microbe in IBD	K
6	Acinetobacter	lwoffii	0.1	Proteobacteria	Gut bacteria in multiple sclerosis patients	W
7	Acinetobacter	s__	0.5	Proteobacteria	Tissue associated intestinal microflora	GF
8	Stenotrophomonas	geniculata	0.1	Proteobacteria	Identified gut microbe in IBD	AG
9	Enterococcus	s__	0.8	Firmicutes	Induces experimental IBD	CV
10	Staphylococcus	sciuri	0.1	Firmicutes	Develops intestinal inflammation in acute and chronic colitis	I

(Continued)

TABLE 3 | Continued

Sl. No.	Bacteria genus	Bacteria species	Proportion (%)	Bacteria phylum	Function in IBD	NCBI genome database link
11	Staphylococcus	aureus	0.6	Firmicutes	Causes Crohn's disease	AU
12	Lactobacillus	zeae	1.9	Firmicutes	Maintains remission of ulcerative colitis	A
13	Lactobacillus	s__	0.4	Firmicutes	Maintains remission of ulcerative colitis	CW
14	Lactococcus	s__	0.7	Firmicutes	used in the treatment of Crohn's disease	CX
15	Pseudomonas	alcaligenes	1.8	Proteobacteria	Identified in the gut microbiota of IBD	AX
16	Pseudomonas	s__	0.1	Proteobacteria	Infection in Children with Early-onset Crohn's Disease	GG
17	Pseudomonas	Other	0.2	Proteobacteria	Gut microbe in children with early onset Crohn's disease	HR
18	Bacillus	s__	0.1	Firmicutes	Increases cytokine levels in IBD	CL
19	Bacteroides	caccae	0.1	Bacteroidetes	Identified in the gut of ulcerative colitis patients	AS
20	Bacteroides	Other	0.2	Bacteroidetes	Commensal bacteria that induces colitis	GR
21	Blautia	producta	0.1	Firmicutes	Gut microbe in Obesity and IBD	N
22	Faecalibacterium	prausnitzii	0.1	Firmicutes	Gut microbe in Crohn's disease patients	O
23	Microbacterium	maritypicum	0.1	Actinobacteria	Fecal microbiome in Obesity	V
24	Eggerthella	lenta	5.1	Actinobacteria	Causes bacteremia in Crohn's disease patient	AA
25	Propionibacterium	acnes	2.8	Actinobacteria	Intestinal microbe in Liver disease	BA
26	Methanobrevibacter	s__	0.3	Euryarchaeota	Identified in the gut of IBD	BB
27	g__	s__	1.8	Acidobacteria	Identified in the gut microbiome of Type 2 Diabetes patients	BD
28	g__	s__	0.3	Actinobacteria	Identified in gut microbiota in IBD	BF
29	Adlercreutzia	s__	0.2	Actinobacteria	Causes dysbiosis in IBD patients	BQ
30	Slackia	s__	0.2	Actinobacteria	Alters human gut microbiome in Multiple Sclerosis	BS
31	g__	s__	0.8	Bacteroidetes	Identified in gut microbiome of IBD patients	CA
32	g__	s__	0.4	Bacteroidetes	Characterized in intestinal biopsies in IBD patients	CB
33	g__	s__	0.1	Bacteroidetes	Human gut microbe in Obesity and IBD	CC
34	Cloacibacterium	s__	0.4	Bacteroidetes	Identified in the rectum of human colorectal adenoma patients	CG
35	g__	s__	0.1	Firmicutes	Causes microbiota dysbiosis in IBD	CO
36	g__	s__	0.1	Firmicutes	Gut microbe in IBD	DA
37	g__	s__	1.7	Firmicutes	A microbial signature of Crohn's disease	DB
38	Clostridium	s__	0.8	Firmicutes	Causes infection of the gut in IBD	DE
39	Dorea	s__	0.1	Firmicutes	Causes dysfunction of the intestinal microbiome in IBD	DJ
40	Lachnospira	s__	0.3	Firmicutes	gut bacteria in Crohn's disease patients	DK
41	Ruminococcus	s__	0.1	Firmicutes	Dominant in gut microbiome of IBD patients	DO
42	g__	s__	0.3	Firmicutes	A microbial signature of Crohn's disease	DQ
43	Oscillospira	s__	0.1	Firmicutes	Gut microbe in IBD patients	DU
44	Ruminococcus	s__	0.9	Firmicutes	Dominant in gut microbiome of IBD patients	DV
45	g__	s__	0.3	Firmicutes	Gut microbe underlying the onset of IBD	DW
46	Acidaminococcus	s__	1.1	Firmicutes	Gut microbe in IBD	DX
47	Phascolarctobacterium	s__	2.2	Firmicutes	Causes dysfunction of the intestinal microbiome in IBD	DZ
48	Schwartzia	s__	0.5	Firmicutes	Causes fecal microbial dysbiosis in IBD	EA
49	Anaerococcus	s__	0.6	Firmicutes	Microbe in Inflammatory Pouch Complications	EE
50	Finegoldia	s__	0.3	Firmicutes	Intestinal microbe in colorectal cancer	EF
51	g__	s__	0.6	Firmicutes	Gut microbe in GI diseases	EI
52	Bulleidia	s__	0.1	Firmicutes	Fecal-associated and mucosalassociated microbiota in irritable bowel syndrome patients	EJ
53	Coprobacillus	s__	0.1	Firmicutes	Alters Gut Microbiota in Psoriatic Arthritis	EL
54	Leptotrichia	s__	0.5	Fusobacteria	Causes gut mucosal inflammation in Rheumatoid arthritis patients	EO

(Continued)

TABLE 3 | Continued

Sl. No.	Bacteria genus	Bacteria species	Proportion (%)	Bacteria phylum	Function in IBD	NCBI genome database link
55	g__	s__	3.6	Proteobacteria	Intestinal microbe in children with severe and complicated acute viral gastroenteritis	EV
56	g__	s__	0.5	Proteobacteria	Causes chronic inflammation in IBD	FB
57	g__	s__	0.1	Proteobacteria	Microbial factor associated with postoperative Crohn's disease	FD
58	g__	s__	1.5	Proteobacteria	Involved in host-microbial cross talk in IBD	FG
59	Sutterella	s__	0.1	Proteobacteria	Gut microbe in experimental colitis	FH
60	Lautropia	s__	0.2	Proteobacteria	Causes fecal microbial dysbiosis in IBD	FJ
61	g__	s__	0.5	Proteobacteria	Fecal and mucosa associated microbe in IBD	FK
62	Citrobacter	s__	0.3	Proteobacteria	Gut microbe in newly diagnosed with treatment-naïve Crohn's disease patients	FY
63	Halomonas	s__	0.8	Proteobacteria	Intestinal microflora in chronic kidney disease	GB
64	g__	s__	0.3	Proteobacteria	Bacteria in human Ulcerative Colitis patients	GH
65	Other	Other	0.2	Actinobacteria	Alters fecal microbiota in pediatric IBD patients	GO
66	Eggerthella	Other	0.1	Actinobacteria	Causes bacteremia in Crohn's disease patient	GQ
67	Other	Other	4.0	Firmicutes	Gut microbe in experimental colitis	GT
68	Other	Other	4.2	Firmicutes	Fecal and mucosa associated microbe in IBD	GW
69	Weissella	Other	1.2	Firmicutes	Gut microbe in IBD patients	GX
70	Other	Other	2.5	Proteobacteria	Causes microbial dysbiosis in pediatric Crohn's disease	HD
71	Other	Other	1.4	Proteobacteria	Fecal and mucosa associated microbe in IBD	HL
DISEASED COLON (CROHN'S COLITIS)						
1	Ochrobactrum	s__	0.1	Proteobacteria	Causes early bacterial dependent induction of inducible nitric oxide synthase (iNOS) in epithelial cells in experimental colitis	EU
2	Sphingomonas	s__	0.1	Proteobacteria	Tissue associated intestinal microflora	FF
3	Burkholderia	s__	1.6	Proteobacteria	Causes dysfunction of GALT and gut flora in IBD	FI
4	Acinetobacter	rhizosphaerae	1.8	Proteobacteria	Identified gut microbe in IBD	K
5	Acinetobacter	lwoffii	0.5	Proteobacteria	Gut bacteria in multiple sclerosis patients	W
6	Acinetobacter	Other	1.6	Proteobacteria	Tissue associated intestinal microflora in colitis patients	HQ
7	Stenotrophomonas	geniculata	0.3	Proteobacteria	Identified gut microbe in IBD	AG
8	Enterococcus	s__	0.1	Firmicutes	Induces experimental IBD	CV
9	Staphylococcus	sciuri	0.1	Firmicutes	Develops intestinal inflammation in acute and chronic colitis	I
10	Staphylococcus	aureus	0.6	Firmicutes	Causes Crohn's disease	AU
11	Lactobacillus	zeae	1.9	Firmicutes	Maintains remission of ulcerative colitis	A
12	Lactobacillus	s__	0.4	Firmicutes	Maintains remission of ulcerative colitis	CW
13	Lactococcus	s__	0.7	Firmicutes	Used in the treatment of Crohn's disease	CX
14	Pseudomonas	alcaligenes	1.8	Proteobacteria	Identified in the gut microbiota of IBD	AX
15	Pseudomonas	s__	0.1	Proteobacteria	Infection in Children with Early-onset Crohn's Disease	GG
16	Pseudomonas	Other	0.2	Proteobacteria	Gut microbe in children with early onset Crohn's disease	HR
17	Bacillus	thermoamylovorans	0.2	Firmicutes	A probiotic- normal flora of the gut	E
18	Bacillus	s__	2.6	Firmicutes	Increases cytokine levels in IBD	CL
19	Bacteroides	eggerthii	0.1	Bacteroidetes	Enhances colitis in mice	AJ
20	Bacteroides	Other	0.4	Bacteroidetes	Commensal bacteria that induces colitis	GR
21	Microbacterium	maritypicum	0.1	Actinobacteria	Fecal microbiome in Obesity	V
22	Eggerthella	lenta	4.5	Actinobacteria	Causes bacteremia in Crohn's disease patient	AA
23	Brevundimonas	diminuta	0.2	Proteobacteria	Identified in the adult fecal microbiota of allergy patients	AO

(Continued)

TABLE 3 | Continued

Sl. No.	Bacteria genus	Bacteria species	Proportion (%)	Bacteria phylum	Function in IBD	NCBI genome database link
24	Propionibacterium	acnes	1.2	Actinobacteria	Intestinal microbe in Liver disease	BA
25	Methanobrevibacter	s__	0.8	Euryarchaeota	Identified in the gut of IBD patients	BB
26	g__	s__	0.7	Acidobacteria	Identified in the gut microbiome of Type 2 Diabetes patients	BD
27	g__	s__	0.2	Actinobacteria	Identified in gut microbiota in IBD	BE
28	g__	s__	0.5	Actinobacteria	Identified in gut microbiota in IBD	BF
29	Microbacterium	s__	0.1	Actinobacteria	Identified in the duodenum of children with ulcerative colitis	BK
30	Bifidobacterium	s__	0.2	Actinobacteria	Identified in gut microbiota of IBD patients	BO
31	g__	s__	0.3	Actinobacteria	Identified in fecal microbiota of pediatric IBD patients	BP
32	Atopobium	s__	0.2	Actinobacteria	Altered intestinal microbiota in Crohn's disease	BR
33	Slackia	s__	1.3	Actinobacteria	Alters human gut microbiome in Multiple Sclerosis	BS
34	g__	s__	0.1	Bacteroidetes	Identified in gut microbiome of IBD patients	CA
35	g__	s__	0.3	Bacteroidetes	Human gut microbe in Obesity and IBD	CC
36	g__	s__	0.7	Firmicutes	Causes microbiota dysbiosis in IBD	CO
37	g__	s__	0.2	Firmicutes	Gut microbe in IBD	DA
38	g__	s__	0.9	Firmicutes	A microbial signature of Crohn's disease	DB
39	Clostridium	s__	0.6	Firmicutes	Causes infection of the gut in IBD	DE
40	Lachnospira	s__	0.6	Firmicutes	Gut bacteria in Crohn's disease patients	DK
41	Moryella	s__	0.1	Firmicutes	Microbe in Inflammatory Pouch Complications	DL
42	g__	s__	0.1	Firmicutes	gut microbe in IBD	DP
43	g__	s__	0.6	Firmicutes	A microbial signature of Crohn's disease	DQ
44	Oscillospira	s__	0.2	Firmicutes	Gut microbe in IBD patients	DU
45	Ruminococcus	s__	0.9	Firmicutes	Dominant in gut microbiome of IBD patients	DV
46	g__	s__	0.2	Firmicutes	Gut microbe underlying the onset of IBD	DW
47	Acidaminococcus	s__	1.0	Firmicutes	Gut microbe in IBD	DX
48	Phascolarctobacterium	s__	0.6	Firmicutes	Causes dysfunction of the intestinal microbiome in IBD	DZ
49	Schwartzia	s__	0.2	Firmicutes	Causes fecal microbial dysbiosis in IBD	EA
50	g__	s__	0.1	Firmicutes	A microbial signature of Crohn's disease	EC
51	Anaerococcus	s__	0.3	Firmicutes	Microbe in Inflammatory Pouch Complications	EE
52	Finegoldia	s__	0.4	Firmicutes	Intestinal microbe in colorectal cancer	EF
53	g__	s__	0.5	Firmicutes	Gut microbe in GI diseases	EI
54	Bulleidia	s__	0.2	Firmicutes	Fecal-associated and mucosalassociated microbiota in irritable bowel syndrome patients	EJ
55	Coprobacillus	s__	0.3	Firmicutes	Alters Gut Microbiota in Psoriatic Arthritis	EL
56	Leptotrichia	s__	0.5	Fusobacteria	Causes gut mucosal inflammation in Rheumatoid arthritis patients	EO
57	g__	s__	4.1	Proteobacteria	Intestinal microbe in children with severe and complicated acute viral gastroenteritis	EV
58	g__	s__	0.2	Proteobacteria	Microbial factor associated with postoperative Crohn's disease	FD
59	g__	s__	1.2	Proteobacteria	Involved in host-microbial cross talk in IBD	FG
60	Sutterella	s__	0.1	Proteobacteria	Gut microbe in experimental colitis	FH
61	Lautropia	s__	0.1	Proteobacteria	Causes fecal microbial dysbiosis in IBD	FJ
62	g__	s__	0.4	Proteobacteria	Fecal and mucosa associated microbe in IBD	FK
63	g__	s__	0.1	Proteobacteria	Bacteria in Mucosal and Submucosal Intestinal Tissues in Advanced Crohn's Disease	FN
64	Ralstonia	s__	0.1	Proteobacteria	Microbiota in the Mucosa of Patients With Ulcerative Colitis	FP
65	Halomonas	s__	0.5	Proteobacteria	Intestinal microflora in chronic kidney disease	GB

(Continued)

TABLE 3 | Continued

Sl. No.	Bacteria genus	Bacteria species	Proportion (%)	Bacteria phylum	Function in IBD	NCBI genome database link
66	Haemophilus	s__	0.7	Proteobacteria	Treatment naïve microbiome in new onset Crohn's disease	GD
67	g__	s__	0.1	Proteobacteria	Microbe in colon tissue from IBD subjects	GE
68	Other	Other	1.1	Actinobacteria	Alters fecal microbiota in pediatric IBD patients	GO
69	Eggerthella	Other	0.1	Actinobacteria	Causes bacteremia in Crohn's disease patient	GQ
70	Other	Other	1.7	Firmicutes	Gut microbe in experimental colitis	GT
71	Other	Other	2.2	Firmicutes	Fecal and mucosa associated microbe in IBD	GW
72	Weissella	Other	2.2	Firmicutes	Gut microbe in IBD patients	GX
73	Other	Other	0.1	Proteobacteria	Causes microbial dysbiosis in pediatric Crohn's disease	HD
74	Methylobacterium	Other	0.1	Proteobacteria	Causes gut microbial dysbiosis in pediatric Crohn's disease patients	HG
75	Other	Other	0.2	Proteobacteria	Fecal and mucosa associated microbe in IBD	HK
76	Other	Other	0.6	Proteobacteria	Fecal and mucosa associated microbe in IBD	HL

Specific Information of functions was adapted from NCBI Genome Database (https://www.ncbi.nlm.nih.gov/genome/).
The bacterial species that could not be identified at the genus level are mentioned as g___ and the bacterial species that could not be identified at the species level are mentioned as s___.

any significant difference between healthy colon specimens and diseased colon specimens (**Table 4**).

Bacterial Species Identified in a Significantly Higher Proportion in Diseased Colon Tissues

As shown in **Figure 3**, diseased colon specimens represented a significantly higher proportion ($p < 0.05$) of gut bacteria belonging to Phylum Firmicutes including *Blautia producta*, *Faecalibacterium prausnitzii*, *Anoxybacillus kestanbolensis*, *Ruminococcus gnavus*, *Eubacterium dolichum*, *Lysinibacillus boronitolerans,* and oral bacteria including *Staphylococcus sciuri*, *Staphylococcus aureus*, *Streptococcus anginosus*.

In contrast, healthy colon specimens were significantly dominated ($p < 0.05$) by oral bacteria belonging to Phylum Actinobacteria that includes; *Corynebacterium kroppenstedtii*, *Corynebacterium durum.* Additionally, healthy colon specimens were dominated by gut bacteria belonging to Phylum Actinobacteria that includes; *Colinsella stercoris*, *Colinsella aerofaciens, Kocuria rhizophila*, *Eggerthella lenta*, *Propionibacterium granulosum*, *Propionibacterium acnes*, *Actinomyces europaeus*, *Rothia dentocariosa,* and Phylum Bacteroidetes that includes; *Bacteroides fragilis*, *Bacteroides eggerthii*, *Bacteroides caccae*, *Parabacteroides distasonis* (**Figure 3**).

Alpha Diversity and Beta Diversity Analyses

Alpha diversity and beta diversity metrics were computed to analyse the diversity of bacterial species within each sample and between samples. To assess our sampling efficiency, we plotted rarefaction curves (Chao1 and Shannon) for all 39 specimens. Increased diversity (Shannon) in the diseased samples compared to control samples was observed. From the rarefaction curves, it is evident that most AA samples require additional sampling whereas Caucasian samples do not (data not shown).

Since, outliers exhibiting different microbiome profiles were observed both in the healthy and disease groups, we performed principle coordinate analysis (PCoA analysis) and hierarchial clustering to obtain a holistic view of the microbiome profile in each sample. Two dimensional PCoA plots revealed that control samples which had similar microbiome profiles as suggested by histograms and OTU heat map clustered together (data not shown).

Pathogenic Oral and Gut Flora Abundantly Colonized in Diseased Colon Specimens

The pathogenic oral bacteria identified abundantly in diseased colon specimens as compared to healthy colon specimens were *Porphyromonas*, *Prevotella*, *Gemella, Staphylococcus, Streptococcus, Abiotrophia, Granulicatella, Lactobacillus, Lactococcus, Peptostreptococcus, Selenomonas, Veillonella, Parvimonas, Eubacterium, Fusobacterium, Pseudomonas*, *Aggregatibacter,* and *Corynebacterium* (**Table 1**).

Pathogenic gut bacteria identified abundantly in diseased colon specimens as compared to healthy colon specimens include *Ochrobactrum, Delftia, Sphingomonas, Burkholderia, Acinetobacter, Stenotrophomonas, Enterococcus*, *Granulicatella*, *Staphylococcus*, *Streptococcus*, *Lactobacillus*, *Lactococcus*, *Pseudomonas*, *Bacillus*, *Campylobacter,* and *Bacteroides* (**Table 3**).

DISCUSSION

Our study demonstrates significant perturbations among bacteria belonging to Phyla Bacteroidetes and Firmicutes in full-thickness diseased colon specimens containing neuromuscular compartment (**Figure 2**). Our studies further show that the proportion of pathogenic bacteria are higher in diseased

TABLE 4 | Functions and Proportions of bacterial species identified in the full thickness human colon specimens of Caucasians and African Americans.

Sl. No.	Bacteria genus	Bacteria species	Proportion (%)	Bacteria phylum	Function in IBD	NCBI genome database link
CAUCASIAN AMERICANS						
1	Lactobacillus	zeae	6.8	Firmicutes	Maintains remission of ulcerative colitis	A
2	Bacillus	thermoamylovorans	0.1	Firmicutes	A probiotic- normal flora of the gut	E
3	Prevotella	tannerae	0.1	Bacteroidetes	Prevalent in colitis	F
4	Collinsella	stercoris	0.0	Actinobacteria	Used for treatment of IBD	G
5	Prevotella	stercorea	1.4	Bacteroidetes	Alters mucosal microbiota in the colon of patients with IBD	H
6	Staphylococcus	sciuri	0.1	Firmicutes	Develops intestinal inflammation in acute and chronic colitis	I
7	Shuttleworthia	satelles	0.0	Firmicutes	Identified in the human ileum	J
8	Acinetobacter	rhizosphaerae	1.1	Proteobacteria	Identified gut microbe in IBD	K
9	Blautia	producta	0.1	Firmicutes	Gut microbe in Obesity and IBD	N
10	Akkermansia	muciniphila	0.1	Verrucomicrobia	Adheres to enterocytes and strengthens the integrity of the epithelial cell layer	S
11	Prevotella	melaninogenica	0.2	Bacteroidetes	Gut microbiome biomarker in ankylosing spondylitis	U
12	Acinetobacter	lwoffii	0.2	Proteobacteria	Gut bacteria in multiple sclerosis patients	W
13	Bifidobacterium	longum	0.2	Actinobacteria	Attenuates acute murine experimental model of IBD	Y
14	Eggerthella	lenta	4.3	Actinobacteria	Causes bacteremia in Crohn's disease patient	AA
15	Rhizobium	leguminosarum	0.1	Proteobacteria	Identified gut microbe in IBD patients	AB
16	Anoxybacillus	kestanbolensis	0.1	Firmicutes	Identified gut microbe in IBD patients	AD
17	Stenotrophomonas	geniculata	0.1	Proteobacteria	Identified gut microbe in IBD patients	AG
18	Corynebacterium	durum	0.1	Actinobacteria	Identified gut microbe in IBD patients	AK
19	Eubacterium	dolichum	0.8	Firmicutes	Causes dysbiosis of the intestinal microbiota	AL
20	Brevundimonas	diminuta	0.1	Proteobacteria	Identified in the adult fecal microbiota of allergy patients	AO
21	Lysinibacillus	boronitolerans	12.3	Firmicutes	Identified gut microbe in IBD patients	AT
22	Staphylococcus	aureus	0.6	Firmicutes	Causes Crohn's disease	AU
23	Peptostreptococcus	anaerobius	4.8	Firmicutes	Causes dysbiosis in IBD	AW
24	Pseudomonas	alcaligenes	1.0	Proteobacteria	Identified in the gut microbiota of IBD	AX
25	Propionibacterium	acnes	3.9	Actinobacteria	Intestinal microbe in Liver disease	BA
26	Methanobrevibacter	s__	0.6	Euryarchaeota	Identified in the gut of IBD	BB
27	g__	s__	0.8	Acidobacteria	Identified in the gut microbiome of Type 2 Diabetes patients	BD
28	g__	s__	0.9	Actinobacteria	Identified in gut microbiota in IBD	BF
29	Varibaculum	s__	0.1	Actinobacteria	Identified in the gut of a premature infant	BH
30	Corynebacterium	s__	0.7	Actinobacteria	Causes experimental colitis	BI
31	Microbacterium	s__	0.1	Actinobacteria	Identified in the duodenum of children with ulcerative colitis	BK
32	Bifidobacterium	s__	0.1	Actinobacteria	identified in gut microbiota of IBD patients	BO
33	g__	s__	0.2	Actinobacteria	Identified in fecal microbiota of pediatric IBD patients	BP
34	Adlercreutzia	s__	0.1	Actinobacteria	Causes dysbiosis in IBD patients	BQ
35	Atopobium	s__	0.1	Actinobacteria	altered intestinal microbiota in Crohn's disease	BR
36	Slackia	s__	0.7	Actinobacteria	Alters human gut microbiome in Multiple Sclerosis	BS
37	Prevotella	s__	0.1	Bacteroidetes	A microbial signature of Crohn's disease	BZ
38	g__	s__	0.4	Bacteroidetes	Identified in gut microbiome of IBD patients	CA
39	g__	s__	0.2	Bacteroidetes	Characterized in intestinal biopsies in IBD patients	CB
40	g__	s__	0.2	Bacteroidetes	Human gut microbe in Obesity and IBD	CC
41	Cloacibacterium	s__	0.7	Bacteroidetes	Identified in the rectum of human colorectal adenoma patients	CG
42	SHD-231	s__	0.1	Chloroflexi	Identified in the fecal microbiome of Gout patients	CH
43	g__	s__	0.1	Cyanobacteria	Identified in the gut microbiome of IBD patients	CI

(Continued)

TABLE 4 | Continued

Sl. No.	Bacteria genus	Bacteria species	Proportion (%)	Bacteria phylum	Function in IBD	NCBI genome database link
44	Calothrix	s__	0.1	Cyanobacteria	Identified gut microbe in IBD patients	CK
45	Bacillus	s__	0.5	Firmicutes	Increases cytokine levels in IBD	CL
46	g__	s__	0.6	Firmicutes	Causes microbiota dysbiosis in IBD	CO
47	Gemella	s__	0.1	Firmicutes	Microbiome in New-Onset Crohn's Disease	CP
48	Abiotrophia	s__	0.1	Firmicutes	Causes fecal microbial dysbiosis in IBD	CS
49	Alloiococcus	s__	3.4	Firmicutes	Identified gut microbe in IBD patients	CT
50	Enterococcus	s__	0.4	Firmicutes	Induces experimental IBD	CV
51	Lactobacillus	s__	0.5	Firmicutes	Maintains remission of ulcerative colitis	CW
52	Lactococcus	s__	0.7	Firmicutes	Used in the treatment of Crohn's disease	CX
53	g__	s__	0.1	Firmicutes	Gut microbe in IBD	DA
54	g__	s__	1.1	Firmicutes	A microbial signature of Crohn's disease	DB
55	Christensenella	s__	1.2	Firmicutes	Identified gut microbe	DC
56	Clostridium	s__	0.9	Firmicutes	causes infection of the gut in IBD	DE
57	Pseudoramibacter_ Eubacterium	s__	1.8	Firmicutes	Metabolizes Linoleic acid in the Gut	DF
58	g__	s__	0.1	Firmicutes	Commensal gut bacteria in IBD	DG
59	Blautia	s__	0.3	Firmicutes	Butyrate-producing bacterial species in Gut	DH
60	Coprococcus	s__	0.2	Firmicutes	Butyrate-producing bacterial species in Gut	DI
61	Dorea	s__	0.1	Firmicutes	Causes dysfunction of the intestinal microbiome in IBD	DJ
62	Lachnospira	s__	0.3	Firmicutes	Gut bacteria in Crohn's disease patients	DK
63	g__	s__	0.1	Firmicutes	Gut microbe in IBD	DP
64	g__	s__	0.6	Firmicutes	A microbial signature of Crohn's disease	DQ
65	Peptostreptococcus	s__	0.3	Firmicutes	Causes gut microbiota dysbiosis in IBD	DR
66	Anaerotruncus	s__	0.1	Firmicutes	Tissue associated intestinal microflora	DT
67	Oscillospira	s__	0.2	Firmicutes	Gut microbe in IBD patients	DU
68	Ruminococcus	s__	0.4	Firmicutes	Dominant in gut microbiome of IBD patients	DV
69	g__	s__	0.3	Firmicutes	Gut microbe underlying the onset of IBD	DW
70	Acidaminococcus	s__	1.2	Firmicutes	Gut microbe in IBD	DX
71	Phascolarctobacterium	s__	1.9	Firmicutes	Causes dysfunction of the intestinal microbiome in IBD	DZ
72	Schwartzia	s__	0.5	Firmicutes	Causes fecal microbial dysbiosis in IBD	EA
73	Selenomonas	s__	0.2	Firmicutes	Causes dysbiosis in colorectal cancer	EB
74	g__	s__	0.1	Firmicutes	A microbial signature of Crohn's disease	EC
75	Anaerococcus	s__	0.7	Firmicutes	Microbe in Inflammatory Pouch Complications	EE
76	Finegoldia	s__	0.3	Firmicutes	Intestinal microbe in colorectal cancer	EF
77	g__	s__	0.4	Firmicutes	Gut microbe in GI diseases	EI
78	Bulleidia	s__	0.1	Firmicutes	Fecal-associated and mucosalassociated microbiota in irritable bowel syndrome patients	EJ
79	Coprobacillus	s__	0.3	Firmicutes	Alters Gut Microbiota in Psoriatic Arthritis	EL
80	Fusobacterium	s__	0.8	Fusobacteria	Identified from colonic biopsies of IBD patients	EN
81	Leptotrichia	s__	0.2	Fusobacteria	Causes gut mucosal inflammation in Rheumatoid arthritis patients	EO
82	g__	s__	0.3	Gemmatimonadetes	Identified gut microbe in IBD patients	EP
83	g__	s__	0.4	Lentisphaerae	Normal gut microbe	EQ
84	Ochrobactrum	s__	0.1	Proteobacteria	Causes early bacterial dependent induction of inducible nitric oxide synthase (iNOS) in epithelial cells in experimental colitis	EU
85	g__	s__	4.7	Proteobacteria	Intestinal microbe in children with severe and complicated acute viral gastroenteritis	EV
86	g__	s__	0.2	Proteobacteria	Causes chronic inflammation in IBD	FB

(Continued)

TABLE 4 | Continued

Sl. No.	Bacteria genus	Bacteria species	Proportion (%)	Bacteria phylum	Function in IBD	NCBI genome database link
87	g__	s__	0.3	Proteobacteria	Identified gut microbe in IBD patients	FC
88	g__	s__	0.1	Proteobacteria	Microbial factor associated with postoperative Crohn's disease	FD
89	Sphingomonas	s__	0.3	Proteobacteria	Tissue associated intestinal microflora	FF
90	g__	s__	1.7	Proteobacteria	Involved in host-microbial cross talk in IBD	FG
91	Sutterella	s__	0.1	Proteobacteria	gut microbe in experimental colitis	FH
92	Burkholderia	s__	1.2	Proteobacteria	Causes dysfunction of GALT and gut flora in IBD	FI
93	Lautropia	s__	0.2	Proteobacteria	Causes fecal microbial dysbiosis in IBD	FJ
94	g__	s__	0.4	Proteobacteria	Fecal and mucosa associated microbe in IBD	FK
95	Comamonas	s__	2.5	Proteobacteria	Identified gut microbe in IBD patients	FL
96	Delftia	s__	0.1	Proteobacteria	Fecal and mucosa associated microbe in IBD	FM
97	Desulfovibrio	s__	0.2	Proteobacteria	Sulfate reducing bacteria in IBD	FV
98	Citrobacter	s__	0.2	Proteobacteria	Gut microbe in newly diagnosed with treatment-naïve Crohn's disease patients	FY
99	Halomonas	s__	0.9	Proteobacteria	Intestinal microflora in chronic kidney disease	GB
100	Aggregatibacter	s__	0.6	Proteobacteria	Causes fungal microbiota dysbiosis in IBD	GC
101	Haemophilus	s__	0.3	Proteobacteria	Treatment naïve microbiome in new onset Crohn's disease	GD
102	Pseudomonas	s__	0.8	Proteobacteria	Infection in Children with Early-onset Crohn's Disease	GG
103	g__	s__	0.2	Proteobacteria	Bacteria in human Ulcerative Colitis patients	GH
104	g__	s__	0.1	TM7	No role in IBD	
105	Other	Other	0.5	Actinobacteria	Alters fecal microbiota in pediatric IBD patients	GO
106	Eggerthella	Other	0.1	Actinobacteria	Causes bacteremia in Crohn's disease patient	GQ
107	Bacteroides	Other	0.1	Bacteroidetes	Commensal bacteria that induces colitis	GR
108	Prevotella	Other	0.7	Bacteroidetes	A microbial signature of Crohn's disease	GS
109	Other	Other	3.2	Firmicutes	Gut microbe in experimental colitis	GT
110	Other	Other	7.5	Firmicutes	Fecal and mucosa associated microbe in IBD	GW
111	Weissella	Other	1.5	Firmicutes	Gut microbe in IBD patients	GX
112	Other	Other	0.1	Firmicutes	Commensal gut bacteria in IBD	HA
113	Other	Other	1.1	Proteobacteria	Causes microbial dysbiosis in pediatric Crohn's disease	HD
114	Paracoccus	Other	0.3	Proteobacteria	Identified gut microbe in IBD patients	HH
115	Other	Other	0.1	Proteobacteria	Fecal and mucosa associated microbe in IBD	HK
116	Other	Other	0.7	Proteobacteria	Fecal and mucosa associated microbe in IBD	HL
117	Other	Other	0.1	Proteobacteria	Identified gut microbe in IBD patients	HN
118	Other	Other	0.5	Proteobacteria	Adult fecal microbe	HO
AFRICAN AMERICANS						
1	Lactobacillus	zeae	1.1	Firmicutes	Maintains remission of ulcerative colitis	A
2	Prevotella	stercorea	4.6	Bacteroidetes	Alters mucosal microbiota in the colon of patients with IBD	H
3	Shuttleworthia	satelles	0.4	Firmicutes	Identified in the human ileum	J
4	Acinetobacter	rhizosphaerae	0.2	Proteobacteria	Identified gut microbe in IBD patients	K
5	Microbacterium	maritypicum	0.2	Actinobacteria	Fecal microbiome in Obesity	V
6	Acinetobacter	lwoffii	0.5	Proteobacteria	Gut bacteria in multiple sclerosis patients	W
7	Eggerthella	lenta	0.7	Actinobacteria	Causes bacteremia in Crohn's disease patient.	AA
8	Stenotrophomonas	geniculata	2.0	Proteobacteria	Identified gut microbe in IBD patients	AG
9	Corynebacterium	durum	0.1	Actinobacteria	Identified gut microbe in IBD patients	AK
10	Eubacterium	dolichum	0.5	Firmicutes	Causes dysbiosis of the intestinal microbiota	AL
11	Brevundimonas	diminuta	0.1	Proteobacteria	Identified in the adult fecal microbiota of allergy patients	AO

(Continued)

TABLE 4 | Continued

Sl. No.	Bacteria genus	Bacteria species	Proportion (%)	Bacteria phylum	Function in IBD	NCBI genome database link
12	Lysinibacillus	boronitolerans	5.0	Firmicutes	Identified gut microbe in IBD patients	AT
13	Staphylococcus	aureus	0.2	Firmicutes	Causes Crohn's disease	AU
14	Peptostreptococcus	anaerobius	24.9	Firmicutes	Causes dysbiosis in IBD	AW
15	Pseudomonas	alcaligenes	1.1	Proteobacteria	Identified in the gut microbiota of IBD	AX
16	Propionibacterium	acnes	0.6	Actinobacteria	Intestinal microbe in Liver disease	BA
17	Methanobrevibacter	s__	0.4	Euryarchaeota	Identified in the gut of IBD	BB
18	g__	s__	0.2	Acidobacteria	Identified in human gut microbiota	BC
19	g__	s__	4.3	Acidobacteria	Identified in the gut microbiome of Type 2 Diabetes patients	BD
20	g__	s__	0.3	Actinobacteria	Identified in gut microbiota in IBD	BE
21	Varibaculum	s__	0.6	Actinobacteria	Identified in the gut of a premature infant	BH
22	Corynebacterium	s__	0.5	Actinobacteria	Causes experimental colitis	BI
23	Arthrobacter	s__	0.2	Actinobacteria	Fecal microflora in chronic IBD patients	BL
24	Slackia	s__	0.2	Actinobacteria	Alters human gut microbiome in Multiple Sclerosis	BS
25	Chryseobacterium	s__	0.3	Bacteroidetes	Fecal and mucosa associated microbe in IBD	CF
26	Cloacibacterium	s__	0.2	Bacteroidetes	Identified in the rectum of human colorectal adenoma patients	CG
27	g__	s__	0.2	Cyanobacteria	Identified in human gut microbiota	CJ
28	Bacillus	s__	2.7	Firmicutes	Increases cytokine levels in IBD	CL
29	Alloiococcus	s__	6.0	Firmicutes	Identified gut microbe in IBD patients	CT
30	Lactobacillus	s__	0.2	Firmicutes	Maintains remission of ulcerative colitis	CW
31	Lactococcus	s__	0.3	Firmicutes	Used in the treatment of Crohn's disease	CX
32	g__	s__	0.1	Firmicutes	Gut microbe in IBD	DA
33	g__	s__	1.3	Firmicutes	A microbial signature of Crohn's disease	DB
34	Christensenella	s__	0.2	Firmicutes	Identified gut microbe	DC
35	Clostridium	s__	0.4	Firmicutes	causes infection of the gut in IBD	DE
36	Pseudoramibacter_Eubacterium	s__	0.9	Firmicutes	Metabolizes Linoleic acid in the Gut	DF
37	Lachnospira	s__	0.3	Firmicutes	Gut bacteria in Crohn's disease patients	DK
38	g__	s__	0.3	Firmicutes	A microbial signature of Crohn's disease	DQ
39	Peptostreptococcus	s__	0.4	Firmicutes	Causes gut microbiota dysbiosis in IBD	DR
40	Oscillospira	s__	0.2	Firmicutes	Gut microbe in IBD patients	DU
41	Ruminococcus	s__	2.2	Firmicutes	Dominant in gut microbiome of IBD patients	DV
42	g__	s__	0.4	Firmicutes	Gut microbe underlying the onset of IBD	DW
43	Acidaminococcus	s__	1.0	Firmicutes	Gut microbe in IBD	DX
44	Phascolarctobacterium	s__	0.5	Firmicutes	Causes dysfunction of the intestinal microbiome in IBD	DZ
45	Schwartzia	s__	0.1	Firmicutes	Causes fecal microbial dysbiosis in IBD	EA
46	Selenomonas	s__	0.5	Firmicutes	Causes dysbiosis in colorectal cancer	EB
47	Anaerococcus	s__	0.5	Firmicutes	Microbe in Inflammatory Pouch Complications	EE
48	Finegoldia	s__	0.4	Firmicutes	Intestinal microbe in colorectal cancer	EF
49	g__	s__	0.8	Firmicutes	Gut microbe in GI diseases	EI
50	Bulleidia	s__	0.1	Firmicutes	Fecal-associated and mucosalassociated microbiota in irritable bowel syndrome patients	EJ
51	Fusobacterium	s__	8.4	Fusobacteria	Identified from colonic biopsies of IBD patients	EN
52	Leptotrichia	s__	1.7	Fusobacteria	Causes gut mucosal inflammation in Rheumatoid arthritis patients	EO
53	g__	s__	0.7	Gemmatimonadetes	Identified gut microbe in IBD patients	EP
54	Ochrobactrum	s__	0.1	Proteobacteria	Causes early bacterial dependent induction of inducible nitric oxide synthase (iNOS) in epithelial cells in experimental colitis	EU
55	g__	s__	1.5	Proteobacteria	Intestinal microbe in children with severe and complicated acute viral gastroenteritis	EV

(Continued)

TABLE 4 | Continued

Sl. No.	Bacteria genus	Bacteria species	Proportion (%)	Bacteria phylum	Function in IBD	NCBI genome database link
56	g__	s__	0.1	Proteobacteria	Involved in host-microbial cross talk in IBD	FG
57	Sutterella	s__	0.2	Proteobacteria	Gut microbe in experimental colitis	FH
58	Burkholderia	s__	0.4	Proteobacteria	Causes dysfunction of GALT and gut flora in IBD	FI
59	Lautropia	s__	0.2	Proteobacteria	Causes fecal microbial dysbiosis in IBD	FJ
60	Comamonas	s__	0.4	Proteobacteria	Identified gut microbe in IBD patients	FL
61	Ralstonia	s__	0.2	Proteobacteria	Microbiota in the Mucosa of Patients With Ulcerative Colitis	FP
62	Bilophila	s__	0.1	Proteobacteria	Causes irritable bowel syndrome	FU
63	Desulfovibrio	s__	0.1	Proteobacteria	Sulfate reducing bacteria in IBD	FV
64	Halomonas	s__	0.7	Proteobacteria	Intestinal microflora in chronic kidney disease	GB
65	g__	s__	0.1	Proteobacteria	Microbe in colon tissue from IBD subjects	GE
66	Acinetobacter	s__	0.7	Proteobacteria	Tissue associated intestinal microflora	GF
67	Pseudomonas	s__	0.1	Proteobacteria	Infection in Children with Early-onset Crohn's Disease	GG
68	g__	s__	0.8	TM7	No role in IBD	
69	Other	Other	0.3	Actinobacteria	Alters fecal microbiota in pediatric IBD patients	GO
70	Eggerthella	Other	0.1	Actinobacteria	Causes bacteremia in Crohn's disease patient	GQ
71	Bacteroides	Other	0.7	Bacteroidetes	Commensal bacteria that induces colitis	GR
72	Prevotella	Other	3.2	Bacteroidetes	A microbial signature of Crohn's disease	GS
73	Other	Other	2.8	Firmicutes	Gut microbe in experimental colitis	GT
74	Paenibacillus	Other	0.1	Firmicutes	Gut microbe in a healthy infant	GU
75	Other	Other	2.2	Firmicutes	Fecal and mucosa associated microbe in IBD	GW
76	Paracoccus	Other	0.1	Proteobacteria	Identified gut microbe in IBD patients	HH
77	Other	Other	0.6	Proteobacteria	Fecal and mucosa associated microbe in IBD	HL
78	Other	Other	0.1	Proteobacteria	Adult fecal microbe	HO
79	Other	Other	0.4	Proteobacteria	Mucosal and fecal microbe	HP
80	Acinetobacter	Other	2.2	Proteobacteria	Tissue associated intestinal microflora in colitis patients	HQ
81	Pseudomonas	Other	0.2	Proteobacteria	Gut microbe in children with early onset Crohn's disease	HR

Specific Information of functions was adapted from NCBI Genome Database (https://www.ncbi.nlm.nih.gov/genome/).
The bacterial species that could not be identified at the genus level are mentioned as g___ and the bacterial species that could not be identified at the species level are mentioned as s___.

compared to adjacent healthy colon specimens. We suggest that pathogenic bacteria belonging to these two phyla have a greater impact on colon motility function in colitis patients (**Tables 1**, **3**). Although the incidence of IBD is increasing among African Americans (AA), the underlying causes are completely unknown (Sofia et al., 2014). Our study further highlight a significant disparity in bacterial dysbiosis among AA compared to CA colitis patients (**Figure 3**).

CA specimens had significantly higher levels of *Fusobacterium*, *Parabacteroides*, *Citrobacter*, *Haemophilus*, *Acinetobacter*, *Pseudomonas,* and *Stenotrophomonas*. *Fusobacterium nucleatum* is known to have a well-characterized role in the oral cavity. We have determined that *Fusobacterium* can be recovered from human full thickness colon specimens and this could indicate their ability to survive and proliferate inside host cells. *Parabacteroides* was found to be dominant in the acute phase of IBD in CA patients. *Citrobacter* is an epithelial cell adherent pathogen and can subvert inflammation in colitis. *Pseudomonas* interacts with the mucosal layer of colon and disrupts the mucosal barrier integrity leading to colitis in CA patients.

The AA specimens had significantly higher levels of *Prevotella* and *Clostridia*. *Prevotella* augments T-helper cells mediated colon mucosal inflammation by activating Toll-like receptor 2 leading to production of T-helper cells polarizing cytokines by antigen-presenting cells, including interleukins. In addition, *Prevotella* induce epithelial cells to produce interleukins and cytokines that can promote recruitment of neutrophils and mucosal T-helper cell immune responses. *Prevotella* can mediate inflammation of the mucosa leading to the circulation of bacteria, bacterial products and other inflammatory mediators. *Prevotella* could augment release of inflammatory mediators from immune cells and various stromal cells in colitis in AA patients. *Clostridium* can disrupt gut immune dormancy and cause infectious colitis in AA patients. Collectively, our data suggest that the presence of pathogenic bacteria in AA

TABLE 5 | Proportions of bacterial species of unknown function colonized in full thickness colon of colitis patients.

Sl. No.	Bacteria genus	Bacteria species	Proportion (%)	Bacteria phylum	Function in IBD	NCBI genome database link
ADJACENT HEALTHY COLON						
1	Micrococcus	luteus	0.01	Actinobacteria	No role in IBD	X
2	Arthrobacter	s__	0.01	Actinobacteria	No role in IBD	BL
3	Propionicimonas	s__	0.01	Actinobacteria	No role in IBD	BN
4	Paludibacter	s__	0.01	Bacteroidetes	No role in IBD	BW
5	Chryseobacterium	s__	0.02	Bacteroidetes	No role in IBD	CF
6	Calothrix	s__	0.03	Cyanobacteria	No role in IBD	CK
7	Novosphingobium	s__	0.02	Proteobacteria	No role in IBD	FE
DISEASED COLON (ULCERATIVE COLITIS)						
1	Micrococcus	luteus	0.01	Actinobacteria	No role in IBD	X
2	Arthrobacter	s__	0.02	Actinobacteria	No role in IBD	BL
3	Propionicimonas	s__	0.1	Actinobacteria	No role in IBD	BN
4	Paludibacter	s__	0.03	Bacteroidetes	No role in IBD	BW
5	Chryseobacterium	s__	0.1	Bacteroidetes	No role in IBD	CF
6	Calothrix	s__	0.1	Cyanobacteria	No role in IBD	CK
7	Novosphingobium	s__	0.04	Proteobacteria	No role in IBD	FE
DISEASED COLON (CROHN'S COLITIS)						
1	Micrococcus	luteus	0.02	Actinobacteria	No role in IBD	X
2	Arthrobacter	s__	0.2	Actinobacteria	No role in IBD	BL
3	Propionicimonas	s__	0.02	Actinobacteria	No role in IBD	BN
4	Paludibacter	s__	0.02	Bacteroidetes	No role in IBD	BW
5	Chryseobacterium	s__	0.3	Bacteroidetes	No role in IBD	CF
6	Calothrix	s__	0.1	Cyanobacteria	No role in IBD	CK
7	Novosphingobium	s__	0.01	Proteobacteria	No role in IBD	FE

Specific Information of functions was adapted from NCBI Genome Database (https://www.ncbi.nlm.nih.gov/genome/).
The bacterial species that could not be identified at the genus level are mentioned as g___ and the bacterial species that could not be identified at the species level are mentioned as s___.

full thickness diseased specimens could adversely affect colon motility.

Additionally, our data in UC and CC specimens show the presence of several orange (*Prevotella*, *Peptostreptococcus*, *Eubacterium*, *Fusobacterium*, and *Campylobacter*), red (*Porphyromonas*), purple (*Veillonella*), and yellow (*Streptococcus*) complex putative oral pathogens known to cause gingivitis and periodontitis among IBD patients (**Tables 1**, **3**). Previous studies using mucosal biopsies and feces have shown that gut microbiota in bowel diseases is characterized by an increase in certain phyla such as Proteobacteria, Firmicutes, genus *Bifidobacterium,* as well as a reduction in the amounts of genera *Ruminococcus*, *Clostridia* and (in some cases) *Faecalibacterium* (Lane et al., 2017; Nishida et al., 2018). However, none of the earlier studies using feces have shown a shift in the balance between Phyla Bacteroidetes and Firmicutes among UC or CC patients; even though this was observed in healthy individuals (Mariat et al., 2009; Koliada et al., 2017). In contrary to our results, one study using mucosal biopsies has shown a significantly decreased Firmicutes to Bacteroidetes ratio in both UC and CC compared with controls (Kabeerdoss et al., 2015). Collectively, our data suggest that the putative oral pathogens found in diseased colon specimens may modulate the proportion of non-detrimental gut bacteria, thus potentially worsening the condition of the colon in colitis patients.

Oral bacterial species like *Porphyromonas*, *Peptostreptococcus*, *Eubacterium*, *Fusobacterium*, *Streptococcus salivarius, S. mitis, S. bovis, Veillonella* spp., *Staphylococcus* aureus, *S. epidermidis,* and *Campylobacter* spp. can convert nitrate to nitrite. A large amount of bioactive NO is found in the gastrointestinal tract, generated by dietary sources and by conversion of anaerobic bacteria in the oral cavity, or by anaerobic reaction with nitrate in the colon by *Escherichia coli* spp. The entero-salivary nitrate conversion pathway provides a rich source of bioactive NO and nitrate-reducing bacteria, such as *Veillonella*. In this pathway, nitrate is obtained by the salivary gland and is then concentrated in the saliva. Various facultative anaerobic bacteria on the top of the tongue effectively reduces nitrate to nitrite. The bacteria then use the nitrate and the nitrite as electron acceptors in their respiration process. This also helps the host in the first steps of converting nitrate to NO. The salivary nitrate then reaches the systemic circulation, various enzymatic reactions occur leading to reduction to NO, and other reactive nitrogen intermediates. The oral cavity plays an important role the production of nitric oxide, and specifically, employs the nitrate-nitrite-NO pathway in the oral cavity. It is well known that oral cavity bacteria can migrate to the colon. Taken together, our data suggest that the

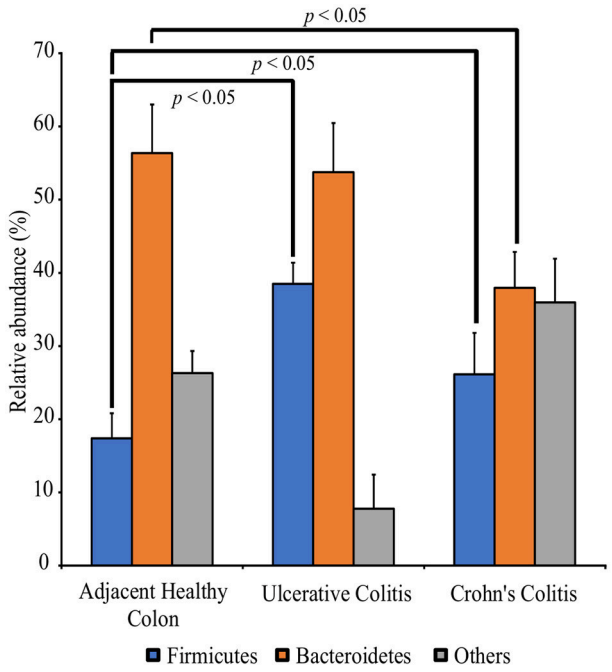

FIGURE 2 | Perturbation of the full thickness colon microbiome in Colitis specimens as compared to adjacent healthy specimens. Specimens are categorized into adjacent healthy colon ($n = 13$), Ulcerative colitis (UC, $n = 13$) and Crohn's colitis (CC, $n = 13$). Data represented are the mean of relative abundances of each phylum identified in specimens belonging to each group while error bars indicate standard error. Diseased specimens demonstrate a balance between the Phyla Firmicutes and Bacteroidetes. Conversely, healthy colon specimens demonstrate a significantly higher proportion of Phyla Bacteroidetes. *$p < 0.05$ by Mann-Whitney *U* Test ($n = 13$ under each group).

putative oral pathogens found in diseased colon specimens may survive by exploiting the nitrate-nitrite-NO pathway to modulate the proportion of non-detrimental gut bacteria, thus potentially worsening the condition of colon in colitis patients (**Figure 4**).

Previous studies suggest that enteric neurons and smooth muscle mediated gut motility is impaired in colitis patients (Snape et al., 1991; Vermillion et al., 1993). IBD associated gut inflammation affects the morphological and functional changes in the myenteric/enteric nervous system (ENS) and nitric oxide (NO) synthesis (Takahashi, 2003; Kono et al., 2004). Experimental studies have also shown that gut bacteria have a role in oxidative stress induced gut inflammation by controlling metabolic endotoxemia in obese mice (Cani et al., 2008). We have shown that polybacterial oral infection decrease the expression of nNOS and NRF2-phase II enzymes in the gut and this could lead to impaired colon motility (Gangula et al., 2015; Walker et al., 2018).

Some of the gut bacteria we have identified in the full thickness colon specimens in the present study, including *Bacteroides*, *Prevotella*, *Pseudomonas*, etc., have been identified in colon mucosal biopsies in earlier studies (Bibiloni et al., 2006). These bacteria evoke inflammatory responses affecting the innermost lining of colon. Many specific beneficial bacteria, including members of *Bacteroides* and *Prevotella* groups, *C. coccoides*, and Lactic acid bacteria were known to be decreased in colitis patients (Gibson et al., 1991). Specimens used in prior studies were colon mucosal biopsies or stool samples; but not full thickness colon specimens (Gibson et al., 1991; Bibiloni et al., 2006). Full-thickness colon consists of four layers of tissue including mucosa, submucosa, muscularis, and serosa.

Novel to this research design, full thickness colon specimens were obtained because colitis patients often experience colon motility abnormalities (Snape et al., 1991; Annese et al., 1997; Vrees et al., 2002). Several lines of evidence suggest that nitrergic neurons that releases NO via nNOS are known to play a pivotal role in colon motility (Kono et al., 2004; Winston et al., 2013). Previous studies have demonstrated that nitrergic neurons are degenerated in colitis (Onori et al., 2005; Sung et al., 2006). Recent studies from our laboratory indicate that nNOS, as well as antioxidants (NRF2 regulated-Phase II enzymes) protein expression are down-regulated in diseased colon specimens (Myers et al., 2014; Gangula et al., 2017). Furthermore, our previous studies demonstrated that polybacterial infection led to a decrease in nNOS, NRF2 and antioxidants protein expression in the colon tissues (Gangula et al., 2015). In addition, studies have shown that NO may play homeostatic role in gut inflammation (Kolios et al., 2004). Taken together, our data suggest that elevated levels of oral and gut pathogens in diseased colon full thickness specimens could contribute to impaired nNOS-NO-NRF2-Phase II system and colon motility abnormalities in IBD patients (**Figure 4**).

To our knowledge, our study is the first to report the presence of several microbiota of unknown function in IBD including *Micrococcus luteus*, Chloracidobacteria, *Arthrobacter*, *Propionicimonas*, *Paludibacter*, *Chryseobacterium*, *Calothrix,* and *Novosphingobium* (**Table 5**). These new microbiota members have not been identified in mucosal/fecal specimens in previous studies, suggesting that these bacteria are primarily colonized in the neuromuscular compartment. Additional studies are warranted to characterize the novel bacteria and investigate their specific role in colon motility and constipation in IBD patients.

In summary, this study have identified specific bacterial pathogens potentially associated with colon motility in IBD patients. The observations showed that some putative oral pathogens belonging to the Phyla Firmicutes (Streptococcus, Staphylococcus, Peptostreptococcus), and Fusobacteria (Fusobacterium) dominated in the microbiomes of CC and UC diseased specimens and might involve the modulation of colon motility in IBD.

STUDY LIMITATIONS

The limitations of the study include the smaller sample size across disease and race groups making this as a preliminary study. In spite of the limitations in sample size and the fact that some of the identified bacteria were not significantly altered in colitis specimens, we were still able to observe differences in the microbiome between CA and AA colitis patients. This could be due to amplicon sequencing of a shorter conserved region of 16S rRNA gene instead of in depth shotgun sequencing.

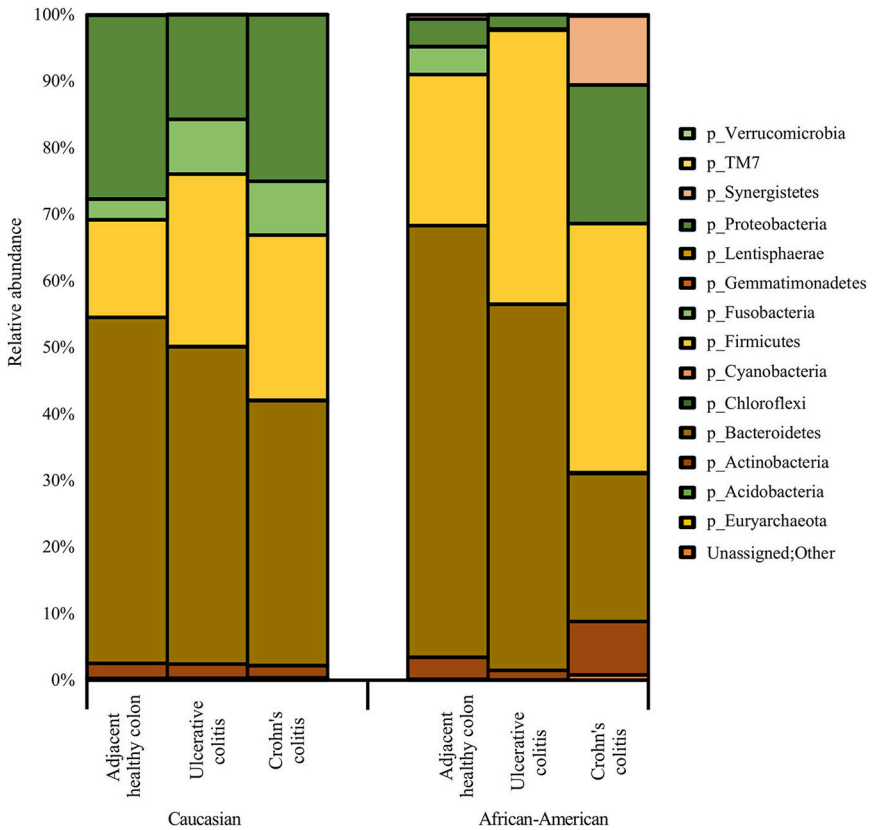

FIGURE 3 | Summary of major bacterial taxa showing the relative abundance of oral and gut bacteria at the Phylum level in the colitis and adjacent healthy specimen groups under each race. Data represented are the mean of relative abundances of each Phyla detected in samples belonging to each group. The dominant phyla across all samples (both diseased and healthy specimens) were Bacteroidetes, followed by Firmicutes and Proteobacteria. Other major phyla observed among these specimens also include Actinobacteria, Fusobacteria, and Synergistetes. The Phylum Proteobacteria did not show any significant difference between healthy colon specimens and diseased colon specimens. A larger proportion of unassigned bacteria (0.3%) was identified in AA Crohn's Colitis patients compared to other groups.

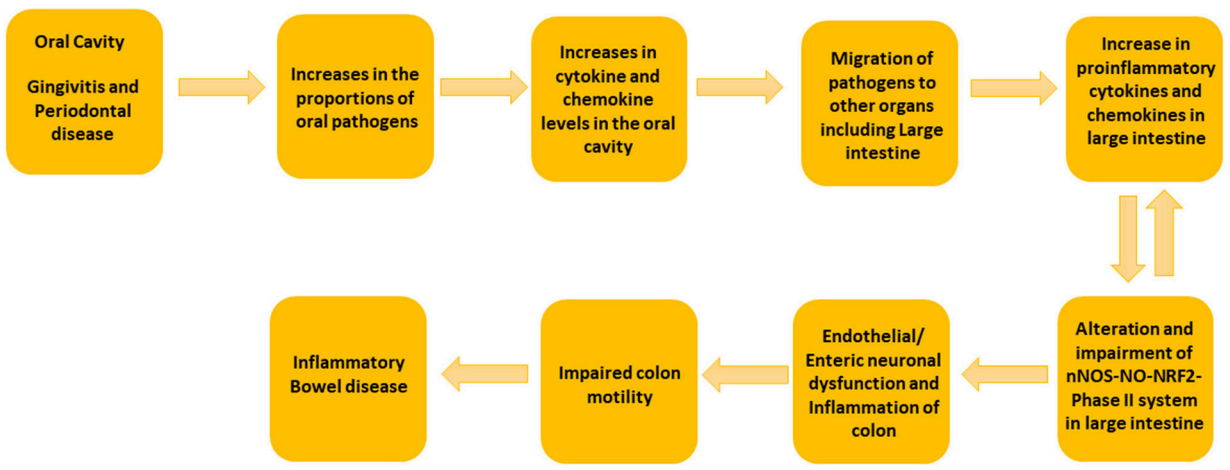

FIGURE 4 | Schematic Representation of the suggested mechanism involved in the development of colitis by oral and gut microbiome. We propose that the increase in the concentrations of putative oral pathogens elevates the cytokine and chemokine levels in oral cavity. When putative oral pathogens travel to the gut, they can colonize locally and lead to the elevated levels of proinflammatory cytokines. This can effect on nNOS-NO-NRF2-Phase II system in the large intestine and could lead to colon dysmotility and colitis.

Moreover, we did not profile the oral microbiome from oral specimens (dental plaque, etc.) in the same IBD patients from whom full thickness colon specimens were collected. Finally, host-microbiome interaction studies are needed to better discern specific roles of the oral and gut bacteria in the development of colitis. Future studies are aimed to collect oral and fecal specimens therefore a comparative experiments in regards to changes in microbiome, along with specific key proteins will be conducted from the same patient.

AUTHOR CONTRIBUTIONS

VD, SM, KS, SP, SS, PG, and MT have contributed both for data analysis and manuscript preparation. DS, CF-D, LK, SA, and JS have contributed in manuscript preparation.

ACKNOWLEDGMENTS

The authors sincerely thank University of North Carolina at Chapel Hill School of Medicine- Microbiome Core Facility (UNC; MC) for performing amplicon sequencing. We thank CHTN for providing diseased and healthy specimens. We further thank dental student doctors Mr. A. Arab and J. Hodges for their initial contribution on this project. The Meharry Bioinformatics Core is funded in part by NIH grants MD007593 and MD007586. SA is supported by NIMHD R-CTR grant No. 54544MD007593 and NCI grant No. 5454CA163069. This work is supported in part by 1SC1GM121282 funded to PG. In addition, Research reported in this publication was supported by the National Institute of General Medical Sciences of the National Institutes of Health under Award Number SG1GM121282 (PG).

REFERENCES

Agossa, K., Dendooven, A., Dubuquoy, L., Gower-Rousseau, C., Delcourt-Debruyne, E., and Capron, M. (2017). Periodontal manifestations of inflammatory bowel disease: emerging epidemiologic and biologic evidence. *J. Periodontal Res.* 52, 313–324. doi: 10.1111/jre.12422

Annese, V., Bassotti, G., Napolitano, G., Usai, P., Andriulli, A., and Vantrappen, G. (1997). Gastrointestinal motility disorders in patients with inactive Crohn's disease. *Scand. J. Gastroenterol.* 32, 1107–1117.

Atarashi, K., Suda, W., Luo, C., Kawaguchi, T., Motoo, I., Narushima, S., et al. (2017). Ectopic colonization of oral bacteria in the intestine drives TH1 cell induction and inflammation. *Science* 358, 359–365. doi: 10.1126/science.aan4526

Bassotti, G., Antonelli, E., Villanacci, V., Salemme, M., Coppola, M., and Annese, V. (2014). Gastrointestinal motility disorders in inflammatory bowel diseases. *World J. Gastroenterol.* 20, 37–44. doi: 10.3748/wjg.v20.i1.37

Bibiloni, R., Mangold, M., Madsen, K. L., Fedorak, R. N., and Tannock, G. W. (2006). The bacteriology of biopsies differs between newly diagnosed, untreated, Crohn's disease and ulcerative colitis patients. *J. Med. Microbiol.* 55, 1141–1149. doi: 10.1099/jmm.0.46498-0

Cani, P. D., Bibiloni, R., Knauf, C., Waget, A., Neyrinck, A. M., Delzenne, N. M., et al. (2008). Changes in gut microbiota control metabolic endotoxemia-induced inflammation in high-fat diet-induced obesity and diabetes in mice. *Diabetes* 57, 1470–1481. doi: 10.2337/db07-1403

Caporaso, J. G., Bittinger, K., Bushman, F. D., DeSantis, T. Z., Andersen, G. L., and Knight, R. (2010a). PyNAST: a flexible tool for aligning sequences to a template alignment. *Bioinform.* 26, 266–267. doi: 10.1093/bioinformatics/btp636

Caporaso, J. G., Kuczynski, J., Stombaugh, J., Bittinger, K., Bushman, F. D., Costello, E. K., et al. (2010b). QIIME allows analysis of high-throughput community sequencing data. *Nat. Methods* 7, 335–336. doi: 10.1038/nmeth.f.303

Edgar, R. C. (2010). Search and clustering orders of magnitude faster than BLAST. *Bioinformatics* 26, 2460–2461. doi: 10.1093/bioinformatics/btq461

Gangula, P., Ravella, K., Chukkapalli, S., Rivera, M., Srinivasan, S., Hale, A., et al. (2015). Polybacterial periodontal pathogens alter vascular and gut BH_4/nNOS/NRF2-phase II enzyme expression. *PLoS ONE* 10:e0129885. doi: 10.1371/journal.pone.0129885.

Gangula, P. R., Smoot, D. T., Izban, M., Ballard, B., and Adunyah, S. (2017). "Expression of NO and NRF2 enzymes in Human Colitis," in *Proceedings of the RCMI Translational Science 2017 Conference* (Washington, DC), 78.

Geboes, K., and Collins, S. (1998). Structural abnormalities of the nervous system in Crohn's disease and ulcerative colitis. *Neurogastroenerol. Motil.* 10, 189–202.

Gibson, G. R., Cummings, J. H., and Macfarlane, G. T. (1991). Growth and activities of sulphate-reducing bacteria in gut contents of healthy subjects and patients with ulcerative colitis. *FEMS Microbiol. Lett.* 86, 103–111. doi: 10.1111/j.1574-6968.1991.tb04799.x

Gower, J. C. (2005). "Principal coordinates analysis," in *Encyclopedia of Biostatistics*, eds P. Armitage and T. Colton, (John Wiley & Sons Ltd). doi: 10.1002/0470011815

Haas, B. J., Gevers, D., Earl, A. M., Feldgarden, M., Ward, D. V., Giannoukos, G., et al. (2011). Chimeric 16S rRNA sequence formation and detection in Sanger and 454-pyrosequenced PCR amplicons. *Genome Res.* 21, 494–504. doi: 10.1101/gr.112730.110

Hajishengallis, G. (2015). Periodontitis: from microbial immune subversion to systemic inflammation. *Nat. Rev. Immunol.* 15, 30–44. doi: 10.1038/nri3785

Kabeerdoss, J., Jayakanthan, P., Pugazhendhi, S., and Ramakrishna, B. S. (2015). Alterations of mucosal microbiota in the colon of patients with inflammatory bowel disease revealed by real time polymerase chain reaction amplification of 16S ribosomal ribonucleic acid. *Indian J Med Res.* 142, 23–32. doi: 10.4103/0971-5916.162091

Keegan, K. P., Glass, E. M., and Meyer, F. (2016). MG-RAST, a metagenomics service for analysis of microbial community structure and function. *Methods Mol. Biol.* 1399, 207–233. doi: 10.1007/978-1-4939-3369-3_13

Koliada, A., Syzenko, G., Moseiko, V., Budovska, L., Puchkov, K., Perederiy, V., et al. (2017). Association between body mass index and Firmicutes/Bacteroidetes ratio in an adult Ukrainian population. *BMC Microbiol.* 17:120. doi: 10.1186/s12866-017-1027-1

Kolios, G., Valatas, V., and Ward, S. G. (2004). Nitric oxide in inflammatory bowel disease: a universal messenger in an unsolved puzzle. *Immunology* 113, 427–437. doi: 10.1111/j.1365-2567.2004.01984.x

Kono, T., Chisato, N., Ebisawa, Y., Asama, T., Sugawara, M., Ayabe, T., et al. (2004). Impaired nitric oxide production of the myenteric plexus in colitis detected by a new bioimaging system. *J. Surg. Res.* 117, 329–336. doi: 10.1016/j.jss.2003.11.004

Lane, E. R., Zisman, T. L., and Suskind, D. L. (2017). The microbiota in inflammatory bowel disease: current and therapeutic insights. *J. Inflamm. Res.* 10, 63–73. doi: 10.2147/JIR.S116088

Lira-Junior, R., and Figueredo, C. M. (2016). Periodontal and inflammatory bowel diseases: is there evidence of complex pathogenic interactions? *World J. Gastroenterol.* 22, 7963–7972. doi: 10.3748/wjg.v22.i35.7963

Mariat, D., Firmesse, O., Levenez, F., Guimaraes, V. D., Sokol, H., Dore, J., et al. (2009). The Firmicutes/Bacteroidetes ratio of the human microbiota changes with age. *BMC Microbiol.* 9:123. doi: 10.1186/1471-2180-9-123

Myers, J. N., Schaffer, M. W., Korolkova, O. Y., Williams, A. D., Gangula, P. R., and M'Koma, A. E. (2014). Implications of the colonic deposition of free hemoglobin-α chain: a previously unknown tissue by-product in inflammatory bowel disease. *Inflamm. Bowel Dis.* 20, 1530–1547. doi: 10.1097/MIB.0000000000000144

Nishida, A., Inoue, R., Inatomi, O., Bamba, S., Naito, Y., and Andoh, A. (2018). Gut microbiota in the pathogenesis of inflammatory bowel disease. *Clin. J. Gastroenterol.* 11, 1–10. doi: 10.1007/s12328-017-0813-5

Onori, L., Aggio, A., D'Alo, S., Muzi, P., Cifone, M. G., Mellillo, G., et al. (2005). Role of nitric oxide in the impairment of circular muscle contractility of distended, uninflamed mid-colon in TNBS-induced acute distal colitis in rats. *World J. Gastroenterol.* 11, 5677–5684. doi: 10.3748/wjg.v11.i36.5677

Poli, E., Lazzeretti, M., Grandi, D., Pozzoli, C., and Coruzzi, G. (2001). Morphological and functional alterations of the myenteric plexus in rats with TNBS-induced colitis. *Neurochem. Res.* 26, 1085–1093. doi: 10.1023/A:1012313424144

Popova, C., Dosseva-Panova, V., and Panov, V. (2013). Microbiology of periodontal diseases. a review. *Biotechnol. Biotechnol. Equip.* 27, 3754–3759. doi: 10.5504/BBEQ.2013.0027

Price, M. N., Dehal, P. S., and Arkin, A. P. (2010). FastTree 2-approximately maximum-likelihood trees for large alignments. *PLoS ONE* 5:e9490. doi: 10.1371/journal.pone.0009490.

Schloss, P. D., Westcott, S. L., Ryabin, T., Hall, J. R., Hartmann, M., Hollister, E. B., et al. (2009). Introducing mothur: open-source, platform-independent, community-supported software for describing and comparing microbial communities. *Appl. Environ. Microbiol.* 75, 7537–7541. doi: 10.1128/AEM.01541-09

Snape, W. J. Jr., Williams, R., and Hyman, P. E. (1991). Defect in colonic smooth muscle contraction in patients with ulcerative colitis. *Am. J. Physiol.* 261, G987–G991. doi: 10.1152/ajpgi.1991.261.6.G987

Sofia, M. A., Rubin, D. T., Hou, N., and Pekow, J. (2014). Clinical presentation and disease course of inflammatory bowel disease differs by race in a large tertiary care hospital. *Dig Dis Sci.* 59, 2228–2235. doi: 10.1007/s10620-014-3160-0

Strauss, J., Kaplan, G. G., Beck, P. L., Rioux, K., Panaccione, R., Devinney, R., et al. (2011). Invasive potential of gut mucosa-derived *Fusobacterium nucleatum* positively correlates with IBD status of the host. *Inflamm. Bowel Dis.* 17, 1971–1978. doi: 10.1002/ibd.21606

Sung, T. S., La, J. H., Kim, T. W., and Yang, I. S. (2006). Alteration of nitrergic neuromuscular transmission as a result of acute experimental colitis in rat. *J. Vet. Sci.* 7, 143–150. doi: 10.4142/jvs.2006.7.2.143

Takahashi, T. (2003). Pathophysiological significance of neuronal nitric oxide synthase in the gastrointestinal tract. *J. Gastroenterol.* 38, 421–430. doi: 10.1007/s00535-003-1094-y

Vavricka, S. R., Manser, C. N., Hediger, S., Vogelin, M., Scharl, M., Biedermann, L., et al. (2013). Periodontitis and gingivitis in inflammatory bowel disease: a case-control study. *Inflamm. Bowel. Dis.* 19, 2768–2777. doi: 10.1097/01.MIB.0000438356.84263.3b

Vermillion, D. L., Huizinga, J. D., Riddell, R. H., and Collins, S. M. (1993). Altered small intestinal smooth muscle function in Crohn's disease. *Gastroenterol.* 104, 1692–1699.

Vrees, M. D., Pricolo, V. E., Ptenti, F. M., and Cao, W. (2002). Abnormal motility in patients with ulcerative colitis: the role of inflammatory cytokines. *Arch. Surg.* 137, 439–445. doi: 10.1001/archsurg.137.4.439

Walker, M. Y., Pratap, S., Southerland, J. H., Farmer-Dixon, C. M., Lakshmyya, K., and Gangula, P. R. (2018). Role of oral and gut microbiome in nitric oxide-mediated colon motility. *Nitric Oxide* 73, 81–88. doi: 10.1016/j.niox.2017.06.003

Winston, J. H., Li, Q., and Sarna, S. K. (2013). Paradoxical regulation of ChAT and nNOS expression in animal models of Crohn's colitis and ulcerative colitis. *Am. J. Physiol. Gastrointest. Liver Physiol.* 305, G295–302. doi: 10.1152/ajpgi.00052.2013

Zhao, L., Huang, Y., Lu, L., Yang, W., Huang, T., Lin, Z., et al. (2018). Saturated long-chain fatty acid-producing bacteria contribute to enhanced colonic motility in rats. *Microbiome* 6:107. doi: 10.1186/s40168-018-0492-6

Conflict of Interest Statement: The authors declare that the research was conducted in the absence of any commercial or financial relationships that could be construed as a potential conflict of interest.

Copyright © 2019 Dinakaran, Mandape, Shuba, Pratap, Sakhare, Tabatabai, Smoot, Farmer-Dixon, Kesavalu, Adunyah, Southerland and Gangula. This is an open-access article distributed under the terms of the Creative Commons Attribution License (CC BY). The use, distribution or reproduction in other forums is permitted, provided the original author(s) and the copyright owner(s) are credited and that the original publication in this journal is cited, in accordance with accepted academic practice. No use, distribution or reproduction is permitted which does not comply with these terms.

frontiers in Microbiology

ORIGINAL RESEARCH
published: 11 January 2019
doi: 10.3389/fmicb.2018.03281

Elucidating the Immune-Related Mechanisms by Which Probiotic Strain *Lactobacillus casei* BL23 Displays Anti-tumoral Properties

*Elsa Jacouton, Marie-Laure Michel, Edgar Torres-Maravilla, Florian Chain, Philippe Langella and Luis G. Bermúdez-Humarán**

Micalis Institute, INRA, AgroParisTech, Université Paris-Saclay, Jouy-en-Josas, France

We have recently described antitumor properties of *Lactobacillus casei* BL23 strain in both a mouse allograft model of human papilloma virus (HPV)-induced cancer and dimethylhydrazine-associated colorectal cancer. However, the mechanisms underlying these beneficial effects are still unknown. Interestingly, *in vitro* cellular models show that this bacterium is able to stimulate the production of high levels of IL-2. Because this cytokine has well-known antitumor properties, we decided to explore its role in the anti-cancer effects of BL23 using the HPV-induced cancer model. We found a negative correlation between IL-2 and tumor size confirming the necessity of IL-2 to protect from tumor development. Then, we blocked IL-2 synthesis using neutralizing monoclonal antibodies in mice that were challenged with lethal levels of tumor cells; this led to a significant reduction in the protective abilities of BL23. Next, we used a genetically modified strain of *Lactococcus lactis* to deliver exogenous IL-2 to the system, and in doing so, we were able to partially mimic the antitumor properties of BL23. Additionally, we showed the systemic role of T-cells in tumor protection through a negative correlation between tumor size and T-cells subpopulations and an increasement of BL23-specific local Foxp3 levels in tumor-bearing mice. Finally, we observed a negative correlation between tumor size and NK+ cells, but local recruitment of NK cells and cytotoxic activity appeared specific to BL23 treatment. Taken together, our data suggest that IL-2 signaling pathway plays an important role in the anti-tumoral effects of probiotic strain *L. casei* BL23. These results encourage further investigation in the use of probiotic strains for potential therapeutic applications to clinical practice, in particular for the treatment of colorectal cancer. Furthermore, our approach could be extended and applied to other potential beneficial microorganisms, such as gut microbiota, in order to better understand the crosstalk between microbes and the host.

Keywords: probiotic, *Lactobacillus casei* BL23, anti-tumor, cancer, IL-2

OPEN ACCESS

Edited by:
Learn-Han Lee,
Monash University Malaysia, Malaysia

Reviewed by:
Zhigang Zhou,
Feed Research Institute (CAAS), China
Simone Guglielmetti,
University of Milan, Italy
Eugenia Bezirtzoglou,
Democritus University of Thrace, Greece
Eric Claassen,
Vrije Universiteit Amsterdam, Netherlands

***Correspondence:**
Luis G. Bermúdez-Humarán
luis.bermudez@inra.fr

Specialty section:
This article was submitted to Microbial Symbioses, a section of the journal Frontiers in Microbiology

Received: *15 September 2018*
Accepted: *17 December 2018*
Published: *11 January 2019*

Citation:
Jacouton E, Michel M-L, Torres-Maravilla E, Chain F, Langella P and Bermúdez-Humarán LG (2019) Elucidating the Immune-Related Mechanisms by Which Probiotic Strain Lactobacillus casei BL23 Displays Anti-tumoral Properties. Front. Microbiol. 9:3281. doi: 10.3389/fmicb.2018.03281

INTRODUCTION

The Food and Agriculture Organization of the United Nations World Health Organization has defined probiotics as "live microorganisms which, when administered in adequate amounts, confer health benefits on the host" (FAO/WHO, 2002). A growing body of evidence suggests that probiotics can reinforce natural defenses, protect against gastrointestinal disorders, and enhance

either innate or adaptive immunity. Indeed, it has been shown that probiotics can induce dendritic cell (DC) maturation (Delcenserie et al., 2008), enhance natural killer (NK) cell cytotoxicity (Takagi et al., 2001), and upregulate cytokine secretion (Delcenserie et al., 2008; Azcarate-Peril et al., 2011).

Lactobacilli, which belong to the group of lactic acid bacteria (LAB), feature prominently among putative probiotics. In addition, some strains are naturally present in human mucosal surfaces (e.g., vagina and gastrointestinal tract), where they make up a small portion of the microbiota and are thus considered commensals (Martin et al., 2014). Some strains of *Lactobacillus* have been used for centuries in the preservation and production of fermented foods (e.g., yogurt and cheese; (Bernardeau et al., 2008)) and are thus "Generally Recognized As Safe" by the U.S. Food and Drug Administration. These microorganisms exert beneficial health effects on the host, mainly by modulating immune response (Martin et al., 2013). In addition, a number of studies have demonstrated that consumption of probiotics, including lactobacilli, may play a preventive role in the onset of different types of cancer (Kato et al., 1994; Aragón et al., 2015; Hu et al., 2015). It has also been reported that some strains of *Lactobacillus* can induce DC maturation and differentiation of the Th1 immune response, which is important for tumor inhibition (Cai et al., 2016). However, despite the number of studies that have shown anti-cancer effects of different strains of *Lactobacillus* (Khazaie et al., 2012; Konishi et al., 2016; Lenoir et al., 2016), the precise host molecular mechanisms of these antitumor properties remain unclear.

Many studies have proposed that the effects of probiotics might involve: (i) modification of gut pH, (ii) an increase in the production of short-chain fatty acids (SCFAs; e.g., acetate, propionate, and butyrate), (iii) antagonistic activity against pathogens through the production of antimicrobial compounds (such as bacteriocins), or (iv) competition with pathogens for available nutrients, receptors, and growth factors (for review see refs. in (Kahouli et al., 2013)). Also, oral administration of LAB has been shown to effectively reduce DNA damage induced by chemical carcinogens, in particular in different animal models of colorectal cancer (CRC; Uccello et al., 2012; Kahouli et al., 2013). However, in all of these studies the proposed antitumor effects are associated with oral intake of the probiotic. Despite this, we recently demonstrated anticancer effects of the dairy strain BL23 of *L. casei* in a mouse allograft model of human papilloma virus (HPV)-induced cancer when the probiotic was administered intranasally (Lenoir et al., 2016). In addition, we also showed that oral administration of this probiotic strain was able to reduce the severity of 1,2-dimethylhydrazine (DMH)-associated CRC (Lenoir et al., 2016). Although the precise mechanisms of this antitumor effect were not clearly established, we hypothesized that *L. casei* BL23 can activate antitumor immunity and retard tumor growth. Indeed, in the model of DMH-associated CRC we showed that the defense against cancer demonstrated by *L. casei* BL23 was associated with the modulation of T-cells toward a Th17-biased immune response, accompanied by the expression of regulatory cytokines (e.g., IL-6, IL-17, IL-10, and TGF-β). In this study, we decided to further examine the mechanisms of this defense by investigating the host cell-signaling pathway associated with the antitumor properties of *L. casei* BL23, using the HPV-induced cancer model. In particular, we sought to evaluate the potential involvement of the IL-2-driven immune response in the antitumor effects of *L. casei* BL23. This cytokine and its associated pathway have been linked with positive effects in cancer therapy (Rosenberg et al., 1985), in particular in HPV-associated tumor cells (Casana et al., 2002). In addition, *L. casei* BL23 has been reported to induce high levels of this cytokine in both *in vivo* (Dorostkar et al., 2016) and *in vitro* models (including DCs and monocytes; personal observations).

MATERIALS AND METHODS

Bacterial Strains and Growth Conditions

Lactobacillus casei BL23 (Acedo-Felix and Perez-Martinez, 2003; Maze et al., 2010) was grown in MRS medium (Difco, KS, Unites States) at 37°C under static conditions. *L. lactis* MG1363 (Gasson, 1983) and recombinant *L. lactis* NZ9000, which secretes murine IL-2 (strain LL-IL2, **Supplementary Data** and **Supplementary Figure S1**), were grown in M17 medium (Difco, KS, United States) supplemented with 0.5% glucose (GM17) at 30°C under static conditions. Strain LL-IL2 was maintained with chloramphenicol at a concentration of 10 μg/ml. For IL-2 production, the strain was grown to an optical density at 600 nm (OD_{600}) of 0.6, then induced with 10 ng/ml of nisin (Sigma) for 1 h (as previously described in (Bermudez-Humaran et al., 2003)). LL-IL2 culture extraction and immunoblotting assays were performed as described in (Bermudez-Humaran et al., 2015) using murine IL-2 antibodies (Peprotech, see **Supplementary Data**).

TC-1 Cell Line

The mouse (C57BL/6) lung tumor line TC-1 (kindly provided by Dr. T.C. Wu, Johns Hopkins University, Baltimore, MD, United States in 2000) was grown in RPMI (Roswell Park Memorial Institute) medium 1640 (Lonza, Switzerland) supplemented with 10% heat-inactivated fetal calf serum (FCS), 50 U/ml penicillin, and 50 U/ml streptomycin (Lonza, Levallois-Perret, France) in a 5% CO_2 atmosphere. The TC-1 cell line was generated by transduction with a retroviral vector that express HPV-16 E6/E7 plus a retrovirus expressing activated c-Ha-*ras* (Lin et al., 1996). The authenticity of TC-1 cells was regularly controlled in our laboratory, first by the addition in each experiment of both 0.4 mg/ml G418 (Geneticin) (Sigma-Aldrich, St. Louis, MO, Unites States) and 0.2 mg/ml hygromycin (Sigma-Aldrich, St. Louis, MO, United States) to maintain the selective pressure for HPV-16 E6/E7 and c-Ha-*ras*, and second, by confirming the presence of the HPV-I6 E7 gene by PCR (once every 6 months). Once a month, TC-1 cells were confirmed to be mycoplasma-free with a PCR-based detection test.

Mice

Specific pathogen-free C57BL/6 mice (females, 6–8 weeks old; Janvier SAS, St. Berthevin, France) were housed in a pathogen-free isolator (four mice per cage) under sterile conditions in 12-h light cycles in the animal facilities of the National Institute

of Agricultural Research (IERP, INRA, Jouy-en-Josas, France). Animals were supplied with water and fed *ad libitum* (normal chow: R 03–40, SAFE). Temperature and moisture were carefully controlled. Mice were observed once a day to ensure their welfare. All protocols were carried out in accordance with the institutional ethical guidelines of the ethics committee COMETHEA (Comité d'Ethique en Expérimentation Animale of the Centre INRA of Jouy-en-Josas and AgroParisTech), which approved this study.

Production of IL-2 by Bone Marrow Dendritic Cells (BMDCs)

Bone Marrow Dendritic Cells (BMDCs) were generated from bone marrow cells isolated from femurs and tibias of specific pathogen-free C57BL/6 mice (males, 4–6 weeks old; Janvier SAS, St. Berthevin, France). BM cells were separated via either Ficoll-Paque density separation (Lympholyte-Mammal, Cedarlane) or 75 μm strainer and cultured at $\sim 1 \times 10^6$ cells/well using 24-well plates and DMEM medium (Sigma-Aldrich, St. Louis, MO, United States) at 37°C with 10% CO_2. The medium was supplemented with 10% heat-inactivated FCS (Lonza, Switzerland), 50 mM 2-mercaptoethanol (Sigma-Aldrich, St. Louis, MO, United States), 1 mM glutamine (Lonza, Switzerland), 50 U/ml penicillin (Lonza, Switzerland), 50 g/ml streptomycin (Lonza, Switzerland), and 20 ng/ml of recombinant murine granulocyte-macrophage colony-stimulating factor (GM-CSF; Peprotech, France). Freshly prepared medium was added every 3 days. After 10 days, BMDC cultures (higher CD11c expression confirmed by FACS analysis) were treated with *L. casei* BL23 or *L. lactis* MG1363 at a dose of 1:1, 1:40 and 1:100 CFUs per BMDC. After 24 h of incubation, supernatant samples were recovered and examined with ELISA (Mabtech) for the presence of IL-2.

Bacterial Administration in TC-1-Challenged Mice

Groups of mice ($n = 8$) were intranasally (*i.n.*) administered 1×10^9 colony-forming units (CFU) of either *L. casei* BL23, *L. lactis* MG1363, or recombinant LL-IL2, which were suspended in 10 μl of PBS and administered using a micropipette after intraperitoneal anesthetization. All cultures were washed three times in PBS before being suspended for administration. Each mouse received 5 μl of the solution in each nostril on days –35, –21, and –7 (**Supplementary Figure S2A**). Control mice received identical quantities of PBS (i.e., 10 μl). Mice were challenged 7 days after the final bacteria administration (D0) by subcutaneous (*s.c.*) injection in the right rear flank with 5×10^4 TC-1 cells in 100 μl of sterile PBS. The dimensions of the tumor at the site of injection were measured every week in two perpendicular directions with a caliper, and tumor volume was estimated as (length × width^2)/2 (Bermudez-Humaran et al., 2005). Mice were sacrificed by vertebral dislocation at D28 (**Supplementary Figures S2A, S2B**).

For IL-2 blocking experiments, mice received (once every 2 days) intraperitoneal (*i.p.*) injections of 100 μl of IL-2-neutralizing monoclonal antibodies (mAb 500-M127; Peprotech, France) prepared in PBS at 50 μg/ml (**Supplementary Figure S2A**).

In a final experiment, mice were administered *s.c.* 1×10^7 CFU of *L. casei* BL23 ($n = 8$) or PBS ($n = 4$) once every 2 days after challenge with a tumor (**Supplementary Figure S2B**).

Lactobacillus casei BL23 Localization After *i.n.* Administration

Lactobacillus casei BL23 was stained with syto 9 (Live/Dead Baclight Bacterial Viability Kit, ThermoFisher Scientific, France) during 15 min at room temperature in the dark according to the manufacturer's instructions. Then, four mice were administered either with 1×10^9 CFU of stained *L. casei* BL23, unstained *L. lactis* MG1363 or equivalent volume of PBS. Broncho-Alveolar Liquid (BAL), Nasal-Associated Lymphoïd Tissue (NALT) and stomach content were collected 30 min, 24 h and 48 h after *i.n.* administration as previously described in Medaglini et al. (2006). NALT and stomach were mechanically crushed in 300 μl or 1 ml of PBS, respectively, prior to be filtered through 40 μm cell stainer. Stained *L. casei* BL23 was detected using a flow cytometer "(Accuri C6)".

Immune Cells Analysis Using Flow Cytometry

Spleens were collected and mononuclear cells isolated via gentle extrusion of the tissue through a 50-μm-mesh nylon cell strainer (BD). Cells were resuspended in DMEM medium supplemented with 10% FCS, 2 mM L-glutamine, 50 U/mg penicillin, and 50 U/mg streptomycin. Erythrocytes were lysed with red-blood-cell lysing buffer (Sigma-Aldrich, St. Louis, MO, United States). Cells collected at D28 were first stained with eFluor 506-labeled fixable viability dye (eBioscience), and a surface staining was then performed with APC-eFluor780-labeled anti-CD3 (145-2C11), PECy7-labeled anti-NKp46 (29A1.4), PE-labeled anti-CD4 (RM4–5), FITC-labeled anti-Foxp3 (FJK-16s) and Brillant Violet 605-labeled anti-CD8α (53–6.7) antibodies. Flow cytometry analyses were carried out using a BD-Fortessa machine. Data were analyzed using FlowJo software (version X10.0.7).

Analysis of Gene Expression Profiles in Tumor Sections

Tumor samples were stored in RNAlater (Sigma Aldrich, St. Louis, MO, United States) at –80°C following animal sacrifice. Total RNA was extracted using the RNeasy mini-kit (Qiagen, Courtaboeuf, France) according to the manufacturer's recommendations. RNA concentration was measured using a NanoDrop spectrophotometer (NanoDrop Technologies, Wilmington, DE,United States) and 1 μg was used to synthesize cDNA using the High Capacity cDNA Reverse Transcription kit (Applied Biosystems, Foster, CA, United States), following the manufacturer's instructions. The qPCR mixture contained Taqman probes (Life Technologies, France; primers are described in **Table 1**) and reactions were carried out according to the manufacturer's instructions using an ABI Prism 7700 thermal cycler (Applied Biosystems, Foster, CA, United States) in a reaction volume of 20 μl. To quantify and normalize the

TABLE 1 | Sequence of Taqman primers used in this study.

Probes	Targets
Mm00446171_m1	mCD3/CD247
Mm00439860_m1	mIL-2/Itk
Mm00607939_s1	mβ-Actin
Mm01337324_g1	mNKp46/Ncr1
Mm00475162_m1	mFoxp3
Mm01182107_g1	mCD8α

expression data, we used the ΔCt method with β-actin as a reference gene.

Cytotoxic Activity of NK Cells

Natural killer (NK) cells were isolated using the NK cell isolation kit II, mouse (Miltenyl Biotec, France), following the manufacturer's instructions, from mice that had been treated with either *L. casei* BL23 or *L. lactis* MG1363. TC-1 cells were grown as described above and cultivated in petri dishes at 5×10^5 cells per dish for 2 days. NK cells were then added at a 1:20 ratio and cultivated for 5 days before microscopic observations (Zeiss microscope Axio observer Z1) as described in Ribelles et al. (2013).

Statistical Analysis

Data Were Analyzed With Prism Software (Version 5)

All data were displayed as mean ± s.e.m. Comparisons between two groups were performed with *T*-test followed by Mann–Whitney post-test. Groups of three or more animals were analyzed by one-way analysis of variance (ANOVA). Mice treated with *L. casei* BL23 and displaying tumors were excluded from the analysis.

RESULTS

Lactobacillus casei BL23 Has a Protective Effect Against Tumors in the TC-1 Allograft Model of HPV-Induced Cancer

We recently reported that *L. casei* BL23 displayed a protective effect in a mouse allograft model of HPV-induced cancer (Lenoir et al., 2016). Here we first validated these prior observations using the same conditions (e.g., bacteria dosage, *i.n.* administration, schema of administration; **Supplementary Figure S2A**) and we compared these results to those obtained with *L. lactis* MG1363, a LAB strain for which no positive effect has been reported in the HPV-induced cancer model (Bermudez-Humaran et al., 2005). Our results showed that *L. casei* BL23 had a significant protective effect against tumor onset at day 28 (the day on which animals were sacrificed): only 58% (14/24) of mice that had been administered *L. casei* BL23 developed tumors, compared to 100% of mice receiving either PBS or *L. lactis* MG1363 (**Figure 1A**). These results confirm the absence of any positive effect of *L. lactis* MG1363, which is consistent with previous reports (Bermudez-Humaran et al., 2005; Cortes-Perez et al., 2007). We then determined bacterial location after *i.n.* administration using Syto 9 bacterial staining. We mainly found *L. casei* BL23 in NALT and stomach (**Figure 1B**) 24 h and 48 h after administration. Despite a higher *L. casei* BL23 concentration was observed (2069 events/μl as mean in NALT vs. 950 events/μl as mean in stomach) in NALT than in stomach 24h post inoculation; we compared the effect on tumor onset in function of the route of bacterial administration (oral vs. *i.n.*). We confirmed previous data obtained with recombinant bacteria showing no protective effect following oral bacterial administration (**Figure 1C**).

Tumor Size Was Negatively Correlated With Levels of IL-2

Several studies have investigated IL-2 for potential use in tumor growth inhibition. So we determined the local IL-2 expression (in tumor sections) of mice bearing tumors by qPCR. Interestingly, we observed a significant negative correlation between tumor size and local IL-2 levels in tumor samples ($r^2 = -0.75$, $p = 0.0008$, **Supplementary Figure S3A**), suggesting a positive role for this cytokine to treat tumors.

To assess if *L. casei* strain BL23 could exerted its anti-tumor effects *via* IL-2, we first investigated its abilities to induce IL-2 expression in an *in vitro* model of BMDCs. Specifically, BMDCs were treated with either *L. casei* BL23 or *L. lactis* MG1363 for 24 h at MOI 100. As shown in **Figure 2A**, the presence of *L. casei* BL23 specifically induced IL-2 expression while *L. lactis* MG1363 did not. Additionally, we determined an IL-2 dose response in presence of *L. casei* BL23. Our results showed that *L. casei* BL23 significantly increased IL-2 production at MOI 1:40 and 1:100 (**Supplementary Figure S1B**).

We next determined the role of IL-2 in the antitumor effects of *L. casei* BL23 *in vivo*. For this, we blocked IL-2 production in mice via *i.p.* injections of IL-2-neutralizing mAb 2 days before and 2 days after *i.n.* bacterial treatments and then once every 2 days following *s.c.* TC-1 challenge (**Supplementary Figure S2A**). As shown in **Figure 2B**, 62.5% of mice (5/8) treated with *L. casei* BL23 developed tumors over the 28-day test period compared to 100% of control mice (8/8) treated with PBS. Conversely, mice treated with anti-IL-2 mAb lost the protective effect of *L. casei* BL23 (**Figure 2B**): 87.5% of mice (7/8) that were treated with both *L. casei* BL23 and anti-IL-2 mAb developed tumors, and the same result was found with control mice receiving PBS.

In order to confirm that IL-2 had a protective effect against tumor development in our model, mice were *i.n.* administered with a recombinant strain of *L. lactis* which secretes murine IL-2 (LL-IL2, **Supplementary Figure S1A**, and **Supplementary Data**). We confirmed IL-2 production via ELISA prior to administration of the recombinant strain to mice (**Supplementary Figure S1C**). As shown in **Figure 2C**, the administration of LL-IL2 prevented tumor development in 25% of mice (2/8), while tumors were observed in 100% of PBS-treated mice.

Altogether, these data suggest that the IL-2 signaling pathway plays an important role in the ability of BL23 to control tumor development in the HPV-induced model of cancer.

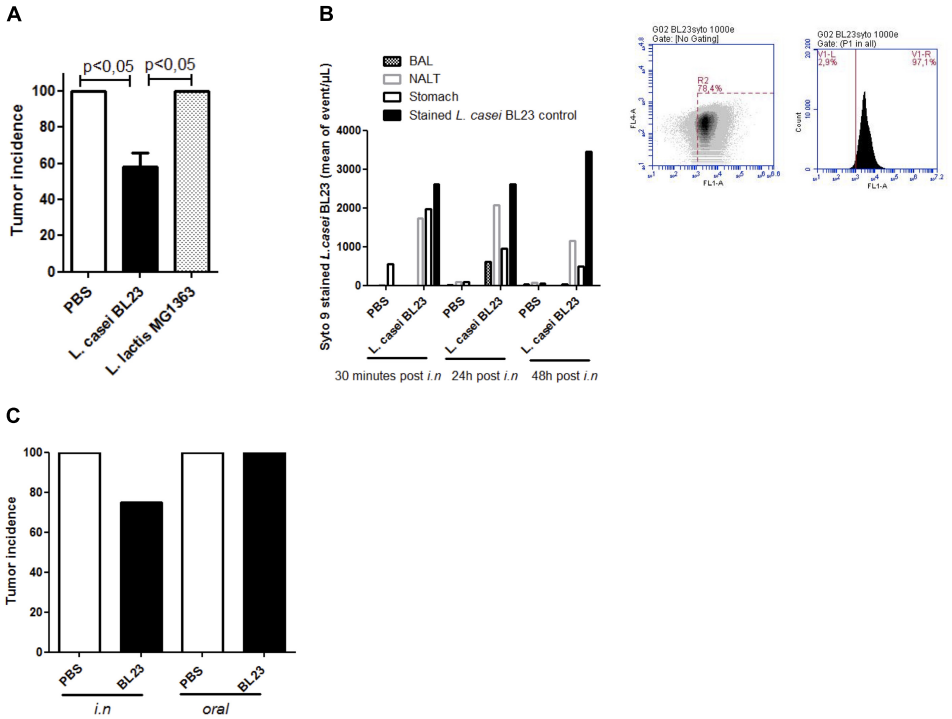

FIGURE 1 | *Lactobacillus casei* BL23 protection against TC1-induced tumors: influence of the route of administration **(A)** Tumor incidence in the TC-1 mouse allograft model of HPV-induced cancer. Mice were intranasally administered either *L. casei* BL23, *L. lactis* MG1363, or sterile PBS three times (bacteria at a concentration of 1×10^9 CFU). A week following the final administration, mice were challenged with 5×10^4 TC-1 tumor cells ($n = 3$ independent *in vivo* experiments at $n = 8$ mice, $p < 0.05$, ANOVA). **(B)** *L. casei* BL23 detection after *i.n.* administration. Mice were *i.n.* administered with stained *L. casei* BL23 ($n = 4$ mice per group), stained *L. casei* BL23 (dilution by 10 after 24 and 48 h of storage at 4°C in the dark) was used as positive control. **(C)** Comparison of tumor incidence between oral and *i.n.* administration protocol ($n = 8$ mice). Data are represented as the mean of each group ± SEM.

Both Systemic and Local T Immune Cells Are Crucial to Protect Against Tumor Growth

To go deeper in the analysis of the immune response related to tumor inhibition observed with BL23, splenocytes and tumor sections were harvested and immune cell populations were assessed using flow cytometry and qPCR, respectively. We first analyzed the systemic expression of immune T cells subpopulation. A negative correlation between tumor size and the abundance of both CD3+ ($r^2 = -0.87$, $p < 0.0001$, **Supplementary Figure S3B**), CD8+ ($r^2 = -0.84$, $p < 0.0001$, **Supplementary Figure S3C**), CD4+ ($r^2 = -0.85$, $p < 0.0001$, **Supplementary Figure S3D**) and FOXP3+ ($r^2 = -0.88$, $p < 0.0001$, **Supplementary Figure S3E**) cells was observed. Furthermore, anti-IL-2 treatment had no effect on the proportion of systemic CD3+ cells compared to PBS treatment. However, mice treated with *L. casei* BL23 exhibited significantly reduced levels of CD3+ cells when anti-IL-2 antibodies were also administered (**Figure 3A**).

In addition, we only observed a negative correlation between tumor size and local CD3+ cells ($r^2 = -0.84$, $p = 0.002$, **Supplementary Figure S3F**). However, mice bearing tumor and treated with *L. casei* BL23 exhibited significantly higher local Foxp3 level (**Figure 3B**).

Interestingly, we also detected a positive correlation between local levels of CD3+ cells and IL-2 in tumor-bearing mice ($r^2 = -0.83$, $p < 0.0001$, **Supplementary Figure S3G**).

These data highlight the crucial role of both systemic and local T-immune response after i.n. administration of BL23 to combat tumor growth, and point out the important role of IL-2 pathway in these anti-cancer effects.

NK Cells Mediated a Cytotoxic Effect of *L. casei* BL23 Toward Cancer Cells

Because of the well-known role of IL-2 in NK cell proliferation and the cytotoxic activities of these cells on tumor development (Takagi et al., 2001), we assessed the systemic expression of NK cells. A negative correlation between tumor size and NKP46+ cells was found confirming the necessity of NK cells in tumor protection ($r^2 = -0.86$, $p < 0.0001$, **Supplementary Figure S3H**).

More interestingly, there was a significant negative correlation between local NKp46 expression and tumor size ($r^2 = -0.94$, $p = 0.016$, **Supplementary Figure S3I**). This correlation was specific to *L. casei* BL23 treatment since no correlation was observed between NK cells and tumor size in control PBS-treated mice (data not shown).

We further analyzed cytotoxicity activity of NK on TC-1 cells *in vitro*. For this, NK cells were isolated from mice that had been

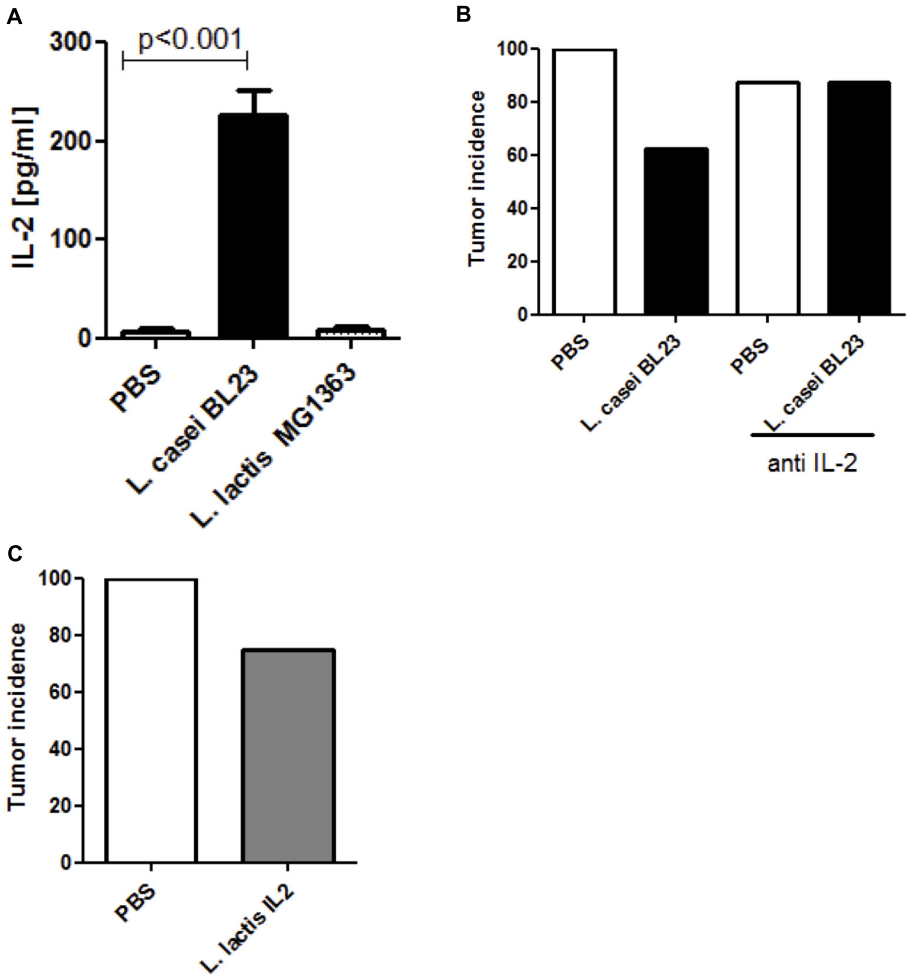

FIGURE 2 | IL-2 involvement in tumor protection. **(A)** IL-2 production by murine DCs (n = 3 independent experiments, $p < 0.001$, ANOVA). BMDCs were exposed to bacteria at MOI = 100 for 24 h. **(B)** Tumor incidence. Mice were administered PBS or *L. casei* BL23 in the presence or absence of anti-IL-2 mAb. **(C)** Effect of *L. lactis*-IL2 treatment on protection against tumors. Data are represented as the mean of each group ± SEM (n = 8 mice per group).

treated *i.n.* with either *L. lactis* MG1363 (negative control) or *L. casei* BL23, and cultivated in the presence of TC-1 cells for 5 days. As shown in **Figure 3C**, TC-1 cells that were exposed to NK cells from *L. casei* BL23-treated mice exhibited a larger lysis area than those exposed to NK cells isolated from *L. lactis* MG1363-treated mice. These data suggest that, unlike *L. lactis* MG1363, *L. casei* BL23 induced the recruitment of NK cells with high potent cytotoxicity toward tumor cells.

Therapeutic *s.c. L. casei* BL23 Administration Resulted in Reduced Tumor Volume

It is well known that some species of anaerobic bacteria can selectively migrate after intravenous injection and grow in the hypoxic regions of solid tumors (Kimura et al., 1980). As *L. casei* BL23 is a facultative anaerobic Gram-positive bacterium, we cannot discard the possibility that this strain has a local effect in the tumor environment, especially in regards of the observed local immune response. To investigate this, we performed local *s.c.* administration of *L. casei* BL23 post-TC-1 injection (**Supplementary Figure S2B**). For this, mice were first challenged with tumor cells and, 1 day later, we administered *s.c.* bacteria at the same injection site. Our results revealed that, in contrast to the prophylactic effect of *i.n.* treatment with *L. casei* BL23 prior to tumor challenge, *s.c.* therapeutic administration had no effect on tumor incidence (**Figure 4A**), however, a significant reduction in tumor size was observed (**Figure 4B**).

Furthermore, as shown in **Figure 5**, *s.c.* therapeutic administration of *L. casei* BL23 increased CD3 (**Figure 5A**) and IL-2 levels (**Figure 5B**) and reduced Nkp46 levels (**Figure 5C**) in tumor sections. No regulation was observed for CD8+ cells (**Figure 5D**).

These results suggest that *L. casei* BL23 can have a beneficial effect in the HPV-induced cancer model following both *i.n.* and local administration (*s.c.*). This highlights the possibility of using *L. casei* BL23 not only as a preventive agent but also as a form of therapy to decrease tumor size.

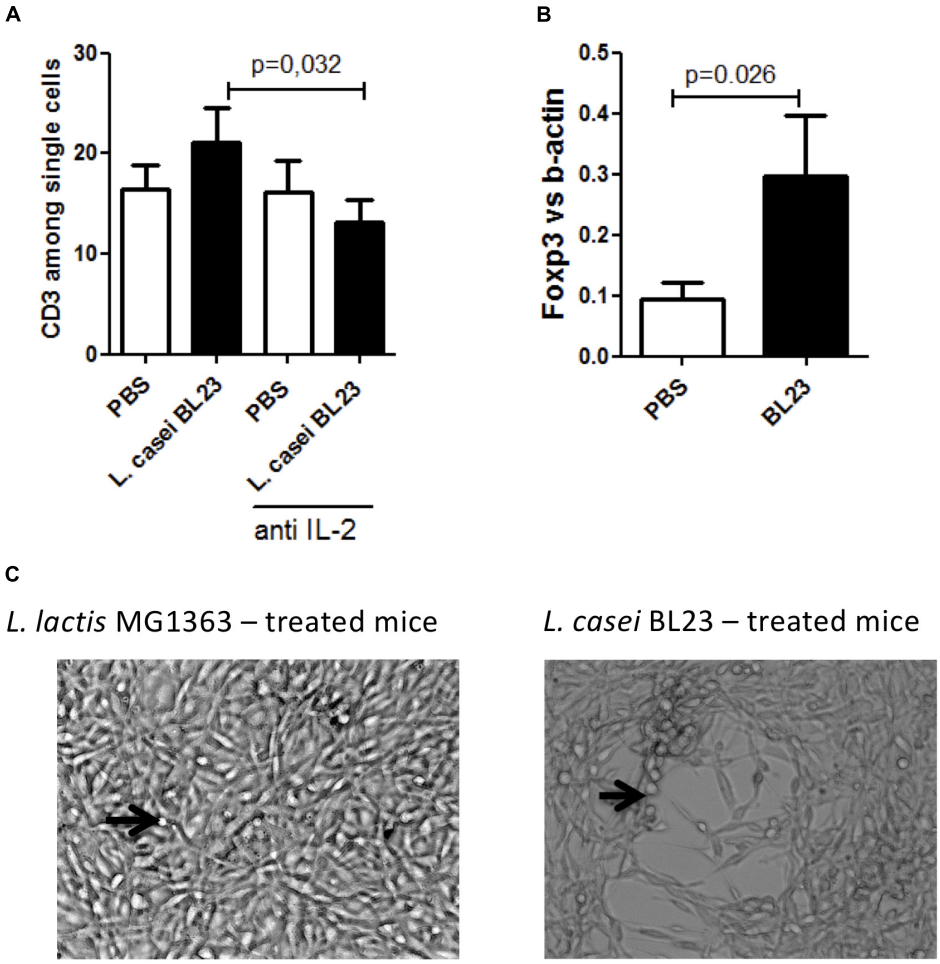

FIGURE 3 | A potent role of immune cells in *L. casei* BL23 tumor protection after i.n adminsitration. **(A)** CD3+ cells level in spleen (n = 8 mice per group; p = 0.0032, T-test followed by Mann–Whitney post-test)). **(B)** Foxp3 level in tumor section (n = 8 mice per group; p = 0.026, T-test followed by Mann–Whitney post-test). **(C)** *In vitro* cytotoxic activity of NK cells isolated from mice treated with (right panel) *L. casei* BL23 or (left panel) *L. lactis* MG1363. TC-1 cells, which formed a dense and well-adhering layer in the presence of NK from *L. lactis* MG1363-administered mice, almost completely disappeared in the presence of NK from mice treated with *L. casei* BL23. TC-1 cells were incubated with NK cells at a ratio of 1:20 for 5 days. Black arrows indicate NK cells.

DISCUSSION

Lactic acid bacteria are widely used in the food industry; they are safe (having been widely consumed by humans for centuries in fermented foods) and can confer many beneficial effects on host health. Indeed, LAB have been linked with several probiotic activities, including the stimulation of the immune system (for a review see (Martin et al., 2013)). In addition, some LAB species are members of healthy human gut microbiota. Recently, several studies have reported the ability of certain LAB strains to inhibit tumor development (Khazaie et al., 2012; Konishi et al., 2016; Lenoir et al., 2016). Among the potential anti-tumoral mechanisms of LAB, two of the most promising are the modulation of the immune response and the induction of cellular apoptosis. For instance, two strains of *L. casei* are able to decrease tumor cell proliferation and enhance apoptosis in allograft models of colorectal cancer (Lee et al., 2004; Baldwin et al., 2010; Konishi et al., 2016). Similarly, oral administration of an *L. casei* strain reduces the onset of chemically induced tumors via the stimulation of IL-12 or NK-cell cytotoxicity mechanisms (Takagi et al., 2001, 2008). Furthermore, our team recently demonstrated the protective effects of the probiotic strain *L. casei* BL23 in different mouse models of cancer, including colorectal-associated cancer (CAC) and the TC-1 allograft model (Lenoir et al., 2016). In the CAC model, *L. casei* BL23 was linked with reduced expression of pro-inflammatory cytokines, but the molecular and cellular mechanisms involved in TC-1 cancer prevention were not elucidated.

First, we investigated the role of the bacterial route of administration: *i.n.* vs. oral. We effectively showed that stained *L. casei* BL23 was mainly founded in NALT after *i.n.* administration with a posterior transit to the stomach. Interestingly, oral administration of BL23 which resulted in a local localization of the bacterium (i.e., digestive tract,

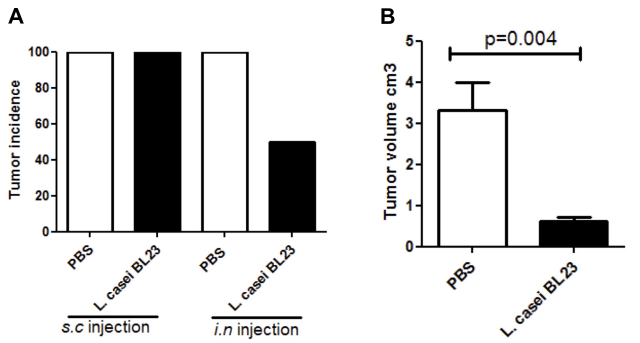

FIGURE 4 | Assessment of therapeutic *s.c.* introduction of *L. casei* BL23 at the site of TC-1 injection. **(A)** Tumor incidence, **(B)** tumor volume. Mice were challenged with TC-1 tumors and, beginning 24h later, received *s.c.* injections of bacteria every 2 days. Data are represented as the mean of each group ± SEM (n = 4 to 8 mice, respectively, for PBS or BL23 treated group; p = 0.004, T-test followed by Mann–Whitney post-test).

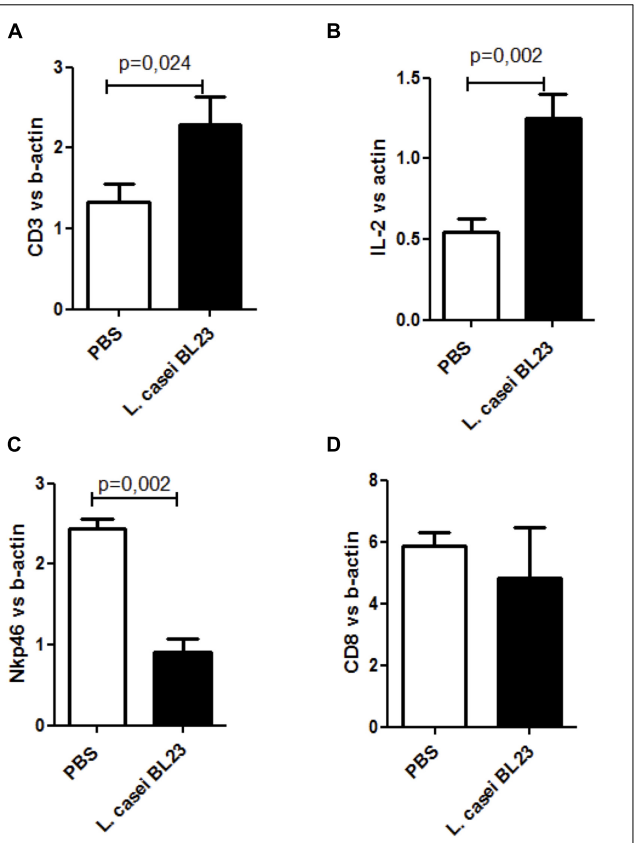

FIGURE 5 | Local immune response induced by *L. casei* BL23 following *s.c.* administration. **(A)** CD3 level (p = 0.024, T-test followed by Mann–Whitney post-test), **(B)**, IL-2 level (p = 0.002, T-test followed by Mann Whitney post-test), **(C)** Nkp46 level (p = 0.002, T-test followed by Mann–Whitney post-test), and **(D)** CD8 level in tumor sections (ns, T-test followed by Mann–Whitney post-test). Data are represented as the mean of each group ± SEM (n = 4 to 8 mice, respectively, for PBS or BL23 treated group).

did not protect mice from tumor onset, confirming that *i.n.* administration of BL23 is crucial in the process of tumor protection in our animal model. Surprisingly, we failed to locate administered bacteria in BAL samples as previously described for other LAB (Grangette et al., 2001), however, in that study, their analyses were performed later (10 days after instillation) and we cannot exclude that we examined bacterial location too early for BAL detection. However, NALT has been described as an important tissue not only for mucosal but also for systemic immune response stimulation (Vintini and Medina, 2014) (Medaglini et al., 2006). Indeed, Vintini et al. reported a specific T-cell response after administration of another *L. casei* strain in NALT and serum samples. So, we cannot rule out a NALT-specific immune response induced by the presence of bacteria after instillation. To test this hypothesis, more investigations concerning NALT-related sequential immune response after BL23 inoculation are necessary.

IL-2 is a polyvalent cytokine with effects on the activation and regulation of immune cells, and is expressed by both lymphoid and non-lymphoid cells (Hoyer et al., 2008). For 15 years, several works have investigated IL-2 for potential use in tumor growth inhibition (Den Otter et al., 1995; Den Otter et al., 1998; Casana et al., 2002; Kusnierczyk et al., 2004). In this context, we hypothesized that the anti-tumoral activity associated with *L. casei* BL23 in our allograft model could be due to IL-2 regulation and the subsequent immune response. Our results showed that, *L. casei* BL23 is able to boost IL-2 secretion *in vitro*. Additionally, we observed that mice with low level of local IL-2 (in tumor sections) presented larger tumors. Strikingly, when mice were treated with IL-2-neutralizing mAb prior to both *i.n.* administration with *L. casei* BL23 and *s.c.* challenge with TC-1 cells, *L. casei* BL23 failed to protect against TC-1 tumor onset. Instead, administration of IL-2 via a recombinant strain of *L. lactis* (LL-IL2) partially mimicked the protective phenotype, although not up to the levels observed with *L. casei* BL23. These results highlight the key, but not exclusive, role of IL-2 signaling in *L. casei* BL23-associated protection against tumors in the mouse allograft model of HPV-induced cancer.

To further decipher the BL23 specific immune response, we first analyzed it at a systemic level. We observed that CD3+ (a marker of T cells), CD8+ (a marker of cytotoxic T-cells), CD4+ (a marker of TH cells) and Foxp3+ (a marker of regulatory T cells) were negatively correlated with tumor size suggesting that most important is the T-cell immune response, lower is tumor grow. We showed that in presence of anti-IL-2, mice which are not protected from tumors had also lower systemic CD3+ cells. In addition, when we specifically investigated the local immune response, we observed a specific up-regulation of Foxp3 in mice treated with BL23 and a negative correlation between tumor size and levels of CD3+ Moreover, in tumor-bearing mice, IL-2 and CD3+ levels were positively correlated with each other, suggesting that in mice with large tumors, CD3+ levels may decrease as a result of IL-2 dependence. These results highlight the efficacy of both T immune cells and IL-2 levels as good prognosis markers in tumor-bearing mice.

Furthermore, when analyzing tumor sections from mice treated with *L. casei* BL23, we detected a specific, negative correlation between NKp46 cell abundance and tumor size. Intrigued by the positive regulation of local and systemic NK cells in mice, we analyzed the effect of *L. casei* BL23 on the cytotoxic activity of NK cells and determined that NK cells from mice treated with *L. casei* BL23 displayed higher lysis activity against TC-1 cells than NK cells from control mice did.

These data are consistent with the results of multiple studies that highlight the role of T-cell subpopulations and NK cells in improved survival for patients suffering from cervical adenocarcinoma as well as in higher resistance in TC-1-challenged mice (Bermudez-Humaran et al., 2005; Brulet et al., 2007; Punt et al., 2015).

Finally, to investigate possibilities for the use of *L. casei* BL23 in a therapeutic approach, we assessed the strain *in vivo* for both local (*s.c.* administration at the same site of tumor injection) and therapeutic (i.e., after tumor challenge) effects. In this context, the presence of the bacteria significantly reduced tumor growth. However, the anti-cancer mechanisms of *s.c. L. casei* BL23 differed from those of *i.n.* administered bacteria. For example, *s.c.* injection of BL23 reduced NKp46 expression in tumor sections, but *i.n.* administration did not. In addition, preventive *i.n.* administration reduced tumor onset through a mechanism linked partially with local and systemic NK cell recruitment, while *s.c.* therapeutic administration had no effect on tumor onset, instead reducing tumor size via a recruitment of IL-2 and CD3 but NK-cell-independent mechanism.

CONCLUSION

In conclusion, this study provides the first clues about the host molecular mechanisms involved in the anti-cancer effects of *L. casei* BL23. Our results may contribute to future efforts to develop probiotic-based food supplements for therapeutic applications in cancer treatment.

AUTHOR CONTRIBUTIONS

EJ and LB-H conceived and designed the study and wrote the manuscript. EJ conducted all the experiments. EJ, M-LM, and LB-H performed the data analysis. ET-M and FC provided technical help for the *in vivo* experiments. EJ, M-LM, PL, and LB-H discussed the experiments and results.

FUNDING

This work was partially funded by the Association pour la Recherche sur le Cancer (ARC, France): action no. PGA12014020851 and the DHU-i2B consortium (Département Hospitalo-Universitaire Inflammation-Immunopathologie-Biothérapie).

ACKNOWLEDGMENTS

We are grateful to the conventional animal facility staff from INRA Jouy-en-Josas. We also thank Laurence Zitvogel for helpful advice.

SUPPLEMENTARY MATERIAL

The Supplementary Material for this article can be found online at: https://www.frontiersin.org/articles/10.3389/fmicb.2018.03281/full#supplementary-material

REFERENCES

Acedo-Felix, E., and Perez-Martinez, G. (2003). Significant differences between *Lactobacillus casei* subsp casei ATCC 393(T) and a commonly used plasmid-cured derivative revealed by a polyphasic study. *Int. J. Syst. Evol. Microbiol.* 53, 67–75. doi: 10.1099/ijs.0.02325-0

Aragón, F., Carino, S., Perdigon, G., and de Moreno de LeBlanc, A. (2015). Inhibition of growth and metastasis of breast cancer in mice by milk fermented with *Lactobacillus casei* CRL 431. *J. Immunother.* 38, 185–196. doi: 10.1097/CJI.0000000000000079

Azcarate-Peril, M. A., Sikes, M., and Bruno-Barcena, J. M. (2011). The intestinal microbiota, gastrointestinal environment and colorectal cancer: a putative role for probiotics in prevention of colorectal cancer? *Am. J. Physiol. Gastrointest. Liver Physiol.* 301, G401–G424. doi: 10.1152/ajpgi.00110.2011

Baldwin, C., Millette, M., Oth, D., Ruiz, M. T., Luquet, F. M., and Lacroix, M. (2010). Probiotic *Lactobacillus acidophilus* and L. casei mix sensitize colorectal tumoral cells to 5-fluorouracil-induced apoptosis. *Nutr. Cancer* 62, 371–378. doi: 10.1080/01635580903407197

Bermudez-Humaran, L. G., Cortes-Perez, N. G., Lefevre, F., Guimaraes, V., Rabot, S., Alcocer-Gonzalez, J. M., et al. (2005). A novel mucosal vaccine based on live *Lactococci* expressing E7 antigen and IL-12 induces systemic and mucosal immune responses and protects mice against human papillomavirus type 16-induced tumors. *J. Immunol.* 175, 7297–7302. doi: 10.4049/jimmunol.175.11.7297

Bermudez-Humaran, L. G., Langella, P., Commissaire, J., Gilbert, S., Le Loir, Y., L'Haridon, R., et al. (2003). Controlled intra- or extracellular production of staphylococcal nuclease and ovine omega interferon in *Lactococcus lactis*. *FEMS Microbiol. Lett.* 224, 307–313. doi: 10.1016/S0378-1097(03)00475-0

Bermudez-Humaran, L. G., Motta, J. P., Aubry, C., Kharrat, P., Rous-Martin, L., Sallenave, J. M., et al. (2015). Langella, Serine protease inhibitors protect better than IL-10 and TGF-beta anti-inflammatory cytokines against mouse colitis when delivered by recombinant *Lactococci*. *Microb. Cell Fact.* 14:26. doi: 10.1186/s12934-015-0198-4

Bernardeau, M., Vernoux, J. P., Henri-Dubernet, S., and Gueguen, M. (2008). Safety assessment of dairy microorganisms: the *Lactobacillus* genus. *Int. J. Food Microbiol.* 126, 278–285. doi: 10.1016/j.ijfoodmicro.2007.08.015

Brulet, J. M., Maudoux, F., Thomas, S., Thielemans, K., Burny, A., Leo, O., et al. (2007). DNA vaccine encoding endosome-targeted human papillomavirus type 16 E7 protein generates CD4+ T cell-dependent protection. *Eur. J. Immunol.* 37, 376–384. doi: 10.1002/eji.200636233

Cai, S., Kandasamy, M., Rahmat, J. N., Tham, S. M., Bay, B. H., Lee, Y. K., et al. (2016). *Lactobacillus rhamnosus* GG Activation of dendritic cells and neutrophils depends on the dose and time of exposure. *J. Immunol. Res.* 2016:7402760. doi: 10.1155/2016/7402760

Casana, P. H., Hernandez, H., and Arana, M. J. (2002). Interleukin-2 inhibits proliferation of HPV-associated tumor cells and halts tumor growth in vivo. *Biochem. Biophys. Res. Commun.* 299, 818–824. doi: 10.1016/S0006-291X(02)02715-8

Cortes-Perez, N. G., Lefevre, F., Corthier, G., Adel-Patient, K., Langella, P., and Bermudez-Humaran, L. G. (2007). Influence of the route of immunization and the nature of the bacterial vector on immunogenicity of mucosal vaccines based on lactic acid bacteria. *Vaccine* 25, 6581–6588. doi: 10.1016/j.vaccine.2007.06.062

Delcenserie, V., Martel, D., Lamoureux, M., Amiot, J., Boutin, Y., and Roy, D. (2008). Immunomodulatory effects of probiotics in the intestinal tract. *Curr. Issues Mol. Biol.* 10, 37–54.

Den Otter, W., Dobrowolski, Z., Bugajski, A., Papla, B., Van Der Meijden, A. P., Koten, J. W., et al. (1998). Intravesical interleukin-2 in T1 papillary bladder carcinoma: regression of marker lesion in 8 of 10 patients. *J. Urol.* 159, 1183–1186.

Den Otter, W., Hill, F. W., Klein, W. R., Koten, J. W., Steerenberg, P. A., De Mulder, P. H., et al. (1995). Therapy of bovine ocular squamous-cell carcinoma with local doses of interleukin-2: 67% complete regressions after 20 months of follow-up. *Cancer Immunol. Immunother.* 41, 10–14. doi: 10.1007/BF01788954

Dorostkar, R., Hashemzadeh, M. S., Jafari, S., Tat, M., Ghalavand, M., Asghari, M. H., et al. (2016). Immunotherapeutic efficacy of a *Lactobacillus casei* lysate as an adjuvant combined with a heated-4T1 mammary carcinoma cell lysate in a murine model of breast cancer. *Asian Biomed.* 10, 327–334. doi: 10.5372/1905-7415.1004.494

FAO/WHO. (2002). *FAO/WHO Working Group Report on Drafting Guidelines for the Evaluation of Probiotics in Food*. London: Food and Agriculture Organization.

Gasson, M. J. (1983). Plasmid complements of Streptococcus lactis NCDO 712 and other lactic streptococci after protoplast-induced curing. *J. Bacteriol.* 154, 1–9.

Grangette, C., Muller-Alouf, H., Goudercourt, D., Geoffroy, M. C., Turneer, M., and Mercenier, A. (2001). Mucosal immune responses and protection against tetanus toxin after intranasal immunization with recombinant *Lactobacillus plantarum*. *Infect. Immun.* 69, 1547–1553. doi: 10.1128/IAI.69.3.1547-1553.2001

Hoyer, K. K., Dooms, H., Barron, L., and Abbas, A. K. (2008). Interleukin-2 in the development and control of inflammatory disease. *Immunol. Rev.* 226, 19–28. doi: 10.1111/j.1600-065X.2008.00697.x

Hu, J., Wang, C., Ye, L., Yang, W., Huang, H., Meng, F., et al. (2015). Anti-tumour immune effect of oral administration of *Lactobacillus plantarum* to CT26 tumour-bearing mice. *J. Biosci.* 40, 269–279. doi: 10.1007/s12038-015-9518-4

Kahouli, I., Tomaro-Duchesneau, C., and Prakash, S. (2013). Probiotics in colorectal cancer (CRC) with emphasis on mechanisms of action and current perspectives. *J. Med. Microbiol.* 62, 1107–1123. doi: 10.1099/jmm.0.048975-0

Kato, I., Endo, K., and Yokokura, T. (1994). Effects of oral administration of *Lactobacillus casei* on antitumor responses induced by tumor resection in mice. *Int. J. Immunopharmacol.* 16, 29–36. doi: 10.1016/0192-0561(94)90116-3

Khazaie, K., Zadeh, M., Khan, M. W., Bere, P., Gounari, F., Dennis, K., et al. (2012). Abating colon cancer polyposis by *Lactobacillus acidophilus* deficient in lipoteichoic acid. *Proc. Natl. Acad. Sci. U S A.* 109, 10462–10467. doi: 10.1073/pnas.1207230109

Kimura, N. T., Taniguchi, S., Aoki, K., and Baba, T. (1980). Selective localization and growth of *Bifidobacterium bifidum* in mouse tumors following intravenous administration. *Cancer Res.* 40, 2061–2068.

Konishi, H., Fujiya, M., Tanaka, H., Ueno, N., Moriichi, K., Sasajima, J., et al. (2016). Probiotic-derived ferrichrome inhibits colon cancer progression via JNK-mediated apoptosis. *Nat. Commun.* 7:12365. doi: 10.1038/ncomms12365

Kusnierczyk, H., Pajtasz-Piasecka, E., Koten, J. W., Bijleveld, C., Krawczyk, K., and Den Otter, W. (2004). Further development of local IL-2 therapy of cancer: multiple versus single IL-2 treatment of transplanted murine colon carcinoma. *Cancer Immunol. Immunother.* 53, 445–452. doi: 10.1007/s00262-003-0490-8

Lee, J. W., Shin, J. G., Kim, E. H., Kang, H. E., Yim, I. B., Kim, J. Y., et al. (2004). Immunomodulatory and antitumor effects in vivo by the cytoplasmic fraction of *Lactobacillus casei* and *Bifidobacterium longum*. *J. Vet. Sci.* 5, 41–48.

Lenoir, M., Del Carmen, S., Cortes-Perez, N. G., Lozano-Ojalvo, D., Munoz-Provencio, D., Chain, F., et al. (2016). *Lactobacillus casei* BL23 regulates treg and Th17 T-cell populations and reduces DMH-associated colorectal cancer. *J. Gastroenterol.* 51, 862–873. doi: 10.1007/s00535-015-1158-9

Lin, K. Y., Guarnieri, F. G., Staveley-O'Carroll, K. F., Levitsky, H. I., August, J. T., Pardoll, D. M., et al. (1996). Treatment of established tumors with a novel vaccine that enhances major histocompatibility class II presentation of tumor antigen. *Cancer Res.* 56, 21–26.

Martin, R., Miquel, S., Langella, P., and Bermudez-Humaran, L. G. (2014). The role of metagenomics in understanding the human microbiome in health and disease. *Virulence* 5, 413–423. doi: 10.4161/viru.27864

Martin, R., Miquel, S., Ulmer, J., Kechaou, N., Langella, P., and Bermudez-Humaran, L. G. (2013). Role of commensal and probiotic bacteria in human health: a focus on inflammatory bowel disease. *Microb. Cell Fact.* 12:71. doi: 10.1186/1475-2859-12-71

Maze, A., Boel, G., Zuniga, M., Bourand, A., Loux, V., Yebra, M. J., et al. (2010). Complete genome sequence of the probiotic *Lactobacillus casei* strain BL23. *J. Bacteriol.* 192, 2647–2648. doi: 10.1128/JB.00076-10

Medaglini, D., Ciabattini, A., Cuppone, A. M., Costa, C., Ricci, S., Costalonga, M., et al. (2006). In vivo activation of naive CD4+ T cells in nasal mucosa-associated lymphoid tissue following intranasal immunization with recombinant *Streptococcus gordonii*. *Infect. Immun.* 74, 2760–2766. doi: 10.1128/IAI.74.5.2760-2766.2006

Punt, S., van Vliet, M. E., Spaans, V. M., de Kroon, C. D., Fleuren, G. J., Gorter, A., et al. (2015). FoxP3(+) and IL-17(+) cells are correlated with improved prognosis in cervical adenocarcinoma. *Cancer Immunol. Immunother.* 64, 745–753. doi: 10.1007/s00262-015-1678-4

Ribelles, P., Benbouziane, B., Langella, P., Suarez, J. E., and Bermudez-Humaran, L. G. (2013). Protection against human papillomavirus type 16-induced tumors in mice using non-genetically modified lactic acid bacteria displaying E7 antigen at its surface. *Appl. Microbiol. Biotechnol.* 97, 1231–1239. doi: 10.1007/s00253-012-4575-1

Rosenberg, S. A., Mule, J. J., Spiess, P. J., Reichert, C. M., and Schwarz, S. L. (1985). Regression of established pulmonary metastases and subcutaneous tumor mediated by the systemic administration of high-dose recombinant interleukin-2. *J. Exp. Med.* 161, 1169–1188. doi: 10.1084/jem.161.5.1169

Takagi, A., Ikemura, H., Matsuzaki, T., Sato, M., Nomoto, K., Morotomi, M., et al. (2008). Relationship between the in vitro response of dendritic cells to *Lactobacillus* and prevention of tumorigenesis in the mouse. *J. Gastroenterol.* 43, 661–669. doi: 10.1007/s00535-008-2212-7

Takagi, A., Matsuzaki, T., Sato, M., Nomoto, K., Morotomi, M., and Yokokura, T. (2001). Enhancement of natural killer cytotoxicity delayed murine carcinogenesis by a probiotic microorganism. *Carcinogenesis* 22, 599–605. doi: 10.1093/carcin/22.4.599

Uccello, M., Malaguarnera, G., Basile, F., D'Agata, V., Malaguarnera, M., Bertino, G., et al. (2012). Potential role of probiotics on colorectal cancer prevention. *BMC Surg.* 12:S35. doi: 10.1186/1471-2482-12-S1-S35

Vintini, E. O., and Medina, M. (2014). Immune response in nasopharynx, lung, and blood elicited by experimental nasal pneumococcal vaccines containing live or heat-killed Lactobacilli as mucosal adjuvants. *Can. J. Physiol. Pharmacol.* 92, 124–131. doi: 10.1139/cjpp-2013-0227

Conflict of Interest Statement: The authors declare that the research was conducted in the absence of any commercial or financial relationships that could be construed as a potential conflict of interest.

Copyright © 2019 Jacouton, Michel, Torres-Maravilla, Chain, Langella and Bermúdez-Humarán. This is an open-access article distributed under the terms of the Creative Commons Attribution License (CC BY). The use, distribution or reproduction in other forums is permitted, provided the original author(s) and the copyright owner(s) are credited and that the original publication in this journal is cited, in accordance with accepted academic practice. No use, distribution or reproduction is permitted which does not comply with these terms.

frontiers in Microbiology

MINI REVIEW
published: 23 January 2019
doi: 10.3389/fmicb.2018.03328

Intestinal Microbiota as a Host Defense Mechanism to Infectious Threats

Simona Iacob[1,2], Diana Gabriela Iacob[2] and Luminita Monica Luminos[1,2]*

[1] Department of Infectious Diseases, Carol Davila University of Medicine and Pharmacy, Bucharest, Romania, [2] National Institute of Infectious Diseases "Prof. Dr. Matei Bals", Bucharest, Romania

The intestinal microbiota is a complex microbial community, with diverse and stable populations hosted by the gastrointestinal tract since birth. This ecosystem holds multiple anti-infectious, anti-inflammatory, and immune modulating roles decisive for intestinal homeostasis. Among these, colonization resistance refers to the dynamic antagonistic interactions between commensals and pathogenic flora. Hence, gut bacteria compete for the same intestinal niches and substrates, while also releasing antimicrobial substances such as bacteriocines and changing the environmental conditions. Short chain fatty acids (SCFAs) generated in anaerobic conditions prompt epigenetic regulatory mechanisms that favor a tolerogenic immune response. In addition, the commensal flora is involved in the synthesis of bactericidal products, namely secondary biliary acids or antimicrobial peptides (AMPs) such as cathellicidin-LL37, an immunomodulatory, antimicrobial, and wound healing peptide. Gut microbiota is protected through symbiotic relations with the hosting organism and by quorum sensing, a specific cell-to-cell communication system. Any alterations of these relationships favor the uncontrollable multiplication of the resident pathobionts or external entero-pathogens, prompting systemic translocations, inflammatory reactions, or exacerbations of bacterial virulence mechanisms (T6SS, T3SS) and ultimately lead to gastrointestinal or systemic infections. The article describes the metabolic and immunological mechanisms through which the intestinal microbiota is both an ally of the organism against enteric pathogens and an enemy that favors the development of infections.

Keywords: intestinal microbiota, infection, commensal flora, bacterial enteropathogens, colonization resistance, mucosal immunity, short chain fatty acids

OPEN ACCESS

Edited by:
Learn-Han Lee,
Monash University Malaysia, Malaysia

Reviewed by:
Amélia M. Sarmento,
Fernando Pessoa University, Portugal
Bei Han,
Xi'an Jiaotong University, China
Claucia Fernanda Volken De Souza,
University of Taquari Valley, Brazil

****Correspondence:***
Diana Gabriela Iacob
dianagiacob@gmail.com

Specialty section:
This article was submitted to Microbial Symbioses, a section of the journal Frontiers in Microbiology

Received: *20 September 2018*
Accepted: *21 December 2018*
Published: *23 January 2019*

Citation:
Iacob S, Iacob DG and Luminos LM (2019) Intestinal Microbiota as a Host Defense Mechanism to Infectious Threats. Front. Microbiol. 9:3328. doi: 10.3389/fmicb.2018.03328

INTRODUCTION

The human body hosts trillions of microorganisms at the level of the skin and mucous membranes. Together they build a complex microbial community, with multiple metabolic and immune functions that are essential for the survival of the human organism (Lin and Zhang, 2017).The most important representation of this community can be found in the gut as the intestinal microbiota. The gut microbiota is a stable and diverse ecosystem established upon birth and that gradually develops complex digestive and metabolic functions. Along with the intestinal epithelium,

the microbiota forms a protective barrier against infectious threats and plays an active role in promoting and maintaining the immune homeostasis during intestinal infections. In order to accomplish these functions, commensal bacteria that colonize the intestinal tract develop symbiotic relationships with the human organism while also competing against microbial pathogens.

The article is centered on the how antiinfectious defense mechanisms intervene during host-microbiota interactions as well as during the direct competition between commensals and pathogens. The review details complex antiinfectious mechanisms ensuring the success of the microbiota in this competition, including quorum sensing (QS), colonization resistance, direct bactericidal activity, cooperation with the immune system and counteracting strategies developed by enteric pathogens to ensure their survival.

MICROBIOTA AND INFECTIOUS THREATS

The cells of the gut microbiota outnumber the somatic cells by 10–100 times, yet most cannot be cultivated *in vitro*. Molecular techniques have revealed that the flora of healthy individuals contains over 99.1% bacterial species and is mainly represented by 4 phyla, *Firmicutes*, *Bacteroidetes, Actinobacteria,* and *Proteobacteria*, the remaining ones being viruses or members of the *Archaea or Eukarya* domain. At birth the microbiota colonizes the intestinal tract and gradually diversifies so that after 3 years the dominant pattern belongs to anaerobic species *Bacteroidetes, Firmicutes* and especially *Clostridium cluster IV/XIV* (Rajilic-Stojanovic et al., 2007). The small intestine predominantly hosts *Streptococcus, Veillonella* and *Lactobacillus* species, while the large intestine and distal gut contain anaerobic species, mainly *Bacteroides*, *Clostridium*, *Fusobacterium,* and *Bifidobacterium* and facultative anaerobic species like *Escherichia*, *Enterobacter, Enterococcus, Klebsiella, Lactobacillus,* and *Proteus* (Donaldson et al., 2016). The relationship between the gut microbiota and the organism can be symbiotic, mutual or commensal, thus allowing the colonization with protective species ("symbionts"), among which the most beneficial are *Lactobacillus* and *Bifidobacterium* (Walter, 2008; O'Callaghan and van Sinderen, 2016). In certain conditions though, pathogenic or potentially pathogenic microorganisms ("pathobionts") may trigger inflammatory, oncogenic or infectious diseases. The pathogens that enter the digestive tract induce diarrheal diseases complicated by dehydration and organ failure. In addition, intestinal pathogens release toxins, penetrate through the mucus layer, adhere to the intestinal epithelium, manipulate the intestinal immunity, and sometimes translocate into the systemic circulation (Stecher and Hardt, 2008). The most threatening enteropathogens include: *Shigella; Campylobacter; Yersinia*; and non-typhoid *Salmonella* species associated with inflammatory diarrhea; toxin producing Vibrio *cholerae* and *Escherichia coli* species responsible for secretory diarrhea; and *S. typhi/parathiphy* endotoxin producers causing systemic life-threatening enteric fevers. Among conditional pathogens, two representatives stand out: *Enterococcus species* responsible for endocarditis and *Clostridium difficile,* a frequent cause of post-antibiotic enterocolitis (Perez-Lopez et al., 2016).

The organism opposes enteric pathogens through an "intestinal barrier" composed of 3 interdependent components, namely the intestinal microbiota, the continuous intestinal epithelium protected by the mucus layer and the mucosal immunity. Within this structure, the microbiota restricts the access of pathogens to the intestinal mucosa through specific competitive mechanisms also termed "colonization resistance" along with QS, a network of communication molecules.

BACTERIAL QUORUM SENSING IN THE ANTIMICROBIAL DEFENSE

Despite the physiological variations and challenging survival conditions in the gut, the microbiota has proved to be an extremely stable structure throughout time. This stability is ensured by QS, an intercellular communication mechanism based on signaling molecules accumulated during bacterial replication and regulated by feed-back (Thompson et al., 2016). These chemical signals referred to as "autoinducers" activate specific receptors and induce bacterial phenotypic changes correlated with adherence, motility and intestinal density of bacteria or with the secretion of protective short chain fatty acids (SCFAs) and antimicrobial peptides (AMPs). QS is employed both by commensals, to ensure gut homeostasis, and by pathogens, to minimize host immune responses and help express pathogenicity. One of these signals is the autoinducer-2 (AI-2), released and recognized by a wide range of commensal bacteria (Pereira et al., 2013). Hence, AI-2 produced by the commensal *R.obeum*, through accumulation and negative feedback, restricts the colonization with the pathogenic *V. cholera* (Hsiao et al., 2014). Enteropathogens (*E. coli, Clostridia, Listeria, and Pseudomonas species*) exploit QS systems against commensals by activating virulence factors, toxin synthesis, sporulation, biofilm formation or by inducing antimicrobial resistance (Chen et al., 2014; Asfour, 2018; Pinheiro et al., 2018). Better knowledge of cell-cell QS signals and the ability to enzymatically block some of the signals (Quorum Quenching) already observed in many plants and demonstrated on animal models could provide alternative solutions in the future for antimicrobial treatment against multiresistant strains.

COLONIZATION RESISTANCE AGAINST PATHOGENS

The concept of colonization resistance refers to the ability of commensals to prevent the colonization and overgrowth of intestinal pathogens (Lawley and Walker, 2013). Colonization resistance is a mechanism of intestinal protection following the direct competition between commensals and pathogens for the intestinal niche and nutritive resources.

Niche Competition: Mucus-Layer Protection

The intestinal epithelium is represented by a monolayer of cells joined through tight junctions which plays a complex role in mucus production and immune response (Rakoff-Nahoum et al., 2004; Kong et al., 2018). Ever since birth, the commensal flora attaches to the intestinal mucus, occupying all available spaces and impeding enteropathogenic colonization (Huang et al., 2011). The mucin-rich mucus layer exhibits O-glycan structures or peptidic motifs that function as receptors for bacterial adhesion, allowing the colonization with health-promoting bacteria such as *Lactobacillus* and *Bifidobacterium* (Kinoshita et al., 2007) and interfering in the metabolism of certain immunoprotective species (*Bacteroides thetaiotaomicron, Bacteroides fragilis)* (Coyne et al., 2005; Martens et al., 2009; Bergstrom and Xia, 2013). Mucin promotes bacterial clearance, modulates virulence factors and biofilm formation, while also ensuring the survival of commensals in the competition with entheropathogens (Sicard et al., 2017). Mucus thus forms the natural habitat of intestinal symbionts and is among the first defense mechanisms of the intestinal epithelia against bacterial invasion. Mucin competition is used for survival by commensal strains of *E. coli* or *Bifidobacterium* versus pathogenic *E. coli or C. difficile* (Collado et al., 2005; O'Callaghan and van Sinderen, 2016). The probiotics have also been shown to stimulate mucus secretion and intestinal colonization (Collado et al., 2005; Caballero-Franco et al., 2007). Some enteropathogens such as *Samonella* and *Helicobacter pylori* have developed strategies to avoid mucus or overcome mucus receptors such as flagellar motility (*Salmonella, Campylobacter, C. difficile, V. cholerae*)., mucinases secretion (*Salmonella typhimurium, E. coli and S. flexneri, V. cholerae*) or lack of adhesins involved in intestinal adherence. Others have developed mechanisms that anchor them better to the mucus through mucin-binding proteins (*Listeria, H. pylori*) or fimbrial adhesins (*S. enterica*) or activate certain virulence mechanisms, namely type VI or III secretion system (T6SS,T3SS) (e.g., *V. cholerae*) (Branka et al., 1997; Tu et al., 2008; Ganesh et al., 2013; Luo et al., 2014; Liu et al., 2015; Sicard et al., 2017). In this context, mucus plays an important role in bacterial pathogenic mechanisms and displays the potential to become a target for future anti-diarrheal drug therapies (Caballero-Franco et al., 2007).

Nutrient Competition: Mucus as a Nutritive Resource

Mucins and dietary complex carbohydrates are essential intestinal nutritive resources (Kim and Ho, 2010) to which commensal species have adapted through specific metabolic pathways (Ndeh and Gilbert, 2018). Enteropathogens frequently use nutritious sources offered by commensal species; pathogenic germs that are unable to metabolize these sources are frequently eliminated. Hence, the pathogenic *C. difficile* survives by metabolizing the succinate from the symbiont *B. thetaiotaomicron*, whereas *C. difficile mutans* unable to metabolize succinate are eliminated (Ferreyra et al., 2014). Furthermore these metabolic pathways also ensure colonization resistance. Thus, the glycan fucosylations predominantly induced by *Bacteroides* provide a source of nutrition to symbionts and favor their colonization. This mechanism is vital for the colonization of *Bacteroides* species as well as for enteropathogens that require fucosis to express virulence (Coyne et al., 2005; Pacheco et al., 2012; Wands et al., 2015). *S. typhimurium, C. difficile, E. coli, Campylobacter jejuni* still use fucose or other metabolic products of commensal species (sialic acid, succinate) to regulate their expansion and pathogenicity (Ng et al., 2013; Curtis et al., 2014; Dwivedi et al., 2016; Sicard et al., 2018).

However, some pathogenic bacteria may use digestive nutrients that commensals cannot metabolize. Thus, ethanolamine, a carbon and nitrogen source for *S. typhimurium*, *Enterohemorrhagic E. coli* (EHEC), *Klebsiella, Pseudomonas, C. difficile* and *Listeria monocytogenes* cannot be used by most commensal species (Garsin, 2010). EHEC species in particular have developed metabolic pathways for distinct sugar resources, some of which are inaccessible to commensal *E. coli* (Fabich et al., 2008). Interestingly, in the presence of multiple distinct strains of commensal *E. coli*, EHEC could fail to colonize the gut according to mice experiments (Maltby et al., 2013). Diversified diets offering a variety of sugars can provide the necessary resources for some pathogenic germs even during their competition with the commensal flora. *Citrobacter rodentium* is such an example as it requires multiple mono or polysaccharides and has a high rate of colonization. However in the case of a diet based solely on monosaccharides, *C. rodentium* cannot survive the competition with several commensal species (Kamada et al., 2012). As a result, the dietary intake of nutrients plays a significant role in the pathogenesis of enteric infections.

The effective colonization of intestinal niches also requires the ability to elude the immune barrier mounted by the mucosal immunity and the specific antimicrobial compounds of the microbiota, such as antimicrobial peptides, secondary bile acids (BA) and SCFA.

THE ROLE OF MUCOSAL IMMUNITY

The mucosal immune response prevents the invasion of intestinal niches by pathogens and ensures the immune tolerance toward commensal germs (Wershil and Furuta, 2008). In particular, DCs belonging to gut-associated lymphoid tissue are a key population able to regulate mucosal immunity and intestinal homeostasis. Thus, DCs are able to mount a tolerant response by downregulating the NF-kB signaling cascade when DC activation is induced by commensals through either epithelial-cell-derived cytokines (TGF-β, IL10), luminal antigens or microfold cells. Tolerogenic DC from mesenteric lymph nodes also display a DC CD103+ profile that enables the conversion of naïve CD4+T cells toward either of the following immunosuppressive lymphocyte lineages: Th3, FoxP3+(TREG) and Th2 which favors IgA secreting B-cells (Coombes and Powrie, 2008). Additionally, anti-inflammatory cytokines (IL4,5,10,TGF-β) and IgA ensure the protection of the intestinal epithelia and the anchorage of the

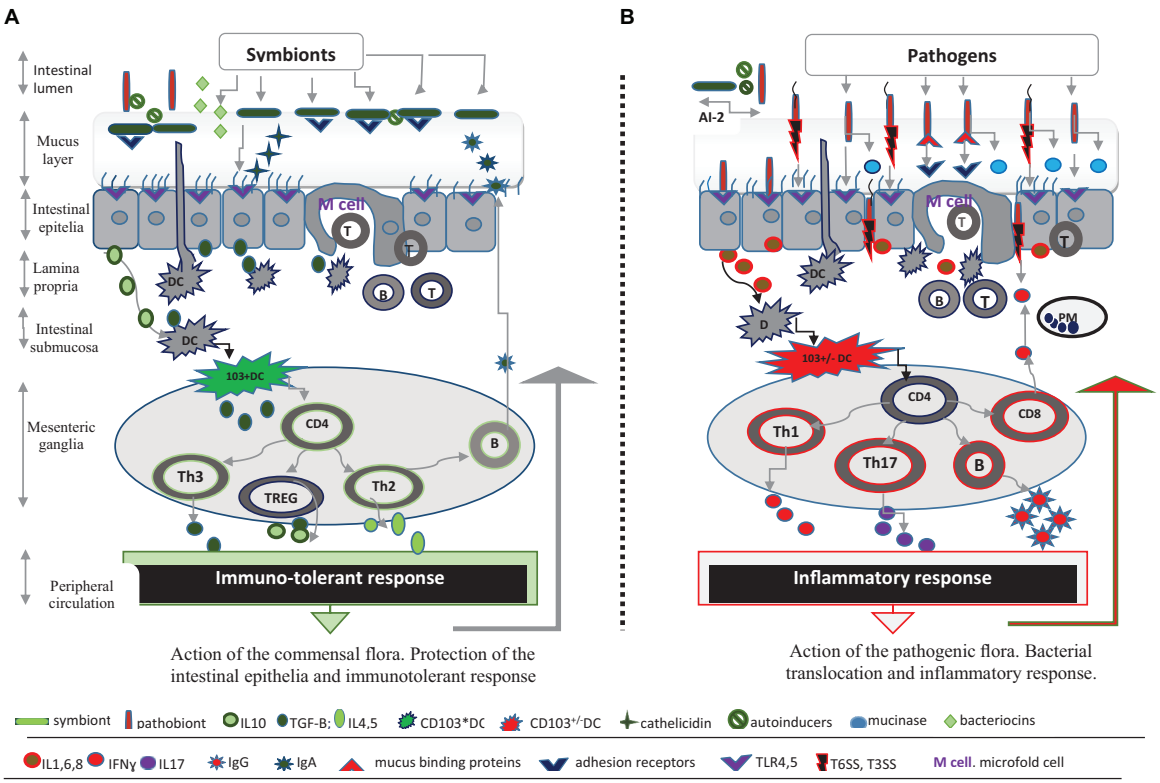

FIGURE 1 | Microbiota and the intestinal barrier against infectious threats. **(A)** Symbionts shape mucosal immunity and protect intestinal epithelia. The commensal flora, intestinal epithelia covered by mucus, and the mucosal immune response form a complex intestinal barrier against infectious threats. The first line of defense is represented by the mucus layer as well as by antimicrobial peptides (cathelicidin), bacteriocins, and intestinal IgA that ensure the integrity of intestinal epithelial cells (IECs). The commensal flora is interconnected through Quorum-sensing signals (e.g., AI-2 inducer) and is anchored to the protective mucus, at a distance from the intestinal epithelia. Thus commensal species reach high densities in mucosal niches and use available nutrient sources contributing to the colonization resistance. The mucosal immunity is best represented by a network of cells and cytokines within the lamina propria, submucosa and mesenteric ganglia that are ultimately modulated by the commensal flora. Commensals activate resident submucosal dendritic cells (DCs) and initiate an immunosuppressive response through NFkB/TGFβ pathway which in turn activates the lymphnode CD103^{+} DCs mesenteric population. These DCs subset have the ability to prime naïve CD4+ T cell lymphocytes from mesenteric ganglia and induce immunosuppressive CD4+ T cells lineages, namely Th3, FoxP3+ (TREG) and Th2-inducing IL10, and TGF-β cytokines. The immune-tolerant response protects IECs and allows symbiotic relationships between the organism and commensal flora. **(B)** Intestinal pathogens activate inflammatory mediators and promote invasion. Pathogenic species possess virulence factors (T6SS or T3SS system, flagella, mucus binding proteins, mucinases, etc.) that enable their mucus diffusion and translocation across IECs. Herein pathogens activate TLR4 and 5 receptors and subsequently induce the release of inflammatory cytokines, IL1, IL6, and IL8. These cytokines further activate the CD103+/-DCs population and either promote CD4 T helper cells polarization into inflammatory Th1, Th17, and CD8-cytotoxic subsets or stimulate B lymphocytes to express IgG, while also reducing the immunosuppressive response. The IgG activity and inflammatory response driven by Th1/Th17-related cytokines, IFN-γ, IL-17, limits the bacterial invasion. The AI-2 inducer produced by certain symbionts can also prevent intestinal colonization with pathogenic species through negative feedback signals. However a significant gut inflammatory response allows bacterial translocation.

commensal flora to the protective mucus (Hasegawa et al., 2014). On the other hand, a proinflammatory response ensues when the TLR mediated response generated by pathogens switches the DC tolerogenic profile to the inflammatory CD103-/+ mesenteric DCs. DCs will further upregulate the NF-kB system and stimulate CD4 differentiation into inflammatory Th1, Th17, and CD8-cytotoxic subsets along with IgG secreting B lymphocytes. Furthermore, proinflammatory cytokines (IL6, IL8, IL17, IL21, IL22, and IFN-γ) will recruit neutrophils to the invaded site (Vandamme et al., 2012; Hunter and De Plaen, 2014; Perez-Lopez et al., 2016). The inflammatory response ensures epithelial integrity and prevents the invasion of the intestinal mucosa by *Salmonella, C. jejuni* or other pathogens (Geddes et al., 2011). Dysregulations of the NF-κB pathway could nevertheless induce an excessive inflammatory response and epithelial disruption, promoting translocations of bacteria and toxins (**Figure 1**).

MICROBIOTA AND ITS DIRECT WEAPONS, THE ANTIMICROBIAL COMPOUNDS

Antimicrobial Peptides

Antimicrobial peptides are innate immune effector molecules with bactericidal, anti-inflammatory and anti-endotoxinic properties (Vandamme et al., 2012). Cathelicidin, a vitamin D mediated AMP, favors mucus synthesis and epithelial repair,

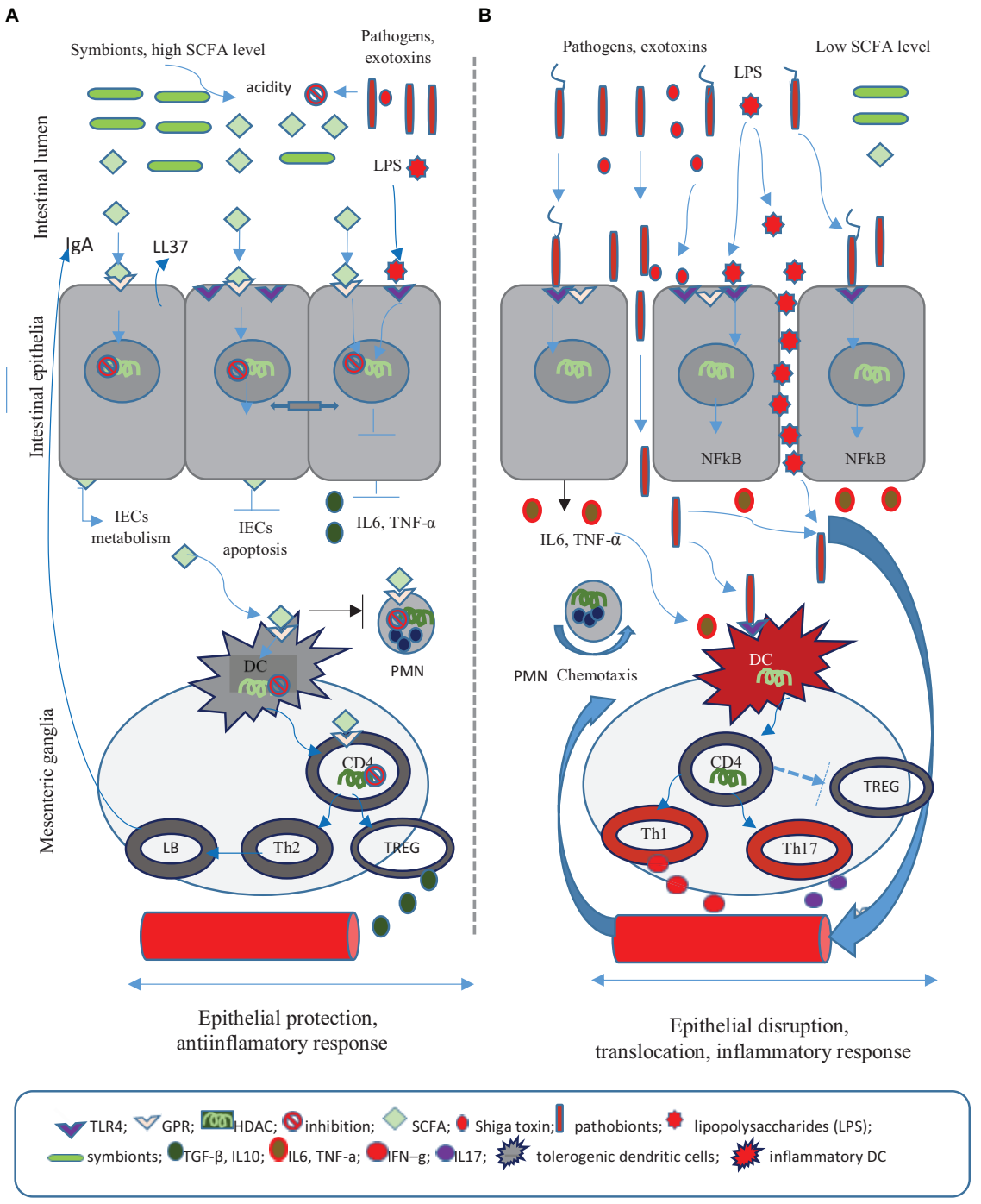

FIGURE 2 | The role of short chain fatty acids (SCFA) in the anti-infectious defense. **(A)** SCFA are fermentation products of the commensal flora and exert anti-inflammatory and trophic roles on the intestinal epithelial cells (IECs). SCFA elicit effects on IECs metabolism increasing colonic acidity and preventing the colonization with pathogenic germs. SCFA play a significant role in the preservation of tight epithelial junctions through the activation of HIF factor and by decreasing enterocyte apopotosis. As a result SCFA decrease epithelial permeability. At a cellular level SCFA activate specific G protein-coupled receptors (GPR), modulate the chromatin through histone deacetylase (HADC) inhibition, supress the nuclear factor (*NF*)-κB and reduce the release of pro-inflammatory cytokines (IL6, TNF-α). SCFA regulate the inflammatory response by promoting tolerogenic dendritic cells (DCs), IL-10-producing T-helper cells (TREG), and Th2 response including *B*-cell IgA production. The immune role of SCFA relies on their ability to induce an anti-inflamatory response and to stimulate antimicrobial molecules, namely cathelicidin (LL37) and intestinal IgA. Consequently SCFA offer protection to IEC and decrease the risk of bacterial invasion and toxin translocation. **(B)** The absence of SCFA leads to epithelial breaches and translocations of bacteria and lipopolysaccharides (LPS). The inflammatory response involves the following: the activation of toll-like receptor 4 (TLR4) by pathogenic flora, HDAC activity, the (NF)-B transcription, DCs stimulation which promotes mesenteric Th1/Th17 cell differentiation, the release of pro-inflammatory cytokines IL6, TNF-α, IFN–γ, IL17, and neutrophil migration.

as well as chemotaxis and T-cell recruitment to the invaded site. The intestinal microbiota facilitates the synthesis of AMP in the intestinal epithelium via a pattern recognition receptor mediated mechanism or indirectly, through its own metabolic products, in particular SCFA (Schauber et al., 2003; Raqib et al., 2012). *B. thetaiotaomicron* and *Listeria innocua* are the main species that induce AMP, especially angiogenins, cathelicidin and several defensines (Hooper et al., 2003; Eckmann, 2005). AMP release can be down-regulated by certain pathogens (*Helycobacter, Schigella*) or up-regulated by probiotics (*Lactobacillus*, *Bifidobacterium),* explaining the success of the experimental use of probiotics in the prophylaxis of intestinal infections in birds (Sunkara et al., 2012).

Bacteriocins

The commensal flora produces cell wall-active bactericidal polypeptides generically called bacteriocins. Bacteriocins are produced by *Eubacteria* and some *Archaea* species and are classified according to their peptidic structure (Garcia-Gutierrez et al., 2018). Bacteriocin-producing species are best represented by the families of the *Lactobacillaceae* and *Bifidobacterium* (Hammami et al., 2013). Each bacterial species produces several types of bacteriocins regulated by QS in a cell density-dependent manner (Kleerebezem, 2004). Bacteriocins significantly limit the colonization with multidrug resistant enterococci (Millette et al., 2008), *L. monocytogenes* (Dabour et al., 2009), *C. difficile* (Crowther et al., 2013), *S.aureus* (Park et al., 2007) and other pathogens (Umu et al., 2016). In addition, probiotics also release bacteriocins responsible for the elimination of certain pathogenic species and for the restoration of commensal intestinal communities. Thus, the probiotic strain *E. coli* Nissle-1917 induces anti *Shiga-toxin* bacteriocins (Mohsin et al., 2015) while PA-1 pediocin acts upon *Listeria* species (Dabour et al., 2009). Sactibiotic thuricin-CD, a bacteriocin produced by a strain of *B.thuringiensis*, exhibits inhibitory concentrations against *C. difficile* that are comparable to vancomycin and metronidazole without the former's toxicity (Mathur et al., 2016). Despite increasing attention, the study of bacteriocins is impeded by unstandardized methods and discordant results on animal models.

Secondary Bile Acids

Bile acids are essential antimicrobial agents controlled by the intestinal microbiota acting through cell membrane-damage or by activating vitamin D and farnesoid X nuclear receptors involved in the regulation of cathelicidin (Ridlon et al., 2014; Martin et al., 2018).

The liver synthesizes cholic acid and chenodeoxycholic acids, two primary BAs deconjugated by bacteria bile salt hydrolases (BSHs) and converted to secondary BAs, namely deoxycholic acid (DCA) and lithocholic acid. It has been suggested that BSHs-producing species of *Lactobacillus, Bifidobacterium, Clostridium,* and *Bacteroides* are protected from the toxicity of BA and are advantaged in the competition for survival (Horáčková, 2018). One example is the invasive BSH-producing *L. monocytogenes* strain versus BSH-negative and non-virulent *L. innocua* (Dussurget et al., 2002). Deconjugation is an attribute of Gram positive bacilli, especially of the commensal *Lactobacillus* and *Clostridium* species (e.g., *C. scindens*) and ensures the colonization resistance toward other species (Buffie et al., 2015). *B.bifidum*-induced DCA diminishes the pathogenicity of certain germs by targeting virulence-associated T6SS or T3SS effectors, used by toxigenic enterobacteria species and *V. cholerae* (Urdaneta and Casadesús, 2017). Furthermore, the absence of DCA-producing commensals allows the expansion of pathogens as in the case of *C. difficile* enterocolitis (Kochan et al., 2018). Increasing the level of BAs through therapy or diets favors the expansion of species involved in BA deconjugation (*Firmicutes* and *Clostridium* in particular) along with the inhibition of *Bacteroidetes* and *Actinobacteria.* Nevertheless, certain invasive species such as *Salmonella* can survive for prolonged periods despite high concentrations of BAs (Urdaneta and Casadesús, 2017). Considering that excessive BAs, especially DCA, are involved in the development of cholesterol gallstones and colon cancer, the intestinal flora can play an additive role to these complications. Concurrently, low concentrations of BAs are correlated with reduced antimicrobial function, favoring Gram negative bacterial overgrowth and translocation (Ridlon et al., 2014).

Short Chain Fatty Acids

Short chain fatty acids are saturated aliphatic organic acids consisting of a chain of 2–6 carbon atoms and a carboxylic acid moiety. SCFAs result from fermentation processes initiated by the gut and perform immune, anti-infectious and metabolic roles. There are three main types of SCFA: acetate, propionate and butyrate. Butyrate is mostly produced by *Firmicutes* in the colon, while acetate and propionate produced by *Bacteroidetes* strains predominate in the systemic circulation (Cummings et al., 1987).

SCFAs are GPR41, GPR43, and GPR109 membrane receptor ligands with immunomodulatory functions. These receptors are located specifically in the intestinal tract but can also be found in leukocytes, hematopoietic tissues (GPR43) or in the enteric nervous system, portal circulation and gut–brain neural circuit (GPR41). GPR109 mainly expressed in the colon epithelia responds to butyrate only. At a cellular level, SCFAs protect the intestinal epithelium and reduce bacterial translocation by stabilizing the hypoxia-inducible transcription factor (Kelly et al., 2015). SCFAs also act as epigenetic regulators of the local and systemic inflammatory response. Thus SCFAs serve as histone acetyltransferases activators or histone deacetylase inhibitors (HDACi) that modulate transcriptional factors (e,g NF-κB, MyoD) (Liu et al., 2012; Koh et al., 2016; Chen et al., 2018). Butyrate, the most potent HDACi, has been shown to modulate the genetic expression of over 19.000 genes in a human colonic epithelial cell line (Daly and Shirazi-Beechey, 2006). SCFAs acting as HDAC is also exert divergent immunologic responses depending on the cell type and its degree of activity and HDACi type (Villagra et al., 2010). SCFAs can thus regulate Th1/Th2 cytokines, often favoring an anti-inflammatory response (DC with a tolerogenic profile, the production of $Foxp3^{+}$(TREG) cells, IL10 release, NF-kB suppression). In addition, SCFAs inhibit inflammatory responses mounted by polymorphonuclear cells, lymphocytes or tissue phagocytes (**Figure 2**). However, once an

inflammatory process has already been initiated, SCFAs further intensify this process.

The action of SCFAs on T lymphocytes depends on their activation – activated T lymphocytes favor SCFA suppression of FoxP3+TREG cells, while decreased T cell activation induces FoxP3+(TREG) cell expansion. Furthermore, in the presence of an infection and of subsequent T cell lymphocyte activation, SCFAs promote the differentiation of Th1 and Th17 and stimulate both effector (pro-inflammatory) and FoxP3+(TREG) cell lines. Still, in the absence of an acute infection SCFAs induce cell production of IL10 and immune tolerance (Cavaglieri et al., 2003; Furusawa et al., 2013; **Figure 2**).

Short chain fatty acids play a trophic role on the intestinal mucosa, enable the proliferation of normal colon cells and maintain the integrity of epithelial tight junctions. By decreasing epithelial permeability, SCFAs oppose bacterial and LPS translocations. Thus the acetate produced by *Bifidobacteria* inhibits the apoptosis of epithelial cells and prevents gut-blood EHEC-*Shiga* toxins translocation (Fukuda et al., 2011). SCFAs interfere with the lipid and glucose metabolism in the liver and various tissues and represent an energy source for gut epithelia. In addition, SCFAs acidify the intestinal environment further preventing the colonization with pathogenic bacteria (den Besten et al., 2013). Thus *Clostridium* butyrate producers (especially *Lachnospiraceae, Ruminococcaceae,* and *F.prausnitzii*) impede the colonization with *Salmonella*, *C. difficile*, and *Campylobacter species* (Goepfert and Hicks, 1969; Van Deun et al., 2008; Antharam et al., 2013; Rivera-Chávez et al., 2016). As a result, pathogenic species will colonize locations where the pH is convenient for the expression of virulence factors, such as the colon for *Shigella* or the ileum and jejunum for the invasive EHEC and *S. tiphy/S. typhimurium* (Speelman et al., 1984; Tazume et al., 1990). On the other hand SCFAs and particularly butyrate, modulate the expression of cellular receptors (e.g., EHEC-*Shiga* toxin receptors), virulence factors (T3SS) or epithelial adherence factors of some enteropathogens (Nakanishi et al., 2009; Tobe et al., 2011; De Nisco et al., 2018). Consequently, some commensal species may support pathogenic bacteria via SCFA release, while others strengthen the barrier function of the intestinal epithelium and prevent translocations or colonization with bacterial pathogens. These observations highlight the idea that the simple presence of SCFAs is not sufficient to balance the gut-microbiota relationship and that further data is needed on SCFA producing probiotics and their administration.

CONCLUSION

The intestinal microbiota is a complex and stable microbial community whose symbiotic relationship with the human organism is crucial for gut homeostasis and colonization resistance against intestinal pathogens. The effective colonization by pathogens is precluded through the competition with commensal flora for the same intestinal niche and nutritional resources, as well as by specific antimicrobial products and mucosal immune response. Pathogens employ multiple strategies to adapt to this hostile environment such as the expression of various virulence factors, structural changes or the manipulation of the QS system. Any changes involving the structure, stability or functional activities of intestinal microbiota could have long-lasting effects and favor intestinal and systemic infections.

AUTHOR CONTRIBUTIONS

SI, DI, and LL contributed equally to the acquisition, analysis, and critical revision of the article. All authors had given their consent for the publication and agreed to be responsible for the accuracy and integrity of the article.

REFERENCES

Antharam, V. C., Li, E. C., Ishmael, A., Sharma, A., Mai, V., Rand, K. H., et al. (2013). Intestinal dysbiosis and depletion of butyrogenic bacteria in *Clostridium difficile* infection and nosocomial diarrhea. *J. Clin. Microbiol.* 51, 2884–2892. doi: 10.1128/JCM.00845-13

Asfour, H. Z. (2018). Anti-quorum sensing natural compounds. *J. Microsc. Ultrastruct. Wolters Kluwer – Medknow Publications* 6, 1–10. doi: 10.4103/JMAU.JMAU_10_18

Bergstrom, K. S. B., and Xia, L. (2013). Mucin-type O-glycans and their roles in intestinal homeostasis. *Glycobiology* 23, 1026–1037. doi: 10.1093/glycob/cwt045

Branka, J. E., Vallette, G., Jarry, A., Bou-Hanna, C., Lemarre, P., Van Pn, et al. (1997). Early functional effects of *Clostridium difficile* toxin A on human colonocytes. *Gastroenterology* 112, 1887–1894. doi: 10.1053/gast.1997.v112.pm9178681

Buffie, C. G., Bucci, V., Stein, R. R., McKenney, P. T., Ling, L., Gobourne, A., et al. (2015). Precision microbiome reconstitution restores bile acid mediated resistance to *Clostridium difficile*. *Nature* 517, 205–208. doi: 10.1038/nature13828

Caballero-Franco, C., Keller, K., De Simone, C., and Chadee, K. (2007). The VSL#3 probiotic formula induces mucin gene expression and secretion in colonic epithelial cells. *Am. J. Physiol. Liver Physiol.* 292, G315–G322. doi: 10.1152/ajpgi.00265.2006

Cavaglieri, C. R., Nishiyama, A., Fernandes, L. C., Curi, R., Miles, E. A., and Calder, P. C. (2003). Differential effects of short-chain fatty acids on proliferation and production of pro- and anti-inflammatory cytokines by cultured lymphocytes. *Life Sci.* 73, 1683–1690. doi: 10.1016/S0024-3205(03)00490-9

Chen, G., Ran, X., Li, B., Li, Y., He, D., Huang, B., et al. (2018). Sodium butyrate inhibits inflammation and maintains epithelium barrier integrity in a TNBS-induced inflammatory bowel disease mice model. *EBioMedicine* 30, 317–325. doi: 10.1016/j.ebiom.2018.03.030

Chen, J., Ma, M., Uzal, F. A., and McClane, B. A. (2014). Host cell-induced signaling causes *Clostridium perfringens* to upregulate production of toxins important for intestinal infections. *Gut Microbes* 10, 96–107. doi: 10.4161/gmic.26419

Collado, M. C., Gueimonde, M., Hernández, M., Sanz, Y., and Salminen, S. (2005). Adhesion of selected *Bifidobacterium* strains to human intestinal mucus and the role of adhesion in enteropathogen exclusion. *J. Food Prot.* 68, 2672–2678. doi: 10.4315/0362-028X-68.12.2672

Coombes, J. L., and Powrie, F. (2008). Dendritic cells in intestinal immune regulation. *Nat. Rev. Immunol.* 8, 435–446. doi: 10.1038/nri2335

Coyne, M. J., Reinap, B., Lee, M. M., and Comstock, L. E. (2005). Human symbionts use a host-like pathway for surface fucosylation. *Science (80-)* 307, 1778–1781. doi: 10.1126/science.1106469

Crowther, G. S., Baines, S. D., Todhunter, S. L., Freeman, J., Chilton, C. H., and Wilcox, M. H. (2013). Evaluation of NVB302 versus vancomycin activity in an in vitro human gut model of *Clostridium difficile* infection. *J. Antimicrob. Chemother.* 68, 168–176. doi: 10.1093/jac/dks359

Cummings, J. H., Pomare, E. W., Branch, W. J., Naylor, C. P., and Macfarlane, G. T. (1987). Short chain fatty acids in human large intestine, portal, hepatic and venous blood. *Gut* 28, 1221–1227. doi: 10.1136/gut.28.10.1221

Curtis, M. M., Hu, Z., Klimko, C., Narayanan, S., Deberardinis, R., and Sperandio, V. (2014). The gut commensal *Bacteroides thetaiotaomicron* exacerbates enteric infection through modification of the metabolic landscape. *Cell Host Microbe* 16, 759–769. doi: 10.1016/j.chom.2014.11.005

Dabour, N., Zihler, A., Kheadr, E., Lacroix, C., and Fliss, I. (2009). In vivo study on the effectiveness of pediocin PA-1 and *Pediococcus acidilactici* UL5 at inhibiting *Listeria monocytogenes*. *Int. J. Food Microbiol.* 133, 225–233. doi: 10.1016/j.ijfoodmicro.2009.05.005

Daly, K., and Shirazi-Beechey, S. P. (2006). Microarray analysis of butyrate regulated genes in colonic epithelial cells. *DNA Cell Biol.* 25, 49–62. doi: 10.1089/dna.2006.25.49

De Nisco, N. J., Rivera-Cancel, G., and Orth, K. (2018). The biochemistry of sensing: enteric pathogens regulate type III secretion in response to environmental and host cues. *MBio. Am. Soc. Microbiol.* 9:e2122-17. doi: 10.1128/mBio.02122-17

den Besten, G., van Eunen, K., Groen, A. K., Venema, K., Reijngoud, D.-J., and Bakker, B. M. (2013). The role of short-chain fatty acids in the interplay between diet, gut microbiota, and host energy metabolism. *J. Lipid Res. Am. Soc. Biochem. Mol. Biol.* 54, 2325–2340. doi: 10.1194/jlr.R036012

Donaldson, G. P., Lee, S. M., and Mazmanian, S. K. (2016). Gut biogeography of the bacterial microbiota. *Nat. Rev. Microbiol.* 14, 20–32. doi: 10.1038/nrmicro3552

Dussurget, O., Cabanes, D., Dehoux, P., Lecuit, M., Buchrieser, C., Glaser, P., et al. (2002). *Listeria monocytogenes* bile salt hydrolase is a PrfA-regulated virulence factor involved in the intestinal and hepatic phases of listeriosis. *Mol. Microbiol.* 45, 1095–1106. doi: 10.1046/j.1365-2958.2002.03080.x

Dwivedi, R., Nothaft, H., Garber, J., Xin Kin, L., Stahl, M., Flint, A., et al. (2016). L-fucose influences chemotaxis and biofilm formation in *Campylobacter jejuni*. *Mol. Microbiol.* 101, 575–589. doi: 10.1111/mmi.13409

Eckmann, L. (2005). Defence molecules in intestinal innate immunity against bacterial infections. *Curr. Opin. Gastroenterol.* 21, 147–151. doi: 10.1097/01.mog.0000153311.97832.8c

Fabich, A. J., Jones, S. A., Chowdhury, F. Z., Cernosek, A., Anderson, A., Smalley, D., et al. (2008). Comparison of carbon nutrition for pathogenic and commensal *Escherichia coli* strains in the mouse intestine. *Infect Immun.* 76, 1143–1152. doi: 10.1128/IAI.01386-07

Ferreyra, J. A., Wu, K. J., Hryckowian, A. J., Bouley, D. M., Weimer, B. C., and Sonnenburg, J. L. (2014). Gut microbiota-produced succinate promotes *C. difficile* infection after antibiotic treatment or motility disturbance. *Cell Host Microbe.* 16, 770–777. doi: 10.1016/j.chom.2014.11.003

Fukuda, S., Toh, H., Hase, K., Oshima, K., Nakanishi, Y., Yoshimura, K., et al. (2011). *Bifidobacteria* can protect from enteropathogenic infection through production of acetate. *Nature* 469, 543–547. doi: 10.1038/nature09646

Furusawa, Y., Obata, Y., Fukuda, S., Endo, T. A., Nakato, G., Takahashi, D., et al. (2013). Commensal microbe-derived butyrate induces the differentiation of colonic regulatory T cells. *Nature* 504, 446–450. doi: 10.1038/nature12721

Ganesh, B. P., Klopfleisch, R., Loh, G., and Blaut, M. (2013). Commensal *Akkermansia muciniphila* exacerbates gut inflammation in *Salmonella Typhimurium*-infected gnotobiotic mice. *PLoS One* 8:e74963. doi: 10.1371/journal.pone.0074963

Garcia-Gutierrez, E., Mayer, M. J., Cotter, P. D., and Narbad, A. (2018). Gut microbiota as a source of novel antimicrobials. *Gut Microbes* 27, 1–21. doi: 10.1080/19490976.2018.1455790

Garsin, D. A. (2010). Ethanolamine utilization in bacterial pathogens: roles and regulation. *Nat. Rev. Microbiol.* 8, 290–295. doi: 10.1038/nrmicro2334

Geddes, K., Rubino, S. J., Magalhaes, J. G., Streutker, C., Le Bourhis, L., Cho, J. H., et al. (2011). Identification of an innate T helper type 17 response to intestinal bacterial pathogens. *Nat. Med.* 17, 837–844. doi: 10.1038/nm.2391

Goepfert, J. M., and Hicks, R. (1969). Effect of volatile fatty acids on *Salmonella typhimurium*. *J. Bacteriol. Am. Soc. Microbiol. (ASM)* 97, 956–958.

Hammami, R., Fernandez, B., Lacroix, C., and Fliss, I. (2013). Anti-infective properties of bacteriocins: an update. *Cell Mol. Life Sci.* 70, 2947–2967. doi: 10.1007/s00018-012-1202-3

Hasegawa, M., Yada, S., Liu, M. Z., Kamada, N., Muñoz-Planillo, R., Do, N., et al. (2014). Interleukin-22 regulates the complement system to promote resistance against pathobionts after pathogen-induced intestinal damage. *Immunity* 41, 620–632. doi: 10.1016/j.immuni.2014.09.010

Hooper, L. V., Stappenbeck, T. S., Hong, C. V., and Gordon, J. I. (2003). Angiogenins: a new class of microbicidal proteins involved in innate immunity. *Nat. Immunol.* 4, 269–273. doi: 10.1038/ni888

Horáčková, Š., Plocková, M., and Demnerová, K. (2018). Importance of microbial defence systems to bile salts and mechanisms of serum cholesterol reduction. *Biotechnol. Adv.* 36, 682–690. doi: 10.1016/j.biotechadv.2017.12.005

Hsiao, A., Ahmed, A. M. S., Subramanian, S., Griffin, N. W., Drewry, L. L., Petri, W. A., et al. (2014). Members of the human gut microbiota involved in recovery from *Vibrio cholerae* infection. *Nature* 515, 423–426. doi: 10.1038/nature13738

Huang, J. Y., Lee, S. M., and Mazmanian, S. K. (2011). The human commensal *Bacteroides fragilis* binds intestinal mucin. *Anaerobe* 17, 137–141. doi: 10.1016/j.anaerobe.2011.05.017

Hunter, C. J., and De Plaen, I. G. (2014). Inflammatory signaling in NEC: role of NF-κB, cytokines and other inflammatory mediators. *Pathophysiol. Off. J. Int. Soc. Pathophysiol.* 21, 55–65. doi: 10.1016/j.pathophys.2013.11.010

Kamada, N., Kim, Y.-G., Sham, H. P., Vallance, B. A., Puente, J. L., Martens, E. C., et al. (2012). Regulated virulence controls the ability of a pathogen to compete with the gut microbiota. *Science* 8, 1325–1329. doi: 10.1126/science.1222195

Kelly, C. J., Zheng, L., Campbell, E. L., Saeedi, B., Scholz, C. C., Bayless, A. J., et al. (2015). Crosstalk between microbiota-derived short-chain fatty acids and intestinal epithelial HIF augments tissue barrier function. *Cell Host Microbe* 17, 662–671. doi: 10.1016/j.chom.2015.03.005

Kim, Y. S., and Ho, S. B. (2010). Intestinal goblet cells and mucins in health and disease: recent insights and progress. *Curr. Gastroenterol. Rep.* 12, 319–330. doi: 10.1007/s11894-010-0131-2

Kinoshita, H., Uchida, H., Kawai, Y., Kitazawa, H., Miura, K., Shiiba, K., et al. (2007). Quantitative evaluation of adhesion of *Lactobacilli* isolated from human intestinal tissues to human colonic mucin using surface plasmon resonance (BIACORE assay). *J. Appl. Microbiol.* 102, 116–123. doi: 10.1111/j.1365-2672.2006.03061.x

Kleerebezem, M. (2004). Quorum sensing control of lantibiotic production; nisin and subtilin autoregulate their own biosynthesis. *Peptides* 25, 1405–1414. doi: 10.1016/j.peptides.2003.10.021

Kochan, T. J., Shoshiev, M. S., Hastie, J. L., Somers, M. J., Plotnick, Y. M., Gutierrez-Munoz, D. F., et al. (2018). Germinant synergy facilitates *Clostridium difficile* spore germination under physiological conditions. *mSphere* 3:e00335-18.

Koh, A., De Vadder, F., Kovatcheva-Datchary, P., and Bäckhed, F. (2016). From dietary fiber to host physiology: short-chain fatty acids as key bacterial metabolites. *Cell* 165, 1332–1345. doi: 10.1016/j.cell.2016.05.041

Kong, S., Zhang, Y. H., and Zhang, W. (2018). Regulation of intestinal epithelial cells properties and functions by amino acids. *Biomed. Res. Int. Hindawi* 2018, 1–10. doi: 10.1155/2018/2819154

Lawley, T. D., and Walker, A. W. (2013). Intestinal colonization resistance. *Immunology* 138, 1–11. doi: 10.1111/j.1365-2567.2012.03616.x

Lin, L., and Zhang, J. (2017). Role of intestinal microbiota and metabolites on gut homeostasis and human diseases. *BMC Immunol.* 18:2. doi: 10.1186/s12865-016-0187-3

Liu, T., Li, J., Liu, Y., Xiao, N., Suo, H., Xie, K., et al. (2012). Short-chain fatty acids suppress lipopolysaccharide-induced production of nitric oxide and proinflammatory cytokines through inhibition of NF-κB pathway in RAW264.7 *cells*. *Inflammation* 35, 1676–1684. doi: 10.1007/s10753-012-9484-z

Liu, Z., Wang, Y., Liu, S., Sheng, Y., Rueggeberg, K.-G., Wang, H., et al. (2015). *Vibrio cholerae* represses polysaccharide synthesis to promote motility in mucosa. *Infect. Immun.* 83, 1114–1121. doi: 10.1128/IAI.02841-14

Luo, Q., Kumar, P., Vickers, T. J., Sheikh, A., Lewis, W. G., Rasko, D. A., et al. (2014). Enterotoxigenic *Escherichia coli* secretes a highly conserved mucin-degrading metalloprotease to effectively engage intestinal epithelial cells. *Infect Immun.* 82, 509–521. doi: 10.1128/IAI.01106-13

Maltby, R., Leatham-Jensen, M. P., Gibson, T., Cohen, P. S., and Conway, T. (2013). Nutritional basis for colonization resistance by human commensal *Escherichia coli* strains HS and Nissle 1917 against *E. coli* O157:H7 in the mouse intestine. *PLoS One* 8:e53957. doi: 10.1371/journal.pone.0053957

Martens, E. C., Roth, R., Heuser, J. E., and Gordon, J. I. (2009). Coordinate regulation of glycan degradation and polysaccharide capsule biosynthesis by a prominent human gut symbiont. *J. Biol. Chem.* 284, 18445–18457. doi: 10.1074/jbc.M109.008094

Martin, G., Kolida, S., Marchesi, J. R., Want, E., Sidaway, J. E., and Swann, J. R. (2018). In vitro modeling of bile acid processing by the human fecal microbiota. *Front. Microbiol.* 9:1153. doi: 10.3389/fmicb.2018.01153

Mathur, H., Rea, M. C., Cotter, P. D., Hill, C., and Ross, R. P. (2016). The efficacy of thuricin CD, tigecycline, vancomycin, teicoplanin, rifampicin and nitazoxanide, independently and in paired combinations against *Clostridium difficile* biofilms and planktonic cells. *Gut Pathog. BioMed Central* 8:20. doi: 10.1186/s13099-016-0102-8

Millette, M., Cornut, G., Dupont, C., Shareck, F., Archambault, D., and Lacroix, M. (2008). Capacity of human nisin- and pediocin-producing lactic acid bacteria to reduce intestinal colonization by vancomycin-resistant enterococci. *Appl. Environ. Microbiol.* 1, 1997–2003. doi: 10.1128/AEM.02150-07

Mohsin, M., Guenther, S., Schierack, P., Tedin, K., and Wieler, L. H. (2015). Probiotic *Escherichia coli* Nissle 1917 reduces growth, *Shiga* toxin expression, release and thus cytotoxicity of enterohemorrhagic *Escherichia coli*. *Int. J. Med. Microbiol.* 305, 20–26. doi: 10.1016/j.ijmm.2014.10.003

Nakanishi, N., Tashiro, K., Kuhara, S., Hayashi, T., Sugimoto, N., and Tobe, T. (2009). Regulation of virulence by butyrate sensing in enterohaemorrhagic *Escherichia coli*. *Microbiology* 155, 521–530. doi: 10.1099/mic.0.023499-0

Ndeh, D., and Gilbert, H. J. (2018). Biochemistry of complex glycan depolymerisation by the human gut microbiota. *FEMS Microbiol. Rev.* 42, 146–164. doi: 10.1093/femsre/fuy002

Ng, K. M., Ferreyra, J. A., Higginbottom, S. K., Lynch, J. B., Kashyap, P. C., Gopinath, S., et al. (2013). Microbiota-liberated host sugars facilitate post-antibiotic expansion of enteric pathogens. *Nature* 502, 96–99. doi: 10.1038/nature12503

O'Callaghan, A., and van Sinderen, D. (2016). *Bifidobacteria* and their role as members of the human gut microbiota. *Front. Microbiol.* 7:925. doi: 10.3389/fmicb.2016.00925

Pacheco, A. R., Curtis, M. M., Ritchie, J. M., Munera, D., Waldor, M. K., Moreira, C. G., et al. (2012). Fucose sensing regulates bacterial intestinal colonization. *Nature* 492, 113–117. doi: 10.1038/nature11623

Park, Y.-S., Shin, W.-S., and Kim, S.-K. (2007). In vitro and in vivo activities of echinomycin against clinical isolates of *Staphylococcus aureus*. *J. Antimicrob. Chemother.* 61, 163–168. doi: 10.1093/jac/dkm421

Pereira, C. S., Thompson, J. A., and Xavier, K. B. (2013). AI-2-medated signalling in bacteria. *FEMS Microbiol. Rev.* 37, 156–181. doi: 10.1111/j.1574-6976.2012.00345.x

Perez-Lopez, A., Behnsen, J., Nuccio, S.-P., and Raffatellu, M. (2016). Mucosal immunity to pathogenic intestinal bacteria. *Nat. Rev. Immunol.* 16, 135–148. doi: 10.1038/nri.2015.17

Pinheiro, J., Lisboa, J., Pombinho, R., Carvalho, F., Carreaux, A., Brito, C., et al. (2018). MouR controls the expression of the *Listeria monocytogenes* Agr system and mediates virulence. *Nucleic Acids Res.* 46, 9338–9352. doi: 10.1093/nar/gky624

Rajilic-Stojanovic, M., Smidt, H., and de Vos, W. M. (2007). Diversity of the human gastrointestinal tract microbiota revisited. *Environ. Microbiol.* 9, 2125–2136. doi: 10.1111/j.1462-2920.2007.01369.x

Rakoff-Nahoum, S., Paglino, J., Eslami-Varzaneh, F., Edberg, S., and Medzhitov, R. (2004). Recognition of commensal microflora by toll-like receptors is required for intestinal homeostasis. *Cell* 118, 229–241. doi: 10.1016/j.cell.2004.07.002

Raqib, R., Sarker, P., Mily, A., Alam, N. H., Arifuzzaman, A. S. M., Rekha, R. S., et al. (2012). Efficacy of sodium butyrate adjunct therapy in shigellosis: a randomized, double-blind, placebo-controlled clinical trial. *BMC Infect. Dis.* 12:111. doi: 10.1186/1471-2334-12-111

Ridlon, J. M., Kang, D. J., Hylemon, P. B., and Bajaj, J. S. (2014). Bile acids and the gut microbiome. *Curr. Opin. Gastroenterol.* 30, 332–338. doi: 10.1097/MOG.0000000000000057

Rivera-Chávez, F., Zhang, L. F., Faber, F., Lopez, C. A., Byndloss, M. X., Olsan, E. E., et al. (2016). Depletion of butyrate-producing *Clostridia* from the gut microbiota drives an aerobic luminal expansion of *Salmonella*. *Cell Host Microbe* 19, 443–454. doi: 10.1016/j.chom.2016.03.004

Schauber, J., Svanholm, C., Termén, S., Iffland, K., Menzel, T., Scheppach, W., et al. (2003). Expression of the cathelicidin LL-37 is modulated by short chain fatty acids in colonocytes: relevance of signalling pathways. *Gut* 52, 735–741. doi: 10.1136/gut.52.5.735

Sicard, J.-F., Le Bihan, G., Vogeleer, P., Jacques, M., and Harel, J. (2017). Interactions of intestinal bacteria with components of the intestinal mucus. *Front. Cell Infect. Microbiol.* 7:387. doi: 10.3389/fcimb.2017.00387

Sicard, J.-F., Vogeleer, P., Le Bihan, G., Rodriguez Olivera, Y., Beaudry, F., Jacques, M., et al. (2018). N-Acetyl-glucosamine influences the biofilm formation of *Escherichia coli*. *Gut Pathog.* 10:26. doi: 10.1186/s13099-018-0252-y

Speelman, P., Kabir, I., and Islam, M. (1984). Distribution and spread of colonic lesions in shigellosis: a colonoscopic study. *J. Infect. Dis.* 150, 899–903. doi: 10.1093/infdis/150.6.899

Stecher, B., and Hardt, W.-D. (2008). The role of microbiota in infectious disease. *Trends Microbiol.* 16, 107–114. doi: 10.1016/j.tim.2007.12.008

Sunkara, L. T., Jiang, W., and Zhang, G. (2012). Modulation of antimicrobial host defense peptide gene expression by free fatty acids. *PLoS One* 7:e49558. doi: 10.1371/journal.pone.0049558

Tazume, S., Takeshi, K., Saidi, S. M., Ichoroh, C. G., Mutua, W. R., Waiyaki, P. G., et al. (1990). Ecological studies on intestinal microbial flora of Kenyan children with diarrhoea. *J. Trop Med. Hyg.* 93, 215–221.

Thompson, J. A., Oliveira, R. A., and Xavier, K. B. (2016). Chemical conversations in the gut microbiota. *Gut Microbes* 7, 163–170. doi: 10.1080/19490976.2016.1145374

Tobe, T., Nakanishi, N., and Sugimoto, N. (2011). Activation of motility by sensing short-chain fatty acids via two steps in a flagellar gene regulatory cascade in enterohemorrhagic *Escherichia coli*. *Infect. Immun.* 79, 1016–1024. doi: 10.1128/IAI.00927-10

Tu, Q. V., McGuckin, M. A., and Mendz, G. L. (2008). *Campylobacter jejuni* response to human mucin MUC2: modulation of colonization and pathogenicity determinants. *J. Med. Microbiol.* 57, 795–802. doi: 10.1099/jmm.0.47752-0

Umu, Ö. C. O., Bäuerl, C., Oostindjer, M., Pope, P. B., Hernández, P. E., Pérez-Martínez, G., et al. (2016). The potential of class II bacteriocins to modify gut microbiota to improve host health. *PLoS One* 11:e0164036. doi: 10.1371/journal.pone.0164036

Urdaneta, V., and Casadesús, J. (2017). Interactions between bacteria and bile salts in the gastrointestinal and hepatobiliary tracts. *Front. Med.* 4:163. doi: 10.3389/fmed.2017.00163

Van Deun, K., Pasmans, F., Van Immerseel, F., Ducatelle, R., and Haesebrouck, F. (2008). Butyrate protects Caco-2 cells from *Campylobacter jejuni* invasion and translocation. *Br. J. Nutr.* 100, 480–484. doi: 10.1017/S0007114508921693

Vandamme, D., Landuyt, B., Luyten, W., and Schoofs, L. (2012). A comprehensive summary of LL-37, the factotum human cathelicidin peptide. *Cell. Immunol.* 280, 22–35. doi: 10.1016/j.cellimm.2012.11.009

Villagra, A., Sotomayor, E. M., and Seto, E. (2010). Histone deacetylases and the immunological network: implications in cancer and inflammation. *Oncogene* 29, 157–173. doi: 10.1038/onc.2009.334

Walter, J. (2008). Ecological role of lactobacilli in the gastrointestinal tract: implications for fundamental and biomedical research. *Appl. Environ. Microbiol.* 74, 4985–4996. doi: 10.1128/AEM.00753-08

Wands, A. M., Fujita, A., McCombs, J. E., Cervin, J., Dedic, B., Rodriguez, A. C., et al. (2015). Fucosylation and protein glycosylation create functional receptors for cholera toxin. *Elife* 4:e09545. doi: 10.7554/eLife.09545

Wershil, B., and Furuta, G. (2008). Gastrointestinal mucosal immunity. *J. Allergy Clin. Immunol.* 121, S380–S383. doi: 10.1016/j.jaci.2007.10.023

Conflict of Interest Statement: The authors declare that the research was conducted in the absence of any commercial or financial relationships that could be construed as a potential conflict of interest.

Copyright © 2019 Iacob, Iacob and Luminos. This is an open-access article distributed under the terms of the Creative Commons Attribution License (CC BY). The use, distribution or reproduction in other forums is permitted, provided the original author(s) and the copyright owner(s) are credited and that the original publication in this journal is cited, in accordance with accepted academic practice. No use, distribution or reproduction is permitted which does not comply with these terms.

frontiers in Microbiology

ORIGINAL RESEARCH
published: 28 January 2019
doi: 10.3389/fmicb.2019.00011

Nasopharyngeal Microbiota in Children With Invasive Pneumococcal Disease: Identification of Bacteria With Potential Disease-Promoting and Protective Effects

Anny Camelo-Castillo[1], Desirée Henares[1,2], Pedro Brotons[1,2], Antonio Galiana[3], Juan Carlos Rodríguez[3], Alex Mira[2,4†] and Carmen Muñoz-Almagro[1,2,5*†] on behalf of the Catalan Study Group of Host-Pathogen Interaction in Patients With IPD[‡]*

[1] Institut de Recerca Sant Joan de Déu, Hospital Sant Joan de Déu, Barcelona, Spain, [2] Network of Epidemiology and Public Health, CIBERESP, Barcelona, Spain, [3] Department of Microbiology, Hospital de Alicante, Alicante, Spain, [4] Center for Advanced Research in Public Health, FISABIO Foundation, Valencia, Spain, [5] School of Medicine, Universitat Internacional de Catalunya, Barcelona, Spain

Background and Aims: The risk of suffering from some infectious diseases can be related to specific microbiota profiles. Specifically, the nasopharyngeal microbiota could play a role as a risk or protective factor in the development of invasive disease caused by *S. pneumoniae.*

Methodology: We analyzed the nasopharyngeal microbiota of children with invasive pneumococcal disease (IPD) and that of healthy controls matched by age, sex, and seasonality from Catalonia, Spain. Epidemiological, microbiological and clinical variables were considered to compare microbiota profiles, analyzed by sequencing the V1–V4 region of the 16S rRNA gene.

Results: Twenty-eight children with IPD (median age 43 months) and 28 controls (42.6 months) were included in the study. IPD children presented a significantly higher bacterial diversity and richness ($p < 0.001$). Principal coordinate analysis revealed three different microbiota profiles: microbiota A, dominated by the genus *Dolosigranulum* (44.3%); Microbiota B, mostly represented by *Streptococcus* (36.9%) and *Staphylococcus* (21.3%) and a high diversity of anaerobic genera including *Veillonella*, *Prevotella* and *Porphyromonas*; and Microbiota C, mainly containing *Haemophilus* (52.1%) and *Moraxella* (31.4%). The only explanatory factor for the three microbiotas was the classification of children into disease or healthy controls ($p = 0.006$). A significant negative correlation was found between *Dolosigranulum* vs. *Streptococcus* ($p = 0.029$), suggesting a potential antagonistic effect against pneumococcal pathogens.

Conclusions: The higher bacterial diversity and richness in children with IPD could suggest an impaired immune response. This lack of immune competence could be aggravated by breastfeeding <6 months and by the presence of keystone pathogens

OPEN ACCESS

Edited by:
Learn-Han Lee,
Monash University Malaysia, Malaysia

Reviewed by:
Emmanuel F. Mongodin,
University of Maryland, Baltimore, United States
Nuria Salazar,
Instituto de Productos Lácteos de Asturias (IPLA), Spain

***Correspondence:**
Alex Mira
mira_ale@gva.es
Carmen Muñoz-Almagro
cma@sjdhospitalbarcelona.org

[†]These authors have contributed equally to this work and are joint senior authors

[‡]Membership of the Catalan Study group of host-pathogen interaction in patients with IPD is provided in the Acknowledgments

Specialty section:
This article was submitted to Microbial Symbioses, a section of the journal Frontiers in Microbiology

Received: *03 April 2018*
Accepted: *07 January 2019*
Published: *28 January 2019*

Citation:
Camelo-Castillo A, Henares D, Brotons P, Galiana A, Rodriguez JC, Mira A and Muñoz-Almagro C (2019) Nasopharyngeal Microbiota in Children With Invasive Pneumococcal Disease: Identification of Bacteria With Potential Disease-Promoting and Protective Effects. Front. Microbiol. 10:11. doi: 10.3389/fmicb.2019.00011

such as *Porphyromonas*, a bacterium which has been shown to be able to manipulate the immune response, and that could favor the overgrowth of many proteolytic anaerobic organisms giving rise to a dramatic dysbiosis. From an applied viewpoint, we found suggestive microbiota profiles associated to IPD or asymptomatic colonization that could be used as disease biomarkers or to pave the way for characterizing health-associated inhabitants of the respiratory tract. The identification of beneficial bacteria could be useful to prevent pneumococcal infections by integrating those microorganisms in a probiotic formula. The present study suggests not only respiratory tract samples, but also breast milk, as a potential source of those beneficial bacteria.

Keywords: nasopharyngeal microbiota, children, invasive pneumococcal disease, *Streptococcus pneumoniae, Dolosigranulum*

INTRODUCTION

The human microbiota communities and their genes are an intriguing ecosystem that play an essential role for human body functions including food digestion, nutrition, regulation of human metabolism, and regulation of immune defense against infections, among others (Zhu et al., 2010). The majority of microorganisms of the human ecosystem act as symbionts that co-evolve and co-adapt with their human host according to their diet, life-style, human genetic characteristics, immune modulation, or environment parameters (Dethlefsen et al., 2007). Particularly in samples from the respiratory tract, the variability in bacterial composition between individuals has been described to be so high that a core microbiome could not be defined at the species level (Bogaert et al., 2011). Despite this inter-individual variability, the bacterial composition of each person has been proposed to fall within discrete categories where some bacterial taxa dominate the community. The presence of these structured microbial consortia was first described in the gut, where three groups or "enterotypes" were found, dominated by *Bacteroides*, *Prevotella*, or *Ruminococcus* (Arumugam et al., 2011). However, the notion of enterotypes is currently under debate, and it is still not clear whether enterotypes can be generalized to the general population, or whether microbiota follows in fact a gradient in taxonomic composition (Jeffery et al., 2012). In children between 1 and 3 months of age, for instance, the hypopharynx was found to contain four or five community types, and these "pneumotypes" followed specific trajectories during the child's development (Mortensen et al., 2016). In adults, bronchoalveolar lavage samples showed two distinct pneumotypes, one of which was enriched with oral microorganisms (particularly *Prevotella* and *Veillonella*) and appeared to be associated with higher inflammatory markers (Segal et al., 2013). Thus, studying the bacterial community structures in the respiratory tract could be important to understand susceptibility to Chronic Obstructive Pulmonary Disease (COPD) or to pulmonary infections like pneumococcal pneumonia or, more extensively, Invasive Pneumococcal Disease (IPD).

It has been proposed that the degree of stability of the microbiota depends partly on the first colonization by keystone species in the first days of life (Relman, 2012). Natural feed of humans in their early days is breastfeeding, so human milk is expected to be a major supplier of keystone species for human microbiota development, including the respiratory tract, given the high microbial diversity in colostrum, transition, and mature milk (Hunt et al., 2011; Cabrera-Rubio et al., 2012). In addition, breast milk provides macronutrients, micronutrients and bioactive molecules that protect against infections and inflammation and are key factors for human growth and development (Ballard and Morrow, 2013). Another source of resilience to infection is provided by the antagonistic interactions between the local microbiota and the invasive species. For instance, the nasal passage inhabitant *Corynebacterium accolens* appears to be over-represented in children without *Streptococcus pneumoniae* nasal colonization and has been shown to release antipneumococcal free fatty acids from human skin surface triacylglycerols (Bomar et al., 2016). Other commensal bacteria produce antimicrobial peptides that have been shown to inhibit oral pathogens (López-López et al., 2017) and prevent pharynx infections in children (Di Pierro et al., 2014). Thus, understanding microbiota composition and structure in respiratory samples will be instrumental for establishing disease risk and for the development of probiotics that could be used to colonize the respiratory tract and contribute to the prevention of infections (Tagg and Dierksen, 2003; Medina et al., 2008).

Our hypothesis is that the nasopharyngeal microbiota plays a role as a risk or protective factor in the development of invasive disease caused by *S. pneumoniae.* To test this hypothesis, the objective of the present study was to characterize the nasopharyngeal microbiota profiles in two groups of children: (i) children with invasive pneumococcal disease (IPD), considered as a case group whose nasopharyngeal microbiota was suffering an important disturbance; and (ii) a matched control group of healthy children representative of a healthy nasopharyngeal niche. A series of epidemiological, microbiological, and clinical variables related with major risk of developing IPD were considered to compare microbiota profiles in the two groups. For robust characterization of bacterial composition, a long-fragment 16S sequencing approach was used, in which a 780 bp region of the gene was

amplified and sequenced in order to improve taxonomic assignment.

MATERIALS AND METHODS

Study Design

This was an observational prospective study including all children and adolescents (<18 years) with IPD admitted to 5 hospitals in Catalonia, Spain: Hospital Sant Joan de Deu, Hospital de Nens, Hospital de Mataro, Hospital de Vic and Hospital de Calella (HC), during the period January 2014 to March 2015. One healthy control that was treated at Sant Joan de Deu hospital for minor surgery (i.e., phimosis or minor dermatologic surgery) was selected for each case. Cases and controls were matched by age, sex, and seasonality, given previous evidence of seasonal influence on the microbiota composition of respiratory samples (Bogaert et al., 2011). Children whose parents or guardians did not sign the informed consent were excluded of the study. The study was performed following the guidelines of the Ethics Committee of Hospital Sant Joan de Deu which approved the study. All information collected has been treated confidentially and in accordance with applicable laws on personal data.

IPD Definition

IPD was defined as the presence of clinical findings of infection (which were used for classification of the disease) together with isolation of *Streptococcus pneumoniae* and/or DNA detection of autolysin (*LytA*) gene and an additional capsular gene of *S. pneumoniae* by Real-Time PCR in plasma, cerebrospinal fluid or pleural fluid. Clinical diagnoses were mutually exclusive.

Data Collection

Relevant clinical, epidemiological, immunological, and microbiological variables were collected for each subject including delivery mode, duration of breastfeeding (mixed or exclusive), fulfillment of breastfeeding world health recommendations (minimum duration of 6 months) exposure to crowding, pneumococcal vaccination status, parents' smoking habits, and previous occurrence of respiratory infections. Among microbiological variables we assessed carriers of 13-valent pneumococcal conjugate vaccine (PCV13) serotypes, invasiveness potential of nasopharyngeal *S. pneumoniae* serotypes and co-colonization with respiratory viruses. Serotypes were classified according to the studies of Brueggemann et al. (2003), Sleeman et al. (2006), and del Amo et al. (2014). Serotypes 1, 3, 4, 5, 7F, 8, 9A, 9V, 12F, 14, 18C, and 19A were considered to have a high-attack rate or highly-invasive serotypes whereas the remainder were considered as low-attack rate or non-highly-invasive or opportunistic serotypes. In addition, we recorded data of clinical diagnosis, presence of underlying disease, previous antibiotic intake, white blood cell count, C-reactive protein level, occurrence of complications, length of hospitalization, provision of intensive care, and course of disease for the cases.

Sample Collection and Laboratory Analyses

Nasopharyngeal aspirate samples collected in sterile plastic tubes from cases and controls and eluted with 0.5 ml of phosphate buffered saline (PBS) were extracted and stored at −80°C until further genomic/microbial analysis. Whenever samples were needed for the sole purposes of the study they were taken by experienced nurses of the Hospital Sant Joan de Deu Clinical Trials Unit.

Microbiological Methods

S. pneumoniae Detection and Characterization

The definition of Invasive Pneumococcal Disease (IPD) is the presence of clinical findings of infection together with isolation of *Streptococcus pneumoniae* by culture and/or DNA detection of *S. pneumoniae* by Real-Time PCR in plasma, cerebrospinal fluid or any other sterile fluid. The microbiological confirmation of the patients is based on one technique, the other or both together. All pneumococcal isolates were identified by standard microbiological methods, including the optochin sensitivity test and an antigenic test targeting the capsular polysaccharide (Slidex pneumo-kit, bioMérieux, Marcy-l'Etolie, France). DNA detection of pneumococcal *LytA* gene was performed by a duplex real-time PCR as previously reported (Selva et al., 2014; del Amo et al., 2015). This duplex real-time PCR also included as target the *Rnase P* human single-copy gene to detect and measure the number of human cells (Brotons et al., 2017), using primers and probes recommended by CDC (Meningitis, 2011). Absolute quantification of RNAseP using PCR can be used to estimate the number of human cells present in the clinical samples. The measure of Human DNA load was then used to normalize by potential differences in sample amount and avoid potential bias between samples. In addition, DNA was measured prior to PCR and concentrations adjusted to minimize amplification bias between samples. Capsular typing was carried out by a molecular technique based on automated fluorescent fragment analysis which allows differentiation of 40 serotypes (Selva et al., 2014). Quellung reaction performed at the National Center for Microbiology (Majadahonda, Madrid) was used to complete serotyping in invasive strains isolated by culture.

Viral Respiratory Study in Nasopharyngeal Samples

All nasopharyngeal samples were tested by AnyplexTM II RV16 Detection v1.1. (Seegene, Seoul, Korea). This multiplex Real-Time PCR assay performs simultaneous amplification, detection and differentiation of DNA/RNA of Adenovirus (AdV), Influenza A virus (FluA), Influenza B virus (FluB), Parainfluenza virus 1 (PIV1), Parainfluenza virus 2 (PIV2), Parainfluenza virus 3 (PIV3), Parainfluenza virus 4 (PIV4) Rhinovirus A/B/C (HRV), Respiratory syncytial virus A (RSV A), Respiratory syncytial virus B (RSV B), Bocavirus 1/2/3/4 (HBoV), Metapneumovirus (MPV), Coronavirus 229E (CoV 229E), Coronavirus NL63 (CoV NL63), Coronavirus OC43 (CoV OC43), Enterovirus (HEV), and an internal control in two PCR sets.

Microbiota Analysis

DNA extraction of nasopharyngeal aspirates was performed by Nuclisens® EasyMag® according to manufacturer instructions (bioMérieux, Marcy-l'Etolie, France). This is an automated system for total nucleic acid extraction based in magnetic silica particles. After extracting the DNA, its quality and quantity was measured with Nanodrop (Thermo Fisher Scientific, Massachusetts, USA) and only samples with a 260/280 absorbance ratio between 1.8 and 2 were processed for Next Generation Sequencing (NGS).

NGS libraries were created with 100 ng of total DNA for each sample, to which a unique multiplex identifier (MID) was assigned. PCR amplification of the 16S rRNA gene was performed using high fidelity Extensor Long Range PCR Enzyme (Thermo Fisher Scientific, Massachusetts, USA), with the degenerate universal bacterial primers of 16S rRNA gene 8F (5′-CAGAGTTTGATCMTGGCTCAG-3′) and 785R (5′-GGCCVGGGTATCTAATCC-3′) (Simón-Soro et al., 2014) and the following cycling conditions to minimize amplification biases (Simón-Soro et al., 2014): 2 min at 94°C, followed by 30 cycles of 10s at 94°C, 30s at 52°C, 90s at 68°C, and a final step of 7 min at 68°C. These primers amplified the variable regions 1 to 4 (V1–V4) of 16S rRNA gene with an expected size of 780 pb. The PCR products were first purified using a Minielute PCR purification Kit (Qiagen, Venlo, The Netherlands) and then using Agencourt AMPure beads (Beckman coulter, Munich, Germany). Finally, the amplicons were pyrosequenced using a 454 GS FLX Titanium chemistry (Roche, Basel, Switzerland) with Lib-L type microspheres, pooling 20 samples per 1/8 of a pyrosequencing plate.

Negative controls (PBS) were extracted by the same method of the studied samples (Easymag) and 16S rRNA gene and Human *Rnase P* gene were analyzed by PCR, producing no amplification. DNA concentrations for negative controls were also below the quality control thresholds required at Macrogen Inc. (Republic of South Korea). In addition, a negative control (water) was included in each sequencing run to discard contamination during library preparation, producing no results.

Bioinformatic Analysis and OTU Assignment

Raw sequences were analyzed using "Quantitative Insights into Microbial Ecology" (QIIME) v1.7.0 software (Caporaso et al., 2010) and were separated using the 8-bp "barcodes" assigned to each sample. Chimeric sequences were eliminated by ChimeraSlayer program (Haas et al., 2011). An end-trimming quality filtering was performed by removing 50-bp windows with quality values <25 using Prinseq. Only reads >500 bp were included for taxonomic classification. Sequences with differences in the primer binding region or with more than four ambiguities in homopolymeric regions were excluded from the analysis. The resulting high quality sequences of the 16S rRNA gene were classified using the RDP database (Ribosomal Database Project) (Cole et al., 2009) with a bootstrap cutoff of 80%. Samples were classified in Operational Taxonomic Units (OTUs) at 97% sequence identity as the standard species-level boundary (Yarza et al., 2008). Only the OTUs representing over 0.1% of the total sequences of each sample were considered for further statistical analysis, as low-frequency reads, including singletons, are more likely to represent sequencing errors, contaminants, or transient organisms without a biological role at the niche under study (de la Cuesta-Zuluaga and Escobar, 2016). Bacterial taxonomic composition was determined for each sample and means for each group (cases and controls) were calculated.

Estimation of Microbial Diversity and Statistical Analysis

Data analysis was performed using QIIME 1.7.0 software. Rarefaction curves (Mean ± S.E.) were calculated by including 1,000 randomly selected reads per sample. Alpha diversity indexes were calculated from rarefied samples (1,000 sequences per sample), using the Shannon index (Shannon, 1948) for diversity and the Chao1 index (Chao, 1984) for richness. Beta diversity was also calculated with the rarefied 1,000 reads per sample using weighted and unweighted UniFrac (Lozupone et al., 2006) distance matrices, and the principal coordinate analysis (PCoA) generated 2D and 3D plots for all mapping fields. In addition, we clustered samples using UPGMA (Unweighted Pair Group Method with Arithmetic mean, also known as average linkage) (Michener and Sokal, 1957). Two-way comparisons in bacterial composition using the UniFrac metric (Lozupone et al. 2006) were used to measure whether the microbial communities in the microbiota types were significantly different. A tree with 1,000 reads from each sample was obtained, and microbiota types were considered significantly different if the UniFrac distance value for the tree was larger than expected if the sequences were randomly distributed. A thousand permutations were performed to obtain a *P*-value, using Bonferroni corrections for multiple comparisons. In addition, we also performed Constrained Correspondence Analysis (CCA), which is a statistic tool which emphasizes variation, and tests whether the factor provided (the microbiota type) can explain part of the total variability. This analysis was performed by the R software ade4 package (Dray and Dufour, 2007) using the Chi-squared distances-based function CCA. Adonis tests were done with the R library "vegan" (Oksanen et al., 2018) to determine corrected *p*-values.

Microbial community comparisons and statistical analysis were performed using the statistical software R v2.15.2 with the packages for Community Ecology (vegan), Euclidean Methods in Environmental Sciences (ade4), The Bee Swarm Plot (beeswarm) and gplots packages (http://R-project.org), R (The R Foundation for Statistical Computing).

We used LEfSe (Linear discriminant analysis Effect Size) with default parameters (Segata et al., 2011), available in the Galaxy Web Server toolkit to determine significant differences (alpha value = 0.05) in the proportions of bacterial genera between cases and controls groups. LEfSe uses the non-parametric factorial Kruskal-Wallis (KW) sum-rank test to detect features with significant differential abundance with respect to the class of interest.

Normality of the data was analyzed with the Shapiro-Wilk test. Continuous data with normal distributions were described using mean and Standard Deviation (SD). In case of non-normal distribution, median and interquartile range (IQR) were used. Significance (p-values) of continuous and normally distributed data was determined using Student's t-test. When data did not follow a normal distribution, Wilcoxon signed-rank test was used. Significance of categorical data was established by using Chi-square test. When Chi-square expected frequency was equal or less than five, Fisher's exact test was applied. When variables followed a normal distribution, the ANOVA test was used to determine if there were statistically significant differences in mean values between the microbiota groups. If distribution was not normal, we used the non-parametric Kruskal-Wallis test. Multiple testing correction was performed when needed.

Ethics Statement

The study was performed following the guidelines of the Ethics Committee of Hospital Sant Joan de Deu which approved the study (project approval code PIC-70-15). All information collected has been treated confidentially and in accordance with applicable laws on personal data. Written consent was obtained from parent or legal guardians of children included in the study.

TABLE 1 | Epidemiological and microbiological characteristics of study groups.

Variable	Cases (n = 28)	Controls (n = 28)	p-value
EPIDEMIOLOGICAL VARIABLES			
Age, months (Md, IQR)	43.0 (20.8–60.2)	42.6 (31.6–58.9)	0.72
Gender, male	16 (57.1)	16 (57.1)	1.00
Influenza season	12 (42.9)	14 (50.0)	0.59
Race, Caucasian	23 (82.1)	25 (89.3)	0.71
Birth weight, gr (Mean, SD)	3,143 (626)	3,298 (579)	0.34
Gestational age, weeks (Mean, SD)	38.5 (2.3)	38.8 (2.0)	0.67
Delivery type, C–section† (cases: n = 25; controls: n = 26)	7 (28.0)	10 (38.5)	0.43
Breastfeeding	23 (82.1)	19 (67.9)	0.22
Breastfeeding duration ≥6 months¶ † (cases: n = 23; controls: n = 19)	9 (39.1)	13 (68.4)	0.06
Breastfeeding duration, months (Md, IQR)† (cases: n = 23; controls: 19)	4 (1–7)	6 (4–10)	0.19
Day-care attendance	25 (89.3)	23 (82.1)	0.45
Shared bedroom† (cases: n = 21; controls: 27)	13 (61.9)	12 (44.4)	0.23
Parental smoking† (cases: n = 26)	11 (42.3)	13 (46.4)	0.76
Vaccinated against influenza	1 (3.6)	0 (0.0)	1.00
Vaccinated against pneumococcal disease	17 (60.7)	19 (67.9)	0.58
PCV13 vaccinated	14 (82.4)	17 (89.5)	0.42
Respiratory infection in the previous 30 days† (Controls: n = 27)	13 (46.4)	13 (48.1)	0.90
MICROBIOLOGICAL VARIABLES			
Sp detection in NP sample by PCR	18 (64.3)	16 (57.1)	0.58
High-attack rate Sp serotype in NP sample	10 (55.5)	2 (12.5)	**0.009**
PCV13 serotype coverage in NP sample	11 (61.1)	2 (12.5)	**0.004**
Viral detection in NP sample by PCR	17 (60.7)	14 (50.0)	0.42
Rinovirus	10 (35.7)	10 (35.7)	1.00
Adenovirus	4 (14.3)	4 (14.3)	1.00
Parainfluenza virus	2 (7.1)	1 (3.6)	1.00
Respiratory siyncytial virus	2 (7.1)	0 (0.0)	0.49
Coronavirus	1 (3.6)	2 (7.1)	1.00
Enterovirus	1 (3.6)	0 (0.0)	1.00
Bocavirus	1 (3.6)	0 (0.0)	1.00
Influenza A virus	2 (7.1)	0 (0.0)	0.49
Influenza B virus	0 (0.0)	1 (3.6)	1.00
Multiple respiratory viral infection	5 (29.4)	4 (28.6)	1.00

Results expressed as counts (%) unless stated otherwise.

Md, median; IQR, interquartile range; SD, standard deviation; PCV13, 13-valent pneumococcal conjugate vaccine; PICU, pediatric intensive care unit.

† missing values.

¶ according to WHO recommendations.

The bold values means statistically significant associations with p-values < 0.05.

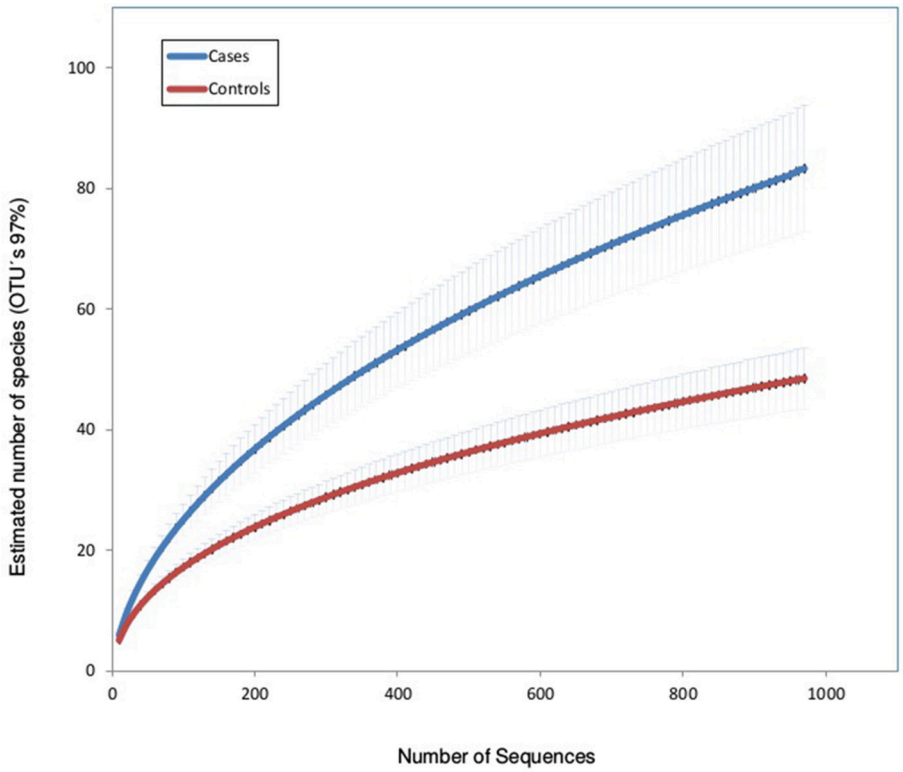

FIGURE 1 | Rarefaction curves of nasopharyngeal samples in patients with invasive pneumococcal disease (cases) and healthy children (controls). The horizontal axis shows the number of reads (sequencing effort) obtained by pyrosequencing the 16S rRNA gene. The vertical axis shows the number (mean ± S.E.) of operational taxonomic units (OTUs) at a level of 97% (estimated mean number of bacterial species).

RESULTS

Epidemiological and Clinical Features of Patients

During the study period a total of 53 patients were diagnosed of IPD in Hospital Sant Joan de Deu ($n = 38$), Hospital de Nens ($n = 6$), Hospital de Mataro ($n = 5$), Hospital de Vic ($n = 2$), and Hospital de Calella ($n = 2$). Fourty-two of them (79.2%) accepted to participate in the study under informed consent. Twenty-eight (52.8%) controls were available for matching with cases so the study finally comprised 56 subjects. No significant differences of total human DNA load was found between samples of cases and controls (Log_{10} 3.6 vs. 3.2 gene copies/reaction, $p = 0.1$), indicating that both types of samples did not differ in the amount of material.

The median age of the 28 cases was 43.0 months (IQR 20.8–60.2 months) and 16 (57.1%) were male. The clinical diagnoses of these patients were 19 pneumonia (including 10 complicated pneumonia with empyema and 3 necrotizing pneumonia), 7 bacteremia, 1 meningitis, and 1 fulminant sepsis. Invasive samples collected for diagnosing IPD included blood ($n = 19$, 67.8%), pleural fluid ($n = 5$, 17.9%), blood and pleural fluid ($n = 3$, 10.7%), and cerebrospinal fluid ($n = 1$, 3.6%). Detection of *S. pneumoniae* in invasive samples was performed by PCR ($n = 14$, 50.0%), by culture ($n = 12$, 42.9%), and both by PCR and culture ($n = 2$, 7.1%). Median white blood cell count of 17,515/L and median C-reactive protein levels of 154.7 mg/L indicated inflammatory activity. An underlying disease was reported in 3 cases with chronic pulmonary disease, neuroblastoma, and splenic dysfunction, respectively. Median length of hospitalization was 7 days (IQR 4–8 days). Five cases (17.9%) received intensive care, 4 (14.3%) suffered sequelae, and one child died.

Pneumococcal nasopharyngeal carriage was observed in 18 (64.3%) cases and 16 (57.1%) controls. A total of 11 PCV13 serotypes were identified among carriers in the case group, specifically serotype 1 ($n = 2$), serotype 3 ($n = 3$), serotype 14 ($n = 2$), serotype 19A ($n = 3$), and serotype 19F ($n = 1$). In contrast, only 2 PCV13 serotypes, classified as serotype 3, were found in control carriers. Nasopharyngeal samples were taken from cases after a mean of 92 h of fever (IQR 48–408 h) and all of them except two (one patient with necrotizing pneumonia and another one with fatal fulminant sepsis and viral respiratory coinfection), were exposed to beta-lactamic antibiotic treatment, during a mean period of 4 days. No patients were exposed to macrolide treatment or other class of antibiotics. **Table 1** shows epidemiological and microbiological variables for cases and controls. Proportions of coinfection with respiratory virus and pneumococcal nasopharyngeal carriage, were higher in cases compared to controls, but the differences between groups did not reach statistical significance. There was a significantly higher proportion of PCV13 pneumococcal serotype carriers

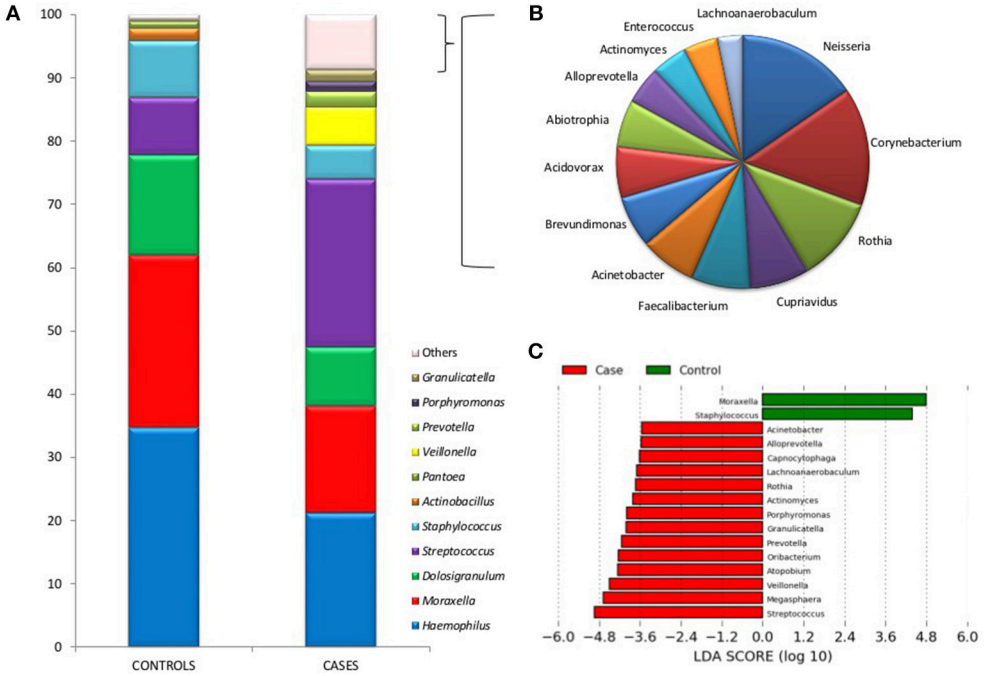

FIGURE 2 | Bacterial taxonomic composition of nasopharyngeal samples in cases and controls. **(A)** Graphs show the mean proportion of the most frequent bacterial genera as inferred by PCR amplification and pyrosequencing of the 16S rRNA gene. The mean proportions were calculated based on 1,000 sequences per sample. Those bacteria at a proportion lower than 1% are indicated as "Others" and were particularly abundant in cases. **(B)** Shows a description of those low-frequency bacteria in patients with IPD, which include many oral organisms (bacteria at a proportion <0.2% are not shown). **(C)** A Linear Discriminant Analysis Effect Size (LEfSe) analysis shows those bacteria with significantly different levels ($\alpha = 0.05$) between cases and controls.

in cases compared to controls (61.1 vs. 12.5%, $p = 0.004$) as well as significantly higher number of high-attack rate serotypes (55.5 vs. 12.5%, $p = 0.009$). A trend for significance was observed for breastfeeding through 6 months (the minimum time recommended by World Health Organization) in cases (39.1 vs. 68.4%, $p = 0.06$).

High Bacterial Diversity in IPD Patients

A total of 284.558 16S rRNA sequence reads were obtained. After sequence length and quality filtering, we obtained 201.888 reads >500 bp (500–780 bp), with an average of 2.549 reads of the 16S rRNA gene per sample (range between 1,085 and 29,370 reads).

Rarefaction curves (using OTUs at 97% sequence identity) showed that mean bacterial richness had higher values in children with IPD compared with healthy patients (**Figure 1**). Individual rarefaction curves with 1,000 reads show that most bacteria present were detected by this level of coverage and show a shift toward higher OTU richness in children with IPD (**Supplementary Figure 1**). Species richness (Chao1 Index) was significantly higher in cases (mean: 79, 95% confidence interval: 57.4–100.58) compared to healthy controls (mean: 47.8, 95% CI: 37.5–58.2, $p < 0.0001$). The Shannon diversity index was also significantly higher in cases (mean: 1.21, 95% CI: 0.94–1.48) vs. healthy controls (mean: 0.77, 95% CI: 0.62–0.92, $p < 0.0001$).

The taxonomic assignment of the 16S rRNA reads revealed that the most common phyla in IPD patients were *Firmicutes* (50.9% of the total number of reads), *Proteobacteria* (41.4%), *Bacteroidetes* (5.0%), *Actinobacteria* (2.2%), and a lower proportion of *Fusobacteria*. Within the control group, the most common phyla were *Proteobacteria* (66.0% of the total number of reads), *Firmicutes* (33.6%), *Bacteroidetes* (0.2%), and *Actinobacteria* (0.2%).

Figure 2A shows differences between the two groups in the mean proportions of each bacterial genera. In the cases group the most prevalent bacteria were *Streptococcus, Haemophilus*, *Moraxella*, *Dolosigranulum*, *Veillonella*, *and Staphylococcus* with 26.4, 21.1, 16.8, 9.3, 6.1, and 5.2% of the total, respectively. Whilst in the control group their proportions were 9.0, 34.5, 27.1, 15.7, 0.1, and 8.9%, respectively. The higher bacterial diversity detected in children with IPD corresponded to the high prevalence of lactate fermenting *Veillonella*, and mainly to genera found at low frequencies. The taxonomic assignment of those genera present at <1% of the total, which accounted for over 9% of the reads in IPD patients, is shown in **Figure 2B** and reveals the presence of many oral species like *Corynebacterium*, *Neisseria*, *Actinomyces*, or *Rothia*, among others.

LEfSE ranking analysis shows that *Moraxella* and *Staphylococcus* were found to be significantly more abundant in healthy individuals, according to this high-dimensional class comparison test. On the other hand, the genera *Streptococcus*, *Megasphaera*, *Veillonella*, *Atopobium*, *Oribacterium*, *Prevotella*, *Granulicatella*, *Porphyromonas*, *Actinomyces*, *Rothia*, *Lachnoanaerobaculum*, *Capnocytophaga*, *Alloprevotella*, and *Acinetobacter* were significantly more abundant in patients

TABLE 2 | Bacterial species identified in the present study.

Genus	Species	Cases ($n = 28$)	Controls ($n = 28$)
Streptococcus	*pneumoniae*	51.08%	91.17%
	mitis	23.10%	2.82%
	oralis	7.02%	0.51%
	sp	6.62%	1.07%
	uncultured sp	5.40%	1.49%
	infantis	3.19%	0.13%
	sp. oral clone	1.84%	0.64%
	peroris	0.74%	–
	sanguinis	0.41%	0.77%
	parasanguinis	0.22%	–
	genomosp	0.12%	–
	pseudopneumoniae	0.10%	–
	cristatus	0.07%	0.47%
	pyogenes	0.02%	0.94%
Dolosigranulum	*pigrum*	83.26%	84.17%
	uncultured sp	16.74%	15.83%
Haemophilus	*influenzae*	80.30%	99,65%
	uncultured sp	11.77%	0,08%
	sp	6.81%	0,03%
	parainfluenzae	1.02%	0,09%
	haemolyticus	0.11%	0,10%
Moraxella	*catarrhalis*	94.89%	79.71%
	lincolnii	2.93%	8.30%
	nonliquefaciens	2.14%	4.46%
	caprae	0.04%	0.40%
	lacunata	–	7.14%
Prevotella	uncultured sp	34.54%	60.00%
	histicola	15.70%	–
	sp	12.80%	20.00%
	sp. oral clone	12.32%	–
	pallens	9.90%	–
	nanceiensis	3.86%	20.00%
	conceptionens	3.38%	–
	oris	2.90%	–
	melaninogenic	1.69%	–
	salivae	0.72%	–
Veillonella	uncultured sp	39,94%	24.00%
	parvula	29,49%	24.00%
	sp	14,23%	8.00%
	dispar	7,37%	24.00%
	sp. oral taxon	6,67%	20.00%
	tobetsuensis	2,24%	–
Porphyromonas	uncultured sp	71.93%	56.25%
	sp. *oral clone*	14.91%	18,75%
	sp	13.16%	25.00%
Staphylococcus	*epidermidis*	65,40%	9.67%
	sp	11,16%	47.12%
	haemolyticus	7,07%	0.05%
	uncultured sp	6,51%	2.23%
	pettenkoferi	3,35%	–
	devriesei	2,51%	–
	cohnii	1,95%	–
	hominis subsp. null	1,40%	–
	pasteuri	0,28%	–
	warneri	0,28%	–
	aureus	–	40.89%

*Data indicate percentages of 16S rRNA reads from a given genus with a hit against each species. Frequencies of each genera are shown in **Figure 2**. To minimize taxonomic assignment errors, only hits with >97% nucleotide identity and >500 bp alignment were selected. Only species with frequencies >0.1% are shown.*

with IPD (**Figure 2C**). Most of these bacteria are common oral inhabitants (Mira et al., 2017). **Supplementary Figure 2** shows a Heatmap profile showing abundances of bacterial genera in individual cases and controls indicating the age of each child.

The use of long-amplicon (780 bp) sequencing allowed us to taxonomically assign the 16S sequences at the species level with a higher degree of accuracy (Shin et al., 2016). In order to minimize errors in taxonomic assignment, only sequence alignments >97% sequence identity over >500 bp were considered, which would encompass the 16S rRNA hypervariable regions v1–v3/v4. Our results are shown in **Table 2**. According to this assignment, the genus *Staphylococcus* would be dominated by *S. aureus* in the controls (>40% of the reads in this genus) whereas this species would be totally absent in IPD patients, that would be dominated by *S. epidermidis* and *S. haemolyticus*. Virtually, all *Haemophilus* species in controls would correspond to *H. influenzae*, whereas in the cases, 18% of the reads in this genus would correspond to uncultured or unknown species. It is surprising to note that over 90% of the reads matching *Streptococcus* would correspond to *S. pneumoniae* in the controls while in IPD patients, only 51% of the streptococcal reads would correspond to *S. pneumoniae* and over 40% of them gave top matches to *S. mitis*, *S. oralis*, or uncultured species.

Microbiota Nasopharyngeal-Types in Health and Disease

When all samples were analyzed by two-dimensional principal coordinates analysis (2D PCoA), 67% of the variability in the data could be explained by the first two components. Samples appeared to cluster in three different groups, corresponding to three different types of respiratory tract microbiota, or nasopharyngeal-types (**Figure 3**). The Microbiota A was mainly composed of reads assigned to the genera *Dolosigranulum* (44.3%), *Moraxella* (29.3%), and *Haemophilus* (10.5%) (**Figure 3A**). The Microbiota B was represented mostly by the genera *Streptococcus* (36.9%), *Staphylococcus* (21.3%), *Veillonella* (9.8%), together with a high diversity of anaerobic genera as *Prevotella* and *Porphyromonas* (**Figure 3B**). Finally, the Microbiota C was composed mainly of the genera *Haemophilus* (52.1%), *Moraxella* (31.4%), and *Streptococcus*

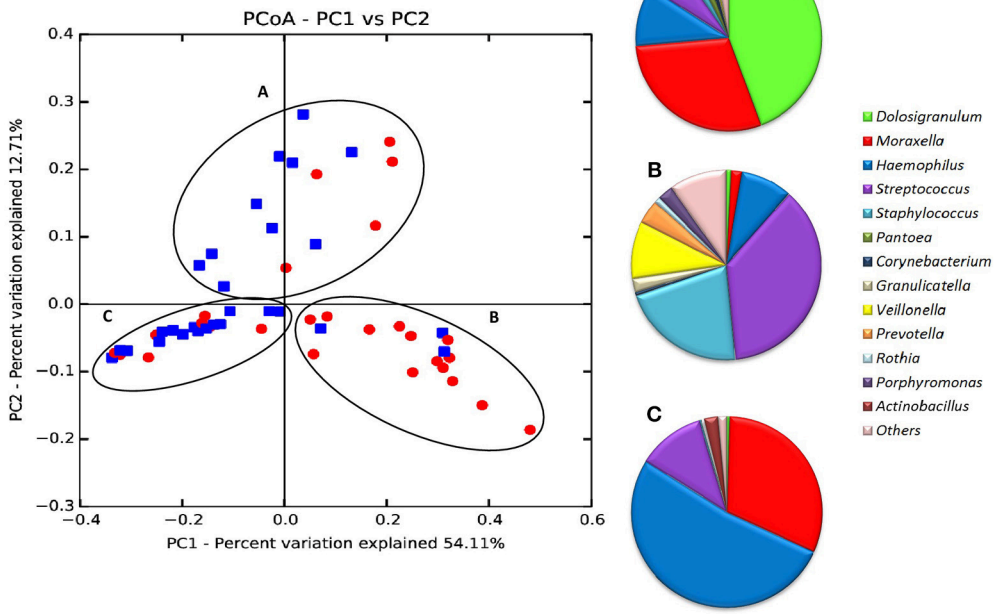

FIGURE 3 | Principal Coordinates Analysis (PCoA) of all 56 nasopharyngeal samples according to bacterial composition. Data include IPD patients (red-dots) and healthy controls (blue dots). PCoAs were performed with weighted UniFrac analysis with clustering at the species taxonomic level (97% sequence identity) with 1,000 reads per sample. The taxonomic composition (proportion of bacterial genera) of the 3 microbiota types ("nasopharyngeal-types") is shown to the right. Data in **(A–C)** were obtained from 1,000 randomly selected sequences per sample.

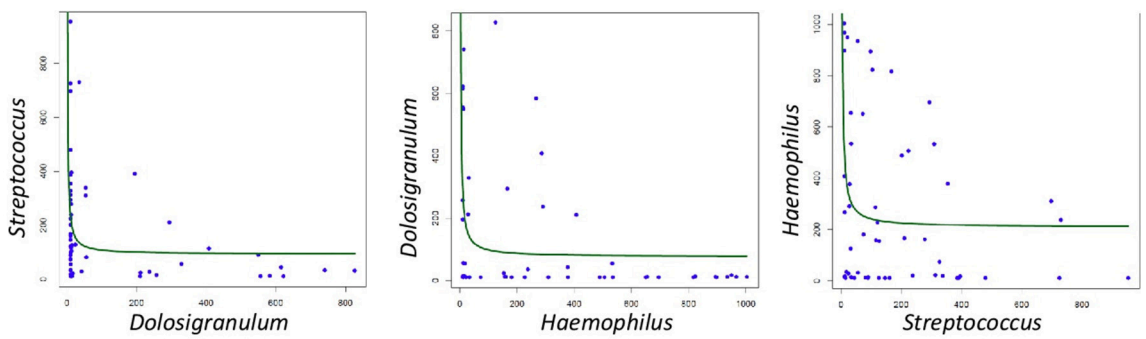

FIGURE 4 | Correlations between the frequency of dominant bacteria in the three nasopharyngeal microbiota types. Data show potential negative associations, as they followed significant hyperbolic regressions.

(11.4%) (**Figure 3C**). Thus, nasopharyngeal-type A was dominated by *Dolosigranulum*, nasopharyngeal-type C by *Haemophilus*, and nasopharyngeal-type B by *Streptococcus*, with a high presence of oral microorganisms. The three microbiota types were found to be significantly different from each other (Unifrac Distance, corrected $p < 0.01$ in all cases). In addition, CCA analysis showed that microbiota type significantly explained the variability in bacterial composition among samples (Adonis *p*-value: 0.002). In agreement with the existence of specific bacterial communities dominated by a given genus, negative correlations were found (**Figure 4**) between the three dominant genera (*p*-values for significant hyperbolic regressions were, respectively, 0.029, 0.011, and 0.029 for comparisons between *Dolosigranulum* and *Streptococcus*, *Dolosigranulum* and *Haemophilus*, and *Streptococus* and *Haemophilus*).

In order to understand the features influencing nasopharyngeal-types, all available epidemiological, microbiological, immunological and clinical variables were compared by bivariate analysis with the three microbiota types. No significant differences were found in any of the variables considered that could explain the grouping in the three different

TABLE 3 | Epidemiological, microbiological, immunological, and clinical characteristics by microbiota type.

A				
Variable	**Microbiota A ($n = 15$)**	**Microbiota B ($n = 17$)**	**Microbiota C ($n = 24$)**	***p*-value**
Case group	5 (17.9)	14 (50.0)	9 (32.1)	**0.006**
EPIDEMIOLOGICAL VARIABLES				
Age, months (Md, IQR)	40.8 (20.8–80.3)	41.4 (32.1–56.6)	44.4 (29.5–61.4)	0.95
Gender, male	8 (53.3)	8 (47.1)	16 (66.7)	0.43
Influenza season	6 (40.0)	6 (35.3)	14 (58.3)	0.29
Race, Caucasian	11 (73.3)	16 (94.1)	21 (87.5)	0.26
Birth weight, gr (Mean, SD)	3,147 (689)	3,329 (749)	3,198 (428)	0.68
Gestational age, weeks (Mean, SD)	38.1 (2.3)	38.6 (2.6)	39.7 (1.7)	0.43
Delivery type, C-section† ($n = 48$)	6 (42.9)	4 (28.6)	7 (30.4)	0.75
Breastfeeding	13 (86.7)	13 (76.5)	16 (66.7)	0.43
Breastfeeding in controls	9 (90.0)	1 (33.3)	9 (60.0)	0.10
Breastfeeding duration ≥ 6 months¶ †(A: $n = 13$, B: $n = 13$, C: $n = 16$)	7 (53.9)	7 (53.9)	8 (50.0)	0.97
Breastfeeding duration, months (Md, IQR)† (A: $n = 13$, B: $n = 13$, C: $n = 16$)	6 (3–10)	6 (3–12)	5.5 (1.5–7)	0.67
Day-care attendance	13 (86.7)	16 (94.1)	19 (79.2)	0.40
Shared bedroom† (B: $n = 12$, C: $n = 21$)	5 (33.3)	7 (58.3)	13 (61.9)	0.21
Parental smoking† (B: $n = 15$)	8 (53.3)	6 (40.0)	10 (41.7)	0.71
Vaccinated against influenza	0 (0.0)	0 (0.0)	1 (4.2)	1.00
Vaccinated against pneumococcal disease	9 (60.0)	13 (46.5)	14 (58.3)	0.45
PCV13 vaccinated	7 (77.8)	11 (84.6)	13 (92.9)	0.61
Respiratory infection in the previous 30 days† ($n = 52$)	6 (42.9)	5 (31.3)	15 (68.2)	0.07*
MICROBIOLOGICAL VARIABLES				
Sp detection in NP sample by PCR	7 (46.6)	9 (52.9)	18 (75.0)	0.16
High-attack rate Sp serotype in NP sample	3 (42.9)	3 (33.3)	6 (33.3)	0.90
PCV13 serotype coverage in NP sample	3 (42.9)	4 (44.4)	6 (33.3)	0.81
Viral detection in NP sample by PCR	7 (46.7)	8 (47.1)	16 (66.7)	0.34
Multiple respiratory viral infection	2 (28.6)	3 (37.5)	4 (25.0)	0.82
IMMUNOLOGICAL VARIABLES (CASE GROUP)				
White blood count, 10^3cells/mm^3 †($n = 21$) (Md, IQR)	24.6 (18.9–33.4)	15.7 (10.0–18.2)	18.2 (7.5–22.7)	0.12
C-reactive protein, mg/L† ($n = 20$) (Md, IQR)	29.2 (10.8–69.0)	113.1 (50.5–237.6)	302.9 (261.5–355.8)	**0.009****
B				
Variable	**Microbiota A ($n = 5$)**	**Microbiota B ($n = 14$)**	**Microbiota C ($n = 9$)**	***p*-value**
CLINICAL VARIABLES (CASE GROUP)				
Underlying disease	1 (20.0)	1 (71.4)	1 (11.1)	0.75
Antibiotic intake in the previous 7 days† ($n = 26$)	5 (100.0)	12 (85.7)	6 (66.7)	1.00
Lenght of hospital stay, days (Md, IQR)	4 (3–6)	7 (7–8)	7.5 (3.5–10)	0.21
Admission to PICU	0 (0.0)	4 (28.6)	1 (11.1)	**0.53**
Lenght of PICU stay, days (Md, IQR)	0 (0.0)	2 (0–6)	1 (1–1)	0.45
Complications	0 (0.0)	2 (14.3)	2 (22.2)	0.80
MAIN CLINICAL DIAGNOSIS				
Complicated pneumonia	0 (0.0)	8 (57.1)	5 (55.6)	0.09
Bacteremia	3 (60.0)	3 (21.4)	1 (11.1)	0.17
Pneumonia	2 (40.0)	2 (14.3)	2 (22.2)	0.51
Meningitis	0 (0.0)	1 (7.1)	0 (0.0)	1.00
Sepsis	0 (0.0)	0 (0.0)	1 (11.1)	0.50
Serious IPD (complicated pneumonia, meningitis, or sepsis)	0 (0.0)	9 (64.9)	6 (66.7)	**0.04**
Course of disease, sequelae or exitus	0 (0.0)	3 (21.4)	2 (22.2)	0.67

Results expressed as counts (%), unless stated otherwise.

Md, median; IQR, Interquartile range; SD, standard deviation; NP, nasopharyngeal; PCV13, 13-valent pneumococcal conjugate vaccine; PICU, Pediatric Intensive Care Unit; IPD, Invasive Pneumococcal Disease.

†Missing values.

¶According to WHO recommendations.

**p = 0.05 comparing Microbiota B and C.*

***p = 0.03 comparing Microbiota A and C; p = 0.04 comparing Microbiota A and B. The bold values means statistically significant associations with p-values < 0.05.*

microbiotas (**Table 3**). However, the classification of patients into case and control groups was significantly associated with the nasopharyngeal-types ($p = 0.006$, Chi-square test). Among cases, nasopharyngeal-type B was the most frequently detected pattern (50.0%), followed by nasopharyngeal-type C (32.1%), while nasopharyngeal-type A was detected only in 17.9% of children with IPD. Conversely, nasopharyngeal-type B was only detected in 3 controls (10.7%).

Overall, children with nasopharyngeal-type A showed to have markedly lower inflammatory activity measured by the C-reactive protein level when compared to those with nasopharyngeal-type C ($p = 0.03$) or nasopharyngeal-type B ($p = 0.04$). In addition, no case with nasopharyngeal-type A was diagnosed with complicated pneumonia, meningitis, and sepsis, in contrast to the relatively high occurrence of these serious IPD manifestations among nasopharyngeal-type B and nasopharyngeal-type C cases (0.0, 64.9, and 66.7%, respectively, $p = 0.04$). Similarly, none of the cases with nasopharyngeal-type A required intensive care but a noticeable proportion of cases with nasopharyngeal-type B and C did (0.0, 28.6, and 11.1%, respectively). Of note, 90% of the ten healthy controls with a Microbiota A were fed with maternal milk whereas breastfeeding was less frequent in controls with Microbiota B (33.3%) and C-types (60.0%). In spite of these differences, the association between breastfeeding and type of microbiota was not found to be statistically significant. On the other hand, there were no significant correlations between any specific bacterial genera over-represented in IPD patients and inflammatory parameters.

DISCUSSION

The current work describes for the first time the nasopharyngeal microbiota in a case-control study of children with IPD and healthy children. Our data show that bacterial richness and diversity were significantly higher in IPD patients. In such cases, a clear dysbiosis was observed with a high frequency of *Veillonella* and other oral microorganisms which appeared to be relatively absent in controls. This over-representation of anaerobic and proteolytic oral species in children with IPD was also found by Segal et al. (2013) in adult bronchoalveolar lavage samples in association with increased inflammation. In our samples, the microbiota related with IPD was also associated with higher levels of the C-reactive protein inflammatory biomarker.

De Steenhuijsen Piters et al. (2016) similarly found higher nasopharyngeal microbiota diversity in elderly pneumonia patients compared to elderly healthy controls, whilst this difference was not found in adult patients. In ecological terms, these results are surprising since higher bacterial diversity is usually related with health (Turnbaugh et al., 2007), while lower bacterial diversity is associated with disease. It is noteworthy that patients with primary immunodeficiencies presented a higher microbiota diversity compared with healthy controls. This fact might correlate with an increase of immune system permissiveness for microbe colonization (Oh et al., 2013). Similarly, a local increase in bacterial diversity has been detected in polyps and tumor biopsies from patients with colorectal cancer (Mira-Pascual et al., 2015), a disease which has been associated with immune suppression at the affected tissues. The best studied case of immune-driven dysbiosis is probably gum disease, where the presence of the "keystone pathogen" *Porphyromonas gingivalis* has been shown to induce a profound alteration of the immune system (Hajishengallis, 2011) facilitating the settlement of many species that produce inflammation. However, the increase in microbial diversity associated with dysbiosis in gum disease and cancer could not only be due to immune alteration but also to a nutritionally richer environment (Mira et al., 2017). In the respiratory tract of children with IPD, future investigations should elucidate whether the observed dysbiosis is a consequence of immune changes, increased nutrient availability or both. In periodontal disease, destructive inflammation generates abundant gum tissue breakdown products that serve as nutrients for proteolytic and saccharolytic bacteria to obtain essential amino-acids and iron, including degraded collagen, and heme-containing compounds (Hajishengallis et al., 2012). It is important to underline that *Porphyromonas* was one of the over-represented genera in IPD patients (**Figure 2C**). However, all reads belonging to this genus appeared to correspond to uncultured or unknown species (**Table 2**). We hope the present study stimulates research into the characterization of these potentially pathogenic species, including their potential involvement as keystone pathogens (Darveau et al., 2012).

In addition, IPD samples presented significantly higher levels of *Veillonella* (**Figure 2C**), which is a bacterium that uses lactate as a carbon source, as a consequence of which it is usually found physically and functionally associated to lactate producers like *Streptococcus* (Dige et al., 2014; Gaspar et al., 2014). In our data, however, the correlation between *Streptococcus* and *Veillonella* levels in cases was not significant ($R^2 = 0.17$, $p > 0.1$, **Supplementary Figure 3**) and therefore it is unknown whether streptococcal serotypes associated with IPD produce more lactate that those found in healthy children. Future work should determine whether the seemingly higher acidic environment in children with IPD is a consequence of lactate production by microorganisms, by lactate-dehydrogenase over-expression in the human tissue (Tan et al., 2002) or both.

Our data identified three bacterial clusters or nasopharyngeal-types, dominated by *Dolosigranulum*, *Streptococcus*, or *Haemophilus*. Similarly, other studies have described the presence of bacterial nasopharyngeal clusters. In a Danish cohort (1–3 months of age) and a Dutch cohort (from birth to 6 months of age), up to 5 and 4 nasopharyngeal-types were described (Mortensen et al., 2016), respectively. Although there are methodological, geographical and age-related differences between these studies, all available data from respiratory tract samples point toward the presence of precise microbial communities with a given dominant bacteria on each nasopharyngeal-type, although larger samples sizes are required to validate this.

In the current manuscript, the only statistically significant explanatory factor for these three microbiota profiles was the classification of patients into case or control groups. *Streptococcus*-dominated community (Microbiota B) was clearly

associated to IPD patients. Given that *Dolosigranulum* abundance in the nasopharynx has been reported to be inversely associated with episodes of wheezing and mild respiratory tract infections (Biesbroek et al., 2014) we speculate that the *Dolosigranulum*-dominated community (Microbiota A) could be more resistant to pneumococcal infection occurrence and severity. Our hypothesis was supported by the lower number of cases with a Microbiota A-type (17.9% of the total) and by the fact that such cases experienced less severe manifestations of IPD and did not require intensive care. In this respect, it is suggestive that *Dolosigranulum* and *Haemophilus* are found in the present study to have a negative correlation with *Streptococcus*, the dominant genera in IPD cases (**Figure 4**). Moreover, the nasopharyngeal presence of *Dolosigranulum* has been associated with breastfeeding. It has been shown that lactation has a profound impact in the microbial community composition of the infant upper respiratory tract, increasing the prevalence and levels of *Dolosigranulum* and reducing the levels of *Staphylococcus*, *Prevotella*, or *Veillonella* (Biesbroek et al., 2014). In agreement with this, we found a considerably higher proportion of Microbiota A healthy controls that were breastfed and a trend for statistical significance in the relation between exclusive breastfeeding up to 6 months of age and case-control classification ($p = 0.06$) (**Table 1**). Despite the lack of statistical power to observe significance in these associations, the results obtained suggest that breastfeeding could have an important role in protection against pneumococcal infection. As far as for *Haemophilus*-dominated community (microbiota C), both IPD cases and healthy controls appear to fall within this microbiota profile. This genus, together with *Moraxella,* has been associated with higher rates of parent-reported upper respiratory infections and wheezing in the first years of life (Hyde et al., 2014; Bogaert et al., 2015). In fact, the group of children with *Haemophilus* and *Moraxella*-dominated microbiota showed a higher percentage of patients presenting a respiratory infection in the previous 30 days before the sample collection (68.2%), with a trend for significance ($p = 0.07$). However, future experimental work with a larger sample size should further explore the significance of these microbiota profiles and test whether the presence of a given nasopharyngeal microbiota makes individuals more sensitive or resistant to pneumococcal infection.

Our study describes the use of a long-amplicon sequencing approach of the 16S rRNA for species-level identification. Computer simulations show that taxonomic assignment accuracy, especially at the species level, decreases dramatically in short reads, like those of current Illumina or Ion Torrent technologies (Claesson et al., 2010), while the use of long-amplicon (≥500 bp) has been postulated as a good tool for species-level taxonomical assignments (Shin et al., 2016) and has been widely used as a diagnostic tool of bacterial infections in clinical samples (Guembe et al., 2013; Martínez et al., 2016). However, we have found surprising results using 16S rRNA for species level identification since *S. pneumoniae* would be more frequent in controls than in cases. These results are discordant with the results generated from a real-time PCR targeting *LytA* gene, the target recommended by CDC for pneumococcal detection. *LytA* PCR indicated the presence of *S. pneumoniae* in 64.4% of cases vs. 57.1% in controls (**Table 1**). According to our results, taxonomic assignment by using 16S rRNA could be limited in some genera and accurate identification at the species level should be done with more conserved genes. It is important to keep in mind that streptococci are particularly similar in the 16S rRNA gene sequence, and therefore species-level assignment in this genus must be treated with caution (Ing et al., 2012). Even more, despite *LytA* is the recommended gene utilized for pneumococcal diagnosis according to CDC (National Center for Immunization and Respiratory Diseases, 2014), this target has been reported to misidentify the pathogen (Morales et al., 2015; Simões et al., 2016), may be showing the occurrence of genetic exchange among streptococcal species and opening the possibility that other etiological agents could be involved. Thus, future work should increase our understanding of these microbial consortia by accurate species-level identification.

CONCLUSION

In conclusion, we found a higher bacterial diversity and richness in children with IPD which could suggest an impaired immune response. This lack of immune competence could be aggravated by limited breastfeeding lower than recommended by WHO and by the presence of keystone pathogens which need to be characterized and that could favor the overgrowth of many proteolytic anaerobic organisms from the oral cavity, giving rise to a dramatic dysbiosis. From an applied point of view, we found suggestive microbiota profiles associated to IPD (*Streptococcus*-dominated microbiota profile) or asymptomatic colonization (*Dolosigranulum*-dominated microbiota profile) that could be used, respectively, as disease biomarkers or to identify health-associated inhabitants of the respiratory tract. The characterization of beneficial bacteria could be useful to prevent pneumococcal infections by integrating those microorganisms in a probiotic formula. The present study suggests not only respiratory tract samples, but also breast milk, as a potential source of those beneficial bacteria.

DATA AVAILABILITY STATEMENT

Sequence files and metadata for all samples used in this study are stored in the MG-RAST server to be publicly available by accessing the project Invasive Pneumococcal Disease (IPD) in children is associated with a highly diverse nasopharyngeal microbiota: a case-control study, ID mgp80930. All remaining data are contained within the paper and/or **Supporting Information Files**.

AUTHOR CONTRIBUTIONS

AM and CM-A contributed to the conception, design, and analysis of data. DH and JR contributed to the case and control recruitment and microbiological characterization of samples. AC-C and AG contributed to the bioinformatics analysis. PB contributed to the coordination, statistical analysis, and data/sample management. AC-C, PB, AM, and CM-A were the major contributors in writing the manuscript. All authors read and approved the final manuscript.

FUNDING

This work was supported in part by Fondo Europeo de Desarrollo Regional (FEDER) and the Ministry of Science and Innovation, Instituto de Salud Carlos III (ISCIII) (http://www.isciii.es), Projects of Research on Health [FIS project number PI16/00174, Principal Investigator: CM-A], Predoctoral contract for training in research into Health [Grant number FI17/00248, Recipient: DH] and Sant Joan de Deu Foundation [Grant number AFR2015, Principal Investigator: CM-A] (http://www.fsjd.org/es). The funders had no role in study design, data collection and interpretation, or the decision to submit the work for publication.

ACKNOWLEDGMENTS

We thank A. Artacho for his help in statistical analysis and The Catalan Study group of host-pathogen interaction in patients with IPD: Maria Andres-Franch, Carlos Bautista, PB, AC-C, Alvaro Díaz, Cristina Esteva, Mariona F. de Sevilla, Ana Fernandez, Miguel Garcia-Fernandez, AG, Carmen Galles, Lourdes Garcia, Juan Jose Garcia-Garcia, Susanna Hernandez-Bou, Cristian Launes, Francisco Lozano, Carles Luaces, AM, CM-A, Marian Navarro, Daniel Penela, JR, Miriam Triviño, Ana Valero-Rello, Goretti Sauca, Edual Sellares.

SUPPLEMENTARY MATERIAL

The Supplementary Material for this article can be found online at: https://www.frontiersin.org/articles/10.3389/fmicb.2019.00011/full#supplementary-material

Supplementary Figure 1 | Rarefaction curves of individual nasopharyngeal samples in **(a)** healthy children (controls) and **(b)** patients with invasive pneumococcal disease (cases). The horizontal axis shows the number of reads (sequencing effort) obtained by pyrosequencing the 16S rRNA gene. The vertical axis shows the number of operational taxonomic units (OTUs) at a level of 97% (estimated number of bacterial species per sample).

Supplementary Figure 2 | Heatmap profile showing average abundances of bacterial genera incases and controls indicating the age of each child. Genera present in <3 patients were removed from the analysis for clarity.

Supplementary Figure 3 | Relationships between the levels of *Streptococcus* and *Veillonella* in children's nasopharyngeal samples. Scatterplots show the number of sequence reads in the two bacterial genera for cases **(A)** and controls **(B)**.

REFERENCES

Arumugam, M., Raes, J., Pelletier, E., Le Paslier, D., Yamada, T., Mende, D. R., et al. (2011). Enterotypes of the human gut microbiome. *Nature* 473, 174–180. doi: 10.1038/nature09944

Ballard, O., and Morrow, A. L. (2013). Human milk composition. *Pediatr. Clin. North Am.* 60, 49–74. doi: 10.1016/j.pcl.2012.10.002

Biesbroek, G., Bosch, A. A. T. M., Wang, X., Keijser, B. J. F., Veenhoven, R. H., Sanders, E. A., et al. (2014). The Impact of breastfeeding on nasopharyngeal microbial communities in infants. *Am. J. Respir. Crit. Care Med.* 190, 298–308. doi: 10.1164/rccm.201401-0073OC

Bogaert, D., De Steenhuijsen Piters, W. A. A., and Sanders, E. A. M. (2015). The role of the local microbial ecosystem in respiratory health and disease. *Philos. Trans. R. Soc. Lond. B Biol. Sci.* 370:20140294. doi: 10.1098/rstb.2014.0294

Bogaert, D., Keijser, B., Huse, S., Rossen, J., Veenhoven, R., van Gils, E., et al. (2011). Variability and diversity of nasopharyngeal microbiota in children: a metagenomic analysis. *PLoS ONE* 6:e17035. doi: 10.1371/journal.pone.0017035

Bomar, L., Brugger, S. D., Yost, B. H., Davies, S. S., and Lemon, K. P. (2016). *Corynebacterium accolens* releases antipneumococcal free fatty acids from human nostril and skin surface triacylglycerols. *mBio* 7, e01725–e01715. doi: 10.1128/mBio.01725-15

Brotons, P., Bassat, Q., Lanaspa, M., Henares, D., Perez-Arguello, A., Madrid, L., et al. (2017). Nasopharyngeal bacterial load as a marker for rapid and easy diagnosis of invasive pneumococcal disease in children from Mozambique. *PLoS ONE* 12:e0184762. doi: doi: 10.1371/journal.pone.0184762

Brueggemann, A. B., Griffiths, D. T., Meats, E., Peto, T., Crook, D. W., and Spratt, B. G. (2003). Clonal relationships between invasive and carriage *Streptococcus pneumoniae* and serotype- and clone-specific differences in invasive disease potential. *J. Infect. Dis.* 187, 1424–1432. doi: 10.1086/374624

Cabrera-Rubio, R., Collado, M. C., Laitinen, K., Salminen, S., Isolauri, E., and Mira, A. (2012). The human milk microbiome changes over lactation and is shaped by maternal weight and mode of delivery. *Am. J. Clin. Nutr.* 96, 544–551. doi: 10.3945/ajcn.112.037382

Caporaso, J. G., Kuczynski, J., Stombaugh, J., Bittinger, K., Bushman, F. D., Costello, E. K., et al. (2010). QIIME allows analysis of high-throughput community sequencing data. *Nat. Methods* 7, 335–336. doi: 10.1038/nmeth.f.303

Chao, A. (1984). Nonparametric estimation of the number of classes in a population. *Scand. J. Stat.* 11, 265–270.

Claesson, M. J., Wang, Q., O'Sullivan, O., Greene-Diniz, R., Cole, J. R., Ross, R. P., et al. (2010). Comparison of two next-generation sequencing technologies for resolving highly complex microbiota composition using tandem variable 16S rRNA gene regions. *Nucleic Acids Res.* 38:e200. doi: 10.1093/nar/gkq873

Cole, J. R., Wang, Q., Cardenas, E., Fish, J., Chai, B., Farris, R. J., et al. (2009). The Ribosomal Database Project: improved alignments and new tools for rRNA analysis. *Nucleic Acids Res.* 37, D141–D145. doi: 10.1093/nar/gkn879

Darveau, R. P., Hajishengallis, G., and Curtis, M. A. (2012). Porphyromonas gingivalis as a potential community activist for disease. *J. Dent. Res.* 91, 816–820. doi: 10.1177/0022034512453589

de la Cuesta-Zuluaga, J., and Escobar, J. S. (2016). Considerations for optimizing microbiome analysis using a marker gene. *Front. Nutr.* 3:26. doi: 10.3389/fnut.2016.00026

De Steenhuijsen Piters, W. A. A., Huijskens, E. G. W., Wyllie, A. L., Biesbroek, G., van den Bergh, M. R., Veenhoven, R. H., et al. (2016). Dysbiosis of upper respiratory tract microbiota in elderly pneumonia patients. *ISME J.* 10, 97–108. doi: 10.1038/ismej.2015.99

del Amo, E., Brotons, P., Monsonis, M., Triviño, M., Iñigo, M., Selva, L., et al. (2014). High invasiveness of pneumococcal serotypes included in the new generation of conjugate vaccines. *Clin. Microbiol. Infect.* 20, 684–689. doi: 10.1111/1469-0691.12422

del Amo, E., Selva, L., de Sevilla, M. F., Ciruela, P., Brotons, P., Triviño, M., et al. (2015). Estimation of the invasive disease potential of *Streptococcus pneumoniae* in children by the use of direct capsular typing in clinical specimens. *Eur. J. Clin. Microbiol. Infect. Dis.* 34, 705–711. doi: 10.1007/s10096-014-2280-y

Dethlefsen, L., McFall-Ngai, M., and Relman, D. A. (2007). An ecological and evolutionary perspective on human-microbe mutualism and disease. *Nature* 449, 811–818. doi: 10.1038/nature06245

Di Pierro, F., Colombo, M., Zanvit, A., Risso, P., and Rottoli, A. S. (2014). Use of *Streptococcus salivarius* K12 in the prevention of streptococcal and viral pharyngotonsillitis in children. *Drug. Healthc. Patient Saf.* 6, 15–20. doi: 10.2147/DHPS.S59665

Dige, I., Grønkjær, L., and Nyvad, B. (2014). Molecular studies of the structural ecology of natural occlusal caries. *Caries Res.* 48, 451–460. doi: 10.1159/000357920

Dray, S., and Dufour, A.-B. (2007). *The ade4 Package: Implementing the Duality Diagram for Ecologists*. Available online at: http://www.jstatsoft.org/ (Accessed January 14, 2019).

Gaspar, P., Al-Bayati, F. A. Y., Andrew, P. W., Neves, A. R., and Yesilkaya, H. (2014). Lactate dehydrogenase is the key enzyme for pneumococcal pyruvate metabolism and pneumococcal survival in blood. *Infect. Immun.* 82, 5099–5109. doi: 10.1128/IAI.02005-14

Guembe, M., Marin, M., Martin-Rabadan, P., Echenagusia, A., Camunez, F., Rodriguez-Rosales, G., et al. (2013). Use of universal 16s RRNA gene PCR as a diagnostic tool for venous access port-related bloodstream infections. *J. Clin. Microbiol.* 51, 799–804. doi: 10.1128/JCM.02414-12

Haas, B. J., Gevers, D., Earl, A. M., Feldgarden, M., Ward, D. V, Giannoukos, G., et al. (2011). Chimeric 16S rRNA sequence formation and detection in Sanger and 454-pyrosequenced PCR amplicons. *Genome Res.* 21, 494–504. doi: 10.1101/gr.112730.110

Hajishengallis, G. (2011). Immune evasion strategies of *Porphyromonas gingivalis*. *J. Oral Biosci.* 53, 233–240. doi: 10.2330/joralbiosci.53.233

Hajishengallis, G., Darveau, R. P., and Curtis, M. A. (2012). The keystone-pathogen hypothesis. *Nat. Rev. Microbiol.* 10, 717–725. doi: 10.1038/nrmicro2873

Hunt, K. M., Foster, J. A., Forney, L. J., Schü Tte, U. M. E., Beck, D. L., Abdo, Z., et al. (2011). Characterization of the diversity and temporal stability of bacterial communities in human milk. *PLoS ONE* 6:e21313. doi: 10.1371/journal.pone.0021313

Hyde, E. R., Petrosino, J. F., Piedra, P. A., Camargo, C. A., Espinola, J. A., Mansbach, J. M., et al. (2014). Nasopharyngeal Proteobacteria are associated with viral etiology and acute wheezing in children with severe bronchiolitis. *J. Allergy Clin. Immunol.* 133, 1220–1222. doi: 10.1016/j.jaci.2013.10.049

Ing, J., Mason, E. O., Kaplan, S. L., Lamberth, L. B., Revell, P. A., Luna, R. A., et al. (2012). Characterization of nontypeable and atypical *Streptococcus pneumoniae* pediatric isolates from 1994 to 2010. *J. Clin. Microbiol.* 50, 1326–1330. doi: 10.1128/JCM.05182-11

Jeffery, I. B., Claesson, M. J., Toole, P. W. O., and Shanahan, F. (2012). Categorization of the gut microbiota: enterotypes or gradients? *Nat. Rev. Microbiol.* 10, 591–592. doi: 10.1038/nrmicro2859

López-López, A., Camelo-Castillo, A., Ferrer, M. D., Simon-Soro, Á., and Mira, A. (2017). Health-associated niche inhabitants as oral probiotics: the case of *Streptococcus dentisani*. *Front. Microbiol.* 8:379. doi: 10.3389/fmicb.2017.00379

Lozupone, C., Hamady, M., and Knight, R. (2006). UniFrac–an online tool for comparing microbial community diversity in a phylogenetic context. *BMC Bioinformatics* 7:371. doi: 10.1186/1471-2105-7-371

Martínez, M. J., Massora, S., Mandomando, I., Ussene, E., Jordao, D., Lovane, L., et al. (2016). Infectious cause of death determination using minimally invasive autopsies in developing countries. *Diagn. Microbiol. Infect. Dis.* 84, 80–86. doi: 10.1016/j.diagmicrobio.2015.10.002

Medina, M., Villena, J., Salva, S., Vintiñi, E., Langella, P., and Alvarez, S. (2008). Nasal administration of *Lactococcus lactis* improves local and systemic immune responses against *Streptococcus pneumoniae*. *Microbiol. Immunol.* 52, 399–409. doi: 10.1111/j.1348-0421.2008.00050.x

Meningitis (2011). *Laboratory Methods for the Diagnosis of Meningitis*. CDC. Available online at: https://www.cdc.gov/meningitis/lab-manual/index.html (Accessed January 14, 2019).

Michener, C. D., and Sokal, R. R. (1957). A quantitative approach to a problem in classification. *Evolution* 11, 130–162. doi: 10.2307/2406046

Mira, A., Simon-Soro, A., and Curtis, M. A. (2017). Role of microbial communities in the pathogenesis of periodontal diseases and caries. *J. Clin. Periodontol.* 44, S23–S38. doi: 10.1111/jcpe.12671

Mira-Pascual, L., Cabrera-Rubio, R., Ocon, S., Costales, P., Parra, A., Suarez, A., et al. (2015). Microbial mucosal colonic shifts associated with the development of colorectal cancer reveal the presence of different bacterial and archaeal biomarkers. *J. Gastroenterol.* 50, 167–179. doi: 10.1007/s00535-014-0963-x

Morales, M., Martín-Galiano, A. J., Domenech, M., and García, E. (2015). Insights into the evolutionary relationships of LytA autolysin and ply pneumolysin-like genes in *Streptococcus pneumoniae* and related Streptococci. *Genome Biol. Evol.* 7, 2747–2761. doi: 10.1093/gbe/evv178

Mortensen, M. S., Brejnrod, A. D., Roggenbuck, M., Abu Al-Soud, W., Balle, C., Krogfelt, K. A., et al. (2016). The developing hypopharyngeal microbiota in early life. *Microbiome* 4:70. doi: 10.1186/s40168-016-0215-9

National Center for Immunization and Respiratory Diseases (2014). *PCR for Detection and Characterization of Bacterial Meningitis Pathogens: Neisseria meningitidis, Haemophilus influenzae, and Streptococcus pneumoniae.*

Oh, J., Freeman, A. F., NISC Comparative Sequencing Program., Park, M., Sokolic, R., Candotti, F., et al. (2013). The altered landscape of the human skin microbiome in patients with primary immunodeficiencies. *Genome Res.* 23, 2103–2114. doi: 10.1101/gr.159467.113

Oksanen, J., Blanchet, F. G., Friendly, M., Kindt, R., Legendre, P., McGlinn, D., et al. (2018). *Community Ecology Package*. Available at: https://cran.r-project.org/web/packages/vegan/vegan.pdf (Accessed November 22, 2018).

Relman, D. A. (2012). The human microbiome: ecosystem resilience and health. *Nutr. Rev.* 70, S2–S9. doi: 10.1111/j.1753-4887.2012.00489.x

Segal, L. N., Alekseyenko, A. V, Clemente, J. C., Kulkarni, R., Wu, B., Gao, Z., et al. (2013). Enrichment of lung microbiome with supraglottic taxa is associated with increased pulmonary inflammation. *Microbiome* 1:19. doi: 10.1186/2049-2618-1-19

Segata, N., Izard, J., Waldron, L., Gevers, D., Miropolsky, L., Garrett, W. S., et al. (2011). Metagenomic biomarker discovery and explanation. *Genome Biol.* 12:R60. doi: 10.1186/gb-2011-12-6-r60

Selva, L., Berger, C., Garcia-Garcia, J. J., de Paz, H., Nadal, D., and Muñoz-Almagro, C. (2014). Direct identification of *Streptococcus pneumoniae* capsular types in pleural fluids by using multiplex PCR combined with automated fluorescence-based capillary electrophoresis. *J. Clin. Microbiol.* 52, 2736–2737. doi: 10.1128/JCM.00906-14

Shannon, C. E. (1948). A mathematical theory of communication. *Bell Syst. Tech. J.* 27, 379–423. doi: 10.1145/584091.584093

Shin, J., Lee, S., Go, M. J., Lee, S. Y., Kim, S. C., Lee, C. H., et al. (2016). Analysis of the mouse gut microbiome using full-length 16S rRNA amplicon sequencing. *Sci. Rep.* 6, 1–10. doi: 10.1038/srep29681

Simões, A. S., Tavares, D. A., Rolo, D., Ardanuy, C., Goossens, H., Henriques-Normark, B., et al. (2016). LytA-based identification methods can misidentify *Streptococcus pneumoniae*. *Diagn. Microbiol. Infect. Dis.* 85, 141–148. doi: 10.1016/j.diagmicrobio.2016.03.018

Simón-Soro, A., Guillen-Navarro, M., and Mira, A. (2014). Metatranscriptomics reveals overall active bacterial composition in caries lesions. *J. Oral Microbiol.* 6:25443. doi: 10.3402/jom.v6.25443

Sleeman, K. L., Griffiths, D., Shackley, F., Diggle, L., Gupta, S., Maiden, M. C., et al. (2006). Capsular serotype-specific attack rates and duration of carriage of *Streptococcus pneumoniae* in a population of children. *J. Infect. Dis.* 194, 682–688. doi: 10.1086/505710

Tagg, J. R., and Dierksen, K. P. (2003). Bacterial replacement therapy: adapting "germ warfare" to infection prevention. *Trends Biotechnol.* 21, 217–223. doi: 10.1016/S0167-7799(03)00085-4

Tan, T. Q., Mason, E. O., Wald, E. R., Barson, W. J., Schutze, G. E., Bradley, J. S., et al. (2002). Clinical characteristics of children with complicated pneumonia caused by *Streptococcus pneumoniae*. *Pediatrics* 110, 1–6. doi: 10.1542/peds.110.1.1

Turnbaugh, P. J., Ley, R. E., Hamady, M., Fraser-Liggett, C. M., Knight, R., and Gordon, J. I. (2007). The human microbiome project. *Nature* 449, 804–810. doi: 10.1038/nature06244

Yarza, P., Richter, M., Peplies, J., Euzeby, J., Amann, R., Schleifer, K.-H., et al. (2008). The All-Species Living Tree project: a 16S rRNA-based phylogenetic tree of all sequenced type strains. *Syst. Appl. Microbiol.* 31, 241–250. doi: 10.1016/j.syapm.2008.07.001

Zhu, B., Wang, X., and Li, L. (2010). Human gut microbiome: the second genome of human body. *Protein Cell* 1, 718–725. doi: 10.1007/s13238-010-0093-z

Conflict of Interest Statement: The authors declare that the research was conducted in the absence of any commercial or financial relationships that could be construed as a potential conflict of interest.

Copyright © 2019 Camelo-Castillo, Henares, Brotons, Galiana, Rodriguez, Mira and Muñoz-Almagro. This is an open-access article distributed under the terms of the Creative Commons Attribution License (CC BY). The use, distribution or reproduction in other forums is permitted, provided the original author(s) and the copyright owner(s) are credited and that the original publication in this journal is cited, in accordance with accepted academic practice. No use, distribution or reproduction is permitted which does not comply with these terms.

frontiers in Microbiology

ORIGINAL RESEARCH
published: 08 February 2019
doi: 10.3389/fmicb.2019.00164

Comparison of Small Gut and Whole Gut Microbiota of First-Degree Relatives With Adult Celiac Disease Patients and Controls

Rahul Bodkhe[1†], Sudarshan A. Shetty[1†‡], Dhiraj P. Dhotre[1], Anil K. Verma[2‡], Khushbo Bhatia[2], Asha Mishra[2], Gurvinder Kaur[3], Pranav Pande[1], Dhinoth K. Bangarusamy[4], Beena P. Santosh[4], Rajadurai C. Perumal[4], Vineet Ahuja[2], Yogesh S. Shouche[1] and Govind K. Makharia[2*]*

[1] National Centre for Microbial Resource, National Centre for Cell Science, Pune, India, [2] Department of Gastroenterology and Human Nutrition, All India Institute of Medical Sciences, New Delhi, India, [3] Department of Transplant Immunology and Immunogenetics, All India Institute of Medical Sciences, New Delhi, India, [4] AgriGenome Labs Pvt. Ltd., Kerala, India

Recent studies on celiac disease (CeD) have reported alterations in the gut microbiome. Whether this alteration in the microbial community is the cause or effect of the disease is not well understood, especially in adult onset of disease. The first-degree relatives (FDRs) of CeD patients may provide an opportunity to study gut microbiome in pre-disease state as FDRs are genetically susceptible to CeD. By using 16S rRNA gene sequencing, we observed that ecosystem level diversity measures were not significantly different between the disease condition (CeD), pre-disease (FDR) and control subjects. However, differences were observed at the level of amplicon sequence variant (ASV), suggesting alterations in specific ASVs between pre-disease and diseased condition. Duodenal biopsies showed higher differences in ASVs compared to fecal samples indicating larger disruption of the microbiota at the disease site. The duodenal microbiota of FDR was characterized by significant abundance of ASVs belonging to *Parvimonas*, *Granulicatella*, *Gemella*, *Bifidobacterium*, *Anaerostipes*, and *Actinomyces* genera. The duodenal microbiota of CeD was characterized by higher abundance of ASVs from genera *Megasphaera* and *Helicobacter* compared to the FDR microbiota. The CeD and FDR fecal microbiota had reduced abundance of ASVs classified as *Akkermansia* and *Dorea* when compared to control group microbiota. In addition, predicted functional metagenome showed reduced ability of gluten degradation by CeD fecal microbiota in comparison to FDRs and controls. The findings of the present study demonstrate differences in ASVs and predicts reduced ability of CeD fecal microbiota to degrade gluten compared to the FDR fecal microbiota. Further research is required to investigate the strain level and active functional profiles of FDR and CeD microbiota to better understand the role of gut microbiome in pathophysiology of CeD.

Keywords: celiac, gut microbiota, gluten, *H. pylori*, butyrate, duodenal microbiota

OPEN ACCESS

Edited by:
Learn-Han Lee,
Monash University Malaysia, Malaysia

Reviewed by:
Steven Thomas Leach,
University of New South Wales, Australia
Daniel Martinez Garcia,
EveryWhere Schools, Spain

****Correspondence:***
Yogesh S. Shouche
yogesh@nccs.res.in
Govind K. Makharia
govindmakharia@gmail.com

[†] These authors have contributed equally to this work

[‡] ***Present address:***
Sudarshan A. Shetty,
Laboratory of Microbiology, Wageningen University and Research, Wageningen, Netherlands
Anil K. Verma,
Celiac Disease Research Laboratory, Department of Pediatrics, Università Politecnica delle Marche, Ancona, Italy

Specialty section:
This article was submitted to Microbial Symbioses, a section of the journal Frontiers in Microbiology

Received: *17 August 2018*
Accepted: *22 January 2019*
Published: *08 February 2019*

Citation:
Bodkhe R, Shetty SA, Dhotre DP, Verma AK, Bhatia K, Mishra A, Kaur G, Pande P, Bangarusamy DK, Santosh BP, Perumal RC, Ahuja V, Shouche YS and Makharia GK (2019) Comparison of Small Gut and Whole Gut Microbiota of First-Degree Relatives With Adult Celiac Disease Patients and Controls. Front. Microbiol. 10:164. doi: 10.3389/fmicb.2019.00164

Abbreviations: ANOSIM, analysis of similarities; ASV, amplicon sequence variant; CeD, celiac disease; DADA2, divisive amplicon denoising algorithm 2; DC, diseased controls (dyspeptic); FDR, first degree relatives; HLA, human leukocyte antigen; KEGG, kyoto encyclopedia of genes and genomes; PCoA, principal coordinates analysis; rRNA, ribosomal ribonucleic acid; SCFA, short chain fatty acids; tTG, tissue transglutaminase.

INTRODUCTION

Celiac disease is a common, chronic immune mediated enteropathy of the small intestine which affects approximately 0.7% of the global population (Singh et al., 2018). Once thought to be uncommon in Asia, CeD is now prevalent in many Asian countries including India (Makharia et al., 2011). Recently, the prevalence of CeD has been on the rise, especially in developing countries (Lohi et al., 2007). This rapid rise in disease prevalence cannot be attributed only to the underlying genetic makeup of the population but rather to the environmental factors including infant feeding practices, reduction in infectious diseases, reovirus infection, and use of antibiotics (Jabri and Sollid, 2006; Lohi et al., 2007; Myléus et al., 2009; Volta and De Giorgio, 2012; Mårild et al., 2013; Bouziat et al., 2017).

CeD is caused by the consumption of gluten proteins present in cereals such as wheat, barley and rye in genetically susceptible individuals (Caminero et al., 2015). While many genes are involved in the development of CeD, thus far only the presence of HLA-DQ2 or DQ8 haplotype is considered to be essential (Sanz et al., 2011). Additional factors that contribute to pathogenesis include other co-genetic factors (genome wide association studies have identified several markers), wheat-related factors (age of ingestion, type and quantity of wheat) and the way gluten is metabolized in the intestine (Van De Wal et al., 1998; Kagnoff, 2007; Verdu et al., 2015). About 30–40% of the gluten protein consists of glutamine and proline. Since humans are unable to enzymatically break the molecular bonds between these two amino-acids, many immunogenic peptides are produced (Jabri and Sollid, 2006). There remains a possibility that enzymes secreted by the small intestinal microbiota convert some of these immunogenic peptides to non-immunogenic peptides.

While 20–30% of individuals in many countries including India are genetic susceptibility to develop CeD and the majority of them are exposed to wheat, only 1% of them develop CeD. This brings forth the role of other factors such as the gut microbiota in the pathogenesis of CeD (Sanz et al., 2011; Sánchez et al., 2012). Recently, numerous studies have highlighted the potential role of gut microbiota in inflammatory gastrointestinal diseases (Png et al., 2010; Fernandez-Feo et al., 2013; de Sousa Moraes et al., 2014; Schneeberger et al., 2015; Rivière et al., 2016; Zeng et al., 2017).

However, whether the changes in the microbial community structure and function in patients with CeD are cause or effect of the disease state remains unclear to date. In order to answer this question, one has to examine the status of the gut microbiota in the pre-disease state. Recently two studies investigated the microbiota of at-risk children who developed CeD few years after birth. One study observed an increase in *Bifidobacterium breve* and *Enterococcus* spp. in infants that developed active CeD (Olivares et al., 2018). Another study, did not observe any association between microbiota composition and development of CeD during the age of 9 and 12 months (Rintala et al., 2018). Nevertheless, potential microbiota related triggers for development of CeD in later adult life still remain unclear. While 70–80% percent of first-degree relatives (FDRs) of patients with CeD have HLADQ2/DQ8 haplotype (compared to 30% in the general population); only approximately 8.5% of FDRs develop CeD (Singh et al., 2015). Thus, the question arises; why do only few FDRs develop CeD and what is the role of the gut microbiome in disease protection? Indirect evidence of altered microbiota in relatives of patients with CeD is suggested by significantly lower levels of acetic acid and total short chain fatty acids (SCFA), and higher fecal tryptic activity (Tjellström et al., 2007). There is a lack of information regarding the gut microbial composition and function in adult FDRs of patients with CeD. Additionally, it is important to explore the status of the microbiota in both the small intestine, the site of the disease, and feces, as representative of whole gut microbiome. To test the hypothesis that gut microbiome of FDR is different from CeD and could potentially play an important role in the pathogenesis of CeD, we explored the composition of both small intestinal and the whole gut microbiome using Illumina MiSeq in a subset of patients with CeD, FDR and controls. We further investigated the potential microbial functions that are characteristic of FDR and CeD microbiota.

MATERIALS AND METHODS

Human Subjects, Duodenal Biopsies and Fecal Sample Collection

A total of 62 subjects participated in this study including 23 treatment naïve patients with CeD [all HLA-DQ2/DQ8+, having high titre of anti-tissue transglutaminase antibodies (tTG Ab) and having villous abnormalities of modified Marsh grade 2 or more], 15 healthy FDRs of patients with CeD [having normal titre of anti-tTG Ab and having no villous abnormalities of modified Marsh grade 0 or 1], and 24 controls (patients with Hepatitis B Virus carriers or those having functional dyspepsia; having normal titre of anti-tTG Ab and having no villous abnormalities; **Table 1**). Duodenal biopsies and fecal samples were collected from each of the above mentioned subjects at All India Institute of Medical Sciences, New Delhi, and sent to National Centre for Cell Sciences, Pune for microbiome analysis. The ethics committees of All India Institute of Medical Sciences, New Delhi, and National Centre for Cell Sciences, Pune, India approved the study. Informed and written consent was obtained from all the participants. There was a significant different in the age between the three groups ($p < 0.05$, Kruskal-Wallis test). Further details of patients and controls have been provided in the (**Supplementary Table S3**).

DNA Extraction and 16S rRNA Gene Sequencing

Total DNA was extracted from duodenal biopsies using QIAGEN DNeasy Blood and Tissue kit (QIAGEN, Germany) and fecal samples using the QIAamp fast DNA stool Mini Kit (QIAGEN, Germany) according to the manufacturer's instructions. We used Illumina MiSeq sequencing to determine the microbial composition of the duodenal biopsies and fecal samples. PCR was set up in 50 μl reaction using AmpliTaq Gold PCR Master Mix (Life Technologies,

TABLE 1 | Demographic characteristics on study subjects.

Groups	No. of subjects	Age (mean ± S.D.)	Gender*		Sampling site		Villous abnormalities (as per Modified Marsh criteria)				HLA Haplotype			tTG Titre (mean ± SD)
			M	F	S	B	0	1	3a	3b	3c	DQ2	DQ8	DQ2+ DQ8+	
CeD	23	23.4 ± 9.5	10	13	21	16	0	0	2	7	14	22	1	0	199.9 ± 72.1
FDR	15	31.6 ± 10.8	6	9	15	13	15	0	0	0	0	13	0	2	4.36 ± 2.6
DC	24	30.6 ± 12.3	22	2	23	14	22	2	0	0	0	6	0	0	4.09 ± 2.8

*M = male, F = female, tTG = Tissue transglutaminase, S = Stool samples, B = Biopsy sample. *For the DC group our samples are biased by the higher representation of males compared to females.*

United States) and with 16S rRNA V4 variable region-specific bacterial primers 515F (5′-GTGCCAGCMGCCGCGGTAA-3′) and 806R (5′- GGACTACHVGGGTWTCTAAT-3′) (Walters et al., 2016).

Sequence Processing and Bacterial Community Analysis

Illumina Miseq platform rendered a total of 76058052 raw 16S rRNA sequence reads for the 102 fecal and biopsy samples of the diagnosis groups, with an average of 745667 ± 194667 reads per sample. Adapter sequences were trimmed by using Cutadapt (1.18) tool (Martin, 2011) and trimmed reads were pooled as Fasta.gz file format for further analysis in DADA2 (v 1.6.0) pipeline (Callahan et al., 2016). In the first step reads were inspected for read quality profile, the read quality score was decreased (< 30) after 240 bases for forward read and 160 bases for reverse reads. We truncated the forward reads at position 240 (trimming the last 10 nucleotides) and reverse reads at position 160 (trimming the last 90 nucleotide). After quality filtering and removal of bases with a total of 70502947 (92.69%) high-quality reads of the 16S rRNA amplicons were obtained, with an average 691205 ± 181263 reads per sample, ranging from 325350 to 1207169 among samples (**Supplementary Table S4**). Finally, taxonomic assignment was done by the naive Bayesian classifier method with default setting as implemented in DADA2, against Human Intestinal 16S rRNA gene reference taxonomy database (HITdb v 1.00). Briefly, HITdb is a 16S rRNA gene database based on high-quality sequences specific for human intestinal microbiota, this database provides improved taxonomic up to the species level (Ritari et al., 2015). Unassigned chimeric and sequences of chloroplast and mitochondria were excluded from downstream analysis. Taxonomic assignment successfully mapped 6567144 ASVs, with an average of 64383 ± 29929 ASVs per sample. Finally, from these ASVs, ASV table was constructed and the ASVs generated by the contaminants were removed by using decontam software (Davis et al., 2018) and the output ASV table was used for downstream analyses.

Microbial diversity and composition analysis were done using the R-package phyloseq (v1.22.3) (McMurdie and Holmes, 2013) and microbiome R package (v1.0.2).[1] To test for similarities in microbial communities between sample types and diagnosis groups Analysis of similarities (ANOSIM) on Bray-Curtis distances was used. ANOSIM is a function in vegan package (v 2.4-4) to calculate significance of PCoA clustering based on the Bray-Curtis distances (Oksanen et al., 2011).

To identify differentially abundant ASVs in pairwise comparisons between diagnosis groups we used DESeq2 (v1.18.0) (Love et al., 2014). All ASVs that were significantly (alpha = 0.01) different in abundance between the diagnosis groups were reported and were adjusted for multiple comparisons using the Benjamini-Hochberg, false discovery

[1]https://github.com/microbiome/microbiome

rate procedure. Data was visualized using ggplot2 (v 2.2.1) in R (Wickham, 2011, 2017).

Analysis of 16S rRNA Gene Copies of *H. pylori*

Available full-length 16S rRNA gene sequences of *H. pylori* were downloaded from LPSN-list of prokaryotic names with standing in nomenclature (Parte, 2013). To identify and extract the V4 regions from these 16S rRNA gene sequences, V4 variable region-specific primers 515F (5′-GTGCCAGCMGCCGCGGTAA-3′) and 806R (5′-GGACTACHVGGGTWTCTAAT-3′) were used. Next, to highlight possible similarities and differences between the V4 regions we performed multiple sequence alignment (MSA) using CLUSTAL W 2.0.11 (Larkin et al., 2007). The full-length 16S rRNA gene sequence of *E. coli* strain U 5/41 was used as a reference sequence (**Supplementary Information**).

Metagenomic Imputation

Piphillin tool was used to infer metagenome from 16S rRNA ASV counts table and representative sequence of each ASV. Briefly, this tool predicts metagenomes with high accuracy by leveraging the most-current genome reference databases (Iwai et al., 2016). It uses direct nearest-neighbor matching between 16S rRNA amplicons and genomes to predict the represented genomes. Latest version (May, 2017) of KEGG database and 97% of the identity cutoff was selected for the prediction. The output from Piphillin was further analyzed by STAMP statistical tool, ANOVA with *post hoc* Tukey-kramer test was used to identify statistically different KEGG orthologies between diagnosis groups (Parks et al., 2014).

RESULTS

Comparison of Fecal and Duodenal Microbial Community in the Study Cohort

The characteristics of the study subjects have been summarized in the **Table 1**. All the participants were on staple gluten containing diet during sampling for this particular study. After diagnosis of CeD the patients underwent therapy with dietary recommendation to avoid gluten in daily diet. However, in the present study, we do not include samples after dietary changes. The duodenal biopsies and fecal samples were included to investigate differences in both site-specific and whole gut microbial diversity and community structure in patients with CeD, FDRs and DC (non-celiac Disease-Control group). Irrespective of the diagnosis group i.e., CeD, FDR, or DC, the microbial community in the fecal samples was different when compared to the microbial community in duodenal biopsies (ANOSIM statistic R: 0.4998, Significance: 0.001), (**Supplementary Figure S1A**).

However, there was no significant difference in alpha diversity between the sampling sites (**Supplementary Figure S1B**).

Site Specific Comparison of Duodenal and Fecal Microbiota of FDRs, CeD and Control Group

To investigate if patients with CeD, FDRs or DC had site specific dissimilarities in microbiota composition, further analysis was divided based on the sampling site.

Pairwise comparison of alpha diversity of the duodenal microbiota of FDRs, CeD and controls showed no significant difference (**Figure 1A**). Similarly, for fecal microbiota, no significant difference was observed in the alpha diversity between the diagnosis groups (**Figure 1B**).

Unconstrained ordination using the Bray-Curtis dissimilarity showed no significant differences in the duodenal microbiota of CeD, FDRs and DC (Analysis of similarities; ANOSIM test; R-statistic = 0.0014, p = 0.427) (**Figure 1C**). Similarly, there was no significant difference in the fecal microbiota of the three diagnosis groups (Analysis of similarities; ANOSIM test; R-statistic = 0.051, p = 0.058) (**Figure 1D**).

Comparison of Duodenal Microbiota Composition Between the Diagnosis Groups

At phylum level, Actinobacteria, Bacteroides, Euryarchaeota, Firmicutes and Proteobacteria were the dominant members in the duodenal microbiota (**Figure 2**).

The phyla, Actinobacteria (p = 0.013) and Bacteroides (p = 0.02) were significantly higher in pre-disease state (FDR) in comparison to the DC microbiota. Although at the phylum level there was no significant difference in the abundance of Firmicutes, the order Clostridiales within this phylum showed significantly higher abundance in FDR microbiota compared to DC microbiota ($p < 0.05$) (**Supplementary Figure S2**). There was no significant difference in abundance of the other major phyla between the FDR and CeD as well as the CeD and DC microbiota (**Figure 2**).

Differences in ASV Abundances in Duodenal Microbiota of the Diagnosis Groups

Differential abundance analysis of ASVs using DESeq2 revealed more than 20-fold higher abundance of ASVs belonging to genera *Parvimonas*, *Granulicatella*, *Gemella*, *Bifidobacterium*, *Anaerostipes*, and *Actinomyces* in the FDR group compared to both CeD and DC groups (p-value < 0.01, **Figures 3A,C**). In the CeD group, ASVs belonging to genera *Helicobacter* and *Megasphaera* were highly abundant compared to both FDR and DC group (**Figures 3B,C**).

Investigation of the differentially abundant ASVs between the FDR and CeD group revealed differences in the abundances of specific ASVs within the same genus (**Figure 3C**). Some ASVs within the archaeal genus *Methanomassiliicoccus* were highly abundant in the CeD group while others were highly abundant in FDR group (**Figure 3C**). Notably, there is only one species of this archaeal genus, *Methanomassiliicoccus luminyensis,* validly described in literature with a single copy of 16S rRNA gene

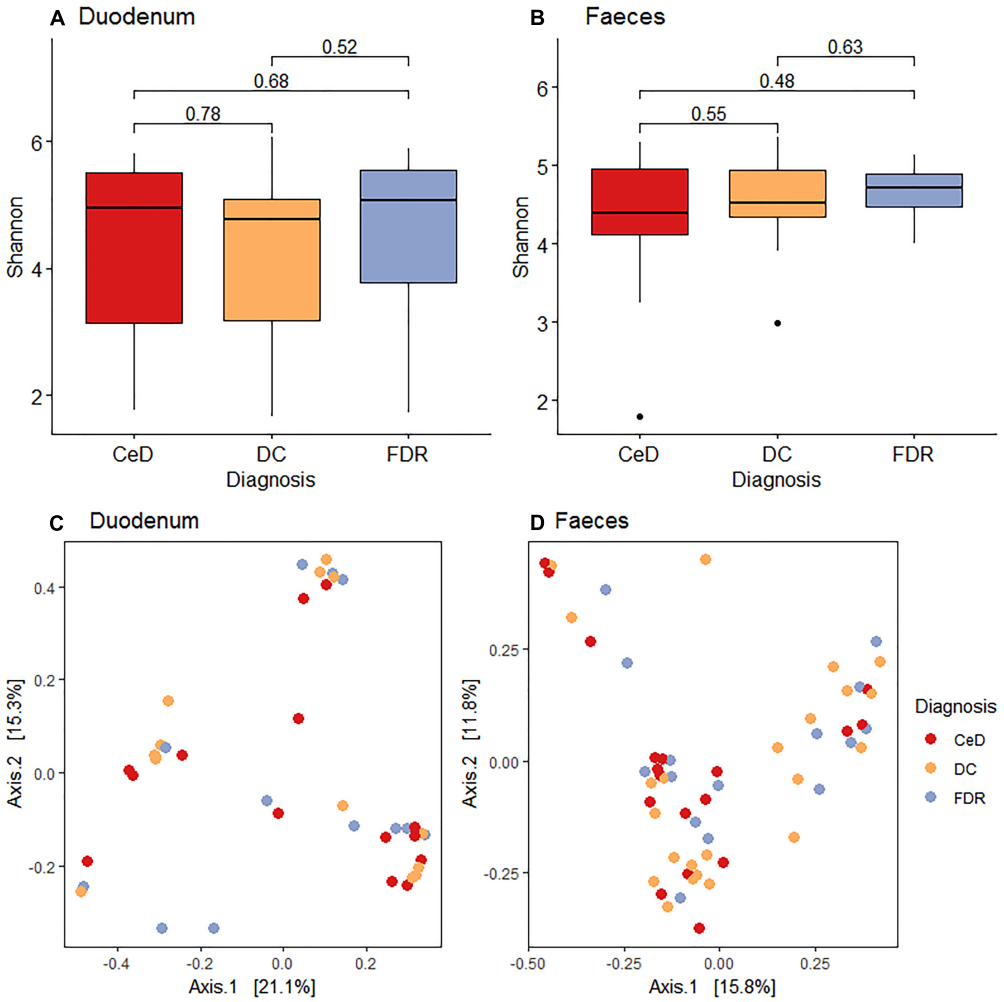

FIGURE 1 | (A) Pairwise comparison of alpha diversity of the duodenal microbiota of diagnosis groups. **(B)** Pairwise comparison of alpha diversity of fecal microbiota of diagnosis groups. **(C)** Principle coordinates analysis of microbial community based on Bray-Curtis distance between diagnosis groups in duodenal microbiota. **(D)** Principle coordinates analysis of microbial community based on Bray-Curtis distance between diagnosis groups in fecal microbiota.

in its genome (Dridi et al., 2012; Gorlas et al., 2012). This suggests a possibility of either species- or strain- level differences in *Methanomassiliicoccus* between the CeD and FDR which requires further investigation. Additionally, ASVs belonging to genera *Eubacterium* and *Catenibacterium* showed ASV level variation in abundance between the CeD and FDR duodenal microbiota (**Figure 3C**).

Comparison of both the FDR and CeD duodenal microbiota with that of the DC duodenal microbiota revealed similarities in the abundances of specific ASVs. Both the CeD and FDR duodenal microbiota were characterized by the abundance of ASVs belonging to genus *Prevotella*, *Megasphaera*, *Helicobacter* and *Catenibacterium* when compared to the DC duodenal microbiota (**Figures 3A,B**).

We further checked for similarities and differences between these *Helicobacter* ASVs because, the ASVs of *Helicobacter* were abundant in FDR and CeD duodenal microbiota when compared to DC duodenal microbiota and one specific ASV was abundant in CeD compared to FDR duodenal microbiota. We observed that the ASV identified as differentially abundant in the CeD duodenal microbiota when compared to both FDR and DC microbiota was ASV1811. Contrary to this, ASV2016 and ASV4095 belonging to *H. pylori* were high in abundance in the FDR duodenal microbiota compared to DC duodenal microbiota (**Supplementary Information**). In view of intra-genomic differences in 16S rRNA gene, we compared the 16S rRNA gene copies of *H. pylori* in publically available genomes. We observed that on average the *H. pylori* genome has two copies of 16S rRNA gene and we did not observe differences between the two copies within a single genome in the V4 region investigated here (**Supplementary Information** text page 3–7). The analysis used for microbial profiling in the present study employs a well-established algorithm to identify finer sequence level variation and differentiate single nucleotide level difference in the 16S rRNA gene amplicon (Callahan et al., 2016). We suggest that future investigation of CeD and FDR

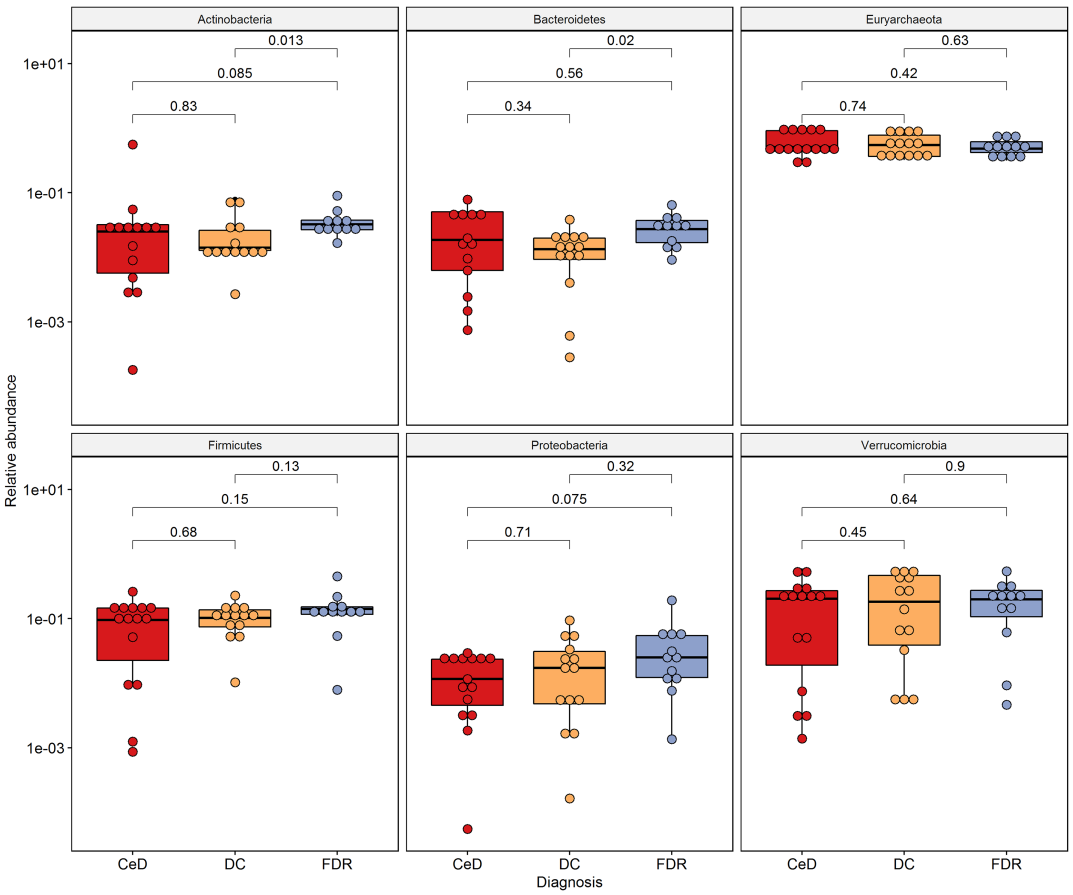

FIGURE 2 | Phylum level distribution of ASVs in duodenal microbiota. Pairwise comparisons were done using Wilcoxon tests.

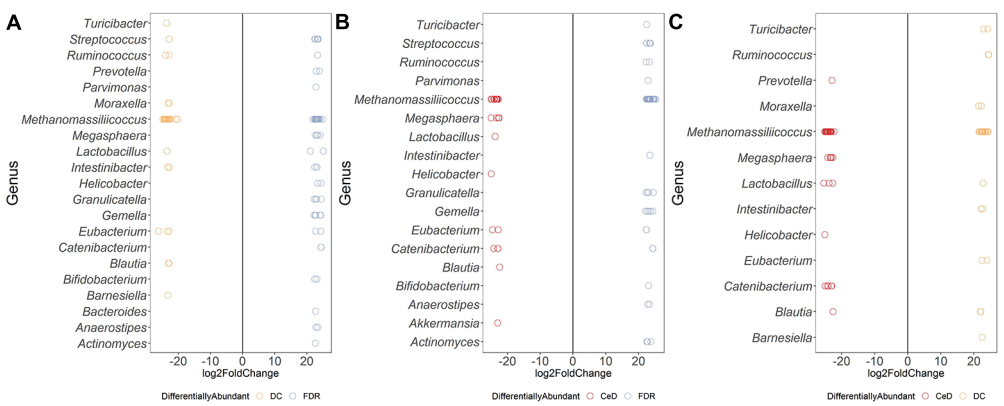

FIGURE 3 | Comparison of differential abundance of microbial ASVs between the diagnosis groups in duodenal microbiota. **(A)** Differential abundance DC vs FDR. **(B)** Differential abundance CeD vs DC **(C)** Differential abundance CeD vs FDR. Only ASVs with significant differences (*P* 0.01) in log2 fold change are depicted.

duodenal microbiota need to focus on strain level variations and functional aspects of *H. pylori* using metagenomics and functional omics.

Both CeD and FDR duodenal microbiota were characterized by low abundance (20-fold) of *Barnesiella* when compared to that in DC (**Figures 3A,B**). Interestingly, the genus *Lactobacillus* showed variation in abundances at ASV level between the three diagnosis groups (**Figures 3A–C**). Strains of *Lactobacillus* are reported to have probiotic effects, ability to degrade gluten and are often associated with health benefits (Lorenzo Pisarello et al., 2014; Orlando et al., 2014). The differences at ASV level observed in our study indicate the need to investigate the potential

impact of species- and/or strain-level differences within the genus *Lactobacillus* in CeD and FDR subjects.

Comparison of Fecal Microbiota Composition Between the Diagnosis Groups

There was no significant difference in abundance of the phyla Proteobacteria, Actinobacteria, Euryarchaeota and Firmicutes (**Figure 4**) between the diagnosis groups. The phylum Bacteroidetes was found to be marginally lower in abundance in the FDR group when compared to the DC group ($p = 0.054$). Similar trend was observed for order Bacteroidales ($p = 0.054$, **Supplementary Figure S3**). The order Clostridiales was significantly abundant in FDRs in comparison to DC group ($p = 0.017$) (**Supplementary Figure S3**). The order Clostridiales was also observed to abundant in duodenal microbiota of FDRs (**Supplementary Figure S2**).

Differences in ASV Abundances in Fecal Microbiota of the Diagnosis Groups

When compared to the duodenal microbiota, fewer ASVs were differentially abundant between the diagnosis groups which suggests a lower variation in fecal microbiota at ASV-level.

Both FDR and CeD fecal microbiota was characterized by a 20-fold decrease in abundance of ASVs belonging to genera *Dorea* and *Akkermansia* (**Figures 5A,B**). In addition, when compared to DC, FDR fecal microbiota showed lower abundance of ASVs belonging to *Lactobacillus* and *Haemophilus* while, fecal microbiota of CeD had lower abundance of *Prevotella* (**Figures 5A,B**). Interestingly, CeD fecal microbiota had ASV level differences in abundance of *Lactobacillus* when compared to DC fecal microbiota ($p < 0.01$, **Figure 5B**). Similarly, *Methanomassiliicoccus* showed ASV level variation in abundances between the three diagnosis groups ($p < 0.01$, **Figures 5A–C**).

Comparison of ASV abundances between the FDR and CeD fecal microbiota revealed higher abundance of ASVs from genera *Pediococcus*, *Intestinibacter*, *Blautia* and *Dorea* in the FDR microbiota ($p < 0.01$) (**Figure 5C**). However, in comparison with DC fecal microbiota, FDR microbiota had 20-fold lower abundance of ASVs related to *Akkermansia* and *Dorea* ($p < 0.01$).

Imputed Metagenome of FDR and CeD Fecal Microbiome Shows Reduced Proportion of Genes Involved in Gluten Metabolism

In addition to differentially abundant microbial ASVs, different study groups might have altered metabolic potential. Of specific interest were the enzymes related to glutenases as they play a role in breakdown of gliadin residues. We followed Piphillin workflow to predict functional profile of fecal and duodenal microbiota (Iwai et al., 2016). A total of 159 KEGG orthologies (KO) were significantly different between diagnosis groups in the fecal microbiota (**Supplementary Table S1**). Among these the KO abundance for Xaa-pro dipeptidase (K01271, Prolidase) enzyme which is known to have role in gluten degradation was found to be significantly reduced in CeD as compared to FDR and DC fecal microbiota (**Figure 6**). Notably, we did not observe any significant difference in the predicted abundance of prolidase in the duodenal microbiota (**Supplementary Table S2**).

DISCUSSION

The aim of the present study was to investigate differences in the duodenal and fecal microbiota of pre-diseased state i.e., FDRs subjects compared to diseased state i.e., CeD and DC. The FDR group was included for two main reasons: (1) They represent a population which is genetically-susceptible to develop CeD; (2) They provide a unique opportunity to identify features of the host as well as of the associated microbiota that may be involved in the protection against developing CeD. We collected both duodenal biopsies and fecal samples to investigate both local and overall changes in the microbiota in FDR, patients with CeD and DC. To the best of our knowledge, reports on site specific microbiota patterns in adult patients with CeD remain scarce, and no results on both site specific and whole gut microbiome on FDRs have been reported to date. Present study provides an overall view on differences of both site-specific changes as well as changes in the fecal microbiota of FDRs, CeD and DC.

The duodenal microbiota of CeD was characterized by high abundance of *Helicobacter* and *Megasphaera* compared to both FDR and DC group. In addition, comparison of *Helicobacter* ASVs suggested ASV-level variation between FDR and CeD duodenal microbiota. Previously, CeD patients with *H. pylori* gastritis were reported to have an increased number of intraepithelial lymphocytes in the duodenal mucosa (Villanacci et al., 2006). On the contrary, there are also reports which have failed to reveal a relationship between *H. pylori* and CeD and found that *H. pylori* presence was inversely associated with CeD (Lebwohl et al., 2013). In the present study, the ASV which is abundant in CeD is different from those ASVs which are enriched in FDR, emphasizing the need for investigating strain level variations in *H. pylori* and its potential impact on pathophysiology of CeD. There were other genera which showed ASV level difference between the microbiota of the CeD, FDR and DC such as, *Streptococcus*, *Ruminococcus*, *Methanomassiliicoccus*, *Catenibacterium*, *Intestinibacter*, and *Blautia*. Specific interest would be for identifying those ASVs that are differentially abundant between the FDR and CeD microbiota. In this comparison between the pre-disease and disease state, we observed a reduced abundance of ASVs related to *Ruminococcus*, *Parvimonas*, *Intestinibacter*, *Granulicatella*, *Gemella*, *Bifidobacterium*, *Anaerostipes*, and *Actinomyces* in the diseased state. The species from genera *Ruminococcus* and *Anaerostipes* are known to produce SCFA such as acetate and butyrate that have beneficial effect on the host (Ze et al., 2012; Morrison and Preston, 2016; Shetty et al., 2017). The genus *Granulicatella* is commonly associated with diseases such as cancer, Crohn's disease and bacteremia (Woo et al., 2003; Nakatsu et al., 2015; Qiu et al., 2017). The bacterial species within the genera *Actinomyces*,

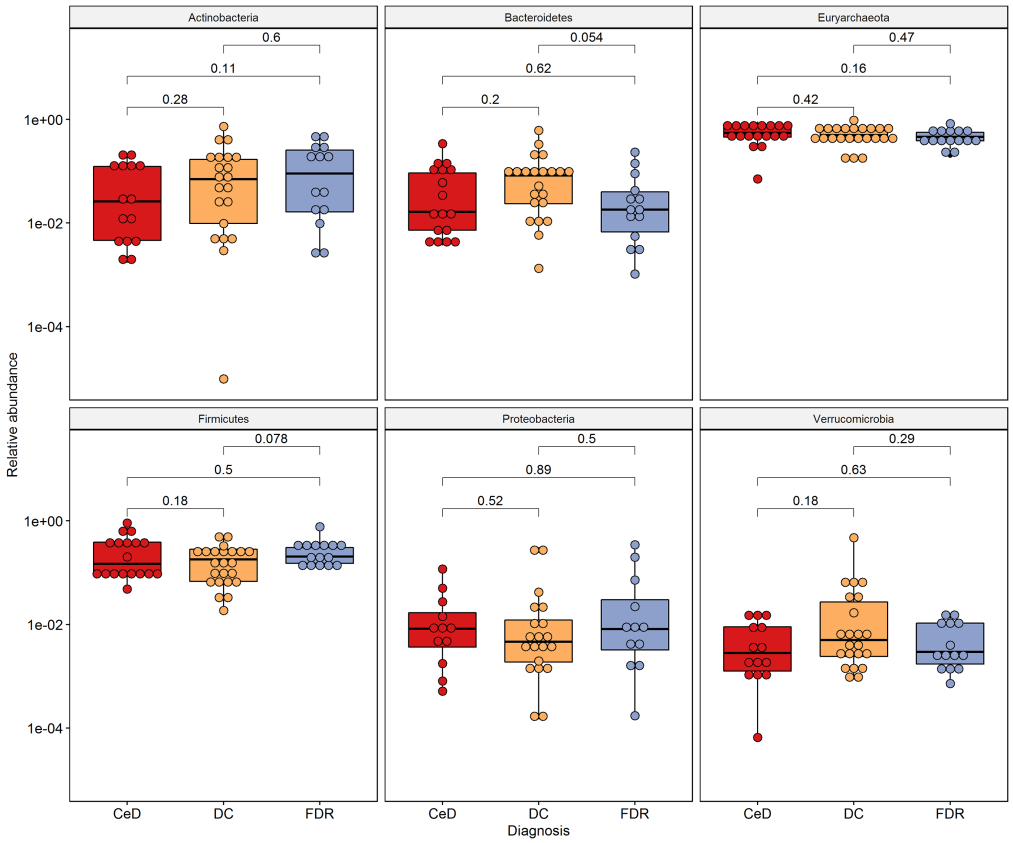

FIGURE 4 | Phylum level distribution of ASVs in fecal microbiota. Pairwise comparisons were done using Wilcoxon tests.

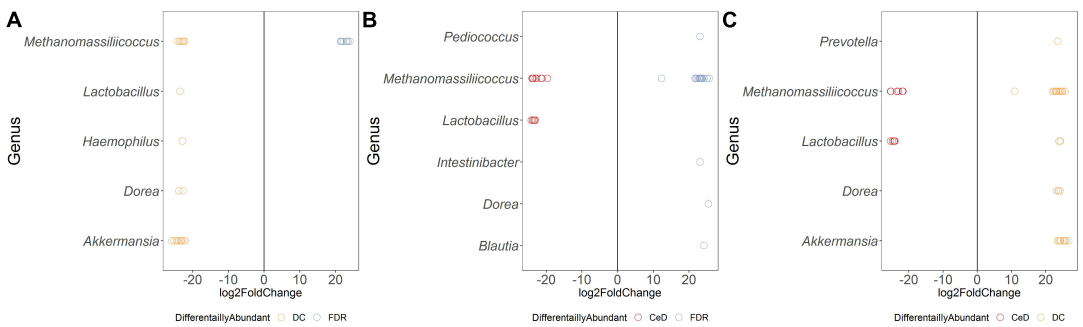

FIGURE 5 | Comparison of differential abundance of microbial ASVs between the diagnosis groups in fecal microbiota. **(A)** Differential abundance DC vs FDR. **(B)** Differential abundance CeD vs FDR. **(C)** Differential abundance CeD vs DC. Only ASVs with significant differences ($P < 0.01$) in average log2 fold change are depicted.

Streptococcus, Bifidobacterium, and *Anaerostipes* are known to possess gluten degrading enzymes, probiotic properties and ability to produce SCFA, respectively (Barrangou et al., 2009; Fernandez-Feo et al., 2013, Couvigny et al., 2015; Morrison and Preston, 2016, Rivière et al., 2016). Moreover, a strain belonging to *Bifidobacterium* was recently reported to prevent gluten-related immunopathology in mice (McCarville et al., 2017). Higher abundances of ASVs belonging to the above-mentioned genera in small intestine of FDRs compared to CeD may indicate their potential protective role in pre-disease state.

In comparison to duodenal biopsies, a smaller number of ASVs were differentially abundant between the diagnosis groups in fecal samples. This indicates more disrupted microbiome at disease site than faecal gut microbiome and highlights the importance of inclusion of biopsy samples in present study. We observed ASV level variation in the both fecal and duodenal microbiota between the diagnosis groups. Previously,

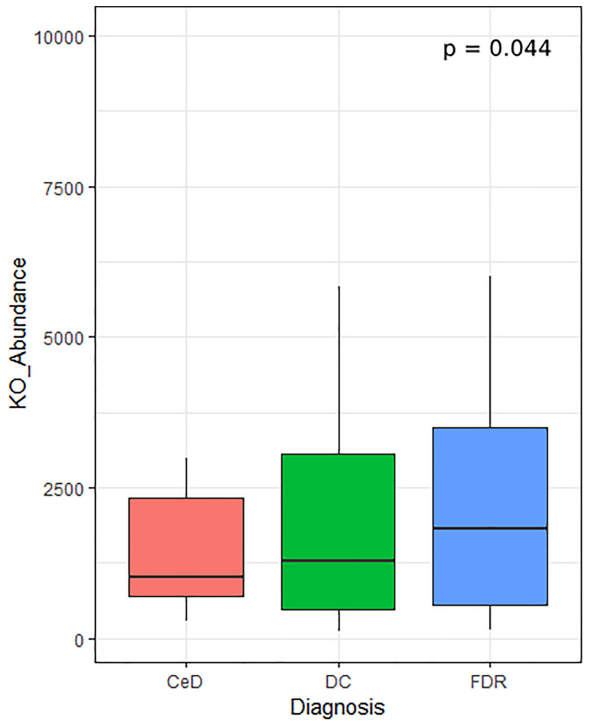

FIGURE 6 | KO abundance for Xaa-pro dipeptidase (K01271) enzyme in feces inferred from predicted metagenome for fecal samples. Comparison was done using ANOVA.

a higher abundance of *Lactobacillus* was observed in the oral microbiome of patients with CeD (Tian et al., 2017). Moreover, there are reports stating that the certain *Lactobacillus* species degrade gliadin and increases the availability of antigenic peptides (Engström et al., 2015). In the present study, higher abundance of different ASVs of *Lactobacillus* in CeD and in FDR microbiota may suggest strain level differences in ability to breakdown gluten into either pro-inflammatory or anti-inflammatory peptides in the small intestine. However, this will require more in-depth characterization of the strain-level variation in functional capabilities of *Lactobacillus* species. Another important observation from differential abundance analysis was the significantly lower abundance of *Barnesiella* in CeD and FDR compared to DC duodenal microbiota and significantly lower abundance of *Akkermansia* in fecal microbiota of both CeD and FDR compared to DC. While *Akkermansia* was highly abundant in CeD microbiota when compared to FDR microbiota. Both of these genera are known to degrade mucus and produce SCFAs which in turn strengthens the health of enterocytes and inhibits intestinal inflammation (Desai et al., 2016; Ravcheev and Thiele, 2017). Therefore, there is a need for more detailed investagion of these bacteria commonly residing in the mucus layer.

Through metagenome prediction method, we found that the gene abundance for Xaa-pro Dipeptidase enzymes was less in CeD as compared to FDR and DC microbiota. This enzyme shows a high specificity for proline residues present in gluten and hydrolyze the peptide bond (Park et al., 2004). These observations suggest that the FDR and CeD fecal microbiota differs in the bacterial composition and that there is a difference in specific bacteria that are capable of gluten degradation. As a consequence, this may impact gluten processing and the presentation of immunogenic gluten epitopes to the immune system. However, the observations of the predicted metagenome have to be validated with *in vitro* enzyme assay.

Overall, we observe differences at ASV level between the FDR and CeD microbiota. We do not observe major differences in community diversity and structure from both alpha diversity and community dissimilarity analysis. The potential species and/or strain level variations and functional aspects identified in this study emphasize the need for well-designed mechanistic follow-up studies using bacteria identified as different between the disease and pre-disease states.

However, metagenomic studies of biopsy samples remain a challenge because of high proportion of host DNA. Thus, predictive metagenomics using 16S rRNA gene as a practical solution was employed for biopsies. In this initial exploratory study, we investigated the gut microbiome with respect to the disease status only and future studies considering other confounding factors such as diet, body mass index age, sex, frequency and quantity of gluten intake among others will be required for a better understanding the gut microbiome in CeD and FDRs. Additionally, the control group in our study was not healthy subjects but patients with functional dyspepsia. These subjects were used as proxy since invasive sampling procedures such as endoscopy from clinically healthy subjects is not permitted under the institutional regulations. Since one of the aims of the present study was to identify similarities and differences between the FDR and CeD microbiota, a control group with a different disease was used as comparison group. This procedure of using a control group with a disease other than the focus of the main study is common practice in epidemiological studies (Coggon et al., 2009). However, this could have also resulted in underestimating the number of ASVs that could be variable between FDR vs DC and CeD vs DC, especially in the CeD group because the proposed disease model for functional dyspepsia includes low-grade duodenal inflammation (Talley et al., 2017). Despite the fact that, *H. pylori* is a recognized causative agent of functional dyspepsia, we observe high abundance of ASVs related to *H. pylori* in CeD and FDR microbiota (Sugano et al., 2015). Therefore, the possible role of *H. pylori* in pathophysiology of CeD requires further investigation. Based on the findings of the present study, it can be hypothesized that the microbiota of FDR represents a potentially balanced, non-inflammatory state as compared to that of microbiota of patients with CeD in genetically pre-disposed subjects. High abundance of known pro-inflammatory bacteria such as those related to *Helicobacter* could have a critical role in the pathogenesis of CeD. In addition, expansion of specific species or strains of gluten degrading bacteria which breakdown gluten into pro-inflammatory peptides may have a pivotal role in the pathogenesis of CeD. Exposure to drugs (e.g., proton pump inhibitors) and antibiotics have been hypothesized to select

particular strains of bacteria in humans (Domínguez-Bello et al., 2008). A long-term follow-up of FDRs of patients with CeD will be crucial to identify triggers such as dietary changes, lifestyle changes, medications, specifically antibiotics that could affect the microbiota homeostasis in them and factors that lead to transition toward a pro-inflammatory microbiota from a non-inflammatory microbiota.

CONCLUSION

Significant differences at ASV level suggest that specific bacteria like *Helicobacter* may be important for pathogenesis of CeD. Higher abundance of potentially beneficial bacterial ASVs especially those belonging to SCFA producing genera in FDRs suggest that there may be a protective role of these in CeD development. Moreover, the predicted differences in gluten metabolism potential by FDR and CeD microbiota point toward the need for investigating functional capabilities of specific bacteria in healthy FDR and CeD patients.

DATA AVAILABILITY

Sequence data generated in this study is available from the NCBI Sequence Read Archive within the Bioproject ID accession PRJNA385740 (https://www.ncbi.nlm.nih.gov/bioproject/?term~=~PRJNA385740) and to reproduce the analysis done in R, the R Markdown file and required data are available at https://github.com/rahulnccs/Comparison-of-Small-Gut-and-Whole-Gut-Microbiota-of-First-Degree-Relatives-with-Adult-Celiac-Disease.

AUTHOR CONTRIBUTIONS

GM, YS, and VA conceived, designed, and supervised the study. GM recruited the patients, and performed the diagnosis and endoscopic examination. GK performed the HLA test. AV, KB, and AM were responsible for storage and maintenance of the collected biological samples (duodenal biopsy/stool). RB and PP extracted the genomic DNA. DB, BS, and RP were involved in amplicon sequencing. SS, DD, and RB performed the bioinformatics analysis for amplicon data. SS, RB, DD and GM acquired and interpreted the data, and drafted the manuscript. YS, DD, and VA critically reviewed the manuscript. All authors have read and approved the final manuscript.

FUNDING

We acknowledge the support of the Food and Nutrition Division of Department of Biotechnology, Government of India who provided the research grant for this study (Sanction No. BT/PR-14956/FNS/20/497/2010).

ACKNOWLEDGMENTS

We acknowledge the help of Aishwairya Sharma, a dietician, who counseled the patients for gluten free diet. We are grateful to Dr. Nachiket Marathe for fruitful discussion related to the project. We thank Johanna Gutleben for proofreading the manuscript. We would like to acknowledge the effort made by the reviewers during the peer review process and for assisting us to improve the overall quality of data presented in this study. We sincerely acknowledge the support of each participant of this study who accepted to participate in this study.

SUPPLEMENTARY MATERIAL

The Supplementary Material for this article can be found online at: https://www.frontiersin.org/articles/10.3389/fmicb.2019.00164/full#supplementary-material

FIGURE S1 | (A) Principal coordinates analysis (PCoA) of the fecal and duodenal microbiota based on Bray–Curtis distance. **(B)** Comparison of alpha diversity measures between sampling sites.

FIGURE S2 | Order level distribution of ASVs in duodenal microbiota. Pairwise comparisons were done using Wilcoxon tests.

FIGURE S3 | Order level distribution of ASVs in fecal microbiota. Pairwise comparisons were done using Wilcoxon tests.

TABLE S1 | Significantly different KEGG orthologies (KO) between diagnosis groups in fecal microbiota. Analyzed using the STAMP statistical tool, ANOVA with *post hoc* Tukey–kramer test was used to identify statistically different KEGG orthologies between diagnosis groups.

TABLE S2 | Significantly different KEGG orthologies (KO) between diagnosis groups in duodenal microbiota. Analyzed using the STAMP statistical tool, ANOVA with *post hoc* Tukey–kramer test was used to identify statistically different KEGG orthologies between diagnosis groups.

TABLE S3 | Details of the study subjects including disease status, Marsh values, age, gender, and tTg titre.

TABLE S4 | Number of sequencing reads per sample at each stage of data analysis is given below.

INFORMATION | Differential Abundance of Amplicon Sequence Variants of *Helicobacter.* Multiple sequence alignment was performed by CLUSTAL 2.0.11.

REFERENCES

Barrangou, R., Briczinski, E. P., Traeger, L. L., Loquasto, J. R., Richards, M., Horvath, P., et al. (2009). Comparison of the complete genome sequences of *Bifidobacterium animalis* subsp. lactis DSM 10140 and Bl-04. *J. Bacteriol.* 191, 4144–4151. doi: 10.1128/JB.00155-09

Bouziat, R., Hinterleitner, R., Brown, J. J., Stencel-Baerenwald, J. E., Ikizler, M., Mayassi, T., et al. (2017). Reovirus infection triggers inflammatory responses to dietary antigens and development of celiac disease. *Science* 356, 44–50. doi: 10.1126/science.aah5298

Callahan, B. J., McMurdie, P. J., Rosen, M. J., Han, A. W., Johnson, A. J. A., and Holmes, S. P. (2016). DADA2: high-resolution sample inference from Illumina amplicon data. *Nat. Methods* 13:581. doi: 10.1038/nmeth.3869

Caminero, A., Nistal, E., Herrán, A. R., Pérez-Andrés, J., Ferrero, M. A., Ayala, L. V., et al. (2015). Differences in gluten metabolism among healthy volunteers, coeliac disease patients and first-degree relatives. *Br. J. Nutr.* 114, 1157–1167. doi: 10.1017/S0007114515002767

Coggon, D., Barker, D., and Rose, G. (2009). *Epidemiology for the Uninitiated*. Hoboken, NJ: John Wiley & Sons.

Couvigny, B., De Wouters, T., Kaci, G., Jacouton, E., Delorme, C., Doré, J., et al. (2015). Commensal *Streptococcus salivarius* modulates PPARγ transcriptional activity in human intestinal epithelial cells. *PLoS One* 10:e0125371. doi: 10.1371/journal.pone.0125371

Davis, N. M., Proctor, D. M., Holmes, S. P., Relman, D. A., and Callahan, B. J. (2018). Simple statistical identification and removal of contaminant sequences in marker-gene and metagenomics data. *Microbiome* 6:226. doi: 10.1186/s40168-018-0605-2

de Sousa Moraes, L. F., Grzeskowiak, L. M., de Sales Teixeira, T. F., and Peluzio, M. D. C. G. (2014). Intestinal microbiota and probiotics in celiac disease. *Clin. Microbiol. Rev.* 27, 482–489. doi: 10.1128/CMR.00106-13

Desai, M. S., Seekatz, A. M., Koropatkin, N. M., Kamada, N., Hickey, C. A., Wolter, M., et al. (2016). A dietary fiber-deprived gut microbiota degrades the colonic mucus barrier and enhances pathogen susceptibility. *Cell* 167, 1339.e21–1353.e21. doi: 10.1016/j.cell.2016.10.043

Domínguez-Bello, M. G., Pérez, M. E., Bortolini, M. C., Salzano, F. M., Pericchi, L. R., Zambrano-Guzman, O., et al. (2008). Amerindian *Helicobacter pylori* strains go extinct, as European strains expand their host range. *PLoS One* 3:e3307. doi: 10.1371/journal.pone.0003307

Dridi, B., Fardeau, M.-L., Ollivier, B., Raoult, D., and Drancourt, M. (2012). *Methanomassiliicoccus luminyensis* gen. nov., sp. nov., a methanogenic archaeon isolated from human faeces. *Int. J. Syst. Evol. Microbiol.* 62, 1902–1907. doi: 10.1099/ijs.0.033712-0

Engström, N., Sandberg, A.-S., and Scheers, N. (2015). Sourdough fermentation of wheat flour does not prevent the interaction of transglutaminase 2 with α2-gliadin or gluten. *Nutrients* 7, 2134–2144. doi: 10.3390/nu7042134

Fernandez-Feo, M., Wei, G., Blumenkranz, G., Dewhirst, F. E., Schuppan, D., Oppenheim, F. G., et al. (2013). The cultivable human oral gluten-degrading microbiome and its potential implications in coeliac disease and gluten sensitivity. *Clin. Microbiol. Infect* 19, E386–E394. doi: 10.1111/1469-0691.12249

Gorlas, A., Robert, C., Gimenez, G., Drancourt, M., and Raoult, D. (2012). Complete genome sequence of *Methanomassiliicoccus luminyensis*, the largest genome of a human-associated Archaea species. *J. Bacteriol.* 194, 4745–4745. doi: 10.1128/JB.00956-12

Iwai, S., Weinmaier, T., Schmidt, B. L., Albertson, D. G., Poloso, N. J., Dabbagh, K., et al. (2016). Piphillin: improved prediction of metagenomic content by direct inference from human microbiomes. *PLoS One* 11:e0166104. doi: 10.1371/journal.pone.0166104

Jabri, B., and Sollid, L. M. (2006). Mechanisms of disease: immunopathogenesis of celiac disease. *Nat. Rev. Gastroenterol. Hepatol.* 3:516. doi: 10.1038/ncpgasthep0582

Kagnoff, M. F. (2007). Celiac disease: pathogenesis of a model immunogenetic disease. *J. Clin. Invest.* 117, 41–49. doi: 10.1172/JCI30253

Larkin, M. A., Blackshields, G., Brown, N., Chenna, R., McGettigan, P. A., McWilliam, H., et al. (2007). Clustal W and Clustal X version 2.0. *Bioinformatics* 23, 2947–2948. doi: 10.1093/bioinformatics/btm404

Lebwohl, B., Blaser, M. J., Ludvigsson, J. F., Green, P. H., Rundle, A., Sonnenberg, A., et al. (2013). Decreased risk of celiac disease in patients with *Helicobacter pylori* colonization. *Am. J. Epidemiol.* 178, 1721–1730. doi: 10.1093/aje/kwt234

Lohi, S., Mustalahti, K., Kaukinen, K., Laurila, K., Collin, P., Rissanen, H., et al. (2007). Increasing prevalence of coeliac disease over time. *Aliment. Pharmacol. Ther.* 26, 1217–1225. doi: 10.1111/j.1365-2036.2007.03502.x

Lorenzo Pisarello, M. J., Vintiñi, E. O., González, S. N., Pagani, F., and Medina, M. S. (2014). Decrease in lactobacilli in the intestinal microbiota of celiac children with a gluten-free diet, and selection of potentially probiotic strains. *Can. J. Microbiol.* 61, 32–37. doi: 10.1139/cjm-2014-0472

Love, M. I., Huber, W., and Anders, S. (2014). Moderated estimation of fold change and dispersion for RNA-seq data with DESeq2. *Genome Biol.* 15:550. doi: 10.1186/s13059-014-0550-8

Makharia, G. K., Verma, A. K., Amarchand, R., Bhatnagar, S., Das, P., Goswami, A., et al. (2011). Prevalence of celiac disease in the northern part of India: a community based study. *J. Gastroenterol. Hepatol.* 26, 894–900. doi: 10.1111/j.1440-1746.2010.06606.x

Mårild, K., Ye, W., Lebwohl, B., Green, P. H., Blaser, M. J., Card, T., et al. (2013). Antibiotic exposure and the development of coeliac disease: a nationwide case–control study. *BMC Gastroenterol.* 13:109. doi: 10.1186/1471-230X-13-109

Martin, M. (2011). Cutadapt removes adapter sequences from high-throughput sequencing reads. *EMBnet J.* 17, 10–12. doi: 10.14806/ej.17.1.200

McCarville, J., Dong, J., Caminero, A., Bermudez-Brito, M., Jury, J., Murray, J., et al. (2017). A commensal *Bifidobacterium longum* strain improves gluten-related immunopathology in mice through expression of a serine protease inhibitor. *Appl. Environ. Microbiol.* doi: 10.1128/AEM.01323-17 [Epub ahead of print].

McMurdie, P. J., and Holmes, S. (2013). phyloseq: an R package for reproducible interactive analysis and graphics of microbiome census data. *PLoS One* 8:e61217. doi: 10.1371/journal.pone.0061217

Morrison, D. J., and Preston, T. (2016). Formation of short chain fatty acids by the gut microbiota and their impact on human metabolism. *Gut Microbes* 7, 189–200. doi: 10.1080/19490976.2015.1134082

Myléus, A., Ivarsson, A., Webb, C., Danielsson, L., Hernell, O., Högberg, L., et al. (2009). Celiac disease revealed in 3% of Swedish 12-year-olds born during an epidemic. *J. Pediatr. Gastroenterol. Nutr.* 49, 170–176. doi: 10.1097/MPG.0b013e31818c52cc

Nakatsu, G., Li, X., Zhou, H., Sheng, J., Wong, S. H., Wu, W. K. K., et al. (2015). Gut mucosal microbiome across stages of colorectal carcinogenesis. *Nat. Commun.* 6:8727. doi: 10.1038/ncomms9727

Oksanen, J., Blanchet, F. G., Kindt, R., Legendre, P., Minchin, P. R., O'hara, R. B., et al. (2011). *vegan: Community Ecology Package. R Package Version 117–118*.

Olivares, M., Walker, A. W., Capilla, A., Benítez-Páez, A., Palau, F., Parkhill, J., et al. (2018). Gut microbiota trajectory in early life may predict development of celiac disease. *Microbiome* 6:36. doi: 10.1186/s40168-018-0415-6

Orlando, A., Linsalata, M., Notarnicola, M., Tutino, V., and Russo, F. (2014). Lactobacillus GG restoration of the gliadin induced epithelial barrier disruption: the role of cellular polyamines. *BMC Microbiol.* 14:19. doi: 10.1186/1471-2180-14-19

Park, M.-S., Hill, C. M., Li, Y., Hardy, R. K., Khanna, H., Khang, Y.-H., et al. (2004). Catalytic properties of the PepQ prolidase from *Escherichia coli*. *Arch. Biochem. Biophys.* 429, 224–230. doi: 10.1016/j.abb.2004.06.022

Parks, D. H., Tyson, G. W., Hugenholtz, P., and Beiko, R. G. (2014). STAMP: statistical analysis of taxonomic and functional profiles. *Bioinformatics* 30, 3123–3124. doi: 10.1093/bioinformatics/btu494

Parte, A. C. (2013). LPSN—list of prokaryotic names with standing in nomenclature. *Nucleic Acids Res.* 42, D613–D616. doi: 10.1093/nar/gkt1111

Png, C. W., Lindén, S. K., Gilshenan, K. S., Zoetendal, E. G., McSweeney, C. S., Sly, L. I., et al. (2010). Mucolytic bacteria with increased prevalence in IBD mucosa augment in vitro utilization of mucin by other bacteria. *Am. J. Gastroenterol.* 105, 2420–2428. doi: 10.1038/ajg.2010.281

Qiu, Z., Yang, H., Rong, L., Ding, W., Chen, J., and Zhong, L. (2017). Targeted metagenome based analyses show gut microbial diversity of inflammatory bowel disease patients. *Indian J. Microbiol.* 57, 307–315. doi: 10.1007/s12088-017-0652-6

Ravcheev, D. A., and Thiele, I. (2017). Comparative genomic analysis of the human gut microbiome reveals a broad distribution of metabolic pathways for the degradation of host-synthetized mucin glycans and utilization of mucin-derived monosaccharides. *Front. Genet.* 8:111. doi: 10.3389/fgene.2017.00111

Rintala, A., Riikonen, I., Toivonen, A., Pietilä, S., Munukka, E., Pursiheimo, J.-P., et al. (2018). Early fecal microbiota composition in children who later develop celiac disease and associated autoimmunity. *Scand. J. Gastroenterol.* 53, 403–409. doi: 10.1080/00365521.2018.1444788

Ritari, J., Salojärvi, J., Lahti, L., and de Vos, W. M. (2015). Improved taxonomic assignment of human intestinal 16S rRNA sequences by a dedicated reference database. *BMC Genomics* 16:1056. doi: 10.1186/s12864-015-2265-y

Rivière, A., Selak, M., Lantin, D., Leroy, F., and De Vuyst, L. (2016). Bifidobacteria and butyrate-producing colon bacteria: importance and strategies for their stimulation in the human gut. *Front. Microbiol.* 7:979. doi: 10.3389/fmicb.2016.00979

Sánchez, E., Laparra, J., and Sanz, Y. (2012). Discerning the role of *Bacteroides fragilis* in celiac disease pathogenesis. *Appl. Environ. Microbiol.* 78, 6507–6515. doi: 10.1128/AEM.00563-12

Sanz, Y., Palma, G. D., and Laparra, M. (2011). Unraveling the ties between celiac disease and intestinal microbiota. *Int. Rev. Immunol.* 30, 207–218. doi: 10.3109/08830185.2011.599084

Schneeberger, M., Everard, A., Gómez-Valadés, A. G., Matamoros, S., Ramírez, S., Delzenne, N. M., et al. (2015). *Akkermansia muciniphila* inversely correlates with the onset of inflammation, altered adipose tissue metabolism and metabolic disorders during obesity in mice. *Sci. Rep.* 5:16643. doi: 10.1038/srep16643

Shetty, S. A., Hugenholtz, F., Lahti, L., Smidt, H., and de Vos, W. M. (2017). Intestinal microbiome landscaping: insight in community assemblage and implications for microbial modulation strategies. *FEMS Microbiol. Rev.* 41, 182–199. doi: 10.1093/femsre/fuw045

Singh, P., Arora, A., Strand, T. A., Leffler, D. A., Catassi, C., Green, P. H., et al. (2018). Global prevalence of celiac disease: systematic review and meta-analysis. *Clin. Gastroenterol. Hepatol.* 16, 823.e2–836.e2. doi: 10.1016/j.cgh.2017.06.037

Singh, P., Arora, S., Lal, S., Strand, T. A., and Makharia, G. K. (2015). Risk of celiac disease in the first-and second-degree relatives of patients with celiac disease: a systematic review and meta-analysis. *Am. J. Gastroenterol.* 110:1539. doi: 10.1038/ajg.2015.296

Sugano, K., Tack, J., Kuipers, E. J., Graham, D. Y., El-Omar, E. M., Miura, S., et al. (2015). Kyoto global consensus report on *Helicobacter pylori* gastritis. *Gut* 64, 1353–1367. doi: 10.1136/gutjnl-2015-309252

Talley, N. J., Goodsall, T., and Potter, M. (2017). Functional dyspepsia. *Austr. Prescr.* 40:209. doi: 10.18773/austprescr.2017.066

Tian, N., Faller, L., Leffler, D. A., Kelly, C. P., Hansen, J., Bosch, J. A., et al. (2017). Salivary gluten degradation and oral microbial profiles in health and celiac disease. *Appl. Environ. Microbiol.* 83:3330-16. doi: 10.1128/AEM.03330-16

Tjellström, B., Stenhammar, L., Högberg, L., Fälth-Magnusson, K., Magnusson, K.-E., Midtvedt, T., et al. (2007). Gut microflora associated characteristics in first-degree relatives of children with celiac disease. *Scand. J. Gastroenterol.* 42, 1204–1208. doi: 10.1080/00365520701320687

Van De Wal, Y., Kooy, Y. M., Van Veelen, P. A., Peña, S. A., Mearin, L. M., Molberg, Ø., et al. (1998). Small intestinal T cells of celiac disease patients recognize a natural pepsin fragment of gliadin. *Proc. Natl. Acad. Sci.* 95, 10050–10054. doi: 10.1073/pnas.95.17.10050

Verdu, E. F., Galipeau, H. J., and Jabri, B. (2015). Novel players in coeliac disease pathogenesis: role of the gut microbiota. *Nat. Rev. Gastroenterol. Hepatol.* 12:497. doi: 10.1038/nrgastro.2015.90

Villanacci, V., Bassotti, G., Liserre, B., Lanzini, A., Lanzarotto, F., and Genta, R. M. (2006). *Helicobacter pylori* infection in patients with celiac disease. *Am. J. Gastroenterol.* 101:1880.

Volta, U., and De Giorgio, R. (2012). New understanding of gluten sensitivity. *Nat. Rev. Gastroenterol. Hepatol.* 9:295. doi: 10.1038/nrgastro.2012.15

Walters, W., Hyde, E. R., Berg-Lyons, D., Ackermann, G., Humphrey, G., Parada, A., et al. (2016). Improved bacterial 16S rRNA gene (V4 and V4-5) and fungal internal transcribed spacer marker gene primers for microbial community surveys. *mSystems* 1:e00009-15. doi: 10.1128/mSystems.00009-15

Wickham, H. (2011). "ggplot2," in *Wiley Interdisciplinary Reviews: Computational Statistics*, Vol. 3, eds J. E. Gentle and D. W. Scott (Hoboken, NJ: Wiley), 180–185. doi: 10.1002/wics.147

Wickham, H. (2017). *Tidyverse: Easily Install and Load'tidyverse'packages. R Package Version 1*.

Woo, P. C.-Y., Fung, A. M.-Y., Lau, S. K.-P., Chan, B. Y.-L., Chiu, S.-K., Teng, J. L.-L., et al. (2003). *Granulicatella adiacens* and *Abiotrophia defectiva* bacteraemia characterized by 16S rRNA gene sequencing. *J. Med. Microbiol.* 52, 137–140. doi: 10.1099/jmm.0.04950-0

Ze, X., Duncan, S. H., Louis, P., and Flint, H. J. (2012). *Ruminococcus bromii* is a keystone species for the degradation of resistant starch in the human colon. *ISME J.* 6:1535. doi: 10.1038/ismej.2012.4

Zeng, M., Inohara, N., and Nuñez, G. (2017). Mechanisms of inflammation-driven bacterial dysbiosis in the gut. *Mucosal Immunol.* 10:18. doi: 10.1038/mi.2016.75

Conflict of Interest Statement: DB, BS, and RP were employed by company AgriGenome Labs Pvt Ltd. Kerala, India.

The remaining authors declare that the research was conducted in the absence of any commercial or financial relationships that could be construed as a potential conflict of interest.

Copyright © 2019 Bodkhe, Shetty, Dhotre, Verma, Bhatia, Mishra, Kaur, Pande, Bangarusamy, Santosh, Perumal, Ahuja, Shouche and Makharia. This is an open-access article distributed under the terms of the Creative Commons Attribution License (CC BY). The use, distribution or reproduction in other forums is permitted, provided the original author(s) and the copyright owner(s) are credited and that the original publication in this journal is cited, in accordance with accepted academic practice. No use, distribution or reproduction is permitted which does not comply with these terms.

frontiers in Microbiology

ORIGINAL RESEARCH
published: 14 February 2019
doi: 10.3389/fmicb.2019.00193

Comparison of the Vaginal Microbiomes of Premenopausal and Postmenopausal Women

*Karol Gliniewicz[1,2], G. Maria Schneider[1,2], Benjamin J. Ridenhour[1], Christopher J. Williams[3], Yuli Song[4], Miranda A. Farage[4], Kenneth Miller[4] and Larry J. Forney[1,2]**

[1] Department of Biological Sciences, University of Idaho, Moscow, ID, United States, [2] Institute for Bioinformatics and Evolutionary Studies, University of Idaho, Moscow, ID, United States, [3] Department of Statistical Science, University of Idaho, Moscow, ID, United States, [4] The Procter and Gamble Company, Cincinnati, OH, United States

For decades hormone therapy (HT) has been prescribed to treat the symptoms of menopause, such as vaginal dryness, itching and burning. Here we sought to compare the vaginal microbiomes of postmenopausal women who received low dose estrogen therapy to those of premenopausal and postmenopausal women, and to do so in conjunction with assessing the alleviation of symptoms associated with vaginal atrophy. In this study vaginal swab samples were obtained from 45 women who were classified as either premenopausal, postmenopausal, or postmenopausal and undergoing HT. The vaginal microbiomes of these women were characterized by *16S rRNA* gene sequencing and bacterial abundances were quantified by qPCR. We found that the vaginal communities from our cohort could be divided into six clusters (A-F) based on differences in the composition and relative abundances of bacterial taxa. Communities in cluster A were dominated by *Lactobacillus crispatus*, and those of cluster B were dominated by *Gardnerella vaginalis*. Communities in cluster C had high proportions of *L. iners,* while those in cluster D were more even and included several co-dominant taxa. Communities in clusters E and F were dominated by *Bifidobacterium* and *L. gasseri*, respectively. The vaginal communities of most postmenopausal women receiving HT (10/15) were dominated by species of lactobacilli and belonged to clusters A, C, and F ($P < 0.001$). This sharply contrasts with vaginal communities of postmenopausal women without HT, most of which (10/15) were in cluster D, depleted of lactobacilli, and had about 10-fold fewer total bacteria ($P < 0.05$). The vaginal communities of women in each study group differed in terms of the dominant bacterial species composition and relative abundance. Those of postmenopausal women receiving HT significantly differed from those of postmenopausal women without HT and were most often dominated by species of *Lactobacillus*. Noteworthy, HT greatly improved vaginal atrophy scores, decreased vaginal pH, and significantly increased bacterial numbers in comparison to postmenopausal women not receiving HT.

Keywords: menopause, vaginal microbiome, vaginal atrophy, hormone replacement therapy, microbial community structure and function, premenopause

OPEN ACCESS

Edited by:
Ana E. Escalante, National Autonomous University of Mexico, Mexico

Reviewed by:
Catherine Putonti, Loyola University Chicago, United States
German Bonilla Rosso, Université de Lausanne, Switzerland

***Correspondence:**
Larry J. Forney
lforney@uidaho.edu

Specialty section:
This article was submitted to Microbial Symbioses, a section of the journal Frontiers in Microbiology

Received: *24 May 2018*
Accepted: *23 January 2019*
Published: *14 February 2019*

Citation:
Gliniewicz K, Schneider GM, Ridenhour BJ, Williams CJ, Song Y, Farage MA, Miller K and Forney LJ (2019) Comparison of the Vaginal Microbiomes of Premenopausal and Postmenopausal Women. Front. Microbiol. 10:193. doi: 10.3389/fmicb.2019.00193

INTRODUCTION

Menopause usually occurs in the fourth or fifth decade of life and is defined as cessation of menstruation for 12 consecutive months marking the end of fertility. Decreased ovary function during menopause results in lower levels of circulating estrogen, which often leads to various symptoms such as hot flashes, night sweats, decreased cognitive functions and mood changes that are experienced by women during the years immediately preceding and during menopause (Takahashi and Johnson, 2015). Additionally, genitourinary tract changes associated with vulvovaginal atrophy (VVA) are common and affect at least 50% of menopausal women (Santoro and Komi, 2009; Nappi and Kokot-Kierepa, 2010, 2012; Simon et al., 2013; Minkin et al., 2014). The most common signs of VVA include dryness, redness, itching, and dyspareunia, with occasional discharge and/or bleeding (Bachmann and Nevadunsky, 2000). For decades, both systemic and local low-dose estrogen therapy have been widely used for management of VVA and vaginal dryness in postmenopausal women (Raymundo et al., 2004; Bachmann et al., 2008; Pinkerton et al., 2009).

Changes in the vaginal environment during menopause are accompanied by changes in the species composition of the vaginal microbiome (Hillier and Lau, 1997; Brotman et al., 2014; Shen et al., 2016). Often this is manifest in decreased proportions of lactobacilli and lactic acid production, causing an increased vaginal pH that possibly renders the vagina more susceptible to infections and exacerbates the vaginal symptoms associated with VVA. Very few studies have been done to compare the vaginal microbiomes of postmenopausal women who receive HT and those that do not (Yoshimura and Okamura, 2001; Heinemann and Reid, 2005; Shen et al., 2016; Mitchell et al., 2017). Findings show that the communities of women who receive HT often resemble those of premenopausal women by essentially restoring high proportions of *Lactobacillus*, but the means by which this occurs is not understood (Mitchell et al., 2017). In this cross-sectional pilot study, we explicitly compared the vaginal microbiomes of premenopausal women to those of postmenopausal women who receive various forms of HT and those that do not. In addition, we determined bacterial abundance, estimated the species richness and evenness of vaginal communities, and measured various biomarkers of inflammation in the vulvo-vaginal area.

MATERIALS AND METHODS

Subject Data and Sample Collection

Healthy adult women enrolled in the study comprised three groups of 15 females each (**Supplementary Table S1** contains detailed demographic data) that were prescreened based on their vaginal pH and vaginal atrophy score as previously described by Farage and coworkers (Farage et al., 2015). Subject recruitment and sample collection were conducted at an independent facility (Radiant Research, Cincinnati, OH). Testing was conducted in compliance with the Good Clinical Practice Regulations [21 Code of Federal Regulations (CFR 50)] and in accordance with the Declaration of Helsinki (WMA Declaration of Helsinki, 2013). Test protocols were approved by the clinical facility's Institutional Review Board. Subjects were healthy adult female volunteers, 23–67 years of age, who had signed an informed consent. Subjects were excluded from participation if they had had a partial or full hysterectomy, irregular menstrual cycle, skin abnormalities in the vulvar area, diabetes, kidney, heart or circulatory disease, were currently pregnant or breast-feeding, took certain immunosuppressive or anti-inflammatory medications that might interfere with test results, or if they were participating in another clinical study.

To obtain vaginal samples subjects were placed in the dorsolithotomy position, and medically trained personnel used COPAN ESwab^{TM} (COPAN Diagnostics Inc.) to obtain samples from the vaginal wall approximately 2 inches into the vagina. Afterward, the swab was placed in a cryogenic tube and stored in a −80°C freezer until they were shipped on dry ice to the laboratory for further analysis.

Microbial Community Analysis

We transferred 250 μL of each sample to bead beating tubes and added 100 μL of lytic enzyme cocktail (50 μL lysozyme 500 kU/mL, 6 μL mutanolysin 25 kU/mL, 4 μL lysostaphin 3000 kU/mL, and 41 μL mixture of 10 mM Tris–HCl and 50 mM EDTA pH 8.0). These mixtures were incubated at 37 °C for 1 h in a dry heat block. Next, 750 mg of zirconia–silica beads (0.1 mm diameter) were added to all samples, and the tubes were placed in Mini-BeadBeater-96 at room temperature for 1 min at 2100 rpm. Once completed, bead beating was followed by a brief centrifugation. Isolation of bacterial genomic DNA was performed with a QIAamp DNA Mini kit (Qiagen Inc., Valencia, CA, United States) according to the manufacturer's protocol. DNA concentrations were quantified with a QuantiFluor dsDNA kit (Promega Inc., Madison, WI, United States) using a Turner TBS-380 mini-fluorometer (Turner BioSystems, United States). DNA size and integrity were verified using an Agilent DNA 1000 kit and an Agilent Bioanalyzer 2100 (Agilent, Santa Barbara, CA, United States) using the manufacturer's protocol.

The V1–V3 region of bacterial *16S rRNA* genes (*Escherichia coli* positions 27F-534R) was amplified using a mixture of degenerate primers that flanked the variable regions (**Supplementary Table S2**). Amplicons were produced by two consecutive rounds of PCR. The first round of PCR amplified the targeted V1–V3 region of the *16S rRNA* gene, while the second round of PCR attached the sample barcode and sequencing adapters. The concentrations of amplicons were determined using a Pico Green assay (Promega Inc.) and a SpectraMax Gemini XPS fluorometer (Molecular Devices, Sunnyvale, CA, United States), then equal amounts (∼100 ng) were pooled in a single tube. The amplicon pool was cleaned to remove short undesirable fragments using the following procedure. First the pool was size selected with using AMPure beads (Beckman Coulter Inc., Pasadena, CA, United States), the product was then run on a 1% gel, excised from the gel, column purified using a Qiagen MinElute PCR purification kit

and size selected again with AMPure beads (Beckman Coulter, Indianapolis, IN, United States). To determine the quality of the amplicons, the pool was PCR amplified with Illumina adaptor specific primers followed by size selection using a DNA1000 chip and an Agilent 2100 Bioanalyzer. The cleaned amplicon pool was then quantified using the KAPA Illumina library quantification kit (KAPA Biosciences) and the Applied Biosystems StepOne plus real-time PCR system. Finally, sequences were obtained using an Illumina MiSeq paired-end 300 bp protocol (Illumina, Inc., San Diego, CA, United States).

Raw DNA sequence reads from the Illumina MiSeq were assigned to samples, demultiplexed and classified in the following manner. The custom python application dbcAmplicons[1] was used to assign reads to samples based on both expected barcode and primer sequences. Sequencing was performed in the IBEST Genomic Resources Core at the University of Idaho. Barcodes could have at most 1 mismatch (Hamming distance) and primers could have at most 4 mismatches (Levenshtein distance) provided the final 4 bases of the primer matched the target sequence perfectly. Sequence reads were then trimmed of their primer sequence and merged into a single amplicon sequence using the application FLASH (Magoč and Salzberg, 2011). Finally, the RDP Bayesian classifier was used to assign sequences to phylotypes (Wang et al., 2007). Reads were assigned to the first RDP taxonomic level with a bootstrap score ≥50. Reads categorized as belonging to the genus *Lactobacillus* were subsequently analyzed to identify which species of this genus were present in the samples. Blastn was used in BLAST+ (Camacho et al., 2009) to compare each read to a database composed of *16S rRNA* gene sequences longer than 1000 bp belonging to the genus *Lactobacillus* (downloaded from NCBI in February 2014). The identity of the different bacterial species reported as the best match for each read was recorded, the number of reads assigned to each of the taxa counted, and their relative abundance in the different samples calculated. These data were cleaned to include only samples with ≥3,000 reads and those taxa that occurred with a relative abundance of at least 0.01 (1%). All less abundant taxa (below 0.01) were aggregated into the category 'Other.' Cleaned data included the relative abundances of 51 OTUs for all 45 test subjects. A species was considered dominant in a given sample or sample cluster, if it reached at least 51% relative abundance.

Quantifying *16S rRNA* Gene Copy Number

We used a broad-coverage *16S qPCR* assay developed by Liu and coworkers (Liu et al., 2012) to quantify the bacteria in samples. DNA yields from samples were quantified fluorometrically and 0.2 ng of template DNA was added to each 10 μl reaction containing 1.8 μM forward and reverse primer, 225 nM TaqMan® probe, 1× Platinum Quantitative PCR SuperMix-UDG w/ROX (Invitrogen™) and molecular grade water. Each assay included a series of standards and a negative control (no DNA template). All assays were done in triplicate. Cycling parameters were: 3 min at 50°C for treatment with uracil-N glycosylase (UNG), 10 min at 95°C for *Taq* activation, 15 s at 95°C (denaturation), 1 min 60°C (annealing) and extension for 40 cycles. PCR amplification and real-time detection of fluorescence were performed using ABI 7900HT Real Time PCR system with StepOne Plus software (Applied Biosystems™).

Statistical Analysis and Data Visualization

We visualized the vaginal microbiomes of the subjects using a clustering analysis and a principle coordinates analysis. Both analyses required calculation of dissimilarity between individual samples. Dissimilarity was calculated using the mean absolute difference between samples, $\frac{1}{n}\sum i\left|x_i - y_i\right|$ where n is the number non-zero OTUs in the samples x and y and x_i and y_i are the relative abundances of the i-th OTU in those samples (Anderson et al., 2006). Principle coordinates analysis (Gower, 1966) was performed using a correction factor (Cailliez, 1983; Legendre and Legendre, 1998). To create a dendrogram, complete-linkage clustering was used to perform hierarchical agglomeration of samples (Legendre and Legendre, 1998). The number of clusters within the data was determined by maximizing the silhouette width (a measure of similarity within clusters) with respect to the number of clusters (Rousseeuw, 1987).

Using the clusters detected, we examined the relationship between cluster and treatment as well as cluster and measured traits. A contingency Chi-squared was calculated to test whether or not study groups were evenly distributed among the six clusters. To test for difference among clusters for measured traits (e.g., pH, histamine concentrations), we used one-way ANOVA with log-transformed dependent variables and the assigned cluster as the explanatory variable (vaginal atrophy scores were not log-transformed). Log-transformation was used to ensure the assumption of i.i.d. errors was met in our statistical models. *Post hoc* linear contrasts to compare trait means of clusters using Tukey's range test (Tukey, 1949).

Similar to the analyses of trait means for clusters, one-way ANOVA with treatment as the explanatory factor and *post hoc* linear contrasts were used to compare DNA concentrations extracted from samples and for estimation of *16S rRNA* gene copies with BactQuant qPCR TaqMan assay (Liu et al., 2012). *Post hoc* linear contrasts were corrected for multiple comparisons using the method proposed by Holm (1979).

RESULTS

Of the women enrolled in the study (**Supplementary Table S1**), one group included only premenopausal women (PRE), mean age of 33 (±6.4) years, with a vaginal pH ≤ 5 and vaginal atrophy score ≤2. The second group included only postmenopausal women (POST) with a vaginal pH ≥ 5 and vaginal atrophy score ≥6, while the third group included postmenopausal women undergoing hormone therapy (POST+HT) who had a vaginal pH ≤ 5 and a vaginal atrophy score ≤2. Women in the POST+HT group had received HT in some form (oral, vaginal, or transdermal patch) for at least 12 consecutive months prior

[1]https://github.com/msettles/dbcAmplicons

to the study. The mean age of postmenopausal women enrolled in the study was 60.5 years, and height, weight and BMI were comparable among the groups.

Vaginal Bacterial Community Composition

We used culture-independent methods to characterize vaginal bacterial communities in these three groups of women. This was done by classifying sequences of the V1–V3 region of bacterial *16S rRNA* genes in vaginal swab samples. Hierarchical clustering of bacterial community composition data showed that the 45 vaginal samples could be assigned to six distinct clusters based on differences in the composition of relative abundances of bacterial taxa (**Figure 1** and **Supplementary Tables S3–S5**). Clustering was dependent on study group (χ^2 = 32.55, *df* = 10, *P*-value < 0.001). With the exception of cluster D, the rank-abundance curves of bacterial taxa were highly skewed and communities within clusters were dominated by a single species. The average proportion of *L. crispatus* in cluster A (*N* = 12) was 0.92 (95% CI: 0.92, 0.92), while the average proportion of *Gardnerella* in cluster B (*N* = 12) was 0.66 (95% CI: 0.65, 0.66), and that of *L. iners* in cluster C (*N* = 6) was 0.73 (95% CI: 0.72, 0.73). The communities in clusters E and F were dominated by *Bifidobacterium* and *L. gasseri*, respectively; each with *N* = 2. Finally, communities in cluster D (*N* = 11) exhibited greater diversity and evenness and included several co-dominant taxa, including *Anaerococcus*, *Atopobium*, *Finegoldia*, *Gardnerella*, *Prevotella*, and *Streptococcus.* The compositions of all samples were visualized by principle coordinates analysis (**Figure 2**), which illustrates the clear distinction between communities that were dominated by either *L. crispatus*, *L. iners*, or *G. vaginalis*.

The vaginal communities of most postmenopausal women undergoing HT were dominated by lactobacilli, namely *L. crispatus* (8/15), *L. iners* (1/15), and *L. gasseri* (1/15) and belonged to clusters A, C, and F, respectively (**Figures 3A,B**). The remaining five communities of women receiving HT had high proportions of either *Gardnerella* (3/15; cluster B) or *Bifidobacterium* (2/15; cluster E). In contrast, the vaginal communities of postmenopausal women not receiving HT were very different and few were dominated by species of *Lactobacillus* (2/15). Instead, they very often included various strictly anaerobic bacteria (cluster D; 10/15) and were sometimes dominated by *Gardnerella* (cluster B; 3/15). Of the 15 premenopausal women in this study only eight had vaginal communities dominated by species of *Lactobacillus*, with three dominated by *L. crispatus*, four dominated by *L. iners* and one dominated by *L. gasseri.*

Quantification of Bacterial Number in Vaginal Communities

We used qPCR to quantify the number of *16S rRNA* gene copies in vaginal samples and these data were used as a proxy for estimating the abundance of bacteria present in vaginal samples (**Figure 4**). The average number of *16S rRNA* genes, and therefore the number of bacteria, varied widely among women in all three study groups. However, on average the number of bacteria in samples from postmenopausal women receiving HT was nearly the same as in samples from premenopausal women. In contrast, the abundance of bacteria in postmenopausal women was roughly 10-fold lower than the other groups (ANOVA; *F*-ratio = 4.18, $P < 0.05$). These differences in bacterial abundance were consistent with the observation that, on average, significantly less genomic DNA was obtained from samples from postmenopausal women not receiving HT ($\bar{x}$ = 1.99 ± 0.61 ng/μl) as compared to samples from postmenopausal women who did receive HT ($\bar{x}$ = 9.25 ± 1.63 ng/μl) or premenopausal women ($\bar{x}$ = 5.59 ± 1.35 ng/μl) (ANOVA, *F*-ratio = 8.13, $P < 0.005$).

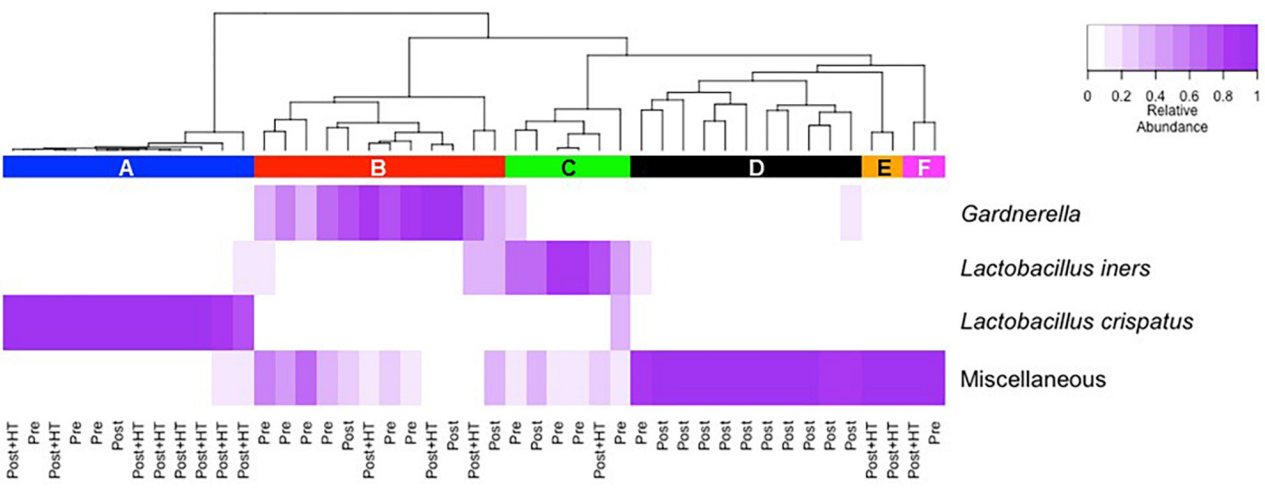

FIGURE 1 | Cluster analysis of vaginal bacterial communities found in 45 women who were either premenopausal, postmenopausal, or postmenopausal and receiving hormone replacement therapy. The dendrogram was created as described in the Materials and Methods section. The number of clusters within the data was determined by maximizing the silhouette width as described by Rousseeuw (1987).

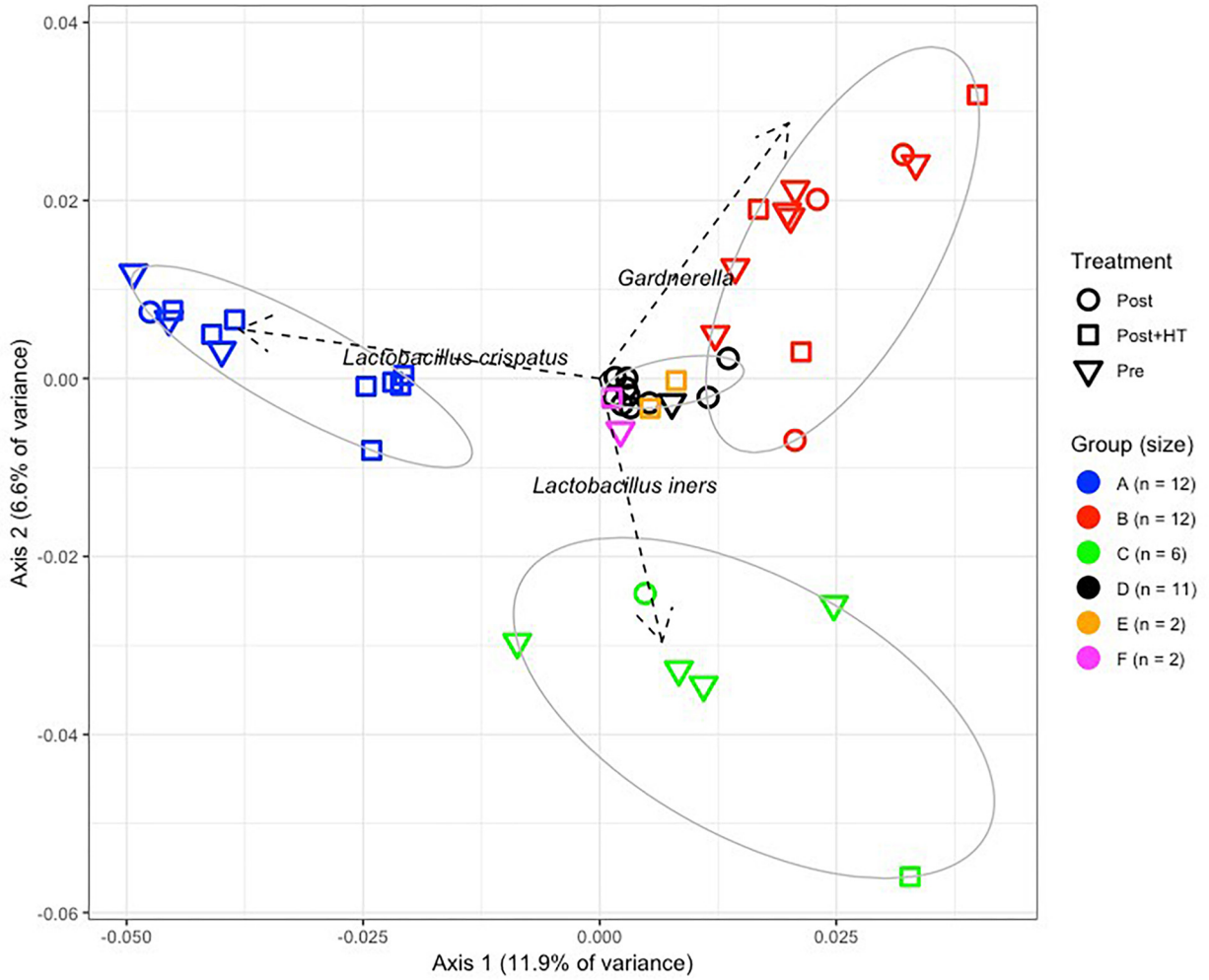

FIGURE 2 | Principle components analysis of vaginal bacterial communities found in 45 women who were either premenopausal, postmenopausal, or postmenopausal and receiving hormone replacement therapy.

Effect of Estrogen Replacement Therapy on Vaginal Atrophy and Biochemical Markers

Farage et al. (2015) used clinical data from these same study subjects to characterize anatomical and physiological changes to the vulvovaginal region that are associated with menopause. Their analyses focused on differences among study groups, whereas here we explored differences among women based on the vaginal microbiome. One-way ANOVA of vaginal atrophy scores and quantified biochemical markers versus cluster membership revealed significant differences among clusters in 8 of the 23 measurements (**Table 1**). Pairwise comparison of cluster means using Tukey's HSD revealed a general pattern for the eight measurements where significant differences were found. In general, women belonging to cluster D had lower histamine levels, a greater ratio of histidine to histamine, a lower IL-1rα to IL-1α ratio, higher pH and higher vaginal atrophy scores (**Supplementary Tables S6, S7**).

DISCUSSION

In this study, we characterized the vaginal bacterial communities of women in three groups: postmenopausal women undergoing hormone replacement therapy who had a vaginal pH $\leq$ 5 and a vaginal atrophy score $\leq$2; postmenopausal women with a vaginal pH $\geq$ 5 and vaginal atrophy score $\geq$6, and premenopausal women with a vaginal pH $\leq$ 5 and vaginal atrophy score $\leq$2. The vaginal communities of women in each group markedly differed from one another in terms of bacterial species composition. Among all women there were six sorts of communities that could be distinguished based on the kinds and relative abundance of the dominant bacterial species. Four of these accounted for most of the community types found in the women studied, and each could be characterized by the bacterial taxa that were dominant. No single community type was exclusively found in a single study group. Indeed, it was quite the opposite. For example, in premenopausal women three sorts of communities were commonly found (13/15)

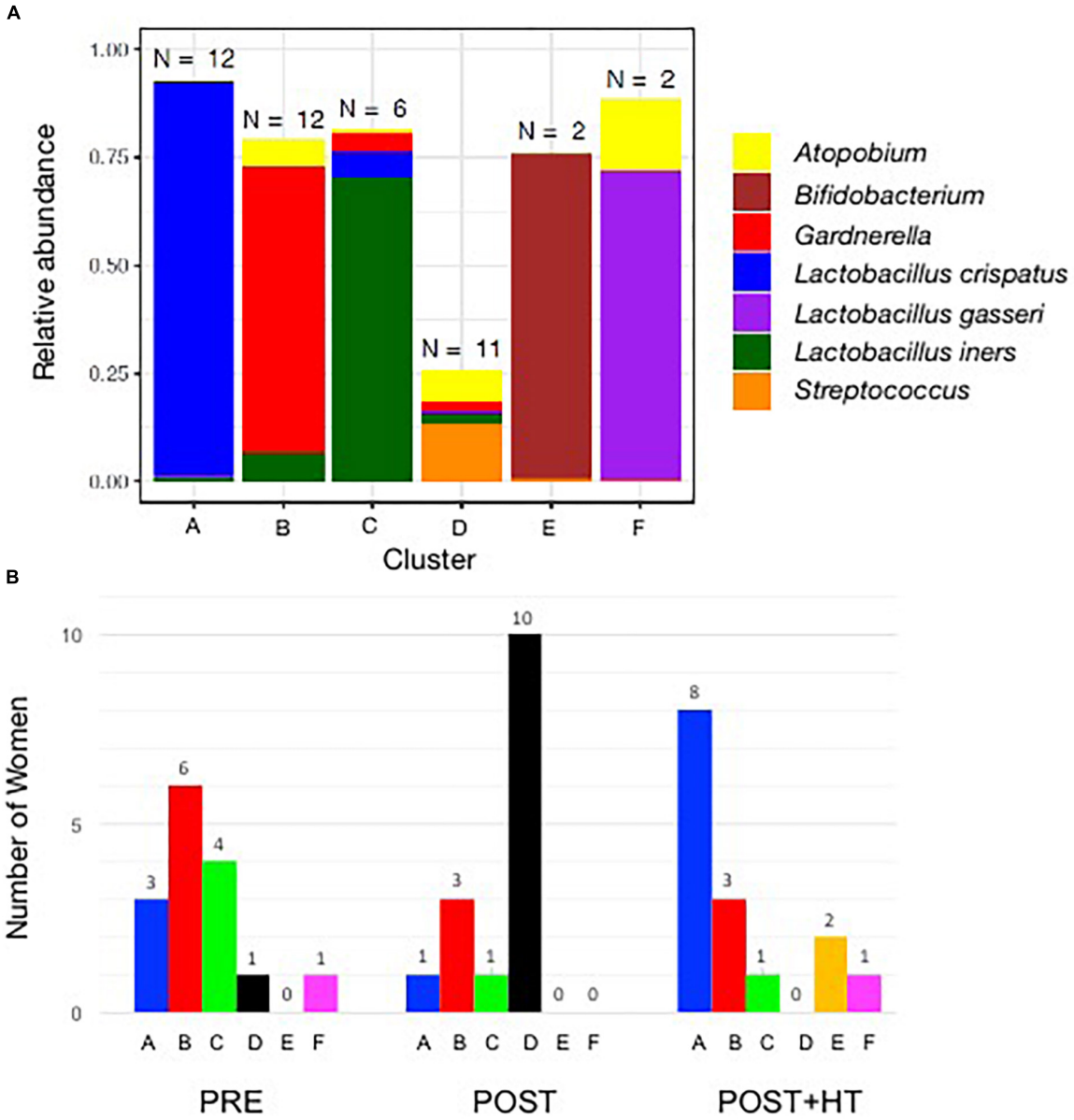

FIGURE 3 | (A) Stacked bar chart showing the predominant taxa that comprised >10% (on average) of communities in at least one cluster. The number of women in each cluster is shown above each bar, and the identity of the taxa are shown in the key on the right of the graph. **(B)** Number of women in clusters A–F in the three treatment groups. One group (PRE) included only premenopausal women with a vaginal pH ≤ 5 and vaginal atrophy score ≤2. The second group (POST) included only postmenopausal women with a vaginal pH ≥ 5 and vaginal atrophy score ≥6, while the third group (POST+H) included postmenopausal women undergoing hormone replacement therapy who had a vaginal pH ≤ 5 and a vaginal atrophy score ≤2.

that were dominated by either *L. crispatus*, *G. vaginalis*, or *L. iners* and clustered in clusters A, B, and C, respectively. These same community types also occurred in postmenopausal women and postmenopausal women undergoing HT, although their frequency varied. Despite the relatively small study cohort these data suggest that the species composition of vaginal communities cannot be used to predict membership in a treatment group.

The vaginal communities of most postmenopausal women receiving HT were dominated by species of lactobacilli (10/15), whereas this was usually not the case in untreated postmenopausal women (3/15). The preponderance of lactobacilli in the vaginal communities of women receiving HT has been previously reported in several studies and is correlated with the alleviation of symptoms associated with VVA (Ginkel et al., 1993; Devillard et al., 2004; Mac Bride et al., 2010; Lethaby et al., 2016; Shen et al., 2016; Mitchell et al., 2017). Our findings suggest that HT may lead to preferential enrichment of *L. crispatus* and not other species of *Lactobacillus*. This could represent an additional benefit of HT therapy since among the

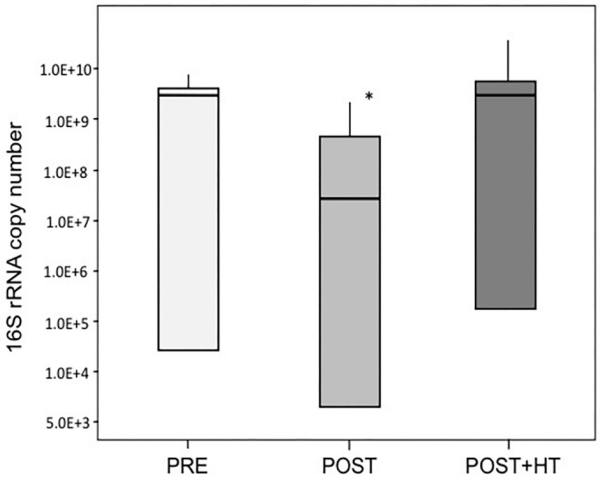

FIGURE 4 | Average *16S rRNA* gene copy number in samples of women in the three treatment groups. One group (PRE) included only premenopausal women with a vaginal pH ≤ 5 and vaginal atrophy score ≤2. The second group (POST) included only postmenopausal women with a vaginal pH ≥ 5 and vaginal atrophy score ≥6, while the third group (POST+H) included postmenopausal women undergoing hormone replacement therapy who had a vaginal pH ≤ 5 and a vaginal atrophy score ≤2. Asterisk denotes statistically significant difference ($P < 0.05$), medians are indicated by thicker lines within the bar graph for each group of women.

TABLE 1 | Pairwise comparison of clusters based on different physiological and biochemical factors.

Variable	*p*	Pairwise differences (*p*)
Histamine (labia majora)	0.04	B > D (0.09)
Histamine (labia minora)	0.04	B > D (0.03)
Histidine:Histamine (labia majora)	0.05	
Histidine:Histamine (labia minora)	0.08	D > B (0.09)
IL-1rα:IL-1α (labia minora)	0.01	A > D (0.01); B > D (0.01); D > C (0.005)
Vaginal atrophy	<0.001	D > A (<0.001); D > B (<0.001); D > C (0.005)
Vaginal pH (mid-vagina)	<0.001	B > A (0.02); B > C (0.1); D > A (<0.001); D > B (<0.001); D > C (<0.001)
Vaginal pH (labia minora)	0.02	D > A (0.01)

Model results were not significant for histamine (introitus), histamine:histidine (introitus), histidine (introitus, labia majora, labia minora), IL-1rα:IL-1α (introitus and labia majora), natural moisturizing factor (introitus, labia majora, and labia minora), temperature (introitus, labia majora, and labia minora), and pH (introitus and labia majora). Clusters: A, dominated by Lactobacillus crispatus; B, Gardnerella vaginalis; C, L. iners; D, several co-dominant taxa.

vaginal lactobacilli it is thought that *L. crispatus* most effectively reduces the risk to sexually transmitted infections and various adverse gynecological sequelae (Barrons and Tassone, 2008; Verstraelen et al., 2009; Stapleton et al., 2011). The underlying circumstances that lead to the enrichment of *L. crispatus* are completely unknown. It has been suggested that estrogen stimulates that proliferation of squamous epithelial cells, which is accompanied by the increased production of glycogen by these cells (Cruickshank, 1934; Buchanan et al., 1998; Krause et al., 2009; Sturdee et al., 2010). Glucose, maltose and maltodextrins produced through the hydrolysis of glycogen are thought to serve as carbon sources that support the proliferation of vaginal lactobacilli. The simplicity of this model is attractive, but it leaves important questions unanswered. These include the source(s) of amylase(s) needed for the depolymerization of glycogen, how lactobacilli effectively compete for these "common goods" that are available to all community members, and whether all vaginal lactobacilli compete equally well for these resources. The last of these seems unlikely. Our findings hint at the possibility that *L. crispatus* may disproportionally benefit from an increase in the production of glycogen or certain other resources produced by the host in response to HT. However, the underlying drivers of vaginal community composition and the basis for differences among women of all ages is unknown.

This study confirms that vaginal bacterial communities of postmenopausal women are usually not dominated by species of *Lactobacillus* (Heinemann and Reid, 2005; Gustafsson et al., 2011; Mirmonsef et al., 2015). In the present study, the communities of just 3 of 15 women were dominated by lactobacilli, which is good agreement with the findings of Shen et al. (2016) who reported that this was the case in only seven of thirty women (when dominance was defined as >25% of a community). It should be noted that various authors describe the vaginal communities of postmenopausal women as being "depleted" of lactobacilli (Hillier and Lau, 1997; Burton and Reid, 2002; Pabich et al., 2003; Zhang et al., 2012) and imply that these communities are rather consistent in terms of species composition. These rather general statements seem misleading. Instead, our findings indicate that the vaginal communities of postmenopausal women most often include high proportions of strictly anaerobic bacteria that are co-dominant (10/15, cluster D), but vary among women, which is consistent with the findings of others (Milsom et al., 1993; Cauci et al., 2002; Shen et al., 2016). While the composition of these communities resembles those of premenopausal women with bacterial vaginosis diagnosed by Nugent criteria (Ravel et al., 2011, 2013; Jung et al., 2017), all subjects were asymptomatic and free of clinical signs of dysbiosis. In general, women belonging to this group had lower histamine levels, a greater ratio of histidine to histamine, a lower IL-1rα to IL-1α ratio, higher pH and higher vaginal atrophy scores. Presently we cannot explain why communities with this composition are sometimes associated with vaginal symptoms such as itching or discharge, while in other cases they are not. However, two possibilities would be genetic differences within bacterial species wherein some strains elicit symptoms while others do not, underlying genetic or physiological differences in subpopulations of women, or a combination of these two. Additionally, the cytokine, histidine/histamine and inflammatory marker measurements have been collected using vulvar skin, which may reflect some general menopause symptoms, rather than directly relate to the vaginal environment. This aspect is one of the limitations of this study. Other limitations would include relatively small sample size and racial diversity or measured estrogen levels, which might have contributed to not being able to detect some

of the significant differences regarding the correlations between biomarkers and vaginal microbiota.

Our findings resemble those of previous reports showing the relatively low proportions of lactobacilli in the vaginal communities of postmenopausal women (Hummelen et al., 2011; Brotman et al., 2014). This might be attributed to low estrogen during menopause that results in atrophy and thinning of the vaginal squamous epithelium and decreased vaginal secretions. We suspect that this also leads to lower levels, and possibly differences in the kinds of nutrients that are available to support the growth of vaginal bacteria. This may well create a less favorable host environment for vaginal microbiota to thrive, especially the vaginal lactobacilli (Mirmonsef et al., 2015). The lower number of bacteria found in samples from postmenopausal women who were not receiving low dose estrogen therapy is consistent with this postulate and the findings of Hillier and Lau (1997). Low-dose local estrogen formulations effectively relieve the symptoms of vulvovaginal atrophy in most, but not all women (Robinson and Cardozo, 2003; Galhardo et al., 2006; Shen et al., 2016; Mitchell et al., 2017). This is most often accompanied by markedly increased proportions of lactobacilli that often exceed 90%, but this is not always the case (Pabich et al., 2003). The reasons for this incongruence are unknown. It could result from genetic or physiological differences between hosts that might be overcome by personalizing the dosage, changing the mode of estrogen administration, the estrogens used, or the timing of treatments (Archer, 2010). Personalizing HT may provide a way to more consistently reshape the vaginal microbiome of women, so they are dominated by lactobacilli while alleviating the symptoms of VVA.

AUTHOR CONTRIBUTIONS

KG was involved in analysis of the microbiome data, performing *16S qPCR* assays, and in preparation of the manuscript. GS extracted gDNA from samples, run QC analyses, and prepared them for DNA sequencing. BR and CW were responsible for statistical analyses of the data and contributed to preparation of the manuscript. YS, MF, and KM were involved in sample collection and study design and contributed to the manuscript preparation. LF was involved in manuscript editing and coordination of all parties engaged in the study.

FUNDING

This study was supported by a grant (P30 GM103324) from the Centers of Biomedical Research Excellence program of the National Institute of General Medical Sciences and by the Procter and Gamble Company.

SUPPLEMENTARY MATERIAL

The Supplementary Material for this article can be found online at: https://www.frontiersin.org/articles/10.3389/fmicb.2019.00193/full#supplementary-material

REFERENCES

Anderson, M. J., Ellingsen, K. E., and McArdle, B. H. (2006). Multivariate dispersion as a measure of beta diversity. *Ecol. Lett.* 9, 683–693. doi: 10.1111/j.1461-0248.2006.00926.x

Archer, D. F. (2010). Efficacy and tolerability of local estrogen therapy for urogenital atrophy. *Menopause* 17, 194–203. doi: 10.1097/gme.0b013e3181a95581

Bachmann, G., Lobo, R. A., Gut, R., Nachtigall, L., and Notelovitz, M. (2008). Efficacy of low-dose estradiol vaginal tablets in the treatment of atrophic vaginitis, a randomized controlled trial. *Obstet. Gynecol.* 111, 67–76. doi: 10.1097/01.AOG.0000296714.12226.0f

Bachmann, G. A., and Nevadunsky, N. S. (2000). Diagnosis and treatment of atrophic vaginitis. *Am. Fam. Physician.* 61, 3090–3096.

Barrons, R., and Tassone, D. (2008). Use of Lactobacillus probiotics for genitourinary infections in women, a review. *Clin. Ther.* 30, 453–468. doi: 10.1016/j.clinthera.2008.03.013

Brotman, R. M., Shardell, M. D., Gajer, P., Fadrosh, D., Chang, K., Silver, M. I., et al. (2014). Association between the vaginal microbiota, menopause status and signs of vulvovaginal atrophy. *Menopause* 21, 450–458. doi: 10.1097/GME.0b013e3182a4690b

Buchanan, D. L., Kurita, T., Taylor, J. A., Lubahn, D. B., Cunha, G. R., and Cooke, P. S. (1998). Role of stromal and epithelial estrogen receptors in vaginal epithelial proliferation, stratification and cornification. *Endocrinology* 139, 4345–4352. doi: 10.1210/endo.139.10.6241

Burton, J. P., and Reid, G. (2002). Evaluation of the bacterial vaginal flora of 20 postmenopausal women by direct (nugent score) and molecular (polymerase chain reaction and denaturing gradient gel electrophoresis) techniques. *J. Infect. Dis.* 186, 1770–1780. doi: 10.1086/345761

Cailliez, F. (1983). The analytical solution of the additive constant problem. *Psychometrika* 48, 305–308. doi: 10.1109/83.777085

Camacho, C., Coulouris, G., Avagyan, V., Ma, N., Papadopoulos, J., Bealer, K., et al. (2009). BLAST+, architecture and applications. *BMC Bioinformatics* 10:421. doi: 10.1186/1471-2105-10-421

Cauci, S., Driussi, S., De Santo, D., Penacchioni, P., Iannicelli, T., Lanzafame, P., et al. (2002). Prevalence of bacterial vaginosis and vaginal flora changes in peri- and postmenopausal women. *J. Clin. Microbiol.* 40, 2147–2152. doi: 10.1128/JCM.40.6.2147-2152.2002

Cruickshank, R. (1934). The biology of the vagina in the human subject. II, the bacterial flora and secretion of the vagina in relation to glycogen in the vaginal epithelium. *J. Obstet. Gynecol. Br. Emp.* 41, 208–226. doi: 10.1111/j.1471-0528.1934.tb08759.x

Devillard, E., Burton, J. P., Hammond, J. A., Lam, D., and Reid, G. (2004). Novel insight into the vaginal microflora in postmenopausal women under hormone replacement therapy as analyzed by PCR-denaturing gradient gel electrophoresis. *Eur. J. Obstet. Gynecol. Reprod. Biol.* 117, 76–81. doi: 10.1016/j.ejogrb.2004.02.001

Farage, M. A., Wehmeyer, K., Fadayel, G., Carpenter, S., Cheng, R., Wang, B., et al. (2015). Urogenital biomolecular and physical measures in pre- and post-menopausal women. *J. Clin. Gynecol. Obstet.* 4, 237–250. doi: 10.14740/jcgo347e

Galhardo, C. L., Soares, J. M., Simoes, R. S., Haidar, M. A., Rodrigues de Lima, G., and Baracat, E. C. (2006). Estrogen effects on the vaginal pH, flora and cytology in late postmenopause after a long period without hormone therapy. *Clin. Exp. Obstet. Gynecol.* 33, 85–89.

Ginkel, P. D., Soper, D. E., Bump, R. C., and Dalton, H. P. (1993). Vaginal flora in postmenopausal women, the effect of estrogen replacement. *Infect. Dis. Obstet. Gynecol.* 1, 94–99. doi: 10.1155/S1064744993000225

Gower, J. C. (1966). Some distance properties of latent root and vector methods used in multivariate analysis. *Biometrika* 53, 325–338. doi: 10.1093/biomet/53.3-4.325

Gustafsson, R. J., Ahrne, S., Jeppsson, B., Benoni, C., Olsson, C., Stjernquist, M., et al. (2011). The Lactobacillus flora in vagina and rectum of fertile and

postmenopausal healthy Swedish women. *BMC Womens Health* 11:17. doi: 10.1186/1472-6874-11-17

Heinemann, C., and Reid, G. (2005). Vaginal microbial diversity among postmenopausal women with and without hormone replacement therapy. *Can. J. Microbiol.* 51, 777–781. doi: 10.1139/w05-070

Hillier, S. L., and Lau, R. J. (1997). Vaginal microflora in postmenopausal women who have not received estrogen replacement therapy. *Clin. Infect. Dis.* 25, S123–S126. doi: 10.1086/516221

Holm, S. (1979). A simple sequentially rejective multiple test procedure. *Scand. J. Stat.* 6, 65–70.

Hummelen, R., Macklaim, J. M., Bisanz, J. E., Hammond, J. A., McMillan, A., Vongsa, R., et al. (2011). Vaginal microbiome and epithelial gene array in post-menopausal women with moderate to severe dryness. *PLoS One* 6:e26602. doi: 10.1371/journal.pone.0026602

Jung, H. S., Ehlers, M. M., Lombaard, H., Redelinghuys, M. J., and Kock, M. M. (2017). Etiology of bacterial vaginosis and polymicrobial biofilm formation. *Crit. Rev. Microbiol.* 43, 651–667. doi: 10.1080/1040841X.2017.1291579

Krause, M., Wheeler, T. L. II, Snyder, T. E., and Richter, H. E. (2009). Local effects of vaginally administered estrogen therapy, a review. *J. Pelvic. Med. Surg.* 15, 105–114. doi: 10.1097/SPV.0b013e3181ab4804

Legendre, P., and Legendre, L. (1998). *Numerical Ecology, 2nd English Edition*. Amsterdam: Elsevier Science BV.

Lethaby, A., Ayeleke, R. O., and Roberts, H. (2016). Local oestrogen for vaginal atrophy in postmenopausal women. *Cochrane Database Syst. Rev.* 8, CD001500. doi: 10.1002/14651858.CD001500.pub3

Liu, C. M., Aziz, M., Kachur, S., Hsueh, P. R., Huang, Y. T., Keim, P., et al. (2012). BactQuant, an enhanced broad-coverage bacterial quantitative real-time PCR assay. *BMC Microbiol.* 12:56. doi: 10.1186/1471-2180-12-56

Mac Bride, M. B., Rhodes, D. J., and Shuster, L. T. (2010). Vulvovaginal atrophy. *Mayo Clin. Proc.* 85, 87–94. doi: 10.4065/mcp.2009.0413

Magoč, T., and Salzberg, S. L. (2011). FLASH, fast length adjustment of short reads to improve genome assemblies. *Bioinformatics* 27, 2957–2963. doi: 10.1093/bioinformatics/btr507

Milsom, I., Arvidsson, L., Ekelund, P., Molander, U., and Eriksson, O. (1993). Factors influencing vaginal cytology, pH and bacterial flora in elderly women. *Acta Obstet. Gynecol. Scand.* 72, 286–291. doi: 10.3109/00016349309068039

Minkin, M. J., Maamari, R., and Reiter, S. (2014). Postmenopausal vaginal atrophy: evaluation of treatment with local estrogen therapy. *Int. J. Womens Health* 6, 281–288. doi: 10.2147/IJWH.S57900

Mirmonsef, P., Modur, S., Burgad, D., Gilbert, D., Golub, E. T., French, A. L., et al. (2015). Exploratory comparison of vaginal glycogen and Lactobacillus levels in premenopausal and postmenopausal women. *Menopause* 22, 702–709. doi: 10.1097/GME.0000000000000397

Mitchell, C. M., Srinivasan, S., Zhan, X., Wu, M. C., Reed, S. D., Guthrie, K. A., et al. (2017). Vaginal microbiota and genitourinary menopausal symptoms, a cross-sectional analysis. *Menopause* 24, 1160–1166. doi: 10.1097/GME.0000000000000904

Nappi, R. E., and Kokot-Kierepa, M. (2010). Women's voices in the menopause, results from and international survey on vaginal atrophy. *Maturitas* 67, 233–238. doi: 10.1016/j.maturitas.2010.08.001

Nappi, R. E., and Kokot-Kierepa, M. (2012). Vaginal health, insights, views and attitudes (VIVA) – results from an international survey. *Climacteric* 15, 36–44. doi: 10.3109/13697137.2011.647840

Pabich, W. L., Fihn, S. D., Stamm, W. E., Scholes, D., Boyko, E. J., and Gupta, K. (2003). Prevalence and determinants of vaginal flora alterations in postmenopausal women. *J. Infect. Dis.* 188, 1054–1058. doi: 10.1086/378203

Pinkerton, J. V., Stovall, D. W., and Kightlinger, R. S. (2009). Advances in the treatment of menopausal symptoms. *Womens Health* 5, 361–384. doi: 10.2217/whe.09.31

Ravel, J., Brotman, R. M., Gajer, P., Ma, B., Nandy, M., Fadrosh, D. W., et al. (2013). Daily temporal dynamics of vaginal microbiota before, during and after episodes of bacterial vaginosis. *Microbiome* 1:29. doi: 10.1186/2049-2618-1-29

Ravel, J., Gajer, P., Abdo, Z., Schneider, G. M., Koenig, S. S., McCulle, S. L., et al. (2011). Vaginal microbiome of reproductive-age women. *Proc. Natl. Acad. Sci. U.S.A.* 108, 4680–4687. doi: 10.1073/pnas.1002611107

Raymundo, N., Yu-cheng, B., Zi-yan, H., Lai, C. H., Leung, K., Subramaniam, R., et al. (2004). Treatment of atrophic vaginitis with topical conjugated equine estrogens in postmenopausal Asian women. *Climacteric* 7, 312–318. doi: 10.1080/13697130400003147

Robinson, D., and Cardozo, L. D. (2003). The role of estrogens in female lower urinary tract dysfunction. *Urology* 62(4 Suppl. 1), 45–51. doi: 10.1016/S0090-4295(03)00676-9

Rousseeuw, P. J. (1987). Silhouettes, a graphical aid to the interpretation and validation of cluster analysis. *J. Comput. Appl. Math.* 20, 53–65. doi: 10.1016/0377-0427(87)90125-7

Santoro, N., and Komi, J. (2009). Prevalence and impact of vaginal symptoms among postmenopausal women. *J. Sex. Med.* 6, 2133–2142. doi: 10.1111/j.1743-6109.2009.01335.x

Shen, J., Song, N., Williams, C. J., Brown, C. J., Yan, Z., Xu, C., et al. (2016). Effects of low-dose estrogen therapy on the vaginal microbiomes of women with atrophic vaginitis. *Sci. Rep.* 6:24380. doi: 10.1038/srep24380

Simon, J. A., Kokot-Kierepa, M., Goldstein, J., and Nappi, R. E. (2013). Vaginal health in the United States, results from the vaginal health, insights, views and attitudes survey. *Menopause* 20, 1043–1048. doi: 10.1097/GME.0b013e318287342d

Stapleton, A. E., Au-Yeung, M., Hooton, T. M., Fredricks, D. N., Roberts, P. L., Czaja, C. A., et al. (2011). Randomized, placebo-controlled phase 2 trial of a Lactobacillus crispatus probiotic given intravaginally for prevention of recurrent urinary tract infection. *Clin. Infect. Dis.* 52, 1212–1217. doi: 10.1093/cid/cir183

Sturdee, D. W., Panay, N., International Menopause, and Society Writing Group. (2010). Recommendations for the management of postmenopausal vaginal atrophy. *Climacteric* 13, 509–522. doi: 10.3109/13697137.2010.522875

Takahashi, T. A., and Johnson, K. M. (2015). Menopause. *Med. Clin. N. Am.* 99, 521–534. doi: 10.1016/j.mcna.2015.01.006

Tukey, J. (1949). Comparing individual means in the analysis of variance. *Biometrics* 5, 99–114. doi: 10.2307/3001913

Verstraelen, H., Verhelst, R., Claeys, G., De Backer, E., Temmerman, M., and Vaneechoutte, M. (2009). Longitudinal analysis of the vaginal microflora in pregnancy suggests that L. Crispatus promotes the stability of the normal vaginal microflora and that L. gasseri and/or L. iners are more conducive to the occurrence of abnormal vaginal microflora. *BMC Microbiol.* 9:116. doi: 10.1186/1471-2180-9-116

Wang, Q., Garrity, G. M., Tiedje, J. M., and Cole, J. R. (2007). Naïve Bayesian classifier for rapid assignment of rRNA sequences into the new bacterial taxonomy. *Appl. Environ. Microbiol.* 73, 5261–5267. doi: 10.1128/AEM.00062-07

WMA Declaration of Helsinki (2013). World Medical association declaration of helsinki ethical principles for medical research involving human subjects. *JAMA* 310, 2191–2194. doi: 10.1001/jama.2013.281053

Yoshimura, T., and Okamura, H. (2001). Short term estriol treatment restores normal premenopausal vaginal flora to elderly women. *Maturitas* 39, 253–257. doi: 10.1016/S0378-5122(01)00212-2

Zhang, R., Daroczy, K., Xiao, B., Yu, L., Chen, R., and Liao, Q. (2012). Qualitative and semiquantitative analysis of Lactobacillus species in the vaginas of healthy fertile and postmenopausal Chinese women. *J. Med. Microbiol.* 61, 729–739. doi: 10.1099/jmm.0.038687-0

Conflict of Interest Statement: YS, MF, and KM were employed by Procter and Gamble Company. LF has consulted for Procter and Gamble Company.

The remaining authors declare that the research was conducted in the absence of any commercial or financial relationships that could be construed as a potential conflict of interest.

Copyright © 2019 Gliniewicz, Schneider, Ridenhour, Williams, Song, Farage, Miller and Forney. This is an open-access article distributed under the terms of the Creative Commons Attribution License (CC BY). The use, distribution or reproduction in other forums is permitted, provided the original author(s) and the copyright owner(s) are credited and that the original publication in this journal is cited, in accordance with accepted academic practice. No use, distribution or reproduction is permitted which does not comply with these terms.

frontiers in Microbiology

ORIGINAL RESEARCH
published: 22 May 2019
doi: 10.3389/fmicb.2019.01137

Elucidation of *Akkermansia muciniphila* Probiotic Traits Driven by Mucin Depletion

Jongoh Shin[1†], Jung-Ran Noh[2†], Dong-Ho Chang[3], Yong-Hoon Kim[2], Myung Hee Kim[4], Eaum Seok Lee[5], Suhyung Cho[1], Bon Jeong Ku[5], Moon-Soo Rhee[6], Byoung-Chan Kim[3,7,8], Chul-Ho Lee[2]* and Byung-Kwan Cho[1,9]**

[1] Department of Biological Sciences and KI for the BioCentury, Korea Advanced Institute of Science and Technology, Daejeon, South Korea, [2] Laboratory Animal Resource Center, Korea Research Institute of Bioscience and Biotechnology, Daejeon, South Korea, [3] Metabolic Regulation Research Center, Korea Research Institute of Bioscience and Biotechnology, Daejeon, South Korea, [4] Infection and Immunity Research Laboratory, Metabolic Regulation Research Center, Korea Research Institute of Bioscience and Biotechnology, Daejeon, South Korea, [5] Department of Internal Medicine, Chungnam National University School of Medicine, Daejeon, South Korea, [6] Korean Collection for Type Cultures, Korea Research Institute of Bioscience and Biotechnology, Jeongeup-si, South Korea, [7] Department of Bioprocess Engineering, Korea Research Institute of Bioscience and Biotechnology (KRIBB), School of Biotechnology, Korea University of Science and Technology, Daejeon, South Korea, [8] 114 Bioventure Center, HealthBiome, Inc., Daejeon, South Korea, [9] Intelligent Synthetic Biology Center, Daejeon, South Korea

Akkermansia muciniphila is widely considered a next-generation beneficial microbe. This bacterium resides in the mucus layer of its host and regulates intestinal homeostasis and intestinal barrier integrity by affecting host signaling pathways. However, it remains unknown how the expression of genes encoding extracellular proteins is regulated in response to dynamic mucosal environments. In this study, we elucidated the effect of mucin on the gene expression and probiotic traits of *A. muciniphila*. Transcriptome analysis showed that the genes encoding most mucin-degrading enzymes were significantly upregulated in the presence of mucin. By contrast, most genes involved in glycolysis and energy metabolic pathways were upregulated under mucin-depleted conditions. Interestingly, the absence of mucin resulted in the upregulation of 79 genes encoding secreted protein candidates, including Amuc-1100 as well as members of major protein secretion systems. These transcript level changes were consistent with the fact that administration of *A. muciniphila* grown under mucin-depleted conditions to high-fat diet-induced diabetic mice reduced obesity and improved intestinal barrier integrity more efficiently than administration of *A. muciniphila* grown under mucin-containing conditions. In conclusion, mucin content in the growth medium plays a critical role in the improvement by *A. muciniphila* of high-fat diet-induced obesity, intestinal inflammation, and compromised intestinal barrier integrity related to a decrease in goblet cell density. Our findings suggest the depletion of animal-derived mucin in growth medium as a novel principle for the development of *A. muciniphila* for human therapeutics.

Keywords: *Akkermansia muciniphila*, extracellular protein, mucus layer, metabolic disorder, microbiome analysis

OPEN ACCESS

Edited by:
M. Pilar Francino, Fundación para el Fomento de la Investigación Sanitaria y Biomédica de la Comunitat Valenciana (FISABIO), Spain

Reviewed by:
Maria de los Angeles Serradell, National Council for Scientific and Technical Research (CONICET), Argentina
Åsa Sjöling, Karolinska Institutet, Sweden

***Correspondence:**
Byoung-Chan Kim
bckim@kribb.re.kr
Chul-Ho Lee
chullee@kribb.re.kr
Byung-Kwan Cho
bcho@kaist.ac.kr

† These authors have contributed equally to this work

Specialty section:
This article was submitted to Microbial Symbioses, a section of the journal Frontiers in Microbiology

Received: *17 November 2018*
Accepted: *06 May 2019*
Published: *22 May 2019*

Citation:
Shin J, Noh J-R, Chang D-H, Kim Y-H, Kim MH, Lee ES, Cho S, Ku BJ, Rhee M-S, Kim B-C, Lee C-H and Cho B-K (2019) Elucidation of Akkermansia muciniphila Probiotic Traits Driven by Mucin Depletion. Front. Microbiol. 10:1137. doi: 10.3389/fmicb.2019.01137

INTRODUCTION

The gastrointestinal (GI) tract harbors complex and diverse microorganisms, termed the gut microbiota, establishing symbiotic interactions between the gut microbiota and the host (Hooper et al., 2012). In particular, the outer layer of the colonic mucus is densely populated by diverse commensal microbes (Johansson et al., 2011). Some of these gut microbes degrade mucin glycans via secretion of glycosyl hydrolases, and the resulting monosaccharides are used as additional energy and carbon sources. In turn, gut microbes also affect mucus composition by degrading mucin and releasing bioactive factors that can alter the gene expression of mucin-producing host cells (Deplancke and Gaskins, 2001; Johansson et al., 2011; Ottman et al., 2012). Due to these significant mucus–microbiota interactions, the mucus layer plays an essential role in shaping the mucus barrier and composition of the gut microbiota (Johansson et al., 2015). Recently, substantial evidence has demonstrated that the host–microbiota interaction has a critical role in obesity and other disorders by affecting several homeostatic (Cani et al., 2012; Everard et al., 2013), metabolic (Cani et al., 2007, 2008), and other physiological interactions with the hosts (Sommer and Bäckhed, 2013).

One of the key members of the colonic mucus-associated microbiota is *Akkermansia muciniphila*. This bacterium is capable of using mucus as a sole carbon and nitrogen source by producing several mucin-degrading enzymes (Derrien, 2004; Ottman et al., 2017a). It is well adapted to the mucous layer, accounting for 1–5% of the fecal microbial composition in healthy adults (Derrien, 2004; Belzer and de Vos, 2012). Thereby, *A. muciniphila* plays a crucial role in the maintenance of GI tract homeostasis and gut barrier integrity. Previous studies demonstrated that the abundance of *A. muciniphila* inversely correlated with several metabolic disorders (Dao et al., 2016; Derrien et al., 2017), such as obesity (Karlsson et al., 2012; Everard et al., 2013), inflammatory bowel disease (Png et al., 2010), type 2 diabetes (Zhang et al., 2013), and autism (Wang et al., 2011) in mice and humans. This correlation was additionally confirmed in several studies where oral administration of *A. muciniphila* bacteria reversed high-fat diet (HFD)-induced intestinal metabolic disorders and altered mucus layer thickness (Everard et al., 2013; Shin et al., 2014). Thus, *A. muciniphila* has garnered much attention as a next-generation probiotic bacterium (Cani and de Vos, 2017).

Among the critical factors that determine probiotic traits, extracellular proteins or vesicles are secreted into the host by probiotic bacteria. Some of these are reported to exhibit immunomodulatory and anti-inflammatory activity, with the secreted proteins potentially interacting directly with relevant immune cells to trigger downstream signaling pathways in the host mucosa (Sánchez et al., 2008, Sanchez et al., 2010; Bernardo et al., 2012; Ruiz et al., 2014). In this regard, the extracellular materials secreted by *A. muciniphila* have been evaluated in several studies. Remarkably, the cell-free supernatant of *A. muciniphila* culture was found to induce the production of an anti-inflammatory cytokine, interleukin-10, and this induction also occurred with the live bacterium (Ottman et al., 2017b), indicating that extracellular materials can activate the downstream signaling pathway of Toll-like receptor 2 (TLR2). A few studies have been conducted to determine the outer membrane proteome of *A. muciniphila* (Ottman et al., 2016, 2017b), leading to the discovery of the extracellular protein Amuc_1100, which recapitulates the effect of *A. muciniphila* on TLR2 activation as well as the improvement of intestinal barrier integrity (Plovier et al., 2016; Ottman et al., 2017b). Furthermore, it was revealed that *Akkermansia*-derived extracellular vesicles act as a functional module for maintaining the integrity of the intestinal barrier in HFD-mice (Chelakkot et al., 2018). However, it remains unknown how the expression of genes encoding extracellular proteins, including Amuc_1100, is regulated in response to dynamic mucosal environments. Such knowledge is imperative for better understanding the mechanisms of the interactions between the bacterium and the host as they relate to obesity, type 2 diabetes, and intestinal barrier integrity.

In the present study, we sought to elucidate the effect of mucin on the gene expression and probiotic traits of *A. muciniphila*. Transcriptome analysis revealed that the genes encoding most mucin-degrading enzymes were significantly upregulated in the presence of mucin [hereafter, mucin (+)]. By contrast, expression of most genes involved in glycolysis and energy metabolic pathways was upregulated in the absence of mucin [hereafter, mucin (−)]. In addition, 79 genes encoding secreted protein candidates, including Amuc_1100, were upregulated in mucin (−) conditions compared to mucin (+) conditions and the corresponding proteins secreted into culture medium. These changes in transcript levels were consistent with the fact that administration of *A. muciniphila* grown under mucin (−) conditions more efficiently reduced obesity and improved intestinal barrier integrity in HFD-induced diabetic mice than administration of *A. muciniphila* grown under mucin (+) conditions. These results suggest that the mucin content is important in the regulation of metabolism and gut permeability by *A. muciniphila*.

MATERIALS AND METHODS

Bacterial Strain and Growth Conditions

Akkermansia muciniphila Muc^T (= DSM 22959^T) was obtained from the German Collection of Microorganisms and Cell Cultures (Leibniz-Institut DSMZ-Deutsche Sammlung von Mikroorganismen und Zellkulturen GmbH, Germany). *A. muciniphila* was cultivated anaerobically at 37 °C on medium supplemented with mucin (DSM medium 1203a with 0.2% (wt/v) mucin) or without mucin[1]. DSM 1203a medium contained 16 g peptone, 7 g yeast extract, 5 g sodium chloride, 1 g starch, 1 g dextrose, 1 g sodium pyruvate, 1 g arginine, 0.5 g sodium succinate, 0.5 g L-cysteine HCl, 0.4 g sodium bicarbonate, 0.5 g ferric pyrophosphate, 0.005 g haemin, 0.0005 g vitamin K, and 0.5 g sodium thioglycollate in 1 l distilled water. All procedures for media preparation were performed under

[1]https://www.dsmz.de/microorganisms/medium/pdf/DSMZ_Medium1203a.pdf

anaerobic condition according to previously established method (Ahn et al., 2016).

DSM 1203a agar plates (1.5%, w/v) were prepared and *A. muciniphila* DSM 22959^T was incubated at 37°C in the anaerobic chamber (Coy Laboratory Products) with a $N_2/CO_2/H_2$ (86:7:7) gas phase.

RNA Extraction and RNA-Seq Analysis

For RNA extraction, *A. muciniphila* grown on solid medium with/without mucin were harvested by scraping the surface using a sterilized scalpel and were resuspended in extraction buffer (200 mM Tris-HCl, pH 7.5, 25 mM EDTA, 250 mM NaCl, and 0.5% SDS). The harvested cells were rapidly frozen in liquid N_2 and then ground to a fine powder using a mortar and pestle. Cell debris was removed by centrifugation at 3,000 × *g* for 30 min at 4°C. Total RNA was extracted using TRIzol® reagent (Thermo Scientific, Rockford, IL, United States) according to the manufacturer's instructions. RNA quality was confirmed by the A260/280 ratio and visualization of two distinct bands of ribosomal RNAs (rRNA) using 2% agarose gel electrophoresis. rRNAs were selectively removed by Ribo-Zero^{TM} rRNA Removal Kit bacteria (Illumina, San Diego, CA, United States). RNA-Seq libraries were constructed in triplicate using TruSeq Strand mRNA LT Sample Prep Kit (Illumina) and then analyzed for size distribution using the Agilent Tapestation 2200 (Santa Clara, CA, United States). Constructed RNA-Seq libraries were sequenced with an Illumina Mi-Seq instrument with a 51 bp single-end sequencing recipe. The sequencing reads obtained were demultiplexed using Bcl2fastq V1.8.4 (Illumina), and low-quality reads and adaptor sequences were additionally trimmed using the CLC Genomics Workbench 6.5.1 (Qiagen, Hilden, Germany). The remaining reads were aligned to the *A. muciniphila* reference genome (CP001071.1) using CLC Genomics Workbench. The following parameters were applied for mapping: mismatch cost = 2, insertion cost = 3, deletion cost = 3, length fraction = 0.9, and similarity fraction = 0.9. The gene-wise read count was obtained using BEDTools suite v2.17.0 (Quinlan and Hall, 2010). Upon counting, reads that mapped only to the sense strand of the respective CDS were considered. Differential gene expression was assessed with the Bioconductor package DEseq2 (Love et al., 2014), and the significance level was set at $Padj < 0.01$. Total gene expression data can be found in **Supplementary Table S2**. Raw transcriptome data in FASTQ format is available in the European Nucleotide Archive (ENA) under study accession PRJEB28544.

Annotation of Extracellular Proteins

All CDSs were analyzed using available prediction programs combined into a bioinformatics pipeline (**Figure 3A**) as described previously (Gomez et al., 2015; Cornejo-Granados et al., 2017). To predict signal peptide-carrying proteins, SignalP 4.1 (Dyrløv Bendtsen et al., 2004) was used with default parameters. Non-classical secreted proteins were additionally predicted with the options for "gram-positive bacteria" using SecretomeP 2.0 (Bendtsen et al., 2005), and all proteins with a SecP score > 0.5 were considered non-classical secreted proteins. Candidate secreted proteins derived from SignalP 4.1 and Secretome P 2.0 were merged and were additionally searched for homology to secreted protein by Blastp. LipoP 1.0 (Juncker et al., 2003) was used to predict lipoprotein motifs with default parameters, and all proteins annotated with "CYT (cytoplasmic)" were removed from the list of putative secreted proteins. Additionally, transmembrane proteins (with ≥ 1 transmembrane motifs) were removed from the set of predicted extracellular proteins using TMHMM 2.0 (Krogh et al., 2001).

Animals and Diet

Eight-week-old male C57BL/6 mice were purchased from The Jackson Laboratory (Bar Harbor, ME, United States) and maintained at the Korea Research Institute of Bioscience and Biotechnology (Daejeon, Korea). Mice were housed under a constant 12 h light/dark cycle. To establish the obese mouse model, they were fed an HFD (60% of kcal from fat; D12492, Research Diet, New Brunswick, NJ, United States) for 6 weeks and then divided into three groups: HFD treated with 25% glycerol in sterile PBS (HFD group) or HFD treated with *A. muciniphila* grown on mucus-based [AK mucin (+)] or mucus-depleted [AK mucin (−)] medium. Mice were treated daily with an oral administration of *A. muciniphila* (1.0×10^8 CFU/day) and treatment was continued for 4 weeks. Age-matched normal chow diet-fed mice were used as a control (ND group). Body weight and blood glucose were recorded once weekly. Oral gavage treatment with *A. muciniphila* was continued for 4 weeks. All animal experiments were approved by the Institutional Animal Care and Use Committee and performed in accordance with the institutional guidelines of the Korea Research Institute of Bioscience and Biotechnology (Approved No.: KRIBB-AEC-16117).

IP-GTT and IP-ITT

After 4 weeks of HFD treatment with *A. muciniphila* administration, intraperitoneal glucose tolerance test (IP-GTT) and intraperitoneal insulin tolerance test (IP-ITT) were performed. After 16 or 4 h of fasting for GTT and ITT, respectively, the basal glucose level of each mouse was measured in blood taken from the tail vein. Then, either glucose (2 g/kg) or insulin (0.1 U/ml) was injected intraperitoneally, and blood glucose levels were monitored at 30, 60, 90, and 120 min. The area under the curve (AUC) was calculated using GraphPad Prism software (La Jolla, CA, United States).

Tissue Sampling

At 4 weeks post-treatment, blood samples were collected from the orbital venous sinuses of the mice to analyze the concentrations of plasma insulin. Plasma was prepared by centrifugation at 10,000 × *g* for 5 min at 4°C. After exsanguination, mice were sacrificed by cervical dislocation. Liver, epididymal, and subcutaneous adipose and brown adipose tissues were collected for histology, and small intestine samples were immediately immersed in liquid nitrogen and stored at −80°C for further analysis.

HOMA-IR

After 4 weeks of HFD treatment with *A. muciniphila* administration, plasma insulin levels were determined using

an ELISA kit (Mercodia, Uppsala, Sweden) according to the manufacturer's instructions. HOMA-IR was calculated using the following formula: fasting blood glucose (mg/dl) × fasting insulin (μU/ml)/405.

Plasma LPS Analysis

Plasma LPS concentration was measured with a commercially available kit [Cambrex Limulus Amebocyte Lysate (LAL) kit; Lonza, Walkersville, MD]. This assay has a sensitivity range of 0.1–1.0 endotoxin units (EU)/ml. Plasma samples were diluted 1:5 in endotoxin-free water and then heated at 75°C for 5 min to remove interfering plasma components. Endotoxin assays were performed using a quantitative turbidimetric Limulus amebocyte lysate assay.

Histological Analysis

At necropsy, liver samples and adipose tissues were immediately fixed in 10% formaldehyde, embedded in paraffin, and cut into 4 μm slices. Slides were stained with hematoxylin and eosin. Then, histology sections were viewed at 100× magnification, and images were obtained with a microscope (Olympus BX51, Tokyo, Japan). The total number and cross-sectional area of adipocytes were calculated with an image analysis program (ImageInside ver. 2.32, Olympus). For goblet cell staining, deparaffinized and rehydrated sections were stained with periodic acid-Schiff's (PAS) reaction. The number of goblet cells per mouse ileum was counted in 10-well-oriented crypt-villus units.

Quantitative Real-Time PCR

At necropsy, Peyer's patches free part in ileum was collected and total RNA was prepared from this intestine samples using TRIzol reagent (Thermo Fisher Scientific). Quantification and integrity analysis of total RNA was performed by NanoDrop™ spectrophotometer (Thermo Fisher Scientific). The cDNA was synthesized by reverse transcription, and real-time qPCR was performed as previously described (Kim et al., 2015). The 18S RNA gene was used as a reference. The sequences of the primers used for real-time qPCR are available in **Supplementary Table S7**.

Statistical Analysis

Data were analyzed and statistical testing (Pearson's correlation coefficient and Student's *t*-test) was performed using GraphPad Prism v8 and R software. Comparisons multiple groups were performed using Tukey-Kramer HSD test after the one-way analysis of variance (ANOVA). The threshold of significance was set at $P < 0.05$. Replicates (n) in this study refer to biological replicates.

RESULTS

Transcriptomic Landscape of *A. muciniphila* Under Mucin-Rich and -Depleted Conditions

To elucidate global changes in gene expression in response to the presence of mucin, RNA-sequencing (RNA-Seq) was employed for *A. muciniphila* cells grown under mucin (+) and mucin (−) conditions (**Figure 1A**). We obtained 1.9–3.8 million high-quality sequencing reads for each triplicate sample that mapped uniquely to the *A. muciniphila* reference genome (CP001071.1) with at least 36-fold sequencing coverage (**Supplementary Table S1**; van Passel et al., 2011). Principal component analysis of the RNA-Seq results showed significant changes in gene expression between the mucin (+) and (−) conditions, suggesting a global change in cellular functions (**Figure 1B**). Pearson correlation coefficient values between three biological replicates confirmed the experimental reproducibility (Pearson correlation coefficient > 0.99) (**Figure 1C**). Among the 1,126 DEGs between the mucin (+) and (−) conditions (**Supplementary Table S2**), 583 genes were downregulated and 543 genes were upregulated in mucin (−) conditions compared to mucin (+) conditions; the DEGs exhibited a considerable dynamic range of gene expression, with fold changes ranging from 0.03-to 41.01-fold (**Figure 1D**).

To gain more insight into the biological functions of the DEGs, Gene Ontology (GO) term enrichment analysis was conducted (Shannon et al., 2003; Saito et al., 2012). All enriched GO molecular function terms are shown in **Figure 1E**, with clear functional differences between up- and downregulated genes. GO terms enriched among upregulated genes included DNA binding (GO:0003677) and NADH dehydrogenase activity (GO:0003954) with Benjamini-Hochberg corrected $P < 0.017$. Furthermore, Kyoto Encyclopedia of Genes and Genomes (KEGG) pathway enrichment analysis showed that Ribosome and oxidative phosphorylation was significantly enriched, with a corrected $P < 0.001$ (**Supplementary Table S3**). Among the genes in this pathway, ATP synthase (Amuc_0505–Amuc_0510), the succinate dehydrogenase gene cluster (Amuc_0984–Amuc_0986), and the NADH dehydrogenase gene cluster (Amuc_1604–Amuc_1614) were significantly upregulated, with fold changes > 2.2 and $Padj < 7.0 \times 10^{-219}$. By contrast, enriched GO molecular function terms among the downregulated genes were significantly associated with hydrolase activity acting on glycosyl bonds (GO:0016798), nucleic acid binding (GO:0003676), and DNA binding (GO:0003677) with corrected $P < 0.046$ (**Figure 1E** and **Supplementary Table S3**). Considering that mucin is composed of heavily O-glycosylated glycoproteins, these results indicate that genes involved in mucin-degrading processes were overexpressed under mucin (+) conditions.

Mucin-Rich Conditions Trigger Expression of Genes Encoding Mucin-Degrading Enzymes

In further detail, we analyzed changes in the expression of genes involved in the mucin-degrading pathway and central carbon metabolism. Mucin oligosaccharides are composed of five different monosaccharides, including *N*-acetyl-D-glucosamine (GlcNAc), *N*-acetylhexosamine (HexNAc), L-fucose (fucose), D-galactose (galactose), and *N*-acetylneuraminic acid (NeuAc). Their heterogeneity is derived from various glycosidic bonds, and the sugar residue can be substituted with sulfate, acetate,

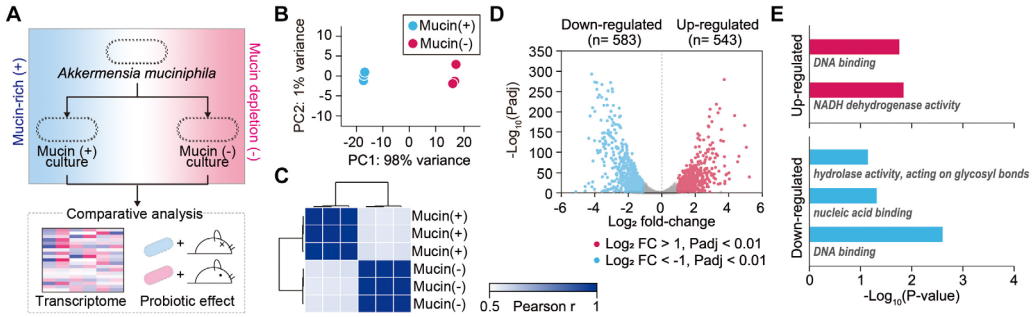

FIGURE 1 | Transcriptomic dynamics of *A. muciniphila* under mucin-rich and mucin-depleted conditions. **(A)** Schematic of experimental design employed in this study. **(B)** Principal component analysis (PCA) of whole-transcriptome RNA data. **(C)** Sample-to-sample Pearson correlation coefficients between the data sets. **(D)** Volcano plot of genes sequenced under mucin-rich and mucin-depleted conditions. Differentially expressed genes (DEGs) are in blue. **(E)** Significantly enriched Gene Ontology (GO) molecular function terms among upregulated (red) and downregulated (blue) differentially expressed genes between mucin-rich and mucin-depleted conditions (Benjamini-Hochberg corrected $P < 0.05$).

or phosphate groups (Tailford et al., 2015). Therefore, the hypothetical mucin complex can typically be degraded by five different enzymatic reactions (A–E), shown in **Figure 2**. The corresponding enzymes are named according to their specific mucin-degrading reactions: *N*-acetylgalactosaminidases (A), L-fucosidases (B), sulfatases (C), galactosidases (D), and neuraminidases (E). For our analysis of the mucin-degrading pathway, we selected 28 enzymes that were predicted to be involved in mucin-degrading reactions by the BioCyc database (Caspi et al., 2016) and metabolic model (iAkkMuc_588) (Ottman et al., 2017a). Transcriptomic data showed that most genes encoding enzymes in the mucin-degrading A, B, and D groups were significantly downregulated under mucin (−) conditions, with fold changes < 0.79 and *Padj* < 0.01, indicating their crucial roles in mucin degradation (**Figure 2** and **Supplementary Table S4**). Furthermore, most genes encoding mucin-degradation-associated transporters, such as fucose, GlcNAc, and sulfate transporters, were also significantly downregulated under mucin (−) conditions, with fold changes < 0.49 and *Padj* < 0.01. However, the transcript abundances of one gene encoding sulfatase in the mucin-degrading C group were highly upregulated under mucin (−) conditions, with fold changes > 3.76 and *Padj* < 0.01. These results are consistent with our previous

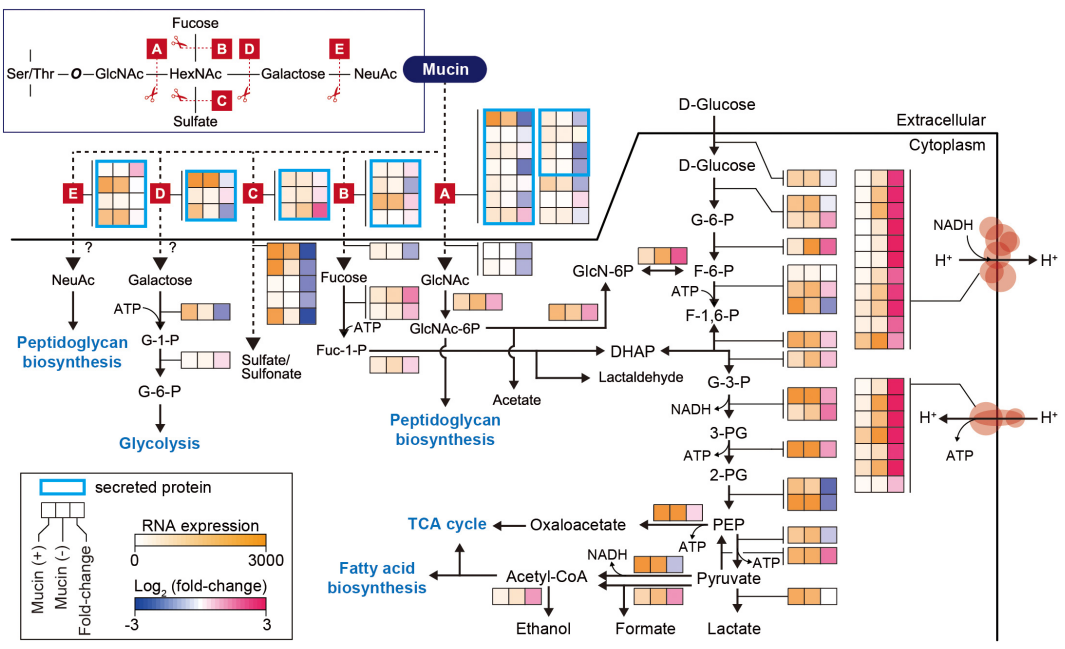

FIGURE 2 | Differentially expressed genes involved in mucin-degradation pathway and glycolytic/gluconeogenesis in *A. muciniphila*. Enzymes are represented according to their corresponding mucin-degrading reactions, as follows: A, *N*-acetylgalactosaminidase; B, L-fucosidase; C, sulfatase; D, galactosidase; E, neuraminidase. The heat map indicates RNA expression levels and $\log_2$ fold changes. Gene list and expression values are also shown in **Supplementary Table S4**.

understanding of transcriptomic and proteomic responses to mucin (Ottman et al., 2016, 2017a).

Additional reactions are necessary for converting monosaccharides into any of the intermediates of central carbon metabolism (**Figure 2**). These corresponding pathways were derived from the BioCyc and KEGG databases (Kanehisa, 2000; Caspi et al., 2016; Ottman et al., 2017a). Galactose is converted into glucose-6-phosphate (glucose-6-P) through the Leloir pathway, whereas GlcNAc is catabolized through glucosamine-6-phosphate (GlcN-6P) to fructose 6-phosphate (F-6-P). Fucose is catabolized through dihydroxyacetone phosphate (DHAP) to glyceraldehyde 3-phosphate (G-3-P) or through fuculose-1-phosphate to lactaldehyde. Additionally, NeuAc and GlcNAc can also be directly converted to peptidoglycan. Thus, the mucin-degrading pathway is also linked to the glycolysis pathway for catabolism. Interestingly, most of the genes involved in the glycolysis pathway showed similar expression levels between the two conditions, with $Padj > 0.01$, or significant upregulation under mucin (−) conditions, with fold changes of 1.4–3.5 and $Padj < 0.01$, with the exception of two enolase genes (Amuc_0844 and Amuc_1184), one dihydrolipoyl dehydrogenase gene (Amuc_1689), and one ATP-dependent 6-phosphofructokinase gene (Amuc_1481) (**Figure 2** and **Supplementary Table S4**). In accordance with the upregulation of genes in the glycolysis pathway, respiratory chain complex genes were also significantly upregulated. As mentioned above, all genes encoding ATP synthase, succinate dehydrogenase, and NADH dehydrogenase were highly upregulated during growth without mucin (**Figure 2** and **Supplementary Table S4**). Presumably, this regulation reflects a strategy to counteract the lower energy status in the absence of mucin, which has previously been shown to limit cell growth (Ottman et al., 2017a; van der Ark et al., 2018).

Identification of Extracellular Proteins Encoded in the *A. muciniphila* Genome

Next, we investigated extracellular or secreted proteins encoded in the *A. muciniphila* genome, as the extracellular materials of *A. muciniphila,* including the cell-free supernatant of *A. muciniphila* culture (Ottman et al., 2017b), purified Amuc_1100 protein (Plovier et al., 2016), and *A. muciniphila*-derived extracellular vesicles (Chelakkot et al., 2018), are able to recapitulate the effect of *A. muciniphila* in improving intestinal barrier integrity and the production of an anti-inflammatory cytokine. To identify genes encoding extracellular or secreted proteins, we set up a bioinformatics pipeline consisting of SignalP 4.1 (Dyrløv Bendtsen et al., 2004), SecretomeP 2.0 (Bendtsen et al., 2005), LipoP 1.0 (Juncker et al., 2003), TMHMM 2.0 (Krogh et al., 2001), and Phobious (Kall et al., 2007; Gomez et al., 2015; Cornejo-Granados et al., 2017; **Figure 3A**). These algorithms exhibited good performance in predicting the signal peptides, subcellular localization, and transmembrane helices of proteins. To predict classical and non-classical secreted proteins among the complete coding domain sequences (CDSs), SignalP 4.1 (Dyrløv Bendtsen et al., 2004) and SecretomeP 2.0 (Bendtsen et al., 2005) were used, respectively. Putative lipoprotein signal peptides were also identified using LipoP 1.0 (Juncker et al., 2003), and the predicted proteins were merged, resulting in a set of 627 unique proteins for *A. muciniphila* (**Figure 3A**). Among these, the presence of transmembrane regions was estimated by TMHMM 2.0 (Krogh et al., 2001), and proteins with no transmembrane domain were considered extracellular proteins. In total, the pipeline predicted 357 extracellular proteins (∼15.9% of the total proteins), which are listed in **Supplementary Table S5**. Amuc_1100, an outer membrane protein that has been shown to exhibit a probiotic effect on diet-induced obesity (Plovier et al., 2016), was also included among the extracellular proteins of *A. muciniphila*. Amuc_1100 was identified as a non-classical secreted protein without signal peptide type I, suggesting that this protein is not transported by the Sec proteins (**Supplementary Table S5**). In addition, the Amuc_1098 and Amuc_0336 proteins, which were found to be the most abundant outer membrane proteins through proteome analysis (Ottman et al., 2016, 2017b), were also classified as extracellular proteins by this analysis.

To understand the cellular functions of these extracellular proteins, we performed KEGG/GO term enrichment analyses for the 357 genes encoding these extracellular proteins. The results showed that 16 GO terms were significantly overrepresented in the biological process, molecular function, and cellular component categories, with $P < 0.025$ (**Figure 3B** and **Supplementary Table S6**). The most overrepresented GO term in the cellular component category was external encapsulating structure (GO:0030312), which is the representative cellular component reported for extracellular proteins (Gomez et al., 2015; **Supplementary Table S6**). Moreover, GO terms related to secretion, homeostasis, and carbohydrate metabolic process were highly enriched in the biological process category (**Figure 3B**). Interestingly, a significantly enriched term in the molecular function category was related to fucosidase, alpha-L-fucosidase, beta-*N*-acetylhexoaminidase, sulfuric ester hydrolase, hexosaminidase, hydrolase hydrolyzing O-glycosyl compounds, and hydrolase acting on glycosyl bonds, reflecting the mucin-degrading activity of the secretome (**Figure 3B** and **Supplementary Table S6**). This is consistent with the previously reported high fucosidase activity in the supernatant (Ottman et al., 2016). Furthermore, only the "other glycan degradation" KEGG pathway (00511) was significantly enriched, with a $P < 4.3 \times 10^{-10}$, indicating that mucin-degrading enzymes were highly enriched among the extracellular proteins. Among the 28 genes encoding mucin-degrading enzymes, 25 (89.3%) were predicted to be extracellular proteins (**Figure 2**). Taken together, the functions of the extracellular proteins are mainly related to mucin-degrading activity and tentative probiotic effectors (e.g., Amuc_1100).

Mucin-Depletion Activates Expression of Genes Encoding 48 Secreted Protein Candidates and Protein Secretion Pathways

Next, we examined how the expression of genes encoding protein secretion systems and secreted proteins is affected by the presence

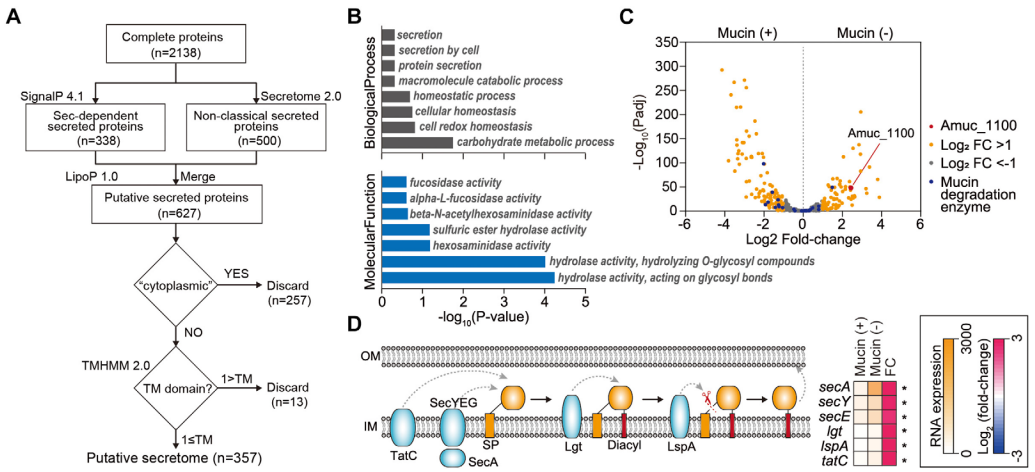

FIGURE 3 | Analysis of extracellular proteins and protein secretion systems in *A. muciniphila*. **(A)** Workflow to identify the extracellular proteins encoded in *A. muciniphila* genome. **(B)** Significantly enriched Gene Ontology (GO) terms among the predicted extracellular proteins. GO terms belonging to the biological process and molecular function categories are shown in gray and blue, respectively. **(C)** Volcano plots summarizing the differentially expressed genes encoding extracellular proteins. The negative $\log_{10}$ of the *Padj* is plotted on the Y-axis, and the $\log_2$ of the fold change is plotted on the X-axis. **(D)** Differentially expressed genes involved in protein secretion pathways in *A. muciniphila*. **Padj* < 0.01.

of mucin. Using *Padj* and fold-change thresholds (*Padj* < 0.01 and $|\log_2$ fold-change$|$ > 1), we identified a total of 197 DEGs, including 79 upregulated and 118 downregulated DEGs in mucin (−) conditions compared to mucin (+) conditions, that encoded extracellular proteins (**Figure 3C**). As mentioned above, genes encoding mucin-degrading enzymes were transcriptionally downregulated under mucin (−) conditions. By contrast, the gene encoding the Amuc_1100 protein was significantly upregulated (fold change = 5.40, *Padj* = 4.0×10^{-44}) under the mucin (−) condition (**Figure 3C**), suggesting the enhancement of probiotic effects (Plovier et al., 2016).

To export these proteins from the cytosol into the host environment, bacteria use unique protein secretion systems. Although several protein secretion systems were not fully identified in the *A. muciniphila* genome, Sec, Tat (twin-arginine targeting), and a part of the type II secretion system were found in the genome. Interestingly, the mucin-depletion condition also significantly enhanced the expression of most genes in the Sec and Tat systems, as well as of those encoding lipoprotein localization-associated proteins (fold change > 2.6, *Padj* < 3.2×10^{-18}) (**Figure 3D**). Taken together, the transcriptome analysis of *A. muciniphila* suggested that the presence or absence of mucin regulates the expression of Amuc-1100, as well as of the major protein secretion systems. These results indicate that the probiotic effect of *A. muciniphila* could be dependent on the mucin content of the culture conditions.

Mucin-Depletion Enhances *A. muciniphila*-Mediated Effects on HFD-Induced Obesity

In order to confirm the above hypothesis, we compared the effects of daily administration of *A. muciniphila* grown either on mucus-based [AK mucin (+)] or mucus-depleted [AK mucin (−)] medium on HFD-induced obesity. HFD-fed mice showed increased body weight (15%) and fasting blood glucose (12%) levels compared to control diet (ND)-fed mice after only 6 weeks of HFD treatment (**Supplementary Figures S1A,B**). These results indicate that HFD induces obesity and high blood glucose levels (Everard et al., 2013; Shin et al., 2014; Plovier et al., 2016). Interestingly, we found that an additional 4 weeks of treatment with AK mucin (−) attenuated HFD-induced changes in body weight and blood glucose levels more effectively than treatment with AK mucin (+) (**Figures 4A,B**).

The fact that treatment with *A. muciniphila* reduced body weight gain despite HFD consumption led us to additionally evaluate the effect of *A. muciniphila* on hepatic steatosis and adipocyte hypertrophy. Mice treated with AK mucin (−) exhibited a significantly lower hepatic triglyceride content ($P < 0.05$) than either untreated HFD-fed mice or HFD-fed mice treated with AK mucin (+) (**Supplementary Figures S1C,D**). Compared with the size distribution of epididymal adipocytes in the ND-fed group, small and medium adipocytes were significantly reduced (size > 1,000 μm^2), but the large adipocyte fraction (size < 3,000 μm^2) was significantly increased in HFD-fed mice ($P < 0.05$). The administration of *A. muciniphila* appeared to reduce adipocyte hypertrophy and increased the proportion of small adipocytes, which were more distinct in the HFD-fed mice treated with AK mucin (−) than in those treated with AK mucin (+) (**Figure 4C**). A similar trend was observed in subcutaneous adipocytes (**Supplementary Figures S1E,F**). Increased fat accumulation in white adipose tissue by various factors, including HFD treatment, has been shown to subsequently lead to ectopic fat deposition in brown adipose tissue (Calderon-Dominguez et al., 2016). When comparing mice treated with AK mucin (−) to HFD-fed mice, fat accumulation in brown adipose tissue was normalized (**Supplementary Figure S1G**).

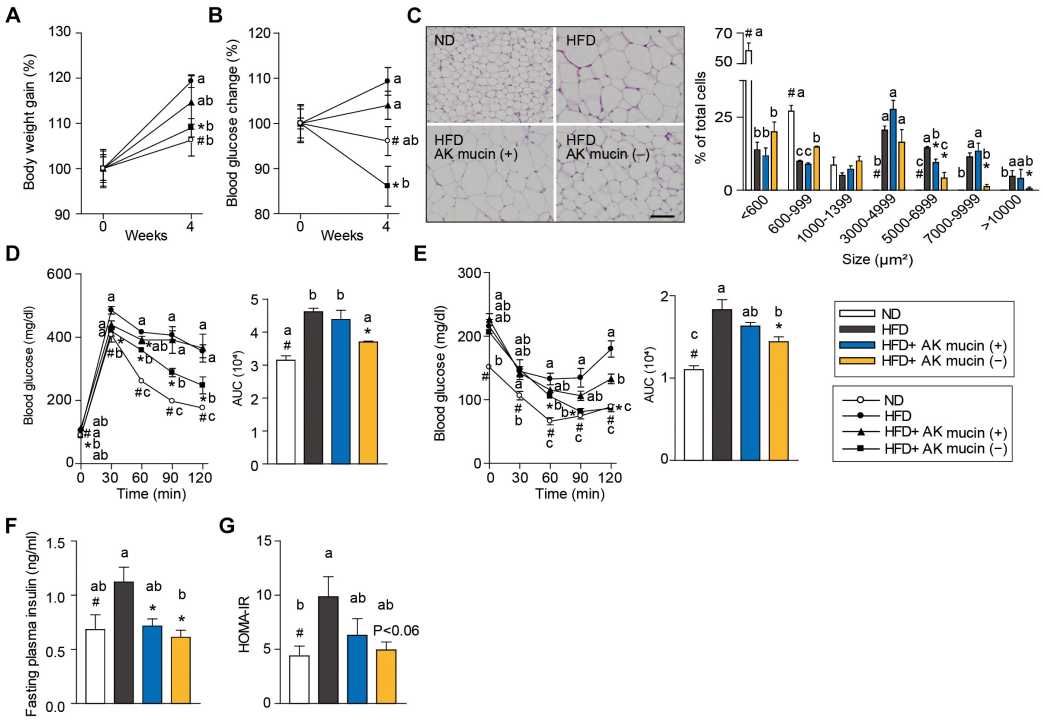

FIGURE 4 | Effects of *A. muciniphila* on HFD-induced obesity. **(A)** Body weight and **(B)** blood glucose change (%) after 4 weeks of treatment. **(C)** Representative H&E-stained images and size distribution of epididymal adipose tissue deposits. Scale bars, 100 μm. **(D)** Blood glucose change and the mean area under the curve (AUC) measured during the IP-GTT. **(E)** Blood glucose change and the mean area under the curve (AUC) measured during the IP-ITT. **(F)** Fasting plasma insulin and **(G)** HOMA-IR index measured after 4 weeks of treatment. Data are means ± SEM (n = 4–5 for each group). $^{\#}P < 0.05$, High fat diet (HFD) vs. Normal chow diet (ND) group, $^{*}P < 0.05$, HFD vs. *A. muciniphila*-treated group (two-tailed Student's t-test). ^{abc}Means not sharing a common letter are significantly different at $P < 0.05$ (Tukey-Kramer HSD test).

To evaluate whether *A. muciniphila* had an effect on glucose intolerance and insulin resistance, intraperitoneal glucose tolerance test (IP-GTT) and insulin tolerance test (IP-ITT) were performed after 4 weeks of *A. muciniphila* treatment (**Figures 4D,E**). As expected, HFD-fed mice exhibited a significant increase in blood glucose levels (**Figure 4D**) and plasma insulin (**Figure 4F**) compared to ND-fed mice, both in the fasting state and during the glucose measurement, suggesting a decrease in glucose tolerance following HFD treatment. Moreover, HFD-fed mice treated with AK mucin (−) showed significant improvements in glucose tolerance and insulin sensitivity ($P < 0.05$), as evidenced by reductions in the area under the curve (AUC) and fasting plasma insulin levels compared to those in the untreated HFD-fed mice (**Figures 4D–F**). In addition, the homeostatic model assessment-insulin resistance (HOMA-IR) index, which is closely linked to insulin resistance status, was also significantly increased in HFD-fed mice. However, *A. muciniphila* treatment appeared to improve insulin resistance (**Figure 4G**). In particular, treatment with AK mucin (−) tend to improve insulin resistance than treatment with AK mucin (+). Although it was reported that there is no significant difference in probiotic effects based on the use of medium with or without mucin (Plovier et al., 2016), our results suggest that mucin-depletion conditions could enhance the beneficial effects of *A. muciniphila* compared to mucin-containing conditions.

Mucin-Depletion Improves *A. muciniphila*-Mediated Effects on Intestinal Barrier Integrity and Inflammation

Altered gut barrier function is associated with increased intestinal permeability through decreased expression of tight junction proteins (Ahmad et al., 2014) in obese and diabetic mice. We therefore assessed the effects of AK mucin (+) or AK mucin (−) on endotoxemia and the expression of genes associated with the gut barrier. While HFD-fed mice displayed higher circulating LPS levels than ND-fed mice (Everard et al., 2013; Shin et al., 2014; Plovier et al., 2016; Chelakkot et al., 2018), suggesting metabolic endotoxemia, treatment with *A. muciniphila* restored LPS levels to that observed in the ND group, regardless of mucin growth conditions (**Figure 5A**). *A. muciniphila* treatment changed the expression of some genes encoding intestinal barrier proteins, as well as mucin. In the ileum, expression of genes encoding barrier-forming tight-junction proteins (CLDN3 and 4) was significantly higher in mice treated with AK mucin (−) ($P < 0.05$) than in untreated HFD-fed mice (**Figure 5B**). In addition, long-term HFD treatment has been shown to

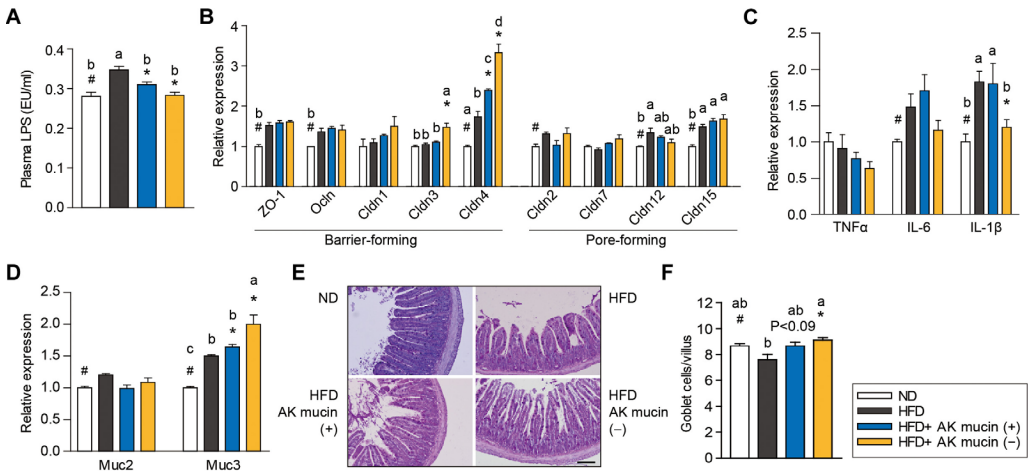

FIGURE 5 | Effects of *A. muciniphila* on intestinal barrier function and inflammation. **(A)** Circulating plasma LPS measured after 4 weeks of treatment. **(B)** Expression of genes encoding barrier- or pore-forming tight junction proteins, **(C)** proinflammatory cytokines, and **(D)** mucin in the ileum. **(E)** Representative PAS-stained images and **(F)** mucus-containing goblet cell density in the ileum. Scale bars, 100 μm. Data are means ± SEM (n = 4–5 for each group). $^{\#}P < 0.05$, High fat diet (HFD) vs. Normal chow diet (ND) group, $^{*}P < 0.05$, HFD vs. *A. muciniphila*-treated group (two-tailed Student's t-test). ^{abc}Means not sharing a common letter are significantly different at $P < 0.05$ (Tukey-Kramer HSD test).

increase the expression of pro-inflammatory cytokines in the gut (Cani et al., 2008), and some cytokines can directly influence goblet cell function. Consistent with this, we observed that HFD treatment increased the expression of genes encoding pro-inflammatory cytokines (IL-6 and IL-1β); however, AK mucin (−) significantly inhibited intestinal inflammation (**Figure 5C**). Although the expression of *Muc2*, encoding a secreted form of mucin, was not altered, the expression of *Muc3*, encoding a membrane-bound mucin, was significantly upregulated by *A. muciniphila* treatment (**Figure 5D**). Moreover, treatment with AK mucin (−) led to greater goblet cell density in the ileum (**Figures 5E,F**). Therefore, this result suggests that in AK mucin (−)-fed mice, as compared to HFD-fed mice, more mucus is produced (McGuckin and Hasnain, 2017).

DISCUSSION

A. muciniphila is widely considered a next-generation beneficial microbe. This bacterium resides in the mucus layer of the host and regulates intestinal homeostasis and intestinal barrier integrity by affecting host signaling pathways (Dao et al., 2016; Cani and de Vos, 2017). Recently, several studies demonstrated that administration of *A. muciniphila* or *A. muciniphila*-derived compounds improves not only body weight and glucose tolerance, but also intestinal barrier integrity (Everard et al., 2013; Shin et al., 2014; Plovier et al., 2016; Chelakkot et al., 2018). Although the interaction between *A. muciniphila* and the mucus layer has been shown to be significant (Johansson et al., 2015), it remained unclear how this bacterium engages in crosstalk with host cells in the dynamic mucus layer environment.

In this study, we elucidated the effect of mucin on the gene expression and probiotic traits of *A. muciniphila*. Transcriptome analysis showed that most genes encoding mucin-degrading enzymes were significantly upregulated under mucin (+) conditions. By contrast, most glycolysis-related and energy metabolic pathway-related genes were upregulated under mucin (−) conditions. The observed changes in transcript levels reflect the fact that mucin-degradation-associated genes, as well as mucin-derived monosaccharide-associated transporters, were induced for cell growth with mucin, showing the adaptation of this gut bacterium to the mucosal niche (Ottman et al., 2017a; Thursby and Juge, 2017). However, the depletion of mucin induced a distinct response in terms of the upregulation of glycolysis and energy metabolic pathways, including NADH dehydrogenase and ATP synthase (**Figure 2**). In particular, the upregulation of these major genes related to energy metabolism indicates that *A. muciniphila* might be switching to preferred energy generation pathways under mucin (−) conditions. This regulation is presumably a strategy to adapt to the lower energy status under mucin-depleted conditions, which have been shown to limit cell growth (Ottman et al., 2017a).

Importantly, the absence of mucin induces expression of the gene encoding Amuc_1100. This result indicates that the beneficial effect of *A. muciniphila* may depend on the mucin content of the corresponding environment. In this context, the 78 upregulated extracellular proteins in mucin (−) conditions compared to mucin (+) conditions (fold change > 2, $Padj < 0.01$), similar to Amuc_1100, can be thought of as potential candidate proteins for beneficial effects of *A. muciniphila* in HFD-induced obesity, but additional confirmation is required. In addition, genes in the Sec and Tat secreted systems, as well as those encoding lipoprotein localization-associated proteins, were upregulated under mucin (−) conditions. Interestingly, prolipoprotein diacylglyceryl transferase (Amuc_1104) is located very close to the gene cluster (Amuc_1098–Amuc_1102) that includes Amuc_1100. Since

various glycolipids and lipoproteins have also been shown to activate TLR2 in a similar manner to *A. muciniphila* (Yan et al., 2007), other lipoproteins besides Amuc-1100 may also be potential candidate proteins.

Several studies have highlighted the probiotic effects of *A. muciniphila* on host physiology, as mentioned above. As an extension of these studies, we demonstrated that the administration of *A. muciniphila* grown under mucin (−) conditions reduced obesity and improved intestinal barrier integrity in HFD-fed mice more efficiently than *A. muciniphila* grown under mucin (+) conditions. We observed that long-term HFD treatment without *A. muciniphila* resulted in reduced goblet cell density in the ileum, but in AK mucin (−)-fed mice, the reduced goblet cell density was restored. Based on these results, we speculate that the mucus layer of mice, which is thinned by obesity or diabetes (Everard et al., 2013; Shin et al., 2014), induces the expression of proteins capable of inducing a probiotic effect in *A. muciniphila*, resulting in the upregulation of the Muc3 gene and the regeneration of mucin, so that *A. muciniphila* is able to restore and colonize the mucus layer. This crosstalk between host cells and *A. muciniphila* is thought to be a strategy that allows the bacterium to survive in the intestinal mucus layer.

CONCLUSION

In conclusion, this study revealed the effect of mucin on the gene expression and beneficial effects of *A. muciniphila* on HFD-induced obesity. The mucin content of the growth environment is crucial in inducing *A. muciniphila*-mediated improvements in the treatment of HFD-induced excessive body weight, glucose intolerance, intestinal inflammation, and compromised intestinal barrier integrity related to a decrease in goblet cell density. Our finding provides a novel principle for the development of *A. muciniphila* for human therapeutics and suggests avoiding animal-derived mucin in the growth medium for better probiotic activity of *A. muciniphila*.

AUTHOR CONTRIBUTIONS

B-CK, C-HL, and B-KC conceived and supervised the study. JS, B-CK, C-HL, and B-KC designed the experiments. JS, J-RN, D-HC, M-SR, and Y-HK performed the experiments. JS, SC, B-CK, C-HL, and B-KC analyzed the data. JS, SC, MK, EL, BK, B-CK, C-HL, and B-KC wrote the manuscript and commented on the manuscript.

FUNDING

This work was supported by the Intelligent Synthetic Biology Center of the Global Frontier Project (2011-0031957 to B-KC), the Bio and Medical Technology Development Program (2018M3A9H3024759 to B-KC, 2015M3C9A4053394 to MK) through the National Research Foundation of Korea (NRF) funded by the Ministry of Science and ICT (MSIT), and the Korea Research Institute of Bioscience and Biotechnology (KRIBB) Research Initiative Program (to C-HL).

SUPPLEMENTARY MATERIAL

The Supplementary Material for this article can be found online at: https://www.frontiersin.org/articles/10.3389/fmicb.2019.01137/full#supplementary-material

REFERENCES

Ahmad, R., Chaturvedi, R., Olivares-Villagómez, D., Habib, T., Asim, M., Shivesh, P., et al. (2014). Targeted colonic claudin-2 expression renders resistance to epithelial injury, induces immune suppression, and protects from colitis. *Mucosal Immunol.* 7, 1340–1353. doi: 10.1038/mi.2014.21

Ahn, S., Jin, T.-E., Chang, D.-H., Rhee, M.-S., Kim, H. J., Lee, S. J., et al. (2016). *Agathobaculum butyriciproducens* gen. nov. sp. nov., a strict anaerobic, butyrate-producing gut bacterium isolated from human faeces and reclassification of *Eubacterium desmolans* as *Agathobaculum desmolans* comb. nov. *Int. J. Syst. Evol. Microbiol.* 66, 3656–3661. doi: 10.1099/ijsem.0.001195

Belzer, C., and de Vos, W. M. (2012). Microbes inside—from diversity to function: the case of *Akkermansia*. *ISME J.* 6, 1449–1458. doi: 10.1038/ismej.2012.6

Bendtsen, J. D., Kiemer, L., Fausbøll, A., and Brunak, S. (2005). Non-classical protein secretion in bacteria. *BMC Microbiol.* 5:58. doi: 10.1186/1471-2180-5-58

Bernardo, D., Sánchez, B., Al-Hassi, H. O., Mann, E. R., Urdaci, M. C., Knight, S. C., et al. (2012). Microbiota/host crosstalk biomarkers: regulatory response of human intestinal dendritic cells exposed to *Lactobacillus* extracellular encrypted peptide. *PLoS One* 7:e36262. doi: 10.1371/journal.pone.0036262

Calderon-Dominguez, M., Mir, J. F., Fucho, R., Weber, M., Serra, D., and Herrero, L. (2016). Fatty acid metabolism and the basis of brown adipose tissue function. *Adipocyte* 5, 98–118. doi: 10.1080/21623945.2015.1122857

Cani, P. D., Amar, J., Iglesias, M. A., Poggi, M., Knauf, C., Bastelica, D., et al. (2007). Metabolic endotoxemia initiates obesity and insulin resistance. *Diabetes* 56, 1761–1772. doi: 10.2337/db06-1491

Cani, P. D., Bibiloni, R., Knauf, C., Waget, A., Neyrinck, A. M., Delzenne, N. M., et al. (2008). Changes in gut microbiota control metabolic endotoxemia-induced inflammation in high-fat diet-induced obesity and diabetes in mice. *Diabetes* 57, 1470–1481. doi: 10.2337/db07-1403

Cani, P. D., and de Vos, W. M. (2017). Next-generation beneficial microbes: the case of *Akkermansia muciniphila*. *Front. Microbiol.* 8:1765. doi: 10.3389/fmicb.2017.01765

Cani, P. D., Osto, M., Geurts, L., and Everard, A. (2012). Involvement of gut microbiota in the development of low-grade inflammation and type 2 diabetes associated with obesity. *Gut Microbes* 3, 279–288. doi: 10.4161/gmic.19625

Caspi, R., Billington, R., Ferrer, L., Foerster, H., Fulcher, C. A., Keseler, I. M., et al. (2016). The MetaCyc database of metabolic pathways and enzymes and the BioCyc collection of pathway/genome databases. *Nucleic Acids Res.* 44, D471–D480. doi: 10.1093/nar/gkv1164

Chelakkot, C., Choi, Y., Kim, D.-K., Park, H. T., Ghim, J., Kwon, Y., et al. (2018). *Akkermansia muciniphila*-derived extracellular vesicles influence gut permeability through the regulation of tight junctions. *Exp. Mol. Med.* 50:e450. doi: 10.1038/emm.2017.282

Cornejo-Granados, F., Zatarain-Barrón, Z. L., Cantu-Robles, V. A., Mendoza-Vargas, A., Molina-Romero, C., Sánchez, F., et al. (2017). Secretome prediction of two *M. tuberculosis* clinical isolates reveals their high antigenic density and potential drug targets. *Front. Microbiol.* 8:128. doi: 10.3389/fmicb.2017.00128

Dao, M. C., Everard, A., Aron-Wisnewsky, J., Sokolovska, N., Prifti, E., Verger, E. O., et al. (2016). *Akkermansia muciniphila* and improved metabolic health during a dietary intervention in obesity: relationship with gut microbiome richness and ecology. *Gut* 65, 426–436. doi: 10.1136/gutjnl-2014-308778

Deplancke, B., and Gaskins, H. R. (2001). Microbial modulation of innate defense: goblet cells and the intestinal mucus layer. *Am. J. Clin. Nutr.* 73, 1131S–1141S. doi: 10.1093/ajcn/73.6.1131S

Derrien, M. (2004). *Akkermansia muciniphila* gen. nov., sp. nov., a human intestinal mucin-degrading bacterium. *Int. J. Syst. Evol. Microbiol.* 54, 1469–1476. doi: 10.1099/ijs.0.02873-0

Derrien, M., Belzer, C., and de Vos, W. M. (2017). *Akkermansia muciniphila* and its role in regulating host functions. *Microb. Pathog.* 106, 171–181. doi: 10.1016/j.micpath.2016.02.005

Dyrløv Bendtsen, J., Nielsen, H., von Heijne, G., and Brunak, S. (2004). Improved prediction of signal peptides: signalP 3.0. *J. Mol. Biol.* 340, 783–795. doi: 10.1016/j.jmb.2004.05.028

Everard, A., Belzer, C., Geurts, L., Ouwerkerk, J. P., Druart, C., Bindels, L. B., et al. (2013). Cross-talk between *Akkermansia muciniphila* and intestinal epithelium controls diet-induced obesity. *Proc. Natl. Acad. Sci. U.S.A.* 110, 9066–9071. doi: 10.1073/pnas.1219451110

Gomez, S., Adalid-Peralta, L., Palafox-Fonseca, H., Cantu-Robles, V. A., Soberón, X., Sciutto, E., et al. (2015). Genome analysis of excretory/secretory proteins in *Taenia solium* reveals their abundance of antigenic regions (AAR). *Sci. Rep.* 5:9683. doi: 10.1038/srep09683

Hooper, L. V., Littman, D. R., and Macpherson, A. J. (2012). Interactions between the microbiota and the immune system. *Science* 336, 1268–1273. doi: 10.1126/science.1223490

Johansson, M. E. V., Jakobsson, H. E., Holmén-Larsson, J., Schütte, A., Ermund, A., Rodríguez-Piñeiro, A. M., et al. (2015). Normalization of host intestinal mucus layers requires long-term microbial colonization. *Cell Host Microbe* 18, 582–592. doi: 10.1016/j.chom.2015.10.007

Johansson, M. E. V., Larsson, J. M. H., and Hansson, G. C. (2011). The two mucus layers of colon are organized by the MUC2 mucin, whereas the outer layer is a legislator of host-microbial interactions. *Proc. Natl. Acad. Sci. U.S.A.* 108(Suppl._1), 4659–4665. doi: 10.1073/pnas.1006451107

Juncker, A. S., Willenbrock, H., von Heijne, G., Brunak, S., Nielsen, H., and Krogh, A. (2003). Prediction of lipoprotein signal peptides in Gram-negative bacteria. *Protein Sci.* 12, 1652–1662. doi: 10.1110/ps.0303703

Kall, L., Krogh, A., and Sonnhammer, E. L. L. (2007). Advantages of combined transmembrane topology and signal peptide prediction–the Phobius web server. *Nucleic Acids Res.* 35, W429–W432. doi: 10.1093/nar/gkm256

Kanehisa, M. (2000). KEGG: Kyoto encyclopedia of genes and genomes. *Nucleic Acids Res.* 28, 27–30. doi: 10.1093/nar/28.1.27

Karlsson, C. L. J., Onnerfält, J., Xu, J., Molin, G., Ahrné, S., and Thorngren-Jerneck, K. (2012). The microbiota of the gut in preschool children with normal and excessive body weight. *Obesity* 20, 2257–2261. doi: 10.1038/oby.2012.110

Kim, Y.-H., Hwang, J. H., Kim, K.-S., Noh, J.-R., Choi, D.-H., Kim, D.-K., et al. (2015). Metformin ameliorates acetaminophen hepatotoxicity via Gadd45β-dependent regulation of JNK signaling in mice. *J. Hepatol.* 63, 75–82. doi: 10.1016/j.jhep.2015.02.008

Krogh, A., Larsson, B., von Heijne, G., and Sonnhammer, E. L. (2001). Predicting transmembrane protein topology with a hidden Markov model: application to complete genomes. *J. Mol. Biol.* 305, 567–580. doi: 10.1006/jmbi.2000.4315

Love, M. I., Huber, W., and Anders, S. (2014). Moderated estimation of fold change and dispersion for RNA-seq data with DESeq2. *Genome Biol.* 15:550.

McGuckin, M. A., and Hasnain, S. Z. (2017). Goblet cells as mucosal sentinels for immunity. *Mucosal Immunol.* 10, 1118–1121. doi: 10.1038/mi.2016.132

Ottman, N., Davids, M., Suarez-Diez, M., Boeren, S., Schaap, P. J., Martins dos Santos, V. A. P., et al. (2017a). Genome-scale model and omics analysis of metabolic capacities of *Akkermansia muciniphila* reveal a preferential mucin-degrading lifestyle. *Appl. Environ. Microbiol.* 83:e01014-17. doi: 10.1128/AEM.01014-17

Ottman, N., Reunanen, J., Meijerink, M., Pietilä, T. E., Kainulainen, V., Klievink, J., et al. (2017b). Pili-like proteins of *Akkermansia muciniphila* modulate host immune responses and gut barrier function. *PLoS One* 12:e0173004. doi: 10.1371/journal.pone.0173004

Ottman, N., Huuskonen, L., Reunanen, J., Boeren, S., Klievink, J., Smidt, H., et al. (2016). Characterization of outer membrane proteome of *Akkermansia muciniphila* reveals sets of novel proteins exposed to the human intestine. *Front. Microbiol.* 7:1157. doi: 10.3389/fmicb.2016.01157

Ottman, N., Smidt, H., de Vos, W. M., and Belzer, C. (2012). The function of our microbiota: who is out there and what do they do? *Front. Cell. Infect. Microbiol.* 2:104. doi: 10.3389/fcimb.2012.00104

Plovier, H., Everard, A., Druart, C., Depommier, C., Van Hul, M., Geurts, L., et al. (2016). A purified membrane protein from *Akkermansia muciniphila* or the pasteurized bacterium improves metabolism in obese and diabetic mice. *Nat. Med.* 23, 107–113. doi: 10.1038/nm.4236

Png, C. W., Lindén, S. K., Gilshenan, K. S., Zoetendal, E. G., McSweeney, C. S., Sly, L. I., et al. (2010). Mucolytic bacteria with increased prevalence in IBD mucosa augment in vitro utilization of mucin by other bacteria. *Am. J. Gastroenterol.* 105, 2420–2428. doi: 10.1038/ajg.2010.281

Quinlan, A. R., and Hall, I. M. (2010). BEDTools: a flexible suite of utilities for comparing genomic features. *Bioinformatics* 26, 841–842. doi: 10.1093/bioinformatics/btq033

Ruiz, L., Hevia, A., Bernardo, D., Margolles, A., and Sánchez, B. (2014). Extracellular molecular effectors mediating probiotic attributes. *FEMS Microbiol. Lett.* 359, 1–11. doi: 10.1111/1574-6968.12576

Saito, R., Smoot, M. E., Ono, K., Ruscheinski, J., Wang, P.-L., Lotia, S., et al. (2012). A travel guide to Cytoscape plugins. *Nat. Methods* 9, 1069–1076. doi: 10.1038/nmeth.2212

Sánchez, B., Bressollier, P., and Urdaci, M. C. (2008). Exported proteins in probiotic bacteria: adhesion to intestinal surfaces, host immunomodulation and molecular cross-talking with the host. *FEMS Immunol. Med. Microbiol.* 54, 1–17. doi: 10.1111/j.1574-695X.2008.00454.x

Sanchez, B., Urdaci, M. C., and Margolles, A. (2010). Extracellular proteins secreted by probiotic bacteria as mediators of effects that promote mucosa-bacteria interactions. *Microbiology* 156, 3232–3242. doi: 10.1099/mic.0.044057-0

Shannon, P., Markiel, A., Ozier, O., Baliga, N. S., Wang, J. T., Ramage, D., et al. (2003). Cytoscape: a software environment for integrated models of biomolecular interaction networks. *Genome Res.* 13, 2498–2504. doi: 10.1101/gr.1239303

Shin, N.-R., Lee, J.-C., Lee, H.-Y., Kim, M.-S., Whon, T. W., Lee, M.-S., et al. (2014). An increase in the *Akkermansia* spp. population induced by metformin treatment improves glucose homeostasis in diet-induced obese mice. *Gut* 63, 727–735. doi: 10.1136/gutjnl-2012-303839

Sommer, F., and Bäckhed, F. (2013). The gut microbiota–masters of host development and physiology. *Nat. Rev. Microbiol.* 11, 227–238. doi: 10.1038/nrmicro2974

Tailford, L. E., Crost, E. H., Kavanaugh, D., and Juge, N. (2015). Mucin glycan foraging in the human gut microbiome. *Front. Genet.* 6:81. doi: 10.3389/fgene.2015.00081

Thursby, E., and Juge, N. (2017). Introduction to the human gut microbiota. *Biochem. J.* 474, 1823–1836. doi: 10.1042/BCJ20160510

van der Ark, K. C. H., Aalvink, S., Suarez-Diez, M., Schaap, P. J., de Vos, W. M., and Belzer, C. (2018). Model-driven design of a minimal medium for *Akkermansia muciniphila* confirms mucus adaptation. *Microb. Biotechnol.* 11, 476–485. doi: 10.1111/1751-7915.13033

van Passel, M. W. J., Kant, R., Zoetendal, E. G., Plugge, C. M., Derrien, M., Malfatti, S. A., et al. (2011). The genome of *Akkermansia muciniphila*, a dedicated intestinal mucin degrader, and its use in exploring intestinal metagenomes. *PLoS One* 6:e16876. doi: 10.1371/journal.pone.0016876

Wang, L., Christophersen, C. T., Sorich, M. J., Gerber, J. P., Angley, M. T., and Conlon, M. A. (2011). Low relative abundances of the mucolytic bacterium *Akkermansia muciniphila* and *Bifidobacterium* spp. in feces of children with autism. *Appl. Environ. Microbiol.* 77, 6718–6721. doi: 10.1128/AEM.05212-11

Yan, F., Cao, H., Cover, T. L., Whitehead, R., Washington, M. K., and Polk, D. B. (2007). Soluble proteins produced by probiotic bacteria regulate intestinal epithelial cell survival and growth. *Gastroenterology* 132, 562–575. doi: 10.1053/j.gastro.2006.11.022

Zhang, X., Shen, D., Fang, Z., Jie, Z., Qiu, X., Zhang, C., et al. (2013). Human gut microbiota changes reveal the progression of glucose intolerance. *PLoS One* 8:e71108. doi: 10.1371/journal.pone.0071108

Conflict of Interest Statement: B-CK was employed by company HealthBiome, Inc.

The remaining authors declare that the research was conducted in the absence of any commercial or financial relationships that could be construed as a potential conflict of interest.

Copyright © 2019 Shin, Noh, Chang, Kim, Kim, Lee, Cho, Ku, Rhee, Kim, Lee and Cho. This is an open-access article distributed under the terms of the Creative Commons Attribution License (CC BY). The use, distribution or reproduction in other forums is permitted, provided the original author(s) and the copyright owner(s) are credited and that the original publication in this journal is cited, in accordance with accepted academic practice. No use, distribution or reproduction is permitted which does not comply with these terms.

frontiers in Microbiology

ORIGINAL RESEARCH
published: 07 June 2019
doi: 10.3389/fmicb.2019.01286

Investigating Host Microbiota Relationships Through Functional Metagenomics

Elisabeth Laville[1], Josette Perrier[2], Nada Bejar[1], Marc Maresca[2], Jeremy Esque[1], Alexandra S. Tauzin[1], Emna Bouhajja[1], Marion Leclerc[3], Elodie Drula[4,5], Bernard Henrissat[4,5], Stephane Berdah[6,7], Eric Di Pasquale[6,7], Patrick Robe[8] and Gabrielle Potocki-Veronese[1]*

[1] INSA, INRA, CNRS, LISBP, Université de Toulouse, Toulouse, France, [2] iSm2, Centrale Marseille, CNRS, Aix-Marseille University, Marseille, France, [3] UMR1319, Micalis, Institut National de la Recherche Agronomique, Jouy-en-Josas, France, [4] CNRS, Architecture et Fonction des Macromolécules Biologiques, Aix-Marseille Université, Marseille, France, [5] USC 1408 AFMB, INRA, Marseille, France, [6] UMRT24 IFSTTAR, Laboratoire de Biomécanique Appliquée, Faculté de Médecine Secteur Nord, Aix-Marseille University, Marseille, France, [7] Inst Neurophysiopathol, INP, CNRS, Aix-Marseille Université, Marseille, France, [8] Givaudan SA, Toulouse, France

OPEN ACCESS

Edited by:
Vishal Singh,
The University of Toledo,
United States

Reviewed by:
Alfonso Benítez-Páez,
Instituto de Agroquímica y Tecnología de Alimentos (IATA), Spain
Mirjam Perner,
GEOMAR Helmholtz Centre for Ocean Research Kiel, Germany

***Correspondence:**
Elisabeth Laville
laville@insa-toulouse.fr

Specialty section:
This article was submitted to Microbial Symbioses, a section of the journal Frontiers in Microbiology

Received: *11 December 2018*
Accepted: *23 May 2019*
Published: *07 June 2019*

Citation:
Laville E, Perrier J, Bejar N, Maresca M, Esque J, Tauzin AS, Bouhajja E, Leclerc M, Drula E, Henrissat B, Berdah S, Di Pasquale E, Robe P and Potocki-Veronese G (2019) Investigating Host Microbiota Relationships Through Functional Metagenomics. Front. Microbiol. 10:1286. doi: 10.3389/fmicb.2019.01286

The human Intestinal mucus is formed by glycoproteins, the O- and N-linked glycans which constitute a crucial source of carbon for commensal gut bacteria, especially when deprived of dietary glycans of plant origin. In recent years, a dozen carbohydrate-active enzymes from cultivated mucin degraders have been characterized. But yet, considering the fact that uncultured species predominate in the human gut microbiota, these biochemical data are far from exhaustive. In this study, we used functional metagenomics to identify new metabolic pathways in uncultured bacteria involved in harvesting mucin glycans. First, we performed a high-throughput screening of a fosmid metagenomic library constructed from the ileum mucosa microbiota using chromogenic substrates. The screening resulted in the isolation of 124 clones producing activities crucial in the degradation of human O- and N-glycans, namely sialidases, β-D-N-acetyl-glucosaminidase, β-D-N-acetyl-galactosaminidase, and/or β-D-mannosidase. Thirteen of these clones were selected based on their diversified functional profiles and were further analyzed on a secondary screening. This step consisted of lectin binding assays to demonstrate the ability of the clones to degrade human intestinal mucus. In total, the structural modification of several mucin motifs, sialylated mucin ones in particular, was evidenced for nine clones. Sequencing their metagenomic loci highlighted complex catabolic pathways involving the complementary functions of glycan sensing, transport, hydrolysis, deacetylation, and deamination, which were sometimes associated with amino acid metabolism machinery. These loci are assigned to several *Bacteroides* and *Feacalibacterium* species highly prevalent and abundant in the gut microbiome and explain the metabolic flexibility of gut bacteria feeding both on dietary and human glycans.

Keywords: functional metagenomics, carbohydrate-active enzymes, human intestinal mucin, human gut microbiota, lectin binding

INTRODUCTION

The human intestinal tract harbors a dense commensal microbial community whose interactions with the host are of paramount importance for its health and well-being, particularly for the development of immunity and protection against invasion by pathogens. One of the best-known functions of the microbiota is its contribution to the digestion of dietary fibers, derived mainly from plant cell walls. Dietary fibers, consisting of polysaccharides of great structural diversity, represent the main energy source for the microbiota. The majority of gut bacterial species possess an enzymatic arsenal in the form of carbohydrate-active enzymes (CAZymes; Lombard et al., 2014) used to depolymerize these fibers. The products are further fermented to provide Short chain fatty acids (SCFAs) to the host. By contrast CAZymes produced by the human digestive system can only act on digestible starch and some other simple sugars such as sucrose or lactose (El Kaoutari et al., 2013). In addition to dietary fibers, intestinal microorganisms use glycans associated with human glycoproteins as a source of energy in particular mucin glycans that are secreted by the goblet cells of the intestinal epithelium. Mucin glycoproteins contain a large panel of mostly O-linked, and some N-linked, glycan structures (Podolsky, 1985; Robbe et al., 2004). Mucins represent a protective barrier for the intestine that is perpetually renewed. Mucus-colonizing bacteria produce both proteins to adhere to mucins and enzymes to degrade them (Tailford et al., 2015). The enzymatic machinery of these bacteria allows mucins to be recycled.

In recent years, growth assays on pig and human mucins, combined with pioneering genomic and transcriptomic studies, have shown that a number of pathogens and commensals (Tailford et al., 2015; Martens et al., 2018), including several *Bacteroides* species (Bäckhed et al., 2005; Sonnenburg et al., 2005; Martens et al., 2008; Marcobal et al., 2013), *Ruminococcus gnavus* (Owen et al., 2017) and the probiotic species *Akkermansia muciniphila* (Derrien et al., 2004), are involved in mucin degradation. This was especially described in cases of dietary fiber deprivation, when certain commensals shift their metabolism from dietary to host glycans (Desai et al., 2016). Furthermore, recent studies have also shown correlations between host diet, a reduction in mucus thickness, microbiota composition, and inflammatory bowel diseases (ulcerative colitis and Crohn's disease) and colorectal cancers (Pickard et al., 2014; Jakobsson et al., 2015; Desai et al., 2016). Despite these recent advances, only a dozen CAZymes (reviewed in Tailford et al., 2015) have been biochemically proven to degrade mucin oligosaccharides, and our understanding of mucin glycan-degrading pathways is almost exclusively restricted to cultured species. To date, only one enzyme has been characterized as involved in the degradation of human N-glycans by an uncultured gut bacterium (Ladevèze et al., 2013, 2015). Considering the fact that the majority of microbiota species are still uncultured, the studies so far conducted into the degradation of human glycans by gut bacteria are thus far from exhaustive.

In this study, we used functional metagenomics to identify mucin-degrading pathways from the uncultured fraction of the human gut microbiota. A two-step activity-based screening strategy was applied to search for mucin catabolic pathways in a mucosal ileal metagenomic library, and to demonstrate their involvement in the structural modification of human colon mucus. Genomic and metagenomic data were integrated to assess the abundance and prevalence of these mucin glycan utilization loci in the human gut microbiome, and to reveal synteny with genomic loci from reference gut bacteria, which had not previously been proven to be involved in these host–microbiota relationships.

MATERIALS AND METHODS

Metagenomic DNA Sampling and Library Construction

Bacterial metagenomic DNA was obtained from the distal ileum sample of a 50-55-year-old patient undergoing colonoscopy and surgery for a suspected cancer of the lower colon after patient had been subjected to a cleansing preparation. The patient did not receive any antibiotics or other drugs in the 6 months before sampling. The sampling protocol was approved by the local ethics committee: the Comité de Protection des Personnes Sud Est V (Ref.: 07-CHUG-21; B. Habozit, J. L. Crakowski, J. Juge, J. Grunwald, E. Svhan, and E. Fontaine on the committee). A segment of 2 cm^2 was obtained from a healthy zone, before being immediately frozen and kept at −80°C until processing. The ileal mucosa was scraped, an enriched bacterial fraction was recovered using the method described in Courtois et al. (2003), and the metagenomic DNA was extracted as described in Tasse et al. (2010). Fragments of between 30 and 40 kb in size were isolated and cloned into the pCC1FOS fosmid (Epicenter Technologies). EPI100 *E. coli* cells were then transfected to obtain a library of 20,000 clones. Recombinant clones were transferred to 384-well microtiter plates containing a Luria-Bertani (LB) medium, supplemented with 12.5 mg/L chloramphenicol and 8% (w/v) glycerol. They were grown for a period of 22 h at 37°C and then frozen and conserved at −80°C. All other culture media mentioned in this study contained 12.5 mg/L chloramphenicol.

Metagenomic Library Screening

The library was gridded using an automated microplate gridder (K2, KBiosystem, Basildon, United Kingdom) on 22 cm × 22 cm trays containing a solid agar medium supplemented with 12.5 mg/L chloramphenicol and with chromogenic substrates at a final concentration of 60 µg/mL (w/v). The chromogenic substrates used – 5-Bromo-4-chloro-3-indolyl a-L-fucopyranoside (X-α-L-Fuc), 5-Bromo-4-chloro-3-indolyl 2-acetamido-2-deoxy-b-D-glucopyranoside (X-β-D-GlcNac), 5-Bromo-4-chloro-3-indolyl N-acetyl-a-D-neuraminic acid (X-α-D-Neu5Ac), 5-Bromo-4-chloro-3-indolyl 2-acetamido-2-deoxy-b-D-galactopyranoside (X-β-D-GalNac), 5-Bromo-4-chloro-3-indolyl a-D-mannopyranoside (X-α-D-Man), and 5-Bromo-4-chloro-3-indolyl b-D-mannopyranoside (X-β-D-Man) – were purchased from Carbosynth[1]. The plates were incubated at 37°C for periods

[1]https://www.carbosynth.com

of between 1 day and 2 weeks, depending on the time needed to observe the blue-colored clones.

Lectin Binding Experiments

On the basis of their multiple activities on the chromogenic X-substrates from the primary screening, a selection of hit clones were tested for their ability to degrade human colon mucus using lectin binding assays. The hit clones were grown at 37°C in 400 mL LB medium, with orbital shaking at 120 rpm. After 16 h, cells were harvested using centrifugation for 5 min at 5,000 rpm, before being re-suspended and concentrated in an activity buffer (RPMI medium from Sigma) to obtain a final OD600 nm of 80. Cell lysis was carried out using sonication. Cell debris were centrifuged at 13,000 rpm for 10 min and cytoplasmic extracts were filtered using a 0.20 μm Minisart RC4 syringe filter. An *E. coli* EPI100 clone containing the pCC1FOS fosmid without a metagenomic DNA fragment was used as a negative control. The human colon mucus was isolated from three patients of both genders, 31–74 years of age and all of European origin as previously described (Ajandouz et al., 2016). The sampling procedures were approved by the French Ethics Committee (CODECOH no. DC-2011-1319). Samples were taken from a macroscopically unaffected area as identified by the surgeon. After resection, the specimens were placed in an ice-cold DMEM solution supplemented with antibiotics. After longitudinal opening of the intestine, the surface of the mucosa was scraped in PBS to collect intestinal mucus. The mucus from the three patients was pooled and stored at −80°C until used. A lectin binding assay was used to test the effect of bacterial enzymes expressed by the positive clones on human mucins. Briefly, 96-well plates (F-Bottom, Nunc Maxisorp®) were coated overnight at 4°C with 100 μL of human mucins (5 μg/mL) diluted in a pH 9.6 bicarbonate/carbonate coating buffer (100 mM). After two washes with 200 μL phosphate saline buffer (pH 7.4) supplemented with Tween20 0.02% (v/v; PBS-T), the plates were incubated at 37°C with 100 μL of the bacterial supernatant (dilution: 1/100) for 5 h. The wells were washed twice with 200 μL PBS-T before being saturated at room temperature for 1 h with 200 μL PBS containing 1% BSA (PBS-B). Finally, the wells were washed twice with 200 μL PBS-Tween, and 100 μL of fluorescein-labeled lectin solution (5 μg/mL) in PBS-B were added. The fluorescein-conjugated lectins used (all from Vector Laboratories, France) were: Concanavalin A (Con A; selective of Manα2/6/3-manβ4-Glc(Nac)-R > α-Man > α-Glc > αGlcNAc), *Sambucus nigra* (soybean) agglutinin (SNA; selective of Neu5Acα1/6 Gal(NAc)-R) and *Triticum vulgaris* (wheat germ) agglutinin (WGA; selective of Galβ4-GlcNacβ6/3-Galβ4-R > GlcNAcβ-R > Neu5Acα3/6/8-R). After 1 h incubation at 37°C, the wells were washed and the fluorescence measured at an excitation/emission of 490 nm using a BioTek Synergy HTX Multi-Mode Microplate Reader (BioTek, France). Each binding experiment for a given lectin was performed in triplicate, using the same microplate for all hit clones including three control clones (*E. coli* host strain transformed with the empty vector Epi100).

The mean fluorescence value for the three control clones, corresponding to 100% binding, was used to calculate the percentage of the lectin binding for each clone, including the three control clones. The variance within biological replicates of each clone was first assessed using the *F*-test against control clones. Subsequently, *p*-values were calculated using the *t*-test to evaluate the statistical significance of differences between a given clone and the controls. *P*-values lower than 0.05 were considered statistically significant.

Metagenomic Sequence Analysis

The fosmid DNA of the clone hits was extracted using the NucleoBond Xtra Midi kit from Macherey-Nagel (France). Fosmids were then sequenced using the Ion Torrent S5 System at the GeT-Biopuces Platform (Toulouse, France). Read assembly was performed using Masurca[2]. The assembled contigs were cleaned from the pCC1FOS vector sequence using Crossmatch[3]. ORF detection and functional annotation was performed using the RAST annotation server[4] (Aziz et al., 2008). CAZyme encoding genes were identified by BLAST analysis of the predicted ORFs against the full-length sequences of glycoside hydrolases (GH), polysaccharide lyases (PL), carbohydrate esterases (CE), carbohydrate-binding modules (CBM), and glycosyltransferases (GT) included in the CAZy database[5], using a cut-off *E*-value of 7·10-6. Sequences that aligned over their entire length with a sequence in the database with >50% identity were directly assigned to the same family as the subject sequence. The remaining ones were subjected in parallel to (i) a BLAST search against a library built with partial sequences corresponding to individual GH, PL, CE, CBM, and GT modules and (ii) a HMMER2 search using Hidden Markov models (HMM2) built for each CAZy module family, allowing a view of CAZyme modularity (Lombard et al., 2014). The contigs' entire nucleotidic sequences were blasted against the non-redundant database of the NCBI and against each other to examine their divergence from the reference strain genomes, and the redundancy between clone hits. Taxonomic assignation of the metagenomic sequences was determined using the PhyloPythias program[6] (model type: Generic 2013–800 Genera). The same results were obtained with a minimum slice at 3% and 50%. The presence of signal peptide cleavage sites in ORF amino acid sequences were predicted using the SignalP server[7] (Nielsen, 2017).

Prevalence Analyses

The homolog sequences of the translated ORFs were searched for in the translated catalog of 9.9 million reference genes using BLASTP (*E*-value = 0, identity ≥ 90%). This catalog consisted of the gut metagenomic sequences of 1,267 subjects from three continents (United States, China and Europe): 139 US HMP samples, 760 European fecal samples from the MetaHIT project and 368 Chinese fecal samples (Li et al., 2014). The microbial gene richness in the human gut was assessed by recovering

[2]http://www.genome.umd.edu/masurca.html

[3]http://bozeman.mbt.washington.edu/phredphrapconsed.html

[4]http://rast.nmpdr.org/

[5]http://www.cazy.org

[6]http://phylopythias.bifo.helmholtz-hzi.de

[7]http://www.cbs.dtu.dk/services/SignalP/

the occurrence frequency data of homologous sequences of the catalog from the 9.9 million gene frequency table in the 1,267 subjects[8]. The frequency values have no unit. They are normalized to account for sampling and sequencing biases generated by the diverse origins of the cohorts constituting the catalog.

Data Deposition

The datasets generated in the course of this study are available in the repository of the DDBJ/EMBL/GenBank Nucleotide Sequence Database under accession numbers LR131274-LR131286[9].

RESULTS AND DISCUSSION

Screening the Human Gut Metagenome for Mucin Glycan-Degrading Activities

The 20,000 clones of the *E. coli* fosmid library constructed from the ileum mucosa microbiota, covering in total 0.7 Gb of metagenomic sequence, were screened for nearly all the α- and β-glycosidase activities required for the degradation of N- and O-glycans. Firstly, α-L-fucosidases, β-D-N-acetyl-glucosaminidases, β-D-N-acetyl-galactosaminidases, α-D-neuraminic-acid hydrolases, α-D- and β-D-mannosidases were searched for using chromogenic reagents (5-Bromo-4-chloro-3-indoxyl-glycosyl, known as X-glycosyl substrates) in a rich solid medium on which the metagenomic clones had been gridded. It was not possible to screen for β-D-galactosidases using this approach due to the high background activity of the *E. coli* host.

These 120,000 assays allowed 158 validated activities to be identified, with this corresponding to 124 positive clones, since 40 clones produced several of the screened activities (**Table 1**). Strikingly, no positive clone was found on the fucosyl substrate, despite α-linked-L-fucosyl residues frequently being found at the non-reducing end of O-linked oligosaccharides, and α-fucosidase activity being widespread in gut bacteria whatever their taxa (Katayama et al., 2005; Tailford et al., 2015). This may be due to the fact that α-fucosidases are known to be inactive on this kind of artificial substrate (Katayama et al., 2005). The hit yields varied from 0.1% (for X-α-D-Man) to 3.3% (for X-β-D-GlcNac) depending on the screening substrate, which is on average 2.2 times higher than the hit rate (0.4–1.3%) obtained when screening the same library for dietary fiber hydrolytic activities (Cecchini et al., 2013).

Assessment of Human Intestinal Mucus Degradation

Since chromogenic substrates do not represent the structural complexity of mucin oligosaccharides, we then confirmed the activity of the hit clones on the physiological substrate targeted by mucus-degrading bacteria. From the 124 positive clones, we selected 13 to be tested on human intestinal mucus and/or sequenced. The clones chosen were those: (i) producing complementary glycosidase activities required to break down complex mucin oligosaccharide structures thanks to the expression of several CAZy-encoding genes clustering in the same metagenomic loci, or thanks to the production of a highly promiscuous CAZyme; and (ii) producing the highest levels of activity, defined as those with the quickest response to chromogenic testing.

The mucus-degrading ability of the metagenomic clones was assessed using the ELISA assay technique, which involves the modification of mucin-specific lectin binding if the epitopes are affected by CAZyme activity. The mucus was incubated with the hit clones' cytoplasmic extracts. After a washing step, it was then incubated with three fluorescent lectins specific to different N- and O-glycan motifs (**Table 2**). A comparison of lectin binding percentages with those obtained for reference clones (*E. coli* host strain transformed with the empty vector Epi100) is provided in **Figure 1** and **Table 2**. We observed considerable variability in the binding inhibition values, likely due to the heterogeneousness of the glycan structures in the human mucus samples. Nevertheless, binding modification was significant for several clone–lectin couples. Overall, most of the

TABLE 1 | Results of primary screening.

Substrates	**Number of positive clones – Hit rate**
X-β-D-GalNac	47 – 2,3‰
X-β-D-GlcNac	67 – 3,3‰
X-α-D-Man	2 – 0,1‰
X-α-D-Neu5Ac	27 – 1,3‰
X-β-D-Man	17 – 0,8‰
X-α-L-Fuc	0
Single activities	**Number of positive clones**
X-β-D-GalNac	15
X-β-D-GlcNac	29
X-α-D-Man	1
X-α-D-Neu5Ac	20
X-β-D-Man	9
Multiple activities	**Number of positive clones**
X-β-D-Man + X-α-D-Neu5Ac	2
X-β-D-GlcNac + X-α-D-Neu5Ac	1
X-β-D-GlcNac + X-β-D-Man	2
X-β-D-GlcNac + X-β-D-GalNac	27
X-β-D-GlcNac + X-α-D-Man	1
X-β-D-GlcNac + X-β-D-GalNac + X-β-D-Man	1
X-β-D-GlcNac + X-β-D-GalNac + X-α-D-Neu5Ac	3
X-β-D-GlcNac + X-α-D-Man+ X-β-D-Man	2
X-β-D-GlcNac + X-β-D-GalNac + X-α-D-Neu5Ac + X-β-D-Man	1

[8]http://meta.genomics.cn/meta/dataTools

[9]https://www.ncbi.nlm.nih.gov/genbank/

TABLE 2 | Functional profile and CAZyme-encoding gene content of the hit clones.

Clone identifier	CAZy families and their substrate target inferred from the activities listed in the CAZy database								Activity on X- substrates (GH family inferred as responsible for the clone phenotype)				Lectins and their binding specificities (GH family inferred as responsible for the clone phenotype)		
													WGA	SNA	ConA
	β-GlcNac	β-GalNac	α-Neu5Ac	β-Gal	α-Gal(Nac)	β-Man	α-Man	α -Fuc	X-β-GlcNac	X-β-GalNac	X-α-Neu5Ac	X-β-Man	Galβ4-GlcNacβ6/3-Galβ4-R > GlcNAcβ-R > R	Neu5Acα1/6 Gal(NAc)-R Neu5Acα3/6/8-	Manα2/6/3-manβ4-Glc(Nac)-R > α-Man > α-Glc > αGlcNAc
9D11				GH1		GH1			X	–	–	X(GH1)	↘(GH1)	↘	–
14N11	GH20	GH20		GH2		GH2	GH92		X(GH20)	X(GH20)	X	X(GH2)	↘(GH2, GH20)	–	–
20L12	GH20	GH20	GH33	GH2	GH27	GH2			X(GH20)	X(GH20)	X(GH33)	–	–	↘(GH33)	–
39E18	GH20	GH20	GH33	GH2	GH27	GH2			X(GH20)	–	–	–	↘(GH2, GH20, GH33)	–	–
47G11	GH20	GH20	GH33	GH2		GH2	GH92	GH29	–	–	X(GH33)	–	–	↘(GH33)	–
3I21	GH20	GH20	GH33					GH29	X(GH20)	X(GH20)	X(GH33)	–	↘(GH20, GH33)	↘(GH33)	–
40B3			GH33						–	–	X(GH33)	–	–	↘(GH33)	↘
41E6	GH3	GH3	GH33						–	–	X(GH33)	–	nt	nt	nt
39O22			GH33						–	–	X(GH33)	–	–	↘(GH33)	–
12O6	GH20	GH20		GH2		GH2			X(GH20)	X(GH20)	–	–	↘(GH2, GH20)	–	↘
47C24	GH20	GH20		GH2		GH2			X(GH20)	X(GH20)	–	–	nt	Nt	nt
13P9				GH2		GH2			–	–	–	X(GH2)	–	–	–
33D18				GH2		GH2			–	–	–	X(GH2)	–	–	–

X, activity on X-substrates;↘, significant decrease of lectin binding to colon mucus after incubation with the hit clones, compared to reference (E. coli host strain transformed with the empty vector Epi100); nt, non-tested; –, no significant activity/no alteration in binding.

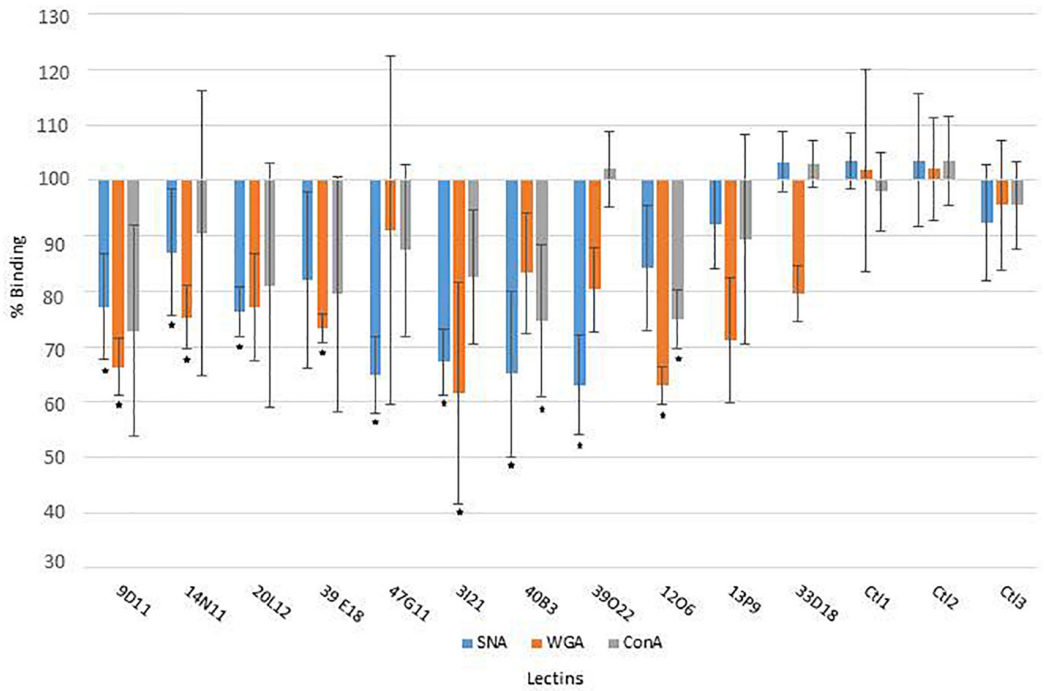

FIGURE 1 | Lectin binding on human colon mucus after incubation with the clone extracts, compared to reference clones (*E. coli* host strain transformed with the empty vector Epi100; *, significant modification of lectin binding).

selected clones, except 13P9 and 33D18, induced a decrease in binding of at least one lectin. The effects were particularly clear for the clones producing activities that target the β-D-GalNAc, β-D-GlcNAc, and α-D-Neu5Ac residues usually found at the terminal extremities of human mucin glycans, which are the most accessible to exo-acting glycosidases. In most cases, the hit clones produced the activities required to degrade the glycan structures targeted by the specific lectins, thus affecting lectin binding.

With respect to the WGA lectin, which is specific to terminal Galβ4-GlcNacβ6/3-Galβ4-R > GlcNAcβ-R, and to a lesser extent, Neu5Acα3/6/8-R motifs, five β-D-N-acetyl-glucosaminidase-producing clones (9D11, 14N11, 39E18, 3I21, and 12O6) induced less lectin binding than was obtained for the reference clones. The terminal Galβ4 residues were likely removed by the *E. coli* β-galactosidase activity, facilitating access to the β-D-N-acetyl-glucosaminidases produced by the hit clones. Binding of the SNA lectin, which is specific to terminal Neu5Acα1/6 Gal(NAc)-R motifs, was reduced after the action of five clones active on X-α-D-Neu5Ac (20L12, 47G11, 3I21, 40B3, and 39O22) and, surprisingly, clone 9D11, which is not active on X-α-D-Neu5Ac. Also surprisingly, ConA lectin binding, which is specific to Manα2/6/3-manβ4-Glc(Nac)-R > α-Man > α-Glc > αGlcNAc motifs, was inhibited after the action of two clones (40B3 and 12O6) which were not detected as being active on X-α-Man. We cannot exclude the possibility that these clones do indeed produce the enzymes required to break down the glycan motifs targeted by ConA, but that their activity cannot be detected on the corresponding X-glycosyl substrates due to the structural modification of the aglycon in chromogenic substrates. Another explanation could be the production by the hit clones of cell wall anchors or glycoprotein adhesins (as further explained in this paper regarding 9D11 sequence annotation), which may compete for binding with mucin-specific lectins.

Identification of Mucin Glycan Utilization Loci

The metagenomic DNA from the 13 clones was sequenced using a high sequencing depth (100X) to ensure reliable sequence assembly. For each clone, one contig of between 27,897 and 50,904 bp in size was obtained. In total, 794,676 bp (containing 316 ORFs) were analyzed. Of these 316 ORFs, 56 were annotated as CAZyme encoding genes.

Forty-nine of these predicted CAZymes contained a GH module (**Supplementary Table S1**), and a further four were esterases. In most of the contig sequences, the CAZyme-encoding genes were organized in operon-like multigenic systems similar to the polysaccharide utilization loci (PULs) described for cultivated species (Terrapon et al., 2018) and other metagnomic DNA fragments (Tasse et al., 2010; **Supplementary Table S1**). The metagenomic PULs retrieved in the present study code for the batteries of CAZymes, carbohydrate sensing/binding proteins and transporters required to achieve the complete breakdown and uptake of mucin glycans. The structural modification of mucin glycans results from the production of several glycosidase activities that could be inferred from the GH families highlighted in their sequences (**Table 2** and **Supplementary Table S1**), and which are all required for the degradation of complex

mucin glycans. Most of the GH sequences presented the signal peptide sequences, indicating their membrane or extracellular location in the bacteria they originate from, necessary to initiate the breakdown of complex glycan structures into simpler oligosaccharides, which are very likely internalized thanks to the various carbohydrate transporters we identified (annotated as ABC transport family, MFS, SusD/SusC systems or outer membrane efflux protein). As with canonical Bacteroidetes PULs, we also identified other genes coding for proteins involved in the regulation of gene expression in these metagenomic loci (AraC family transcriptional regulator, chemotaxis protein CheY/response regulator receiver domain protein). Finally, as described in greater detail later in this section, we also identified in these loci several genes coding for putative enzymes involved in central carbohydrate metabolism, especially sialic acid metabolism.

Partial or complete sequence redundancy was observed in clones 14N11, 20L12, 47G11, and 39E18, in clones 3I21, 40B3 41E6, and 39O22, in clones 12O6 and 47C24, and in clones 13P9 and 33D18 (**Figures 2A–D**, respectively). These 12 sequences finally correspond to four loci, all assigned to the *Bacteroides* genus using PhyloPythiaS which is in agreement with the syntenies detailed hereafter.

Locus A Assigned to *Bacteroides vulgatus* or *Bacteroides massiliensis*

The three partially redundant sequences of the sialidase-, β-D-NAcetylgalactosaminidase- and/or β-D-NAcetylglucosaminidase-producing clones 14N11, 20L12, and 39E18 presented high sequence identity (99–100%) onto their coverage areas (**Figure 2A**). The 39E18 contig is included in that of 20L12. The 14N11 and 20L12 sequences can be combined to form a longer, single contig containing eight GH-encoding genes assigned to the GH2 (2 sequences), GH20 (3 sequences), GH27, GH33, and GH92 families. These families all host already characterized members which are able to depolymerize human N- and O-glycans; β-galactosidases, β-N-acetylglucosaminidases, α-N-acetylgalactosaminidases, sialidases and α-mannosidases, respectively. Synteny was detected between contigs 14N11, 20L12, and 39E18 and a locus from *Bacteroides vulgatus* ATCC 8482 corresponding to the predicted PUL 67. The synteny with PUL 67 is, however, disrupted by the insertion of four genes in the metagenomic DNA (ORFs 13–16 in clone 20L12), including the GH27 encoding gene and two genes involved in nutrient binding and transport. This insertion confers an ecological advantage to the uncultured strain containing this metagenomic locus over *B. vulgatus* for O-GalNAc glycan foraging, especially the core 3 structure from human colonic mucins (Brockhausen et al., 2009). Sialidase activity was observed for contig 47G11 on the chromogenic substrate and mucus. This contig contained a similar gene series to 14N11 and 20L12, albeit with two additional CAZyme-encoding genes (GH29 and 97), and shared, respectively 82 and 90% sequence identity with contigs 14N11 and 20L12. The percentage of its CAZyme sequences' identity with the homologous sequences in contigs 14N11 and 20L12 (79–90%) indicates that these metagenomic fragments originate from different strains or species. Contig 47G11 indeed presents an almost perfect synteny with the predicted PUL 4 from *B. massiliensis* B84634 (100% Cov, 99% ID), but with two additional genes in the metagenomic sequence.

The *B. vulgatus* strain ATCC 8482 is one of the most prevalent strains in the human gut *Bacteroides* group. It is thought to be responsible for the development of inflammation and exacerbated immune response in the pathogenesis of IBD (Shiba et al., 2003). However, in our study, we found the genes of contigs 20L12 and 14N11 to be highly prevalent and abundant in the human gut metagenomic gene catalog, regardless of the geographic origin or medical status of the subjects (**Figure 3** and **Supplementary Table S1**). The locus identified in this study, which is not a biomarker of IBD, is thus unlikely to be involved in IBD. Besides, the *B. vulgatus* strain ATCC 8482, which is known to produce a whole panel of glycolytic activities required to degrade mucus glycoproteins (Ruseler-van Embden et al., 1989), has previously been found to degrade pig gastric mucin, but not human mucin glycans (Hoskins et al., 1992; Png et al., 2010). These data could thus be revisited by more specifically assessing the growth of this strain on specific structures of sialylated mucin glycans. As *B. vulgatus* strain ATCC8482, *B. massiliensis* B84634 was also reported to be able to grow on pig gastric mucin, resulting in the activation of six of its 33 PULs, including PUL 4 (Pudlo et al., 2015). The prevalence of the cluster's genes is lower than those of corresponding genes in the *B. vulgatus* strain, and their abundance is lower in European subjects (**Figure 3** and **Supplementary Table S1**).

Finally, in the contigs of these sialidase-producing clones, we also identified genes encoding putative sialic acid-specific 9-O-acetylesterase, N-acetylglucosamine-6-phosphate deacetylase, glucosamine-6-phosphate deaminase and sialic acid-induced mutarotase, constituting the denominated Nan system for *N*-acylneuraminate (Vimr et al., 2004; Egan et al., 2014). Marcobal et al. (2011) stressed that a certain number of bacterial species do not possess all the enzymes for the complete catabolism of sialic acid: *B. tetaiotaomicron*, for example, has sialidases but not the Nan system to metabolize sialic acid. Conversely, other species such as *Clostridium difficile* do not have sialidases but possess the Nan system to metabolize sialic acid released by other bacteria. Here, the uncultured bacteria from which contigs 14N11, 20L12, and 39E18 originated evolved to cluster all the sialidase-encoding genes and the Nan operon on the same locus, as well as other CAZyme-encoding genes likely to release other monosaccharides belonging to the sialylated mucin glycans. This confers an important ecological advantage to colonize the mucosal layer.

Locus B Assigned to *Bacteroides plebeius*

The four partially redundant sequences 3I21, 40B3, 39O22, and 41E6 have high sequence similarity (99–100%) (**Figure 2B**). The 3I21 and 41E6 sequences can be combined to form a longer, single contig containing seven GH-encoding genes, including the GH20, GH29, GH33, GH3 families, which are known to contain members able to depolymerize O-glycans

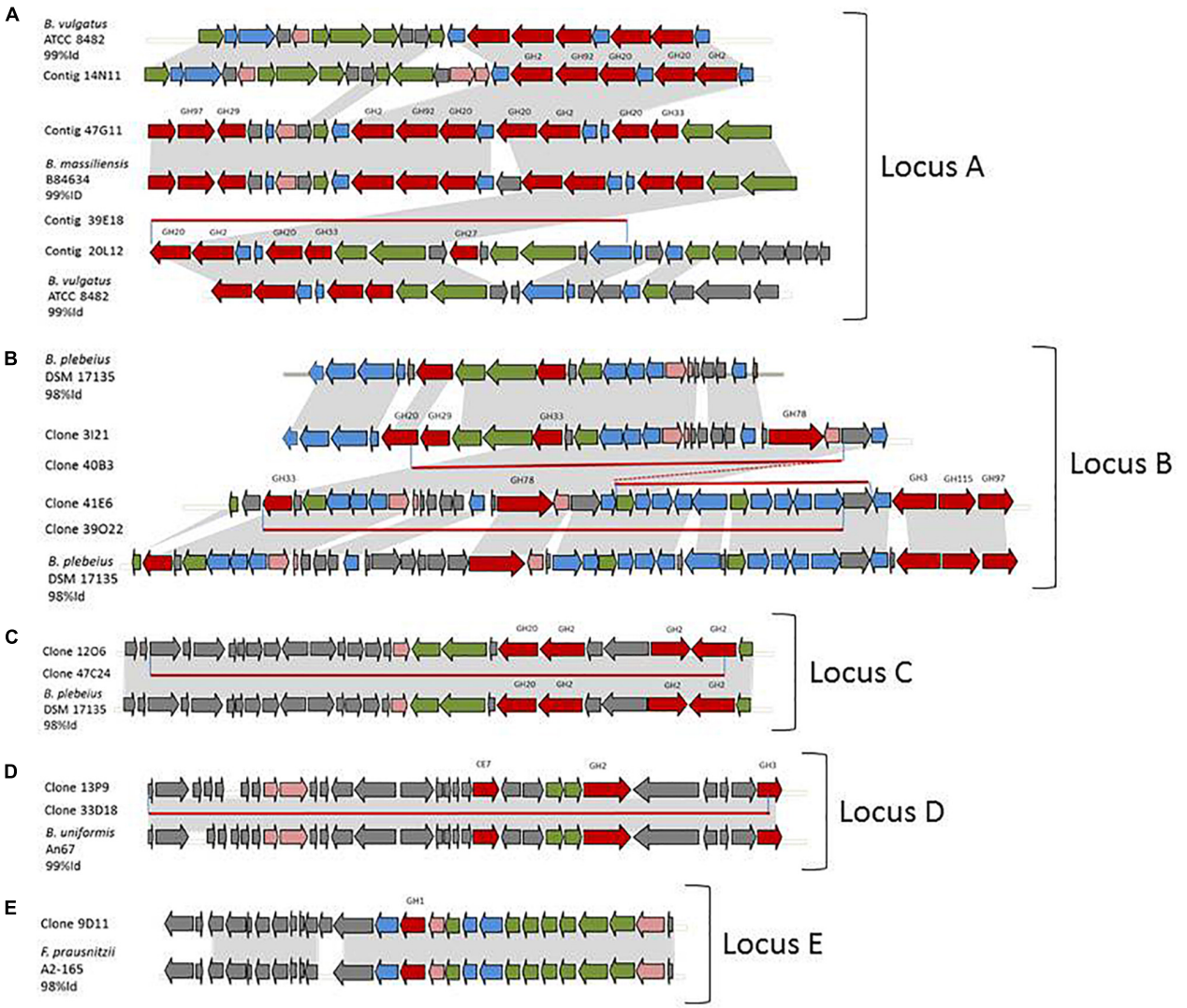

FIGURE 2 | Metagenomic loci of the hit clones and syntenies with reference genomes. **(A)** partial redundancy between clones 14N11, 47G11, 39E18, and 20L12 and their synteny with *B. vulgatus* ATCC 8482 and *B. massiliensis* B84634. **(B)** partial redundancy between clones 3I21, 40B3, 41E6, and 39O22 and their synteny with *B. plebeius* DSM 17135. **(C)** partial redundancy between clones 12O6 and 47C24 and their synteny with *B. plebeius* DSM 17135. **(D)** partial redundancy between clones 13P9 and 33D18 and their synteny with *B. uniformis* An67. **(E)** synteny of 9D11 and *F. prausnitzii* A2-165. In gray, identical genome parts; red arrows, CAZymes; blue arrows, other enzymes of carbohydrate metabolism; green arrows, transporters; pink arrows, transcription/transduction signal; gray arrows, others; and red lines, redundant metagenomic sequences.

(β-1,6-N-acetylglucosaminidases, α-L-fucosidases, sialidases). The remaining GH78-, GH115-, and GH97-encoding genes belong to another gene cluster best suited to the degradation of plant glycans, which highlights the probable metabolic flexibility of the uncultured bacterium from which this metagenomic DNA fragment originated. The functional profile of the clones matches their content in GH families (**Table 2** and **Figure 1**). Additional genes involved in carbohydrate binding and transport (annotated as substrate-binding protein, SusC/SusD, and major facilitator family transporter) and gene expression regulation were also present in these metagenomic sequences. These contigs present a nearly perfect synteny with the predicted PUL 9 from the *B. plebeius* DSM 17135 strain (93% Cov, 98% Id for 3I21 and 95% Cov, 98% Id for 41E6), although this was disrupted by the insertion of two genes coding for a GH29 putative α-L-fucosidase (ORF6 in contig 3I21) and one putative transporter (ORF18 in contig 3I21), adding a complementary function to the bacterium's glycan degradation pathway. In this mucin-targeting metagenomic PUL, GH-encoding genes were also surrounded by genes conferring complementary functions for N-acetylhexosamine catabolism and sialylation processes – methyl transferase, N-acetylneuraminate cytidylyltransferase, N-acetylneuraminic mutarotase, sialic acid-specific 9-O-acetylesterase, N-acetylneuraminate lyase and N-acylglucosamine 2-epimerase – whose roles in carbohydrate metabolism have previously been described for symbiotic

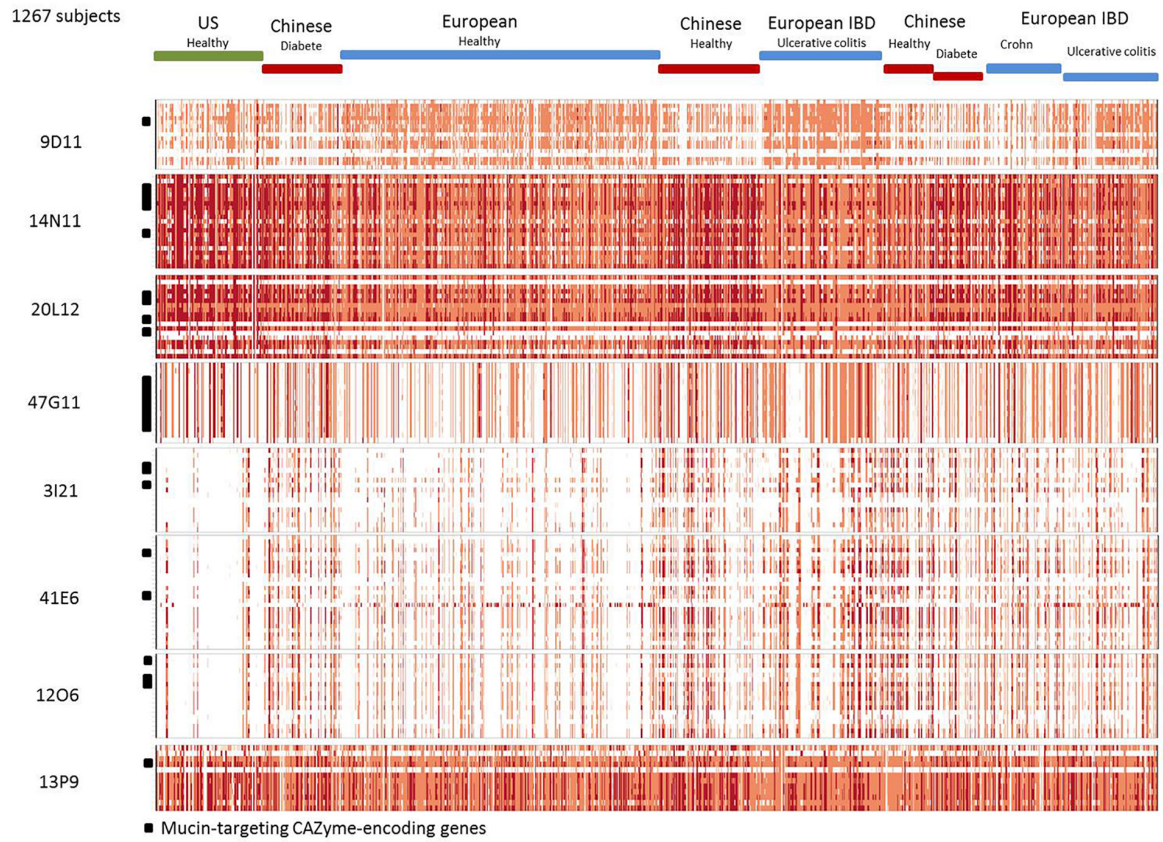

FIGURE 3 | Abundance and prevalence of the genes of the contigs in the human gut metagenome. Genes are in rows. Individuals are in columns. The normalized abundance is represented by a color scale, white, not detected; pink, orange, and red, increasing abundance with a 100-fold change between colors.

and pathogenic bacteria (Vimr and Lichtensteiger, 2002; Ringenberg et al., 2003; Bravo et al., 2004; Vimr et al., 2004; Mizanur and Pohl, 2008). This gene cluster thus combines genes dedicated to the depolymerization of sialylated mucin glycans with genes involved in the synthesis, activation and transfer of sialic acid onto bacterial cell surfaces. Such a process of carbohydrate harvesting and reuse for bacterial glycan synthesis would permit bacteria to mimic vertebrate cell surfaces and evade the host's immune system. In mammals, sialic acids are widespread molecules usually at the terminal position of oligosaccharide chains of cell-surface or serum glycoconjugates. Their functions in regulation of host innate defense mechanisms make it a key substance for microorganisms to survive in the environment (Vimr et al., 2004). Although they were all prevalent in the sample, these metagenomic genes are not evenly distributed among the population (**Figure 3**). Except for one gene (ORF1, contig 41E6), a mobile element appearing in the heat map as a biomarker of European subjects, the entire locus (including the additional GH29 compared to *B. plebeius* DSM 17135 PUL9) is significantly more abundant in the European IBD cohort than the healthy cohort. At the same time, it is abundant and prevalent in the Chinese subjects, including the healthy ones, and almost absent in the United States subjects.

Locus C Assigned to *Bacteroides plebeius*

Contig 47C24 is included in contig 12O6, with which it shares 99% sequence identity. Contig 12O6 has 98% identity with a *B. plebeius* DSM 17135 locus, which includes a part of the predicted PUL 4 (**Figure 2C**). This part of PUL 4 contains one GH20- and three GH2-encoding genes, with the former gene explaining the β-D-Nacetylgalactosaminidase and β-D-Nacetylglucosaminidase activities of clones 47C24 and 12O6. Surrounding the CAZymes, we also found three genes likely involved in the binding and transport of nutrients. Finally, not surprisingly, the prevalence and abundance pattern of this locus was similar to that of contigs 3I21, 40B3, 39O22, and 41E6, which also showed synteny with other *B. plebeius* DSM 17135 loci.

Locus D Assigned to *Bacteroides uniformis*

The last *Bacteroides* contig, namely contig 13P9, which includes sequence 33D18 (**Figure 2D**), shared 99% identity with a genomic locus from *B. uniformis* An67, a strain which is not included in the PUL database. This metagenomic PUL contains a GH2-, a GH3-, and a CE7-encoding gene. The GH2 family contains β-D-mannosidases, explaining activity on X-β-D-Man (**Table 2** and

Figure 1). Due to its position at the end of the contig, the GH3-encoding gene is truncated and probably not functional here, but some of the characterized proteins of the family are known to act on β-N-acetylhexosamines, of which the acetyl groups could be hydrolysed by the CE7 enzyme. This metagenomic locus is probably involved in the catabolism of human N-glycans by uncultured bacteria, and/or *B. uniformis* strains, which have a high potential to utilize both dietary (Tasse et al., 2010; Patrascu et al., 2017) and endogenous glycans (Benítez-Páez et al., 2017). This considerable metabolic flexibility of *B. uniformis*, which gives it a significant advantage when it comes to easily colonizing the human gut ecosystem, could explain why the locus identified in this study is so prevalent and abundant in the microbiome, regardless of the geographic origin or medical status of the individual (**Supplementary Table S1** and **Figure 3**).

Locus E Assigned to *Faecalibacterium prausnitzii*

The last metagenomic locus identified here, that of the β-D-mannosidase and β-N-acetylglucosaminidase clone 9D11, was assigned to Feacalibacterium using PhylophythiaS. It was indeed found to share 98% identity with a locus of *Faecalibacterium prausnitzii* A2-165 F (**Figure 2E**). It contains only one CAZyme-encoding gene (GH1), which was probably responsible for the activity detected on X-β-Man. Conversely, neither activity on X-β-GlcNac nor modification of WGA and SNA lectin binding to mucus could be explained by the presence of this GH1 enzyme, indicating that one or several of the numerous putative proteins encoded in this locus (some presenting distant homologies with adhesins and agglutinins) may perform these functions, and/or that the encoded GH1 is a highly promiscuous enzyme, which will have to be characterized. Additionally, five genes coding for a putative peptidic transport system (oppABCDF operon) were clustered in this locus. The opp transport system is involved in peptide uptake for nutrition, sensing environmental changes and recycling peptides from, for instance, muropeptides; that is, peptidoglycans from bacterial cell walls consisting of alternating residues of β-N-acetylglucosamine (NAG) and N-acetylmuramic acid (NAM) linked to a peptide chain (Monnet, 2003). In this pathway, peptides internalized by the oppABCDF system are hydrolysed into amino acids by a set of peptidases, a role that may have been performed here by the putative CocE/NonD hydrolase belonging to the aminopeptidase family identified in the 9D11 locus. With respect to the functioning of *F. prausnitzii* in the human gut microbiota, most strains grew on N-acetylglucosamine, highlighting their probable ability to utilize host-derived substrates (Lopez-Siles et al., 2012). This is consistent with the CAZy gene content of the *F. prausnitzii* genomes. We indeed found several *F. prausnitzii* sequences in the CAZy database that had been assigned to families as GH2- and GH3-containing members active on β-D-N-acetylglucosamine, β-D-N-acetylhexosamine and β-D-glucosamine linkages, although none of these *F. prausnitzii* enzymes has been biochemically characterized to date. In any case, *F. prausnitzii* is far from being as well equipped with glycan-degrading enzymes as the *Bacteroides* species described above. Nevertheless, our results demonstrate that this species has the potential to interact with mucus. This could explain the above mentioned modulation of the effect of *B. thetaiotaomicron* on the intestinal mucus barrier, resulting in a modification in goblet cell differentiation and mucin glycosylation (Wrzosek et al., 2013). Moreover, *F. prausnitzii* belongs to the most abundant Firmicutes species in the human gut, which is consistent with the high abundance and prevalence of the locus we identified in this study (**Figure 3**). The gene abundance heat map indicates a lower prevalence of 9D11 genes in Chinese subjects, regardless of their medical status, than in European ones. What is more, compared to healthy subjects, these genes are more abundant in the microbiome of patients suffering from ulcerative colitis, but less abundant in patients with Crohn's disease (CD). This is perfectly consistent with the low abundance of *F. prausnitzii* in the microbiome of CD patients, particularly those with ileal involvement (Sokol et al., 2009), which could be connected with the ability of this species to interact with mucus through its glycan and proteic fractions, as highlighted here with the 9D11 locus.

CONCLUSION

To conclude, our work constitutes the first activity-based metagenomic study targeting the glycan-mediated relationships between the human gut microbiota and the host. Until now, the identification of bacterial species and metabolic pathways involved in mucus degradation was restricted to cultured bacteria, tested for growth on complex mucin glycan structures of porcine origin. When combined to genomic and transcriptomic analyses, these studies allowed to identify mucin glycan utilization loci for the few dozen of targeted strains. Nevertheless, to date only a very small number of these pathways have been biochemically proven to degrade human mucin structures.

In the present study, we designed a two-step functional screening strategy, which allowed us, for the first time, both to identify mucus degrading pathways from uncultured species of the microbiota, and to prove their ability to degrade specific motives of human colonic mucus. The mucin glycan utilization loci we discovered are highly prevalent and abundant in the microbiome, and present marked synthenies with loci from several prominent commensal strains from the Bacteroidetes and Firmicutes phyla, most of them being known to forage on dietary glycans, but which had never been described to feed on mucin glycans. Our data highlight the metabolic flexibility of these abundant commensals, which would have the ability to easily redirect their metabolism from dietary polysaccharides to host-derived glycans, depending on the availability of resources. In addition, we highlighted the overabundance of certain of these (meta) genomic loci in the microbiome of patients suffering from inflammatory diseases. This particular trait, together with the proof of their involvement in the modification of human mucus, makes them new targets to study the host response to the degradation of the mucus firewall, and to elaborate new strategies to restore gut homeostasis, for example by using specific functional foods to divert over-abundant mucus foragers toward dietary glycans.

ETHICS STATEMENT

Bacterial metagenomic DNA was obtained from the distal ileum sample of a 51-year-old male patient undergoing colonoscopy and surgery for a suspected cancer of the lower colon after he had been subjected to a cleansing preparation. The patient did not receive any antibiotics or other drugs in the 6 months before sampling. The sampling protocol was approved by the local ethics committee: the Comité de Protection des Personnes Sud Est V (Ref.: 07-CHUG-21; B. Habozit, J. L. Crakowski, J. Juge, J. Grunwald, E. Svhan, and E. Fontaine on the committee) and informed written consent was obtained from the subject before sampling. The human colon mucus was isolated from patients (Ajandouz et al., 2016). Briefly, human intestinal colonic resections (5–10 cm long) were obtained from patients undergoing surgery for colonic adenocarcinoma at the Hospital Nord of Marseille's general and gastrointestinal surgery unit as part of a collaborative "clinical transfer" project. The sampling procedures were approved by the French Ethics Committee (CODECOH no. DC-2011-1319).

AUTHOR CONTRIBUTIONS

EL conceived the study, designed the work, acquired, analyzed and interpreted the data, and drafted the work. JP and MM conceived the study, designed the work, acquired and analyzed the data, and drafted the final revision of the manuscript. NB and JE acquired, analyzed and interpreted the data, and drafted the final revision of the manuscript. AT, EB, ED, and BH analyzed and interpreted the data, and drafted the final revision of the manuscript. ML, SB, EDP, and PR conceived the study and designed the work, and drafted the final revision of the manuscript. GP-V conceived the study, designed the work, analyzed and interpreted the data, and drafted the final revision of the manuscript.

FUNDING

This research was funded by the French Ministry of Education and Research (Ministère de l'Enseignement Supérieur et de la Recherche), the INRA's M2E Metaprogramme (the Metascreen project), and the European Union's Horizon 2020 Framework Program (LEITBIO-2015-685474, Metafluidics).

SUPPLEMENTARY MATERIAL

The Supplementary Material for this article can be found online at: https://www.frontiersin.org/articles/10.3389/fmicb.2019.01286/full#supplementary-material

REFERENCES

Ajandouz, E. H., Berdah, S., Moutardier, V., Bege, T., Birnbaum, D. J., Perrier, J., et al. (2016). Hydrolytic fate of 3/15-acetyldeoxynivalenol in humans: specific deacetylation by the small intestine and liver revealed using in Vitro and ex Vivo approaches. *Toxins* 8:232. doi: 10.3390/toxins8080232

Aziz, R. K., Bartels, D., Best, A. A., DeJongh, M., Disz, T., Edwards, R. A., et al. (2008). The RAST server: rapid annotations using subsystems technology. *BMC Genomics* 9:75. doi: 10.1186/1471-2164-9-75

Bäckhed, F., Ley, R. E., Sonnenburg, J. L., Peterson, D. A., and Gordon, J. I. (2005). Host-bacterial mutualism in the human intestine. *Science* 307, 1915–1920. doi: 10.1126/science.1104816

Benítez-Páez, A., Gómez del Pulgar, E. M., and Sanz, Y. (2017). The glycolytic versatility of *Bacteroides* uniformis CECT 7771 and its genome response to oligo and polysaccharides. *Front. Cell Infect. Microbiol.* 7:383. doi: 10.3389/fcimb.2017.00383

Bravo, I. G., Garcıìa-Vallvé, S., Romeu, A., and Reglero, Á. (2004). Prokaryotic origin of cytidylyltransferases and α-ketoacid synthases. *Trends Microbiol.* 12, 120–128. doi: 10.1016/j.tim.2004.01.004

Brockhausen, I., Schachter, H., and Stanley, P. (2009). "O-GalNAc Glycans," in *Essentials of Glycobiology*, eds A. Varki, R. D. Cummings, J. D. Esko, H. H. Freeze, P. Stanley, C. R. Bertozzi, et al. (Cold Spring Harbor, NY: Cold Spring Harbor Laboratory Press).

Cecchini, D. A., Laville, E., Laguerre, S., Robe, P., Leclerc, M., Doré, J., et al. (2013). Functional metagenomics reveals novel pathways of prebiotic breakdown by human gut bacteria. *PLoS One* 8:e72766. doi: 10.1371/journal.pone.0072766

Courtois, S., Cappellano, C. M., Ball, M., Francou, F.-X., Normand, P., Helynck, G., et al. (2003). Recombinant environmental libraries provide access to microbial diversity for drug discovery from natural products. *Appl. Environ. Microbiol.* 69, 49–55. doi: 10.1128/aem.69.1.49-55.2003

Derrien, M., Vaughan, E. E., Plugge, C. M., and de Vos, W. M. (2004). Akkermansia muciniphila gen. nov., sp. nov., a human intestinal mucin-degrading bacterium. *Int. J. Syst. Evol. Microbiol.* 54, 1469–1476. doi: 10.1099/ijs.0.02873-0

Desai, M. S., Seekatz, A. M., Koropatkin, N. M., Kamada, N., Hickey, C. A., Wolter, M., et al. (2016). A dietary fiber-deprived gut microbiota degrades the colonic mucus barrier and enhances pathogen susceptibility. *Cell* 167, 1339–1353.e21. doi: 10.1016/j.cell.2016.10.043

Egan, M., O'Connell Motherway, M., Ventura, M., and van Sinderen, D. (2014). Metabolism of sialic acid by Bifidobacterium breve UCC2003. *Appl. Environ. Microbiol.* 80, 4414–4426. doi: 10.1128/AEM.01114-14

Hoskins, L. C., Boulding, E. T., Gerken, T. A., Harouny, V. R., and Kriaris, M. S. (1992). Mucin glycoprotein degradation by mucin oligosaccharide-degrading strains of human faecal bacteria. Characterisation of saccharide cleavage products and their potential role in nutritional support of larger faecal bacterial populations. *Microb. Ecol. Health Dis.* 5, 193–207. doi: 10.3109/08910609209141586

Jakobsson, H. E., Rodríguez-Piñeiro, A. M., Schütte, A., Ermund, A., Boysen, P., Bemark, M., et al. (2015). The composition of the gut microbiota shapes the colon mucus barrier. *EMBO Rep.* 16, 164–177. doi: 10.15252/embr.201439263

El Kaoutari, A., Armougom, F., Gordon, J. I., Raoult, D., and Henrissat, B. (2013). The abundance and variety of carbohydrate-active enzymes in the human gut microbiota. *Nat. Rev. Microbiol.* 11, 497–504. doi: 10.1038/nrmicro3050

Katayama, T., Fujita, K., and Yamamoto, K. (2005). Novel bifidobacterial glycosidases acting on sugar chains of mucin glycoproteins. *J. Biosci. Bioeng.* 99, 457–465. doi: 10.1263/jbb.99.457

Ladevèze, S., Cioci, G., Roblin, P., Mourey, L., Tranier, S., and Potocki-Véronèse, G. (2015). Structural bases for N-glycan processing by mannoside phosphorylase. *Acta Crystallogr. Sect. D Biol. Crystallogr.* 71, 1335–1346. doi: 10.1107/S1399004715006604

Ladevèze, S., Tarquis, L., Cecchini, D. A., Bercovici, J., Andre, I., Topham, C. M., et al. (2013). Role of glycoside phosphorylases in mannose foraging by human gut bacteria. *J. Biol. Chem.* 288, 32370–32383. doi: 10.1074/jbc.M113.483628

Li, J., Jia, H., Cai, X., Zhong, H., Feng, Q., Sunagawa, S., et al. (2014). An integrated catalog of reference genes in the human gut microbiome. *Nat. Biotech.* 32, 834–841. doi: 10.1038/nbt.2942

Lombard, V., Golaconda Ramulu, H., Drula, E., Coutinho, P. M., and Henrissat, B. (2014). The carbohydrate-active enzymes database (CAZy) in 2013. *Nucleic Acids Res.* 42, D490–D495. doi: 10.1093/nar/gkt1178

Lopez-Siles, M., Khan, T. M., Duncan, S. H., Harmsen, H. J. M., Garcia-Gil, L. J., and Flint, H. J. (2012). Cultured representatives of two major phylogroups of

human colonic faecalibacterium prausnitzii can utilize pectin, uronic acids, and host-derived substrates for growth. *Appl. Environ. Microbiol.* 78, 420–428. doi: 10.1128/AEM.06858-11

Marcobal, A., Barboza, M., Sonnenburg, E. D., Pudlo, N., Martens, E. C., Desai, P., et al. (2011). *Bacteroides* in the infant gut consume milk oligosaccharides via mucus-utilization pathways. *Cell Host Microbe* 10, 507–514. doi: 10.1016/j.chom.2011.10.007

Marcobal, A., Southwick, A. M., Earle, K. A., and Sonnenburg, J. L. (2013). A refined palate: bacterial consumption of host glycans in the gut. *Glycobiology* 23, 1038–1046. doi: 10.1093/glycob/cwt040

Martens, E. C., Chiang, H. C., and Gordon, J. I. (2008). Mucosal glycan foraging enhances fitness and transmission of a saccharolytic human gut bacterial symbiont. *Cell Host Microbe* 4, 447–457. doi: 10.1016/j.chom.2008.09.007

Martens, E. C., Neumann, M., and Desai, M. S. (2018). Interactions of commensal and pathogenic microorganisms with the intestinal mucosal barrier. *Nat. Rev. Microbiol.* 16, 457–470. doi: 10.1038/s41579-018-0036-x

Mizanur, R. M., and Pohl, N. L. (2008). Bacterial CMP-sialic acid synthetases: production, properties, and applications. *Appl. Microbiol. Biotechnol.* 80, 757–765. doi: 10.1007/s00253-008-1643-7

Monnet, V. (2003). Bacterial oligopeptide-binding proteins. *Cell. Mol. Life Sci.* 60, 2100–2114. doi: 10.1007/s00018-003-3054-3

Nielsen, H. (2017). "Predicting Secretory Proteins with SignalP," in *Protein Function Prediction: Methods and Protocols*, ed. D. Kihara (New York, NY: Springer), 59–73. doi: 10.1007/978-1-4939-7015-5_6

Owen, C. D., Tailford, L. E., Monaco, S., Šuligoj, T., Vaux, L., Lallement, R., et al. (2017). Unravelling the specificity and mechanism of sialic acid recognition by the gut symbiont *Ruminococcus gnavus*. *Nat. Commun.* 8:2196. doi: 10.1038/s41467-017-02109-8

Patrascu, O., Béguet-Crespel, F., Marinelli, L., Le Chatelier, E., Abraham, A.-L., Leclerc, M., et al. (2017). A fibrolytic potential in the human ileum mucosal microbiota revealed by functional metagenomic. *Sci. Rep.* 7:40248. doi: 10.1038/srep40248

Pickard, J. M., Maurice, C. F., Kinnebrew, M. A., Abt, M. C., Schenten, D., Golovkina, T. V., et al. (2014). Rapid fucosylation of intestinal epithelium sustains host–commensal symbiosis in sickness. *Nature* 514, 638–641. doi: 10.1038/nature13823

Png, C. W., Lindén, S. K., Gilshenan, K. S., Zoetendal, E. G., McSweeney, C. S., Sly, L. I., et al. (2010). Mucolytic bacteria with increased prevalence in IBD mucosa augment *In Vitro* utilization of mucin by other bacteria. *Am. J. Gastroenterol.* 105, 2420–2428. doi: 10.1038/ajg.2010.281

Podolsky, D. K. (1985). Oligosaccharide structures of human colonic mucin. *J. Biol. Chem.* 260, 8262–8271.

Pudlo, N. A., Urs, K., Kumar, S. S., German, J. B., Mills, D. A., and Martens, E. C. (2015). Symbiotic human gut bacteria with variable metabolic priorities for host mucosal glycans. *mBio* 6:e1282-15. doi: 10.1128/mBio.01282-15

Ringenberg, M. A., Steenbergen, S. M., and Vimr, E. R. (2003). The first committed step in the biosynthesis of sialic acid by *Escherichia coli* K1 does not involve a phosphorylated N-acetylmannosamine intermediate. *Mol. Microbiol.* 50, 961–975. doi: 10.1046/j.1365-2958.2003.03741.x

Robbe, C., Capon, C., Coddeville, B., and Michalski, J.-C. (2004). Structural diversity and specific distribution of O-glycans in normal human mucins along the intestinal tract. *Biochem. J.* 384, 307–316. doi: 10.1042/bj20040605

Ruseler-van Embden, J. G., van der Helm, R., and van Lieshout, L. M. (1989). Degradation of intestinal glycoproteins by *Bacteroides* vulgatus. *FEMS Microbiol. Lett.* 58, 37–41. doi: 10.1016/0378-1097(89)90338-8

Shiba, T., Aiba, Y., Ishikawa, H., Ushiyama, A., Takagi, A., Mine, T., et al. (2003). The suppressive effect of bifidobacteria on *Bacteroides* vulgatus, a putative pathogenic microbe in inflammatory bowel disease. *Microbiol. Immunol.* 47, 371–378. doi: 10.1111/j.1348-0421.2003.tb03368.x

Sokol, H., Seksik, P., Furet, J. P., Firmesse, O., Nion-Larmurier, I., Beaugerie, L., et al. (2009). Low counts of faecalibacterium prausnitzii in colitis microbiota. *Inflamm. Bowel Dis.* 15, 1183–1189. doi: 10.1002/ibd.20903

Sonnenburg, J. L., Xu, J., Leip, D. D., Chen, C.-H., Westover, B. P., Weatherford, J., et al. (2005). Glycan foraging in vivo by an intestine-adapted bacterial symbiont. *Science* 307, 1955–1959. doi: 10.1126/science.1109051

Tailford, L. E., Crost, E. H., Kavanaugh, D., and Juge, N. (2015). Mucin glycan foraging in the human gut microbiome. *Front. Genet.* 6:81. doi: 10.3389/fgene.2015.00081

Tasse, L., Bercovici, J., Pizzut-Serin, S., Robe, P., Tap, J., Klopp, C., et al. (2010). Functional metagenomics to mine the human gut microbiome for dietary fiber catabolic enzymes. *Genome Res.* 20, 1605–1612. doi: 10.1101/gr.108332.110

Terrapon, N., Lombard, V., Drula, É., Lapébie, P., Al-Masaudi, S., Gilbert, H. J., et al. (2018). PULDB: the expanded database of polysaccharide utilization loci. *Nucleic Acids Res.* 46, D677–D683. doi: 10.1093/nar/gkx1022

Vimr, E., and Lichtensteiger, C. (2002). To sialylate, or not to sialylate: that is the question. *Trends Microbiol.* 10, 254–257. doi: 10.1016/s0966-842x(02)02361-2

Vimr, E. R., Kalivoda, K. A., Deszo, E. L., and Steenbergen, S. M. (2004). Diversity of microbial sialic acid metabolism. *Microbiol. Mol. Biol. Rev.* 68, 132–153. doi: 10.1128/mmbr.68.1.132-153.2004

Wrzosek, L., Miquel, S., Noordine, M.-L., Bouet, S., Chevalier-Curt, M. J., Robert, V., et al. (2013). *Bacteroides* thetaiotaomicron and *Faecalibacterium prausnitzii* influence the production of mucus glycans and the development of goblet cells in the colonic epithelium of a gnotobiotic model rodent. *BMC Biol.* 11:61. doi: 10.1186/1741-7007-11-61

Conflict of Interest Statement: PR was employed by company Givaudan SA.

The remaining authors declare that the research was conducted in the absence of any commercial or financial relationships that could be construed as a potential conflict of interest.

Copyright © 2019 Laville, Perrier, Bejar, Maresca, Esque, Tauzin, Bouhajja, Leclerc, Drula, Henrissat, Berdah, Di Pasquale, Robe and Potocki-Veronese. This is an open-access article distributed under the terms of the Creative Commons Attribution License (CC BY). The use, distribution or reproduction in other forums is permitted, provided the original author(s) and the copyright owner(s) are credited and that the original publication in this journal is cited, in accordance with accepted academic practice. No use, distribution or reproduction is permitted which does not comply with these terms.

frontiers in Microbiology

REVIEW
published: 10 June 2019
doi: 10.3389/fmicb.2019.01136

The Microbiome and Irritable Bowel Syndrome – A Review on the Pathophysiology, Current Research and Future Therapy

Pei Pei Chong[1], Voon Kin Chin[1], Chung Yeng Looi[1], Won Fen Wong[2], Priya Madhavan[3] and Voon Chen Yong[1]*

[1] School of Biosciences, Taylor's University, Subang Jaya, Malaysia, [2] Department of Medical Microbiology, Faculty of Medicine, University of Malaya, Kuala Lumpur, Malaysia, [3] School of Medicine, Faculty of Health and Medical Sciences, Taylor's University, Subang Jaya, Malaysia

Irritable bowel syndrome (IBS) is a functional disorder which affects a large proportion of the population globally. The precise etiology of IBS is still unknown, although consensus understanding proposes IBS to be of multifactorial origin with yet undefined subtypes. Genetic and epigenetic factors, stress-related nervous and endocrine systems, immune dysregulation and the brain-gut axis seem to be contributing factors that predispose individuals to IBS. In addition to food hypersensitivity, toxins and adverse life events, chronic infections and dysbiotic gut microbiota have been suggested to trigger IBS symptoms in tandem with the predisposing factors. This review will summarize the pathophysiology of IBS and the role of gut microbiota in relation to IBS. Current methodologies for microbiome studies in IBS such as genome sequencing, metagenomics, culturomics and animal models will be discussed. The myriad of therapy options such as immunoglobulins (immune-based therapy), probiotics and prebiotics, dietary modifications including FODMAP restriction diet and gluten-free diet, as well as fecal transplantation will be reviewed. Finally this review will highlight future directions in IBS therapy research, including identification of new molecular targets, application of 3-D gut model, gut-on-a-chip and personalized therapy.

Keywords: irritable bowel syndrome, microbiome, microbiota dysbiosis, fecal transplant, IBS animal model

OPEN ACCESS

Edited by:
Vishal Singh,
The University of Toledo,
United States

Reviewed by:
Konstantinos Papadimitriou,
Agricultural University of Athens,
Greece
Ruggiero Francavilla,
University of Bari Aldo Moro, Italy

****Correspondence:***
Pei Pei Chong
PeiPei.Chong@taylors.edu.my

Specialty section:
This article was submitted to Microbial Symbioses, a section of the journal Frontiers in Microbiology

Received: *13 September 2018*
Accepted: *06 May 2019*
Published: *10 June 2019*

Citation:
Chong PP, Chin VK, Looi CY, Wong WF, Madhavan P and Yong VC (2019) The Microbiome and Irritable Bowel Syndrome – A Review on the Pathophysiology, Current Research and Future Therapy. Front. Microbiol. 10:1136. doi: 10.3389/fmicb.2019.01136

INTRODUCTION

Irritable bowel syndrome (IBS) is a common functional gastrointestinal disorder characterized by chronic, recurrent abdominal discomfort and pain, with changes in bowel habits. Patients with IBS can be categorized into four major subtypes depending on the predominant stool pattern, including IBS with constipation (IBS-C), IBS with diarrhea (IBS-D), IBS with mixed bowel habits (IBS-M) and unclassified IBS (Lacy et al., 2016). IBS is frequently encountered in clinical setting, with a prevalence of 10–15% recorded worldwide, despite variations in the criteria used to delineate IBS among countries (Canavan et al., 2014; Sperber et al., 2017). Currently, the Rome IV Diagnostic Criteria, which provides symptom-based criteria is generally applied for diagnosis of IBS and other functional gastrointestinal disorders (Lacy et al., 2016). The impact of IBS on the risk of mortality and socioeconomic status remains elusive, as different epidemiological studies yielded

varying results (Canavan et al., 2014). Nevertheless, patients with IBS do account for an increase in health resource utilization and decreased work productivity when compared to healthy individuals (Lembo, 2007).

The onset of IBS-related symptoms often occurrs during adolescence, with females being more susceptible than males in the development of IBS (Canavan et al., 2014). Patients with IBS typically experience abdominal discomfort or pain, and get relief upon defecation, with changes in the stool pattern. Additionally, patients with IBS may experience a range of altered bowel habits, including diarrhea, constipation or alternating constipation and diarrhea. Besides that, digestive symptoms such as dyspepsia, dysphagia, non-cardiac chest pain and nausea are also frequently encountered in patients with IBS. On the other hand, IBS also showed comorbidity with other functional gastrointestinal disorders and association with non-gastrointestinal disorders such as chronic pelvic pain, temporomandibular joint disorder, fibromyalgia and chronic fatigue syndrome (Noddin et al., 2005; Soares, 2014). Most profoundly, psychiatric associated comorbidities such as anxiety, depression and somatoform disorders are highly linked with IBS where these comorbidities require further medical attention. If left untreated, these psychiatric comorbidities will impose negative impact on the quality of life (Bonavita and De Simone, 2008; Soares, 2014).

The human gut is a complex structure and is inhabited by trillions of microorganisms including bacteria, fungi, viruses, eukaryotes, and archae. These vibrant microbial communities are imperative in maintaining gastrointestinal homeostasis (Turnbaugh et al., 2007; Marchesi, 2010). Studies have shown that more than 2000 bacterial species reside in the gut with the majority of these species originating from four main phyla: Bacteroidetes, Firmicutes, Actinobacteria, and Proteobacteria (Li et al., 2014; Hugon et al., 2015). The human gut is highly dynamic and undergoes temporal changes from birth to adulthood. As reviewed by Dominguez-Bello et al. (2011), gut microbiota undergoes a few stages of evolution, whereby its initial composition is strongly determined by mode of delivery (either C-section or vaginal delivery), which will then determine the microbiome profile in later stages of development. Subsequently, the gut microbial community continues to grow and diversify in the first few years of life, stabilizes in the adolescence and starts to decline in the adult. Furthermore, the gut microbiome profiles tend to vary between different geographical regions, populations and development stages, indicating that the gut microbiota is constantly evolving throughout life (Dominguez-Bello et al., 2011).

Recent research suggests that the human gut is likely to be affected by environmental factors including xenobiotics, stress, diet and lifestyle throughout the individual's lifespan. Furthermore, recent studies also suggest that gut microbiome is likely a good predictor for metabolic variables and clinical phenotypes and is an important key player in IBS pathogenesis (Rothschild et al., 2018). Hence, this review aims to expound the pathophysiology of IBS and the influence of gut microbiome on IBS pathogenesis, and shed light on current advances and future directions in IBS research and therapeutic interventions.

METHODS

The content and information of this review were based on literature published in PubMed, Scopus, and JCR-ISI. This article does not involve any human or animal experimental studies. Articles published before August 2018 in the aforementioned databases were included. A topic-centric search was performed for each particular section in order to explain and describe the topic. The relevant articles related to the section were identified and the bibliographies were used to perform recursive search to obtain original as well as additional references. The search terms included "irritable bowel syndrome," "microbiota," "microbiome," and "IBS treatment." These search items were combined with the AND operator to additional search terms for the relevant sections of the review, including "pathophysiology," "animal studies," "metagenomics," "prebiotics," "probiotics," "fecal transplantation," "symbiotic," "postbiotic," "metagenome," "fungal treatment," "archaebiotics," "phage therapy," "3-D gut modeling," "dietary intervention," "pathogenesis," "FODMAP," "diet," "meta-analysis," and "future therapy." All authors contributed toward the literature search.

PATHOPHYSIOLOGY OF IBS

The pathophysiology of IBS remains poorly understood. Though non-specific, certain pathogenic factors including genetic predisposition, visceral hypersensitivity, food intolerance, altered gut-brain axis and gut dysmotility, dysfunction of innate immunity and dysbiosis may contribute to this disorder (Bellini et al., 2014) (**Figure 1**). It remains unclear which among these pathogenic factors trigger or augment the IBS as symptoms vary among different individuals.

Genetic Influence

Accumulating evidences have shown that genetic risk in IBS ranges from complex polygenic cases with mixtures of common variants to rare single gene aberration (D'Amato, 2013). The discovery of mutation in the *SC5NA* gene encoding a sodium channel ion, which is associated with abdominal pain experienced by IBS patients, was a notable example of the ability of gene aberration to induce IBS clinical symptoms (Beyder et al., 2014). Subsequently, a number of single nucleotide polymorphisms (SNPs) studies have identified polymorphisms in genes associated with IBS pathogenesis including genes coding for serotonin signaling (Jun et al., 2011; Grasberger et al., 2013), immune regulation and epithelial barrier function (Wouters et al., 2013), bile acid synthesis (Wong et al., 2012) and cannabinoid receptors (Camilleri et al., 2013). Findings from a GWAS in 2015 also identified *GRID2IP* [glutamate receptor, ionotropic, delta 2 (Grid2) interacting protein] and *KDELR2* (KDEL endoplasmic reticulum protein retention receptor 2) to be linked to risk of IBS development (Ek et al., 2015). Meanwhile, report from another GWAS could not confirm the dominant roles for most of the SNPs in immune-related genes in IBS development, except for SNPs in *TNFSF15* (Czogalla et al., 2015). Overall, the impact of genetic influence on IBS development remains obscure due

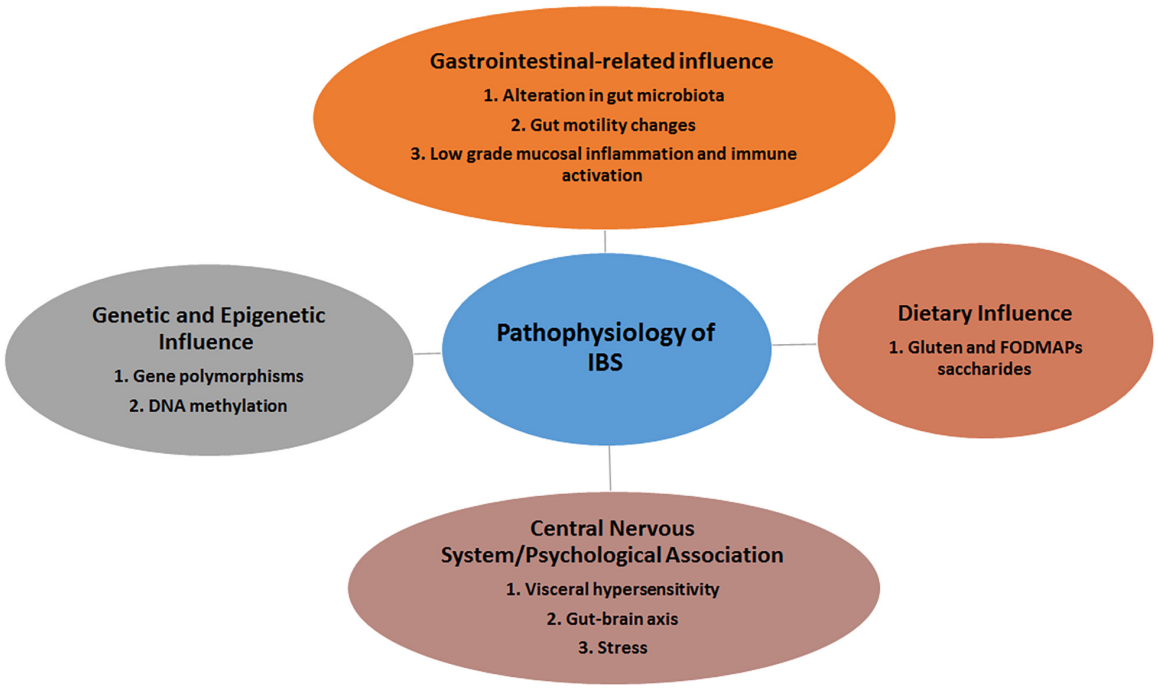

FIGURE 1 | The various players involved in the development of IBS.

to relatively small cohort studies and the absence of prominent structural abnormalities. The susceptibility of common and rare gene variants in IBS remains largely unknown. Additionally, epigenetic factors such as DNA methylation could manifest in IBS (Mahurkar et al., 2016). Hence, further inspection on gene-gene interactions, gene-environment interactions, and gene-pathways interactions are warranted and are more likely to give us clues in understanding IBS pathogenesis.

Gastrointestinal Associated IBS Pathophysiology

Alteration in Gut Microbiota

Under normal circumstances, mucus epithelium barrier confines microbes to the epithelial surface or intestinal lumen where homeostatic immune responses are induced to maintain barrier integrity and tolerance among commensal microbes. This enables microbes to persistently colonize the intestine and perform symbiotic functions. However, once the barrier is breached by influx of inflammatory mediators, pathogens or any agents that provoke intense immune reactions, severe inflammation occurs and this will affect the intestinal environment, and changes the gut microbiota composition (Pedron and Sansonetti, 2008). Briefly, alteration in gut microbiota could contribute to IBS pathogenesis by altering gut immunity and integrity, and modulation of gut neuromuscular junction and gut-brain axis. Multiple reports have linked IBS pathogenesis with dysbiosis, a condition that refers to decrease/loss of microbial diversity and richness, owing to the changes from commensal bacteria to pathogens in the human gut (Carroll et al., 2011, 2012). For example, the composition and activities of *Lactobacilli* and *Bifidobacteria* are heavily compromised in IBS patients (Bellini et al., 2014). A recent study also identified a specific intestinal microbiota signature that could be linked to the severity of IBS (Tap et al., 2017). In this study, the authors reported that the severity of IBS was positively correlated with low CH_4 exhaled, low microbial richness, absence of *Methanobacteriales* and enrichment with *Bacteroides* enterotypes. On the other hand, growing evidence of the involvement of mycobiome alterations in IBS patients and the development of visceral hypersensitivity indicates fungi dysbiosis may have indispensable role in IBS pathogenesis (Botschuijver et al., 2017). The beneficial effects of probiotics on alleviating visceral sensitivity, intestinal permeability and inflammation further support the role of gut microbiota in IBS (Ohman and Simrén, 2013).

Low Grade Mucosal Inflammation and Immune Activation

Recent studies have linked IBS pathogenesis with low grade mucosal inflammation. Combination of low grade mucosal inflammation with visceral hypersensitivity and impaired bowel motility could be the underlying etiology for IBS pathogenesis. This condition may arise from compromised epithelial barrier (Piche et al., 2009), post-infectious alterations (Beatty et al., 2014), dysbiosis (Simrén et al., 2013), and altered stress levels (Qin et al., 2014), which stimulate aberrant immune responses. Associated mucosal inflammation in IBS patients is often linked with history of infectious gastroenteritis induced by bacteria, parasites or viruses, which is referred to as post-infectious IBS (PI-IBS) (Beatty et al., 2014). This association is

further consolidated by findings from several studies including a meta-analysis which demonstrated an approximately sevenfold of increased risk of developing PI-IBS (Halvorson et al., 2006). A number of risk factors have been identified for the development of PI-IBS, including young age, female gender, depression, anxiety and prolonged initial infection with fever (Thabane et al., 2007). Additionally, alteration in immune responses due to inflammation provoked by dysbiotic microbiota, increased number of immune cells such as mast cells and lymphocytes seen in the intestinal mucosal biopsies from PI-IBS patients, and increased cytokine production (Jalanka-Tuovinen et al., 2014; Sundin et al., 2014; Downs et al., 2017) further suggest the pivotal role of post infectious syndrome in IBS development.

A substantial number of studies also documented the role of innate immune dysfunction in IBS pathogenesis and its impact on low-grade inflammation, at both systemic and mucosal level. Activation of immune system in colonic mucosa followed by infiltration of numerous immune cells and release of inflammatory cytokines are observed in IBS patients as compared to healthy subjects (Martin-Viñas and Quigley, 2016; Lazaridis and Germanidis, 2018). Additionally, elevated pro-inflammatory cytokines in isolated PBMCs from patients with IBS-D, particularly IL-6, TNF-α, and IL-1β were observed. These secreted cytokines are also highly associated with depression and anxiety, suggesting the role of gut in regulating brain function (Liebregts et al., 2007). A recent study highlighted the association of inflammatory cytokines IL-17 and TNF-α with disease symptoms and quality of life (IBS-QoL) in different subtypes of IBS patients (Choghakhori et al., 2017). The underlying cause for this altered immune response remains unclear. Nevertheless, impairment in the integrity of mucosal epithelial barrier is likely to be the cause for this condition. Studies in IBS patients with and without infective etiology also showed increased levels of intestinal permeability, suggesting that altered intestinal permeability aroused from defective mucosal epithelial barrier might interfere with gut immune homeostasis, which subsequently promote gut inflammation and aberrant immune responses (Marshall et al., 2004; Shulman et al., 2014).

Currently, most of the studies had focused on specific immune cells, pathogen recognition receptors and cytokines independently, which have yielded varying results and failed to depict the precise role of innate immune dysfunction in the pathophysiology of IBS. More comprehensive approaches should be incorporated to elucidate specific immune signaling pathways involved and the interaction between gut microbiota, enteric nervous system and immune activation during IBS pathogenesis (Lazaridis and Germanidis, 2018). Further examination of immune responses from biopsy samples might provide useful information in elucidating the IBS pathophysiology and identify any potential disease indicators (Choghakhori et al., 2017). Consequently, specific therapeutic interventions can be designed to help combat or mitigate the burden of this disease.

Gut Motility Changes

Patients with IBS often have changes in their gut motility, which is usually driven and augmented by stress via gut-brain axis (Drossman, 2016). These changes are observed in patients with diarrhea, constipation or both and is likely influenced by alteration in serotonin (5-HT) metabolism. Serotonin has a prominent role in controlling gastrointestinal motility. High serotonin levels were observed in patients with diarrhea predominant IBS while low levels of serotonin is associated with constipation predominant IBS (Crowell, 2004; Camilleri, 2009).

Dietary Influence

Diet plays a crucial role in IBS pathogenesis through modulating the normal gut microenvironment including decrease in colonic fermentation, altered gut microbiome composition and reduced antigen activation by the gut immune system (Muegge et al., 2011; David et al., 2014). Growing evidence has supported the importance of diet in IBS etiopathogenesis. Food and breakdown products of food can affect many aspects of gut physiology including motility, permeability, microbiome, visceral sensation, brain-gut interactions, immune regulation and neuro-endocrine function; which are all relevant to the pathogenesis of IBS (Chey, 2016). Thus, a diet that limits intake of "offending" foods that trigger these alterations, or a diet that corrects the microbiota dysbiosis, would be beneficial to manage IBS symptoms.

Exacerbation of symptoms with ingestion of specific foods such as gluten and FODMAPs saccharides are often reported in patients with IBS. Abdominal pain and other GI-related symptoms were reported in IBS patients after consumption of gluten, without the clear evidence of celiac disease based on histology and serology assessments. This condition, so called "non-celiac gluten sensitivity (NCGS)" may be pertinent in IBS-like symptoms development (Elli et al., 2015). The effects of gluten on IBS most likely include alteration of intestinal permeability and activation of autonomous and enteric nervous system (Biesiekierski et al., 2013; Elli et al., 2015).

Ingestion of FODMAPs have been shown to lead to bloating, abdominal pain and other IBS symptoms in about 70% of patients (Staudacher et al., 2012; Böhn et al., 2015). FODMAPs are short-chain carbohydrates that are easily fermentable by gut bacteria into methane and hydrogen gasses but are poorly absorbed (Eswaran et al., 2016). Short chain fatty acids are also another byproduct of FODMAPs fermentation. The gasses produced by FODMAPs lead to bloating symptoms in IBS. The osmotic effects of FODMAPs also increase intraluminal fluid which may cause GI distension and stimulate abnormal intestinal motility.

Central Nervous System/Psychological Association in IBS Pathophysiology

Visceral Hypersensitivity

Visceral hypersensitivity, a condition of increased pain sensation in the bowel due to physiological stimuli is crucial in IBS pathogenesis. Patients with visceral hypersensitivity tend to have lower colonic distension pain threshold where a normal stimulus will intensify the pain in the patients (Camilleri et al., 2001). Visceral hypersensitivity may occur at both peripheral and central nervous system and is the key pathogenesis for IBS (Aziz et al., 2007). Epidemiological data from various studies reveal that prevalence of visceral hypersensitivity in IBS patients varied from

33 to 90%, with a higher tendency to develop in IBS-D patients (Kanazawa et al., 2008; Gwee et al., 2009; Ludidi et al., 2014). Additionally, clinical evidence also showed that IBS patients with visceral hypersensitivity developed more severe complications than those without visceral hypersensitivity (Ludidi et al., 2014). The pathophysiology of visceral hypersensitivity in IBS remains poorly understood. Multiple factors are involved in this altered visceral sensation including dysbiosis, brain–gut communication, diet, psychological factors, genetic predisposition, inflammation and immunological factors. Additionally, altered intestinal permeability may contribute toward visceral sensitization and severity of IBS complications (Farzaei et al., 2016). Findings from clinical studies also revealed high expression of circulating microRNAs (miRNAs) in the colonic tissues of IBS patients, suggesting the involvement of epigenetic and genetic events in modulating intestinal signaling pathways, particularly serotonin receptor gene with a *cis*-regulatory variant on the somatic hypersensitivity and intestinal permeability of IBS patients (Kapeller et al., 2008). On the other hand, sensitization of distal peripheral afferent, particularly serosal and mesenteric afferents within the splanchnic pathway could be the underlying factors for visceral hypersensitivity in IBS patients. These distal peripheral afferents possess chemosensitivity which could prolong visceral sensitization and induce post-inflammatory effects (Anand et al., 2007). Hence, targeting microbiota-gut-brain and local neuroimmune pathways could be potential therapeutic intervention in managing visceral hypersensitivity in IBS patients.

Alteration in Gut-Brain Axis

The brain-gut axis (GBA) is a bidirectional communication system between the gut and the brain. Along this conduit, the brain interacts with the gut through neural components (CNS and ANS), endocrine system (hypothalamic-pituitary-adrenal axis), immune components (cytokines and metabolic) and gastrointestinal components (microbiota, intestinal barrier and intestinal immune response) (Oświęcimska et al., 2017). Studies have shown that disturbances in GBA drive the pathogenesis in neurodegenerative disorders (Cenit et al., 2017) and gastrointestinal diseases including inflammatory bowel syndromes and inflammatory bowel diseases (IBDs) (Bonaz and Bernstein, 2013; Oświęcimska et al., 2017).

The most notable IBS comorbid disorders, anxiety and depression are highly seen in community samples and outpatients. However, the linkage between these disorders and IBS patients were not fully elucidated by healthcare seeking behavior alone. Hence, it was postulated that the brain drives these psychiatric comorbidities seen in IBS patients, which leads to the conclusion that IBS is a primary brain disorder or somatic symptom disorder whereby the brain is involved in manifesting the gastrointestinal symptoms (Henningsen et al., 2003; Tanaka et al., 2011; Patel et al., 2015). Nevertheless, several prospective studies reported that at least in half of the IBS cases, gastrointestinal symptoms appeared first, followed by mood disorders (Jones et al., 2012; Koloski et al., 2012, 2016). In another independent study, incidence of mood and anxiety disorders after the onset of IBS were around 40 and 23% respectively. These findings likely suggest that the gut is driving the brain manifestations (Sykes et al., 2003). Additionally, studies related with gut microbiome, intestinal inflammation and immune response further suggest the concept that the gut drives brain alterations (Liebregts et al., 2007; Mayer et al., 2014). Eventually, if these findings are ultimately accurate, reversing gastrointestinal dysfunction could serve as potential therapeutic interventions in curing IBS and other concomitant mood disorders.

Stress

On the other hand, psychological stress may have critical influence on gut-brain axis. IBS is considered as a stress sensitive disorder. The main effects of stress are mainly on intestinal motility and permeability, visceral sensitivity, immune responses and gut microbiota composition (Qin et al., 2014). The underlying mechanism is likely through secretion of pro-inflammatory cytokines such as interleukin-6 (IL-6) and interleukin-8 (IL-8) which activate hypothalamic-pituitary-adrenal (HPA) and hypothalamic-autonomic nervous system axes, trigger the release of corticotrophin releasing factor (CRF), adrenocorticotropic hormone and cortisol, which consequently affect gut homeostasis (Dinan et al., 2006). The influence of stress on IBS is indisputable. Thus, managing stress and stress-induced responses are imperative as part of the therapeutic intervention in IBS patients. Other psychological factors including abuse (physical, sexual, verbal, and adverse life events), posttraumatic stress disorders and somatization are also likely involved in gut–brain interaction and IBS pathogenesis (Qin et al., 2014).

MICROBIOTA AND MICROBIOME IN IBS

Gut Microbiota Composition in IBS

The human microbiota in the intestines is a complex assemblage of microbes, a dynamic environment comprising pro- and anti-inflammatory bacterial species (Dupont, 2014). Apart from bacteria, intestinal microorganisms such as archae, fungi and viruses exist in symbiosis in healthy individuals. Most bacteria in the gastrointestinal tract include members from the following phyla in a descending order: Firmicutes (64%), Bacteroidetes (23%), Proteobacteria (8%), and Actinobacteria (3%) (Gill et al., 2006; Bäckhed et al., 2012). However, only about one third from the ∼1000 different bacterial species had been identified and characterized so far. Many of the species from Archae that had been isolated are methanogens and halophilic archae. The methanogens associated with gut include *Methanobrevibacter smithii* (94%), *M. stadtmanae* (23%), *Candidatus* "*Methanomethylophilus alvus*" and *Candidatus* "*Methanomassiliicoccus intestinalis,*" among others (Dridi et al., 2009). As polysaccharides get fermented by gut bacteria, gasses such as hydrogen (H_2) and methane (CH_4) are generated as by-products (Pimentel et al., 2006). In addition, short-chain fatty acids (SCFAs) such as acetate, propionate and butyrate are also produced by the colonic bacteria whereby these SCFAs and gasses could affect bowel movement as well as gut permeability. One study by Pozuelo et al. (2015) found a lower abundance of butyrate-producing bacteria in IBS patients, particularly in

IBS-D and IBS-M. As butyrate-producing bacteria are known to improve intestinal barrier function, decreased amount of these bacteria in IBS-D and IBS-M patients could have led to impairment in intestinal permeability and activate the nociceptive sensory pathways, which manifest in the symptoms observed. They also found that IBS patients not undergoing any therapy had lower abundance of Methanobacteria (Pozuelo et al., 2015). This observation was in agreement with several other studies which found that methane production was seen at lower levels in IBS-D and higher levels in IBS-C (Jahng et al., 2012; Tap et al., 2017). Besides the sulfate-reducing bacteria, methanogens from the Archaea kingdom are the main gut microbe responsible for removing excess hydrogen by converting it to methane. Methane production capacity is linked to low transit time and anti-inflammatory effects in the colon. In IBS patients, lower counts of methanogens imply reduced ability for hydrogen gas removal from the colon, and hence this could attribute to flatulence or excess gas in the abdomen.

Among the common trends reported in previous studies on the composition of intestinal bacteria in IBS subjects relative to healthy controls were increase in abundance of Proteobacteria, including from the phyla *Veillonella*, and Firmicutes, including *Lactobacillus* and *Ruminococcus* (Tana et al., 2010; Rigsbee et al., 2012). This was usually accompanied by a decreased quantity of *Bifidobacterium*, *Faecalibacterium, Erysipelotrichaceae* and methanogens (Rajilić-Stojanović et al., 2011; Pozuelo et al., 2015). The halophilic archae such as *Halorubrum koreense*, *Halorubrum alimentarium*, *Halorubrum saccharovorum,* and *Halococcus morrhuae* were isolated from a study on Korean subjects (Nam et al., 2008). This could also be due to Koreans' high-salt food intake, which warrant further studies on the prevalence of these halophilic archae in relation to diet. Out of the 62 fungal genera that were isolated from 98 healthy individuals in the US, the predominant fungi were *Saccharomyces* (present in 89% of the samples), followed by *Candida* (57%) and *Cladosporium* (42%) (Hoffmann et al., 2013). However, thus far gut microbiome studies had reported the distribution of total fungi present as part of the microbiome as only 0.1% (Underhill and Iliev, 2014; Tang et al., 2015). It is possible that this could be an under-representation due to depth limitations of current metagenomics techniques, where sequences of dominant microbes will "crowd out" the detection of less abundant fungi.

Microbiome – From Symbiosis to Dysbiosis and Pathogenesis

The gastrointestinal microbial flora inhabits in the human host through an intriguing relationship of symbiosis or "commensalisms." This delicate symbiosis starts at birth when the infant crosses the birth canal and develops in a regulated and coordinated manner as the infant matures and develops into adulthood. It is widely believed that the GI microbiota in an infant is derived from its mother's microbes during either vaginal delivery or cesarean section and possesses low complexity as well as species diversity. As the infant grows, the microbiota also dynamically matures and gradually attains richness in diversity that approximates the adult microbiota profile by the first year of life. Distinct life events, such as weaning from breast milk to solid foods are postulated to be the cause of the increase in species diversity. It has been postulated that the presence of a microbial flora that co-exist within the individual host in well-established symbiosis may act as a deterrent for pathogenic microbes from colonizing and disrupting the resident microbiota.

Dysbiosis is a condition of having imbalance in the microbial community in or on the body and is sometimes known as impaired microbiota. In a study conducted in Sweden, Norway, Denmark, and Spain, on patients between 17 and 76 years old (Casén et al., 2015), dysbiosis was investigated in 236 IBS and 135 IBD patients who were diagnosed according to Rome II and III-criteria. A dysbiosis frequency of 73% was observed among IBS patients. Dysbiosis in healthy individuals occur at a rate of around 16% (Karantanos et al., 2010; Jeffery et al., 2012; Collins, 2014). In the Casén et al. (2015) study, pre-dominant bacteria contributing to dysbiosis in IBS include Firmicutes such as *Bacillus* and *Ruminococcus gnavus*; Proteobacteria such as *Shigella* or *Escherichia*; and Actinobacteria. *Bacteroides stercoris* and *Bifidobacterium* were also known to contribute to dysbiosis among this patient cohort, which could be affected by the dietary differences between the Scandinavian countries and the Mediterranean region.

A meta-analysis which was performed on 13 studies up until 2016 had shown that there were significant differences in expression in IBS patients compared to healthy controls for *Lactobacillus*, *Bifidobacterium,* and *Faecalibacterium prausnitzii*. However, no significant dysbiosis was shown among the Bacteroides–Prevotella group, *Enterococcus*, *Escherichia coli*, *Clostridum coccoides* and other genera or species among these patients (Liu et al., 2017). Patients involved in this meta-analysis were from China, Finland, France, India, Japan, Netherlands, and United States. Further analysis revealed that IBS-D patients had significant decrease of *Lactobacillus* and *Bifidobacterium*, as compared to their healthy counterparts and constipated-predominant IBS patients. Among Chinese IBS patients, it was reported that *Lactobacilli* showed significant reduction, contrary to patients from other countries (Liu et al., 2017; Zhuang et al., 2017). Therefore, further investigations are required in the case of *Lactobacilli* to identify whether it can survive and adapt well to the pro-inflammatory gut environment or is a contributor to IBS. Increase of *Pseudomonas aeruginosa* was found in two studies indicating a relationship between this bacterium with IBS (Kerckhoffs et al., 2011; Shukla et al., 2015). Other studies reported that increased levels of Bacteroidetes were from the family Enterobacteriaceae such as *Ruminococcus* sp., *Lactobacilli* sp., and *Clostridium* sp. in the IBS patients (Si et al., 2004; Malinen et al., 2010; Ponnusamy et al., 2011). Another organism related to post-infection in IBS patients is the parasite, *Giardia duodenalis* (Beatty et al., 2017). From experiments involving *G. duodenalis* and bacterial biofilms, it was observed that the thickness of the microbiota biofilm was reduced from 100–210 μM to 10–105 μM in the presence of this parasite (Beatty et al., 2017). Further analysis revealed that extracellular matrix (ECM) compositions of the mucosal microbiota biofilms were also altered, along with the structural integrity of the biofilm, with an over-representation of *Clostridiales* bacteria and

a decreased amount of *Phascolarctobacterium* sp. Studies have shown that *G. duodenalis*-infected IBS patients from Italy and Norway had disruptions in their mucosal microbiota, leading to chronic post-infections.

Repeated observations from various studies for bacterial dysbiosis in IBS are generally increased or decreased levels of Firmicutes and Bacteriodetes with ratios that differ between study groups. The dysbiosis would also lead to disruptions in the immune function, which contributes to post-infections in IBS patients which could become chronic. A study by Wadhwa et al. (2016) found that around 25% of *Clostridium difficile* infected patients developed IBS, particularly mixed-IBS, 6 months or more post-infection. When compared to healthy individuals, a few studies have demonstrated that there were increased levels of C-reactive proteins, inflammatory mediators such as IL-6 and IL-8 and inflammatory cytokines in IBS patients (Matricon et al., 2012; Ringel and Maharshak, 2013; Hod et al., 2016). Apart from these, selective inhibition of mast cells was also suggested with the presence of bacterial lipopolysaccharides (Ludidi et al., 2015). Some reports have also indicated an increase of *Streptococcus* spp., a pathogenic bacterium which causes increased levels of IL-6, and mucin degraders such as *Ruminococcus* spp. (Rajilić-Stojanović et al., 2011). In some patients, an increased expression of Toll-like receptor (TLR)-4 which recognizes bacterial LPS, TLR-5 which recognizes bacterial flagellin and increased levels of anti-flagellin antibodies were found in post-infection IBS (Anitha et al., 2012).

There had been many instances when commensals (normal microbiota) reportedly turned pathogenic such as the case of *Enterococcus faecalis* which had inadvertently acquired a number of virulence genes that conferred vancomycin resistance (Paulsen et al., 2003). In another study, activation of latent virulence genes in non-invasive *E. coli* was found to be due to the exposure to *C. jejuni* secretory-excretory products (Reti et al., 2015). Sharing such genes with their co-inhabitants may allow adaptation for better adhesions, acquiring new nutritional pathways and antibiotic resistance, all of which lead to evasion from the immune system as a possible pathogenesis step. In the acute phase of giardiasis, dysbiosis has also been indicated to contribute to CD8 T lymphocyte-mediated impairment (Keselman et al., 2016). Clearly, there is a robust connection between bacteria dysbiosis and the severity of IBS. Nonetheless, the relative abundance of the microbiota in different IBS-subtypes remains largely unexplored. Hence, we summarized the microbiota diversity in different IBS-subtypes in this section, as indicated in **Table 1**.

METHODOLOGIES FOR STUDYING IBS AND ASSOCIATED MICROBIOME

In this section, we review several methodologies available for studying IBS, including the establishment of animal models, and *in vitro* models with the latest innovations of gut-on-a-chip systems. The importance of fecal sample collection for assessing the intestinal microbiota composition and other associated applications are also highlighted. The technological platforms for studying the microbiome (sets of genes), the metagenome and metabolome, along with high-throughput culture (culturomics) are also presented.

Experimental Animal Models for IBS

The Wrap Restraint Stress (WRS)

Currently, there is no single animal model that can best mimic the human IBS. The WRS model which involves immobilizing the animal for a minimum duration of 2 h, is commonly applied in acute tests. This model often demonstrates morphological changes of the entire colonic wall that shows visceral hypersensitivity similar to human IBS symptoms (Gue et al., 1997). The WRS model is established on the premise that psychosocial stress have an indispensable role in the etiology of IBS. Experimental results show that dysmotility and hypersensitivity in these animals could have resulted from alterations in glial cells and both excitatory and inhibitory neurotransmitters (Traini et al., 2016).

Chemical Irritation

Abdominal pain is the main symptom present in most IBS patients (Bray et al., 2006). Animal models of visceral pain are crucial for aiding researchers in unraveling the possible mechanisms that contribute toward IBS etiopathology. The abdominal pain-related behavioral model can be induced by administration of neostigmine, mustard oil, capsaicin and acetic acid solution (Fichna et al., 2012). Pain behaviors in the animals which are measurable include specific postures like licking of the abdomen, forced pressure onto the abdomen and abdominal contractions. Chemical irritation models are useful to study abdominal pain-related signaling pathways in IBS as evidenced by the blockage of pain-related responses in animal by morphine. This model is also frequently applied in drug discovery and therapeutics development for IBS. For example, Chen et al. (2015) showed that berberine can improve intestinal motility and visceral pain in IBS via the opioid receptor dependent manner using chemical irritation method in mice.

Chronic Stressors

Apart from acute stress, there is evidence suggesting that IBS may be associated with childhood traumas of varying root causes or the presence of recurring stress in adulthood (Mayer et al., 2015), indicating prolonged stress may be involved in the development and maintenance of IBS. These clinical data prompted scientists to develop IBS animal models with chronic as opposed to acute stressors. The maternal separation (MS) model and the water avoidance stress (WAS) model are two animal models of chronic stress which were established to mimic infancy trauma, and stress in adulthood, respectively. The symptoms produced by these two behavioral animal models resemble human IBS with WAS being considered as a milder chronic stress compared to MS. Interestingly, these models show that there is a gender-difference in response to stress.

Maternal Separation

In this model, young puppies were removed from the mother for a few hours per day during the first 2 weeks of life. The MS in the first 2 weeks of life appeared to have long-term effects on

TABLE 1 | Alterations in microbiota diversity in different subtypes of IBS.

IBS subtypes	Microbiota diversity (Family/Phylum/Genus/Species)	Alteration in microbiota (compared with healthy subjects)	References
IBS-C	*Veillonella* spp.	Increased	Malinen et al., 2005
	Lactobacilli spp.	Increased	
	R. bromii-like phylotype	Increased	Lyra et al., 2009
	B. catenulatum	Decreased	Kerckhoffs et al., 2009
	Methanobrevibacter	Decreased	Rajilić-Stojanović et al., 2011
	Methanobrevibacter smithii	Increased	Kim G. et al., 2012
	Unknown Ruminococcaceae, unknown Christensenellaceae, *Akkermansia*, and *Methanobrevibacter*	Increased Increased Increased	Pozuelo et al., 2015
	Clostridiales	Increased	Tap et al., 2017
	Bacteroides	Decreased	
	Prevotella	Decreased	
IBS-D	*Lactobacillus* spp.	Decreased	Malinen et al., 2005
	Clostridium symbiosum-like	Decreased	Rajilić-Stojanović, 2007
	Proteobacteria	Increased	Krogius-Kurikka et al., 2009
	Firmicutes (*Lachnospiraceae*)	Increased	
	Actinobacteria	Decreased	
	Bacteroidetes	Decreased	
	B. catenulatum	Decreased	Kerckhoffs et al., 2009
	C. thermosuccinogenes	85% phylotype increased	Lyra et al., 2009
	R. torques	94% phylotype increased	
	Collinsella aerofaciens	Decreased	
	B. intestinalis-like phylotype	Decreased	
	Lactobacillus spp.	Increased	Carroll et al., 2010
	Enterobacteriaceae	Increased	Carroll et al., 2012
	Fecalibacterium (Faecalibacterium prausnitzii)	Decreased	
	Bifidobacteria	Decreased	Parkes et al., 2012
	Ruminococcaceae, unknown Clostridiales, Erysipelotrichaceae, Methanobacteriaceae	Decreased	Pozuelo et al., 2015
	Clostridiales	Increased	Tap et al., 2017
	Bacteroides	Increased	
	Prevotella	Decreased	
	Lachnospira	Decreased	Zhuang et al., 2018
	Parasutterella	Decreased	
	Lachnospiraceae_UCG-010	Decreased	
	Ruminococcaceae_UCG-003	Decreased	
	Lactobacillus	Decreased	
	Turicibacter	Decreased	
	Enterococcus	Decreased	
	Weissella	Decreased	
	Oxalobacter	Decreased	
	Oceanobacillus	Decreased	
	Lachnospiraceae_NK4A136_group	Decreased	
	Faecalitalea	Increased	
	Prevotella	Increased	Su et al., 2018
	Bacteroides	Decreased	
	Bifidobacteria	Decreased	
	Lactobacillus	Decreased	

(Continued)

TABLE 1 | Continued

IBS subtypes	Microbiota diversity (Family/Phylum/Genus/Species)	Alteration in microbiota (compared with healthy subjects)	References
	Faecalibacterium	Decreased	Maharshak et al. (2018)
	Dorea	Increased	
IBS-A	*C. symbiosum*	Decreased	Rajilić-Stojanović, 2007
	Prevotella oralis	Decreased	
	Ruminococcus torques (*R. torques* 93% phylotype)	Increased	Lyra et al., 2009
	B. intestinalis-like phylotype	Highest	
	R. torques 93 %	Decreased	
	C. cocleatum 88%	Increased	
	B. catenulatum	Decreased	Kerckhoffs et al., 2009
	Veillonella	Increased	Tana et al., 2010
	Faecalibacterium spp.	Increased	Rajilić-Stojanović et al. (2011)
	Erysipelotrichaceae	Decreased	Pozuelo et al., 2015
	Clostridiales	Increased	Tap et al., 2017
	Bacteroides	Increased	
	Prevotella	Decreased	

the stress response and subsequent visceral pain sensitivity in the pups. Independent researchers have reported similar heightened visceral sensitivity using these animal models (Coutinho et al., 2002; Ren et al., 2007; Moloney et al., 2012), with results indicating that female animals demonstrated greater sensitivity to MS compared to males.

Water Avoidance Stress

As the name suggests, animals were subjected to periods of water avoidance (WA) as a form of stress. In this model, male Wistar rats were subjected to either WA or sham WA for 1-h daily, 10 days sequentially. Previous data showed that rats subjected to chronic application of WAS for 10 days had visceral hyperalgesia which persisted for at least a month, increased rate of fecal pellet excretion, and evidence of low-grade immune activation such as expression of IL-1β and IFN-γ stress (Bradesi et al., 2005).

In vitro Models for IBS

Human Gut-on-a-Chip

The innovation and development of microfluidic organ-on-a-chip models of human intestine have revolutionized the way in which we can study intestinal physiology and pathophysiology. Previously it was a great challenge to co-culture intestine microbes with viable epithelium for longer than 1 day using conventional culture models, and this was not achievable even with intestinal organoid cultures. Using a 2-D cell culture format with monolayer Caco-2 cells, for example, it is not possible to reproduce the physiological conditions present in the intestines, such as the unique intestinal tissue morphology of villi formation and mucus production, as well as key intestinal differentiated functions including cytochrome P-450-based drug metabolism. Moreover, the commensal bacteria will rapidly overgrow and contaminate the human cell cultures in these co-culture models. Recently, with the invention of microfluidic Organ Chip models of human intestine, these challenges have been overcome (Bein et al., 2018).

One of the earliest "human gut-on-a-chip" devices was developed by Kim and co-workers which was a revolutionary peristaltic, microfluidic, 2-channel Gut Chip model comprising a porous flexible membrane serving as a scaffold for intestinal epithelial cells and coated with ECM, that is sandwiched between 2 microfluidic channels. This microgut device mimics the dynamics (peristalsis), structure and physiological functions (absorption and transport) of human intestine and allows the growth of not only human intestinal cells but also capillary endothelial cells, immune cells, and even microorganisms (Kim H.J. et al., 2012). Interestingly, a normal intestinal microbe (*Lactobacillus rhamnosus* GG) was able to be co-cultured with the intestinal cells on the luminal surface for more than 1 week using this gut-on-a-chip. Huh et al. (2013) described the microengineering behind the fabrication of these organs-on-chips, detailing the materials and dimensions used to construct the structures of these microdevices, as well as the mechanical engineering principles that reproduce the peristalsis-like motions and fluid flow which closely mimic the real *in vivo* situation in the live intestine.

The microfluidic device was intended for drug permeability test, and pharmacokinetics (PK) and pharmacodynamics (PD) evaluation whereby the test drug could be delivered either to the upper or bottom channel via a pressure-driven flow to mimic dynamic *in vivo* conditions, but it could also be adapted to microbiome studies (Kimura et al., 2015). A notable application of the Gut Chip is to investigate the crosstalk between the immune system and the microbiome, a hallmark of chronic inflammatory diseases including IBD (Kim et al., 2016). It is foreseeable that applications of the Gut Chip will be extended

to other disease models including IBS models in the future. A commercialized gut-on-a-chip system is the perfused gut epithelium tubules – 3D intestinal tubules in the OrganoPlate® (MIMETAS, 2018)[1].

Methodologies for Studying Microbiome

Fecal Sample Collection

The last few years had seen the formation of research consortia to investigate the human gut microbiome through metagenome analysis (Qin et al., 2010). These large-scale projects need efficient techniques and standardized methods for sample collection and processing to ensure accurate analysis and interpretation. In particular, DNA extraction from fecal/intestinal samples is one of the crucial steps in determining the composition of microbiota flora. Besides the presence of certain inhibitors from fecal samples, the differences in morphological and physicochemical properties, as well as the phylogenetic diversity will affect DNA extraction and subsequent downstream analysis. A number of studies had compared different sample collection methods, and found that fecal occult blood test card and RNAlater were deemed to be more stable without freezing for 4 days, but if the samples had to be frozen, then swab, FOBT, and 70% ethanol gave the highest accuracy (Sinha et al., 2016; Vogtmann et al., 2017; Wu et al., 2018).

Culture-Independent Approach

Besides that, different approaches have been developed to study the microbiome, including clone libraries, terminal restriction fragment length polymorphism (T-RFLP), quantitative PCR (qPCR), transcriptome microarrays, as well as high throughput sequencing technologies (Illumina sequencing and 454 pyrosequencing). Notably, pyrosequencing of 16S rRNA amplicons and Illumina sequencing are two robust methods for investigating the genome diversity and the differential gene expression of microbial communities in human guts (Qin et al., 2010) and oral cavities (Lazarevic et al., 2009). These technologies not only accelerated metatranscriptomic studies of microbiome, but together with metagenomic data sets, they also provide a great opportunity for exploring the structure and function of microbial communities. Moreover, these methods are culture-independent, allowing further studies and the identification of non-culturable microorganisms in the microbiome.

Culturomics

Nevertheless, one major limitation of metagenomic studies is the depth bias as current metagenomics technologies are unable to detect bacteria at concentrations of $< 10^5$ bacteria per gram of stools. Although metagenomics techniques are able to yield the DNA sequences of many "uncultivable" bacteria, we still require viable microorganisms in pure culture for downstream applications such as for development of microbiota-based therapeutics. Under this circumstance, "Culturomics," which is diversification of culture conditions together with identification by matrix-assisted laser desorption ionization–time of flight mass spectrometry [MALDI-TOF MS], is a set of methodologies aimed at increasing the bacterial repertoire from a microbiota flora. Cultured isolates will not only expand the reference genome databases, they may also reveal novel genes/functions for development of new therapeutics. A landmark culturomics study by Lagier and coworkers which utilized 212 different culture conditions in conjunction with MALDI-TOF-MS for identification, have produced 340 species of bacteria, 5 fungi and 1 giant virus from three stool samples (Lagier et al., 2012). This had led to the rebirth of culture techniques and the development of taxogenomics for classification of new bacteria (Lagier et al., 2015).

Metabolomics

The gut microbiota is the chief "organ" responsible for some crucial metabolic functions that include biosynthesis of amino acids, short chain fatty acids, essential vitamins (e.g. K and B12), bile acid biotransformation and hydrolysis as well as fermentation of non-digestible polysaccharides (Putignani et al., 2014). Therefore, metabolomics, which is the large-scale study of small molecule metabolic products (the metabolome) of cells, tissues, biofluids and organisms at a specific point in time; is a powerful approach to unravel the complex interactions of the metabolites from gut microbiota (metabolome). Comparative studies of metabolome for unhealthy and healthy subjects' microbiota can lead to discovery of unique metabolites that could be developed as diagnostic or prognostic biomarkers. Two principal technologies that can be exploited for metabolomics are mass spectrometry (MS) and nuclear magnetic resonance (NMR) spectroscopy as these offer a good range of coverage, sensitivity and quantification (Vernochi et al., 2016).

Using metabolomics approach, a previous study demonstrated that the metabolite profile of fecal extracts from ulcerative colitis patients with and without IBS had alterations compared to healthy controls (Le Gall et al., 2011). It was also found that perturbed microbial metabolism results in an increased production of hydrogen gas in IBS, as well as indole, phenols and other compounds (Kumar et al., 2010). Volatile organic compounds (VOCs) are released by bacteria as by-products of metabolism, which could be determined by SPME-GC-MS. These specific microbial VOCs profiles could potentially serve as specific biomarker candidates for diagnostic purposes (Bunge et al., 2008). Overall, the current approaches and their applications in studying microbiome is summarized in **Table 2**.

IBS THERAPY OPTIONS

Nowadays, a great myriad of therapeutic options are available for IBS. However, treatment outcome is still unsatisfactory for both the patient and doctor (Moayyedi et al., 2017). An important consequence of the associated comorbidities and treatment failure of IBS is reduced quality of life, and decreased work productivity. To illustrate this point specifically, IBS patients were found to be absent from work 2 days/month on average, with reduced work productivity for 9 days/month, according to a report (Buono et al., 2017).

[1]https://mimetas.com/overview-mimetas-applications/perfused-gut-epithelium-tubules

TABLE 2 | Current methodologies for studying microbiome.

Approach	Examples	Advantages/Features
Culture-independent approach	• Clone libraries • terminal restriction fragment length polymorphism (T-RFLP) • quantitative PCR (qPCR), • transcriptome microarrays, • high throughput sequencing technologies • metagenomics	(1) Enables the discovery of non-cultivable species in the gut (2) Unravel the structure and function of microbial communities (3) Untangle the genome diversity and the differential gene expression of microbial communities (4) Identification of the role of microbes in disease development
Culture-dependent approach	Culturomics (different culture conditions, with identification performed via microbiological methods as well as MALDI-TOF MS)	(1) Enables the recovery of microbes from the samples for downstream applications (2) Expansion of available reference genome databases (3) Potential approach to discover novel genes/functions for development of new therapeutics
Metabolomics	Mass Spectrometry (MS) and Nuclear Magnetic Resonance (NMR) Spectroscopy	(1) Enables the identification of metabolic products at specific time interval (2) Unravel the complexity between metabolites and gut microbiome (3) Enables the discovery of unique metabolic signature for diagnostic/prognostic applications

The fecal microbiota of IBS patients has been known to exhibit several qualitative and quantitative alterations (Dupont, 2014). There has also been a theory of microbial etiology which pinpoints bacterial, viral and parasitic infections for causing IBS (Klem et al., 2017). Therefore, targeting the microbiome in IBS could be an effective therapeutic approach. A subset of IBS patients show good response to non-absorbable antibiotics (Pimentel et al., 2011) and prebiotic/probiotic administration (Moraes-Filho and Quigley, 2015). Fecal transplantation is a new mode of IBS treatment which has gained traction and is lauded as a very promising therapeutic option in the near future. **Figure 2** summarizes the therapeutic options available for alleviating the symptoms of IBS. The various treatment options are discussed in the sections below.

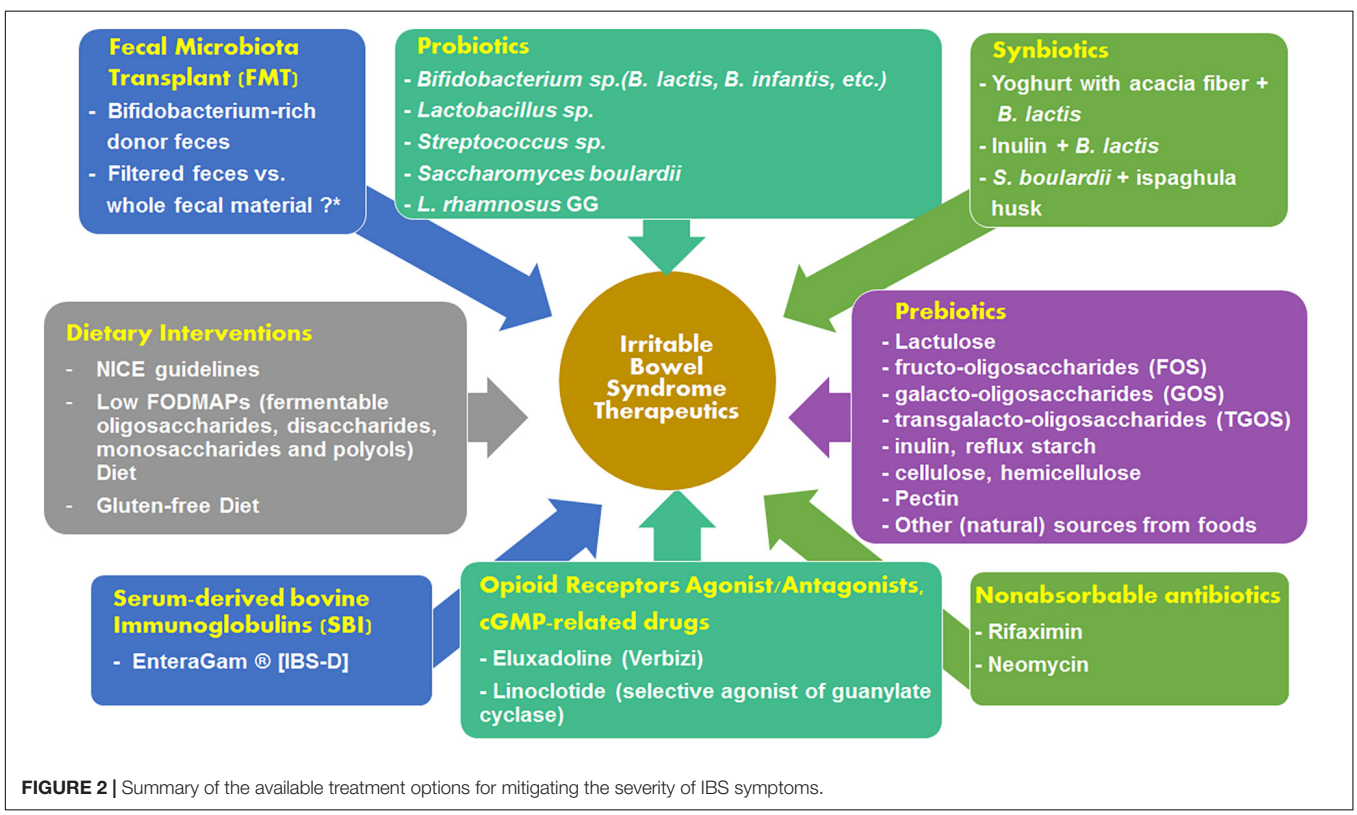

FIGURE 2 | Summary of the available treatment options for mitigating the severity of IBS symptoms.

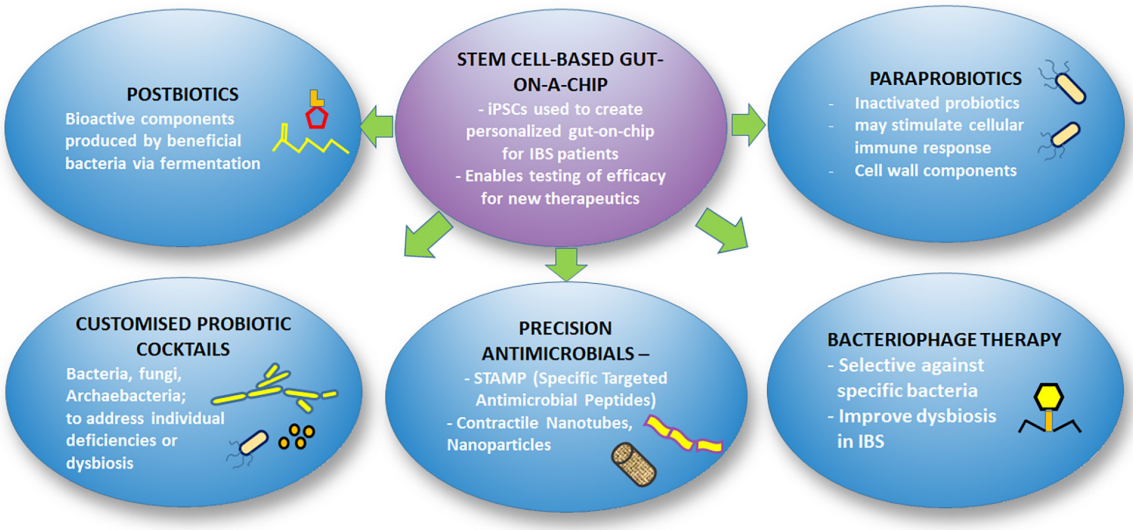

FIGURE 3 | Overview of future therapeutics for IBS.

Microbiota-Based Therapies: Prebiotics, Probiotics, and Synbiotics

Probiotics

Probiotics are living microorganisms which commonly comprises gut-friendly bacteria and sometimes also yeast, and are ingested in the form of foodstuffs and supplements. With the known pathophysiology of IBS, consistent use of probiotics has been demonstrated in previous studies to improve symptoms associated with IBS particularly with the *Biofidobacterium* and *Lactobacillus* strains (Guyonnet et al., 2007; Simrén et al., 2013). Several meta-analyses of randomized controlled trials (RCTs) that compared the effects of probiotics against placebo in reducing IBS symptoms (Ford et al., 2014; Didari et al., 2015; Zhang et al., 2016) found probiotics to be more superior to placebo in reducing overall IBS symptoms and abdominal pain. These meta-analyses looked at single probiotic strains, but other meta-analyses had examined the effects of combinations of strains *Bifidobacterium*, *Lactobacillus,* and *Streptococcus* genera (Jafari et al., 2014). Meta-analyses with less common probiotic genera or species were also conducted, such as with the yeast *Saccharomyces boulardii* (McFarland, 2010), bacteria *B. infantis* (Yuan et al., 2017) and *Lactobacillus rhamnosus* GG (Horvath et al., 2011) albeit with differing results. *S. boulardii* was reportedly able to lead to increase in bowel frequency, whereas *L. rhamnosus* reduced the intensity and frequency of abdominal pain. *B. infantis* in combination probiotics was able to reduce IBS symptoms (bloating and abdominal pain), but not *B. infantis* alone (Yuan et al., 2017).

Although in general terms, probiotics seem to have beneficial effects on improving IBS, how they function is still relatively unknown. Previous studies that attempted to illuminate their mode of action suggest that the probiotics strains played a role in modulating gut inflammation, producing antimicrobial peptides that help to eliminate pathogenic bacteria, and improving the mucosal barrier function. Much remains to be answered as to which strains is/are most effective across the broad spectrum of IBS patients and whether single or combination of strains work best. At the moment it seems to be a case of trial and error. This leads to the question of whether individual differences among IBS patients in terms of immune profile and microbiome diversity could affect the efficacy of probiotics therapy. Personalized or customized probiotics therapy guided by individual microbiota profiling may be the way forward in future.

Prebiotics

A disadvantageous feature of probiotics is that most have a short lifespan and thus repeated doses are necessary. Prebiotics may serve as an alternative treatment as they provide the metabolizable substrates for growth of specific bacteria and hence can alter the microbiota. According to the Food and Agriculture Organization of the United Nations (FAO), prebiotics are defined as non-viable food components that improve host gut health via altering the microbiota (Pineiro et al., 2008). One of the earliest synthetic prebiotics developed is lactulose, which is shown to increase gut bacteria, enhance water retention in stools, and is thus associated with laxative effects. Other prebiotics include fructo-oligosaccharides (FOS), soybean oligosaccharides, galacto-oligosaccharides (GOS), isomalto-oligosaccharides, xylo-oligosaccharides, and transgalacto-oligosaccharides (TGOS). The fructan inulin, cellulose, hemicellulose, reflux starch, and pectin are polysaccharide prebiotics. Many sources of prebiotics exist in nature including cereals, fruits and vegetables. Lactulose, lactosaccharose, FOS, GOS, and cyclodextrins are artificially synthesized prebiotics that can be commonly found as food additives or components in food production.

The benefits of prebiotics to gut health are multi-pronged. Commensal bacteria in the colon can ferment prebiotics to

produce short chain fatty acids (SCFAs) such as acetate, butyrate and propionate. For instance, most strains of *Bifidobacterium* and *Lactobacillus* can utilize FOS (Kaplan and Hutkins, 2000). In fact, recent data showed that different *Bifidobacterium* strains have complementary pathways for utilizing the prebiotics inulin-type fructans and arabinoxylan oligosaccharides (AXOS) (Rivière et al., 2018). The SCFAs produced as metabolic end-products of prebiotics fermentation are capable to bind to GPR43, GPR41 and GPR109A, 'metabolite-sensing' G-protein coupled receptors which regulate the inflammatory responses, thereby affecting gut homeostasis. Moreover, prebiotics can help to correct dysbiosis by promoting positive alterations in the microbial flora, for instance enhancing the proliferation of gut bacteria including *Bifidobacterium* (Paineau et al., 2008; Silk et al., 2009). Prebiotics can also regulate cholesterol biosynthesis and lipid production in the host, as well as satiety (Rivière et al., 2016).

Synbiotics

As its name implies, synbiotics refer to the combination of probiotics and prebiotics in food ingredients or supplements in a form of synergism. In theory, synbiotics should be more potent or efficacious than their probiotics or prebiotics components used in singularity. However, the relatively limited number of clinical trials on synbiotic therapies in IBS patients have thus far produced varying results which could be due to the different probiotic and prebiotic components used in different trials, as well as the different subsets of IBS patients studied (Harris and Baffy, 2017).

It is interesting to note that an open, uncontrolled, multicenter study involving 43 centers focused on 636 IBS constipation-predominant patients who were given a synbiotic composed of *Bifidobacterium longum* W11 and the short chain oligosaccharide prebiotic Fos Actilight, had reported significant improvements in stool frequency, bloating and abdominal pain (Colecchia et al., 2006). One randomized controlled study found that a synbiotic consisting of a mix of 29 soil-based microbes with a prebiotic, leonardite (a complex of humic substances) had resulted in significant reductions in IBS symptoms compared to placebo. Nonetheless, >80% of patients had remission of IBS at the 52-week follow-up (Bittner et al., 2005). Another study on 130 IBS patients revealed that a synbiotic of composite yogurt enriched with acacia fiber and *Bifidobacterium lactis* was associated with significant improvement on IBS symptoms and bowel habit vs. a placebo yogurt (Min et al., 2012). Moreover, Baştürk and coworkers found that a *B. lactis* B94 and 900 mg inulin synbiotic had more pronounced efficacy in reducing belching-abdominal fullness, bloating after meals, constipation and mucus in the feces than the synbiotic alone in IBS children (Baştürk et al., 2016). On the contrary, Abbas and colleagues found that a 6-week course of *S. boulardii* plus ispaghula husk combination therapy did not improve overall symptom severity scores in IBS-D patients; although it had led to diminished proinflammatory cytokines interleukin-8 and TNF-α, and an increase in the anti-inflammatory cytokine IL-10 (Abbas et al., 2014). Clearly, conflicting results from the limited studies thus far warrant the need for more RCTs to prove the virtues of synbiotics in managing IBS.

Non-absorbable Antibiotics

Several large-scale treatment trials and meta-analyses have shown that non-absorbable antibiotics such as Rifaximin and neomycin are effective for treatment of IBS. An antibiotic with a broad range of antibacterial effects against aerobic and anaerobic organisms that inhabit the GI tract, Rifaximin (Xifaxan®, Salix Pharmaceuticals, Bridgewater, NJ, United States) is a rifamycin derivative that was approved by the US Food and Drug Administration in 2015 for the treatment of IBS-D in adults. It is interesting to note that less than 0.5% of the oral dose is absorbed. Because it is poorly absorbed, rifaximin has low toxicity, insignificant adverse effects and drug interactions (Saadi and McCallum, 2013).

Three multicenter double-blind, placebo-controlled, phase 3 trials (TARGET 1–3), had demonstrated the efficacy and safety of rifaximin in improving the symptoms of IBS. The symptom relief was defined as a decrease of at least 30% from baseline in weekly IBS-related abdominal pain or discomfort and a weekly stool consistency score of less than 4 (Pimentel, 2018). TARGET 1 and TARGET 2 trials on IBS patients without constipation had resulted in global symptom relief for at least 2 weeks within a treatment-free month. The patients had received either rifaximin (550 mg) or placebo three times daily for a 2-week duration; and were subsequently subjected to a 10-week observation period (Pimentel et al., 2011). In the TARGET 3 trial, patients who had relapse of IBS-D after a short, 2-week duration first treatment were given repeat treatment of rifaximin. A significantly higher number of patients who were treated again with rifaximin vs. placebo were responders for abdominal pain but not stool consistency (Lembo A. et al., 2016). From this study, it was also shown that the repeat treatment was able to prevent recurrence besides prolonging the period of IBS symptom relief. Previous studies suggest that subpopulations of IBS patients have overgrowth of bacteria in the small bowel, which is known as small intestinal bacterial overgrowth (SIBO) (Giamarellos-Bourboulis et al., 2016). In patients with SIBO, rifaximin treatment had caused remarkable improvements from baseline in IBS symptoms (Meyrat et al., 2012). On the other hand, another antibiotic, neomycin has been shown to improve global IBS symptoms by 50%. Nonetheless, unlike rifaximin, neomycin had adverse effects and induced rapid bacterial resistance or *Clostridium difficile* infection (Distrutti et al., 2016).

Opioid Receptors Agonist/Antagonists and cGMP-Related Drugs

Eluxadoline (Viberzi, Allergan) is a drug having mixed effects against opioid receptors (mixed μ-opioid receptor agonist–δ-opioid receptor antagonist and κ-opioid receptor agonist). Two phase 3 trials which compared 70 and 100 mg twice-daily doses of eluxadoline indicated that the higher dose brought about reduction of overall IBS symptoms, and improved quality of life compared to placebo (Lembo A.J. et al., 2016). The efficacy of treatment effects of eluxadoline on relief of IBS symptoms was on par with rifaximin.

Nonetheless, eluxadoline is associated with side effects. Common side effects from the two phase 3 trials were constipation, abdominal pain, nausea, vomiting, abdominal bloating, and gastroenteritis. Long term usage was cautioned due to the occurrence of serious adverse events (SAEs) linked to eluxadoline use in 4% of the patients (Cash, 2016). From 2015 until 2017, 120 cases of pancreatitis were reported. In 2017, a Drug Safety Communication was issued by the FDA about an association between eluxadoline use in patients without a gallbladder and increased risk of severe pancreatitis that could be fatal.

Linaclotide (Constella®, Allergan Inc.) is a selective guanylate cyclase C (GC-C) agonist which is efficacious in treating constipation-predominant IBS, based on latest meta-analysis of three phase III trials specific for IBS-C (Chey et al., 2012; Rao et al., 2012; Shah et al., 2018). Plecanatide is another GC-C agonist that was found to be effective for IBS-C management (Shah et al., 2018). In a mouse model, linaclotide binds to GC-C receptor expressed on the luminal surface of intestinal epithelial cells, which leads to stimulation of cyclic guanosine monophosphate (cGMP) release. The cGMP inhibits colonic nociceptors and acts as a second messenger in the downstream facilitation of intestinal fluid secretion (Castro et al., 2013). GC-C receptor and its effectors can also modulate intestinal fluid homeostasis and afferent gut nerve activity (Busby et al., 2010). These could be the underlying mechanisms for the ability of linaclotide to reduce abdominal pain in IBS-C patients.

Serum-Derived Bovine Immunoglobulins

Serum-derived bovine immunoglobulin (SBI), marketed under the brand name EnteraGam®, has been approved by the US Food and Drug Administration for use in patients with chronic loose and frequent stools including IBS-D and IBD under physician supervision (EnteraGam Product Information Sheet, 2015). The EnteraGam SBI is essentially a formulation containing > 90% protein, with > 50% being immunoglobulin G (IgG) which is the active ingredient. In general, SBI had been shown by various small open-label studies to improve GI symptoms (i.e., stools frequency per day, ease of passage, and sense of evacuation). The mechanistic basis for the improvement of symptoms was investigated in a study and the findings showed that SBI therapy had led to alterations in the microbiome, particularly for Proteobacteria *Burkholderiales* and Firmicutes *Catonella* in the duodenum brushings but not in the stools. The SBI treatment had also not resulted in any changes in intestinal permeability nor bile acid synthesis. Hence the underlying mechanism for SBI's benefit toward IBS-D patients is still unknown (Valentin et al., 2017).

A pilot study on a small number of subjects had shown the efficacy of SBI in IBS-D treatment (Wilson et al., 2013). A recent study on a total of 1,377 patients with IBS or IBD based on a one-page survey found that a remarkable number of patients had their stool frequency normalized to less than or equal to 4 times/day. The study assumed that the patients with IBS had IBS-D since SBI was prescribed mainly for IBS patients with IBS-D (Shaw et al., 2017).

Dietary Interventions

Dietary interventions have been helpful for IBS patients as most of them report aggravation of symptoms associated with the ingestion of certain foods. In fact, modification or restriction of dietary intake in IBS patients had been implemented to improve or prevent gastrointestinal symptoms (Hayes et al., 2014). Two such diets are the FODMAP restriction and the gluten-free diet.

Low-FODMAPs Diet

FODMAP is an acronym for Fermentable – Oligosaccharides – Disaccharides – Monosaccharides – And – Polyols. Briefly, FODMAPs consist of short chain carbohydrates such as fructans, polyols and galacto-oligosaccharides that are poorly absorbed in the small intestine (Gibson and Shepherd, 2005). Fructose and lactose are also on the FODMAPs list as the absorption mechanism (in the case of fructose) or the enzyme responsible for breaking down the sugar (lactose) are impaired in IBS patients. Consumption of FODMAPs are closely linked with IBS development (Staudacher et al., 2012; Böhn et al., 2015). There are many randomized, controlled trials in the literature which reported the effectiveness of FODMAPs restriction diet in improving global IBS symptoms, visceral pain, bloating and quality of life (QOL) in >50% of IBS sufferers (Dolan et al., 2018). According to Britain's National Institute for Health and Care Excellence (NICE) guidelines for dietary and lifestyle advice, dietary and nutritional perspectives should be considered in administering appropriate advice to IBS patients. Particular attention was given to limitation on intake of insoluble fibers and starch, with ispaghula powder (a soluble fiber) or foods high in soluble fiber being encouraged. The NICE guidelines recommend a more restrictive diet such as low FODMAPs if the IBS symptoms still persist after following the general dietary guidelines (National Institute for Health and Care Excellence [NICE], 2017).

A meta-analysis on the low FODMAP diet based on six RCTs on a total of 182 patients and 172 controls demonstrated an improvement in severity of IBS symptoms and QOL scores (Marsh et al., 2016). Interestingly, a recent paper on a randomized, controlled crossover study showed that a low-FODMAP diet was more superior to a standard Australian diet in improving global IBS symptom scores. Improvement in stool consistency was seen in all patients regardless of IBS subtypes although stool frequency was improved only in IBS-D patients (Halmos et al., 2014).

In a recent meta-analysis, Varjú et al. (2017) conducted pooled analysis from 10 studies comprising RCTs, non-randomized controlled trials and non-controlled prospective trials. A standardized complex outcome score, the IBS-Symptom Severity Score (IBS-SSS) was used for the endpoint scoring. This meta-analysis proved statistically that a low-FODMAP diet does have beneficial effect on IBS-SSS, as compared to a high-FODMAP standard IBS diet recommended by the guidelines (Varjú et al., 2017). Nonetheless, in a more updated systematic review and meta-analysis, Dionne and coworkers looked at the effects of a gluten-free diet (GFD) and a low FODMAPS diet in alleviating the symptoms of IBS (Dionne et al., 2018). Patients on GFD had reduced global symptoms

compared with those on a control diet, although this was not statistically significant. On the other hand, there is evidence that a low FODMAPs diet could help in reducing global IBS symptoms (Dionne et al., 2018).

Despite its potential positive value, a low FODMAPs diet is associated with limitations particularly with regards to its highly restrictive nature, its possible adverse effects on nutritional status in the long term, and the importance of close monitoring by dieticians. A low FODMAPs diet also poses the danger of reducing the abundance of commensal bacteria. A recent study had shown that fecal bacteria such as *Actinobacteria*, *Bifidobacterium,* and *Faecalibacterium prausnitzii*, in patients on a low FODMAPs diet were reduced significantly along with reduction in pro-inflammatory cytokines (Hustoft et al., 2017). Further studies with more defined patient cohorts and symptoms as well as clear and standardized measurements of IBS symptoms pre- and post-intervention should be conducted to investigate the overall effect of a low FODMAPs diet compared to traditional IBS diet.

Gluten-Free Diet

Gluten, a protein found in grains such as wheat, rye, spelt and barley has been touted as the culprit for a wide range of gastrointestinal related disorders. Several studies had investigated the efficacy of a gluten-free diet (GFD) in reducing IBS-related symptoms. Vazzquez-Roque and coworkers conducted a 4-week RCT of gluten-free diet in 23 IBS-D patients who were further subgrouped according to their HLA genotype (12 HLA-DQ2/8-negative and 11 HLA-DQ2/8–positive), with 22 patients in the control group on gluten-containing diet. They found that gluten-free diet had impacted the stool frequency, with statistically significant decrease in stool frequency in individuals on a GFD versus subjects on a gluten-containing diet, and the effect was more pronounced in HLA-DQ2 or 8 positive patients than HLA-DQ2/8 negative patients. Gluten-containing diet was associated with higher small bowel mucosal permeability which was measured using urine sugars excretion as biomarkers (Vazquez-Roque et al., 2013).

In another study, 41 patients with IBS-D who were either HLA-DQ2/8-positive or -negative were placed on a 6-week GFD. The GFD was associated with markedly reduced IBS-SSS score in 71% of patients in total. In the study, HLA-DQ2/8-positive subjects reportedly had greater reduction in depression as well as in vitality score than HLA-DQ2/8-negative subjects (Aziz et al., 2016). The observation that HLA-DQ genotype had a bearing on usefulness of gluten-free diet in improving IBS symptoms suggests that an adaptive immune response may play a role in gluten's effects on gut barrier function. Furthermore, there is speculation that an innate immune response could also be involved, since toll-like receptors (TLR) expression is increased in mucosa of gluten-sensitive patients.

Fecal Microbiota Transplant

Strong evidence for the role of dysbiosis in IBS pathogenesis has elicited the proposition to cure IBS patients through fecal microbiota transplantation (FMT). FMT is an approach which involves the application of a solution of fecal material from a healthy donor into the gut of a receiver, with the intention of restoring the aberrant microbial composition in the gut to a healthy homeostasis. Treatment via FMT had become popular in the past 5 years but in fact, this therapeutic approach has been long practiced since the 4th century in ancient China, by a physician called Ge Hong, whereby he had suggested to patients with severe diarrhea to use fresh stool as a choice of treatment (Rossen et al., 2015).

Numerous studies have clearly linked abnormal gut microbiota composition with IBS development (King et al., 1998; Malinen et al., 2005; Kassinen et al., 2007). Nevertheless, these studies also questioned the suitability of FMT as a form of treatment against IBS. This is owing to the lack of understanding on the microbial pathophysiology. Furthermore, there is no robust, definitive conclusion regarding the exact mechanism underlying IBS pathogenesis, whether IBS is caused by changes in the gut microbiota composition or due to a consequence of the alteration of intestinal secretion and motility.

Based on a systematic review conducted by Halkjær et al. (2017) on IBS and FMT, the authors reported that 28 out of 48 patients (58%) experienced positive outcomes after FMT treatments. Moreover, there were no serious adverse events reported. Meanwhile, in another study by Mizuno et al. (2017) in Japan, the authors revealed that FMT treatment had improved the psychological status and stool form of IBS patients. Additionally, the authors showed that presence of *Bifidobacterium*-rich donor feces could be a promising indicator for successful FMT treatment in IBS. The authors speculate that *Bifidobacterium*-rich feces trigger the minor strains formation of the microbiota growth which could help to increase the diversity after FMT treatment. In another study, it was demonstrated that the effect of using oral fecal capsules was comparable to colonoscopy-administered transplantation in alleviation of IBS symptoms (Kao et al., 2017).

Johnsen et al. (2017) had assessed the effect of FMT on moderate-to-severe IBS-D and IBS-M patients through a randomized, double-blind and placebo-controlled trial. The authors demonstrated that a significant number of patients in the active treatment group versus the placebo group (65% vs. 43%) responded well to the treatment and had reduced IBS symptom severity after 3 months. However, the severity was not alleviated after 12 months. These results serve as an important breakthrough in evaluating the efficacy of FMT treatment in IBS. Nevertheless, larger multicenter studies are warranted to confirm these findings. The efficacy of FMT is still debatable at this stage, owing to newer findings that filtered feces could have the similar effects as whole fecal material transplantation (Ott et al., 2017). This raises the concern of whether bacteriophages and postbiotics, or metabolites secreted by the microbiota are actually the effective agents as these substances are able to get through the filters. More studies are in demand to confirm the actual mechanism and beneficial effect of FMT and the therapeutic agents responsible for the success of FMT treatment in IBS.

STRATEGIES FOR FUTURE IBS THERAPEUTICS

As our understanding of the microbiome gradually unravels, the potential to manipulate the microbiome for improvement in health and disease treatment is widening. As the costs of metagenomics sequencing become more affordable, the ability to obtain the microbiome profile of individuals for diagnostic purposes has been made possible. Along with this, soon we might be able to determine the exact profile of microbiota dysbiosis in each patient and devise personalized treatment such as customized probiotic formulations, targeted antimicrobials or immunotherapeutics for the individual patients. **Figure 3** illustrates the framework of future therapeutic strategies for IBS.

Stem Cell-Based Gut-on-a-Chip

A stem cell-based gut-on-a-chip had been created with cutting-edge technology and are virtually miniature versions of a human intestinal lining, termed organoids, derived from induced pluripotent stem cells (iPSCs). The iPSCs were derived from skin or blood samples collected from a patient and reprogrammed into intestinal villi stem cells (Workman et al., 2018). The gut-on-a-chip is combined with microfluidic engineering to mimic the dynamic microenvironment around the gut cells. By creating a personalized gut-on-a-chip for selected IBS patients, we can gain valuable understanding on the efficacy of new drugs on individual patients, instead of subjecting a patient to needless possible side effects. Emulate, a company that specializes on development of organ-on-chips including Intestine-Chip for toxicology testing, was born out of a commercialization effort of the founding team that created the organ-on-chips[2].

Microbiome-Based Future Therapeutics

Bacteriophage Therapy

Bacteriophages (viruses that infect bacteria) are ubiquitous, naturally occurring entities that control microbial populations and have an important role in controlling the microbial communities in the GI tract. From a metagenomics analysis, an estimated 1,200 viral genotypes, mostly siphophages and prophages within bacterial genomes in fecal contents were reported in the intestines of healthy humans (Mills et al., 2013). Changes in bacteriophage diversity have been reported in the diseased state, but different studies have shown contradictory results where some studies reported a decrease in diversity versus other studies which stated an enhanced diversity (McCarville et al., 2016). Since bacteriophages can exert selective pressure on targeted members of the bacterial community in intestinal microbiome, they may be manipulated for developing IBS therapies. Potential applications of bacteriophages include designing phage to "correct" microbiota dysbiosis, creating phage therapies to target certain bacterial species that causes a gut disease, and developing compounds that block phage induction to inhibit the growth of certain bacteria that requires phage to remain viable. In February 2018, the FDA has approved a phase 1/2a study of bacteriophages specifically designed against adherent-invasive *Escherichia coli* (AIEC), to treat IBD. More studies are needed for probing the possibility of including bacteriophage therapy among the limited arsenal of IBS therapy options available.

Postbiotics, Paraprobiotics, and New Probiotics Formulations

Recent studies have shown that live bacteria are not required for achieving beneficial effects when utilizing probiotics in treating symptoms of gut disorders. New names such as paraprobiotic and postbiotic have been minted to represent these non-living components of the microbiome. Postbiotics and parabiotics have biological activity and provide benefits to the host (Tsilingiri and Rescigno, 2013). Postbiotics are non-viable soluble factors (such as bacterial cell wall components, enzymes, peptides like glutathione, polysaccharides, organic acids, and short chain fatty acids) secreted by live bacteria or released upon cell lysis (Cicenia et al., 2014; Aguilar-Toalá et al., 2018). Other names for postbiotics are metabiotics, biogenics, or metabolites or cell-free supernatants. On the other hand, paraprobiotics, also known as "non-viable probiotics," "inactivated probiotics" or "ghost probiotics," refer to inactivated (non-viable) microbial cells that provide health benefits when given in appropriate doses (Taverniti and Guglielmetti, 2011; Tsilingiri and Rescigno, 2013). The advantage of postbiotics lies in its safety profile and longer shelf-life versus probiotics while conferring health benefits that are comparable to those of probiotics (Shenderov, 2013). Indeed, an interesting study by Tsilingiri and co-workers found that a postbiotic was more superior to a *Lactobacillus* probiotic in protecting the intestine (in this case an organ culture system of IBD model was used) against inflammatory response resulting from *Salmonella* invasion. This study suggested that live microorganisms in probiotics may not always be beneficial as it was found that certain probiotics could elicit a local inflammatory response, and hence postbiotics may be a safer alternative (Tsilingiri et al., 2012). In a recent study, it was shown that *L. casei* DG and its postbiotic attenuated the inflammatory mucosal response in an *ex vivo* organ culture model of post-infection IBS-D (Compare et al., 2017). Nonetheless, more studies are required to validate the beneficial effects of postbiotics either alone or in combination with probiotics for IBS treatment.

As the fungal and archaebacterial components of the gut microbiota as well as their role in maintaining gut health becomes clearer through new culturomics and metabolomics studies, it may be beneficial to formulate new probiotic cocktails that include these microorganisms. Theoretically, it may be possible to also design recombinant probiotics using bioengineering procedures to combine the beneficial attributes of specific bacteria or fungi.

Precision Antimicrobial Compounds

Can biofilm-destroying compounds help to facilitate the antibiotics penetration into "resistant areas" or channel the antimicrobial to less accessible areas of the intestines and thus

[2]https://emulatebio.com/system/

regulate these dysbiosis or imbalances? Or can one design a precision antimicrobial peptide that can specifically target a particular species *in situ*, while sparing the other members of the microbiota? One such example is the clever innovation of a specific targeted antimicrobial peptide (known as STAMP) which was designed by Eckert et al. (2006) to destroy *Streptococcus mutans* in a complex community of the oral biofilm. *Streptococcus mutans* is the chief culprit for dental caries. Similar strategies can be employed for modifying the gut microbiome dynamics and composition by targeting specific microbial species that has been identified to be associated with IBS symptoms. For example, in theory one could design precision antimicrobials or even use CRISPR-Cas9 technology to reduce the population of bacteria such as *Methanobrevibacter smithii* that produces methane for IBS-C patients who have methane breath.

Leveraging on the extensive database of peptides encoded by the gut microbes which are available freely on the MAHMI database[3], the same group of researchers who developed the database had demonstrated that bacterial peptides FR-16 and LR-17 that are encoded by genes in *B. longum* DJ010A and *B. fragilis* YCH46, respectively, could modulate the immune response by elevating the Th17 and decreasing the Th1 cell response (Hidalgo-Cantabrana et al., 2017). Using bioinformatics *in silico* screening tools, we could screen the library of millions of peptides contained in the database to zoom in on manageable number of selected peptides for actual experimental studies to search for those with desired antimicrobial activity.

Precision Nanotubes or Nanoparticles

Contractile nanotubes produced by certain bacteria, such as the R-type bacteriocins produced by *Pseudomonas aeruginosa*, as well as the contractile DNA injection systems produced by Myovirus bacteriophage T4, are naturally occurring precision antimicrobials. These contractile systems bind to receptors on bacterial cell surfaces, then inject a hollow tube into the cell wall, allowing ionic flux and depolarization of the inner membrane, thus killing the bacterial cell (Ge et al., 2015). Exploiting this unique property of contractile nanotubes, we can engineer nanotubes with different specificities to target microbes, by substituting the ligand-recognition domains of receptor-binding proteins from phages or from contractile bacteriocins.

[3]www.mahmi.org

CONCLUSION

The global incidence of IBS is increasing as countries become more modernized. The pathogenesis of IBS is multifactorial, although consensus opinion within the medical profession holds that the gut microbiota plays a central role in disease development. Various existing and in-development treatment options are available but each IBS patient may require personalized treatment. It is believed that a holistic approach with a multi-disciplinary team of healthcare professionals that includes gastroenterologists, dieticians, clinical microbiologist and molecular genomics experts is required for effective diagnosis and management of IBS. IBS-C, IBS-M and IBS-D patients may require different treatment modalities. Currently there are still existing gaps of knowledge in terms of the state of dysbiosis in the microbiota in IBS and the pathophysiological mechanisms whereby targeted therapies can mitigate these imbalances. Further studies including large-scale, controlled trials of existing and new treatments are pertinent for enhancing our understanding in this field. Once these "missing links" have been uncovered, it is highly likely that precision medicine tailored for not only the different IBS subtypes but also for individual genetic and dietary differences can be engineered. In the imminent future, every patient may be able to get their complete genome and gut microbiome sequenced, as well as the gut metabolome data analyzed. These integrated multi-omic data will hopefully aid in decoding the microbiota community present in the patient, and serve as a guide for personalized treatment.

AUTHOR CONTRIBUTIONS

PC conceptualized and coordinated the work. PC, VC, CL, PM, WW, and VY contributed to this article in terms of data collection and writing. PC and VC performed critical revision for the work.

FUNDING

This work was supported by the Taylor's Research Grant Scheme (TRGS), Taylor's University, Malaysia (Award No. TRGS/MFS/2/2016/SOM/013) and Taylor's University (Award No. TRGS/ERFS/2/2018/SBS/025).

REFERENCES

Abbas, Z., Yakoob, J., Jafri, W., Ahmad, Z., Azam, Z., Usman, M. W., et al. (2014). Cytokine and clinical response to *Saccharomyces boulardii* therapy in diarrhea-dominant irritable bowel syndrome: a randomized trial. *Eur. J. Gastroenterol. Hepatol.* 26, 630–639. doi: 10.1097/MEG.0000000000000094

Aguilar-Toalá, J. E., Garcia-Varela, R., Garcia, H. S., Mata-Haro, V., González-Córdova, A. F., Vallejo-Cordoba, B., et al. (2018). Postbiotics: an evolving term within the functional foods field. *Trends Food. Sci. Technol.* 75, 105–114. doi: 10.1016/j.tifs.2018.03.009

Anand, P., Aziz, Q., Willert, R., and van Oudenhove, L. (2007). Peripheral and central mechanisms of visceral sensitization in man. *Neurogastroenterol. Motil. J.* 19, 29–46.

Anitha, M., Vijay-Kumar, M., Sitaraman, S. V., Gewirtz, A. T., and Srinivasan, S. (2012). Gut microbial products regulate murine gastrointestinal motility via Toll-like receptor 4 signaling. *Gastroenterology* 143, 1006–1016.e4. doi: 10.1053/j.gastro.2012.06.034

Aziz, I., Trott, N., Briggs, R., North, J. R., Hadjivassiliou, M., and Sanders, D. S. (2016). Efficacy of a gluten-free diet in subjects with irritable bowel syndrome-diarrhea unaware of their HLA-DQ2/8 genotype. *Clin. Gastroenterol. Hepatol.* 14, 696–703.e1. doi: 10.1016/j.cgh.2015.12.031

Aziz, Q., Willert, R., and van Oudenhove, L. (2007). Peripheral and central mechanisms of visceral sensitization in man. *Neurogastroenterol. Motil.* 19, 29–46. doi: 10.1111/j.1365-2982.2006.00873.x

Bäckhed, F., Fraser, C. M., Ringel, Y., Sanders, M. E., Sartor, R. B., Sherman, P. M., et al. (2012). Defining a healthy human gut microbiome: current concepts,

future directions, and clinical applications. *Cell Host Microbe* 12, 611–622. doi: 10.1016/j.chom.2012.10.012

Baştürk, A., Artanm, R., and Yılmaz, A. (2016). Efficacy of synbiotic, probiotic, and prebiotic treatments for irritable bowel syndrome in children: a randomized controlled trial. *Turk. J. Gastroenterol.* 27, 439–443. doi: 10.5152/tjg.2016.16301

Beatty, J. K., Akierman, S. V., and Motta, J. P. (2017). Giardia duodenalis induces pathogenic dysbiosis of human intestinal microbiota biofilms. *Int. J. Parasitol.* 47, 311–326. doi: 10.1016/j.ijpara.2016.11.010

Beatty, J. K., Bhargava, A., and Buret, A. G. (2014). Post-infectious irritable bowel syndrome: mechanistic insights into chronic disturbances following enteric infection. *World J. Gastroenterol.* 20, 3976–3985. doi: 10.3748/wjg.v20.i14.3976

Bein, A., Shin, W., Jalili-Firoozinezhad, S., Park, M. H., Sontheimer-Phelps, A., Tovaglieri, A., et al. (2018). Microfluidic organ-on-a-chip models of human intestine. *Cell. Mol. Gastroenterol. Hepatol.* 5, 659–668. doi: 10.1016/j.jcmgh.2017

Bellini, M., Gambaccini, D., Stasi, C., Urbano, M. T., Marchi, S., and Usai-Satta, P. (2014). Irritable bowel syndrome: a disease still searching for pathogenesis, diagnosis and therapy. *World J. Gastroenterol.* 20, 8807–8820. doi: 10.3748/wjg.v20.i27.8807

Beyder, A., Mazzone, A., Strege, P. R., Tester, D. J., Saito, Y. A., Bernard, C. E., et al. (2014). Loss-of-function of the voltage-gated sodium channel NaV1.5 (channelopathies) in patients with irritable bowel syndrome. *Gastroenterology* 146, 1659–1668. doi: 10.1053/j.gastro.2014.02.054

Biesiekierski, J. R., Peters, S. L., Newnham, E. D., Rosella, O., Muir, J. G., and Gibson, P. R. (2013). No effects of gluten in patients with self-reported non-celiac gluten sensitivity after dietary reduction of fermentable, poorly absorbed, short-chain carbohydrates. *Gastroenterology* 145, 320–328. doi: 10.1053/j.gastro.2013.04.051

Bittner, A. C., Croffut, R. M., and Stranahan, M. C. (2005). Prescript-Assist probiotic-prebiotic treatment for irritable bowel syndrome: a methodologically oriented, 2-week, randomized, placebo controlled, double-blind clinical study. *Clin. Ther.* 27, 755–761. doi: 10.1016/j.clinthera.2005.06.005

Böhn, L., Störsrud, S., Liljebo, T., Collin, L., Lindfors, P., Törnblom, H., et al. (2015). Diet low in FODMAPs reduces symptoms of irritable bowel syndrome as well as traditional dietary advice: a randomized controlled trial. *Gastroenterology* 149, 1399–1407.e2 doi: 10.1053/j.gastro.2015.07.054

Bonavita, V., and De Simone, R. (2008). Towards a definition of comorbidity in the light of clinical complexity. *Neurol. Sci.* 29, S99–S102. doi: 10.1007/s10072-008-0898-1

Bonaz, B. L., and Bernstein, C. N. (2013). Brain-gut interactions in inflammatory bowel disease. *Gastroenterology* 144, 36–49. doi: 10.1053/j.gastro.2012.10.003

Botschuijver, S., Roeselers, G., Levin, E., Jonkers, D. M., Welting, O., Heinsbroek, S. E., et al. (2017). Intestinal fungal dysbiosis is associated with visceral hypersensitivity in patients with irritable bowel syndrome and rats. *Gastroenterology* 153, 1026–1039. doi: 10.1053/j.gastro.2017.06.004

Bradesi, S. I, Schwetz, H. S., Ennes, C. M., Lamy, G., Ohning, M., Fanselow, C., et al. (2005). Repeated exposure to water avoidance stress in rats: a new model for sustained visceral hyperalgesia. *Am. J. Physiol. Gastrointest. Liver Physiol.* 289, G42–G53. doi: 10.1152/ajpgi.00500.2004

Bray, B. D., Nicol, F., Penman, I. D., and Ford, M. J. (2006). Symptom interpretation and quality of life in patients with irritable bowel syndrome. *Br. J. Gen. Pract.* 56, 122–126.

Bunge, M., Araghipour, N., Mikoviny, T., Dunkl, J., Schnitzhofer, R., Hansel, A., et al. (2008). On-line monitoring of microbial volatile metabolites by proton transfer reaction-mass spectrometry. *Appl. Environ. Microbiol.* 74, 2179–2186. doi: 10.1128/AEM.02069-07

Buono, J. L., Carson, R. T., and Flores, N. M. (2017). Health-related quality of life, work productivity, and indirect costs among patients with irritable bowel syndrome with diarrhea. *Health Qual. Life Outcomes* 15:35. doi: 10.1186/s12955-017-0611-2

Busby, R. W., Bryant, A. P., Bartolini, W. P., Cordero, E. A., Hannig, G., Kessler, M. M., et al. (2010). Linaclotide, through activation of guanylate cyclase C, acts locally in the gastrointestinal tract to elicit enhanced intestinal secretion and transit. *Eur. J. Pharmacol.* 649, 328–335. doi: 10.1016/j.ejphar.2010.09.019

Camilleri, M. (2009). Serotonin in the gastrointestinal tract. *Curr. Opin. Endocrinol. Diabetes Obes.* 16, 53–59.

Camilleri, M., Coulie, B., and Tack, J. F. (2001). Visceral hypersensitivity: facts, speculations, and challenges. *Gut* 48, 125–131.

Camilleri, M., Kolar, G. J., Vazquez-Roque, M. I., Carlson, P., Burton, D. D., and Zinsmeister, A. R. (2013). Cannabinoid receptor 1 gene and irritable bowel syndrome: phenotype and quantitative traits. *Am. J. Physiol. Gastrointest. Liver Physiol.* 304, G553–G560. doi: 10.1152/ajpgi.00376.2012

Canavan, C., West, J., and Card, T. (2014). The epidemiology of irritable bowel syndrome. *Clin. Epidemiol.* 6, 71–80. doi: 10.2147/CLEP.S40245

Carroll, I. M., Chang, Y. H., Park, J., Sartor, R. B., and Ringel, Y. (2010). Luminal and mucosal-associated intestinal microbiota in patients with diarrhea-predominant irritable bowel syndrome. *Gut Pathog.* 2:19. doi: 10.1186/1757-4749-2-19

Carroll, I. M., Ringel-Kulka, T., Keku, T. O., Chang, Y. H., Packey, C. D., Sartor, R. B., et al. (2011). Molecular analysis of the luminal- and mucosal-associated intestinal microbiota in diarrhea-predominant irritable bowel syndrome. *Am. J Physiol. Gastrointest. Liver Physiol.* 301, G799–G807. doi: 10.1152/ajpgi.00154.2011

Carroll, I. M., Ringel-Kulka, T., Siddle, J. P., and Ringel, Y. (2012). Alterations in composition and diversity of the intestinal microbiota in patients with diarrhea-predominant irritable bowel syndrome. *Neurogastroenterol. Motil.* 24, 521–530. doi: 10.1111/j.1365-2982.2012.01891.x

Casén, C., Vebø, H. C., Sekelja, M., Hegge, F. T., Karlsson, M. K., Ciemniejewska, E., et al. (2015). Deviations in human gut microbiota: a novel diagnostic test for determining dysbiosis in patients with IBS or IBD. *Aliment. Pharmacol. Ther.* 42, 71–83. doi: 10.1111/apt.13236

Cash, B. D. (2016). Eluxadoline: a promising therapy that raises many questions. *Transl. Gastroenterol. Hepatol.* 1:76. doi: 10.21037/tgh.2016.09.06

Castro, J., Harrington, A. M., Hughes, P. A., Martin, C. M., Ge, P., Shea, C. M., et al. (2013). Linaclotide inhibits colonic nociceptors and relieves abdominal pain via guanylate cyclase-C and extracellular cyclic guanosine 3',5'-monophosphate. *Gastroenterology* 145, 1334–1346.e1-11. doi: 10.1053/j.gastro.2013.08.017

Cenit, M. C., Sanz, Y., and Codoñer-Franch, P. (2017). Influence of gut microbiota on neuropsychiatric disorders. *World J. Gastroenterol.* 23, 5486–5498. doi: 10.3748/wjg.v23.i30.5486

Chen, C., Lu, M., Pan, Q., Fichna, J., Zheng, L., Wang, K., et al. (2015). Berberine improves intestinal motility and visceral pain in the mouse models mimicking diarrhea-predominant irritable bowel syndrome (IBS-D) symptoms in an opioid-receptor dependent manner. *PLoS One* 10:e0145556. doi: 10.1371/journal.pone.0145556

Chey, W. D. (2016). Food: the main course to wellness and illness in patients with irritable bowel syndrome. *Am. J. Gastroenterol.* 111, 366–371. doi: 10.1038/ajg.2016.12

Chey, W. D., Lembo, A. J., Lavins, B. J., Shiff, S. J., Kurtz, C. B., Currie, M. G., et al. (2012). Linaclotide for irritable bowel syndrome with constipation: a 26-week, randomized, double-blind, placebo-controlled trial to evaluate efficacy and safety. *Am. J. Gastroenterol.* 107, 1702–1712. doi: 10.1038/ajg.2012.254

Choghakhori, R., Abbasnezhad, A., Hasanvand, A., and Amani, R. (2017). Inflammatory cytokines and oxidative stress biomarkers in irritable bowel syndrome: association with digestive symptoms and quality of life. *Cytokine* 93, 34–43. doi: 10.1016/j.cyto.2017.05.005

Cicenia, A., Scirocco, A., Carabotti, M., Pallotta, L., Marignani, M., and Severi, C. (2014). Postbiotic activities of Lactobacilli-derived factors. *J. Clin. Gastroenterol.* 48, 18–22. doi: 10.1097/MCG.0000000000000231

Colecchia, A., Vestito, A., La Rocca, A., Pasqui, F., Nikiforaki, A., Festi, D., et al. (2006). Effect of a symbiotic preparation on the clinical manifestations of irritable bowel syndrome, constipation-variant. Results of an open, uncontrolled multicenter study. *Minerva Gastroenterol. Dietol.* 52, 349–358.

Collins, S. M. (2014). A role for the gut microbiota in IBS. *Nat. Rev. Gastroenterol. Hepatol.* 11, 497–505. doi: 10.1038/nrgastro.2014.40

Compare, D., Rocco, A., Coccoli, P., Angrisani, D., Sgamato, C., Iovine, B., et al. (2017). Lactobacillus casei DG and its postbiotic reduce the inflammatory mucosal response: an ex-vivo organ culture model of post-infectious irritable bowel syndrome. *BMC Gastroenterol.* 17:53. doi: 10.1186/s12876-017-0605-x

Coutinho, S. V., Plotsky, P. M., Sablad, M., Miller, J. C., Zhou, H., Bayati, A. I., et al. (2002). Neonatal maternal separation alters stress-induced responses to viscerosomatic nociceptive stimuli in rat. *Am. J. Physiol. Gastrointest. Liver Physiol.* 282, G307–G316. doi: 10.1152/ajpgi.00240.2001

Crowell, M. D. (2004). Role of serotonin in the pathophysiology of the irritable bowel syndrome. *Br. J. Pharmacol.* 141, 1285–1293. doi: 10.1038/sj.bjp.0705762

Czogalla, Á, Schmitteckert, S., Houghton, L. A., Sayuk, G. S., Camilleri, M., Olivo-Diaz, A., et al. (2015). A meta-analysis of immunogenetic Case–Control Association Studies in irritable bowel syndrome. *Neurogastroenterol. Motil.* 27, 717–727. doi: 10.1111/nmo.12548

D'Amato, M. (2013). Genes and functional GI disorders: from casual to causal relationship. *Neurogastroenterol. Motil.* 25, 638–649. doi: 10.1111/nmo.12173

David, L. A., Maurice, C. F., Carmody, R. N., Gootenberg, D. B., Button, J. E., Wolfe, B. E., et al. (2014). Diet rapidly and reproducibly alters the human gut microbiome. *Nature* 505, 559–563. doi: 10.1038/nature12820

Didari, T., Mozaffari, S., Nikfar, S., and Abdollahi, M. (2015). Effectiveness of probiotics in irritable bowel syndrome: Updated systematic review with meta-analysis. *World J. Gastroenterol.* 21, 3072–3084. doi: 10.3748/wjg.v21.i10.3072

Dinan, T. G., Quigley, E. M., Ahmed, S. M., Scully, P., O'Brien, S., O'Mahony, L., et al. (2006). Hypothalamic-pituitary-gut axis dysregulation in irritable bowel syndrome: plasma cytokines as a potential biomarker? *Gastroenterology* 130, 304–311. doi: 10.1053/j.gastro.2005.11.033

Dionne, J., Ford, A. C., Yuan, Y., Chey, W. D., Lacy, B. E., Saito, Y. A., et al. (2018). Systematic review and meta-analysis evaluating the efficacy of a gluten-free diet and a low FODMAPs Diet in treating symptoms of irritable bowel syndrome. *Am. J. Gastroenterol.* 113, 1290–1300. doi: 10.1038/s41395-018-0195-4

Distrutti, E., Monaldi, L., Ricci, P., and Fiorucci, S. (2016). Gut microbiota role in irritable bowel syndrome: new therapeutic strategies. *World J. Gastroenterol.* 22, 2219–2241. doi: 10.3748/wjg.v22.i7.2219

Dolan, R., Chey, W. D., and Eswaran, S. (2018). The role of diet in the management of irritable bowel syndrome: a focus on FODMAPs. *Expert Rev. Gastroenterol. Hepatol.* 12, 607–615. doi: 10.1080/17474124.2018.1476138

Dominguez-Bello, M. G., Blaser, M. J., Ley, R. E., and Knight, R. (2011). Development of the human gastrointestinal microbiota and insights from high-throughput sequencing. *Gastroenterology* 140, 1713–1719. doi: 10.1053/j.gastro.2011.02.011

Downs, I. A., Aroniadis, O. C., Kelly, L., and Brandt, L. J. (2017). Postinfection irritable bowel syndrome: the links between gastroenteritis, inflammation, the microbiome, and functional disease. *J. Clin. Gastroenterol.* 51, 869–877. doi: 10.1097/MCG.0000000000000924

Dridi, B., Henry, M., El Khechine, A., Raoult, D., and Drancourt, M. (2009). High prevalence of *Methanobrevibacter smithii* and *Methanosphaera stadtmanae* detected in the human gut using an improved DNA detection protocol. *PLoS One* 4:e7063. doi: 10.1371/journal.pone.0007063

Drossman, D. A. (2016). Functional gastrointestinal disorders: history, pathophysiology, clinical features and Rome IV. *Gastroenterology* 150, 1262–1279. doi: 10.1053/j.gastro.2016.02.032

Dupont, H. L. (2014). Review article: evidence for the role of gut microbiota in irritable bowel syndrome and its potential influence on therapeutic targets. *Aliment. Pharmacol. Ther.* 39, 1033–1042. doi: 10.1111/apt.12728

Eckert, R., He, J., Yarbrough, D. K., Qi, F., Anderson, M. H., and Shi, W. (2006). Targeted killing of Streptococcus mutans by a pheromone-guided "Smart" antimicrobial peptide. *Antimicrob. Agents Chemother.* 50, 3651–3657. doi: 10.1128/AAC.00622-06

Ek, W. E., Reznichenko, A., Ripke, S., Niesler, B., Zucchelli, M., Rivera, N. V., et al. (2015). Exploring the genetics of irritable bowel syndrome: a GWA study in the general population and replication in multinational case-control cohorts. *Gut* 64, 1774–1782. doi: 10.1136/gutjnl-2014-307997

Elli, L., Branchi, F., Tomba, C., Villalta, D., Norsa, L., Ferretti, F., et al. (2015). Diagnosis of gluten related disorders: celiac disease, wheat allergy and non-celiac gluten sensitivity. *World J. Gastroenterol.* 21, 7110–7119. doi: 10.3748/wjg.v21.i23.7110

EnteraGam Product Information Sheet (2015). EnteraGam [Product Information Sheet]. Cary, NC: Entera Health, Inc. Available at: https://enteragam.com/assets/lib/Enter-aGam_Product_Information.pdf (accessed September 02, 2018).

Eswaran, S. L., Chey, W. D., Han-Markey, T., Ball, S., and Jackson, K. (2016). A randomized controlled trial comparing the low FODMAP diet vs. modified NICE guidelines in US adults with IBS-D. *Am. J. Gastroenterol.* 111, 1824–1832. doi: 10.1038/ajg.2016.434

Farzaei, M. H., Bahramsoltani, R., Abdollahi, M., and Rahimi, R. (2016). The role of visceral hypersensitivity in irritable bowel syndrome: pharmacological targets and novel treatments. *J. Neurogastroenterol. Motil.* 22, 558–574. doi: 10.5056/jnm16001

Fichna, J., Lapointe, T., Chapman, K., Janecka, A., Vergnolle, N., Altier, C., et al. (2012). New neostigmine-based behavioral mouse model of abdominal pain. *Pharmacol. Rep.* 64, 1146–1154.

Ford, A. C., Quigley, E. M. M., and Lacy, B. E. (2014). Efficacy of prebiotics, probiotics, and synbiotics in irritable bowel syndrome and chronic idiopathic constipation: systematic review and metaanalysis. *Am. J. Gastroenterol.* 109, 1547–1561.

Ge, P., Scholl, D., Leiman, P. G., Yu, X., Miller, J. F., and Zhou, Z. H. (2015). Atomic structures of a bactericidal contractile nanotube in its Pre- and Postcontraction states. *Nat. Struct. Mol. Biol.* 22, 377–382. doi: 10.1038/nsmb.2995

Giamarellos-Bourboulis, E. J., Pyleris, E., Barbatzas, C., Pistiki, A., and Pimentel, M. (2016). Small intestinal bacterial overgrowth is associated with irritable bowel syndrome and is independent of proton pump inhibitor usage. *BMC Gastroenterol.* 16:67. doi: 10.1186/s12876-016-0484-6

Gibson, P. R., and Shepherd, S. J. (2005). Personal view: food for thought–western lifestyle and susceptibility to Crohn's disease. The FODMAP hypothesis. *Aliment. Pharmacol. Ther.* 21, 1399–1409. doi: 10.1111/j.1365-2036.2005.02506.x

Gill, S. R., Pop, M., DeBoy, R. T., Eckburg, P. B., Turnbaugh, P. J., Samuel, B. S., et al. (2006). Metagenomic analysis of the human distal gut microbiome. *Science* 312, 1355–1359. doi: 10.1126/science.1124234

Grasberger, H., Chang, L., Shih, W., Presson, A. P., Sayuk, G. S., Newberry, R. D., et al. (2013). Identification of a functional tph1 polymorphism associated with irritable bowel syndrome bowel habit subtypes. *Am. J. Gastroenterol.* 108, 1766–1774. doi: 10.1038/ajg.2013.304

Gue, M., Del Rio-Lacheze, C., Eutamene, H., Theodorou, V., Fioramonti, J., and Bueno, L. (1997). Stress-induced visceral hypersensitivity to rectal distension in rats: role of CRF and mast cells. *Neurogastroenterol. Motil.* 9, 271–279.

Guyonnet, D., Chassany, O., Ducrotte, P., Picard, C., Mouret, M., Mercier, C. H., et al. (2007). Effect of a fermented milk containing *Bifidobacterium animalis* DN-173 010 on the health-related quality of life and symptoms in irritable bowel syndrome in adults in primary care: a multicentre, randomized, double-blind, controlled trial. *Aliment. Pharmacol. Ther.* 26, 475–486. doi: 10.1111/j.1365-2036.2007.03362.x

Gwee, K. A., Lu, C. L., and Ghoshal, U. C. (2009). Epidemiology of irritable bowel syndrome in Asia: something old, something new, something borrowed. *J. Gastroenterol. Hepatol.* 24, 1601–1607. doi: 10.1111/j.1440-1746.2009.05984.x

Halkjær, S. I., Boolsen, A. W., Günther, S., Christensen, A. H., and Petersen, A. M. (2017). Can fecal microbiota transplantation cure irritable bowel syndrome? *World J. Gastroenterol.* 23, 4112–4120. doi: 10.3748/wjg.v23.i22.4112

Halmos, E. P., Power, V. A., Shepherd, S. J., Gibson, P. R., and Muir, J. G. (2014). A diet low in FODMAPs reduces symptoms of irritable bowel syndrome. *Gastroenterology* 146, 67–75.e5. doi: 10.1053/j.gastro.2013.09.046

Halvorson, H. A., Schlett, C. D., and Riddle, M. S. (2006). Post-infectious irritable bowel syndrome-a meta-analysis. *Am. J. Gastroenterol.* 101, 1894–1899. doi: 10.1111/j.1572-0241.2006.00654.x

Harris, L. A., and Baffy, N. (2017). Modulation of the gut microbiota: a focus on treatments for irritable bowel syndrome. *Postgrad. Med.* 129, 872–888. doi: 10.1080/00325481.2017.1383819

Hayes, P., Corish, C., O'mahony, E., and Quigley, E. M. M. (2014). A dietary survey of patients with irritable bowel syndrome. *J. Hum. Nutr. Diet.* 27, 36–47. doi: 10.1111/jhn.12114

Henningsen, P., Zimmermann, T., and Sattel, H. (2003). Medically unexplained physical symptoms, anxiety and depression: a meta-analytic review. *Psychosom. Med.* 65, 528–533.

Hidalgo-Cantabrana, C., Moro-García, M. A., Blanco-Míguez, A., Fdez-Riverola, F., Lourenço, A., Alonso-Arias, R., et al. (2017). In silico screening of the human gut metaproteome identifies Th17-promoting peptides encrypted in proteins of commensal bacteria. *Front. Microbiol.* 8:1726. doi: 10.3389/fmicb.2017.01726

Hod, K., Ringel-Kulka, T., Martin, C. F., Maharshak, N., and Ringel, Y. (2016). High-sensitive C-reactive protein as a marker for inflammation in irritable bowel syndrome. *J. Clin. Gastroenterol.* 50, 227–232. doi: 10.1097/MCG.0000000000000327

Hoffmann, C., Dollive, S., Grunberg, S., Chen, J., Li, H., Wu, G. D., et al. (2013). Archaea and fungi of the human gut microbiome: correlations with

diet and bacterial residents. *PLoS One* 8:e66019. doi: 10.1371/journal.pone.0066019

Horvath, A., Dziechciarz, P., and Szajewska, H. (2011). Meta-analysis: Lactobacillus rhamnosus GG for abdominal pain-related functional gastrointestinal disorders in childhood. *Aliment. Pharmacol. Ther.* 33, 1302–1310. doi: 10.1111/j.1365-2036.2011.04665.x

Hugon, P., Dufour, J. C., Colson, P., Fournier, P. E., Sallah, K., and Raoult, D. (2015). A comprehensive repertoire of prokaryotic species identified in human beings. *Lancet Infect. Dis.* 15, 1211–1219. doi: 10.1016/S1473-3099(15)00293-5

Huh, D., Kim, H. J., Fraser, J. P., Shea, D. E., Khan, M., Bahinski, A., et al. (2013). Microfabrication of human organs-on-chips. *Nat. Protoc.* 8, 2135–2157. doi: 10.1038/nprot.2013.137

Hustoft, T. N., Hausken, T., Ystad, S. O., Valeur, J., Brokstad, K., Hatlebakk, J. G., et al. (2017). Effects of varying dietary content of fermentable short-chain carbohydrates on symptoms, fecal microenvironment, and cytokine profiles in patients with irritable bowel syndrome. *Neurogastroenterol. Motil.* 29:e12969. doi: 10.1111/nmo.12969

Jafari, E., Vahedi, H., Merat, S., Momtahen, S., and Riahi, A. (2014). Therapeutic effects, tolerability and safety of a multi-strain probiotic in Iranian adults with irritable bowel syndrome and bloating. *Arch. Iran. Med.* 17, 466–470.

Jahng, J., Jung, I. S., Choi, E. J., Conklin, J. L., and Park, H. (2012). The effects of methane and hydrogen gases produced by enteric bacteria on ileal motility and colonic transit time. *Neurogastroenterol. Motil.* 24:e92. doi: 10.1111/j.1365-2982.2011.01819.x

Jalanka-Tuovinen, J., Salojärvi, J., Salonen, A., Immonen, O., Garsed, K., Kelly, F. M., et al. (2014). Faecal microbiota composition and host-microbe cross-talk following gastroenteritis and in postinfectious irritable bowel syndrome. *Gut* 63, 1737–1745. doi: 10.1136/gutjnl-2013-305994

Jeffery, I. B., O'toole, P. W., Öhman, L., Claesson, M. J., Deane, J., Quigley, E. M., et al. (2012). An irritable bowel syndrome subtype defined by species-specific alterations in faecal microbiota. *Gut* 61, 997–1006. doi: 10.1136/gutjnl-2011-301501

Johnsen, P. H., Hilpüsch, F., Cavanagh, J. P., Leikanger, I. S., Kolstad, C., Valle, P. C., et al. (2017). Faecal microbiota transplantation versus placebo for moderate-to-severe irritable bowel syndrome: a double-blind, randomised, placebo-controlled, parallel-group, single centre trial. *Lancet Gastroenterol. Hepatol.* 3, 17–24. doi: 10.1016/S2468-1253(17)30338-2

Jones, M. P., Van Oudenhove, L., and Talley, N. J. (2012). Functional gastrointestinal disorders (FGIDs) and psychological disorders: strong evidence that the link is bidirectional, but psychological distress is more likely to precede a new diagnosis of an FGID. *Gastroenterology* 142:S570.

Jun, S., Kohen, R., Cain, K. C., Jarrett, M. E., and Heitkemper, M. M. (2011). Associations of tryptophan hydroxylase gene polymorphisms with irritable bowel syndrome. *Neurogastroenterol. Motil.* 23, 233–239.e116. doi: 10.1111/j.1365-2982.2010.01623.x

Kanazawa, M., Palsson, O. S., Thiwan, S. I., Turner, M. J., Van Tilburg, M. A., Gangarosa, L. M., et al. (2008). Contributions of pain sensitivity and colonic motility to IBS symptom severity and predominant bowel habits. *Am. J. Gastroenterol.* 103, 2550–2561. doi: 10.1111/j.1572-0241.2008.02066.x

Kao, D., Roach, B., Silva, M., Beck, P., Rioux, K., Kaplan, G. G., et al. (2017). Effect of oral capsule- vs colonoscopy delivered fecal microbiota transplantation on recurrent clostridium difficile infection: a randomized clinical trial. *JAMA* 318, 1985–1993. doi: 10.1001/jama.2017.17077

Kapeller, J., Houghton, L. A., Mönnikes, H., Walstab, J., Möller, D., Bönisch, H., et al. (2008). First evidence for an association of a functional variant in the microRNA-510 target site of the serotonin receptor-type 3E gene with diarrhea predominant irritable bowel syndrome. *Hum. Mol. Genet.* 17, 2967–2977. doi: 10.1093/hmg/ddn195

Kaplan, H., and Hutkins, R. W. (2000). Fermentation of fructooligosaccharides by lactic acid bacteria and bifidobacteria. *Appl. Environ. Microbiol.* 66, 2682–2684.

Karantanos, T., Markoutsaki, T., Gazouli, M., Anagnou, N. P., and Karamanolis, D. G. (2010). Current insights in to the pathophysiology of irritable bowel syndrome. *Gut Pathog.* 2:3. doi: 10.1186/1757-4749-2-3

Kassinen, A., Krogius-Kurikka, L., Mäkivuokko, H., Rinttilä, T., Paulin, L., Corander, J., et al. (2007). The fecal microbiota of irritable bowel syndrome patients differs significantly from that of healthy subjects. *Gastroenterology* 133, 24–33. doi: 10.1053/j.gastro.2007.04.005

Kerckhoffs, A. P., Ben-Amor, K., Samsom, M., van der Rest, M. E., de Vogel, J., Knol, J., et al. (2011). Molecular analysis of faecal and duodenal samples reveals significantly higher prevalence and numbers of *Pseudomonas aeruginosa* in irritable bowel syndrome. *J. Med. Microbiol.* 60, 236–245. doi: 10.1099/jmm.0.022848-0

Kerckhoffs, A. P., Samsom, M., van der Rest, M. E., de Vogel, J., Knol, J., Ben-Amor, K., et al. (2009). Lower Bifidobacteria counts in both duodenal mucosa-associated and fecal microbiota in irritable bowel syndrome patients. *World J. Gastroenterol.* 15, 2887–2892.

Keselman, A., Li, E., Maloney, J., and Singer, S. M. (2016). The microbiota contributes to $CD8^+$ T cell activation and nutrient malabsorption following intestinal infection with Giardia duodenalis. *Infect. Immun.* 84, 2853–2860. doi: 10.1128/IAI.00348-16

Kim, G., Deepinder, F., Morales, W., Hwang, L., Weitsman, S., Chang, C., et al. (2012). *Methanobrevibacter smithii* is the predominant methanogen in patients with constipation-predominant IBS and methane on breath. *Dig. Dis. Sci.* 57, 3213–3218.

Kim, H. J., Huh, D., Hamilton, G., and Ingber, D. E. (2012). Human gut-on-achip inhabited by microbial flora that experiences intestinal peristalsis-like motions and flow. *Lab Chip* 12, 2165–2174. doi: 10.1039/c2lc40074j

Kim, H. J., Li, H., Collins, J. J., and Ingber, D. E. (2016). Contributions of microbiome and mechanical deformation to intestinal bacterial overgrowth and inflammation in a human gut-on-a-chip. *Proc. Natl. Acad. Sci. U.S.A.* 5, E7–E15. doi: 10.1073/pnas.1522193112

Kimura, H., Ikeda, T., Nakayama, H., Sakai, Y., and Fujii, T. (2015). An onchip small intestine–liver model for pharmacokinetic studies. *J. Lab. Autom.* 20, 265–273. doi: 10.1177/2211068214557812

King, T. S., Elia, M., and Hunter, J. O. (1998). Abnormal colonic fermentation in iirritable bowel syndrome. *Lancet* 352, 1187–1189.

Klem, F., Wadhwa, A., Prokop, L. J., Sundt, W. J., Farrugia, G., Camilleri, M., et al. (2017). Prevalence, risk factors, and outcomes of irritable bowel syndrome after infectious enteritis: a systematic review and meta-analysis. *Gastroenterology* 152, 1042–1054.e1. doi: 10.1053/j.gastro.2016.12.039

Koloski, N. A., Jones, M., Kalantar, J., Weltman, M., Zaguirre, J., and Talley, N. J. (2012). The brain-gut pathway in functional gastrointestinal disorders is bidirectional: a 12-year prospective population-based study. *Gut* 61, 1284–1290. doi: 10.1136/gutjnl-2011-300474

Koloski, N. A., Jones, M. P., and Talley, N. J. (2016). Evidence that independent gut-to-brain and brain-to-gut pathways operate in the irritable bowel syndrome and functional dyspepsia: a 1-year population-based prospective study. *Aliment. Pharmacol. Ther.* 44, 592–600. doi: 10.1111/apt.13738

Krogius-Kurikka, L., Lyra, A., Malinen, E., Aarnikunnas, J., Tuimala, J., Paulin, L., et al. (2009). Microbial community analysis reveals high level phylogenetic alterations in the overall gastrointestinal microbiota of diarrhoea-predominant irritable bowel syndrome sufferers. *BMC Gastroenterol.* 9:95. doi: 10.1186/1471-230X-9-95

Kumar, S., Misra, A., and Ghoshal, U. C. (2010). Patients with irritable bowel syndrome exhale more hydrogen than healthy subjects in fasting state. *J. Neurogastroenterol. Motil.* 16, 299–305. doi: 10.5056/jnm.2010.16.3.299

Lacy, B. E., Mearin, F., Chang, L., Chey, W. D., Lembo, A. J., Simren, M., et al. (2016). Bowel disorders. *Gastroenterology* 150, 1393–1407. doi: 10.1053/j.gastro.2016.02.031

Lagier, J. C., Armougom, F., Million, M., Hugon, P., Pagnier, I., Robert, C., et al. (2012). Microbial culturomics: paradigm shift in the human gut microbiome study. *Clin. Microbiol. Infect.* 18, 1185–1193. doi: 10.1111/1469-0691.12023

Lagier, J. C., Hugon, P., Khelaifia, S., Fournier, P. E., La Scola, B., and Raoult, D. (2015). The rebirth of culture in microbiology through the example of culturomics to study human gut microbiota. *Clin. Microbiol. Rev.* 28, 237–264. doi: 10.1128/CMR.00014-14

Lazarevic, V., Whiteson, K., Huse, S., Hernandez, D., Farinelli, L., Østerås, M., et al. (2009). Metagenomic study of the oral microbiota by Illumina high-throughput sequencing. *J. Microbiol. Methods* 79, 266–271. doi: 10.1016/j.mimet.2009.09.012

Lazaridis, N., and Germanidis, G. (2018). Current insights into the innate immune system dysfunction in irritable bowel syndrome. *Ann. Gastroenterol.* 31, 171–187. doi: 10.20524/aog.2018.0229

Le Gall, G., Noor, S. O., Ridgway, K., Scovell, L., Jamieson, C., Johnson, I. T., et al. (2011). Metabolomics of fecal extracts detects altered metabolic activity of gut microbiota in ulcerative colitis and irritable bowel syndrome. *J. Proteome Res.* 10, 4208–4218. doi: 10.1021/pr2003598

Lembo, A., Pimentel, M., Rao, S. S., Schoenfeld, P., Cash, B., Weinstock, L. B., et al. (2016). Repeat treatment with rifaximin is safe and effective in patients with diarrhea-predominant irritable bowel syndrome. *Gastroenterology* 151, 1113–1121. doi: 10.1053/j.gastro.2016.08.003

Lembo, A. J. (2007). The clinical and economic burden of irritable bowel syndrome. *Pract. Gastroenterol.* 31, 3–9.

Lembo, A. J., Lacy, B. E., Zuckerman, M. J., Schey, R., Dove, L. S., Andrae, D. A., et al. (2016). Eluxadoline for irritable bowel syndrome with diarrhea. *N. Engl. J. Med.* 374, 242–253. doi: 10.1056/NEJMoa1505180

Li, J., Jia, H., Cai, X., Zhong, H., Feng, Q., Sunagawa, S., et al. (2014). An integrated catalog of reference genes in the human gut microbiome. *Nat. Biotechnol.* 32, 834–41. doi: 10.1038/nbt.2942

Liebregts, T., Adam, B., Bredack, C., Roth, A., Heinzel, S., Lester, S., et al. (2007). Immune activation in patients with irritable bowel syndrome. *Gastroenterology* 132, 913–920. doi: 10.1053/j.gastro.2007.01.046

Liu, H. N., Wu, H., Chen, Y. Z., Chen, Y. J., Shen, X. Z., and Liu, T. T. (2017). Altered molecular signature of intestinal microbiota in irritable bowel syndrome patients compared with healthy controls: a systematic review and meta-analysis. *Dig. Liver Dis.* 49, 331–337. doi: 10.1016/j.dld.2017.01.142

Ludidi, S., Jonkers, D., Elamin, E., Pieters, H. J., Schaepkens, E., Bours, P., et al. (2015). The intestinal barrier in irritable bowel syndrome: subtype-specific effects of the systemic compartment in an in vitro model. *PLoS One* 10:e0123498. doi: 10.1371/journal.pone.0123498

Ludidi, S., Mujagic, Z., Jonkers, D., Keszthelyi, D., Hesselink, M., Kruimel, J., et al. (2014). Markers for visceral hypersensitivity in patients with irritable bowel syndrome. *Neurogastroenterol. Motil.* 26, 1104–1111. doi: 10.1111/nmo.12365

Lyra, A., Rinttilä, T., Nikkilä, J., Krogius-Kurikka, L., Kajander, K., Malinen, E., et al. (2009). Diarrhoea-predominant irritable bowel syndrome distinguishable by 16S rRNA gene phylotype quantification. *World J. Gastroenterol.* 15, 5936-5945.

Maharshak, N., Ringel, Y., Katibian, D., Lundqvist, A., Sartor, R. B., Carroll, I. M., et al. (2018). Fecal and mucosa-associated intestinal microbiota in patients with diarrhea-predominant irritable bowel syndrome. *Dig. Dis. Sci.* 63, 1890–1899. doi: 10.1007/s10620-018-5086-4

Mahurkar, S., Polytarchou, C., Iliopoulos, D., Pothoulakis, C., Mayer, E. A., and Chang, L. (2016). Genome-wide DNA methylation profiling of peripheral blood mononuclear cells in irritable bowel syndrome. *Neurogastroenterol. Motil.* 28, 410–422. doi: 10.1111/nmo.12741

Malinen, E., Krogius-Kurikka, L., Lyra, A., Nikkilä, J., Jääskeläinen, A., Rinttilä, T., et al. (2010). Association of symptoms with gastrointestinal microbiota in irritable bowel syndrome. *World J. Gastroenterol.* 16, 4532–4540.

Malinen, E., Rinttilä, T., Kajander, K., Mättö, J., Kassinen, A., Krogius, L., et al. (2005). Analysis of the fecal microbiota of irritable bowel syndrome patients and healthy controls with real-time PCR. *Am. J. Gastroenterol.* 100, 373–382. doi: 10.1111/j.1572-0241.2005.40312.x

Marchesi, J. R. (2010). Prokaryotic and eukaryotic diversity of the human gut. *Adv. Appl. Microbiol.* 72, 43–62. doi: 10.1016/S0065-2164(10)72002-5

Marsh, A., Eslick, E. M., and Eslick, G. D. (2016). Does a diet low in FODMAPs reduce symptoms associated with functional gastrointestinal disorders? A comprehensive systematic review and meta-analysis. *Eur. J. Nutr.* 55, 897–906. doi: 10.1007/s00394-015-0922-1

Marshall, J. K., Thabane, M., Garg, A. X., Clark, W., Meddings, J., Collins, S. M., et al. (2004). Intestinal permeability in patients with irritable bowel syndrome after a waterborne outbreak of acute gastroenteritis in Walkerton, Ontario. *Aliment. Pharmacol. Ther.* 20, 1317–1322. doi: 10.1111/j.1365-2036.2004.02284.x

Martin-Viñas, J. J., and Quigley, E. M. (2016). Immune response in irritable bowel syndrome: a systematic review of systemic and mucosal inflammatory mediators. *J. Dig. Dis.* 17, 572–581. doi: 10.1111/1751-2980.12379

Matricon, J., Meleine, M., Gelot, A., Piche, T., Dapoigny, M., Muller, E., et al. (2012). Review article: associations between immune activation, intestinal permeability and the irritable bowel syndrome. *Aliment. Pharmacol. Ther.* 36, 1009–1031. doi: 10.1111/apt.12080

Mayer, E. A., Labus, J. S., Tillisch, K., Cole, S. W., and Baldi, P. (2015). Towards a systems view of IBS. *Nat. Rev. Gastroenterol. Hepatol.* 12, 592–605. doi: 10.1038/nrgastro.2015.121

Mayer, E. A., Savidge, T., and Shulman, R. J. (2014). Brain-gut microbiome interactions and functional bowel disorders. *Gastroenterology* 146, 1500–1512. doi: 10.1053/j.gastro.2014.02.037

McCarville, J. L., Caminero, A., and Verdu, E. F. (2016). Novel perspectives on therapeutic modulation of the gut microbiota. *Therap. Adv. Gastroenterol.* 9, 580–593. doi: 10.1177/1756283X16637819

McFarland, L. V. (2010). Systematic review and meta-analysis of *Saccharomyces boulardii* in adult patients. *World J. Gastroenterol.* 16, 2202–2222.

Meyrat, P., Safroneeva, E., and Schoepfer, A. M. (2012). Rifaximin treatment for the irritable bowel syndrome with a positive lactulose hydrogen breath test improves symptoms for at least 3 months. *Aliment. Pharmacol. Ther.* 36, 1084–1093. doi: 10.1111/apt.12087

Mills, S., Shanahan, F., Stanton, C., Hill, C., Coffey, A., and Ross, R. P. (2013). Review: movers and shakers: influence of bacteriophages in shaping the mammalian gut microbiota. *Gut Microbes* 4, 4–16. doi: 10.4161/gmic.22371

MIMETAS. (2018). *Perfused Gut Epithelium Tubules– 3D Intestinal Tubules in the OrganoPlate*. Available at: https://mimetas.com/overview-mimetas-applications/perfused-gut-epithelium-tubules (accessed September 02, 2018).

Min, Y. W., Park, S. U., Jang, Y. S., Kim, Y. H., Rhee, P. L., Ko, S. H., et al. (2012). Effect of composite yogurt enriched with acacia fiber and *Bifidobacterium lactis*. *World J. Gastroenterol.* 18, 4563–4569. doi: 10.3748/wjg.v18.i33.4563

Mizuno, S., Masaoka, T., Naganuma, M., Kishimoto, T., Kitazawa, M., Kurokawa, S., et al. (2017). Bifidobacterium-rich fecal donor may be a positive predictor for successful fecal microbiota transplantation in patients with irritable bowel syndrome. *Digestion* 96, 29–38. doi: 10.1159/000471919

Moayyedi, P., Mearin, F., Azpiroz, F., Andresen, V., Barbara, G., Corsetti, M., et al. (2017). Irritable bowel syndrome diagnosis and management: a simplified algorithm for clinical practice. *United European Gastroenterol. J.* 5, 773–788. doi: 10.1177/2050640617731968

Moloney, R. D., O'Leary, O. F., Felice, D., Bettler, B., Dinan, T. G., and Cryan, J. F. (2012). Early-life stress induces visceral hypersensitivity in mice. *Neurosci. Lett.* 512, 99–102. doi: 10.1016/j.neulet.2012.01.066

Moraes-Filho, J. P., and Quigley, E. M. M. (2015). The intestinal microbiota and the role of probiotics in irritable bowel syndrome: a review. *Arq. Gastroenterol.* 52, 331–338. doi: 10.1590/S0004-28032015000400015

Muegge, B. D., Kuczynski, J., Knights, D., Clemente, J. C., González, A., Fontana, L., et al. (2011). Diet drives convergence in gut microbiome functions across mammalian phylogeny and within humans. *Science* 332, 970–974. doi: 10.1126/science.1198719

Nam, Y. D., Chang, H. W., Kim, K. H., Roh, S. W., Kim, M. S., Jung, M. J., et al. (2008). Bacterial, archaeal, and eukaryal diversity in the intestines of Korean people. *J. Microbiol.* 46, 491–501. doi: 10.1007/s12275-008-0199-7

National Institute for Health and Care Excellence [NICE] (2017). *Irritable Bowel Syndrome In Adults: Diagnosis And Management. Clinical guideline (CG61), National Institute for Health and Care Excellence (NICE) guidelines for dietary and lifestyle advice*. Available at: https://www.nice.org.uk/guidance/cg61 (accessed April, 2017).

Noddin, L., Callahan, M., and Lacy, B. E. (2005). Irritable bowel syndrome and functional dyspepsia: different diseases or a single disorder with different manifestations? *MedGenMed* 7:17.

Ohman, L., and Simrén, M. (2013). Intestinal microbiota and its role in irritable bowel syndrome (IBS). *Curr. Gastroenterol. Rep.* 15:323. doi: 10.1007/s11894-013-0323-7

Ott, S. J., Waetzig, G. H., Rehman, A., Moltzau-Anderson, J., Bharti, R., Grasis, J. A., et al. (2017). Efficacy of sterile fecal filtrate transfer for treating patients with clostridium difficile infection. *Gastroenterology* 152, 799–811.e7. doi: 10.1053/j.gastro.2016.11.010

Oświęcimska, J., Szymlak, A., Roczniak, W., Girczys-Połedniok, K., and Kwiecien, J. (2017). New insights into the pathogenesis and treatment of irritable bowel syndrome. *Adv. Med. Sci.* 62, 17–30. doi: 10.1016/j.advms.2016.11.001

Paineau, D., Payen, F., Panserieu, S., Coulombier, G., Sobaszek, A., Lartigau, I., et al. (2008). The effects of regular consumption of short-chain fructo-oligosaccharides on digestive comfort of subjects with minor functional bowel disorders. *Br. J. Nutr.* 99, 311–318. doi: 10.1017/S000711450779894X

Parkes, G. C., Rayment, N. B., Hudspith, B. N., Petrovska, L., Lomer, M. C., Brostoff, J., et al. (2012). Distinct microbial populations exist in the mucosa-associated microbiota of sub-groups of irritable bowel syndrome. *Neurogastroenterol. Motil.* 24, 31–39. doi: 10.1111/j.1365-2982.2011.01803.x

Patel, P., Bercik, P., Morgan, D. G., Bolino, C., Pintos-Sanchez, M. I., Moayyedi, P., et al. (2015). Irritable bowel syndrome is significantly associated with somatisation in 840 patients, which may drive bloating. *Aliment. Pharmacol. Ther.* 41, 449–458. doi: 10.1111/apt.13074

Paulsen, I. T., Banerjei, L., Myers, G. S. A., Nelson, K. E., Seshadri, R., Read, T. D., et al. (2003). Role of mobile DNA in the evolution of vancomycin-resistant *Enterococcus faecalis*. *Science* 299, 2071–2074. doi: 10.1126/science.1080613

Pedron, T., and Sansonetti, P. (2008). Commensals, bacterial pathogens and intestinal inflammation: an intriguing menage a trois. *Cell Host Microbe* 3, 344–347. doi: 10.1016/j.chom.2008.05.010

Piche, T., Barbara, G., Aubert, P., Bruley des Varannes, S., Dainese, R., Nano, J. L., et al. (2009). Impaired intestinal barrier integrity in the colon of patients with irritable bowel syndrome: involvement of soluble mediators. *Gut* 58, 196–201. doi: 10.1136/gut.2007.140806

Pimentel, M. (2018). Evidence-based management of irritable bowel syndrome with diarrhea. *Am. J. Manag. Care* 24(3 Suppl), S35–S46.

Pimentel, M., Lembo, A., Chey, W. D., Zakko, S., Ringel, Y., Yu, J., et al. (2011). Rifaximin therapy for patients with irritable bowel syndrome without constipation. *N. Engl. J. Med.* 364, 22–32. doi: 10.1056/NEJMoa1004409

Pimentel, M., Lin, H. C., Enayati, P., van den Burg, B., Lee, H. R., Chen, J. H., et al. (2006). Methane, a gas produced by enteric bacteria, slows intestinal transit and augments small intestinal contractile activity. *Am. J. Physiol. Gastrointest. Liver Physiol.* 290, G1089–G1095. doi: 10.1152/ajpgi.00574.2004

Pineiro, M., Asp, N. G., Reid, G., Macfarlane, S., Morelli, L., Brunser, O., et al. (2008). FAO technical meeting on prebiotics. *J. Clin. Gastroenterol.* 42, S156–S159. doi: 10.1097/MCG.0b013e31817f184e

Ponnusamy, K., Choi, J. N., Kim, J., Lee, S. Y., and Lee, C. H. (2011). Microbial community and metabolomics comparison of irritable bowel syndrome faeces. *J. Med. Microbiol.* 60, 817–827. doi: 10.1099/jmm.0.028126-0

Pozuelo, M., Panda, S., Santiago, A., Mendez, S., Accarino, A., Santos, J., et al. (2015). Reduction of butyrate- and methane-producing microorganisms in patients with Irritable Bowel Syndrome. *Sci. Rep.* 5:12693. doi: 10.1038/srep12693

Qin, H. Y., Cheng, C. W., Tang, X. D., and Bian, Z. X. (2014). Impact of psychological stress on irritable bowel syndrome. *World J. Gastroenterol.* 20, 14126–14131. doi: 10.3748/wjg.v20.i39.14126

Qin, J., Li, R., Raes, J., Arumugam, M., Burgdorf, K. S., Manichanh, C., et al. (2010). A human gut microbial gene catalogue established by metagenomic sequencing. *Nature* 464, 59–65. doi: 10.1038/nature08821

Rajilić-Stojanović, M., Biagi, E., Heilig, H. G., Kajander, K., Kekkonen, R. A., Tims, S., et al. (2011). Global and deep molecular analysis of microbiota signatures in fecal samples from patients with irritable bowel syndrome. *Gastroenterology* 141, 1792–1801. doi: 10.1053/j.gastro.2011.07.043

Rajilić-Stojanović, M. (2007). *Diversity of the Human Gastrointestinal Microbiota – Novel Perspectives from High Throughput Analyses*. Ph.D. thesis, University of Wageningen, Wageningen.

Rao, S., Lembo, A. J., Shiff, S. J., Lavins, B. J., Currie, M. G., Jia, X. D., et al. (2012). A 12-week, randomized, controlled trial with a 4-week randomized withdrawal period to evaluate the efficacy and safety of linaclotide in irritable bowel syndrome with constipation. *Am. J. Gastroenterol.* 107, 1714–1724. doi: 10.1038/ajg.2012.255

Ren, T. H., Wu, J., Yew, D., Ziea, E., Lao, L., Leung, W. K., et al. (2007). Effects of neonatal maternal separation on neurochemical and sensory response to colonic distension in a rat model of irritable bowel syndrome. *Am. J. Physiol. Gastrointest. Liver Physiol.* 292, G849–G856. doi: 10.1152/ajpgi.00400.2006

Reti, K. L., Tymensen, L. D., Davis, S. P., Amrein, M. W., and Buret, A. G. (2015). Campylobacter jejuni increases flagellar expression and adhesion of non-invasive *Escherichia coli*: effects on enterocytic TLR-4 and CXCL-8 expression. *Infect. Immun.* 83, 4571–4581. doi: 10.1128/IAI.00970-15

Rigsbee, L., Agans, R., Shankar, V., Kenche, H., Khamis, H. J., Michail, S., et al. (2012). Quantitative profiling of gut microbiota of children with diarrhea-predominant irritable bowel syndrome. *Am. J. Gastroenterol.* 107, 1740–1751.

Ringel, Y., and Maharshak, N. (2013). Bacteria, inflammation, and immune activation in the pathogenesis of irritable bowel syndrome. *Am. J. Physiol. Gastrointest. Liver Physiol.* 305, G529–G541. doi: 10.1152/ajpgi.00207.2012

Rivière, A., Selak, M., Geirnaert, A., Van den Abbeele, P., and De Vuyst, L. (2018). Complementary mechanisms for degradation of inulin-type fructans and arabinoxylan oligosaccharides among bifidobacterial strains suggest bacterial cooperation. *Appl. Environ. Microbiol.* 84:e02893-17. doi: 10.1128/AEM.02893-17

Rivière, A., Selak, M., Lantin, D., Leroy, F., and De Vuyst, L. (2016). Bifidobacteria and butyrate-producing colon bacteria: importance and strategies for their stimulation in the human gut. *Front. Microbiol.* 7:979. doi: 10.3389/fmicb.2016.00979

Rossen, N. G., MacDonald, J. K., de Vries, E. M., D'Haens, G. R., de Vos, W. M., Zoetendal, E. G., et al. (2015). Fecal microbiota transplantation as novel therapy in gastroenterology: a systematic review. *World J. Gastroenterol.* 21, 5359–5371. doi: 10.3748/wjg.v21.i17.5359

Rothschild, D., Weissbrod, O., Barkan, E., Kurilshikov, A., Korem, T., Zeevi, D., et al. (2018). Environment dominates over host genetics in shaping human gut microbiota. *Nature* 555, 210–215. doi: 10.1038/nature25973

Saadi, M., and McCallum, R. W. (2013). Rifaximin in irritable bowel syndrome: rationale, evidence and clinical use. *Ther. Adv. Chronic Dis.* 4, 71–75. doi: 10.1177/2040622312472008

Shah, E. D., Kim, H. M., and Schoenfeld, P. (2018). Efficacy and tolerability of guanylate cyclase-C agonists for irritable bowel syndrome with constipation and chronic idiopathic constipation: a systematic review and meta-analysis. *Am. J. Gastroenterol.* 113, 329–338. doi: 10.1038/ajg.2017.495

Shaw, A. L., Tomanelli, A., Bradshaw, T. P., Petschow, B. W., and Burnett, B. P. (2017). Impact of serum-derived bovine immunoglobulin/protein isolate therapy on irritable bowel syndrome and inflammatory bowel disease: a survey of patient perspective. *Patient Prefer. Adherence* 11, 1001–1007. doi: 10.2147/PPA.S134792

Shenderov, B. A. (2013). Metabiotics: novel idea or natural development of probiotic conception. *Microb. Ecol. Health Dis.* 24:20399. doi: 10.3402/mehd.v24i0.20399

Shukla, R., Ghoshal, U., Dhole, T. N., and Ghoshal, U. C. (2015). Fecal microbiota in patients with irritable bowel syndrome compared with healthy controls using real-time polymerase chain reaction: an evidence of dysbiosis. *Dig. Dis. Sci.* 60, 2953–2962. doi: 10.1007/s10620-015-3607-y

Shulman, R. J., Jarrett, M. E., Cain, K. C., Broussard, E. K., and Heitkemper, M. M. (2014). Associations among gut permeability, inflammatory markers, and symptoms in patients with irritable bowel syndrome. *J. Gastroenterol.* 49, 1467–1476. doi: 10.1007/s00535-013-0919-6

Si, J. M., Yu, Y. C., Fan, Y. J., and Chen, S. J. (2004). Intestinal microecology and quality of life in irritable bowel syndrome patients. *World J. Gastroenterol.* 10, 1802–1805.

Silk, D. B. A., Davis, A., Vulevic, J., Tzortzis, G., and Gibson, G. R. (2009). Clinical trial: the effects of a trans-galactooligosaccharide prebiotic on faecal microbiota and symptoms in irritable bowel syndrome. *Aliment. Pharmacol. Ther.* 29, 508–518. doi: 10.1111/j.1365-2036.2008.03911.x

Simrén, M., Barbara, G., Flint, H. J., Spiegel, B. M., Spiller, R. C., Vanner, S., et al. (2013). Rome Foundation Committee. Intestinal microbiota in functional bowel disorders: a Rome foundation report. *Gut* 62, 159–176. doi: 10.1136/gutjnl-2012-302167

Sinha, R., Chen, J., Amir, A., Vogtmann, E., Shi, J., Inman, K. S., et al. (2016). Collecting fecal samples for microbiome analyses in epidemiology studies. *Cancer Epidemiol. Biomarkers Prev.* 25, 407–416. doi: 10.1158/1055-9965.EPI-15-0951

Soares, R. L. (2014). Irritable bowel syndrome: a clinical review. *World J. Gastroenterol.* 20, 12144–12160. doi: 10.3748/wjg.v20.i34.12144

Sperber, A. D., Dumitrascu, D., Fukudo, S., Gerson, C., Ghoshal, U. C., Gwee, K. A., et al. (2017). The global prevalence of IBS in adults remains elusive due to the heterogeneity of studies: a Rome Foundation working team literature review. *Gut* 66, 1075–1082. doi: 10.1136/gutjnl-2015-311240

Staudacher, H. M., Lomer, M. C. E., Anderson, J. L., Barrett, J. S., Muir, J. G., Irving, P. M., et al. (2012). Fermentable carbohydrate restriction reduces luminal

bifidobacteria and gastrointestinal symptoms in patients with irritable bowel syndrome. *J. Nutr.* 142, 1510–1518. doi: 10.3945/jn.112.159285

Su, T., Liu, R., Lee, A., Long, Y., Du, L., Lai, S., et al. (2018). Altered intestinal microbiota with increased abundance of *Prevotella* is associated with high risk of diarrhea-predominant irritable bowel syndrome. *Gastroenterol. Res. Pract.* 2018:6961783. doi: 10.1155/2018/6961783

Sundin, J., Rangel, I., Kumawat, A. K., Hultgren-Hörnquist, E., and Brummer, R. J. (2014). Aberrant mucosal lymphocyte number and subsets in the colon of post-infectious irritable bowel syndrome patients. *Scand. J. Gastroenterol.* 49, 1068–1075. doi: 10.3109/00365521.2014.926982

Sykes, M. A., Blanchard, E. B., Lackner, J., Keefer, L., and Krasner, S. (2003). Psychopathology in irritable bowel syndrome: support for a psychophysiological model. *J. Behav. Med.* 26, 361–372.

Tana, C., Umesaki, Y., Imaoka, A., Handa, T., Kanazawa, M., and Fukudo, S. (2010). Altered profiles of intestinal microbiota and organic acids may be the origin of symptoms in irritable bowel syndrome. *Neurogastroenterol. Motil.* 22, 512–519. doi: 10.1111/j.1365-2982.2009.01427.x

Tanaka, Y., Kanazawa, M., Fukudo, S., and Drossman, D. A. (2011). Biopsychosocial model of irritable bowel syndrome. *J. Neurogastroenterol. Motil.* 17, 131–139. doi: 10.5056/jnm.2011.17.2.131

Tang, J., Iliev, I. D., Brown, J., Underhill, D. M., and Funari, V. A. (2015). Mycobiome: approaches to analysis of intestinal fungi. *J. Immunol. Methods* 421, 112–121. doi: 10.1016/j.jim.2015.04.004

Tap, J., Derrien, M., Törnblom, H., Brazeilles, R., Cools-Portier, S., Doré, J., et al. (2017). Identification of an intestinal microbiota signature associated with severity of irritable bowel syndrome. *Gastroenterology* 152, 111–123. doi: 10.1053/j.gastro.2016.09.049

Taverniti, V., and Guglielmetti, S. (2011). The immunomodulatory properties of probiotic microorganisms beyond their viability (ghost probiotics: proposal of paraprobiotic concept). *Genes Nutr.* 6, 261–274. doi: 10.1007/s12263-011-0218-x

Thabane, M., Kottachchi, D. T., and Marshall, J. K. (2007). Systematic review and meta-analysis: the incidence and prognosis of post-infectious irritable bowel syndrome. *Aliment. Pharmacol. Ther.* 26, 535–544. doi: 10.1111/j.1365-2036.2007.03399.x

Traini, C., Evangelista, S., Girod, V., Faussone-Pellegrini, M. S., and Vannucchi, M. G. (2016). Changes of excitatory and inhibitory neurotransmitters in the colon of rats underwent to the wrap partial restraint stress. *Neurogastroenterol. Motil.* 28, 1172–1185. doi: 10.1111/nmo.12816

Tsilingiri, K., Barbosa, T., Penna, G., Caprioli, F., Sonzogni, A., Viale, G., et al. (2012). Probiotic and postbiotic activity in health and disease: comparison on a novel polarised ex-vivo organ culture model. *Gut* 61, 1007–1015. doi: 10.1136/gutjnl-2011-300971

Tsilingiri, K., and Rescigno, M. (2013). Postbiotics: what else? *Benef Microbes* 4, 101–107. doi: 10.3920/BM2012.0046

Turnbaugh, P. J., Ley, R. E., Hamady, M., Fraser-Liggett, C. M., Knight, R., and Gordon, J. I. (2007). The human microbiome project. *Nature* 449, 804–810. doi: 10.1038/nature06244

Underhill, D. M., and Iliev, I. D. (2014). The mycobiota: interactions between commensal fungi and the host immune system. *Nat. Rev. Immunol.* 14, 405–416. doi: 10.1038/nri3684

Valentin, N., Camilleri, M., Carlson, P., Harrington, S. C., Eckert, D., O'Neill, J., et al. (2017). Potential mechanisms of effects of serum-derived bovine immunoglobulin/protein isolate therapy in patients with diarrhea-predominant irritable bowel syndrome. *Physiol. Rep.* 5:e13170. doi: 10.14814/phy2.13170

Varjú, P., Farkas, N., Hegyi, P., Garami, A., Szabó, I., Illés, A., et al. (2017). Low fermentable oligosaccharides, disaccharides, monosaccharides and polyols (FODMAP) diet improves symptoms in adults suffering from irritable bowel syndrome (IBS) compared to standard IBS diet: a meta-analysis of clinical studies. *PLoS One* 12:e0182942. doi: 10.1371/journal.pone.0182942

Vazquez-Roque, M. I., Camilleri, M., Smyrk, T., Murray, J. A., Marietta, E., O'Neill, J., et al. (2013). A controlled trial of gluten-free diet in patients with irritable bowel syndrome-diarrhea: effects on bowel frequency and intestinal function. *Gastroenterology* 144, 903–911.e3. doi: 10.1053/j.gastro.2013.01.049

Vernochi, P., Del Chierico, F., and Putignani, L. (2016). Gut microbiota profiling: metabolomics based approach to unravel compounds affecting human health. *Front. Microbiol.* 7:1144. doi: 10.3389/fmicb.2016.01144

Vogtmann, E., Chen, J., Amir, A., Shi, J., Abnet, C. C., Nelson, H., et al. (2017). Comparison of collection methods for fecal samples in microbiome studies. *Am. J. Epidemiol.* 85, 115–123. doi: 10.1093/aje/kww177

Wadhwa, A., Al Nahhas, M. F., Dierkhising, R. A., Patel, R., Kashyap, P., Pardi, D. S., et al. (2016). High risk of post-infectious irritable bowel syndrome in patients with Clostridium difficile infection. *Aliment. Pharmacol. Ther.* 44, 576–582. doi: 10.1111/apt.13737

Wilson, D., Evans, M., Weaver, E., Shaw, A. L., and Klein, G. L. (2013). Evaluation of serum-derived bovine immunoglobulin protein isolate in subjects with diarrhea-predominant irritable bowel syndrome. *Clin. Med. Insights Gastroenterol.* 6, 49–60. doi: 10.4137/CGast.S13200

Wong, B. S., Camilleri, M., Carlson, P., McKinzie, S., Busciglio, I., Bondar, O., et al. (2012). Increased bile acid biosynthesis is associated with irritable bowel syndrome with diarrhea. *Clin. Gastroenterol. Hepatol.* 10, 1009–1015.e3. doi: 10.1016/j.cgh.2012.05.006

Workman, M. J., Gleeson, J. P., Troisi, E. J., Estrada, H. Q., Kerns, S. J., Hinojosa, C. D., et al. (2018). Enhanced utilization of induced pluripotent stem cell–derived human intestinal organoids using microengineered chips. *Cell. Mol. Gastroenterol. Hepatol.* 5, 669–677.e2. doi: 10.1016/j.jcmgh.2017.12.008

Wouters, M. M., Lambrechts, D., Knapp, M., Cleynen, I., Whorwell, P., Agréus, L., et al. (2013). Genetic variants in *CDC42* and *NXPH1* as susceptibility factors for constipation and diarrhoea predominant irritable bowel syndrome. *Gut* 63, 1103–1111. doi: 10.1136/gutjnl-2013-304570

Wu, W. K., Chen, C. C., Panyod, S., Chen, R. A., Wu, M. S., Sheen, L. Y., et al. (2018). Optimization of fecal sample processing for microbiome study - The journey from bathroom to bench. *J. Formos. Med. Assoc.* 118, 545–555. doi: 10.1016/j.jfma.2018.02.005

Yuan, F., Ni, H., Asche, C. V., Kim, M., Walayat, S., and Ren, J. (2017). Efficacy of *Bifidobacterium infantis* 35624 in patients with irritable bowel syndrome: a meta-analysis. *Curr. Med. Res. Opin.* 33, 1191–1197. doi: 10.1080/03007995.2017.1292230

Zhang, Y., Li, L., Guo, C., Mu, D., Feng, B., Zuo, X., et al. (2016). Effects of probiotic type, dose and treatment duration on irritable bowel syndrome diagnosed by Rome III criteria: a meta-analysis. *BMC Gastroenterol.* 16:62. doi: 10.1186/s12876-016-0470-z

Zhuang, X., Xiong, L., Li, L., Li, M., and Chen, M. (2017). Alterations of gut microbiota in patients with irritable bowel syndrome: a systemic review and meta-analysis. *J. Gastroenterol. Hepatol.* 32, 28–38. doi: 10.1111/jgh.13471

Zhuang, X., Xiong, L., Tian, Z., Li, L., Zeng, Z., and Chen, M. (2018). Fecal microbiota alterations associated with diarrhea-predominant irritable bowel syndrome. *Front. Microbiol.* 9:1600. doi: 10.3389/fmicb.2018.01600

Conflict of Interest Statement: The authors declare that the research was conducted in the absence of any commercial or financial relationships that could be construed as a potential conflict of interest.

Copyright © 2019 Chong, Chin, Looi, Wong, Madhavan and Yong. This is an open-access article distributed under the terms of the Creative Commons Attribution License (CC BY). The use, distribution or reproduction in other forums is permitted, provided the original author(s) and the copyright owner(s) are credited and that the original publication in this journal is cited, in accordance with accepted academic practice. No use, distribution or reproduction is permitted which does not comply with these terms.

frontiers in Microbiology

CORRECTION
published: 13 August 2019
doi: 10.3389/fmicb.2019.01870

Corrigendum: The Microbiome and Irritable Bowel Syndrome – A Review on the Pathophysiology, Current Research and Future Therapy

Pei Pei Chong[1]*, *Voon Kin Chin*[1], *Chung Yeng Looi*[1], *Won Fen Wong*[2], *Priya Madhavan*[3] and *Voon Chen Yong*[1]

[1] School of Biosciences, Taylor's University, Subang Jaya, Malaysia, [2] Department of Medical Microbiology, Faculty of Medicine, University of Malaya, Kuala Lumpur, Malaysia, [3] School of Medicine, Faculty of Health and Medical Sciences, Taylor's University, Subang Jaya, Malaysia

Keywords: irritable bowel syndrome, microbiome, microbiota dysbiosis, fecal transplant, IBS animal model

OPEN ACCESS

Approved by:
Frontiers Editorial Office, Frontiers Media SA, Switzerland

***Correspondence:**
Pei Pei Chong
PeiPei.Chong@taylors.edu.my

Specialty section:
This article was submitted to Microbial Symbioses, a section of the journal Frontiers in Microbiology

Received: *03 July 2019*
Accepted: *29 July 2019*
Published: *13 August 2019*

Citation:
Chong PP, Chin VK, Looi CY, Wong WF, Madhavan P and Yong VC (2019) Corrigendum: The Microbiome and Irritable Bowel Syndrome – A Review on the Pathophysiology, Current Research and Future Therapy. Front. Microbiol. 10:1870. doi: 10.3389/fmicb.2019.01870

A Corrigendum on

The Microbiome and Irritable Bowel Syndrome – A Review on the Pathophysiology, Current Research and Future Therapy

by Chong, P. P., Chin, V. K., Looi, C. Y., Wong, W. F., Madhavan, P., and Yong, V. C. (2019) Front. Microbiol. 10:1136. doi: 10.3389/fmicb.2019.01136

In the original article "Won Fen Wong" was incorrectly assigned as the second corresponding author. The sole corresponding author is "Pei Pei Chong."

In addition, we neglected to include the funder "Taylor's University, TRGS/ERFS/2/2018/SBS/025" to Pei Pei Chong.

A correction has therefore been made to the **Funding** statement:

"This work was supported by the Taylor's Research Grant Scheme (TRGS), Taylor's University, Malaysia (Award No. TRGS/MFS/2/2016/SOM/013) and Taylor's University, (Award No. TRGS/ERFS/2/2018/SBS/025)."

The authors apologize for these errors and state that they do not change the scientific conclusions of the article in any way. The original article has been updated.

Copyright © 2019 Chong, Chin, Looi, Wong, Madhavan and Yong. This is an open-access article distributed under the terms of the Creative Commons Attribution License (CC BY). The use, distribution or reproduction in other forums is permitted, provided the original author(s) and the copyright owner(s) are credited and that the original publication in this journal is cited, in accordance with accepted academic practice. No use, distribution or reproduction is permitted which does not comply with these terms.

frontiers in Microbiology

ORIGINAL RESEARCH
published: 12 June 2019
doi: 10.3389/fmicb.2019.01316

Micronutrient Requirements and Sharing Capabilities of the Human Gut Microbiome

Dmitry A. Rodionov[1,2†], Aleksandr A. Arzamasov[1,2†], Matvei S. Khoroshkin[2†], Stanislav N. Iablokov[2,3], Semen A. Leyn[1,2], Scott N. Peterson[1], Pavel S. Novichkov[4] and Andrei L. Osterman[1*]*

[1] Sanford Burnham Prebys Medical Discovery Institute, La Jolla, CA, United States, [2] A.A. Kharkevich Institute for Information Transmission Problems, Russian Academy of Sciences, Moscow, Russia, [3] Department of Physics, P.G. Demidov Yaroslavl State University, Yaroslavl, Russia, [4] Lawrence Berkeley National Laboratory, Berkeley, CA, United States

OPEN ACCESS

Edited by:
Siok-Fong Chin,
UKM Medical Molecular Biology Institute (UMBI), Malaysia

Reviewed by:
Sergio Uzzau,
University of Sassari, Italy
Sandip Paul,
Indian Institute of Chemical Biology (CSIR), India

***Correspondence:**
Dmitry A. Rodionov
rodionov@sbpdiscovery.org;
rodionov@burnham.org
Andrei L. Osterman
osterman@sbpdiscovery.org

[†] These authors have contributed equally to this work

Specialty section:
This article was submitted to Microbial Symbioses, a section of the journal Frontiers in Microbiology

Received: 09 January 2019
Accepted: 27 May 2019
Published: 12 June 2019

Citation:
Rodionov DA, Arzamasov AA, Khoroshkin MS, Iablokov SN, Leyn SA, Peterson SN, Novichkov PS and Osterman AL (2019) Micronutrient Requirements and Sharing Capabilities of the Human Gut Microbiome. Front. Microbiol. 10:1316. doi: 10.3389/fmicb.2019.01316

The human gut microbiome harbors a diverse array of metabolic pathways contributing to its development and homeostasis via a complex web of diet-dependent metabolic interactions within the microbial community and host. Genomics-based reconstruction and predictive modeling of these interactions would provide a framework for diagnostics and treatment of dysbiosis-related syndromes via rational selection of therapeutic prebiotics and dietary nutrients. Of particular interest are micronutrients, such as B-group vitamins, precursors of indispensable metabolic cofactors, that are produced *de novo* by some gut bacteria (prototrophs) but must be provided exogenously in the diet for many other bacterial species (auxotrophs) as well as for the mammalian host. Cross-feeding of B vitamins between prototrophic and auxotrophic species is expected to strongly contribute to the homeostasis of microbial communities in the distal gut given the efficient absorption of dietary vitamins in the upper gastrointestinal tract. To confidently estimate the balance of microbiome micronutrient biosynthetic capabilities and requirements using available genomic data, we have performed a subsystems-based reconstruction of biogenesis, salvage and uptake for eight B vitamins (B1, B2, B3, B5, B6, B7, B9, and B12) and queuosine (essential factor in tRNA modification) over a reference set of 2,228 bacterial genomes representing 690 cultured species of the human gastrointestinal microbiota. This allowed us to classify the studied organisms with respect to their pathway variants and infer their prototrophic vs. auxotrophic phenotypes. In addition to canonical vitamin pathways, several conserved partial pathways were identified pointing to alternative routes of syntrophic metabolism and expanding a microbial vitamin "menu" by several pathway intermediates (vitamers) such as thiazole, quinolinate, dethiobiotin, pantoate. A cross-species comparison was applied to assess the extent of conservation of vitamin phenotypes at distinct taxonomic levels (from strains to families). The obtained reference collection combined with 16S rRNA gene-based phylogenetic profiles was used to deduce phenotype profiles of the human gut microbiota across in two large cohorts. This analysis provided the first estimate of B-vitamin requirements, production and sharing capabilities in the

human gut microbiome establishing predictive phenotype profiling as a new approach to classification of microbiome samples. Future expansion of our reference genomic collection of metabolic phenotypes will allow further improvement in coverage and accuracy of predictive phenotype profiling of the human microbiome.

Keywords: gut microbiome, vitamin metabolism, metagenomics, 16S, comparative genomics

INTRODUCTION

The human intestinal microbiota is host to trillions of microbes representing thousands of different species and strains and harboring over ten million genes that are organized into complex metabolic and transcriptional networks (Human Microbiome Project Consortium, 2012; Li et al., 2014). These networks are driving numerous metabolic interactions within the microbial community and with the human host in the context of highly variable dietary supply of nutrients (Yatsunenko et al., 2012; David et al., 2014; Zhang et al., 2014; Wu et al., 2015; Blanton et al., 2016; Hibberd et al., 2017; Sheflin et al., 2017). Mapping and predictive modeling of these networks would significantly impact our understanding of associations between the microbiota composition, human health and a large spectrum of human disease states (Subramanian et al., 2014; Zeller et al., 2014; Kostic et al., 2015; Ejtahed et al., 2016; Imhann et al., 2018). Elucidation of metabolic capabilities and nutrient requirements of gut microbial communities is expected to open new opportunities for diagnostics, prevention and treatment of dysbiosis-related syndromes via rational and personalized selection of probiotics, prebiotics and dietary nutrients. Metabolism of micronutrients that can be produced *de novo* by some but not all gut bacteria, such as B-group vitamins, represents a particularly interesting case as it has the potential to combine metabolic interactions, that may be competitive and cooperative.

Six out of eight B-vitamins analyzed in this study, B1 (thiamin), B2 (riboflavin), B3 (niacin), B5 (pantothenate), B9 (folate) and B6 (pyridoxine), are common biosynthetic precursors of major metabolic cofactors, TPP, FMN/FAD, NAD(P), CoA, THF, and PLP, respectively, essential in all microbes as well as in the mammalian host (McCormick, 2003). Vitamin B7 (biotin) serves as an essential carboxylation/decarboxylation cofactor upon covalent attachment to biotin carboxyl carrier protein (BCCP) playing an important role in lipogenesis, carbohydrate and amino acid metabolism (Marquet, 2010). Vitamin B12 (cobalamin), a precursor of the B12 coenzyme family including cyanocobalamin, methylcobalamin, and adenosylcobalamin (AdoCbl), is essential for all animals and many, but not all bacterial species (Degnan et al., 2014; Danchin and Braham, 2017). B12 is synthesized by bacteria in two phases via: (i) either anaerobic or aerobic upstream coring ring synthesis pathway including pre- or post-synthesis incorporation of a cobalt ion; and (ii) a universal downstream pathway that involves adenylation and attachment of aminopropanol and nucleotide components (**Supplementary Figure S1**). Another dietary micronutrient included in our analysis, queuine (Q), is a precursor of a sugar nucleotide queuosine, an essential factor of tRNA modification in both prokaryotes and eukaryotes (Fergus et al., 2015). Availability of these micronutrients in the growth media can influence the structure of various microbial communities (Sanudo-Wilhelmy et al., 2014). On the other hand, recent studies of self-sustaining microbial communities in abiotic environments confirmed the importance of syntrophic metabolism and revealed potential mechanisms for community-wide B-vitamins exchange (Romine et al., 2017). Cross-feeding of these micronutrients between producers and non-producers may also play an important role in the human gut microbiome (HGM) given the efficient absorption of dietary vitamins in the upper gastrointestinal tract.

Previously, we combined genomic and functional context analysis in SEED genome integration and analysis platform to identify novel gene families (enzymes, transporters, transcriptional regulators) and pathway variants involved in microbial B-vitamin metabolism (Rodionov et al., 2002a,b, 2003, 2009, 2017; Vitreschak et al., 2002; Osterman et al., 2010; Rodionova et al., 2017). The earlier SEED subsystems-based analysis revealed a comparable representation and mosaic distribution of B vitamin producers and non-producers within a smaller set of 256 HGM genomes (Magnusdottir et al., 2015), supporting the micronutrient sharing hypothesis.

In the current study, we have focused on a detailed reconstruction of all aspects of biogenesis of nine micronutrients (eight B-vitamins and queuosine) including inference of salvage pathways for non-canonical vitamers and specificity for transport systems on a greatly expanded set of reference genomes. This allowed us to establish genomic signatures for numerous functional pathway variants and to classify all studied species by their simplified *binary phenotypes*, as either having the capability to *de novo* synthesize a given cofactor (*prototrophy*) or being strictly dependent on salvage of its precursor(s) from exogenous sources (*auxotrophy*). Binarization of metabolic phenotypes allows us to develop a computational approach to estimate and compare fractional representation of auxotrophs/prototrophs in publicly available HGM samples. The proposed novel metric, *Community Phenotype Index* (CPI), provides a probabilistic estimate of fractional representation of organisms (on a scale 0 – 100%) with a particular vitamin production capability in a metagenomic sample.

A predictive phylotype-to-phenotype profiling approach established in this study can be extended to a broader range of metabolic phenotypes and applied for comparative

Abbreviations: BPM, Binary Phenotype Matrix; CPI, Community Phenotype Index; CPM, Community Phenotype Matrix; ECF, Energy-Coupling Factor; HGM, Human Gut microbiota/Microbiome; MFS, Major Facilitator Superfamily; NVP, Number of Variable Phenotypes; OPV, Overall Phenotype Variability score; OTU, Operational Taxonomic Unit; TF, Transcription factor; VPR, Vitamin Prototrophy Rank.

analysis of general metabolic capabilities vs. nutrient requirements of gut microbial communities as a function of various factors defining their healthy vs. pathological development (Gehrig et al., 2019). The observed correlations and dependencies are expected to provide guidelines for rational development of therapeutic foods and nutrient supplementation.

MATERIALS AND METHODS

Reference Set of HGM Genomes

To build a comprehensive reference collection of genomes representing diverse bacterial HGM species we utilized the following approach. First, we obtained a list of 194 public HGM genomes collected by the MetaHIT consortium in 2010 (Qin et al., 2010). This list included 151 bacterial genomes sequenced by the Human Microbiome Project (HMP), 17 genomes sequenced by MetaHIT and 26 genomes collected from Genbank. The list was combined with 450 HGM genomes from the Human Microbiome Reference Genome Database in 2012[1] (Human Microbiome Project Consortium, 2012). Finally, we analyzed the collection of ∼1,000 cultured HGM species published in Rajilic-Stojanovic and de Vos (2014). By mapping the HGM species onto the PATRIC genomic database[2] (Wattam et al., 2017) we selected 2,228 bacterial strains represented by either complete or high-quality draft genomes (**Supplementary Table S1**). Phylogenetic trees of analyzed species were generated using concatenated alignments of 11 ribosomal proteins (L5, L6, L9, L10, L15, L20, S2, S4, S5, S6, S8). Ribosomal protein sequences were aligned using MUSCLE (Edgar, 2004). The maximum likelihood phylogenetic tree was constructed using RAxML version 8 (Stamatakis, 2015) and visualized via iTOL (Letunic and Bork, 2016).

In silico Metabolic Reconstruction and Phenotype Prediction

For genomic reconstruction and prediction of metabolic phenotypes for eight B-vitamins and queuosine across the entire set of 2,228 reference genomes, we extended a subsystems-based approach implemented in the SEED platform[3] (Overbeek et al., 2005, 2014) (see **Supplementary Figure S2A** for workflow overview). For each of the nine studied vitamins/cofactors, all known and inferred components (enzymes, transporters and transcriptional regulators) of biosynthetic and salvage pathways (**Supplementary Figure S1**) were captured in a respective mcSEED (microbial community SEED) subsystem propagated to all selected HGM genomes (**Supplementary Table S2**). *In silico* metabolic reconstructions in mcSEED subsystems were based on functional gene annotation using homology-based methods and three genome context techniques: (i) clustering of genes on the chromosome (operons), (ii) co-regulation of genes by a common regulator or a riboswitch, and (iii) co-occurrence of genes in a set of related genomes. Transcriptional regulons for transcription factors (TFs) (BirA, BioQ, NrtR, NiaR, PdxR) and riboswicthes (TPP, FMN, THF, B12) as captured in the RegPrecise database (Novichkov et al., 2013) were used to disambiguate paralogs with related but distinct functions (most importantly, transporters).

Many vitamin biosynthesis pathways contain alternative biochemical modules (routes) implemented by different subsets of enzymes, as well as diverse vitamin transporters. For all identified pathway variants, we established *genomic signatures* represented by a subset of functional roles (signature genes) that are required for *de novo* vitamin/cofactor biosynthesis and/or vitamin salvage (**Table 1**). These were further translated to *phenotype rules* underlying the assignment of a prototrophic or auxotrophic phenotype for each respective vitamin/cofactor. For the purposes of further quantitative analysis, all identified pathway variants (**Supplementary Table S2**) are translated to simplified numeric *binary phenotypes* values corresponding to prototrophy ("1") or auxotrophy ("0"). These values, combined together for all 2,228 reference genomes, comprise a *binary phenotype matrix* (BPM), which was used to assess microbiome-wide biosynthetic capabilities and requirements for nine analyzed micronutrients (**Supplementary Table S1**).

Microbiome-Wide Phenotype Profiling From 16S rRNA Gene Data

The overall workflow for predictive phenotype profiling is provided in **Supplementary Figure S2B**. The 16S rRNA gene sequences of the V3–V5 region for 313 stool samples were obtained from HMP website[4] (Human Microbiome Project Consortium, 2012). We also analyzed a large dataset of stool samples obtained by the American Gut Project (AGP) (McDonald et al., 2018). The V4 region sequencing results for 12,828 AGP samples were obtained from European Nucleotide Archive at EBI (project PRJEB11419). First, we filtered both datasets by read number and length distribution. For HMP, we included samples containing more than 5,000 reads with minimal length 250 nt. For AGP dataset we filtered out samples containing short reads (<150 nt) and less than 10,000 reads per sample. For AGP samples containing a significant fraction of microbial blooms, which are common due to room-temperature storage of samples additional filtering was applied (Amir et al., 2017). As a result, we retained 2,863 AGP and 245 HMP samples for further analysis.

The amplicon sequencing data from HMP and AGP projects were analyzed using the QIIME version 2 (Caporaso et al., 2010). Raw demultiplexed reads were quality filtered, denoised and clustered into Operational Taxonomic Units (OTUs) with representative sequences and calculated read counts (abundances) using the DADA2 plugin with default parameters (p-trunc-len = 250; max-ee = 2.0). As a result, 4,335 and 42,595 OTUs were generated for HMP and AGP datasets, respectively. After filtering OTUs with low abundance, the resulting sets contained 1,298 OTUs for HMP and 3,360 OTUs for the AGP dataset, at that average percentage of removed reads per sample was ∼1.5%. Taxonomic classification of the obtained representative sequences was performed using the NCBI BLAST

[1] https://hmpdacc.org/hmp/HMRGD/

[2] https://www.patricbrc.org

[3] http://www.theseed.org

[4] www.hmpdacc.org

TABLE 1 | *In silico* reconstruction and phenotype prediction for vitamin/cofactor metabolism in a collection of 2,228 HGM reference genomes.

Vitamin [Vitamers][1]	Cofac-tor[2]	Pathways signature [3]	Bas. Path. Var.[4]	BP[5]	No. Gen.[6]	Growth requirements [7]	Transporters for vitamins or vitamers
B1: Thiamine [HET, HMP]	TPP	(ThiF), (ThiS), ThiH/ThiO, ThiG, ThiC, ThiD, ThiE, ThiL/ThiN	P1	1	975	–	B1: ThiT/ThiBPQ/ PnuT/ThiV/ThiXYZ2/ YkoEDC2 HMP: CytX/ThiXYZ/ YkoEDC HET: ThiW/ThiU
		(ThiF), (ThiS), ThiG, ThiC, ThiD, ThiE,ThiL/ThiN	P1*	1	89	(Ig source?)	
		Thi4, ThiC, ThiD, ThiE, ThiL/ThiN	P2	1	45	–	
		(ThiF), (ThiS), ThiH/ThiO, ThiG, ThiD, ThiE, ThiL/ThiN	Ah	0	199	B1; HMP	
		ThiC, ThiD, ThiE, ThiM, ThiL/ThiN	Az	0	114	B1; HET	
		ThiD, ThiE, ThiM, ThiL/ThiN	Ahz	0	452	B1; (HMP+HET)	
		ThiL/ThiN	A	0	354	B1	
B2: Riboflavin	FMN, FAD	(RibA), RibB, RibD, RibH, RibE, RibF	P	1	1644	–	B2: RibU/PnuX/ImpX/ RibN/RfnT/RibZ/ RibXY/RfnT
		RibF	A	0	584	B2	
B3: Niacin (Nicotinate or Nicotinamide) [Qn, Nr]	NAD, NADP	NadA, NadB/NadB2, NadC, NadD/NadM, NadE	P1	1	1170	–	B3: NiaP/NiaX/NiaY Nr: PnuC
		NadA, NadC, NadD/NadM, NadE	P1*	1	34	(missing NadB?)	
		Tdo, (Kfa), Kmo, Kyn, (Had), NadC, NadD/NadM, NadE	P2	1	12	–	
		PncB/NadV, (PncA), NadD/NadM, NadE	A	0	895	B3	
		PncB, (PncA), NadC, NadD/NadM, NadE	Aq	0	86	B3; Qn	
		NadR	Ar	0	31	Nr	
B5: Pantothenate [Pne, Pnt]	CoA	PanD/PanP, PanB, (PanE/PanG), PanC, CoaA/CoaX/CoaW, CoaB, CoaC, CoaD, CoaE	P	1	1168	–	B5: PanT/PanF Pnt: PanS
		PanB, (PanE/PanG), PanC, CoaA/CoaX/CoaW, CoaB, CoaC, CoaD, CoaE	P*	1	95	(β-ala source?)	
		PanD/PanP, PanC, CoaA/CoaX/CoaW, CoaB, CoaC, CoaD, CoaE	Apt	0	39	B5; Pnt	
		PanC, CoaA/CoaX/CoaW, CoaB, CoaC, CoaD, CoaE	Apt*	0	17	B5; Pnt (b-ala source?)	
		CoaA/CoaX/CoaW, CoaB, CoaC, CoaD, CoaE	A	0	793	B5	
		CoaA/CoaX/CoaW, CoaD, CoaE	Apn	0	91	Pantetheine	
		–	A*	0	25	CoA uptake	
B6: Pyridoxine	PLP, PMP	PdxS, (PdxT)	P1	1	862	–	B6: PdxU/PdxU2
		PdxJ, (PdxA), (PdxH/PdxO)	P2	1	711	–	
		PdxK/PdxK2	A	0	541	B6	
		–	A*	0	114	B6 (missing PdxK?)	
B7: Biotin [Dtb, KAPA, DAPA]	Biotin-(BCCP)	BioF, BioA, BioB, BioD, BioC, (BioG/BioH/BioZ/BioV), BirA	P1	1	797	–	B7: BioY/YigM
		BioF, BioA, BioB, BioD, BioW, BirA	P2	1	246	–	
		BioF, BioA, BioB, BioD, BirA	P*	1	74	(pimeloyl source?)	
		BioA, BioB, BioD, BirA	A3	0	68	B7; Dtb; DAPA; KAPA	
		BioD, BioB, BirA	A2	0	38	B7; Dtb; DAPA	
		BioB, BirA	A1	0	169	B7; Dtb	
		BirA	A	0	836	B7	
B9: Folate	THF-$(Glu)_n$	FolE1/FolE2, (FolQ/FolQ1/FolQ2), (FolB/FolB2), FolK, FolP, FolC, PabC, (PabAB), FolA/FolA2/FolM	P	1	1471	–	B9: FolT
		FolE1/FolE2, (FolQ/FolQ1/FolQ2), (FolB/FolB2), FolK, FolP, FolC, FolA/FolA2/FolM	P*	1	415	(pABA source?)	
		FolA/FolA2/FolM	A	0	342	B9	

(Continued)

TABLE 1 | Continued

Vitamin [Vitamers][1]	Cofac-tor[2]	Pathways signature [3]	Bas. Path. Var.[4]	BP[5]	No. Gen.[6]	Growth requirements [7]	Transporters for vitamins or vitamers
B12: Cobalamin [Cbi, Cbr, Ba]	Ado-B12	CbiK/CbiX/CbiX2, CbiL, CbiH, CbiF, CbiG, CbiD, CbiJ, CbiT, CbiE, CbiC, CbiA, Co transporter, CbiP, CbiB, CobU, CobS, CobC/CblZ, CobT, CobD, BtuR/PduO	P1	1	628	–	B12: CbrUVT/BtuBCDF
		ChlID, CobN, CbiL, CobG, CbiH, CbiF, CobF, CbiJ, CbiT, CbiE, CbiC, CbiA, Co transporter, CbiP, CbiB, CobU, CobS, CobC/CblZ, CobT, CobD, BtuR/PduO	P2	1	97	–	
		CbiA, CbiP, CbiB, CobU, CobS, CobC/CblZ, CobT, CobD, BtuR/PduO	Aba	0	32	B12; Cbi; Cbr; Ba	
		CbiP, CbiB, CobU, CobS, CobC/CblZ, CobT, CobD, BtuR/PduO	Acbr	0	43	B12; Cbi; Cbr	
		CobU, CobS, CobC/CblZ, CobT, CobD, BtuR/PduO	Acbi	0	193	B12; Cbi	
		BtuR/PduO	A	0	1235	B12	
Q: Queuosine [preQ1, preQ0, CDG]	Q-(tRNA)	QueA, QueG/QueH, QueC, QueF, GCYHI1/GCYHI2, (QueD), QueE, qTGT	P	1	1109	–	Q: QueT/QrtTUVW/YhhQ
		QueA, QueG/QueH, QueC, QueF, qTGT	Ac	0	62	Q; preQ1; preQ0; CDG	
		QueA, QueG/QueH, QueF, qTGT	Ao	0	42	Q; preQ1; preQ0	
		QueA, QueG/QueH, qTGT	Ap	0	601	Q; preQ1	
		qTGT	Aq	0	297	Q	
		–	A	0	117	Not used	

[1]Abbreviations for vitamers and precursors: HMP, 4-Amino-5-phydroxymethyl-2-methylpyrimidine; HET, 5-(2-Hydroxyethyl)-4-methyltiazole; Ig, iminoglycine; Qn, quinolinate; Nr, N-ribosyl-nicotinamide; Pne, pantetheine; Pnt, pantoate; β-ala, β-alanine; Dtb, dethiobiotin; KAPA, 7-Keto-8-aminopelargonic acid; DAPA, 7,8-Diaminopelargonic acid; pABA, p-aminobenzoate; Cbi, cobinamide; Cbr, cobyrinate diamide; Ba, cobyrinate; Q, queuine; preQ1, 7-aminomethyl-7-deazaguanine; preQ0, 7-cyano-7-deazaguanine; CDG, 7-carboxy-7-deazaguanine. [2]Abbreviations for cofactors: TPP, thiamine pyrophosphate; FMN, flavin mononucleotide; FAD, flavin adenylyl dinucleotide; NAD, nicotinamide adenylyl dinucleotide; NADP, nicotinamide adenylyl dinucleotide phosphate; CoA, Coenzyme A; (BCCP), biotin carboxyl carrier protein; THF-(Glu)n, (polyglutamyl) tetrahydrofolate; Ado-B12, adenosyl cobalamine; Q-(tRNA), modified tRNA. [3]Special characters used in pathway signatures: Parentheses denote functional roles that are NOT required to be present corresponding to enzymes that were not detected in all prototrophs. '/' denotes alternative enzymes with the same functional role (at least one of them is required to be present). Enzymes in red denote universal enzymes that are present in both auxotrophs and prototrophs. [4]Basic Pathway Variants. Asterisk denotes incomplete pathways with one or two essential enzymes missing. [5]Binary Phenotypes. [6]Number of genomes possessing a basic pathway variant. [7]'–' denotes no growth requirement in predicted prototrophs; comments in parentheses describe missing biosynthetic reactions/enzymes.

ToolKit with two reference 16S rRNA gene databases: (i) RDP (Cole et al., 2014, database release 11.5 with taxonomies updated to be consistent with the NCBI Taxonomy database), and (ii) NCBI (version of December 2018 containing 20,792 sequences). A heuristic approach was used to select a species-level consensus taxonomy from a subset of the top blast hits (ordered by identity percent) derived from both reference databases. If species-level consensus assignment was not obtained, then we used the QIIME2-provided feature-classifier plugin with three alternative classifiers (consensus-blast, consensus-vsearch and naive Bayes). Outputs of all three methods were compared and taxonomic assignments with the highest confidence level (equal or exceeding 0.8) were selected. In the case of low confidence levels obtained at the species level or other ambiguities, we repeated the whole procedure to assign consensus taxonomy at the genus level and further at higher taxonomic ranks.

Read counts for each OTU taxonomically assigned by the QIIME2 pipeline were weighted (renormalized) by 16S rRNA gene copy number to account for its variability between different species and to minimize the strongest biases in estimated values of their relative abundances. For this purpose we used the pan-taxa statistics for the rRNA gene copy number provided by the rrnDB database (Stoddard et al., 2015). For each OTU, this number was estimated as a simple mean of respective values provided by rrnDB for the best matching taxonomic group, at species, genus or family level of taxonomic assignment. The obtained renormalized OTU table, along with calculated BPM values, was used as input for predictive phenotype profiling as outlined below.

To assess vitamin production capabilities and requirements for selected HMP and AGP samples, we utilized a beta-version of Phenobiome Profiler tool (PhenoBiome Inc., Walnut Creek, CA, United States[5]). This tool uses BPM and OTU tables to approximate microbiome-wide metabolic phenotypes while minimizing limitations arising from: (i) imprecise and incomplete correspondence of OTUs to reference genomes; (ii) intrinsic heterogeneity of phenotypes within mapped taxonomic groups. To reach a reasonable compromise between coverage

[5]www.phenobiome.com

and precision, we use a *hierarchical averaging approach*. Briefly, in the first step, OTU taxonomic assignments are mapped onto the reference genome collection at three taxonomic levels (species, genus, and family). For the purpose of further averaging and probabilistic phenotype assignment, every mapped OTU is assigned a mapping weight (w) reflecting representation of corresponding genomes in the collection. Thus, for an OTU precisely mapped at the species level, equal weights are assigned to genomes of all strains/isolates of this species that are present in the collection. For OTUs that could not be mapped at the species level, phenotype averaging is performed at the genus level assigning equal weights to all available species within a genus. A similar approach to averaging/weighting is applied to OTUs mapped only at the family level. OTUs that do not map at the family level (typically $\leq$ 5–7% by abundance) were excluded from phenotype prediction. As a result, a Community Phenotype Matrix (CPM) is computed where an approximate (averaged) phenotype value for every mapped OTU is calculated from respective binary phenotype values (p) multiplied by respective weights (w) of each genome (m). Each value in CPM reflects a probabilistic relative contribution of each OTU (i) to the community-wide phenotype:

$$P_i = \sum\nolimits_m w_{i,m} p_m$$

At the next step, a Community Phenotype Index (CPI, %) for each phenotype in a given sample is then calculated as the total of all respective CPM values (P) multiplied by the relative abundances (A) of all individual OTUs:

$$\mathrm{CPI} = \sum\nolimits_i A_i P_i$$

CPI provides a probabilistic estimate of fractional representation (from 0 to 100%) of the analyzed phenotype, in this case a particular micronutrient production capability or prototrophy. Computing CPI for auxotrophy, which is more convenient for assessing micronutrient requirements, is performed the same way but replacing all binary phenotype values (P) in BPM by (1-P). A prediction error for CPI values (reflecting imprecise mapping and phenotype microheterogeneity) was calculated as:

$$\sigma = \sqrt{\sum\nolimits_i A_i^2 (1 - P_i) P_i}$$

The above described phylogeny-based mapping of the obtained taxonomic profiles to the reference collection of genomes with reconstructed BPM yielded on average ∼77% coverage of mapped OTUs by relative abundance at the level of species for either HMP or AGP datasets. At the genus level, the average coverage increased to 96% for HMP and 91% for AGP datasets. Finally, the addition of OTUs mapped only at the family level further increased the overall coverage of mapping to our current reference HGM collection up to 99 and 97% across all samples from HMP and AGP datasets, respectively.

To analyze the distribution of various combinations of vitamin phenotypes in individual taxa we considered possible combinations of individual binary phenotypes as ordered nine-digit strings, termed *phenotypic barcodes*. For instance, the '111111101' barcode corresponds to a prototroph for all vitamins except B12 (multi-prototroph), while '010000000' is an auxotroph for all vitamins except B2 (mono-prototroph). For each sample, we calculated relative contribution of each of 512 possible vitamin barcodes (P_{obs}), using *binary phenotypes* for individual reference genomes from BPM and previously described OTU mapping weights. The same hierarchical averaging/weighting approach was used for calculation of the relative contribution of vitamin barcodes, where each barcode is treated as an individual feature (composite phenotype). To facilitate further manipulations we switched from barcodes to their cumulative representation, termed *vitamin prototrophy rank* (VPR). For instance, the '111111101' and '000000010' barcodes correspond to ranks 8 and 1, respectively. We further predicted a theoretical distribution for VPRs in each sample assuming that vitamin binary phenotypes in all organisms are independent of each other (the null hypothesis). Stated this way, the null hypothesis follows the Poisson binomial distribution for the expected frequencies (P_{exp}) of VPRs in a sample, with CPIs acting as independent trials probabilities. To compare the observed vs. expected VPR distributions we computed the ratio of their corresponding probabilities in each sample ($P_{\mathrm{obs}}/P_{\mathrm{exp}}$) and presented these ratios in logarithmic scale.

Comparison of Phenotype Predictions With PICRUSt2

The Phylogenetic Investigation of Communities by Reconstruction of Unobserved States (PICRUSt) pipeline allows one to predict the following functional information for 16S metagenomic samples: (i) functional gene content based on KEGG database annotations for reference genomes (Kanehisa et al., 2014); and (ii) metabolic pathway abundances using the pathway rules from MetCyc database (Caspi et al., 2012) and MinPath (Minimal set of Pathways) tool (Ye and Doak, 2009). The latest version of the software (PICRUSt2) was installed in a conda environment under Linux CentOS 7 as specified in the GitHub Wiki manual[6]. To predict MetCyc/MinPath-based abundances of vitamin biosynthetic pathways in the HMP and AGP samples (provided as OTU abundance tables and files with representative sequences), the PICRUSt2 pipeline was used with default parameters. We further used PICRUSt2 to predict phenotype abundances in the same samples using the BPM for vitamin biosynthesis pathways in 2,228 reference genomes. First, we prepared the custom traits table for 2,581 leaves of the PICRUSt2 reference tree that overlapped by NCBI TaxID with the reference HGM genomes analyzed in this work. We then used the PICRUSt2 pipeline with BPM-based custom trait table provided as an input. As the input BPM describes capabilities of reference species to produce vitamins, we did not need to run the MinPath pathway abundance prediction. All pathway and phenotype abundances obtained by PICRUSt2 were normalized by a number of reads

[6]https://github.com/picrust/picrust2/wiki

in each sample Scattered plots were produced in R using ggplot2 package.

RESULTS AND DISCUSSION

Genomic Signatures of Vitamin/Cofactor Metabolism

We began this study by selection of the reference collection of bacterial genomes representing the human gastrointestinal microbiota (see Materials and Methods). The selected set included 2,228 genomes representing eleven phyla, 42 orders, 93 families, 226 genera, and 690 species, as well as 173 genomes that have no taxonomically defined species names (**Supplementary Table S1**). The largest number of reference genomes in this set belong to the Firmicutes (1046 genomes), Proteobacteria (588 genomes), Actinobacteria (311 genomes) and Bacteroidetes (205 genomes) phyla. The Fusobacteria and Tenericutes phyla are represented by 41 and 25 genomes, respectively. The remaining five phyla (Verrucomicrobia, Synergistetes, Spirochaetes, Lentisphaerae, and Planctomycetes) contain from one to five reference genomes.

We used a subsystems-based comparative genomics approach (Overbeek et al., 2005; Osterman et al., 2010) to reconstruct biosynthetic pathways for nine universally essential cofactors along with biogenesis, salvage and transport systems for their respective metabolic precursors (eight B-group vitamins and queuosine). The overall workflow for metabolic pathway reconstruction and phenotype assignments is provided in **Supplementary Figure S2A**. The analyzed functional roles include 127 distinct enzymes involved in 9 vitamin biosynthesis/salvage pathways, and 83 transporters (or their components) involved in salvage of exogenous vitamins or their metabolic precursors (**Figure 1**). Detailed pathway diagrams capturing variations in vitamin and cofactor biosynthetic and salvage pathways at the level of individual enzymes (non-orthologous replacements) and topologies (alternative biochemical routes) are presented in **Supplementary Figure S1**. From the obtained genomic distribution of vitamin/cofactor biosynthetic enzymes and transporters we deduced *phenotype rules* (generalized genomic signatures, as captured in **Table 1**) and then assigned individual pathway variants (Ye et al., 2005) to each analyzed genome (**Supplementary Table S2**). Phenotype rules describe sets of genes whose presence or absence in the analyzed genomes permit confident distinction between metabolic pathway variants and prediction of vitamin transport capabilities. For each vitamin/cofactor, all metabolic pathway variants were subdivided into two major categories: (i) *prototrophic* (variant code "P") that are capable of *de novo* cofactor synthesis, and (ii) *auxotrophic* (variant code "A") that are dependent on the uptake and salvage of a respective vitamin or an alternative metabolic precursor from an exogenous source. Distinct P-variants were assigned to prototrophs with alternative *de novo* biosynthetic routes. Thus, variations in B1/TPP biogenesis include two alternative routes for the synthesis of a hydroxyethylthiazole (HET) moiety: a common bacterial variant P1 (ThiFGHS signature) and a eukaryotic-like variant P2 (Thi4 signature). Likewise, two alternative routes to synthesize the quinolinate precursor of NAD comprise the most common bacterial variant P1 (NadAB) and a relatively rare eukaryotic-like variant P2 (Tdo-Kmo-Kyn). Similar variations occur in PLP synthesis (PdxAJ vs. PdxST routes) and in the synthesis of pimeloyl-CoA precursor of biotin (via BioC vs. BioW). B12 is synthesized via either anaerobic or aerobic pathway for corin ring biosynthesis that are characterized by either early or late insertion of cobalt via specific chelatases (CbiK/X vs. CobN) and pathway-specific enzymes (CbiDG vs. CobFG).

Many bacterial genomes that completely lack the *de novo* biosynthetic machinery but typically have vitamin uptake, salvage and downstream biotransformation pathways yielding physiologically active cofactors are generally classified as auxotrophic A-variants. Despite substantial variations in salvage of cofactor precursors (see below), this classification is strengthened by indisputable universal essentiality of these cofactors (with the exception of B12 as discussed below). Downstream pathways common for both P- and A-variants that include from one to five conserved enzymatic steps are characteristic of all analyzed cofactors, except PLP (marked red in **Table 1**). For the latter, *de novo* and salvage routes are topologically non-overlapping (**Figure 1**). The only other exception is A*-variant of Coenzyme A biosynthesis (**Table 1**) in parasitic species of Mollicutes (such as *Mycoplasma/Ureaplasma*) due to their unique capability to uptake a mature cofactor.

Signature salvage enzymes (those that are not involved in *de novo* or downstream pathways) are characteristic of vitamins B1 (ThiK, ThiM, and ThiN), B3 (PncA, PncB and, more rarely, NadV) and B6 (PdxK/K2). Other vitamins and metabolic precursors can feed directly into respective cofactor biosynthetic pathways upon uptake from the media via specific transporter systems. In this study, we have performed a comprehensive mapping of all known and predicted components of salvage enzymes and transporters (see below), which in many cases provided important details on metabolic requirements and capabilities of respective species. However, the presence of particular salvage genes is not required for the general inference of auxotrophy (A-variants). Thus, PdxK/K2 kinase was missing in 116 B6 auxotrophs, suggesting existence of yet unknown alternative forms of this essential salvage enzyme. Such requirement would be particularly unsustainable with respect to uptake transporters that represent a substantial bioinformatic challenge due to their evolutionary plasticity (poorly resolved paralogs) and incomplete knowledge (missing genes).

It is important to note that salvage machinery is often, but not always, present in species with complete P-variants, which allows them to implement an *opportunistic* lifestyle switching from energetically expensive *de novo* synthesis to a more economic salvage depending on the availability of vitamins. Therefore, we have included such capabilities in our overall reconstruction (**Supplementary Table S2**), despite a caveat of presently incomplete and imprecise knowledge of uptake transporters. It is also recognized that salvage enzymes are often involved in cofactor recycling within the cell, as best studied for the case of NAD(P) cofactors (**Figure 1**) (Sorci et al., 2010).

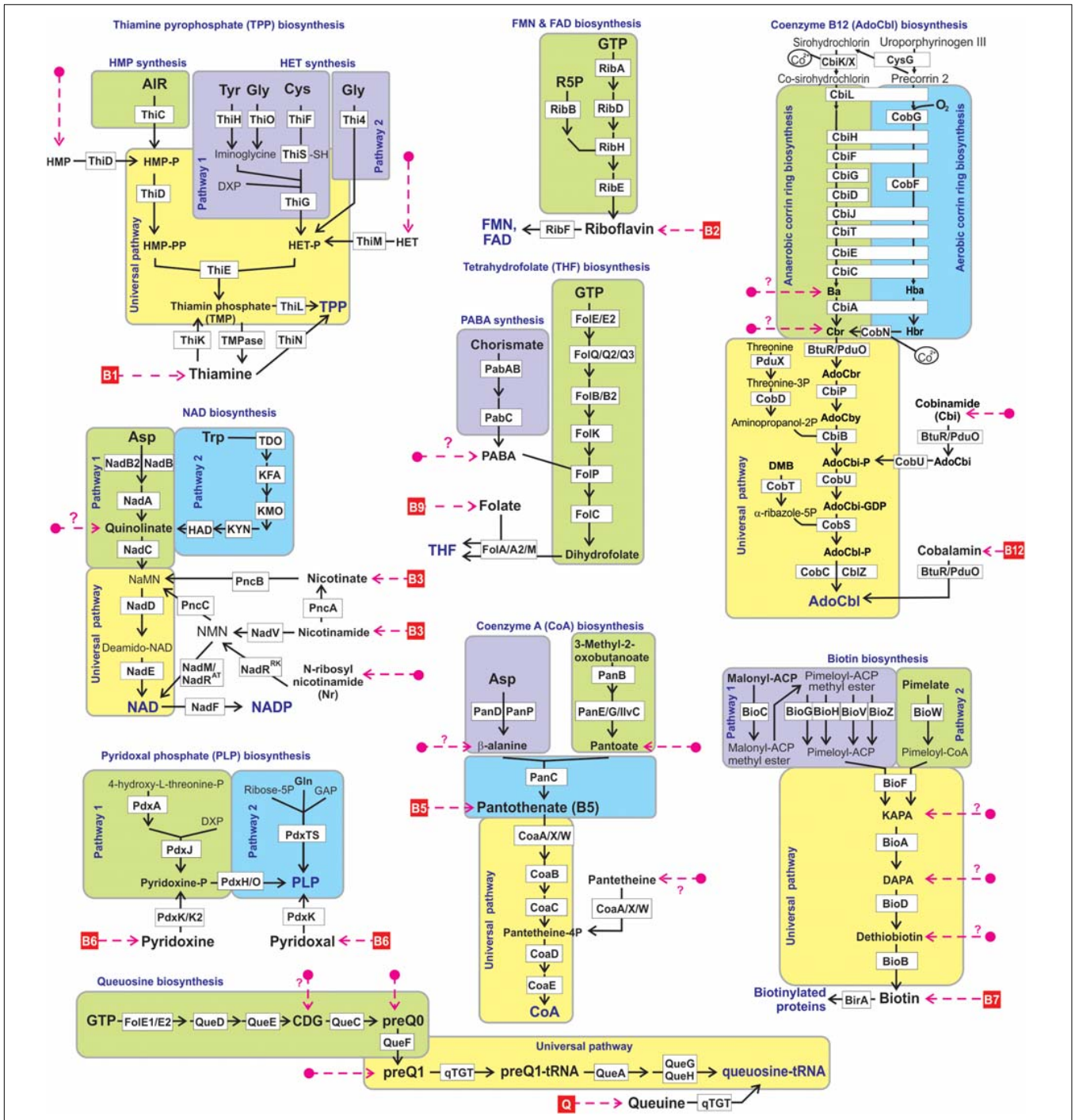

FIGURE 1 | Reconstructed vitamin/cofactor biosynthesis and salvage pathways in HGM genomes. Eight B-vitamins, and queuine (Q) are shown in red boxes. Alternative and universal biosynthetic pathways are marked in blue text and highlighted in colored blocks. Biosynthetic reactions and vitamin/vitamer uptake are depicted by solid black and red dashed lines, respectively. Enzymes are shown by white boxes. The detailed information of enzyme commission (EC) numbers, functional annotations, metabolite abbreviations, and transporter names are provided in **Supplementary Figure S1**.

Moreover, it is tempting to speculate that at least some of the vitamin transporters may contribute to a hypothesized B-vitamin sharing in microbial communities (Romine et al., 2017) (as further discussed below).

Finally, taking into account that the auxotrophy is inferred based mostly on "negative" evidence, the absence of biosynthetic capabilities, we recognize that, at least in principle, the existence of yet unknown and radically different *de novo*

cofactor biosynthetic routes in rare bacterial species cannot be excluded. However, our current analysis of vitamin subsystems in thousands of sequenced bacterial genomes strongly argues against this theoretical possibility. Instead, some species harbor "incomplete" variants of known pathways with one or two "missing genes" (see the next section). It is important to emphasize that the variety of incomplete pathway variants and their representation in the entire reference collection are relatively small confirming that our current understanding and genomic reconstruction of bacterial of vitamin/cofactor biosynthetic machinery are nearly complete.

Incomplete Pathway Variants and Salvage of Alternative Vitamers

Distinguishing between incomplete P-variants with "missing genes" (Osterman and Overbeek, 2003) (variant code P*), which reflect yet unknown non-orthologous gene displacements or alternative biochemical routes, and non-canonical A-variants presents a particular bioinformatic challenge, requiring a detailed case-by-case analysis (**Table 1**) (note that genome sequencing or gene calling gaps do not affect this analysis as pathway variants are only considered when detected in multiple genomes). Thus, 89 genomes including 62 *Bifidobacterium* strains possess an incomplete B1 pathway with missing iminoglycine synthase (ThiO or ThiH), however, all other B1 biosynthetic enzymes are present (**Figure 1**). Based on these considerations, these species were tentatively assigned as prototrophs with yet unknown enzyme/route supplying the iminoglycine precursor (P*-variant). In the B3 pathway, NadB (or an alternative enzyme NadB2) catalyzing the synthesis of iminoaspartate from aspartate is missing in 34 predicted B3 prototrophs (P* including 17 strains of *Helicobacter pylori* and 8 strains of *Micrococcus luteus*, suggesting the presence of a yet unknown alternative iminoaspartate synthesis enzyme in these species. In the B5 pathway, we identified 95 strains with missing aspartate decarboxylase (PanD or PanP) that possess all other *de novo* B5 synthesis enzymes, suggesting the existence of yet uncharacterized alternative enzyme(s) or biochemical route(s) for β-alanine synthesis in these bacteria. Indeed, alternative routes generating β-alanine unrelated to cofactor metabolism (e.g., via alanine racemase or catabolism of pyrimidines) are known. Moreover, β-alanine can be theoretically salvaged, if available, from the growth media. Based on these considerations, we classify the respective pathway variants as P*-type prototrophs rather than auxotrophs salvaging non-canonical vitamers (discussed below).

In the B7 pathway, 74 species from diverse phyla lack the upstream enzymes involved in the synthesis of pimeloyl precursor but possess all downstream biosynthetic enzymes required for assembly of the fused heterocyclic rings of biotin (BioF, BioA, BioD, and BioB). Given the known variability of pathways and isozymes involved in the upstream biotin biosynthesis, we propose the existence of yet uncharacterized enzymes for pimeloyl precursor synthesis in these species. Finally, in the B9 pathway, 454 strains lack the complete pathway for the synthesis of para-aminobenzoate (pABA) precursor, while all other folate biosynthetic enzymes are present in their genomes. There are two potential explanations for these incomplete B9 pathways: (i) presence of yet unknown pABA synthesis routes/enzymes, and/or (ii) salvage of pABA from the diet or other community members. In agreement with the latter hypothesis, it is known that *Lactobacillus* strains having this pathway variant can produce folate only when pABA is added to the medium (Santos et al., 2008; Wegkamp et al., 2010). We chose to classify this variant as P* despite its similarity with salvage of alternative vitamers in A-variants discussed below, mainly because pABA, a known intermediate in the synthesis of other essential metabolites (e.g., aromatic amino acids), may not be considered a true B9 vitamer. At the same time, a number of other identified incomplete pathway variants in metabolism of B1/TPP, B3/NAD, B5/CoA, B7, B12, and queuosine were classified as *bona fide* auxotrophic A-variants with a potential to salvage alternative vitamers, non-canonical metabolic precursors of respective cofactors (**Table 1**).

The largest variety of such variants is observed in the biogenesis of *thiamine pyrophosphate (TPP) cofactor*, which is synthesized via coupling of the phosphorylated hydroxymethylpyrimidine (HMP-PP) and thiazole (HET-P) moieties (**Figure 1**). Nearly half of the analyzed genomes contain complete signatures for the *de novo* biosynthesis of both HMP-PP and HET-P biosynthesis (B1 prototrophs). Auxotrophic variants comprising another half were subdivided into four major sub-variants with distinct biosynthetic/salvage capabilities. The first group of auxotrophs (452 genomes) is unable to synthesize either B1 precursor but possess the ThiM and ThiD kinases, which can convert salvaged HET and HMP precursors into TPP (Ahz-variant in **Table 1**). Two other groups encode partial TPP biosynthetic pathways: (i) HMP auxotrophs (199 genomes) are capable of synthesizing only HET-P *de novo* and use ThiD kinase to generate HMP-PP from salvaged HMP precursor (Ah-variant in **Table 1**); (ii) conversely, HET auxotrophs (114 genomes) have only HMP-PP biosynthetic capabilities and generate HET-P via uptake of exogenous HET and its phosphorylation by ThiM kinase (Az-variant in **Table 1**). Importantly, in all these variants the ability to utilize alternative B1 vitamers or combination thereof is in addition and not instead of a common B1 salvage capability. The remaining group of B1 auxotrophs (354 genomes) can only salvage vitamin B1 but lack the machinery to salvage HET or HMP and combine them into TMP intermediate (A-variant in **Table 1**).

Biogenesis of *NAD(P) redox cofactors* is also associated with a variety of salvage/recycling pathways from one or both forms of vitamin B3: (i) nicotinic acid (or niacin), the most common form, via PncB salvage enzyme; and (ii) nicotinamide, via one of the three alternative routes, via PncA-PncB or, more rarely in bacteria, via NadV-PncC or NadV-NadM route bypassing otherwise nearly universal downstream enzymes NadD-NadE (**Figure 1**). Among B3 auxotrophs (1012 strains), we found 86 strains representing diverse taxa such as *Campylobacter*, *Corynebacterium*, *Lactobacillus*, and *Streptococcus* that contain a truncated *de novo* NAD biosynthetic pathway variant (Aq-variant in **Table 1**) comprised of a single enzyme NadC but none of the upstream enzymes involved in quinolinate production. This genomic signature suggests that, in addition to

canonical B3 salvage, these species can also salvage quinolinate as previously demonstrated for *Streptococcus pyogenes*, (Sorci et al., 2013). Notably, quinolinate is a common intermediate of NAD biosynthesis not only in bacteria but in some host tissues that synthesize NAD via aerobic degradation of tryptophan (kynurenine pathway). Yet another rare salvage pathway is a two-step conversion of nicotinamide riboside (Nr) to NAD via bifunctional NadR enzyme. This pathway is the only route of NAD biogenesis in *Haemophilus influenza* and related species from the Pasteurellales order that should be considered Nr auxotrophs rather than B3 auxotrophs (Ar-variant in **Table 1**). However, in a limited number of NadR-containing HGM genomes, it is present in addition to (not instead of) B3 salvage pathways.

A five-step universal downstream pathway (**Figure 1**) of *Coenzyme A (CoA)* synthesis from pantothenate (vitamin B5) is present (with some non-orthologous variations in the first step) in both, prototrophs (1,263 genomes, 57%) and most, but not all predicted B5 auxotrophs (874 strains, 39%). In addition, 91 strains (mostly *Bifidobacterium* and diverse Clostridiales) lacking *de novo* synthesis have an incomplete universal pathway variant with missing CoaBC bifunctional enzyme catalyzing the conversion of phosphopantothenate to phosphopantetheine. We propose that these bacteria are dependent on an earlier hypothesized "pantetheine shunt," a salvage of an alternative vitamer pantetheine (CoA degradation product) via a secondary activity of pantothenate kinase converting it directly to phosphopantetheine, thus by-passing both steps requiring a missing CoaBC enzyme (Ye et al., 2005; Osterman, 2009). Indeed, an additional pantetheine kinase activity was experimentally demonstrated for selected pantothenate kinases (Strauss et al., 2010). Notably, this genomic pattern (Apn-variant in **Table 1**) also cannot be classified as genuine B5 auxotrophy as respective species would not be able to synthesize CoA from pantothenate. Among B5 auxotrophs with incomplete *de novo* pathways are two variants lacking pantoate biosynthesis: (i) Apt-variant in 40 genomes that contain two *de novo* enzymes, PanD and PanC; (ii) Apt*-variant in 16 genomes that retain only one *de novo* enzyme, PanC. Similar to an Aq-variant in NAD biogenesis, this genomic signature suggests the possibility of salvaging pantoate (with known or unknown source of β-alanine, respectively) in addition to vitamin B5.

More than 80% of identified *B7 auxotrophs* (836 genomes) lack all four enzymes responsible for the conversion of pimeloyl-CoA precursor to biotin (**Figure 1**). The remaining auxotrophs possessing incomplete biosynthetic pathways were classified into three variants (**Table 1**) characterized by the presence of: (i) only the last enzyme, BioB (A1-variant); (ii) the last two enzymes, BioB and BioD (A2-variant); and (iii) the last three enzymes, BioA, BioD, and BioB (A3-variant). Several considerations suggest that the sustainability of these variants is due to salvage of all three pathway intermediates, namely dethiobiotin, 7-keto-8-aminopelargonic acid (KAPA) and 7,8-diaminopelargonic acid (DAPA) as alternative vitamers, rather than due to the existence of yet unknown alternative enzymes or biosynthetic routes. *First*, the fact that only upstream (but not midstream or downstream) truncations are observed makes this interpretation more consistent with pathway topology. *Second*, a sporadic phylogenetic distribution of these variants among diverse Actinobacteria, Proteobacteria and Firmicutes genomes is more consistent with gene loss rather than non-orthologous replacement.

In contrast to other B-vitamin related cofactors, various *derivatives of B12* are not universally essential in bacteria. While most bacteria have B12-dependent methionine synthase and ribonucleotide reductase, these enzymes are often dispensable due to the presence of alternative B12-independent enzymes and metabolic routes (Rodionov et al., 2003). This points to a distinction between beneficial but not mandatory salvage of B12 by respective A-variants (**Table 1**) and *life-or-death* requirements of the exogenous supply of metabolic precursors of all other analyzed cofactors. Nevertheless, the effect of B12 availability on fitness of some gut-colonizing *Bacteroides* spp. was reported (Degnan et al., 2014) providing the first experimental evidence of vitamin exchange in gut microbial consortia.

As in the case of biotin, more than 80% of B12 auxotrophs (1235 strains) lack all enzymes of anaerobic or aerobic upstream corin ring synthesis, as well as most downstream enzymes, except BtuR/PduO family adenosyltransferase converting vitamin B12 (cobalamin) to an active coenzyme B12 (adenosylcobalamin). Likewise and following the same reasoning, the three observed incomplete pathway variants (Aba, Acbr, and Acbi, **Table 1**) appear to point to salvage of alternative B12 vitamers, cobinamide (Cbi), cobyrinate diamide (Cbr) and cobyrinic acid (Ba), respectively (**Figure 1**).

Our current knowledge of salvage pathways related to *Queuosine,* an essential micronutrient, which, despite many similar metabolic features, is not considered a B-vitamin. A fully prototrophic P-variant, for the *de novo* synthesis of queuosine-tRNA from GTP is present in nearly half of the analyzed genomes (**Table 1**). A minimal salvage route (Aq-variant) containing only one conserved downstream enzyme, qTGT tranglycosylase, which can generate the same final product directly from the salvaged queuine (Q) precursor, occurs in nearly 300 genomes. However, the most frequent incomplete variant (Aq in 601 genomes, see **Table 1**) likely entails salvage of preQ1 precursor (see **Figure 1**). Two other variants of incomplete pathways (Ac and Ao) identified in 62 and 42 genomes, respectively, point to two other pathway intermediates, 7-carboxy-7-deazaguanine (CDG) and 7-cyano-7-deazaguanine (preQ0), as alternative salvageable vitamers. Finally, 117 strains including *Mycoplasma/Ureaplasma* and many *Lactobacillus* spp. lack all queuosine biosynthetic enzymes including qTGT. However, unlike in the case of A*-variant in CoA-related auxotrophs, this entirely "void" genomic signature likely reflects a complete loss of Q-modified tRNAs, at least in parasitic Mollicutes (De Crecy-Lagard et al., 2007).

Overall, the current analysis of incomplete pathways allowed us to reconcile most of the gaps and inconsistencies in the *in silico* reconstruction of vitamin/cofactor biogenesis and salvage. It confirmed a rather comprehensive understanding of these aspects of metabolism across the entire set of reference HGM genomes setting the stage for the further microbiome-wide predictive phenotype profiling (as described

in further sections). Of no less importance, it revealed a set of well-defined open problems, such as missing genes and yet unknown biochemical routes, a subject of bioinformatics-driven gene and pathway discovery. Additionally, this analysis tentatively implicated several vitamers as additional or alternative metabolic precursors of respective cofactors as a subject of non-canonical salvage, at least in the species carrying particular partial pathways. These metabolic precursors along with canonical B-vitamins are a likely subject of cross-feeding between donors (at least some prototrophs) and acceptor (auxotrophs) mediated by a variety of specialized transport systems.

Genomic Distribution of Vitamin Transport Systems

A paramount importance of transporters for vitamin uptake and salvage notwithstanding, especially in auxotrophs, we typically did not include them in gene signatures defining major phenotype rules (for the reasons discussed above). On the other hand, specificity assignment of candidate transporters can be achieved with higher accuracy in the genomic and functional context of auxotrophs (as constrained by their well-defined metabolic requirements) and then conservatively projected to prototrophs. Vitamin/vitamer transport systems that are present in many prototrophs can contribute to their opportunistic (energy-saving) lifestyle and, potentially, to cross-feeding as discussed below. All identified and tentatively assigned transport systems are captured in respective subsystems (**Supplementary Table S2**) and corresponding pathway diagrams (**Supplementary Figure S1**). In this brief overview we highlight only some of them focusing on tentatively identified transport systems for alternative vitamers implicated by the analysis of incomplete salvage pathways in the previous section.

Thus, the analyzed distribution of potential uptake transporters for B1 vitamers allowed us to establish the presence of candidate HMP transporters in most HMP auxotrophs (97%), while the HET transporter ThiW was identified in only 64% of HET auxotrophs. In the group of dual HMP/HET auxotrophs, both HET and HMP transporters are present in 259 genomes (57%), and additional ∼100 genomes from this group contain one of the two transporter types. Incomplete knowledge of transporters for thiamine precursors notwithstanding, this analysis suggests that salvage of B1 and its vitamers plays a prominent role in metabolic interaction within gut microbial communities. These transporters are also present in many genomes with P-variants providing the respective species with additional salvaging and, potentially, cross-feeding capabilities.

Incomplete knowledge of transport systems and mechanisms is particularly obvious in otherwise well-studied B3/NAD metabolism. Thus, despite many attempts, no committed B3 transporter has been yet identified even in *Escherichia coli* K12, which is well-known to have a robust nicotinate and nicotinamide salvage capability via PncA-PncB pathway seamlessly compensating for gene deletions in its *de novo* NadB-NadA-NadC pathway (Rowe et al., 1985). Indeed, the presence of B3 transporters from three known families (NiaP, NiaX, and NiaY) were confidently detected only in 25% of all B3 auxotrophs in our reference HGM genome collection (mostly in various Firmicutes but also in some Actinobacteria and Enterobacterales). No specific transporter has been yet identified in the genomes with quinolinate salvage pathway. On the other hand, a committed Nr transporter, PnuC, is consistently present in 31 analyzed genomes from the Pasteurellales order that is solely dependent on the Nr salvage pathway.

Uptake of vitamin B5 in bacteria is mediated by either PanF or PanT transporters, whereas PanS was characterized as a pantoate transporter in *Salmonella* (Ernst and Downs, 2015). Orthologs of known B5 transporters were identified in 75% of all B5 auxotrophs but only in 12% of ∼90 pantetheine auxotrophs pointing to the incomplete knowledge of respective transport systems. Orthologs of PanS transporter were identified in 153 genomes including 35 auxotrophs from the Clostridiales, Tissierellales and Veillonellales orders of Firmicutes. Each of these auxotrophs as well as five prototrophs contain the conserved *panD-panC-panS* operon encoding the complete pantoate salvage pathway pointing to the relevance of this B5 vitamer salvage (and, potentially, cross-feeding) in HGM.

The majority of B7 auxotrophs (78%) contain the Energy-Coupling Factor (ECF) family BioY transporters. An even higher fraction of auxotrophs with incomplete biotin salvage pathways (240 out of 275, 87%) also harbor one or two copies of BioY-family transporters. In addition, a secondary transporter YigM enabling an optional B7 salvage in prototrophic *E. coli* and many other enterobacteria was found in 13 genomes of ε-proteobacteria from the Campylobacterales order that are characterized by either A1 or A3 incomplete pathway variants. These observations suggest that both types of biotin transporters may have a wider specificity for at least some B7 vitamers. So, for the closest B7 precursor, dethiobiotin, this conjecture is supported by their uptake competition observed in *E. coli* (Prakash and Eisenberg, 1974). The reported excretion of B7 vitamers by prototrophic strains of enterobacteria (Ohsugi et al., 1990) supports the hypothesis about their potential role in cross-feeding in microbial communities.

Orthologs and paralogs of known B12 uptake transporters, namely BtuFCD(B) of ATP-binding Cassette (ABC) family and CbrT of the ECF family, were found in one or several copies in nearly half of A-variants including 268 genomes with incomplete pathways suggesting their involvement in the uptake of alternative B12 vitamers. Indeed, representatives of both B12 transporter families were experimentally shown to import both B12 and Cbi (Kenley et al., 1978; Butzin et al., 2013; Santos et al., 2018; Wexler et al., 2018). Therefore, identification of transport systems for B12 and its metabolic precursors in numerous HGM genomes remains an open problem.

The ECF-family preQ1 transporters QueT and QrtT have previously been predicted in diverse bacterial species (Rodionov et al., 2009) and recently validated experimentally in *C. difficile* (de Crecy-Lagard, personal communication). Besides, a previously uncharacterized transporter family YhhQ (COG1738) was implicated in the import of queuosine precursors (Zallot et al., 2017; de Crecy-Lagard, personal communication). Representatives of these three families of transporters are

widely distributed among the analyzed genomes including 72% of Q auxotrophs and 95% of preQ1/preQ0/CDG auxotrophs (**Supplementary Table S2**) supporting a potential physiological relevance of HGM-wide salvage and sharing of Q vitamers.

Metabolite cross-feeding in microbial communities, which, according to some reports, extends beyond micronutrients and includes some amino acids (Mee et al., 2014), may be mediated by at least two distinct supply mechanisms: (i) "passive" mechanism, via partial cell lysis; and (ii) "active" mechanism, via specific or/and general efflux transport systems. Although, at first glance, the passive mechanism, (which, for HGM communities, may also include lysis of the host epithelial cells) appears more straightforward, it is tempting to hypothesize the co-existence of a more symbiotic active mechanism of vitamin sharing. Moreover, while all genomes contain numerous relatively non-specific efflux transport systems, which theoretically may contribute to vitamin/vitamers excretion (e.g., in case of their excessive accumulation), the existence and exact nature of such systems is a subject of experimental rather than bioinformatic analysis. Therefore, in our current analysis, we set out to explore another theoretical possibility that active and specific vitamin excretion can be mediated by at least some families of vitamin uptake transporters working "in reverse." Such hypothesis emphasizing secondary active transporters or active facilitators (e.g., permeases from Major Facilitator Superfamily or MFS family) and channel-type facilitators (Shi, 2013; Saier et al., 2014) as more natural candidates for bi-directional transport as compared to primary active vitamin transporters (such as ABC or ECF family transporters), was previously examined in the context of environmental microbial consortia (Romine et al., 2017).

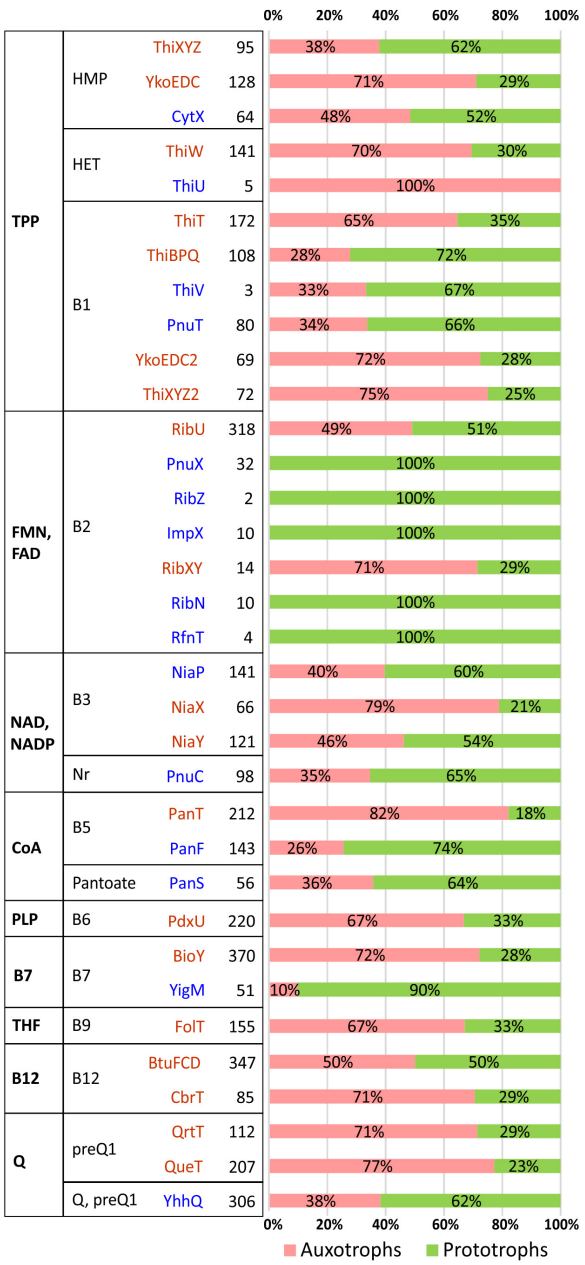

FIGURE 2 | Distribution of vitamin/vitamer transporters in HGM species. Transporters are grouped by a cofactor **(first column)** and vitamin/vitamer **(second column)**. Primary active transporters from the ABC or ECF family are shown in dark red, while secondary active transporters/facilitators (e.g., permeases from MFS family) are in blue. The total number of species possessing a specific transporter is shown in bold with relative contribution of corresponding vitamin auxotrophs/prototrophs shown as a pink/green bar.

It is important to emphasize that while our knowledge of vitamin uptake transporters is incomplete, the knowledge of vitamin efflux is nearly non-existent. Some anecdotal evidence implicating vitamin transporters is available for industrial vitamin producers such as for riboflavin-producing microbial strains (Hemberger et al., 2011; McAnulty and Wood, 2014). For a more systematic bioinformatic analysis, we surveyed distribution and co-occurrence of various families of vitamin transporters and predicted metabolic phenotypes across bacterial species from our collection (**Figure 2**).

Despite a predominantly mosaic distribution, some potentially interesting trends were also observed. Thus, facilitator-class riboflavin transporters (PnuX, RibZ, ImpX, RibN, RfnT) were observed only in B2 prototrophs, whereas the primary active transporters, RibU (ECF family) and RibXY (ABC superfamily) are present in both, prototrophs and auxotrophs. Among similar, albeit less contrasting trends are: (i) the presence of the biotin permease, YigM in the majority of B7 prototrophs contrasting with BioY (ECF family) preferential occurrence in auxotrophs; (ii) more frequent occurrence of pantothenate facilitator transporter PanF in B5 prototrophs vs. the opposing trend of PanT (ECF family) to occur mostly in B5 auxotrophs; (iii) similar co-occurrence trends for thiamine permease PnuT vs. ThiT (ECF family). The observed trends, with the caveats pertaining to incomplete data, statistical significance and possible alternative interpretations, are consistent with a possible role of at least some secondary transporters in the excretion and community-wide sharing of respective vitamins/vitamers. If experimentally confirmed, these trends may provide presently unknown genomic signatures distinguishing potential vitamin donors from

other prototrophs with opportunistic salvaging rather than sharing capabilities.

Comparison of Predicted B-Vitamin Phenotypes With Published Experimental Data

To assess robustness of the predicted vitamin auxotrophic and prototrophic phenotypes, we searched published experimental data on nutritional requirements and B-vitamin production capabilities of human gut bacteria. Analysis of minimal media growth requirements for seven B-vitamins (except B12, see below) in 30 bacterial strains revealed that 75 out of 89 experimentally determined phenotypes (85%) matched the predicted vitamin auxotrophies (**Supplementary Table S3A**). Approximately half of inconsistencies between predicted and experimental phenotypes can be reconciled considering the salvage of alternative metabolic precursors. Thus, five species including *Lactobacillus plantarum*, *Clostridium sporogenes*, *Clostridium tyrobutyricum*, *Clostridium botulinum* A str. Hall, and *Veillonella parvula* required folate for growth. According to our reconstruction, all these species were assigned a special B9 phenotype variant (P*), which corresponds to a conditional prototrophy in the presence (but not in the absence) of the pABA precursor (**Supplementary Table S2G**). Likewise, *Clostridium difficile* and *Megasphaera elsdenii* experimentally established as B5 auxotrophs were also assigned a conditional B prototrophy (P*) phenotype (**Supplementary Table S2F**) due to the unknown source of β-alanine, that in the case of these two species, apparently has to be salvaged exogenous sources. The remaining inconsistencies (∼8%) may originate from a variety of factors including strain-specific phenotype variations (see the next section).

In contrast to other B-vitamins, B12 is not essential for growth of some bacterial strains that either lack B12-dependent enzymes or possess alternative B12-independent enzymes that can substitute their B12-dependent functional analogs (Rodionov et al., 2003). Indeed, the analysis of published experimental data confirms that B12 is not essential for growth of 17 auxotrophic species (**Supplementary Table S3B**). These include 9 *Staphylococcus* spp. that lack any B12-dependent enzyme and *Bacillus cereus* that has a single B12-dependent enzyme, the methionine synthase MetH, and its B12-independent analog MetE (Zhang et al., 2009). In contrast, vitamin B12 is required for growth of 20 other species, most of which lack *de novo* B12 biosynthetic genes (**Supplementary Table S3B**). However, six B12-requiring strains including four species from the *Bacteroidales* order, *Collinsella aerofaciens* and *Clostridium scindens* possess a complete set of B12 synthesis genes. One plausible explanation of these inconsistent B12 phenotypes might be the absence of upstream genes required for the biosynthesis of precorrin-2, a common precursor of B12 and heme (Roper et al., 2000), that were not included in our B12 phenotype analysis. Such species might be classified as precorrin-2 (rather than B12) auxotrophs.

We further analyzed experimentally characterized B-vitamin production capabilities of 24 members of the gut microbiota (**Supplementary Table S3C**). All 50 experimentally established phenotypes are fully consistent with the predicted vitamin prototrophy phenotypes. Interestingly, all members of the *Lactobacillus* genus as well as two *bifidobacteria* are able to synthesize B9 only in the presence of pABA precursor, which is in agreement with the absence of pABA biosynthesis genes in these genomes. Overall, the examined experimental data on B-vitamin requirements and production are in good agreement with our *in silico* reconstruction and prediction of B-vitamin phenotypes.

Binary Vitamin Phenotypes: Phylogenetic Distribution and Variability

To enable a computational microbiome-wide phenotype assessment and comparison between different HGM samples, we have introduced a concept of *digital binary phenotypes* where a numeric value of a particular vitamin phenotype in a reference genome can be either "1" (prototrophy) or "0" (auxotrophy). For the purpose of this analysis, we have converted all the detailed variant codes (**Supplementary Table S2**) to a simplified binary form assigning the value of "1" to all P-variants and "0" to all A-variants. The obtained values for each of the nine phenotypes across 2,228 reference HGM genomes were combined into a Binary Phenotype Matrix (BPM) (**Supplementary Table S1**). This simplified representation allows us to address several important questions.

First, it provides a simple way to assess a phylogenetic distribution of micronutrient requirements and production capabilities across a broad range of HGM genomes. For this purpose, we used BPM to calculate *averaged vitamin prototrophy phenotype values* at various taxonomic ranks: species, genus, family, order, class, and phylum (**Supplementary Table S4**). These averaged values vary on the scale from 0 to 1 (0–100%) providing an estimate of probability (frequency) of an organism in a group to be a prototroph. The obtained distribution of predicted vitamin prototrophy across 690 species was visualized on the phylogenetic tree of HGM species for 230 genera (**Figure 3**), also the percentages of vitamin producers were calculated for each analyzed phylum (**Supplementary Figure S3**). The Proteobacteria and Bacteroidetes phyla contain mostly prototrophs that are capable of synthesizing all vitamins, excluding cobalamin (B12), which is synthesized only by 30 and 42% representatives of these phyla in the reference collection, respectively. The majority of representatives of the Fusobacteria phylum (except *Cetobacterium* and *Leptotrichia*) are capable of synthesizing all vitamins except pantothenate (B5) and queuosine. The Verrucomicrobia phylum represented by five *Akkermansia* strains, as well as a single HGM strain from the Planctomycetes phylum, have biosynthetic capabilities for all vitamins except B12. The Lentisphaerae phylum represented by a single HGM species, *Victivalis vadensis*, produces all vitamins except B5. Both HGM species from the Spirochaetes phylum are auxotrophic for all vitamins except riboflavin (B2). The *Ureaplasma* and *Mycoplasma* strains from the Tenericutes phylum are auxotrophic for all nine micronutrients. The Firmicutes, Actinobacteria and Synergistetes phyla contain the largest number of auxotrophs for the

majority of vitamins. Among Actinobacteria, vitamin B12 is synthesized by species from three orders (Propionibacterales, Corynebacterales, Coriobacteriales), whereas among Firmicutes the majority of B12 producers belong to the Clostridiales, Selenomonadales and Veillonellales orders. Finally, queuosine is not synthesized by most Actinobacteria except two Coriobacteria species, whereas among Firmicutes it is mostly synthesized by Bacillales and Negativicutes. Overall, this analysis reveals general correlational trends between phylogeny (even at higher taxonomic ranks) and vitamin phenotypes, but also points to substantial phenotype variations as visualized by fractional averaged phenotype values (between 0 and 1).

Estimating intraspecies as well as interspecies variations of binary vitamin phenotypes is essential to assess boundaries of confident phylogeny-based phenotype projection for the purpose of microbiome-wide predictive phenotype profiling of HGM samples (see next section). To assess these variations within species or at higher taxonomic levels we used two metrics: (i) *number of variable phenotypes* (NVP, ranges from 0 to 9 for nine phenotypes); and (ii) *overall phenotype variability score* calculated as a sum of variances for each vitamin phenotype (OPVS, ranges between 0 and 4.5 for nine phenotypes) (**Supplementary Table S4A**). The highest individual vitamin variability score 0.5 corresponds to a case when a species is represented by an equal number of vitamin auxotrophic and prototrophic strains.

Overall, 282 out of 694 analyzed HGM species are represented by more than one strain, including 34 species with 10 or more strains (**Supplementary Table S1**). Of those, 45 species (∼15%) have at least one variable vitamin phenotype (**Figures 4A,B**) including 10 species characterized by more than one variable phenotype (NVP > 1). *Ruminococcus torques* represented by two strains in the analyzed set of genomes shows the highest variability of vitamin phenotypes (NVP = 6; OPVS = 3), suggesting that these strains could be incorrectly classified. Indeed, based on phenotypic, biochemical, phylogenetic and genomic evidence one of these strains has recently been reclassified as *Mediterraneibacter torques* ATCC 27756 (Togo et al., 2018). From an evolutionary perspective, the observed cases of intraspecies variability of vitamin phenotypes can be explained by either loss or acquisition of vitamin biosynthesis genes, which are often co-localized into gene clusters on the chromosome. For example, comparative analysis of 62 strains of *Enterococcus faecalis* revealed that 27 strains presumably have lost the *panDBGC* gene locus encoding all essential enzymes from the *de novo* pantothenate biosynthesis pathway (**Supplementary Table S2**). Four out of five strains of *Faecalibacterium prausnitzii* and three out of five strains of *Lactobacillus reuteri* possess the riboflavin biosynthesis operon *ribADHBE*, while their closely related strains apparently have lost the B2 biosynthetic gene clusters. In contrast, one out of five strains of *Streptococcus parasanguinis* likely has acquired a contiguous gene locus encoding 20 enzymes required for B12 biosynthesis (**Supplementary Table S2**).

The same metrics were used to assess interspecies variations and variations at higher taxonomic levels (**Supplementary Table S4**). At the genus level, 139 out of 230 analyzed genera are represented by more than one species, and 76 of them (55%) demonstrated various degrees of phenotype variability. Genera with the highest NVP and OPVS values belong to the Clostridia, Bacilli and Tissierellia classes from the Firmicutes phylum, as well as some genera from the Actinobacteria and Proteobacteria phyla (**Figure 4C**). Variability of vitamin phenotypes gradually increases at higher taxonomic ranks. At the family level, 82 out of 96 families are represented by more than one genus, and 61 of them (74%) exhibit various degrees of phenotype variability. Interestingly, the top four families with the greatest variability scores, namely *Eubacteriaceae*, *Ruminococcaceae*, *Clostridiaceae*, and *Lachnospiraceae*, belong to the Clostridia class further emphasizing its contribution to vitamin phenotype variability in the gut microbiome. At the order level, 30 out of 36 taxa represented by more than one genome (83%) demonstrate highly variable vitamin phenotypes. At the phylum and class levels, Actinobacteria and Firmicutes (including Clostridia, Bacilli and Tissierellia) demonstrate the highest degree of phenotype variability (OPVS > 2) with 8 and 9 variable phenotypes, respectively.

We also calculated vitamin-specific variability scores that take into account variability of phenotypes in all taxa at a given taxonomic rank (**Figure 4D**). At the species level, biosynthesis of vitamin B2 (riboflavin) and B12 (cobalamin) are the least and most variable phenotypes, respectively. Vitamin B1 (thiamine) shows the highest variability scores both at the genus and family levels.

Based on this analysis, we conclude that an accurate phylogeny-based vitamin phenotype projection from reference genomes to OTUs or phylotypes mapped by 16S rRNA gene profiling of HGM samples, is generally impossible at the taxonomic level higher than a family. Moreover, the projection at lower levels, of families, genera and even species may be affected by varying phenotype heterogeneity within respective groups. Therefore, to optimize the accuracy and coverage of microbiome-wide phenotype predictions, we have to account for phenotype heterogeneity characteristic of each phylotype/OTU (see next section).

Microbiome-Wide Predictive Vitamin/Cofactor Phenotype Profiling

We applied the obtained BPM that captures vitamin/cofactor production capabilities and requirements across a collection of curated reference genomes in a simplified digital form for prediction of community-wide phenotypes from HGM 16S samples profiling data. This analysis is performed in two stages, each enabling a particular type of community phenotype profiling (**Supplementary Figure S2B**).

The goal of the *first stage* is to tentatively assign prototrophy/auxotrophy phenotypes to all OTUs (or phylotypes) identified in a sample (above a certain abundance threshold) that are subsequently confidently mapped to our reference collection at least at the family level. As discussed in the previous section, unlike the case of reference genomes,

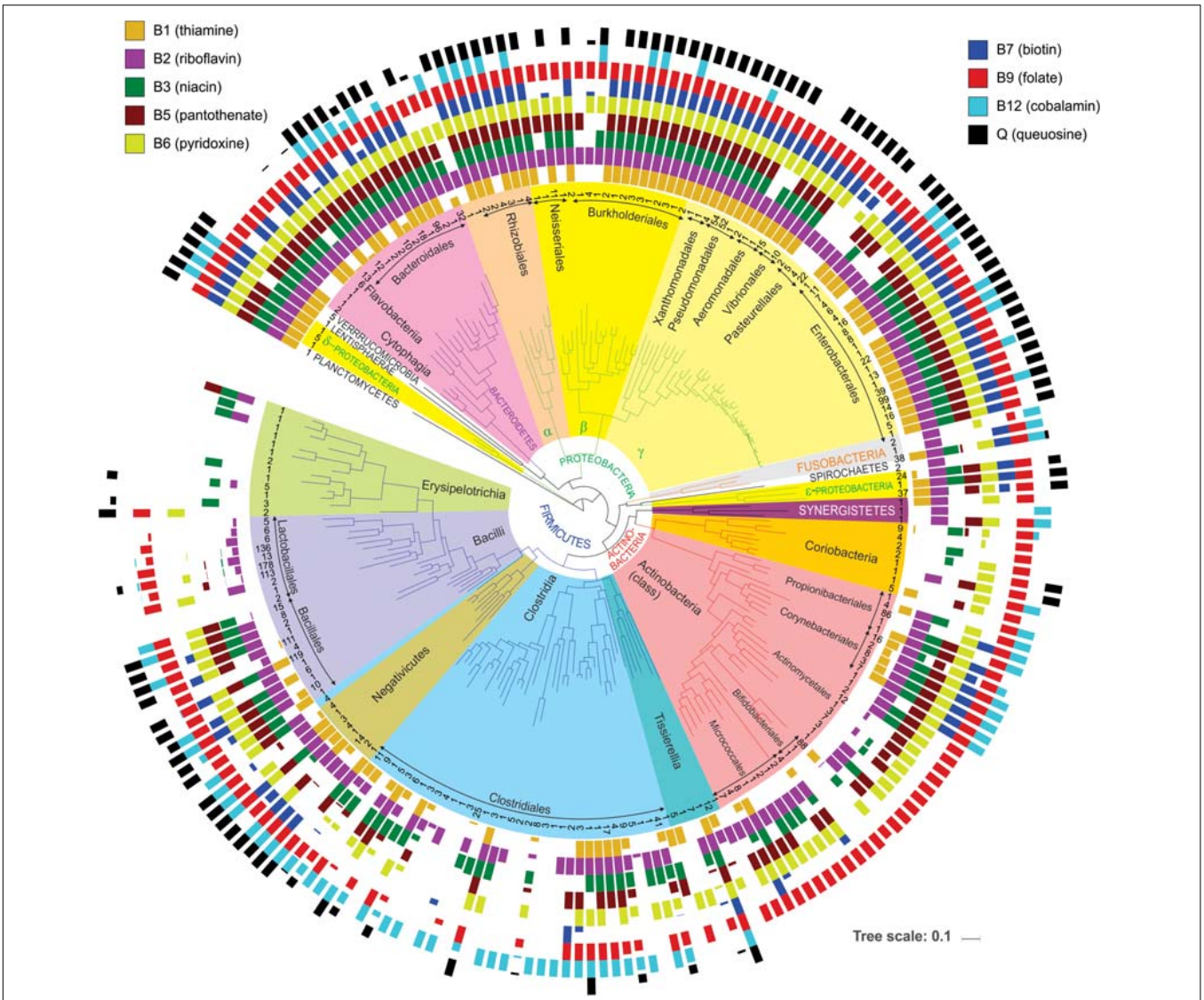

FIGURE 3 | Distribution of vitamin producers among analyzed HGM strains. The phylogenetic tree of HGM genera was obtained from the larger tree constructed by RAxML based on concatenated sequences of ribosomal proteins from the analyzed HGM species. Number of analyzed strains per genus is shown in the inner circle; higher-level taxonomic groups such as orders, classes, and phyla are highlighted inside the tree. Colored bars show average vitamin production phenotypes (prototrophy) of each genus. Empty bars correspond to auxotrophic phenotypes.

some of these assignments (especially those mapped at higher phylogenetic level) are bound to have fractional values (between 0 and 1). In the current implementation of the Phenotype Profiler pipeline (by Phenobiome Inc.), this is achieved by OTU taxonomic assignment mapping to reference genomes using a hierarchical averaging approach (see Materials and Methods for computational details). A final product at this stage of the analysis is a Community Phenotype Matrix (CPM) containing nine columns with respective weighted average phenotype values computed for all mapped OTUs. Similar to BPM, each line in CPM is a nine-digit string reflecting a metabolic potential, biosynthetic capabilities (prototrophy) vs. micronutrient requirements (auxotrophy = 1-prototrophy) of each OTU.

The main product of the *second stage* is a value, which is obtained via transformation of the OTU-abundance-phenotype table into a string of nine values reflecting fractional representation (%) of nine prototrophy phenotypes in the analyzed HGM sample. For each phenotype, this value, termed CPI, is computed as a sum of probabilistic phenotypes in each of the nine columns weighted (multiplied) by relative abundance of respective OTUs. A nine-value CPI string reflects the vitamin prototrophy/auxotrophy phenotype representation extended from an individual OTU to the entire community. Using CPI strings as simplified microbiome-wide metrics of vitamin/cofactor metabolic capabilities and requirements, enables a comparative analysis of multiple samples in model studies [as applied in the accompanying publication (Sharma

et al., in review)] or across large datasets, as illustrated here by the analysis of HMP and AGP collections.

We applied the Phenotype Profiler pipeline to the comparative analysis of two large HGM 16S rRNA datasets from the HMP and AGP projects containing 245 and 2,863 samples, respectively. Both datasets were pre-processed using the QIIME2 pipeline and the obtained OTUs were taxonomically assigned using our custom heuristic-based procedure (see Materials and Methods). The OTU-abundance values were further renormalized to take into account substantial variations in 16S rRNA gene copy number between different species of HGM bacteria (**Supplementary Table S5** and **Supplementary Figure S4**). CPI values and respective prediction errors were calculated for each vitamin (B1, B2, B3, B5, B6, B7, B9, B12, and Q) and each sample from the HMP and AGP datasets using both, original phylogenetic profiles and renormalized by 16S rRNA gene copy number (**Supplementary Table S6**). The prediction errors for individual CPI values were in the range 1–7% for HMP and 2–5% for AGP showing only a moderate impact of imprecise phenotype mapping and phenotype microheterogeneity. The distribution of CPI values for B-vitamins and Q across all samples in the two analyzed datasets is illustrated here for the original taxonomic

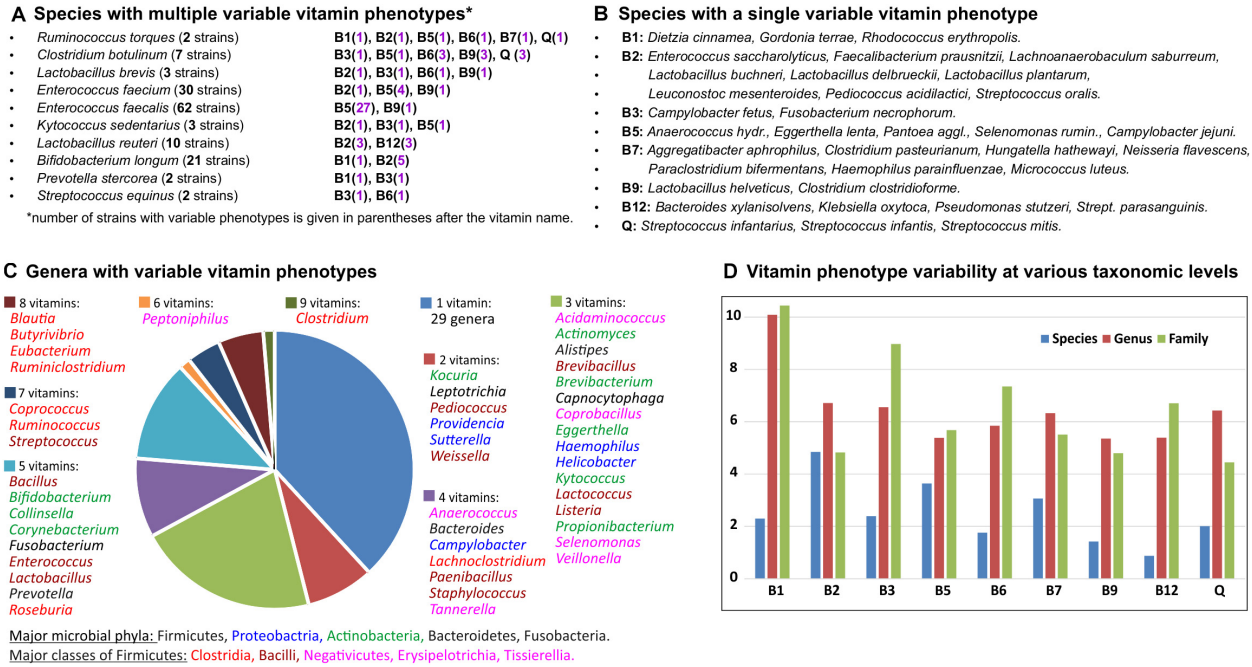

FIGURE 4 | Inter-and intra-species variability of binary vitamin production phenotypes in HGM genomes. **(A)** Species with multiple variable vitamin phenotypes. **(B)** Species with a single variable vitamin phenotype. **(C)** Genera with variable vitamin phenotypes. **(D)** Vitamin phenotype variability at various taxonomic levels.

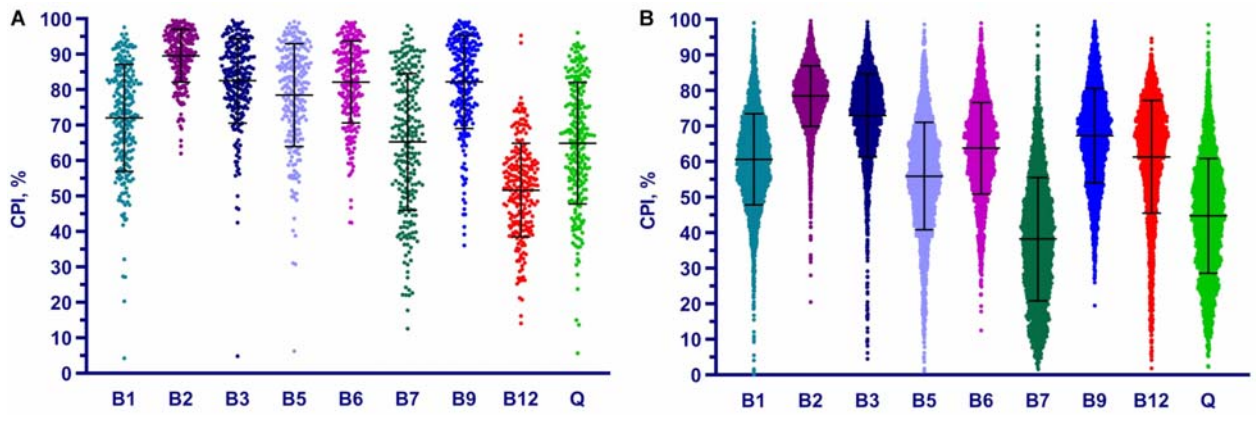

FIGURE 5 | Distribution of Community Phenotype Indices for B and Q vitamins in HGM samples from HMP **(A)** and AGP **(B)** datasets. CPIs are calculated based on taxonomic assignments before 16S count renormalization.

TABLE 2 | Mean CPI values for B-vitamins and Q in HMP and AGP datasets before and after renormalization of taxonomic profiles by 16S gene counts.

Dataset	B1	B2	B3	B5	B6	B7	B9	B12	Q
HMP (original)	72.1	89.7	82.6	78.5	82.2	65.3	82.3	51.7	64.9
HMP (renormalized)	66.4	90.4	81.8	79.1	81.8	59.9	82.2	43.9	58.2
AGP (original)	60.7	78.6	73.1	56.0	63.9	38.3	67.4	61.4	44.8
AGP (renormalized)	58.9	78.9	73.7	57.9	65.4	35.6	68.4	56.8	42.4

profiles (**Figure 5**). The impact of renormalization by 16S rRNA gene copy number is shown in a **Supplementary Figure S5**. In both datasets, CPI values are significantly variable between samples suggesting distinct micronutrient requirements of the respective gut communities. Although the obtained vitamin phenotype profiles for HMP and AGP datasets differ substantially we also noted common trends for certain vitamins (see **Figure 5** and **Table 2** for mean CPI values). Thus, both datasets show the highest mean CPI values for B2, B3, B6, and B9. The HMP dataset is characterized by the lowest mean CPI value for B12. In contrast, vitamin B7 and Q demonstrate the lowest average CPIs in the AGP dataset.

Overall, the phenotype profiling approach proposed in this study complements the established taxonomic profiling approach commonly used for description and comparative analysis of microbial communities. Thus, vitamin-specific CPIs provide useful metrics to compare and contrast micronutrient requirements of HGM communities, while the community-wide distribution of phenotype strings points to major vitamin acceptors and potential donors in these communities.

Lifestyle Preferences in the Human Gut Microbial Communities

A more granular analysis of phenotype profiles of numerous HGM samples allowed us to implicate specific taxa providing major contributions to predominantly prototrophic vs. auxotrophic phenotypes in gut microbial communities. To compare fitness (by relative abundance) of various combinations of vitamin phenotypes in individual species from HGM samples representing different "lifestyles" (e.g., multi-prototrophy vs. multi-auxotrophy lifestyles), we calculated relative contribution of ordered nine-digit strings of individual binary phenotypes (as described in Materials and Methods). As a first approximation of such lifestyles, we introduced a simple metric, *vitamin prototrophy rank* (VPR), ranging from 0 (complete auxotrophy) to 9 (complete prototrophy) with respect to all nine analyzed micronutrients. Intermediate VPR values, 1 through 8, are assigned to groups of species showing prototrophy with respect to 1 through 8 (out of 9) micronutrients. For each sample in the analyzed HMP and AGP communities, we calculated two values: (i) the observed VPR frequencies (P_{obs}), and (ii) the expected VPR probabilities obtained in the assumption of independence of individual phenotypes in each organism (P_{exp}) (**Supplementary Figure S6**).

The results of this analysis are illustrated by ratios of the observed over expected frequency of nine aggregated lifestyles across all samples in HMP and AGP datasets (**Figure 6**). Despite differences in absolute frequencies of distinct VPRs (such as a clear prevalence of multi-prototrophs with VPR = 8 or 9, see **Supplementary Figure S6A**), the comparison of relative frequencies (P_{obs}/P_{exp}) reveals enrichment for both extreme lifestyles, multi-prototrophy and multi-auxotrophy (VPR $\leq$ 3). This trend, which is observed in both datasets, may reflect fundamental properties of organization of syntrophic microbial communities where species with an extreme "parasitic" lifestyle are not only tolerated but gain certain selective advantages as long as multi-prototrophic donors of micronutrients are sufficiently abundant. Major genera contributing to the extreme prototrophic, auxotrophic and intermediate lifestyles are enlisted in **Table 3**. The *Bacteroides* spp. are major contributors to a multi-prototrophic lifestyle in both HMP and AGP datasets. Among major multi-auxotrophs, *Faecalibacterium* spp. are common in both datasets representing the most successful B-vitamin acceptors in microbial gut communities. It is tempting to consider major taxa representing multi-prototrophic lifestyles as potential vitamin donors enabling sustainability of numerous auxotrophic acceptors. Identity of such donors and genomic features distinguishing *sharing* from *non-sharing* prototrophs (e.g., a particular class of efflux transporters or/and regulators) remain an important direction of future research, which would impact our understanding of metabolic interactions in microbial communities.

TABLE 3 | Taxonomic genera mostly contributing to VPR ranks in HGM samples from the HMP and AGP datasets.

Ranks	HMP*	AGP*
7–9	*Bacteroides* (61%), *Alistipes* (15%), *Parabacteroides* (5%), *Paraprevotella* (3%)	*Bacteroides* (44%), *Ruminococcus* (8%), *Akkermansia* (5%), *Anaerostipes* (4%) *Parabacteroides* (4%)
4–6	*Alistipes* (28%), *Blautia* (10%), *Roseburia* (8%), *Eubacterium* (7%), *Prevotella* (5%)	Alistipes (16%), *Roseburia* (14%), *Blautia* (13%), *Prevotella* (9%), *Bifidobacterium* (7%)
0–3	*Faecalibacterium* (17%), *Oscillibacter* (13%), *Lactobacillus* (8%), *Parasutterella* (5%)	*Faecalibacterium* (22%), *Lachnoclostridium* (7%), *Oscillospira* (5%), *Lactobacillus* (4%)

**Average contribution of a genus to a subset of VPR ranks (by abundance) is given in parentheses.*

Comparison of Phenotype Profiling and Pathway Abundance Approach

Of several approaches to functional description of microbial communities, a combination of PICRUSt [an ancestral-state reconstruction algorithm (Langille et al., 2013)] with the MinPath tool (Ye and Doak, 2009) and MetaCyc pathways collection (Caspi et al., 2012) implemented in the PICRUSt2 pipeline enables a similar analysis. Indeed, this analysis yields pathway abundances, which, at least for the case of eight B-vitamins, may be directly compared to respective CPI values. For the purpose of such comparison, we used our BPM for 2,228 reference HGM genomes as an input trait table to predict *vitamin phenotype abundances* in HGM samples from HMP and AGP

datasets by using PICRUSt algorithm (**Supplementary Table S7**). The obtained PICRUSt-based relative phenotype abundances (termed this way by analogy with pathway abundances) are essentially equivalent to CPIs, and their distributions show similar trends (compare **Figure 7** and **Figure 5**). Thus, we consider a combination of BPM with PICRUSt-based phenotype abundances as a potential alternative approach to community phenotype profiling.

We further compared the PICRUSt-based phenotype abundance profiles with vitamin biosynthesis pathway abundances computed for the same HMP and AGP metagenomic datasets using the default PICRUSt2/MinPath approach (see Materials and Methods). We selected a subset of metabolic pathways in MetaCyc database that most closely describe the reconstructed in this work *de novo* vitamin biosynthetic capabilities. For B3, B7, and B12 we included in the analysis two alternative biosynthetic pathways captured in MetaCyc, and their abundances were summed up to get cumulative values for each vitamin (**Table 4**). The obtained MinPath/MetaCyc pathway abundances (**Supplementary Table S7**) were compared with the BPM-based phenotype abundances for each vitamin pathway (except B12) and dataset (**Supplementary Figure S7**). For most compared B-vitamins, the observed correlation coefficients exceeded 0.75 (with the exception of B12, where the predicted MinPath/MetaCyc-based pathway abundances of both anaerobic and aerobic pathways were too low reflecting some technical problem, and vitamin B6, see below). The best correlation was observed for B3, B5, and B9 in both HMP and AGP datasets (**Table 4**). A weaker correlation for vitamin B6 is potentially explained by the absence of the alternative pathway 2 variant in MetaCyc database, while according to our analysis this pathway is very common among HGM bacteria. Likewise, a relatively weak correlation for vitamin B1 can be explained by the absence in MetaCyc collection of the alternative pathway 2 for biosynthesis of the HET moiety.

TABLE 4 | Correlation coefficients for comparison of phenotype abundances produced by PICRUSt2 with binary phenotype and MetaCyc pipelines.

Vitamin	AGP	HMP	MetaCyc pathway(s)
B1	0.62	0.88	Superpathway of thiamin diphosphate biosynthesis I
B2	0.79	0.87	Flavin biosynthesis I (bacteria and plants)
B3	0.84	0.89	NAD biosynthesis I (from aspartate); NAD biosynthesis II (from tryptophan)
B5	0.86	0.94	Pantothenate and coenzyme A biosynthesis I
B6	0.57	0.62	Pyridoxal 5′-phosphate biosynthesis I
B7	0.82	0.76	Biotin biosynthesis I; biotin biosynthesis II
B9	0.89	0.93	Superpathway of tetrahydrofolate biosynthesis
B12*	–	–	Adenosylcobalamin biosynthesis II (late cobalt incorporation); adenosylcobalamin biosynthesis I (early cobalt insertion)
Q	0.78	0.91	preQ0 biosynthesis

**Both anaerobic (early cobalt insertion) and aerobic (late cobalt incorporation) pathways of B12 biosynthesis received very low or zero abundances in most analyzed HGM samples using MinPath/MetaCyc approach, thus we did not compare them with predicted phenotype abundances for vitamin B12.*

CONCLUSION AND FUTURE PERSPECTIVES

By applying the subsystem-based genomic reconstruction, we have analyzed pathways for biosynthesis, salvage and uptake of eight B-group vitamins (and queuosine) for HGM bacteria represented by a diverse reference set of 2,228 genomes. Overall, nine reconstructed metabolic subsystems include over two hundred functional roles encoded by distinct protein families (**Figure 1** and **Supplementary Figure S1**). Specific combinations of the inferred components of biosynthetic pathways and transporters for vitamins and precursors provide genomic signatures, which allowed us to classify all organisms in the collection with respect to their biosynthetic and uptake capabilities (pathway variants) and predict their prototrophic vs. auxotrophic phenotypes (**Table 1**). The obtained results further supported the importance of vitamin cross-feeding and pointed to specific families of transporters potentially contributing to this type of metabolic interactions in HGM communities (**Figure 2**). We detected subsets of auxotrophs encoding partially truncated pathway variants implicating some precursors and derivatives of canonical vitamins (such as thiazole, quinolinate, dethiobiotin, and pantoate) as alternative vitamers potentially broadening the vitamin exchange "market" in HGM consortia (**Table 1**). Robustness of the predicted nutritional requirements and

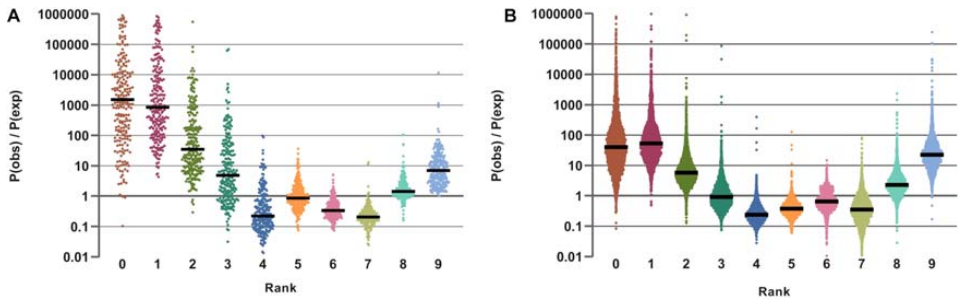

FIGURE 6 | Distribution of ratio of observed and expected probabilities for Vitamin Prototrophy Ranks in HGM samples from HMP **(A)** and AGP **(B)** datasets. Distributions are presented on a logarithmic scale.

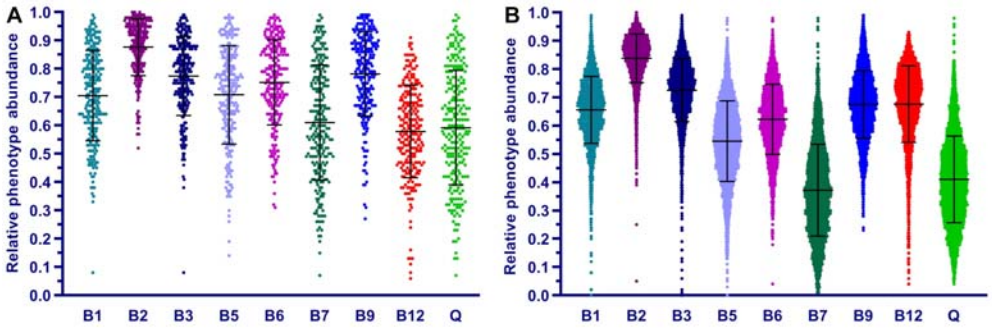

FIGURE 7 | Distribution of relative phenotype abundance for B and Q vitamins in HGM samples from HMP **(A)** and AGP **(B)** datasets. Relative phenotype abundances are calculated using PICRUSt based on external traits from BPM for 2,228 reference genomes obtained in this study.

vitamin production capabilities is supported by the observed consistency between the *in silico* phenotype predictions and published experimental data.

To enable quantitative comparative analysis of community-wide phenotype profiles, we have converted all detailed pathway variant codes to a simplified form of *digital binary phenotypes* with 1 or 0 values corresponding to prototrophy and auxotrophy, respectively. These values computed for each of the nine vitamin phenotypes across 2,228 HGM genomes capture our reference collection in a compact form of a Binary Phenotype Matrix (BPM). Overall, auxotrophic phenotypes are very common in HGM species, and only a small subset of microorganisms can synthesize all vitamins further supporting the micronutrient sharing hypothesis (**Figure 3**). The analysis of phylogenetic distribution of phenotypes within the entire BPM reveals substantial intraspecies and interspecies variations of micronutrient requirements and production capabilities (**Figure 4**). It also allowed us to establish taxonomic boundaries of phenotype conservation, which is essential for phylogeny-based projection of phenotypes from reference genomes to a variety of phylotypes (OTUs) comprising HGM samples. This analysis shows that most vitamin phenotypes are largely conserved at the level of species although some variations between strains and isolates are observed and need to be accounted for by phenotype projection tools. While the phenotype heterogeneity is gradually increasing at higher taxonomic levels, reasonably accurate probabilistic phenotype prediction (weighted for the observed frequency of alternative phenotypes within given taxa) is still feasible at the genus and, to a lesser extent, at the family (but not higher) level. Quite obviously, a well-anticipated growth in the number of sequenced and analyzed reference genomes as well as the increased accuracy of phylogenetic mapping (e.g., by using longer 16S rRNA gene sequences or/and additional phylogenetic signatures) will improve accuracy of phylogeny-based phenotype assignments and provide better estimates of prediction confidence.

Combining the BPM with phylogenetic profiles of HGM samples (e.g., obtained by 16S profiling) enables a new computational approach to *in silico* phylotype-to-phenotype predictive profiling. Application of this approach to the analysis of a broad range of HGM samples from HMP and AGP data sets yielded a comprehensive coverage (in most cases > 95% by relative abundance of mapped OTUs) and high confidence (estimated average error < 10%) of microbiome-wide phenotype predictions. The output of this analysis, in the simplest aggregated form of Community Phenotype Indexes (CPIs), provides an estimate for a fractional representation (relative abundance, from 0 to 100%) of auxotrophy vs. prototrophy for all nine analyzed phenotypes in each analyzed HGM sample. Substantial variations of CPI values are observed between individual samples as well as between these two data sets (**Figure 5**) potentially reflecting some technical differences between HMP and AGP sample and data acquisition pipelines. Indeed, we have compared the average Shannon alpha diversities between HMP and AGP datasets (**Supplementary Table S6**) and found that the HMP dataset is characterized by relatively lower diversity (4.3 for HMP vs. 5.2 for AGP, see **Supplementary Figure S4C**). Quite likely this difference in diversity may at least partially account for the observed phenotypic differences between these datasets. Nevertheless, some common trends are also observed providing the first estimate of micronutrient requirements (auxotrophy) as well as production/sharing (prototrophy) capabilities of HGM communities. Thus, despite the aforementioned high frequency of auxotrophic phenotypes in reference genomes, in real-life HGM samples, the abundance-weighted prototrophy is a dominant phenotype with mean CPI values above 50–60% for most (but not all) vitamins. This analysis confirmed a substantial level of auxotrophy and, thus, a requirement for the exogenous supply of the entire set of nine analyzed micronutrients (eight B vitamins and queuosine), as a characteristic feature of HGM communities across a broad range of samples.

Overall, in addition to further supporting a hypothesized role of syntrophic micronutrient metabolism in HGM communities, a comparative phenotype profiling approach established in this study has provided a computational framework for the experimental testing of this hypothesis (Sharma et al., in review). This approach is extending methodology of a functional

description of microbial communities, which, presently, is not as established as phylogenetic profiling methods. A side-by-side comparison of our phenotype-based approach with the most advanced existing approach, PICRUSt2, predicting pathway abundance via a combination of MinPath algorithm with MetaCyc pathways, revealed a generally good agreement (**Table 4**) for most (but not all) vitamin phenotypes, as well as substantial differences, which could be partially explained by the differences in the applied rules and in the extent of gene/pathway curation.

An anticipated further advancement of microbiome genomics, most importantly: (i) deeper coverage of relevant microbial communities by complete reference genomes and (ii) increased coverage and resolution of phylogenetic profiling (e.g., via better amplicon-based or shotgun metagenomics methodology), is expected to substantially improve the accuracy of predictive phenotype profiling of complex microbial communities. This approach can be further expanded via inclusion of additional digitized phenotypes covering other nutrient requirements (e.g., amino acids), utilization capabilities (e.g., carbohydrates) (Yatsunenko et al., 2012; David et al., 2014; Zhang et al., 2014; Wu et al., 2015; Blanton et al., 2016; Hibberd et al., 2017; Sheflin et al., 2017; Gehrig et al., 2019), catabolic end-products (e.g., production of short-chain fatty acids, other physiologically active metabolites) as well as some non-metabolic phenotypes (antibiotic resistance, virulence, etc.) and by taking into consideration other characteristics of metagenomic samples (diversity, advanced metadata). Future practical applications employing comparative analyses of phenotype profiles across numerous HGM samples may include diagnostics (classification and correlations with patients' data) and prevention/treatment of disbyosis-related syndromes via rational and personalized selection of probiotics and nutritional supplements.

AUTHOR CONTRIBUTIONS

AO and DR conceived and designed the research project. MK and AA performed the comparative genomic analysis, reconstruction of pathways and subsystem encoding. AA compared the obtained phenotypes to experimentally published data. DR provided the quality control of the obtained data. SI, MK, and SL analyzed metabolic phenotypes in the 16S datasets. DR, AA, PN, SP, and AO wrote the manuscript. All authors read and approved the final manuscript.

FUNDING

This research was supported by NIH (R01 GM108527-02 to SP and AO and RO1 DK030292-35 to AO), and the Russian Science Foundation (Grant No. #14-14-00289 to DR).

ACKNOWLEDGMENTS

We thank Robert Olson from the SEED/RAST development team at Argonne National Lab for dedicated support of the mcSEED-based genomic analyses. We are grateful to PhenoBiome Inc. (Walnut Creek, CA, United States, www.phenobiome.com) for providing us with the access to a development version of *Phenobiome Phenotype Profiler* tool.

SUPPLEMENTARY MATERIAL

The Supplementary Material for this article can be found online at: https://www.frontiersin.org/articles/10.3389/fmicb.2019.01316/full#supplementary-material

REFERENCES

Amir, A., Mcdonald, D., Navas-Molina, J. A., Debelius, J., Morton, J. T., Hyde, E., et al. (2017). Correcting for microbial blooms in fecal samples during room-temperature shipping. *mSystems* 2:e00199-16. doi: 10.1128/mSystems.00199-16

Blanton, L. V., Charbonneau, M. R., Salih, T., Barratt, M. J., Venkatesh, S., Ilkaveya, O., et al. (2016). Gut bacteria that prevent growth impairments transmitted by microbiota from malnourished children. *Science* 351:aad3311. doi: 10.1126/science.aad3311

Butzin, N. C., Secinaro, M. A., Swithers, K. S., Gogarten, J. P., and Noll, K. M. (2013). Thermotoga lettingae can salvage cobinamide to synthesize vitamin B12. *Appl. Environ. Microbiol.* 79, 7006–7012. doi: 10.1128/AEM.01800-13

Caporaso, J. G., Kuczynski, J., Stombaugh, J., Bittinger, K., Bushman, F. D., Costello, E. K., et al. (2010). QIIME allows analysis of high-throughput community sequencing data. *Nat. Methods* 7, 335–336.

Caspi, R., Altman, T., Dreher, K., Fulcher, C. A., Subhraveti, P., Keseler, I. M., et al. (2012). The MetaCyc database of metabolic pathways and enzymes and the BioCyc collection of pathway/genome databases. *Nucleic Acids Res.* 40, D742–D753. doi: 10.1093/nar/gkr1014

Cole, J. R., Wang, Q., Fish, J. A., Chai, B., Mcgarrell, D. M., Sun, Y., et al. (2014). Ribosomal database project: data and tools for high throughput rRNA analysis. *Nucleic Acids Res.* 42, D633–D642. doi: 10.1093/nar/gkt1244

Danchin, A., and Braham, S. (2017). Coenzyme B12 synthesis as a baseline to study metabolite contribution of animal microbiota. *Microb. Biotechnol.* 10, 688–701. doi: 10.1111/1751-7915.12722

David, L. A., Maurice, C. F., Carmody, R. N., Gootenberg, D. B., Button, J. E., Wolfe, B. E., et al. (2014). Diet rapidly and reproducibly alters the human gut microbiome. *Nature* 505, 559–563. doi: 10.1038/nature12820

De Crecy-Lagard, V., Marck, C., Brochier-Armanet, C., and Grosjean, H. (2007). Comparative RNomics and modomics in Mollicutes: prediction of gene function and evolutionary implications. *IUBMB Life* 59, 634–658. doi: 10.1080/15216540701604632

Degnan, P. H., Taga, M. E., and Goodman, A. L. (2014). Vitamin B12 as a modulator of gut microbial ecology. *Cell Metab.* 20, 769–778. doi: 10.1016/j.cmet.2014.10.002

Edgar, R. C. (2004). MUSCLE: a multiple sequence alignment method with reduced time and space complexity. *BMC Bioinformatics* 5:113. doi: 10.1186/1471-2105-5-113

Ejtahed, H. S., Soroush, A. R., Angoorani, P., Larijani, B., and Hasani-Ranjbar, S. (2016). Gut microbiota as a target in the pathogenesis of metabolic disorders: a new approach to novel therapeutic agents. *Horm. Metab. Res.* 48, 349–358. doi: 10.1055/s-0042-107792

Ernst, D. C., and Downs, D. M. (2015). The STM4195 gene product (PanS) transports coenzyme a precursors in *Salmonella enterica*. *J. Bacteriol.* 197, 1368–1377. doi: 10.1128/JB.02506-14

Fergus, C., Barnes, D., Alqasem, M. A., and Kelly, V. P. (2015). The queuine micronutrient: charting a course from microbe to man. *Nutrients* 7, 2897–2929. doi: 10.3390/nu7042897

Gehrig, J. G., Venkatesh, S., Chang, H., Hibberd, M. C., Kung, V. L., Cheng, J., et al. (2019). Effects of microbiota-directed therapeutic foods in gnotobiotic mice, gnotobiotic piglets, and undernourished children. *Science* (in press). doi: 10.1126/science.aau4732

Hemberger, S., Pedrolli, D. B., Stolz, J., Vogl, C., Lehmann, M., and Mack, M. (2011). RibM from *Streptomyces davawensis* is a riboflavin/roseoflavin transporter and may be useful for the optimization of riboflavin production strains. *BMC Biotechnol.* 11:119. doi: 10.1186/1472-6750-11-119

Hibberd, M. C., Wu, M., Rodionov, D. A., Li, X., Cheng, J., Griffin, N. W., et al. (2017). The effects of micronutrient deficiencies on bacterial species from the human gut microbiota. *Sci. Transl. Med.* 9:eaal4069. doi: 10.1126/scitranslmed.aal4069

Human Microbiome Project Consortium (2012). Structure, function and diversity of the healthy human microbiome. *Nature* 486, 207–214. doi: 10.1038/nature11234

Imhann, F., Vich Vila, A., Bonder, M. J., Fu, J., Gevers, D., Visschedijk, M. C., et al. (2018). Interplay of host genetics and gut microbiota underlying the onset and clinical presentation of inflammatory bowel disease. *Gut* 67, 108–119. doi: 10.1136/gutjnl-2016-312135

Kanehisa, M., Goto, S., Sato, Y., Kawashima, M., Furumichi, M., and Tanabe, M. (2014). Data, information, knowledge and principle: back to metabolism in KEGG. *Nucleic Acids Res.* 42, D199–D205. doi: 10.1093/nar/gkt1076

Kenley, J. S., Leighton, M., and Bradbeer, C. (1978). Transport of vitamin B12 in *Escherichia coli*. corrinoid specificity of the outer membrane receptor. *J. Biol. Chem.* 253, 1341–1346.

Kostic, A. D., Gevers, D., Siljander, H., Vatanen, T., Hyotylainen, T., Hamalainen, A. M., et al. (2015). The dynamics of the human infant gut microbiome in development and in progression toward type 1 diabetes. *Cell Host Microbe* 17, 260–273. doi: 10.1016/j.chom.2015.01.001

Langille, M. G., Zaneveld, J., Caporaso, J. G., Mcdonald, D., Knights, D., Reyes, J. A., et al. (2013). Predictive functional profiling of microbial communities using 16S rRNA marker gene sequences. *Nat. Biotechnol.* 31, 814–821. doi: 10.1038/nbt.2676

Letunic, I., and Bork, P. (2016). Interactive tree of life (iTOL) v3: an online tool for the display and annotation of phylogenetic and other trees. *Nucleic Acids Res.* 44, W242–W245. doi: 10.1093/nar/gkw290

Li, J., Jia, H., Cai, X., Zhong, H., Feng, Q., Sunagawa, S., et al. (2014). An integrated catalog of reference genes in the human gut microbiome. *Nat. Biotechnol.* 32, 834–841. doi: 10.1038/nbt.2942

Magnusdottir, S., Ravcheev, D., De Crecy-Lagard, V., and Thiele, I. (2015). Systematic genome assessment of B-vitamin biosynthesis suggests co-operation among gut microbes. *Front. Genet.* 6:148. doi: 10.3389/fgene.2015.00148

Marquet, A. (2010). "Biosynthesis of Biotin," in *Comprehensive Natural Products II: Chemistry and Biology*, eds L. N. Mander and H. Liu (Kidlington: Elsevier Ltd), 161–180. doi: 10.1016/b978-008045382-8.00136-2

McAnulty, M. J., and Wood, T. K. (2014). YeeO from *Escherichia coli* exports flavins. *Bioengineered* 5, 386–392. doi: 10.4161/21655979.2014.969173

McCormick, D. B. (2003). Metabolism of vitamins in microbes and mammals. *Biochem. Biophys. Res. Commun.* 312, 97–101. doi: 10.1016/j.bbrc.2003.09.241

McDonald, D., Hyde, E., Debelius, J. W., Morton, J. T., Gonzalez, A., Ackermann, G., et al. (2018). American gut: an open platform for citizen science microbiome research. *mSystems* 3:e00031-18. doi: 10.1128/mSystems.00031-18

Mee, M. T., Collins, J. J., Church, G. M., and Wang, H. H. (2014). Syntrophic exchange in synthetic microbial communities. *Proc. Natl. Acad. Sci. U.S.A.* 111, E2149–E2156. doi: 10.1073/pnas.1405641111

Novichkov, P. S., Kazakov, A. E., Ravcheev, D. A., Leyn, S. A., Kovaleva, G. Y., Sutormin, R. A., et al. (2013). RegPrecise 3.0–a resource for genome-scale exploration of transcriptional regulation in bacteria. *BMC Genomics* 14:745. doi: 10.1186/1471-2164-14-745

Ohsugi, M., Imanishi, Y., Teraoka, T., Nishimura, K., and Nakao, S. (1990). Biosynthesis of biotin-vitamers by family *Enterobacteriaceae*. *J. Nutr. Sci. Vitaminol.* 36, 447–456. doi: 10.3177/jnsv.36.447

Osterman, A., and Overbeek, R. (2003). Missing genes in metabolic pathways: a comparative genomics approach. *Curr. Opin. Chem. Biol.* 7, 238–251. doi: 10.1016/s1367-5931(03)00027-9

Osterman, A. L. (2009). Genomic variations on a CoA biosynthetic theme. *Nat. Chem. Biol.* 5, 871–872. doi: 10.1038/nchembio.267

Osterman, A. L., Overbeek, R., and Rodionov, D. A. (2010). "The Use of Subsystems to Encode Biosynthesis of Vitamins and Cofactors," in *Comprehensive Natural Products II: Chemistry and Biology*, eds L. N. Mander and H. Liu (Kidlington: Elsevier Ltd), 141–159. doi: 10.1016/b978-008045382-8.00710-3

Overbeek, R., Begley, T., Butler, R. M., Choudhuri, J. V., Chuang, H. Y., Cohoon, M., et al. (2005). The subsystems approach to genome annotation and its use in the project to annotate 1000 genomes. *Nucleic Acids Res.* 33, 5691–5702. doi: 10.1093/nar/gki866

Overbeek, R., Olson, R., Pusch, G. D., Olsen, G. J., Davis, J. J., Disz, T., et al. (2014). The SEED and the rapid annotation of microbial genomes using subsystems technology (RAST). *Nucleic Acids Res* 42, D206–D214.

Prakash, O., and Eisenberg, M. A. (1974). Active transport of biotin in *Escherichia coli* K-12. *J. Bacteriol.* 120, 785–791.

Qin, J., Li, R., Raes, J., Arumugam, M., Burgdorf, K. S., Manichanh, C., et al. (2010). A human gut microbial gene catalogue established by metagenomic sequencing. *Nature* 464, 59–65. doi: 10.1038/nature08821

Rajilic-Stojanovic, M., and de Vos, W. M. (2014). The first 1000 cultured species of the human gastrointestinal microbiota. *FEMS Microbiol. Rev.* 38, 996–1047. doi: 10.1111/1574-6976.12075

Rodionov, D. A., Hebbeln, P., Eudes, A., Ter Beek, J., Rodionova, I. A., Erkens, G. B., et al. (2009). A novel class of modular transporters for vitamins in prokaryotes. *J. Bacteriol.* 191, 42–51. doi: 10.1128/JB.01208-08

Rodionov, D. A., Leyn, S. A., Li, X., and Rodionova, I. A. (2017). A novel transcriptional regulator related to thiamine phosphate synthase controls thiamine metabolism genes in archaea. *J. Bacteriol.* 199:e00743-16. doi: 10.1128/JB.00743-16

Rodionov, D. A., Mironov, A. A., and Gelfand, M. S. (2002a). Conservation of the biotin regulon and the BirA regulatory signal in Eubacteria and Archaea. *Genome Res.* 12, 1507–1516. doi: 10.1101/gr.314502

Rodionov, D. A., Vitreschak, A. G., Mironov, A. A., and Gelfand, M. S. (2002b). Comparative genomics of thiamin biosynthesis in procaryotes. New genes and regulatory mechanisms. *J. Biol. Chem.* 277, 48949–48959. doi: 10.1074/jbc.m208965200

Rodionov, D. A., Vitreschak, A. G., Mironov, A. A., and Gelfand, M. S. (2003). Comparative genomics of the vitamin B12 metabolism and regulation in prokaryotes. *J. Biol. Chem.* 278, 41148–41159. doi: 10.1074/jbc.m305837200

Rodionova, I. A., Vetting, M. W., Li, X., Almo, S. C., Osterman, A. L., and Rodionov, D. A. (2017). A novel bifunctional transcriptional regulator of riboflavin metabolism in Archaea. *Nucleic Acids Res.* 45, 3785–3799. doi: 10.1093/nar/gkw1331

Romine, M. F., Rodionov, D. A., Maezato, Y., Osterman, A. L., and Nelson, W. C. (2017). Underlying mechanisms for syntrophic metabolism of essential enzyme cofactors in microbial communities. *ISME J.* 11, 1434–1446. doi: 10.1038/ismej.2017.2

Roper, J. M., Raux, E., Brindley, A. A., Schubert, H. L., Gharbia, S. E., Shah, H. N., et al. (2000). The Enigma of Cobalamin (Vitamin B_{12}) biosynthesis in *Porphyromonas gingivalis*. identification and characterization of a functional corrin pathway. *J. Biol. Chem.* 275, 40316–40323. doi: 10.1074/jbc.M007146200

Rowe, J. J., Lemmon, R. D., and Tritz, G. J. (1985). Nicotinic acid transport in *Escherichia coli*. *Microbios* 44, 169–184.

Saier, M. H. Jr., Reddy, V. S., Tamang, D. G., and Vastermark, A. (2014). The transporter classification database. *Nucleic Acids Res.* 42, D251–D258. doi: 10.1093/nar/gkt1097

Santos, J. A., Rempel, S., Mous, S. T., Pereira, C. T., Ter Beek, J., De Gier, J. W., et al. (2018). Functional and structural characterization of an ECF-type ABC transporter for vitamin B12. *eLife* 7:e35828. doi: 10.7554/eLife.35828

Santos, F., Wegkamp, A., de Vos, W. M., Smid, E. J., and Hugenholtz, J. (2008). High-Level Folate Production in Fermented Foods by the B_{12} Producer *Lactobacillus reuteri* JCM1112. *Appl. Environ. Microbiol.* 74, 3291–3294. doi: 10.1128/AEM.02719-07

Sanudo-Wilhelmy, S. A., Gomez-Consarnau, L., Suffridge, C., and Webb, E. A. (2014). The role of B vitamins in marine biogeochemistry. *Ann. Rev. Mar. Sci.* 6, 339–367. doi: 10.1146/annurev-marine-120710-100912

Sheflin, A. M., Melby, C. L., Carbonero, F., and Weir, T. L. (2017). Linking dietary patterns with gut microbial composition and function. *Gut Microbes* 8, 113–129. doi: 10.1080/19490976.2016.1270809

Shi, Y. (2013). Common folds and transport mechanisms of secondary active transporters. *Annu. Rev. Biophys.* 42, 51–72. doi: 10.1146/annurev-biophys-083012-130429

Sorci, L., Blaby, I. K., Rodionova, I. A., De Ingeniis, J., Tkachenko, S., De Crecy-Lagard, V., et al. (2013). Quinolinate salvage and insights for targeting NAD biosynthesis in group A streptococci. *J. Bacteriol.* 195, 726–732. doi: 10.1128/JB.02002-12

Sorci, L., Kurnasov, O., Rodionov, D. A., and Osterman, A. L. (2010). "Genomics and Enzymology of NAD Biosynthesis," in *Comprehensive Natural Products II: Chemistry and Biology*, eds L. N. Mander and H. Liu (Kidlington: Elsevier Ltd), 213–257. doi: 10.1016/b978-008045382-8.00138-6

Stamatakis, A. (2015). Using RAxML to infer phylogenies. *Curr. Protoc. Bioinform.* 51, 11–14.

Stoddard, S. F., Smith, B. J., Hein, R., Roller, B. R., and Schmidt, T. M. (2015). rrnDB: improved tools for interpreting rRNA gene abundance in bacteria and archaea and a new foundation for future development. *Nucleic Acids Res.* 43, D593–D598. doi: 10.1093/nar/gku1201

Strauss, E., De Villiers, M., and Rootman, I. (2010). Biocatalytic production of coenzyme a analogues. *ChemCatChem* 2, 929–937. doi: 10.1021/jacs.5b12252

Subramanian, S., Huq, S., Yatsunenko, T., Haque, R., Mahfuz, M., Alam, M. A., et al. (2014). Persistent gut microbiota immaturity in malnourished Bangladeshi children. *Nature* 510, 417–421. doi: 10.1038/nature13421

Togo, A. H., Diop, A., Bittar, F., Maraninchi, M., Valero, R., Armstrong, N., et al. (2018). Description of *Mediterraneibacter massiliensis*, gen. nov., sp. nov., a new genus isolated from the gut microbiota of an obese patient and reclassification of *Ruminococcus faecis*, *Ruminococcus lactaris*, *Ruminococcus torques*, *Ruminococcus gnavus* and *Clostridium glycyrrhizinilyticum* as *Mediterraneibacter faecis* comb. nov., *Mediterraneibacter lactaris* comb. nov., *Mediterraneibacter torques* comb. nov., *Mediterraneibacter gnavus* comb. nov. and *Mediterraneibacter glycyrrhizinilyticus* comb. nov. *Antonie Van Leeuwenhoek* 111, 2107–2128. doi: 10.1007/s10482-018-1104-y

Vitreschak, A. G., Rodionov, D. A., Mironov, A. A., and Gelfand, M. S. (2002). Regulation of riboflavin biosynthesis and transport genes in bacteria by transcriptional and translational attenuation. *Nucleic Acids Res.* 30, 3141–3151. doi: 10.1093/nar/gkf433

Wegkamp, A., Teusink, B., de Vos, W. M., and Smid, E. J. (2010). Development of a minimal growth medium for Lactobacillus plantarum. *Lett. Appl. Microbiol.* 50, 57–64. doi: 10.1111/j.1472-765X.2009.02752.x

Wattam, A. R., Davis, J. J., Assaf, R., Boisvert, S., Brettin, T., Bun, C., et al. (2017). Improvements to PATRIC, the all-bacterial bioinformatics database and analysis resource center. *Nucleic Acids Res.* 45, D535–D542. doi: 10.1093/nar/gkw1017

Wexler, A. G., Schofield, W. B., Degnan, P. H., Folta-Stogniew, E., Barry, N. A., and Goodman, A. L. (2018). Human gut *Bacteroides* capture vitamin B12 via cell surface-exposed lipoproteins. *eLife* 7:e37138. doi: 10.7554/eLife.37138

Wu, M., Mcnulty, N. P., Rodionov, D. A., Khoroshkin, M. S., Griffin, N. W., Cheng, J., et al. (2015). Genetic determinants of in vivo fitness and diet responsiveness in multiple human gut *Bacteroides*. *Science* 350:aac5992. doi: 10.1126/science.aac5992

Yatsunenko, T., Rey, F. E., Manary, M. J., Trehan, I., Dominguez-Bello, M. G., Contreras, M., et al. (2012). Human gut microbiome viewed across age and geography. *Nature* 486, 222–227. doi: 10.1038/nature11053

Ye, Y., and Doak, T. G. (2009). A parsimony approach to biological pathway reconstruction/inference for genomes and metagenomes. *PLoS Comput. Biol.* 5:e1000465. doi: 10.1371/journal.pcbi.1000465

Ye, Y., Osterman, A., Overbeek, R., and Godzik, A. (2005). Automatic detection of subsystem/pathway variants in genome analysis. *Bioinformatics* 21(Suppl. 1), i478–i486. doi: 10.1093/bioinformatics/bti1052

Zallot, R., Yuan, Y., and De Crecy-Lagard, V. (2017). The *Escherichia coli* COG1738 Member YhhQ Is Involved in 7-Cyanodeazaguanine (preQ(0)) Transport. *Biomolecules* 7:E12. doi: 10.3390/biom7010012

Zeller, G., Tap, J., Voigt, A. Y., Sunagawa, S., Kultima, J. R., Costea, P. I., et al. (2014). Potential of fecal microbiota for early-stage detection of colorectal cancer. *Mol. Syst. Biol.* 10:766. doi: 10.15252/msb.20145645

Zhang, J., Guo, Z., Lim, A. A., Zheng, Y., Koh, E. Y., Ho, D., et al. (2014). Mongolians core gut microbiota and its correlation with seasonal dietary changes. *Sci. Rep.* 4:5001. doi: 10.1038/srep05001

Zhang, Y., Rodionov, D. A., Gelfand, M. S., and Gladyshev, V. N. (2009). Comparative genomic analyses of nickel, cobalt and vitamin B12 utilization. *BMC Genomics* 10:78. doi: 10.1186/1471-2164-10-78

Conflict of Interest Statement: The authors declare that the research was conducted in the absence of any commercial or financial relationships that could be construed as a potential conflict of interest.

Copyright © 2019 Rodionov, Arzamasov, Khoroshkin, Iablokov, Leyn, Peterson, Novichkov and Osterman. This is an open-access article distributed under the terms of the Creative Commons Attribution License (CC BY). The use, distribution or reproduction in other forums is permitted, provided the original author(s) and the copyright owner(s) are credited and that the original publication in this journal is cited, in accordance with accepted academic practice. No use, distribution or reproduction is permitted which does not comply with these terms.

frontiers in Microbiology

ORIGINAL RESEARCH
published: 02 July 2019
doi: 10.3389/fmicb.2019.01485

B-Vitamin Sharing Promotes Stability of Gut Microbial Communities

Vandana Sharma[1†], Dmitry A. Rodionov[1,2†], Semen A. Leyn[1,2], David Tran[1], Stanislav N. Iablokov[2,3], Hua Ding[4], Daniel A. Peterson[4‡], Andrei L. Osterman[1] and Scott N. Peterson[1*]*

[1] Infectious and Inflammatory Disease Center, Sanford Burnham Prebys Medical Discovery Institute, La Jolla, CA, United States, [2] A.A. Kharkevich Institute for Information Transmission Problems, Russian Academy of Sciences, Moscow, Russia, [3] P.G. Demidov Yaroslavl State University, Yaroslavl, Russia, [4] Department of Pathology, The Johns Hopkins University School of Medicine, Baltimore, MD, United States

OPEN ACCESS

Edited by:
Siok-Fong Chin,
UKM Medical Molecular Biology Institute (UMBI), Malaysia

Reviewed by:
Karoline Faust,
KU Leuven, Belgium
Muriel Derrien,
Nutricia Research, France

***Correspondence:**
Andrei L. Osterman
osterman@sbpdiscovery.org
Scott N. Peterson
speterson@sbpdiscovery.org

[†]These authors have contributed equally to this work

[‡]**Present address:**
Daniel A. Peterson,
Eli Lilly and Company, Indianapolis, IN, United States

Specialty section:
This article was submitted to Microbial Symbioses, a section of the journal Frontiers in Microbiology

Received: 08 January 2019
Accepted: 14 June 2019
Published: 02 July 2019

Citation:
Sharma V, Rodionov DA, Leyn SA, Tran D, Iablokov SN, Ding H, Peterson DA, Osterman AL and Peterson SN (2019) B-Vitamin Sharing Promotes Stability of Gut Microbial Communities. Front. Microbiol. 10:1485. doi: 10.3389/fmicb.2019.01485

Cross-feeding on intermediary and end-point metabolites plays an important role in the dynamic interactions of host-associated microbial communities. While gut microbiota possess inherent resilience to perturbation, variations in the intake of certain nutrients may lead to changes in the community composition with potential consequences on host physiology. Syntrophic relationships and mutualism at the level of major carbon and energy sources have been documented, however, relatively little is known about metabolic interactions involving micronutrients, such as B-vitamins, biosynthetic precursors of essential cofactors in the mammalian host and numerous members of the gut microbiota alike. *In silico* genomic reconstruction and prediction of community-wide metabolic phenotypes for eight major B-vitamins (B1, B2, B3, B5, B6, B7, B9, and B12), suggests that a significant fraction of microbial gut communities (>20% by abundance) are represented by auxotrophic species whose viability is strictly dependent on acquiring one or more B-vitamins from diet and/or prototrophic microbes *via* committed salvage pathways. Here, we report the stability of gut microbiota using humanized gnotobiotic mice and *in vitro* anaerobic fecal culture in the context of extreme variations of dietary B-vitamin supply as revealed by phylotype-to-phenotype prediction from 16S rRNA profiling and metabolomic measurements. The observed nearly unaltered relative abundance of auxotrophic species in gut communities in the face of diet or media lacking B-vitamins or containing them in great excess (∼30-fold above normal) points to a strong contribution of metabolic cooperation (B-vitamin exchange and sharing) to the stability of gut bacterial populations.

Keywords: gut microbiota, B-vitamins, syntrophy, genome reconstruction, community stability

INTRODUCTION

Understanding metabolic interactions underlying assembly, maintenance, and dietary response of gut microbial communities is expected to provide a foundation for diagnostics, disease prevention, and therapeutic treatment of dysbiosis-related syndromes and diseases *via* rational nutritional supplementation. This concept is illustrated by studies evaluating the effects of complementary foods on healthy maturation of infant gut microbiota that were convincingly demonstrated in the context of severe acute malnutrition (Blanton et al., 2016). The human microbiota represents a complex assemblage of member species and a significantly larger set of gene functions.

Collectively these gene functions provide the driving force for the establishment and maintenance of mutualistic relationships including both microbe-microbe and host-microbe interactions. One strategy microbes utilize to gain fitness advantage in the population is to engage in metabolic cooperation (Chassard and Bernalier-Donadille, 2006; Samuel and Gordon, 2006; Sonnenburg et al., 2006). The intensive selective pressure and fierce competition for nutrients in the gut, particularly in the colon, where bacterial populations are extremely dense ($\sim 1 \times 10^{12}$ bacteria/gram feces), may drive the subsequent shedding of genes involved in metabolic coding capacity thereby creating and/or deepening co-dependent relationships between groups of microbial species. It has been speculated that mutualism and synthrophic relationships abound in human microbiota. Evidence is accumulating to support this conjecture (Backhed et al., 2005; Mahowald et al., 2009; Fischbach and Sonnenburg, 2011). A combination of *in vitro* microbiological co-culture studies and the use of gnotobiotic mice have led to a broadened appreciation of the evolutionary strategies underlying functional interactions that define higher-order networks within microbial communities (Faith et al., 2010; Rey et al., 2010).

Metabolic interactions and the impact of dietary components on the microbiota have been studied in various ways. One of the best studied syntrophic networks operating in gut microbiota-host interactions pertain to processes involved in energy extraction from dietary glycans, sugar fermentation, and production of short chain fatty acids (Reichardt et al., 2018). When cultured with resistant starch 2 (RS2), *Ruminococcus bromii* generated significant quantities of reducing sugars but displayed a poor capacity for generalized carbohydrate utilization. However, when co-cultured with *Bacteroides thetaiotaomicron*, the total carbohydrate utilization of both species was increased (Ze et al., 2012). *Desulfovibrio piger* consumes ammonia, lactate, formate, and H_2 generated by fermentation producing H_2S. Fermentation efficiency is reduced by the accumulation of H_2 that inhibits bacterial NADH dehydrogenases. Mutualism between *B. thetaiotaomicron* and *D. piger* has been reported (Rey et al., 2013). In co-colonized mice, *B. thetaiotaomicron* increases the fitness of *D. piger* by providing sulfate, compensating for the lack of sulfatase functions encoded by the *D. piger* genome. *D. piger* consumes products of fermentation H_2 allowing fermentation efficiency of *B. thetaiotaomicron* to be maintained. The activities of some species alter the metabolic preferences of others. *Methanobrevibacter smithii* by an unknown mechanism directs *B. thetaiotaomicron* to preferentially ferment dietary fructans that generate acetate and formate that are subsequently consumed by *M. smithii* for methanogenesis (Samuel and Gordon, 2006). Mice co-colonization with *M. smithii* and *B. thetaiotaomicron* promoted increases in cell number of both species, indicating a mutualistic interaction.

In studies of dietary micronutrients, the impact of selenium was demonstrated using germ-free and gnotobiotic mice, revealing competition between the host and microbiota (Kasaikina et al., 2011). A selective effect of dietary vitamin A on fitness of distinct *Bacteroides* spp. was recently elucidated in gnotobiotic mice colonized by a defined consortium of human gut microbes (Wu et al., 2015). The metabolism of B-vitamins is of high significance since they are biosynthetic precursors of the universally essential cofactors such as TPP (derived from B1), FMN/FAD (from B2), NAD(P) (from B3), etc., drivers of numerous indispensable biochemical reactions in mammalian host and microbes alike. The mammalian host is strictly dependent on the dietary supply of all B-vitamins with the exception of niacin (B3), since in certain mammalian tissues NAD can be synthesized from tryptophan *via* by-passing nicotinate (-amide) requirement. Unlike other micronutrients mentioned, B-vitamins can be synthesized by many bacterial species. However, our *in silico* analysis of available reference genomes revealed that on average 20–30% of species in gut microbial communities (by relative abundance) lack the machinery to synthesize some of the essential B-vitamins (Rodionov et al., 2019). The large fraction of B-vitamin auxotrophs in human gut microbiota implies their strong dependence on the exogenous supply of these micronutrients from the diet and/or v*ia* syntrophic sharing between prototrophic and auxotrophic species.

A potentially important contribution of B-vitamin sharing in microbial communities is supported by several considerations: (i) a limited bioavailability of dietary B-vitamins for microbes in the distal gut due to their active absorption by the host; (ii) relatively low micronutrient requirements (as compared to essential amino acids or other building blocks) (iii) reported precedents of community-wide B-vitamin exchange illustrated by a prototroph-centered microbial consortium from Hot Lake (Romine et al., 2017), and a positive fitness impact provided by B12 prototrophs to a B12 auxotroph in gnotobiotic mice (Goodman et al., 2009).

Based on these considerations, we sought to evaluate the hypothesis that members of microbial communities engage in B-vitamin sharing as a potentially dominant form of mutualism. We hypothesized that a strong contribution of metabolic cooperation would manifest in relatively small or no changes in relative abundance of auxotrophic species even upon substantial changes in the supply of B-vitamins from growth media or diet. To address this hypothesis, we have applied our methodology of genomics-based predictive phenotype profiling, based on projection of 16S rRNA species enumeration of microbiome samples over a curated collection of ∼2,200 sequenced gut resident genomes (Rodionov et al., 2019) for the analysis of fecal samples from humanized gnotobiotic mice that were fed diets supplemented with varying B-vitamin levels (from complete deprivation to 30-fold excess over normal). To reduce the complexity of three-way (microbiota-diet-host) interactions, these studies were extended to *in vitro* anaerobic fecal cultivation and metabolomic measurements. We also used diagnostic *Escherichia coli* B3 and B5 auxotroph mutant strains to test the ability of a panel of prototrophic isolates from human microbiome to support their growth in the absence of respective vitamins in the growth media.

The obtained results, both *in vivo* and *in vitro*, provided strong support of our central hypothesis revealing a remarkable stability with respect to widely varying levels of exogenously supplied micronutrients (B-vitamins). We use the term stability in this

TABLE 1 | Experimental media and diets used *in vitro* and *in vivo*.

B-vitamins:		**B1**	**B2**	**B3**	**B5**	**B7**	**B6**	**B9**	**B12**
		Thiamine	**Riboflavin**	**Niacin**	**Pantothenate**	**Biotin**	**Pyridoxine**	**Folate**	**Cobalamin**
Respective cofactors:		**TPP**	**FMN/FAD**	**NAD/NADP**	**Coenzyme A**	**Biotinyl-ACP**	**PLP/PMP**	**THF/DHF**	**(Ado)-Cob**
Diet (Media)		**Vitamin supplementation (mg/L):**							
AD	All vitamins deficient	–	–	–	–	–	–	–	–
AN	All vitamins normal	6	6	30	16	0.2	7	2	2.5
AE	All vitamins in excess	180	180	900	480	6	210	60	75
4D4N	4 deficient/4 normal	–	–	30	–	–	7	2	2.5
4E4N	4 in excess/4 normal	180	180	30	480	6	7	2	2.5
7D1N	7 deficient/1 normal	–	–	–	–	–	–	–	2.5
7E1N	7 in excess/1 normal	180	180	900	480	6	210	60	2.5

context of the robustness of the auxotrophic component of the studied microbial communities. This observation implies that at least some of the prototrophic species operate as efficient *donors* of micronutrients (B-vitamins), to satisfy the growth requirements of a sizeable fraction of gut auxotrophs.

In addition to the fundamental and practical implications of these findings, the established integrative methodology will enable an extension of these studies toward microbial communities with varying auxotroph representation, under different types of diets or other physiological conditions of the mammalian host, e.g., health vs. disease.

MATERIALS AND METHODS

Escherichia coli K-12 Growth Conditions

Escherichia coli knockout mutants. ΔNadA (B3 auxotroph), ΔPanC (B5 auxotroph), and ΔUxaC (as an isogenic proxy for wild-type with respect to B-vitamin synthesis) from KEIO collection (Baba et al., 2006) were grown at 37°C in M9 solid or liquid medium with or without vitamin B3/B5.

Isolation of Gut Prototrophs

A pool of four human feces was plated on chemically defined medium without any B-vitamin under anaerobic conditions. 90 colonies were picked, grown in liquid culture and glycerol stocks were prepared. 85 out of 90 isolates grew well aerobically. Full-length 16S rRNA amplicons were subjected to Sanger sequencing followed by BLAST search against bacterial 16S rRNA database at NCBI for taxonomic identification of each isolate. All but four were *E. coli* strains.

Rescue Experiments With Wild Type (WT) *E. coli*

Wild type *E. coli* K-12 was grown in M9 medium without any B-vitamin. Culture supernatant or conditioned medium was collected, filter sterilized and stored at −20°C. $O.D._{600}$ of cultures were measured to normalize the volume of culture supernatant to be used for ΔNadA or ΔPanC rescue. To prepare recipient cells, ΔNadA or ΔPanC was grown overnight in M9 medium with 20 μM vitamin B3 or B5, respectively. The cells were collected by centrifugation, washed with vitamin free M9 medium and resuspended in M9 medium without vitamin B3 or B5, respectively. Cells were incubated at 37°C for 6 h to deplete endogenous pools of B-vitamin. Cells were diluted in fresh medium to an $O.D._{600} < 0.001$ and 100 μL of culture were mixed with 100 μL conditioned medium derived from fecal *E. coli* isolates in a 96 well plate and growth was monitored every 20 min.

In vitro Anaerobic Cultivation

Anaerobic culture was performed in an anaerobic chamber containing 9% hydrogen and 91% nitrogen (Coy Laboratory Products, Grass Lake MI). A chemically defined medium (CDM) was used for all cultures. CDM contains 50 mM HEPES, 2.2 mM KH_2PO_4, 10 mM Na_2HPO_4, 60 mM $NaHCO_3$, 4 mM of each amino acid, except leucine (15 mM), 10 mL ATCC, Trace Mineral Supplement. CDM contained nucleoside bases (100 mg/L), inosine, xanthine, adenine, guanine, cytosine, thymidine and uracil (400 mg/L). CDM contained choline (100 mg/L), ascorbic acid (500 mg/L), lipoic acid (2 mg/L), hemin (1.2 mg/L) and myo-inositol (400 mg/L). Resazurin (1 mg/L) was added to visually monitor dissolved oxygen. The pH of the media was adjusted to 7.4. Porcine gastric mucin (1% w/v) replaced glucose. Normal B-vitamin concentrations were as follows: B1 (6 mg/L); B2 (6 mg/L); B3 (30 mg/L); B5 (16 mg/L); B6 (7 mg/L); B7 (0.2 mg/L); B9 (2 mg/L); and B12 (2.5 mg/L). Excess B-vitamin concentrations were as follows: B1 (180 mg/L); B2 (180 mg/L); B3 (900 mg/L); B5 (480 mg/L); B6 (210 mg/L); B7 (6 mg/L); B9 (60 mg/L); and B12 (75 mg/L). Approximately 1×10^6 pooled fecal bacteria were inoculated in pre-reduced CDM with and without B-vitamins (**Table 1**) and grown to approximate saturation for 3 days at 37°C.

Humanized Gnotobiotic Mice and B-Vitamin Diets

The accuracy of B-vitamin biosynthesis phenotypic predictions is robust but highly dependent on the accuracy of species enumeration based on 16S rRNA profiles. The HMP reference genome sequencing efforts, while highly useful, are heavily biased to human isolates. We therefore elected to use humanized gnotobiotic mice to study the impact of B-vitamin dietary extremes. In order to establish gnotobiotic mice harboring gut microbes with high diversity and without bias that may be contributed by a single human donor, we conducted fecal gavage using five healthy human donor samples (IRB 2009019551EP,

under written informed consent) sequentially at 1 week intervals. After the final gavage, mice were maintained for 4 weeks and fecal pellets from humanized gnotobiotic mice were collected. New germ free mice were gavaged twice (day 0 and day 2) with fecal pellets derived from humanized mice. Fecal pellets were collected on Day 7 (controls). B-vitamin supplementation in drinking water (**Table 1**) was maintained for 4 weeks and fecal pellets were collected for 16S rRNA sequencing and cecal contents were collected for LC/MS measurement of B-vitamins. Vitamin deficient and surplus diet studies were performed using a modified AIM-93M diet produced at Harlan Laboratories as has been published (Benight et al., 2011). This diet uses a vitamin free casein base, with cornstarch, maltodextrin sucrose, soybean oil and cellulose as the main source of calories, lipids, and fiber. All diets were vacuum-sealed and irradiated for sterility by the manufacturer prior to introduction into the gnotobiotic environment (Kasaikina et al., 2011). All mouse experiments were performed using protocols approved by Johns Hopkins University Animal care and Use Committee (IACUC number MO14M345).

Bacterial DNA Extraction and 16S rRNA Sequencing

Fresh mouse stool samples were collected and frozen on dry ice and stored at −80°C. The bacterial DNA was extracted using the QIAmp Fast DNA Stool Mini Kit (Qiagen) with the additional step of using a Mini-Beadbeater-16 (Biospec Products) for 5 min to ensure uniform and efficient cell lysis. Library preparation was performed following Illumina's protocols, targeting the V3–V4 region. 16S ribosomal DNA was amplified with PCR using forward:

> 5′-TCGTCGGCAGCGTCAGATGTGTATAAGAGACAG CCTACGGGNGGCWGCAG 3′, and reverse: 5′GTCTCGTGGGCTCGGAGATGTGTATAAGAGACA GGACTACHVGGGTATCTAATCC 3′.

Adapter and barcode sequences for dual indexing were also used as described in the 16S Metagenomic Sequencing Library Preparation protocol. PCR clean-up steps were done with QIAquick 96-PCR Clean-up kit (QIAgen), and library quantification was done using KAPA Library Quantification Kit for Illumina platforms (KAPA Biosystems). The Experion system (Bio-Rad) was used to analyze the DNA concentration and purity of pooled libraries. All 16S rRNA sequence reads from *in vivo* and *in vitro* analyses have been deposited at NCBI under the Bioproject accession numbers PRJNA545546 and PRJNA545535, respectively.

Predictive B-Vitamin Phenotype Profiling

Genomics-based phenotype profiling was performed using our *phylotype-to-phenotype prediction pipeline*, which allows us to translate the 16S rRNA-based phylogenetic profiles (list of phylotypes and their relative abundance) of gut microbiome samples into respective *Community Phenotype Profiles* providing tentative fractional representation of B-vitamin auxotrophy/prototrophy phenotypes in these samples. These predictions are based on genomics-based metabolic reconstruction of respective subsystems (pathways) in RAST/SEED genomic platform (Overbeek et al., 2014) as described in details (Rodionov et al., 2019). Briefly, all identified phylotypes were mapped onto a reference collection of RAST-annotated genomes representing the human microbiome. The reference collection of 2,228 genomes representing the human gut microbiota was compiled based on (i) genomes collected by the MetaHIT consortium (Qin et al., 2010); (ii) genomes of bacteria isolated from the human gastrointestinal tract collected by the human microbiome reference genome database (Human Microbiome Project Consortium, 2012); (iii) collection of ∼1,000 cultured species of the human gastrointestinal microbiota (Rajilic-Stojanovic and De Vos, 2014), and by their mapping into the PATRIC genomic database (Antonopoulos et al., 2017) and further adding of ∼250 additional genomes of their closely related species.

In silico metabolic reconstructions in SEED subsystems were based on functional gene annotation using homology-based methods and three genome context techniques: (i) clustering of genes on the chromosome (operons), (ii) co-regulation of genes by a common regulator or a riboswitch, and (iii) co-occurrence of genes in a set of related genomes. These context-based techniques were used to disambiguate paralogs with related but distinct functions (most notably transporters) and fill-in gaps ("missing genes") in the inferred biochemical pathways. The subsystems-based approach to reconstruction B-vitamin metabolism (Osterman et al., 2010) and its extension to human gut microbial species (Magnusdottir et al., 2015) were previously described.

Based on metabolic pathway topology and the genomic distribution of vitamin metabolism enzymes and transporters, we established phenotype rules describing various pathway variants for each vitamin/cofactor. Binary phenotype values ("1" for prototrophy and "0" for auxotrophy) for each out of eight analyzed B-vitamins and each of individual genomes were obtained via translation of the assigned vitamin pathway variants and combined together into a binary phenotype matrix (BPM).

We used a development version of *Phenobiome Phenotype Profiler* tool (courtesy of PhenoBiome Inc., Walnut Creek, CA, United States)[1] to map phylotypes to the reference collection of genomes based on their taxonomic assignments and calculated weights (w) at three taxonomic levels as described in more details in Rodionov et al. (2019). Briefly, this procedure includes the following steps: (i) mapping of all identified phylotypes to our reference collection of 2,228 curated genomes representing human gut microbiome; (ii) for each mapped phylotype, a phenotype value assignment (on the scale 0–1) is performed by averaging of binary phenotypes (0 or 1) for individual genomes comprising a phylogenetic neighborhood of each phylotype; (iii) multiplying a deduced phenotype value of each detected phylotype by its relative abundance (%); (iv) taking a total of obtained individual values for each replicate; and (v) averaging the obtained total amounts for all replicates within the group and computing respective STDEV (errors). For phylotypes precisely

[1] www.phenobiome.com

mapped at the species level, equal weights are assigned to genomes of all strains in the collection that belong to same species (for the purpose of averaging and probabilistic phenotype assignment). For phylotypes that could not be mapped at species level, phenotype averaging is performed at genus level applying with equal weights assigned to all species within a genus. A similar approach to averaging/weighting is applied to phylotypes mapped only at family level. Phylotypes that do not map at the family level (typically $\leq$0.5% by abundance) were excluded from phenotype prediction.

The mapped phylotypes and the reference BPM were further used to calculate Community Phenotype Matrix (CPM) capturing all individual binary phenotype values (p) multiplied by weights (w). Each value in CPM reflects a relative contribution of each phylotype to the analyzed phenotype (**Supplementary Tables S1B**, **S2B**). Each Community Phenotype Index (CPI), a probabilistic estimate of a fraction (%) of prototrophic cells in a given community that have a functional pathway for the *de novo* biosynthesis of a given B-vitamin, was calculated as total of respective CPM values (contributions) multiplied by relative abundances (A) of all individual phylotypes in a given sample:

$$\mathrm{CPI} = \sum_i A_i \sum_m w_{i,m} p_m$$

To account for variations in 16S rRNA gene copy number in different species, renormalization of OTU count data was optionally performed using pan-taxa statistics for the ribosomal RNA operon copy number provided by the rrnDB database (Stoddard et al., 2015). Each OTU's relative abundance was divided by the simple mean of all known 16S rRNA gene copy numbers for a particular species, genus or family based on the best match between the OTU's assigned taxonomy and the corresponding rrnDB taxonomy. At the end all relative abundances for each sample were rescaled to sum up to one.

LC/MS Measurements of Selected B-Vitamins in *in vitro* Cultures and Cecal Samples

Human fecal pools were used to inoculate chemically defined medium with B-vitamins (conditions as indicated in **Table 1**). The cultures were grown anaerobically for 48 h. $O.D._{600}$ was determined. Cells were collected by centrifugation and supernatants were stored separately at −80°C until further processing. At the time of sacrifice, cecal contents were collected and immediately frozen. The samples were stored at −80°C until further processing.

RESULTS

Community-Wide B-Vitamin Sharing *in vivo*: Humanized Gnotobiotic Mouse Model

To test whether the abundance of B-vitamin auxotrophs in gut microbial communities are affected by the dietary supply of these micronutrients, we have established a model using gnotobiotic mice colonized with human fecal samples. In order to increase the diversity of gut communities we sequentially introduced fecal communities one subject at a time. Fecal slurries from subject 1 was introduced into C57BL/6 germ free (GF) mice (n = 5) by oral gavage. After 1 week, fecal samples from subject two were introduced and so on for a total of five donors (**Figure 1A** and **Supplementary Table S1F**). The composition and β-diversity of communities following the first through third fecal gavage cleanly separated in PCoA plots. Subsequent gavage had no discernable impact in altering community composition (**Figure 1B**). We did not observe significant differences in microbiota diversity using sequential colonization, although the source of phylotypes (strains) in the final mice were derived from distinct donors (not shown).

To achieve greater microbiota uniformity at baseline, 1 week after the final oral gavage, feces were collected and pooled in equal mass and used to colonize new GF mice (**Figure 1A**).

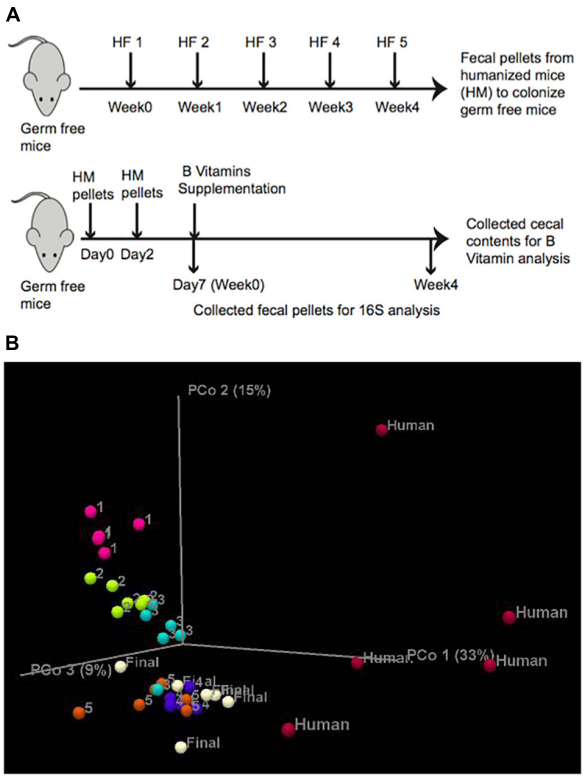

FIGURE 1 | *In vivo* experimental design. **(A)** Humanization of germ free mice was carried out by successive gavage with human feces derived from 5 healthy human subjects (HF) at 1 week intervals. After the final gavage, mice were maintained for 4 weeks and fecal pellets from humanized mice (HM) were collected. Lower panel. Germ free mice were gavaged twice with fecal pellets derived from humanized mice at an interval of 2 days. Fecal pellets were collected on Day 7 (controls). B-vitamin supplementation in drinking water (**Table 1**) was maintained for 4 weeks and fecal pellets were collected for 16S rRNA sequencing and cecal contents were collected for LC/MS measurement of B-vitamins. **(B)** PCoA analysis of mouse humanization. Unweighted Uni-Frac β-diversity of communities at different stages of humanization.

The resulting humanized gnotobiotic mice (n = 5/group) were provided a custom chow devoid of B-vitamins. B-vitamins were supplied in the drinking water in varying quantities to assess the impact of extremes in B-vitamin availability on phylogenetic and predicted phenotype profiles of gut microbial communities. Seven formulations were tested representing vitamin *D*eficiency, *N*ormal or *E*xcessive supply of *A*ll 8 B-vitamins ("AD", "AN," and AE", respectively) along with four intermediate formulations containing various levels of different subsets of these vitamins (**Table 1**). Normal B-vitamin concentrations were defined as that present in a standard diet. Mice were maintained on these diets for 4 weeks. 16S rRNA sequence analysis was performed on fecal samples collected at 0 and 4 weeks after initiating B-vitamin varied diets. The analysis of varied B-vitamin diets required the use of a custom chow that altered the gut microbiota (not shown), therefore, we focused on end-point analysis of microbial communities after 4 weeks of specified B vitamin diets.

Phylogenetic Profiling of Microbial Communities

We sequenced the V3–V4 region of 16S rRNA present in fecal communities. In order to obtain the highest precision enumeration of observed taxa, we used phylotype-based, rather than OTU-based analyses to avoid over-binning of distinct bacterial species (see Methods). This approach allowed us to map over 90% of the relative total abundance of taxa to named species with >98% sequence identity. Approximately 8% of taxa displayed sequence identity to named taxa of 95–98%, approximating genus level assignments and less than 2% of enumerated taxa could only be assigned at the family-level (**Supplementary Table S1A**). The high precision of species enumeration facilitated high confidence B-vitamin biosynthetic phenotype predictions using available reference genome sequence assemblies. We observed inter-mouse variation in the composition of fecal microbiota at baseline. The relative abundance of Akkermansia genus (∼ 27%), driven almost exclusively by a single taxon with high similarity to *Akkermansia muciniphila*, is significantly higher than typically observed in human microbiome samples (**Supplementary Figure S2**). Similarly, taxa with identity to *Muribaculum intestinale* colonized the mouse efficiently and established relative abundance higher than that observed in HMP data sets. With those exceptions, the humanized mouse model is reasonably representative of taxa and proportionality observed in human microbiota. A longitudinal comparison of phylogenetic profiles in fecal samples at baseline and at the end of 4 week on B-vitamin varied diet revealed no trends above mouse-to-mouse variations attributable to dietary effects (**Supplementary Tables S1A,B**).

Predictive Phenotype Profiling of Microbial Communities

All bacterial phylotypes enumerated by 16S rRNA analysis were assigned predicted auxotrophy/prototrophy phenotypes for eight B-vitamins (see Section Materials and Methods). Results of these predictions are illustrated for the 20 phylotypes displaying the highest average relative abundance (**Table 2**), and for the complete set of 207 mapped phylotypes (**Supplementary Table S1C**). Predicted B-vitamin prototrophy phenotypes are captured in a format of Binary Phenotype Matrix (BPM) where the probability of *de novo* synthesis of each B-vitamin-related essential cofactor is deduced from genomics-based reconstruction of respective biosynthesis/salvage pathways (Rodionov et al., 2019). The species for which phenotype predictions were available was compared to profiled species. Matching at the species (S) level achieved ∼90% coverage by relative abundance, yielding precise phenotype predictions with deduced probability values, 1 = prototrophy or 0 = auxotrophy. In relatively rare cases, phenotype microheterogeneity at the strain level was noted. This probability (phenotype index) is approximated by the average values for all available reference genomes. Thus, for *Akkermansia muciniphila*, only one out of four reference genomes has a complete pathway of B12 *de novo* synthesis (prototrophy), while the other three strains lack this pathway and rely on salvage of exogenous B12 (auxotrophy), therefore, a B12 prototrophy index is estimated by a value 0.25 (**Table 2**).

Predictive precision is generally lower for species that are not present in the current Reference Collection, necessitating matching at the genus level (G), representing ∼8.5% by relative abundance of the community. Notably, many B-vitamin phenotypes are rather conserved even at the genus level yielding predominantly binary (1 or 0) values as in *Bacteroides, Parabacteroides,* whereas *Peptoniphilus* spp., display significant strain level heterogeneity (**Table 2**). Such heterogeneity limits the predictive precision. Only ∼2% by relative abundance were mapped at low resolution to the family (F) level. No phenotype assignments were made for phylotypes mapping at higher taxonomic levels.

Notably, B12 mono-auxotrophs (12 species) and omni-prototrophs (14 species) account for the largest fraction of the analyzed microbiota with a combined average relative abundance of 47–50% and 16–19%, respectively (**Supplementary Table S1C**). Indeed, the two most abundant species, *Akkermansia muciniphila* (26%) and *Muribaculum intestinale* (10%) are B12 mono-auxotrophs (**Table 2**). Nevertheless, a number of multi-auxotrophs, most notably *Faecalibacterium prausnitzii* (average abundance ∼9.8%), are maintained in high abundance. A total of 28 species auxotrophic for at least 3 (and up to 6) distinct B-vitamins comprise ∼20% of the population by relative abundance (**Supplementary Table S1B**). The observation that auxotrophy for vitamin B12 is generally higher as compared to other B-vitamins may be explained by the fact that B12 is the only representative of B-vitamins, which is truly dispensable in many microbial species. Indeed, the main (although not the only) essential metabolic role of B12 is in the biosynthesis of methionine as cofactor of cobalamin-dependent methionine synthase MetH. However, many microbial species contain an alternative cobalamin-independent methionine synthase MetE. Greater than 60% of methionine prototrophs (among 1,750 genomes) in our mcSEED reference collection, encode only MetE (680 genomes) or both MetH and MetE (460 genomes). The latter group of organisms may still improve fitness in the presence of exogenous B12 (MetH is known to be more

TABLE 2 | Binary Phenotype Matrix of predicted B-vitamin phenotypes (prototophy) for most abundant 20 species representing microbial community established in gnotobiotic mouse model with humanized gut microbiome.

Mapping to reference collection			Predicted B-vitamin prototrophy[3]								Abund.[4]
Matching species	**Mapping level[1]**	**Genomes[2]**	**B1**	**B2**	**B3**	**B5**	**B6**	**B7**	**B9**	**B12**	**%**
Akkermansia muciniphila	**S**	4	1	1	1	1	1	1	1	0.25	26.3%
Muribaculum intestinale	**S**	1	1	1	1	1	1	1	1	0	10.2%
Faecalibacterium prausnitzii	**S**	6	0	0.67	0	0	1	0	0	1	9.8%
Bacteroides xylanisolvens	**S**	4	1	1	1	1	1	1	1	0.25	4.5%
Blautia glucerasea	**S**	1	1	0	1	0	1	0	1	1	3.6%
Parabacteroides distasonis	**S**	4	1	1	1	1	1	1	1	1	3.1%
Murimonas intestini	**F**	224	0.48	0.56	0.7	0.25	1	0.15	0.49	0.81	3.0%
Phascolarctobacterium faecium	**G**	1	1	1	0	1	1	1	1	1	2.5%
Bacteroides fragilis	**S**	6	1	1	1	1	1	1	1	1	2.3%
Bacteroides uniformis	**S**	7	1	1	1	1	1	1	1	1	2.2%
Bacteroides vulgatus	**S**	6	1	1	1	1	1	1	1	1	2.0%
Coprococcus eutactus	**S**	1	1	1	1	1	1	0	1	0	1.6%
Sutterella massiliensis	**G**	4	0	1	0	0	1	0.5	1	0	1.6%
[Eubacterium] rectale	**S**	3	1	1	1	1	1	0	0	1	1.4%
Bacteroides stercoris	**S**	2	1	1	1	1	1	1	1	1	1.2%
Blautia faecis	**G**	23	0.75	0.31	0.77	0.07	1	0.19	0.86	1	1.1%
Bacteroides stercorirosoris	**S**	1	1	1	1	1	1	1	1	0	0.9%
Bacteroides cellulosilyticus	**S**	3	1	1	1	1	1	1	1	1	0.8%
Ruminococcus champanellensis	**S**	2	0	0	1	0	1	0	1	0	0.8%
Parabacteroides goldsteinii	**S**	3	1	1	1	1	1	1	1	1	0.8%

*[1] "Mapping level": indicates whether a given phylotype (represented by species names in the first column) could be matched to our Reference Collection of genomes at the level of individual species ("S") or only at the level of a corresponding genus ("G") or family ("F"). [2] "Genomes": the number of genomes available in Reference Collection corresponding to the indicated mapping level of a given phylotype that were used for B-vitamin phenotype prediction (as explained in the next comment). [3] "B-vitamin prototrophy (Community Phenotype Index, CPI)": CPI values reflect a likelihood (probability on a scale from 0 to 1) of a given phylotype to be a prototroph for a respective B-vitamin (B1 thru B12). For phylotypes mapped at the level of species (S in column B), CPI value is estimated by averaging respective values ("1" for protortophy and "0" for auxotrophy) predicted from metabolic reconstruction of B-vitamin pathways in individual genomes of all strains/isolates of this species that are presently captured in Reference Collection. For phylotypes mapped at the level of genus, CPI values are first computed for every species within this genus (as described above) and the mean of the obtained values is assigned as a G-level CPI. A similar two-step procedure (species-level averaging) is applied to phylotypes mapped at family level. A complete set of predictions for all mapped phylotypes are provided in **Supplementary Table S1C**). [4] "Abund.": relative abundance averaged for all fecal samples obtained before the start Variable B-vitamin feeding arm of the study (Week 0), see **Supplementary Table S1A**. Gray-white values are in the range from 0 to 1.*

catalytically processive than MetE), but this requirement is much less stringent than any other B-vitamin auxotrophy. Therefore, it is not surprising that this pathway, one of the longest and most costly among B-vitamin related co-factors, is readily lost in many MetE-driven species. A completely different situation exists in many *Bacteroides* spp. and some other prominent groups of gut microbial species that possess only MetH but are at the same time B12 auxotrophs that are fully dependent on its exogenous supply (Goodman et al., 2009).

These observations led us to pose two important questions. Does the ability to carry out *de novo* synthesis of all essential co-factors dictate their abundance relative to multi-auxotrophs? Second, to what extent is the fitness of multi-auxotrophs impacted by the dietary supply of B-vitamins compared to possible B-vitamin sharing provided by prototrophic donors? To address these questions, we first performed a global comparison of Community Phenotype Signatures (CPS_ of B-vitamin auxotrophy computed for all samples obtained in B-vitamin varied diets studies. Each of the eight values (one for each vitamin) comprising CPS is calculated as a community-wide total of contributions to auxotrophy (%) by each individual phylotype. These contributions are computed by multiplication of inverse phenotype values (1 – Prototrophy Index) from **Supplementary Table S2B** over their respective relative abundances. The resulting CPS values are averaged within each dietary group (**Supplementary Table S1D**).

For nearly all B-vitamins the observed auxotrophy representation was in the 20–30% range, with a notable exception of B12 auxotrophy level (∼50%), which is consistent with a trend discussed above. Most importantly, no vitamin-specific dependencies (beyond intragroup variations) could be detected between different diets lacking B-vitamins as well as containing them in normal or excess quantities as illustrated for AD, AN, and AE dietary groups (**Figure 2**). PCoA using Bray-Curtis β-diversity of communities after 4 weeks of AD, AN, and AE did display separation (**Supplementary Figure S1A**), however, the observed differences did not show any diet-dependent trends and did not impact the frequency of B-vitamin auxotrophs.

To assess whether the observed stability manifests only at the community level as a result of gross (community-wide) averaging, we compared the relative abundance of numerous individual multi-auxotrophic species present in extreme dietary conditions (**Supplementary Table S1B**).

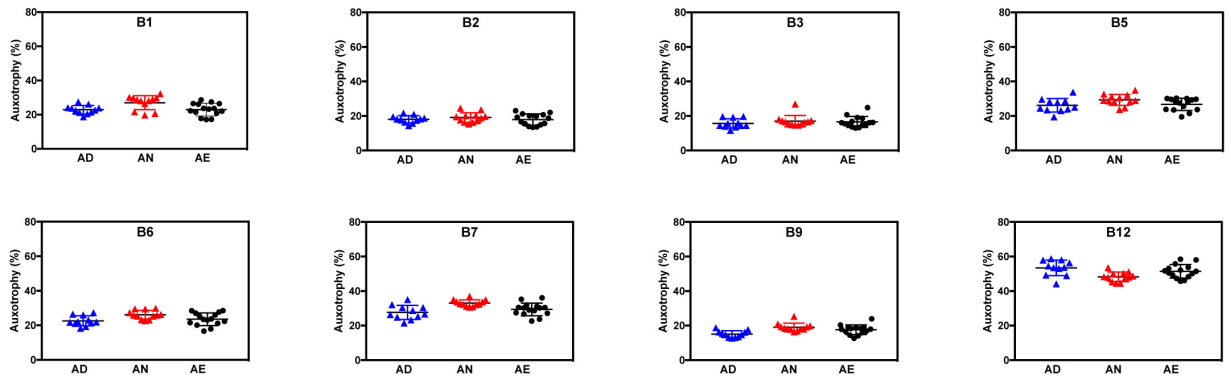

FIGURE 2 | Representation of B-vitamin auxotrophs in microbial communities from humanized gnotobiotic mice fed diets supplemented with different levels of B-vitamins. Community-wide phenotype signatures in the form of auxotrophy representation (%) for each of the eight B-vitamins (as indicated), which were deduced from 16S rRNA profiling of fecal samples (based on data in **Supplementary Tables S1A,B**), are plotted for all individual animals from three groups provided one of the three diets for 4 weeks; (*AD*) a vitamin-free chow with no B-vitamins in the drinking water or the same chow but B-vitamins *normal* (*AN*) or *excessive* (*AE*) were supplemented in drinking water (**Table 1**).

To improve statistics, we aggregated the results obtained for three vitamin-deficient diets (AD, 4D4N, and 7D1N), which have a common subset of deficient vitamins B1, B2, B5, and B7. These were compared to aggregated results from three other diets (AE, 4E4N, and 7E1N), where the same subset of B-vitamins is present in excessive amounts. Notably, of 26 reliably detectable species (≥0.01%) with unambiguous auxotrophy for at least 3 out of 4 B-vitamins (B1, B2, B5, and B7), only five showed a modest (average 0.2–0.8%) but statistically significant increase (P-value < 0.04) in the presence of excessive supply of respective vitamins (**Supplementary Table S1B**). The most consistent increase in relative abundance (∼2-fold) was observed for two B1/B2/B5/B7 auxotrophs, *Romboutsia timonensis* and *Negativibacillus massiliensis,* and one B1/B2/B5 auxotroph [*Clostridium*] *saccharolyticum* (**Supplementary Figure S3**). Most other multi-auxotrophs, including the most prominent *Faecalibacterium prausnitzii*, showed only minor and statistically insignificant differences in abundance between the two extreme dietary series (**Supplementary Table S1B**).

Overall, both types of data analysis (community-wide and species-by-species) described above yield consistent results and suggest tentative answers to both questions formulated above. Since the excessive supply of all B-vitamins (diet AE) fails to increase the overall representation of any B-vitamin auxotrophs as compared to both AN and AD diets (**Figure 2**), none of these vitamins appears to be a limiting micronutrient for respective auxotrophs. Therefore, it is unlikely that the observed overall higher representation of prototrophs is defined solely by their independence from the supply of exogenous B-vitamins but rather driven by other fitness determinants. Additionally, the observation that B-vitamin-deficient diet did not drive decreases in the overall representation of auxotrophs suggests that they are not dependent on dietary vitamin supply and capable of satisfying their micronutrient requirements by the salvage of B-vitamins released by prototrophic members of the community.

LC/MS Measurements of Selected B-Vitamins in Unfractionated Cecal Samples

Our ability to interpret the diet-dependent phylogenetic and phenotype profiling results is contingent on the assumption that extreme changes in dietary B-vitamin supply (excess or deficiency) may indeed affect the availability of these micronutrients in the distal gut. Given the unknown efficiency of intestinal absorption, which may differ for different vitamins, we have tested this assumption by LC/MS measurements of four reliably detected B-vitamins (B1, B2, B3, and B5) in cecal samples collected from all seven groups of mice (**Supplementary Table S1E**). With the exception of niacin (B3), the measured levels of B-vitamins in all samples displayed changes that were in qualitative agreement with their dietary supply (**Figure 3**). The largest fold-change between all three diets was observed for vitamins B1 and B5. The highest basal levels (in AD diet) was observed for vitamins B2 and B3, likely reflecting the higher net production of these vitamins by the microbial community. This effect may be masked by a particularly active absorption by the host combined with robust biogenesis (and sharing) by prototrophs, e.g., vitamin B3. Furthermore, the measured B-vitamin levels do not distinguish intracellular and extracellular pools of cecal material. Despite these limitations, the observed trends generally confirm that B-vitamin levels can be manipulated in the distal gut, thus supporting that microbiota-wide vitamin sharing contributes to community stability in the face of varying dietary supply of these micronutrients.

Community-Wide B-Vitamin Sharing *in vitro*: Anaerobic Fecal Culture Model

We used *in vitro* anaerobic culturing to further test the vitamin sharing hypothesis in a simplified model system, which allows us to eliminate uncertainties related to vitamin absorption or sharing by the host. We performed a series of *in vitro* anaerobic cultivation studies of fecal pools, derived from four

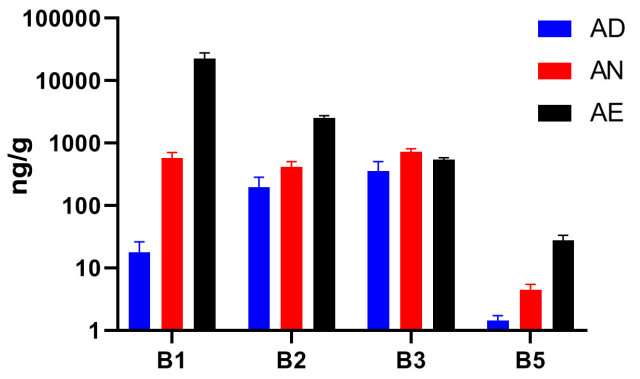

FIGURE 3 | Levels of selected B-vitamins in cecal samples from humanized gnotobiotic mice fed diets supplemented with varying B-vitamins. The levels of four vitamins (B1, B2, B3, and B5) were determined by LC–MS in the cecal samples from mice fed the same three diets (AD, AN, and AE) as in **Figure 2** (using 3 replicates for each of the three diets) and plotted as averaged values (in ng/g cecal material) with *SD* as error bars.

human subjects used for mouse humanization. We employed a chemically defined media (CDM) supplemented with porcine gastric mucin to enhance bacterial diversity. We generated seven media compositions representing deficiency, normal or excessive supply of different vitamin subsets (**Table 1**), to mirror the *in vivo* studies. Approximately 1×10^6 fecal bacteria were inoculated in pre-reduced (CDM + mucin) media. For each media composition, the community outgrowth was conducted in replicate ($n = 6$).

Phylogenetic Profiling

We sequenced the V3–V4 region of 16S rRNA present in fecal culture collected after 48 h of anaerobic growth, which led to ∼10 doublings. Data analysis was performed as for *in vivo* samples and yielded similar precision in mapping. More than 90% of the total relative abundance displayed >98% identity to a named species. The phylogenetic distribution of *in vitro* cultures was distinct from those observed *in vivo*. A comparison of the two datasets (**Supplementary Figure S2**) shows that only 5 out of the most abundant 20 genera are common to both. PCoA of resulting communities in AD, AN, and AE cultures failed to display any diet-dependent separation that achieved statistical significance between groups (**Supplementary Figure S1B**). A rank order of these shared families is also quite different, with the most notable decrease in representation of *Akkermansia*, *Muribaculum*, *Flavonifractor* and *Escherichia* show the most substantial expansion in the *in vitro* subcultures. We noted that variation between replicate cultures ($n = 6$) was greater than that observed *in vivo*. Despite this, no statistically significant media-dependent differences or even trends in phylogenetic profiles could be detected over the entire range of B-vitamin levels in the growth media (**Supplementary Table S2A**).

Predictive Phenotype Profiling

The assignment of auxotrophy/prototrophy phenotypes for eight B-vitamins over the entire set of enumerated species (**Supplementary Tables S2B,C**) and computing community-wide phenotype signatures (**Supplementary Table S2D**) were performed as described for *in vivo* samples. Among the 95 taxa, accounting for 99.8% of reads, 81 (∼95%) were mapped at the level of species and 11 (∼4.5%) at the level of genus, leaving only a minor fraction unmapped or mapped at the family level (∼0.2% each). Notably, despite substantially different phylogenetic profiles of *in vitro* communities, B-vitamin phenotype signatures showed many similar trends, compared to those observed *in vivo*. Thus, the largest fraction of *in vitro* communities was represented by B12 mono-auxotrophs (10 species; ∼60% by relative abundance) (**Supplementary Table S2C**). Likewise, multi-auxotrophs (26 species, 3–8 B-vitamins) accounted for ∼26–27% of microbial communities. As in case of B12 mono-auxotrophs, the most abundant taxa in this category (**Table 3**) were distinct from those observed *in vivo*. Thus, *Flavonifractor plautii*, *Peptoniphilus grossensis* and *Finegoldia magna* are among the most prominent multi-auxotrophs *in vitro*, but not *in vivo* (compare with **Table 2**), while *Faecalibacterium prausnitzii,* the top multi-auxotroph *in vivo*, is below the detection level *in vitro*. The unique communities formed *in vitro* provided an independent means of comparing trends in B-vitamin prototrophy/auxotrophy representation to better distinguish host-dependent vs. microbial-dependent effects. Despite notable phylogenetic differences, the phenotype signatures of both *in vivo* and *in vitro* microbial communities are remarkably similar for nearly all B-vitamins except B12 (**Supplementary Figure S4**). Aggregated data on auxotrophy representation spanning all diets and time points, vary in a much narrower range as compared to microbial gut samples from the human microbiome project (HMP) dataset (**Figure 4**).

Variations of media B-vitamin provisions in the *in vitro* cultures did not cause any significant changes at the level of community phenotype signatures in AD, AN, and AE media (**Figure 5**). Auxotrophy representation remained at the level of 20–30% for most B-vitamins and 10–15% for B9 (**Supplementary Table S2D**). The fraction of B12 auxotrophs in the community is substantially higher (65–75%), including mono- and multi-auxotrophs. We compared individual multi-auxotrophs in the cultures (AD, 4D4N, 7D1N) and (AE, 4E4N, and 7E1N). The growth rates of cultures in all media were comparable and no discernable differences in $O.D._{600}$ were evident. None of these taxa displayed significant changes in relative abundance between extremes in B-vitamin provision in culture media (**Supplementary Table S2C**). We conclude that the observed higher representation of B12 mono-auxotrophs and prototrophs over multi-auxotrophs is not defined solely by the difference in their B-vitamin requirements, since a drastic increase of these (apparently non-limiting) micronutrients in the AE growth media as compared to AN media does not provide any detectable fitness advantages to the latter subset of species. B-vitamin requirements of multi-auxotrophic species are fully satisfied by vitamins released (excreted) by their prototrophic neighbors, as the observed auxotrophy representation is not decreased in B-vitamin-deficient AD media (**Figure 5**). These observations corroborated by direct metabolic

TABLE 3 | Binary Phenotype Matrix of predicted B-vitamin phenotypes (prototophy) for most abundant 20 species representing microbial community established in anaerobic subculturing model of human gut microbiome.

Mapping to reference collection			Predicted B-vitamin prototrophy[3]								Abund.[4]
Matching species	**Mapping level[1]**	**Genomes[2]**	**B1**	**B2**	**B3**	**B5**	**B6**	**B7**	**B9**	**B12**	**%**
Bacteroides thetaiotaomicron	**S**	3	1	1	1	1	1	1	1	0	25.5%
Escherichia fergusonii	**S**	5	1	1	1	1	1	1	1	0	21.0%
Flavonifractor plautii	**S**	3	0	0	0	0	0	0	0	1	6.9%
Peptoniphilus grossensis	**S**	2	0	1	0.5	0	0	0	1	0	6.7%
Finegoldia magna	**S**	6	1	0	0	0	1	0	1	0	5.0%
Bacteroides faecis	**S**	2	1	1	1	1	1	1	1	0	4.5%
Bacteroides vulgatus	**S**	6	1	1	1	1	1	1	1	1	3.1%
Bacteroides caccae	**S**	3	1	1	1	1	1	1	1	0	3.1%
Clostridium perfringens	**S**	4	1	1	1	0	0	0	1	1	2.5%
Phascolarctobacterium faecium	**G**	1	1	1	0	1	1	1	1	1	1.8%
Bacteroides massiliensis	**S**	1	1	1	1	1	1	1	1	0	1.7%
Bacteroides uniformis	**S**	7	1	1	1	1	1	1	1	1	1.7%
Agathobaculum desmolans	**S**	1	0	0	0	0	0	0	0	1	1.2%
Akkermansia muciniphila	**S**	4	1	1	1	1	1	1	1	0.25	1.2%
Pseudoflavonifractor phocaeensis	**G**	3	0	0.5	0	0	0	0	0	0.5	1.2%
Bacteroides ovatus	**S**	7	1	1	1	1	1	1	1	0	1.0%
Parabacteroides merdae	**S**	4	1	1	1	1	1	1	1	1	0.9%
Eggerthella lenta	**S**	3	1	0	0	0.67	1	0	1	0	0.6%
Flintibacter butyricus	**S**	3	0	0	0	0	0	0	0	1	0.2%
Pseudoflavonifractor capillosus	**S**	1	0	0	0	0	0	0	0	1	0.2%

[1] *"Mapping level": see comments to* ***Table 2****.* [2] *"Genomes": see comments to* ***Table 2****.* [3] *"B-vitamin prototrophy (Community Phenotype Index, CPI)": see comments to* ***Table 2****. A complete set of predictions for all mapped phylotypes are provided in* ***Supplementary Table S2B****).* [4] *"Ave. abundance": relative abundance averaged for samples obtained in media with normal levels of all B-vitamins (AN, n = 6), see* ***Supplementary Table S2A****. Gray-white values are in the range from 0 to 1.*

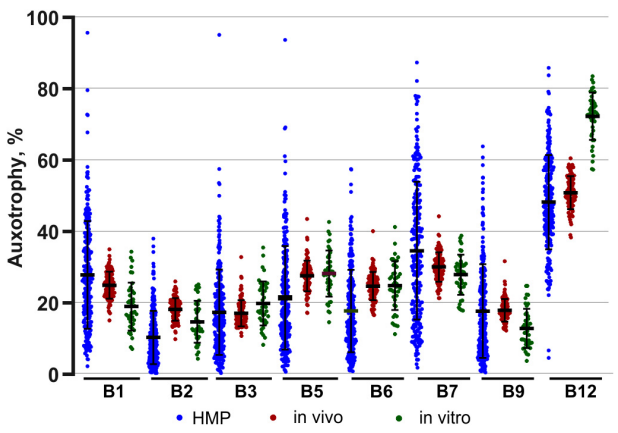

FIGURE 4 | Comparison of B-vitamin auxotrophy phenotype signatures of *in vivo* and *in vitro* microbial communities and samples from human microbiome project (HMP). Phenotype signatures computed for samples obtained in all tested diets/media are shown by dot plots next to the aggregated signatures computed by the same approach for a subset of 313 fecal HMP samples.

measurements (see below) provided additional evidence in support of our central hypothesis that prototrophic microbes actively share B-vitamins enabling the sustained fitness of B-vitamin auxotrophs.

One of the important limitations of 16S rRNA-based community profiling is a well-appreciated non-equivalence of the measured relative abundance of reads and relative abundance of respective phylotypes. This is primarily due to substantial variations in 16S rRNA copy number between different species (and even strains). Indeed, renormalization on species-specific copy number data (see Section Materials and Methods) has an appreciable effect on phylogenetic profiles and respective phenotype profiles, both *in vivo* and *in vitro* (**Supplementary Figure S5** and **Supplementary Table S3**). Notably, this renormalization did not reveal any new trends in the diet-dependent representation of auxotrophs in either dataset. For consistency, the illustrations in this article are shown without renormalization, which by itself, is not a perfect procedure due to incomplete and imprecise nature of 16S rRNA operon multiplicity data.

LC/MS Measurements of Selected B-Vitamins

To leverage the key advantage of host independent effects of B-vitamin sharing in *in vitro* communities we measured the quantities of the same four B-vitamins (B1, B2, B3, and B5) in spent culture supernatants and cell pellets from samples grown in three media AD, AN, and AE (**Supplementary Table S2E** and **Figure 6**). A comparison of fresh AD media (**Figure 6A**) and supernatants from samples grown in this media (**Figure 6B**) shows a net increase in the levels of all vitamins

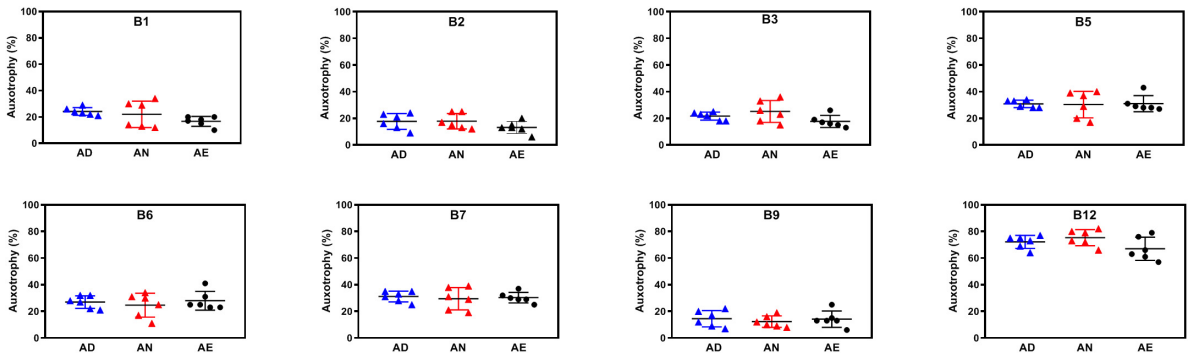

FIGURE 5 | Representation of B-vitamin auxotrophs in microbial communities in anaerobic subcultures grown with different levels of B-vitamins. Community-wide phenotype signatures in the form of auxotrophy representation (%) *for* each of the eight B-vitamins (as indicated), which were deduced from 16S rRNA profiling of microbial cultures grown in defined media containing no added B-vitamins (*AD* – all deficient) and the same media supplemented with *normal* (*AN*) or *excessive* (*AE*) dietary levels of all eight B-vitamins (**Table 1**), are plotted for each replicate (n = 6).

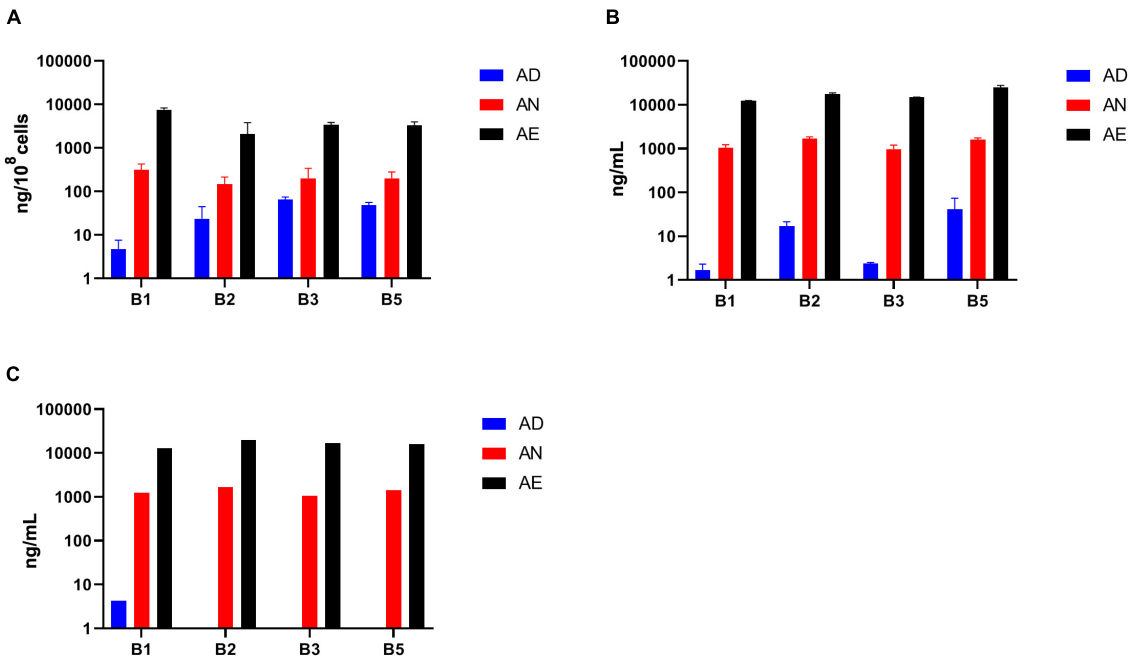

FIGURE 6 | Levels of selected B-vitamins measured by LC-MS in samples of anaerobic subcultures grown with different levels of B-vitamins. **(A)** The levels of four vitamins (B1, B2, B3, and B5) in cell pellet samples (using three replicates for each of the three diets) from *in vitro* subcultures grown in the same three media (AD, AN, AE) as in **Figure 5**) and plotted as averages (ng/10^8 cells) with *SD* as error bars. **(B)** B-vitamin measurements of respective supernatants (ng/mL). **(C)** B-vitamin measurements of respective media prior to inoculation (ng/mL).

except B1 supporting the conclusion about the availability of B-vitamins in the shared extracellular pool, which in the case of *in vitro* cultures could originate only from respective prototrophs. This effect appears to be masked for B1 by its unexpected presence, albeit in relatively low quantities, in the fresh AD media. Not surprisingly, the quantities of all four B-vitamins in the cell pellets (**Figure 6C**) and supernatants (**Figure 6B**) of samples grown in AN and AE media showed no significant difference compared to the respective fresh media. These levels were, however, substantially higher than samples grown under vitamin deficiency. Taken together with unaltered phenotype profiles (**Figure 5**), these results are consistent with the conclusion that B-vitamins are not limiting nutrients for auxotrophic species in these microbial communities under the tested growth conditions.

B-VITAMIN SHARING *IN VITRO* USING *E. COLI* K-12 KNOCKOUT STRAINS

To assess feasibility of vitamin exchange in a simple *in vitro* model, we used two knockout (KO) strains Δ*nadA* (B3

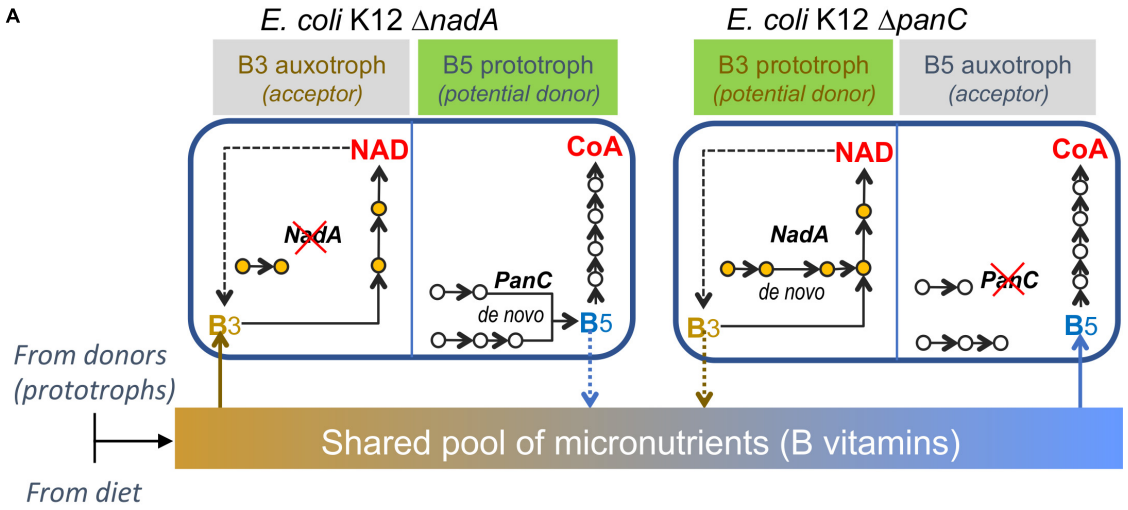

B

Acceptor strains	Vitamin supplementation			Spent media supplementation by potential donors (*E.coli*, isolates)					
	none	B3 (≥10 nM)	B5 (≥2.5 nM)	K12 WT	Isolate P20	Isolate P26	Isolate P33	Isolate P34	Isolate P43
E. coli K12 Δ*nadA*	−	+	−	−	+	−	+	+	−
E. coli K12 Δ*panC*	−	−	+	+	+	+	+	+	−

FIGURE 7 | Modeling vitamin sharing *in vitro*. **(A)**. B-vitamin sharing hypothesis illustrated by the example of two *E. coli* K-12 knockout strains, B3 (ΔNadA) and B5 (ΔPanC) auxotrophs. **(B)**. Summary of growth rescue studies using the same *E. coli* K12 ΔNadA and ΔPanC tester strains as auxotrophic acceptors in B-vitamin-free liquid media supplemented by respective vitamins or supernatants from the cultures of *E. coli,* wild-type (K12-WT) or selected isolates from human fecal samples (**Figure 1** and **Supplementary Figure S1A** for additional data).

auxotroph) and Δ*panC* (B5 auxotroph) from the Keio *E. coli* mutant collection (Baba et al., 2006) as acceptors of respective vitamins and Δ*uxaC* strain (prototroph for both vitamins) as a potential donor (**Figure 7A**). The quantities of exogenous B-vitamin required to rescue and support maximal growth density of Δ*nadA* and Δ*panC* strains in M9 media are relatively low for both strains (2.5 nM and 10 nM, respectively (**Supplementary Figure S6A**). The ability of a prototroph to rescue the growth of these auxotrophs was tested by two methods: (i) by streaking Δ*nadA* and Δ*panC* strains side-by-side with Δ*uxaC* strain on M9 plates lacking B3 and B5; and (ii) by cultivating auxotrophic strains Δ*nadA* or Δ*panC* in liquid media lacking B3 and B5 and supplemented by supernatants of a prototrophic Δ*uxaC* culture grown in the same media for 6 h at 37°C. Both tests resulted in successful rescue of Δ*panC* but not Δ*nadA* strain (**Supplementary Figure S6B**), which may reflect relatively higher B3 requirement of Δ*nadA* strain and/or lower B3 sharing capacity of the prototrophic Δ*uxaC* strain. A potential strain-dependent ability of wild-type *E. coli* to function as B-vitamin donors was further tested using multiple *E. coli* isolates selected using CDM without B3 or B5 (B3 and B5 prototrophs) from human fecal samples. Surprisingly, the sequencing of full-length 16S rRNA revealed that the great majority of isolates recovered on solid media lacking B3 and B5 were *E. coli,* despite the fact that this species was not observed in appreciable abundance in the fecal inoculum (**Supplementary Table S1F**). We speculate that the selection procedure particularly the colony isolation step on solid media may have favored the recovery of this taxonomic group. The latter (liquid culture-based) approach to growth supplementation, showed that while most isolates tested (∼90) displayed some rescue capacity, the efficiency of growth rescue of either auxotroph varied significantly among the tested isolates (**Figure 7B** and **Supplementary Figures S6C,D**) suggesting that B-vitamin prototroph sharing capability in this proof of concept experiment is a quantitative trait controlled by yet unknown regulatory mechanisms.

DISCUSSION

This study of syntrophic metabolism of B-vitamins was to a large extent inspired by groundbreaking work by Goodman et al. (2009) which provided the first strong evidence of syntrophy in metabolism of vitamin B12 in the gut microbial community. Here, we extend the range of tested vitamins focusing mostly on those B-vitamins (B1, B2, B3, and B5) that (unlike B12) need to undergo a multi-step metabolic transformation upon uptake to yield functionally active essential cofactors. Therefore, the respective auxotrophs may be considered as having

partial (downstream) pathways involved in "distributed" (or syntrophic) biogenesis of respective essential cofactors (TPP, FMN/FAD, NAD/NADP, and CoA). The analysis of multiple B-vitamin auxotrophies allowed us to define a widespread form of syntrophy as a basis of mutualism in host-associated microbial communities.

We demonstrate that feeding humanized gnotobiotic mice diets lacking all or some B-vitamins does not alter the fractional representation of B1, B2, B3, B5, B6, B7, B9 or B12 auxotrophic species (including numerous multi-auxotrophs). Our *in vivo* and *in vitro* model studies of human gut microbial communities showed that the fitness of B-vitamin auxotrophs is unaltered by B-vitamin depleted or replete growth conditions. This result strongly supports our hypothesis that the maintenance of B-vitamin auxotrophic segment of microbial populations occurs *via* community-wide B-vitamin sharing through as yet unknown mechanisms. These studies do not allow us to unambiguously state to what extent the observed vitamin sharing is driven by genuine excretion vs. cell lysis, we speculate that at least some B-vitamin prototrophs possess a general capacity to secrete B-vitamins into the extracellular milieu that are subsequently taken up by auxotrophic species thus ensuring their maintenance in the community.

We also tested whether the excess of B-vitamins exerts a selective pressure that favors B-vitamin auxotrophs whose fitness is no longer constrained by B-vitamin limitations and competition for these key substrates. The provision of excess B-vitamins did not impact the frequency of auxotrophs in the gut microbiota *in vitro* or *in vivo*. Taken together, these results provide an impressive example of microbiota stability in the face of extreme essential nutrient deprivation or excess. We speculate that in the absence of B-vitamin sharing, microbiota would be unable to harbor stable communities featuring auxotrophic species. In the event of periods of fasting or dietary limitations that may have been commonplace throughout evolutionary history, may have selected for B-vitamin sharing to maintain stable communities and functionally interacting taxa. It is likely that the evolution of B-vitamin sharing preceded the widespread loss of genes encoding B-vitamin biosynthetic capacity, thereby enabling gene loss of these pathways. A sizeable representation of auxotrophs (at least 20–30% by abundance) may reflect that B-vitamin sharing is highly efficient. These results are consistent with the black queen hypothesis that posits that fitness gain accompanying gene loss is frequency dependent, demanding the B-vitamin donors must remain in sufficient abundance in communities to ensure that auxotrophs are not subject to negative selection (Morris et al., 2012). It will be of interest to evaluate this further by colonization of GF mice with defined communities comprised of B-vitamin prototrophs/auxotrophs in various proportions under vitamin restricted diets to more directly establish the dependency of B-vitamin auxotrophs on adequate abundance of prototrophs.

Our proof of concept studies on growth supplementation of *E. coli* tester strains (B3 and B5 auxotrophs), illustrates B-vitamin sharing, in a simple model system that not all prototrophs (and/or not in all conditions) display uniform efficiency as B-vitamin donors (**Supplementary Figure S6C**). Further studies are required to elucidate genomic features (e.g., a particular kind of vitamin-sharing transporters as well as regulatory and physiological/biochemical factors) defining this capability across major prototrophs in gut microbial communities. Notably, the observed higher propensity for B5 vs. B3 sharing may reflect a fundamental difference in pathway topology. Indeed, pantothenate (B5) is a true intermediate in Coenzyme A biosynthesis, whereas niacin (B3) is a degradation product of the cofactor, NAD (**Figure 7A**). Therefore, one would expect the extent of NAD degradation and, thus, niacin accumulation (followed by recycling and/or excretion) to vary between strains and growth conditions.

It is important to note that the extreme stability was observed in this study for a particular microbial consortium with relatively low level of auxotrophy for nearly all B-vitamins. Without further studies, it may not be generalized to other gut microbial consortia, e.g., with a relatively high content of B-vitamin auxotrophs, which, based on our analysis of numerous HMP samples (Rodionov et al., 2019), is not uncommon. The latter notion may be illustrated by the comparison of B-vitamin auxotrophy levels observed in both *in vivo* and *in vitro* microbial communities (over the entire range of B-vitamin levels in tested diets/media) with a much wider distribution of the same phenotypes over 313 analyzed human fecal samples from HMP dataset (**Figure 4**).

The established extreme stability of gut microbiota in the face of extremes of B-vitamin bioavailability represent an important aspect of metabolite sharing occurring in host-associated microbial communities. This type of cooperative mutualism is likely to be commonplace in gut communities, which extends beyond B-vitamins *per se,* and may be viewed as a component of a large network of cooperative interactions involving cross-feeding and sharing of key metabolites. These interactions enable and highlight the capacity of bacterial communities to carry out complex biochemical transformations exceeding the capacity of its individual components. This study combined *in silico* phenotype predictions with experimental analysis of gut microbial communities, in this case focused on B-vitamin sharing. The curation and reconstruction of additional biochemical pathways encoded in gut resident genomes is highly expandable and may be effectively applied to a wide variety of studies focused on diet-microbiota, microbe-microbe and microbiota-host interactions.

B-vitamin auxotrophs are not limited to gut microbiota and exist in all human-associated microbiomes. An open question of interest relates to the efficiency of B-vitamin sharing in other domains of the human body, e.g., skin, where lower density communities and constrained diffusion of secreted factors may hamper cross-feeding phenomena. It also remains unclear whether B-vitamin donor phenotypes are broadly shared among prototrophs or a community service provided by subset of the community. Identification of gene functions that secrete B-vitamins is expected to greatly enhance our ability to address this open question. The evolution of B-vitamin auxotrophy in gut microbiota is thought to be the result of consistent B-vitamin availability from diet and/or microbial sources, permitting

B-vitamin pathway gene shedding to occur. In the context of the studies presented here, we may further speculate that the overall "fitness" of microbiota is enhanced by an untold number of functional interactions and metabolic dependencies that make the whole greater than the sum of its parts. In the absence of mechanisms to share B-vitamins, communities, even in short-term deprivation of B-vitamin availability would be expected to result in the loss of auxotrophic species, resulting in the large-scale disruption of functional interactions occurring in a well-balanced community.

ETHICS STATEMENT

All mouse experiments were performed using protocols approved by Johns Hopkins University Animal Care and Use Committee (IACUC number MO14M345).

AUTHOR CONTRIBUTIONS

SP and DP conceived and designed the research project. DP and HD performed the animal studies. VS and DT performed *in vitro* studies and DNA extraction for sequence analysis. DR, SL, and AO performed metabolic reconstructions and phenotype predictions. SI performed phylotype-to-phenotype computational analysis. SP and AO wrote the manuscript. All authors read and approved the final manuscript.

FUNDING

This research was supported by the NIH (R01 GM108527-02 to SP and R01 DK030292-35 to AO) and the Russian Science Foundation (Grant #14-14-00289 to DR).

ACKNOWLEDGMENTS

We thank Bob Olson from the SEED/RAST development team at Argonne National Lab for dedicated support of the SEED-based genomic analyses. We are grateful to PhenoBiome Inc., (Walnut Creek, CA, United States, www.phenobiome.com) for providing us with the access to a development version of *Phenobiome Phenotype Profiler* tool. We also thank Matvei Khoroshkin and Alexandr Arzamasov for assistance with metabolic reconstruction of vitamin biosynthetic pathways in reference bacterial genomes. We are grateful to Sid Venkatesh and Jiye Cheng in Prof. Jeffrey Gordon's lab (WUSTL) for performing LC-MS analysis of vitamins in the *in vitro* and *in vivo* samples.

SUPPLEMENTARY MATERIAL

The Supplementary Material for this article can be found online at: https://www.frontiersin.org/articles/10.3389/fmicb.2019.01485/full#supplementary-material

REFERENCES

Antonopoulos, D. A., Assaf, R., Aziz, R. K., Brettin, T., Bun, C., Conrad, N., et al. (2017). PATRIC as a unique resource for studying antimicrobial resistance. *Brief. Bioinform.* [Epub ahead of print]

Baba, T., Ara, T., Hasegawa, M., Takai, Y., Okumura, Y., Baba, M., et al. (2006). Construction of *Escherichia coli* K-12 in-frame, single-gene knockout mutants: the Keio collection. *Mol. Syst. Biol.* 2:2006.0008.

Backhed, F., Ley, R. E., Sonnenburg, J. L., Peterson, D. A., and Gordon, J. I. (2005). Host-bacterial mutualism in the human intestine. *Science* 307, 1915–1920. doi: 10.1126/science.1104816

Benight, N. M., Stoll, B., Chacko, S., Da Silva, V. R., Marini, J. C., Gregory, J. F., et al. (2011). B-vitamin deficiency is protective against DSS-induced colitis in mice. *Am. J. Physiol. Gastrointest. Liver Physiol.* 301, G249–G259. doi: 10.1152/ajpgi.00076.2011

Blanton, L. V., Charbonneau, M. R., Salih, T., Barratt, M. J., Venkatesh, S., Ilkaveya, O., et al. (2016). Gut bacteria that prevent growth impairments transmitted by microbiota from malnourished children. *Science* 351:aad3311. doi: 10.1126/science.aad3311

Chassard, C., and Bernalier-Donadille, A. (2006). H2 and acetate transfers during xylan fermentation between a butyrate-producing xylanolytic species and hydrogenotrophic microorganisms from the human gut. *FEMS Microbiol. Lett.* 254, 116–122. doi: 10.1111/j.1574-6968.2005.00016.x

Faith, J. J., Rey, F. E., O'donnell, D., Karlsson, M., Mcnulty, N. P., Kallstrom, G., et al. (2010). Creating and characterizing communities of human gut microbes in gnotobiotic mice. *ISME J.* 4, 1094–1098. doi: 10.1038/ismej.2010.110

Fischbach, M. A., and Sonnenburg, J. L. (2011). Eating for two: how metabolism establishes interspecies interactions in the gut. *Cell Host Microbe* 10, 336–347. doi: 10.1016/j.chom.2011.10.002

Goodman, A. L., Mcnulty, N. P., Zhao, Y., Leip, D., Mitra, R. D., Lozupone, C. A., et al. (2009). Identifying genetic determinants needed to establish a human gut symbiont in its habitat. *Cell Host Microbe* 6, 279–289. doi: 10.1016/j.chom.2009.08.003

Human Microbiome Project Consortium (2012). A framework for human microbiome research. *Nature* 486, 215–221. doi: 10.1038/nature11209

Kasaikina, M. V., Kravtsova, M. A., Lee, B. C., Seravalli, J., Peterson, D. A., Walter, J., et al. (2011). Dietary selenium affects host selenoproteome expression by influencing the gut microbiota. *FASEB J.* 25, 2492–2499. doi: 10.1096/fj.11-181990

Magnusdottir, S., Ravcheev, D., De Crecy-Lagard, V., and Thiele, I. (2015). Systematic genome assessment of B-vitamin biosynthesis suggests co-operation among gut microbes. *Front. Genet.* 6:148. doi: 10.3389/fgene.2015.00148

Mahowald, M. A., Rey, F. E., Seedorf, H., Turnbaugh, P. J., Fulton, R. S., Wollam, A., et al. (2009). Characterizing a model human gut microbiota composed of members of its two dominant bacterial phyla. *Proc. Natl. Acad. Sci. U.S.A.* 106, 5859–5864. doi: 10.1073/pnas.0901529106

Morris, J. J., Lenski, R. E., and Zinser, E. R. (2012). The black queen hypothesis: evolution of dependencies through adaptive gene loss. *mBio* 3:e00036-12. doi: 10.1128/mBio.00036-12

Osterman, A., Overbeek, R., and Rodionov, D. (2010). "The Use of Subsystems to Encode Biosynthesis of Vitamins and Cofactors," in *Comprehensive Natural Products II*, eds M. Lew and L. Hung-Wen (Oxford: Elsevier), 141–159. doi: 10.1016/b978-008045382-8.00710-3

Overbeek, R., Olson, R., Pusch, G. D., Olsen, G. J., Davis, J. J., Disz, T., et al. (2014). The SEED and the Rapid Annotation of microbial genomes using subsystems technology (RAST). *Nucleic Acids Res.* 42, D206–D214.

Qin, J., Li, R., Raes, J., Arumugam, M., Burgdorf, K. S., Manichanh, C., et al. (2010). A human gut microbial gene catalogue established by metagenomic sequencing. *Nature* 464, 59–65. doi: 10.1038/nature08821

Rajilic-Stojanovic, M., and De Vos, W. M. (2014). The first 1000 cultured species of the human gastrointestinal microbiota. *FEMS Microbiol. Rev.* 38, 996–1047. doi: 10.1111/1574-6976.12075

Reichardt, N., Vollmer, M., Holtrop, G., Farquharson, F. M., Wefers, D., Bunzel, M., et al. (2018). Specific substrate-driven changes in human faecal microbiota composition contrast with functional redundancy in short-chain fatty acid production. *ISME J.* 12, 610–622. doi: 10.1038/ismej.2017.196

Rey, F. E., Faith, J. J., Bain, J., Muehlbauer, M. J., Stevens, R. D., Newgard, C. B., et al. (2010). Dissecting the in vivo metabolic potential of two human gut acetogens. *J. Biol. Chem.* 285, 22082–22090. doi: 10.1074/jbc.M110.117713

Rey, F. E., Gonzalez, M. D., Cheng, J., Wu, M., Ahern, P. P., and Gordon, J. I. (2013). Metabolic niche of a prominent sulfate-reducing human gut bacterium. *Proc. Natl. Acad. Sci. U.S.A.* 110, 13582–13587. doi: 10.1073/pnas.1312524110

Rodionov, D. A., Arzamasov, A. A., Khoroshkin, M. S., Iablokov, S. N., Leyn, S. A., Peterson, S. N., et al. (2019). Micronutrient requirements and sharing capabilities of the human gut microbiome. *Front. Microbiol.* 10:1316. doi: 10.3389/fmicb.2019.01316

Romine, M. F., Rodionov, D. A., Maezato, Y., Osterman, A. L., and Nelson, W. C. (2017). Underlying mechanisms for syntrophic metabolism of essential enzyme cofactors in microbial communities. *ISME J.* 11, 1434–1446. doi: 10.1038/ismej.2017.2

Samuel, B. S., and Gordon, J. I. (2006). A humanized gnotobiotic mouse model of host-archaeal-bacterial mutualism. *Proc. Natl. Acad. Sci. U.S.A.* 103, 10011–10016. doi: 10.1073/pnas.0602187103

Sonnenburg, J. L., Chen, C. T., and Gordon, J. I. (2006). Genomic and metabolic studies of the impact of probiotics on a model gut symbiont and host. *PLoS Biol.* 4:e413. doi: 10.1371/journal.pbio.0040413

Stoddard, S. F., Smith, B. J., Hein, R., Roller, B. R. K., and Schmidt, T. M. (2015). *rrn*DB: improved tools for interpreting rRNA gene abundance in bacteria and archaea and a new foundation for future development. *Nucleic Acids Res.* 43, D593–D598. doi: 10.1093/nar/gku1201

Wu, M., Mcnulty, N. P., Rodionov, D. A., Khoroshkin, M. S., Griffin, N. W., Cheng, J., et al. (2015). Genetic determinants of in vivo fitness and diet responsiveness in multiple human gut *Bacteroides*. *Science* 350:aac5992. doi: 10.1126/science.aac5992

Ze, X., Duncan, S. H., Louis, P., and Flint, H. J. (2012). Ruminococcus bromii is a keystone species for the degradation of resistant starch in the human colon. *ISME J.* 6, 1535–1543. doi: 10.1038/ismej.2012.4

Conflict of Interest Statement: The authors declare that the research was conducted in the absence of any commercial or financial relationships that could be construed as a potential conflict of interest.

Copyright © 2019 Sharma, Rodionov, Leyn, Tran, Iablokov, Ding, Peterson, Osterman and Peterson. This is an open-access article distributed under the terms of the Creative Commons Attribution License (CC BY). The use, distribution or reproduction in other forums is permitted, provided the original author(s) and the copyright owner(s) are credited and that the original publication in this journal is cited, in accordance with accepted academic practice. No use, distribution or reproduction is permitted which does not comply with these terms.

frontiers in Microbiology

ORIGINAL RESEARCH
published: 03 July 2019
doi: 10.3389/fmicb.2019.01518

Fecal Microbiome Data Distinguish Liver Recipients With Normal and Abnormal Liver Function From Healthy Controls

Hai-Feng Lu[1†], Zhi-Gang Ren[2,3†], Ang Li[1,2], Hua Zhang[1], Shao-Yan Xu[3], Jian-Wen Jiang[3,4,5], Lin Zhou[3,4], Qi Ling[3,4], Bao-Hong Wang[1], Guang-Ying Cui[2], Xin-Hua Chen[3,4], Shu-Sen Zheng[3,4] and Lan-Juan Li[1]**

[1] State Key Laboratory for Diagnosis and Treatment of Infectious Disease, Collaborative Innovation Center for Diagnosis and Treatment of Infectious Diseases, The First Affiliated Hospital, School of Medicine, Zhejiang University, Hangzhou, China, [2] Department of Infectious Diseases, Precision Medicine Center, The First Affiliated Hospital of Zhengzhou University, Zhengzhou, China, [3] Department of Hepatobiliary and Pancreatic Surgery, The First Affiliated Hospital, School of Medicine, Zhejiang University, Hangzhou, China, [4] Key Laboratory of Combined Multi-Organ Transplantation, Ministry of Public Health, Hangzhou, China, [5] Health Management Center, The First Affiliated Hospital, School of Medicine, Zhejiang University, Hangzhou, China

OPEN ACCESS

Edited by:
Sunny Hei Wong, The Chinese University of Hong Kong, China

Reviewed by:
Chenyang Wang, Nanjing University Medical School, China
Miguel Gueimonde, Institute of Dairy Products of Asturias (IPLA), Spain

***Correspondence:**
Shu-Sen Zheng
shusenzheng@zju.edu.cn
Lan-Juan Li
ljli@zju.edu.cn

[†] *These authors have contributed equally to this work*

Specialty section:
This article was submitted to Microbial Symbioses, a section of the journal Frontiers in Microbiology

Received: *30 August 2018*
Accepted: *18 June 2019*
Published: *03 July 2019*

Citation:
Lu H-F, Ren Z-G, Li A, Zhang H, Xu S-Y, Jiang J-W, Zhou L, Ling Q, Wang B-H, Cui G-Y, Chen X-H, Zheng S-S and Li L-J (2019) Fecal Microbiome Data Distinguish Liver Recipients With Normal and Abnormal Liver Function From Healthy Controls. Front. Microbiol. 10:1518. doi: 10.3389/fmicb.2019.01518

Emerging evidence suggests that altered intestinal microbiota plays an important role in the pathogenesis of many liver diseases, mainly by promoting inflammation via the "intestinal microbiota-immunity-liver" axis. We aimed to investigate the fecal microbiome of liver recipients with abnormal/normal liver function using 16S rRNA gene sequencing. Fecal samples were collected from 90 liver recipients [42 with abnormal liver function (Group LT_A) and 48 with normal liver function (Group LT_N)] and 61 age- and gender-matched healthy controls (HCs). Fecal microbiomes were analyzed for comparative composition, diversity, and richness of microbial communities. Principal coordinates analysis successfully distinguished the fecal microbiomes of recipients in Group LT_A from healthy subjects, with the significant decrease of fecal microbiome diversity in recipients in Group LT_A. Other than a higher relative abundance of opportunistic pathogens such as *Klebsiella* and *Escherichia/Shigella* in all liver recipients, the main difference in gut microbiome composition between liver recipients and HC was the lower relative abundance of beneficial butyrate-producing bacteria in the recipients. Importantly, we established a fecal microbiome index (specific alterations in *Staphylococcus* and *Prevotella*) that could be used to distinguish Group LT_A from Group LT_N, with an area under the receiver operating characteristic curve value of 0.801 and sensitivity and specificity values of 0.771 and 0.786, respectively. These findings revealed unique gut microbial characteristics of liver recipients with abnormal and normal liver functions, and identified fecal microbial risk indicators of abnormal liver function in liver recipients.

Keywords: liver transplantation, intestinal microbiota, 16S rRNA gene sequencing, butyrate-producing bacteria, opportunistic pathogens

Abbreviations: AUC, the area under the parasitemia curve; HC, healthy controls; HE, hepatic encephalopathy; LDA, linear discriminant analysis; LT, liver transplant; MELD, model for end-stage liver disease; OTUs, operational taxonomic units; PICRUSt, Phylogenetic Investigation of Communities by Reconstruction of Unobserved States software; ROC, receiver operating characteristic curve; rRNA, ribosomal RNA; SCFA, short chain fatty acids.

INTRODUCTION

Liver transplantation is a common and effective therapy for end-stage liver diseases. As of 2015, more than 1,700 living-donor liver transplantations had been successfully performed at the First Affiliated Hospital, College of Medicine of Zhejiang University, China, with an overall 3 years post-surgery survival rate of more than 70%. Despite advances in low-toxicity immunosuppressive drugs, the long-term success of liver transplantation is still limited by the development of chronic liver allograft dysfunction (Starzl et al., 1985). Many studies have emphasized improving the liver transplantation surgery procedure and instituting personalized management of post-transplant patients, including minimization strategies for transplant immunosuppression, to decrease the development of unpredictable clinical complications such as acute and chronic rejection (Reyes et al., 2000), *de novo* autoimmunity (Fedoseyeva et al., 1999), fibrosing cholestatic hepatitis (Hori et al., 2016), infections, and chronic dysfunction (Kok et al., 2017). Additionally, underlying chronic illnesses such as hypertension, diabetes, dyslipidemia, and graft impairment all have severe impacts on the recovery of liver function, thus affecting longevity and quality of life of post-transplant patients (Schoening et al., 2013).

The human intestinal tract harbors about 100 trillion microbes. They play a role in the development of mucosal and systemic immunity and are also involved in host liver disease (Lu et al., 2011; Qin et al., 2014; Chen et al., 2016). Intestinal dysbiosis not only disturbs intestinal immune homeostasis but can also cause immune dysfunction of other non-enteric organs (Jiang et al., 2011; Smolinska and O'Mahony, 2016; Zeevi et al., 2016), which is associated with the induction and progression of liver damage (Garcia-Tsao and Wiest, 2004; Ren et al., 2013). Although liver disease is not necessarily a consequence of these disruptions, diseases of the liver always result in downstream intestinal microbiome and immune dysbiosis (Qin et al., 2014; Lv et al., 2016). Malnutrition, ischemia-reperfusion injury (Ren et al., 2013), and immunosuppression therapy in liver transplant (LT) recipients directly lead to dysbiosis, disrupted intestinal barriers, and alterations in the innate immune response. Importantly, most LT patients have had severe liver disease and complications for a long period prior to receiving a transplant, and are subject to immunosuppression (Fenkel and Halegoua-DeMarzio, 2016) and antibiotic therapy after transplantation (Lu et al., 2013). Although immunosuppressors (e.g., FK506 and CsA) were initially reported to impair intestinal permeability in animals (Gabe et al., 1998), clinical studies on the chronic effects of FK506 and CsA on the intestine of liver recipients 2–4 years post-orthotopic LT (Parrilli et al., 2003) showed that these immunosuppressors did not affect intestinal permeability.

An understanding of variations in the intestinal microbial profile of LT recipients is critical for appropriately managing these patients in the early post-LT period. This knowledge will allow calculated modulation of intestinal microbiome components to benefit restoration of the intestinal microbiota and the recovery of liver function soon after LT, thus improving quality of life and long-term survival. Therefore, in this study we examined the fecal microbiomes of LT recipients (Group LT, 24 months < post-LT period < 48 months) and HCs (Group HC) to uncover the characteristics of the repopulated intestinal microbiota of LT recipients within the stable post-LT period in the absence of any microbiome-targeted therapeutic interventions.

MATERIALS AND METHODS

Study Design and Enrolled Patients

This study was approved by the Institutional Review Board of the First Affiliated Hospital, School of Medicine, Zhejiang University (IRB no. 2014-336). All experiments were performed in accordance with the Helsinki Declaration and the Rules of Good Clinical Practice, and no organs from executed prisoners were used in these recipients. Patients were considered for enrollment if they diagnosed with pathologically-diagnosed hepatitis B virus (HBV)-associated hepatocellular carcinoma with the Barcelona Clinic Liver Cancel (BCLC) stage A or B, and the Child -Pugh class A or B who met the Hangzhou criteria and had undergone liver transplantation more than 24 months but less than 48 months prior to the study period. Each participant filled out a baseline questionnaire (**Supplementary Table S1**). The inclusion criteria were: (a) aged 35–65 years with normal body weight, (b) diagnosed with hepatocellular carcinoma prior to LT and without microbial infection during the perioperative period (based on the patient's medical history), (c) no obvious bodily discomfort, (d) no antibiotic use in the 12 weeks prior to enrollment and no probiotics and/or prebiotics after LT, and (e) FK506 tacrolimus used as the sole immunosuppressive therapy for more than 12 months. The exclusion criteria for patients were: (a) presence of severe complications such as liver abscess, recurrence of hepatocellular carcinoma (HCC), liver trauma, diabetes, hypertension, biliary and/or vascular complications through measuring serum CRP, PCT, and imaging examination, etc. (b) infection with human immunodeficiency virus, hepatitis C virus, or other types of hepatitis virus except HBV, (c) presence of any other organ-specific diseases, including intestinal diseases, pancreatic diseases, and/or tumor recurrence, (d) consumption of alcohol, tobacco, Chinese herbal medicine, and/or recreational drugs, and (e) staying up late, work fatigue and so on. Fecal samples and patient information (including data on diet, drug use, and alcohol consumption) were collected during periodic outpatient follow-up appointments between 1 December, 2014, and 31 December, 2016, at one of the two participating hospitals (First Affiliated Hospital School of Medicine, Zhejiang University, and Shulan (Hangzhou) Hospital). HCs (Group HC) matched to the age, gender, and BMI of the LT group were correspondingly screened and enrolled according to the inclusion and exclusion criteria described in our previous study (Lu et al., 2011). This study included a total of 151 fecal samples (90 from LT patients and 61 from HC) from the participants described above. Written informed consent and questionnaires addressing previous and current diseases, lifestyles, and medications were obtained from all subjects. The data of personalized perioperative medication management and professional postoperative care were extracted from electronic medical records.

Sample Collection and DNA Extraction

Fecal samples were collected in sterile bags, refrigerated, and then taken directly to the laboratory. The samples were then divided into 200 mg aliquots, frozen rapidly in liquid nitrogen, and stored at −80°C until use.

Phenol trichloromethane was used to extract DNA from each frozen fecal sample aliquot using a bead beater to mechanically disrupt the cells, followed by phenol-chloroform extraction (Qin et al., 2014). Extracted DNA was quantified using a Qubit 2.0 Fluorometer (Invitrogen, Carlsbad, CA, United States), and molecular sizes were estimated using agarose gel electrophoresis. All fecal microbial DNA samples were diluted to a concentration of 10 ng/μl for microbial analysis.

PCR and Sequencing

16S rRNA gene sequences were amplified from each of the extracted DNA samples using a set of primers targeting the hyper-variable V3-V4 region (338F/806R) of the gene: 338F, 5′-barcode-ACTCCTACGGGAGGCAGCA-3′ and 806R, 5′-GGACTACHVGGGTWTCTAAT-3′. PCR amplification was performed as described in our previous study (Lu et al., 2016). DNA libraries were constructed using kits provided by Illumina Inc. according to the manufacturer's instructions, and DNA sequencing was performed using the Illumina MiSeq 2000 platform (San Diego, CA, United States) at the State Key Laboratory for Diagnosis and Treatment of Infectious Diseases (Zhejiang University, Hangzhou, China) according to standard protocols.

Nucleotide Sequence Accession Number

Sequence data have been deposited under NCBI BioProject accession number PRJNA544155.

Computational and Statistical Analyses of Bacterial Profiles

Clean data were extracted from raw data using USEARCH 8.0 (Edgar et al., 2011) with the following criteria: (i) sequences from each sample were extracted using each index with zero mismatch, (ii) sequences with an overlap of <50 bp were discarded, (iii) sequences in which the error rate of the overlap was >0.1 were discarded, and (iv) sequences <400 bp in length after the merge were discarded. Quality-filtered sequences were clustered into unique sequences and sorted in order of decreasing abundance to identify representative sequences using UPARSE (Edgar, 2013) according to the UPARSE operational taxonomic unit (OTU) analysis pipeline. Singletons were omitted in this step. OTUs were classified based on 97% similarity after removal of chimeric sequences using the UPARSE values (version 7.1[1]; Zhang Y. et al., 2015). The phylogenetic affiliation of each 16S rRNA gene sequence was analyzed using RDP Classifier[2] (Wang et al., 2007) against the Silva (SSU132) 16S rRNA database with a confidence threshold of 70%.

Bacterial diversity was determined via sampling-based analysis of OTUs and displayed as a rarefaction curve. Bacterial richness and diversity across the samples were calculated using the following indexes: Chao1, ACE, and Shannon (Oksanen et al., 2015). To equalize the differences in sequencing depths among samples, the sequences were downsized to 5,000 per sample (20 permutations) (Zhang Q. et al., 2016). A non-parametric Mann–Whitney *U*-test was used to test for significant differences between two groups. Principal component analyses (PCAs) using weighted and unweighted UniFrac distance metrics were conducted, and the R package[3] was used to visualize interactions among the bacterial communities from different samples (McMurdie and Holmes, 2013).

The specific characterization of fecal microbiota to distinguish taxonomic types was conducted using a linear discriminant analysis (LDA) effect size (LEfSe) method[4] (Segata et al., 2011). Applying a normalized relative abundance matrix, LEfSe was used to: (i) identify key bacteria in fecal samples from the LT_A, LT_N, and HC groups at multiple levels in datasets, (ii) grade the key bacteria according to the results of a Mann–Whitney *U*-test, which determines features with significant differences in abundance between assigned taxa and uses LDA to assess the effect size of each feature (Ling et al., 2014), and (iii) visualize the results using taxonomic bar charts and cladograms. The *P*-values were adjusted as described by Benjamini and Hochberg (Jiang and Yu, 2017). Differences were considered significant when the false discovery rate was < 0.05.

Random forest models (Heitner et al., 2010) were introduced to identify key discriminatory OTUs between Group LT_A, LT_N, and Group HC. And to verify the key discriminatory OTUs which selected by random forest analysis, a 10-fold corss-validation analysis has been performed using rfcv function in R-package "randomForest" (R version 3.2.1). Firstly, random forest and Wilcox rank sum test were used to select differential species with both the value of Mean_decrease_in_accuracy above 0.001, and $p < 0.05$ by the Wilcox rank sum test (Zhang Q. et al., 2016); secondly, 10 times cross-validation analysis was performed to sift through the minimum OTU combination with the lowest error rate and the lowest number that can accurately separate the two groups; and receiver operating characteristics (ROC) analysis was then performed to measure of quality of the classification models by the R software package pROC (Robin et al., 2011). ROC curves were constructed, and the area under the curve (AUC) was used to designate the ROC effect.

Spearman's correlation analyses were also used to assess potentially clinically relevant associations between the relative abundance of fecal bacterial genera and serum markers of liver dysfunction using Hmisc package in R.

RESULTS

Clinical Characteristics of the Participants

After applying the strict inclusion and exclusion criteria described above, we enrolled 90 LT recipients (Group LT_A,

[1]http://drive5.com/uparse/

[2]http://rdp.cme.msu.edu/

[3]http://www.R-project.org/

[4]http://huttenhower.sph.harvard.edu/lefse/

n = 42; Group LT_N, n = 48) and 61 HC subjects (Group HC). There were no significant differences between the groups in terms of age, sex distribution, or body mass index. All liver recipients had previously been diagnosed as having hepatocellular carcinoma with cirrhosis, and all were HBV soluble antigen (HBsAg)-positive prior to LT. Serum levels of alanine aminotransferase, aspartate aminotransferase, and glutamyltranspeptidase were all significantly elevated in Group LT_A compared with Group HC and Group LT_N (all $P < 0.001$). Further details on the clinical characteristics of the subjects are provided in **Table 1**. Antibiotic treatments during the perioperative period (for at least 5 consecutive days) differed among patients because the use of prophylactic antimicrobial agents varied based on the perceived risks and willingness of the patients. The antimicrobial agents used included piperacillin-tazobactam, cefepime dihydrochloride, imipenem-cilastatin sodium, and micafungin sodium. The immunosuppressive therapies prescribed in the 6 months post-LT included simulect, mycophenolate mofetil, glucocorticoids, and FK506 tacrolimus; all drugs were used at doses adjusted according to patient situation based on several factors, including their patient status, platelet count, and white blood cell count. After 6 months post-LT, FK506 tacrolimus (at a serum level of 5–6 ng/ml) with or without mycophenolate mofetil (1 g/day) was used. General liver protective drugs combined with appropriately increasing dosage of anti-immunosuppressive agents were treated in those recipients of Group LT_A. And prophylaxis with high-dose hepatitis B immunoglobulin (HBIG) and Entecavir [nucleos(t)ide analogs] was used after the transplantation to suppress viral replication. As follows: for each recipient, entecavir capsule (oral medication): one capsule daily for life; and HBIG: 2000 intl units/day through intravenous drip within postoperative week 1, 2000 intl units/week through intravenous drip within postoperative week 2–5, then 800 intl units twice a week though intramuscular injection if patients fail to reach anti-HBs levels of 100 intl units/L. The whole blood concentration of HBIG after liver transplantation is needed to monitor for life. If patients fail to reach anti-HBs levels of 500 intl units/L, which tested in the 2th day after using HBIG, within the first month post-liver transplantation, dosage adjustments would be required. We enrolled recipients who were in the post-LT period of >24 months and <48 months because patients were in a stable condition during this period and were not exposed to antibiotics in the 12 weeks prior to participation in the study. In addition, all LT recipients only took FK506 tacrolimus as an immunosuppressive therapy during this period.

Recipients in Group LT_A Showed Decreased Fecal Microbial Diversity

We generated 4,723,696 filtered sequences from the fecal samples of 90 LT recipients and 61 HCs. The qualified reads were clustered into 588 qualified species-level OTUs using 97% as the similarity cutoff. Overall, 88.3 and 60.4% of all reads could be assigned to the family and genus levels, respectively (**Supplementary Dataset S1A**). Species-level OTUs and species richness and diversity estimates were obtained for each microbiome (**Supplementary Dataset S1B**). The species richness of individual samples and of the total gut bacterial communities was estimated by rarefaction analysis. The resulting rarefaction curves indicated that the microbial richness of the sampled guts was near saturation at the applied sequencing depth (**Supplementary Figures S1A,B**), which was sufficient to identify most of the bacterial community members of each individual microbiome. Fecal microbiome estimated richness in ascending order was Group LT_A, Group LT_N, and Group HC (**Supplementary Figure S1C**). The abundance of OTUs in Group LT_A was significantly lower than that in Group LT_N and Group HC (P = 0.007 and <0.001, respectively, **Figure 1A**). Additionally, only 78.2% (460 bacterial OTUs) of the microbiome was shared by the three groups, with 35, 2, and 18 bacterial OTUs unique to Group HC, Group LT_A, and Group LT_N, respectively (**Supplementary Figure S1D**).

Subjects in Group LT_A exhibited an obviously different fecal microbiome composition compared with those in Groups LT_N and HC. In particular, the microbial diversity was significantly decreased in Group LT_A compared with the other two groups

TABLE 1 | Clinical information in liver recipients and healthy controls.

Clinical and pathologicalIndexes		Group LT_A		Group LT_N		Healthy controls		*P*-value		
		N = 42	%	*N* = 48	%	*N* = 61	%	HC vs. LT_A	HC vs. LT_N	LT_A vs. LT_N
Gender	Female	10	23.81	10	20.83	15	24.59	0.999	0.819	0.802
	Male	32	76.19	38	79.17	46	75.41			
Age (year)		46.62 ± 1.51		46.90 ± 1.36		48.21 ± 0.84		0.324	0.391	0.892
BMI (kg/m^2)		23.72 ± 0.32		23.50 ± 0.41		23.72 ± 0.32		0.174	0.432	0.677
Time of post-LT (month)		28.05 ± 2.21		32.79 ± 2.02		–				0.117
ALT (5–40 U/L)		105.12 ± 21.96		22.15 ± 1.03		20.56 ± 1.05		1.047E-05	0.289	0.0001
AST (8–40 U/L)		68.38 ± 8.76		22.17 ± 0.69		22.16 ± 0.60		6.39E-09	0.998	2.165E-07
GGT (11–50 U/L)		121.74 ± 19.37		43.98 ± 4.87		22.59 ± 1.79		1.733E-08	1.77E-05	8.297E-05
Total bilirubin (0–21 μmol/L)		119.67 ± 23.77		15.33 ± 0.86		13.79 ± 0.70		4.926E-07	0.162	9.826E-06

The continuous variables were presented as mean ± standard error of mean (SEM); the continuous variables were compared with the independent t-test between both groups. Fisher's exact test was used to compare categorical variables. – without LT. Group LT_A, liver transplantation recipients with abnormal liver function; Group LT_N, liver transplantation recipients with normal liver function; HC, healthy controls. BMI, body mass index; ALT, alanine aminotransferase; AST, aspartate aminotransferase; GGT, glutamyl transpeptidase.

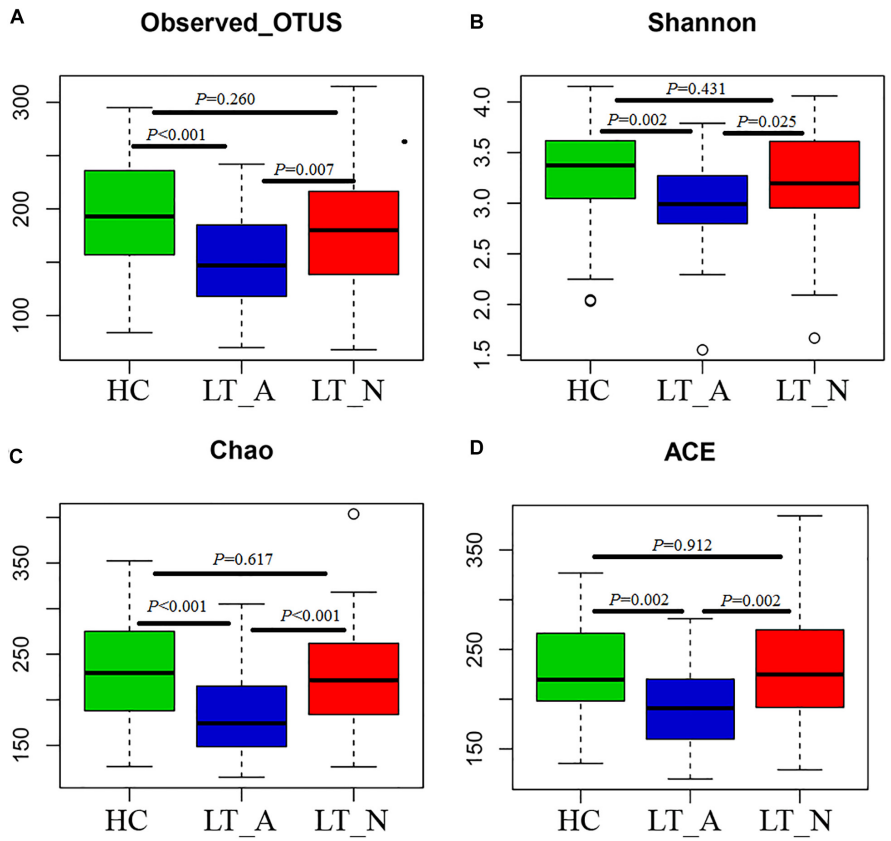

FIGURE 1 | Phylogenetic diversity of fecal microbiomes between liver transplant recipients and healthy subjects. **(A–D)** Box plots depicting microbiome diversity differences according to the number of OTUs detected, the Shannon index, the Chao 1 index, and the ACE index, respectively. "+" represents the median value, while the upper and lower ranges of the box represent the 75 and 25% quartiles, respectively. LT_A, fecal microbiomes of the liver recipients with abnormal liver function; LT_N, fecal microbiomes of the liver recipients with normal liver function; HC, fecal microbiomes of the healthy control group; OTU, operational taxonomic unit.

(P = 0.025 and 0.002, respectively), as estimated by the Shannon index (**Figure 1B**). This finding was validated by the other applied diversity parameters, namely the Chao1 and ACE indexes (Chao1 index: $P < 0.000$ vs. Group LT_N and $P < 0.000$ vs. Group HC, **Figure 1C**; ACE index: $P = 0.002$ vs. Group LT_N and $P = 0.002$ vs. Group HC, **Figure 1D**).

The Bray-Curtis (OTU number dissimilarity, **Figures 2A,B**), unweighted-UniFrac (qualitative, **Figures 2C,D**), and weighted-UniFrac (quantitative, **Figures 2E,F**) PCA plots, which measure the phylogenetic similarities between microbial communities, showed that the fecal microbiota of subjects in Group LT_A differed from that of the HCs, while the fecal microbiota of subjects in Group LT_N overlapped with that of subjects belonging to Groups LT_A and HC. The lower fecal microbiome diversity in Group LT compared with Group HC is also depicted in the PCA plots (**Figures 2B,D,F**).

Bacterial Taxonomic Differences Between LT Recipient Groups and HCs

Many of the taxa were differentially abundant in LT_A, LT_N, and HC. Analysis at the class level (**Supplementary Figure S2A**) showed that the relative abundance of Negativicutes, Gammaprotobacteria and Bacilli were significantly higher in both the LT_N and LT_A groups compared with the HC group; additionally, Fusobacteriia were significantly increased, and Firmicutes_unclassified and Lentisphaerae were significantly decreased in LT_A when compared with HC. We also performed comparisons at the phylum level (**Supplementary Figure S2B**) between the patient groups and healthy controls, and found that Firmicutes were significantly decreased in both the LT_N and LT_A groups compared with the HC group. Interestingly, when compared with healthy controls, LT_A showed higher relative abundance of Proteobacteria and Fusobacteria, while LT_N showed higher relative abundance of Bacteroidetes.

The results of heatmap analysis (a hierarchical clustering analysis) of the fecal microbiomes using a random forests model revealed a discriminatory intestinal microbiome between LT recipient groups and healthy subjects. Comparison of the Group LT_A and Group HC fecal microbiomes revealed 50–97%-identity OTUs assigned to 20 different families/genera that were significantly differently distributed between the two groups (**Figure 3**). Of these 50 OTUs, 35 OTUs corresponding to the families/genera *Butyricicoccus* (2 OTUs), *Prevotella*

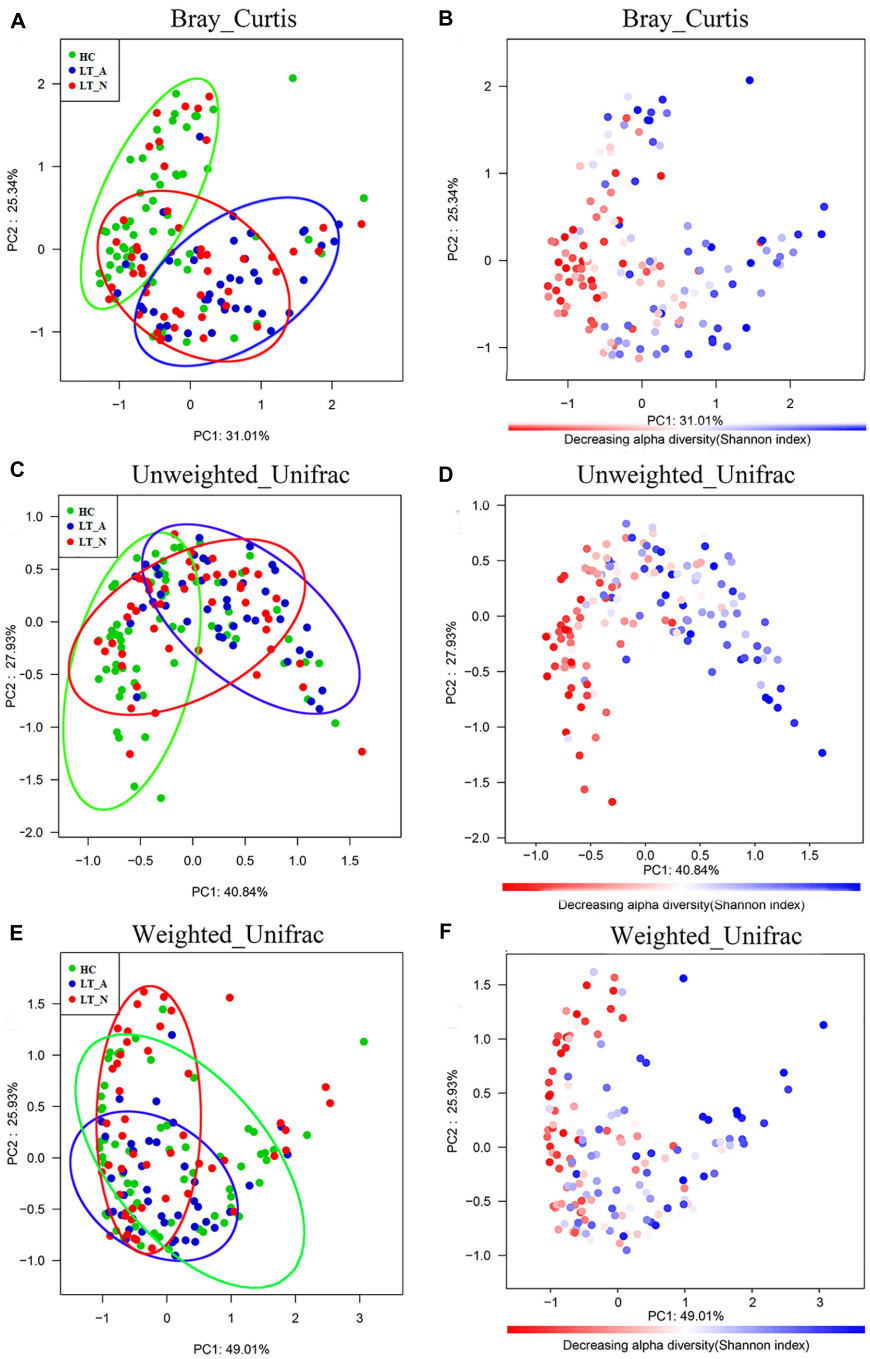

FIGURE 2 | Bacterial diversity clustering determined by combining the results of Bray-Curtis analysis and unweighted and weighted UniFrac PCoA of fecal microbiota. The beta diversity is different between LT_A and HC, and LT_A and LT_N ($P < 0.05$ using PERMANOVA analyses with R-vegan function Adonis). The variance explained by the principal components is indicated in parentheses on the axis, and the ellipses highlight the clustering of the fecal microbiomes according to groups (green, Group HC; blue, Group LT_A; red, Group LT_N). **(A,B)** Indicate the results of Bray-Curtis analysis, **(C,D)** are the results based on unweighted UniFrac (qualitative) analysis, and **(E,F)** show the results of weighted UniFrac (qualitative) analysis. Each point represents a sample. **(A,C,E)** The samples from Group LT_A, Group LT_N, and Group HC are represented in blue, red, and green, respectively. **(B,D,F)** Microbial diversity maps. A highly diverse core (colored in red) indicates the bacterial diversity of Group HC is highest among the three groups (the color scale of red to blue reflects the decreasing alpha diversity of the fecal microbiome). LT_A, fecal microbiomes of the liver recipients with abnormal liver function; LT_N, fecal microbiomes of the liver recipients with normal liver function; HC, fecal microbiomes of the healthy control group; PCoA, principal coordinates analysis.

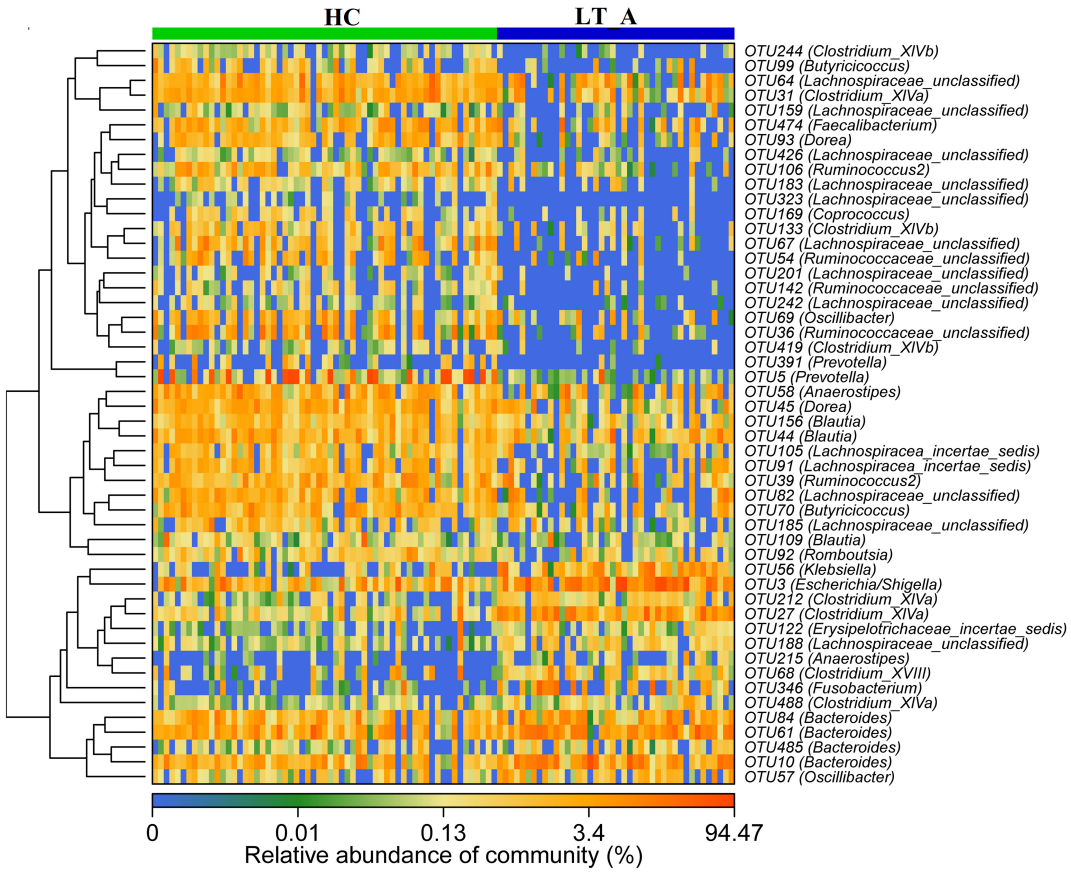

FIGURE 3 | Heat maps showing the relative abundance of the discriminatory OTUs that drive the differences between groups LT_A and HC. For each sample, the columns show the relative abundance data for the discriminatory OTUs listed to the right of the figure. Abundance values for each of the genera were clustered using unsupervised hierarchical clustering [the relative abundance of each genus is indicated by a gradient of color from blue (low abundance) to red (high abundance)]. The corresponding genus of each key OTU is noted to the right of the figure. The heat map on the left shows Spearman hierarchical clustering of relative abundance values for each of the 50 most discriminatory 97%-identity OTUs in a random forest-based model of the fecal microbiota of the LT_A and HC groups. LT_A, fecal microbiomes of the liver recipients with abnormal liver function; HC, fecal microbiomes of the healthy control group; OTU, operational taxonomic unit.

(2 OTUs), *Clostridium*_XIVb (3 OTUs), *Clostridium*_XIVa (1 OTU), *Lachnospiraceae* (12 OTUs), *Faecalibacterium* (1 OTU), *Dorea* (2 OTUs), *Ruminococcaceae* (5 OTUs), *Romboutsia* (1 OTU), *Anaerostipes* (1 OTU), *Coprococcus* (1 OTU), *Blautia* (3 OTUs), and *Oscillibacter* (1 OTU) were more abundant in Group HC than in Group LT_A. The remaining OTUs, including those corresponding to *Klebsiella* (1 OTU), *Escherichia*/*Shigella* (1 OTU), *Clostridium*_XIVa (3 OTUs), *Bacteroides* (4 OTUs), *Fusobacterium* (1 OTU), *Lachnospiraceae* (1 OTU), *Anaerostipes* (1 OTU), *Erysipelotrichaceae*_incertae_sedis (1 OTU), and *Clostridium*_XVIII (1 OTU) were more abundant in Group LT_A than in Group HC.

Comparison of the Group LT_A and Group LT_N fecal microbiomes revealed 26 most-discriminatory-OTUs. Of these, five OTUs, corresponding to *Anaerostipes* (1 OTU), *Clostridium*_IV (1 OTU), and *Clostridium*_XIVa (3 OTUs), were more abundant and 21 OTUs, including *Prevotella* (3 OTUs), *Staphylococcus* (1 OTU), *Burkholderiales* (1 OTU), *Clostridium*_XIVa (2 OTUs), *Ruminococcaceae* (2 OTUs), *Lachnospiracea* (8 OTUs), *Bacteroidales* (1 OTU), *Clostridium*_XVIII (1 OTU), *Butyricicoccus* (1 OTU), and *Dorea* (1 OTU), were less abundant in Group LT_A than in Group LT_N (**Figure 4**). Additionally, heatmap analysis of the fecal microbiomes delineated 29 distinguishing OTUs, which were assigned to 18 different genera, between groups LT_N and HC. Of these most-discriminatory-OTUs, 14 OTUs corresponding to *Lachnospiraceae* (7 OTUs), *Dorea* (1 OTU), *Clostridium*_XIVb (1 OTU), *Ruminococcus* 2 (1 OTU), Firmicutes (1 OTU), *Victivallis* (1 OTU), and *Bacteroides* (2 OTUs) were decreased, while 15 OTUs, including *Megamonas* (1 OTU), *Prevotella* (1 OTU), *Lactobacillus* (1 OTU), *Enterococcus* (1 OTU), *Klebsiella* (1 OTU), *Veillonella* (2 OTUs), *Streptococccus* (1 OTU), *Clostridium*_XIVa (1 OTU), *Bacteroides* (2 OTUs), *Erysipelotrichaceae*_incertae_sedis (1 OTU), *Ruminococcaceae* (1 OTU), and *Lachnospiraceae* (2 OTUs), were increased in the fecal microbiome of Group LT_N compared with that of Group HC (**Supplementary Figure S3**).

We also used LEfSe to compare the estimated phylotypes of the recipient groups with the Group HC microbiota (**Figures 5A,B**), with the results confirming that dysbiosis was

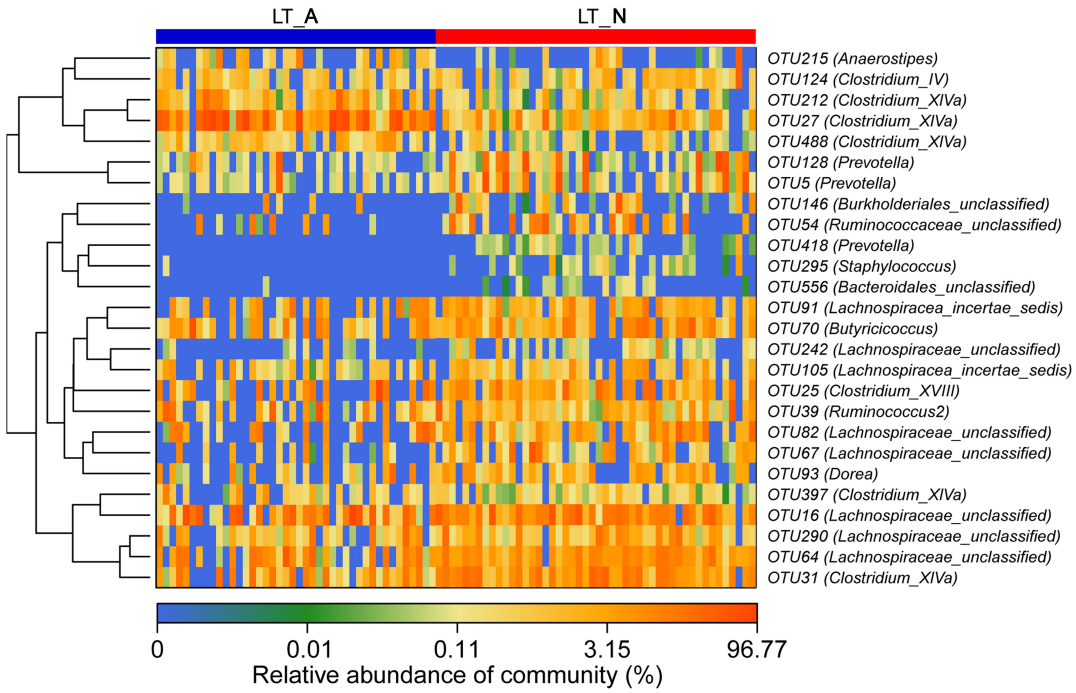

FIGURE 4 | Heat maps showing the relative abundance of the discriminatory OTUs that drive the differences between groups LT_A and LT_N. For each sample, the columns show the relative abundance data for the discriminatory OTUs listed to the right of the figure. The abundance values for each of the genera were clustered using unsupervised hierarchical clustering [the relative abundance of each genus is indicated by a gradient of color from blue (low abundance) to red (high abundance)]. The corresponding genus of each key OTU is noted to the right of the figure. The heat map on the left shows Spearman hierarchical clustering of relative abundance values for each of the 26 most discriminatory 97%-identity OTUs in a random forest-based model of the fecal microbiota of groups LT_A and LT_N. LT_A, fecal microbiomes of the liver recipients with abnormal liver function; LT_N, fecal microbiomes of the liver recipients with normal liver function; OTU, operational taxonomic unit.

indeed present at various phylogenetic levels. At the family level, the Group LT_A fecal microbiome was characterized by a preponderance of *Bacteroidaceae*, *Fusobacteriaceae*, *Streptococcaceae*, *Coriobacteriaceae*, and *Lachnospiraceae* (all LDA scores ($\log_{10}$) >3 and $P < 0.05$; **Supplementary Dataset S2**), while the Group LT_N fecal microbiome was characterized by a higher prevalence of *Enterobacteriaceae*, *Veillonellaceae*, and *Ruminococcaceae* (all LDA scores ($\log_{10}$) > 3 and $P < 0.05$; **Supplementary Dataset S2**). In comparison, the HC fecal microbiomes were dominated by *Prevotellaceae*, *Porphyromonadaceae*, *Lachnospiraceae*, *Coriobacteriaceae*, *Peptostreptococcaceae*, *Ruminococcaceae*, and *Erysipelotrichaceae* (all LDA scores ($\log_{10}$) > 3 and $P < 0.05$; **Supplementary Dataset S2**). At the genus level, opportunistic pathogens (including *Bacteroides*, *Fusobacterium*, and *Streptococcus*) and butyrate-producing bacteria (including *Clostridium*_XIVa and *Dorea*) were enriched in the Group LT_A fecal microbiome (all LDA scores ($\log_{10}$) > 3 and $P < 0.05$; **Supplementary Dataset S2**), while opportunistic pathogens (including *Escherichia_Shigella*, *Klebsiella*, and *Veillonella*), *Megasphaera* (lactate-utilizing bacteria), and *Butyricicoccus* (butyrate-producing bacteria) were enriched in the Group LT_N fecal microbiome (all LDA scores ($\log_{10}$) > 3 and $P < 0.05$; **Supplementary Dataset S2**). In comparison, *Prevotella*, *Collinsella*, *Romboutsia*, *Odoribacter*, and butyrate-producing bacteria (including *Faecalibacterium*, *Clostridium*_IV, *Ruminococcus* 2, *Coprococcus*, *Fusicatenibacter*, and *Clostridium*_XIVb) were enriched in the HC microbiome (all LDA scores ($\log_{10}$) > 3 and $P < 0.05$; **Supplementary Table S2**).

Additionally, *Prevotella*, *Romboutsia,* opportunistic pathogens (including *Klebsiella* and *Escherichia_Shigella*), and butyrate-producing bacteria (including *Butyricicoccus*, *Clostridium*_IV, *Clostridium*_XIVb, and *Clostridium*_XIVa) could be used to distinguish Group LT_A samples from those belonging to Group HC, with ROC-plot AUC values of 0.903 and sensitivity and specificity values of 0.863 and 0.857, respectively **(Figure 6A**; ROC-AUC values shown in **Supplementary Dataset S2A**), while *Staphylococcus* and *Prevotella* could be used to distinguish the fecal microbiomes of Group LT_A from those of Group LT_N, with ROC-AUC values of 0.801 and sensitivity and specificity values of 0.771 and 0.786, respectively (**Figure 6B**; ROC-AUC values shown in **Supplementary Dataset S2B**). Further, *Victivallis*, *Romboutsia*, *Megasphaera*, *Megamonas*, *Veillonella*, *Lactobacillus*, opportunistic pathogens (including *Klebsiella*, *Escherichia/Shigella*, *Enterococcus*, and *Streptococcus*), and butyrate-producing bacteria (including *Ruminococcus* 2, *Fusicatenibacter*, *Dorea*, *Clostridium*_XIVb, and XIVa) could be used to distinguish fecal microbiomes of Group LT_N recipients from those of Group HC, with ROC-AUC values of 0.823 and sensitivity and specificity values of 0.738 and

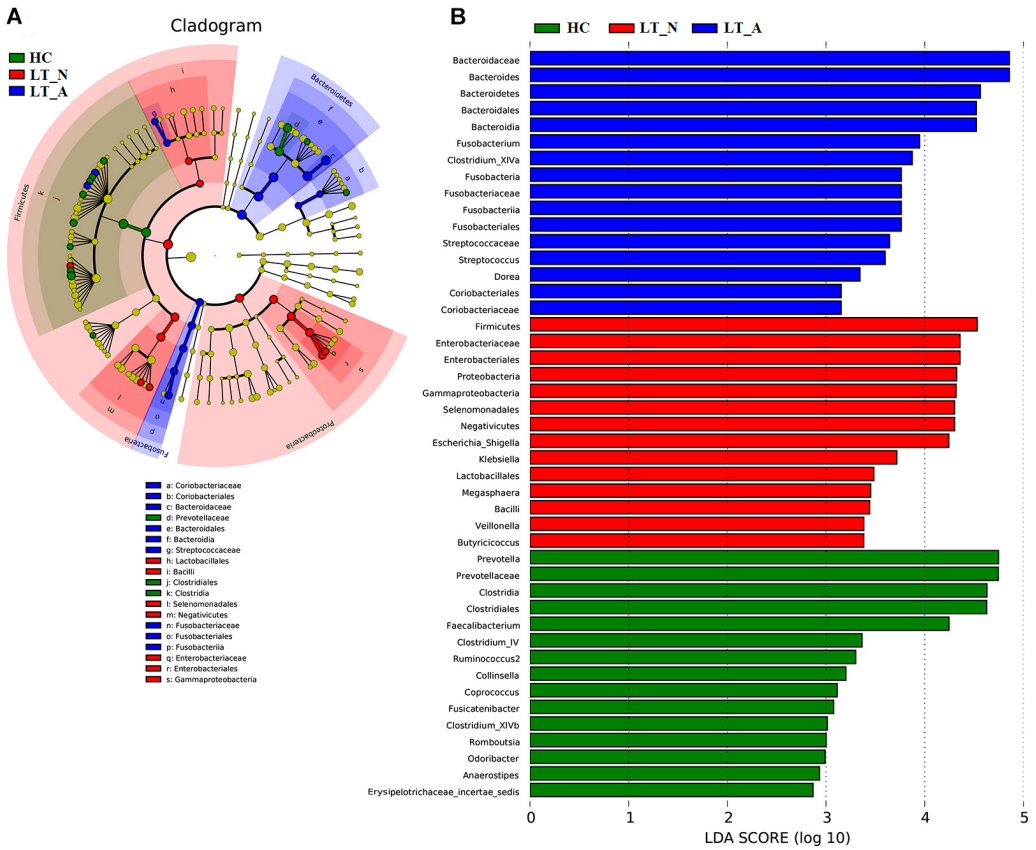

FIGURE 5 | LEfSe and LDA based on divergent OTUs between the fecal microbiomes of the LT_A, LT_N, and HC groups, which identified the most differentially-abundant taxa between the three groups. **(A)** Taxonomic cladogram generated using the LEfSe method. LT_A-enriched taxa, blue; LT_N-enriched taxa, red; taxa enriched in healthy controls, green. **(B)** LDA scores indicating significant differences in microbiota between the three groups (LT_A, LT_N, and HC). HC-enriched taxa, green; LT_A-enriched taxa, blue; LT_N-enriched taxa, red. LT_A, fecal microbiomes of the liver recipients with abnormal liver function; LT_N, fecal microbiomes of the liver recipients with normal liver function; HC, fecal microbiomes of the healthy control group; LEfSE, linear discriminant analysis effect size; LDA, linear discriminant analysis; OTU, operational taxonomic unit.

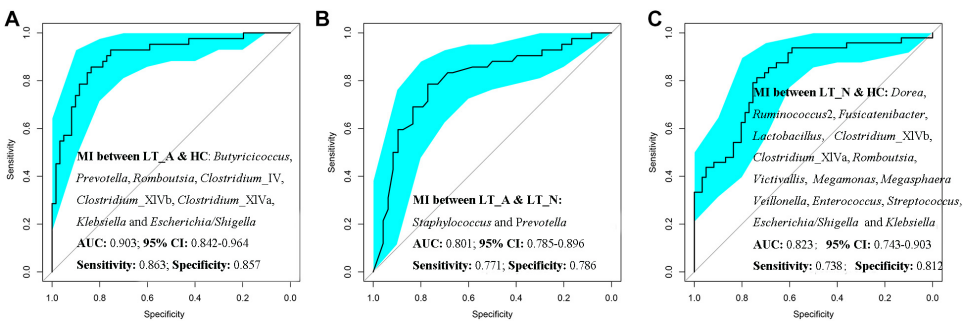

FIGURE 6 | Prediction of the key genera (microbiotal index, MI) in the fecal microbiomes of LT_A, LT_N, and HC. **(A)** ROC curves for *Prevotella*, *Romboutsia*, *Klebsiella*, *Escherichia_Shigella*, *Butyricicoccus*, *Clostridium*_IV, *Clostridium*_XlVb, and *Clostridium*_XlVa could be used to distinguish samples belonging to Group LT_A from those of Group HC, with ROC plot AUC values of 0.903 and sensitivity and specificity values of 0.812 and 0.690, respectively. **(B)** ROC plots for *Staphylococcus* and *Prevotella* could distinguish fecal microbiomes of Group LT_A recipients from those of Group LT_N, with ROC-AUC values of 0.801 and sensitivity and specificity values of 0.771 and 0.786, respectively. **(C)** ROC plots for *Victivallis*, *Romboutsia*, *Megasphaera*, *Megamonas*, *Veillonella*, *Lactobacillus*, *Klebsiella*, *Escherichia/Shigella*, *Enterococcus*, *Streptococcus*, *Ruminococcus* 2, *Fusicatenibacter*, *Dorea*, *Clostridium*_XlVb, and *Clostridium* XlVa could distinguish fecal microbiomes from Group LT_N recipients from those of Group HC, with ROC-AUC values of 0.823 and sensitivity and specificity values of 0.738 and 0.812, respectively. LT_A, fecal microbiomes of the liver recipients with abnormal liver function; LT_N, fecal microbiomes of the liver recipients with normal liver function; HC, fecal microbiomes of the healthy control group; ROC, receiver operating characteristic; AUC, the area under the parasitemia curve.

0.812, respectively (**Figure 6C**; ROC_AUC values shown in **Supplementary Dataset S2C**).

Next to better understand the profile of LT-associated fecal microbiome, we computed covariations between the relative abundance of the discriminatory fecal bacterial genera, and between these genera and clinical indices for liver function including ALT, AST, TB, and GGT (**Supplementary Figure S4**), and we noted that bacteria in most LT_A-associated bacteria including *Bacteroides*, *Fusobacterium*, *Clostridium*_XIVa, *Streptococcus*, and opportunistic pathogens (including *Klebsiella* and *Escherichia_Shigella*) especially *Bacteroides* and *Klebsiella* (Spearman's correlation >0.3, $p < 0.05$ for the correlations of both genera with all serum markers; **Supplementary Figure S4**), positively correlated with serum markers of liver dysfunction; while HC-associated bacteria including *Butyricicoccus*, *Clostridium*_IV, *Clostridium*_XIVb, *Prevotella*, *Collinsella*, *Romboutsia*, *Faecalibacterium*, *Ruminococcus* 2, *Coprococcus*, *Fusicatenibacter*, especially *Butyricicoccus* and *Prevotella* (Spearman's correlation <-0.3, $p < 0.05$ for the correlations of both genera with all serum markers; **Supplementary Figure S4**), negatively correlated with serum markers of liver dysfunction.

DISCUSSION

The host immune system controls the composition, diversity, and location of the microbiota (Thaiss et al., 2016). Alterations in the intestinal microbiome are associated with changes in immunity and metabolism, which play critical roles in the pathogenesis of human liver diseases. Therefore, the restoration of the post-LT microbiota is a dynamic process between the host immune system and bacterial colonization. Mounting evidence has shown that disruption of this complex and delicate homeostasis may worsen liver pathogenetic conditions. The restoration of the microbiota in the early-stages of post-LT recovery is important for long-term complication management (Doycheva et al., 2016). Our previous large, clinical cohort study explored changes to the six predominant gut bacterial genera and to the immune indices of patients who underwent liver transplantation (Wu et al., 2012). That work was the first to report the dysbiosis of gut microbiota in subjects undergoing liver transplantation. Here, we used high-throughput sequencing platforms to identify key bacterial families and genera in the fecal microbiomes of liver recipient cohorts with normal/abnormal liver function, which may help provide targets for microbiota restoration following surgery and immunosuppressant treatments. As pre-transplant intestinal microbiota dysbiosis in LT recipients has a more powerful influence on the post-transplant microbiota than the LT itself (Xie et al., 2011), the present study only included recipients who were diagnosed with HBV-associated hepatocellular carcinoma.

An abundance of opportunistic pathogens in the intestinal microbiota may be detrimental to long-term health after LT. Among the 20 most-discriminatory bacteria enriched in the liver recipients, several are opportunistic pathogens, including *Fusobacterium* (Aliyu et al., 2004), *Streptococcus*, *Klebsiella*, and *Escherichia/Shigella*. Although *Fusobacterium* species are members of the normal gut microbiota of humans, certain species (adherent, invasive, and/or pro-inflammatory) are recognized as opportunistic pathogens and are enriched in the gut microbiomes of patients with liver cirrhosis (Qin et al., 2014) and liver cancer (Ren et al., 2018). *Streptococcus* species, which form part of the commensal human intestinal microbiota, are also enriched in the intestinal microbiomes of patients with liver cirrhosis (Qin et al., 2014). In the present study, both genera were enriched in the fecal microbiomes of recipients with abnormal liver function. *Enterobacteriaceae* enrichment in the disturbed microbiota is associated with an increase of endotoxin production, which leading to endotoxemia, increased intestinal permeability, and liver injury (Arai et al., 1998). There is a positive correlation between overgrowth of *Enterobacteriaceae* and the development of liver dysfunction, as Gram-negative bacterial cell components such as lipopolysaccharide induce over-expression of pro-inflammatory cytokines, chemokines, and some reactive oxygen/nitrogen species by luminal epithelial cells and Kupffer cells (Racanelli and Rehermann, 2006; Szabo and Bala, 2010). In present study, we found relative abundance of opportunistic pathogens had a positive correlation with serum markers of liver dysfunction. The finding that the relative abundance of *Klebsiella* and *Escherichia/Shigella* was much higher in the recipients with normal liver function than in those with abnormal liver function and in the HCs indicates the need for personalized management of individual patients post-transplant.

Our compositional analysis of the fecal microbiota of both LT groups and HCs suggests that the major difference between the three groups is not in the composition of opportunistic bacteria, but rather, in butyrate-producing bacteria. *Lachnospiraceae*, *Odoribacteraceae*, and some clusters of *Clostridiaceae* are known butyrate producers. We found that the recipient groups showed less diversity in butyrate-producing bacteria compared with HCs. *Clostridium* cluster IV (*Faecalibacterium* and *Ruminococcus*) (Schwiertz et al., 2002b; Fang et al., 2017), *Clostridium* cluster XI (*Anaerostipes*) (Schwiertz et al., 2002a; Kant et al., 2015), *Clostridium* cluster XIVb, *Clostridium* cluster XIVa (*Coprococcus* and *Lachnospiraceae*), and *Odoribacter* (belonging to *Odoribacteraceae*) (Gomez-Arango et al., 2016; Callejo et al., 2018) were enriched in control subjects, while *Dorea* (belong to *Clostridium* cluster XIVa) and *Butyricicoccus* (belonging to *Clostridium* cluster IV) were enriched in Groups LT_A and LT_N, respectively. Evidence has shown that butyrate is essential for the maintenance of colonic mucosal health, with roles such as inducing the development of regulatory T cells (Furusawa et al., 2013) and regulating the Treg/Th17 balance, which helps to restore intestinal homeostasis (Zhang M. et al., 2016). *Clostridium* clusters XIVa and IV are reported to stimulate over-expression of interleukin 10 (IL-10) and cytotoxic T lymphocyte-associated antigen 4 (CTLA4) by colon Treg cells (Atarashi et al., 2011). Over-expression of IL-10 and CTLA4 plays an important role in the development of liver injury (Knolle and Gerken, 2000), graft rejection, and in the long-term clinical outcome of organ transplantation patients (Alegre et al., 2001; Guo et al., 2012). Additionally, a decreased abundance of butyrate-producing bacteria (*Ruminococcaceae* and *Clostridiales* family XI Incertae Sedis) was also observed in patients with inflammatory bowel

disease, cirrhosis, and early hepatocellular carcinoma compared with controls (Chen et al., 2011; Joossens et al., 2011; Ren et al., 2018). Butyrate mediates suppression of inflammation and carcinogenesis by interacting with metabolite-sensing G protein-coupled receptors in gut epithelial and immune cells (Sivaprakasam et al., 2016). In present study, the relative abundance of fecal butyrate-producing bacteria had a negative correlation with serum markers of liver dysfunction. Therefore, dysbiosis of intestinal butyrate-producing bacterial populations might result in the progression of chronic liver injury in the liver recipient cohorts.

Although the shifts in the intestinal microbiome of LT recipients under the pressure of long-term immunosuppressant use are uncertain, the known relationship between the host immune system and the intestinal microbiota suggests that immunosuppressors likely affect the repopulation of the intestinal microbiome in LT recipients. Additionally, antibiotic treatments to prevent or eradicate a pathogen are likely to have both short- and long-term impacts on the commensal microbiota (Jernberg et al., 2010; Sommer and Dantas, 2011). These effects can change the relative proportions of different species in the microbiota, with the introduction of a new species or the eradication of an existing species. Finally, the intestinal microbiome and the liver are closely connected (Henao-Mejia et al., 2013); thus, abnormal liver function in LT recipients also contributes to the perturbation of microbiota-host mutualism. The occurrence and development of liver disease are always accompanied by intestinal microbial variation, while structural shifts in the intestinal microbiota always contribute to liver injury or its recovery following hepatic surgery (Ren et al., 2011). Our previous study showed that fecal bacterial populations could serve as non-invasive independent biomarkers for early detection of hepatocellular carcinoma (Ren et al., 2018). Previous animal experiments revealed that alterations in the intestinal microbiota predated hepatic rejection injury in rats following LT (Ren et al., 2014), suggesting that intestinal microbial variation might predict early acute rejection after LT and could become a therapeutic target to improve rejection rates after orthotopic LT. Chronic rejection following LT was always accompanied by abnormal liver function. Here, the fecal microbiota heat map and LEfSe analysis revealed that patients in group LT_A had serious fecal microbiome dysbiosis, with lower butyrate-producing bacterial diversity and a higher prevalence of opportunistic pathogens compared with HCs and liver recipients with normal liver function. Interestingly, enrichment of *Klebsiella* and *Escherichia/Shigella* was observed in liver recipients from both groups compared with HCs.

The gut microbiota is increasingly being recognized as an attractive target for therapeutic intervention, and stimulation of butyric acid production in the intestine of LT recipients could be achieved via the repopulation of butyrate-producers through microbiota-targeted therapies. This novel strategy could reduce chronic liver allograft dysfunction and other complications (Loguercio et al., 2005), as well as improve the quality of life for LT recipients. Understanding the ecological and evolutionary processes that determine the diversity and composition of the repopulated intestinal microbiome in LT recipients with abnormal/normal liver function is a critical first step for achieving these goals.

It should be noted that our findings on the complex discriminatory fecal microbiomes of both LT groups and HCs is only a snapshot, and that we only analyzed the bacterial composition of the fecal microbiota. As such, the current study has several limitations. First, this study didn't include the microbiota profiling prior to liver transplantation. Although we could enroll HBV-associated hepatocellular carcinoma patients with similar pathophysiology and disease severity, patients could not be asked to receive the same medical interventions and treatment within perioperative period, because the use of prophylactic antimicrobial and immunosuppressant agents varied by the targeted disease and the recipient's perceived risks and willingness. Second, the present study was not designed to compare microbiota alterations before and after orthotopic LT surgeries. Future long-term follow-up microbiome studies including pre- and post-orthotopic LT recipients should include multiple cohorts and a later post-operative sampling point to characterize the architecture of a healthy LT recipient microbiome.

In summary, these results demonstrated that the variations in fecal microbiota profiles of LT patients, and identified fecal butyrate-producing bacteria enriched in healthy control samples were negatively correlated with serum markers of liver dysfunction. Lastly, microbiota-directed therapeutic strategies should be considered after orthotopic LT surgeries.

ETHICS STATEMENT

This study was approved by the Institutional Review Board of the First Affiliated Hospital, School of Medicine, Zhejiang University (IRB No. 2014-336). All experiments were performed in accordance with the Helsinki Declaration and the Rules of Good Clinical Practice, and no organs from executed prisoners were used in these recipients.

AUTHOR CONTRIBUTIONS

L-JL and S-SZ conceived and designed the experiments. H-FL, Z-GR, HZ, S-YX, J-WJ, LZ, QL, and B-HW performed the experiments. H-FL, Z-GR, AL, G-YC, and X-HC analyzed the data. LZ, S-SZ, and L-JL contributed reagents, materials, and analysis tools. Z-GR prepared the figures and the tables. H-FL wrote the manuscript.

FUNDING

This study was supported by the National Natural Science Foundation of China (81501431, 81600506, and 81874038), Major program of National Natural Science Foundation of China (91542205), National S&T Major Project of China (2018ZX10301201 and 2017ZX10203205), and the opening foundation of the State Key Laboratory for Diagnosis and Treatment of Infectious Diseases and Collaborative Innovation

Center for Diagnosis and Treatment of Infectious Diseases, The First Affiliated Hospital, College of Medicine, Zhejiang University (Grant SKLID2019KF03).

ACKNOWLEDGMENTS

We would like to thank all of the patients who participated in this study and the physicians in the Department of Infectious Disease, Department of Hepatobiliary and Pancreatic Surgery, The First Affiliated Hospital, School of Medicine, Zhejiang University and Shulan (Hangzhou) Hospital for their collaboration and fecal samples collection. We thank Tamsin Sheen, Ph.D., and Katie Oakley, Ph.D., from Liwen Bianji, Edanz Editing China (www.liwenbianji.cn/ac), for editing the English text of a draft of this manuscript; and Dr. Chao Liu, from the Shanghai Mobiohealth Biomedical Technology Co., Ltd., for Spearman's correlation analysis.

SUPPLEMENTARY MATERIAL

The Supplementary Material for this article can be found online at: https://www.frontiersin.org/articles/10.3389/fmicb.2019.01518/full#supplementary-material

REFERENCES

Alegre, M. L., Frauwirth, K. A., and Thompson, C. B. (2001). T-cell regulation by CD28 and CTLA-4. *Nat. Rev. Immunol.* 1, 220–228. doi: 10.1038/35105024

Aliyu, S. H., Marriott, R. K., Curran, M. D., Parmar, S., Bentley, N., Brown, N. M., et al. (2004). Real-time PCR investigation into the importance of *Fusobacterium necrophorum* as a cause of acute pharyngitis in general practice. *J. Med. Microbiol.* 53, 1029–1035. doi: 10.1099/jmm.0.45648-0

Arai, M., Mochida, S., Ohno, A., Arai, S., and Fujiwara, K. (1998). Selective bowel decontamination of recipients for prevention against liver injury following orthotopic liver transplantation: evaluation with rat models. *Hepatology* 27, 123–127. doi: 10.1002/hep.510270120

Atarashi, K., Tanoue, T., Shima, T., Imaoka, A., Kuwahara, T., Momose, Y., et al. (2011). Induction of colonic regulatory T cells by indigenous *Clostridium* species. *Science* 331, 337–341. doi: 10.1126/science.1198469

Callejo, M., Mondejar-Parreno, G., Barreira, B., Izquierdo-Garcia, J. L., Morales-Cano, D., Esquivel-Ruiz, S., et al. (2018). Pulmonary arterial hypertension affects the rat gutmicrobiome. *Sci. Rep.* 8:9681. doi: 10.1038/s41598-018-27682-w

Chen, Y., Ji, F., Guo, J., Shi, D., Fang, D., and Li, L. (2016). Dysbiosis of small intestinal microbiota in liver cirrhosis and its association with etiology. *Sci. Rep.* 6:34055. doi: 10.1038/srep34055

Chen, Y., Yang, F., Lu, H., Wang, B., Chen, Y., Lei, D., et al. (2011). Characterization of fecal microbial communities in patients with liver cirrhosis. *Hepatology* 54, 562–572. doi: 10.1002/hep.24423

Doycheva, I., Leise, M. D., and Watt, K. D. (2016). The intestinal microbiome and the liver transplant recipient: what we know and what we need to know. *Transplantation* 100, 61–68. doi: 10.1097/TP.0000000000001008

Edgar, R. C. (2013). UPARSE: highly accurate OTU sequences from microbial amplicon reads. *Nat. Methods* 10, 996–998. doi: 10.1038/nmeth.2604

Edgar, R. C., Haas, B. J., Clemente, J. C., Quince, C., and Knight, R. (2011). UCHIME improves sensitivity and speed of chimera detection. *Bioinformatics* 27, 2194–2200. doi: 10.1093/bioinformatics/btr381

Fang, D., Shi, D., Lv, L., Gu, S., Wu, W., Chen, Y., et al. (2017). Bifidobacterium pseudocatenulatum LI09 and Bifidobacterium catenulatum LI10 attenuate D-galactosamine-induced liver injury by modifying the gut microbiota. *Sci. Rep.* 7:8770. doi: 10.1038/s41598-017-09395-8

Fedoseyeva, E. V., Zhang, F., Orr, P. L., Levin, D., Buncke, H. J., and Benichou, G. (1999). De novo autoimmunity to cardiac myosin after heart transplantation and its contribution to the rejection process. *J. Immunol.* 162, 6836–6842.

Fenkel, J. M., and Halegoua-DeMarzio, D. L. (2016). Management of the liver transplant recipient: approach to allograft dysfunction. *Med. Clin. North Am.* 100, 477–486. doi: 10.1016/j.mcna.2016.01.001

Furusawa, Y., Obata, Y., Fukuda, S., Endo, T. A., Nakato, G., Takahashi, D., et al. (2013). Commensal microbe-derived butyrate induces the differentiation of colonic regulatory T cells. *Nature* 504, 446–450. doi: 10.1038/nature12721

Gabe, S. M., Bjarnason, I., Tolou-Ghamari, Z., Tredger, J. M., Johnson, P. G., Barclay, G. R., et al. (1998). The effect of tacrolimus (FK506) on intestinal barrier function and cellular energy production in humans. *Gastroenterology* 115, 67–74.

Garcia-Tsao, G., and Wiest, R. (2004). Gut microflora in the pathogenesis of the complications of cirrhosis. *Best Pract. Res. Clin. Gastroenterol.* 18, 353–372.

Gomez-Arango, L. F., Barrett, H. L., Mcintyre, H. D., Callaway, L. K., Morrison, M., DekkerNitert, M., et al. (2016). Increased systolic and diastolic blood pressure is associated with altered gut microbiota composition and butyrate production in early pregnancy. *Hypertension* 68, 974–981. doi: 10.1161/HYPERTENSIONAHA.116.07910

Guo, Y., Fan, Y., Qiu, J., Liu, Y., Gao, J., and Guo, F. (2012). Polymorphisms in CTLA4 influence incidence of drug-induced liver injury after renal transplantation in Chinese recipients. *PLoS One* 7:e51723. doi: 10.1371/journal.pone.0051723

Heitner, S. B., Hollenberg, S. M., and Colilla, S. A. (2010). Heat maps, random forests, and nearest neighbors: a peek into the new molecular diagnostic world. *Crit. Care Med.* 38, 296–298. doi: 10.1097/CCM.0b013e3181c545ed

Henao-Mejia, J., Elinav, E., Thaiss, C. A., Licona-Limon, P., and Flavell, R. A. (2013). Role of the intestinal microbiome in liver disease. *J. Autoimmun.* 46, 66–73. doi: 10.1016/j.jaut.2013.07.001

Hori, T., Onishi, Y., Kamei, H., Kurata, N., Ishigami, M., Ishizu, Y., et al. (2016). Fibrosing cholestatic hepatitis C in post-transplant adult recipients of liver transplantation. *Ann. Gastroenterol.* 29, 454–459. doi: 10.20524/aog.2016.0069

Jernberg, C., Lofmark, S., Edlund, C., and Jansson, J. K. (2010). Long-term impacts of antibiotic exposure on the human intestinal microbiota. *Microbiology* 156, 3216–3223. doi: 10.1099/mic.0.040618-0

Jiang, J. W., Ren, Z. G., Chen, L. Y., Jiang, L., Xie, H. Y., Zhou, L., et al. (2011). Enteral supplementation with glycyl-glutamine improves intestinal barrier function after liver transplantation in rats. *Hepatobiliary Pancreat. Dis. Int.* 10, 380–385.

Jiang, W., and Yu, W. (2017). Controlling the joint local false discovery rate is more powerful than meta-analysis methods in joint analysis of summary statistics from multiple genome-wide association studies. *Bioinformatics* 33, 500–507. doi: 10.1093/bioinformatics/btw690

Joossens, M., Huys, G., Cnockaert, M., De Preter, V., Verbeke, K., Rutgeerts, P., et al. (2011). Dysbiosis of the faecalmicrobiota in patients with Crohn's disease and their unaffected relatives. *Gut* 60, 631–637. doi: 10.1136/gut.2010.223263

Kant, R., Rasinkangas, P., Satokari, R., Pietila, T. E., and Palva, A. (2015). Genome sequence of the butyrate-producing anaerobic bacterium anaerostipes hadrus PEL 85. *Genome. Announc.* 3:e00224-15. doi: 10.1128/genomeA.00224-15

Knolle, P. A., and Gerken, G. (2000). Local control of the immune response in the liver. *Immunol. Rev.* 174, 21–34.

Kok, B., Ewasiuk, A., and Karvellas, C. J. (2017). Liver transplant in acute-on-chronic liver failure: evaluating the impact of organ dysfunction. *Liver Int.* 37, 651–652. doi: 10.1111/liv.13365

Ling, Z., Liu, X., Jia, X., Cheng, Y., Luo, Y., Yuan, L., et al. (2014). Impacts of infection with different toxigenic *Clostridium* difficile strains on faecal microbiota in children. *Sci. Rep.* 4:7485. doi: 10.1038/srep07485

Loguercio, C., Federico, A., Tuccillo, C., Terracciano, F., D'auria, M. V., De Simone, C., et al. (2005). Beneficial effects of a probiotic VSL#3 on parameters of liver dysfunction in chronic liver diseases. *J. Clin. Gastroenterol.* 39, 540–543.

Lu, H., He, J., Wu, Z., Xu, W., Zhang, H., Ye, P., et al. (2013). Assessment of microbiome variation during the perioperative period in liver transplant

patients: a retrospective analysis. *Microb. Ecol.* 65, 781–791. doi: 10.1007/s00248-013-0211-6

Lu, H., Ren, Z., Li, A., Zhang, H., Jiang, J., Xu, S., et al. (2016). Deep sequencing reveals microbiota dysbiosis of tongue coat in patients with liver carcinoma. *Sci. Rep.* 6:33142. doi: 10.1038/srep33142

Lu, H., Wu, Z., Xu, W., Yang, J., Chen, Y., and Li, L. (2011). Intestinal microbiota was assessed in cirrhotic patients with hepatitis B virus infection. Intestinal microbiota of HBV cirrhotic patients. *Microb. Ecol.* 61, 693–703. doi: 10.1007/s00248-010-9801-8

Lv, L. X., Fang, D. Q., Shi, D., Chen, D. Y., Yan, R., Zhu, Y. X., et al. (2016). Alterations and correlations of the gut microbiome, metabolism and immunity in patients with primary biliary cirrhosis. *Environ. Microbiol.* 18, 2272–2286. doi: 10.1111/1462-2920.13401

McMurdie, P. J., and Holmes, S. (2013). phyloseq: an R package for reproducible interactive analysis and graphics of microbiome census data. *PLoS One* 8:e61217. doi: 10.1371/journal.pone.0061217

Oksanen, J., Blanchet, F. G., Kindt, R., Legendre, P., Minchin, P. R., O'hara, R. B., et al. (2015). *Ordination Methods, Diversity Analysis and Other Functions for Community and Vegetation Ecologists*. Vegan: Community Ecology Package.

Parrilli, G., Abazia, C., Sarnelli, G., Corsaro, M. M., Coccoli, P., Viglione, L., et al. (2003). Effect of chronic administration of tacrolimus and cyclosporine on human gastrointestinal permeability. *Liver Transpl.* 9, 484–488. doi: 10.1053/jlts.2003.50088

Qin, N., Yang, F., Li, A., Prifti, E., Chen, Y., Shao, L., et al. (2014). Alterations of the human gut microbiome in liver cirrhosis. *Nature* 513, 59–64. doi: 10.1038/nature13568

Racanelli, V., and Rehermann, B. (2006). The liver as an immunological organ. *Hepatology* 43, S54–S62. doi: 10.1002/hep.21060

Ren, Z., Cui, G., Lu, H., Chen, X., Jiang, J., Liu, H., et al. (2013). Liver ischemic preconditioning (IPC) improves intestinal microbiota following liver transplantation in rats through 16s rDNA-based analysis of microbial structure shift. *PLoS One* 8:e75950. doi: 10.1371/journal.pone.0075950

Ren, Z., Jiang, J., Lu, H., Chen, X., He, Y., Zhang, H., et al. (2014). Intestinal microbial variation may predict early acute rejection after liver transplantation in rats. *Transplantation* 98, 844–852. doi: 10.1097/TP.0000000000000334

Ren, Z., Li, A., Jiang, J., Zhou, L., Yu, Z., Lu, H., et al. (2018). Gut microbiome analysis as a tool towards targeted non-invasive biomarkers for early hepatocellular carcinoma. *Gut* 68, 1014-1023. doi: 10.1136/gutjnl-2017-315084

Ren, Z. G., Liu, H., Jiang, J. W., Jiang, L., Chen, H., Xie, H. Y., et al. (2011). Protective effect of probiotics on intestinal barrier function in malnourished rats after liver transplantation. *Hepatobiliary Pancreat. Dis. Int.* 10, 489–496.

Reyes, J., Jain, A., Mazariegos, G., Kashyap, R., Green, M., Iurlano, K., et al. (2000). Long-term results after conversion from cyclosporine to tacrolimus in pediatric liver transplantationfor acute and chronic rejection. *Transplantation* 69, 2573–2580.

Robin, X., Turck, N., Hainard, A., Tiberti, N., Lisacek, F., Sanchez, J. C., et al. (2011). pROC: an open-source package for R and S+ to analyze and compare ROC curves. *BMC Bioinform.* 12:77. doi: 10.1186/1471-2105-12-77

Schoening, W. N., Buescher, N., Rademacher, S., Andreou, A., Kuehn, S., Neuhaus, R., et al. (2013). Twenty-year longitudinal follow-up after orthotopic liver transplantation: a single-center experience of 313 consecutive cases. *Am. J. Transplant.* 13, 2384–2394. doi: 10.1111/ajt.12384

Schwiertz, A., Hold, G. L., Duncan, S. H., Gruhl, B., Collins, M. D., Lawson, P. A., et al. (2002a). *Anaerostipes caccae* gen. nov., sp. nov., a new saccharolytic, acetate-utilising, butyrate-producing bacterium from human faeces. *Syst. Appl. Microbiol.* 25, 46–51. doi: 10.1078/0723-2020-00096

Schwiertz, A., Lehmann, U., Jacobasch, G., and Blaut, M. (2002b). Influence of resistant starch on the SCFA production and cell counts of butyrate-producing *Eubacterium* spp. in the human intestine. *J. Appl. Microbiol.* 93, 157–162.

Segata, N., Izard, J., Waldron, L., Gevers, D., Miropolsky, L., Garrett, W. S., et al. (2011). Metagenomic biomarker discovery and explanation. *Genome Biol.* 12:R60. doi: 10.1186/gb-2011-12-6-r60

Sivaprakasam, S., Prasad, P. D., and Singh, N. (2016). Benefits of short-chain fatty acids and their receptors in inflammation and carcinogenesis. *Pharmacol. Ther.* 164, 144–151. doi: 10.1016/j.pharmthera.2016.04.007

Smolinska, S., and O'Mahony, L. (2016). Microbiome-host immune system interactions. *Semin. Liver Dis.* 36, 317–326. doi: 10.1055/s-0036-1593883

Sommer, M. O., and Dantas, G. (2011). Antibiotics and the resistant microbiome. *Curr. Opin. Microbiol.* 14, 556–563. doi: 10.1016/j.mib.2011.07.005

Starzl, T. E., Iwatsuki, S., Shaw, B. W. Jr., Gordon, R. D., and Esquivel, C. O. (1985). Immunosuppression and other nonsurgical factorsin the improved results of liver transplantation. *Semin. Liver Dis.* 5, 334–343. doi: 10.1055/s-2008-1040630

Szabo, G., and Bala, S. (2010). Alcoholic liver disease and the gut-liver axis. *World J. Gastroenterol.* 16, 1321–1329.

Thaiss, C. A., Zmora, N., Levy, M., and Elinav, E. (2016). The microbiome and innate immunity. *Nature* 535, 65–74. doi: 10.1038/nature18847

Wang, Q., Garrity, G. M., Tiedje, J. M., and Cole, J. R. (2007). Naive Bayesian classifier for rapid assignment of rRNA sequences into the new bacterial taxonomy. *Appl. Environ. Microbiol.* 73, 5261–5267. doi: 10.1128/AEM.00062-07

Wu, Z. W., Ling, Z. X., Lu, H. F., Zuo, J., Sheng, J. F., Zheng, S. S., et al. (2012). Changes of gut bacteria and immune parameters in liver transplant recipients. *Hepatobiliary Pancreat. Dis. Int.* 11, 40–50.

Xie, Y. R., Liu, S. L., Liu, X., Luo, Z. B., Zhu, B., Li, Z. F., et al. (2011). Intestinal microbiota and innate immunity-related gene alteration in cirrhotic rats with liver transplantation. *Transplant. Proc.* 43, 3973–3979. doi: 10.1016/j.transproceed.2011.08.113

Zeevi, D., Korem, T., and Segal, E. (2016). Talking about cross-talk: the immune system and the microbiome. *Genome Biol.* 17:50. doi: 10.1186/s13059-016-0921-4

Zhang, M., Zhou, Q., Dorfman, R. G., Huang, X., Fan, T., Zhang, H., et al. (2016). Butyrate inhibits interleukin-17 and generates Tregs to ameliorate colorectalcolitis in rats. *BMC. Gastroenterol.* 16:84. doi: 10.1186/s12876-016-0500-x

Zhang, Q., Wu, Y., Wang, J., Wu, G., Long, W., Xue, Z., et al. (2016). Accelerated dysbiosis of gut microbiota during aggravation of DSS-induced colitis by a butyrate-producing bacterium. *Sci. Rep.* 6:27572. doi: 10.1038/srep27572

Zhang, Y., Wang, X., Hu, M., and Li, P. (2015). Effect of hydraulic retention time (HRT) on the biodegradation of trichloroethylene wastewater and anaerobic bacterial community in the UASB reactor. *Appl. Microbiol. Biotechnol.* 99, 1977–1987. doi: 10.1007/s00253-014-6096-6

Conflict of Interest Statement: The authors declare that the research was conducted in the absence of any commercial or financial relationships that could be construed as a potential conflict of interest.

Copyright © 2019 Lu, Ren, Li, Zhang, Xu, Jiang, Zhou, Ling, Wang, Cui, Chen, Zheng and Li. This is an open-access article distributed under the terms of the Creative Commons Attribution License (CC BY). The use, distribution or reproduction in other forums is permitted, provided the original author(s) and the copyright owner(s) are credited and that the original publication in this journal is cited, in accordance with accepted academic practice. No use, distribution or reproduction is permitted which does not comply with these terms.

frontiers in Microbiology

ORIGINAL RESEARCH
published: 05 July 2019
doi: 10.3389/fmicb.2019.01517

miRNA-Gene Regulatory Network in Gnotobiotic Mice Stimulated by Dysbiotic Gut Microbiota Transplanted From a Genetically Obese Child

*Liman Deng[1], Ruirui Wang[1], Hui Li[1], Chenhong Zhang[1], Liping Zhao[1,2] and Menghui Zhang[1]**

[1] State Key Laboratory of Microbial Metabolism and Joint International Research Laboratory of Metabolic and Developmental Sciences, School of Life Sciences and Biotechnology, Shanghai Jiao Tong University, Shanghai, China, [2] Department of Biochemistry and Microbiology, School of Environmental and Biological Sciences, Rutgers New Jersey Institute for Food, Nutrition, and Health, Rutgers University–New Brunswick, New Brunswick, NJ, United States

OPEN ACCESS

Edited by:
Sunny Hei Wong, The Chinese University of Hong Kong, China

Reviewed by:
Emilie Viennois, Georgia State University, United States
Bruno Melo Carvalho, Universidade de Pernambuco, Brazil
Gerben D. A. Hermes, Wageningen University & Research, Netherlands

***Correspondence:**
Menghui Zhang
mhzhang@sjtu.edu.cn

Specialty section:
This article was submitted to Microbial Symbioses, a section of the journal Frontiers in Microbiology

Received: *26 October 2018*
Accepted: *18 June 2019*
Published: *05 July 2019*

Citation:
Deng L, Wang R, Li H, Zhang C, Zhao L and Zhang M (2019) miRNA-Gene Regulatory Network in Gnotobiotic Mice Stimulated by Dysbiotic Gut Microbiota Transplanted From a Genetically Obese Child. Front. Microbiol. 10:1517. doi: 10.3389/fmicb.2019.01517

Gut microbiota (GM) dysbiosis has been considered a pathogenic origin of many chronic diseases. In our previous trial, a shift in GM structure caused by a complex fiber-rich diet was associated with the health improvement of obese Prader-Willi syndrome (PWS) children. The pre- and post-intervention GMs (pre- and post-group, respectively) from one child were then transplanted into gnotobiotic mice, which resulted in significantly different physiological phenotypes, each of which was similar to the phenotype of the corresponding GM donor. This study was designed to investigate the miRNA-gene regulatory networks involved in causing these phenotypic differences. Using the post-group as a reference, we systematically identified and annotated the differentially expressed (DE) miRNAs and genes in the colon and liver of the pre-group in the second and fourth weeks after GM inoculation. Most of the significantly enriched GO terms and KEGG pathways were observed in the liver and were in the second week after GM transplantation. We screened 23 key genes along with their 73 miRNA regulators relevant to the host phenotype changes and constructed a network. The network contained 92 miRNA-gene regulation relationships, 51 of which were positive, and 41 of which were negative. Both the colon and liver had upregulated pro-inflammatory genes, and genes involved in fatty acid oxidation, lipolysis, and plasma cholesterol clearance were downregulated in only the liver. These changes were consistent with lipid and cholesterol accumulation in the host and with a high inflammation level. In addition, the colon showed an impacted glucagon-like peptide 1 (GLP-1) signaling pathway, while the liver displayed decreased insulin receptor signaling pathway activity. These molecular changes were mainly found in the second week, 2 weeks before changes in body fat occurred. This time lag indicated that GM dysbiosis might initially induce cholesterol and lipid metabolism-related miRNA and gene expression disorder and then lead to

lipid accumulation and obesity development, which implicates a causative role of GM dysbiosis in obesity development rather than a result of obesity. This study provides fundamental molecular information that elucidates how dysbiotic GM increases host inflammation and disturbs host lipid and glucose metabolism.

Keywords: gut microbiota, gnotobiotic mice, miRNA, gene expression, regulatory network, inflammation, lipid and glucose metabolism

INTRODUCTION

There is increasing evidence to suspect the pathogenic role of GM dysbiosis in many diseases, particularly in gastrointestinal and metabolic disorders (Lynch and Pedersen, 2016). It has been recognized that GM can affect host phenotypes by modulating host gene expression. MicroRNAs (also called miRNAs) are very important regulators of gene expression that are active in various biological processes, such as development, immunity, adipocyte differentiation, and lipid metabolism (He and Hannon, 2004; Taganov et al., 2007; Peng et al., 2014). Recently, some studies reported that the modulation of gene expression by GM occurred via prior changes in miRNA expression (Dalmasso et al., 2011; Singh et al., 2012). With the rapidly decreasing cost of high-throughput sequencing, there is growing interest in understanding how miRNAs respond to GM and in turn affect gene expression.

Prader-Willi syndrome is a genetically inherited disease caused by deficiencies in imprinted paternal genes in chromosome region 15q11-q13. Patients with PWS have intense hyperphagia, which results in extreme adiposity, a major cause of death (Butler, 2011). Previously, we significantly improved the health status of 17 PWS children using a GM targeted modulation diet (called the WTP diet, composed of whole grains, traditional Chinese medicine food and prebiotics). Evidence and data analysis suggested that the poor clinical status of the PWS children before the intervention was related to dysbiotic GM. To validate this suspicion, the pre- and post-intervention GMs from an intervened PWS child were transplanted into two randomized groups (pre- and post-group, respectively) of genetically identical germ-free male C57BL/6J mice. As expected, the pre-group had a higher inflammation level and more fat accumulation than the post-group (Zhang et al., 2015; Wang et al., 2018). This animal experiment demonstrated the effect of the disturbance of dysbiotic GM on host health. However, the underlying mechanism remains unclear.

This study focused on the effect of the transplanted dysbiotic GM on miRNA expression and aimed to determine the miRNA–mRNA interactions that link GM and host phenotypes. Using sequencing technology, we first obtained the miRNA expression profiles in the liver and colon samples of gnotobiotic mice taken from the previous fecal microbiota transplantation animal experiment. To elucidate the molecular mechanism behind the differences between the two groups, the previously measured gene expression profiling data of the same samples were integrated into this study. Then, we identified DE miRNAs and their target genes between the two groups in the second and fourth weeks after microbiota inoculation and annotated their biological functions. After that, with emphasis on the phenotypic changes in the host, a regulatory network of DE miRNAs, DE target genes and biological functions relevant to lipid and cholesterol metabolism, glucose homeostasis and inflammation was constructed. Finally, GMs that correlated with the key members in the network were studied to decipher how miRNAs along with their target genes were involved in affecting the phenotype of gnotobiotic mice under the pressure of dysbiotic microbiota.

Abbreviations: AMPK, adenosine monophosphate activated protein kinase; ATGL, adipose triglyceride lipase; DE, differentially expressed; GLP-1, glucagon-like peptide 1; GM, gut microbiota; HDL, high density lipoprotein; IACUC, Institutional Animal Care and Use Committee; IFN, interferon; IL, interleukin; IRS, insulin receptor substrate; LBP, lipopolysaccharide binding protein; LDL, low density lipoprotein; LPS, lipopolysaccharide; MMPs, matrix metalloproteinases; NFAT, nuclear factor of activated T cells; PWS, Prader-Willi syndrome; SAA, serum amyloid A; TLR, toll-like receptor; TNF, tumor necrosis factor; WTP, whole grains, traditional Chinese medicine food and prebiotics.

MATERIALS AND METHODS

Animal Experiment

The animal experiment was previously performed as described (Zhang et al., 2015). Briefly, a PWS obese child had received a 90-day WTP dietary intervention. Patient fecal samples before (on day 0) and after (on day 90) the intervention were collected and preserved at −80°C. For the animal transplantation experiment, the two fecal samples were individually diluted in sterile Ringer working buffer. Then, the clarified supernatants of each sample were mixed with an equal volume of 20% skim milk and transferred into two randomized groups (pre- and post-group) of C57BL/6J germ-free male mice through 2 days of continuous oral gavage. During the experiment, the mice were raised in flexible-film plastic isolators with a regular 12-h light cycle and fed a sterile normal chow diet (D12450B, Research Diets, Inc., New Brunswick, NJ, United States) *ad libitum* in SLAC Inc. (Shanghai, China). Half of the mice in each group were sacrificed in the second week (Pre_2W group, $n = 4$ and Post_2W group, $n = 4$) and the rest in the fourth week (Pre_4W group, $n = 5$ and Post_4W group, $n = 4$) after GM transplantation. Colon and liver tissues were collected for RNA sequencing analysis.

The clinical trial of the PWS children was approved by the Ethics Committee of the School of Life Sciences and Biotechnology, Shanghai Jiao Tong University with No. 2012-016 and registered at Chinese Clinical Trial Registry with No. ChiCTR-ONC-12002646. Written informed consent was obtained from the guardian of the PWS donor. The animal experimental protocols were approved and performed

in accordance with relevant guidelines and regulations recommended by the IACUC of Shanghai SLAC Laboratory Animal Co., Ltd. All potential biologically hazardous materials in this study were properly handled according to Chinese biosafety laws and regulations.

Sequencing of miRNAs and mRNAs

For miRNA sequencing, total RNAs were extracted from tissue samples using a mirVana™ miRNA Isolation Kit (Cat. # AM1560; Austin, TX, United States) according to the manufacturer's instructions. The concentration and purity of the RNA samples were quantified by a NanoDrop spectrophotometer (NanoDrop Technologies, Inc.), and the RNA quality was assessed by an Agilent Bioanalyzer 2100 (Agilent Technologies, Santa Clara, CA, United States). The A260/A280 ratio of the RNA samples was between 2.14 and 2.20. An Illumina TruSeq Small RNA Sample Kit was used to prepare cDNA libraries according to the TruSeq Small RNA Sample Preparation Guide. The concentration and size distribution of the final cDNA libraries were confirmed by a Qubit® 2.0 Fluorometer and an Agilent Bioanalyzer 2100. The sequencing was performed on an Illumina Genome Analyzer IIx with a single-end 1 × 50 nt multiplex procedure.

mRNA sequencing was performed as previously described (Wang et al., 2018). Briefly, total RNAs were extracted using an RNeasy Mini Kit (Qiagen, Germany) and purified using an RNase-Free DNase Set (Qiagen). The cDNA libraries were prepared following the Illumina TruSeq protocol. The mRNA sequencing was performed on an Illumina HiSeq 2500 with a pair-end 2 × 125 nt or 2 × 100 nt multiplex procedure.

The miRNA and mRNA sequencing reads can be accessed in the NCBI SRA database with accession numbers SRP145202, SRP132325 and SRP144862.

Bioinformatics and Statistics

The raw miRNA reads were first clipped to remove the 3′-adapter. Then, the reads were trimmed with a threshold Q30 and were filtered to exclude reads with an N base or outside 16–36 nt. The high-quality unique sequences were aligned to the mouse mature miRNA database in miRBase (Release 21)[1] using Bowtie v1.1.1 (Langmead et al., 2009) with parameters -a –best –strata and -v 2. After non-specifically aligned unique sequences were discarded, the remaining specifically aligned sequences constituted the miRNA expression profile.

The raw mRNA reads were first trimmed with a threshold Q20. Then, reads shorter than 30 nt or with an N base were removed. The remaining data were mapped to the *Mus musculus* reference genome GRCm38 (Genome Reference Consortium mouse build 38)[2] using HISAT version 0.1.7-beta (Kim et al., 2015). The gene expression profiling was calculated using the counts of aligned reads with the mouse genome annotation GTF file[3] by HTSeq-count version 0.6.1p1 (Anders et al., 2015).

[1] ftp://mirbase.org/pub/mirbase/21/mature.fa.gz

[2] ftp://ftp.ensembl.org/pub/release-80/fasta/mus_musculus/dna/

[3] ftp://ftp.ensembl.org/pub/release-80/gtf/mus_musculus

Differential expression analysis between the pre- and post-group was performed using the DESeq2 package (Love et al., 2014). miRNAs and genes with $|\log_2 \text{foldchange}| \geq 1$ were considered to be DE.

For target gene prediction of the DE miRNAs, three target gene prediction algorithms, TargetScan (Agarwal et al., 2015), miRDB (Wong and Wang, 2015), and DIANA-microT-CDS (Reczko et al., 2012), were used to maximally cover the DE miRNAs. To improve the stringency of the prediction, only the genes predicted by at least two algorithms were considered as putative target genes. To ensure that the target genes were specifically expressed in response to the GM, only the putative target genes that were DE were selected as DE target genes.

The GO and KEGG pathway enrichment analyses and functional annotation of the DE target genes were performed using DAVID 6.8 (Huang da et al., 2009). Biological process GO terms and KEGG pathways with gene counts ≥2 and EASE score (modulated p-value) < 0.05 were considered to be significantly enriched.

Spearman's correlation analysis between miRNAs and their target genes was performed, and the p-value was adjusted by the method of Benjamini and Hochberg using R statistical language (R 3.2.2). The regulatory network containing miRNAs, target genes and biological functions was constructed by Cytoscape 3.5.1 (Shannon et al., 2003).

RESULTS

DE miRNAs and Genes in the Colon and Liver of the Gnotobiotic Mice Between the Pre- and Post-groups

After data preprocessing and reference mapping (**Supplementary Table S1**), we detected 1,818 mouse mature miRNAs and 26,876 genes in colon tissues, whereas 1,831 miRNAs and 21,635 genes were detected in liver tissues. Setting the post-group as a baseline, the pre-group had 313 DE miRNAs and 313 DE genes in the colon and 230 DE miRNAs and 1,248 DE genes in the liver (**Table 1**). Most of the identified DE miRNAs and genes displayed time- and tissue-specific characteristics in that they appeared only at one time point and in one tissue. Liver tissue had fewer DE miRNAs but many more DE genes than colon tissue, which suggested that the liver might be more affected by the pre-intervention GM. Both colon and liver tissues had many more DE miRNAs and

TABLE 1 | Numbers of DE miRNAs and genes under the stress of the pre-intervention GM.

		Colon			Liver		
		Total	**Down**	**Up**	**Total**	**Down**	**Up**
miRNA	2W	212	52	160	163	26	137
	4W	101	24	77	67	22	45
Gene	2W	216	83	133	903	393	510
	4W	97	13	84	345	125	220

N = 4 or 5 for each group.

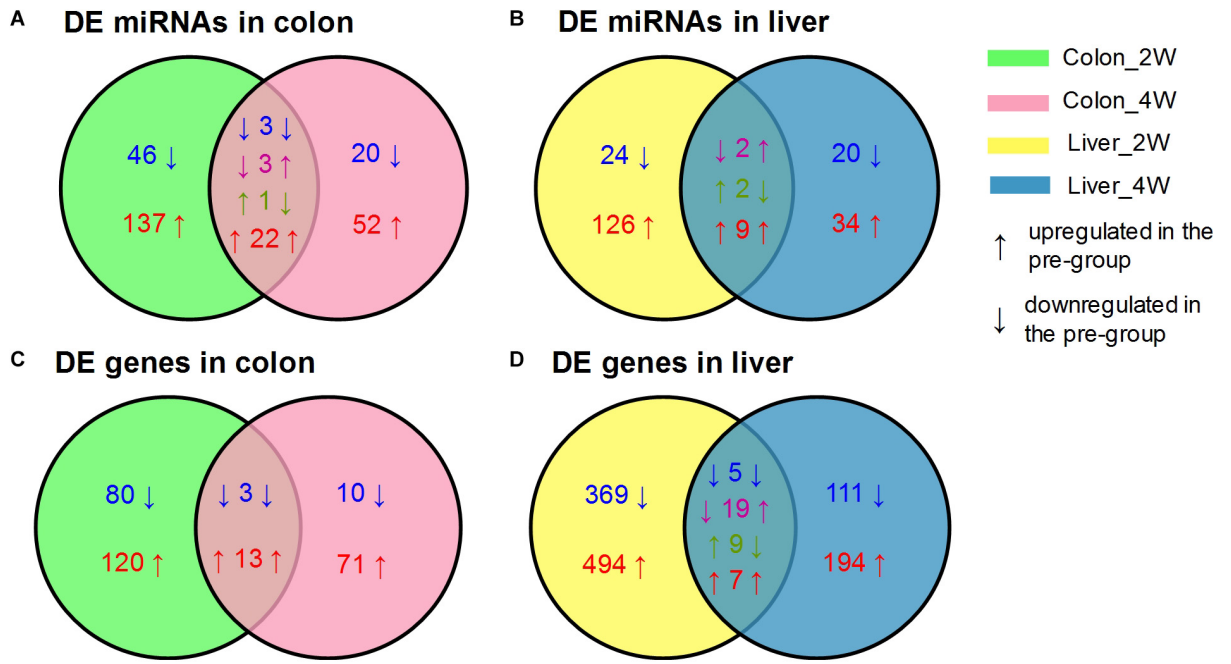

FIGURE 1 | Venn diagrams of the DE miRNAs and genes between the pre-group and the post-group in the second and fourth week after GM transplantation. **(A)** DE miRNAs in colon, **(B)** DE miRNAs in liver, **(C)** DE genes in colon, **(D)** DE genes in liver. DE miRNAs and genes were screened by DESeq2 with the criterion of $|\log_2 \text{FoldChange}| \geq 1$ (pre-group vs. post-group), $n = 4$ or 5 for each group.

genes in the second week than in the fourth week. Although, we could not obtain the exact influencing time-curve of the GM on host miRNAs and genes due to sampling limitation, this result indicated that the effects of the GM mainly occurred in the initial stage of the transplantation and declined with time. The DE miRNAs identified in colon tissue are an example of this observation. There were 46 downregulated and 137 upregulated miRNAs uniquely identified in the second week, while another 20 downregulated and 52 upregulated miRNAs were identified in the fourth week. In addition, the 29 DE miRNAs that appeared at both time points showed different expression patterns: 3 were downregulated and 22 were upregulated at both time points, 3 were downregulated in the second week but upregulated in the fourth week, and 1 displayed opposite of the previous (**Figure 1A**). Similar results were also observed for DE miRNAs in the liver (**Figure 1B**) and for DE genes (**Figures 1C,D**).

DE Target Genes Regulated by the DE miRNAs

Based on the DE miRNA results, large numbers of putative target genes were found. In colon tissue, the 207 DE miRNAs in the second week had 13,606 putative target genes, and the 98 DE miRNAs in the fourth week had 10,855 putative target genes. In liver tissue, 13,352 putative target genes were identified for 161 DE miRNAs in the second week, and 9,923 putative target genes were found for 67 DE miRNAs in the fourth week. Seven DE miRNAs (mmu-miR-8109, mmu-miR-7662-3p, mmu-miR-6539, mmu-miR-5124b, mmu-miR-6402, mmu-miR-142a-3p, and mmu-miR-6352) were removed from further analysis since they did not fulfill our target gene prediction criterion mentioned in the "Materials and Methods" Section.

To be more confident in the target gene selection, the putative target genes were further filtered so that only the DE genes were selected as DE target genes. As a result, in colon tissue, there were 102 DE target genes for 136 DE miRNAs in the second week and 26 DE target genes for 45 DE miRNAs in the fourth week. In liver tissue, 437 DE target genes remained for 148 DE miRNAs in the second week, and 116 DE target genes remained for 53 DE miRNAs in the fourth week (**Supplementary Table S2**).

Significantly Enriched Biological Process GO Terms and KEGG Pathways of the DE Target Genes

In the analysis of the DE target genes, 55 biological process GO terms were significantly enriched (**Figure 2**). Most of these terms were identified in liver tissue, especially in the second week (Liver_2W), where 39 of the 55 significantly enriched GO terms were found. Among these significantly enriched terms, the terms "regulation of lipid transport by positive regulation of transcription from RNA polymerase II promoter" and "cholesterol metabolic process" are associated with lipid and cholesterol metabolism. The terms "negative regulation of insulin receptor signaling pathway" and "negative regulation of glucose import" are relevant to glucose homeostasis, and "response to cytokine" is related to inflammation and immune response. In Liver_4W, the number of significantly enriched GO terms was reduced to 11, with one of the terms, "cellular response to

	Colon_2W	Colon_4W	Liver_2W	Liver_4W
regulation of lipid transport by positive regulation of transcription from RNA polymerase II promoter			*	
cholesterol metabolic process			*	
negative regulation of insulin receptor signaling pathway			*	
negative regulation of glucose import			*	
cellular response to glucose stimulus				**
positive regulation of interleukin-1 production	*			
negative regulation of calcineurin-NFAT signaling cascade		**		
response to cytokine			*	
transcription, DNA-templated			**	*
regulation of transcription, DNA-templated			*	
positive regulation of transcription, DNA-templated			*	
regulation of transcription from RNA polymerase II promoter			*	
positive regulation of transcription from RNA polymerase II promoter			**	*
DNA methylation			*	
DNA recombination			*	
histone H3-K4 methylation			*	
base-excision repair			*	
cellular response to DNA damage stimulus			**	
regulation of apoptotic process			**	
negative regulation of extrinsic apoptotic signaling pathway via death domain receptors			*	
negative regulation of intrinsic apoptotic signaling pathway in response to DNA damage			*	
negative regulation of autophagy			*	
negative regulation of cell death			*	
positive regulation of fibroblast proliferation			*	
endodermal cell differentiation			*	
positive regulation of cell growth			*	
homeostasis of number of cells within a tissue			*	
positive regulation of neuron death				**
thyroid hormone metabolic process		*		
hyaluronan metabolic process			*	
metabolic process			*	
ion transport	*			
transport		*		
positive regulation of sodium ion transport			*	
transmembrane transport				*
multicellular organism growth	*			
angiogenesis			**	
blood vessel morphogenesis			*	
regulation of axonogenesis				*
hair follicle development				*
tube morphogenesis				*
cellular response to hydroxyurea	*			
response to drug			*	
response to oxidative stress			**	
regulation of defense response to virus by host				*
positive regulation of proteasomal ubiquitin-dependent protein catabolic process			**	
amyloid precursor protein catabolic process			**	
positive regulation of establishment of protein localization to plasma membrane			*	
negative regulation of catalytic activity			**	
plasminogen activation			*	
platelet activation			*	
cell-cell adhesion			**	
insulin-like growth factor receptor signaling pathway			*	
peptidyl-threonine phosphorylation				*
spindle localization				*

lipid/cholesterol metabolism | glucose homeostasis | inflammation/immune response | transcription | cell processes | others

FIGURE 2 | The 55 significantly enriched biological process GO terms of the DE target genes. Most GO terms were identified in the liver, especially in Liver_2W. Some of these terms were associated with lipid and cholesterol metabolism, glucose homeostasis and inflammation. **EASE score < 0.01 and *EASE score < 0.05.

	Colon_2W	Colon_4W	Liver_2W	Liver_4W
Regulation of lipolysis in adipocytes			*	
Adipocytokine signaling pathway			*	
Insulin secretion	**			
AMPK signaling pathway			*	
Tuberculosis	**			
Leishmaniasis	**			
Toxoplasmosis	*		*	
Amyotrophic lateral sclerosis (ALS)	*			
Small cell lung cancer			**	
Renal cell carcinoma			*	
Butanoate metabolism			*	
Tryptophan metabolism			*	
Metabolic pathways	*		*	
GnRH signaling pathway	**			
Retrograde endocannabinoid signaling	*			
Sphingolipid signaling pathway	*			
Adrenergic signaling in cardiomyocytes	*			
Estrogen signaling pathway			**	
PI3K-Akt signaling pathway			**	
Jak-STAT signaling pathway			**	
Prolactin signaling pathway			*	
Neurotrophin signaling pathway			*	
Ras signaling pathway			*	
Vascular smooth muscle contraction	*			
Osteoclast differentiation			*	
Apoptosis			*	
Focal adhesion			*	
SNARE interactions in vesicular transport			*	

lipid/cholesterol metabolism glucose homeostasis energy homeostasis diseases and cancers others

FIGURE 3 | The 28 significantly enriched KEGG pathways of the DE target genes. All pathways were found in the second week in the colon and liver. Some of these pathways were associated with lipid metabolism, glucose homeostasis, and energy homeostasis. **EASE score < 0.01 and *EASE score < 0.05.

glucose stimulus," being related to glucose homeostasis. Colon tissue had many fewer significantly enriched GO terms, with only four in Colon_2W and three in Colon_4W. Two of these terms, "positive regulation of interleukin 1 production" enriched in Colon_2W and "negative regulation of calcineurin-NFAT signaling cascade" in Colon_4W, are both associated with inflammation and immune response.

A total of 28 KEGG pathways were significantly enriched in the analysis of the DE target genes (**Figure 3**). Different from the results obtained by GO enrichment analysis, all significantly enriched KEGG pathways were found in the second week. There were 11 KEGG pathways significantly enriched in Colon_2W, and one of them, "Insulin secretion," is related to glucose homeostasis. In Liver_2W, 19 KEGG pathways were significantly enriched, more than what was observed in Colon_2W. Among these pathways, "Regulation of lipolysis in adipocytes" and "Adipocytokine signaling pathway" are associated with lipid metabolism, and the "AMPK signaling pathway" is crucial in the regulation of energy homeostasis.

Regulatory Network Among miRNAs, Target Genes, and Biological Functions Relevant to Host Lipid and Cholesterol Metabolism, Glucose Homeostasis, and Inflammation

To focus our study on functions relevant to changes in host phenotypes, 12 significantly enriched biological process GO

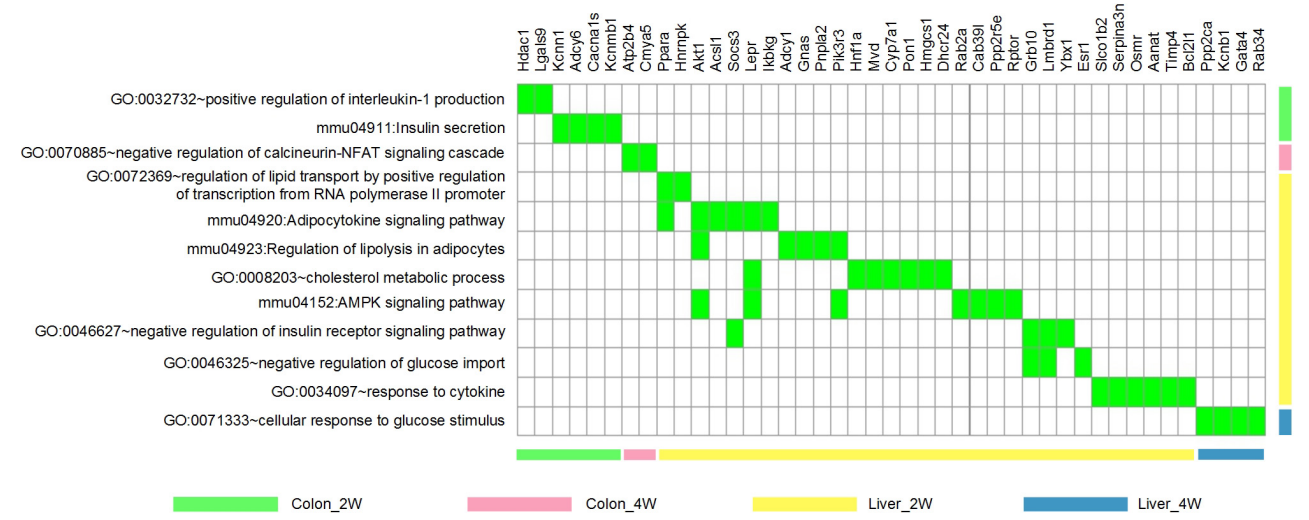

FIGURE 4 | The 12 phenotype-related GO terms and KEGG pathways and the 43 DE target genes involved. These GO terms and KEGG pathways were associated with lipid/cholesterol metabolism, glucose homeostasis, inflammation/immune response and energy homeostasis. Green indicates that the gene is involved in the corresponding term or pathway.

terms and KEGG pathways (associated with lipid metabolism, cholesterol metabolism, glucose homeostasis, inflammation and immune response, and energy homeostasis mentioned in the above section) were selected for further analysis. There were 43 DE target genes involved in these terms and pathways, particularly, 7 of which found in Liver_2W, *Ppara, Akt1, Socs3, Lepr, Pik3r3*, *Grb10*, and *Lmbrd1*, were shared by several terms and pathways (**Figure 4**).

After careful manual checking of the information from functional annotation and literature research (**Table 2**), 23 out of 43 DE target genes that may be more involved in the phenotype development were finally retained. These 23 key genes were regulated by 73 DE miRNAs (**Table 3**). A regulatory network of the miRNAs, target genes and biological functions was then constructed as shown in **Figure 5** that contained 92 miRNA-target gene regulatory relationships: 51 were positively correlated, while 41 were negatively correlated (**Supplementary Table S3**). Four of the 92 relationships, miR-1249-5p—*Ppara*, miR-409-3p—*Akt1*, miR-301b-3p—*Grb10* and miR-130b-3p—*Grb10*, had confirmed records in miRTarBase (Chou et al., 2018), an experimentally validated miRNA target gene database. From the constructed network, we found that the relationship between miRNA and mRNA was not simply one-to-one. Many key genes were often regulated by multiple miRNAs. Some of the key genes were even co-regulated by miRNAs with positive and negative correlations. For instance, in Colon_4W, gene *Cmya5* was negatively regulated by miR-705 and positively regulated by miR-6922-5p. Furthermore, a biological function was always contributed by multiple genes, and these genes might also have contradictory relationships with the same function.

In Colon_2W, 10 upregulated and 2 downregulated miRNAs jointly regulated 4 target genes, *Adcy6*, *Kcnn1*, *Hdac1*, and *Lgals9* (**Figure 5**). *Adcy6* has been reported to be involved in the GLP-1 (an incretin secreted by the intestine to promote insulin secretion)-mediated signaling pathway. *Kcnn1* could inhibit GLP-1 secretion. *Adcy6* and *Kcnn1* were both upregulated in the pre-group, indicating disturbed glucose homeostasis in the colon under the stress of the pre-intervention GM. Expression of *Hdac1* and *Lgals9*, which can enhance the immune response and inflammation, was promoted in the pre-group, indicating that the pre-intervention GM increased pro-inflammatory gene expression in the colon in the second week.

In Colon_4W, five promoted and three inhibited miRNAs collectively increased the expression of two anti-inflammatory genes, *Atp2b4* and *Cmya5* (**Figure 5**), which suggested that inflammation was suppressed in the colon in the fourth week, contrary to that in Colon_2W.

In Liver_2W, 53 microbiota-responsive miRNAs (7 were downregulated and 46 were upregulated) regulated the expression of 17 target genes (eight were downregulated and nine were upregulated) (**Figure 5**). Among these 17 genes, four pro-inflammatory genes, *Lepr*, *Socs3*, *Akt1*, and *Osmr*, were upregulated, and an anti-inflammatory gene, *Ppara*, was downregulated in the pre-group, which indicated that the pre-intervention GM enhanced the inflammatory response in the liver in the second week. However, opposite results were also observed; the expression of two anti-inflammatory genes, *Serpina3n* and *Timp4*, was increased in the pre-group. Expression of *Pnpla1*, *Acsl1* and *Ppara*, which promote fatty acid oxidation or lipolysis, was suppressed, and expression of *Socs3* and *Akt1*, which inhibit fatty acid oxidation, was increased in the pre-group, which suggested that lipid catabolism was restrained in the liver in the second week under the pressure of the pre-intervention GM. *Pon1* and *Hnf1a,* whose expression is closely associated with HDL levels, and *Hnrnpk*, which can promote plasma LDL clearance, were all downregulated in the pre-group. This downregulation may decrease HDL levels and plasma LDL clearance, resulting in inhibition of reverse cholesterol transport

TABLE 2 | Annotations of the 23 key genes associated with lipid and cholesterol metabolism, glucose homeostasis and inflammation.

Group	Gene symbol	Gene ID	Log_2FC (pre/post-group)	Annotations	References
Colon_2W	Kcnn1	ENSMUSG00000002908	1.02	Insulin secretion, potassium ion transport	Encodes potassium voltage-gated channel and some medicines promote GLP-1 secretion via inhibition of its expression (Shin et al., 2012, 2014).
	Adcy6	ENSMUSG00000022994	1.42	Insulin secretion, inflammatory mediator regulation of TRP channels, regulation of lipolysis in adipocytes	Involved in GLP-1 mediated signaling pathway (Dillon et al., 2005; Doyle and Egan, 2007).
	Hdac1	ENSMUSG00000028800	1.23	Positive regulation of interleukin-1 production, positive regulation of tumor necrosis factor production, negative regulation of insulin secretion	Promote B cell proliferation (Yamaguchi et al., 2010) and IFN mediated innate immunity (Xu et al., 2009).
	Lgals9	ENSMUSG00000001123	1.21	Positive regulation of interleukin-1 production, positive regulation of tumor necrosis factor production, response to lipopolysaccharide, positive regulation of defense response to bacterium, positive regulation of innate immune response, positive regulation of macrophage activation, positive regulation of T cell migration	Encode galectin-9 which could induce T helper cells to secrete pro-inflammatory cytokine IFNγ and TNFα (Su et al., 2011) and synergized with LPS to activate transcriptional factor NF-IL6, then transactivated inflammatory cytokine genes *IL1A*, *IL1B,* and *IFN*γ (Matsuura et al., 2009).
Colon_4W	Cmya5	ENSMUSG00000047419	1.01	Negative regulation of calcineurin-NFAT signaling cascade	Inhibit the activity of NFAT (Kielbasa et al., 2011) which are key regulators of T cell development and function (Macian, 2005).
	Atp2b4	ENSMUSG00000026463	1.07	Negative regulation of calcineurin-NFAT signaling cascade	Inhibit the activity of NFAT (Buch et al., 2005).
Liver_2W	Pon1	ENSMUSG00000002588	−1.36	Cholesterol metabolic process, aromatic compound catabolic process, response to fatty acid	Associated with HDL level and important in lipid and cholesterol metabolism and cardiovascular health (Macharia et al., 2012).
	Dhcr24	ENSMUSG00000034926	−1.29	Cholesterol metabolic process, lipid metabolic process, cholesterol biosynthetic process	Encode enzyme catalyzing the first step of cholesterol biosynthesis (Waterham et al., 2001).
	Hmgcs1	ENSMUSG00000093930	−1.19	Cholesterol metabolic process, lipid metabolic process, cholesterol biosynthetic process	Encode enzyme catalyzing the last step of cholesterol biosynthesis (Mathews et al., 2014).
	Hnf1a	ENSMUSG00000029556	−1.28	Cholesterol metabolic process, reverse cholesterol transport, fatty acid biosynthetic process, fatty acid transport, regulation of insulin secretion, glucose homeostasis, maturity onset diabetes of the young	Encode HNF-1α which activates the transcription of apoM, a major component of HDL particles (Richter et al., 2003), and it can affect plasma levels of HDL, reverse cholesterol transport and cholesterol metabolism (Babaya et al., 2003). Hnf1a$^{-/-}$ mice had abnormal HDL particles and suffered from hypercholesterolemia (Shih et al., 2001). Besides, HNF-1α can transactivate insulin I gene (Emens et al., 1992) and it had been reported that Hnf1a knockout mice developed non-insulin-dependent diabetes mellitus (Lee et al., 1998).
	Cyp7a1	ENSMUSG00000028240	1.43	Cholesterol metabolic process, cholesterol homeostasis, cholesterol catabolic process, lipid metabolic process, PPAR signaling pathway, cellular response to glucose stimulus	Encode the rate-limiting enzyme in the conversion of cholesterol to bile acids and plays an important role in bile acid biosynthesis and cholesterol homeostasis (Russell and Setchell, 1992; Pullinger et al., 2002).

(Continued)

TABLE 2 | Continued

Group	Gene symbol	Gene ID	Log_2FC (pre/post-group)	Annotations	References
	Ppara	ENSMUSG00000022383	−1.22	Regulation of lipid transport by positive regulation of transcription from RNA polymerase II promoter, lipid metabolic process, Adipocytokine signaling pathway, positive regulation of fatty acid oxidation, negative regulation of cholesterol storage, PPAR signaling pathway, non-alcoholic fatty liver disease, glucose metabolic process, response to insulin, positive regulation of gluconeogenesis, regulation of glycolytic process by positive regulation of transcription from RNA polymerase II promoter, insulin resistance, negative regulation of inflammatory response, negative regulation of leukocyte cell–cell adhesion	Play a major regulatory function in lipid catabolism, activation of which can induce fatty acid oxidation, enhance lipolysis and increase energy utilization (Reddy and Hashimoto, 2001; Guzmán et al., 2004). In addition, activation of it can inhibit inflammation and many preclinical experiments demonstrated benefits of PPARα agonists in various inflammation-associated diseases (Gervois and Mansouri, 2012). Moreover, activation of it can lead to improvement of insulin sensitivity (Haluzik and Haluzik, 2006).
	Hnrnpk	ENSMUSG00000021546	−1.20	Regulation of lipid transport by positive regulation of transcription from RNA polymerase II promoter, regulation of low-density lipoprotein particle clearance, cellular response to insulin stimulus	Encode hnRNP K protein, a transactivator of *LDLR* gene which mediates plasma LDL clearance (Li and Liu, 2010).
	Acsl1	ENSMUSG00000018796	−1.14	Adipocytokine signaling pathway, lipid metabolic process, lipid biosynthetic process, fatty acid metabolic process, fatty acid transport, triglyceride metabolic process, PPAR signaling pathway	Activate fatty acids (Ellis et al., 2010a) and directed fatty acid toward β-oxidation (Ellis et al., 2010b). Acsl1 specific knockout could significantly decrease fatty acid oxidation rates (Li et al., 2009; Ellis et al., 2010b).
	Akt1	ENSMUSG00000001729	1.02	Adipocytokine signaling pathway, regulation of lipolysis in adipocytes, negative regulation of fatty acid beta-oxidation, positive regulation of lipid biosynthetic process, non-alcoholic fatty liver disease, glucose metabolic process, glucose homeostasis, insulin resistance, inflammatory response, T cell receptor signaling pathway, B cell receptor signaling pathway, TNF signaling pathway, AMPK signaling pathway	Involved in the development of acute inflammation (Di Lorenzo et al., 2009). Overexpressing a constitutively active *Akt1* in transgenic mice and isolated neonatal cardiac myocytes decreased AMPK activity, resulting in suppressed fatty acid oxidation and glucose uptake and glycolysis (Kovacic et al., 2003). *Akt1* was suspected to decrease insulin sensitivity, since improved glucose tolerance and insulin sensitivity was observed in $Akt1^{-/-}$ mice (Buzzi et al., 2010).
	Lepr	ENSMUSG00000057722	2.17	Adipocytokine signaling pathway, cholesterol metabolic process, non-alcoholic fatty liver disease, leptin-mediated signaling pathway, response to leptin, positive regulation of insulin secretion involved in cellular response to glucose stimulus, glucose homeostasis, cytokine–cytokine receptor interaction, T cell differentiation, regulation of energy homeostasis, AMPK signaling pathway	Leptin enhanced immune response via acting on its receptor which is encoded by *Lepr* (Zarkesh-Esfahani et al., 2001) and mice deficient in *Lepr* are resistant to inflammation (Siegmund et al., 2004). Besides, leptin can interact with its receptor LEPR, inhibiting the expression of genes involved in lipogenesis and fatty acid synthesis and increasing the expression of genes mediating fatty acid oxidation, and stimulating fatty acid oxidation by activating AMPK (Liang and Tall, 2001; Minokoshi et al., 2002).
	Socs3	ENSMUSG00000053113	4.18	Adipocytokine signaling pathway, non-alcoholic fatty liver disease, negative regulation of insulin receptor signaling pathway, type II diabetes mellitus, insulin resistance, negative regulation of inflammatory response, TNF signaling pathway	Promote inflammation (Liu et al., 2008; Liu et al., 2015). Negative regulator of leptin receptor signaling, can inhibit fatty acid oxidation and mediate leptin resistance and diet-induced obesity (Bjorbak et al., 2000; Steinberg et al., 2006). Can impair insulin sensitivity via degradation of IRS1 and IRS2 or inhibition of receptor tyrosine phosphorylation (Rui et al., 2002; Senn et al., 2003). Socs3 tissue specific deficiency enhanced insulin sensitivity and protected against obesity-associated insulin resistance (Sachithanandan et al., 2010; Jorgensen et al., 2013).

(Continued)

TABLE 2 | Continued

Group	Gene symbol	Gene ID	Log_2FC (pre/post-group)	Annotations	References
	Pnpla2	ENSMUSG00000025509	−1.02	Regulation of lipolysis in adipocytes, lipid metabolic process, lipid catabolic process, triglyceride catabolic process, lipid storage, lipid homeostasis	Encode ATGL which catalyzes the first step of triglyceride hydrolysis (Zimmermann et al., 2004). In Pnpla2$^{-/-}$ mice, fatty acid release was reduced and massive triglyceride was accumulated (Haemmerle et al., 2006).
	Lmbrd1	ENSMUSG00000073725	1.49	Negative regulation of glucose import, negative regulation of insulin receptor signaling pathway, insulin receptor internalization	Encodes the LMBD1 protein that mediates endocytosis of the insulin receptor. A single-allele knockout of *Lmbrd1* resulted in an enhancement of insulin receptor signaling pathway and increased glucose uptake (Tseng et al., 2013).
	Grb10	ENSMUSG00000020176	1.58	Negative regulation of glucose import, negative regulation of insulin receptor signaling pathway, negative regulation of glycogen biosynthetic process	Interacts with insulin receptor and is a negative regulator of insulin signaling and action (Wick et al., 2003). Loss of Grb10 in mice resulted in enhanced insulin signaling and increased insulin sensitivity (Wang et al., 2007), while overexpression of it caused postnatal insulin resistance (Shiura et al., 2005).
	Serpina3n	ENSMUSG00000021091	1.06	Response to cytokine, acute-phase response	Encode serine protease inhibitor SERPINA3, which inhibits inflammation-associated serine proteases, such as cathepsin G, granzyme B and elastase, to prevent tissue damage during inflammatory responses (Gettins, 2002; Hsu et al., 2014).
	Osmr	ENSMUSG00000022146	1.16	Response to cytokine, cytokine–cytokine receptor interaction	Encode OSM receptor, through which OSM can increase the expression of diverse pro-inflammatory molecules, including IL-6, gp130, and IL1-R1 (Le Goff et al., 2014; West et al., 2017).
	Timp4	ENSMUSG00000030317	1.42	Response to cytokine, response to lipopolysaccharide	Encode matrix metalloproteinases (MMPs) inhibitor, which plays anti-inflammatory function by inhibiting MMPs activity and decreasing TNF-α and IL-1 expression (Celiker et al., 2002).

and plasma cholesterol clearance in the pre-group. Similar to what was observed in the inflammatory response, reverse changes were also found in lipid and cholesterol metabolism. Expression of *Lepr*, which promotes fatty acid oxidation, was increased in the pre-group. Two cholesterol synthetase genes, *Hmgcs1* and *Dhcr24*, were downregulated, and a cholesterol invertase gene, *Cyp7a1*, was upregulated in the pre-group, which implied that cholesterol biosynthesis was inhibited and cholesterol conversion was promoted in the liver in the second week under the stress of the pre-intervention GM. In addition to inflammation and lipid and cholesterol metabolism, molecular changes related to glucose homeostasis were also found in Liver_2W. Expression of *Socs3*, *Akt1*, *Lmbrd1*, and *Grb10*, negative regulators of the insulin signaling pathway, was increased, and expression of *Hnf1a* and *Ppara*, which can enhance insulin sensitivity, was decreased in the pre-group, which indicated that the pre-intervention GM inhibited the insulin signaling pathway and reduced insulin sensitivity in the liver in the second week. Among these 17 target genes, the suppression of *Ppara* was validated by RT-PCR and Western blot in our previous work (Wang et al., 2018). Functional annotation of these 17 genes suggested that the liver in the second week mainly exhibited disorders in cholesterol and lipid metabolism, glucose homeostasis and inflammation. In comparison with the colon, the liver had a larger regulatory network with not only more miRNAs and genes involved but also more biological functions influenced.

In contrast to Liver_2W, there was no regulatory network formed in Liver_4W, implying that the response of the liver to the pre-intervention GM mainly occurred in the second week.

Correlation Relationships Among Key miRNAs/Genes, Key OTUs and Some Physiological/Biochemical Parameters

In our previous work, 45 key OTUs were found to characterize the GMs of the pre- and post-groups. The pre-group had more Bacteroidetes (*Bacteroides* and *Parabacteroides*), Firmicutes (*Ruminococcus*) and Proteobacteria (*Bilophila*), while the post-group had more *Bifidobacterium* and *Lactobacillus*. The transplanted GMs inherited the major features of the corresponding donor samples, and there was no significant change over the first 4 weeks after transplantation (Wang et al., 2018).

TABLE 3 | The 73 miRNA regulators of the 23 key genes.

Group	miRNA	Log_2FC (pre/post-group)	Regulated key genes	Group	miRNA	Log_2FC (pre/post-group)	Regulated key genes
Colon_2W	mmu-miR-3547-5p	2.4738	Hdac1	Liver_2W	mmu-miR-3071-3p	1.72877	Lepr
	mmu-miR-6368	1.22617	Hdac1		mmu-miR-3072-3p	1.20282	Lepr
	mmu-miR-344e-3p	1.04254	Hdac1		mmu-miR-3090-3p	1.26417	Acsl1
	mmu-miR-3103-5p	−1.2423	Lgals9		mmu-miR-3091-3p	1.14713	Socs3
	mmu-miR-3076-5p	1.02201	Lgals9		mmu-miR-3095-3p	1.18135	Hmgcs1, Pnpla2
	mmu-miR-542-3p	2.06234	Kcnn1		mmu-miR-329-3p	1.5288	Socs3
	mmu-miR-7679-5p	1.02946	Adcy6		mmu-miR-33-3p	1.20094	Grb10, Lepr, Lmbrd1, Socs3
	mmu-miR-875-5p	1.21167	Adcy6		mmu-miR-338-5p	1.65017	Cyp7a1
	mmu-miR-6356	1.02966	Adcy6		mmu-miR-342-3p	2.50052	Cyp7a1
	mmu-miR-1197-3p	1.38913	Adcy6		mmu-miR-344g-5p	1.17696	Hnf1a
	mmu-miR-1955-5p	−1.2704	Adcy6		mmu-miR-350-5p	1.16633	Grb10
	mmu-miR-466n-3p	1.20615	Adcy6		mmu-miR-365-2-5p	−1.28404	Ppara
Colon_4W	mmu-miR-6481	1.54255	Atp2b4		mmu-miR-376c-3p	1.65018	Acsl1
	mmu-miR-344g-3p	1.15315	Atp2b4		mmu-miR-377-3p	1.53095	Cyp7a1, Dhcr24
	mmu-miR-1933-5p	1.10568	Atp2b4		mmu-miR-3971	1.11239	Hnf1a, Socs3
	mmu-miR-6912-5p	−1.0309	Atp2b4		mmu-miR-409-3p	1.53844	Akt1, Hnrnpk
	mmu-miR-760-3p	1.43912	Atp2b4		mmu-miR-411-3p	1.75709	Lmbrd1
	mmu-miR-7090-5p	−1.2088	Atp2b4		mmu-miR-421-5p	1.53348	Lmbrd1, Socs3
	mmu-miR-705	−1.0281	Cmya5		mmu-miR-484	1.49636	Hnf1a, Serpina3n
	mmu-miR-6922-5p	1.13032	Cmya5		mmu-miR-495-3p	1.18952	Hnrnpk, Lmbrd1
Liver_2W	mmu-miR-103-1-5p	1.08093	Lmbrd1		mmu-miR-5106	1.99096	Osmr
	mmu-miR-1249-5p	−1.4106	Akt1, Ppara		mmu-miR-5107-5p	1.10158	Lmbrd1
	mmu-miR-129-5p	−1.4207	Hnrnpk, Lmbrd1		mmu-miR-5112	1.97171	Lepr
	mmu-miR-130b-3p	1.05918	Acsl1, Grb10		mmu-miR-5130	1.87501	Dhcr24
	mmu-miR-134-5p	1.41304	Acsl1		mmu-miR-543-3p	1.03476	Acsl1, Cyp7a1, Lmbrd1
	mmu-miR-150-5p	1.84003	Osmr		mmu-miR-654-3p	1.06343	Pon1
	mmu-miR-15b-5p	1.77209	Acsl1		mmu-miR-654-5p	2.19462	Cyp7a1
	mmu-miR-1934-5p	1.28486	Acsl1		mmu-miR-672-5p	1.19394	Serpina3n
	mmu-miR-1948-3p	−1.2602	Lmbrd1		mmu-miR-677-3p	1.13387	Grb10, Timp4
	mmu-miR-1956	−1.0114	Grb10		mmu-miR-6971-5p	−1.02436	Pnpla2
	mmu-miR-196b-5p	1.54465	Acsl1, Osmr		mmu-miR-700-3p	1.07922	Grb10
	mmu-miR-20b-5p	1.17708	Ppara		mmu-miR-7079-3p	1.01557	Osmr
	mmu-miR-223-3p	1.98	Hmgcs1		mmu-miR-721	−1.27276	Acsl1, Grb10
	mmu-miR-301a-5p	1.27932	Ppara		mmu-miR-760-5p	1.37697	Acsl1
	mmu-miR-301b-3p	1.30687	Acsl1, Grb10		mmu-miR-7658-3p	1.45679	Acsl1
	mmu-miR-302d-5p	1.01566	Hmgcs1		mmu-miR-8101	1.47626	Dhcr24
	mmu-miR-3062-3p	1.07836	Grb10				

We calculated the correlations among the 45 key OTUs (listed in **Supplementary Table S4**) and the key miRNAs/genes. As shown in **Figure 6**, the more abundant OTUs (such as *Bacteroides*) in the pre-group were positively correlated with pro-inflammatory genes (*Hdac1*, *Lgals9*, *Osmr*, *Akt1*, *Socs3*, and *Lepr*), inflammation negative regulator genes (*Cmya5*, *Atp2b4*, *Serpina3n*, and *Timp4*), lipid catabolism-inhibiting genes (*Akt1* and *Socs3*), insulin sensitivity-inhibiting genes (*Akt1*, *Socs3*, *Kcnn1*, *Lmbrd1*, and *Grb10*) and these genes' positively correlated miRNA regulators. On the other hand, less abundant OTUs (such as *Bifidobacterium*) in the pre-group were positively correlated with lipid catabolism or cholesterol clearance-promoting genes (*Ppara*, *Pnpla2*, *Pon1*, *Hnrnpk*, and *Hnf1a*), insulin sensitivity-enhancing genes (*Ppara* and *Hnf1a*) and these genes' positively correlated miRNA regulators. Among these key genes and miRNAs, *Lgals9*, miR-5112 and miR-342-3p were significantly correlated with the key OTUs.

We also checked the correlations among some physiological/biochemical parameters (listed in **Supplementary Table S5**) and the key miRNAs/genes (**Figure 7**). Compared with the post-group, the pre-group had higher expression of inflammatory factors (TNFα, IL6, and TLR4) in the liver and colon and higher concentrations of serum LBP and SAA in the second week after GM transplantation (Zhang et al., 2015). These inflammation-related biochemical parameters exhibited an obvious positive correlation with key pro-inflammatory genes and miRNAs. In the fourth week after GM transplantation, histological images showed that the pre-group

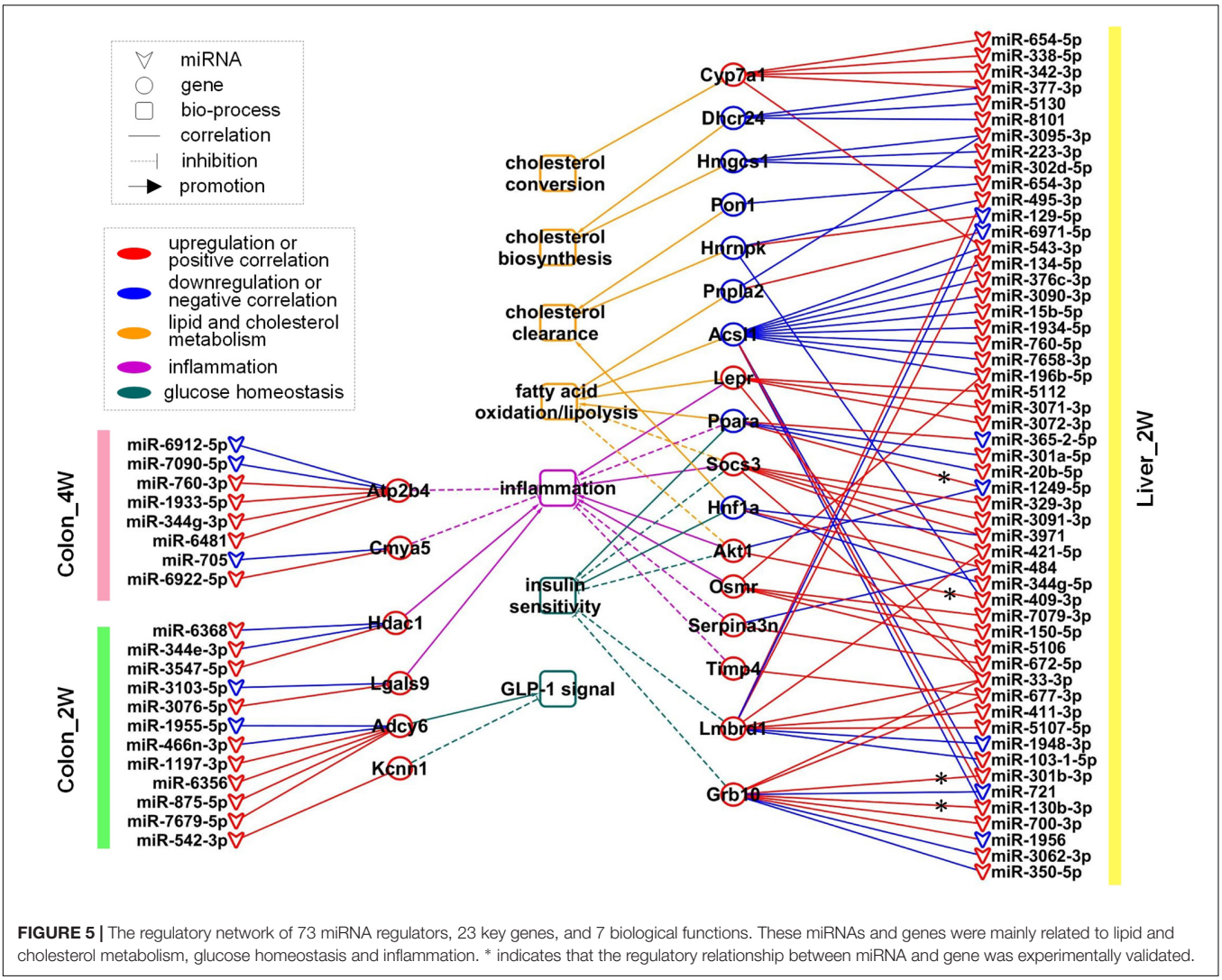

FIGURE 5 | The regulatory network of 73 miRNA regulators, 23 key genes, and 7 biological functions. These miRNAs and genes were mainly related to lipid and cholesterol metabolism, glucose homeostasis and inflammation. * indicates that the regulatory relationship between miRNA and gene was experimentally validated.

developed liver macrovesicular steatosis and they had higher concentrations of hepatic triglyceride and total cholesterol, larger adipocytes, greater fat mass and higher concentrations of serum triglyceride and leptin (Zhang et al., 2015; Wang et al., 2018). However, genes and miRNAs relevant to cholesterol and lipid metabolism, such as *Akt1*, *Socs3*, *Ppara*, *Acsl1*, *Pnpla2*, *Pon1*, *Hnrnpk*, *Hnf1a* and their miRNA regulators, did not show an obvious and consistent correlation with these body fat-related physiological/biochemical parameters.

DISCUSSION

By combining miRNA and mRNA sequencing data of the colon and liver, this study found that dysbiotic GM indeed changed the expression of miRNAs and their target genes involved in host lipid and cholesterol metabolism, glucose homeostasis and inflammation, which indicated that host miRNAs and genes were important in mediating the effect of the GM and in turn impacting host phenotypes.

In this study, we first screened the DE miRNAs responding to the dysbiotic GM, then sought their targeted DE genes, and finally tracked the key GM members and the biological functions closely correlated with these miRNAs/genes. This strategy resulted in a clear GM-miRNA-gene-biological function regulatory path under the stress of the dysbiotic GM.

We found that the changed expression of miRNAs and their target genes in response to the dysbiotic GM was tissue specific. The pre-intervention GM triggered inflammation in both the colon and liver, but the affected miRNAs and corresponding target genes in these tissues varied. In Colon_2W, the changed miRNAs upregulated the pro-inflammatory genes *Hdac1* and *Lgals9*. In contrast, in Liver_2W, the changed miRNA upregulated the pro-inflammatory genes *Osmr*, *Akt1*, *Socs3*, and *Lepr* and downregulated the anti-inflammatory gene *Ppara*. The GM of the pre-group had more LPS-producing bacteria, such as Gram-negative bacteria *Bacteroides*, *Parabacteroides*, and *Bilophila* (**Supplementary Table S4**), leading to a higher level of endotoxin load that was reflected by a higher level of serum LBP (**Supplementary Table S5**). These LPS-producing bacteria

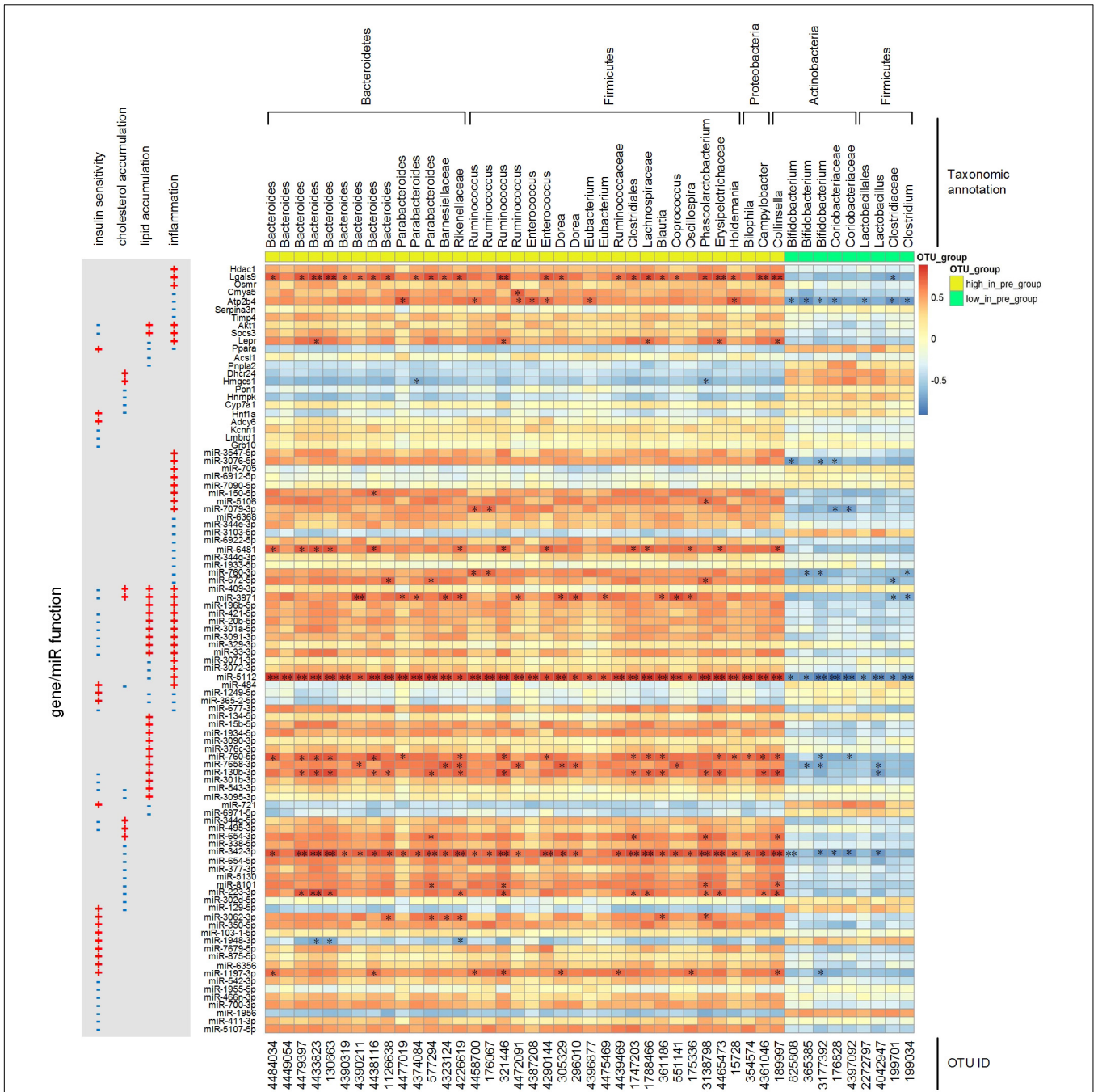

FIGURE 6 | Spearman correlations among the abundances of key OTUs and the expression levels of key miRNAs/genes. The *p*-value was post adjusted by the method of Benjamini and Hochberg. $N = 4$ or 5 for each group. ** adjusted p-value < 0.01 and * adjusted p-value < 0.05.

had a positive correlation with pro-inflammatory genes along with their positively correlated miRNA regulators (**Figure 6**), indicating that the enrichment of these LPS-producing bacteria might be responsible for the increase in the expression of pro-inflammatory genes in the pre-group. It has been reported that *Lgals9* could synergize with LPS to activate inflammatory cytokine gene expression (Matsuura et al., 2009). *Hdac1* (Xu et al., 2009; Yamaguchi et al., 2010), *Osmr* (Le Goff et al., 2014; West et al., 2017), *Akt1* (Di Lorenzo et al., 2009), *Socs3* (Liu et al., 2008; Liu et al., 2015) and *Lepr* (Zarkesh-Esfahani et al., 2001; Siegmund et al., 2004) have also been reported to promote the immune response and inflammation. On the other hand, many preclinical experiments have demonstrated the benefits of PPARα agonists in various inflammation-associated diseases (Gervois and Mansouri, 2012). Thus, these inflammation-related molecular changes in the colon and liver might result in

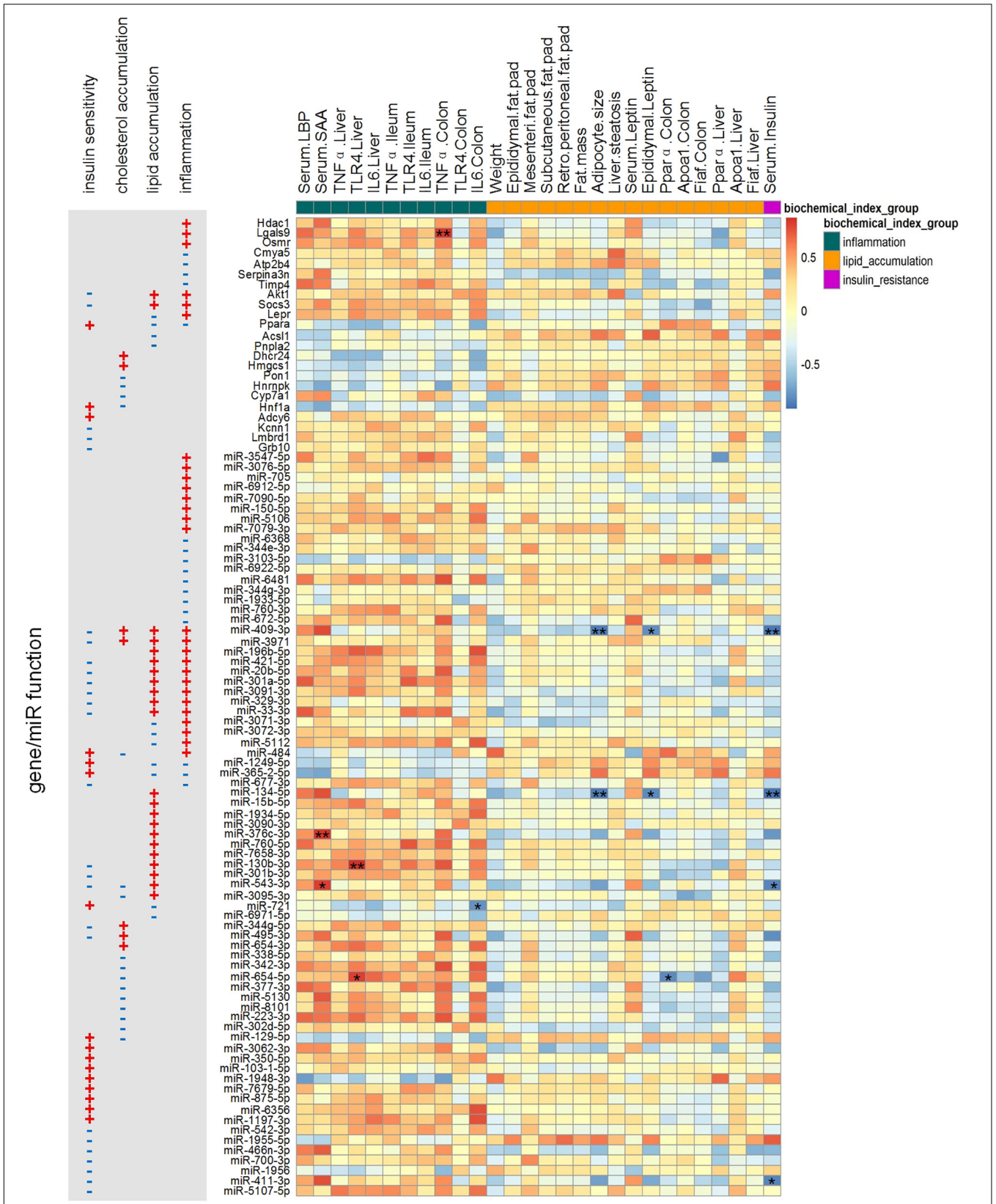

FIGURE 7 | Spearman correlations between physiological/biochemical parameters and the expression levels of key miRNAs/genes. The *p*-value was post adjusted by the method of Benjamini and Hochberg. $N = 4$ or 5 for each group. ** adjusted p-value < 0.01 and * adjusted p-value < 0.05.

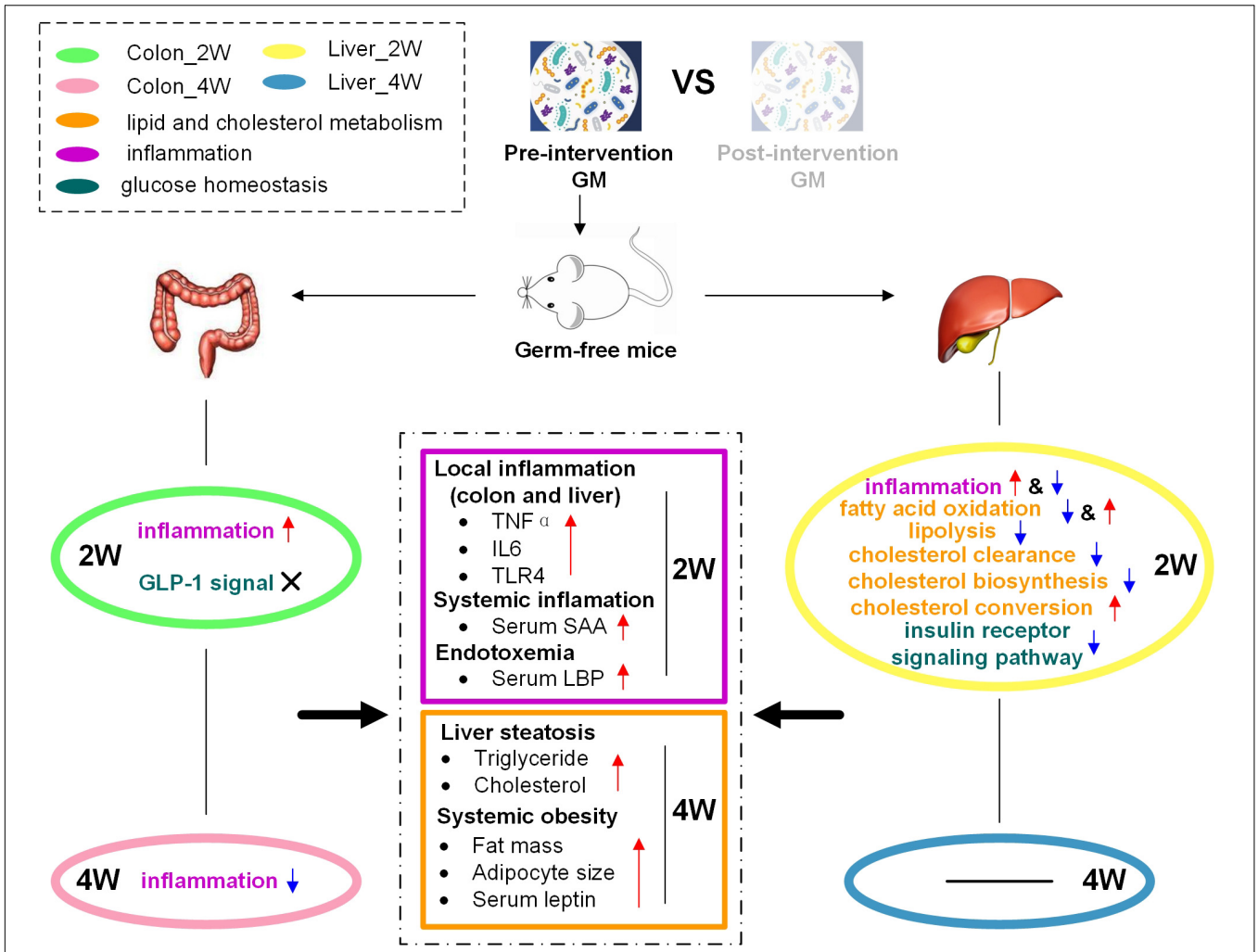

FIGURE 8 | Schematic diagram illustrating how dysbiotic GM affected the host phenotype through the regulation of miRNA and target genes. The pre-intervention GM promoted inflammation and inhibited lipid and cholesterol catabolism and insulin signaling in the colon and liver, resulting in high levels of inflammation and fat accumulation in gnotobiotic mice.

higher inflammation levels in the pre-group (**Figure 8**). Genes and miRNAs that promote inflammation in the colon and liver exhibited obvious positive correlations with inflammatory biochemical parameters (**Figure 7**). This phenomenon also indicated that the molecular changes induced by dysbiotic GM led to higher levels of inflammation in the pre-group. The host immunity could be regulated in many ways. The intestinal barrier is considered to have an important role in GM-induced host inflammation (Cheru et al., 2019). Lim et al. found that *Lactobacillus sakei* OK67 increased colon tight junction protein expression in high-fat diet-induced obese conventional mice (Lim et al., 2016). In our study, the expression levels of the tight junction proteins ZO-1 and Occludin were very low and were not significantly different between the two groups in the colon, as detected by both mRNA sequencing and RT-PCR (**Supplementary Table S6**), suggesting that in germ-free mice, the inflammation caused by dysbiotic GM might not, at least not mainly, through the modulation of tight junction protein expression. We could not deduce that the low and unchanged tight junctions expression after fecal microbiota transplantation was mouse specific, as germ-free mice, instead of conventionally raised mice, were used in this study. We were also not sure whether the expression of gut tight junction proteins in germ-free mice was truly lower than that in conventionally raised mice since the latter were not used as a control in our experiment. However, we found that many genes, such as *Hdac1* and *Lgals9,* that can activate inflammatory cytokine gene expression, and *Tlr4*, which is a surface receptor involved in microbial recognition, were expressed at higher levels in the pre-group transplanted with dysbiotic GM. These changes might be the way that the host defended to the GM. Similar to our study, El Aidy et al. (2012) investigated the change in the intestinal mucosa during the conventionalization of germ-free mice and found induced expression of surface receptors, antimicrobial peptides, and pro-inflammatory cytokines and enhanced antigen presentation, although they did not report changes in tight junction proteins.

In addition, the liver had disturbed lipid and cholesterol metabolism, which was not observed in the colon. The expression of target genes that promote fatty acid oxidation or lipolysis, *Ppara*, *Acsl1*, and *Pnpla2*, was suppressed, and the expression of target genes that inhibit fatty acid oxidation, *Socs3* and *Akt1*, was increased in the pre-group in Liver_2W. *Ppara* plays a major regulatory function in lipid catabolism (Reddy and Hashimoto, 2001; Guzmán et al., 2004), and its suppression has also been reported in conventionalized mice that was easier to obtain fat than GF mice (El Aidy et al., 2013). Studies have indicated that specific knockout of *Acsl1* could significantly decrease fatty acid oxidation rates (Li et al., 2009; Ellis et al., 2010b). In *Pnpla2*$^{-/-}$ mice, fatty acid release was reduced, and massive triglycerides accumulated (Haemmerle et al., 2006). *Socs3*, a negative regulator of leptin receptor signaling, can inhibit fatty acid oxidation and mediate leptin resistance and diet-induced obesity (Bjorbak et al., 2000; Steinberg et al., 2006). Overexpression of *Akt1* can decrease AMPK activity, leading to suppressed fatty acid oxidation, glucose uptake, and glycolysis (Kovacic et al., 2003). Thus, these lipid catabolism-relevant molecular changes suggested that dysbiotic GM could promote lipid accumulation in gnotobiotic mouse liver via inhibition of fatty acid oxidation and lipolysis. In addition, we observed that the cholesterol clearance-related genes *Pon1*, *Hnf1a*, and *Hnrnpk* were suppressed in the pre-group in Liver_2W. Many studies have shown that the expression of *Pon1* is closely associated with HDL levels and is important in lipid and cholesterol metabolism (Macharia et al., 2012). Shih et al. (2001) reported that *Hnf1a*$^{-/-}$ mice had abnormal HDL particles and suffered from hypercholesterolemia. *Hnrnpk* has been implicated as a transactivator of the *LDLR* gene that mediates LDL clearance (Li and Liu, 2010). The suppression of these molecules might decrease HDL levels and plasma LDL clearance, resulting in the inhibition of reverse cholesterol transport and plasma cholesterol clearance in the pre-group. These lipid and cholesterol metabolism-related molecular changes might explain why more triglyceride and cholesterol accumulated in the liver or even the whole body in the pre-group (**Figure 8**). We noted that genes and miRNAs relevant to cholesterol and lipid metabolism did not show an obvious correlation with body fat-related biochemical parameters (**Figure 7**). Time lag might be the reason for this result as the change of molecular expression occurred in the second week, 2 weeks before changes in body fat. GM dysbiosis might initially induce cholesterol and lipid metabolism-related miRNA and gene expression disorders and then lead to lipid accumulation and obesity development. This lagging obesity phenotype phenomenon implicates a causative role of GM dysbiosis in obesity development, rather than a result of obesity. Considering these observations, we think that a dysbiotic GM from a genetically obese child promoted lipid and cholesterol accumulation in mice on a normal chow diet by inhibiting fatty acid oxidation, lipolysis and plasma cholesterol clearance rather than by enhancing lipogenesis and cholesterol biosynthesis.

Although serum insulin was not significantly different between the two groups of mice (**Supplementary Table S5**), we identified that GLP-1 and insulin signaling pathways were disturbed in the pre-group. In Colon_2W, two genes relevant to GLP-1 secretion or action, *Adcy6* and *Kcnn1*, were upregulated in the pre-group. In Liver_2W, the expression of four negative regulators of the insulin signaling pathway, *Socs3*, *Lmbrd1*, *Grb10*, and *Akt1*, was increased, and the expression of two genes, *Hnf1a* and *Ppara*, which can enhance insulin sensitivity, was decreased in the pre-group. *Adcy6* has been reported to be involved in the GLP-1-mediated signaling pathway (Dillon et al., 2005; Doyle and Egan, 2007). Some medications promote GLP-1 secretion by inhibiting *Kcnn1* expression (Shin et al., 2012, 2014). It has been reported that *Socs3* can degrade IRSs or inhibit receptor tyrosine phosphorylation (Rui et al., 2002; Senn et al., 2003). *Socs3* tissue-specific deficiency in liver and skeletal muscle could enhance insulin sensitivity and protect against obesity-associated insulin resistance (Sachithanandan et al., 2010; Jorgensen et al., 2013). *Lmbrd1* has been reported to mediate endocytosis of the insulin receptor, and a single-allele knockout of *Lmbrd1* resulted in enhancement of the insulin receptor signaling pathway and increased glucose uptake (Tseng et al., 2013). *Grb10* is a negative regulator of insulin signaling and action (Wick et al., 2003). Overexpression of *Grb10* caused postnatal insulin resistance (Shiura et al., 2005). In *Akt1*$^{-/-}$ mice, improved glucose tolerance and insulin sensitivity were observed (Buzzi et al., 2010). It has been reported that *Hnf1a* could transactivate the insulin I gene (Emens et al., 1992) and that *Hnf1a* knockout mice developed non-insulin-dependent diabetes mellitus (Lee et al., 1998). Many studies have shown that activation of *Ppara* can lead to improvement of insulin sensitivity (Haluzik and Haluzik, 2006). Thus, these molecular changes showed that the pre-intervention GM disturbed GLP-1 signaling and secretion in the colon, inhibited the insulin signaling pathway and reduced insulin sensitivity in the liver.

Moreover, we found that the influence of GM on host molecular expression was time-dependent. Most of the differences between the two groups found in the second week decreased or disappeared in the fourth week, and at different time points, there were different miRNAs and genes responding to the GM. It is well known that diet plays a dominant role in shaping the GM (Zhang et al., 2010). Since the two groups of mice in our study were both on a sterile normal chow diet after microbiota transplantation, there was no environmental pressure to keep the initial GM differences between the two groups. Thus, the GM discrepancy between the two groups decreased as time went on. Another possible reason is that organisms are prone to maintain homeostasis under stimulation via their complex negative feedback regulatory networks. El Aidy et al. found that in addition to the induction of the immune response, the expression of tolerance-associated molecules increased since day 8 after conventionalization. The induction of pro- and anti-inflammatory signals jointly drives a balanced, tolerant immune response to microbiota, establishing immune homeostasis in conventionalized mice (El Aidy et al., 2012). In our study, we also detected increased expression of negative regulators in the pre-group. Two negative regulators of NFAT, *Cmya5* and *Atp2b4*, were upregulated in the pre-group in Colon_4W. The expression of two protease inhibitors, *Serpina3n* and *Timp4*, was increased in the pre-group in Liver_2W. Increased expression of inflammatory negative regulators in the pre-group indicated that inflammatory negative feedback regulation was

activated by the higher inflammatory environment induced by the pre-intervention GM. This activation could maintain an organism's inflammatory homeostasis, prevent tissue damage during inflammatory responses and might explain why most of the inflammatory markers were significantly increased in the pre-group in the second week and were not different between the two groups in the fourth week. Similar negative feedback was also detected in lipid and cholesterol metabolism. *Lepr*, which encodes the leptin receptor was upregulated in the pre-group in Liver_2W. Higher plasma levels of leptin were commonly found in obese humans and rats, and some of these humans and rats even developed leptin resistance (Maffei et al., 1995). Consistently, in our study, *Socs3*, which can mediate leptin resistance, was upregulated in the liver in the second week, and serum leptin levels were significantly higher in the fourth week in the pre-group, which implied that the pre-group might develop leptin resistance. Two genes, *Hmgcs1* and *Dhcr24*, which are involved in cholesterol biosynthesis, decreased, and *Cyp7a1*, which encodes an enzyme that converts cholesterol to bile acids, increased in the pre-group in Liver_2W. These molecular changes might be an organism's antagonistic responses to cholesterol accumulation. As the mice generated a tolerance to the stimulation by the GM in our study, the GM effects on the host declined as time went on.

Our previous study found that GMs of recipient mice preserved major features of the corresponding donor GMs. Similar to the phenotype differences observed in the PWS donor, gnotobiotic mice that received pre-intervention GM also developed higher inflammation and lipid accumulation (Wang et al., 2018). It is necessary to note that although the PWS child had improved phenotypes after the dietary intervention, it is not certain whether he was already healthy or whether his post-intervention GM was beneficial. However, setting the post-intervention GM as a reference helped us to identify the miRNAs whose expression was disturbed by the dysbiotic pre-intervention GM.

In our animal experiment, fecal microbiota transplantation was performed with only one PWS child as a GM donor. The purpose of this design was to minimize GM variations among individual subjects due to genetic and environmental background (Human Microbiome Project Consortium, 2012) and thus focus on physiological consequences caused by the GM. Indeed, through this pilot investigation, we found that dysbiotic GM could change the expression of miRNAs and their target genes. Bioinformatics analysis indicated that these changes were relevant to host inflammation and to lipid and glucose metabolism. It is worth noting that since this result was from just one donor, the detailed correlation of miRNA and mRNA found in this investigation could be varied upon changing donors. However, the corresponding affected biological functions relevant to these molecules should not change much since they are consistent with the modulation of the host phenotype. In our previous clinical trial, all participants had similar improvement in their physiological metabolic parameters, and their GM structure became similar after the intervention (Zhang et al., 2015). Since the GM donor was randomly selected, we think the results from this donor could be considered representative to a certain degree. Nevertheless, to obtain more generalized conclusions about the relationships among the miRNA, mRNA and host phenotypes, future investigation and validation should be performed with more donors.

In our study, we used deep sequencing rather than microarray to observe host miRNA and gene expression. This approach allowed us to find more DE miRNAs and genes. However, some limitations were also found. Among the large number of miRNAs and genes collected in public databases, information about miRNA function and experimentally verified target genes is extremely scarce. If only verified target genes could be used, many genes obtained by deep sequencing would be out of consideration. Hence, we applied prediction algorithms to identify target genes. However, miRNA target gene prediction algorithms have very high false-positive rates. To improve the stringency, we only considered the target genes predicted by at least two algorithms and further screened them by differential expression. This strategy results in a clear miRNA-gene regulatory path with more confidence; otherwise, the DE miRNAs can cover almost all of the genes detected. To promote miRNA-associated studies, projects that experimentally validate miRNA function and target genes are highly called for in the future.

Through this study, we obtained fundamental molecular information elucidating how a dysbiotic GM increases host inflammation and disturbs host lipid and glucose metabolism by modulating host miRNA and gene expression. These findings provide the possibility for researching microbiota-targeted precision medicine in the future.

ETHICS STATEMENT

The clinical trial of the PWS children was approved by the Ethics Committee of the School of Life Sciences and Biotechnology, Shanghai Jiao Tong University with No. 2012-016 and registered at Chinese Clinical Trial Registry with No. ChiCTR-ONC-12002646. Written informed consent was obtained from the guardian of the PWS donor. The animal experimental protocols were approved and performed in accordance with relevant guidelines and regulations recommended by the Institutional Animal Care and Use Committee (IACUC) of the Shanghai SLAC Laboratory Animal Co., Ltd. All the potential biologically hazardous materials in this study were properly handled according to the Chinese Biosafety Laws and Regulations.

AUTHOR CONTRIBUTIONS

RW, CZ, and LZ designed the research. RW performed the experimental procedure. LD, HL, and MZ performed the data analysis and annotation. LD and MZ wrote the manuscript.

FUNDING

This study was supported by a grant from the National Natural Science Foundation of China (Grant No. 31330005).

ACKNOWLEDGMENTS

We thank Guojun Wu, Jing Wang, and other members of the Lab of Molecular Microbial Ecology and Ecogenomics for suggestions regarding the analysis and writing.

SUPPLEMENTARY MATERIAL

The Supplementary Material for this article can be found online at: https://www.frontiersin.org/articles/10.3389/fmicb.2019.01517/full#supplementary-material

REFERENCES

Agarwal, V., Bell, G. W., Nam, J. W., and Bartel, D. P. (2015). Predicting effective microRNA target sites in mammalian mRNAs. *eLife* 4:e05005. doi: 10.7554/eLife.05005

Anders, S., Pyl, P. T., and Huber, W. (2015). HTSeq–a Python framework to work with high-throughput sequencing data. *Bioinformatics* 31, 166–169. doi: 10.1093/bioinformatics/btu638

Babaya, N., Ikegami, H., Fujisawa, T., Nojima, K., Itoi-Babaya, M., Inoue, K., et al. (2003). Association of I27L polymorphism of hepatocyte nuclear factor-1 alpha gene with high-density lipoprotein cholesterol level. *J. Clin. Endocrinol. Metab.* 88, 2548–2551. doi: 10.1210/jc.2002-021891

Bjorbak, C., Lavery, H. J., Bates, S. H., Olson, R. K., Davis, S. M., Flier, J. S., et al. (2000). SOCS3 mediates feedback inhibition of the leptin receptor via Tyr985. *J. Biol. Chem.* 275, 40649–40657. doi: 10.1074/jbc.M007577200

Buch, M. H., Pickard, A., Rodriguez, A., Gillies, S., Maass, A. H., Emerson, M., et al. (2005). The sarcolemmal calcium pump inhibits the calcineurin/nuclear factor of activated T-cell pathway via interaction with the calcineurin A catalytic subunit. *J. Biol. Chem.* 280, 29479–29487. doi: 10.1074/jbc.M501326200

Butler, M. G. (2011). Prader-Willi syndrome: obesity due to genomic imprinting. *Curr. Genomics* 12, 204–215. doi: 10.2174/138920211795677877

Buzzi, F., Xu, L., Zuellig, R. A., Boller, S. B., Spinas, G. A., Hynx, D., et al. (2010). Differential effects of protein kinase B/Akt isoforms on glucose homeostasis and islet mass. *Mol. Cell Biol.* 30, 601–612. doi: 10.1128/MCB.00719-09

Celiker, M. Y., Ramamurthy, N., Xu, J. W., Wang, M., Jiang, Y., Greenwald, R., et al. (2002). Inhibition of adjuvant-induced arthritis by systemic tissue inhibitor of metalloproteinases 4 gene delivery. *Arthritis Rheum.* 46, 3361–3368. doi: 10.1002/art.10648

Cheru, L., Saylor, C. F., and Lo, J. (2019). Gastrointestinal barrier breakdown and adipose tissue inflammation. *Curr. Obes. Rep.* 8, 165–174. doi: 10.1007/s13679-019-00332-6

Chou, C. H., Shrestha, S., Yang, C. D., Chang, N. W., Lin, Y. L., Liao, K. W., et al. (2018). miRTarBase update 2018: a resource for experimentally validated microRNA-target interactions. *Nucleic Acids Res.* 46, D296–D302. doi: 10.1093/nar/gkx1067

Dalmasso, G., Hang, T. T. N., Yan, Y., Laroui, H., Charania, M. A., Ayyadurai, S., et al. (2011). Microbiota modulate host gene expression via microRNAs. *PLoS One* 6:e19293. doi: 10.1371/journal.pone.0019293

Di Lorenzo, A., Fernandez-Hernando, C., Cirino, G., and Sessa, W. C. (2009). Akt1 is critical for acute inflammation and histamine-mediated vascular leakage. *Proc. Natl. Acad. Sci. U.S.A.* 106, 14552–14557. doi: 10.1073/pnas.0904073106

Dillon, J. S., Lu, M., Bowen, S., and Homan, L. L. (2005). The recombinant rat glucagon-like peptide-1 receptor, expressed in an alpha-cell line, is coupled to adenylyl cyclase activation and intracellular calcium release. *Exp. Clin. Endocrinol. Diabetes* 113, 182–189. doi: 10.1055/s-2005-837526

Doyle, M. E., and Egan, J. M. (2007). Mechanisms of action of glucagon-like peptide 1 in the pancreas. *Pharmacol. Ther.* 113, 546–593. doi: 10.1016/j.pharmthera.2006.11.007

El Aidy, S., Merrifield, C. A., Derrien, M., van Baarlen, P., Hooiveld, G., Levenez, F., et al. (2013). The gut microbiota elicits a profound metabolic reorientation in the mouse jejunal mucosa during conventionalisation. *Gut* 62, 1306–1314. doi: 10.1136/gutjnl-2011-301955

El Aidy, S., van Baarlen, P., Derrien, M., Lindenbergh-Kortleve, D. J., Hooiveld, G., Levenez, F., et al. (2012). Temporal and spatial interplay of microbiota and intestinal mucosa drive establishment of immune homeostasis in conventionalized mice. *Mucosal Immunol.* 5, 567–579. doi: 10.1038/mi.2012.32

Ellis, J. M., Frahm, J. L., Li, L. O., and Coleman, R. A. (2010a). Acyl-coenzyme A synthetases in metabolic control. *Curr. Opin. Lipidol.* 21, 212–217. doi: 10.1097/mol.0b013e32833884bb

Ellis, J. M., Li, L. O., Wu, P. C., Koves, T. R., Ilkayeva, O., Stevens, R. D., et al. (2010b). Adipose acyl-CoA synthetase-1 directs fatty acids toward beta-oxidation and is required for cold thermogenesis. *Cell Metab.* 12, 53–64. doi: 10.1016/j.cmet.2010.05.012

Emens, L. A., Landers, D. W., and Moss, L. G. (1992). Hepatocyte nuclear factor 1 alpha is expressed in a hamster insulinoma line and transactivates the rat insulin I gene. *Proc. Natl. Acad. Sci. U.S.A.* 89, 7300–7304. doi: 10.1073/pnas.89.16.7300

Gervois, P., and Mansouri, R. M. (2012). PPARalpha as a therapeutic target in inflammation-associated diseases. *Expert Opin. Ther. Targets* 16, 1113–1125. doi: 10.1517/14728222.2012.715633

Gettins, P. G. (2002). The F-helix of serpins plays an essential, active role in the proteinase inhibition mechanism. *FEBS Lett.* 523, 2–6. doi: 10.1016/s0014-5793(02)02924-1

Guzmán, M., Lo Verme, J., Fu, J., Oveisi, F., Blázquez, C., and Piomelli, D. (2004). Oleoylethanolamide stimulates lipolysis by activating the nuclear receptor peroxisome proliferator-activated receptor α (PPAR-α). *J. Biol. Chem.* 279, 27849–27854. doi: 10.1074/jbc.M404087200

Haemmerle, G., Lass, A., Zimmermann, R., Gorkiewicz, G., Meyer, C., Rozman, J., et al. (2006). Defective lipolysis and altered energy metabolism in mice lacking adipose triglyceride lipase. *Science* 312, 734–737. doi: 10.1126/science.1123965

Haluzik, M. M., and Haluzik, M. (2006). PPAR-alpha and insulin sensitivity. *Physiol. Res.* 55, 115–122.

He, L., and Hannon, G. J. (2004). MicroRNAs: small RNAs with a big role in gene regulation. *Nat. Rev. Genet.* 5, 522–531. doi: 10.1038/nrg1379

Hsu, I., Parkinson, L. G., Shen, Y., Toro, A., Brown, T., Zhao, H., et al. (2014). Serpina3n accelerates tissue repair in a diabetic mouse model of delayed wound healing. *Cell Death Dis.* 5:e1458. doi: 10.1038/cddis.2014.423

Huang da, W., Sherman, B. T., and Lempicki, R. A. (2009). Systematic and integrative analysis of large gene lists using DAVID bioinformatics resources. *Nat. Protoc.* 4, 44–57. doi: 10.1038/nprot.2008.211

Human Microbiome Project Consortium (2012). Structure, function and diversity of the healthy human microbiome. *Nature* 486, 207–214. doi: 10.1038/nature11234

Jorgensen, S. B., O'Neill, H. M., Sylow, L., Honeyman, J., Hewitt, K. A., Palanivel, R., et al. (2013). Deletion of skeletal muscle SOCS3 prevents insulin resistance in obesity. *Diabetes* 62, 56–64. doi: 10.2337/db12-0443

Kielbasa, O. M., Reynolds, J. G., Wu, C. L., Snyder, C. M., Cho, M. Y., Weiler, H., et al. (2011). Myospryn is a calcineurin-interacting protein that negatively modulates slow-fiber-type transformation and skeletal muscle regeneration. *FASEB J.* 25, 2276–2286. doi: 10.1096/fj.10-169219

Kim, D., Langmead, B., and Salzberg, S. L. (2015). HISAT: a fast spliced aligner with low memory requirements. *Nat. Methods* 12, 357–360. doi: 10.1038/nmeth.3317

Kovacic, S., Soltys, C. L., Barr, A. J., Shiojima, I., Walsh, K., and Dyck, J. R. (2003). Akt activity negatively regulates phosphorylation of AMP-activated protein kinase in the heart. *J. Biol. Chem.* 278, 39422–39427. doi: 10.1074/jbc.M305371200

Langmead, B., Trapnell, C., Pop, M., and Salzberg, S. L. (2009). Ultrafast and memory-efficient alignment of short DNA sequences to the human genome. *Genome Biol.* 10:R25. doi: 10.1186/gb-2009-10-3-r25

Le Goff, B., Singbrant, S., Tonkin, B. A., Martin, T. J., Romas, E., Sims, N. A., et al. (2014). Oncostatin M acting via OSMR, augments the actions of IL-1 and TNF in synovial fibroblasts. *Cytokine* 68, 101–109. doi: 10.1016/j.cyto.2014.04.001

Lee, Y. H., Sauer, B., and Gonzalez, F. J. (1998). Laron dwarfism and non-insulin-dependent diabetes mellitus in the Hnf-1alpha knockout mouse. *Mol. Cell Biol.* 18, 3059–3068. doi: 10.1128/mcb.18.5.3059

Li, H., and Liu, J. (2010). Identification of heterogeneous nuclear ribonucleoprotein K as a transactivator for human low density lipoprotein receptor gene transcription. *J. Biol. Chem.* 285, 17789–17797. doi: 10.1074/jbc.M109.082057

Li, L. O., Ellis, J. M., Paich, H. A., Wang, S., Gong, N., Altshuller, G., et al. (2009). Liver-specific loss of long chain acyl-CoA synthetase-1 decreases triacylglycerol synthesis and beta-oxidation and alters phospholipid fatty acid composition. *J. Biol. Chem.* 284, 27816–27826. doi: 10.1074/jbc.M109.022467

Liang, C. P., and Tall, A. R. (2001). Transcriptional profiling reveals global defects in energy metabolism, lipoprotein, and bile acid synthesis and transport with reversal by leptin treatment in ob/ob mouse liver. *J. Biol. Chem.* 276, 49066–49076. doi: 10.1074/jbc.M107250200

Lim, S. M., Jeong, J. J., Woo, K. H., Han, M. J., and Kim, D. H. (2016). Lactobacillus sakei OK67 ameliorates high-fat diet-induced blood glucose intolerance and obesity in mice by inhibiting gut microbiota lipopolysaccharide production and inducing colon tight junction protein expression. *Nutr. Res.* 36, 337–348. doi: 10.1016/j.nutres.2015.12.001

Liu, X., Zhang, Y., Yu, Y., Yang, X., and Cao, X. (2008). SOCS3 promotes TLR4 response in macrophages by feedback inhibiting TGF-beta1/Smad3 signaling. *Mol. Immunol.* 45, 1405–1413. doi: 10.1016/j.molimm.2007.08.018

Liu, Z., Gan, L., Zhou, Z., Jin, W., and Sun, C. (2015). SOCS3 promotes inflammation and apoptosis via inhibiting JAK2/STAT3 signaling pathway in 3T3-L1 adipocyte. *Immunobiology* 220, 947–953. doi: 10.1016/j.imbio.2015.02.004

Love, M. I., Huber, W., and Anders, S. (2014). Moderated estimation of fold change and dispersion for RNA-seq data with DESeq2. *Genome Biol.* 15:550. doi: 10.1186/s13059-014-0550-8

Lynch, S. V., and Pedersen, O. (2016). The human intestinal microbiome in health and disease. *N. Engl. J. Med.* 375, 2369–2379. doi: 10.1056/NEJMra1600266

Macharia, M., Hassan, M. S., Blackhurst, D., Erasmus, R. T., and Matsha, T. E. (2012). The growing importance of PON1 in cardiovascular health: a review. *J. Cardiovasc. Med.* 13, 443–453. doi: 10.2459/JCM.0b013e328354e3ac

Macian, F. (2005). NFAT proteins: key regulators of T-cell development and function. *Nat. Rev. Immunol.* 5, 472–484. doi: 10.1038/nri1632

Maffei, M., Halaas, J., Ravussin, E., Pratley, R. E., Lee, G. H., Zhang, Y., et al. (1995). Leptin levels in human and rodent: measurement of plasma leptin and ob RNA in obese and weight-reduced subjects. *Nat. Med.* 1, 1155–1161. doi: 10.1038/nm1195-1155

Mathews, E. S., Mawdsley, D. J., Walker, M., Hines, J. H., Pozzoli, M., and Appel, B. (2014). Mutation of 3-hydroxy-3-methylglutaryl CoA synthase I reveals requirements for isoprenoid and cholesterol synthesis in oligodendrocyte migration arrest, axon wrapping, and myelin gene expression. *J. Neurosci.* 34, 3402–3412. doi: 10.1523/JNEUROSCI.4587-13.2014

Matsuura, A., Tsukada, J., Mizobe, T., Higashi, T., Mouri, F., Tanikawa, R., et al. (2009). Intracellular galectin-9 activates inflammatory cytokines in monocytes. *Genes Cells* 14, 511–521. doi: 10.1111/j.1365-2443.2009.01287.x

Minokoshi, Y., Kim, Y. B., Peroni, O. D., Fryer, L. G., Muller, C., Carling, D., et al. (2002). Leptin stimulates fatty-acid oxidation by activating AMP-activated protein kinase. *Nature* 415, 339–343. doi: 10.1038/415339a

Peng, Y., Yu, S., Li, H., Xiang, H., Peng, J., and Jiang, S. (2014). MicroRNAs: emerging roles in adipogenesis and obesity. *Cell Signal* 26, 1888–1896. doi: 10.1016/j.cellsig.2014.05.006

Pullinger, C. R., Eng, C., Salen, G., Shefer, S., Batta, A. K., Erickson, S. K., et al. (2002). Human cholesterol 7alpha-hydroxylase (CYP7A1) deficiency has a hypercholesterolemic phenotype. *J. Clin. Invest.* 110, 109–117. doi: 10.1172/JCI15387

Reczko, M., Maragkakis, M., Alexiou, P., Grosse, I., and Hatzigeorgiou, A. G. (2012). Functional microRNA targets in protein coding sequences. *Bioinformatics* 28, 771–776. doi: 10.1093/bioinformatics/bts043

Reddy, J. K., and Hashimoto, T. (2001). Peroxisomal beta-oxidation and peroxisome proliferator-activated receptor alpha: an adaptive metabolic system. *Annu. Rev. Nutr.* 21, 193–230. doi: 10.1146/annurev.nutr.21.1.193

Richter, S., Shih, D. Q., Pearson, E. R., Wolfrum, C., Fajans, S. S., Hattersley, A. T., et al. (2003). Regulation of apolipoprotein M gene expression by MODY3 gene hepatocyte nuclear factor-1alpha: haploinsufficiency is associated with reduced serum apolipoprotein M levels. *Diabetes* 52, 2989–2995. doi: 10.2337/diabetes.52.12.2989

Rui, L., Yuan, M., Frantz, D., Shoelson, S., and White, M. F. (2002). SOCS-1 and SOCS-3 block insulin signaling by ubiquitin-mediated degradation of IRS1 and IRS2. *J. Biol. Chem.* 277, 42394–42398. doi: 10.1074/jbc.C200444200

Russell, D. W., and Setchell, K. D. (1992). Bile acid biosynthesis. *Biochemistry* 31, 4737–4749.

Sachithanandan, N., Fam, B. C., Fynch, S., Dzamko, N., Watt, M. J., Wormald, S., et al. (2010). Liver-specific suppressor of cytokine signaling-3 deletion in mice enhances hepatic insulin sensitivity and lipogenesis resulting in fatty liver and obesity. *Hepatology* 52, 1632–1642. doi: 10.1002/hep.23861

Senn, J. J., Klover, P. J., Nowak, I. A., Zimmers, T. A., Koniaris, L. G., Furlanetto, R. W., et al. (2003). Suppressor of cytokine signaling-3 (SOCS-3), a potential mediator of interleukin-6-dependent insulin resistance in hepatocytes. *J. Biol. Chem.* 278, 13740–13746. doi: 10.1074/jbc.M210689200

Shannon, P., Markiel, A., Ozier, O., Baliga, N. S., Wang, J. T., Ramage, D., et al. (2003). Cytoscape: a software environment for integrated models of biomolecular interaction networks. *Genome Res.* 13, 2498–2504. doi: 10.1101/gr.1239303

Shih, D. Q., Bussen, M., Sehayek, E., Ananthanarayanan, M., Shneider, B. L., Suchy, F. J., et al. (2001). Hepatocyte nuclear factor-1alpha is an essential regulator of bile acid and plasma cholesterol metabolism. *Nat. Genet.* 27, 375–382. doi: 10.1038/86871

Shin, M. H., Choi, E. K., Kim, K. S., Kim, K. H., Jang, Y. P., Ahn, K. S., et al. (2014). Hexane fractions of bupleurum falcatum L. stimulates glucagon-like peptide-1 secretion through G beta gamma -mediated pathway. *Evid. Based Complement. Alternat. Med.* 2014:982165. doi: 10.1155/2014/982165

Shin, M.-H., Suh, H.-W., Lee, K.-B., Kim, K.-S., Yang, H. J., Choi, E.-K., et al. (2012). Gentiana scabra extracts stimulate glucagon-like peptide-1 secretion via G protein-coupled receptor pathway. *BioChip J.* 6, 114–119. doi: 10.1007/s13206-012-6202-8

Shiura, H., Miyoshi, N., Konishi, A., Wakisaka-Saito, N., Suzuki, R., Muguruma, K., et al. (2005). Meg1/Grb10 overexpression causes postnatal growth retardation and insulin resistance via negative modulation of the IGF1R and IR cascades. *Biochem. Biophys. Res. Commun.* 329, 909–916. doi: 10.1016/j.bbrc.2005.02.047

Siegmund, B., Sennello, J. A., Jones-Carson, J., Gamboni-Robertson, F., Lehr, H. A., Batra, A., et al. (2004). Leptin receptor expression on T lymphocytes modulates chronic intestinal inflammation in mice. *Gut* 53, 965–972. doi: 10.1136/gut.2003.027136

Singh, N., Shirdel, E. A., Waldron, L., Zhang, R. H., Jurisica, I., and Comelli, E. M. (2012). The murine caecal microRNA signature depends on the presence of the endogenous microbiota. *Int. J. Biol. Sci.* 8, 171–186. doi: 10.7150/ijbs.8.171

Steinberg, G. R., McAinch, A. J., Chen, M. B., O'Brien, P. E., Dixon, J. B., Cameron-Smith, D., et al. (2006). The suppressor of cytokine signaling 3 inhibits leptin activation of AMP-kinase in cultured skeletal muscle of obese humans. *J. Clin. Endocrinol. Metab.* 91, 3592–3597. doi: 10.1210/jc.2006-0638

Su, E. W., Bi, S., and Kane, L. P. (2011). Galectin-9 regulates T helper cell function independently of Tim-3. *Glycobiology* 21, 1258–1265. doi: 10.1093/glycob/cwq214

Taganov, K. D., Boldin, M. P., and Baltimore, D. (2007). MicroRNAs and immunity: tiny players in a big field. *Immunity* 26, 133–137. doi: 10.1016/j.immuni.2007.02.005

Tseng, L. T., Lin, C. L., Tzen, K. Y., Chang, S. C., and Chang, M. F. (2013). LMBD1 protein serves as a specific adaptor for insulin receptor internalization. *J. Biol. Chem.* 288, 32424–32432. doi: 10.1074/jbc.M113.479527

Wang, L., Balas, B., Christ-Roberts, C. Y., Kim, R. Y., Ramos, F. J., Kikani, C. K., et al. (2007). Peripheral disruption of the Grb10 gene enhances insulin signaling and sensitivity in vivo. *Mol. Cell Biol.* 27, 6497–6505. doi: 10.1128/MCB.00679-07

Wang, R., Li, H., Yang, X., Xue, X., Deng, L., Shen, J., et al. (2018). Genetically obese human gut microbiota induces liver steatosis in germ-free mice fed on normal diet. *Front. Microbiol.* 9:1602. doi: 10.3389/fmicb.2018.01602

Waterham, H. R., Koster, J., Romeijn, G. J., Hennekam, R. C., Vreken, P., Andersson, H. C., et al. (2001). Mutations in the 3beta-hydroxysterol Delta24-reductase gene cause desmosterolosis, an autosomal recessive disorder of cholesterol biosynthesis. *Am. J. Hum. Genet.* 69, 685–694. doi: 10.1086/323473

West, N. R., Hegazy, A. N., Owens, B. M. J., Bullers, S. J., Linggi, B., Buonocore, S., et al. (2017). Oncostatin M drives intestinal inflammation and predicts response to tumor necrosis factor-neutralizing therapy in patients with inflammatory bowel disease. *Nat. Med.* 23, 579–589. doi: 10.1038/nm.4307

Wick, K. R., Werner, E. D., Langlais, P., Ramos, F. J., Dong, L. Q., Shoelson, S. E., et al. (2003). Grb10 inhibits insulin-stimulated insulin receptor substrate (IRS)-phosphatidylinositol 3-kinase/Akt signaling pathway by disrupting the association of IRS-1/IRS-2 with the insulin receptor. *J. Biol. Chem.* 278, 8460–8467. doi: 10.1074/jbc.M208518200

Wong, N., and Wang, X. (2015). miRDB: an online resource for microRNA target prediction and functional annotations. *Nucleic Acids Res.* 43, D146–D152. doi: 10.1093/nar/gku1104

Xu, D., Holko, M., Sadler, A. J., Scott, B., Higashiyama, S., Berkofsky-Fessler, W., et al. (2009). Promyelocytic leukemia zinc finger protein regulates interferon-mediated innate immunity. *Immunity* 30, 802–816. doi: 10.1016/j.immuni.2009.04.013

Yamaguchi, T., Cubizolles, F., Zhang, Y., Reichert, N., Kohler, H., Seiser, C., et al. (2010). Histone deacetylases 1 and 2 act in concert to promote the G1-to-S progression. *Genes Dev.* 24, 455–469. doi: 10.1101/gad.552310

Zarkesh-Esfahani, H., Pockley, G., Metcalfe, R. A., Bidlingmaier, M., Wu, Z., Ajami, A., et al. (2001). High-dose leptin activates human leukocytes via receptor expression on monocytes. *J. Immunol.* 167, 4593–4599. doi: 10.4049/jimmunol.167.8.4593

Zhang, C., Yin, A., Li, H., Wang, R., Wu, G., Shen, J., et al. (2015). Dietary modulation of gut microbiota contributes to alleviation of both genetic and simple obesity in children. *EBioMedicine* 2, 968–984. doi: 10.1016/j.ebiom.2015.07.007

Zhang, C., Zhang, M., Wang, S., Han, R., Cao, Y., Hua, W., et al. (2010). Interactions between gut microbiota, host genetics and diet relevant to development of metabolic syndromes in mice. *ISME J.* 4, 232–241. doi: 10.1038/ismej.2009.112

Zimmermann, R., Strauss, J. G., Haemmerle, G., Schoiswohl, G., Birner-Gruenberger, R., Riederer, M., et al. (2004). Fat mobilization in adipose tissue is promoted by adipose triglyceride lipase. *Science* 306, 1383–1386. doi: 10.1126/science.1100747

Conflict of Interest Statement: The authors declare that the research was conducted in the absence of any commercial or financial relationships that could be construed as a potential conflict of interest.

Copyright © 2019 Deng, Wang, Li, Zhang, Zhao and Zhang. This is an open-access article distributed under the terms of the Creative Commons Attribution License (CC BY). The use, distribution or reproduction in other forums is permitted, provided the original author(s) and the copyright owner(s) are credited and that the original publication in this journal is cited, in accordance with accepted academic practice. No use, distribution or reproduction is permitted which does not comply with these terms.

frontiers in Microbiology

ORIGINAL RESEARCH
published: 19 July 2019
doi: 10.3389/fmicb.2019.01664

The Microbiome of Prostate Fluid Is Associated With Prostate Cancer

Xiaowei Ma[1,2†], Chenfei Chi[1†], Liancheng Fan[1†], Baijun Dong[1], Xiaoguang Shao[1], Shaowei Xie[3], Min Li[2*‡] and Wei Xue[1*‡]*

[1] Department of Urology, Renji Hospital, School of Medicine, Shanghai Jiao Tong University, Shanghai, China, [2] Department of Clinical Laboratory, Renji Hospital, School of Medicine, Shanghai Jiao Tong University, Shanghai, China, [3] Department of Ultrasound in Medicine, Renji Hospital, School of Medicine, Shanghai Jiao Tong University, Shanghai, China

OPEN ACCESS

Edited by:
Siok-Fong Chin,
UKM Medical Molecular Biology Institute (UMBI), Malaysia

Reviewed by:
Séamus Fanning,
University College Dublin, Ireland
Ernst Holler,
University of Regensburg, Germany

***Correspondence:**
Xiaowei Ma
m138902y@hotmail.com
Min Li
ruth_limin@126.com
Wei Xue
xuewei@renji.com

†These authors have contributed equally to this work as co-first authors

‡These authors have contributed equally to this work as co-corresponding authors

Specialty section:
This article was submitted to Microbial Symbioses, a section of the journal Frontiers in Microbiology

Received: 29 October 2018
Accepted: 04 July 2019
Published: 19 July 2019

Citation:
Ma X, Chi C, Fan L, Dong B, Shao X, Xie S, Li M and Xue W (2019) The Microbiome of Prostate Fluid Is Associated With Prostate Cancer. Front. Microbiol. 10:1664. doi: 10.3389/fmicb.2019.01664

Objectives: To explore the microbiome of the prostatic fluid in high prostate-specific antigen (PSA) patients.

Patients and Methods: The microbiome profiles of prostatic fluid samples from 32 prostate cancer (PCa) patients and 27 non-PCa people were assessed. Microbiome analysis was assessed by massive 16S ribosomal RNA gene sequencing.

Results: Compared with the NCA group, the microbial diversity was lower in the CA group. There were no specific microbial species in the CA group or NCA group. However, many species, such as those in the genera *Alkaliphilus*, *Enterobacter*, *Lactococcus*, *Cronobacter*, *Carnobacterium*, and *Streptococcus*, showed a significant difference between the CA group and NCA group.

Conclusion: The prostate contains reduced bacteria, suggesting a possible pathophysiological correlation between the composition of the microbiome and PCa. Meanwhile, this study uncovered that the microbiome may be beneficial in maintaining the stability of the microenvironment of the prostate and provides interesting perspectives for the identification of novel biomarkers in high-PSA patients.

Keywords: prostate cancer, prostatic fluid, microbiome, cancer, prostate

INTRODUCTION

Prostate cancer (PCa) is one of the commonest male malignant tumors, and it is the second most diagnosed malignant tumor and the fifth leading cause of tumor-associated death in the world (Wong et al., 2016). At the moment, PCa is the third highest cause of tumor-associated mortality in the United States (Siegel et al., 2017). In addition, the incidence of PCa shows, recently, a trend of fast increase in Asian countries, including China (Bray et al., 2010). Moreover, PCa seriously influences sexual functions, male urinary and decreases the quality of life (Chipman et al., 2014). Despite great efforts made worldwide to explore the novel treatment strategies of PCa, the patients generally relapse and develop resistance in advanced stages. Therefore, we should draw great attention to and search for better approaches for the diagnosis and treatment of PCa.

Prostate-specific antigen (PSA), an enzyme secreted by the prostate gland, increases in the blood of patients with PCa; therefore, it is widely used as an established laboratory test for PCa. However, as it is commonly used to diagnose PCa, misdiagnosis events frequently occur due to its high sensitivity and low specificity, and its value in screening, particularly in asymptomatic males, is controversial when considering the risks and benefits of early detection. Tumors and inflammation can both lead to damage to the prostate gland, causing increased levels of PSA.

Chronic prostatitis (CPS), a common chronic inflammation disease in adult males, accounts for more than 90%. In addition, studies have shown that chronic inflammation in the prostate has been especially relevant for the progression, pathogeny, and prognosis of PCa (Taverna et al., 2015; He et al., 2017), and CPS (Giunchi et al., 2017) is one of the causes of elevated PSA. According to different inflammatory and tumor conditions in previous researches, the modifications of bacterial populations were also founded in PCa samples and partly promote the development of cancer by enhancing the pro-inflammatory responses or changing the extracellular environment of the prostate (Cohen et al., 2005; Shinohara et al., 2013; Cavarretta et al., 2017). It has been reported that many pathogenic microorganisms could induce symptomatic asymptomatic and symptomatic inflammatory reactions in the prostate, including *Escherichia coli* (Buerfent et al., 2015), *Pseudomonas* spp. (Souto et al., 2014), *Neisseria gonorrhoeae* (Churchward et al., 2017), *Chlamydia trachomatis* (Koroleva et al., 2015), and *Trichomonas vaginalis* (Lee et al., 2012). In addition, *Propionibacterium acnes*, detected in PCa patients' samples through direct genomic amplification and culture, has been associated with enhanced inflammatory response in patients with PCa. Now that CPS and PCa have been closely associated with the microbiome, revealing the connection in the microorganisms associated with PCa and CPS might be important.

Until now, a comprehensive and detailed comparison of the microbial ecosystems of the prostatic fluid of PCa patients and non-PCa people has not been conducted. Therefore, the objectives of the current study are to characterize the microbiomes associated with the non-tumor and tumor prostatic fluid microenvironment in high-PSA people using 16S ribosomal RNA (rRNA) gene sequencing and assess their relevance in terms of the pathogenesis of PCa as well as to find a connection in the microorganisms associated with PCa and CPS with the hope to seek out a new means for the diagnosis of PCa.

TABLE 1 | The clinical characteristics and pathological parameters of the two groups.

	CA (n = 32)	NCA (n = 27)	P
Age (years)	68.21 ± 1.04	65.00 ± 1.67	0.0516
WBC (10^9/L)	5.91 ± 0.43	6.87 ± 0.27	0.0594
PSA (ng/μl)	17.48 ± 2.60	31.72 ± 15.67	0.5866
fPSA/PSA	9.12 ± 1.87	13.57 ± 1.36	0.0679
Gleason 6	43.75% (14/32)		
Gleason 7	46.8% (15/32)		
Gleason 8	9.4% (3/32)		

CA, prostate cancer; NCA, non-prostate cancer; PSA, prostate specific antigen; fPSA, free prostate specific antigen; Gleason, Prostate Gleason Grading system; WBC, white blood count.

PATIENTS AND METHODS

Patient Selection and Specimen Processing

From May 2015 to October 2016, prostatic fluid specimens from 59 patients who had a high level of PSA (>4 ng/ml) before prostate biopsy were chosen for our study. None of the patients had recent urinary tract infections or sexually transmitted infections. Patients with a pathologic International Prostate Symptom Score (IPSS) or lower urinary tract symptoms (LUTS) were excluded. Nobody have any antimicrobial exposure

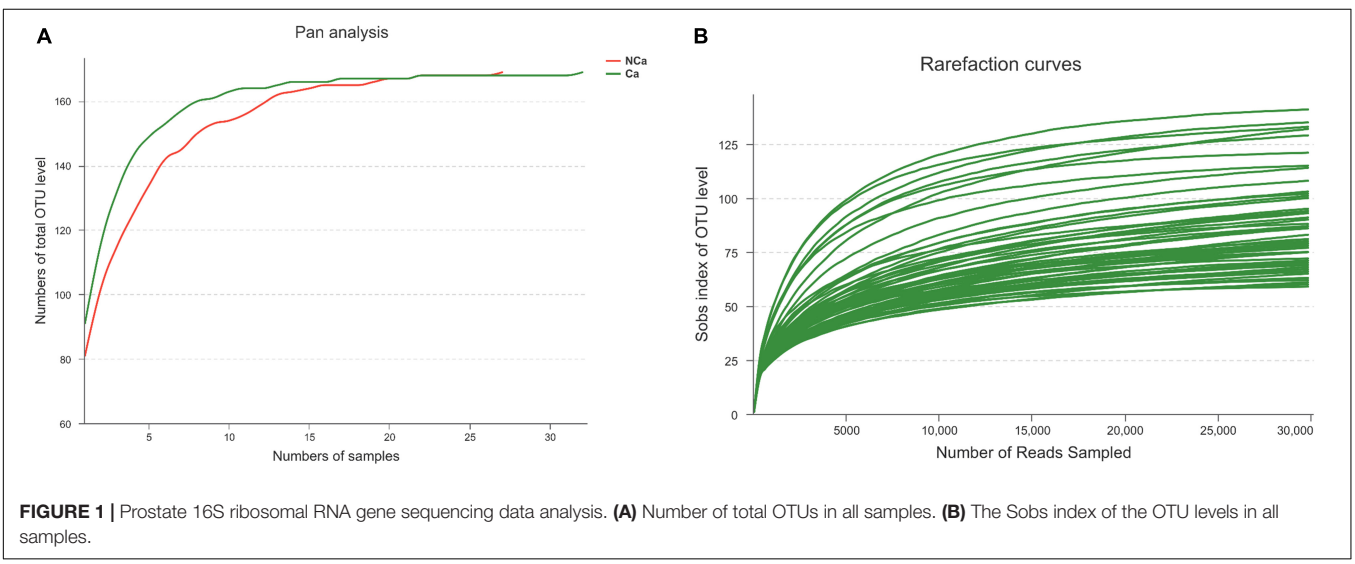

FIGURE 1 | Prostate 16S ribosomal RNA gene sequencing data analysis. **(A)** Number of total OTUs in all samples. **(B)** The Sobs index of the OTU levels in all samples.

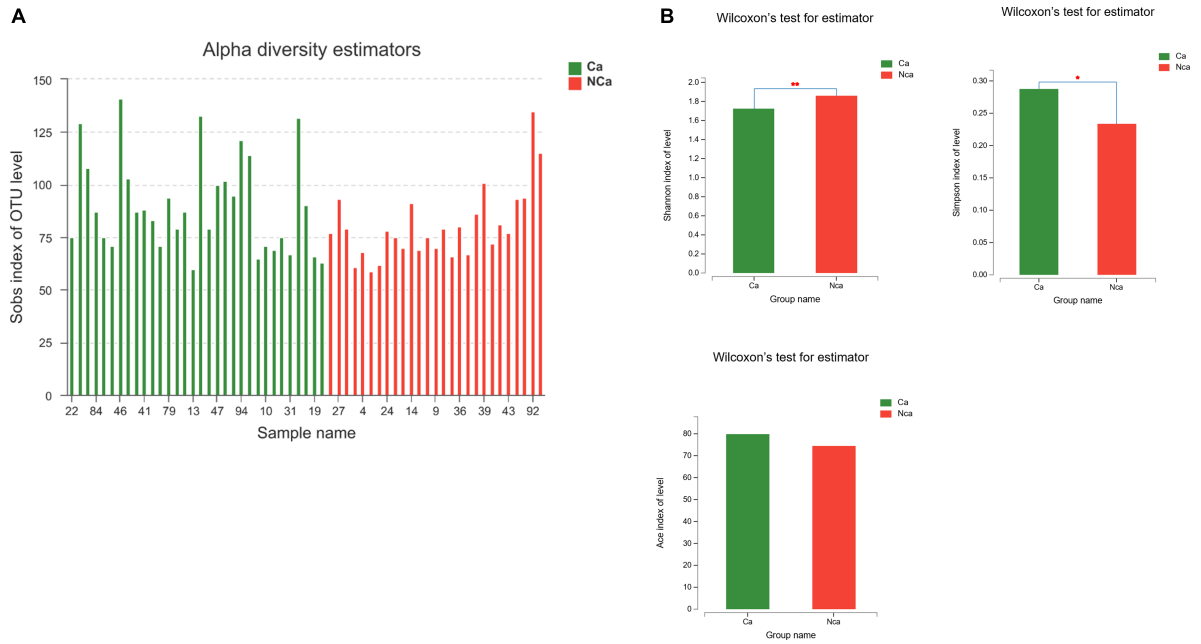

FIGURE 2 | PCa samples showed reduced microbial diversity. **(A)** The alpha microbial diversity presented in all samples. **(B)** The Shannon–Wiener index, Simpson index, and Ace index in the CA group and NCA group.

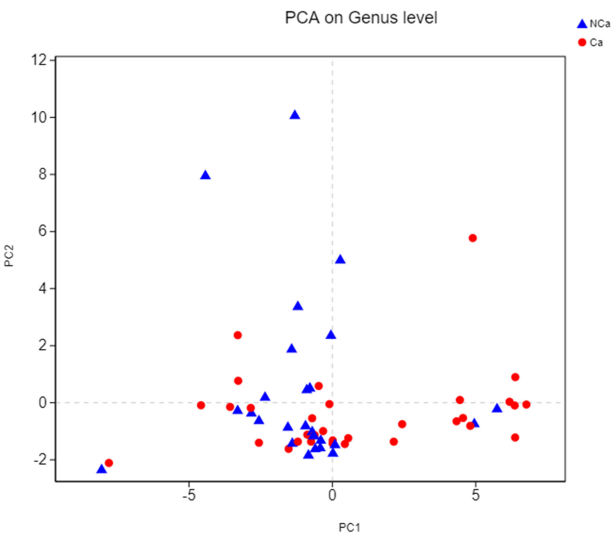

FIGURE 3 | PCA on genus level.

within the preceding 4 week. The diagnosis of 32 PCa patients and 27 non-PCa people was determined by pathology after prostate biopsy. Data collection was conducted according to the principles outlined in the Declaration of Helsinki. All participants signed an informed consent form agreeing to provide their own anonymous information for future research. The study was approved by the ethical committee of the Renji Hospital (Renji/2013126). **Table 1** details the clinical characteristics and pathological parameters of the participators.

Sample Collection and DNA Extraction

Prostatic fluid samples were collected at the hospital through massaging the prostate before prostate biopsy under sterile acquisition and stored at −80°C within 1 h. DNA extraction was performed using a QIAamp DNA Mini Kit (Qiagen, Valencia, CA, United States). The concentration of bacterial DNA was measured using a Nanodrop 2000 (Thermo Fisher Scientific, United States). Data on demographics and clinical variables were collected during the clinic visits.

16S Ribosomal RNA Gene Sequencing

The V3–V4 region of the bacterial 16S rRNA gene was amplified using PCR with the barcode-indexed primers 338F and 806R using a PCR thermocycler system (GeneAmp 9700, ABI, United States). A negative control was simultaneously amplified. If the negative control was negative, the resulting PCR products were extracted from a 2% agarose gel and further purified using the AxyPrep DNA Gel Extraction Kit (Axygen Biosciences, Union City, CA, United States) and quantified using QuantiFluor^{TM}-ST (Promega, United States) according to the manufacturer's protocol. The purified amplicons were pooled in equimolar concentrations, and paired-end sequencing (2 × 300) was performed using an Illumina MiSeq instrument (Illumina, San Diego, CA, United States).

Processing of the Sequencing Data

Raw FASTQ files were demultiplexed, quality-filtered with Trimmomatic and merged using FLASH with the following

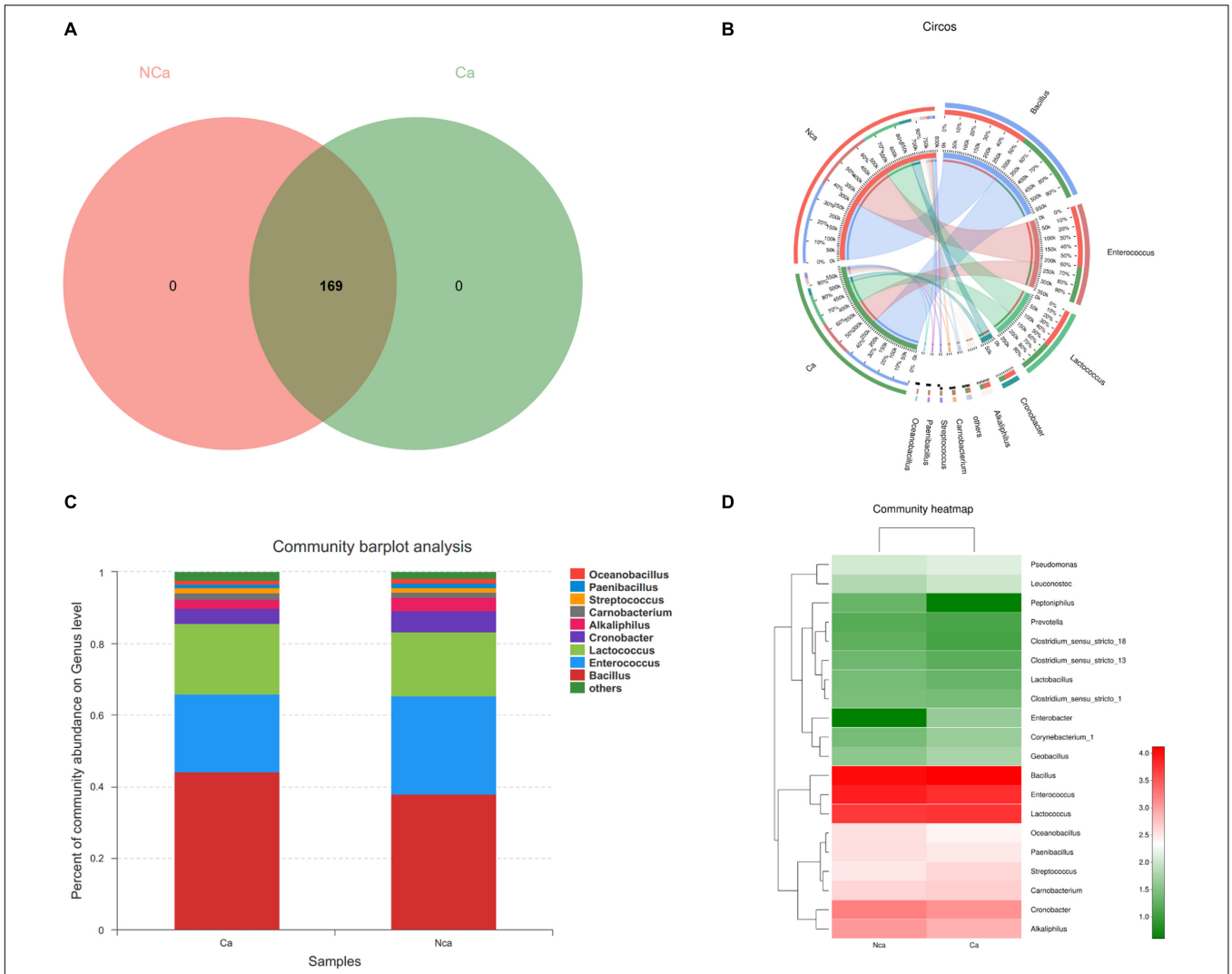

FIGURE 4 | Species composition analysis. **(A)** The two groups did not show a specific composition. **(B)** The community pie chart shows the microbial composition of the two groups. **(C)** The community barplot for the two groups. **(D)** The heatmap demonstrates the compositions of the two groups.

criteria: (i) the reads were truncated at any site receiving an average quality score <20 over a 50 bp sliding window. (ii) Primers were exactly matched, allowing two nucleotide mismatching, and reads containing ambiguous bases were removed. (iii) Sequences whose overlap was longer than 10 bp were merged according to their overlap sequence.

Operational taxonomic units (OTUs) were clustered with a 97% similarity cutoff using UPARSE (version 7.1[1]), and chimeric sequences were identified and removed using UCHIME. Then, the singletons were also removed. The taxonomy of each 16S rRNA gene sequence was analyzed using the RDP Classifier algorithm[2] against the Silva (SSU123) 16S rRNA database using a confidence threshold of 70%. OTUs with a number of sequences <0.005% of the total number of sequences were removed from the OTU table. In addition, rarefaction was performed on the OTU table to prevent methodological artifacts arising from varying sequencing depths. α-Diversity was measured by species richness from the rarefied OTU table. β-Diversity was estimated by computing the unweighted UniFrac distance and was visualized using principal coordinate analysis. In an effort to identify the possible species represented by the OTUs, we performed a MegaBLAST search to align the reads of the OTUs against reference sequences in the National Center for Biotechnology Information (NCBI) 16S rRNA database. The data has been uploaded to SRA database (SRP197683).

Statistical Analysis

All statistical analyses were performed using R packages (V.2.15.3) and SPSS 16.0 (SPSS Inc., Chicago, IL, United States). For the comparison of continuous variables, data are presented as the median (first quartile to the third quartile). The statistical

[1]http://drive5.com/uparse/

[2]http://rdp.cme.msu.edu/

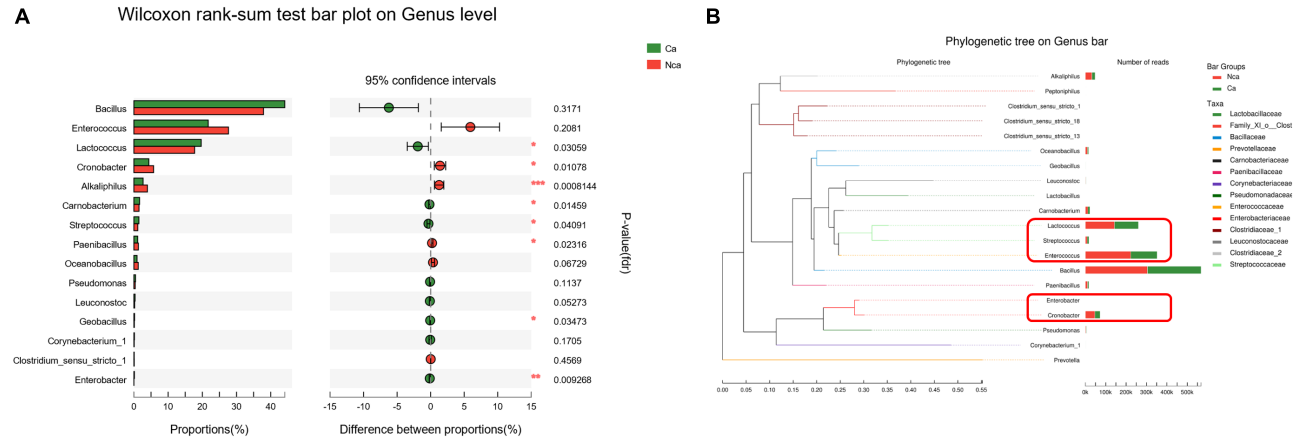

FIGURE 5 | Analysis of the specific microbial species differences. **(A)** The differences in microbial species between the two groups were explored. **(B)** The evolution of the different microbial species in the two groups.

significance of the differences among different groups was tested using Friedman's test, with the Wilcoxon rank-sum test for CA (cancer group) versus NCA (non-PCa) (according to the data distribution). For the correlation analysis, Spearman's rank test was performed. Multiple hypothesis tests were adjusted using the Benjamini and Hochberg false discovery rate (FDR), and a significant association was considered to occur when the FDR was below the threshold of 0.05. A random forest model (randomForest 4.6-7 package) using the 12-genera signature was applied for the data from the PBC and control samples. To evaluate the discriminatory ability of the random forest model, operating characteristic curves (receiving operational curve, ROC) were constructed, and the area under the curve (AUC) was calculated.

RESULTS

Sequencing Data Quality Analysis

Prostatic fluid from 32 PCa patients and 27 non-PCa (NCA) people was submitted to 16S rRNA gene sequencing. The pan analysis was smooth and steady after 20 samples, indicating that the number of samples was sufficient for the analysis (**Figure 1A**). The rarefaction curves of all samples were smooth and steady (**Figure 1B**), indicating that the depth of sequencing was sufficient for the diversity analysis.

PCa Samples Showed Reduced Microbial Diversity

Then, we compared the microbial alpha diversity of the two groups (the CA group represented samples from the PCa patients, and the NCA group represented the samples from non-PCA people) by calculating the Shannon–Wiener, Simpson and Ace diversity indexes. The alpha diversity was determined based on community richness and community evenness. There did not appear to be a difference in the Sobs index for the OTU level between the two groups in **Figure 2A**. Therefore, the Ace index showed no difference in community richness between the two groups. Meanwhile, the difference in the Shannon–Wiener and Simpson indexes in **Figure 2B** indicated that there was a significant difference in community evenness between the two groups. The data demonstrated reduced microbial diversity in the prostatic fluid from people with PCa. The PCA analysis at the genus level showed that the NCA and CA groups had some clustering with members of their own group (**Figure 3**).

Species Composition Analysis

The results show that there were no unique microbial species in the CA group or NCA group (**Figure 4A**). All samples consisted of *Oceanobacillus*, *Paenibacillus*, *Streptococcus*, *Carnobacterium*, *Alkaliphilus*, *Cronobacter*, *Lactococcus*, *Enterococcus*, *Bacillus*, and others (**Figures 4B,C**). However, there were some differences in species between the two groups (**Figure 4D**).

Analysis of the Specific Microbial Species Differences

To further study the differences in microbial species between the two groups, we explored the differences in the specific microbial species between the two groups. The proportions of *Alkaliphilus*, *Enterobacter*, *Lactococcus*, *Cronobacter*, *Carnobacterium*, *Streptococcus*, *Paenibacillus*, and *Geobacillus* showed a significant difference between the CA group and the NCA group ($P < 0.05$, **Figure 5A**). In addition, some of the different microbial species in the two groups were evolutionarily similar, such as *Lactococcus*, *Streptococcus*, and *Enterococcus* (**Figure 5B**).

Disease Status Discrimination With the Microbiome

Finally, to explore the potential ability of the prostate fluid microbiome to identify PCa status, we constructed a random forest model based on the prostate fluid microbiome signature composed of 8 associated genera. We constructed an ROC to analyse the clinical accuracy of using the gut microbiome for

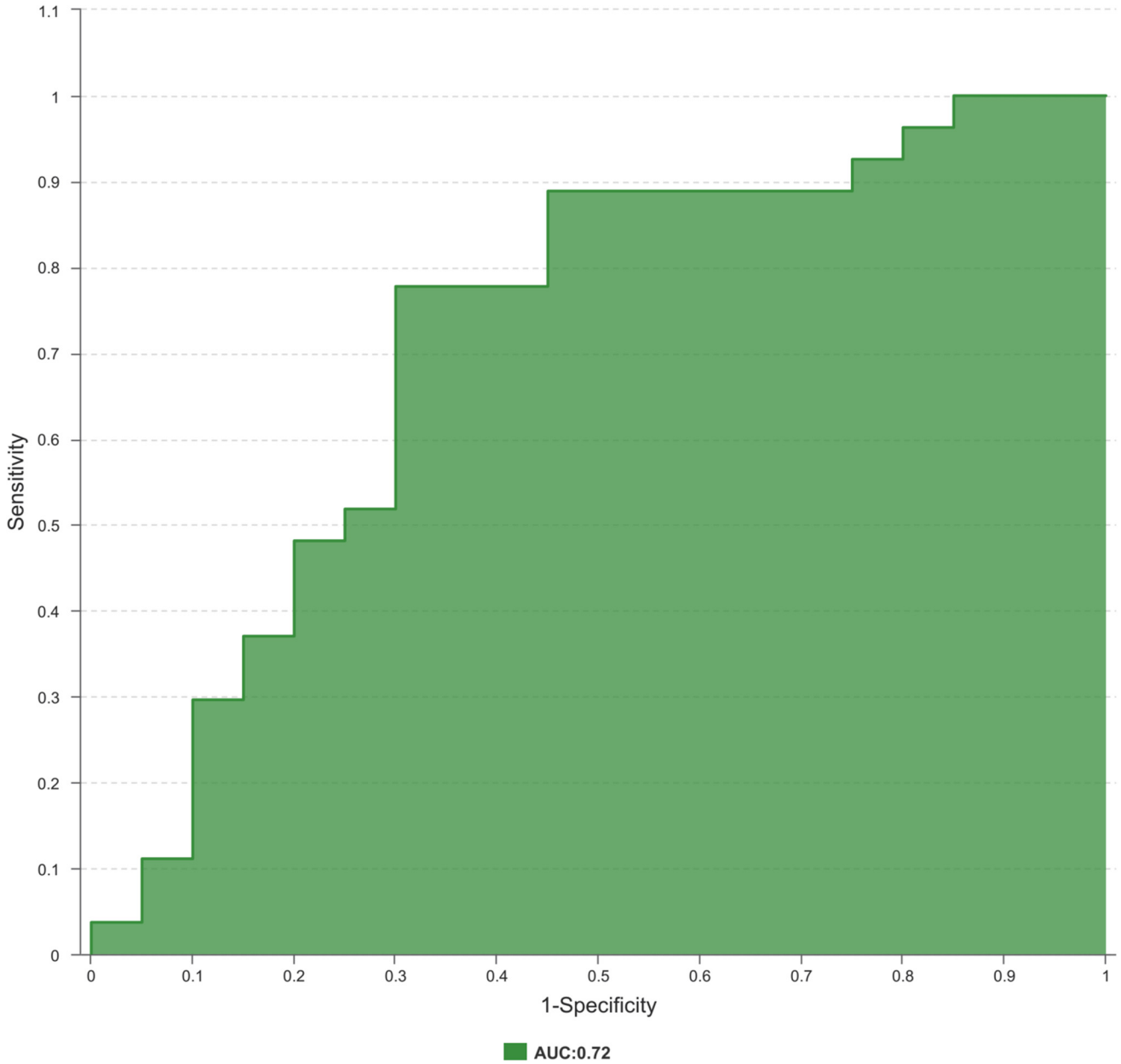

FIGURE 6 | The ROC curve used to analyze the clinical accuracy of using differential bacteria obtained from the CA group and NCA group for the diagnosis of PCa.

the diagnosis of PCa, and the AUC (area under the curve) was 0.72 (**Figure 6**), suggesting that it might play a role in the diagnosis of PCa.

DISCUSSION

PCa is one of the top malignancies in the male population worldwide. Although age, ethnicity, and family history are the risk factors for PCa, some other factors were recognized in the development and progression of PCa, such as infections of bacteria and virus, inflammation, and other environmental factors (Bosland, 1988; Maitland and Collins, 2008; Sutcliffe and Platz, 2008; Sfanos et al., 2013; Delcaru et al., 2017). All of above mentioned factors could influence the microbiological composition, the community of the fungi, viruses, bacteria and parasites living within the human body. These eventually impact human health and disease by interacting with each other and with the host (Holmes et al., 2011; Giorgetti et al., 2015; Pagliari et al., 2015). In recent

years, the development of high throughput molecular-based methods for the identification of complex microbiomes has promoted the research in microbiome, which reveals the novel relationship between microbiological composition and human pathological conditions, such as colorectal cancer, PCa, diabetes and obesity (van Olden et al., 2015; Wang et al., 2015; Cavarretta et al., 2017; Komaroff, 2017; Liu et al., 2017).

In the present study, we revealed the microbiome of the prostatic fluid from PCa patients by using a massive 16S rRNA gene sequencing approach. In addition to confirming the existence of a prostate-specific microbiome, we also identified different microbial species between the CA group and the NCA group.

We collected prostatic fluid specimens from 32 patients with PCa and 27 non-PCa people, all participants with a high level of PSA. The rarefaction curves of all samples indicated that the depth of sequencing catered to the needs of 16S rRNA gene sequencing analysis. Then, we compared the microbial diversity of the CA and NCA groups by calculating the Shannon–Wiener index and Simpson diversity index. The results suggest that the NA group showed reduced microbial diversity when compared with the NCA group, demonstrating that microbial diversity may have a role in the progression of PCa. We further analyzed the specific microbial species in the two groups, but the results demonstrated that there were no idiosyncrasies in the microbial species in the CA group when compared with the NCA group. All samples consisted of *Oceanobacillus*, *Paenibacillus*, *Streptococcus*, *Carnobacterium*, *Alkaliphilus*, *Cronobacter*, *Lactococcus*, *Enterococcus*, *Bacillus*, and others. However, there were many differences of the abovementioned species between the two groups, such as *Alkaliphilus*, *Enterobacter*, *Lactococcus*, *Cronobacter*, *Carnobacterium*, *Streptococcus*, *Paenibacillus*, and *Geobacillus*. Nevertheless, some of the different microbial species in the two groups were evolutionarily similar, as shown in the phylogenetic tree.

In a recent prostate microbiome study, Riley et al. (1998) reported that 16S rDNA could be detected in prostate tissues with CPS at first. Ilaria Cavarretta et al. (2017) reported that the *Streptococcus* was almost exclusive presented in non-tumor regions, supporting the idea that the *Lactobacillales* might belong to a normal prostatic microbiome and might contribute to the balance of the host extracellular environment. In addition, in our study, the proportion of *Streptococcus* in the CA group was significantly higher than that in the NCA group. The difference might come from the sample type. The microbiome has been seen as a key factor in disease, controlling multiple pathways involved with metabolism (Shreiner et al., 2015). Some recent studies indicated that bile acids, lactate, fatty lipids and others could maintain endocrine functions to regulate tricarboxylic acid cycle, cholesterol, glucose and energy homeostasis via some bacteria (Swann et al., 2011; Serino et al., 2012; Hui et al., 2017). The host and its microbiota coproduce a great diversity of small molecules during metabolism, many of which might play critical roles in the occurrence and development of disease. In our study, some of the different microbial species in the two groups, such as *Lactococcus* spp. and *Streptococcus* spp., could change the environment through variety metabolites, which is thought to play a role in tumor growth.

This pilot study has several limitations. It is difficult to control for bacteria possibly introduced from the urinary tract, and the small sample number was a limitation of this study. A major innovation point of this analysis was that it provided the first detailed description of the microbiome environment in prostate fluid in CA and NCA patients.

CONCLUSION

This 16S rRNA gene sequencing approach suggested novel findings of a large population of bacteria within the prostatic fluid, found differences in the microbial species in the prostatic fluid from non-PCa people and PCa patients, and demonstrated that bacteria may be beneficial in maintaining the stability of the microenvironment of the prostate, providing new ideas for the diagnosis of PCa with high PSA. Further studies might place more focus on clarifying the possible pathogenic role of bacteria and exploring the microbiome in other body fluids associated with PCa.

ETHICS STATEMENT

Data collection followed the principles outlined in the Declaration of Helsinki; all participants had signed an informed consent document agreeing to deliver their own anonymous information for future studies. The study was approved by our local ethical committee (Renji/2013126).

AUTHOR CONTRIBUTIONS

XM and CC drafted the manuscript and designed the study. CC and LF carried out the DNA extraction and the sample collection. BD, XS, and SX collected the patients' materials and clinical and patients' information. XM and ML performed the sequencing. XM and WX performed the data interpretation, bioinformatical and statistical analyses, drafted the manuscript, and designed the study. All authors read and approved the final version of the manuscript.

FUNDING

This study was supported by the National Natural Science Foundation of China (Nos. 81671975, 81371875, 81572536, and 81672850) and the Shanghai Municipal Commission of Health and Family Planning (201640247).

REFERENCES

Bosland, M. C. (1988). The etiopathogenesis of prostatic cancer with special reference to environmental factors. *Adv. Cancer Res.* 51, 1–106. doi: 10.1016/s0065-230x(08)60220-1

Bray, F., Lortet-Tieulent, J., Ferlay, J., Forman, D., and Auvinen, A. (2010). Prostate cancer incidence and mortality trends in 37 European countries: an overview. *Eur. J. Cancer* 46, 3040–3052. doi: 10.1016/j.ejca.2010.09.013

Buerfent, B. C., Gondorf, F., Wohlleber, D., Schumak, B., Hoerauf, A., Hübner, M. P., et al. (2015). *Escherichia coli*-induced immune paralysis is not exacerbated during chronic filarial infection. *Immunology* 145, 150–160. doi: 10.1111/imm.12435

Cavarretta, I., Ferrarese, R., Cazzaniga, W., Saita, D., Lucianò, R., Ceresola, E. R., et al. (2017). The microbiome of the prostate tumour microenvironment. *Eur. Urol.* 72, 625–631. doi: 10.1016/j.eururo.2017.03.029

Chipman, J. J., Sanda, M. G., Dunn, R. L., Wei, J. T., Litwin, M. S., Crociani, C. M., et al. (2014). Measuring and predicting prostate cancer related quality of life changes using EPIC for clinical practice. *J. Urol.* 191, 638–645. doi: 10.1016/j.juro.2013.09.040

Churchward, C. P., Alany, R. G., Kirk, R. S., Walker, A. J., and Snyder, L. A. S. (2017). Prevention of ophthalmia neonatorum caused by *neisseria gonorrhoeae* using a fatty acid-based formulation. *MBio* 8, e534–e517. doi: 10.1128/mBio.00534-17

Cohen, R. J., Shannon, B. A., McNeal, J. E., Shannon, T., and Garrett, K. L. (2005). Propionibacterium acnes associated with inflammation in radical prostatectomy specimens: a possible link to cancer evolution? *J. Urol.* 173, 1969–1974. doi: 10.1097/01.ju.0000158161.15277.78

Delcaru, C., Podgoreanu, P., Alexandru, I., Popescu, N., Măruţescu, L., Bleotu, C., et al. (2017). Antibiotic resistance and virulence phenotypes of recent bacterial strains isolated from urinary tract infections in elderly patients with prostatic disease. *Pathogens* 6:E22. doi: 10.3390/pathogens6020022

Giorgetti, G., Brandimarte, G., Fabiocchi, F., Ricci, S., Flamini, P., Sandri, G., et al. (2015). Interactions between innate immunity, microbiota, and probiotics. *J. Immunol. Res.* 2015:501361. doi: 10.1155/2015/501361

Giunchi, F., Jordahl, K., Bollito, E., Colecchia, M., and Patriarca, C. (2017). Interpathologist concordance in the histological diagnosis of focal prostatic atrophy lesions, acute and chronic prostatitis. PIN, and prostate cancer. *Virchows Arch.* 470, 711–715. doi: 10.1007/s00428-017-2123-1

He, Y., Zeng, H., Yu, Y., Zhang, J., Zeng, X., Gong, F., et al. (2017). Resveratrol improved the progression of chronic prostatitis via the downregulation of c-kit/SCF by activating sirt1. *J. Agric. Food Chem.* 65, 5668–5673. doi: 10.1021/acs.jafc.7b01879

Holmes, E., Li, J. V., Athanasiou, T., Ashrafian, H., and Nicholson, J. K. (2011). Understanding the role of gut microbiome-host metabolic signal disruption in health and disease. *Trends Microbiol.* 19, 349–359. doi: 10.1016/j.tim.2011.05.006

Hui, S., Ghergurovich, J. M., Morscher, R. J., Jang, C., Teng, X., Lu, W., et al. (2017). Glucose feeds the TCA cycle via circulating lactate. *Nature* 551, 115–118. doi: 10.1038/nature24057

Komaroff, A. L. (2017). The microbiome and risk for obesity and diabetes. *JAMA* 317, 355–356.

Koroleva, E. A., Kobets, N. V., Zayakin, E. S., Luyksaar, S. I, Shabalina, L. A., Zigangirova, N. A., et al. (2015). Small molecule inhibitor of type three secretion suppresses acute and chronic *Chlamydia trachomatis* infection in a novel urogenital Chlamydia model. *Biomed. Res. Int.* 2015:484853. doi: 10.1155/2015/484853

Lee, J. J., Moon, H. S., Lee, T. Y., Hwang, H. S., Ahn, M. H., and Ryu, J. S. (2012). PCR for diagnosis of male *Trichomonas vaginalis* infection with chronic prostatitis and urethritis. *Korean J. Parasitol.* 50, 157–159. doi: 10.3347/kjp.2012.50.2.157

Liu, F., Wang, X., Shi, H., and Wang, Y. (2017). Polymannuronic acid ameliorated obesity and inflammation associated with a high-fat and high-sucrose diet by modulating the gut microbiome in a murine model. *Br. J. Nutr.* 117, 1332–1342. doi: 10.1017/S0007114517000964

Maitland, N. J., and Collins, A. T. (2008). Inflammation as the primary aetiological agent of human prostate cancer: a stem cell connection? *J. Cell Biochem.* 105, 931–939. doi: 10.1002/jcb.21843

Pagliari, D., Piccirillo, C. A., Larbi, A., and Cianci, R. (2015). The interactions between innate immunity and microbiota in gastrointestinal diseases. *J. Immunol. Res.* 2015:898297.

Riley, D. E., Berger, R. E., Miner, D. C., and Krieger, N. J. (1998). Diverse and related 16S rRNA-encoding DNA sequences in prostate tissues of men with chronic prostatitis. *J. Clin. Microbiol.* 36, 1646–1652.

Serino, M., Luche, E., Gres, S., Baylac, A., Bergé, M., Cenac, C., et al. (2012). Metabolic adaptation to a high-fat diet is associated with a change in the gut microbiota. *Gut* 61, 543–553. doi: 10.1136/gutjnl-2011-301012

Sfanos, K. S., Isaacs, W. B., and De Marzo, A. M. (2013). Infections and inflammation in prostate cancer. *Am. J. Clin. Exp. Urol.* 1, 3–11.

Shinohara, D. B., Vaghasia, A. M., Yu, S. H., Mak, T. N., Brüggemann, H., Nelson, W. G., et al. (2013). A mouse model of chronic prostatic inflammation using a human prostate cancer-derived isolate of Propionibacterium acnes. *Prostate* 73, 1007–1015. doi: 10.1002/pros.22648

Shreiner, A. B., Kao, J. Y., and Young, V. B. (2015). The gut microbiome in health and in disease. *Curr. Opin. Gastroenterol.* 31:2015.

Siegel, R. L., Miller, K. D., and Jemal, A. (2017). Cancer statistics, 2017. *CA Cancer J. Clin.* 67, 7–30. doi: 10.3322/caac.21387

Souto, R., Silva-Boghossian, C. M., and Colombo, A. P. (2014). Prevalence of *Pseudomonas aeruginosa* and *Acinetobacter* spp. in subgingival biofilm and saliva of subjects with chronic periodontal infection. *Braz. J. Microbiol.* 45, 495–501. doi: 10.1590/s1517-83822014000200017

Sutcliffe, S., and Platz, E. A. (2008). Inflammation and prostate cancer: a focus on infections. *Curr. Urol. Rep.* 9, 243–249. doi: 10.1007/s11934-008-0042-z

Swann, J. R., Want, E. J., Geier, F. M., Spagou, K., Wilson, I. D., Sidaway, J. E., et al. (2011). Systemic gut microbial modulation of bile acid metabolism in host tissue compartments. *Proc. Natl. Acad. Sci. U.S.A.* 108, 4523–4530. doi: 10.1073/pnas.1006734107

Taverna, G., Pedretti, E., Di Caro, G., Borroni, E. M., Marchesi, F., Grizzi, F., et al. (2015). Inflammation and prostate cancer: friends or foe? *Inflamm. Res.* 64, 275–286. doi: 10.1007/s00011-015-0812-2

van Olden, C., Groen, A. K., and Nieuwdorp, M. (2015). Role of intestinal microbiome in lipid and glucose metabolism in diabetes mellitus. *Clin. Ther.* 37, 1172–1177. doi: 10.1016/j.clinthera.2015.03.008

Wang, C. Z., Zhang, C. F., Chen, L., Anderson, L., Fang, L. U., Yuan, C. S., et al. (2015). Colon cancer chemopreventive effects of baicalein, an active enteric microbiome metabolite from baicalin. *Int. J. Oncol.* 47, 1749–1758. doi: 10.3892/ijo.2015.3173

Wong, M. C., Goggins, W. B., Wang, H. H., Fung, F. D., Leung, C., Wong, S. Y., et al. (2016). Global incidence and mortality for prostate cancer: analysis of temporal patterns and trends in 36 countries. *Eur. Urol.* 70, 862–874. doi: 10.1016/j.eururo.2016.05.043

Conflict of Interest Statement: The authors declare that the research was conducted in the absence of any commercial or financial relationships that could be construed as a potential conflict of interest.

Copyright © 2019 Ma, Chi, Fan, Dong, Shao, Xie, Li and Xue. This is an open-access article distributed under the terms of the Creative Commons Attribution License (CC BY). The use, distribution or reproduction in other forums is permitted, provided the original author(s) and the copyright owner(s) are credited and that the original publication in this journal is cited, in accordance with accepted academic practice. No use, distribution or reproduction is permitted which does not comply with these terms.

Advantages of publishing in Frontiers

OPEN ACCESS
Articles are free to read for greatest visibility and readership

FAST PUBLICATION
Around 90 days from submission to decision

HIGH QUALITY PEER-REVIEW
Rigorous, collaborative, and constructive peer-review

TRANSPARENT PEER-REVIEW
Editors and reviewers acknowledged by name on published articles

Frontiers
Avenue du Tribunal-Fédéral 34
1005 Lausanne | Switzerland

Visit us: www.frontiersin.org
Contact us: frontiersin.org/about/contact

REPRODUCIBILITY OF RESEARCH
Support open data and methods to enhance research reproducibility

DIGITAL PUBLISHING
Articles designed for optimal readership across devices

FOLLOW US
@frontiersin

IMPACT METRICS
Advanced article metrics track visibility across digital media

EXTENSIVE PROMOTION
Marketing and promotion of impactful research

LOOP RESEARCH NETWORK
Our network increases your article's readership